Chair of Waste Processing Technology and Waste Management

Doctoral Thesis

Origins, Distribution, and Fate of Contaminants and Ash Constituents in Waste for SRF Production and Co-Processing

Sandra Antonia Viczek, BSc MSc MSc

March 2021

MONTANUNIVERSITÄT LEOBEN
www.unileoben.ac.at

AFFIDAVIT

I declare on oath that I wrote this thesis independently, did not use other than the specified sources and aids, and did not otherwise use any unauthorized aids.

I declare that I have read, understood, and complied with the guidelines of the senate of the Montanuniversität Leoben for "Good Scientific Practice".

Furthermore, I declare that the electronic and printed version of the submitted thesis are identical, both, formally and with regard to content.

Date 24.03.2021

Signature Author
Sandra Antonia Viczek

To my family

Partial funding for this work was provided by: The Center of Competence for Recycling and Recovery of Waste 4.0 (acronym ReWaste4.0) (contract number 860 884) under the scope of the COMET – Competence Centers for Excellent Technologies – financially supported by BMK, BMDW, and the federal states of Styria, managed by the FFG.

DANKSAGUNG

Diese Dissertation würde in dieser Form nicht vorliegen, hätten mich nicht zahlreiche Menschen auf meinem Weg unterstützt oder wären nicht Teile des Weges mit mir mitgegangen.

Mein besonderer Dank gilt natürlich meinem Betreuer Prof. Roland Pomberger für die konstruktiven Betreuungsgespräche und die Möglichkeit, diese Dissertation zu verfassen. Ich möchte mich auch bei Renato Sarc bedanken, der mich während den letzten Jahren stets unterstützt hat und immer für fachliche und projektbezogene Fragen zur Verfügung stand. Weiters möchte ich mich herzlich bei Prof. Karl E. Lorber und Lisa Kandlbauer für das Korrekturlesen dieser Dissertation und einiger Publikationen bedanken, sowie bei meiner Mentorin Doris Kühnelt.

Besonders dankbar bin ich all meinen Kolleginnen und Kollegen, vor allem dem ReWaste4.0 Team. Gemeinsam haben wir unzählige Stunden im Büro verbracht, oft auch lange Abende und Nächte beim Schreiben unserer Paper. Egal wie hoch der Druck war, wir konnten immer auf die gegenseitige Unterstützung zählen und haben in all den Jahren auch sehr viel gelacht. Es war mir eine Freude, diesen Weg gemeinsam mit euch zu gehen.

Ich möchte mich auch bei Alexia Aldrian bedanken, die mir beim Planen der chemischen Analysen immer für Diskussionen beratend zur Seite gestanden ist. Weiters möchte ich mich bei unserem Labor bedanken, da meine Proben und Anforderungen oft nicht die einfachsten waren.

Ein großes Dankeschön verdienen auch unsere zahlreichen studentischen Mitarbeiter und Mitarbeiterinnen im ReWaste4.0 Projekt, die uns über viele Wochen und Monate tatkräftig bei der Umsetzung der praktischen Versuche unterstützt haben, und dabei trotz der oft unangenehmen Arbeit nie ihre Motivation und gute Laune verloren haben.

Weiters möchte ich mich bei allen Partnern im Projekt ReWaste4.0 für die tolle und konstruktive Zusammenarbeit bedanken, insbesondere der IFE Aufbereitungstechnik, Komptech, Lafarge, Mayer Recycling, Redwave und Saubermacher, die ihr Technikum, ihre Aggregate, Daten, Abfallproben oder einen Standort für Versuche zur Verfügung gestellt haben.

Mein besonderer Dank gilt außerdem Prof. Kevin Francesconi, der im Zuge meiner Masterarbeit mein Interesse für die Wissenschaft geweckt und gefördert hat, und mich so zur Überzeugung gebracht hat, eine Dissertation zu schreiben.

Vor allem aber möchte ich mich bei meiner gesamten Familie, allen voran bei meinen Eltern, bedanken. Ihr habt es mir ermöglicht, diesen Weg zu gehen, und habt mich dabei immer unterstützt, ein offenes Ohr gehabt und mir voller Zuversicht und Überzeugung gesagt: „Du machst das schon“. Vielen Dank für alles!

KURZFASSUNG

Herkunft, Verteilung und Verbleib von Schadstoffen und Aschebestandteilen in Abfällen für SRF Herstellung und Co-Processing

Bei der Herstellung verschiedenster Produkte und Konsumgüter kommen häufig Rohstoffe bzw. chemische Verbindungen zum Einsatz, die anorganische Schadstoffe wie Schwermetalle und Metalloide enthalten. Wenn diese Produkte das Ende ihres Lebenszyklus erreicht haben und entsorgt werden, können die enthaltenen Schadstoffe für viele Abfallbehandlungswege aufgrund existierender Grenzwerte, Richtwerte oder Qualitätsanforderungen ein Problem darstellen. Das betrifft auch Ersatzbrennstoffe (refuse-derived fuels; RDF) und deren Einsatz in der Zementindustrie (Co-Processing), der international zunehmend an Bedeutung gewinnt. In vielen Ländern werden aus festen, nicht gefährlichen Abfällen auch qualitätsgesicherte Ersatzbrennstoffe (solid recovered fuels; SRF) hergestellt. SRF Hersteller müssen dabei ggf. Maßnahmen ergreifen, um die Einhaltung der Vorgaben sicherzustellen, z.B. zur Verringerung der Konzentration bestimmter Schadstoffe. Dies erfordert jedoch Wissen über Abfallfraktionen, Materialien oder Produkte, die größere Mengen der relevanten chemischen Elemente enthalten. Neben Schadstoffen spielt beim Co-Processing von SRF und anderen RDF auch eine weitere Gruppe von Elementen eine wichtige Rolle, nämlich Aschebestandteile, da diese in den Zementklinker eingebunden und somit aus technischer Sicht stofflich verwertet werden.

Diese Dissertation befasst sich in drei verschiedenen Bereichen mit Schadstoffen und/oder Aschebestandteilen: Herkunft, Verteilung & Entfernung sowie Verbleib. Auf Basis von Literaturdaten wurden Schadstoffträger identifiziert und das Vorkommen von aschebildenden Elementen in Abfallfraktionen erörtert. Anhand praktischer Versuche wurden die Verteilung chemischer Elemente, Möglichkeiten zur Entfernung von Schadstoffträgern sowie der Effekt solcher Maßnahmen auf die SRF Qualität untersucht. Dabei wurden auch die bisher wenig erforschten Feinfraktionen chemisch und mineralogisch charakterisiert. Hinsichtlich des Verbleibs liegt der Fokus der Arbeit auf Aschebestandteilen und der Bestimmung des stofflich verwertbaren Anteils von SRF beim Co-Processing (R-Index) sowie der Identifizierung jener Material- bzw. Abfallfraktionen, die am meisten zum R-Index beitragen. Darauf basierend wird der potentielle Beitrag der Zementindustrie zur Erreichung der europäischen Recyclingziele berechnet und die Rolle der Zementindustrie in einer modernen Kreislaufwirtschaft diskutiert.

Die Ergebnisse zeigen, dass die Entfernung der Feinfraktion die Schadstoffkonzentrationen im Abfallstrom signifikant verringern kann, insbesondere in Kombination mit der Entfernung von PVC mit Nahinfrarot (NIR) Sortierern. Allerdings enthalten die Feinfraktionen auch den größten Anteil an wertvollen Aschebestandteilen für die Zementindustrie. Diese können nicht stofflich verwertet werden, wenn die Feinfraktion bei der SRF-Herstellung aus dem Abfallstrom entfernt wird. Dadurch kommt es zu einem Interessenkonflikt zwischen Ressourcenschonung und Umweltschutz. Die Analyse konventioneller SRF zeigte, dass 13 bis 18 Masse-% der SRF beim Co-Processing als stofflich verwertet angesehen werden können. In einer modernen Kreislaufwirtschaft kann die Zementindustrie daher eine attraktive ergänzende Recyclingoption darstellen, die Mischfraktionen oder Sortierreste aus etablierten Recyclingprozessen nicht nur thermisch, sondern auch stofflich verwerten kann.

ABSTRACT

Origins, Distribution, and Fate of Contaminants and Ash Constituents in Waste for SRF Production and Co-Processing

Raw materials or chemical compounds containing inorganic contaminants such as heavy metals or metalloids are frequently applied for the industrial production of various goods and consumer products. When these products are discarded at the end of their life cycle, the contained contaminants may pose a problem to various waste treatment options because of existing limit values, guidance values, or quality requirements. This also applies to the co-processing of refuse-derived fuels (RDF) in the cement industry, which is increasingly attractive throughout the world. In several countries, mixed solid wastes are frequently processed to solid recovered fuels (SRF), a quality-assured subgroup of RDF solely produced from non-hazardous solid wastes. SRF producers may need to take measures to ensure that the requirements are met, including measures to decrease contaminant concentrations in SRF. However, this requires prior knowledge of the waste fractions, materials, or products that may contain large amounts of these elements. Besides contaminants, another group of chemical elements plays an essential role in the co-processing of SRF and other RDF, namely ash constituents, which are incorporated into the cement clinker and are, therefore, from a technical perspective, recycled on a material level.

This Doctoral Thesis focuses on three different domains concerning contaminants and/or ash constituents: origins, distribution & removal, and fate. An extensive literature review was conducted to identify contaminant carriers and to discuss the occurrence of ash-forming elements in waste fractions. The element distribution, removal options for contaminant carriers and effects on SRF quality were investigated by practical experiments. Special attention was paid to chemically and mineralogically characterizing the fine fractions, which have hardly been investigated before. Concerning the fate of elements, this Thesis focused on ash constituents and determining the material-recyclable share of SRF (R-index) during co-processing, as well as identifying those material or waste fractions that contribute most to the R-index. Consequently, the potential contribution of the cement industry towards reaching European recycling targets was estimated, and the role of the cement industry in a modern circular economy was assessed.

The obtained results show that removing the fine fraction can significantly decrease contaminant concentrations in the treated waste stream, especially in combination with near-infrared (NIR) sorters removing PVC. However, the fine fractions also contain the largest share of valuable ash constituents for the cement industry. These materials would be prevented from being recycled when the fraction is removed from the waste during SRF production. This leads to a conflict of interest between resource utilization/conservation and environmental protection. Analyses of conventional SRF showed that 13 to 18 mass-% of the SRF may be considered as recycled on a material level in the cement industry. Therefore, in a modern circular economy, the cement industry may represent an attractive complementary recycling option, offering the material recycling of mixed fractions or sorting residues from established recycling processes in addition to their thermal recovery.

PUBLICATIONS AND CONTRIBUTIONS

- **Articles in peer-reviewed journals**

Viczek, S.A., Kandlbauer, L., Khodier, K., Aldrian, A., Sarc, R. (under review, 2021): *Sampling and analysis of coarsely shredded mixed commercial waste. Part II: particle size-dependent element determination*.

Viczek, S.A., Aldrian, A., Pomberger, R., Sarc, R. (in press, 2021): *Origins of major and minor ash constituents of solid recovered fuel for co-processing in the cement industry.* Waste Management.

Viczek, S.A., Lorber, K.E., Pomberger, R., Sarc, R. (2021): *Production of contaminant-depleted solid recovered fuel from mixed commercial waste*. Fuel 294, 120414, https://doi.org/10.1016/j.fuel.2021.120414

Viczek, S.A., Khodier, K., Kandlbauer, L., Aldrian, A., Redhammer, G., Tippelt, G., Sarc, R. (2021): *The particle size-dependent distribution of chemical elements in mixed commercial waste and implications for enhancing SRF quality*. Science of the total Environment 776, 145343. https://doi.org/10.1016/j.scitotenv.2021.145343

Viczek, S.A., Aldrian, A., Pomberger, R., Sarc, R. (2020): *Determination of the material-recyclable share of SRF during co-processing in the cement industry*. Resources, Conservation and Recycling 156, 104696. https://doi.org/10.1016/j.resconrec.2020.104696

Aldrian, A., Viczek, S.A., Pomberger, R., Sarc, R. (2020): *Methods for identifying the material-recyclable share of SRF during co-processing in the cement industry*. Methods X 7, 100837. https://doi.org/10.1016/j.mex.2020.100837

Viczek, S.A., Aldrian, A., Pomberger, R., Sarc, R. (2020): *Origins and carriers of Sb, As, Cd, Cl, Cr, Co, Pb, Hg, and Ni in mixed solid waste – A literature-based evaluation*. Waste Management 103, 87-112. https://doi.org/10.1016/j.wasman.2019.12.009

Khodier, K., Viczek, S.A., Curtis, A., Aldrian, A., O'Leary, P., Lehner, M., Sarc, R. (2020): *Sampling and analysis of coarsely shredded mixed commercial waste. Part I: procedure, particle size and sorting analysis*. International Journal of Environmental Science and Technology 17, 959-972. https://doi.org/10.1007/s13762-019-02526-w

- **Peer-reviewed conference contributions**

Sarc, R., Viczek, S.A., Aldrian, A., Lorber, K.E., Pomberger, R. (2020): *Stoffliche Verwertung bei der energetischen Nutzung von Ersatzbrennstoffen in der Zementindustrie*. **Written contribution (peer reviewed)**. In: Energie aus Abfall 17, 761-772.

Viczek, S.A., Khodier, K., Pomberger, R., Sarc, R. (2019): *Grain Size-Dependent Distribution of Contaminants in Coarse-shredded Commercial Waste – As, Cd, Co, Cr, Hg, Ni, Pb, Sb, and*

Cl. **Oral presentation & written contribution (peer-reviewed)**. At: IRRC Waste to Energy, Vienna, 14.-15.10.2019. Waste Management 9, 413-429.

- **Other conference contributions, posters, and presentations**

Viczek, S.A., Lampl, C., Aldrian, A., Sarc, R. (2020): *Co-Processing von Ersatzbrennstoffen: Beitrag der Zementindustrie zur Recyclingrate*. **Oral presentation & written contribution.** At: Recy&DepoTech 2020, Virtual, 18.–20.11.2020.

Viczek, S.A. (2020): *Production of Pollutant-Depleted SRF from Mixed Commercial Waste for Co-Processing in the Cement Industry.* **Oral presentation**. At: IRRC Waste-to-Energy, Virtual, 15.–16.10.2020.

Viczek, S.A. (2019): *Facts about SRF co-processing in the cement industry.* **Oral presentation**. At: Current issues of Waste Management in Preparation for the 'Circular Economy'/Aktuális Hulladékgazdálkodási kérdések a 'Körkörös Gazdaságra' való felkészülés jegyében, Miskolc, 20.11.2019.

Viczek, S.A., Aldrian, A., Pomberger, R., Sarc, R. (2019): *Analytical determination of the material-recyclable share of SRF through co-processing in the cement industry - Comparison of ashing temperatures.* **Oral presentation & written contribution**. At: Sardinia 2019: 17th international waste management and landfill symposium, Cagliari, 30.09–04.10.2019.

Viczek, S.A., Khodier, K., Pomberger, R., Sarc, R. (2019): *Grain size-dependent distribution of As, Cd, Cl, Co, Cr, Fe, Hg, Ni, Pb, Sb, Sn, Ti, V, W, and Zn in coarse-shredded commercial waste.* **Oral presentation & written contribution**. At: Sardinia 2019: 17th international waste management and landfill symposium, Cagliari, 30.09.–04.10.2019.

Viczek, S.A., Aldrian, A., Pomberger, R., Sarc, R. (2019): *Analytical determination of recycling quota through SRF co-processing in the cement industry.* **Oral presentation & written contribution**. At: 7th International Conference on Sustainable Solid Waste Management, Heraklion, 26.–29.06.2019.

Viczek, S.A., Khodier, K., Aldrian, A., Pomberger, R., Sarc, R. (2019): *Grain size-dependent distribution of contaminants in coarse-shredded commercial waste – results for As, Ba, Cd, Co, Cr, Cu, Hg, Mn, Mo, Ni, Pb, and Sb.* **Oral presentation & written contribution**. At: 7th International Conference on Sustainable Solid Waste Management, Heraklion, 26.–29.06.2019.

Viczek, S.A. (2019): *Characterization and treatment of selected contaminants and impurities in mixed solid waste*. **Oral presentation.** At: PhD Doctoral Colloquium, University of Graz, 20.–21.05.2019.

Aldrian, A., Abi-Fadel, A., Viczek, S.A., Sarc, R. (2019): *Untersuchungen zur Bestimmung des organisch und anorganisch gebundenen Chlorgehaltes in Ersatzbrennstoffen*. **Written**

contribution. In: Tagungsband 9. Wissenschaftskongress Abfall- und Ressourcenwirtschaft, 243-247.

Viczek, S.A., Aldrian, A., Pomberger, R., Sarc, R. (2019): *Bestimmung des stofflich verwertbaren Anteils des EBS bei der energetischen Verwertung in der Zementindustrie*. **Poster & written contribution**. In: Österreichische Abfallwirtschaftstagung 2019, Eisenstadt, 15.–17.05.2019.

Viczek, S.A, Sarc, R. (2018): *Identifizierung von Sb-, Cd-, Cr- und Ni-Trägern in gemischten Abfällen auf Basis von Literaturdaten*. **Poster & written contribution**. In: Recy&DepoTech 2018: Vorträge-Konferenzband zur 14. Recy&DepoTech, Leoben, 07.–09.11.2018, 773–780.

- **(Co-)supervised Bachelor's and Master's Theses**

Häring, L. (2021): *PVC Recycling in einer Kreislaufwirtschaft – Stand der Wissenschaft und Technik.* Bachelor's Thesis, Montanuniversitaet Leoben.

Jansch, L. (2020): *Bilanzierung eines österreichischen Zementwerks: Al, Ca, Fe, K, Mg, Na, P, S, Si, Ti.* Bachelor's Thesis, Montanuniversitaet Leoben.

Schaller, A. (2020): *Hydrothermale Verfahren und Dampfbehandlung von Abfällen – Stand der Wissenschaft und Technik*. Bachelor's Thesis, Montanuniversitaet Leoben.

Lauschensky, J. (2019): *Auswirkungen des Einsatzes von EBS aus nicht gefährlichen Abfällen auf Schadstoffgehalte im Zement und im Recyclingkreislauf*. Master's Thesis, FH Technikum Wien.

Warchol, T. (2019): *Zusammensetzung und Chlorgehalt von Rejekten aus der Papierindustrie und Ersatzbrennstoffen für die Zementindustrie*. Bachelor's Thesis, Montanuniversitaet Leoben.

- **Participation in committees**

Austrian Standards Committee 157 "Waste Management", ISO TC 300 "Solid Recovered Fuels" and CEN TC 343 "Solid Recovered Fuels" for the elaboration of the new ISO EN standard "Solid Recovered Fuels – Determination of the Recycling-Index".

TABLE OF CONTENTS

Page

1 INTRODUCTION

Every year the world generates approximately 2 billion tonnes (2.01 billion tonnes in year 2016, Kaza et al. (2018)) of municipal solid waste (MSW) from residential, commercial, and institutional sources. This amount is expected to rise to 3.4 billion tonnes by 2050 (Kaza et al., 2018). These numbers emphasize the importance of the principle that waste shall be treated in a way that minimizes its effect on the environment and enables the highest possible waste valorization (i.e., reuse, recycling, or recovery, cf. Kabongo (2013), Arancon et al. (2013)). This principle is also reflected by the EU waste hierarchy (EC, 2018, 2008a) (Figure 1).

Figure 1: Waste hierarchy as defined in the EU waste framework directive (EC, 2018, 2008a).

According to the EU waste hierarchy defined in Directive 2008/98/EC on waste and repealing certain Directives (waste framework directive) (EC, 2008a) as well as Directive 2018/851 amending Directive 2008/98/EC on waste (EC, 2018), preventing waste is the most preferable option, which implies taking measures before an object even becomes waste. The next favorable option is to prepare waste products or product components for their reuse. Recycling comprises reprocessing materials into substances, materials, or products. However, it does not include reprocessing into fuels. The production of fuels and subsequent energy recovery is included in the category “recovery”, which includes processes where waste replaces other materials (R operations, listed in Annex II of directive 2008/98/EC). By definition, recovery includes the use of waste as a fuel or other means for energy generation, including incineration facilities if an energy efficiency of ≥ 0.60 (for installations permitted before January 1, 2009) or ≥ 0.65 (for installations permitted after December 31, 2008) is achieved. Incineration facilities with lower energy efficiencies are considered disposal facilities. Disposal includes operations that are not recovery (D operations, outlined in Annex I of directive 2008/98/EC), even if substances or energy are reclaimed as a secondary consequence (EC, 2008a).

While most MSW generated worldwide is currently disposed or dumped in landfills, a trend of increased recycling and composting is observable on a global level. Generally, the amount of

recyclable material, especially plastics, is growing with increasing income levels (Kaza et al., 2018). However, not every material in waste can be recycled due to various reasons, including being mixed with other materials, being soiled or contaminated, or not being present in amounts large enough to make recycling economically viable (Pomberger, 2020). Consequently, in upper-middle-income countries, waste-to-energy incineration is increasing (Kaza et al., 2018).

The European Union, specifically Directive 2010/75/EU on industrial emissions (EC, 2010), strictly distinguishes between "waste incineration plants" and "waste co-incineration plants". While a waste incineration plant is *"dedicated to the thermal treatment of waste, with or without recovery of the combustion heat generated (…)"* (EC, 2010), a waste co-incineration plant is a "*technical unit whose main purpose is the generation of energy or production of material products and which uses waste as a regular or additional fuel or in which waste is thermally treated for the purpose of disposal (…)"* (EC, 2010). One option for waste co-incineration that has become increasingly popular in the past decades is the utilization of refuse-derived fuels (RDF) in the cement industry to substitute fossil fuels. The thermal substitution rate (TSR) expresses the degree of substitution, i.e., the percentage of thermal energy demand covered by alternative fuels and biomass. Figure 2 illustrates the development of the TSR in different countries, the EU-28, and worldwide. While the TSR is continually increasing on a global scale, the highest overall TSR is achieved by the Austrian cement industry (GCCA, 2021).

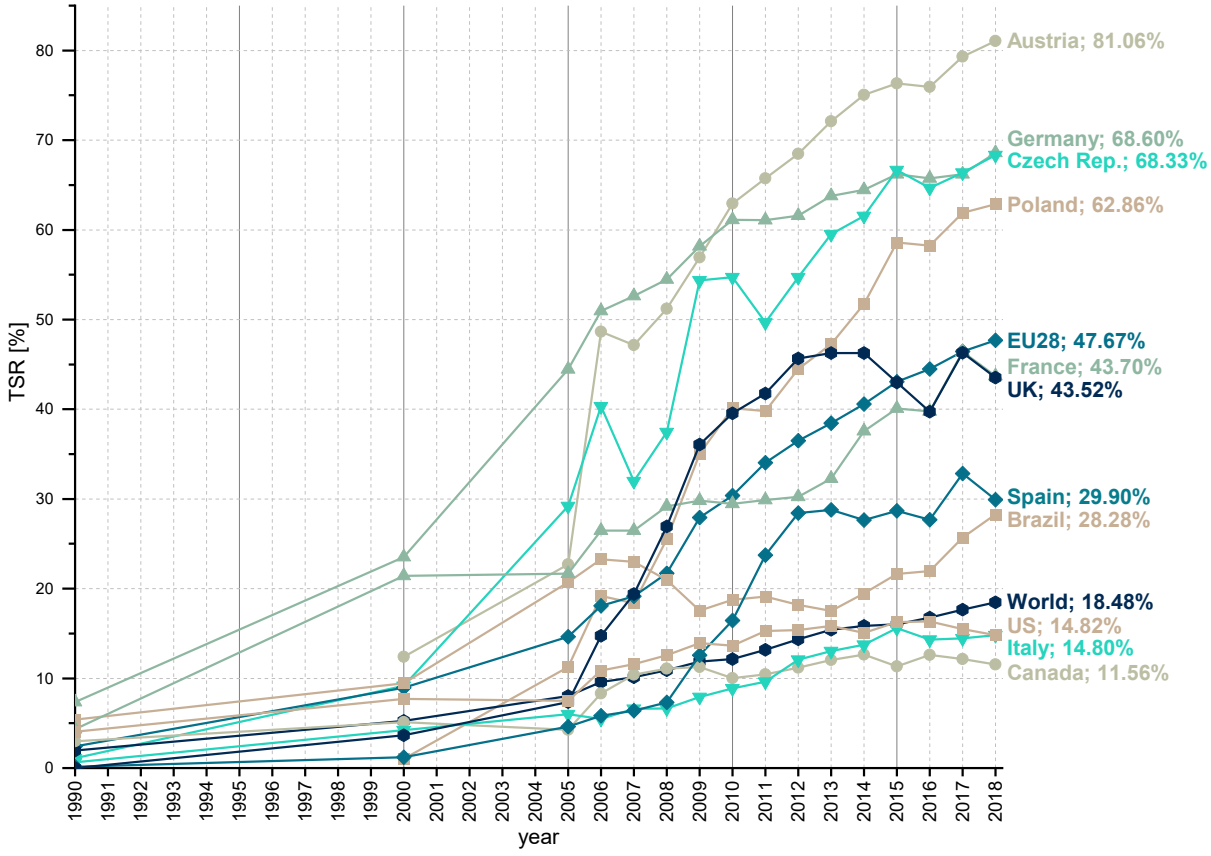

Figure 2: Development of the thermal substitution rates (TSR in %) in different countries, the EU, and worldwide between 1990 and 2018 (GCCA, 2021).

1.1 State of the art

To a large extent, the Austrian cement industry reaches its high substitution rates by utilizing plastic-rich waste (Mauschitz, 2020), i.e., solid recovered fuels (SRF) (Sarc et al., 2019; Sarc et al., 2014). SRF is a subgroup of RDF and comprises quality-assured fuels exclusively produced from solid, non-hazardous sorted or mixed waste, e.g., municipal waste fractions, mixed commercial waste (MCW), and production or packaging wastes (ASI, 2011b; Lorber et al., 2012; Sarc et al., 2014). Several processing steps are usually involved when waste is processed to fuel for co-incineration plants such as the cement industry. Furthermore, compliance with defined requirements, guidance and limit values must be assured.

State-of-the-art SRF production plants typically apply multiple shredding steps and various separation techniques to process MSW or MCW to SRF (Sarc et al., 2014). Typically, a coarse shredder or bag opener is used at the beginning of the process to increase the accessibility and processability of the waste. Screening, e.g., at 60 or 80 mm, may be used to generate a coarser and a finer fraction, both of which may differ in their lower heating value (LHV). The coarse fraction usually contains more plastic foils, which increases its LHV compared to the screen underflow. Both particle size fractions may be treated by magnetic separators to remove Fe-metals, air classifiers to remove unwanted heavy materials such as stones, and eddy current separators to remove non-Fe metals (Sarc et al., 2014). Furthermore, near-infrared (NIR) sorters are frequently applied to remove valuable polyethylene terephthalate (PET) for recycling, or unwanted polyvinyl chloride (PVC) (Pomberger and Sarc, 2014; Sarc et al., 2014), a chlorine carrier having negative effects on the cement manufacturing process if present in higher concentrations (Gerassimidou et al., 2021; Lorber et al., 2012). While the finer fraction <60 mm may be directly applied as a fuel for secondary firing in the cement industry, the coarser fraction with a higher LHV may be further comminuted to a size <30 mm and used as a fuel for primary firing (Sarc et al., 2014).

Besides chlorine concentrations, an important aspect that needs consideration is the fact that MSW and MCW frequently contain heavy metals or metalloids (e.g., Hg, Pb, Sb, Cd) as a consequence of their current or former use in the industrial production of various goods (e.g., Rotter, 2002; Turner, 2019; Turner and Filella, 2017; Viczek et al., 2020b; Yan et al., 2020). Apart from impacting waste properties and being decisive factors for waste categorization (hazardous, non-hazardous (EC, 2008b, 2008a)), heavy metals and metalloids in non-hazardous waste play a role in landfilling, composting, recycling, and incineration (Götze et al., 2016; Pomberger et al., 2015; Viczek et al., 2021 under review). However, studies have shown that mechanical waste treatment steps influence heavy metal concentrations in RDF (Nasrullah et al., 2016; Nasrullah et al., 2015; Rotter, 2002). Specific heavy metals can be removed together with materials they usually occur in; for example, the removal of PET and PVC with NIR sorters can also decrease Sb and Cd levels (Kreindl, 2007; Pieber et al., 2012).

Removing such “contaminant carriers” may be necessary for some waste streams because several limit values or guidance values exist on different levels for SRFs and their utilization. They range from regional emission legislation (e.g., the US Clean Air Act (US EPA, 2019) or

EU industrial emissions directive (EC, 2010)) to national limit values for the SRF itself, for example, in Austria (BMLFUW, 2010) or Switzerland (Swiss Federal Council, 2015). Furthermore, the classification system for SRF in the standard EN 15359 (ASI, 2011b) includes limit values for Cl and Hg that define five SRF classes. Additionally, requirements for SRF may be defined by quality marks (e.g., RAL GZ 724 for quality assured SRF in Germany (Flamme and Geiping, 2012)) or cement manufacturers (Lorber et al., 2012; Pomberger, 2008). Examples for guidance and limit values for SRF intended to be co-incinerated in the cement industry are compared in Table 1.

Table 1: Comparison of guidance values and limit values for heavy metals, metalloids, and other chemical elements in SRF (Flamme and Geiping, 2012), adapted and updated.

Element	Austria, legal limit values (BMLFUW, 2010)		Germany, RAL quality mark 724 (BGS e.V., 2014)		Switzerland, legal limit values (Swiss Federal Council, 2015)
	mg/MJ		mg/MJ		mg/kg
	median	80th percentile	median	80th percentile	
As	2	3	0.31	0.81	30
Cd	0.23	0.46	0.25	0.56	5
Co	1.5	2.7	0.38	0.75	250
Cr	25	37	7.8	16	500
Hg	0.075	0.15	0.038	0.075	1
Ni	10	18	5.0	10	500
Pb	20	36	12	25	500
Sb	7	10	3.1	7.5	300
Cu	-	-	-	-	500
Mn	-	-	16	31	-
Sn	-	-	1.9	4.4	100
Tl	-	-	0.063	0.13	3
V	-	-	0.63	1.6	-
Zn	-	-	-	-	4,000

The co-incineration of RDF in the cement industry is frequently referred to as co-processing. This term is used for industrial processes that enable the simultaneous recovery of energy and the mineral content of waste material, therewith enabling the substitution of both fossil fuels and mineral raw materials (Basel Convention, 2012; Lamas et al., 2013; Vodegel et al., 2018). This is the case for the co-incineration of RDF in the cement industry because not only is the energy used, but the ash formed during the combustion process is introduced into the kiln and incorporated into the product, the cement clinker.

Although the fuel ash becomes part of the product, which could technically be seen as partial recycling on a material level, from a legal point of view, co-processing of RDF is considered a recovery operation, more specifically an R1 operation ("*use principally as a fuel or other means to generate energy*") according to the EU waste framework directive (EC, 2008a). In single European countries such as Hungary, France, or Portugal, a mixed recovery, i.e., the simultaneous recovery of energy and materials, is already legally established (Viczek et al., 2020a). The European Union is also considering acknowledging the incorporation of mineral constituents of RDF into the cement clinker and potentially counting these minerals towards the EU recycling targets in the future (EC, 2018). However, under current EU legislation,

"*metals incorporated in the mineral output of the co-incineration process of municipal waste shall not be reported as recycled*" (EC, 2019).

In any case, more information and reliable data are necessary to evaluate whether the chemical components present in SRF ash are the same chemical components that are required to produce cement clinker. Scientific studies investigating ashes from MSW incineration (MSWI) and/or their potential application as substitute raw materials for the cement industry (Ashraf et al., 2019; Clavier et al., 2020; Gao et al., 2017; Garcia-Lodeiro et al., 2016; Krammart and Tangtermsirikul, 2004; Lam et al., 2011; Pan et al., 2008; Saikia et al., 2007; Sarmiento et al., 2019), as well as analyses of SRF ashes (Dunnu et al., 2010; Hilber et al., 2007; Kuna, 2015; Pohl et al., 2011; Wagland et al., 2011), lend support to this assumption. The composition of SRF ash, MSWI ash, and the role of different element oxides in the cement manufacturing process is given in Table 2.

Table 2: The role of selected chemical components in the cement manufacturing process and examples for their concentrations in SRF and MSWI ashes, adapted from Viczek et al. (2020a).

Chemical compound	Role in cement manufacturing	SRF ash composition in % (from MSW and MCW)				MSWI bottom ash composition in %			MSWI fly ash composition in %		
		Hilber et al. (2007)	Pohl et al. (2011)	Dunnu et al. (2010)	Wagland et al. (2011)	Sarmiento et al. (2019)	Ashraf et al. (2019)	Pan et al. (2008)	Pan et al. (2008)	Sarmiento et al. (2019)	Saikia et al. (2007)
CaO	Four main chemical components for cement clinker production, giving the clinker its crucial properties	25.77	40.13	25.41	18.5	16.2–37.6	12.71–14.78	50.39	45.42	34.2–54.9	13.86
SiO_2		26.52	23.87	38.12	48.1	33.4–50.6	18.88–25.91	13.44	13.6	3.93–15.6	12.01
Al_2O_3		13.68	10.47	11.18	9.5	5.39–11.6	9.55–10.57	1.26	0.92	1.51–3.72	8.1
Fe_2O_3		3.33	4.83	2.88	2.7	2.64–11.1	4.64–4.81	8.84	3.83	0.12–2.23	1.21
MgO	Clinker phase	2.43	3.23	3.68	2	1.52–2.07	1.75–1.81	2.26	3.16	0.98–5.81	2.62
TiO_2	Clinker phase	2.28	2.68	2.33	1.8	0.69–1.39	1.87–2.17	2.36	3.12	0.41–0.95	-
SO_3	Required to transfer alkali oxides into alkali sulfates	1.34	3.4*	4.5	0.8*	0.97–3.84	1.5*	1.79	6.27	5.54–13.3	4.6*
Na_2O	In the form of sulfates: altering the chemical reactivity of clinker with water	5.27	2.2	4.18	3.3	2.22–5.13	1.53–2.09	12.66	4.16	3.53–4.65	17.19
K_2O		2.02	0.78	2.34	1.9	0.61–1.02	0.88–1.16	1.78	3.85	2.28–2.40	7.41
P_2O_5	-	1.26	0.51	1.18	1.5	0.87–2.22	1.44–1.46	3.19	1.72	0.49–1.11	-

*calculated from total S or SO_4^{2-}.

1.2 Problem identification and formulation

Although contaminants in SRF need close monitoring to assure compliance with limit values and guidance values (Table 1) or requested quality criteria (Pomberger, 2008), only few technical measures are taken in SRF production plants that aim at reducing contaminant concentrations. The most common technology applied to remove specific materials is Fe- and non-Fe metals separation, targeting valuable metals or metal alloys for recycling. Furthermore, NIR sorting is frequently applied, but the reduction of Sb and Cd is only a secondary effect of removing the Cl carrier PVC or valuable PET, which is the primary purpose of applying this technology. Therefore, Cl is the only SRF-relevant contaminant frequently and targetedly removed from the waste stream in SRF production plants. However, legal limit values may sometimes require reducing the concentration of other contaminants when the SRF is intended for utilization in the cement industry. As a prerequisite to finding suitable methods for reducing the concentrations of specific contaminants, knowledge about their distribution and the waste fractions, waste materials, waste objects, or products they may occur in is crucial. This information is often very limited; it is collected and extended in this Thesis and used as a basis to test and determine potential technologies that may result in the reduction of specific contaminants.

With a potential recognition of energy recovery and simultaneous material recycling during SRF co-processing in the cement industry being discussed in the European Commission, a second group of chemical elements, namely ash constituents, comes into play. Literature has demonstrated that SRF ash consists of chemical compounds that are valuable to the cement industry because they can substitute primary raw materials. If this mixed recovery is recognized on the EU level (which shall be assessed until the end of 2028 (EC, 2018)), the cement industry will contribute towards reaching the EU recycling targets. However, the share of SRF that can be considered as recycled on a material level has not been investigated with a large number of SRF samples before. Thus, the determination of the material-recyclable share is now addressed in this Thesis. The information is subsequently used to estimate the potential contribution of the cement industry towards the recycling targets by co-processing of SRF and to evaluate the role of the cement industry in a circular economy.

Furthermore, the possibility of recycling mineral constituents in the cement industry raises the question of whether elements other than typical contaminants need to be considered when assessing SRF quality. Because some of the major constituents of SRF ash represent valuable chemical compounds for the cement industry, it is evident that a genuine evaluation of the quality of SRF intended for co-processing requires taking both the concentrations of contaminants as well as ash constituents into consideration. This is particularly important when specific waste fractions are removed in the SRF production process, and represents an entirely new aspect for SRF quality assessment, which in terms of chemical elements is currently limited to certain heavy metals, metalloids, and chlorine, besides considering other parameters such as the LHV, particle size, ash content, or water content.

2 METHODOLOGY AND SCOPE

2.1 Scope of investigations

This Thesis focuses on two groups of chemical elements relevant to SRF and co-processing: contaminants and ash constituents (Figure 3). As outlined in section 1.1, contaminants matter because of legal limit values, guidance values, or quality criteria requested by cement plant operators. Ash constituents are important because they may represent valuable raw materials for the cement industry. The most relevant chemical elements are listed in the sections “main” and “further” of Figure 3. Other elements that were determined in this Thesis, either in unprocessed waste or SRF ash, are listed in the section “other”. Analyses of unprocessed waste comprised both contaminants as well as major and minor ash constituents. Thereby, this Thesis follows a new approach for evaluating SRF quality that considers both valuable and unwanted chemical elements or compounds.

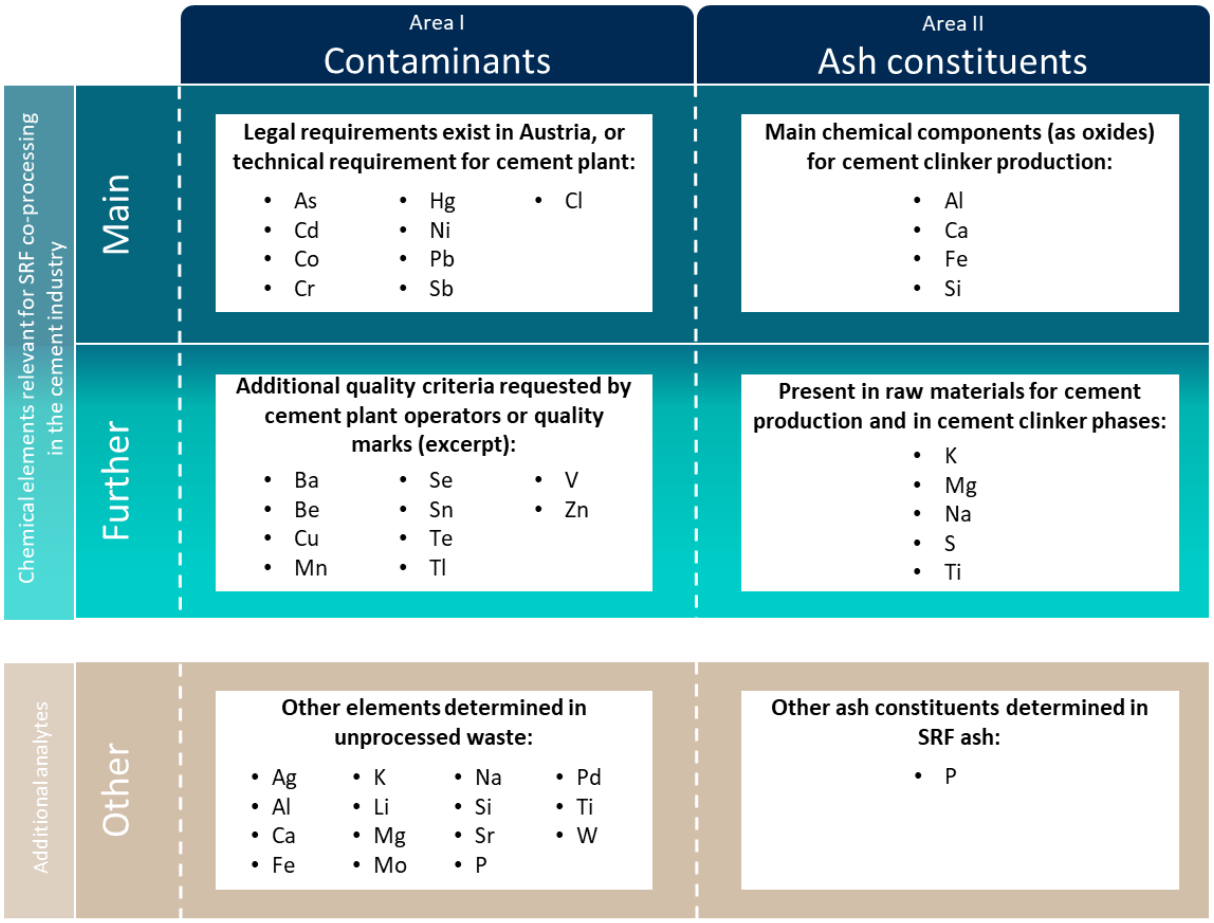

Figure 3: Chemical elements (contaminants and ash constituents) relevant to SRF for co-processing in the cement industry and other elements analyzed in this Thesis. The elements were grouped based on Table 1, Table 2, and the quality requirements requested by a cement plant as reported by Pomberger (2008).

The system in which these chemical elements are investigated is outlined in Figure 4. It comprises the SRF production process and SRF application in the cement industry and deals with three domains in relation to the chemical elements concerned:

1. **Origins** of elements in waste and their industrial applications,
2. **Distribution** of elements in waste or waste fractions and potential removal options during mechanical waste processing, and
3. **Fate** of elements in the cement clinker kiln.

Because numerous studies (e.g., Achternbosch et al., 2003; Cipurkovic et al., 2014; Lederer et al., 2015; Zeschmar-Lahl, 2003) have already reported the behavior and transfer coefficients of contaminants in cement plants, there is limited need for further research regarding the fate of these heavy metals or metalloids in the cement industry. Therefore, this Thesis focuses on the fate of typical ash constituents, many of which represent valuable materials for cement manufacturers, and the potential material recycling of mixed solid wastes that SRF co-processing is offering.

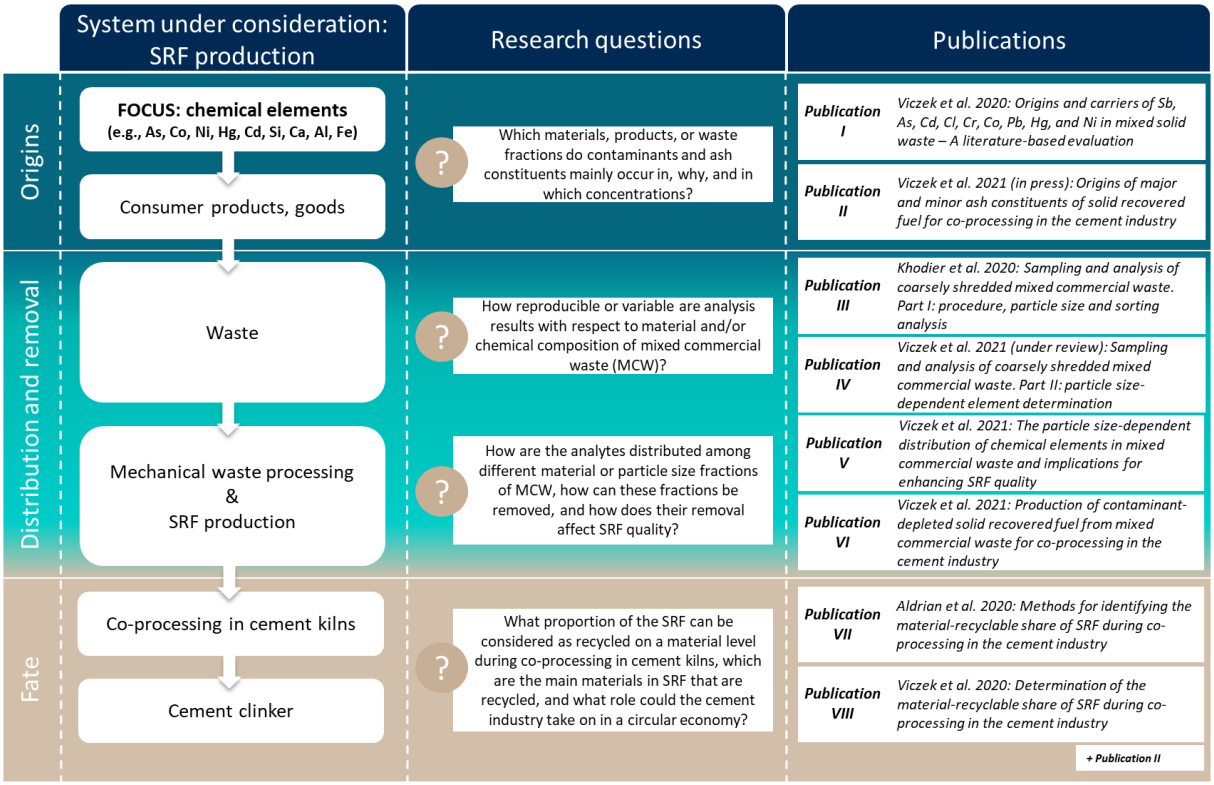

Figure 4: Thesis structure, outline of the system under consideration, and assignment of research questions and publications.

2.2 Research questions

Research Question 1:

Which materials, products, or waste fractions do contaminants and ash constituents mainly occur in, why, and in which concentrations?

Knowledge of the materials or fractions containing SRF-relevant contaminants (As, Cd, Cl, Co, Cr, Hg, Ni, Pb, Sb) is the prerequisite for all subsequent steps aiming at removing these unwanted contaminants from the waste stream. Various literature exists on the presence of contaminants in consumer products, materials, waste, or waste fractions. Therefore, ***Publication I*** aims to identify the main carriers of As, Cd, Cl, Co, Cr, Hg, Ni, Pb, Sb in waste based on extensive literature research. Concentrations reported for consumer products, waste fractions, and certain materials are elaborated in the form of concise tables. By comparing the element concentrations reported for the respective material, waste fraction, or product with the reported concentrations in the mixed waste stream, contaminant carriers are identified and classified according to their strength. Additionally, Publication I is dedicated to explaining why these chemical elements occur in the identified contaminant carriers and includes additional information regarding the occurrence and industrial applications of the investigated elements. Because not all contaminant carriers may be reflected by the analysis results due to common laboratory practice in the field of environmental analysis, the publication also assesses the influence of some standard sample preparation procedures, especially the removal of hard impurities, on analysis results.

Publication II addresses the origins of the second group of chemical elements relevant to SRF: the ash constituents Al, Ca, K, Fe, Mg, Na, P, S, Si, and Ti. Because existing studies reporting chemical analyses of waste or waste fractions rarely focused on these elements, a combined approach is chosen, complementing a literature review on the occurrence and industrial applications of these elements with chemical ash analyses of material fractions extracted from SRF.

Research Question 2:

How reproducible or variable are analysis results with respect to material and/or chemical composition of mixed commercial waste (MCW)?

Despite sensor-based continuous analysis methods for waste being developed, sampling is still unavoidable for determining various parameters in modern waste management. However, sampling of waste is a complicated task due to waste heterogeneity and because very large items may be present, as is often the case with MCW. In this regard, it is also necessary to know how much the analysis results for the same pile of mixed commercial waste can vary. To determine the relative sampling variability (RSV; a measure of the total sampling variance normalized by the arithmetic mean), a replication experiment designed according to the principles of the Theory of Sampling (TOS) (cf. DS, 2013; Esbensen and Wagner, 2014; Gy, 1995) and ÖNORM S 2127 (ASI, 2011a) is carried out. Ten composite samples are taken from

the falling waste stream after shredding a pile of 45 tons of MCW. The composite samples are screened to yield nine different particle size classes, which were manually sorted and chemically analyzed. ***Publication III*** focuses on the basic setup, the theoretical background of the experiments, as well as the RSVs of sorted material fractions. ***Publication IV*** is dedicated to the RSVs of 30 elements and evaluating correlations between sorting analyses and chemical analyses.

Research Question 3:

How are the analytes distributed among different material or particle size fractions of mixed commercial waste (MCW), how can these fractions be removed, and how does their removal affect SRF quality?

Contaminants can be distributed among or enriched in different material classes (see Research Question 1), but also in different particle size classes, as indicated in literature reporting elevated contaminant concentrations in the fine fractions (Curtis et al., 2019; Sarc, 2015; Viczek et al., 2020b). If SRF-relevant contaminants were "accumulated" in the fine fractions, this would offer SRF producers the possibility to simply improve SRF quality by screening, while defined material fractions would require other technologies, e.g., NIR sorting. However, it needs to be assessed how removing these contaminant-rich fractions affects the overall SRF quality, including parameters such as the LHV and ash constituents. Furthermore, a thorough characterization of the fine fraction has never been carried out before but is necessary to evaluate possible treatment options if this fraction is removed from the waste stream in the SRF production process.

Publication V is dedicated to the particle size-dependent distribution of 30 chemical elements, which was determined in the course of the replication experiment (see research question 2). Furthermore, the publication chemically and mineralogically characterizes the fine fraction <5 mm with different analytical techniques. ***Publication VI*** focuses on possible combinations of technologies to remove contaminant-rich materials and waste fractions, like screening, NIR sorting to remove the prominent Sb, Cd, or Cl carriers PET and PVC, and the removal of black and grey colored materials which cannot be recognized by state-of-the-art NIR sorters. Both publications assess and discuss how removing the investigated waste fractions affects SRF quality, taking both contaminants and ash constituents into account.

Research Question 4:

What proportion of the SRF can be considered as recycled on a material level during co-processing in cement kilns, which are the main materials in SRF that are recycled, and what role could the cement industry take on in a circular economy?

To support the European Commission's pending decision on recognizing the material recycling of mineral matter during co-processing, more information on the ash composition of SRF is required. If the European Commission decides to acknowledge the recycling of mineral

constituents in the cement industry, the cement industry could support the EU Member States in reaching the EU recycling targets. This is especially the case in countries with an already high TSR. In countries with a low TSR, recognizing a mixed recovery could cause a shift of waste streams away from conventional waste incineration or landfilling towards co-processing. Because the European Commission has defined recycling targets for different waste streams, e.g., MSW or plastics packaging waste, information on the extent to which different materials or waste fractions from SRF are recycled in the cement industry is of interest.

To answer the posed research question, ***Publication VII*** focuses on developing and validating a suitable analysis procedure by testing different ashing temperatures, sample digestion/fusion techniques, and instrumental analysis methods. ***Publication VIII*** applies the method to a large variety of SRF samples (plastic-rich SRF from mixed municipal and commercial solid waste) calculates the potential contribution of the cement industry towards reaching the EU recycling targets. Furthermore, the ash analyses of material fractions performed in ***Publication II*** (using the methods published in Publication VII) serve to identify the materials that are mainly responsible for this material-recyclable proportion of SRF, i.e., those materials that contribute most to the ash content and large amounts of the valuable element oxides in SRF ash. Based on this information, the role the cement industry can take on in a circular economy is assessed.

3 RESULTS

3.1 Publication I

Origins and carriers of Sb, As, Cd, Cl, Cr, Co, Pb, Hg, and Ni in mixed solid waste – A literature-based evaluation

S.A. Viczek, A. Aldrian, R. Pomberger, R. Sarc

Waste Management 103 (2020), 87-112,
https://doi.org/10.1016/j.wasman.2019.12.009

Author Contributions (CRediT Contributor Roles Taxonomy):

SV: Conceptualization, Methodology, Formal analysis, Investigation, Data curation, Writing – original draft preparation, Writing – review and editing, Visualization, Project administration;

AA: Writing – original draft preparation (section 5), Writing – review and editing;

RP: Resources, Funding acquisition;

RS: Writing – review and editing, Supervision, Funding acquisition.

Waste Management 103 (2020) 87–112

Contents lists available at ScienceDirect

Waste Management

journal homepage: www.elsevier.com/locate/wasman

Origins and carriers of Sb, As, Cd, Cl, Cr, Co, Pb, Hg, and Ni in mixed solid waste – A literature-based evaluation

S.A. Viczek, A. Aldrian, R. Pomberger, R. Sarc *

Chair of Waste Processing Technology and Waste Management, Montanuniversität Leoben, Leoben, Austria

ARTICLE INFO

Article history:
Received 12 July 2019
Revised 29 November 2019
Accepted 5 December 2019
Available online 24 December 2019

Keywords:
Commercial solid waste
Contaminant carriers
Heavy metals
Municipal solid waste
Solid recovered fuel

ABSTRACT

Antimony, arsenic, cadmium, chlorine, chromium, cobalt, lead, mercury, nickel and their compounds are commonly used in the industrial production of various goods. At the end of the product life cycle, these elements enter the waste system as constituents of the products. Mixed municipal and commercial wastes are landfilled, biologically treated, incinerated, and/or processed in mechanical treatment plants to yield solid recovered fuel (SRF). In all these cases, inorganic contaminants that are present in the input waste material play a significant role. In mechanical waste treatment, materials containing high concentrations of these elements (contaminant carriers) can be selectively removed (e.g. by infrared sorters) to improve the output quality, but prior knowledge about the contaminant carriers is required.

This paper reviews several waste-related publications in order to identify carriers of Sb, As, Cd, Cl, Cr, Co, Pb, Hg, and Ni in mixed municipal and commercial waste. Identified contaminant carriers are listed alongside ranges for expected concentrations. Furthermore, the data are combined with information on industrial applications and contaminant concentrations in products in order to discuss the reasons for the presence of the respective elements in the carriers. Generally, besides inerts or metals, identified contaminant carriers often include plastics, composite materials, leather products, textiles, rubber, electronic waste, and batteries. Moreover, it is evaluated how individual contaminant carriers are reflected by chemical waste analyses. While the findings of the paper can be applied to different waste treatment options, the discussion focuses on SRF, which is the main output of mechanical treatment plants.

Contents

* Corresponding author.
E-mail address: renato.sarc@unileoben.ac.at (R. Sarc).

https://doi.org/10.1016/j.wasman.2019.12.009
0956-053X/

1. Introduction

Several chemical elements, including heavy metals and their compounds, are widely used in the industrial production of various goods and commercial products. At the end of the product life cycle, these chemical elements – as constituents of the products – enter the waste system as a mixed waste stream consisting of various materials. Such mixed, non-hazardous municipal solid waste (MSW), as well as commercial waste, can be processed in mechanical sorting plants to yield solid recovered fuel (SRF). This is common practice in several European countries including Austria (Sarc et al., 2019), which is why the discussion of this paper focuses on SRF. However, depending on the legal regulations in individual countries, other possibilities to treat mixed, non-hazardous municipal and commercial waste include landfilling, incineration, or composting. For all these treatment options, inorganic contaminants such as heavy metals that are present in the waste are relevant on an international level, as they will finally end up in the landfill leachate, off-gas, or output (compost and/or SRF) (Pollak and Favoino, 2004; Saveyn and Eder, 2014).

When mixed municipal solid waste and commercial solid waste is processed to SRF that is co-incinerated in cement kilns, gaseous emissions of the combustion process have to comply with legal limit values. In Europe, the EU Industrial Emission Directive (EC, 2010) lists limit values for hydrogen chloride (HCl), cadmium (Cd), thallium (Tl), mercury (Hg), antimony (Sb), arsenic (As), lead (Pb), chromium (Cr), cobalt (Co), copper (Cu), manganese (Mn), nickel (Ni), and vanadium (V) (Table 1). These elements and their compounds are also part of the US Clean Air Act from 1990 listing 187 hazardous air pollutants (US EPA, 2019), underlining the international relevance of these pollutants, which can also be emitted during the incineration of waste or SRF. In order to comply with the limit values at the end of the process, i.e. the exhaust system, Austria has additionally transferred these 'output' limit values from the gaseous emissions to the SRF (i.e. 'input') that is co-incinerated or co-processed, respectively. The Austrian Waste Incineration Ordinance (WIO) 2010 (BMLFUW, 2010) therefore specifies calorific-value-dependent limit values (i.e. in mg/MJ_{DM} (DM = dry mass)) for As, Cd, Co, Cr, Hg, Ni, Pb, and Sb (cf. Table 1). Depending on their volatility, these elements are either transferred into the cement clinker (Genon and Brizio, 2008), or become part of the emissions, e.g. by adsorbing to small dust particles while cooling down (Sarc et al., 2014). Limiting the contaminant concentrations in SRF similar to the Austrian WIO therefore leads to smaller amounts of trace elements in both emissions and clinker.

Besides these legally stipulated quality criteria, the cement industry also aims for low chlorine concentrations in SRF because high loads of chlorine may reduce the quality of the cement (Kikuchi et al., 2008). Chlorine can also impair the clinker burning process as volatilization of chlorides in hot zones and condensation in cooler zones can induce the formation of chlorine deposits and undesired chlorine-cycles (Lorber et al., 2011). Technical solutions, such as the installation of a chlorine bypass, may help avoid these problems, however, in addition to these measures low chlorine concentrations in SRF (below 1.0 or rather 0.8 $w\%_{DM}$) are still strived for (Lorber et al., 2012).

Table 1
European (output-related) and Austrian (input-related) legal requirements and limit values for the co-incineration of waste or SRF in the cement industry (BMLFUW, 2010; EC, 2010).

European IED (output related)		Austrian WIO (input related)		
Parameter	Limit value [mg/Nm^3]	Parameter	Limit values [mg MJ$^{-1}_{DM}$]	
			median	80th percentile
Sb + As + Pb + Cr + Co + Cu + Mn + Ni + V	0.5	Sb	7	10
		As	2	3
		Pb	20	36
		Cr	25	37
		Co	1.5	2.7
		Ni	10	18
Cd + Tl	0.05	Cd	0.23 (0.45)	0.46 (0.7)
Hg	0.05	Hg	0.075	0,15
HCl	10			
		() for SRF with quality assurance		

Such legal and technical requirements for SRF coming into force triggered the demand for additional technological solutions like near-infrared (NIR) sorters (Sarc et al., 2014). They are used to selectively remove materials in which a specific chemical element is strongly present. These materials are referred to as contaminant carriers in this paper. In SRF production plants, NIR sorters are typically used to remove PVC (polyvinyl chloride), a well-known chlorine carrier. Also PET (polyethylene terephthalate) bottles are removed from the waste stream for economic reasons, as they are directed towards recycling (Pomberger and Sarc, 2014).

Studies have shown that removing certain materials positively affects the concentrations of some of the elements that are subject to legal and technical requirements. For example, experiments have demonstrated that removing PVC from the waste stream using NIR sorters does not only decrease the chlorine content of the SRF, but can also reduce cadmium and lead in certain cases (Pieber et al., 2012). Removing PET bottles also reduces concentrations of antimony in the SRF (Kreindl, 2007). These findings indicate that (taking potential adverse effects on the calorific value of the SRF into account) the targeted removal of specific material fractions can reduce contaminant concentrations and increase the quality of SRF. A necessary precondition for this is the identification of contaminant carriers in the respective waste stream.

Depending on the waste stream and its type and origin, contaminant carriers are expected to vary. To allow for a first assessment of problematic fractions, and to facilitate the identification of contaminant carriers in different waste streams in practice, an extensive literature review on the heavy metal, metalloid, or chlorine concentrations in different waste fractions represents a reasonable basis.

Various publications presenting data on the chemical composition of waste and specific fractions are available. These data have been recently reviewed, assigned to fit 11 waste fractions, and statistically evaluated by Götze et al. (2016a). Their results are summarized in Table 2 and enable a first identification of waste

Table 2
Summary of selected results from Götze et al. (2016a) for concentrations (0.75-percentiles) of antimony, arsenic, cadmium, chlorine, chromium, cobalt, lead, mercury, and nickel in waste fractions.

	Sb [mg/kg$_{DM}$]	As [mg/kg$_{DM}$]	Cd [mg/kg$_{DM}$]	Cl [%$_{DM}$]	Cr [mg/kg$_{DM}$]	Co [mg/kg$_{DM}$]	Pb [mg/kg$_{DM}$]	Hg [mg/kg$_{DM}$]	Ni [mg/kg$_{DM}$]
Gardening waste	0.11 *n = 13*	3.080 *n = 18*	0.60 *n = 23*	0.283 *n = 26*	23.0 *n = 19*	2.7 *n = 14*	23.7 *n = 25*	0.198 *n = 20*	9.0 *n = 20*
Paper & cardboard	2.45 *n = 8*	6.100 *n = 57*	1.25 *n = 88*	0.300 *n = 75*	40.3 *n = 65*	2.0 *n = 8*	39.8 *n = 88*	0.265 *n = 84*	13.3 *n = 57*
Organic	2.60 *n = 12*	18.605 *n = 48*	0.60 *n = 71*	0.700 *n = 58*	56.3 *n = 62*	2.6 *n = 17*	89.1 *n = 68*	0.396 *n = 34*	10.5 *n = 51*
Food waste	0.50 *n = 2*	28.350 *n = 54*	1.28 *n = 100*	1.173 *n = 20*	69.0 *n = 103*	2.0 *n = 43*	56.9 *n = 105*	0.870 *n = 59*	20.4 *n = 99*
Composites	-	0.200 *n = 3*	5.50 *n = 15*	2.550 *n = 41*	708.5 *n = 6*	-	363.3 *n = 15*	0.380 *n = 14*	47.1 *n = 6*
Glass	31.70 *n = 6*	280.475 *n = 36*	2.95 *n = 49*	0.000 *n = 10*	275.7 *n = 49*	9.0 *n = 3*	189.1 *n = 51*	0.200 *n = 49*	37.1 *n = 40*
Inert	6.07 *n = 7*	25.000 *n = 39*	3.28 *n = 50*	0.550 *n = 13*	167.5 *n = 50*	68.0 *n = 4*	382.3 *n = 50*	0.285 *n = 49*	67.7 *n = 44*
Combustibles	13.00 *n = 23*	11.340 *n = 89*	3.93 *n = 158*	1.248 *n = 114*	142.2 *n = 122*	3.7 *n = 14*	147.0 *n = 155*	0.470 *n = 140*	22.0 *n = 97*
Metal	48.73 *n = 8*	29.800 *n = 45*	5.20 *n = 71*	0.001 *n = 19*	304.3 *n = 50*	43.5 *n = 5*	90.0 *n = 67*	0.200 *n = 60*	147.3 *n = 40*
Plastic	129.23 *n = 14*	10.075 *n = 46*	16.50 *n = 103*	8.125 *n = 90*	187.0 *n = 73*	53.3 *n = 5*	247.0 *n = 102*	0.400 *n = 89*	19.6 *n = 44*
Waste mix	200.10 *n = 34*	30.068 *n = 50*	5.04 *n = 141*	1.000 *n = 81*	182.3 *n = 116*	11.9 *n = 20*	544.6 *n = 102*	1.375 *n = 113*	75.2 *n = 104*

Dark gray: highest concentrations (≥0.67-percentile).
Light grey: medium concentrations (≥0.33-percentile).
White: lowest concentrations (<0.33-percentile).
n = number of data points.

fractions containing high concentrations of certain contaminants. The highest concentrations of Sb, As, Cd, Cl, Cr, Co, Pb, Hg, and Ni are often found in composites, glass, inert, combustibles, metal, and plastic fractions. Note that electronic or hazardous materials are not part of the literature review of Götze et al. (2016a). However, electronic devices or batteries are significant sources of heavy metals and other contaminants and regularly end up in MSW.

Although grouped data show fractions that are likely to contain contaminant carriers, original data are required to identify the contaminant carriers because the fractions have been described in the original publications in more detail. The purpose of this paper is to review primary sources to identify and list specific waste and material fractions found in MSW that contain high concentrations of As, Cd, Cl, Cr, Co, Hg, Ni, Pb, and Sb. Furthermore, an overview of the industrial applications of each element is given and combined with information from waste-related publications or information on the product level in order to discuss why these elements are present in waste and material fractions, and to identify specific contaminant carriers, i.e. materials or products that are responsible for increased concentrations of the element in the waste fraction. Finally, identified contaminant carriers are listed and ranges of expected concentrations of the chemical element from literature are provided.

Note that the paper intends to list as many contaminant carriers as possible, even though in some countries they may not be significant any longer. Legal regulations that restrict their use in some countries, usually affecting the waste sector with some delay, are pointed out where possible.

2. Materials and methods

2.1. Literature selection

Potential contaminant carriers have been identified reviewing literature sources and combining the extracted information. The exact procedure of identifiying contaminant carriers is depicted in Fig. 1.

Peer-reviewed journal articles, online reports from governmental institutions and other organizations as well as theses in English, German, French, Italian, and Dutch have been reviewed. The screening of references included all accessible publications reviewed by Götze et al. (2016a) and other sources. Only publications listing values for separate waste fractions were included, those listing values for the waste mix only were excluded. No age limit was set for publications because certain contaminant carriers might still be relevant either due to their longevity or in countries where they are not legally restricted. Where publications presented data derived from other papers, the primary source was identified and referenced, if accessible. Otherwise, the secondary source is referenced. Only publications including tables that provide exact numbers for analyte concentrations have been used in the evaluation. Table 3 lists the publications as well as the number of datasets used for identifying contaminant carriers.

2.2. Choosing reference values

Götze et al. (2016a) was drawn on to identify the main contaminated fractions (cf. Table 2). The 0.75-percentiles have been considered appropriate values for this purpose, as they are more likely to be affected by outliers caused by single contaminant carriers than the median values.

In order to identify contaminant carriers and relevant material fractions in more detail, the published concentrations of an element in single fractions need to be compared with either concentrations in other fractions, or concentrations in the waste mix. In the current approach, a comparison with the waste mix was chosen because this value will be directly influenced by the contaminant carriers present in the waste stream. Comparing fractions, on the other hand, would simply result in a list of fractions containing high contaminant concentrations not related to the overall concentration in the waste mix. In addition, removing a contaminant car-

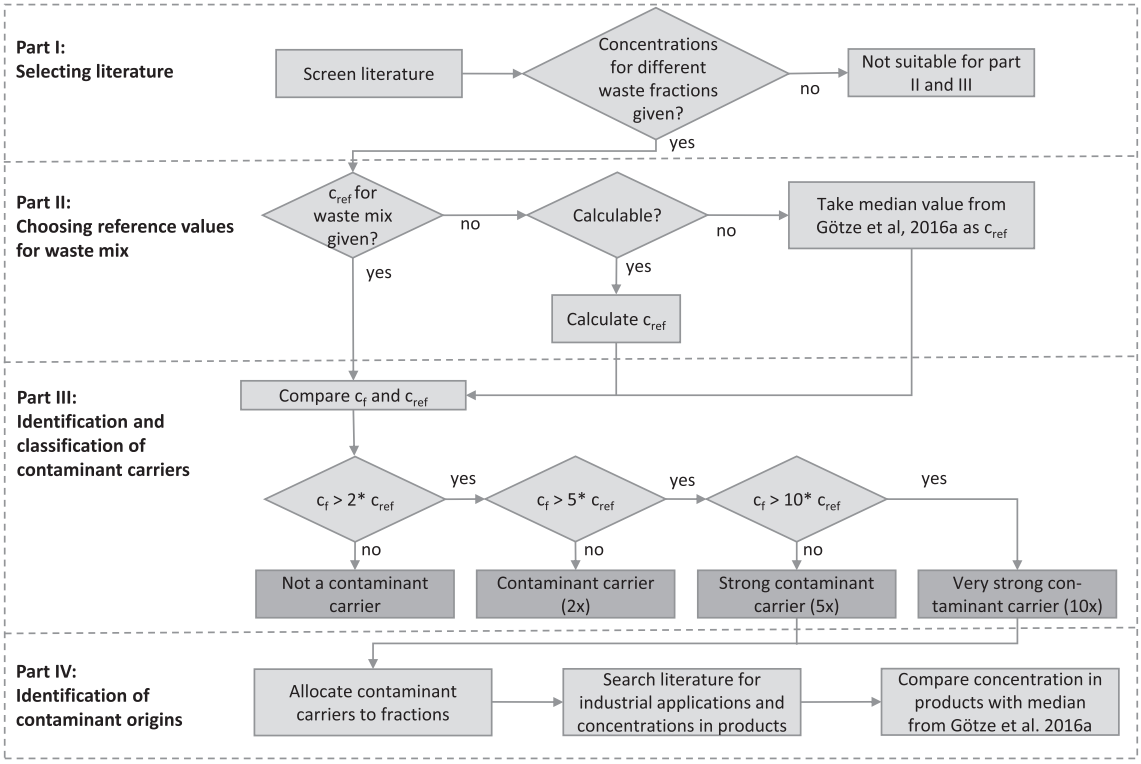

Fig. 1. Procedure used to identify contaminant carriers.

Table 3
Literature used for identifying contaminant carriers in MSW.

Literature source	Cl	Cr	Co	Cd	As	Sb	Ni	Hg	Pb	Reference value for waste mix available
(Viczek et al., 2019b)	1	1	1	1	1	1	1	1	1	Yes
(Götze et al., 2016b)	1	1	1	1	1	1	1	1	1	(Götze et al., 2016a)
(Nasrullah et al., 2016)	1	1	1	1	1	1	1	1	1	Yes
(Nasrullah et al., 2015)	1	1	1	1	1	1	1	1	1	Yes
(Astrup et al., 2011)	1		1	1	1			1	1	Yes
(Eisted and Christensen, 2011)	1	1	1	1	1	1	1	1	1	Calculated
(Komilis et al., 2011)		1	1	1			1		1	(Götze et al., 2016a)
(Rizza, 2011)	1									(Götze et al., 2016a)
(ADEME (2010))	1	1		1	1		1	1		Yes
(Janz, 2010)		1		1			1		1	(Götze et al., 2016a)
(Ma et al., 2010)	1									Yes
(Österlund et al., 2009)	1									(Götze et al., 2016a)
(Riber et al., 2009)	1	1		1	1		1	1	1	(Götze et al., 2016a)
(Choi et al., 2008)	1									Yes
(Pomberger, 2008)	1	1	1	1	1	1	1	1	1	(Götze et al., 2016a)
(Burnley, 2007)		2		2	2			2	2	(Götze et al., 2016a)
(Penque, 2007)	1									Yes
(Hoffmann et al., 2006)	1									Yes
(Prochaska et al., 2005)	1	1	1	1	1	1	1	1	1	Yes
(LfU Bayern, 2003)	1	1		1	1		1	1	1	Yes
(Rotter, 2002)				1				1	1	(Götze et al., 2016a)
(Kost, 2001)	1									(Götze et al., 2016a)
(Ferrari et al., 2000)	1	1		1			1	1	1	(Götze et al., 2016a)
(Beker and Cornelissen, 1999)	1	2	2	2	2	2	2	2	2	Yes
(Liu and Liptak, 1999)	1	2		2	2		2	2	2	(Götze et al., 2016a) *
(Watanabe et al., 1999)						10				Yes
(Nakamura et al., 1996)				1		1			1	(Götze et al., 2016a)
(Maystre and Viret, 1995)	1			1				1	1	Calculated
(Otte, 1994)		1	1	1	1	1	1	1	1	Yes
(Rugg and Hanna, 1992)		1		1	1		1	1	1	Yes
(Bode et al., 1990)		1		1	1			1	1	(Götze et al., 2016a)
Total number of datasets	22	22	12	26	20	21	19	23	25	
Total number of studies	22	19	11	23	17	11	17	20	22	

* Except for chlorine: Cl waste mix reference value was available in the original publication.

rier that constitutes a large part of the waste fraction, and whose concentration therefore is similar to that of the whole mix, would not be practicable at all. The required reference value of the waste mix is ideally found in the same publication that provides the concentrations in single fractions, otherwise it is either calculated or the median value given by Götze et al. (2016a) (cf. Fig. 1) is used. Note that in this case the median value is preferred to the 0.75-percentile for the purpose of comparing fractions with average waste rather than with contaminated waste. Table 3 lists all publications used and the origins of the reference values of the waste mix.

2.3. Identification and classification of contaminant carriers

A fraction (or a product or good) has been identified as a contaminant carrier based on the ratio between the fraction's concentration (c_f) and the reference concentration (c_{ref}). Contaminant carriers have been allocated to three classes of different strengths in order to assess the impact of single objects or small amounts of the carrier on the waste stream. Classes, definitions for the classification, and the labeling that is used in the summarizing tables for each element are given in Table 4.

2.4. Identifying the origins of contaminants

In a final step, the identified contaminant carriers were allocated to the material fractions listed by Götze et al. (2016a) so that elevated levels reported in certain fractions may be explained. Sources from outside the waste sector, e.g. regarding industrial applications of the elements, have been screened for plausible causes of elevated concentrations of certain elements in the identified carriers. The concentration of elements in products has been researched and compared with the median values for mixed waste provided by Götze et al. (2016a) to assess the impact of products or individual materials on the waste stream. Unless calculations were necessary, e.g. to convert concentrations of oxides into concentrations of elements, were necessary, values were rarely rounded, and apart from some exceptions, significant figures have been adopted from the sources.

3. Contaminants in waste and their origin

3.1. Antimony (Sb)

3.1.1. Antimony in waste fractions

The extensive literature review of Götze et al. (2016a) demonstrates that the highest concentrations of Sb (0.75 quantiles) in household waste are met in the plastic fraction (129.23 mg/kg_{DM}), followed by metals (48.73 mg/kg_{DM}), glass (31.70 mg/kg_{DM}), and the combustible fraction (13.00 mg/kg_{DM}). Sources of antimony in municipal solid waste have already been examined by Nakamura et al. (1996) and are taken into account although some of the listed 'little discharge/high content' materials may not be common any more. For this paper, a detailed evaluation of 21 datasets from 11 publications has been used to identify contaminant carriers in waste based on the procedure described in Section 2.

In the following section, causes of elevated levels of antimony in the above-mentioned and other important waste fractions are discussed and allocated to industrial applications of antimony. A comprehensive summary of antimony carriers (waste fractions, materials, or products) and expected or published concentrations is presented in Table 5.

Table 4
Identification and classification of contaminant carriers.

Condition	Classification	Symbol (used in summarizing tables)
$c_f \leq 2 * c_{ref}$	Not a contaminant carrier	–
$c_f > 2 * c_{ref}$	Contaminant carrier	○
$c_f > 5 * c_{ref}$	Strong contaminant carrier	●
$c_f > 10 * c_{ref}$	Very strong contaminant carrier	●

3.1.2. Origins of antimony in waste fractions

3.1.2.1. Antimony in plastics. In the plastics fraction, especially PET and unlabeled plastics packaging (Götze et al., 2016b), hard plastics (Nasrullah et al., 2015), tubes and hard cable sheaths (Pomberger, 2008) are considered contaminant carriers according to the definition introduced in Section 2. Common uses of antimony in the plastics industry imply that these observations are related to the element's use for flame retardancy, as a catalyst, or as a pigment.

Antimony trioxide (Sb_2O_3), which is also a white pigment (Pfaff, 2017), is a known catalyst for polymerizing PET (Kiyataka et al., 2018), and partially remains in the material (Welle, 2016). This explains the high values reported for PET bottles or similar fractions. According to Ranta-Korpi et al. (2014), 100 to 300 mg/kg of antimony can be expected where Sb_2O_3 is used as a catalyst for PET. Other non-antimony-based catalysts are available (Thiele, 2004) but antimony-based catalysts are still applied in more than 90% of the global polyester production (Dupont et al., 2016). Scientific reports analyzing PET bottles show varying antimony contents. In Japan, which is at the forefront of non-antimony catalysts application (Thiele, 2004), some PET bottles have been found to contain less than 0.1 mg/kg of Sb, while others contained antimony in the range of 170 to 220 mg/kg (Shotyk et al., 2006). Kreindl (2007) reports Sb concentrations of 250 to 310 mg/kg for colorless, green and blue PET bottles in Austria. A Brazilian study (Kiyataka et al., 2018) reports similar values (272.2 to 317.2 mg/kg) for colorless and for colored PET bottles but significantly higher concentrations (561.4 – 640.5 mg/kg) for some green PET bottles. Brandão et al. (2014) report antimony concentrations of 89.9 to 388 mg/kg in PET bottles for sparkling and non-sparkling water.

One of the main industrial applications of antimony trioxide is imparting flame retardancy to various materials, including poly-

Table 5
Selected antimony carriers, expected concentrations in products or waste fractions, comparison with mixed waste and classification.

Material or waste fraction	Sb [mg/kg$_{DM}$]	Literature source	Level of Sb carrier
Mixed waste	62.90	(Götze et al., 2016a), median	
Plastics (wf)	129.23	(Götze et al., 2016a), 0.75-percentile	
PET bottles	89.9–388	(Brandão et al., 2014; Götze et al., 2016b; Kiyataka et al., 2018; Kreindl, 2007)[b;b;b;b]	○ ●
For comparison: PET bottles, non-Sb catalyst	< 0.1	(Shotyk et al., 2006)[b]	–
Individual green PET bottles, Brazil	561.4–640.5	(Kiyataka et al., 2018)[b]	●
Plastics* with Sb pigments	30–600	(Ranta-Korpi et al., 2014)[b]	○ ●
Flame retarded plastics*	4200–42,000	(Ranta-Korpi et al., 2014)[b]	●
PVC, flame retarded	26,300	(Belarra et al., 1998)[b]	●
For comparison: PVC (wf)	2.4–12	(David, 2014)[b]	–
Tubes (wf) **	160	(Pomberger, 2008)[b]	○
Cable sheaths (wf) **	180	(Pomberger, 2008)[b]	○
Paint buckets (wf)	250	(Pomberger, 2008)[b]	○
Expanding foam (wf)	375	(Pomberger, 2008)[b]	●
Metals (wf)	48.73	(Götze et al., 2016a) 0.75-percentile	
Lead alloys	10,000–150,000	(Tercero Espinoza et al., 2015)[b]	●
Glass (wf)	31.70	(Götze et al., 2016a) 0.75-percentile	
CRT glass, funnel	0–3340	(The Waste & Resources Action Programme (2004))[b]	○ ● ●
CRT glass, panel	1670–5850	(The Waste & Resources Action Programme (2004))[b]	●
Combustibles (wf)	13.00	(Götze et al., 2016a) 0.75-percentile	
Clothes (polyester)	11–270	(Nakamura et al., 1996; Schäfer, 2013)[b;b]	○
Textiles	247	(Nakamura et al., 1996)[b]	○
Mattresses (polyester or flame retarded cotton)	15–150	(Danish EPA (2015))[b]	○
Curtains	2100	(Nakamura et al., 1996)[b]	●
Stuffed toys	156	(Nakamura et al., 1996)[b]	○
Bedding clothes	156	(Nakamura et al., 1996)[b]	○
Carpets (wf)	17.1	(Otte, 1994)[a]	○
Rubber (wf)	27–230	(Nasrullah et al., 2016; Nasrullah et al., 2015; Pomberger, 2008)[a;a;b]	○
Subfraction: Colored rubber (wf)	83.3	(Otte, 1994)[a]	●
For comparison: Sub-fraction: Other rubber (wf)	10.1	(Otte, 1994)[a]	–
For comparison: Tires	0.2–2.4	(Bally, 2003; Hjortenkrans et al., 2007; Kennedy and Gadd, 2000)[b]	–
Styrene-butadiene rubber, ethylene propylene rubber	42000–251000	(United states antimony corporation (2017))[b]	●
Leather (wf)	28.6	(Otte, 1994)[a]	○
Other Sb-carriers			
Children's jewelry parts (necklaces, bracelets)	2124	(Negev et al., 2018)[b]	●
Fine fraction (wf)	7.2–479.6	(Watanabe et al., 1999)[a]	○

wf = waste fraction.
○: contaminant carrier.
●: strong contaminant carrier.
●: very strong contaminant carrier.
* used for PVC, PE, PP, PS, polyesters or PET, PA, ABS, PU.
** probably contains PVC.
[a] : reference value for mixed waste obtained or calculated from the same publication as the listed fraction.
[b] : median from Götze et al. (2016a) used as a reference.

mers (Tercero Espinoza et al., 2015). It can be used either as an individual flame retardant in halogenated polymers (e.g. PVC), or in combination with halogenated compounds (e.g. chlorine-paraffins) in order to achieve flame retardancy in non-halogenated polymers such as polyethylene (PE) or polypropylene (PP) (Ranta-Korpi et al., 2014; Troitzsch, 2016). The resulting concentrations of Sb in flame-retarded materials depend on the kind of polymer, varying between 4.2 and 42 g/kg (Ranta-Korpi et al., 2014). In general, antimony is mainly used as a flame-retarding additive in products with moderate to long lifetimes (Månsson et al., 2009), implying that antimony will remain a relevant element in waste streams in future.

High values of Sb observed in tubes and hard cable sheaths (often made of PVC) may also be explained by the use of Sb_2O_3 for flame retardancy. In the past, however, antimony compounds such as antimony mercaptides have also been used as stabilizers for PVC, especially for PVC-U (unplasticized PVC) and records (LPs, etc.). Such Sb-based stabilizers are still in use outside of Europe (Hopfmann et al., 2016) and due to the longevity of PVC products they are expected to keep entering the waste system.

Besides applications as a catalyst, flame retardant synergist, or stabilizer, several heat-, light- and chemically resistant inorganic pigments containing antimony are used in plastics. Some examples are nickel titanium yellow (Ti, Sb, Ni)O_2, manganese titanium yellow (Ti, Sb, Mn)O_2, or chromium titanium yellow (Ti, Sb, Cr)O_2. Depending on the pigment, antimony concentrations ranging from 30 to 600 mg/kg may be expected in plastics (Ranta-Korpi et al., 2014).

3.1.2.2. Antimony in metals. In the metals fraction, elevated Sb concentrations are observed especially for non-ferrous metals (Beker and Cornelissen, 1999; Otte, 1994). The metal industry applies Sb in alloys with lead and tin for Babbitt metals, plumbs, or plates for lead batteries. Sb contents of such alloys are ranging from 1 to 15%. Applications include cable sheathing and lead pipes, ammunition, and storage batteries. Also, Sb is used for doting semiconductors (Holleman et al., 2007; Tercero Espinoza et al., 2015).

3.1.2.3. Antimony in glass, and ceramics. Based on data published by Eisted and Christensen (2011), glass can be considered a contaminant carrier in some waste streams. Antimony compounds such as sodium hexahydroxoantimonate or antimony trioxide are used in the glass industry for several purposes: as opacifiers for glass and enamels, as decolorizing and refining agents, or to remove bubbles. Examples of Sb-containing glass include optical glasses or CRT glass formerly used for television tubes (Anderson, 2012; Schmidt, 2013; Tercero Espinoza et al., 2015). Although the present approach has not identified ceramic waste fractions as Sb carriers, it should be noted that Sb compounds can be used as pigments (such as rutile pigments) in the ceramics industry as well (Gazulla et al., 2007; Večeřa et al., 2013).

3.1.2.4. Antimony in the combustible fraction. A more detailed view at the combustible fraction reveals the following contaminant carriers: textile products (Nakamura et al., 1996), rubber, leather (Nasrullah et al., 2016; Nasrullah et al., 2015; Otte, 1994; Pomberger, 2008; Watanabe et al., 1999), as well as foams (Nasrullah et al., 2015; Pomberger, 2008).

Similar to plastics, observed elevated levels of Sb in textiles, e.g. clothes (Schäfer, 2013), mattresses (Danish EPA (2003)), or curtains and stuffed toys (Nakamura et al., 1996) are either related to antimony used as a flame retardant or as a catalyst because the textile material can consist of PET-based synthetic fibers (Danish EPA (2003); Nakamura et al., 1996; Schäfer, 2013). Apart from plastics and textiles, Sb-based flame-retarding systems in combination with halogen donors are also used to impart flame retardancy to leather, coatings, paints, electrical devices, and rubber products (Dick and Rader, 2014; Pfaff, 2017; United states antimony corporation (2017)). For this reason, elastomers such as styrene butadiene rubber or ethylene propylene rubber may contain between 5 and 30% of Sb_2O_3 (United states antimony corporation (2017)). Tires in contrast, which might be part of the rubber fraction in sorting analyses, do not seem to be responsible for elevated levels of antimony in the rubber fraction. They contain low amounts of antimony ranging from 0.2 to 2.4 mg/kg (Bally, 2003; Hjortenkrans et al., 2007; Kennedy and Gadd, 2000).

The fractions leather and rubber, which often include shoes, are mostly analyzed as mixed fractions in waste-related publications and are only rarely reported as separate rubber, leather, or textile fractions. Otte (1994) has analyzed the sub-fractions of the leather/rubber fraction more closely. Results show that the highest antimony concentrations are found in leather and colored rubber, being much higher than in shoes and other rubber. High antimony concentrations in colored rubber may be consistent with the use of Sb_2S_5 as a red pigment and as a rubber accelerator in the vulcanization of red rubber (Anderson, 2012; Larrañaga et al., 2016).

3.1.2.5. Antimony in fine fractions. Besides the above-listed fractions, Watanabe et al. (1999) report antimony concentrations in the fine fraction that are more than four times as high as the overall concentration in the waste. Available sources, however, do not allow for making meaningful conclusions on the origin of Sb in the fine fraction.

3.1.3. Summary: Antimony carriers

In combustible fractions and plastics, which are the main relevant fractions for the production of SRF, antimony is primarily present because it is used as a flame retardant, catalyst, pigment, or (formerly) as a stabilizer. These results are largely consistent with the findings of Nakamura et al. (1996). Table 5 summarizes selected examples of potential antimony carriers in mixed municipal solid waste and lists the respective antimony concentrations reported for these carriers on a product level or in waste sorting analyses.

3.2. Arsenic (As)

3.2.1. Arsenic in waste fractions

Götze et al. (2016a) report the highest arsenic concentrations (0.75-percentiles) in the waste fraction of glass (280.475 mg/kg_{DM}), followed by the fractions metal (29.800 mg/kg_{DM}), food waste (28.350 mg/kg_{DM}), inert (25.000 mg/kg_{DM}), and organic (18.605 mg/kg_{DM}). A total of 20 datasets from 17 publications have been used to identify arsenic carriers in waste. A summarizing table of potential arsenic carriers and reported concentrations is presented in Table 6.

3.2.2. Origins of arsenic in waste fractions

3.2.2.1. Arsenic in glass. Glass can be identified as a possible contaminant carrier in waste according to the concentrations listed in various studies (ADEME (2010); Beker and Cornelissen, 1999; Eisted and Christensen, 2011; LfU Bayern, 2003; Otte, 1994). Remarkably high concentrations of arsenic are reported for kitchen and table ware glass by Götze et al. (2016b). The fact that this was only observed in a sample from source segregated waste but not in residual waste implies that variations between samples can be high. High concentrations of arsenic in glass can be explained by the use of arsenic trioxide (As_2O_3) as a clarifier or fining agent for removing gases, as a decolorizing agent, and as an oxidizing-reducing agent in the glass industry (Atkarskaya and Bykov, 2003; NRC, 1977; Rohr and Meckel, 1992). Former applications included the production of bottle glass and other glassware (U.S.

Table 6
Selected arsenic carriers, expected concentrations in products or waste fractions, comparison with mixed waste and classification.

Material or waste fraction	As [mg/kg$_{DM}$]	Literature source	Level of As carrier
Mixed waste	10.950	(Götze et al., 2016a), median	
Glass (wf)	280.475	(Götze et al., 2016a), 0.75-percentile	
Glass	2000–10000	(NRC, 1977)[b]	●
Kitchen and tableware glass (wf)	1534.95	(Götze et al., 2016b)[b]	●
For comparison: Glass packaging, various colors (wf)	6.8–13.56	(Götze et al., 2016b)[b]	–
Clear glass ampoules (medical use) *	1850–2930	(Bohrer et al., 2006)[b]	●
Amber glass ampoules (medical use) *	190–600	(Bohrer et al., 2006)[b]	●
Glass bottle (medical use) *	54–99	(Bohrer et al., 2006)[b]	◍
For comparison: Raw material quartz sand (pure)	0.37	(Rohr and Meckel, 1992)[b]	–
CRT glass, panel	0–2300	(The Waste & Resources Action Programme (2004))[b]	○ ◍ ●
CRT glass, funnel	0–1500	(The Waste & Resources Action Programme (2004))[b]	○ ◍ ●
Metals (wf)	29.800	(Götze et al., 2016a) 0.75-percentile	
Brass	200–500	(NRC, 1977)[b]	●
Copper (for specific uses)	1500–5000	(NRC, 1977)[b]	●
Food waste (wf)	28.350	(Götze et al., 2016a) 0.75-percentile	
Fish, Cephalopods, Crustaceans, ** wet weight	0.005–26.0	(Taylor et al., 2017)[b]	○
For comparison: Rice**	0.14	(Das et al., 2004)[b]	–
For comparison: Poultry (As in feed) **	0.001–0.01	(Nachman et al., 2013)[b]	–
Inert (wf)	25.000	(Götze et al., 2016a) 0.75-percentile	
Ceramics (wf)	18.42–65.87	(Götze et al., 2016b)[b]	○
Comparison: raw material clay	0.317–45.1	(Reeuwijk et al., 2013)[b]	○
Non-combustible	132	(Eisted and Christensen, 2011)[a]	●
Organic (wf)	18.605	(Götze et al., 2016a) 0.75-percentile	
Impregnated wood (wf)	400	(Astrup et al., 2011)[a]	●
For comparison: press boards (new)	0.05–9.8	(Schrägle, 2015)[b]	–
For comparison: Old wood fractions for press boards***	0.05–1.8	(Schrägle, 2010)[b]	–
Electronic devices/batteries (wf)			
Household batteries (wf)	83	(Riber et al., 2009)[b]	◍
Electrical goods (wf)	71	(Burnley, 2007)[b]	◍
Other As-carriers			
Children's jewelry parts (necklaces, bracelets)	483	(Negev et al., 2018)[b]	●
Fine fractions of mixed commercial waste < 5 mm or 5–10 mm	8–31	(Viczek et al., 2019b)[a]	○

wf = waste fraction.
○: contaminant carrier.
◍: strong contaminant carrier.
●: very strong contaminant carrier.
* Ampoules for storing intravenous formulations, glass bottle for amino acids injections.
** food known to contain high levels of arsenic.
*** solid wood, coated wood with PVC or non-PVC plastics, composite wood without coating, fines.
[a] : reference value for mixed waste obtained or calculated from the same publication as the listed fraction.
[b] : median from Götze et al. (2016a) used as a reference.

Department of health and human services (2007)), but today substitutes for arsenic compounds are available and applied by the glass industry. Glass that was not treated with arsenicals, however, also contains trace amounts of arsenic originating from the raw materials (Rohr and Meckel, 1992).

3.2.2.2. Arsenic in metals. In the metals fraction, arsenic carriers comprise ferrous metals (Beker and Cornelissen, 1999; Burnley, 2007; Götze et al., 2016b; Ma et al., 2010; Rugg and Hanna, 1992) as well as non-ferrous metals (Beker and Cornelissen, 1999; Rugg and Hanna, 1992). One of the main uses of arsenic in the metals industry is its application in alloys, e.g. in bismuth-alloys, alloys for lead batteries, ammunition and solders, or CuSn alloys for mirrors, and as an anti-friction additive to metals used for bearings (Holleman et al., 2007; U.S. Department of health and human services (2007)). Furthermore, adding arsenic can improve the high-temperature properties of copper and can decrease the dezincification of brass (NRC, 1977).

3.2.2.3. Arsenic in food waste. According to the analysis of Götze et al. (2016b), food waste contains the third-highest concentration of arsenic, yet, the conditions defined in Section 2 and the publications reviewed in this paper did not help identifying any contaminant carriers consistent with this fraction. This is also related to the fact that reviewed articles rarely divide the food waste fraction into other fractions, e.g. 'meat waste' or 'vegetable waste'. It is well known that inorganic and organic arsenic compounds are present in several food products such as rice (Das et al., 2004) or seafood (Taylor et al., 2017) and that arsenic-based compounds are constituents of feed in poultry production (Nachman et al., 2013). These food products, however, cannot explain the above observation, as their reported arsenic levels are much lower than the 0.75-percentile value of arsenic in mixed waste given by Götze et al. (2016a).

Inorganic arsenic, especially As_2O_3, has formerly been used as a pesticide in agriculture, primarily on orchards and cotton fields. (Holleman et al., 2007; U.S. Department of health and human services (2007)). The Bavarian State Ministry for the Environment, however, states that the former application of arsenic as a pesticide does not seem to affect arsenic levels in municipal solid waste any longer (LfU Bayern, 2003). The data available therefore does not yield plausible explanations for the observed levels of arsenic in food waste.

3.2.2.4. Arsenic in inert materials. Ceramics (Götze et al., 2016b) and non-combustibles in general (Eisted and Christensen, 2011; Riber et al., 2009) have been identified as contaminant carriers using the method outlined in Section 2. Arsenic is naturally present in clay (Archer et al., 2011; Reeuwijk et al., 2013), and arsenic compounds are furthermore used as pigments (LfU Bayern, 2003; Sharma, 2014) and in the ceramics industry (Sharma, 2014; Wares et al., 2014).

3.2.2.5. Arsenic organic fractions and combustibles. Arsenic used to be chiefly applied as a wood preservative, with more than 90% of the global arsenic produced being used for this application (U.S. Department of health and human services (2007)). Chromated copper arsenate (CCA) was a preservative used to prevent rotting and decay. It is a reason for the high levels of arsenic observed in the wood fraction of several sorting campaigns (Astrup et al., 2011; Beker and Cornelissen, 1999; Götze et al., 2016b; Liu and Liptak, 1999; Rugg and Hanna, 1992). In 2003, the use of CCA as a wood preservative was phased out in the US (U.S. Department of health and human services (2007)). The European Union as well has prohibited this application of arsenic in 2006, but CCA-treated wood that has entered the market before 2007 remains in use until it reaches the end of its life cycle (EC, 2006b). This suggests that - depending on the input waste - increased levels of arsenic may still be observed in wooden waste fractions, as can be seen from more recent publications such as Götze et al. (2016b) or Astrup et al. (2011). Since sorting analyses may also allocate wood to the combustible fraction, this application can also impact arsenic levels observed for combustibles.

3.2.2.6. Arsenic in batteries and electronic devices. The use of As in alloys to strengthen lead-acid storage battery grids (IARC, 2012) is a potential explanation for elevated arsenic contents in batteries. However, Riber et al. (2009) report increased As concentrations in a fraction of household batteries and the amount of lead batteries potentially present in this fraction is not known. Furthermore, electrical goods (Burnley, 2007) have been identified as contaminant carriers for arsenic, which can be explained by the element's application in the semiconductor and electronics industry where gallium arsenide and arsine are widely used, including telecommunication, solar cells, transistors or optoelectronics such as lasers or light-emitting diodes (LEDs) (Hassan, 2018; IARC, 2012; Ratnaike, 2003).

3.2.3. Summary: Arsenic carriers

High levels of arsenic can be observed especially in glass, some metal alloys, and impregnated or CCA-treated wood. CCA-treated wood is probably the most relevant combustible arsenic carrier in MSW and mixed commercial waste, but it is not assumed to be generally present in every waste stream in Europe, the US or other countries where the use of CCA has been restricted. As-concentrations, however, may peak from time to time when a lot or batch of CCA-impregnated wood has reached the end of its life cycle and enters the waste stream. The reasons for arsenic values observed in food waste remain unclear. Table 6 summarizes selected arsenic carriers in mixed municipal solid waste and provides ranges of arsenic concentrations.

3.3. Cadmium (Cd)

3.3.1. Cadmium in waste fractions

The highest concentrations (0.75-percentiles) of cadmium are reported for plastics (16.50 mg/kg_{DM}), followed by composites (5.50 mg/kg_{DM}), metal (5.20 mg/kg_{DM}), combustibles (3.93 mg/kg_{DM}), and inert materials (3.28 mg/kg_{DM}) (Götze et al., 2016a). Nakamura et al. (1996) and Franklin Associates (1989) have already reported some sources of cadmium in municipal solid waste. Their findings are compared with 21 other studies, yielding a total of 26 datasets used to identify further cadmium carriers. A recent review of cadmium in consumer products is also provided by Turner (2019). A summarizing table of potential cadmium carriers and expected ranges of concentrations is presented in Table 7.

3.3.2. Origins of cadmium in waste fractions

3.3.2.1. Cadmium in batteries and electronic devices. By far the highest concentrations of cadmium are observed in nickel-cadmium (NiCd) batteries, which have already been identified as important cadmium carriers by Nakamura et al. (1996) and Franklin Associates (1989). In Europe, NiCd batteries were prohibited by the EU Battery Directive in 2008 because their cadmium content exceeds 0.002% by weight. With some exceptions, these batteries are no longer allowed to enter the market (BMLFUW, 2008). However, NiCd batteries are estimated to remain in use for 12.3 years on average (Colin, 2017). Due to their high product lifetime, NiCd batteries are expected to remain relevant for the European waste management in the near future.

Besides NiCd batteries, dry batteries (Nakamura et al., 1996), zinc-carbon, and alkaline batteries (Komilis et al., 2011; Liu and Liptak, 1999; Maystre and Viret, 1995; Rotter, 2002) contain cadmium, although in much smaller concentrations. The study of Komilis et al. (2011) observed only small amounts of cadmium in alkaline and zinc-carbon batteries while one non-alkaline battery was identified as a contaminant carrier with the present approach. Another study performed by Recknagel et al. (2009) has shown that cadmium levels were generally higher in zinc-carbon batteries than in alkaline batteries.

High cadmium concentrations are also observed in electronic devices (Burnley, 2007; LfU Bayern, 2003; Maystre and Viret, 1995; Pomberger, 2008), circuit boards, and electronic parts (Janz, 2010; Rotter, 2002). Elevated cadmium concentrations in the electronic fraction can be attributed to NiCd batteries, plastics, galvanic coatings, chip resistors, semiconductors, and solar cells (Janz, 2010; LfU Bayern, 2003).

3.3.2.2. Cadmium in plastics. Regarding the plastics fraction, especially PVC fractions (Astrup et al., 2011; Burnley, 2007; Nakamura et al., 1996; Pomberger, 2008) and other plastic fractions that are likely to contain PVC, e.g. 'other plastics' (Liu and Liptak, 1999; Rotter, 2002; Rugg and Hanna, 1992), cable sheaths, and flooring (Pomberger, 2008; Rotter, 2002) were identified as cadmium carriers. This is probably caused by the use of Cd-compounds (e.g. cadmium stearate, cadmium laureate) for the thermal stabilization of polyvinyl chloride (PVC), resulting in cadmium concentrations of 300–1400 mg/kg (Ranta-Korpi et al., 2014). In Europe, the cadmium content of new PVC-articles was restricted by the REACH regulation introducing limit values of 100 mg/kg were introduced. For certain PVC products required in the construction sector that contain recycled PVC, the limit value for cadmium was set to 1000 mg/kg (EC (2011)).

Cadmium is furthermore used in the form of pigments in various plastics, including PVC, polyethylene (PE), polypropylene (PP), and PET giving the plastics a yellow or red color. In combination with other pigments, shades of yellowish-green, orange and brown are achieved as well (Ranta-Korpi et al., 2014). Especially red, orange and yellow plastic items have also been identified by Bode et al. (1990) as a source for cadmium in household waste (Snedeker, 2014). Using cadmium as a pigment results in Cd concentrations of about 300 to 3900 mg/kg (Ranta-Korpi et al., 2014). Such pigments still play an important role in plastics requiring high temperature processing (International Cadmium Association (2018)). Limit values defined by the European REACH regulation, however, also apply to plastics with cadmium pigments (EC (2011)).

3.3.2.3. Cadmium in composites. The reasons for elevated cadmium levels in the composite fraction are hard to determine because the exact composition of the fraction is not known. Elevated levels of cadmium have been reported for shoes (Astrup et al., 2011; Rotter, 2002). Apart from that, other materials listed in the other

Table 7
Selected cadmium carriers, expected concentrations in products or waste fractions, comparison with mixed waste and classification.

Material or waste fraction	Cd [mg/kg$_{DM}$]	Literature source	Level of Cd carrier
Mixed waste	2.17	(Götze et al., 2016a), median	
Electronic devices/batteries (wf)			
Electronic material (wf)	8.7–509	(Burnley, 2007; LfU Bayern, 2003; Maystre and Viret, 1995; Pomberger, 2008)[b;a;a;b]	○ ● ●
Circuit boards	4852	(Rotter, 2002)[b]	●
Circuit boards (without electrical components)	1.2–21.5	(Janz, 2010)[b]	○ ●
Electrical equipment (plastics)	18.8–1370	(Rotter, 2002; Turner, 2019)[b;b]	● ●
Electrical components radio, computer	8.9–27.0	(Janz, 2010)[b]	● ●
Electrical components calculator*	9945	(Janz, 2010)[b]	●
NiCd batteries	30000–280000	(Liu and Liptak, 1999; Nakamura et al., 1996; Saft, 2008a; SBS, 2015; Yuasa, 2015)[b;b;b;b;b]	●
Dry batteries (wf)	48	(Nakamura et al., 1996)[b]	●
Zinc-carbon and alkaline batteries (wf)	53–1027	(Liu and Liptak, 1999)[b]	●
Zinc-carbon batteries	0.441–135	(Komilis et al., 2011; Recknagel et al., 2009; Rotter, 2002)[b;b;b]	○
For comparison: Alkaline batteries	0.1 - <5	(Komilis et al., 2011; Recknagel et al., 2009; Varta, 2018a)[b;b;b]	–
Plastics (wf)	16.50	(Götze et al., 2016a), 0.75-percentile	
PVC (Cd, stabilized; declining)	300–1400	(Ranta-Korpi et al., 2014)[b]	●
Plastics with Cd pigments**	300–3900	(Ranta-Korpi et al., 2014)[b]	●
Plastics consumer products with suspected Cd pigments	236–19600	(Turner, 2019)[b]	●
Red plastics, Cd pigments***	1598–2490	(Bode et al., 1990)[b]	●
Yellow plastics, Cd pigments***	8050	(Bode et al., 1990)[b]	●
PVC (wf)	1.5–120	(Astrup et al., 2011; Burnley, 2007; David, 2014; Pomberger, 2008)[a;b;b;b]	● ●
Plastics consumer products with food contact	27.2–148.4	(Turner, 2019)[b]	●
Plastics consumer products storage and construction	18.6–10000	(Turner, 2019)[b]	● ●
Plastics consumer products clothing and accessories	35.3–35000	(Turner, 2019)[b]	●
Plastics consumer products toys and hobbies	36.3–19600	(Turner, 2019)[b]	●
Plastics consumer products office and garden	21.1–13400	(Turner, 2019)[b]	● ●
Composites (wf)	5.50	(Götze et al., 2016a) 0.75-percentile	
Shoes (wf)	23.6 – 250	(Astrup et al., 2011; Otte, 1994; Rotter, 2002) [a;a;b]	●
Metal (wf)	5.20	(Götze et al., 2016a) 0.75-percentile	
Non-ferrous (wf)	16–391	(Beker and Cornelissen, 1999; Burnley, 2007; Rugg and Hanna, 1992)[a;b;a]	● ●
Ferrous (wf)	5.2–15	(Beker and Cornelissen, 1999; Burnley, 2007; Rugg and Hanna, 1992)[a;b;a]	○ ●
Aluminum scraps (wf)	53.0	(Maystre and Viret, 1995)[a]	●
Combustibles (wf)	3.93	(Götze et al., 2016a) 0.75-percentile	
Mix containing leather, rubber, textile, or shoes (wf)	18–81.3	(Beker and Cornelissen, 1999; Janz, 2010; Otte, 1994; Rugg and Hanna, 1992)[a;b;a;a]	○ ● ●
Leather (wf)	4.5–61.7	(Otte, 1994; Rotter, 2002)[a;b]	○ ● ●
Rubber (wf)	11.0–11.7	(Nasrullah et al., 2015; Rotter, 2002)[a;b]	●
Subfraction: Colored rubber (wf)	87.1	(Otte, 1994)[a]	●
For comparison: Sub-fraction: Other rubber (wf)	10.4	(Otte, 1994)[a]	–
For comparison: Tyres	8	(Bally, 2003)[b]	○
Textiles (wf)	3.1	(Nasrullah et al., 2016)[a]	○
Carpets (wf)	8.8	(Beker and Cornelissen, 1999)[a]	○
Inert materials (wf)	3.28	(Götze et al., 2016a) 0.75-percentile	
Inert, non-combustible (wf)	7.91–32.6	(LfU Bayern, 2003; Riber et al., 2009)[a;b]	○
Ceramics (wf)	4.98–34.1	(Otte, 1994; Riber et al., 2009)[a;b]	○ ●
Ceramics (Cd pigments glaze)	46.6–38100	(Turner, 2019)[b]	●
For comparison: raw material clay	0.133–0.75	(Reeuwijk et al., 2013)[b]	–
Clay for glass clay containers	557.99–757.99	(Valadez-Vega et al., 2011)[b]	●
Enamel “litargirio” for glass clay containers	63.32–65.95	(Valadez-Vega et al., 2011)[b]	●
Ash (wf)	69.5	(Janz, 2010)[b]	●
Other Cd carriers			
Glass (wf)	1.42	(Eisted and Christensen, 2011)[a]	○
Cd pigment enamels - drinking glassware glaze	285–70900	(Turner, 2019)[b]	●
Cd pigment enamels - glass bottles	1170–19400	(Turner, 2019)[b]	●
Paint buckets (wf)	20.0	(Pomberger, 2008)[b]	●
Renovation waste (wf)	24.5	(LfU Bayern, 2003)[a]	○
Children’s jewelry parts (necklaces, bracelets)	211.961	(Negev et al., 2018)[b]	●

wf = waste fraction.
○: contaminant carrier.
●: strong contaminant carrier.
●: very strong contaminant carrier.
* high Cd and Ni values can be explained by incomplete removal of NiCd batteries (Janz, 2010).
** Cadmium selenide or sulfide, used in PVC, PE, PP, PS, PET, PA, PU.
*** In the study of Bode et al. (1990) red, orange and yellow colored products showed higher Cd contents than other colors, but not all red, orange and yellow plastics were colored with Cd pigments. Low concentrations (<0.9 mg/kg) of Cd were observed in these plastics as well.
[a] : reference value for mixed waste obtained or calculated from the same publication as the listed fraction.
[b] : median from Götze et al. (2016a) used as a reference.

sections (e.g. plastics or combustibles) may have been part of composites and thereby might have caused the observed cadmium concentrations.

3.3.2.4. Cadmium in metals. Ferrous as well as non-ferrous metal appears to be a cadmium carrier based on the evaluation of data of several publications (Beker and Cornelissen, 1999; Burnley, 2007; Liu and Liptak, 1999; Maystre and Viret, 1995; Rugg and Hanna, 1992). Cadmium is used for galvanically deposited coatings, especially on iron, steel, brass, and aluminum (Holleman et al., 2007; International Cadmium Association (2019)). Such coatings are commonly used for nuts and bolts but this application is declining because of the element's toxicity (Schweitzer, 2009). Another possible reason for the high cadmium concentrations in the metal fraction is that batteries and electronic parts, which contain high concentrations of cadmium, could be attributed to the metal fraction in sorting analyses if no separate fraction is defined.

3.3.2.5. Cadmium in combustibles. Apart from plastics, rubber (Nasrullah et al., 2015; Rotter, 2002), textiles (Nasrullah et al., 2016), leather (Rotter, 2002), shoes (Astrup et al., 2011; Rotter, 2002), and mixed fractions thereof (Beker and Cornelissen, 1999; Janz, 2010; Liu and Liptak, 1999; Otte, 1994; Rugg and Hanna, 1992) have been identified as contaminant carriers. This could be related to the use of cadmium pigments in textile dyes (Franklin Associates, 1989), rubber products (International Cadmium Association (2018)) and the leather industry (Dixit et al., 2015). All these materials are also likely to appear in composites, suggesting a potential explanation for the values reported by Götze et al. (2016a) in the composite fraction as well.

3.3.2.6. Cadmium in inert materials. Besides metals, other inert materials (LfU Bayern, 2003), ceramics (Otte, 1994), and glass (Eisted and Christensen, 2011) can be considered as cadmium carriers. This could be related to cadmium pigments used in glass, ceramic glazes, and enamels, or as a phosphor (Franklin Associates, 1989; International Cadmium Association (2018); Turner, 2019). Furthermore, high concentrations of cadmium have been reported for raw clay used for manufacturing glass-clay containers (Valadez-Vega et al., 2011). According to Turner (2019), ceramics currently constitute the main application of cadmium pigments.

Moreover, high cadmium concentrations are reported for ash (Janz, 2010), indicating that cadmium concentrations in waste and the fine fraction may well increase in winter or during the heating season.

3.3.3. Summary: Cadmium carriers

Electronic devices and batteries are still important cadmium carriers. Franklin Associates (1989) and Nakamura et al. (1996) have already identified NiCd batteries as important sources for cadmium in MSW, and due to the longevity of this product, they are expected to keep entering the waste system despite existing regulations for the cadmium content of new batteries. Other cadmium carriers are often related to the use of cadmium as a pigment, which is still relevant in some applications, or to its use as a PVC stabilizer. Identified cadmium carriers and ranges for expected cadmium concentrations are given in Table 7.

3.4. Chlorine (Cl)

3.4.1. Chlorine in waste fractions

Götze et al. (2016a) have observed the highest concentrations of chlorine (0.75-percentiles) in plastics (8.125 $\%_{DM}$) followed by composites (2.550 $\%_{DM}$), combustibles (1.248 $\%_{DM}$), and food waste (1.173 $\%_{DM}$). Sources for chlorine in household waste, bio-waste, bulky waste, packaging waste, and commercial waste have already been investigated by Hoffmann et al. (2006). The authors identified the main chlorine carriers in these waste streams and determined whether the chlorine is bound organically or inorganically in these fractions. In the present paper, a total of 22 datasets from 22 studies was used to identify chlorine carriers in municipal solid waste. A summary of identified chlorine carriers including expected chlorine contents is given in Table 8.

3.4.2. Origins of chlorine in waste fractions

3.4.2.1. Chlorine in plastics. Hoffmann et al. (2006) have identified plastics, composites, textiles and electronic devices as the fractions containing the highest amount of chlorine, leading to the conclusion that PVC represents the main source of chlorine in these fractions. The same fractions have also been identified as chlorine carriers using the method introduced in section 2. The highest chlorine concentrations have been were observed in PVC products including electric sheaths and tubes (Astrup et al., 2011; Liu and Liptak, 1999; Maystre and Viret, 1995; Österlund et al., 2009; Pomberger, 2008) and in non-packaging plastics (Ma et al., 2010), which are also likely to contain PVC. Formally, PVC contains 56.7% of chlorine, but the actual chlorine content can vary significantly depending on the amount of additives. Especially soft PVC may contain up to 60 wt-% of additives (Windsperger et al., 2007), and therefore have a lower chlorine content. Furthermore, additional chlorine can be added to PVC, yielding chlorinated PVC (cPVC) with chlorine contents of about 66% (Patrick, 2005). David (2014) determined the chlorine content in different waste PVC fractions that were removed from the waste stream by an NIR sorter, demonstrating that fractions of soft or colored waste-PVC contain less chlorine than hard or colorless PVC, which is consistent with the higher amount of additives in soft and colored PVC. Also non-PVC plastics may contain chlorine because chlorinated paraffins might be used in combination with antimony to impart flame retardancy to polyolefins and polystyrene (Troitzsch, 2016).

Besides these fractions, unlabeled packaging plastics (Götze et al., 2016b) and plastics from foodstuff (Maystre and Viret, 1995) can be considered as chlorine carriers. The elevated chlorine content in packaging may originate from the former contents, or from PVC used for packaging.

3.4.2.2. Chlorine in composites and combustibles. Besides plastics, synthetic foams (Kost, 2001; Maystre and Viret, 1995; Pomberger, 2008), and the mixed or separate fractions of rubber, textiles, leather, carpets, and shoes (Astrup et al., 2011; Beker and Cornelissen, 1999; Götze et al., 2016b; LfU Bayern, 2003; Liu and Liptak, 1999; Ma et al., 2010; Nasrullah et al., 2016; Nasrullah et al., 2015; Österlund et al., 2009; Penque, 2007; Pomberger, 2008; Riber et al., 2009; Rizza, 2011) have been identified as chlorine carriers. This may also be the result of the broad range of applications of flame retardants (Pfaff, 2017; United states antimony corporation (2017)). On the other hand, neoprene (polychloroprene $(C_4H_5Cl)_n$) parts also contain chlorine and may be part either of the textiles or the composite fraction.

In the case of shoes, which may be part either of the composite or of the combustible fractions as well, PVC can also cause elevated chlorine levels (Ma et al., 2008). Apart from PVC, elevated levels in the composites fraction (Götze et al., 2016b; Hoffmann et al., 2006; LfU Bayern, 2003; Pomberger, 2008) can be caused by polyvinylidene chloride (PVDC) which is applied as a coating to packaging. It serves as a barrier, reduces the permeability to flavors and

Table 8
Selected chlorine carriers, expected concentrations in products or waste fractions, comparison with mixed waste and classification.

Material or waste fraction	Cl [$\%_{DM}$]	Literature source	Level of Cl carrier
Mixed waste	0.670	(Götze et al., 2016a), median	
Plastics (wf)	8.125	(Götze et al., 2016a), 0.75-percentile	
PVC (formal)	56.7	calculated[b]	●
Various PVC fractions (flooring, bottles, etc.) (wf)	6.49–41	(Astrup et al., 2011; Maystre and Viret, 1995; Pomberger, 2008)[a;a;b]	○ ●
PVC soft, transparent (wf)	11–16	(David, 2014)[b]	●
PVC soft, colored (wf)	4–7	(David, 2014)[b]	●
PVC hard, transparent (wf)	43–45	(David, 2014)[b]	●
PVC hard, colored (wf)	34–39	(David, 2014)[b]	●
Cable sheaths (wf)	3.5–22.3	(Maystre and Viret, 1995; Österlund et al., 2009; Pomberger, 2008)[a;b;b]	●
Plastic tubes (wf)	7.3	(Pomberger, 2008)[b]	●
Non packaging plastics (wf)	1.38	(Ma et al., 2010)[a]	○
Packaging plastics, unlabeled (wf)	1.61–2.45	(Götze et al., 2016b)[b]	○
Plastics from foodstuff	12.6	(Maystre and Viret, 1995)[a]	●
Synthetic foams, expanding foams (wf)	1.47–9.1	(Kost, 2001; Maystre and Viret, 1995; Pomberger, 2008)[b;a;b]	○ ●
Composites (wf)	2.550	(Götze et al., 2016a) 0.75-percentile	
Shoes (wf)	2.404–23	(Astrup et al., 2011; LfU Bayern, 2003)[a;a]	○ ●
Mixed fractions with leather, rubber, shoes, cork (wf)	0.665–4.4	(Beker and Cornelissen, 1999; Götze et al., 2016b; LfU Bayern, 2003; Liu and Liptak, 1999; Pomberger, 2008; Riber et al., 2009)[a;b;a;a;b;b]	○ ●
Office articles	2.76	(Riber et al., 2009)[b]	○
Paper-plastics packaging	3.73	(Hoffmann et al., 2006)[a]	○
Plastics-aluminum packaging	1.81	(Hoffmann et al., 2006)[a]	○
Vacuum cleaner bags	1.24	(LfU Bayern, 2003)[a]	○
Combustibles (wf)	1.248	(Götze et al., 2016a) 0.75-percentile	
Rubber (wf)	3.5–9.38	(Nasrullah et al., 2016; Nasrullah et al., 2015; Österlund et al., 2009; Pomberger, 2008; Riber et al., 2009; Rizza, 2011)[a;a;b;b;b;b]	●
Neoprene (formal)	39.8	calculated[b]	●
Textiles (wf) *	1.06–12.5	(Ma et al., 2010; Österlund et al., 2009; Penque, 2007)[a;b;a]	○
Carpets, mats	4.7092	(Beker and Cornelissen, 1999)[a]	●
Wood, mixed (wf)	12.5	(Penque, 2007)[a]	○
For comparison: Massive wood (wf)	0.016–0.107	(Schrägle, 2010)[b]	–
For comparison: Press boards, new	0.016–0.069	(Schrägle, 2015)[b]	–
For comparison: Press boards with non-PVC plastics coating (wf)	0.04–0.297	(Schrägle, 2010)[b]	–
For comparison: Press boards with PVC coating (wf)	1.56–16.46	(Schrägle, 2010)[b]	○ ●
For comparison: Composite wood without plastics coating (wf)	0.05–0.12	(Schrägle, 2010)[b]	–
Food waste (wf)	1.173	(Götze et al., 2016a) 0.75-percentile	
Meat scraps	2.3	(Maystre and Viret, 1995)[a]	○
Animal food	1.63	(Riber et al., 2009)[b]	○
Batteries and electronic devices (wf)			
Electronic materials (wf)	3.577	(LfU Bayern, 2003)[a]	●
Batteries, problematic materials (wf)	1.58–2.7125	(Pomberger, 2008; Riber et al., 2009)[b;b]	○
Zinc-carbon batteries	3.2551	(Maystre and Viret, 1995)[a]	○
Fine fraction < 10 mm (wf) **	0.19–4.21	(Hoffmann et al., 2006)[a]	○ ●
Wood shavings from press boards		Refer to press boards (combustibles section)	
Table salt (NaCl formal)	60.7	calculated[b]	●

wf = waste fraction.
○: contaminant carrier.
●: strong contaminant carrier.
●: very strong contaminant carrier.
* may include shoes.
** highest values occurred due to table salt residues (Hoffmann et al., 2006).
[a] : reference value for mixed waste obtained or calculated from the same publication as the listed fraction.
[b] : median from Götze et al. (2016a) used as a reference.

extends the shelf life. Uses include but are not limited to cookie and chocolate bar packaging (Hoffmann et al., 2006).

High chlorine values observed for the wood fraction (Penque, 2007) can originate from press boards (Hoffmann et al., 2006) because wood glue can contain up to 10% of aluminum chloride as a hardener (Schrägle, 2015; Wittchen et al., 2008). Some more recent analyses of new press boards (Schrägle, 2015), however, find the use of chlorides in this context to have declined.

3.4.2.3. Chlorine in food waste and other organics. Elevated chlorine levels have been observed specifically in the organics fraction (ADEME (2010)), in meat scraps (Maystre and Viret, 1995), and animal food (Riber et al., 2009). In biowaste fractions like these, major part of chlorine is inorganically bound, as it is present mainly in the form of sodium chloride (NaCl) in food waste, or as potassium chloride (KCl) in gardening waste, respectively (Hoffmann et al., 2006).

3.4.2.4. Chlorine in batteries and electronic devices. Electronic devices (LfU Bayern, 2003), batteries (Maystre and Viret, 1995; Riber et al., 2009), and the fraction of problematic substances, including batteries and pharmaceuticals (Pomberger, 2008), are identified as chlorine carriers as well. Reasons for the elevated chlorine levels in batteries include the use of PVC (Saft, 2008b) or the use of chlorides in electrolytes, such as in zinc-carbon batteries containing ammonium chloride (Taylor, 2000). The chlorine content in pharmaceuticals can either be attributed to the pharmaceutical itself or to its blister packaging which is often made from PVC (Raju et al., 2016).

3.4.2.5. Chlorine in the fine fraction. Elevated levels of chlorine in the fine fraction have been reported by Hoffmann et al. (2006), who explained this observation with the presence of salts or glue-containing wood shavings from press boards.

3.4.3. Summary: Chlorine carriers

Hoffmann et al. (2006) report that most chlorine carriers or chlorine-containing fractions are related to PVC. This polymer represents the main chlorine carrier and contributes to the chlorine levels in various fractions and products, including composites, combustibles, and plastics. Flame retardants may also play a role in some applications where chlorine-paraffins are used instead of brominated flame retardants. In the fraction of biowaste, inorganic salts like NaCl and KCl are responsible for the chlorine content. In general, in waste with a high plastics content, the share of organically bound chlorine is expected to prevail, while in wastes containing large amounts of biowaste, chlorine will be predominantly present as inorganic chlorine (Beckmann et al., 2006). Table 8 lists potential chlorine carriers and gives reported ranges for their chlorine contents.

3.5. Chromium (Cr)

3.5.1. Chromium in waste fractions

Götze et al. (2016a) report the highest concentrations (0.75-percentiles) of chromium in composites (708.5 mg/kg$_{DM}$), followed by metal (304.3 mg/kg$_{DM}$), glass (275.7 mg/kg$_{DM}$), and plastics (187.0 mg/kg$_{DM}$). Chromium carriers have been identified assessing 22 datasets from 19 different publications. A list of potential chromium carriers including reported chromium concentrations is given in Table 9.

3.5.2. Origins of chromium in waste fractions

3.5.2.1. Chromium in composites and combustibles. The composite fraction of waste is very heterogeneous, and composite materials might even be allocated to combustibles in other studies. For example, depending on the other fractions that may or may not be defined, leather articles, shoes, and similar materials can be attributed to both the composite and the combustible fraction. These materials therefore may have led to the high chromium concentrations in the composite fraction reported by Götze et al. (2016a).

Textiles, rubber, shoes, leather, and mixed fractions thereof (Astrup et al., 2011; Beker and Cornelissen, 1999; Eisted and Christensen, 2011; Götze et al., 2016b; LfU Bayern, 2003; Liu and Liptak, 1999; Nasrullah et al., 2016; Nasrullah et al., 2015; Otte, 1994; Pomberger, 2008; Prochaska et al., 2005) have been identified as chromium carriers based on the definitions in Section 2. Leather seems to be the major chromium carrier present in these fractions and is also likely to be part of the shoes and the textile fractions.

The high concentration of chromium in leather and leather products is a result of the tanning process, during which chromium(III) salts are applied. Usually, about 60% of the added chromium is taken up by the leather (Matlack, 2010). For this reason, total chromium contents of up to 3.8% (38,000 mg/kg) have been reported for leather products like wristbands from watches, shoes, working gloves, jackets, and other clothes (Rydin, 2002; Thyssen et al., 2012). Although chromium compounds are used to dye certain textiles (e.g. wool) in black, dark green, or dark blue shades (Mahapatra, 2016), the major part of chromium found in the textile fraction is suspected to be caused by leather parts.

Since only hexavalent chromium is considered carcinogenic, REACH regulations only regulate Cr(VI) in leather articles (EC (2014)). Trivalent chromium, however, constitutes the major part of chromium found in leather (Thyssen et al., 2012).

Although no wood fraction has been identified as a contaminant carrier in the reviewed publications, high values of chromium can be observed in certain fractions of old wood, e.g. pressure-impregnated palisade poles (Gras, 2002). Chromium salts have been used to pickle wood (Gras, 2002), which might be a possible explanation for the observed chromium levels.

3.5.2.2. Chromium in metals. Ferrous and non-ferrous metals were identified as chromium carriers based on the data available (Beker and Cornelissen, 1999; Burnley, 2007; Götze et al., 2016b; Liu and Liptak, 1999; Otte, 1994; Pomberger, 2008; Rugg and Hanna, 1992). This was expected because chromium is used extensively in the metal industry. Its applications include the use in alloys (e.g. stainless steels, ferrochromium, chromium-nickel, and chromium-cobalt alloys), solders, as well as surface coatings (Cunat, 2004; Holleman et al., 2007; Janz, 2010; Morf and Taverna, 2006).

3.5.2.3. Chromium in glass and other inert materials. Glass has been identified as a contaminant carrier based on the high chromium concentrations reported in some studies (ADEME (2010); Beker and Cornelissen, 1999; Burnley, 2007; Eisted and Christensen, 2011). Reported chromium concentrations for glass fractions sorted by color (Götze et al., 2016b; Riber et al., 2009) reveal that especially green glass and, to some extent, brown glass is a chromium carrier. This can be explained by the use of the pigment Cr_2O_3, which is used to achieve green shades in glass (Holleman et al., 2007).

Ceramics have not been identified as chromium carriers based on the defined conditions, but certain ceramics, namely cermets, require chromium for their production (Holleman et al., 2007).

3.5.2.4. Chromium in plastics. 'Other plastics' (except HDPE, PET, and films) have only been identified as chromium carriers based on the data presented in Liu and Liptak (1999). The plastics industry applies chromium compounds as pigments, e.g. Cr_2O_3 is used to give a green color to HDPE containers or items for outdoor use. Cr-pigments may also be present in PVC, PP, PS, PET, PA, ABS, and PU. Cr is furthermore used as a catalyst for the polymerization of polyethylenes such as linear low-density polyethylene (LLDPE) and high-density polyethylene (HDPE). Where chromium compounds are used as catalysts, residual chromium concentrations after a cleanup step are not expected to exceed 5 mg/kg in the material. While the chromium content in plastics after polymerization is not suspected to be high, pigmentation with Cr-based compounds is a major source of chromium in plastics (Ranta-Korpi et al., 2014). Furthermore, similar to metals, plastic surfaces can also be coated with chromium (Janz, 2010).

3.5.2.5. Chromium in electronic devices. The electronic fraction (Burnley, 2007), circuit boards and electronic parts (Janz, 2010), as well as problematic materials and batteries (Pomberger, 2008) can be considered as chromium carriers, which is probably related to the use of chromium in metal alloys and solders (cf. section 3.5.2.2).

3.5.2.6. Chromium in the fine fraction. Beker and Cornelissen (1999) and Viczek et al. (2019b) report elevated levels of chromium in the fine fractions of waste. This observation could be related to small metal parts, metal shavings or metal abrasions. There is not enough information on the fractions, however, to draw conclusions on the exact reason for elevated chromium levels.

Note that for other elements that are typically used in metal alloys, i.e. Co, Ni, and Pb, the fine fractions have been identified as contaminant carriers based on the definitions in Section 2 as well. Stainless steels, for example, typically consist of iron, chro-

Table 9
Selected chromium carriers, expected concentrations in products or waste fractions, comparison with mixed waste and classification.

Material or waste fraction	Cr [mg/kg$_{DM}$]	Literature source	Level of Cr carrier
Mixed waste	111.8	(Götze et al., 2016a), median	
Composites (wf)	708.5	(Götze et al., 2016a), 0.75-percentile	
Mixed leather, rubber, shoes (wf)	833.3–7885	(Beker and Cornelissen, 1999; LfU Bayern, 2003; Otte, 1994; Pomberger, 2008; Riber et al., 2009)[a;a;a;b;b]	● ●
Shoes (wf)	5490–5992	(LfU Bayern, 2003; Otte, 1994)[a;a]	●
Leather (wf)	5070	(Otte, 1994)[a]	●
Leather products (shoes, jackets etc.)	< 100–38000	(Rydin, 2002; Thyssen et al., 2012)[b;b]	○ ● ●
Subfraction: Colored rubber (wf)	346	(Otte, 1994)[a]	○
For comparison: Sub-fraction: Other rubber (wf)	95	(Otte, 1994)[a]	–
Metals (wf)	304.3	(Götze et al., 2016a) 0.75-percentile	
Non-ferrous metals (wf)	300–2340	(Beker and Cornelissen, 1999; Pomberger, 2008)[a;b]	○ ● ●
Ferrous metals (wf)	230–5998	(Beker and Cornelissen, 1999; Burnley, 2007; Otte, 1994; Pomberger, 2008; Rugg and Hanna, 1992)[a;b;a;b;a]	○ ● ●
Stainless steels	105000–300000	(Cunat, 2004)[b]	●
Cr-Ni stainless steel (Nirosta)	180,000	(Holleman et al., 2007)[b]	●
Glass (wf)	275.7	(Götze et al., 2016a) 0.75-percentile	
Green glass (wf)	970.15–1190	(Götze et al., 2016b; Riber et al., 2009)[b;b]	● ●
Brown glass (wf)	152.43–398.25	(Götze et al., 2016b)[b]	○
For comparison: clear glass (wf)	12.29–15.87	(Götze et al., 2016b)[b]	–
Plastics (wf)	187.0	(Götze et al., 2016a) 0.75-percentile	
Other plastics (wf)	279	(Liu and Liptak, 1999)[b]	○
Plastics with Cr-based pigments*	30–3.400	(Ranta-Korpi et al., 2014)[b]	○ ● ●
For comparison: plastics after polymerization with Cr_2O_3**	1–5	(Ranta-Korpi et al., 2014)[b]	–
Electronic devices/batteries			
Electronic materials (wf)	728–1304	(Burnley, 2007; LfU Bayern, 2003)[b;a]	○ ● ●
Circuit boards	200–498	(Janz, 2010)[b]	○
Electronic parts from circuit boards	515–818	(Janz, 2010)[b]	○ ●
Problematic materials	3230	(Pomberger, 2008)[b]	●
Fine fraction (wf)			
< 3 mm	270–450	(Beker and Cornelissen, 1999)[a]	○
3 – 8 mm	176.7–280	(Beker and Cornelissen, 1999)[a]	○
8 – 20 mm	240–363.3	(Beker and Cornelissen, 1999)[a]	○
Coarsely shredded commercial waste < 5 mm	180–400	(Viczek et al., 2019b)[a]	○
Coarsely shredded commercial waste 10–20 mm	58–888	(Viczek et al., 2019b)[a]	○ ●
Other Cr-carriers			
Wooden palisade poles, pressure impregnated	1110	(Gras, 2002)[b]	● ●
Children's jewelry parts (necklaces, bracelets)	8821	(Negev et al., 2018)[b]	●
Cermets (77% Cr, 23% Al_2O_3)	770,000	(Holleman et al., 2007)[b]	●
For comparison: Raw material clay	0.777–205	(Reeuwijk et al., 2013)[b]	–

wf = waste fraction.
○: contaminant carrier.
●: strong contaminant carrier.
●: very strong contaminant carrier.
* used for PVC, PE, PP, PS, PET, PA, ABS, PU.
** used for LLDPE, HDPE.
[a] : reference value for mixed waste obtained or calculated from the same publication as the listed fraction.
[b] : median from Götze et al. (2016a) used as a reference.

mium, and nickel (ISSF (2019)). For the waste stream characterized by Beker and Cornelissen (1999), the fine fraction has been identified as a contaminant carrier for Pb, Ni, Cr and Co. Similarly, the fine fraction in the waste analyzed by Nasrullah et al. (2015) is a contaminant carrier for Pb, Ni and Co. If the same method is applied to iron, which was only determined by Nasrullah et al. (2015), the fine fraction is identified as a contaminant carrier for iron as well, which supports the hypothesis that small metal parts could be responsible for the elevated concentrations of these elements reported in some publications.

3.5.3. Summary: Chromium carriers

Apart from metal alloys, the main chromium carriers present in MSW are leather and leather products. Applications using chromium oxide as a pigment, for example green glass or plastics, lead to the presence of chromium carriers in waste as well. Electronic devices, including circuit boards, have also been identified as chromium carriers. Selected identified chromium carriers and the corresponding expected chromium concentrations are given in Table 9.

3.6. Cobalt (Co)

3.6.1. Cobalt in waste fractions

The highest concentrations of cobalt are reported in the fractions inert materials (68.0 mg/kg$_{DM}$), plastics (53.3 mg/kg$_{DM}$), metals (43.5 mg/kg$_{DM}$), glass (9.0 mg/kg$_{DM}$), and combustibles (3.7 mg/kg$_{DM}$) (Götze et al., 2016a). A total of 12 datasets from 11 publications was used to identify individual fractions or products that may be contaminant carriers. A summary of results is presented in Table 10.

3.6.2. Origins of cobalt in waste fractions

3.6.2.1. Cobalt in inert materials. In inert or non-combustible material fractions, elevated concentrations of cobalt are observed for ceramics (Beker and Cornelissen, 1999; Götze et al., 2016b). Cobalt compounds are used as pigments for ceramics, where it is a traditional and widely spread source of blue color (Llusar et al., 2001). Besides the enamel, the clay used for ceramics also contains cobalt (Valadez-Vega et al., 2011).

Table 10
Selected cobalt carriers, expected concentrations in products or waste fractions, comparison with mixed waste and classification.

Material or waste fraction	Co [mg/kg$_{DM}$]	Literature source	Level of Co carrier
Mixed waste	7.6	(Götze et al., 2016a), median	
Inert (wf)	68.0	(Götze et al., 2016a), 0.75-percentile	
Ceramics (wf)	9.3–279	(Beker and Cornelissen, 1999; Götze et al., 2016b)[a;b]	○ ●
Clay for glass-clay containers	468–563	(Valadez-Vega et al., 2011)[b]	●
Enamel "litargirio" for glass-clay containers	43.20–44.00	(Valadez-Vega et al., 2011)[b]	●
Plastics (wf)	53.3	(Götze et al., 2016a) 0.75-percentile	
Plastics soft (wf)	180	(Nasrullah et al., 2015)[a]	●
non-packaging plastic-identification code 7–19 (wf)	18.88	(Götze et al., 2016b)[b]	○
Co-catalyzed PET, PBT	5–50	(Ranta-Korpi et al., 2014)[b]	○ ●
Plastics with Co pigments*	80–1500	(Ranta-Korpi et al., 2014)[b]	●
Metals (wf)	43.5	(Götze et al., 2016a) 0.75-percentile	
Ferrous metals (wf)	37–64.2	(Beker and Cornelissen, 1999; Otte, 1994)[a;a]	○ ●
Non-ferrous metals (wf)	8–28.9	(Beker and Cornelissen, 1999)[a]	●
Metal packaging ferrous	19.6–24.1	(Götze et al., 2016b)[b]	○
Non-packaging metal ferrous	39.1	(Götze et al., 2016b)[b]	●
Cobalt-chromium alloys	350000–650000	(Cunat, 2004; Holleman et al., 2007)[b;b]	●
Glass (wf)	9.0	(Götze et al., 2016a) 0.75-percentile	
Combustibles (wf)	3.7	(Götze et al., 2016a) 0.75-percentile	
Textiles (wf)	31.0	(Nasrullah et al., 2015)[a]	●
Wood (wf)	38.7	(Eisted and Christensen, 2011)[a]	●
Organics, residue (wf)	67.2	(Otte, 1994)[a]	○
Electronic devices/batteries (wf)			
Batteries (wf)	2200	(Astrup et al., 2011)[a]	●
Zinc-carbon batteries	13.0 – 33.0	(Komilis et al., 2011)[b]	○
Alkaline batteries	3.70–242	(Komilis et al., 2011)[b]	○ ●
NiCd batteries	4000–20,000	(Saft, 2008a; Yuasa, 2015)[b]	●
NiMH batteries	6300–19,000	(Johnson Controls, 2015)[b]	●
Li-ion batteries	210,000	(Entel, 2016)[b]	●
Fine fraction (wf)	0.5–42	(Beker and Cornelissen, 1999; Nasrullah et al., 2015; Viczek et al., 2019b)[a;a;a]	○ ●

wf = waste fraction.
○: contaminant carrier.
●: strong contaminant carrier.
●: very strong contaminant carrier.
* Used for PVC, PE, PP, PS, PET, PA, ABS, PU.
[a] : reference value for mixed waste obtained or calculated from the same publication as the listed fraction.
[b] : median from Götze et al. (2016a) used as a reference.

3.6.2.2. Cobalt in plastics. Plastics (Beker and Cornelissen, 1999; Eisted and Christensen, 2011), soft plastics (Nasrullah et al., 2015), and non-packaging plastics with identification codes 7–19 (Götze et al., 2016b) have been identified as contaminant carriers. In the plastics industry, cobalt is used as a catalyst or pigment. Catalytic applications include polymerization catalysts for polyurethanes and polyesters (e.g. PET) as well as polybutadiene rubber, an important impact modifier for high impact polystyrene (HIPS) and acrylonitrile butadiene styrene (ABS). Cobalt is not the leading catalyst for PET polymerization, but it is the most important catalyst for polybutadiene rubber (Ranta-Korpi et al., 2014).

Inorganic and organic cobalt based pigments are used for PVC, PE, PP, PS, PET, PA, ABS, and PU. Inorganic cobalt compounds are thermally and chemically resistant and therefore applied in plastics processed at high temperatures. Examples include the green pigments cobalt zinc chromite (Co, Zn)Cr_2O_4, cobalt nickel zinc titanate (Co, Ni, Zn)$_2TiO_4$, blue pigments such as cobalt chromium aluminate Co(Al, Cr)$_2O_4$ or cobalt aluminate $CoAl_2O_4$, or 'pigment black' Co(Cr, Fe, Mn)$_2O_4$. However, cobalt pigments are often replaced by cheaper copper pigments where shades of blue and green are required. Besides inorganic cobalt compounds, less thermally stable organometallic azo-cobalt complexes can be used (Jandke and Reinicker, 2016; Ranta-Korpi et al., 2014).

3.6.2.3. Cobalt in metals. Ferrous metals (Beker and Cornelissen, 1999; Otte, 1994), packaging and non-packaging ferrous metals (Götze et al., 2016b), and one sample of non-ferrous metal (Beker and Cornelissen, 1999) have been identified as cobalt carriers. Cobalt is commonly used in the metal industry asa constituent of heat-, corrosion-, or wear-resistant metal alloys, often paired with chromium or nickel (Campbell, 2008; Holleman et al., 2007).

3.6.2.4. Cobalt in glass. From the data presented in the reviewed publications, no glass fraction has been identified as a cobalt carrier using the present approach. However, in the glass industry used cobalt to taint glass blue or to decolorize glass that appears yellowish due to its iron content (Holleman et al., 2007).

3.6.2.5. Cobalt in combustibles. Apart from plastics, textiles (Nasrullah et al., 2015), organics (Otte, 1994), and wood (Eisted and Christensen, 2011) have also been identified as cobalt carriers in individual publications. Elevated levels in textiles could be due to the use of cobalt pigments for dyeing (Aspland, 1993), while cobalt-containing wood protection products, e.g. siccatives in alkyd paints and coatings, could explain the elevated levels in wood. (Danish EPA (2015); Llusar et al., 2001).

3.6.2.6. Cobalt in batteries and electrical devices. Astrup et al. (2011) list batteries as a critical element (i.e. a material with high concentrations of a certain chemical element) in waste with respect to cobalt. NiCd batteries contain cobalt, more precisely cobalt oxide or hydroxide (Saft, 2008a; Yuasa, 2015), as do nickel metal hydride (NiMH) batteries (Johnson Controls, 2015; Saft, 2008b), or zinc-carbon and alkaline batteries (Komilis et al., 2011). Li-ion batteries

can contain up to 35% of lithium cobalt oxide ($LiCoO_2$) as well (Ansmann, 2011; Entel, 2016).

3.6.2.7. Cobalt in the fine fraction. Viczek et al. (2019b), Nasrullah et al. (2015) and Beker and Cornelissen (1999) report elevated levels of cobalt in the fine fractions. This observation could be related to small metal parts, metal shavings or metal abrasions (as proposed for chromium in Section 3.5.2.6), or even small ceramics or glass parts in the fine fraction. Insufficient information on these fractions is available to determine the source of cobalt with certainty, however.

3.6.3. Summary: Cobalt carriers

Apart from metals where cobalt is used for alloys, cobalt occurs in MSW due to its use as a pigment in ceramics, plastics, or textiles. It is also used for wood applications, as a catalyst for certain polymers, and in various batteries. Table 10 gives an overview of the identified cobalt carriers and reported cobalt concentrations.

3.7. Lead (Pb)

3.7.1. Lead in waste fractions

Götze et al. (2016a) report that the highest lead concentrations (0.75-percentiles) are observed in the individual waste fractions of inert materials (382.3 mg/kg_{DM}), composites (363.3 mg/kg_{DM}), plastics (247.0 mg/kg_{DM}), glass (189.1 mg/kg_{DM}), combustibles (147.0 mg/kg_{DM}), and metals (90.0 mg/kg_{DM}). Contaminant carriers in these fractions were identified more specifically by using 25 datasets from 22 publications. As for Cadmium, products containing lead in municipal solid waste have already been characterized by Franklin Associates (1989) and Nakamura et al. (1996), the findings are compared in section 3.7.3. The identified potential contaminant carriers including reported concentrations are presented in Table 11.

3.7.2. Origins of lead in waste fractions

3.7.2.1. Lead in inert materials. Elevated lead levels have been observed in ceramics (Beker and Cornelissen, 1999; Götze et al., 2016a; Otte, 1994; Riber et al., 2009), other non-combustibles (Burnley, 2007; Eisted and Christensen, 2011), other inorganics (Liu and Liptak, 1999), or the inert fraction (LfU Bayern, 2003; Maystre and Viret, 1995) in cases when no separate ceramics fraction was established. This can be related to the presence of lead in the raw material for ceramics: clay contains lead (Reeuwijk et al., 2013; Valadez-Vega et al., 2011) in concentrations that could explain the elevated levels of lead in the inert fraction. Furthermore, lead oxide (PbO) is used for ceramic enamels (Holleman et al., 2007), which according to LfU Bayern (2003) is responsible for elevated levels of lead in the inert fraction.

3.7.2.2. Lead in composites. The origin of lead concentrations in composite fractions is hard to analyze, as the detailed composition of this fractions is not known. Elevated levels of lead have been reported for shoes (Rotter, 2002), which in some sorting campaigns may have been part of the composite fractions. In addition, the materials discussed in the following paragraphs may have been part of the composites fraction and may have contributed to the observed lead concentrations.

3.7.2.3. Lead in plastics. In the plastics fraction, elevated levels of Pb are reported for PVC flooring (Pomberger, 2008) and the 'other plastics' (LfU Bayern, 2003) or 'dense plastics' (Burnley, 2007) fractions, both of which are likely to contain PVC as well. Concentrations range from 473 to 879 mg/kg. Lead compounds have been used as a stabilizer in PVC and as a pigment component in many resins (Franklin Associates, 1989; Ranta-Korpi et al., 2014). While the use of lead-based pigments has significantly decreased since the 1970s (Franklin Associates, 1989), lead-based heat stabilizers are still common. Although their use has been impaired by environmental concerns regarding the toxicity of lead, the share of lead-based heat stabilizers still amounted for more than 50% in 2007 (Ranta-Korpi et al., 2014). They are used in flexible as well as rigid PVC applications, including wire insulation, PVC foams, rigid vinyl pipes, fittings, and window profiles. Lead stabilizers with a heat- and light-stabilizing effect are used in PVC roofing and items for outdoor use. For this reason, lead contents in PVC range from 4500 to 33,000 mg/kg (Ranta-Korpi et al., 2014).

Elevated levels of lead have also been reported for plastic films (Burnley, 2007; Liu and Liptak, 1999) and LDPE bags and films (Rugg and Hanna, 1992). The use of lead for the production of technical films (LfU Bayern, 2003) may help explain this observation, but available sources are insufficient to determine the exact cause.

3.7.2.4. Lead in glass. Reviewed reports (Beker and Cornelissen, 1999; Eisted and Christensen, 2011; LfU Bayern, 2003) suggest that the glass fraction, especially leaded glass (Nakamura et al., 1996), can be considered a contaminant carrier for lead. PbO is usually used for decorative glassware but also for some special optical glasses when a high refractive index is needed. It makes the glass dense, hard, and X-ray absorbing (Hasanuzzaman et al., 2016). It has also been used in cathode ray tubes (CRTs) for monitors and TV screens (Restrepo et al., 2016; The Waste & Resources Action Programme (2004)).

3.7.2.5. Lead in metals. High concentrations of lead are also reported for metals, especially for non-ferrous metals (Burnley, 2007; Maystre and Viret, 1995; Otte, 1994; Pomberger, 2008; Rugg and Hanna, 1992). On a more detailed level, Götze et al. (2016b) report elevated lead concentrations for non-ferrous and ferrous non-packaging metals while Rugg and Hanna (1992) report high lead concentrations in tin cans. However, some publications (Burnley, 2007; Pomberger, 2008) also observe elevated concentrations for ferrous metals. Lead is used in various alloys, for example in bearing metals with a lead content of 60 to 80%, or in type metal with a lead content of 70 to 90% (Holleman et al., 2007).

3.7.2.6. Lead in other combustible materials. Wood (Janz, 2010; Liu and Liptak, 1999), particularly impregnated wood (Astrup et al., 2011), can also be considered a lead carrier. Publications demonstrate that especially waste wood from demolition, renovation, furniture, and packaging features high values (40 to 700 mg/kg DM) of lead, compared to natural wood (0 to 5 mg/kg DM) and wood residues from the wood industry or from construction sites (40 to 20 mg/kg DM) (BUWAL (1996)). It is likely that the observed levels of lead originate from impregnations or paints.

There are various lead pigments, such as the yellow pigment $PbCrO_4$, or the white pigment $PbCO_3$ that have been used as paints (Holleman et al., 2007). Pomberger (2008), for example, reports high Pb concentrations in paint buckets found in waste, Nakamura et al. (1996) observed them in the paint itself. In Europe, lead carbonate and lead sulfate are not permitted in mixtures intended to be used as paints, except for restoration and maintenance purposes (EC, 2006a).

Rubber has been identified as a source of lead by Franklin Associates (1989), one of the reasons being lead pigments. The concentrations of lead observed in the rubber fraction (Nasrullah et al., 2015; Rotter, 2002) are furthermore similar to the concentrations that have been observed in old tires (Bally, 2003). However, the exact cause for elevated levels of lead cannot be determined from the available data.

Table 11
Selected lead carriers, expected concentrations in products or waste fractions, comparison with mixed waste and classification.

Material or waste fraction	Pb [mg/kg$_{DM}$]	Literature source	Level of Pb carrier
Mixed waste	191.9	(Götze et al., 2016a), median	
Inert (wf)	382.3	(Götze et al., 2016a), 0.75-percentile	
Ceramics (wf)	917–1967	(Beker and Cornelissen, 1999; Götze et al., 2016b; Otte, 1994; Riber et al., 2009)[a;b;a;b]	○ ●
For comparison: Raw material clay	0.510–99.7	(Reeuwijk et al., 2013)[b]	–
Clay for glass-clay containers	608–805	(Valadez-Vega et al., 2011)[b]	○
Enamel "litargirio" for glass-clay containers	62.60–64.75	(Valadez-Vega et al., 2011)[b]	–
Composites (wf)	363.3	(Götze et al., 2016a) 0.75-percentile	
Shoes (wf)	565	(Rotter, 2002)[b]	○
Office articles (wf)	576	(Riber et al., 2009)[b]	○
Combustibles (wf)	147.0	(Götze et al., 2016a) 0.75-percentile	
Rubber (wf)	250–459	(Nasrullah et al., 2015; Rotter, 2002)[a;b]	○
Wood (wf)	30.9–6900	(Astrup et al., 2011; Janz, 2010; Liu and Liptak, 1999)[a;b;b]	○ ●
Wood waste with residues of coatings, colors, press boards	623–821	(Gras, 2002)[b]	○
Waste wood, solid	36.8–452	(Schrägle, 2010)[b]	○
Press boards, PVC coated	7.7–279	(Schrägle, 2010)[b]	–
Wood composites without plastics coating	6.4–121	(Schrägle, 2010)[b]	–
Press boards (product)	3.16–150	(Schrägle, 2015)[b]	–
For comparison: untreated wood	< 2.5–6.5	(Gras, 2002)[b]	–
Plastics (wf)	247.0	(Götze et al., 2016a) 0.75-percentile	
PVC flooring (wf)	500	(Pomberger, 2008)[b]	○
Plastics, hard (wf)	400	(Nasrullah et al., 2015)[a]	○
Dense plastics (wf)	879	(Burnley, 2007)[b]	○
Other plastics (without packaging, foils, Styrofoam) (wf)	473	(LfU Bayern, 2003)[a]	○
Film plastics (wf)	1595	(Burnley, 2007)[b]	●
LDPE bags and film (wf)	565	(Rugg and Hanna, 1992)[a]	○
PVC pipes, lead stabilized	4500–9000	(Ranta-Korpi et al., 2014)[b]	●
PVC fittings, lead stabilized	10000–14000	(Ranta-Korpi et al., 2014)[b]	●
PVC window profiles, lead stabilized	12500–17000	(Ranta-Korpi et al., 2014)[b]	●
PVC wire cables, lead stabilized	15500–27000	(Ranta-Korpi et al., 2014)[b]	●
PVC roofing, lead stabilized	24000–33000	(Ranta-Korpi et al., 2014)[b]	●
Plastics with Pb pigments (PVC, LDPE, HDPE)	300–3000	(Ranta-Korpi et al., 2014)[b]	○ ●
Glass (wf)	189.1	(Götze et al., 2016a) 0.75-percentile	
Leaded glass	167000–353000	(Hasanuzzaman et al., 2016)[b]	●
CRT glass (panel)	up to 30,600	(The Waste and Resources Action Programme, 2004)[b]	●
CRT glass (funnel)	102000–228000	(Restrepo et al., 2016; The Waste and Resources Action Programme, 2004)[b;b]	●
CRT glass (neck)	260,000	(Restrepo et al., 2016)[b]	●
Crystal glassware	270,000	(Nakamura et al., 1996)[b]	●
Metals (wf)	90.0	(Götze et al., 2016a) 0.75-percentile	
Non-ferrous metals (wf)	4000–38529	(Burnley, 2007; Maystre and Viret, 1995; Otte, 1994; Pomberger, 2008; Rugg and Hanna, 1992)[b;a;a;b;a]	●
Non-ferrous non-packaging metals (wf)	680	(Götze et al., 2016b)[b]	○
Ferrous metals (wf)	1300–10000	(Burnley, 2007; Pomberger, 2008)[b;b]	●
Ferrous non-packaging metals	865	(Götze et al., 2016b)[b]	○
Tin cans (wf)	350	(Rugg and Hanna, 1992)[a]	○
Bearing metals	600000–800000	(Holleman et al., 2007)[b]	●
Type metals	700000–900000	(Holleman et al., 2007)[b]	●
Electronic devices/batteries (wf)			
Electrical goods	2713–77000	(Burnley, 2007; LfU Bayern, 2003; Maystre and Viret, 1995; Nakamura et al., 1996)[b;a;a;b]	●
Circuit boards	53,031	(Rotter, 2002)[b]	●
Circuit boards (without electrical components)	18722–69548	(Janz, 2010)[b]	●
Plastic casings	1755	(Rotter, 2002)[b]	●
Electrical components radio, computer	15787–38879	(Janz, 2010)[b]	●
Cables (wf)	5354	(Rotter, 2002)[b]	●
Batteries (wf)	10,800	(Burnley, 2007)[b]	●
Dry battery	526	(Nakamura et al., 1996)[b]	○
Small sealed lead battery	650,000	(Nakamura et al., 1996)[b]	●
Alkaline batteries	2.8–24.3	(Komilis et al., 2011)[b]	–
Zinc-carbon batteries	690–1400	(Komilis et al., 2011)[b]	○ ●
Primary zinc/air button cell	100–300	(Conrad Electronics (2014))[b]	–
Fine fraction (wf)	42–706	(Beker and Cornelissen, 1999; Burnley, 2007; Ferrari et al., 2000; Nasrullah et al., 2015; Rugg and Hanna, 1992)[a;b;b;a;a]	○
Ash	4200	(Janz, 2010)[b]	●
Coarsely shredded commercial waste < 10 mm	37–1350	(Viczek et al., 2019b)[a]	○ ●
Other Pb-carriers			
Children's jewelry parts (necklaces, bracelets)	1420	(Negev et al., 2018)[b]	●
Paint buckets	400	(Pomberger, 2008)[b]	○
Paint	710,000	(Nakamura et al., 1996)[b]	●
Glow lamp	120,000	(Nakamura et al., 1996)[b]	●

(*continued on next page*)

Table 11 (*continued*)

Material or waste fraction	Pb [mg/kg$_{DM}$]	Literature source	Level of Pb carrier
Lead tubes	970,000	(Nakamura et al., 1996)[b]	●
Incandescent bulbs	5700	(Nakamura et al., 1996)[b]	●
Fluorescent lamp	78,000	(Nakamura et al., 1996)[b]	●

wf = waste fraction.
◯: contaminant carrier.
◍: strong contaminant carrier.
●: very strong contaminant carrier.
[a] : reference value for mixed waste obtained or calculated from the same publication as the listed fraction.
[b] : median from Götze et al. (2016a) used as a reference.

3.7.2.7. Lead in batteries and electronic devices. According to the defined criteria, electronic devices, especially circuit boards and electronic parts of computers, radios or calculators (Janz, 2010; Nakamura et al., 1996; Rotter, 2002), cables (Rotter, 2002), and batteries (Komilis et al., 2011; Nakamura et al., 1996; Pomberger, 2008) can be considered lead carriers as well.

Lead is commonly used in electronic products (LfU Bayern, 2003), e.g. in the form of lead-containing solders (Morf and Taverna, 2006). Regarding batteries, lead accumulators have been the main source of lead in municipal solid waste in the US in the 1980s (Franklin Associates, 1989). Lead concentrations in lead accumulators are much higher than in dry batteries (Nakamura et al., 1996) or in zinc-carbon and alkaline-manganese batteries (Komilis et al., 2011). Lead contents of several zinc-carbon and alkaline-manganese batteries differ by a factor of approximately 100, with non-alkaline batteries being classified as lead carriers, while for alkaline batteries, lead concentrations similar to office paper or compost have been observed (Komilis et al., 2011). Alkaline batteries can therefore not be considered lead carriers. However, the European Union restricted the use of lead in 2003 (EC, 2011b, 2003), decline of the lead content in electronic materials and MSW should therefore be expected (LfU Bayern, 2003)

Furthermore, the following goods, which may have declined in use in some countries, have been identified as sources for lead by Franklin Associates (1989) and Nakamura et al. (1996): light bulbs, which contain lead in solders and in the glass, incandescent bulbs, fluorescent lamps, and lead tubes.

3.7.2.8. Lead in the fine fraction. Some publications (Beker and Cornelissen, 1999; Burnley, 2007; Nasrullah et al., 2015; Rugg and Hanna, 1992; Viczek et al., 2019b) report fine fractions containing high concentrations of lead, which led to the fine fractions being identified as lead-carrying fractions. Since no more information on the fine fraction is available, the origin of these elevated levels of lead cannot be determined. Potential explanations include small metal parts, metal shavings or metal abrasions. Another possibility is the presence of ash, which according to Janz (2010) displays high concentrations of lead (Janz, 2010).

3.7.3. Summary: Lead carriers

In their report from the late 1980s, Franklin Associates (1989) state that lead-acid batteries contributed the main part of lead present in municipal solid waste. They also identify consumer electronics since they comprise soldered circuit boards containing lead, leaded glass in television sets, and plated steel chassis. These materials are followed by glass and ceramics, including optical glass. Although the use of lead has decreased for several applications, the contaminant carriers Franklin Associates (1989) listed in their report are still quite similar while the relative amount of lead introduced by these fractions has probably changed. Nakamura et al. (1996) also observe that a major part of the lead is found in high-concentration items constituting only a minor part of municipal solid waste. Lead carriers identified in the present approach furthermore include ceramics, leaded glass, PVC, electronic parts, waste wood, and ash. Results and expected concentrations are summarized in Table 11.

3.8. Mercury (Hg)

3.8.1. Mercury in waste fractions

The literature review of Götze et al. (2016a) shows that the highest concentrations of mercury (0.75 quantiles) in household waste are allocated to food waste (0.870 mg/kg$_{DM}$), followed by combustibles (0.470 mg/kg$_{DM}$), plastic (0.400 mg/kg$_{DM}$), organics (0.396 mg/ kg$_{DM}$), and composites (0.380 mg/ kg$_{DM}$). Concentrations in all other fractions, however, range from 0.198 to 0.285 mg/kg$_{DM}$, which is not much lower. A detailed evaluation of 23 datasets from 20 publications was used to identify contaminant carriers in waste. A comprehensive table of contaminant carriers and reported concentrations of mercury is presented in Table 12.

3.8.2. Origins of mercury in waste fractions

3.8.2.1. Mercury in food waste. In their study, Götze et al. (2016a) point out the high mercury content in food waste reported in some sources. They removed data points below the detection limit, since some sources had quite high detection limits of 2 mg/kg$_{DM}$, but they also point out that other publications such as Ferrari et al. (2000) and Zhang et al. (2008) report high values > 2 mg/kg$_{DM}$ Hg in food waste. While seafood is known to contain mercury (Harrison, 2005), largely present as methylmercury (Batista et al., 2011), it is unclear whether the levels are high enough to explain the values observed for mixed food waste (compare Table 12). Mercury concentrations typically range from 0.1 to 0.2 mg/kg and are usually below 0.5 mg/kg (Balshaw et al., 2007). These values presumably refer to wet mass, meaning that the impact fish waste has on the mercury levels in food waste is determined by the amount and water content of fish waste.

A closer look at the publications observing high Hg concentrations in food waste shows that Ferrari et al. (2000) report a concentration of 2.5 mg/kg$_{DM}$ in canteen waste, which was mainly composed of organic waste of biological origin from vegetables and animals, but the reported Hg concentrations are comparably high for all fractions (lowest value: 1.20 mg/kg$_{DM}$). When these are compared with the mean value in mixed waste from Götze et al. (2016a), the method defined in this paper would identify all these fractions as contaminant carriers.

Zhang et al. (2008) in contrast report values higher than 2 mg/kg$_{DM}$ for a fraction that mainly consists of putrescible waste (food, fruits) but also contains various indistinguishable and fine particles that may also be responsible for the elevated mercury levels. It is, therefore, possible that the observed Hg-concentrations do not originate from food waste itself, but from small impurities or contaminations.

Table 12
Selected mercury carriers, expected concentrations in products or waste fractions, comparison with mixed waste and classification.

Material or waste fraction	Hg [mg/kg$_{DM}$]	Literature source	Level of Hg carrier
Mixed waste	0.580	(Götze et al., 2016a), median	
Food waste (wf)	0.870	(Götze et al., 2016a), 0.75-percentile	
Seafood, general*, probably referred to wet mass	0.1–0.2 usually < 0.5	(Balshaw et al., 2007)[b]	–
Shrimp, octopus, wish, canned tuna, mussels, squid (range), probably wet mass	0.0038–0.1739	(Batista et al., 2011)[b]	–
Combustibles (wf)	0.470	(Götze et al., 2016a) 0.75-percentile	
Wood (wf)	0.2–2	(Beker and Cornelissen, 1999; Eisted and Christensen, 2011; LfU Bayern, 2003; Liu and Liptak, 1999)[a;a;a;b]	○ ● ●
Old wood, solid	0.05 – 1.4	(Schrägle, 2010)[b]	○
Wooden boards, painted or treated	0.36–0.91	(Gras, 2002)[b]	–
For comparison: press boards (product)	0.02–0.2	(Gras, 2002; Schrägle, 2015)[b;b]	–
For comparison: untreated wood	< 0.05	(Gras, 2002)[b]	–
Leather, rubber, cork	1.630	(LfU Bayern, 2003)[a]	●
Newspaper	0.3–2	(Liu and Liptak, 1999)[b]	○
Plastics (wf)	0.400	(Götze et al., 2016a) 0.75-percentile	
Organics (wf)	0.396	(Götze et al., 2016a) 0.75-percentile	
Composites (wf)	0.380	(Götze et al., 2016a) 0.75-percentile	
Vacuum cleaner bags (wf)	0.714	(LfU Bayern, 2003)[a]	○
Metals (wf)	0.200	(Götze et al., 2016a) 0.75-percentile	
Ferrous metals (wf)	3	(Beker and Cornelissen, 1999)[a]	●
Non-ferrous metals (wf)	8.5	(Beker and Cornelissen, 1999)[a]	●
Electronic devices/batteries (wf)			
Electronic material (wf)	1.688	(LfU Bayern, 2003)[a]	●
Batteries (wf)	127–2900	(Astrup et al., 2011; Burnley, 2007; Riber et al., 2009; Rotter, 2002; Rugg and Hanna, 1992)[a;b;b;b;a]	○ ● ●
Alkali-manganese batteries (wf)	836	(Maystre and Viret, 1995)[a]	●
Zinc-carbon batteries (wf)	72–136	(Liu and Liptak, 1999; Maystre and Viret, 1995)[b;a]	●
Button cell battery	4000–10000; < 20,000	(Conrad Electronics (2014); Sperlich et al., 2014)[b]	●
For comparison: Button cell battery, Hg-free	< 1	(Varta, 2018b)[b]	–
Problematic materials (wf)	100	(Pomberger, 2008)[b]	●
Compact fluorescent lamps (energy saving bulbs)	1.5–4.0 mg/lamp	(LGL Bayern, 2012; Sperlich et al., 2014)[b]	●
Fluorescent tubes	< 5 mg/lamp	(Sperlich et al., 2014)[b]	●
Fine fraction (wf)	0.2–0.9	(Beker and Cornelissen, 1999; LfU Bayern, 2003; Nasrullah et al., 2015)[a;a;a]	○ ●
< 20 mm	0.2–11.8	(Ferrari et al., 2000)[b]	○ ● ●
Coarsely shredded commercial waste, < 5 mm	0.7–3.6	(Viczek et al., 2019b)[a]	○ ●
Other Hg-carriers			
Raw material: Clay	0.0280–2.20	(Reeuwijk et al., 2013)[b]	○
Children's jewelry parts (necklaces, bracelets)	110	(Negev et al., 2018)[b]	●
Thermometer	150–3000 mg/piece	(LGL Bayern, 2012)[b]	●
Barometers	1000–3000 mg/piece	(LGL Bayern, 2012)[b]	●

wf = waste fraction.
○: contaminant carrier.
●: strong contaminant carrier.
●: very strong contaminant carrier.
[a] : reference value for mixed waste obtained or calculated from the same publication as the listed fraction.
[b] : median from Götze et al. (2016a) used as a reference.

3.8.2.2. Mercury in combustible fractions including plastics. The detailed evaluation of the sources reveals that, based on the principles defined in section 2, composites and plastics (ADEME (2010)), wood (Beker and Cornelissen, 1999; Eisted and Christensen, 2011; LfU Bayern, 2003; Liu and Liptak, 1999), vacuum cleaner bags and a mixed fraction of leather, cork, and rubber (LfU Bayern, 2003) as well as newspaper (Liu and Liptak, 1999) can be considered mercury carriers. Note, though, that all these materials except wood stand out only in single publications, and there is not enough information to name specific reasons. The elevated level of mercury observed in the organic fraction (Götze et al., 2016a) could also originate from these fractions because it is not known which materials were included in the organic fraction of individual publications. In general, mercury has formerly been used as a pigment and pesticide (Holleman et al., 2007). At low concentrations, however, contamination from other materials cannot be excluded. Such contaminations could originate from broken mercury-thermometers or fluorescent lamps (cf. section 3.8.2.5). In any case, the concentrations in all these fractions and the 0.75 percentile values listed by Götze et al. (2016a) are significantly lower than the concentrations in the main mercury carriers, i.e. batteries, and electronic devices.

3.8.2.3. Mercury in electronic devices and batteries. The highest values of mercury are reported for batteries (Astrup et al., 2011; Riber et al., 2009; Rotter, 2002; Rugg and Hanna, 1992), electronic devices (LfU Bayern, 2003) and the battery-containing fraction of problematic materials (Pomberger, 2008). Riber et al. (2009) state that batteries are expected to be the main source of mercury in waste. Batteries with high concentrations of mercury include alkali-manganese batteries, carbon zinc batteries (Liu and Liptak, 1999; Maystre and Viret, 1995) and coin-cell batteries (Astrup

et al., 2011). Regarding electronic devices, mercury is used in relays and switches. Furthermore, gas discharge lamps contain mercury (Chandrappa and Das, 2012).

3.8.2.4. Mercury in metal fractions. Apart from batteries, electronic devices, and single combustible fractions, the ferrous and non-ferrous metal fractions in Beker and Cornelissen (1999) have been identified as mercury carriers in the analyzed waste steam. Burnley (2007) suggests that metals are a key source of mercury. However, available information prevents any reliable conclusion on the exact origin of mercury in this fraction.. An example of metallic parts containing mercury is amalgam. Silver amalgam was used for dental fillings, and in the past mirrors have been coated with tin amalgam (Holleman et al., 2007).

3.8.2.5. Mercury in the fine fraction. Elevated mercury levels have been observed in the fine fraction (Beker and Cornelissen, 1999; LfU Bayern, 2003; Nasrullah et al., 2015; Viczek et al., 2019b). Vacuum cleaner bags (LfU Bayern, 2003), which usually contain fine material, have also been identified as a mercury carrier. Depending on the screen size, individual coin-cell batteries may in theory end up in the fine fraction. Also other mercury-containing devices such as broken mercury thermometers (LGL Bayern, 2012) might have caused elevated levels in single samples. Furthermore, fluorescent tubes or compact fluorescent lamps (energy saving bulbs) contain mercury which is released when the lamps break (Jang et al., 2005; LGL Bayern, 2012; Sperlich et al., 2014). According to the LfU Bayern (2003), elemental mercury is likely to attach to materials with a high specific surface area, causing the elevated levels of mercury detected in the fine fraction and in vacuum cleaner bags. However, similar to lead and cobalt, the data do not lend support to conclusions on the exact origins of mercury in the fine fraction because there is only limited information available.

Table 13
Selected nickel carriers, expected concentrations in products or waste fractions, comparison with mixed waste and classification.

Material or waste fraction	Ni [mg/kg$_{DM}$]	Literature source	Level of Ni carrier
Mixed waste	44.2	(Götze et al., 2016a), median	
Metals (wf)	147.3	(Götze et al., 2016a), 0.75-percentile	
Ferrous metals (wf)	180–10000	(Beker and Cornelissen, 1999; Otte, 1994; Rugg and Hanna, 1992)[a;a;a]	○ ●
Non-ferrous metals (wf)	56–15000	(Beker and Cornelissen, 1999; Otte, 1994; Pomberger, 2008; Rugg and Hanna, 1992)[a;a;b;a]	○ ●
Metal packaging ferrous (wf)	183–271	(Götze et al., 2016b)[b]	○ ●
Non-packaging ferrous (wf)	1810	(Götze et al., 2016b)[b]	●
Non-packaging non-ferrous (wf)	687	(Götze et al., 2016b)[b]	●
Al trays, foils	201	(Riber et al., 2009)[b]	○
Cr-Ni stainless steel (Nirosta)	80,000	(Holleman et al., 2007)[b]	●
Nickel steels	250000–360000	(Holleman et al., 2007)[b]	●
Other steels	10000–320000	(Cunat, 2004)[b]	●
Inert materials (wf)	67.7	(Götze et al., 2016a) 0.75-percentile	
Glass (wf)	11–313	(Beker and Cornelissen, 1999)[a]	○
Clear glass (wf)	143	(Riber et al., 2009)[b]	○
Green glass (wf)	162	(Riber et al., 2009)[b]	○
Brown glass (wf)	163	(Riber et al., 2009)[b]	○
Other glass (wf)	146.9	(Riber et al., 2009)[b]	○
Ceramics (wf)	322	(Riber et al., 2009)[b]	●
Composites (wf)	47.1	(Götze et al., 2016a) 0.75-percentile	
Office articles	476	(Riber et al., 2009)[b]	●
Other composites*	148.3	(LfU Bayern, 2003)[a]	○
Electronic devices/batteries (wf)			
Electronic materials	1543.8	(LfU Bayern, 2003)[b]	●
Circuit boards**	787–13103	(Janz, 2010)[b]	●
Electronic components	2057–85377	(Janz, 2010)[b]	●
NiCd batteries	30000–250000	(Rydh and Svärd, 2003; Saft, 2008a; SBS, 2015; Yuasa, 2015)[b;b;b;b]	●
NiMH batteries	250000–460000	(Johnson Controls, 2015; Rydh and Svärd, 2003; Saft, 2008b)[b;b;b]	●
Lithium-ion batteries	120000–150000	(Rydh and Svärd, 2003)[b]	●
Alkaline batteries	984–3730	(Komilis et al., 2011)[b]	●
ZiZinc-carbon batteries	22.2–672	(Komilis et al., 2011)[b]	○ ●
Other Ni-carriers			
Children's jewelry parts (necklaces, bracelets)	35,956	(Negev et al., 2018)[b]	●
Plastics with Ni-based pigments***	20–1200	(Ranta-Korpi et al., 2014)[b]	○ ●
PP, LDPE Ni-stabilized	100–500	(Ranta-Korpi et al., 2014)[b]	○ ●
Non-packaging plastics, no label (wf)	214	(Götze et al., 2016b)[b]	○
Plastic foils (wf)	200	(Pomberger, 2008)[b]	○
Wood (wf)	34.9–151.3	(Janz, 2010)[b]	○
Construction material: press boards without coating or paint	342–359	(Gras, 2002)[b]	●
For comparison: untreated wood	1.5–2.6	(Gras, 2002)[b]	–
Fine fraction (wf)	44–550	(ADEME (2010); Beker and Cornelissen, 1999; Nasrullah et al., 2015; Prochaska et al., 2005; Viczek et al., 2019b)[a;a;a;a;a]	○ ●

wf = waste fraction.
○: contaminant carrier.
●: strong contaminant carrier.
●: very strong contaminant carrier.
* composites other than electronic waste, packaging, vehicle parts, renovation waste, and vacuum cleaner bags.
** high Cd and Ni values can be explained by incomplete removal of NiCd batteries (Janz, 2010).
*** used for PVC, LDPE, HDPE, ABS, PA, PET, PP, PS, PU.
[a] : reference value for mixed waste obtained or calculated from the same publication as the listed fraction.
[b] : median from Götze et al. (2016a) used as a reference.

3.8.3. Summary: Mercury carriers

Electronic devices and batteries seem to be the most important mercury carriers in municipal solid waste. For many other fractions, the origin of mercury remains unclear and contaminations cannot be excluded. Potential mercury carriers in separate fractions are listed in Table 12 and expected mercury concentrations are given.

3.9. Nickel (Ni)

3.9.1. Nickel in waste fractions

The highest concentrations (0.75-percentiles) of nickel have been reported in metals (147.3 mg/kg DM), inert materials (67.7 mg/kg DM), and composites (47.1 mg/kg DM) by Götze et al. (2016a). A total of 19 datasets from 17 publications were used to identify the contaminant carriers more specifically. Table 13 lists the identified contaminant carriers and reported nickel concentrations.

3.9.2. Origins of nickel in waste fractions

3.9.2.1. Nickel in metals. High values of nickel are reported for both ferrous and non-ferrous metal fractions (Beker and Cornelissen, 1999; Otte, 1994; Rugg and Hanna, 1992), packaging and non-packaging metals (Götze et al., 2016b), ferrous food and beverage containers (Liu and Liptak, 1999), tin cans (Rugg and Hanna, 1992), and aluminum trays and foil (Riber et al., 2009). The major part of nickel is used in the metal industry where it is a prominent and common constituent of alloys. Nickel increases the corrosion resistance and the toughness of stainless steel and other alloys (Holleman et al., 2007).

3.9.2.2. Nickel in glass and ceramics. Elevated concentrations of Ni have been observed in different fractions of glass, including clear, green, brown, and other glass (Beker and Cornelissen, 1999; Riber et al., 2009), as well as in ceramics (Riber et al., 2009) and other non-combustibles (Eisted and Christensen, 2011; Riber et al., 2009). One reason may be the use of nickel compounds in intensifying the color and shade of pigments and in enhancing the look of glass and ceramics intended for food contact (Szynal et al., 2016).

3.9.2.3. Nickel in composites. High nickel values have been observed in office articles (Riber et al., 2009) and a fraction called 'other composites' (LfU Bayern, 2003) inclduding all composites except packaging, electronic materials, renovation waste, vacuum cleaner bags, and vehicle parts. The data available do not allow to determine the exact reasons for the observed levels of nickel in the composite fraction.

3.9.2.4. Nickel in batteries and electronic devices. High concentrations of nickel can be found in batteries, including zinc-carbon and alkaline batteries as well as NiCd batteries (Komilis et al., 2011; Liu and Liptak, 1999), electronic devices (LfU Bayern, 2003), circuit boards and electronic parts (Janz, 2010). Nickel and nickel compounds are used in Li-ion and nickel metal hydride (NiMH) batteries as well (Rydh and Svärd, 2003; Saft, 2008a, 2008b).

3.9.2.5. Nickel in plastics and other combustible fractions. Elevated levels of nickel have been reported in non-packaging unlabeled plastics (Götze et al., 2016b) and plastic foils (Pomberger, 2008). The plastics industry applies nickel compounds as a catalyst for the production of an important impact modifier for high impact polystyrene (HIPS) and acrylonitrile butadiene styrene (ABS). Due to a purification step, only small Ni-concentrations of less than 10 mg/kg are expected. Nickel compounds have also been used as stabilizers for polypropylene (PP) and low-density polyethylene (LDPE), resulting in Ni-concentrations of 100–500 mg/kg in the resin. The use of Ni for this purpose is declining but it is still used in combination with UV absorbers and in agricultural films. Furthermore, Ni-pigments are used to dye plastic resin in yellow, orange, or green shades. In this case, depending on the pigment, nickel concentrations of 20 to 1200 mg/kg are expected (Ranta-Korpi et al., 2014).

Besides plastics, elevated nickel concentrations were reported for wood (Janz, 2010), probably because nickel salts have been used to pickle and colorize wood (Gras, 2002).

3.9.2.6. Nickel in the fine fraction. Similar to cobalt, lead, and mercury, elevated concentrations of nickel have been observed in the fine fraction (ADEME (2010); Beker and Cornelissen, 1999; Nasrullah et al., 2015; Prochaska et al., 2005; Viczek et al., 2019b). Again, this could be explained by small metal parts or abraded metal present in this fraction, but there is not enough information to tell with certainty.

3.9.3. Summary: Nickel carriers

Batteries, electronic devices and parts, metals as well as glass and ceramics have been identified as nickel carriers. While combustible fractions and plastics play a more important role for the production of SRF, the origins of nickel in these fractions largely remain unclear. The identified nickel carriers and expected nickel concentrations are summarized in Table 13.

4. Implications for the removal of contaminant carriers

Depending on the kind of contaminant carrier or contaminant carrying fractions, different technologies can be used. These technologies include but are not limited to NIR (e.g. for PVC, PET, etc. (Pieber et al., 2012; Vrancken et al., 2017)) or XRF sorters (e.g. for heavy metal-containing plastic parts (Aldrian et al., 2015; Turner and Filella, 2017) or contaminated wood (Vrancken et al., 2017)), magnetic separators (ferrous metal parts), or screening (removal of certain grain size fractions). While some contaminant carriers may be easily removed using existing techniques, for others there may not be a suitable technique for their large-scale removal on the market yet. For example, contaminant carriers in the composite fraction are not only hard to determine, but probably even harder to remove from the waste stream. The same problem applies to batteries, which are often still located in devices, making their detection difficult.

In any case, when any of the contaminant carriers or contaminant-carrying fractions listed are removed, attention has to be paid to how this affects other parameters, e.g. the lower heating value or concentrations of other chemical elements in the waste stream. Especially in case of SRF with limit values given in mg/MJ_{DM}, a decrease in heating value may adversely affect the product quality.

In general, a decrease in LHV is observed when plastics such as PVC or PET, both of which are fractions of high calorific value, are removed (Kreindl, 2007; Pieber et al., 2012). Removing inert contaminant carriers, on the other hand, would result in a higher heating value. A theoretical increase in heating value was also calculated for a stream of coarsely shredded commercial waste when the fine fraction < 5 or < 10 mm is removed (Viczek et al., 2019b; Viczek et al., 2019a). While the concentration of As, Co, Cr, Hg, Ni, Pb, and several other elements in the remaining waste stream above 5 or 10 mm, respectively, was decreased, the concentration of Cd, Cl and Sb in mg/kg increased. When concentrations were calculated in mg/MJ, a lower concentration was observed for all reported elements except for chlorine, due to the raised

LHV (Viczek et al., 2019b). This implies that there are links between the different elements and parameters and that the effect of removing waste fractions on the parameter of interest has to be investigated for every waste stream or waste processing facility because the outcome strongly depends on the properties of every single waste stream (e.g. the amount of the contaminant carrier that needs to be removed). When removing certain fractions is feasible and performed, less emissions of the respective elements during incineration are expected as well. The contaminant-carrying waste fraction that is removed, however, has to be treated or recovered as well, but this should ideally be done in facilities that are specialized on the respective waste fractions, provided that suitable or specialized options are available.

5. Implications for chemical analyses

As always in analytical chemistry, sampling and the sample preparation procedure that is chosen will significantly affect the analysis results. With respect to the heterogeneous materials waste and solid recovered fuel (SRF) are composed of, and considering the contaminant carriers that were identified in chapter 3, two important influence factors need to be highlighted to allow for a more correct interpretation of analysis results: the selected digestion method and the exact sample preparation procedure.

5.1. Selection of digestion method

When waste samples, e.g. SRF, are analyzed with respect to metal concentrations, the digestion method chosen to convert the sample matrix into a solution, thereby making it suitable for ICP-MS or ICP-OES measurements, is essential and can significantly influence the obtained results. European standards such as EN 15411 (ASI, 2011a) or EN 13656 (ASI, 2002a) recommend acid digestion with hydrofluoric acid (HF), hydrochloric acid (HCl), and nitric acid (HNO_3) for SRF. Several laboratories, however, avoid the use of HF due to its hazard potential or do not possess the required equipment for working with HF, therefore performing a digest with aqua regia (HCl and HNO_3) (ASI, 2002b) to prepare the SRF samples for subsequent analyses. When this digestion method is used, metals incorporated in glasses or silicate phases are either only partially determined or not determined at all since the silicate matrix is not fully digested when these reagents are applied. This will most likely result in an underestimation of the concentrations of elements like As, Cr, or Co, if they are present in glass in the sample (see chapters 3.2.2.1, 3.5.2.3, and 3.6.2.4). Using a digestion method involving HF, the silicate matrix is degraded, and the metal ions are transferred into the digest solution where they can be determined.

5.2. Sample preparation (drying, comminution, homogenization, subsampling)

In general, the primary requirement for the analysis of waste samples is sample preparation, which strongly affects the analysis results. The aim of sample preparation is to make the samples accessible for analysis in the first place, since most analytical methods require a small amount of a pre-dried sample with a particle size < 1 mm (usually < 0.5 mm, occasionally even < 0.25 mm). For this reason, sample preparation includes drying, comminution (reduction of particle size), homogenization and sub-sampling (reduction of the sample mass). These steps can be carried out in different orders and can be repeated.

During all steps of sample preparation, the representativeness of the sample needs to be maintained, which means that even after sample preparation the sample needs to reflect all features of the sampled mass and shall not be altered during these steps (ASI, 2011b, 2011c).

Contaminations, e.g. by abrasions of the material the mill is made of, or evaporation of e.g. volatile components need to be prevented. Although the abrasion of mill material cannot be fully prevented and strongly depends on the hardness of the material that needs to be comminuted, the influence on the analysis results for waste materials is usually rather small.

To maintain the representativeness of the sample, in general it is required that every particle present in the sample before sample preparation must have the sample probability of ending up in the residual subsample after sample preparation (ASI, 2011c). However, some common laboratory procedures may counteract this rule will be shown in the following subchapters.

5.2.1. Removal of hard impurities

European standards EN 15443 (ASI, 2011c) and EN 15413 (ASI, 2011b) list the following aggregates for the comminution of SRF samples: coarse cutting mills or wood crushers, cutting mills and shredders for coarse comminution, and cutting mills for fine comminution. Unfortunately, these aggregates, especially the cutting mills for fine comminution, are not suitable for adequately comminuting all components present in a mixed solid waste or SRF sample. Based on experience, cutting mills can comminute the fractions of plastics, paper/cardboard, textiles, and wood very well. Also, small (<5 mm) metal parts (e.g. pieces of aluminum cans, copper wires) or inert materials (e.g. stones, glass) can be successfully comminuted by cutting mills. However, SRF samples frequently contain larger particles (>5 mm) of metal or inert materials. Such particles cannot be processed or comminuted with the aggregates intended for use by the standard because they may damage the screen insert of the mill. For this reason, such 'impurities' are removed from the sample during the sample preparation process. Environmental analysis provides two principal ways of dealing with these impurities:

a) They are removed and processed separately using another, suitable aggregate. Before analysis, all separately processed subsamples are reunited and homogenized. With this methodology, the representativeness of the sample is preserved.
b) The second possibility is to remove and weigh the impurities. Subsequently, only their weight is accounted for by correcting all analysis results based on the 'impurity content'. In this case, these impurities are assumed to be materials that do not affect the analysis results, which is true for parameters like the lower heating value (LHV) because metals and stones do not contribute to this parameter, only their mass is important. When concentrations of e.g. heavy metals are determined, this methodology distorts the results, because – as discussed in chapter 3 and subchapters - heavy metals can also occur in glass, stones, and metal parts of different kinds.

In the area of solid recovered fuels, usually, the second methodology is chosen. This is not a matter of convenience, but separately processing the impurities is often not a viable option. Metal parts can be milled to small particle sizes using vibratory disk mills, while glass or stones can be comminuted using ball mills, planetary ball mills, rotor impact mills, or cross beater mills (Retsch GmbH, 2019). These aggregates often cannot be used because the amounts of impurities are too small (e.g. only one single piece of metal), and many of these aggregates require a minimum filling quantity for proper operation. Moreover, such aggregates are not foreseen by the European standards EN 15443 (ASI, 2011b) and EN 15413 (ASI, 2011c). The procedure of removing impurities is

also considered in the Austrian Waste Incineration Ordinance (BMLFUW, 2010) that was introduced in chapter 1, which demands that the amount of impurities that is removed during sample preparation is documented.

5.2.2. Impact on analysis results

In the laboratory of the Chair of Waste Processing Technology and Waste Management at Montanuniversitaet Leoben, Austria, the content of "impurities" in SRF samples processed between January and July 2019 ranged from 0 to 7.3 mass-% (in single cases above 10%). In many cases, this mass share originated from only one piece of inert material or metal. Amounts of heavy metals in metal parts are significant, however, as was also shown by Aldrian et al. (2016) who determined the amount of Al, Fe, Cu, Zn, Cr, Co, Ni, As, Cd, Sn, Sb, Hg, and Pb in the metal parts present in 10 SRF samples. All visible metal parts were removed from the SRF samples by hand and processed separately before ICP-MS analysis. While the amount of metal impurities was 0.8 mass-% for premium quality SRF and 1.3 mass-% for medium quality SRF, 42% of the total Cr in premium quality SRF (medium quality: 32%), 25% of the total amount of Ni (medium quality: 46%), and 27% of Co (medium quality: 22%) were present in these metal parts.

Such results may justify asking, whether the sample preparation procedure applied in single laboratories working with SRF or waste affects the conclusions on the metal content of the sample and whether the true metal content can even be fully determined by means of routine analysis. Note as well that SRF is already the result of a production process, in the course of which metal parts and other heavy particles have already been removed. The effect of these sample preparation practices, therefore, is expected to be significantly higher for untreated waste samples.

In summary, this suggests that, depending on the procedure that was chosen, not all contaminant carriers are equally reflected by analysis results. Especially the element contents of metals, which have been identified as carriers of many of the examined elements in chapter 3, will probably not be fully accounted for, unless the metal parts are very small or present as abrasions. Determining the origin of certain contaminants needs the analytical procedures to be examined more intensively and beyond routine analysis, and analytical procedures that reflect the contribution of all contaminant carriers need to be applied.

6. Conclusion

Several potential contaminant carriers that might occur in MSW and commercial waste have been identified. With the origins of high concentrations of specific elements in single waste processing plants often remaining unknown, this paper may help develop practical experiments on characterizing and removing different waste fractions while monitoring the impact on output waste material quality. The information provided can be applied to various real waste streams and treatment options to assess or determine particular contaminant carriers that cause elevated levels of the element.

In the combustible fractions, several types of plastics have been identified as contaminant carriers because of the use of pigments or stabilizers. For this reason, future work could focus on colored plastics because they can be easily detected in the visible range of the spectrum and can subsequently be removed.

Although there are technologies available to remove many of the identified contaminant carriers, some might not be easily removed from the waste stream, e.g. due to a large heterogeneity within the group, a lack of available technologies, or because their relative amount in the waste stream is too large, or too small to make their removal economically justifiable. It also needs to be discussed whether elements present in specific contaminant carriers are captured and reflected by the laboratory analyses and therefore may even be the ones causing the elevated concentrations. To prevent a deterioration of the quality of the output material, in particular SRF quality, by removing a specific fraction, several contributing factors and correlations that have to be taken into account need to be investigated for individual waste streams. Even if contaminant carriers are identified, removing them may still remain a challenge to modern waste management.

Declaration of Competing Interest

The authors declare no conflict of interest.

Acknowledgments

The Center of Competence for Recycling and Recovery of Waste 4.0 (acronym ReWaste4.0) (contract number 860 884) under the scope of the COMET – Competence Centers for Excellent Technologies – financially supported by BMVIT, BMDW, and the federal state of Styria, managed by the FFG.

References

ADEME (Agence de l'Environnement et de la Maîtrise de l'Energie), 2010. La composition des ordures ménagères et assimilées en France. French Environmental Protection Agency. ADEME, Angers.

Aldrian, A., Eggenbauer, P., Sarc, R., Pomberger, R., 2016. Metallisch vorliegender Anteil des Gesamtmetallgehalts für verschiedene Elemente in Ersatzbrennstoffen, in: Pomberger, R. et al. (Eds.), Recy & DepoTech 2016. Conference Proceedings of the 13th Recy & DepoTech-Conference (8th to 11th November 2016, Leoben, Austria), pp. 769–772.

Aldrian, A., Ledersteger, A., Pomberger, R., 2015. Monitoring of WEEE plastics in regards to brominated flame retardants using handheld XRF. Waste Manage. 36, 297–304. https://doi.org/10.1016/j.wasman.2014.10.025.

Anderson, C.G., 2012. The metallurgy of antimony. Chem. Erde 72, 3–8. https://doi.org/10.1016/j.chemer.2012.04.001.

Ansmann, 2011. Material Safety Data Sheet (MSDS) for Ansmann Lithium-Ion Batteries, single cells and multi-cell battery packs.

Archer, A.R., Elmore, A.C., Bell, E., Rozycki, C., 2011. Field investigation of arsenic in ceramic pot filter-treated drinking water. Water Sci. Technol.: J. Int. Assoc. Water Pollut. Res. 63, 2193–2198.

ASI (Austrian Standards Institute), 2002a. Characterization of waste – Digestion for subsequent determination of aqua regia soluble portion of elements, Vienna.

ASI (Austrian Standards Institute), 2002b. Characterization of waste – Microwave assisted digestion with hydrofluoric (HF), nitric (HNO3) and hydrochloric (HCl) acid mixture for subsequent determination of elements, Vienna.

ASI (Austrian Standards Institute), 2011a. Solid recovered fuels – Methods for the determination of the content of trace elements (As, Ba, Be, Cd, Co, Cr, Cu, Hg, Mo, Mn, Ni, Pb, Sb, Se, Tl, V and Zn), Vienna.

ASI (Austrian Standards Institute), 2011b. Solid recovered fuels – Methods for the preparation of the laboratory sample, Vienna.

ASI (Austrian Standards Institute), 2011c. Solid recovered fuels – Methods for the preparation of the test sample from the laboratory sample, Vienna.

Aspland, J.R., 1993. Pigments as textile colorants: Pigmenting or pigmentation. Text. Chem. Color. 10, 31–37.

Astrup, T., Riber, C., Pedersen, A.J., 2011. Incinerator performance: effects of changes in waste input and furnace operation on air emissions and residues. Waste Manage. Res.: J. Int. Solid Wastes Public Clean. Assoc., ISWA 29, 57–68. https://doi.org/10.1177/0734242X11419893.

Atkarskaya, A.B., Bykov, V.N., 2003. Clarification of glass using arsenic and antimony oxides. Glass Ceram. 60, 389–391.

Balshaw, S., Edwards, J., Daughtry, B., Ross, K., 2007. Mercury in seafood: Mechanisms of accumulation and consequences for consumer health. Rev. Environ. Health 22, 37. https://doi.org/10.1515/REVEH.2007.22.2.91.

Bally, A., 2003. Altreifenentsorgung: Was ist ökologisch sinnvoll?. BiCon AG.

Batista, B.L., Rodrigues, J.L., de Souza, S.S., Oliveira Souza, V.C., Barbosa, F., 2011. Mercury speciation in seafood samples by LC-ICP-MS with a rapid ultrasound-assisted extraction procedure: Application to the determination of mercury in Brazilian seafood samples. Food Chem. 126, 2000–2004. https://doi.org/10.1016/j.foodchem.2010.12.068.

Beckmann, M., Scholz, R., Horeni, M., 2006. Energetische Verwertung von Ersatzbrennstoffen mit hohem Chlorgehalt, in: Wiemer, K. (Ed.), Bio- und Sekundärrohstoffverwertung. Stofflich, energetisch, 1st ed. Witzenhausen-Inst. für Abfall Umwelt und Energie, Witzenhausen.

Beker, D., Cornelissen, A.A.J., 1999. Chemische analyse van huishoudelijk restafval: Resultaten 1994 en 1995. Rijksinstituut voor Volksgezondheid en Milieu (RIVM), Rapport-nummer 776221002.

Belarra, M.A., Belategui, I., Lavilla, I., Anzano, J.M., Castillo, J.R., 1998. Screening of antimony in PVC by solid sampling-graphite furnace atomic absorption spectrometry. Talanta 46, 1265–1272. https://doi.org/10.1016/S0039-9140(97)00390-1.

BMLFUW (Bundesministerium für Land- und Forstwirtschaft, Umwelt und Wasserwirtschaft), 2008. Verordnung über die Abfallvermeidung, Sammlung und Behandlung von Altbatterien und -akkumulatoren (Batterienverordnung). Austrian Federal Ministry for the Environment, BGBl. II Nr. 159/2008, Wien.

BMLFUW (Bundesministerium für Land- und Forstwirtschaft, Umwelt und Wasserwirtschaft), 2010. Verordnung über die Verbrennung von Abfällen (Abfallverbrennungsverordnung - AVV). Austrian Federal Ministry for the Environment, BGBl. II Nr. 476/2010, Wien.

Bode, P., de Bruin, M., Aalbers, T.G., Meyer, P.J., 1990. Plastics from Household Waste as a Source of Heavy Metal Pollution. In: Zeisler, R., Guinn, V.P. (Eds.), Nuclear analytical methods in the life sciences. Springer Science+Business Media, New York, pp. 377–383.

Bohrer, D., Becker, E., Nascimento, P.C., Mörschbächer, V., Machado de Carvalho, L., da Silva Marques, M., 2006. Arsenic release from glass containers by action of intravenous nutrition formulation constituents. Int. J. Pharm. 315, 24–29. https://doi.org/10.1016/j.ijpharm.2006.02.008.

Brandão, J., Moyo, M., Okonkwo, J., 2014. Determination of antimony in bottled water and polyethylene terephthalate bottles: a routine laboratory quality check. Water Sci. Technol. Water Supply 14, 181–188. https://doi.org/10.2166/ws.2013.187.

Burnley, S.J., 2007. The use of chemical composition data in waste management planning - a case study. Waste Manage. 27, 327–336. https://doi.org/10.1016/j.wasman.2005.12.020.

BUWAL (Bundesamt für Umwelt, Wald und Landwirtschaft), 1996. Verbrennen von Abfällen, Alt- oder Restholz in Holzfeuerungen und im Freien. Swiss Federal Office for the Environment.

Campbell, F.C., 2008. Elements of metallurgy and engineering alloys. ASM Int.

Chandrappa, R., Das, D.B., 2012. Solid Waste Management: Principles and Practice. Springer, Berlin, Heidelberg.

Choi, K.-I., Lee, S.-H., Lee, D.-H., Osako, M., 2008. Fundamental characteristics of input waste of small MSW incinerators in Korea. Waste Manage. 28, 2293–2300. https://doi.org/10.1016/j.wasman.2007.10.008.

Colin, J., 2017. How battery life cycle influences the collection rate of battery collection schemes. IBCR 2017, 20 September 2017, Lisbon, Portugal.

Conrad Electronics SE, 2014. Material Safety Data Sheet - primary zinc/air button cell (size ZA13/PR48). http://www.produktinfo.conrad.com/datenblaetter/650000-674999/650496-si-01-en-HOERGERAETEBATTERIEN_ZINK_LUFT_ZA13__6ER.pdf.

Cunat, P.-J., 2004. Alloying elements in stainless steel and other chromium-containing alloys. ICDA, Paris.

Danish EPA (Danish Environmental Protection Agency), 2003. Survey of chemical substances in consumer products: Survey of the content of certain chemical substances in mattress pads.

Danish EPA (Danish Environmental Protection Agency), 2015. Substitution of cobalt in wood protection products.

Das, H.K., Mitra, A.K., Sengupta, P.K., Hossain, A., Islam, F., Rabbani, G.H., 2004. Arsenic concentrations in rice, vegetables, and fish in Bangladesh: a preliminary study. Environ. Int. 30, 383–387. https://doi.org/10.1016/j.envint.2003.09.005.

David, R., 2014. Materialanalyse und Verwertungsmöglichkeiten einer aus der Ersatzbrennstoff-Produktion ausgeschleusten Polyvinylchlorid-Fraktion. Masterarbeit.

Dick, J.S., Rader, C.P., 2014. Raw Materials Supply Chain for Rubber Products. Carl Hanser Verlag, München.

Dixit, S., Yadav, A., Dwivedi, P.D., Das, M., 2015. Toxic hazards of leather industry and technologies to combat threat: a review. J. Cleaner Prod. 87, 39–49. https://doi.org/10.1016/j.jclepro.2014.10.017.

Dupont, D., Arnout, S., Jones, P.T., Binnemans, K., 2016. Antimony recovery from end-of-life products and industrial process residues: a critical review. J. Sustain. Metall. 2, 79–103. https://doi.org/10.1007/s40831-016-0043-y.

EC (European Commission), 2003. Directive 2002/95/EC of the European Parliament and of the Council of 27 January 2003 on the restriction of the use of certain hazardous substances in electrical and electronic equipment.

EC (European Commission), 2006a. Annex XVII to Regulation No 1907/2006, entry 16.

EC (European Commission), 2006b. Commission directive 2006/139/EC of 20 December 2006 amending Council Directive 76/769/EEC as regards restrictions on the marketing and use of arsenic compounds for the purpose of adapting its Annex I to technical progress.

EC (European Commission), 2010. Directive 2010/75/EU of the European Parliament and of the Council of 24 November 2010 on industrial emissions (integrated pollution prevention and control).

EC (European Commission), 2011a. Commission Regulation (EU) No 494/2011 of 20 May 2011 amending Regulation (EC) No 1907/2006 of the European Parliament and of the Council on the Registration, Evaluation, Authorisation and Restriction of Chemicals (REACH) as regards Annex XVII (Cadmium).

EC (European Commission), 2011b. Directive 2011/65/EU of the European Parliamant and of the Council of 8 June 2011 on the restriction of the use of certain hazardous substances in electrical and electronic equipmen (recast).

EC (European Commission), 2014. Commission Regulation (EU) No 301/2014 of 25 March 2014 amending Annex XVII to Regulation (EC) No 1907/2006 of the European Parliament and of the Council on the Registration, Evaluation, Authorisation and Restriction of Chemicals (REACH) as regards chromium VI compounds.

Eisted, R., Christensen, T.H., 2011. Characterization of household waste in Greenland. Waste Manage. 31, 1461–1466. https://doi.org/10.1016/j.wasman.2011.02.018.

Entel, 2016. Battery Material Safety Data Sheet: Product CNB451E, CNB550E and CNB950E.

Ferrari, G., Gregorio, P., Sammito, R., 2000. La valutazione delle caratteristiche dei rifiuti per una gestione dei rifiuti ambientalmente compatibile, in: . 39° Congr. Naz. SItI "La Promozione della salute nel Terzo Millennio". SItI.

Franklin Associates, L., 1989. Characterization of products containing lead and cadmium in municipal solid waste in the United States, 1970 - 2000.

Gazulla, M.F., Gómez, M.P., Barba, A., Orduña, M., 2007. Chemical and phase characterisation of ceramic pigments. X-Ray Spectrom. 36, 82–91. https://doi.org/10.1002/xrs.943.

Genon, G., Brizio, E., 2008. Perspectives and limits for cement kilns as a destination for RDF. Waste Manage. 28, 2375–2385. https://doi.org/10.1016/j.wasman.2007.10.022.

Götze, R., Boldrin, A., Scheutz, C., Astrup, T.F., 2016a. Physico-chemical characterisation of material fractions in household waste: Overview of data in literature. Waste Manage. 49, 3–14. https://doi.org/10.1016/j.wasman.2016.01.008.

Götze, R., Pivnenko, K., Boldrin, A., Scheutz, C., Astrup, T.F., 2016b. Physico-chemical characterisation of material fractions in residual and source-segregated household waste in Denmark. Waste Manage. 54, 13–26. https://doi.org/10.1016/j.wasman.2016.05.009.

Gras, B., 2002. Schadstoffe in Altholz.

Harrison, N., 2005. Inorganic contaminants in food, in: Watson, D.H. (Ed.), Food chemical safety. CRC Press, Boca Raton, pp. 148–168.

Hasanuzzaman, M., Rafferty, A., Sajjia, M., Olabi, A.-G., 2016. Properties of Glass Materials. In: Hashmi, S. (Ed.), Reference Module in Materials Science and Materials Engineering. Elsevier, Amsterdam.

Hassan, M.M., 2018. Arsenic in Groundwater: Poisoning and Risk. Assessment. CRC Press.

Hjortenkrans, D.S.T., Bergbäck, B.G., Häggerud, A.V., 2007. Metal Emissions from Brake Linings and Tires: Case Studies of Stockholm, Sweden 1995/1998 and 2005. Environ. Sci. Technol. 41, 5224–5230. https://doi.org/10.1021/es070198o.

Hoffmann, G., Schirmer, M., Bilitewski, B., 2006. Chlorstudie - Untersuchungen zu Hauptchlorträgern in verschiedenen Abfallströmen.

Holleman, A.F., Wiberg, E., Wiberg, N., 2007. Lehrbuch der anorganischen Chemie. de Gruyter, Berlin.

Hopfmann, T., Kuhn, K.-J., Kaufhold, J., Schiller, M., 2016. PVC Stabilisatoren. In: Maier, R.-.D., Schiller, M. (Eds.), Handbuch Kunststoff-Additive. 4th ed. Carl Hanser Verlag, München, pp. 469–547.

IARC (IARC Working Group on the Evaluation of Carcinogenic Risk to humans), 2012. Arsenic and arsenic compounds. International Agency for Research on Cancer.

International Cadmium Association, 2018. Cadmium Pigments. https://www.cadmium.org/cadmium-applications/cadmium-pigments. Accessed 30 July 2018.

International Cadmium Association, 2019. Cadmium coatings. https://www.cadmium.org/cadmium-applications/cadmium-coatings. Accessed 29 March 2019.

ISSF (International Stainless Steel Forum), 2019. The Stainless Steel Family. http://www.worldstainless.org/Files/issf/non-image-files/PDF/TheStainlessSteelFamily.pdf. Accessed 7 April 2019.

Jandke, J., Reinicker, R.A., 2016. Farbmittel. In: Maier, R.-.D., Schiller, M. (Eds.), Handbuch Kunststoff-Additive. 4th ed. Carl Hanser Verlag, München.

Jang, M., Hong, S.M., Park, J.K., 2005. Characterization and recovery of mercury from spent fluorescent lamps. Waste Manage. 25, 5–14. https://doi.org/10.1016/j.wasman.2004.09.008.

Janz, A., 2010. Schwermetalle aus Elektroaltgeräten und Batterien im kommunalen Restabfall. Potenziale, Mobilisierung und Freisetzung während der Deponierung. Dissertation. Forum für Abfallwirtschaft und Altlasten e.V, Pirna.

Johnson Controls, 2015. Safety Data Sheet Nickel-Metal Hydride Battery: Version 2, Issue date 04/01/2015, Revision Date 12/07/2015.

Kennedy, P., Gadd, J., 2000. Preliminary Examination of Trace elements in Tyres. Brake Pads and Road Bitumen in New Zealand. https://wwwtransport.govt.nz/assets/Import/Documents/stormwater-inorganic3.pdf.

Kikuchi, R., Kukacka, J., Raschman, R., 2008. Grouping of mixed waste plastics according to chlorine content. Sep. Purif. Technol. 61, 75–81. https://doi.org/10.1016/j.seppur.2007.10.001.

Kiyataka, P.H.M., Dantas, S.T., Albino, A.C., Pallone, J.A.L., 2018. Antimony assessment in PET bottles for soft drink. Food Anal. Methods 11, 1–9. https://doi.org/10.1007/s12161-017-0951-x.

Komilis, D., Bandi, D., Kakaronis, G., Zouppouris, G., 2011. The influence of spent household batteries to the organic fraction of municipal solid wastes during composting. Sci. Total Environ. 409, 2555–2566. https://doi.org/10.1016/j.scitotenv.2011.02.044.

Kost, T., 2001. Brennstofftechnische Charakterisierung von Haushaltsabfällen. Dissertation. Forum für Abfallwirtschaft und Altlasten e.V, Pirna, p. 61.

Kreindl, G., 2007. Schwermetallherkunft in den Inputfraktionen einer Alternativbrennstoffverwertungsanlage. Diplomarbeit.

Larrañaga, M.D., Lewis, R.J., Lewis, R.A., 2016. Hawley's Condensed Chemical Dictionary. Wiley.

LfU Bayern (Bayerisches Landesamt für Umweltschutz), 2003. Zusammensetzung und Schadstoffgehalt von Siedlungsabfällen: Abschlussbericht. Bavarian Authority for Environmental Protection (Germany).
LGL Bayern (Bayerisches Landesamt für Gesundheit und Lebensmittelsicherheit), 2012. Arbeit, Umwelt und Gesundheit aktuell: Quecksilber aus Energiesparlampen. https://www.bestellen.bayern.de/application/eshop_app000004?SID=578279100&ACTIONxSESSxSHOWPIC(BILDxKEY:%27lgl_arbuges_00005%27,BILDxCLASS:%27Artikel%27,BILDxTYPE:%27PDF%27). Accessed 9 July 2019.
Liu, D.H.F., Liptak, B.G., 1999. Hazardous Waste and Solid Waste. Taylor & Francis.
Llusar, M., Forés, A., Badenes, J.A., Calbo, J., Tena, M.A., Monrós, G., 2001. Colour analysis of some cobalt-based blue pigments. J. Eur. Ceram. Soc. 21, 1121–1130. https://doi.org/10.1016/S0955-2219(00)00295-8.
Lorber, K.E., Sarc, R., Aldrian, A., 2012. Design and quality assurance for solid recovered fuel. Waste Manage. Res. 30, 370–380. https://doi.org/10.1177/0734242X12440484.
Lorber, K.E., Sarc, R., Pomberger, R., 2011. Österreichische Erfahrungen zum Einsatz verschiedener Abfälle als Ersatzbrennstoffe (EBS) und mögliche Anwendungsprobleme. I. Wissenschaftskongress Abfall-und Ressourcenwirtschaft, Österreich.
Ma, W., Hoffmann, G., Schirmer, M., Chen, G., Rotter, V.S., 2010. Chlorine characterization and thermal behavior in MSW and RDF. J. Hazard. Mater. 178, 489–498. https://doi.org/10.1016/j.jhazmat.2010.01.108.
Ma, W., Rotter, S., Hoffmann, G., Lehmann, A., 2008. Origins of chlorine in MSW and RDF: Species and analytical methods, in: Waste management 2008, Granada, Spain. 02.06.2008 - 04.06.2008. WIT Press Southampton, UK, pp. 551–558.
Mahapatra, N.N., 2016. Textile Dyes. Woodhead Publishing India Pvt. Ltd., Neu Dehli.
Månsson, N.S., Hjortenkrans, D.S.T., Bergbäck, B.G., Sörme, L., Häggerud, A.V., 2009. Sources of antimony in an urban area. Environ. Chem. 6, 160. https://doi.org/10.1071/EN08078.
Matlack, A., 2010. Introduction to Green Chemistry. Taylor & Francis, Boca Raton.
Maystre, L.Y., Viret, F., 1995. A goal-oriented characterization of urban waste. Waste Manage. Res. 13, 207–218. https://doi.org/10.1177/0734242X9501300303.
Morf, L.S., Taverna, R., 2006. Ermittlung von Quellen der Schwermetalle in Restmüll. Projekt MOVE Endbericht.
Nachman, K.E., Baron, P.A., Raber, G., Francesconi, K.A., Navas-Acien, A., Love, D.C., 2013. Roxarsone, inorganic arsenic, and other arsenic species in chicken: A U.S.-based market basket sample. Environ. Health Perspect. 121, 818–824. https://doi.org/10.1289/ehp.1206245.
Nakamura, K., Kinoshita, S., Takatsuki, H., 1996. The origin and behavior of lead, cadmium and antimony in MSW incinerator. Waste Manage. 16, 509–517. https://doi.org/10.1016/S0956-053X(96)00093-1.
Nasrullah, M., Vainikka, P., Hannula, J., Hurme, M., 2015. Elemental balance of SRF production process: solid recovered fuel produced from commercial and industrial waste. Fuel 145, 1–11. https://doi.org/10.1016/j.fuel.2014.12.071.
Nasrullah, M., Vainikka, P., Hannula, J., Hurme, M., Oinas, P., 2016. Elemental balance of SRF production process: solid recovered fuel produced from municipal solid waste. Waste Manage. Res. 34, 38–46. https://doi.org/10.1177/0734242X15615697.
Negev, M., Berman, T., Reicher, S., Sadeh, M., Ardi, R., Shammai, Y., 2018. Concentrations of trace metals, phthalates, bisphenol A and flame-retardants in toys and other children's products in Israel. Chemosphere 192, 217–224. https://doi.org/10.1016/j.chemosphere.2017.10.132.
NRC (National Research Council), 1977. Arsenic. National Academy of Sciences.
Österlund, H., Rodushkin, I., Ylinenjärvi, K., Baxter, D.C., 2009. Determination of total chlorine and bromine in solid wastes by sintering and inductively coupled plasma-sector field mass spectrometry. Waste Manage. 29, 1258–1264. https://doi.org/10.1016/j.wasman.2008.07.017.
Otte, P.F., 1994. Analyse van metalen en calorische waarde in componenten uit huishoudelijk afval 1988-1992.Rijksinstituut voor Volksgezondheid en Milieu (RIVM), Rapport-nummer 776201012.
Patrick, S.G., 2005. Practical Guide to Polyvinyl Chloride. Rapra Technology.
Penque, A., 2007. Examination of Chlorides in Municipal Solid Waste to Energy Combustion Residue: Origins, Fate and. Potential for Treatment.
Pfaff, G., 2017. Inorganic Pigments. de Gruyter.
Pieber, S., Ragossnig, A., Pomberger, R., Curtis, A., 2012. Biogenic carbon-enriched and pollutant depleted SRF from commercial and pretreated heterogeneous waste generated by NIR sensor-based sorting. Waste Manage. Res. 30, 381–391. https://doi.org/10.1177/0734242X12437567.
Pollak, M., Favoino, E., 2004. Heavy metals and organic compounds from wastes used as organic fertilizers: Annex 2 - Compost quality definition - legislation and standards.
Pomberger, R., 2008. Entwicklung von Ersatzbrennstoff für das HOTDISC-Verfahren und Analyse der abfallwirtschaftlichen Relevanz. Dissertation.
Pomberger, R., Sarc, R., 2014. Use of Solid Recovered Fuels in the Cement Industry. In: Thomé-Kozmiensky, K.J., Thiel, S. (Eds.), Waste management. TK-Verl, Thomé-Kozmiensky, Neuruppin, pp. 417–488.
Prochaska, M., Raber, G., Lorber, K.E., 2005. Herstellung von Ersatzbrennstoffen. Projekt-Endbericht.
Raju, G., Sarkar, P., Singla, E., Singh, H., Sharma, R.K., 2016. Comparison of environmental sustainability of pharmaceutical packaging. Perspect. Sci. 8, 683–685. https://doi.org/10.1016/j.pisc.2016.06.058.
Ranta-Korpi, M., Vainikka, P., Konttinen, J., Saarimaa, A., Rodriguez, M., 2014. Ash forming elements in plastics and rubbers. VTT Public. Series, 186.
Ratnaike, R.N., 2003. Acute and chronic arsenic toxicity. Postgrad. Med. J. 79, 391–396. https://doi.org/10.1136/pmj.79.933.391.
Recknagel, S., Richter, A., Richter, S., 2009. Investigation on the heavy metal content of zinc-carbon and alkaline manganese dry cells. Waste Manage. 29, 1213–1217. https://doi.org/10.1016/j.wasman.2008.06.042.
Reeuwijk, N.M., Klerx, W.N.M., Kooijman, M., Hoogenboom, L.A.P., Rietjens, I.M.C.M., Martena, M.J., 2013. Levels of lead, arsenic, mercury and cadmium in clays for oral use on the Dutch market and estimation of associated risks. Food additives & contaminants. Part A, Chemistry, analysis, control, exposure & risk assessment 30, 1535–1545. https://doi.org/10.1080/19440049.2013.811297.
Restrepo, E., Widmer, R., Schluep, M., 2016. A critical review of recycling and disposal options for leaded glass from cathode ray tubes (CRTs), in: 2016 Electronics Goes Green 2016+ (EGG). Electronics Goes Green 2016+ (EGG), Berlin. 6/9/2016 - 9/9/2016. IEEE, pp. 1–7.
Retsch GmbH, 2019. Official website – Laboratory mills, grinders & crushers. https://www.retsch.com/products/milling/. Accessed 2 July 2019.
Riber, C., Petersen, C., Christensen, T.H., 2009. Chemical composition of material fractions in Danish household waste. Waste Manage. 29, 1251–1257. https://doi.org/10.1016/j.wasman.2008.09.013.
Rizza, C.S., 2011. Analisi e ottimizzazione di un inceneritore di rifiuti. Master's Thesis.
Rohr, U., Meckel, L., 1992. Determination of arsenic in glass and raw materials for glass via quartz-tube hydride generation AAS after separation by solvent extraction. Fresenius' J. Anal. Chem. 342, 370–375. https://doi.org/10.1007/BF00322188.
Rotter, S., 2002. Schwermetalle in Haushaltsabfällen. Potenzial, Verteilung und Steuerungsmöglichkeiten durch Aufbereitung. Dissertation. Forum für Abfallwirtschaft und Altlasten e.V, Pirna.
Rugg, M., Hanna, N.K., 1992. Metals concentrations in compostable and noncompostable components of municipal solid waste in cape may county, new jersey. Second United States Conference on Municipal Solid Waste Management, 2 June 1992, Arlington, Virginia.
Rydh, C.J., Svärd, B., 2003. Impact on global metal flows arising from the use of portable rechargeable batteries. Sci. Total Environ. 302, 167–184. https://doi.org/10.1016/S0048-9697(02)00293-0.
Rydin, S., 2002. Survey of Chemical Substances in Consumer Products: Investigation of the Content of Cr(VI) and Cr(III) in Leather Products on the Danish Market.
Saft, 2008a. Safety Data Sheet Secondary Nickel-Cadmium Sealed Cells.
Saft, 2008b. Safety Data Sheet Secondary Nickel-Metal Hydride Sealed Cells.
Sarc, R., Lorber, K.E., Pomberger, R., Rogetzer, M., Sipple, E.M., 2014. Design, quality, and quality assurance of solid recovered fuels for the substitution of fossil feedstock in the cement industry. Waste Manage. Res. 32, 565–585. https://doi.org/10.1177/0734242X14536462.
Sarc, R., Seidler, I.M., Kandlbauer, L., Lorber, K.E., Pomberger, R., 2019. Design, quality and quality assurance of solid recovered fuels for the substitution of fossil feedstock in the cement industry – update 2019. Waste Manage. Res. 37, 885–897. https://doi.org/10.1177/0734242X19862600.
Saveyn, H., Eder, P., 2014. End-of-waste criteria for biodegradable waste subjected to biological treatment (compost & digestate): Technical proposals.
SBS (Storage Battery Systems LLC.), 2015. Safety Data Sheet Nickel Cadmium Batteries.
Schäfer, B., 2013. Antimon-Freisetzung aus Polyethylenterephthalat-(PET-)haltigen Textilien, in: Bundesamt für Verbraucherschutz und Lebensmittelsicherheit (Ed.), Berichte zur Lebensmittelsicherheit 2011. Springer, Basel, pp. 41–43.
Schmidt, M., 2013. Rohstoffrisikobewertung - Antimon. DERA Rohstoffinformationen 18.
Schrägle, R., 2010. Kaskadennutzung kann an Grenzwerten scheitern. Holz-Zentralblatt 10.12.2010, 1250–1251.
Schrägle, R., 2015. Schadstoffe in Spanplatten. Holz-Zentralblatt 16.01.2015, 56–57.
Schweitzer, P.A., 2009. Fundamentals of Corrosion: Mechanisms, Causes, and Preventative Methods. CRC Press.
Sharma, S.K., 2014. Heavy Metals In Water: Presence. Royal Society of Chemistry, Removal and Safety.
Shotyk, W., Krachler, M., Chen, B., 2006. Contamination of Canadian and European bottled waters with antimony from PET containers. J. Environ. Monit. 8, 288–292. https://doi.org/10.1039/B517844B.
Snedeker, S.M., 2014. Toxicants in Food Packaging and Household Plastics: Exposure and Health Risks to Consumers. Springer, London.
Sperlich, K., Oehme, I., Kraus, K., Süring, K., Gleis, M., Butz, W., Schnee, E., Lehmann, C., Friedrich, B., Krüger, F., Mordziol, C., 2014. Quecksilber in Umwelt und Produkten - Schwerpunkt Lampen. http://www.umweltbundesamt.de/publikationen/quecksilber-in-umwelt-produkten-schwerpunkt-lampen. Accessed 9 July 2019.
Szynal, T., Rebeniak, M., Mania, M., 2016. Migration studies of nickel and chromium from ceramic and glass tableware into food simulants. Rocz. Panstw. Zakl. Hig. 67, 247–252.
Taylor, C., 2000. The Kingfisher. Science Encyclopedia, Kingfisher.
Taylor, V., Goodale, B., Raab, A., Schwerdtle, T., Reimer, K., Conklin, S., Karagas, M.R., Francesconi, K.A., 2017. Human exposure to organic arsenic species from seafood. Sci. Total Environ. 580, 266–282. https://doi.org/10.1016/j.scitotenv.2016.12.113.
Tercero Espinoza, L., Hummen, T., Brunot, A., Hovestad, A., Garay, I.P., Velte, D., Smuk, J., Todorovic, J., van der Ejik, C., Joce, C., 2015. CRM InnoNet Report: Critical Raw Materials Substitution Profiles - Revised May 2015. Karlsruhe, Germany.

The Waste & Resources Action Programme, 2004. Materials recovery from waste cathode ray tubes (CRTs). R&D Report: Glass.
Thiele, U.K., 2004. RAW MATERIALS - Quo vadis polyester catalyst? Chem. Fibers Int. 54, 162–163.
Thyssen, J.P., Strandesen, M., Poulsen, P.B., Menné, T., Johansen, J.D., 2012. Chromium in leather footwear - risk assessment of chromium allergy and dermatitis. Contact Dermatitis 66, 279–285. https://doi.org/10.1111/j.1600-0536.2011.02053.x.
Troitzsch, J., 2016. Flammschutzmittel. In: Maier, R.-.D., Schiller, M. (Eds.), Handbuch Kunststoff-Additive. 4th ed. Carl Hanser Verlag, München, pp. 1015–1068.
Turner, A., 2019. Cadmium pigments in consumer products and their health risks. Sci. Total Environ. 657, 1409–1418. https://doi.org/10.1016/j.scitotenv.2018.12.096.
Turner, A., Filella, M., 2017. Field-portable-XRF reveals the ubiquity of antimony in plastic consumer products. Sci. Total Environ. 584–585, 982–989. https://doi.org/10.1016/j.scitotenv.2017.01.149.
U.S. Department of health and human services, 2007. Toxicological profile for arsenic.
United states antimony corporation, 2017. Uses and Formulations. http://usantimony.com/uses_formulations.htm. Accessed 25 July 2018.
US EPA (United States Environmental Protection Agency), 2019. Initial List of Hazardous Air Pollutants with Modifications. https://www.epa.gov/haps/initial-list-hazardous-air-pollutants-modifications. Accessed 4 October 2019.
Valadez-Vega, C., Zúñiga-Pérez, C., Quintanar-Gómez, S., Morales-González, J.A., Madrigal-Santillán, E., Villagómez-Ibarra, J.R., Sumaya-Martínez, M.T., García-Paredes, J.D., 2011. Lead, cadmium and cobalt (Pb, Cd, and Co) leaching of glass-clay containers by pH effect of food. Int. J. Mol. Sci. 12, 2336–2350. https://doi.org/10.3390/ijms12042336.
Varta, 2018a. Safety Data Sheet MSDS 2.001.003. Primary Alkaline Cylindrical.
Varta, 2018b. Safety Data Sheet MSDS 2.001.022, Primary zinc/silver oxide button cell, mercury free (series V... MF).
Večeřa, J., Čech, J., Mikulášek, P., Šulcová, P., 2013. The study of rutile pigments Ti1−3xCrxM2xO2. Cent. Eur. J. Chem. 11, 1447–1455. https://doi.org/10.2478/s11532-013-0287-3.
Viczek, S.A., Khodier, K., Aldrian, A., Pomberger, R., Sarc, R., 2019a. Grain size dependent distribution of contaminants in coarse-shredded commercial waste–results for As, Ba, Cd, Co, Cr, Cu,Hg, Mn, Mo, Ni, Pb, and Sb. Proceedings of the Heraklion 2019 7th International Confrerence on Sustainable Solid Waste Management, 26 - 29 June 2019. http://uest.ntua.gr/heraklion2019/proceedings/pdf/HERAKLION2019_Viczek2_etal.pdf. Accessed 3 October 2019.
Viczek, S.A., Khodier, K., Pomberger, R., Sarc, R., 2019b. Grain size dependent distribution of As, Cd, Cl, Co, cr, Fe, Hg, Ni, Pb, Sb, Sn, Ti, V, W, and Zn in coarse-shredded commercial waste. Proceedings of the 17th international waste management and landfill symposium. 30 Sept - 04 Oct 2019, Santa Margherita di Pula, Italy.
Vrancken, C., Longhurst, P.J., Wagland, S.T., 2017. Critical review of real-time methods for solid waste characterisation: Informing material recovery and fuel production. Waste Manage. 61, 40–57. https://doi.org/10.1016/j.wasman.2017.01.019.
Wares, M.A., Awal, M.A., Das, S.K., Alam, J., 2014. Environmentally persistant toxicant arsenic affects uterus grossly and histologically. Bangl. J. Vet. Med. 11, 61–68. https://doi.org/10.3329/bjvm.v11i1.13175.
Watanabe, N., Inoue, S., Ito, H., 1999. Antimony in municipal waste. Chemosphere 39, 1689–1698. https://doi.org/10.1016/S0045-6535(99)00069-7.
Welle, F., 2016. Verpackungsmaterial aus Polyethylenterephthalat. DLG Expertenwissen 4/2016.
Windsperger, A., Windsperger, B., Tuschl, R., 2007. PVC heute. Die aktuelle Situation des Werkstoffs Weich-PVC in den relevanten Themenbereichen.
Wittchen, B., Josten, E., Reiche, T., 2008. Holzfachkunde: Ein Lehr-, Lern- und Arbeitsbuch für Tischler/Schreiner und Holzmechaniker. Vieweg+Teubner Verlag.
Yuasa, 2015. NiCd Material Safety Data Sheet.
Zhang, H., He, P.-J., Shao, L.-M., 2008. Implication of heavy metals distribution for a municipal solid waste management system — a case study in Shanghai. Sci. Total Environ. 402, 257–267. https://doi.org/10.1016/j.scitotenv.2008.04.047.

3.2 Publication II

Origins of major and minor ash constituents of solid recovered fuel for co-processing in the cement industry

S.A. Viczek, A. Aldrian, R. Pomberger, R. Sarc

Waste Management, accepted March 24, 2021.

Author Contributions (CRediT Contributor Roles Taxonomy):

SV: Conceptualization, Methodology, Formal analysis, Investigation, Writing – original draft preparation, Writing – review and editing, Visualization, Project administration;

AA: Methodology, Formal analysis;

RP: Funding acquisition, Resources;

RS: Writing – review and editing, Supervision, Funding acquisition.

Manuscript – Waste management (2021 in press)

Origins of major and minor ash constituents of solid recovered fuel for co-processing in the cement industry

S.A. Viczek, A. Aldrian, R. Pomberger, and R. Sarc*

Chair of Waste Processing Technology and Waste Management, Department of Environmental and Energy Process Engineering, Montanuniversitaet Leoben, Franz-Josef-Strasse 18, 8700 Leoben, Austria

*Corresponding author. E-mail address: renato.sarc@unileoben.ac.at (R. Sarc)

Abstract: Solid recovered fuel (SRF) ash consists of element oxides, which are valuable materials for cement manufacturers. When SRF is co-processed in the cement industry, its mineral content is incorporated into the clinker. Therefore, from a technical perspective, SRF ash is recycled. However, since recycling processes for materials that may be present in SRF exist, and since recycling goals are defined for different waste types, understanding the origin of these ash constituents and the contribution of different materials to the Recycling-index (R-index, i.e., the material-recyclable share of SRF) is important. In this work, the origins of Al, Ca, Fe, Si, Ti, Mg, Na, K, S, and P were first reviewed. Subsequently, ten SRF samples were sorted, and the ash content and composition of the sorting fractions (e.g., < 10 mm, plastics, paper&cardboard) determined. Additionally, selected samples of polyethylene (PE), polypropylene (PP), polystyrene (PS), polyethylene terephthalate (PET), polyvinyl chloride (PVC), liquid packaging board (LPB), wood, and paper&cardboard (P&C) extracted from SRF were investigated. The results demonstrated that the materials that contributed most of the valuable oxides and ash content, and thereby to the R-index of SRF, are mixed or composite fractions, for example, the fine fraction, composites, and sorting residues. Except for the composite LPB, no other material recovery options exist for most of these fractions. For this reason, the recycling of mixed and soiled materials or residues in the cement industry may be considered a complementary option to existing recycling processes.

Keywords: ash composition, cement manufacturing, co-incineration, material recycling, refuse-derived fuel (RDF), waste processing.

1 Introduction

In the cement industry, primary fuels required for the clinker burning process are increasingly substituted by alternative fuels, including solid recovered fuels (SRF). SRF is a quality-assured subgroup of refuse-derived fuel (RDF) exclusively produced from non-hazardous solid waste, including mixed municipal and commercial waste (ASI, 2011b; Sarc et al., 2014). Thermal substitution rates (TSRs), that is, the share of energy supplied via alternative fuels, are increasing worldwide (Sarc et al., 2019) and have reached ~80% (on average) in some countries such as Austria (Mauschitz, 2020). Legally, various countries have recognized the utilization of SRF and other RDFs in the cement industry as an energy recovery pathway, including members of the European Union (EC, 2017). However, from a technical perspective, co-processing of RDF can be considered a mixture of energy and material recovery often referred to as "mixed recovery", which is acknowledged in some countries (Viczek et al., 2020a). This mixed recovery arises from the fact that the ash of RDF is incorporated into the cement clinker. Since the ashes are composed of various chemical compounds that are valuable raw materials for cement production, their incorporation into a new product, such as the clinker, can technically be considered as recycling at the material level.

This material recovery option is also supported by considerable research on the application of municipal soil waste incinerator (MSWI) ash as a mineral source or substitute raw material for the cement industry (Clavier et al., 2019; Kikuchi et al., 2008; Lam et al., 2011; Saikia et al., 2007; Sarmiento et al., 2019). Various studies have demonstrated that these ashes contain the necessary elemental composition for cement manufacturing and are a potential substitute for traditional raw materials (Clavier et al., 2020). While the recycling of MSWI ash in the cement industry involves two or more processes, that is, waste incineration in a separate suitable facility and subsequent application of (pre-treated) ash in the cement industry (Clavier et al., 2020), SRF ashes are directly produced in the clinker burning process at the primary or secondary firing system and are incorporated into the clinker in the same process step.

Analyses of 80 SRF samples prepared from mixed commercial waste have demonstrated that approximately 77% of the ash consists of the four main chemical components required for the production of cement clinker: CaO (28.5%), SiO_2 (31.5%), Al_2O_3 (13.2%), and Fe_2O_3 (3.6%). In addition to these four components, SRF ash contains small amounts of other elements, many of which are frequently introduced into the cement kiln as part of the raw materials, namely SO_3 (5.6%), MgO (3.1%), Na_2O (1.6%), K_2O (1.7%), TiO_2 (2.1%), and P_2O_5 (0.8%) (Viczek et al., 2020a).

Aldrian et al. (2020) proposed the following calculation method for the "R-index", i.e., the share of SRF (in $\%_{DM}$) that can be considered as recycled on a material level:

$$R - index = \frac{AC}{100} \cdot (w_1 + w_2 + \cdots + w_n) \qquad \text{Formula 1}$$

where AC is the ash content [$wt\%_{DM}$] and w_1, w_2, ..., w_n are the mass shares of selected element oxides in ash [$wt\%_{DM}$].

Depending on the elements selected for the calculation of the R-index, the values can range from 13.5% (CaO, SiO_2, Al_2O_3, Fe_2O_3) to 17.6% (R-index = AC at 950°C) (Viczek et al., 2020a). This indicates that in countries with already high thermal substitution rates, the cement industry could readily contribute toward reaching set recycling goals, as defined by the European Union (EC, 2018a, 2018b), provided that the minerals incorporated into the clinker are recognized as recycled. Because different recycling targets for different types of waste have been defined, such as for packaging waste or municipal waste, material

recycling in the cement industry would need to be divided and assigned to the right waste type.

The required assignment to different waste types raises the question of where the most relevant SRF ash constituents come from, that is, which materials contribute most to the R-index, or what is the share of each material class that can be considered recycled in the cement kiln. To answer these questions, this paper presents the analysis of 10 ash constituents (Al_2O_3, CaO, Fe_2O_3, SiO_2, MgO, TiO_2, K_2O, Na_2O, SO_3, and P_2O_5) for two test series. The first test series aims to investigate the distribution of these elements among broader material categories of SRF (e.g., plastics, textiles, fine fraction, residue), thereby evaluating the contribution of each waste fraction to the final SRF ash content and composition. The second test series comprises ashes of particular material fractions, such as polyethylene (PE) and polypropylene (PP) extracted from different SRF samples, and aims to investigate the detailed ash composition, including the determination of additional chemical elements. Literature data on the occurrence of these elements in waste fractions, their origins, and technical applications (Section 2) serve as a basis for discussing and interpreting the results. Consequently, the role and position of the cement industry as part of a recycling industry can be evaluated based on the materials that contribute most to the R-index.

2 Origins of ash-forming elements and their occurrence in waste fractions: Literature review

In the following sections, the occurrence of major and minor constituents of SRF ash in different waste fractions is discussed through the review of industrial applications or the natural occurrence of the elements. The focus of the discussion is directed towards fractions that are likely to remain part of the SRF and are not likely to be removed from the waste stream in state-of-the-art SRF production plants. Note that all of the discussed elements are major constituents of the earth's crust (Clarke and Washington, 1924) and therefore are naturally abundant in rocks, soils, and other inorganic, inert, or fine materials that frequently end up in waste and SRF. However, these inorganic or inert materials are considered to be impurities in SRF because they do not contribute to the energy content. The median concentrations of Al, Ca, Fe, Si, Mg, Ti, K, Na, S, and P in different waste fractions reported by Götze et al. (2016a), who performed a thorough literature review on element concentrations in waste fractions, are summarized in Tab. 1.

2.1 Aluminum (Al)

In the review by Götze et al. (2016a), the highest Al concentrations were reported for the metal, composite, and inert fractions (Tab. 1). High concentrations were also observed in the paper and cardboard fraction, which may be linked to liquid packaging board (LPB) (cf. analyses of Götze et al. (2016b)) which typically contains a layer of Al. Furthermore, Al in paper can originate from the use of kaolin as a filler, coating in papermaking, or calcium sulfoaluminate as a pigment in high-quality paper (Bajpai, 2015).

Aluminum is the most prominent non-Fe metal and is used for various purposes in the metal industry (Holleman et al., 2007). While non-Fe metals (e.g., aluminum cans) are usually removed from the waste stream during SRF production using eddy-current separators (Sarc et al., 2014), small parts of aluminum foil might still end up in the SRF. The high Al content of the inert fraction may be linked to gravel, sand, stones, aluminosilicates, such as clay and ceramic materials (cf. analyses of Götze et al. (2016b)), or residues from building activities (e.g., cement or bricks) (Holleman et al., 2007). These materials may well end up in the fine fraction of the SRF, owing to their brittle fracturing behavior during shredding. Analyses of the particle size-dependent distribution of Al in coarsely shredded mixed commercial waste (MCW) revealed that the highest median Al concentrations occurred in the fine fractions < 5 mm and 5–10 mm (Viczek et al., 2021b; Viczek et al., 2021a). X-ray diffraction (XRD) analysis of the < 5 mm MCW fractions showed the presence of clinochlore, muscovite, and traces of albite (Viczek et al., 2021a).

Although the median concentration of Al in mixed waste plastics is low compared to other material fractions listed by Götze et al. (2016a), Al compounds are widely used in plastic manufacturing for polymerization catalysis, stabilization, as pigments, or as fillers (Ranta-Korpi et al., 2014). Al concentrations in plastics[1] are relatively low when used as a catalyst (10–100 mg/kg), co-stabilizer (300–2,700 mg/kg), or aluminate and aluminosilicate pigments (90–1,600 mg/kg) compared to its application in fillers, flame retardants, or metallic aluminum pigments. Typical fillers containing Al include glass fiber (containing Si, Ca, Al, and B), kaolin (Si and Al), or mica (Si, Al, and K), and cause Al concentrations of 6,300–58,000 mg/kg (Ranta-Korpi et al., 2014). Furthermore, plastic packaging coated with Al (e.g., chips packaging) may contain Al in high concentrations (Götze et al., 2016b).

2.2 Calcium (Ca)

The highest median concentrations of Ca in various waste fractions have been reported for glass, inert materials, and paper/cardboard (Götze et al., 2016a). The most prevalent type of glass, accounting for almost 90% of all glass produced, is soda-lime glass (Robertson, 2006). It is used as packaging glass (jars and bottles) and flat glass, and consists of 68%–73% SiO_2, 10%–13% CaO, 12%–15% Na_2O, 1.5–2% Al_2O_3, and 0.05–0.25% FeO (Robertson, 2006). In the inert materials fraction, Ca may originate from ceramics, gravel, sand, stones (Götze et al., 2016b), or residues from building materials (e.g., cement, mortar, plaster, and gypsum) (Holleman et al., 2007). Chemical analyses of waste fractions reported by Götze et al. (2016b) revealed high Ca concentrations in animal-derived food waste, probably originating from bones or eggshells, which may also be attributed to the fraction "inert materials."

Tab. 1 Median concentrations of 10 ash constituting elements and ash content of waste fractions reported in the literature review of Götze et al. (2016a). Note: For Si, the number of data points from the literature was limited

	Al [mg/kg$_{DM}$]	Ca [mg/kg$_{DM}$]	Fe [mg/kg$_{DM}$]	Si [mg/kg$_{DM}$]	Mg [mg/kg$_{DM}$]	Ti [mg/kg$_{DM}$]	K [mg/kg$_{DM}$]	Na [mg/kg$_{DM}$]	P [mg/kg$_{DM}$]	S [mg/kg$_{DM}$]	Ash content [%$_{DM}$]
Organic	8400	14000	4700	488	1695	120	10000	3720	3000	2000	15.7
Food waste	46	3611	48	-	274	45	8989	2980	5200	3780	20.9
Gardening waste	11178	11256	5270	143733	1850	788	7695	3441	1184	1000	14.0
Paper&Cardboard	11700	34600	755	12400	1210	13	743	1090	164	1400	13.0
Composites	28615	12555	1585	-	1060	-	1096	1820	340	2000	16.0
Plastics	820	4160	849	1670	344	4200	750	1170	244	1125	3.0
Combustibles	1570	9510	733	5110	917	150	1640	1630	300	2600	8.7
Metal	171500	1143	492500	168	756	1100	501	648	232	297	96.7
Glass	7620	67775	1350	342000	9370	250	5730	25500	98	687	98.9
Inert	22000	36400	11500	270000	2350	2000	12600	5760	439	1920	97.0

[1] concentrations refer to the final, clean polymer product; in most cases, "as received" (OS) may be considered equal to the dry mass (DM)

High Ca contents can be observed for various paper wastes (e.g., books, magazines, or newsprint), and range from ca. 1.5 to 9.6%$_{DM}$, (Götze et al., 2016b). They are probably linked to $CaCO_3$ as a filler for paper gaining preference over kaolin (Bajpai, 2015). In the pulp and paper industry, fillers are typically added in amounts of 10%–30% (Biermann, 1996). Furthermore, ground or precipitated $CaCO_3$ or gypsum can be applied as a coating agent for paper, while calcium sulfoaluminate is the oldest known pigment for paper (Bajpai, 2015).

Mixed waste plastics contain significantly lower amounts of Ca than the fractions mentioned above (Götze et al., 2016a), although Ca is commonly used in the plastic industry. Ca compounds are primarily used as fillers or reinforcements, which implies that they are added at very high loadings, and may also be used as pigments or PVC heat stabilizers (Ranta-Korpi et al., 2014). $CaCO_3$ is the most commonly used inorganic compound in plastics. Loading levels range from 1 wt% to several tens of percent, resulting in Ca concentrations of up to 15% in the final product. Other common Ca-containing fillers include dolomite ($CaMg(CO_3)_2$) and wollastonite ($CaSiO_3$), with Ca concentrations of 3%–10% in the final product. $CaSO_4$ may be used as a filler for PVC, polyesters, or plastic foam, resulting in Ca contents of 1–9%. Furthermore, glass fibers are used to reinforce plastics at high loadings (up to 30%). Because the most common types of glass fibers used in plastics contain Ca, this may result in a high Ca content of 1%–5% in reinforced plastics. The use of Ca-containing compounds as pigments does not result in similarly high Ca concentrations (Ranta-Korpi et al., 2014).

High concentrations of Ca were also observed in fine fractions < 5 mm of coarsely shredded mixed commercial waste (Viczek et al., 2021b; Viczek et al., 2021a). XRD analyses of fine fractions (< 5 mm) revealed that, in addition to being present as carbonates in the form of calcite ($CaCO_3$) and dolomite ($CaMg(CO_3)_2$), crystalline Ca is also present as sulfate, that is, anhydrite ($CaSO_4$), bassanite ($CaSO_4 \cdot 0.5\ H_2O$), and gypsum ($CaSO_4 \cdot 2\ H_2O$) (Viczek et al., 2021a). The fine fractions also contained small glass particles, which cannot be determined by XRD.

2.3 Iron (Fe)

Götze et al. (2016a) reported the highest median Fe concentrations in metals, followed by inert materials, gardening waste, and organics. While large metal parts are usually removed during SRF production by magnetic separators (Sarc et al., 2014), small metal parts or metal abrasions remain in the SRF. High Fe contents of up to 22%$_{DM}$ were observed for the fine fractions of MCW < 5 mm, which featured the highest Fe content of all investigated particle size classes of the study of Viczek et al. (2021a). The prevalent iron compounds in the investigated fractions were magnetite (Fe_3O_4), wuestite (FeO), and hematite (Fe_2O_3). No clear evidence was found for metallic Fe.

The inert fraction may contain Fe because of its natural occurrence in clay minerals and soils (Stucki et al., 1987) and consequently in ceramics and pottery (Götze et al., 2016b). As discussed in the previous sections, after shredding, these materials are expected to end up in the fine fraction. The high content of Fe in gardening waste (Götze et al., 2016b) may also be linked to soil residues.

Plastic wastes contain relatively low concentrations of Fe, although iron compounds are used in plastics and rubbers (Ranta-Korpi et al., 2014). Its primary purpose is the coloration of plastics in yellow, red, brown, and black hues, resulting in Fe concentrations of 60–3,600 mg/kg. Furthermore, Fe is present as a residue in inorganic fillers or reinforcements, including chalk, talc, calcium carbonate, dolomite, glass fibers, wollastonite, mica, and kaolin. The potential presence of Fe in these materials causes Fe concentrations in the final product of up to 630 mg/kg or 700–14,000 mg/kg in the case of mica (Ranta-Korpi et al., 2014).

2.4 Silicon (Si)

The highest median concentrations of Si can be observed for the waste fractions of glass, inert materials, and gardening waste (Götze et al., 2016a) (Tab. 1). SiO_2 is usually the main constituent in most types of glass (Holleman et al., 2007). Common glass such as soda-lime glass (Section 2.2) is used in packaging, bottles, windows, or mirrors, and contains ~70% SiO_2 (Holleman et al., 2007; Robertson, 2006). Similar to Al (see section 2.1), Si in the "inert" fraction may originate from aluminosilicates, i.e., clay or ceramic products (Götze et al., 2016b) or residues from building activities (e.g., cement, mortar, bricks) (Holleman et al., 2007). Because these materials are expected to break into several smaller pieces during the comminution steps, they are likely to end up in the fine fraction of SRF, as would glass.

The high Si content of gardening waste may be linked to soil residues, as indicated by the analysis results of (Götze et al., 2016b), who reported high Si concentrations in gravel, sand, stones, plants with dust and soil residues, as well as hummus and soil fractions. Soil residues or inorganic matter containing SiO_2 or other silicates may be present in the fine fraction of MCW for SRF production. Viczek et al. (2021a) reported the highest concentrations of Si in different particle size classes of coarsely shredded MCW in the fine fraction < 5 mm. While amorphous Si compounds in glass were only optically identified in the samples and could not be detected by XRD, the largest part of crystalline Si was present as quartz. In addition, Si was present in the form of muscovite and traces of albite (Viczek et al., 2021a).

Further applications of Si in the manufacturing of materials that are desired in SRF (e.g., plastics and paper) include the use of Si compounds as fillers. For example, talc ($Mg_3Si_4O_{10}(OH)_2$) is used as a filler or coating pigment in the pulp and paper industry (Bajpai, 2015). Si-containing fillers for plastics also include talc, glass fibers, mica, kaolin, or wollastonite. These compounds are added to plastics at usage levels of 10%–30% (Ranta-Korpi et al., 2014), which may lead to a high percentage of Si in the plastic products.

2.5 Magnesium (Mg)

Götze et al. (2016a) reported the highest median concentrations of Mg in the waste fractions glass, inert materials, and gardening waste. The occurrence of Mg in glasses is probably linked to its use in soda-lime glass to replace some of the Ca and adjust the glass properties (Pedone et al., 2008). Mg occurs at high concentrations in inert materials such as ceramics or cat litter (Götze et al., 2016b), the latter consisting of bentonite, which is primarily composed of montmorillonite (Eisenhour and Brown, 2009), a Mg-containing silicate. $MgCO_3$ is used in the building sector to prepare mortar (Holleman et al., 2007). These materials are likely to end up in the fine fractions of waste, where the highest median Mg concentrations of all particle size classes were observed for MCW (Viczek et al., 2021b; Viczek et al., 2021a). In the fine fraction < 5 mm investigated by Viczek et al. (2021a), crystalline Mg was present as dolomite, clinochlore, and small amounts of magnesite.

The high Mg content in gardening waste may be linked to the occurrence of Mg in the plant material itself, because it is essential for plant growth and is the central metal ion of chlorophyll. Concentrations of Mg in leaves are typically above 2,000 mg/kg$_{DM}$ (Hermans et al., 2013), but the content may vary depending on the plant species (Hauer-Jákli and Tränkner, 2019). Although the woody plant material from gardening waste might contain less Mg than leaves or humus (Götze et al., 2016b), Mg levels seem to fit the expected levels of plants and leaves, considering that gardening waste is a mixture of several plant parts and soil residues.

While plastics and paper contain lower amounts of Mg, they represent important fractions in the SRF. Magnesium compounds are often used as catalysts in the plastics industry, but the Mg concentrations in the polymer are typically below 100 mg/kg (Ranta-Korpi et al., 2014). High concentrations are expected when magnesium hydroxide ($Mg(OH)_2$) is

used as a flame retardant at high usage levels of 20%–60%, resulting in Mg concentrations of up to 250,000 mg/kg. Furthermore, Mg is used as a filler or impact modifier (e.g., dolomite, talc, and glass fibers), resulting in Mg contents of 100 to 60,000 mg/kg depending on the material used (Ranta-Korpi et al., 2014). Mg-containing fillers, such as talc, are also frequently used in the paper industry (Bajpai, 2015).

2.6 Titanium (Ti)

The highest median concentrations in waste are, by far, reported for the waste fraction plastics, followed by inerts and metals Götze et al. (2016a). Considering the ash content of these materials, it is expected that the Ti concentration in plastic ash exceeds that of inert materials and metals, even more significantly. Generally, Ti is used in a broad range of applications in the form of titanium dioxide (TiO_2). It is present in most white or brightly tinted items, including paints, plastics, fibers, paper, cardboard, enamels, and ceramics (Holleman et al., 2007).

While various Ti compounds are used in the plastics industry (Ranta-Korpi et al., 2014), the highest Ti concentrations can be observed when TiO_2 is used as a pigment or filler, as the usage level is typically between 0.5–5 wt%, resulting in Ti concentrations of ca. 3,000–30,000 mg/kg. Ti concentrations are usually lower when Ti compounds are used as catalysts (10–70 mg/kg) or when Ti-containing pigments, other than TiO_2, are used (100–2,700 mg/kg) (Ranta-Korpi et al., 2014). In the paper industry, TiO_2 is used as a specialty filler or coating agent (Bajpai, 2015).

2.7 Potassium (K)

Inert materials, organics, food, and gardening are waste fractions for which the highest median concentrations of K have been observed (Götze et al., 2016a). Potassium naturally occurs in feldspars, which are part of clay minerals (Locher, 2000), occurring in several inert materials, such as ceramics, gravel, stones, and sand (Götze et al., 2016b). Furthermore, because of its occurrence in clay, K also occurs as a common minor phase in cement clinker as a sulfate (Locher, 2000). The particle size-dependent distribution of K in MCW showed the highest median concentrations in the fine fractions (< 5 mm and < 10 mm). In the finer fraction < 5 mm, K was present in the form of muscovite, which belongs to the group of micas (Viczek et al., 2021a). As discussed in the previous sections, mica is also used as a filler or pigment in plastics, which is why K is introduced into various plastic products (Ranta-Korpi et al., 2014).

As an essential nutrient for all living organisms, K occurs in various organic materials. Consequently, it also occurs in organic, gardening, and food waste fractions. For example, K concentrations in plants can range from 10,000 to 60,000 mg/kg_{DM} (Kirkby, 2005). Higher concentrations have been found in vegetable food waste and plant material compared to animal-derived food waste (Götze et al., 2016b).

2.8 Sodium (Na)

By far, the highest Na concentrations have been reported for glass (Tab. 1). As discussed in Section 2.2, the most common glass type, soda-lime glass, contains significant amounts of sodium. Similar to K, Na also occurs in feldspars and is thereby part of clay minerals, pottery, or cement clinker, which may explain the high Na concentrations in the inert fractions. Götze et al. (2016b) also reported high Na concentrations in the waste fraction gravel, sand, stones, and cat litter because montmorillonite, the main component of bentonite, contains Na. As discussed, these materials are likely to end up in the fine fractions, which have exhibited significantly higher concentrations of Na than larger particle size fractions, as reported by Viczek et al. (2021a). XRD analyses showed the presence of small amounts of albite in the fine fraction (< 5 mm). The high concentrations of Na in organic and food waste fractions (Götze et al., 2016b) may be linked to the presence of NaCl in food (Gerassimidou et al., 2021; Viczek et al., 2020b) and living organisms.

2.9 Sulfur (S)

Götze et al. (2016a) listed the highest median concentrations of S for food waste, combustibles, and organics. Sulfur is naturally present in various organic materials, biomolecules, and living organisms, explaining the high concentrations in various fractions of food, organic, and gardening wastes. In the combustible fraction, Götze et al. (2016b) reported high concentrations in wood, sanitary products, vacuum cleaner bags, textiles, leather, and rubber.

Paper and cardboard, as well as plastics, also contain S (Tab. 1). In the pulp and paper industry, gypsum or calcium sulfoaluminate may be used as coating pigments. Furthermore, S compounds can be used in several applications such as pulping chemicals (Bajpai, 2015). In the plastics industry, S is a chemical component of different plastics and rubbers (Ranta-Korpi et al., 2014), including polyphenylene sulfide (PPS; ca. 30 wt% S), polysulfones (PSF, 7–8 wt% S), polyehtersulfones (PES, 13–14 wt% S), polyphenylsulfones (PPSF, 7.5–8.5 wt% S), polysulfide polymers, or chlorosulfonated polyethylene (CSM, 0.5–1.5 wt% S). Sulfur and its components are also used in the vulcanization of rubbers as accelerators or retarders, resulting in S contents of 0.3–1.0 wt%. Fillers and inorganic or organic pigments in plastics, including $BaSO_4$ and $CaSO_4$, and result in S concentrations of 0.1–4.1 wt% in the final product. Further applications of S compounds in polymers include their use as stabilizers, antimicrobials, blowing or fluorescent whitening agents, and antistatic additives (Ranta-Korpi et al., 2014).

2.10 Phosphorus (P)

The highest P concentrations were reported for the organic, food, and gardening waste fractions, while other fractions contained much lower amounts of P (Tab. 1). Phosphorus is an essential element for most organisms and is commonly found in soil, rocks, plants, and animal tissues (Robles, 2014). Phosphorus concentrations in plants range from 500 to 5,000 mg/kg_{DM} (Malhotra et al., 2018). Significantly higher contents, however, are present in animal excrements (28,000–39,000 mg/kg_{DM}; Götze et al. (2016b)) as well as sewage sludge (up to 60,000 mg/kg_{DM}; Scheidig et al. (2013)).

3 Materials and Methods

3.1 Samples

3.1.1 Sample series I

Sample series I comprised material fractions from 10 samples of SRF from mixed solid waste intended for primary firing ("SRF primary" suitable as a main burner fuel in the primary firing system of cement plants) provided by an Austrian SRF producer. Samples were collected according to EN 15442 (ASI, 2011a) between August and September 2020 and dried at 105 °C (EN 14346 (ASI, 2007)). After removing the fine fraction < 10 mm, the samples were manually sorted into the material fractions glass, wood, inert, plastic, metal, paper&cardboard (P&C), textiles, composite, and the sorting residue, which consisted of all other material classes as well as heavily entangled materials.

3.1.2 Sample series II

Sample series II included defined material fractions extracted from five composite samples of "SRF primary" produced from mixed solid waste. The same samples were investigated at the particle level by Weissenbach and Sarc (2021). The samples were taken from Austrian SRF production plants in four runs between September and November 2019. Particles belonging to the following material classes were sorted manually: paper&cardboard (P&C), wood, liquid packaging board (LPB), and plastics. The plastic fractions were sorted into polyethylene (PE), polypropylene (PP), polystyrene (PS), polyethylene terephthalate (PET), and polyvinyl chloride (PVC) using a lab-scale NIR sorter (engineered by Binder+Co AG (Gleisdorf, Austria) using the EVK HELIOS NIR G2-320 sensor (EVK, Graz, Austria) with a spectral range of 0.9–1.7 µm). For further details on the procedure, refer to Weissenbach and Sarc (2021). Composite samples of the sorted

material fractions of the same manufacturers were formed by combining the fractions from the four runs. In total, 39 samples were used for chemical analyses (sufficient PVC material was only available from four of the five SRF manufacturers).

3.2 Chemical analyses

3.2.1 Sample series I: comprehensive analysis of SRF fractions

Samples were dried to constant mass at 105°C according to EN 14346 (ASI, 2007), comminuted to < 0.5 mm, and ashed at 815 °C according to DIN 51719 (DIN, 1997). For further analyses, Method D proposed by Aldrian et al. (2020) was chosen, that is, lithium metaborate fusion according to DIN 51729-11 (DIN, 1998b), dissolution of the fused bead in 2 M HCl, and analysis of Al, Ca, Fe, K, Mg, Na, P, S, Si, and Ti via inductively coupled plasma optical emission spectrometry (ICP-OES) according to DIN 11885 (DIN, 1998a). For details, see Aldrian et al. (2020).

3.2.2 Sample series II: analysis of defined materials classes (e.g., PE, PP, and PS)

Samples were dried to constant mass at 105°C according to EN 14346 (ASI, 2007), comminuted to < 0.5 mm, and ashed at 815 °C according to DIN 51719 (DIN, 1997). Owing to the low ash content of the materials and the small remaining sample mass, and because more analytes were targeted, ash samples were digested by microwave-assisted acid digestion with HCl, HNO_3, and HF according to EN 13656 (ASI, 2002). This approach is based on method B proposed by Aldrian et al. (2020) who demonstrated equivalent results for the analyses of ash constituents as method D, used for sample series I. The concentrations of Ag, Al, As, Ba, Be, Ca, Cd, Co, Cr, Cu, Fe, Hg, K, Li, Mg, Mn, Mo, Na, Ni, P, Pb, Pd, Sb, Se, Si, Sn, Sr, Te, Ti, Tl, V, W, and Zn were determined by inductively coupled plasma mass spectrometry (ICP-MS) based on EN 17294-2 (ASI, 2017), while the concentration of S was determined by ICP-OES according to EN 11885 (DIN, 1998a).

3.2.3 Thermogravimetric analysis of SRF

Three of the original, unsorted SRF samples of series I were dried to constant mass at 105° C and comminuted to a size < 0.25 mm. The samples were investigated by simultaneous thermal analysis (STA 449C Jupiter (Netzsch)) with FTIR gas analysis (Bruker). The systems were coupled with a heated tube, and measurements were performed in a heated cuvette. For the analyses, approximately 25 mg of each sample was heated to 1300° C under normal atmospheric conditions with an airflow of 40 mL/min at a rate of 10 °C/min.

3.2.4 Calculations

R-indices were calculated according to Formula 1. For simplicity, it was assumed that the analyzed ash forming elements were mainly present as oxides in the ash, and the corresponding concentrations of the respective oxides (e.g., Al_2O_3, CaO, Fe_2O_3, K_2O, MgO, Na_2O, P_2O_5, SO_3, SiO_2, and TiO_2) were calculated. It needs to be emphasized that while this is the conventional way of expressing elemental ash compositions, the prevalent element species in ashes are rather silicates and aluminosilicates. Statistical analyses were performed using OriginPro 2020 (version 9.7.0.188).

4 Results and Discussion

4.1 Thermogravimetric analysis of SRF – confirmation of suitable ashing temperatures

Thermogravimetric analysis was conducted to obtain a more detailed evaluation of the effect of ashing temperatures, as discussed by Aldrian et al. (2020). The analysis showed that most freed CO_2 originated from combustion processes; however, starting at approximately 600 °C, a further release of CO_2 resulting from endothermic reactions was observed. These reactions may be due to the decomposition of carbonates (e.g., $CaCO_3$) in the sample, which supports the work by Aldrian et al. (2020). The diagrams (Figures S1-S3 in the Supplementary Material) show ongoing combustion and mass changes after 550 °C. In comparison, only minor changes were observed between 815 °C and 950 °C, supporting the assumption that these ashing temperatures yield equivalent results for the ash content, and, consequently, the determination of the R-index.

4.2 Ash composition of combustible SRF fractions (sample series I)

Sorting analyses showed that small amounts of inert materials, glass, or metals were present in some of the SRF samples (see Fig. 1 for average SRF composition; detailed results are found in the Supplementary Material). These fractions were not separately analyzed owing to the insufficient amount available. Additionally, due to their size (> 10 mm because only the screen overflow was sorted) they are unlikely to be fully recycled, i.e., incorporated into clinker phases. Large metal parts are commonly removed from the clinker using magnetic separators after the clinker burning process. Therefore, this work focuses on the characterization of the ashes from combustible and fine fractions. Larger parts of inert materials, metals, and glass are not considered for calculating the R-index.

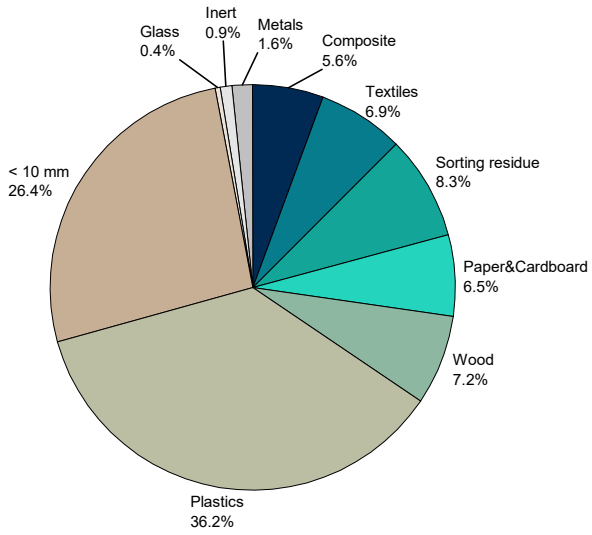

Fig. 1. Average composition of the solid recovered fuel (SRF) samples (sample series I; n=10). Data for single samples is provided in the Supplementary Material.

The average ash composition of the combustible fractions of SRF is shown in Fig. 2. The ash of composite materials showed the highest concentrations of Al_2O_3, while the highest SiO_2 concentrations were observed in the fine fraction < 10 mm. The highest CaO concentrations were found in the ash of the paper&cardboard fractions. Fe oxide is present in similar concentrations in the ash of the sorting residue, textiles, and the fine fraction. Furthermore, Fig. 2 shows a very good correspondence of the ash composition of the investigated SRF with the 80 SRF samples investigated by Viczek et al. (2020a).

It is evident that the materials with the highest ash content may have the largest influence on the overall composition of SRF ashes, provided they are present in sufficient quantities. The materials contributing the largest shares of Al_2O_3, CaO, Fe_2O_3, K_2O, MgO, Na_2O, P_2O_5, SiO_2, SO_3, and TiO_2 are displayed in Fig. 3.

With an average ash content of 22%$_{DM}$ and the second highest mass share of all material fractions from sorted SRF, the fine fraction < 10 mm contributed the most considerable amounts of all investigated element oxides except for TiO_2. The highest amount of TiO_2, as well as the second-highest amounts of the other elements, were contributed by the mixed plastic fraction. However, while the ash content in the wood and paper fractions corresponded well with previously reported values (Weissenbach and Sarc, under review), the 8%–13% (average: 10%)

ash content of the mixed plastics fraction was significantly higher than the 3% reported by Götze et al. (2016a), or the 2–3% found in common plastics types (except for PVC, which contained 9–20% of ash) (Weissenbach and Sarc, under review). In this context, it must be emphasized that the SRF was only sorted and the fractions were not washed. Therefore, the samples were not clean, but as soiled as they occur in mixed waste. For materials with a very low ash content and a high surface area, such as plastics, fine particles attached to the surface may have a significant influence on the ash content and composition. Note that the overall mass share of the fraction is not expected to be affected as significantly as the ash content. For this reason, sample series II comprised cleaner fractions and aimed to investigate certain material classes more thoroughly.

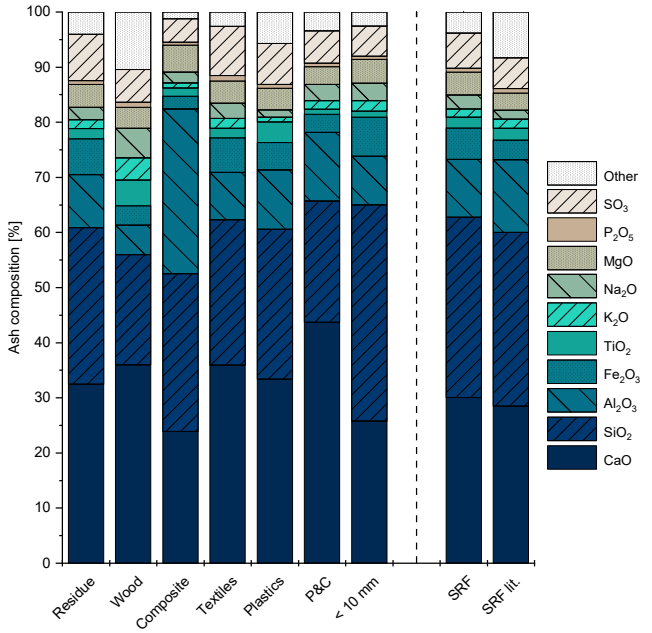

Fig. 2. Average ash composition (n=10) of material factions from SRF and comparison with the average calculated SRF ash composition (n=10) and SRF ash composition from Viczek et al. (2020a) ("SRF lit.")

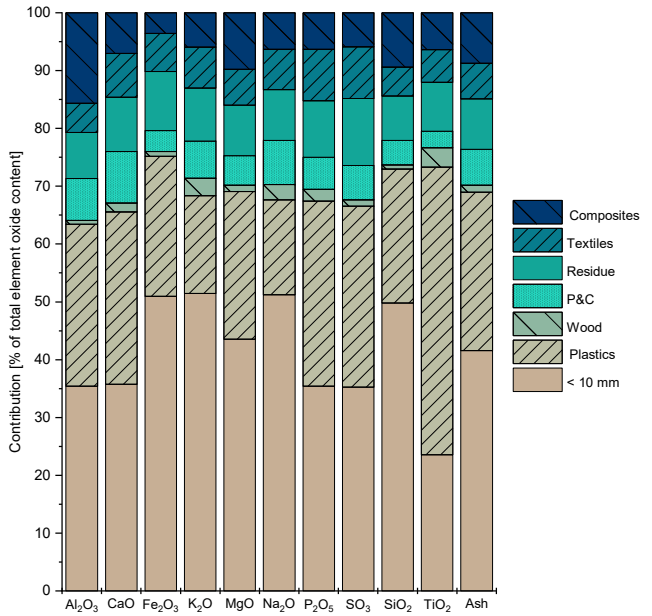

Fig. 3. Average contribution (n=10) of the different material classes to the total amount of element oxides and ash of the SRF ash samples

4.3 Ash composition of defined materials (sample series II)

The ash composition of sample series II with respect to the main ash constituents is shown in Fig. 4, oxides of other elements (e.g., Ba, Sb, and Zn) usually made up less than 2% of the ash. The detailed results are provided in the Supplementary Material. A comparison of the ash composition of defined material fractions with that of SRF published by Viczek et al. (2020a) found that the ashes of all investigated materials, that is, plastic types, wood, paper&cardboard, and LPB, displayed much lower SiO_2 contents than SRF ash, suggesting that another fraction was the main source of SiO_2 (e.g., the fine fraction).

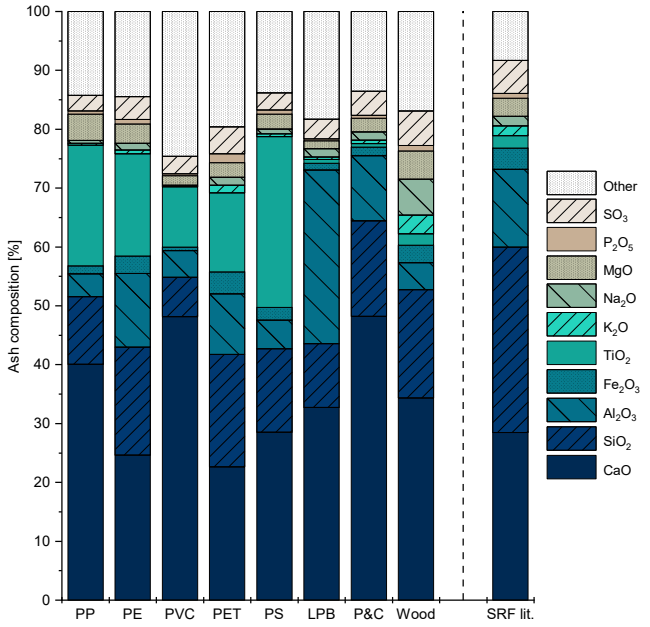

Fig. 4. Ash composition of the material fractions polypropylene (PP; n=5), polyethylene (PE; n=5), polyvinyl chloride (PVC; n=4), polyethylene terephthalate (PET; n=5), polystyrene (PS; n=5), liquid packaging board (LPB; n=5), paper&cardboard (P&C; n=5), wood (n=5), and comparison with the average SRF ash composition (SRF lit.) as published by Viczek et al. (2020a) (n=80).

While both the ash content (Table S4, Supplementary Material) and composition of the wood and paper&cardboard fractions of sampling series II were consistent with those of sampling series I, this was not the case for plastics. First, the ash content in the plastic fractions was much lower than that in the mixed plastics fraction of sampling series I, but within the expected range reported in the literature (Götze et al., 2016a; Götze et al., 2016b; Weissenbach and Sarc, under review). Second, the investigated plastic types contain significant concentrations of TiO_2, suggesting that the highest share of TiO_2 in the SRF ash originates from the plastic fraction.

Compared to sample series II, the TiO_2 concentration is strongly suppressed in the mixed plastics samples from sample series I, and the concentration of SiO_2 is enhanced. Together with the differences in ash content of the plastic samples in both sample series, this observation supports the hypothesis that mixed plastic fractions from sample series I (Section 4.2) were contaminated with fine particles. Consequently, their contribution to the ash content is expected to be significantly lower with fewer surface-adhering particles.

4.4 Comparison of the SiO_2 : CaO : Al_2O_3+Fe_2O_3 ratio with other fuels and raw materials

On average, 65%–85% and 50%–77% of the ashes from different material fractions of sample series I and II, respectively, consisted of the four main chemical compounds required for the production of cement clinker: Al_2O_3, CaO, Fe_2O_3, and SiO_2. The right ratio of these elements in

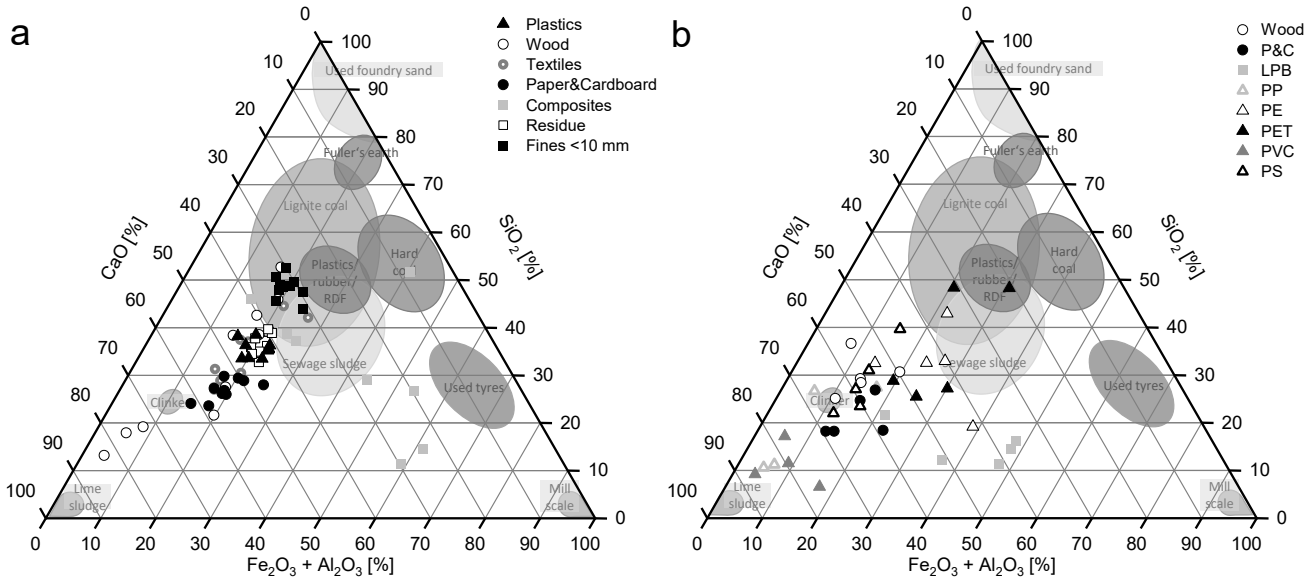

Fig. 5. Comparison of the ash composition of different materials, fuels and raw materials relevant to the cement industry, as well as clinker. Ternary diagram reproduced from VDZ (2019) and extended with a) sample series I, and b) sample series II.

the raw meal and the cement clinker is essential for cement manufacturing, which is why the raw meal mix is adjusted to suit the utilized fuels (Viczek et al., 2020a). In Fig. 5, the SiO_2 : CaO : Al_2O_3+Fe_2O_3 ratio of the ashes of sample series I and II are compared with other common fuels, raw materials, and the desired ratio in the clinker. The ashes of wood, paper&cardboard, and some samples of textiles are rich in Ca and therefore the element ratio is similar to the desired ratio in the clinker. This also applies to PP and PS; however, some of the PP samples and all PVC samples are closer to lime sludge because of their even higher Ca content. This implies that, depending on the material composition of the SRF, the SRF ashes may be located in different areas of the ternary diagram and may require different actions to account for their effect on the clinker composition.

4.5 Implications for the Recycling index and the role of the cement industry

The compositional analyses and observations discussed in sections 4.2 and 4.3, as well as the R-indices calculated for the materials (Fig. 6), demonstrate that the materials that contribute most to the R-Index of SRF are fractions that are typically not subjected to other recycling processes. This is the case for the fine fractions, which are a mixture of various materials and have not been widely investigated, and the sorting residue. Composite materials, contributing 20% of the Al_2O_3 in the SRF, are also a very heterogeneous fraction. Except for LPB, most composites are typically not recycled because of the difficulty to separate each material. While paper&cardboard are commonly recycled, once they are mixed with municipal or commercial waste these materials may be too soiled for recycling.

Except for PVC, which had the highest ash content of the investigated plastic types, most plastic types had rather low R-indices. In the case of PVC, a significantly higher R-index was calculated under the scenario "R-index ash" than for "R-index 9 oxides", calculated with the ash content or nine of the constituents, respectively. This is likely attributable to the high chlorine content in PVC, as seen in Fig. 4, which displays a higher content of "other" components in the ash of PVC than in the ashes of other polymers. Despite the higher ash content or R-index, PVC is not desired in SRF because the chlorine concentration is technically limited due to corrosion issues or the degradation of the cement clinker quality (Gerassimidou et al., 2021).

Based on the combined results of sample series I and II and the literature review, the proportion of mixed plastics in SRF that contributed the most to the ash content, valuable element oxides in the ash, and thereby the recycling index, are likely fillers and surface contamination (indicated by the elevated ash content, suppressed Ti, and high Si concentrations in the mixed plastics fraction from sampling series I compared to the cleaner materials in sampling series II). Without surface contamination, the ash content of the investigated mixed plastic fraction is likely reduced to a third or a quarter of the observed ash content. Therefore, this contribution may also be assigned to the fine fraction; depending on the origin of the SRF, (e.g., packaging or construction and demolition waste), the extent of surface contamination may vary. The low ash content of PET and polyolefins indicated that these materials are mainly subject to energy recovery (~97%) when they enter the cement kiln as part of the SRF. Thus, for these materials, material recovery plays a subordinate role.

A statistically significant (p<0.05) negative correlation (r=-0.78) was found between the ash content and the share of plastics in the SRF, indicating that the ash content may decrease with increasing amounts of plastics. Because sorting data are compositional data, this correlation may have resulted from the decreasing percentage of other materials when the share of plastics increases. However, the results showed that the ash composition and content of SRF are likely to vary depending on the waste used for its production. Plastic-rich SRF, for example, produced from packaging waste, with only low amounts of fines or other material classes, may display lower ash contents and a different element oxide pattern (e.g., more TiO_2), and therefore lower R-indices.

The R-indices calculated for the 10 SRF samples (sample series I, without hard impurities) investigated in this work ranged from 7.8% to 11.9% when Al_2O_3, CaO, Fe_2O_3, and SiO_2 were considered, 9.4 to 14.5% with Al_2O_3, CaO, Fe_2O_3, SiO_2, TiO_2, MgO, SO_3, Na_2O, and K_2O, and 10.3 to 15.5% when the R-index was equal to the ash content.

5 Conclusions

The literature review has shown that inorganic materials often contain significant amounts of Al, Ca, Fe, Si, Ti, and Mg, but so do combustible materials, albeit in smaller concentrations. The role of combustible fractions may increase when they are combusted, as the concentrations in the ash are higher than in the original material. However, despite being considered impurities, inorganic materials frequently end up in SRF, e.g., in the fine fraction, and can be recycled in the cement industry.

The primary SRF material fractions recycled in the cement industry are mixed materials, including fine fractions, composite materials, or other

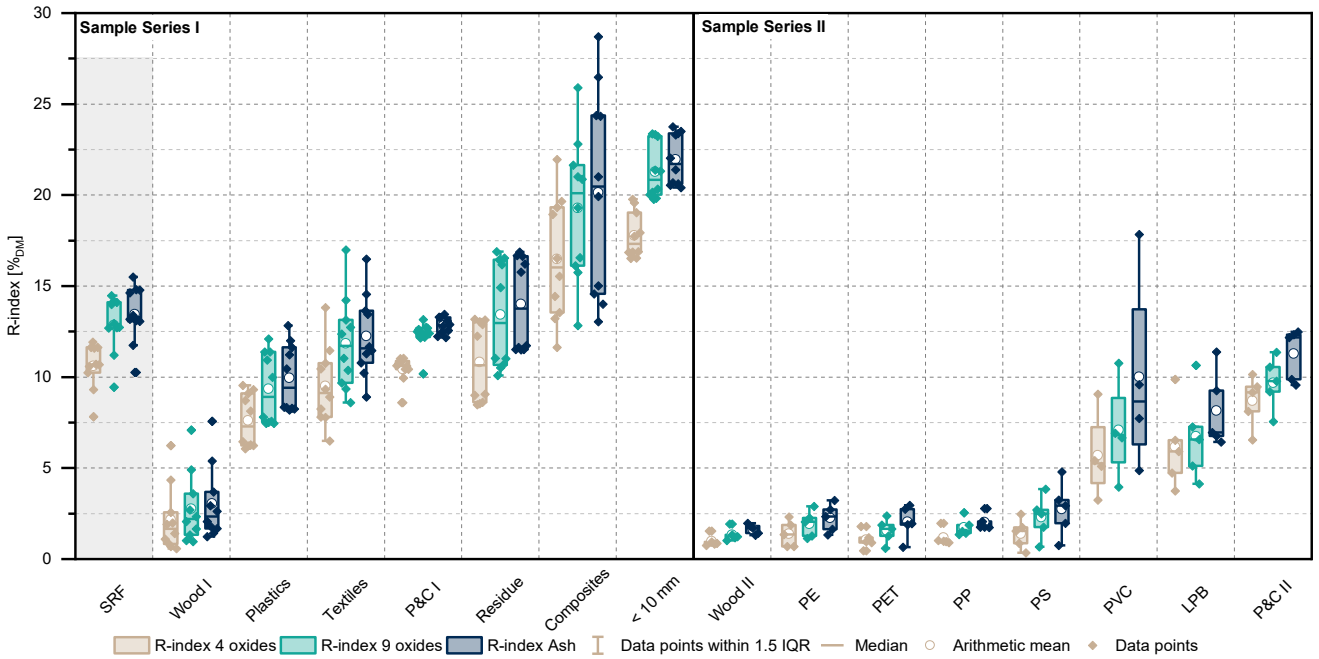

Fig. 6. Calculated R-indices for the materials of the two sample series as well as SRF from sample series I. R-indices were calculated for three scenarios: "R-index 4 oxides" considering Al_2O_3, CaO, Fe_2O_3, and SiO_2; "R-index 9 oxides" considering Al_2O_3, CaO, Fe_2O_3, SiO_2, TiO_2, MgO, SO_3, Na_2O, and K_2O; and "R-index Ash" where the R-index equals the ash content.

not clearly identifiable materials (sorting residue), for which no other state-of-the-art recycling options are currently available. Therefore, the cement industry's role in a circular economy is likely to be a complementary recycling option to existing recycling processes. In addition to SRF from mixed wastes, residue materials from established recycling processes such as tire fluff from recycled old tires, reject materials from polymer or paper recycling, residues from primary sorting of mixed packaging waste, and similar fractions, may be recycled in the cement industry and substitute a certain share of primary raw materials.

Conflict of interest

The authors declare no conflict of interest.

Acknowledgments

Partial funding for this work was provided by the Center of Competence for Recycling and Recovery of Waste 4.0 (acronym ReWaste4.0) (contract number 860 884) under the scope of the COMET Competence Centers for Excellent Technologies, financially supported by BMK, BMDW, and the federal state of Styria, managed by the FFG.

References

Aldrian, A., Viczek, S.A., Pomberger, R., Sarc, R., 2020. Methods for identifying the material-recyclable share of SRF during co-processing in the cement industry. Methods X, 100837. https://doi.org/10.1016/j.mex.2020.100837.

ASI (Austrian Standards Institute), 2002. ÖNORM EN 13656 Characterization of waste – Microwave assisted digestion with hydrofluoric (HF), nitric (HNO3) and hydrochloric (HCl) acid mixture for subsequent determination of elements. Issued on 01/12/2002, Vienna.

ASI (Austrian Standards Institute), 2007. ÖNORM EN 14346 Characterization of waste - Calculation of dry matter by determination of dry residue or water content. Issued on 01/03/2007, Vienna.

ASI (Austrian Standards Institute), 2011a. ÖNORM EN 15442 Solid recovered fuels - Methods for sampling. Issued on 01/05/2011, Vienna.

ASI (Austrian Standards Institute), 2011b. ÖNORM EN 15359 Solid recovered fuels - Specifications and classes. Issued on 15/12/2011, Vienna.

ASI (Austrian Standards Institute), 2017. ÖNORM EN ISO 17294-2 Water quality - Application of inductively coupled plasma mass spectrometry (ICP-MS) - Part 2: Determination of selected elements including uranium isotopes. Issued on 15/01/2017, Vienna.

Bajpai, P., 2015. Pulp and paper industry: Chemicals. Elsevier, Amsterdam, Netherlands.

Biermann, C.J., 1996. Handbook of pulping and papermaking, 2nd ed. Academic Press, San Diego, Calif., 754 pp.

Clarke, F.W., Washington, H.S., 1924. The composition of the Earth's crust. US Geological Survey. https://doi.org/10.3133/pp127.

Clavier, K.A., Paris, J.M., Ferraro, C.C., Townsend, T.G., 2020. Opportunities and challenges associated with using municipal waste incineration ash as a raw ingredient in cement production – a review. Resour Conserv Recy 160, 104888. https://doi.org/10.1016/j.resconrec.2020.104888.

Clavier, K.A., Watts, B., Liu, Y., Ferraro, C.C., Townsend, T.G., 2019. Risk and performance assessment of cement made using municipal solid waste incinerator bottom ash as a cement kiln feed. Resour Conserv Recy 146, 270–279. https://doi.org/10.1016/j.resconrec.2019.03.047.

DIN (Deutsches Institut für Normung), 1997. DIN 51719 Testing of solid fuels – Solid mineral fuels – Determination of ash content. Issued 07/1997.

DIN (German Institute for Standardization), 1998a. DIN EN ISO 11885 Water quality - determination of 33 elements by inductively coupled plasma atomic emission spectroscopy. Issued 04/1998.

DIN (German Institute for Standardization), 1998b. DIN 51729-11 Testing of solid fuels - Determination of chemical composition of fuel ash - Part 11: Determination by inductively coupled plasma emission spectrometry (ICP-OES). Issued 11/1998.

EC (European Commission), 2017. Communication from the Commission to the European Parliament, the Council, the European Economic and Social Committee and the Committee of the Regions. The role of waste-to-energy in the circular economy.

EC (European Commission), 2018a. Directive (EU) 2018/852 of the European Parliament and of the Council of 30 May 2018 amending Directive 94/62/EC on packaging and packaging waste.

EC (European Commission), 2018b. Directive 2018/851 of the European Parliament and the Council of 30th May 2018 amending Directive 2008/98/EC on waste.

Eisenhour, D.D., Brown, R.K., 2009. Bentonite and Its Impact on Modern Life. Elements, 83–88.

Gerassimidou, S., Velis, C.A., Williams, P.T., Castaldi, M.J., Black, L., Komilis, D., 2021. Chlorine in waste-derived solid recovered fuel (SRF), co-combusted in cement kilns: A systematic review of sources, reactions, fate and implications. Crit Rev Env Sci Tec 51(2), 140–186. https://doi.org/10.1080/10643389.2020.1717298.

Götze, R., Boldrin, A., Scheutz, C., Astrup, T.F., 2016a. Physico-chemical characterisation of material fractions in household waste: Overview of data in literature. Waste Manage 49, 3–14. https://doi.org/10.1016/j.wasman.2016.01.008.

Götze, R., Pivnenko, K., Boldrin, A., Scheutz, C., Astrup, T.F., 2016b. Physico-chemical characterisation of material fractions in residual and source-

segregated household waste in Denmark. Waste Manage 54, 13–26. https://doi.org/10.1016/j.wasman.2016.05.009.
Hauer-Jákli, M., Tränkner, M., 2019. Critical Leaf Magnesium Thresholds and the Impact of Magnesium on Plant Growth and Photo-Oxidative Defense: A Systematic Review and Meta-Analysis From 70 Years of Research. Frontiers in plant science 10, 766. https://doi.org/10.3389/fpls.2019.00766.
Hermans, C., Chen, J., Verbruggen, N., 2013. Magnesium in Plants, in: Kretsinger, R.H., Uversky, V.N., Permyakov, E.A. (Eds.), Encyclopedia of Metalloproteins. Springer, New York, NY, pp. 1269–1276.
Holleman, A.F., Wiberg, E., Wiberg, N., 2007. Lehrbuch der anorganischen Chemie, 102nd ed. de Gruyter, Berlin.
Kikuchi, R., Kukacka, J., Raschman, R., 2008. Grouping of mixed waste plastics according to chlorine content. Separation and Purification Technology 61, 75–81. https://doi.org/10.1016/j.seppur.2007.10.001.
Kirkby, E.A., 2005. Essential elements, in: Hillel, D. (Ed.), Encyclopedia of soils in the environment. Elsevier, Amsterdam, pp. 478–485.
Lam, C.H.K., Barford, J.P., McKay, G., 2011. Utilization of municipal solid waste incineration ash in Portland cement clinker. Clean Technol Envir 13, 607–615. https://doi.org/10.1007/s10098-011-0367-z.
Locher, F.W., 2000. Zement: Grundlagen der Herstellung und Verwendung, 1st ed. Verlag Bau+Technik, s.l., 540 pp.
Malhotra, H., Vandana, Sharma, S., Pandey, R., 2018. Phosphorus Nutrition: Plant Growth in Response to Deficiency and Excess, in: Hasanuzzaman, M., Fujita, M., Oku, H., Nahar, K., Hawrylak-Nowak, B. (Eds.), Plant nutrients and abiotic stress tolerance. Springer, Singapore, pp. 171–190.
Mauschitz, G., 2020. Emissionen aus Anlagen der österreichischen Zementindustrie. Berichtsjahr 2019.
Pedone, A., Malavasi, G., Menziani, M.C., Segre, U., Cormack, A.N., 2008. Role of Magnesium in Soda-Lime Glasses: Insight into Structural, Transport, and Mechanical Properties through Computer Simulations. J. Phys. Chem. C 112, 11034–11041. https://doi.org/10.1021/jp8016776.
Ranta-Korpi, M., Vainikka, P., Konttinen, J., Saarimaa, A., Rodriguez, M., 2014. Ash forming elements in plastics and rubbers. The VTT publication series 186.
Robertson, G.L., 2006. Food packaging: Principles and practice, 2nd ed. CRC Press, Boca Raton, 550 pp.
Robles, H., 2014. Phosphorus, in: Wexler, P. (Ed.), Encyclopedia of Toxicology, 3rd ed. Elsevier Science, Burlington, pp. 920–921.
Saikia, N., Kato, S., Kojima, T., 2007. Production of cement clinkers from municipal solid waste incineration (MSWI) fly ash. Waste Manage 27, 1178–1189. https://doi.org/10.1016/j.wasman.2006.06.004.
Sarc, R., Lorber, K.E., Pomberger, R., Rogetzer, M., Sipple, E.M., 2014. Design, quality, and quality assurance of solid recovered fuels for the substitution of fossil feedstock in the cement industry. Waste Manag Res 32, 565–585. https://doi.org/10.1177/0734242X14536462.
Sarc, R., Seidler, I.M., Kandlbauer, L., Lorber, K.E., Pomberger, R., 2019. Design, Quality and Quality Assurance of Solid Recovered Fuels for the Substitution of Fossil Feedstock in the Cement Industry – Update 2019. Waste Manag Res 37, 885–897. https://doi.org/10.1177/0734242X19862600.
Sarmiento, L.M., Clavier, K.A., Paris, J.M., Ferraro, C.C., Townsend, T.G., 2019. Critical examination of recycled municipal solid waste incineration ash as a mineral source for portland cement manufacture – A case study. Resour Conserv Recy 148, 1–10. https://doi.org/10.1016/j.resconrec.2019.05.002.
Scheidig, K., Lehrmann, F., Mallon, J., Schaaf, M., 2013. Klärschlamm-Monoverbrennung mit integriertem Phosphor-Recycling. Energie aus Abfall 10, 1039–1046.
Stucki, J.W., Goodman, B.A., Schwertmann, U., 1987. Iron in Soils and Clay Minerals. Springer Netherlands, Dordrecht, 902 pp.
VDZ (Verein Deutscher Zementwerke e.V.), 2019. Personal message on ternary diagram with fuel ash composition. E-mail, 14.05.2019.
Viczek, S.A., Aldrian, A., Pomberger, R., Sarc, R., 2020a. Determination of the material-recyclable share of SRF during co-processing in the cement industry. Resour Conserv Recy 156, 104696. https://doi.org/10.1016/j.resconrec.2020.104696.
Viczek, S.A., Aldrian, A., Pomberger, R., Sarc, R., 2020b. Origins and carriers of Sb, As, Cd, Cl, Cr, Co, Pb, Hg, and Ni in mixed solid waste – A literature-based evaluation. Waste Manage 103, 87–112. https://doi.org/10.1016/j.wasman.2019.12.009.
Viczek, S.A., Khodier, K., Kandlbauer, L., Aldrian, A., Redhammer, G., Tippelt, G., Sarc, R., 2021a. The particle size-dependent distribution of chemical elements in mixed commercial waste and implications for enhancing SRF quality. Sci Total Environ 776, 145343. https://doi.org/10.1016/j.scitotenv.2021.145343.
Viczek, S.A., Lorber, K.E., Sarc, R., 2021b. Production of contaminant-depleted solid recovered fuel from mixed commercial waste for co-processing in the cement industry. Fuel 294, 120414. https://doi.org/10.1016/j.fuel.2021.120414.
Weissenbach, T., Sarc, R., under review. Investigation of particle-specific characteristics of non-hazardous, coarse-shredded mixed waste.
Weissenbach, T., Sarc, R., 2021. Investigation of particle-specific characteristics of non-hazardous, fine shredded mixed waste. Waste Manage, 162–171. https://doi.org/10.1016/j.wasman.2020.09.033.

3.3 Publication III

Sampling and analysis of coarsely shredded mixed commercial waste. Part I: procedure, particle size and sorting analysis

K. Khodier, **S.A. Viczek**, A. Curtis, A. Aldrian, P. O'Leary, M. Lehner, R. Sarc

International Journal of Environmental Science and Technology 17 (2020), 959-972, https://doi.org/10.1007/s13762-019-02526-w

Author Contributions (CRediT Contributor Roles Taxonomy):

KK: Conceptualization, Methodology, Software, Formal analysis, Investigation, Data curation, Writing – original draft preparation, Writing – review and editing, Visualization, Project administration;

SV: Conceptualization, Methodology, Investigation, Writing – review and editing;

AC: Methodology, Investigation;

AA: Methodology;

PO: Supervision;

ML: Writing – review and editing, Supervision;

RS: Methodology, Investigation, Writing – review and editing, Supervision, Funding acquisition.

International Journal of Environmental Science and Technology
https://doi.org/10.1007/s13762-019-02526-w

ORIGINAL PAPER

Sampling and analysis of coarsely shredded mixed commercial waste. Part I: procedure, particle size and sorting analysis

K. Khodier[1] · S. A. Viczek[2] · A. Curtis[2] · A. Aldrian[2] · P. O'Leary[3] · M. Lehner[1] · R. Sarc[2]

Received: 28 March 2019 / Revised: 6 August 2019 / Accepted: 27 August 2019

Abstract

Performing experiments with mixed commercial waste, sampling is unavoidable for material analysis. Thus, the procedure of sampling needs to be defined in a way that guarantees sufficient accuracy regarding the estimation of the examined analytes. In this work, a sampling procedure for coarsely shredded mixed commercial waste, based on the Austrian Standard ÖNORM S 2127, the horizontal sampling standard DS 3077 and the theory of sampling, was established, described and examined through a replication experiment determining the relative sampling variability. The analytes are described through a matrix of nine (9) material classes and nine (9) particle size classes. It turns out that the typical threshold value of 20% can be reached for some fractions of the particle size–material matrix (for example, wood 20–40 mm and cardboard 60–80 mm) but gets as bad as 231% (wood 200–400 mm) for others. Furthermore, a decrease in the relative sampling variability with the mass share of a fraction is observed. Part of the observed variability is explainable through the fundamental sampling error, while contributions of other types of sampling errors are also evident. The results can be used for estimating confidence intervals for experimental outcomes as well as assessing required sample sizes for reaching a target precision when working with mixed commercial waste.

Keywords Theory of sampling · Relative sampling variability · Commercial waste · Coarse shredder · Increment mass · Sample mass

List of symbols

$\mathbf{A}_v$	Binary matrix for combining adjacents of v particle size fractions [–]
$\mathbf{B}_w$	Binary matrix for combining 1 to w material classes [–]
c	Constitutional parameter [kg/m^3]
CV	Coefficient of variance [–]
d_{05}	5th percentile particle size [mm], [cm]
d_{95}	95th percentile particle size [cm]
$d_{\max}$	Maximum particle diameter [mm]
f	Particle shape parameter [–]
f_{red}	Mass reduction factor [–]
f^*_{red}	Real mass reduction factor [–]
$f^*_{\text{red},r}$	f^*_{red} when reducing the fine fraction of the $(r-1)$ th screening step [–]
g	Particle size parameter [–]
HI_{lot}	Heterogeneity invariant of the lot [g]
$\mathbf{M}$	Particle size–material matrix (masses) [kg]
m_c	Average particle mass of the constituent c [g]
m_{disc}	Mass discarded during mass reduction [kg]
m_{ij}	Mass of the ith particle size fraction and jth material class in the primary sample [kg]
m^*_{ij}	Weighed mass of the ith particle size fraction and jth material class [kg]
m_{inc}	Minimum increment mass [kg]
m_k	Average particle masses of the constituents k [g]
m_{lot}	Mass of the lot to be sampled [g]
m_{part}	Mass of sample part [kg]
m_{pres}	Mass preserved during mass reduction [kg]

Editorial responsibility: Binbin Huang.

✉ R. Sarc
renato.sarc@unileoben.ac.at

[1] Chair of Process Technology and Industrial Environmental Protection, Department of Environmental and Energy Process Engineering, Montanuniversitaet Leoben, Franz-Josef-Strasse 18, 8700 Leoben, Austria

[2] Chair of Waste Processing Technology and Waste Management, Department of Environmental and Energy Process Engineering, Montanuniversitaet Leoben, Franz-Josef-Strasse 18, 8700 Leoben, Austria

[3] Chair of Automation, Department Product Engineering, Montanuniversitaet Leoben, Peter-Tunner-Strasse 25/II, 8700 Leoben, Austria

Published online: 07 September 2019

m_{sam}	Minimum sample mass [g]
$m_{sam,k}$	Mass of the kth sample [kg]
n	Number of samples [–]
p	Fraction of particles with a specific characteristic [–]
q	Number of constituents [–]
RSV	Relative sampling variability [%]
s	Standard deviation [conc. u.]
t_{inc}	Increment extraction time [s]
$\dot{V}$	Volume flow [kg/m^3]
v	Number of particle size fractions [–]
$\mathbf{W}$	Particle size-material matrix (mass shares) [kg/kg]
$\mathbf{W}_{mp}$	Matrix of all regarded particle size fraction and material class combinations (mass shares) [kg/kg]
w	Number of material classes [–]
w_c	Mass share of the constituent c [g]
w_{ij}	Mass share of the ith particle size fraction and jth material class in the primary sample [kg/kg]
w_k	Mass shares of the constituents k [g]
$\bar{x}$	Weighted arithmetic mean [conc. u.]
x_k	Concentration of a specific analyte according to sample k [conc. u.]
β	Liberation parameter [–]
ρ	Bulk density [kg/m^3]
σ^2_{FSE}	Variance caused by the fundamental sampling error [–]

Introduction

Coarse shredding followed by one or more screening stages is often the first step when processing mixed commercial waste (MCW). Besides size reduction and definition, this combination contributes to the concentration of different materials as well as their contained chemical elements in different fractions. Reasons for this are the different particle size distributions of the material classes in the original material, as well as differences in comminution behaviour—e.g. brittle fracturing of glass and passing through or tearing of plastic foils.

Aiming at systematically steering this concentration process, optimal shredder and screen parametrization are intended to be found through empirical regression models for the particle size–material matrix as well as for the distribution of the concentrations of contained elements over particle sizes, based on experimental results. Because of the high inherent inhomogeneity of MCW, performing such experiments demands processing of large amounts of material to homogenize the variability of the input stream regarding composition and particle size between the single runs. These high amounts of material cause the infeasibility of analysing the complete shredding product so that samples need to be taken.

Various standards and recommendations concerning sampling of MCW are available, giving guidelines on sample extraction, increment sizes, sample numbers and sizes, and sample processing for different applications. Regarding masses, they aim at ensuring that the amount of analyte contained in the sample is sufficient to keep the effect of single particles ending up in the sample—or not—at an insignificant level. This is, for example, done through average particle masses and shares of sorting fractions by Felsenstein and Spangl (2017). In contrast, the technical report CEN/TR 15310 (European Committee for Standardization 2006) for uses inhomogeneity descriptors in combination with the cubic diameter of the largest particles, as well as bulk density, as an estimate for maximum particle contributions to the analyte.

In Austria, the Austrian Standard ÖNORM S 2127—Basic characterization of waste heaps or solid waste from containers and transport vehicles (Austrian Standards Institute 2011)—is usually applied, demanding a minimum increment mass m_{inc} [kg] according to Eq. (1)—where d_{95} is the 95th percentile particle size [mm]—and a minimum number of 10 increments per (representative) sample. Furthermore, at least one sample per 200 t of waste investigated is required. Multiplying these requirements leads to a minimum for the total sample mass.

$$m_{inc\,[kg]} \geq 0.06 \cdot d_{95[mm]} \tag{1}$$

However, the standard does not give information about the statistical significance of the sampling result. Furthermore, the linear consideration of the diameter for the resulting sample mass is very likely to underestimate the masses required to get reliable information about coarse fractions. It is a compromise between reliability and practicability in terms of comprehensibility and economically feasible (sorting) analyses of the resulting sample masses. According to Wavrer (2018), a comparable practically oriented approach called MODECOM™ is used in France.

The technical report CEN/TR 15310—characterization of waste—sampling of waste materials (European Committee for Standardization 2006) is another available reference. It defines the minimum increment mass m_{inc} [kg] according to Eq. (2), where ρ [kg/m^3] is the bulk density of the material.

$$m_{inc\,[kg]} \geq 2.7 \cdot 10^{-8} \cdot \rho_{\left[\frac{kg}{m^3}\right]} \cdot d_{95\,[mm]} \tag{2}$$

The equation describes the resulting mass, when using a sampling device which is at least three times as long as the

maximum particle diameter (practically determined through d_{95}) in each dimension, as demanded by the report. This shall ensure that all particles can easily enter the sampling device. The resulting increment mass is about 50 times the maximum particle mass, according to the report. It furthermore suggests a minimum sample mass m_{sam} [g], calculated according to Eq. (3), where p [m/m] is the fraction of the particles with a specific characteristic, g [–] is the correction factor for the particle size distribution of the material to be sampled, and CV [–] is the desired coefficient of variation caused by the fundamental error.

$$m_{\mathrm{sam}\,[\mathrm{g}]} \geq \frac{1}{6} \cdot \pi \cdot \left(d_{95\,[\mathrm{cm}]}\right)^3 \cdot \rho_{\left[\frac{\mathrm{g}}{\mathrm{cm}}\right]} \cdot g_{[-]} \cdot \frac{\left(1 - p_{[\mathrm{m/m}]}\right)}{\mathrm{CV}^2_{[-]} \cdot p_{[\mathrm{m/m}]}} \tag{3}$$

The value of g depends on the quotient of the 95th and 5th percentile particle sizes (d_{95}/d_{05}), according to Eq. (4). 0.1 is suggested as a well-accepted value for CV, and p needs to be determined from knowledge about waste consistency.

$$g = \begin{cases} 0.25 & \text{if } 4 < d_{95}/d_{05} \\ 0.50 & \text{if } 2 < d_{95}/d_{05} \leq 4 \\ 0.75 & \text{if } 1 < d_{95}/d_{05} \leq 2 \\ 1 & \text{if } d_{95}/d_{05} = 1 \end{cases} \tag{4}$$

While the report also provides formulae for calculating the significance of the analytical results, determining it requires a priori knowledge about the material, as does the determination of minimum increment and sample masses.

Another reference is the Guidelines for statistical evaluation of sorting and particle gravimetric analyses from Vienna University of Technology (TU Wien) and the University of Natural Resources and Life Sciences in Vienna (BOKU) (Felsenstein and Spangl 2017). It provides theory-based instructions on required sample masses for different significance levels, while mainly addressing the sampling of the total mixed municipal waste of Austrian federal provinces and demanding prior particle weight analyses for calculating sample masses.

Gy (2004a), the founder of the theory of sampling (TOS), also provides formulae supporting the determination of required sample masses by calculating the minimum possible sampling error—the fundamental sampling error (FSE). It is calculated according to Eq. (5), where σ^2_{FSE} [–] is the variance caused by the FSE, m_{sam} [g] and m_{lot} [g] are the masses of the sample and of the lot to be sampled and $\mathrm{HI}_{\mathrm{lot}}$ [g] is the heterogeneity invariant of the lot (Gy 2004a). $\mathrm{HI}_{\mathrm{lot}}$ can be calculated through Eq. (6), which contains the following parameters:

- c [g/cm^3]: constitutional parameter, which can vary from values lower than 1, up to millions
- β [–]: liberation parameter with $0 \leq \beta \leq 1$
- f [–]: particle shape parameter with $0 \leq f \leq 1$ and common values near 0.5
- g [–]: size range parameter with $0 \leq g \leq 1$
- d_{95} [cm]: 95th percentile particle size

$$\sigma^2_{\mathrm{FSE}\,[-]} = \left(\frac{1}{m_{\mathrm{sam}\,[\mathrm{g}]}} - \frac{1}{m_{\mathrm{lot}\,[\mathrm{g}]}}\right) \cdot \mathrm{HI}_{\mathrm{lot}\,[\mathrm{g}]} \tag{5}$$

$$\mathrm{HI}_{\mathrm{lot}\,[\mathrm{g}]} = c_{\left[\frac{\mathrm{g}}{\mathrm{cm}^3}\right]} \cdot \beta_{[-]} \cdot f_{[-]} \cdot g_{[-]} \cdot d^3_{95\,[\mathrm{cm}]} \tag{6}$$

While Gy states that values for these parameters can be found for different materials in literature, no references were found for MCW. Furthermore, according to Gy (2004a), no satisfactory formula is known yet for determining f. Hence, the heterogeneity invariant needs to be evaluated experimentally.

However, according to Wavrer (2018), a simplified formula exists for "simple particles," meaning cases where the particles are assumed to consist either of 0% or 100% of an analyte—as is typically the case for waste sorting analyses, where each particle is assigned to a sorting fraction. In that case, the FSE can be calculated through Eq. (7), where m_c and m_k are the average particle masses of the constituent of interest c and the other constituents k, and w_c and w_k are their mass shares, respectively. q stands for the number of constituents.

$$\sigma^2_{\mathrm{FSE}\,[-]} = \left(\frac{1}{m_{\mathrm{sam}\,[\mathrm{g}]}} - \frac{1}{m_{\mathrm{lot}\,[\mathrm{g}]}}\right) \cdot \left(m_{c\,[\mathrm{g}]} \frac{1 - 2\,w_{c[-]}}{w_{c[-]}} + \sum_{k=1}^{q} w_{k[-]} \cdot m_{k[\mathrm{g}]}\right) \tag{7}$$

Still, a priori knowledge is needed in terms of average particle masses and assumptions about the composition of the constituents, as is the case in Felsenstein and Spangl's (2017) guideline. Moreover, applying the formulae for the FSE does not provide information about the real sampling error beyond the contribution of the fundamental one.

In conclusion, no satisfactory guidance was found for a priori determination of required increment masses or sample masses for achieving a certain level of significance when sampling MCW. Furthermore, the general estimation error (GEE) for the elements of the particle size–material

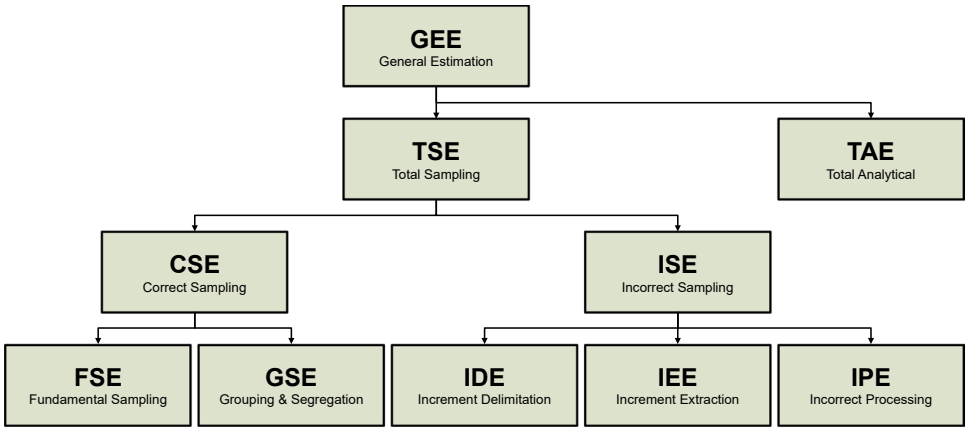

Fig. 1 Contributions to the general estimation error

matrix as well as for the distribution of chemical elements throughout particle sizes is the result of several processing steps and subsampling steps. Thus, to evaluate analytical data quality for modelling purposes, as well as for interpreting experiments, the total error of the data acquisition process, from primary sampling to chemical analysis (which is the GEE), needs to be determined experimentally. This is done through a replication experiment (REx) as described in the Danish standard DS 3077, which is a horizontal sampling standard based on the TOS (Danish Standards Foundation 2013).

Even though the other described references may deliver more profound statements regarding necessary sample masses, the Austrian standard ÖNORM S 2127 was chosen for the REx in this work for multiple reasons: the necessary information about the material (which is only d_{95}) was available and analysing the resulting masses was expected to be feasible in practice. Furthermore, the REx offered the opportunity to evaluate this standard, which is widely applied in Austria.

The investigation to be presented will be published in two parts. In part I (i.e. the present contribution), a procedure for sampling MCW-shredding experiments is developed, based on TOS, DS 3077 and ÖNORM S 2127. Furthermore, the applied steps of sample processing from the primary sample to the particle size–material matrix are described. Finally, the results of a REx are presented, providing information about data quality when applying the described procedure. The corresponding experimental work was conducted from October to December 2018 in Allerheiligen im Mürztal, Styria, Austria.

Part II, presented by Viczek et al. (2019), deals with the distribution of several chemical elements, especially heavy metals, in different grain size fractions of coarsely shredded MCW. Post-sorting processing of the material for analysing the concentrations of these elements is described. Furthermore, the GEE is evaluated for the concentrations in different particle size classes through the REx. Ultimately, the distribution of the chemical elements throughout particle sizes, as well as correlations to the results of sorting analysis are presented.

Materials and methods

Theory of sampling

According to Esbensen and Wagner (2014), the theory of sampling is a universal, scale-invariant fundamentum for understanding sampling and the potential errors caused by it. It is based on the fundamental sampling principle, requiring all increments of the lot to have the same likelihood of ending up in the (representative) sample. It describes all errors contributing to the total sampling error (TSE). The GEE consists of this TSE in addition to the, often well-determined, total analytical error (TAE) (Esbensen and Wagner 2014). Its components are shown in Fig. 1.

Gy (2004b) divides the contributions to the TSE into correct sampling errors (CSE) and incorrect sampling errors (ISE). The first are caused by constitutional and distributional heterogeneities of the material to be sampled and are unavoidable, whereas the latter come from avoidable sampling mistakes and should, therefore, be avoided as far as possible.

CSE consists of two kinds of errors, the FSE and the grouping and segregation error (GSE). The FSE is caused by the constitutional heterogeneity, which describes chemical and physical differences between fragments of the lot—in the case of MCW: particles—and can only be altered

through physical interventions like comminution. The GSE, on the other hand, is present due to the distributional heterogeneity, meaning the spatial distribution of different particles, e.g. through segregation, or regarding MCW because of compositional differences of different, joined but not homogenized, waste sources (Esbensen and Julius 2009). The distributional heterogeneity is the reason why samples need to consist of a number of increments spaced around the lot to achieve acceptable levels of GSE.

ISEs are the sum of incorrect delimitation errors (IDEs), incorrect extraction errors (IEEs) and incorrect processing errors (IPEs). The IDEs describe errors in defining geometrical domains to be potentially taken as a sample. According to Gy (2004b), they can be avoided when collecting materials of a stream using equal time intervals. The IEEs appear, when the delimited domain (including all particles whose centre of mass is contained) cannot be precisely extracted, meaning particles end up in the sample that should not have and vice versa. Finally, IPEs mean all errors caused by incorrect processing of the sample after extraction and consist of six elements: contamination by foreign material, loss of material (e.g. dust), alteration in chemical and alteration in physical composition, involuntary operator faults and deliberate faults for manipulating results (Gy 2004b).

Replication experiment

The GEE manifested as the variability of repeated sampling can be quantified through a REx as described in DS 3077 (Danish Standards Foundation 2013). It is performed by extracting and analysing replicate samples of the same lot. The variability in analytical results obtained for these repeated samples is then expressed through the relative sampling variability (RSV), giving a measure for sampling quality evaluation. It is calculated according to Eq. (8), where s [arbitrary concentration unit (conc. u.)] is the standard deviation and $\bar{x}$ [conc. u.] is the arithmetic mean of the concentrations of a specific analyte in the repeated samples—functioning as an estimate for the true value.

$$\mathrm{RSV}_{[\%]} = \frac{s}{\bar{x}} \cdot 100_{[\%]} \tag{8}$$

In this investigation, the single samples cover equal time spans in which material falls from the conveyor belt. Hence, for calculating $\bar{x}$, the contribution of each sample needs to be weighted by sample mass, as time spans with lower throughputs contribute less to the concentrations in the total lot. Therefore, $\bar{x}$ is calculated according to Eq. (9), where $m_{\mathrm{sam},k}$ is the sample mass [kg] of the kth replicate sample and x_k [conc. u.] is the concentration of a specific analyte according to sample k. As each of the samples is equally likely to be taken, s is calculated without weighting, according to Eq. (10), where n [–] is the number of samples.

$$\bar{x} = \frac{\sum_k x_k \cdot m_{\mathrm{sam},k}}{\sum_k m_{\mathrm{sam},k}} \tag{9}$$

$$s = \sqrt{\frac{1}{n-1} \cdot \sum_k \left(x_k - \bar{x}\right)^2} \tag{10}$$

According to DS 3077, the absolute minimum number of replicates for performing a REx is 10 (Danish Standards Foundation 2013). Due to the enormous amount of manual work needed in waste sorting analytics, this minimum number of samples is chosen for this work. Furthermore, the standard gives guidance for RSV interpretation, stating that 20% is a consensus acceptance threshold. This value is to be understood as a rough indication—the threshold applied in practice needs to be defined based on the potential impacts of analytical uncertainties.

Shredding experiment and primary sampling

Experimental set-up

The shredding experiment in this investigation was performed using a mobile single-shaft coarse shredder Terminator 5000 SD with the F-type cutting unit from the Austrian company Komptech (Fig. 2). It was fed using an ordinary wheel loader. The shredding product was discharged using the conveyor belt included in the machine, forming a windrow.

The experiment was performed operating the machine on 60% of the maximum shaft rotation speed (18.6 rpm) and with the cutting gap completely closed. The waste used was MCW from Styria in Austria.

Sample and increment mass

For defining the total sample mass to be taken, in this work the Austrian standard ÖNORM S 2127 was considered as a reference. Multiplying the minimum increment mass from Eq. (1) with the minimum number of increments, which is 10, and considering that the expected amount of waste to be processed in the experiment is less than 200 t, the minimum sample mass m_{sam} is calculated according to Eq. (11). With

400 mm being a conservative estimate for d_{95} from prior experiments, a minimum sample mass of 240 kg is defined.

$$m_{\mathrm{sam}\,[\mathrm{kg}]} \geq 0.6 \cdot d_{95[\mathrm{mm}]} \tag{11}$$

As a rising number of increments forming a sample of a mass m_{sam} leads to better spatial coverage of the lot, it is very likely that dividing this mass into more than 10 increments—resulting in values for m_{inc} lower than defined by Eq. (1)—does not negatively influence sampling quality, but rather improve it while keeping the total mass to be analysed constant. For practical reasons consisting of the manageable sample device volume and increment mass when sampling by hand, as well as the maximum practicable sampling frequency and the target of keeping the experimental duration as short as possible because of the high throughput, 20 was chosen as the number of increments, resulting in a minimum increment mass of 12 kg.

Practical implementation of primary sampling

For reasons of practical implementation, sampling during the shredding experiments was performed by hand. This was done by holding a suitable open container into the falling stream at the end of the product conveyor belt, allowing preferable one-dimensional sampling. The container was held by two people standing at each side of the conveyor belt. At certain times, they received a starting signal to introduce the container into the stream. After a defined time (determination described below), the container was removed, containing one increment. To guarantee the accessibility of the belt, it was kept low during sampling intervals, needing the shredder to keep moving in the opposite direction of the output material stream, forming a long windrow.

According to CEN/TR 15310, each dimension of the sampling device should be at least three times as long as d_{95}, to allow the entry of all particles (European Committee for Standardization 2006). For the described sampling method, a container of $(1.2\ \mathrm{m})^3$ would have been unmanageable. The inner dimensions of the sampling device used (built from two mortar buckets) are $1.17 \times 0.37 \times 0.30$ (length × width × depth in m), which corresponds to a volume of $0.13\ \mathrm{m}^3$. With the width of the conveyor belt being 1 m and holding the device very close to the belt, it was observed that all falling material entered the container.

Fig. 2 Feeding of Komptech Terminator 5000 SD

For determining the duration of each sampling step, the mass flow was estimated at the beginning of the experiment. To do so, the mean volume flow on the conveyor belt was measured for a duration of 3 min using a laser triangulation measurement bar above the end of the belt. The REx was part of an experimental series: prior to the experiment, a calibration experiment was performed, processing a total mass of 3.5 t for linking volume flows to mass flows. It showed a bulk density of $161.8\ \mathrm{kg/m}^3$. At the end of the three minutes, the sampling duration for the extraction of an increment, t_{inc} was calculated from the average volume flow $\dot{V}$, the bulk density estimate ρ and the target increment mass m_{inc} of 12 kg, according to Eq. (12), rounding up to time intervals of 0.5 s. This resulted in a t_{inc} value of 4 s.

$$t_{\mathrm{inc}\,[\mathrm{s}]} = 0.5 \cdot \left\lceil 2 \cdot \frac{m_{\mathrm{inc}\,[\mathrm{kg}]}}{\dot{V}_{[\mathrm{m}^3/\mathrm{s}]} \cdot \rho_{[\mathrm{kg/m}^3]}} \right\rceil \tag{12}$$

The first sample was taken after an operation time of 5 min, three for averaging mass flow and two for performing the corresponding calculation and for instructing the sampling teams.

Having four sampling teams of two people each and four sampling devices, a sampling interval of 30 s was feasible. The assignment of the increments to the ten samples was alternated, leading to a sampling interval of 5 min for each sample. After a total time of 107 min, the experiment was completed.

Sample processing

Each sample taken was collected in seven waste disposal bins of 220 l each. From there, the path to the particle size–material matrix is a sequence of mass reduction, screening and sorting, as shown in Fig. 3. The single steps are described in the following subchapters.

Mass check and mass reduction

The lower the sample mass, the lower the efforts for screening and sorting. Thus, the primary samples, as well as fine fractions produced through screening, are subject to a mass check. There, it is evaluated whether mass reduction is applicable. Reasons for masses higher than needed are high momentary throughputs during primary sampling time intervals, as well as low coarse fraction shares, while minimum fine fraction masses are recalculated with the new maximum particle diameter, according to Eq. (11). In this work, it was

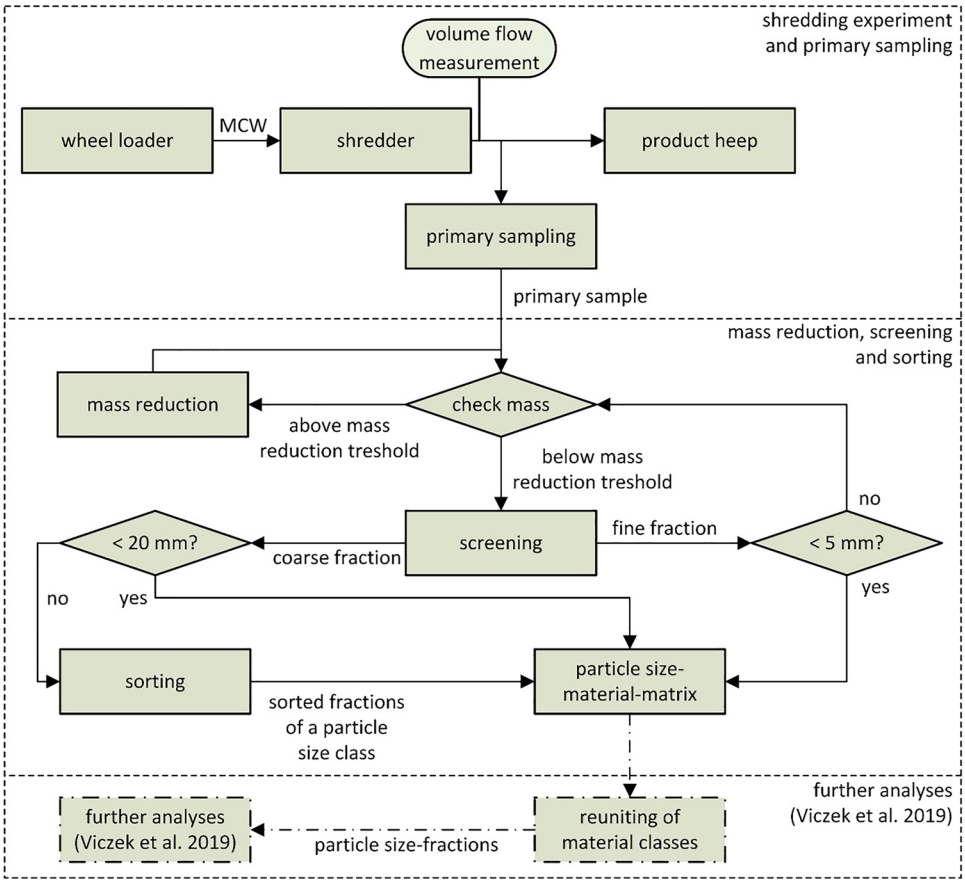

Fig. 3 Sample processing flowsheet

decided to apply mass reduction, when at least 30% of the material can be discarded while adding a safety buffer of 10% of the minimum mass to be kept. This is the case if the inequality shown in Eq. (13) is true for the mass of the evaluated sample part m_{part}, the maximum particle diameter d_{max}, as defined by the preceding screening step (400 mm for the primary sample), and a mass reduction factor f_{red} [–] of 0.7. Discarding less material was considered as not being feasible due to the needed effort for mass reduction. The mass reduction factor defines the fraction of the sample that is preserved. Three possible values for f_{red} were defined, being 0.5, 0.6, and 0.7, respectively. The lowest valid one according to Eq. (13) is chosen. Lower values were not applied, to support spatial coverage of the sample part by taking at least five increments when applying mass reduction, which is a process of subsampling. Being such, it needs to be kept in mind, that all of the described potential sampling errors also apply to subsampling and are added to the primary sampling error. On the other hand, the latter is smaller for these fractions than for coarse ones, due to lower average particle masses, leading to more contained particles per mass.

$$m_{\text{part}\,[\text{kg}]} \geq \frac{0.66 \cdot d_{\text{max}\,[\text{mm}]}}{f_{\text{red}\,[-]}} \tag{13}$$

Various implementations of mass reduction were described and evaluated by Petersen et al. (2004). Most of them, like riffle splitters, revolver splitters or Boerner dividers are not applicable, as they require the material to be pourable. This is not the case with coarse MCW, which has a high agglomeration tendency. Others, like alternate or fractional shovelling (Petersen et al. 2004) or coning and quartering (Wagner and Esbensen 2012), which are often used for waste mass reduction, show high sampling errors according to the references. Therefore, a mass reduction procedure based on the method of bed blending as described by Wagner and Esbensen (2012) was applied—a comparable approach was used by Pedersen and Jensen (2015) while sampling impregnated wood waste in Denmark.

The sample to be reduced was emptied onto a plastic foil to avoid contamination from the floor or possible loss of material. On this foil, it was spread out, forming an evenly distributed windrow of a length of 5 m (Fig. 4). Using random numbers from 1 to 10 a number of 5–7 segments (0.5 m each)—depending on f_{red}—was chosen for preservation. The other segments were extracted from the windrow and pushed to the floor beside the plastic foil, using a broom. To support this, lines with a distance of 0.5 m were drawn on the

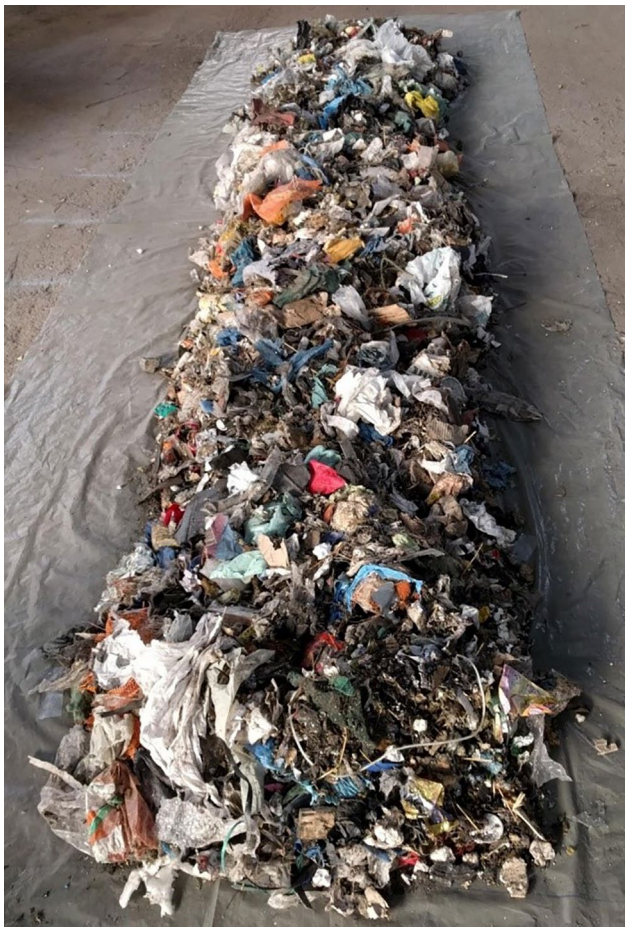

Fig. 4 Windrow for mass reduction

floor next to the foil and on the foil in advance for increment delimitation. The material to be preserved as well as the material to be discarded was shovelled into containers to be weighed. From these masses (i.e. preserved: m_{pres}, discarded: m_{disc}) the real reduction factor f^{*}_{red} [–] is calculated according to Eq. (14).

$$f^{*}_{\mathrm{red}} = \frac{m_{\mathrm{pres}}}{m_{\mathrm{pres}} + m_{\mathrm{disc}}} \tag{14}$$

Screening

The samples were screened into nine different particle size classes, using screen plates with circular holes of eight different diameters. Screening was performed using a batch drum screen, which has the shape of an equilateral octagonal prism formed by the screen plates. The dimensions are shown in Fig. 5. Screen plates with the following hole diameters were used (in mm): 200, 100, 80, 60, 40, 20, 10, and 5. The screen was operated using material batches of 75 l for screen cuts of 20–200 mm. The volumetric batch size was reduced by 50% for the smaller ones, as the high mass of the material, caused by the higher bulk density of finer fractions, would have overworked the motor of the screen. Screening times were chosen based on experience, ensuring mass constancy: 180 s for screen cuts of 40–200 mm and 270 s for the smallest three screen cuts. The rotation speed of the screen was set to 5 rpm.

Sorting and mixing

Coarse fractions produced in the screening steps that have particle sizes larger than 20 mm (i.e. in total six fractions), were hand-sorted into nine different material classes. Finer material (i.e. three fractions having particle sizes smaller than 20 mm) was not sorted due to infeasibility, considering the immense amount of work needed to sort such fine materials. Furthermore, finer materials are rarely sorted in practical analyses, as processing them in treatment plants for extracting valuable materials is often disproportionately costly. The material classes were chosen in regard to potential valuables (i.e. from the waste management point of view) contained in the waste, they are: metals (ME), wood (WO), paper (PA), cardboard (CB), plastics 2D (2D), plastics 3D (3D), inert materials including glass (IN), textiles (TX), and a residual fraction (RE). Fractions finer than 20 mm were assigned to the residual fraction. After weighing the sorted fractions, they were joined again, as the subsequent chemical analysis was performed for each particle size class, but not for individual sorting fractions.

Weighing

The weighing was carried out using two different scales. The bigger scale was used for containers with a filled weight higher than 30 kg. With a maximum container weight of about 16 kg, this corresponds to partial samples with a weight of up to 14 kg. The uncertainty of this scale is 100 g. Lighter containers were weighed using a scale with an uncertainty of 0.1 g.

In practice, this means that screening fractions and mass reduction fractions were usually weighed using the big scale. Sorting results were always weighed using the more precise small scale.

Calculations

Particle size–material matrices

The particle size–material matrices regarding masses $\mathbf{M}$ are $v \times w$ matrices, where the elements m_{ij} represent the mass of

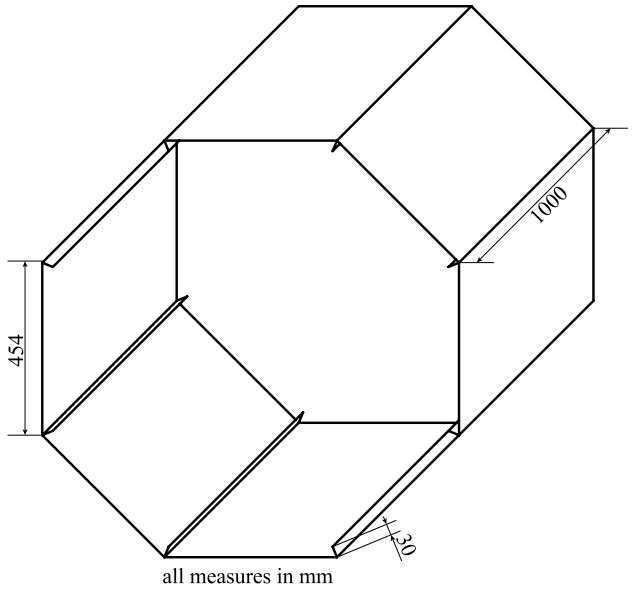

Fig. 5 Dimensions of the screening drum

the ith of v particle size classes and the jth of w material classes in an original sample. The assignment of the indices to the classes is shown in Table 1. For calculating the masses in the original sample, mass reduction steps must be considered mathematically. Thus, the mass m_{ij} is calculated according to Eq. (15), where m_{ij}^* is the mass weighed in the sorting analysis and $f_{\mathrm{red},r}^*$ is the real mass reduction factor (according to Eq. 14), when reducing the fine fraction produced in the $(r-1)$th screening step. $r = 1$ stands for the original material (0–400 mm) and $f_{\mathrm{red},r}^*$ is 1 if no mass reduction was performed.

$$m_{ij} = \frac{m_{ij}^*}{\prod_{r=1}^{i} f_{\mathrm{red},r}^*} \tag{15}$$

The elements w_{ij} of the particle size–material matrices regarding mass fractions $\mathbf{W}$ represent the shares of masses m_{ij} of the total sample mass and are calculated according to Eq. (16):

$$w_{ij} = \frac{m_{ij}}{\sum_{i=1}^{v}\sum_{j=1}^{w} m_{ij}} \tag{16}$$

As the definition of material classes as well as the choice of screen cuts is arbitrary, further classes can be defined and evaluated by summing up the masses of specific fractions. This allows calculating standard deviations and RSV values for the mass shares of larger fractions, up to the total material. To calculate all different combinations of materials, a binary matrix $\mathbf{B}_w$ containing all possible combinations of ones and zeros for w digits is needed. To generate it, the j column of the matrix contains the w-digit binary representation of the number j, while each of the w rows contains one digit. For w digits, the matrix has $(w^2 - 1)$ columns. For the actual data, w is 9. Equation (17) shows the matrix $\mathbf{B}_4$ as an example.

$$\mathbf{B}_4 = \begin{bmatrix} 0&0&0&0&0&0&0&1&1&1&1&1&1&1&1 \\ 0&0&0&1&1&1&1&0&0&0&0&1&1&1&1 \\ 0&1&1&0&0&1&1&0&0&1&1&0&0&1&1 \\ 1&0&1&0&1&0&1&0&1&0&1&0&1&0&1 \end{bmatrix} \tag{17}$$

Regarding particle size, only adjacent classes are combined, corresponding to an alternating choice of screen cuts. For v particle size classes a binary matrix $\mathbf{A}_v$ is needed, containing all possible combinations of zeros and 1 to v adjacent ones in its rows. The matrix has v columns and $(v \cdot (v+1)/2)$ rows. For the present data, v is 9. Equation (18) shows the matrix $\mathbf{A}_4$ as an example.

$$\mathbf{A}_4 = \begin{bmatrix} 0&0&0&1&0&0&1&0&1&1 \\ 0&0&1&0&0&1&1&1&1&1 \\ 0&1&0&0&1&1&0&1&1&1 \\ 1&0&0&0&1&0&0&1&0&1 \end{bmatrix}^{\mathrm{T}} \tag{18}$$

The matrices $\mathbf{W}_{\mathrm{mp}}$, containing the weight fractions of all possible combinations of materials and adjacent particle sizes, are calculated according to Eq. (19) and have 45 rows and 511 columns.

$$\mathbf{W}_{\mathrm{mp}} = \mathbf{A}_9 \cdot \mathbf{W} \cdot \mathbf{B}_9 \tag{19}$$

Table 1 Assignment of indices to particle size classes (i) and materials classes (j)

index *i*/*j*	1	2	3	4	5	6	7	8	9
Size class [mm]	200–400	100–200	80–100	60–80	40–60	20–40	10–20	5–10	0–5
Material class	ME	WO	PA	CB	2D	3D	IN	TX	RE

Results and discussion

Process and material analysis and primary sampling mass

The mean throughput—determined at the end of the experiment—was 25.2 t/h or 71.8 m^3/h, resulting in a total mass of 45.0 t, a total bulk volume of 128.1 m^3 on the product conveyor belt and thus a bulk density of 351.4 kg/m^3. This means that the bulk density of the shredded material of the REx is much higher than the expected density of 161.8 kg/m^3. Still, the target primary sample masses were approximately achieved, with a mean of 241 kg, a standard deviation of 22 kg, a minimum of 215 kg, and a maximum of 284 kg. The weighted mean values of the particle size–material matrix as well as of the sums of size classes and material classes are shown in Table 2.

Sampling error

The relative sampling variabilities related to the material classes in Table 2 are shown in Table 3. Beyond that, Fig. 6 shows the RSV values as well as the standard deviations *s* for all 22,995 classes in the matrices $\mathbf{W}_{mp}$, plotted against the correspondent weighted mean values. The grey triangles mark the data corresponding to the original matrices **W**.

Table 2 Weighted means of particle size–material fractions' mass shares

Particle class [mm]	ME (%)	WO (%)	PA (%)	CB (%)	2D (%)	3D (%)	IN (%)	TX (%)	RE (%)	Sum (%)
0–5	0.0[a]	0.0[a]	0.0[a]	0.0[a]	0.0[a]	0.0[a]	0.0[a]	0.0[a]	17.1[a]	17.1
5–10	0.0[a]	0.0[a]	0.0[a]	0.0[a]	0.0[a]	0.0[a]	0.0[a]	0.0[a]	6.5[a]	6.5
10–20	0.0[a]	0.0[a]	0.0[a]	0.0[a]	0.0[a]	0.0[a]	0.0[a]	0.0[a]	11.0[a]	11.0
20–40	0.7	1.4	0.8	2.1	0.4	2.3	2.1	0.1	2.2	12.1
40–60	0.8	1.8	0.9	2.5	0.5	2.0	1.0	0.1	2.2	11.8
60–80	1.0	2.0	1.0	2.1	0.7	2.3	0.5	0.5	2.2	12.3
80–100	0.7	1.0	0.7	1.3	0.6	1.7	0.2	0.4	1.4	7.9
100–200	1.0	0.9	0.9	4.7	2.2	3.3	0.4	1.7	2.6	17.6
200–400	0.1	0.0	0.0	0.2	1.1	0.7	0.0	1.1	0.7	3.8
Sum	4.4	7.1	4.3	12.8	5.5	12.2	4.1	3.9	45.8	100.0

[a]Particle size fraction was not sorted: complete material was assigned to the residual fraction with: metals (ME), wood (WO), paper (PA), cardboard (CB), plastics 2D (2D), plastics 3D (3D), inert material (IN), textiles (TX) and residual fraction (RE)

Table 3 RSV values

Particle class [mm]	ME (%)	WO (%)	PA (%)	CB (%)	2D (%)	3D (%)	IN (%)	TX (%)	RE (%)	Sum (%)
0–5	-	-	-	-	-	-	-	-	12.3	12.3
5–10	-	-	-	-	-	-	-	-	12.3	12.3
10–20	-	-	-	-	-	-	-	-	10.4	10.4
20–40	41.4	17.7	24.3	39.3	18.4	17.1	19.7	29.3	22.7	11.6
40–60	47.3	21.5	16.8	25.6	14.2	8.7	37.2	43.4	16.4	8.8
60–80	39.4	23.3	22.9	18.1	17.7	10.0	49.9	30.4	8.9	8.1
80–100	62.0	34.7	38.0	14.2	19.3	17.5	210.7	43.4	17.2	7.7
100–200	74.0	47.7	69.0	21.6	28.9	35.2	131.8	40.9	40.0	10.9
200–400	153.0	230.9	203.9	126.2	38.3	39.8	-	42.9	52.2	28.8
Sum	16.4	18.3	10.5	15.0	16.6	12.1	31.2	26.6	3.6	0.0

RSV < 20% | 20% ˜ RSV < 50 % | RSV ° 50%

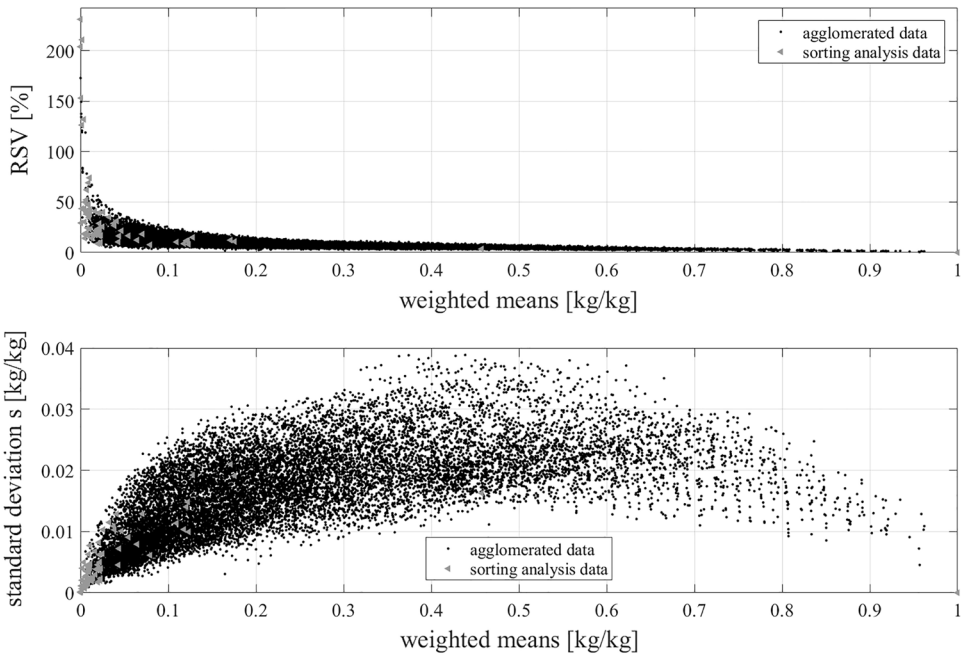

Fig. 6 RSV and standard deviation versus weighted mean of mass shares

Incorrect sampling errors

Primary sampling

Increment delimitation is done by defining time intervals during which all material falling from the product conveyor belt of the shredder is collected. Therefore, no IDEs are expected.

Correct increment extraction, on the other hand, turns out to be challenging: some increments could not be taken at the defined time, because the end of the conveyor belt was too high. The reason for this was the wheel loader feeding material into the shredder, not allowing the latter to move forward. Because of this, the belt had to be elevated, producing a higher heap. In these situations, increment extraction started as soon as it was possible again. Furthermore, communication between the samplers and the person responsible for timing was difficult during sampling, due to the loudness of the machine. Because of this, the end of the defined 4 s of sampling was determined by the samplers through counting. Considering the real mass flow of 25.2 t/h, the average sample mass with 20 increments of 4 s each would have been 560 kg, while the observed average was less than half of that, i.e. about 241 kg. Consequently, it can be assumed that the real sampling time was less than 2 s, because of the subjective sense of time, which might also have been influenced by the weight of the increments taken. Nonetheless, this did not negatively affect the target sample mass of 240 kg. Furthermore, all samples fulfil Eq. (11) as the empirical value for d_{95} is 194 mm (calculated through linear interpolation from Table 2). Still, the deviation from the defined sampling time of 4 s is not very likely to be uniform, leading to scattering of real sampling time and thus to IEE.

Regarding IPE, it cannot be assured that all particles of the taken increments reached the final samples, as handling the bulky sampling device, which is also heavy when filled, might have led to unintentional falling out of some particles.

Mass reduction

Mass reduction is a subsampling process. Consequently, all potential sampling errors might as well occur at this step. Regarding increment delimitation, drawing the equidistant lines on the foil is a quite exact process. So—if IDEs occur at all—the order of magnitude should be negligible compared to IEE:

Extracting the increments correctly turned out to be problematic, especially for coarse fractions. This is because of material wedging, impeding pourability. Because of this, when pushing the segments to be discarded from the foil, it was unavoidable to extract material from the neighbouring segments as well. Therefore, IEE could not be completely avoided with the mass reduction method applied.

Regarding increment preparation, the main expectable error is loss of dust blown away when handling the material.

Screening and sorting

As screening and sorting are not sampling operations, IDE and IEE cannot occur. IPE, on the other hand, are expected

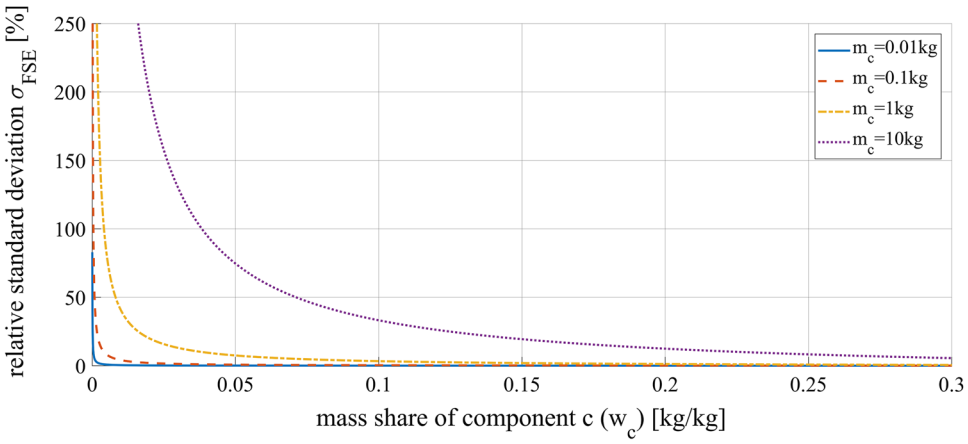

Fig. 7 Relative standard error caused by FSE versus mass share of a constituent c of a two-component composition, according to Eq. (7), for different average particle masses m_c of constituent c with a lot mass of 45,000 kg, a sample mass of 240 kg and an average particle mass for the other constituent k of 0.1 kg

due to blowing away of dust, as well as the loss of particles falling from the sorting table unnoticed.

Loss of water

The samples taken were processed during several weeks. Although stored in closed disposal bins, loss of humidity is possible as the bins are not hermetical, leading to IPE.

The total loss of material, calculated comparing the sum of the individual fraction masses according to Eq. (14) to the primary sample masses, shows a mean value of 5.6% and ranges between 4.6 and 7.2%.

Container and equipment contamination

For practical reasons, before reusing containers, and equipment like the screen or shovels, they could only be cleaned using hand brushes. Thus, cross-contamination of different samples and subsamples cannot be completely excluded, leading to further potential IPE. These contaminations are expected to be low, due to small contact areas in relation to sample masses.

Sampling quality

Applying an RSV of 20% as a threshold for good sampling, Table 3 shows that the applied procedure only produces good results for some of the examined fractions. Figure 6 further shows that RSV tends to be better for large fractions, indicating that small fractions require better sampling and analytics for achieving acceptable relative errors. This is the case, although the absolute standard deviation seems to increase with mass share, reaching a maximum for fraction ratios of 50%.

Figure 7 shows the RSV contribution of the FSE over the mass share (according to Eq. 7) of a constituent c for different average particle masses m_c for the present lot mass and target primary sample mass, assuming a two-component composition. For the average particle mass of the other constituent m_k a value of 0.1 kg was chosen. m_k has little influence on σ_{FSE}, as long as it is significantly smaller than the sample mass m_{sam}. Comparing Figs. 6 and 7, it is apparent that the general trend of the empirical RSV shows similarities to the trend of the FSE's contribution to the sampling error. Especially for coarse particles which are either heavy (e.g. metal 100–200), have very low mass shares (e.g. paper 200–400), or both (e.g. metal 200–400), the FSE explains very well why RSVs far beyond 20% were observed.

However, keeping in mind that only few particle size-material fractions—if any—have average particle masses as high as 1 kg, the figures show that primary sampling FSE only explains part of the observed sampling errors. For example, for a fraction with a mass share of 0.1 σ_{FSE} is 3.4% in Fig. 7, while the RSV values in Fig. 6 range somewhere between 5 and 25%. Therefore, other sampling errors obviously also show significant contributions. Wavrer (2018) highlights the high distributional heterogeneity of municipal solid waste. For MCW, it is known to be even higher, therefore the GSE is likely to significantly contribute to the sampling error. Furthermore, the described ISEs, as well as CSEs and ISEs from subsampling also contribute to the observed RSVs. These contributions, along with the different average particle masses and numbers of subsampling stages for the different data points, as well as errors in estimating RSV due to the low number of 10 taken samples, also explain the scattering of the data in Fig. 6 along the ordinate axis.

Knowing the standard deviation, confidence intervals for estimated concentrations can be calculated as a corresponding

measure. But doing so, care has to be taken for very large RSVs: the high relative errors indicate a positively skewed distribution of the values (and therefore not a normal distribution), as commonly used confidence intervals like 95% would otherwise include negative percentages. Ultimately, the quality of sampling needs to be rated dependent on the analytical target.

Conclusion

A sampling and sample processing procedure for screening and sorting analysis of shredded mixed (i.e. commercial) solid waste was established and is reported, based on the TOS, the Danish horizontal sampling standard DS 3077 and the Austrian standard ÖNORM S 2127. Assessment of sampling quality, rated through the relative sampling variability, shows that the procedure gives good results for some values of the particle size-material matrix (at a threshold of 20%) but not for all of them—it gets as bad as 231%. It is further shown that the RSV is better for larger fractions. In conclusion, especially when analysing small fractions, a reduction in the occurring sampling errors is necessary. Regarding the CSEs, in a first step, it should be assured that the sample mass suffices to keep the FSE within a reasonable range. For this, building a database of typical particle masses, as suggested by Wavrer (2018), is highly encouraged. Equation (7) then provides a (necessary, but not sufficient) minimum sample mass.

As it was shown that FSE only contributes a part of the observed RSVs, compensating the high distributional heterogeneity of the waste by increasing the number of increments might also significantly improve sampling quality by reducing GSE. To handle the resulting higher sampling frequencies, automated primary sampling, e.g. using a reversible conveyor belt, is encouraged.

Such automated sampling might as well contribute to reducing ISEs, i.e. IEEs, as it allows to extract samples exactly in time, while still preserving the benefits of sampling from a falling stream (one-dimensional sampling and good separation of agglomerated particles). Moreover, IEEs during mass reduction (caused by agglomerations, especially for coarse fractions) could as well be reduced by (automatic) subsampling from a falling stream. Furthermore, the analytical error can be decreased by using a more precise big scale.

Finally, when evaluating very small fractions through screening and sorting, increasing sample masses will be unavoidable for reliable analyses. In addition to the discussed estimation of the FSE, the determined values for the RSV help to estimate them in advance.

Acknowledgements Open access funding provided by Montanuniversität Leoben. The Competence Center Recycling and Recovery of Waste 4.0—ReWaste4.0—(Grant Number 860 884) is funded by the Austrian Federal Ministry of Transport, Innovation and Technology (BMVIT), Austrian Federal Ministry of Science, Research and Economy (BMWFW) and the Federal Province of Styria, within COMET—Competence Centers for Excellent Technologies. The COMET programme is administered by the Austrian Research Promotion Agency (FFG).

Compliance with ethical standards

Conflict of interest The authors declare that they have no conflict of interest.

References

Austrian Standards Institute (2011) ÖNORM S 2127 Grundlegende Charakterisierung von Abfallhaufen oder von festen Abfällen aus Behältnissen und Transportfahrzeugen [Basic characterization of waste heaps or solid wastes from containers and transport vehicles]. Austrian Standards Institute, Vienna. ICS: 13.030.01

Danish Standards Foundation (2013) DS 3077 Representative sampling—Horizontal standard. Danish Standards Foundation, Charlottenlund. ICS: 03.120.30, 13.080.05

Esbensen KH, Julius LP (2009) Representative sampling, data quality, validation—a necessary trinity in chemometrics. In: Tauler R, Walczak B, Brown SD (eds) Comprehensive chemometrics: chemical and biochemical data analysis, 1st edn. Elservier, Burlington, pp 1–20

Esbensen KH, Wagner C (2014) Theory of sampling (TOS) versus measurement uncertainty (MU)—a call for integration. TrAC. https://doi.org/10.1016/j.trac.2014.02.007

European Committee for Standardization (2006) CEN/TR 15310-1 characterisation of waste—sampling of waste materials—part 1: guidance on selection and application of criteria for sampling under various conditions. European Committee for Standardization, Brussels. ICS: 13.030.10, 13.030.20

Felsenstein K, Spangl B (2017) Richtlinien für die statistische Auswertung von Sortieranalysen und Stückgewichtsanalysen [Guidelines for statistical evaluation of sorting and particle mass analyses], pp 34–68. http://www.argeabfallverband.at/fileadmin/bilder/PDFs/Anhaenge_RA_OOE_2018.pdf. Accessed 19 Mar 2019

Gy P (2004a) Sampling of discrete materials: II. Quantitative approach—sampling of zero-dimensional objects. Chemom Intell Lab Syst 74(1):25–38. https://doi.org/10.1016/j.chemolab.2004.05.015

Gy P (2004b) Sampling of discrete materials—a new introduction to the theory of sampling: I. Qualitative approach. Chemom Intell Lab Syst 74(1):7–24. https://doi.org/10.1016/j.chemolab.2004.05.012

Pedersen PB, Jensen JH (2015) Representative sampling for a full-scale incineration plant test—how to succeed with TOS facing

unavoidable logistical and practical constraints. TOS Forum 3(1):213–217

Petersen L, Dahl KD, Esbensen KH (2004) Representative mass reduction in sampling—a critical survey of techniques and hardware. Chemom Intell Lab Syst 74(1):95–114. https://doi.org/10.1016/j.chemolab.2004.03.020

Viczek SA, Khodier K, Aldrian A, Sarc S (2019) Sampling and analysis of coarsely shredded mixed commercial waste; part II: grain size dependent elemental distribution. In preparation for submission in a peer reviewed process (status Aug 2019)

Wagner C, Esbensen KH (2012) A critical review of sampling standards for solid biofuels—missing contributions from the theory of sampling (TOS). Renew Sustain Energy Rev 16(1):504–517. https://doi.org/10.1016/j.rser.2011.08.016

Wavrer P (2018) Theory of sampling (TOS) applied to characterisation of municipal solid waste (MSW)—a case study from France. TOS Forum 5(1):3–11

3.4 Publication IV

Sampling and analysis of coarsely shredded mixed commercial waste. Part II: particle size-dependent element determination

S.A. Viczek, L. Kandlbauer, K. Khodier, A. Aldrian, R. Sarc

Submitted to journal: January 04, 2021;
Status on March 24, 2021: Under review since January 13, 2021.

Author Contributions (CRediT Contributor Roles Taxonomy):

SV: Conceptualization, Methodology, Formal analysis, Investigation, Data curation, Writing – original draft preparation, Writing – review and editing, Visualization, Project administration;

LK: Formal Analysis, Investigation, Writing – original draft preparation, Writing – review and editing, Visualization;

KK: Conceptualization, Methodology, Formal Analysis, Investigation, Writing – review and editing;

AA: Methodology, Resources;

RS: Conceptualization, Writing – review and editing, Supervision, Funding acquisition.

Manuscript – under review

Sampling and analysis of coarsely shredded mixed commercial waste. Part II: particle size-dependent element determination

S.A. Viczek[a], L. Kandlbauer[a], K. Khodier[b], A. Aldrian[a], and R. Sarc[a]*

[a] *Chair of Waste Processing Technology and Waste Management, Department of Environmental and Energy Process Engineering, Montanuniversitaet Leoben, Franz-Josef-Strasse 18, 8700 Leoben, Austria*

[b] *Chair of Process Technology and Industrial Environmental Protection, Department of Environmental and Energy Process Engineering, Montanuniversitaet Leoben, Franz-Josef-Strasse 18, 8700 Leoben, Austria*

*Corresponding author. E-mail address: renato.sarc@unileoben.ac.at (R. Sarc)

Abstract: In contemporary waste management, sampling of waste is essential whenever a specific parameter needs to be determined. Although sensor-based continuous analysis methods are being developed and enhanced, many parameters still require conventional analytics. Therefore, sampling procedures that provide representative samples of waste streams and enable sufficiently accurate analysis results are crucial. While Part I estimated the relative sampling variabilities (RSV) for material classes in a replication experiment, Part II focuses on RSVs for 30 chemical elements and the lower heating value (LHV) of the same samples, i.e., 10 composite samples screened to yield 9 particle size classes (< 5 mm to 400 mm). RSVs <20% were achieved for 39% of element-particle size class combinations but ranged up to 203.5%. When calculated for the original composite samples, RSVs <20% were found for 57% of the analysis parameters. High RSVs were observed for elements that are expectedly subject to high constitutional heterogeneity. Besides depending on the element, RSVs were found to depend on particle size and the mass of the particle size fraction in the sample. Furthermore, Part I and Part II results were combined, and the correlations between material composition and element concentrations in the particle size classes were interpreted and discussed. For interpretation purposes, log-ratios were calculated from the material compositions. They were used to build a regression model predicting element concentration based on material composition only. In most cases, a prediction accuracy of +/-20% of the expected value was reached, implying that a mathematical relationship exists.

Keywords: contaminants, element-material correlation, heavy metals, mixed commercial waste (MCW), replication experiment, solid recovered fuel (SRF)

1 Introduction

The assessment of the quality and the categorization of waste are usually based on various analytical results. Chemical parameters that are particularly important for quality assessment are the concentrations of various heavy metals, metalloids, and other inorganic contaminants (cf. EC 2008a Annex III; EC 2008b Annex VI). These elements frequently occur in mixed commercial waste (MCW) and mixed municipal solid waste (MMSW) because they are present in various consumer goods and materials (e.g. Turner 2019; Turner and Filella 2017; Viczek et al. 2020). Their concentrations play a decisive role in various waste processing options (see section 1.1). However, because usually "analytical results are estimates of unknown quantities" (Gy 1995), they are subject to uncertainties, many of which are related to heterogeneity. Since mixed solid wastes are usually highly heterogeneous and tend to segregate (Pomberger et al. 2015), sampling of waste can be challenging.

Fig. 1 shows an example of uncertainties related to the different steps of the analytical procedure at the example of lead (Pomberger et al. 2015). Flamme and Gallenkemper (2001) state even higher analysis uncertainties: the uncertainty related to sampling can range up to 1000% if the sample is taken from a stationary waste pile, and uncertainties of 100 to 300% can be expected for sample preparation. While the propagation of uncertainties in all process steps leads to a general variance of the analysis results (Krämer et al. 2016), the contribution of primary sampling to the measurement uncertainty and variability is often dominant (Ellison and Williams 2012; Esbensen and Julius 2009; Ramsey et al. 2019). For this reason, reliable and representative sampling is crucial. Although various sampling standards exist, the sampling quality can still be influenced by on-site circumstances (e.g., the possibility to take the sample from the falling stream or a stationary pile).

Because of the effort, errors, and uncertainties related to the sampling of heterogeneous waste materials, researchers are also looking for continuous, real-time methods to determine specific parameters in waste. The investigated methods are usually sensor-based and aiming at ideally generating results without sampling and sample preparation procedures. Real-time methods for the characterization of solid waste are reviewed in detail by Vrancken et al. (2017) and include laser-induced breakdown spectroscopy (LIBS), X-ray, or near-infrared (NIR) technology. The most established of these techniques in the waste sector is NIR, which has been used for sorting purposes since the 1990s (Krämer et al. 2016). NIR technology was found to deliver good real-time results for solid recovered fuels for the higher heating value (HHV), lower heating value (LHV), water, ash, and Cl content. However, results achieved for Sb, Cd, Pb, and Cr are currently considered insufficient for quantitative analyses, and real-time measurements should be limited to qualitative analyses (Krämer et al. 2016; Krämer 2017).

However, as long as real-time technologies are not applicable for all relevant parameters, need further enhancement or comparison with results from conventional analyses, and are not state of the art in waste treatment plants, sampling remains crucial to determine the properties of waste streams and the related uncertainties need to be known and handled correctly.

Fig. 1 Uncertainties related to the single steps of the analytical procedure at the example of lead in mixed solid waste. Adapted from Pomberger et al. (2015)

1.1 Importance of heavy metal and metalloid concentrations

Concentrations of heavy metals and metalloids are not only relevant in the consumer products sector but also in the post-consumer regime. In the latter, contaminant concentrations play a significant role in determining suitable waste treatment pathways. Generally, contaminant concentrations determine whether or not a waste is considered hazardous (EC 2008a, 2008b), and in the case of non-hazardous waste, which is in the focus of this study, they can be a decisive factor for the selection or applicability of several waste treatment options:

When landfilled, leaching of certain elements from waste can pose a possible risk to the environment (Kjeldsen et al. 2002). When composted, compost quality and composition depend on the purity of the input waste (e.g., separately collected organic waste or the separated undersize fraction from mechanical biological treatment of MSW) (Andersen et al. 2010; Smith 2009), and heavy metal limits for compost standards exist in several countries (Amlinger et al. 2004). When incinerated, the amount of inorganic contaminants in the gaseous emissions which have to comply with limit values (e.g., Industrial Emissions Directive (EC 2010)) is strongly related to their amounts in the input waste (Astrup et al. 2011; Brunner and Rechberger 2015; Morf et al. 2000). Even when waste fractions are directed towards recycling, the concentration of inorganic contaminants can - among other factors - determine whether or not a particular material can indeed be recycled. Examples include plastics containing selected brominated flame retardants (Pivnenko et al. 2017; Slijkhuis 2018) or cadmium-containing PVC products (EC 2011). Another popular waste treatment option is to produce solid recovered fuels (SRF) for co-processing in cement kilns (Sarc et al. 2019). This option also requires the contaminants to be monitored because the contaminant concentrations in input fuel as well as the resulting output gaseous emissions and the product shall be kept at a low level (BMLFUW 2010). Depending on the country, compliance with limit values for certain chemical elements can either be requested directly by the cement manufacturers (Lorber et al. 2012), by quality marks (e.g., RAL GZ 724 quality mark for quality assured SRF in Germany (Flamme and Geiping 2012)), or by the legislature (e.g., Austrian Waste incineration ordinance (WIO) (BMLFUW 2010)). Limit values for inorganic contaminants in SRF may be given in mg/MJ, taking the lower heating value (LHV) into account. This is the case for mercury in EN 15359 (ASI 2011d) and the eight heavy metals regulated by the Austrian WIO (BMLFUW 2010).

Due to the importance of contaminant concentrations for all these different waste treatment options, it is evident that knowledge on their distributions in waste and possibilities for their removal before the final waste treatment is of interest. To gain this information, sampling is unavoidable and required to enable a sufficiently accurate examination of the analytes. MCW typically contains large items, e.g., mattresses or furniture parts, which is why coarse shredding followed by one or more screening stages is typically the first step of MCW processing. While this step significantly facilitates sampling, as a vision of Khodier et al. (2020), varying shredder parameters could enable waste processors to steer the concentration of different material and contaminant streams into certain particle size fractions. To assess whether this is possible, prior knowledge about sampling variability and sampling errors is required.

1.2 Theory of sampling

In the theory of sampling (TOS), variability and sampling errors can be expressed by the global estimation error (GEE), which is the relative difference between the obtained analytical result and the actual, unknown value of the parameter. It is furthermore defined as the sum of the total sampling errors (TSE) and the total analytical errors (TAE) (Gy 2004). For significantly heterogeneous materials, the TAE plays a minor role as the sum of all sampling errors is usually significantly larger. The TSE originates from the sampling process or material heterogeneity and consists of correct sampling errors (CSE) and incorrect sampling errors (ISE) (Wagner and Esbensen 2012).

CSEs are caused by heterogeneity (Wagner and Esbensen 2012), two types of which are distinguished in TOS: constitutional heterogeneity (CH) and distributional heterogeneity (DH) (Gy 2004). CH depends on the physical and/or chemical differences between individual fragments, i.e., the fact that single particles can contain small or only trace amounts of the analyte or can be almost entirely made of the analyte (e.g., iron traces in waste plastics vs. an iron particle in waste). With increasing compositional differences between the fractions, CH increases, thereby causing the fundamental sampling error. This correct sampling error can never be eliminated but can be decreased by comminution (Gy 1998; Wagner and Esbensen 2012). In contrast to CH being only dependent on material properties, DH reflects the irregular spatial distribution of the fragments in a lot (Esbensen and Wagner 2014; Wagner and Esbensen 2012). DH is caused by the tendency of fragments to locally segregate and group in space and time and is responsible for the second type of correct sampling error, the grouping, and segregation error. It can be counteracted by mixing and composite sampling, i.e., taking several small sample increments rather than fewer, larger sample increments (Wagner and Esbensen 2015).

While CSEs comprise material-specific errors that are always present in sampling situations, ISE concern the sampling equipment and procedure (Wagner and Esbensen 2015). ISE need to be minimized or eliminated where possible as they are generating bias (Wagner and Esbensen 2012). ISE consists of the increment delimitation error (IDE), the increment extraction error (IEE), and the increment preparation error (IPE). While IDE and IEE concern errors occurring during the sampling process, IPE comprises all changes to the sample during or after sampling stages, including the loss of material (moisture, dust) and contamination. (Wagner and Esbensen 2015)

One approach to estimate the GEE is to conduct a replication experiment, as described in DS 3077 (DS 2013). The replication experiment yields the relative sampling variability (RSV), also referred to as the relative coefficient of variation CV_{rel}, a measure of the total sampling variance normalized by the arithmetic mean (Esbensen and

Wagner 2014). RSV or CV_{rel}, respectively, represent the GEE and are calculated according to Equation (1), with s being the standard deviation and $\bar{x}$ being the average of a set of analytical results (DS 2013; Wagner and Esbensen 2012):

$$RSV\ [\%] = \left[\frac{s}{\bar{x}}\right] \times 100 = CV_{rel} \quad (1)$$

1.3 Connection to Part I and aim of the study

Part I of this study presented by Khodier et al. (2020) introduced the theoretical background of the TOS in greater detail and reported the results of a replication experiment for MCW and the distribution of materials in terms of sorting fractions (e.g., metal, wood, paper, cardboard, plastics 2D, plastics 3D) among nine different particle size classes. The study reports RSVs of up to 231% and found that RSVs below 20%, which is the general consensus acceptance threshold according to DS 3077, can only be achieved for less than half of the examined fractions. Furthermore, a decrease of the RSV with increasing mass shares of the fractions was observed.

The current paper, Part II, focuses on the chemical analysis of the different particle size fractions examined in Part I. While the RSVs reported by Khodier et al. (2020) mostly result from DH, the chemical analyses presented in this paper are significantly influenced by CH as well. For example, different fragments that were merely classified as plastics for the material distribution can contain significantly different concentrations of heavy metals that will be reflected by the chemical analyses. Therefore, Part II determines the RSVs and thereby the GEEs for 30 elements and compares them with the results of Khodier et al. (2020). The current study focuses on sampling aspects; therefore, analysis results are only briefly summarized to facilitate interpretations of the results. The corresponding concentrations are presented and discussed in detail, focusing on SRF production in Viczek et al. (2021b). Furthermore, the results of Part I and Part II are combined by investigating correlations between material composition and chemical analysis results, aiming to investigate whether a mathematical relationship between the element concentrations and the compositions determined by sorting analyses can be found. This may open up the opportunity to create models that enable predicting specific chemical analysis parameters based on online or manual sorting analyses.

2 Materials and Methods

2.1 Samples

A replication experiment was carried out sampling approximately 45 metric tons of MCW from the area of Graz, Austria, collected in October 2018. The waste was coarsely shredded using a mobile single-shaft coarse shredder (Komptech Terminator 5000 SD with F-type cutting unit) operating at 18.6 rpm (i.e., 60% of the maximum shaft rotation speed) and with a completely closed cutting gap. A wheel loader was used to feed the shredder that was slowly moving forward, forming a windrow of the discharge material via the shredder's discharge conveyor belt. A total of 200 sample increments (with a mass of ~12 kg each) were taken from the falling waste stream at the end of the conveyor belt using sampling troughs (length x width x height: 1.17x0.37x0.30 m) in time intervals of 30 seconds. Ten composite samples (each with a mass of ~ 240 kg) were created by combining 20 sample increments taken in time intervals of 5 minutes.

Each of the 10 composite samples was screened using a batch drum screen in multiple steps to generate 9 particle size fractions: 0–5 mm, 5–10 mm, 10–20 mm, 20–40 mm, 40–60 mm, 60–80 mm, 80–100 mm, 100–200 mm, 200–400 mm. In total, 90 samples were generated. After each screen cut, the mass of the screen underflow was determined, and the sample mass was reduced, if appropriate, see Fig. 2. Every particle size fraction > 20 mm was manually sorted to determine the material composition and was reunited for chemical analyses. For details on the procedure and calculations, cf. Khodier et al. (2020).

2.2 Chemical analyses

All 90 samples were chemically analyzed, for detailed analysis results cf. Viczek et al. (2021b). The samples were dried to constant mass at 105°C[1] to determine the dry residue according to EN 14346 (process A) (ASI 2007). Hard impurities (e.g., metal parts, stones) were removed to avoid damages to the mills. The removed impurities were weighed and can be accounted for in terms of their weight, but they were not separately analyzed, which corresponds to common laboratory practice (for a more detailed discussion, cf. Viczek et al. (2020)). The effects of this practice are discussed in section 2.3. Further sample processing included comminution to a size < 0.5 mm using cutting mills, homogenization, and mass reduction.

Concentrations of silver (Ag), aluminum (Al), arsenic (As), barium (Ba), beryllium (Be), calcium (Ca), cadmium (Cd), cobalt (Co), chromium (Cr), copper (Cu), iron (Fe), mercury (Hg), potassium (K), lithium (Li), magnesium (Mg), manganese (Mn), molybdenum (Mo), sodium (Na), nickel (Ni), phosphorus (P), lead (Pb), palladium (Pd), antimony (Sb), selenium (Se), silicon (Si), tin (Sn), strontium (Sr), tellurium (Te), titanium (Ti), thallium (Tl), vanadium (V), tungsten (W), and zinc (Zn) were determined by ICP-MS (based on EN 15411 (ASI 2011a) and EN ISO 17294-2 (ASI 2017)) after microwave-assisted acid-digestion with hydrofluoric acid (HF), nitric acid (HNO_3) and hydrochloric acid (HCl) (ÖNORM EN 13656 (ASI 2002)). Calorimetric digestion (ÖNORM EN 14582 (ASI 2016)) followed by ion chromatography (EN ISO 10304-1 (DIN 2009)) was applied to determine the chlorine (Cl) content. The lower heating value (LHV) was calculated according to DIN 51900-1 (DIN 2000), and the ash content was determined according to DIN 51719 (DIN 1997). Samples were measured as duplicates.

2.3 Handling of hard impurities

EN 15443 (ASI 2011c) states that it is essential that all materials are included in the sample when the particle size is reduced, as, e.g., removing metals significantly influences the results regarding these and other accompanying metals. However, the tools for particle size reductions listed in the standard are not suitable for the comminution of hard materials to particle sizes suitable for preparing tests or laboratory samples. According to EN 15413 (ASI 2011b), different visible fractions can be separately analyzed when this procedure enhances subsequent comminution, homogenization, or sub-sampling processes. In the case of non-shreddable materials being present, the standard suggests manual separation. The mass of every removed fraction needs to be documented to enable reporting a weighted combination of analysis results.

Separately analyzing the hard impurities is often not a viable option when either the equipment is not available to laboratories or suitable comminution aggregates require a minimum filling amount that cannot be reached. In the area of solid recovered fuels, the most common approach is to account for these fractions of hard impurities only in terms of their weight, which means the analyte concentration is considered zero. This is a legit assumption when the analysis results are not affected by the impurity, e.g., for iron parts and the lower heating value (LHV), which technically is zero for metals. However, if the analytes are heavy metals, this practice leads to a distortion of results.

[1] Because of the volatility of elemental Hg, EN 15411 proposes not to expose samples to temperatures above 40°C before determining the Hg content. However, the waste samples that are subject to chemical analyses in this study have already passed several process steps (coarse shredding, sieving, lab scale comminution). Temperatures exceeding 40°C therefore cannot be excluded, especially during comminution steps. For this reason, and because elemental Hg is also volatilized when the samples are dried at 40°C, the Hg that is determined in this study is somehow bound. Drying at 105°C is therefore considered suitable for this purpose.

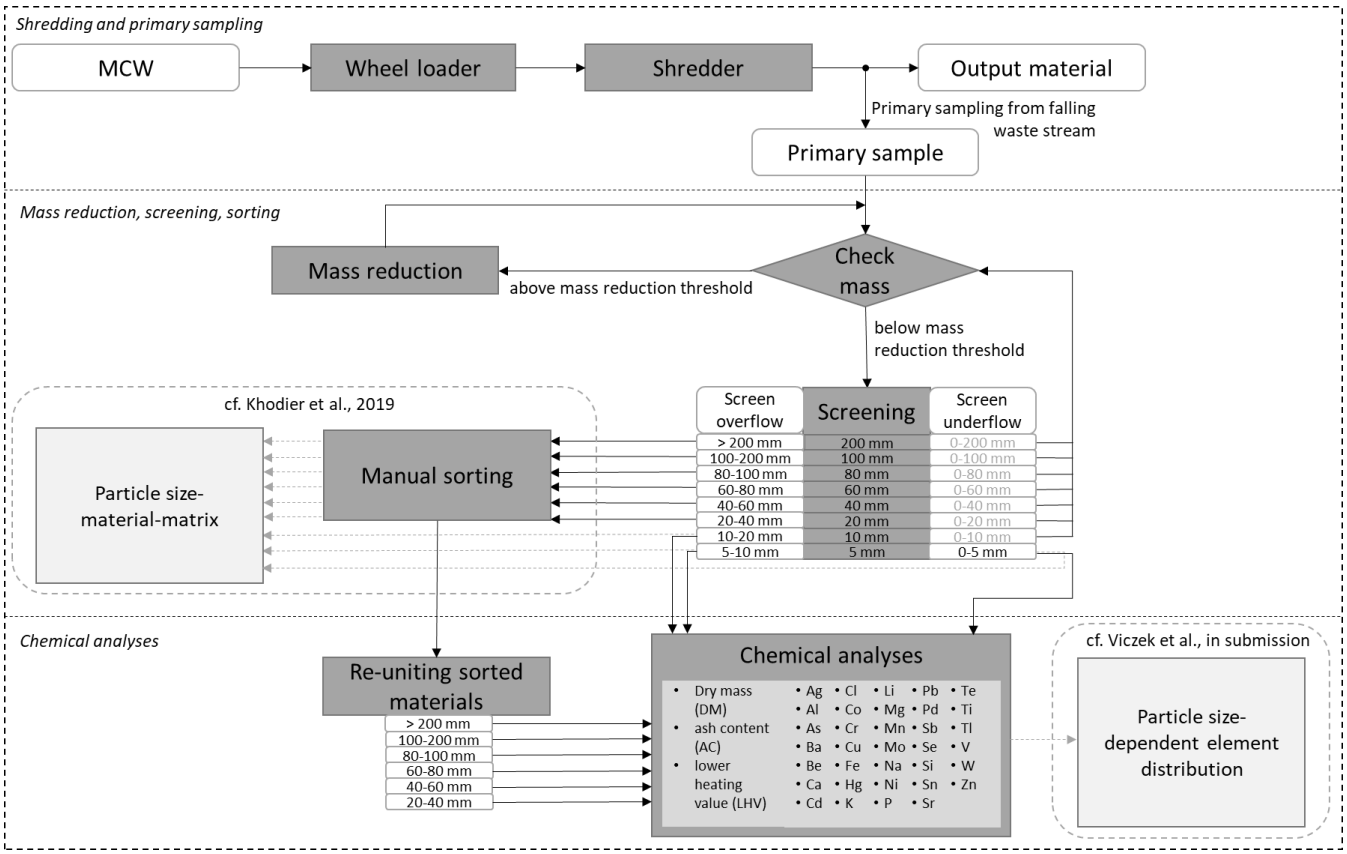

Fig. 2 Sampling and sample processing flowsheet

2.4 Calculations and data analysis

2.4.1 Correlations and RSVs

To interpret the correlation through significant Pearson correlation coefficients normally distributed data are necessary. Spearman correlation coefficients allow interpretations if the data are distributed differently. Therefore, the logarithmic normal distribution of each analyte (element, LHV), as well as the normal distribution (α=0.05) of the material fractions and log-ratios (see section 2.4.2) of the fractions, were tested separately in each particle size class above 20mm using the Kolmogorov-Smirnov test (MathWorks 2020b) in MATLAB (version 9.6 R2019a). Statistically significant ($p < 0.05$) correlations (Pearson and Spearman coefficients) for elements and materials were calculated with RStudio (R version 4.0.2) using only particle size fractions above 20 mm, as the smaller fractions have not been manually sorted. Furthermore, the material classes "inert" and "metal" were excluded because they were not part of the chemical analyses. The detailed results of the sorting analyses summarized in Khodier et al. (2020) are given in Appendix E.

RSV values were calculated based on Formula 1 with concentrations (c) below the limit of quantification (L.O.Q.) being considered with c = L.O.Q. Correlation coefficients (Pearson r, Spearman ρ) for RSVs with other parameters, e.g., particle size classes (using the mean value for each particle size fraction, e.g., 7.5 mm for the fraction 5–10 mm) were calculated using OriginPro 2020 (Version 9.7.0.188). The strength of the correlation was assessed based on Cohen (1988): strong ($|r| > 0.5$), moderate ($0.3 < |r| < 0.5$), and weak correlation ($0.1 < |r| < 0.3$).

2.4.2 Log-ratios

To consider the fact that data from sorting analyses are compositional data providing information about relative values, log-ratios were calculated to interpret the influence on the element concentration of the varying composition of the material. In this case, the additive log-ratio transformation was used because it allows comprehensible interpretation for the given case since only two components are considered in one log-ratio. Here, one material fraction needs to be defined as the denominator of a set of logarithmic ratios (natural logarithms were used, following common practice) defined by the other material fraction as numerators (Greenacre 2019). In this case, each of the material fractions was once chosen as the denominator to allow to interpret the influence of all material fractions to each other individually, while the remaining fractions were used as the numerators, resulting in six ratios for each particle size class above 20mm, i.e., the samples that were manually sorted. Similar to the interpretation of element-material correlations, the fractions "metal" and "inert" were not considered in the calculation since they were removed before chemical analyses. In general, "zero values" are problematic in a data set for computing ratios, but several different options for replacing the zeros are available. In the given case, zero values were only present in the particle size class 200–400mm in the material fractions wood, paper, and cardboard (see Appendix E), and they were replaced with the small value 0.005, which is a common method according to Greenacre (2019) (if a larger amount of zero values is present a sensitivity analyses can be conducted to compare the effect of different zero replacement methods). With this adaption, the data were rescaled to 100%, which in the field of compositional data is called "closing the data" (Greenacre 2019) for the following calculations. To compare and interpret the correlations between material fractions and element concentration, the results were calculated in RStudio and consider the log-ratios of the material fractions and the element concentrations. The latter were calculated as logarithmic values (natural logarithm) for interpretation purposes.

2.4.3 Prediction models for element concentration and LHV

The prediction models aim to project the element concentration without chemical analysis, based on the information of material composition only, and is a possibility to combine the information from Part I and the results from the present paper. Since only materials above 20mm were sorted in separate material classes, prediction models were only built considering the six particle size classes in 20–400mm (20–40mm, 40–60mm, 60–80mm, 80–100mm, 100–200mm, 200–400mm). Since prior investigations during this work confirmed

highly correlated multi-dimensional data, the Partial Least Squares Regression (PLS) was chosen. It enables to build a linear regression model from the original data by transforming the data in a new space, with the option to reduce dimensions for easier visualization. To find the ideal number of considered dimensions (factors), different approaches are possible. Here, the criterion was to consider the number of factors that leads to the smallest predicted residual sum of squares (PRESS) (Vandeginste et al. 1998) in the process of cross-validation. Cross-validation (CV), in general, is an option to evaluate the performance of the model and can be done in various ways. The underlying principle of all CV options is to split the dataset into two groups. One is used to build the model (calibration data), and the rest is used for evaluation (test data). Most methods use multiple rounds of CV to reduce variability by building different calibration and test data sets and calculate a combined result for the validation result over all the rounds (Massart et al. 1997). Since the given dataset, in this case, has a rather small amount of entries (31 measurements for 60 samples), the CV method "leave-one-out" was chosen. Here, one entry was chosen to be the test data, while the model was built on the residual data, and the PRESS for each considered dimension was calculated as the average of all rounds. From this, the ideal number of factors was evaluated by finding the value corresponding to the lowest PRESS, which was then used in MATLAB (version 9.6 R2019a) with the function "plsregress" (MathWorks 2020c) to build the regression model and calculate regression coefficients. A list of the number of considered factors for each element is given in Appendix C. With the underlying idea of developing a model for replacing chemical analyses with the involved sampling and preparation steps, the models were firstly built from the data for all particle size classes combined. It was found that the overall results highly improve when considering the particle size classes individually, due to the high variability of the element concentration in the individual particle size classes (see section 3.3). This led to the development of six prediction models per element, which can predict the concentration of 29 individual elements (see section 0, without Be, Pd, Se, Te, Tl (because values were mostly below L.O.Q.)) as well as the LHV based on the information form the calculated log-ratios.

In the case of the prediction model, the fraction of 3D-plastics was chosen as the denominator for the log-ratios since it showed plausible results in the correlation plot, while the fractions cardboard, paper, textile, wood, 2D-plastics, and residual fraction were used for the numerators. This resulted in six ratios for each particle size class above 20mm, i.e., manually sorted fractions. Elements with concentrations < L.O.Q. were considered with the value for L.O.Q. to consider as many values as possible for the regression model. Especially for the elements Cd and Hg, a large proportion of the measured values was below L.O.Q. in the larger particle size fractions. Pd was overall excluded from the prediction because the chemical analysis found over 90% (cf. Viczek et al. 2021b) of the available values to be below L.O.Q., which would not allow a meaningful prediction. To further allow to find a model with good prediction purposes in most cases, outliers of the available element concentrations were removed for the creation of the model. These were identified when the value was more than three scaled standard median absolute deviations away from the median (MathWorks 2020a). In general, ten data points for each regression model were available, but because outliers were excluded for building the models, a smaller amount of data points was left in some cases. The minimum number of values necessary for the model was set to seven, since it allows to calculate and interpret the median values, which concluded that a prediction model was not possible for all elements in all particle size classes (e.g., Cr (200–400mm) and Sn (80–100mm)). A list with the number of the available datasets is given in Appendix C. The accuracy of the models was tested with the same data that was used to build the models. This is not an ideal approach to assess the models' prediction abilities but was necessary since only a limited number of analyses was available.

3 Results and Discussion

3.1 Possible incorrect sampling errors

Measures were set to minimize and eliminate incorrect sampling errors where possible during and after the experiment. However, due to the on-site circumstances and the duration of sample processing and analysis, IEE and especially IPE cannot be entirely excluded. Incorrect sampling errors during primary sampling, mass reduction, screening, and sorting were already discussed in Part I (Khodier et al. 2020). The loss of material and possible contamination of containers and equipment on-site were briefly discussed as well but require a more detailed discussion because these factors play an essential role in chemical analyses.

3.1.1 Material and water loss

One of the main IPEs occurring is the bias caused by material loss. Material may have been lost in the form of dust (e.g., during screening) or as single particles during sorting. This loss likely influences the analysis results as the dust may have contained the determined elements in different concentrations than the rest of the waste stream. Furthermore, water loss has occurred during the time-intensive sample processing and sorting steps. The water content of the primary sample or each particle size fraction was not determined directly, but in the laboratory, i.e., after several on-site processing steps (screening, sorting) and storage. For this reason, the exact water content at the time of the sampling is unknown. The extent of the water loss is expected to differ for each particle size fraction because of different processing steps. The small fractions < 20 mm were not sorted and were transported and stored in buckets with sealable lids (after being stored in closed disposal bins on-site). Particle size fractions > 20 mm were sorted, which was a time-consuming process. Because the sorting process of smaller particle size classes took longer, more water evaporation is expected to have taken place for smaller particle size fractions than larger ones. After being stored in closed disposal bins on site as well, these fractions were transported and stored in closed garbage bags before analysis. Consequently, it is assumed that the small fractions < 20 mm have experienced the smallest water loss. However, in contrast to the loss of dust, the IPE caused by water loss does not influence analysis results for chemical elements as they refer to mg/kg dry mass (DM).

IPEs caused by material and water losses, however, may influence the calculations of the overall analyte concentration in the initial waste mix or calculations regarding the removal of specific fractions (cf. Viczek et al. 2021b). The water evaporated during screening and sorting is not accounted for by the determination of the water content in the laboratory. This may lead to underestimating the water content for fractions > 20 mm based on the laboratory results and may cause an overestimation of the total load of an element in the larger fractions. For this reason, the concentrations in the waste mix were calculated using the final fraction weights after sorting instead of the fraction weights after screening. Because of the IPE caused by material and water loss, however, the exact original composition is unknown. With a total mass loss (e.g., dust, water) between screening and the final sorting results of 5.6% on average (range 4.6–7.2%), the losses are manageable.

3.1.2 Contamination of on-site equipment

Another critical incorrect sampling error is possible contamination during sample processing, as the containers and equipment on-site could only be cleaned using hand brushes. Cross-contamination between the 10 representative samples and sub-samples (particle size fractions) – all originating from the same pile of waste – can therefore not be excluded entirely. However, potential contaminations are expected to be low due to small contact areas in relation to the sample masses.

3.1.3 Chemical analyses and subsampling

In addition to the possible errors discussed above and in Part I, additional sampling errors in Part II include sample processing in the laboratory (including subsampling) and the total analytical error (TAE). Besides the removal of hard impurities, which was discussed in section 2.3, the errors occurring in the laboratory include the potential loss of analytes, for example, the potential loss of Hg while drying the samples in the oven at 105°C, see section 2.2 for a brief discussion of this issue. However, as the volatility of Hg is well known, this error needs to be considered when interpreting the results, as is the case for hard impurities. Further errors may be caused by incomplete digestion, which was counteracted by choosing microwave-assisted acid digestion with HNO_3, HCl, and HF. Other errors that may occur, e.g., by subsampling or contamination by mills, were minimized by good laboratory practice in the EN ISO/IEC 17025 accredited laboratory performing the sample preparation and analyses.

3.2 Particle size-dependent distribution of elements

The analysis results for 30 elements, which the calculations in the present paper are based on, are presented in detail and discussed with respect to SRF production in Viczek et al. (2021b). Four elements were mostly below the limit of quantification (L.O.Q.: Be, Se: 2.5 mg/kg_{DM}; Te, Tl: 0.25 mg/kg_{DM}). Viczek et al. (2021b) identified three different groups based on the observed correlation patterns between ln(particle size) and ln(element concentration), see Fig. 3. A negative correlation between element concentrations and the particle size was the predominant pattern observed for 27 of the 30 investigated elements. The fine fraction < 5 mm was found to contain the highest concentrations and most considerable total amounts of these elements. The different distribution of these elements among different particle size classes, their industrial applications, and the corresponding implications regarding heterogeneity-induced sampling errors are expected to influence the observed RSVs, see section 3.3.

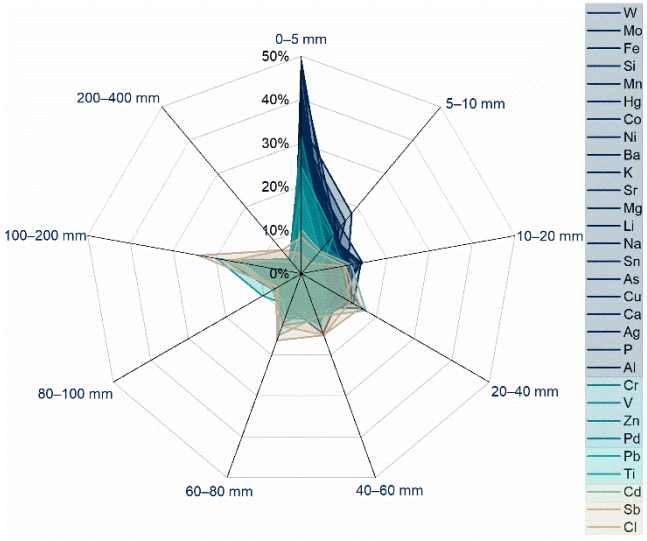

Fig. 3. Share of each element [%] in the different particle size classes. The elements are colored according to the groups identified in Viczek et al. (2021b) based on the observed statistically significant ($p < 0.05$) correlations for ln(particle size) and ln(element concentration). Pattern A: strong ($r > 0.5$, dark blue), moderate ($0.3 > r > 0.5$, lighter blue) or weak ($0.1 > r > 0.3$, turquoise) negative correlation. Pattern B: No statistically significant correlation (light green, only observed for Cd). Pattern C: positive correlation (beige)

3.3 RSV and GEE

Relative sampling variabilities (RSVs) were calculated for five cases: mg/kg_{DM} without hard impurities, mg/kg_{DM} including hard impurities, mg/kg_{OS} including hard impurities, mg/MJ, and for the percentual share of the element concerting the total mass of the primary sample (dry mass without hard impurities), thereby taking the mass of the particle size fraction into account. In all these scenarios, the lowest RSVs are observed for concentrations in mg/kg_{DM} without hard impurities. RSVs increase with every additional factor involved, e.g., hard impurities, water content, or LHV, for which RSVs are substantially higher. Exact numbers for all scenarios are given in Appendix A. Applying the general consensus acceptance threshold of an RSV of 20% (DS 2013), Table A.1 in Appendix A shows that even in the best setting (mg/kg_{DM} without hard impurities), this acceptance threshold can only be achieved for 19% of the element-fraction combinations.

3.3.1 RSVs for different elements

Box-whisker diagrams of the relative sampling variabilities (RSV) observed for the investigated elements (mg/kg_{DM} without hard impurities) in different particle size fractions are depicted in Fig. 4. The smallest RSVs are observed for Pd, which was often observed in concentrations below the L.O.Q. Therefore, the small RSVs originate from the fact that the same concentration, i.e., the L.O.Q., was assumed as the concentration in all these fractions. Small RSVs are furthermore observed for the LHV and Ti. In the case of the LHV, this is probably linked to the initial size and the comminution behavior of different materials, transferring them into certain particle size fractions. Furthermore, the range of possible values for the LHV is rather small compared to the possible range of element concentrations, especially considering that hard impurities with a potential LHV of 0 MJ/kg_{DM} were removed from the larger fractions. Typical ranges for LHVs are 15-20 MJ/kg_{DM} for paper, wood, and liquid packaging board; around 20-25 MJ/kg_{DM} for PET, PVC, and textiles; and around 35-42 MJ/kg_{DM} for PS, PE, and PP (Viczek et al. 2021a; Weissenbach and Sarc 2021). This indicates that the LHV of the most abundant materials in waste only differs by a factor of 2-3.

The low RSVs for Ti, in contrast, may be linked to its presence in similar concentrations among all particle size fractions (cf. Viczek et al. 2021b), indicating that the element is well distributed in the waste material. This is likely to result from the broad range of applications of titanium dioxide (TiO_2), which is present in most white or brightly tinted items, including paints, plastics, fibers, paper or cardboard, enamels, or ceramics (Holleman et al. 2007).

The example of Ti highlights the role distributional heterogeneity plays for chemical analyses of waste. The results of the elements for which the highest RSVs were observed additionally strongly reflect the large effect of constitutional heterogeneity. As illustrated in Fig. 4, the highest RSVs were observed for Cd, followed by Pb, Cu, W, Sn, and Cr. Concentrations of all these elements were highly variable in almost all particle size fractions. These elements are not broadly present in all typical materials occurring in waste but rather occur in high concentrations in specific materials or particles (cf. Viczek et al. 2020), which means a high constitutional heterogeneity is expected. For example, the Cu concentration in a copper wire fragment is a lot higher than in the surrounding particles. Consequently, single fragments of copper wire ending up in the sample significantly alter the analysis results. The case is similar for Cd, as it was formerly used as a pigment or stabilizer in plastics but has been banned for this purpose in the European Union (EC 2011). Therefore, it will be less abundant in plastic items that were produced in Europe more recently. As both distributional and constitutional heterogeneity cause correct sampling errors, it has to be assumed that the correct sampling error and, consequently, the minimal possible error (MPE) is already high for certain chemical elements in mixed commercial waste analyses. For this reason, the sampling can only be improved with higher efforts (e.g., increasing the number of increments, increasing the total sample mass).

3.3.2 RSVs for different particle size classes

The smallest particle size fractions < 20 mm exhibit slightly better RSVs than larger fractions, indicating a better sampling quality for smaller particle size fractions (see Fig. 5). The worst median RSVs are observed

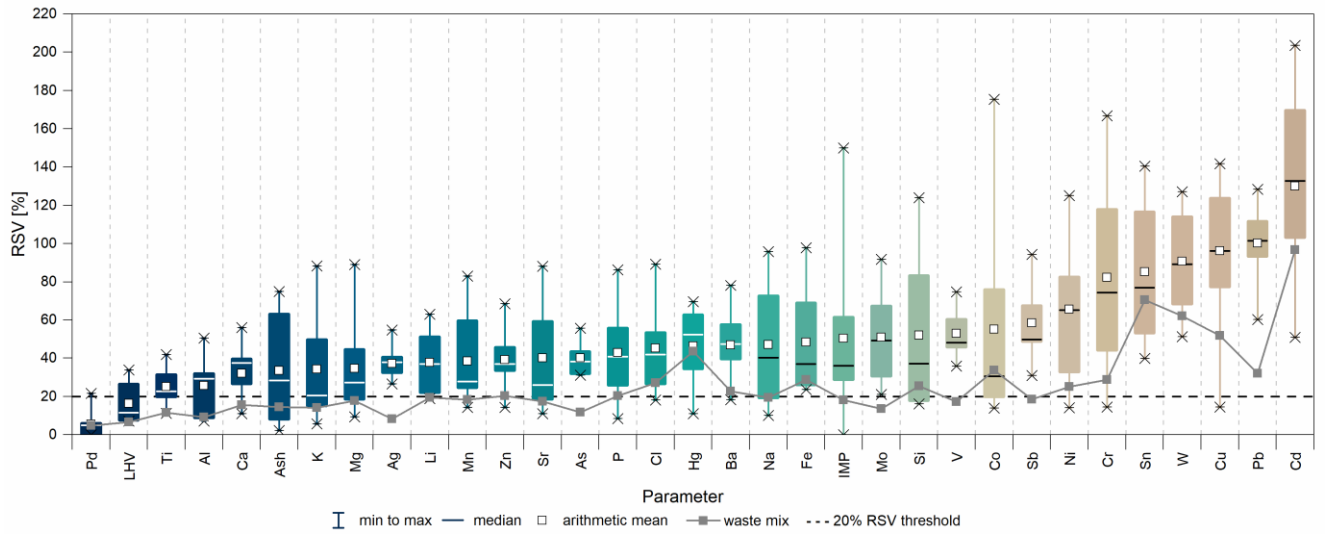

Fig. 4 RSVs of element concentrations, LHV, ash content, and hard impurities (IMP) in the different particle size classes sorted from low to high RSVs based on their mean RSVs. The solid grey line represents the RSVs for element concentrations in the whole waste mix, i.e., of the united particle size fractions

for the fraction 80–100 mm. Linear correlation analysis of ln(particle size) vs. ln(RSV) confirms that there is a statistically significant ($p < 0.05$) moderate positive correlation (Pearson $r = 0.37$, Spearman $\rho = 0.31$) between the particle size and the RSV. Furthermore, a weak ($r = -0.17$, $\rho = -0.12$) but statistically significant ($p < 0.05$) negative correlation between the mass share of the particle size fraction and the RSV is observable, indicating that the RSV of element concentrations in a particle size fraction decreases with increasing mass shares of the particle size fraction. This is consistent with the observations reported in Part I, although a much smaller proportion of the initial sample mass was ultimately subject to chemical analyses.

However, higher concentrations alone do not cause better RSVs, as there is no statistically significant correlation between the RSV and the element concentration (average concentration in the particle size fraction in relation to the maximum observed average concentration: c_i/c_{max}).

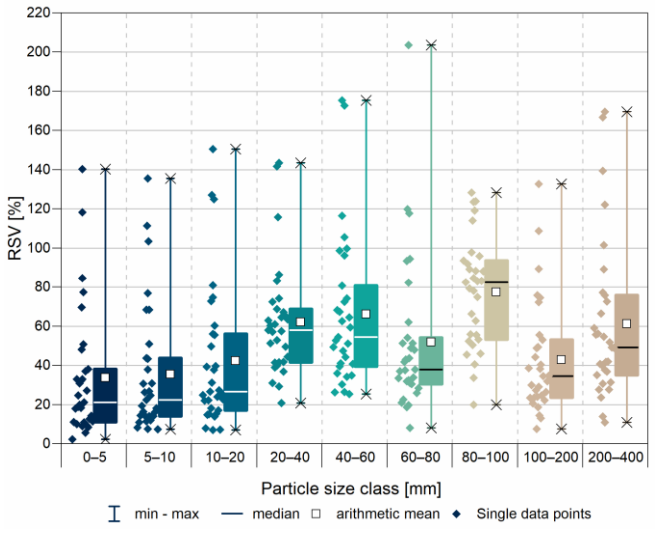

Fig. 5 RSVs of all parameters (excluding Pd, water content, and impurities) for different particle size classes

3.3.3 RSVs calculated for the original waste mix

Combining the different particle size classes and calculating the RSVs for the overall concentrations of each element in the waste mix (grey line in Fig. 4) shows that despite the high RSVs in single fractions, good RSVs < 20% can be achieved for 15 of 30 elements (mg/kg_{DM}) and the LHV, impurities, ash content, dry matter, and water content (Table A.6 in Appendix A). RSVs between 20% and 50% can be achieved for 11 elements. These RSVs are achieved even though the single fractions underwent additional processing (screening, sorting) and are therefore affected by additional errors, which leads to the suggestion that even better RSVs can be achieved when the original samples are directly analyzed.

3.4 Mathematical relations for elements and material fractions

3.4.1 Interpretation of correlations via correlation plot

Statistically significant ($p < 0.05$) correlations between chemical elements, LHV, and the mass share of materials listed in Appendix E (excluding metals and inert materials, see section 2.3) in the particle size classes above 20 mm are presented in Fig. 6. The correlation plot shows, inter alia, a negative correlation of the LHV with wood (WO), paper (PA), and the residual fraction (RE), and a positive correlation with 2D plastics (2D) and textile (TX). This may lead to the interpretation that a higher share of wood, paper, and residuals leads to a lower LHV, and a larger share of 2D plastics and textile increases the LHV, while the amount of 3D plastics (3D), as well as cardboard (CB), does not significantly influence the LHV. While the correlation between 2D plastics and the LHV is consistent with the observation that the LHV of waste plastics (especially PE from foils) is usually higher than that of wood, paper, or cardboard (Weissenbach and Sarc 2021), attention has to be paid to the fact that data from sorting analyses are compositional data. Therefore, the decrease of the LHV might not be entirely attributable to the increase of the mass fraction of wood, paper, and residuals, but rather to the fact that the increase of their share (in %) results in a decrease in the share (in %) of other materials, e.g., plastics 2D and 3D. This is also shown by the calculated log-ratios for the material fractions (Fig. 7, full results given in Appendix B), as strong negative correlations between the material-ratios PA/3D, WO/3D, and the LHV are observed, indicating a lower LHV when the share of PA or WO is increasing compared to the amount of 3D (Fig. 7 (A)). These observations are also consistent with the report of Weissenbach and Sarc (2021), as many of the plastics that may be present in the 3D fraction (e.g., PE, PP, PS) feature a higher LHV than wood and paper.

Additionally, Fig. 7 (B) indicates a decreasing LHV when the share of WO increases compared to the share of PA. This statement contradicts literature results (e.g., Beilicke and Wesenigk 1987; Weissenbach and Sarc 2021) and makes an interpretation of compositional data only based on the correlation plots complex. Further, Fig. 7 (A) shows that a higher share of wood compared to plastics 3D leads to a larger amount of Al in the sample. At the same time, the ratios CB/3D, as well as PA/3D and RE/3D, are positively correlated with the ratio WO/3D. With this additional information, the increasing amount of Al cannot be clearly

assigned to a rising share of wood in the sample but might also arise from the paper and/or cardboard and/or residual fraction. This is consistent with the literature review of Götze et al. (2016), indicating that the median Al concentrations in waste plastics are usually lower than in paper, gardening waste, combustibles, and the waste mix, suggesting that the observations in Fig. 7 may be connected to the low Al content of plastics. This emphasizes again that interpretations are possible, but their complexity often requires additional research and evaluation methods. Nevertheless, the results from the prediction models in section 1.1.1 state that the correlation between elements and material fractions is, in most cases, sufficient to forecast specific element concentrations for the median value.

3.4.2 Possibilities for prediction models for element concentration and LHV

To show the mathematical relation between element concentrations and sorting analyses, in total, prediction models for 29 elements and the LHV in six particle size classes were obtained. The log-ratios as observable variables, the original measured value of the element concentration as the predicted variable, as well as the ideal number of considered factors (based on cross-validation, see section 2.4.3) served as the input for the models. As an immediate result, the models calculated regression coefficients for predicting values for new data. The regression coefficients k for the individual models are given in Appendix C and are used in Equation (2) for calculating the element concentration or the LHV. Here, the calculated concentration $c_{j_{PSC}}$ of element j in the particle size class PSC is defined by the regression coefficients k and log-ratios for the material fractions $w_{i,PSC}$.

$$c_{j_{PSC}} = k_{0,PSC} + \sum_i k_{i,PSC} * \ln(\frac{w_{i,PSC}}{w_{3D,PSC}}) \qquad (2)$$

For the evaluation of the models, all the available data (including datasets that were previously identified as outliers) was applied to the models, and the calculated/predicted value of the element concentration/LHV was compared with the chemically determined value due to a limited number of samples (10 replicates). Additionally, the results for the predicted values in the whole sample in all particle size classes above 20mm were calculated and compared with the original value as well. The results are presented in box plots, where each predicted value was compared with the original one (y_{fit}/y) to show the accuracy of the models in percent. Taking Fe as an example, Fig. 8. shows that most of the predicted Fe values for all particle size classes reach the original value in a range of +/- 20%. Additionally, the mean values, as well as the median values, lie within that range too. The plots for the remaining elements as well as the LHV are given in Appendix D. As a summarized result of the models, the median values from the ten available samples for the reached percentage of the predicted values are presented in Tab. 1. Except for Ba, Cd, Cl, Cu, Mo,

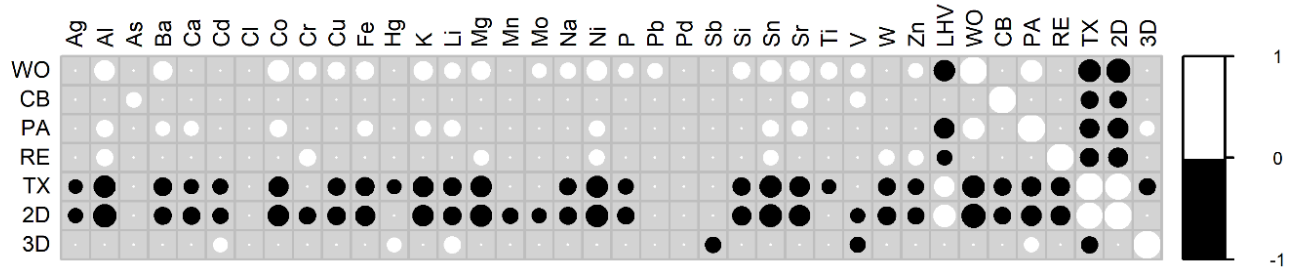

Fig. 6 Statistically significant (p < 0.05) positive (white) and negative (black) Spearman correlations of analysis parameters and sorting analyses for particle size classes >20mm from Part I (Khodier et al. 2020). The size of the circles is proportional to the strength of the linear correlation (for numbers of Pearson and Spearman correlation coefficients see Appendix B). Abbreviations: Cardboard (CB), paper (PA), textile (TX), wood (WO), 2D-plastics (2D), 3D-plastics (3D), residual fraction (RE)

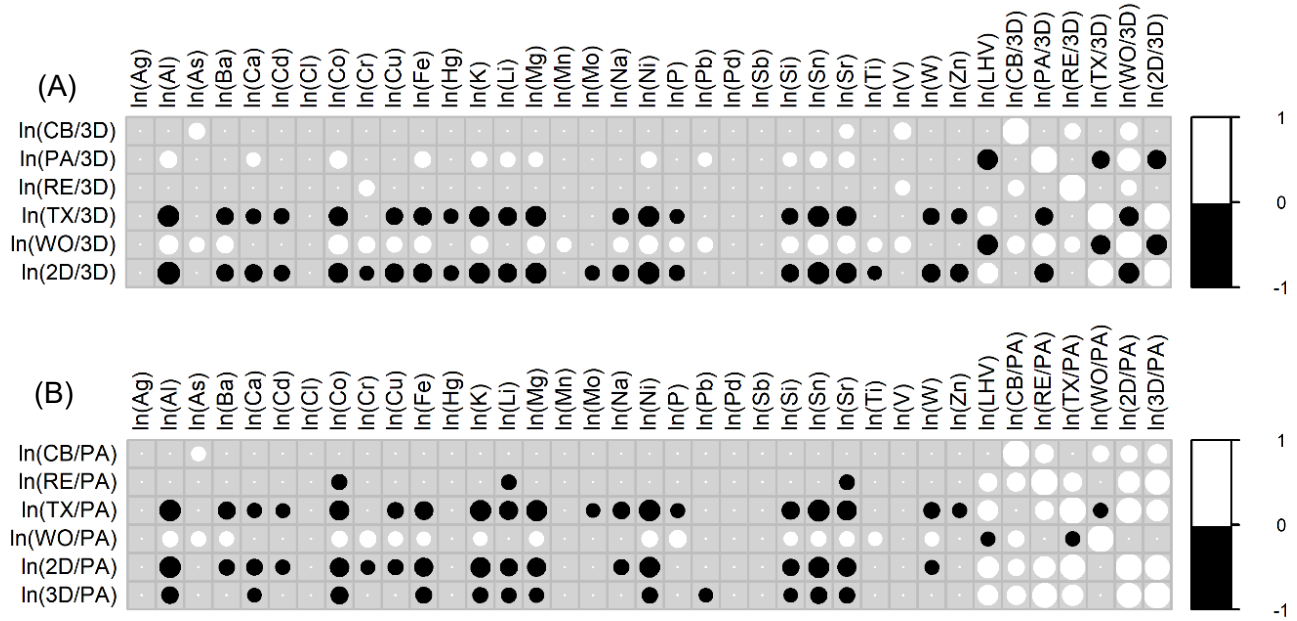

Fig. 7 Statistically significant (p < 0.05) positive (white) and negative (black) Spearman correlations of logarithmic values of the analysis parameters and log-ratios based on results from sorting analyses for particle size classes >20mm from Part I (see Appendix E) with the reference material (A) 3D and (B) PA. The size of the circles is proportional to the strength of the linear correlation (for numbers of Pearson as well as Spearman correlation coefficients see Appendix B). Abbreviations: Cardboard (CB), paper (PA), textile (TX), wood (WO), 2D-plastics (2D), 3D-plastics (3D), residual fraction (RE)

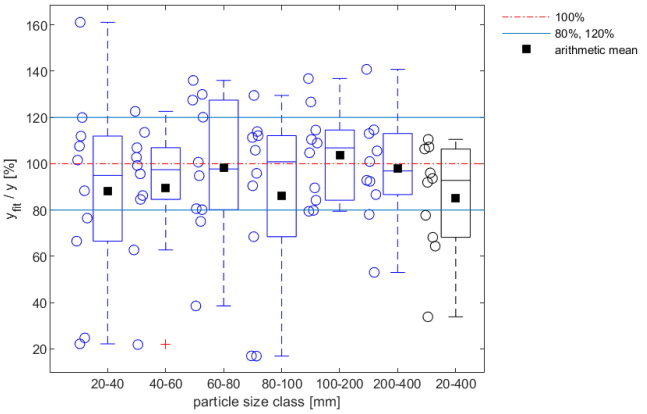

Fig. 8 Box plot of iron (Fe) for the results of the prediction models in different particle size classes and the material mix in the particle size classes >20mm. Here, the boxes in the diagrams show the range from the 25th (lower quartile) to the 75th (upper quartile) percentile of the values, while the horizontal line inside the box defines the median. The whiskers, which are the extending vertical lines from the boxes, indicate variability outside the upper and lower quartile and consider a range for data points within the 1.5 interquartile range. Outliers are marked with a '+'-symbol, and additionally, the mean of each box plot, as well as the individual data points, are plotted.

V, and W, all the medians for the individual particle size classes (20–40mm, 40–60mm, 60–80mm, 80–100mm, 100–200mm, 200–400mm) are in a range of +/- 20% of a correct prediction, the majority is even in a range of +/- 10%. Considering the median values of the material mix with the particle size 20–400mm, an even better accuracy was reached for most elements. By taking into account the median of the material mix, this approach would likely be the most practicable, e.g., for production plants of solid recovered fuels, since the quality must be defined for the overall output mix. Additionally, investigations for the consideration of the material fractions below 20mm are required since they contain a high concentration and a large total amount of the analyte (Viczek et al. 2021b). Besides the quantitative determination of the element content, the technical limitations for optical detection of fine particles also require further research. Here, except for the elements Cd, Cr, Cu, Ni, Pb, Sn, the prediction of the median was approximately between 80 and 100% (Cr, Sn: no values because of too little available values for regression model). This clearly states that there is a relation between material composition and element concentration and a possibility to estimate the results from chemical analysis mathematically by just the information from sorting analyses. According to literature from Krämer (2017), real-time measurements from NIR-technology deliver insufficient quantitative analyses for several heavy metals (Cd, Cr, Sb, Pb). The presented method results show poor quality for the prediction of Cd and Pb in the material mix (20–400mm, median value). This is probably linked to their uneven distribution, which is also reflected by the fact that the highest RSVs were calculated for these two elements (see section 3.3). For Sb, in contrast, an over 80% accuracy in predicting the concentration of Sb in the material mix was achieved. Due to the high number of outliers, no regression model for the overall value in the material mix of Cr could be built. The evaluation of the concentration of Cl and the LHV over NIR-technology was significantly better than for the heavy metals in the results from Krämer (2017). The determined results from the models also showed very good accuracy for the values from LHV in all particle size classes, and in most cases, for Cl.

3.4.3 Study limitations

The used data set in this example is limited in its size, which is not typical for prediction models and shows in some cases a broad scattering of the values, which is typical for the considered waste material and its heterogeneity. However, such a detailed chemical analysis of a broad range of chemical elements and analytical parameters is rarely available for waste materials and a good opportunity to investigate the connections and correlations mentioned in the present article. Overall, the results show that a correlation between material composition and element concentration is recognizable, which might allow calculating chemical parameters based on information from, e.g., an NIR-sorter combined with a model for sensor-based particle size determination. The latter was investigated on single particles in a mixed commercial waste stream by Kandlbauer et al. (2020). This combination could enable the evaluation of chemical

Tab. 1 Median of the ratios between the predicted values and the original one (y_{fit}/y) for the individual particle size classes and elements (values in %)

Element	20–40 mm	40–60 mm	60–80 mm	80–100 mm	100–200 Mm	200–400 mm	20–400mm
Ag	104.9	100.3	99.3	101.3	100.6	100.4	94.4
Al	98.1	99.0	97.3	99.1	103.4	112.6	101.3
As	106.0	106.6	105.1	111.6	102.4	104.1	101.2
Ba	97.7	95.7	99.4	94.3	122.1	90.5	87.9
Ca	96.6	98.9	102.6	119.2	96.7	97.2	97.1
Cd	85.8	93.9	90.4	94.7	59.8	100.0	39.0
Cl	100.5	94.6	103.3	95.2	79.9	104.5	89.5
Co	93.9	100.5	102.8	97.7	99.6	98.0	94.0
Cr	90.3	88.8	102.5	104.3	92.4	-	-
Cu	67.8	82.6	99.5	81.3	103.5	95.7	60.2
Fe	95.0	97.5	97.8	100.8	106.9	96.9	92.8
Hg	96.9	100.0	100.0	100.0	100.0	100.0	92.84
K	96.0	99.6	102.7	98.1	102.1	94.6	93.7
Li	102.9	91.5	94.8	96.1	100.3	99.7	89.3
Mg	93.9	98.2	97.9	90.7	95.7	99.3	94.3
Mn	99.1	101.9	106.0	90.7	100.0	97.9	93.1
Mo	97.8	98.7	108.3	96.4	112.5	124.3	91.4
Na	91.5	99.9	101.8	99.1	93.6	117.1	88.0
Ni	95.7	96.7	98.4	93.5	102.3	99.3	79.8
P	96.9	99.8	103.5	99.6	104.7	106.4	94.8
Pb	116.3	90.6	97.8	90.6	100.4	90.3	71.7
Sb	92.4	102.0	81.2	95.7	98.2	105.3	83.3
Si	96.2	98.8	113.9	101.7	92.6	105.5	92.5
Sn	103.3	100.4	96.8	-	103.5	101.6	-
Sr	90.4	99.9	107.9	94.2	100.3	101.7	88.9
Ti	95.9	103.9	95.8	95.2	98.5	99.5	101.4
V	101.9	102.3	101.1	91.5	97.3	123.6	99.1
W	84.3	87.3	99.0	90.6	105.3	132.8	87.1
Zn	97.5	98.6	97.5	91.1	96.6	97.7	102.2
LHV	103.4	100.5	99.5	100.9	99.7	99.5	101.4

properties without the expensive and time-consuming act of sampling, sample preparation, and chemical analysis since the information regarding material and particle size from NIR-sorters and sensor-based particle size determination models could be evaluated while the material is still in the treatment process (in-line analytics). Here, the necessity of in-line analytics is also shown by the fact that the results from the prediction models are best for the median values of the individual samples, requiring a large number of samples for a good prediction of the actual values. Additionally, in-line analytics would allow timely results which, combined with suitable actuators in a processing plant, further enable influencing the quality and reacting to certain deviations by adapting treatment steps (screening, shredding).

Further investigations must deal with the fact that fine materials below 20mm were not considered in the models but will contribute significantly to the heavy metal and metalloid content in waste samples. Here, methods to detect or determine the influence of particles that are smaller than a critical size determined by the camera resolution must be examined or may be considered with a correction factor in the models (Krämer 2017). Additionally, fractions with smaller particle sizes could be removed by a prior screening step, which would result in a decrease of the concentrations of most elements in the screen overflow. However, treatment options for the removed material streams need to be investigated (Viczek et al. 2021b).

4 Conclusions

While the applied procedure gives good results for some parameters, RSVs range up to 203.5% for others. This may be linked to the high distributional and constitutional heterogeneity caused by the industrial applications of the chemical elements and their compounds, leading to a high minimum possible errors (MPE) for these elements. However, better RSVs were achieved when calculated for the original waste stream rather than the single fractions, which would be the usual way of sampling and analyzing waste or SRF. As the waste stream in this study has undergone some additional procedures, which are always accompanied by additional errors, the RSVs are expected to be lower when the waste is directly analyzed without additional screening or sorting steps. The conclusion of Part I, stating that the quality of the sampling can only be rated in relation to the analytical target, also applies to chemical analyses. The developed regression models show a first attempt to predict element concentrations based on data from sorting analyses. While the majority of the results for most elements showed good accuracy (+/-20% of the original value), several aspects need to be further investigated. Firstly, the fact that the data comes from one replication experiment and shows high heterogeneity in material composition and element content concludes that several calibration datasets for different waste streams or waste streams with different origins must be available for a significant analysis of unknown datasets. This procedure is complex and time-consuming but must be considered if the need for a real-time method for chemical analysis should be continued. Nevertheless, the available data and the results from the regression models can be used to investigate and evaluate a model for a digital sampling procedure and interpret the effects of a varying number of samples, sample mass, and the time interval between sampling.

Funding: Partial funding for this work was provided by: The Center of Competence for Recycling and Recovery of Waste 4.0 (acronym ReWaste4.0) (contract number 860 884) under the scope of the COMET – Competence Centers for Excellent Technologies – financially supported by BMK, BMDW, and the federal states of Styria, managed by the FFG.

Conflict of interest: The authors declare no conflict of interest.

Availability of data and material (data transparency): Data is part of the supporting material of this manuscript as well as another manuscript (Viczek et al. in submission b) that is under consideration for publication in a peer-reviewed journal focusing on different aspects of the investigations.

References

Amlinger F, Pollak M, Favoino E (2004) Heavy metals and organic compounds from wastes used as organic fertilizers: Annex 2 - Compost quality definition - legislation and standards

Andersen JK, Boldrin A, Christensen TH, Scheutz C (2010) Mass balances and life-cycle inventory for a garden waste windrow composting plant (Aarhus, Denmark). Waste Manag Res 28:1010–1020. https://doi.org/10.1177/0734242X09360216

Astrup T, Riber C, Pedersen AJ (2011) Incinerator performance: Effects of changes in waste input and furnace operation on air emissions and residues. Waste Manag Res 29:57–68. https://doi.org/10.1177/0734242X11419893

ASI (Austrian Standards Institute) (2002) ÖNORM EN 13656 Characterization of waste – Microwave assisted digestion with hydrofluoric (HF), nitric (HNO3) and hydrochloric (HCl) acid mixture for subsequent determination of elements. Issued on 01/12/2002

ASI (Austrian Standards Institute) (2007) ÖNORM EN 14346 Characterization of waste - Calculation of dry matter by determination of dry residue or water content. Issued on 01/03/2007

ASI (Austrian Standards Institute) (2011a) ÖNORM EN 15411 Solid recovered fuels – Methods for the determination of the content of trace elements (As, Ba, Be, Cd, Co, Cr, Cu, Hg, Mo, Mn, Ni, Pb, Sb, Se, Tl, V and Zn). Issued on 15/10/2011

ASI (Austrian Standards Institute) (2011b) ÖNORM EN 15413 Solid recovered fuels – Methods for the preparation of the test sample from the laboratory sample. Issued on 15/10/2011

ASI (Austrian Standards Institute) (2011c) ÖNORM EN 15443 Solid recovered fuels – Methods for the preparation of the laboratory sample. Issued on 15/10/2011

ASI (Austrian Standards Institute) (2011d) ÖNORM EN 15359 Solid recovered fuels - Specifications and classes. Issued on 15/12/2011

ASI (Austrian Standards Institute) (2016) ÖNORM EN 14582 Characterization of waste — Halogen and sulfur content — Oxygen combustion in closed systems and determination methods

ASI (Austrian Standards Institute) (2017) ÖNORM EN ISO 17294-2 Water quality - Application of inductively coupled plasma mass spectrometry (ICP-MS) - Part 2: Determination of selected elements including uranium isotopes

Beilicke G, Wesenigk H (1987) Zusammenstellung von Heizwerten für die Brandlastberechnung

Brunner PH, Rechberger H (2015) Waste to energy--key element for sustainable waste management. Waste Manag 37:3–12. https://doi.org/10.1016/j.wasman.2014.02.003

BMLFUW (Bundesministerium für Land- und Forstwirtschaft, Umwelt und Wasserwirtschaft) (2010) Verordnung über die Verbrennung von Abfällen

Cohen J (1988) Statistical Power Analysis for the Behavioral Sciences, 2nd ed. Taylor and Francis, Hoboken

DS (Danish Standards) (2013) DS 3077 Representative sampling - horizontal standard 03.120.30; 13.080.05

DIN (Deutsches Institut für Normung) (1997) DIN 51719 Testing of solid fuels – Solid mineral fuels – Determination of ash content

DIN (Deutsches Institut für Normung) (2000) DIN 51900-1 Testing of solid and liquid fuels - Determination of gross calorific value by the bomb calorimeter and calculation of net calorific value - Part 1: Principles, apparatus, methods

DIN (Deutsches Institut für Normung) (2009) DIN EN ISO 10304-1 Water quality - Determination of dissolved anions by liquid chromatography of ions - Part 1: Determination of bromide, chloride, fluoride, nitrate, nitrite, phosphate and sulfate

Ellison SLR, Williams A (2012) EURACHEM/CITAC Guide CG 4 Quantifying Uncertainty in Analytical Measurement. QUAM:2012.P1, 3rd edition.
Esbensen KH, Julius LP (2009) Representative Sampling, Data Quality, Validation – A Necessary Trinity in Chemometrics. In: Tauler R, Walczak B, Brown SD (eds) Comprehensive Chemometrics: Chemical and Biochemical Data Analysis. Elsevier, Burlington, pp 1–20
Esbensen KH, Wagner C (2014) Theory of sampling (TOS) versus measurement uncertainty (MU) – A call for integration. TrAC-Trend Anal Chem 57:93–106. https://doi.org/10.1016/j.trac.2014.02.007
European Commission (2008a) Directive 2008/98/EC of the European Parliament and of the Council of 19 November 2008 on waste and repealing certain directives (waste framework directive)
EC (European Commission) (2008b) Regulation (EC) No 1272/2008 of the European Parliament and the Council of December 16 2008 on classification, labelling and packaging of substances and mixtures
EC (European Commission) (2010) Directive 2010/75/EU of the European Parliament and of the Council of 24 November 2010 on industrial emissions (integrated pollution prevention and control)
EC (European Commission) (2011) Commission Regulation (EU) No 494/2011 of 20 May 2011 amending Regulation (EC) No 1907/2006 of the European Parliament and of the Council on the Registration, Evaluation, Authorisation and Restriction of Chemicals (REACH) as regards Annex XVII (Cadmium)
Flamme S, Gallenkemper B (2001) Inhaltsstoffe von Sekundärbrennstoffen, Ableitung der Qualitätssicherung der Bundesgütegemeinschaft Sekundärbrennstoffe e. V. Muell und Abfall:699–704
Flamme S, Geiping J (2012) Quality standards and requirements for solid recovered fuels: a review. Waste Manag Res 30:335–353. https://doi.org/10.1177/0734242X12440481
Götze R, Boldrin A, Scheutz C, Astrup TF (2016) Physico-chemical characterisation of material fractions in household waste: Overview of data in literature. Waste Manag 49:3–14. https://doi.org/10.1016/j.wasman.2016.01.008
Greenacre MJ (2019) Compositional data analysis in practice. Chapman & Hall/CRC Interdisciplinary statistics series
Gy P (1998) Sampling for analytical purposes. John Wiley & Sons
Gy P (2004) Sampling of discrete materials—a new introduction to the theory of sampling. Chemometrics and Intelligent Laboratory Systems 74:7–24. https://doi.org/10.1016/j.chemolab.2004.05.012
Gy PM (1995) Introduction to the theory of sampling I. Heterogeneity of a population of uncorrelated units. TrAC-Trend Anal Chem 14:67–76. https://doi.org/10.1016/0165-9936(95)91474-7
Holleman AF, Wiberg E, Wiberg N (2007) Lehrbuch der anorganischen Chemie, 102. Aufl. de Gruyter, Berlin
Kandlbauer L, Khodier K, Ninevski D, Sarc R (2020) Sensor-based Particle Size Determination of Shredded Mixed Commercial Waste based on two-dimensional Images. Waste Manag. https://doi.org/10.1016/j.wasman.2020.11.003
Khodier K, Viczek SA, Curtis A, Aldrian A, O'Leary P, Lehner M, Sarc R (2020) Sampling and analysis of coarsely shredded mixed commercial waste. Part I: procedure, particle size and sorting analysis. Int J Environ Sci Technol 17:959–972. https://doi.org/10.1007/s13762-019-02526-w
Kjeldsen P, Barlaz MA, Rooker AP, Baun A, Ledin A, Christensen TH (2002) Present and Long-Term Composition of MSW Landfill Leachate: A Review. Crit Rev Env Sci Tec 32:297–336. https://doi.org/10.1080/10643380290813462
Krämer P, Flamme S, Schubert S, Gehrmann H, Glorius T (2016) Entwicklungen zur Echtzeitanalytik von Ersatzbrennstoffen. In: Thomé-Kozmiensky KJ (ed) Energie aus Abfall. TK Verlag Karl Thomé-Kozmiensky, Neuruppin
Krämer P (2017) Entwicklung von Berechnungsmodellen zur Ermittlung relevanter Einflussgrößen auf die Genauigkeit von Systemen zur nahinfrarotgestützten Echtzeitanalytik von Ersatzbrennstoffen, 1. Auflage. Schriftenreihe zur Aufbereitung und Veredlung, vol 66. Shaker, Aachen
Lorber KE, Sarc R, Aldrian A (2012) Design and quality assurance for solid recovered fuel. Waste Manag Res 30:370–380. https://doi.org/10.1177/0734242X12440484
Massart DL, Vandeginste, B. G. M., Buydens, L. M. C., Jong S de, Lewi PJ, Smeyers-Verbeke J (1997) Handbook of Chemometrics and Qualimetrics: Part A. Data Handling in Science and Technology. Elsevier
MathWorks (2020a) isoutlier. https://de.mathworks.com/help/matlab/ref/isoutlier.html. Accessed 3 December 2020
MathWorks (2020b) kstest. https://de.mathworks.com/help/stats/kstest.html. Accessed 3 December 2020
MathWorks (2020c) plsregress. https://de.mathworks.com/help/stats/plsregress.html. Accessed 3 December 2020
Morf LS, Brunner PH, Spaun S (2000) Effect of operating conditions and input variations on the partitioning of metals in a municipal solid waste incinerator. Waste Manag Res 18:4–15. https://doi.org/10.1034/j.1399-3070.2000.00085.x
Pivnenko K, Granby K, Eriksson E, Astrup TF (2017) Recycling of plastic waste: Screening for brominated flame retardants (BFRs). Waste Manag 69:101–109. https://doi.org/10.1016/j.wasman.2017.08.038
Pomberger R, Aldrian A, Sarc R (2015) Grenzwerte - Technische Sicht zur rechtlichen Notwendigkeit. In: Piska C, Lindner B (eds) Abfallwirtschaftsrecht Jahrbuch 2015. NWV Neuer wissenschaftlicher Verlag, Wien, Graz, pp 269–289
Ramsey MH, Ellsion SLR, Rostron P (2019) Eurachem/EUROLAB/CITAC/Nordtest/AMC Guide: Measurement uncertainty arising from sampling: a guide to methods and approaches. Second Edition: A guide to methods and approaches
Sarc R, Seidler IM, Kandlbauer L, Lorber KE, Pomberger R (2019) Design, Quality and Quality Assurance of Solid Recovered Fuels for the Substitution of Fossil Feedstock in the Cement Industry – Update 2019. Waste Manag Res 37:885–897. https://doi.org/10.1177/0734242X19862600
Slijkhuis C (2018) Recycling von Kunststoffen aus EAG bei gleichzeitiger Eliminierung von Schadstoffen. In: Pomberger R, et al. (eds) Vorträge-Konferenzband zur 14. Recy & DepoTech-Konferenz, pp 261–264
Smith SR (2009) A critical review of the bioavailability and impacts of heavy metals in municipal solid waste composts compared to sewage sludge. Environ Int 35:142–156. https://doi.org/10.1016/j.envint.2008.06.009
Turner A (2019) Cadmium pigments in consumer products and their health risks. Sci Total Environ 657:1409–1418. https://doi.org/10.1016/j.scitotenv.2018.12.096
Turner A, Filella M (2017) Field-portable-XRF reveals the ubiquity of antimony in plastic consumer products. Sci Total Environ 584-585:982–989. https://doi.org/10.1016/j.scitotenv.2017.01.149
Vandeginste BGM, Massart DL, Buydens LMC, Jong S de, Lewi PJ, Smeyers-Verbeke, J. (1998) Multivariate calibration. In: Vandeginste BGM (ed) Handbook of chemometrics and qualimetrics: Part B. Elsevier, Amsterdam, Boston
Viczek SA, Lorber KE, Sarc R (2021a) Production of contaminant-depleted solid recovered fuel from mixed commercial waste for co-processing in the cement industry. Fuel 294:120414. https://doi.org/10.1016/j.fuel.2021.120414
Viczek SA, Khodier K, Kandlbauer L, Aldrian A, Redhammer G, Tippelt G, Sarc R (2021b) The particle size-dependent distribution of chemical elements in mixed commercial waste and implications for enhancing SRF quality. Sci Total Environ 776:145343. https://doi.org/10.1016/j.scitotenv.2021.145343
Viczek SA, Aldrian A, Pomberger R, Sarc R (2020) Origins and carriers of Sb, As, Cd, Cl, Cr, Co, Pb, Hg, and Ni in mixed solid waste – A literature-based evaluation. Waste Manag 103:87–112. https://doi.org/10.1016/j.wasman.2019.12.009
Vrancken C, Longhurst PJ, Wagland ST (2017) Critical review of real-time methods for solid waste characterisation: Informing material recovery and fuel production. Waste Manag 61:40–57. https://doi.org/10.1016/j.wasman.2017.01.019
Wagner C, Esbensen KH (2012) A critical review of sampling standards for solid biofuels – Missing contributions from the Theory of Sampling (TOS). Renew Sust Energ Rev 16:504–517. https://doi.org/10.1016/j.rser.2011.08.016
Wagner C, Esbensen KH (2015) Theory of sampling: four critical success factors before analysis. J AOAC Int 98:275–281. https://doi.org/10.5740/jaoacint.14-236
Weissenbach T, Sarc R (2021) Investigation of particle-specific characteristics of non-hazardous, fine shredded mixed waste. Waste Manag:162–171. https://doi.org/10.1016/j.wasman.2020.09.033

3.5 Publication V

The particle size-dependent distribution of chemical elements in mixed commercial waste and implications for enhancing SRF quality

S.A. Viczek, K. Khodier, L. Kandlbauer, A. Aldrian, G. Redhammer, G. Tippelt, R. Sarc

Science of the total environment 776 (2021), 145343,
https://doi.org/10.1016/j.scitotenv.2021.145343

Author Contributions (CRediT Contributor Roles Taxonomy):

SV: Conceptualization, Methodology, Formal Analysis, Investigation, Resources, Data curation, Writing – original draft preparation, Writing – review and editing, Visualization, Project administration;

KK: Methodology, Investigation, Writing – review and editing;

LK: Formal analysis, Investigation, Writing – original draft preparation (section PCA), Writing – review and editing, Visualization;

AA: Methodology, Resources, Writing – review and editing;

GR: Formal analysis, Investigation, Resources, Writing – original draft preparation (sections regarding XRD and Mössbauer Spectroscopy), Writing – review and editing, Visualization;

GT: Formal analysis, Investigation;

RS: Conceptualization, Resources, Writing – review and editing, Supervision, Funding acquisition.

Science of the Total Environment 776 (2021) 145343

Contents lists available at ScienceDirect

Science of the Total Environment

journal homepage: www.elsevier.com/locate/scitotenv

The particle size-dependent distribution of chemical elements in mixed commercial waste and implications for enhancing SRF quality

S.A. Viczek [a], K. Khodier [b], L. Kandlbauer [a], A. Aldrian [a], G. Redhammer [c], G. Tippelt [c], R. Sarc [a,*]

[a] Chair of Waste Processing Technology and Waste Management, Department of Environmental and Energy Process Engineering, Montanuniversitaet Leoben, Franz-Josef-Strasse 18, 8700 Leoben, Austria
[b] Chair of Process Technology and Industrial Environmental Protection, Department of Environmental and Energy Process Engineering, Montanuniversitaet Leoben, Franz-Josef-Strasse 18, 8700 Leoben, Austria
[c] Department of Chemistry and Physics of Materials, University of Salzburg, Hellbrunnerstrasse 34, 5020 Salzburg, Austria

HIGHLIGHTS

- The particle size-dependent distribution of 30 elements in MCW was studied.
- Analyses were performed for 9 particle size fractions and 10 replicate samples.
- 27 elements show a negative correlation between concentration and particle size.
- Fine fractions <5 mm carry most contaminants & valuable minerals for cement clinker.
- Therefore, removing the fine fraction can significantly reduce heavy metal contents.

GRAPHICAL ABSTRACT

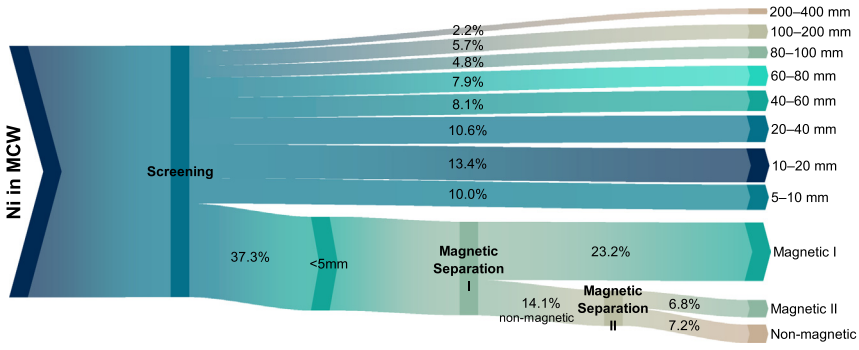

ARTICLE INFO

Article history:
Received 20 December 2020
Received in revised form 14 January 2021
Accepted 17 January 2021
Available online 22 January 2021

Editor: Huu Hao Ngao

Keywords:
Heavy metals
Mixed commercial waste
Particle-size investigation
Screening
Solid recovered fuel (SRF)
Waste characterization

ABSTRACT

Mixed commercial waste (MCW) contains contaminants that are important for several waste treatment options, e.g. the production and utilization of SRF for which limit values exist. Because these contaminants can be linked to specific materials but also occur in certain particle size classes, this paper presents the particle size-dependent distribution of 30 elements (Ag, Al, As, Ba, Ca, Cd, Cl, Co, Cr, Cu, Fe, Hg, K, Li, Mg, Mn, Mo, Na, Ni, P, Pb, Pd, Sb, Si, Sn, Sr, Ti, V, W, Zn) in nine particle size classes (<5 mm, 5–10 mm, 10–20 mm, 20–40 mm, 40–60 mm, 60–80 mm, 80–100 mm, 100–200 mm and 200–400 mm) of coarsely shredded mixed commercial waste collected in the area of Graz, Austria. For 27 elements a negative correlation between concentration and particle size was observed, i.e., increasing concentrations with decreasing particle size. The fine fraction <5 mm contained the highest concentrations and the most considerable total amount of most analytes (e.g., > 40% of Hg, Mn, Mo, Sn, W). The removal of this fraction therefore theoretically reduces concentrations [mg/kg_{DM}] of the 27 negatively-correlated elements in the screen overflow by 2.1 to 38%, while Cd (+10%), Sb (+12%), and Cl concentrations (+17%) and the lower heating value (+16%) increase. Besides containing contaminants, the fine fraction <5 mm consisted of ~11% Fe, 12% Ca, 12% Si, and 1.5% Al, all of which are valuable raw materials for the cement industry. Fe was found to be present as oxides, primarily as magnetite and wuestite. Calcium was present as carbonates (calcite, dolomite), but also considerable amounts of calcium sulfates (bassanite, gypsum, anhydrite). Concludingly, while screening can significantly improve SRF quality with respect to heavy metals, valuable raw materials for the cement industry may be removed as well, potentially resulting in a conflict between environmental protection and resource utilization.

* Corresponding author.
E-mail addresses: sandra.viczek@unileoben.ac.at (S.A. Viczek), karim.khodier@unileoben.ac.at (K. Khodier), lisa.kandlbauer@unileoben.ac.at (L. Kandlbauer), alexia.aldrian@unileoben.ac.at (A. Aldrian), guenther.redhammer@sbg.ac.at (G. Redhammer), gerold.tippelt@sbg.ac.at (G. Tippelt), renato.sarc@unileoben.ac.at (R. Sarc).

https://doi.org/10.1016/j.scitotenv.2021.145343

1. Introduction

Various inorganic contaminants (e.g., Hg, Pb, Sb, Cd) are commonly present in municipal solid waste (MSW) and mixed commercial waste (MCW)[1] because these elements and heavy metals are - or have formerly been - used in the industrial production of numerous consumer goods (e.g., Turner, 2019; Turner and Filella, 2017; Viczek et al., 2020b; Yan et al., 2020).

Heavy metal and metalloid concentrations are not only important during the product life cycle but also in the post-consumer regime. These contaminants impact waste properties and determine whether a waste is considered hazardous or non-hazardous (EC, 2008a; 2008b). For non-hazardous waste, contaminant concentrations determine whether a waste treatment pathway is suitable (Götze et al., 2016b; Pomberger et al., 2015; Viczek et al., in submission) as they are highly relevant for landfilling, composting, and incineration of waste. Consequently, limit values exist for different waste treatment options (Viczek et al., in submission).

One of these options, for which limit values are of high importance, has become increasingly popular: the production of solid recovered fuel (SRF) with subsequent co-incineration for energy recovery (Dunnu et al., 2009; Hilber et al., 2007) or co-processing in the cement industry (Lorber et al., 2012; Sarc et al., 2014; Sarc et al., 2019). Relevant limit values for SRF or gaseous emissions from its combustion exist on different levels, ranging from regional emission legislation (e.g., US Clean Air Act (US EPA, 2019) or EU industrial emissions directive (EC, 2010)) to national limit values for SRF (e.g., Austrian Waste Incineration Ordinance (AT WIO) referring to mg/MJ (BMLFUW Bundesministerium für Land- und Forstwirtschaft, Umwelt und Wasserwirtschaft, 2010), or Switzerland referring to mg/kg (Swiss Federal Council, 2015)). Furthermore, requirements for SRF are set by standards (e.g., EN 15359 (ASI, 2011b)), cement manufacturers (Lorber et al., 2012), or quality marks (e.g., RAL GZ 724 for quality assured SRF in Germany (Flamme and Geiping, 2012)). It is evident that possibilities to reduce contaminant concentrations are of specific interest to SRF producers and co-incineration or co-processing facilities. As a prerequisite, knowledge about the distribution of contaminants is required.

Inorganic contaminants in waste are often discussed with respect to the materials or waste fractions containing these elements in high concentrations (cf. Götze et al. (2016a) and Viczek et al. (2020b) and references therein). The presence of such contaminant carriers in the input waste directly influences contaminant concentrations in SRF (Nasrullah et al., 2015b). State-of-the-art SRF production facilities include several processing steps, e.g., shredding, magnetic separation, screening, air classification, or eddy-current separation (Sarc et al., 2014; Sarc et al., 2019). Furthermore, they may rely on near-infrared (NIR) technology to remove polyethylene terephthalate (PET) bottles (valuable material for recycling) and polyvinyl chloride (PVC; Cl carrier), thereby reducing the Sb, Cl, and occasionally the Cd content of the SRF (Pieber et al., 2012). However, sorting out specific materials might not be sufficient to decrease the heavy metal content of waste (Zhang et al., 2008).

As suggested by literature (Adam et al., 2018; Curtis et al., 2019; Sarc, 2015), inorganic contaminants in (comminuted) waste can not only be enriched in specific material fractions but also in defined particle size classes. This can result from various factors such as a) the materials' original particle size; b) its comminution behavior (e.g., passing through or tearing of plastic foils or textiles, brittle fracturing of glass) that leads to different particle size distributions of material classes (Khodier et al., 2020) or plastic types (Möllnitz et al., 2020)); c) the different heavy metals these materials typically contain (Viczek et al., 2020b); and d) the physicochemical properties of the elements (e.g., adsorption of elemental Hg to materials with a high specific surface area (LfU Bayern, 2003)).

In literature reporting waste compositions and contaminants (cf. comparison in appendix A), elevated levels of certain heavy metals often occur in the "fine fraction", a barely investigated residual fraction that is not sorted but sometimes chemically analyzed. Although the fine fraction has a different particle size in almost every study, a comparison of these fractions with the coarser, sorted fractions of the same studies reveals that the fine fractions often contain considerably higher concentrations of specific chemical elements (Viczek et al., 2020b).

Compared to the original waste mix, the fine fractions are reported to contain more than twice as much Cr (Beker and Cornelissen, 1999; Sarc, 2015), Co (Beker and Cornelissen, 1999; Curtis et al., 2019; Nasrullah et al., 2015a), Hg (Beker and Cornelissen, 1999; Curtis et al., 2019; LfU Bayern, 2003; Nasrullah et al., 2015a; Sarc, 2015), Ni (ADEME Agence de l'Environnement et de la Maîtrise de l'Energie, 2010; Beker and Cornelissen, 1999; Nasrullah et al., 2015a; Prochaska et al., 2005; Sarc, 2015), and Pb (Beker and Cornelissen, 1999; Nasrullah et al., 2015a; Rugg and Hanna, 1992; Sarc, 2015), to name some examples (cf. Appendix A). All these elements (or certain elemental species) are considered as pollutants severely impacting human health and the environment (Bharagava, 2017). Elemental Hg is assumed to attach to materials with a high specific surface area (LfU Bayern, 2003) and, therefore, occurs in the fine fraction. Furthermore, it can originate from broken Hg thermometers or fluorescent tubes (LGL Bayern, 2012). In contrast, Cr, Ni, Co, and Pb are frequent metal alloy constituents (Holleman et al., 2007; ISSF, 2019). In some reports, elevated concentrations of these alloying elements occur together (Beker and Cornelissen, 1999; Nasrullah et al., 2015a) or together with high Fe concentrations (Nasrullah et al., 2015a), indicating that the observed contaminant levels in the fine fraction could be related to metal abrasions (Viczek et al., 2020b). High Pb concentrations were also reported in ash (Janz, 2010), implying that Pb concentrations in the fine fraction could rise especially during the heating season.

On the other hand, the fine fractions often feature low concentrations (i.e., less than half the concentration of the waste mix) of Sb (Beker and Cornelissen, 1999; Curtis et al., 2019) and Cd (Beker and Cornelissen, 1999; Curtis et al., 2019; LfU Bayern, 2003; Rugg and Hanna, 1992). These elements are often found in plastics, where Sb_2O_3 is used as a flame retardant synergist or polymerization catalyst for PET, and Cd compounds were formerly used as pigments or PVC stabilizers (Viczek et al., 2020b). Due to the comminution behavior and original particle size of plastics or textiles, these materials are expected to occur in medium or larger particle size fractions (Khodier et al., 2020; Möllnitz et al., 2020). In some publications, however, high Sb concentrations are reported in the fine fractions as well (Nasrullah et al., 2015a; Watanabe et al., 1999) (cf. Appendix A).

The review of the analytical data published in these studies (cf. Appendix A) indicates the existence of a relation between waste particle size classes and concentrations of several elements and higher heavy metal concentrations in the fine fraction. Despite these indications, the fine fraction of MCW is still poorly characterized, and the particle size-dependent element distribution was not yet thoroughly investigated. A first characterization of four composite MCW samples based on their particle-size classes was performed for Adam et al. (2018) and Curtis et al. (2019) for nine elements (As, Cd, Cl, Co, Cr, Hg, Ni, Pb, Sb) and four particle size classes. Due to the small number of samples and screen cuts, the study discusses the concentrations in the four single samples rather than testing statistical significance or looking for distribution patterns. However, such patterns, i.e., the particle size-dependent element distribution, represent valuable information to waste processors and SRF producers. Knowledge on the accumulation of contaminants in specific particle size classes or fractions offers the possibility to manage contaminant flows and maintain SRF quality with comparably simple means such as screening or even as a

[1] By MSW and MCW, this article refers to solid, non-hazardous, mixed wastes from the municipal sector or commercial sectors (e.g., restaurants, production facilities, various stores or businesses) that may include bulky waste items. These wastes typically consist of paper and cardboard, plastics, metals, glass, textiles, wood, organic waste, etc.

complementary technique to existing NIR sorters. The present study, therefore, reports the distribution of 30 chemical elements in nine different particle size classes of a recent MCW stream, identifies patterns, calculates the effect of removing certain particle size classes, and interprets the results based on the intended utilization of the SRF, i.e., co-processing in the cement industry or co-incineration for energy recovery. Complementary results on the material composition, element-material correlations, and relative sampling variabilities (RSVs) of the same waste stream are reported by Khodier et al. (2020) and Viczek et al. (in submission). Furthermore, the fine fraction <5 mm is characterized chemically and mineralogically and treatment options are discussed taking the fraction's composition into account.

2. Materials and methods

2.1. Samples

Approximately 45 metric tons of MCW consisting of different deliveries from the urban area of Graz, Austria, collected in October 2018, were coarsely shredded using a mobile single-shaft coarse shredder (Terminator 5000 SD, F-type cutting unit, Komptech GmbH) operating with a closed cutting gap at 18.6 rpm (i.e., 60% of the maximum shaft rotation speed). For sampling, a replication experiment (DS, 2013) was carried out. In time intervals of 30 s, 200 sample increments (with a mass of ~12 kg each) were taken from the falling waste stream using sampling troughs (length × width × height: 1.17 × 0.37 × 0.30 m). Combining 20 increments taken in time intervals of 5 min yielded 10 composite samples, each with a mass of ~240 kg. For details, calculations, and results of the replication experiment, cf. Khodier et al. (2020) and Viczek et al. (in submission).

Further sample processing was a sequence of screening and mass reduction (cf. Fig. 1). Each of the 10 composite samples was screened using a batch drum screen to generate 9 particle size fractions: 0–5 mm, 5–10 mm, 10–20 mm, 20–40 mm, 40–60 mm, 60–80 mm, 80–100 mm, 100–200 mm, 200–400 mm, giving a total of 90 samples. After each screen cut, the mass of the screen underflow was determined, and the sample mass was reduced, if appropriate, cf. Khodier et al. (2020). Particle size fractions >20 mm were manually sorted to determine the material composition and were reunited for chemical analyses.

2.2. Chemical and further analyses

2.2.1. Particle size-dependent element distribution

The samples were dried to constant mass at 105 °C[2], and the dry residue was determined according to EN 14346 (process A) (ASI, 2007). Further sample processing included comminution to a size <0.5 mm with cutting mills, homogenization, and mass reduction. To avoid damage to the mills, hard impurities (visible metal parts, stones) were removed, weighed, and their weight was recorded, but they were not separately analyzed. While this corresponds to common laboratory practice (for a more detailed discussion cf. Viczek et al. (2020b)), it affects analysis results, as discussed in Section 3. All particle size fractions were analyzed by ICP-MS (based on EN 15411 (ASI, 2011a) and EN ISO 17294-2 (ASI, 2017)) after microwave-assisted acid-digestion (ÖNORM EN 13656 (ASI, 2002)) to determine the concentrations of Ag, Al, As, Ba, Be, Ca, Cd, Co, Cr, Cu, Fe, Hg, K, Li, Mg, Mn, Mo, Na, Ni, P, Pb, Pd, Sb, Se, Si, Sn, Sr, Te, Ti, Tl, V, W, and Zn. The Cl content was determined by ion chromatography (EN ISO 10304-1 (DIN, 2009)) after calorimetric digestion (ÖNORM EN 14582 (ASI, 2016)). Samples were analyzed as duplicates. Limits of quantification (L.O.Q.) are given in appendix B. The ash content was determined according to DIN 51719 (DIN, 1997), and the lower heating value (LHV) was calculated according to DIN 51900-1 (DIN, 2000).

2.2.2. Characterization of the fine fractions <5 mm

The comminuted analysis samples (< 0.5 mm) of the fine fractions <5 mm were subjected to a high speed permanent magnetic drum (HPG 500 × 650/13, IFE Aufbereitungstechnik GmbH) working at 172 millitesla (mT). The non-magnetic residue was subsequently treated with a high-intensity magnetic drum (KHP 300 × 2000–9/1H, IFE Aufbereitungstechnik GmbH) working at 630 mT. The two magnetic fractions and the non-magnetic residue were analyzed by ICP-MS as described in Section 2.2.1.

In the magnetic and non-magnetic fractions of composite sample 1, Fe oxidation states were determined by ^{57}Fe Mössbauer spectroscopy using an apparatus (Halder Electronics, Germany) in horizontal arrangement (^{57}Fe Co/Rh single-line thin source, constant acceleration mode with symmetric triangular velocity shape, multi-channel analyzer with 1024 channels, regular velocity calibration against metallic Fe). Data evaluation was performed with the program Recoil using the full static hyperfine interaction Hamiltonian analysis with Lorentzian-shaped doublets (Lagarec and Rancourt, 1997; Rancourt and Ping, 1991).

Powder X-ray diffraction (XRD) data were collected for the magnetic and non-magnetic fractions of composite samples 1 and 8 in coupled Theta-Theta mode on a Bruker D8 Advance diffractometer equipped with a solid-state Lynxeye detector and an automatic sample changer. Data were acquired using Cu $K_{\alpha 1,2}$ radiation between 10° and 90° 2Theta, with a step size of 0.01°, integration time of 1 s, with the divergence slit and the receiving slits opened at 0.3° and 2.5° respectively. A primary and secondary side 2.5° Soller slit was used to minimize axial divergence, and a detector window opening angle of 2.95° was chosen. For Rietveld analyses, the background was modeled with a Chebychev function of 10th order, and the fundamental parameter approach was used to describe the peak shape of the Bragg reflections.

2.3. Calculations and data analysis

Concentrations in mg/MJ were calculated from the concentrations (mg/kg_{DM}) and the corresponding LHV (MJ/kg_{DM}) of the same sample and particle size fraction. The (log)normal distribution of each element's concentration in each particle size class was tested using the Kolmogorov-Smirnov test in OriginPro 2020 (version 9.7.0.188). Statistically significant ($p < 0.05$) correlations between ln(concentration) and ln(mean value of particle size class, e.g., 7.5 for particle size class 5–10 mm) – referred to as element-particle size correlations – were identified in Microsoft Excel 2013 using a one-way ANOVA followed by linear regression analysis. Pearson and Spearman correlation coefficients were computed using MATLAB (version 9.6 R2019a). The strength of the correlations was evaluated as follows: $r \geq 0.5$ or $r \leq -0.5$ strong; $r \geq 0.3$ or $r \leq -0.3$ moderate; $r \geq 0.1$ or $r \leq -0.1$ weak, or $0.1 > r > -0.1$ no correlation (Cohen, 1988). Statistically significant ($p < 0.05$) element-element correlations were calculated using all data points of all particle size fractions applying RStudio (version 1.3.959). Principal Component Analysis (PCA) was carried out using MATLAB® (MathWorks, 2020b). The biplot was created using the MATLAB® function "biplot" (MathWorks, 2020a), considering all the available element concentrations as well as the lower heating value (LHV). It depicts scores and loadings that are calculated by Singular Value Decomposition (SVD) (Massart et al., 1997) with the MATLAB® function "svd" (MathWorks, 2020c). To compare influences of individual variables independent of size and unit, the variables were

[2] For Hg analyses, EN 15411 suggests to avoid heating samples to more than 40 °C during sample processing, because of the volatility of elemental Hg. However, it is assumed, that elemental Hg is also volatilized when the samples are dried at 40 °C. Furthermore, the samples analyzed in this study have already passed several process steps (coarse shredding, sieving, etc.) and were further comminuted in the laboratory. Especially during comminution, temperatures can easily exceed 40 °C. It is, therefore assumed that mainly Hg that is somehow bound is determined in this study, and that drying at 105 °C is suitable for this purpose.

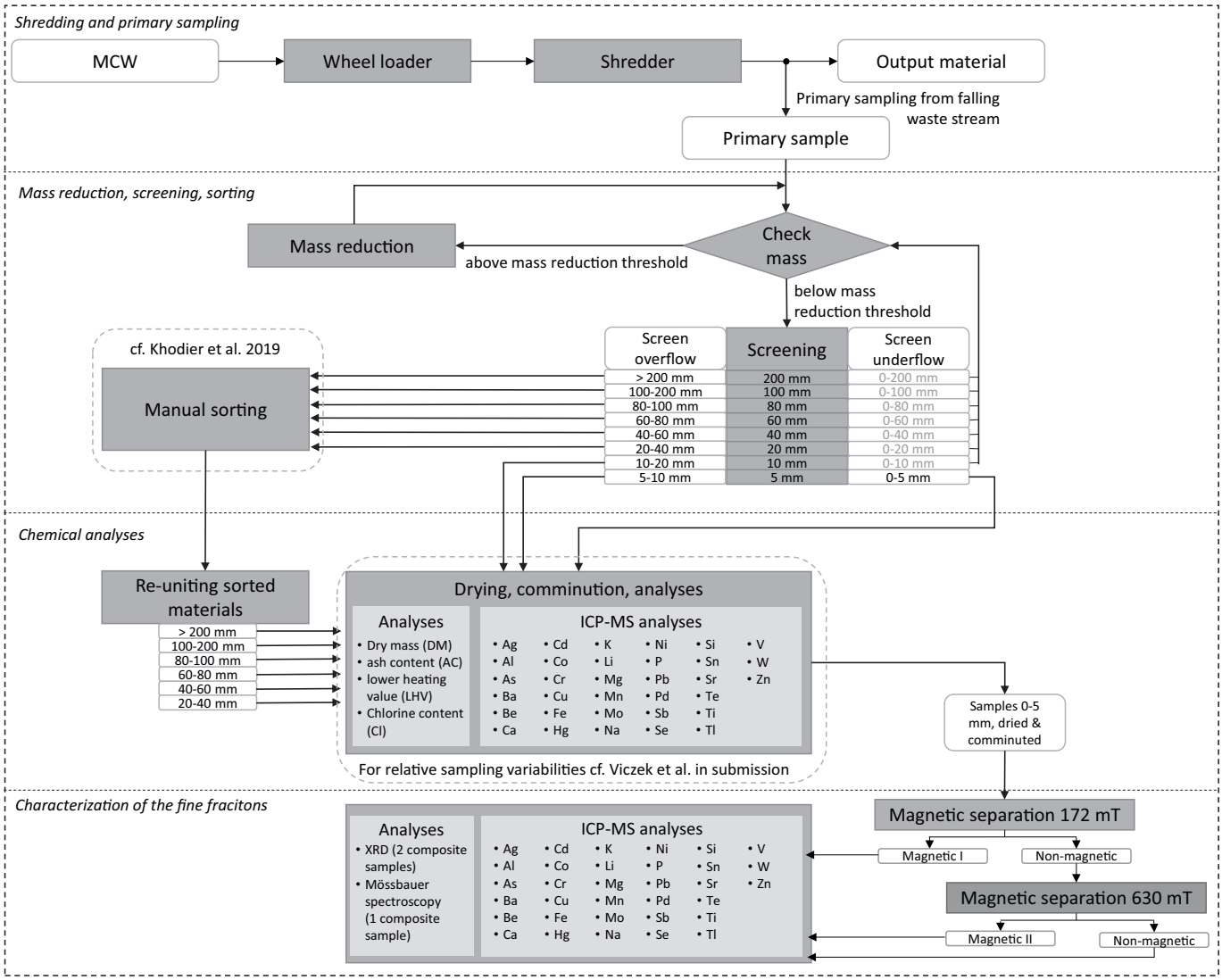

Fig. 1. Sampling and sample processing flowsheet.

standardized so that each column in the data set had a mean of 0 and a standard deviation of 1 before SVD was applied.

3. Results and discussion

Results were obtained for 30 elements; 4 elements were mostly below the limit of quantification (L.O.Q.: Be, Se: 2.5 mg/kg$_{DM}$; Te, Tl: 0.25 mg/kg$_{DM}$). To facilitate the correct interpretation of the results, the fact that hard impurities were manually removed during sample preparation (cf. Section 2.2.1) has to be emphasized.

The common practice in the waste and SRF sector of accounting for hard impurities only in terms of weight (Viczek et al., 2020b), thereby assuming an analyte concentration of 0, would distort the results for the particle size-dependent element distribution.[3] Therefore, all analyte concentrations presented in this paper refer to dry mass without accounting for the mass of hard impurities. Because only sufficiently large particles can be manually removed, hardly any impurities were extracted from particle size class <5 mm (cf. Appendix B). The chosen approach thereby mimics modern SRF production plants, where metals and other heavy particles are removed from the waste stream by magnetic separators, eddy current separators, and wind sifters (Lorber et al., 2012), whereas small impurities (e.g., metal abrasions, metal shavings, glass shards) remain in the waste stream and are reflected in the analyses. Therefore, the analysis results obtained using this approach resemble the concentrations that would likely be achieved if the crude MCW had been processed in modern SRF production plants.

3.1. Element-particle size correlations and concentrations in particle size classes

The subsequent sections present the results for selected elements to give examples for observable patterns. For the full results of 30 analytes (box whisker plots and tables) cf. Appendix B.

3.1.1. Element concentrations in mg/kg$_{DM}$ and element distributions

Three different patterns A, B, and C, were observed for the element concentrations in different particle size classes (cf. Fig. 2a-c, Table 1).

[3] Accounting only for the weight of impurities is a legitimate assumption when the analysis results are not affected by the impurity, e.g., for the lower heating value (LHV), which technically is zero for most hard impurities (metal, glass, inert etc.). This increase in weight, however, would decrease the element concentrations in medium particle size fractions, while concentrations in small particle size fractions would remain almost unaltered. This would amplify trends towards higher concentrations in the smallest, and possibly also in the largest particle size fractions.

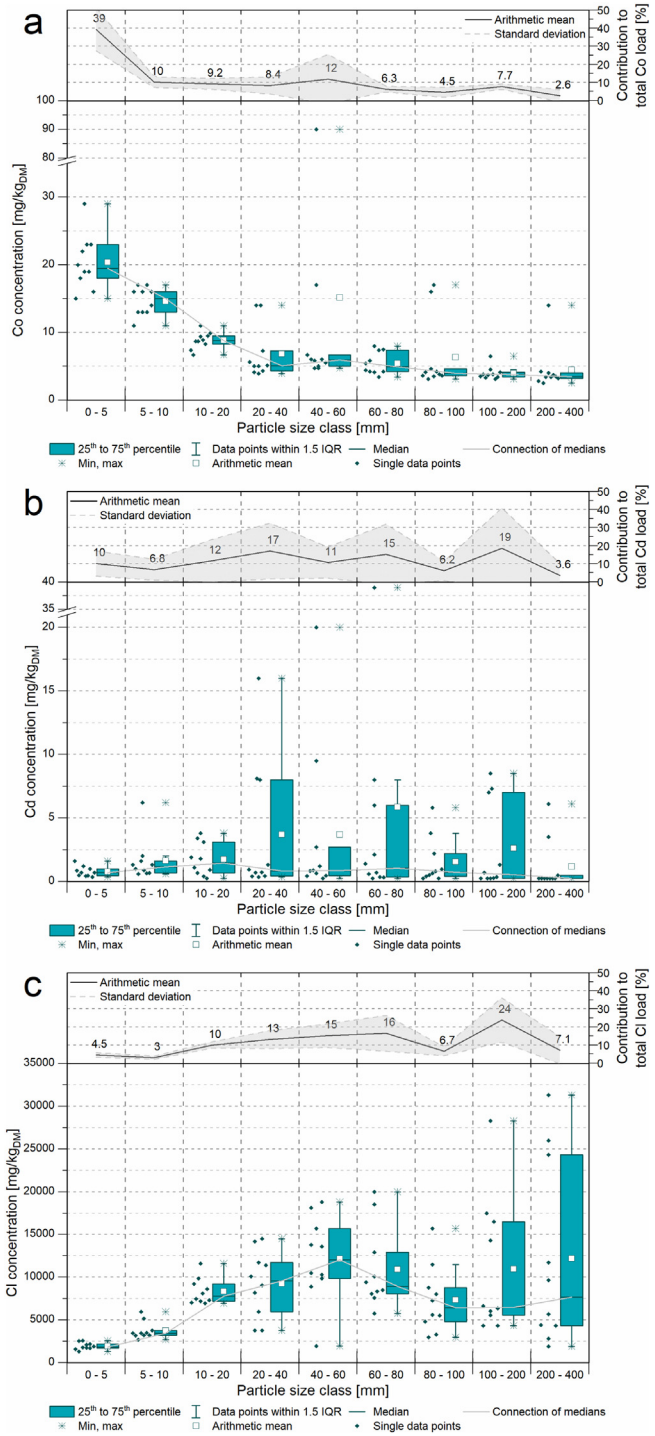

Fig. 2. Analysis results for Co, Cd, and Cl depicted as boxplots, illustrating three observable patterns: (a) Pattern "A": negative correlation - higher concentrations in smaller particle size fractions (b) Pattern "B": no linear correlation (c) Pattern "C": positive correlation - higher concentrations in medium to large particle size classes. The upper part of the graphs illustrates the contribution of each particle size fraction (mean ± standard deviation, $n = 10$) to the absolute amount of the element present in the waste mix.

The patterns are mostly reflected in the box whisker plots, and linear regression analysis of ln(concentration) vs. ln(particle size) confirmed the element concentration-particle size correlations and their statistical significance ($p < 0.05$). Pearson (r) and Spearman (ρ) correlation coefficients, R^2, and p-values are listed in Table C.1 in Appendix C. For most elements except Pd, Hg (many observations < L.O.Q), and the LHV, a lognormal distribution was observed in all particle size classes.

A. Negative linear correlation - Higher concentrations in smaller particle size fractions

Pattern A, by far, represents the predominant correlation pattern for ln(concentration) vs. ln(particle size). It is observable with statistical significance ($p < 0.05$) but varying correlation strengths for 27 of the 30 elements and the ash content. In total, 21 elements (Ag, Al, As, Ba, Ca, Co, Cu, Fe, Hg, K, Li, Mg, Mn, Mo, Na, Ni, P, Si, Sn, Sr, W) and the ash content show strong ($r \leq -0.5$) negative correlations. Another 4 elements (Cr, Pd, V, Zn) show a moderate correlation ($-0{,}5 < r \leq -0.3$). Pb and Ti show weak correlations ($r = -0.27$ and -0.22, respectively). However, the high variability in Pb concentrations in all particle sizes implies that single items or particles present in waste contain high concentrations of Pb. Some elements (e.g., Na) exhibit features that are not well reflected by a linear correlation. Predictions may, therefore, require quadratic or higher-order polynomial models.

The distribution of the total element content among the particle size fractions (taking the masses of each particle size fraction into account) is depicted above each box whisker plot in Fig. 2. Fig. 2a shows that, on average, 39% of the total Co present in the waste is located in the fraction 0–5 mm, and 49% in the fraction 0–10 mm. The fraction 0–5 mm also contains the largest part (21 to 49%) of the other 24 elements attributable to pattern "A" with a strong or moderate correlation. For Ti, the fractions' contributions rather depend on the fractions' masses. Pb contributions are highly variable due to the high variability of analyte concentrations.

B. No linear correlation - low concentration in smallest and largest particle size classes

No statistically significant correlation was found for Cd (Fig. 2b), because a linear regression model cannot reflect the concentration pattern (highest concentrations and variabilities in medium particle size fractions). While the mean values reflect this pattern, the medians, being less prone to outliers, are similar in all particle size fractions. Each fraction's contribution to the total amount of Cd is highly variable, with several peaks in different particle size fractions.

C. Positive linear correlation - Higher concentrations in medium to large particle size classes

Higher concentrations in medium or large particle size classes were observed for Cl (Fig. 2c) and Sb. Furthermore, the LHV increases with increasing particle size (Fig. 3a). Linear regression analysis showed moderate ($r \geq 0.3$, Sb) or strong ($r \geq 0.5$, Cl) positive correlations between ln (particle size) and ln(analyte concentration). Due to their industrial uses, both Cl and Sb are often associated with plastics. Because of their flexibility and dimensionality, most plastics in MCW are not expected to be comminuted to very small particle sizes during one coarse shredding step, and therefore end up in larger particle size fractions. Furthermore, the high variability within the particle classes reflects the fact that single items contain high concentrations of these elements (e.g., Sb in flame-retarded plastics or textiles, Sb catalyst residues in PET bottles, Cl in PVC). These single items might not always end up in the primary sample or subsamples.

Larger particle size fractions also contribute the main share of elements following pattern "C". With an average of 24%, most Cl in the investigated waste stream is present in the particle size fraction 100–200 mm. The same fraction also carries the most considerable amounts of Sb (17%), but the fractions 20–40 mm and 40–60 mm contribute similar amounts (16% and 15%, respectively).

3.1.2. Element concentrations in mg/MJ

Official or legal limit values for SRF are often given in mg/MJ (e.g., EN 15359 (ASI, 2011B), AT WIO (BMLFUW Bundesministerium für Land- und Forstwirtschaft, Umwelt und Wasserwirtschaft, 2010)). Because

Table 1
Assignment of elements to the three different patterns determined by the correlations between particle size and analyte concentration in mg/kg$_{DM}$ (ash: %$_{DM}$, LHV: MJ/kg$_{DM}$) or mg/MJ.

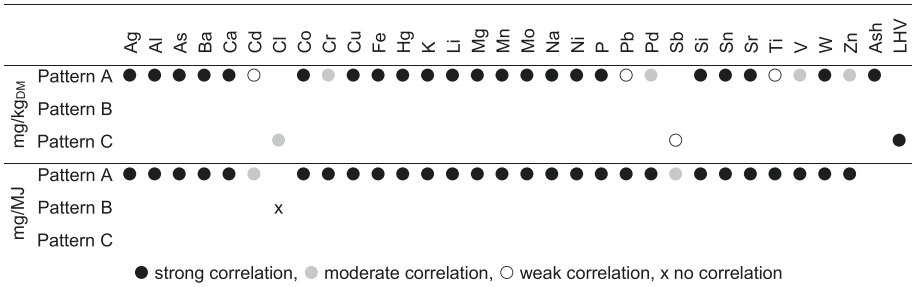

of the positive correlation between particle size and the LHV (see Section 3.1.1), the consideration of concentrations in mg/MJ affects the patterns presented in Section 3.1.1 (Fig. 3a). Pattern "A" (higher concentrations in small particle size fractions) is further enhanced, and the strength of the negative correlations is increased. This effect is illustrated in Fig. 3 b-c at the example of Hg. When considering analyte concentrations in mg/MJ, statistically significant moderate or strong negative correlations are found for 29 of the 30 elements, which could then be attributed to pattern "A" (Table 1). In this setting, Cd and Sb exhibit moderate negative correlations, and no positive correlation is observable for Cl any more ($r = -0.09$, cf. Appendix C). As a result, the importance of the small particle size fractions increases when limit values are given in mg/MJ, and the effect of their removal (see Section 3.6) is even larger.

3.2. Average concentrations in the investigated waste mix and comparison with literature values

To assess whether the overall element concentrations in the examined waste stream are within the expected range, or if some concentrations stand out, the overall analyte concentrations in the examined waste stream (mean values, $n = 10$) are compared to the literature review performed by Götze et al. (2016a) (Fig. 4). Because the review comprises different kinds of municipal waste and the handling of hard impurities is unclear, the values are not fully comparable. Nevertheless, extraordinarily high or low concentrations can be pointed out. Fig. 4 shows that – while single elements exceed the maximum observed value (Mo, Sr) or are below the minimum concentration (Li, P) reported by Götze et al. (2016a) – most concentrations are between the 25th and 75th percentile, i.e., within an expected range. A direct comparison with the single studies, from which an accumulation of contaminants in the fine fraction can be suggested (see Appendix A, Table A.1) shows that – even though some studies are from the 1990s and different countries (different legislation, different products) – the concentrations of many elements in the MCW mix and fine fractions are still in similar orders of magnitude. The enrichment of element concentrations in the fine fraction compared to the waste mix, however, is not as significant as reported in previous studies (Beker and Cornelissen, 1999; Nasrullah et al., 2015a), see Table A.2. This might be due to the fine fraction's large mass share in the present study, which significantly affects overall element concentrations.

3.3. Characterization of the fine fractions <5 mm

3.3.1. Elemental distribution after magnetic separation

ICP-MS analyses of the fine fractions <5 mm showed an average Fe concentration of approx. 113 g/kg$_{DM}$, i.e., 11.3%, which is 10 times higher than the concentrations reported in the literature, cf. Appendix A. Besides Fe, other typical alloying elements occur in these fractions. Treatment of the fine fraction with magnetic separators and subsequent analysis by ICP-MS demonstrated that the largest share of Fe is transferred into the fraction "Magnetic I", i.e., the magnetic fraction after magnetic separation at 172 mT (Fig. 5).

Together with iron, the largest shares of Co, Cr, Mn, Mo, Ni, and W were transferred into the fraction Magnetic I. In the case of Hg, the fractions Magnetic I and Non-magnetic contain similar shares. The observed results and the correlation analysis in Section 3.1.1 support the hypothesis that metal abrasions may be responsible for the high concentrations of these elements, as proposed, e.g., by Viczek et al. (2020b). Magnetic fraction I mainly consists of Fe (350 g/kg) and Si (313 g/kg). Si likely originates from dust and other non-magnetic particles, indicating that the very small particle size (comminuted to <0.5 mm) of the analysis sample was not ideal for magnetic separation (dust, particles being carried along, likely electrostatic charge). This "contamination" and the presence of organic matter (C was not determined) in the magnetic fractions (I and II) have to be considered when interpreting the results. It also causes a loss of material that would otherwise contribute to the LHV of the residual non-magnetic fraction.

Magnetic Fraction II contains large amounts of Si (421 g/kg), Ca (108 g/kg), and Fe (40 mg/kg). The non-magnetic fractions also contain large amounts of Si (146 g/kg), Ca (97 g/kg), and probably the largest amount of organic matter. For full results of 29 elements (concentrations, distribution among fractions, visualization) cf. Appendices E and F.

Although the recovery after magnetic separation was between 80 and 120% for most elements, it ranged from 49 to 184% (compared to the original concentration in the fraction <5 mm, cf. Table E.1). However, the recovery is in a similar range as the RSVs observed in Viczek et al. (in submission). It may result from material losses during magnetic separation and sample segregation, which was observed for all fractions. Nevertheless, elements can be assigned to fractions carrying the highest concentrations, and the fraction into which most of the element was transferred in the process can be identified (Table 2). Due to the smaller masses of Magnetic fraction I and II, they do not always carry the highest share of the element, despite carrying the highest concentrations.

3.3.2. Mineral phases

The phase content of crystalline phases in the samples is complex, especially in the non-magnetic concentrates, which prevented the identification of all phases. The results of the Rietveld analysis to obtain phase contents are given in Table 3. It is evident that in the Magnetic I concentrates, the dominating phases are calcite $CaCO_3$ and bassanite $CaSO_4 \cdot 0.5\ H_2O$. Small amounts of other $CaSO_4$ phases (anhydrite and gypsum) are also present besides small amounts of dolomite $CaMg(CO_3)_2$. As expected, the Magnetic I concentrates show the highest content of iron-containing phases, predominately as magnetite Fe_3O_4, wuestite $Fe_{1-x}O$ and most probably magnesio-wuestite (labeled wuestite 2 in Table 3). Furthermore, they contain minor amounts of hematite Fe_2O_3. There is no clear evidence for metallic iron. However, there is evidence for further iron-containing phases such as micas and iron-rich chlorites (clinochlore).

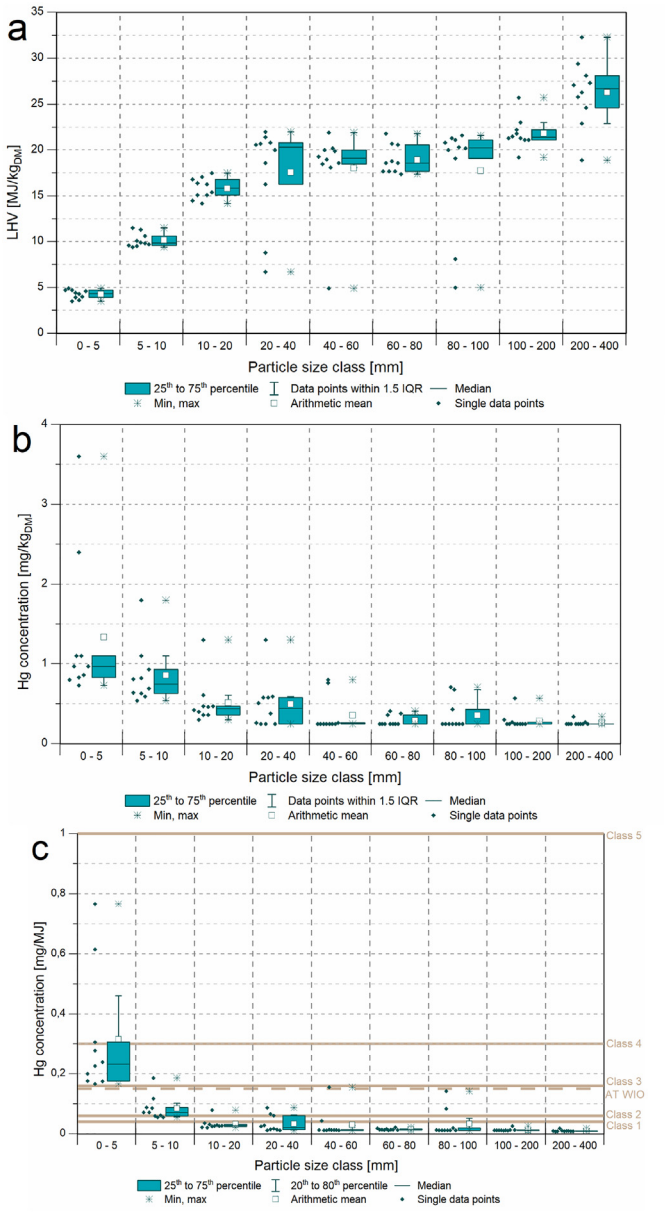

Fig. 3. (a) Lower heating value of different particle size classes of coarsely shredded MCW without accounting for the weight of impurities, (b) Hg concentrations in mg/kg_{DM}, (c) Hg concentrations in mg/MJ including the 80th percentile limit values for the five SRF classes defined in EN 15359 (solid lines) and the Austrian waste incineration ordinance (AT WIO, dashed line).

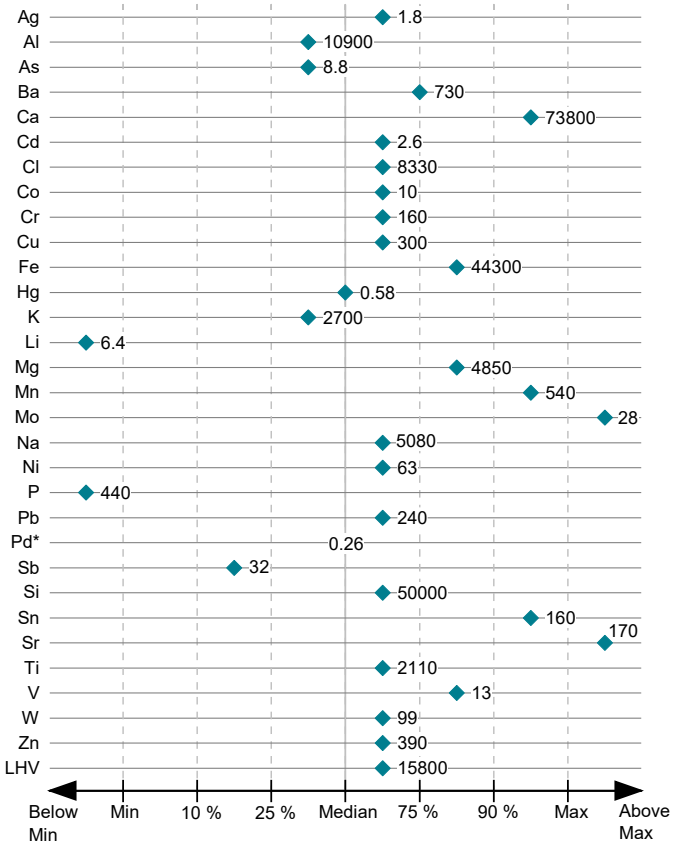

Fig. 4. Comparison of overall analyte concentrations in the investigated MCW stream with the statistical evaluation of literature data performed by Götze et al. (2016a). The marker's labels represent the mean concentrations of the examined waste stream (n = 10; mg/kg_{DM} for elements, kJ/kg_{DM} for LHV, both without hard impurities). The marker position shows between which percentile values of Götze et al. (2016a) the concentration is located. Overall concentrations are calculated from the mass shares of particle size classes and analyte concentrations therein. Mean values, standard deviation, and median are given in Table D.1 in Appendix D. * No statistical evaluation of Pd was available.

Most iron phases are reduced in Magnetic fraction II, and only minor amounts of wuestite, magnetite, and hematite are found. In these concentrates, quartz is enriched, as is bassanite, dolomite, and to some extent, calcite. The main crystalline phases in the non-magnetic fractions are quartz and calcite, and bassanite for one sample (see Table 3). Concludingly, the main crystalline (mineral) phases determined by XRD correspond well to the main elements identified in these fractions in Section 3.3.1. However, differences can be observed for some elements and may be connected to the presence of non-crystalline compounds such as glass particles.

3.3.3. Mössbauer analysis

As determined from XRD analysis, there is no firm evidence for metallic iron in the concentrates. The ^{57}Fe Mössbauer spectrum (cf. Appendix E) of magnetic fraction I (composite sample 1) is the superimposition of spectra contributions of the oxidic phases magnetite, hematite, two types of wuestite, and a paramagnetic Fe^{3+} component, which corresponds to Fe^{3+} in octahedral coordination, most probably an iron-rich sheet silicate (clinochlore as evidenced by X-ray diffraction). The need for two different components for wuestite is based on the fact that only with two doublets of the strong absorption contribution around Doppler velocities of +1.0 mm/s can be satisfactorily matched. From the evaluation of the Magnetic I Mössbauer spectrum, ~ 54% of total iron is in the high spin divalent state; the remaining is ferric iron. Half of the area fraction of the sextet for the octahedral site of magnetite was assigned to Fe^{2+} and Fe^{3+}, respectively, as due to fast electron hopping it is not possible to discern between the two valence states at this crystallographic position in magnetite, one observes Mössbauer parameters intermediate between Fe^{2+} and Fe^{3+}.

In Magnetic fraction II, the spectral signatures of magnetite and hematite have significantly decreased and are on the border to being resolved. It is evident that the spectral features of paramagnetic high spin Fe^{3+} in octahedral coordination has significantly increased. Besides, there is a need for a doublet for Fe^{2+} in wuestite and an additional Fe^{2+} component, which has typical values for octahedral coordination and might arise from an iron-rich mica. Consequently, based on the Mössbauer data, this concentrate shows iron in oxidic form, and ~ 39% are in the divalent state. However, most of the iron seems to be enriched in (sheet) silicates.

In the non-magnetic concentrate, the overall iron content is very low, and thus the spectrum appears noisy. Here, the Mössbauer spectrum still indicates the presence of some hematite; around 18% of

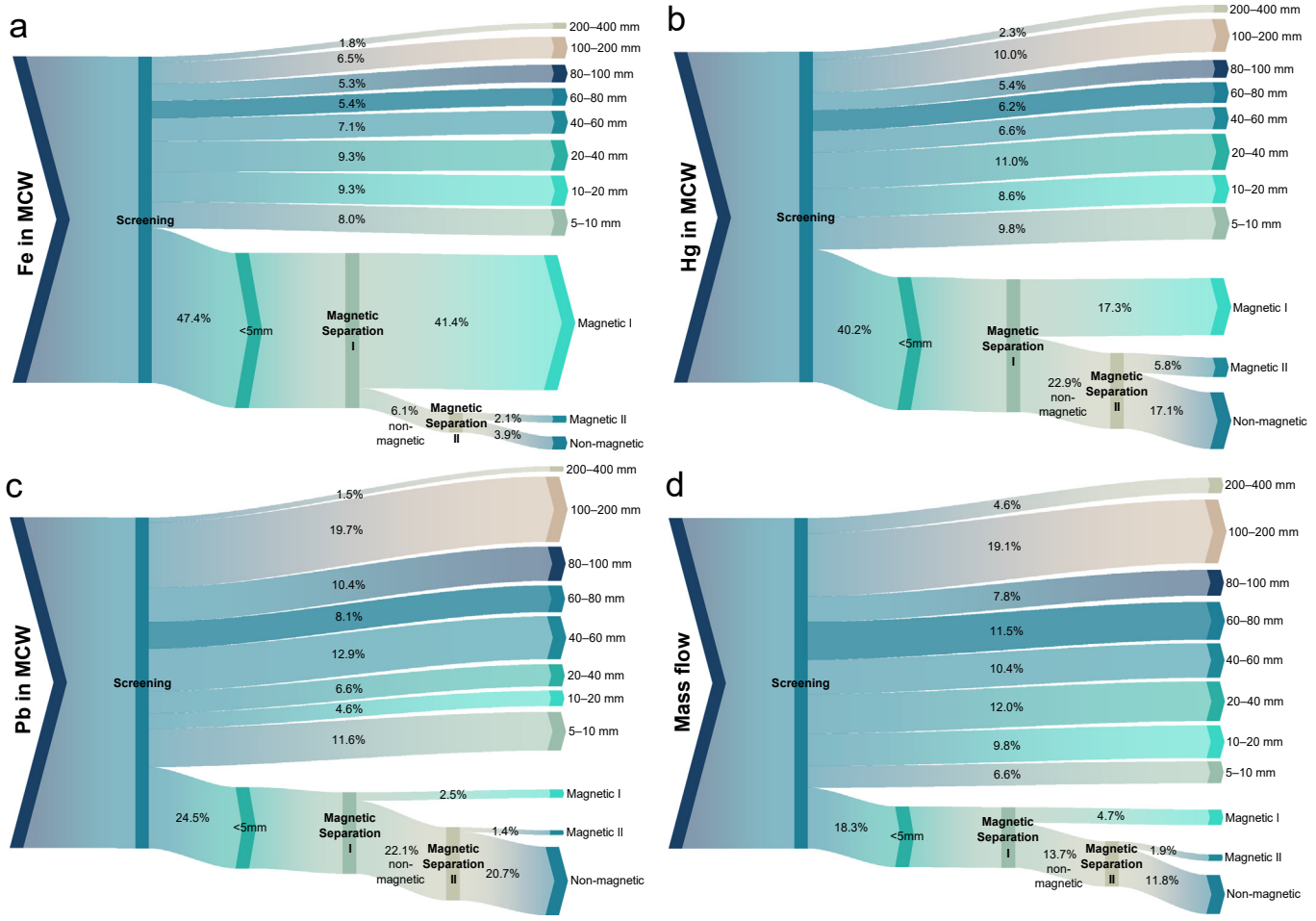

Fig. 5. (a) Fe flows, (b) Hg flows, (c) Pb flows, and (d) mass flows after screening and magnetic separation.

total iron can be assigned to this mineral. For satisfactory evaluation of the paramagnetic resonance absorption contribution, 5 additional doublets are necessary. Two of them correspond to ferric iron in octahedral coordination. The remaining have Mössbauer parameters typical for Fe^{2+}; from this, ~ 30% of total iron is in the divalent state.

3.4. Element-element correlations

Statistically significant ($p < 0.05$) element-element and element-LHV correlations are depicted in Fig. 6. The strongest correlations with $r \geq 0.9$ are Mn-Fe (0.98), Si-K (0.95), W-Hg (0.95), Mg-K (0.94), Sr-Mg (0.93), Mo-Mn (0.92), Sr-K (0.92), Mo-Fe (0.91), Sr-Si (0.91), LHV-K (−0.91), LHV-Si (−0.91), LHV-Sr(−0.91), LHV-Mg (−0.9), Na-K (0.9), and Si-Mg (0.9), cf. Fig. C.2 in Appendix C. While some correlations can be explained by the common industrial uses of these elements, it is important to note that correlation does not imply causation. Correlations for which possible explanations can be given include the strong negative correlations between the LHV and K, Mg, Si, and other elements whose oxides are typical ash-constituents. In the five samples for which the ash content was determined, there is also a strong positive correlation ($r \geq 0.96$) between these elements and the ash content, and, as expected, a strong negative correlation ($r = -0.97$) between the LHV and the ash content (Fig. C.3 in Appendix C). On the other hand, the positive correlations between the LHV and Cl ($r = 0.53$) or Sb ($r = 0.4$) are probably linked to their presence in plastics.

When correlation coefficients are calculated only for the fractions below 20 mm (Fig. C.4 in Appendix C), a strong correlation between Cr and Ni ($r = 0.99$) can be observed. This could indicate the presence of abrasions from Cr and Ni-containing alloys in the fine fractions.

3.5. Principal component analysis (PCA)

The PCA results are displayed in the biplot given in Fig. 7, where the first two Principal Components are considered. Here, the explainable variance in the first two dimensions reaches 57% but gives a good overview of the data and supports the statements from the ANOVA. The

Table 2
Assignment of elements to the fractions with their highest concentration and the fractions carrying the highest total share of the element load.

Highest concentration			Highest share		
Magnetic Fraction I	Magnetic Fraction II	Non-magnetic Fraction	Magnetic Fraction I	Magnetic Fraction II	Non-magnetic Fraction
Ag[a], As, Co, Cr, Cu[a], Fe, Hg, Mn, Mo, Ni, W, Zn[a]	Ag[a], Al, Ca, Cd, Cu[a], K, Li, Mg, P, Si, Sr, Ti, V, Zn[a]	Ba, Na, Pb, Sb, Sn	Co, Cr, Fe, Hg[a], Mn, Mo, Ni, W		Ag, Al, As, Ba, Ca, Cd, Cu, Hg[a], K, Li, Mg, Na, P, Pb, Sb, Si, Sn, Sr, Ti, V, Zn

[a] Similar concentrations/shares in 2 fractions.

Table 3
Crystalline phase content of the investigated fine fractions in wt% and standard deviations from refining obtained by Rietveld analysis of powder X-ray diffraction pattern.

Phase	Composite sample 1			Composite sample 8		
	Magnetic Fraction I	Magnetic Fraction II	Non-magnetic	Magnetic Fraction I	Magnetic Fraction II	Non-magnetic
Quartz	8.8 ± 0.6	14.6 ± 0.7	23.4 ± 0.8	19.0 ± 0.7	19.8 ± 0.9	46.8 ± 0.9
Calcite	21.3 ± 0.8	26.6 ± 0.9	22.9 ± 0.8	15.6 ± 0.8	26.4 ± 1.2	25.1 ± 0.9
Dolomite	4.3 ± 0.8	6.6 ± 0.6	10.6 ± 0.7	3.3 ± 0.7	4.0 ± 0.8	7.7 ± 0.8
Magnesite	0.8 ± 0.7	–	–	3.0 ± 0.7	–	–
Anhydrite	5.4 ± 0.9	6.4 ± 0.6	5.8 ± 0.8	2.6 ± 0.6	2.1 ± 0.8	0.7 ± 0.3
Bassanite	29.3 ± 0.9	34.8 ± 1.2	26.9 ± 0.9	8.6 ± 0.8	13.9 ± 1.2	7.3 ± 0.9
Gypsum	2.3 ± 0.6	1.5 ± 0.7	1.1 ± 0.4	12.4 ± 0.5	17.9 ± 1.3	8.6 ± 1.2
Lime	0.6 ± 0.4	–	–	–	–	–
Magnetite	10.0 ± 0.7	1.0 ± 0.4	–	13.7 ± 0.8	1.0 ± 0.6	–
Hematite	1.8 ± 0.7	0.3 ± 0.1	0.1 ± 0.1	2.9 ± 0.4	0.2 ± 0.1	–
Wuestite	7.2 ± 0.4	0.3 ± 0.1	0.2 ± 0.1	10.6 ± 0.4	0.5 ± 0.2	0.2 ± 0.1
Wuestite 2	3.2 ± 0.6	0.1 ± 0.1	0.2 ± 0.1	5.1 ± 0.4	0.4 ± 0.1	–
Clinochlore	4.2 ± 0.6	1.3 ± 0.4	2.8 ± 0.6	3.2 ± 0.7	3.9 ± 0.7	1.5 ± 0.4
Muscovite	0.2 ± 0.1	5.6 ± 1.5	4.9 ± 0.9	0.4 ± 0.1	–	1.6 ± 0.2
Albite	0.8 ± 0.3	0.9 ± 0.4	0.1 ± 0.1	0.1 ± 0.1	9.7 ± 0.9	0.1 ± 0.1
Rutile	–	–	0.7 ± 0.4	–	0.3 ± 0.1	0.3 ± 0.1

biplot graphically reflects the three patterns outlined in Section 3.1.1, as all elements that were assigned to pattern "A" (negative correlation with particle size) are located on the right side of the coordinate origin of the biplot, while elements of pattern "C" (positive correlation) on the left side. The correlation strength is reflected by the endpoint location of the parameter vectors on Principal Component 1 (PC1). While elements with a strong negative correlation (higher element concentration in smaller particle sizes - acc. to the classification in Section 3.1.1) are plotted furthest away from the origin regarding PC1, the elements with weak correlation appear in a position closer to the origin. Consequently, elements for which no linear correlation between particle size and element concentration is detected, e.g., Cd – assigned to pattern "B" – are located close to the origin. Slight deviations in correlation strengths can be explained by the fact that the biplot only shows the results in the first two dimensions. This leads to a loss of information in the plot, which is contained in the remaining dimensions. Nevertheless, the plot allows for visualization of the data and their basic structure, which matches the statements presented in Section 3.1.1.

Further information provided by PCA in Fig. 7 is the interpretation of the element distribution in different particle size classes. The plot shows that small particle size fractions appear on the right side. Despite the overlapping of the data points on the left side, the plot shows a trend that fractions belonging to larger particle sizes tend to be positioned further left. The combined visualization of variables and objectives allows to state the correlation between elements and particle size classes based on the position in the plot. If data points and elements appear

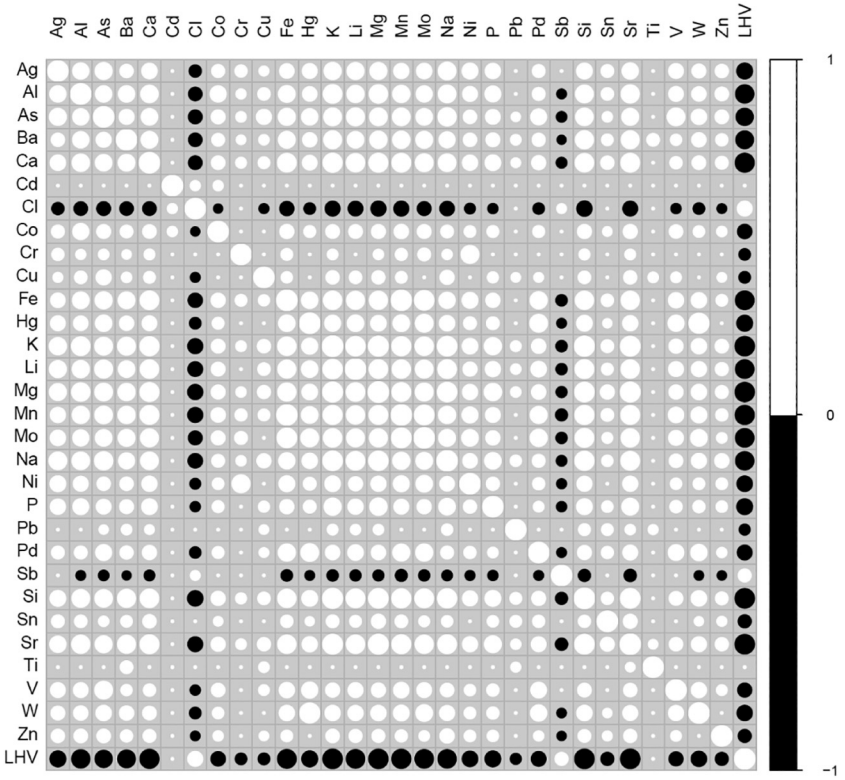

Fig. 6. Statistically significant ($p < 0.05$) positive (white) and negative (black) element-element and element-LHV correlations. The size of the circles is proportional to the strength of the linear correlation (Pearson correlation coefficients; for numbers cf. Appendix C).

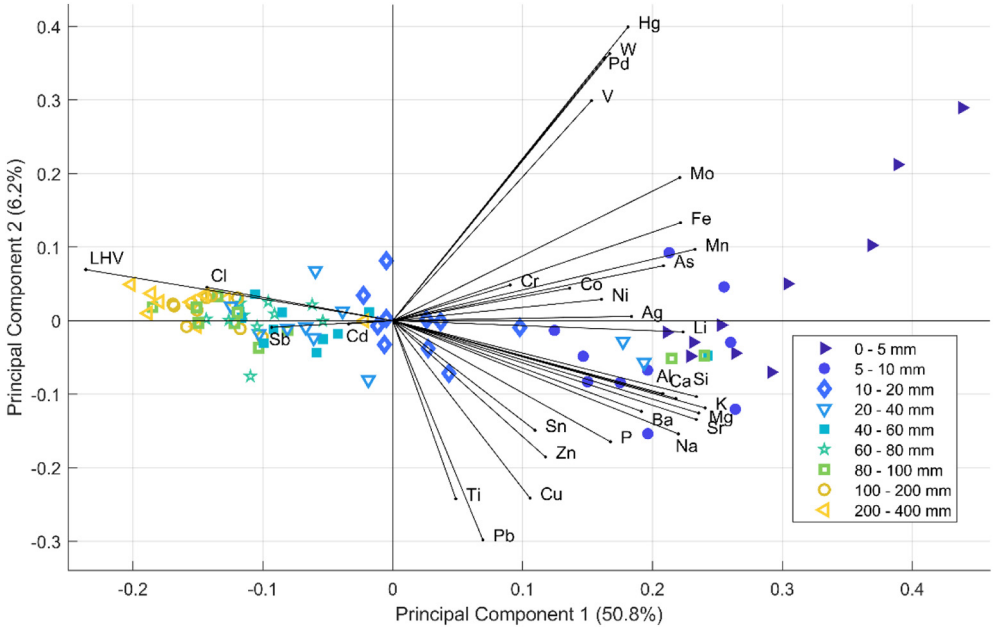

Fig. 7. Visualization of the PCA results (biplot) in the first two dimensions. Markers represent the scores of the individual objectives, which are in this work the 90 available samples. Lines represent the loadings and describe the variables from the given data set (30 elements and LHV, see Table 1). The explained variance of each Principal Component is given in parentheses at the axes.

in the same area in the plot, a positive correlation can be found; if they are plotted far away from each other on opposite sides, a negative correlation is present. Based on this, small particle size classes (0–5 mm, 5–10 mm) show a higher concentration of most metals and typical ash-constituents (Si, Ca, Al, etc.) and a smaller LHV as well as Cl concentration. Particles belonging to a larger particle size class generally show a higher LHV and tend to have lower concentrations of major ash-constituents and metals.

The PCA also enables the visual detection of outliers, an example being the two data points categorized as 80–100 mm that are positioned on the right side of the plot. A closer investigation showed that these samples contain higher concentrations of Si, K, Mg, Sr, Al, and Na, which explains the differentiated position far off the remaining data points of the same particle size class.

Besides the element-particle size correlations, Fig. 7 also visually reflects element-element correlations (cf. Section 3.1.1). Information about the correlations is given through the position of the vectors. If they appear close together or in the same area of the plot, variables show a strong positive correlation to one another. Different orientations of the lines indicate a shift from strong positive towards no or negative correlations. Therefore, the strong negative correlation between LHV and K, Mg, Si, or Sr is stated by the position of the elements on opposite sides of the origin on the horizontal axis. A positive correlation between, for example, Mg, K, Sr, and Na, or W and Hg can be seen by the same direction of the respective vectors, which can also be observed for LHV and Cl.

3.6. Effect of the removal of specific particle size fractions

By calculating the expected concentrations in screen overflow and comparing these concentrations to the initial concentration in the waste stream (Fig. 4 and Table D.1), the theoretical effect of a screening step can be simulated. This effect is depicted in Fig. 8, referring to relative concentration changes in mg/kg$_{DM}$ (Fig. 8a) and mg/MJ (Fig. 8b). Removing small particle size classes is expected to impact the properties of the waste stream as follows:

- Removing fractions with a low LHV leads to an average LHV-increase in the screen overflow by 16% (removal of fraction 0–5 mm) or 21% (removal of fraction 0–10 mm) compared to the LHV of the initial waste stream.
- This LHV increase is achieved by removing 18 to 25% of the mass (DM without hard impurities), i.e., ~1% LHV increase per 1% of mass decrease.
- Considering concentrations in mg/kg$_{DM}$, all 27 elements assigned to pattern “A” an average decrease of 2.1 to 38% (removal of fraction 0–5 mm) or 2.3 to 47% (removal of fraction 0–10 mm) is observed.
- Since the small fractions only contain small concentrations of Cd, Sb, and Cl but amount to 18 to 25% of the mass, their removal is accompanied by a concentration increase of elements of pattern “B” and “C” by 10 to 17%, or 11 to 23%, respectively.
- When concentrations are considered in mg/MJ, the concentration of 29 elements, even Sb and Cd, is decreased by 3.6 to 46%, or 5.9 to 56%, respectively. This indicates that the increased LHV compensates the increased Cd and Sb concentrations that were observed on a mg/kg$_{DM}$ basis. Only Cl concentrations are still slightly increased by 0.5 to 1.8%. However, as the Cl content is usually expressed in %$_{DM}$ rather than in mg/MJ, the Cl content, in any case, needs to be considered as experiencing a significant increase when smaller fractions are removed.
- While the quality of the screen overflow is increased concerning several parameters, the screen underflow represents a waste fraction with poor quality and a low LHV, exceeding many limit values, e.g., those for SRF defined by the Austrian WIO.

The low quality of the screen underflow makes comparing the expected element concentrations in the screen overflow and underflow with limit values essential. Fig. 9 depicts the expected (calculated) Hg concentrations in the screen underflow (U) and overflow (O) after a single screening step at different mesh sizes. While the average concentration of the investigated MCW mix is close to the 80th percentile limit value for class 1 SRF, the concentration in the screen overflows (80th percentile) is usually below this limit irrespective of the screen cut. The screen underflows, however, often exceed the defined limit values significantly. For example, based on the Hg concentration only (and not considering the LHV and other parameters), the screen underflow <5 mm could only be classified as class 5 SRF. In Austria, this fraction alone could

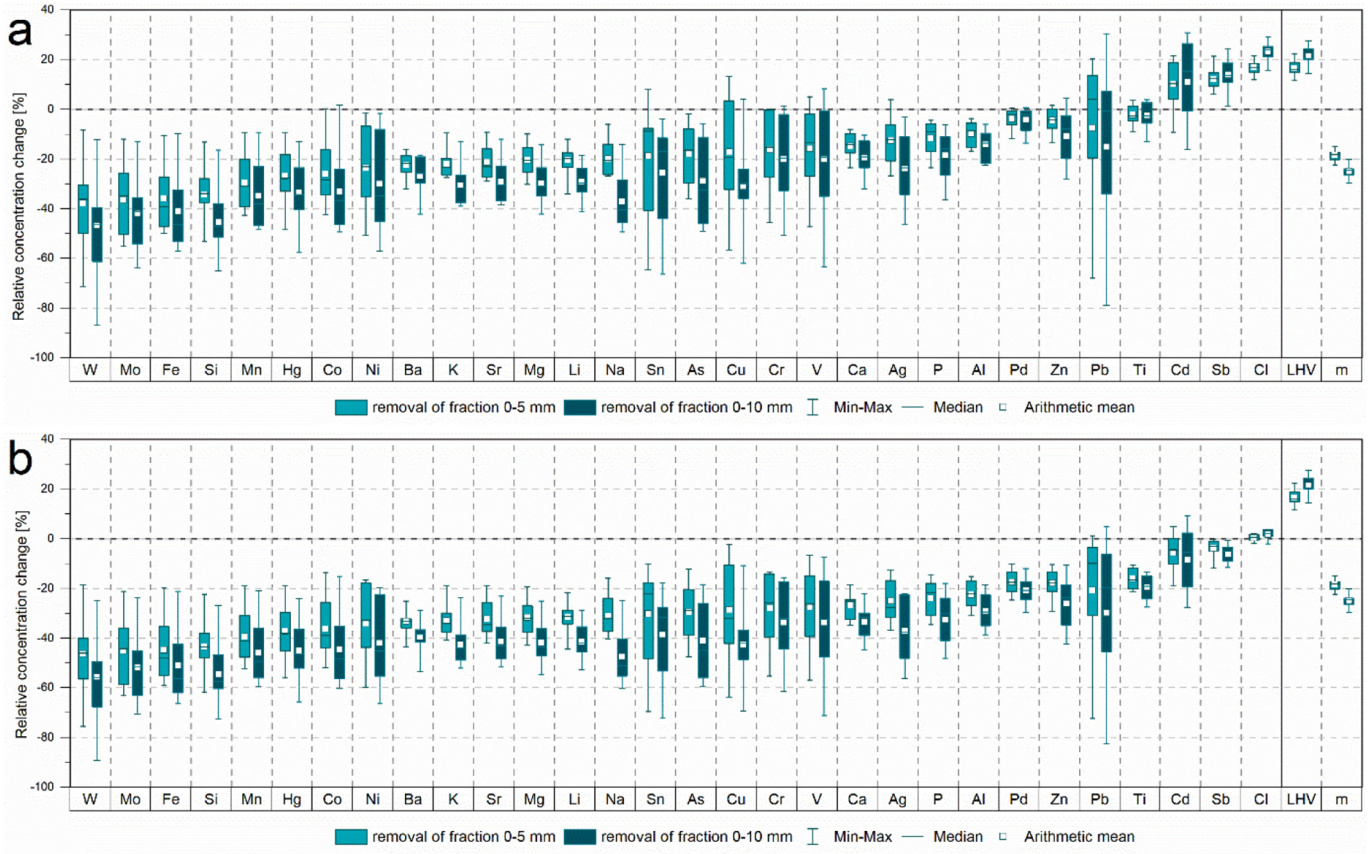

Fig. 8. Effect of the removal of the fractions 0–5 mm and 0–10 mm: relative concentration change in the screen overflow referring to (a) mg/kg_{DM} and (b) mg/MJ. "m" represents the mass loss [%] by removing the fraction from the waste stream and refers to dry mass, LHV always refers to MJ/kg_{DM}.

not be used as SRF in the cement industry anymore. This emphasizes the importance of choosing the right screen cut suiting the purpose and, if applicable, finding separate treatment pathways for the low-grade fractions in which the contaminants are enriched.

Appendix D lists the expected average LHV and concentrations of all analytes in the screen underflow and overflow after a single screening step at 5, 10, 20, 40, 60, 80, 100, and 200 mm, and provides charts similar to Fig. 9 for As, Cd, Cl, Co, Cr, Ni, Pb, and Sb.

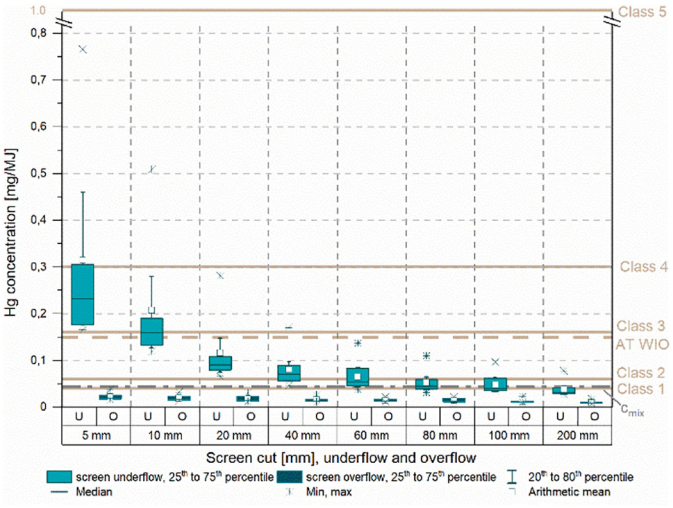

Fig. 9. Calculated Hg concentrations [mg/MJ] in screen underflow (U) and overflow (O) after a single screening step and comparison with 80th percentile limit values from EN 15359 (solid lines) and the Austrian waste incineration ordinance (AT WIO, dashed line). The dash-dotted line represents the concentration (80th percentile, i.e., 0.043 mg/MJ) in the investigated waste mix.

3.6.1. Implications for SRF intended for (co)-incineration other than cement kilns

Removing the fine fraction from MCW for the production of SRF intended for co-incineration facilities other than the cement industry (e.g., power plants) (Thiel and Thomé-Kozmiensky, 2012) could be beneficial for all parameters assessed, provided that Cl carriers can be removed. This can, for example, be done with an NIR sorter. Apart from its heavy metal content, the fine fraction is not a valuable fraction for this application as it increases the ash content of the fuel, thereby increasing the amount of slag that has to be treated or disposed of, e.g., landfilled. Removing the fine fraction could also increase the amount of SRF that can be co-incinerated as capacities become available. Therefore, screening can be considered worthwhile for this application.

3.6.2. Implications for SRF intended for co-processing in the cement industry

The situation is more complex for co-processing. In the cement kiln, the SRF ash is incorporated into the clinker and thereby substitutes some of the raw materials (Aldrian et al., 2020; Viczek et al., 2020a). The main chemical compounds for cement manufacturing are SiO_2, Al_2O_3, CaO, and Fe_2O_3. They are either present in the SRF or formed when the SRF is combusted. These element oxides were found to make up 76.8% of the ash of SRF produced from MCW (Viczek et al., 2020a). While, technically, this share can be considered as recycled on a material level, SRF co-processing is still considered as energy recovery in most EU member countries from the legal perspective. However, a decision of the European Commission on the recognition of material recovery in this process is pending (EC, 2018).

Considering the high ash content (71%) of the fine fraction <5 mm, and that approx. 37% of this whole fraction consists of Si, Al, Ca, Fe, Mg, Ti, Na, and K (calculated as oxides: 62%), it becomes clear that the fine fraction contains the largest amount of recyclable material for cement manufacturing of all particle size fractions. Therefore, screening would not only remove significant amounts of the contaminants that are subject to limit values, but also 46% of the total Si, 26% of Al, 30% of Ca, 47% of Fe, and large shares of other elements that are typically present in cement clinker. Apart from the significant heavy metal content, the fine fraction represents a valuable fraction to cement manufacturers and should ideally remain as a part of the SRF or be applied in a different way in the cement plant (cf. Section 3.6.3), with or without prior treatment.

Furthermore, the observation of Ca in the form of sulfates is likely relevant for the cement industry. Cement manufacturers use gypsum and anhydrite as sulfate sources. Small amounts of these minerals are added to correct the raw meal composition when the sulfate content is too low, as it is required to bind alkali metals (Viczek et al., 2020a). Consequently, both the calcium and the sulfate are valuable and incorporated into the clinker, and small parts of the $CaCO_3$, the primary Ca-containing raw material, are substituted without the arising CO_2 emissions. This indicates, that besides biogenic carbon (Lorber et al., 2012) SRF may contain other chemical compounds that may contribute to reducing CO_2 emissions.

3.6.3. Options for the fine fractions

No matter where the SRF is used, when the fine fraction is removed during SRF production, a suitable treatment pathway for the high contaminant concentrations and the low LHV of this fraction must be found. In Austria, for example, the investigated fractions <5 mm (as mono fractions) exceed national limit values for SRF for the cement industry. Conventional waste incineration, for example, legally and technically represents a possibility as there are no input limit values, provided that the waste fraction is legally defined as non-hazardous waste.

The fact that the fine fraction contained large amounts of Fe that could easily be removed with magnetic separation makes this fraction interesting for recycling. This could be a viable and profitable option, depending on the fine fractions' average Fe content. In literature, values about 1% are reported (cf. Appendix A), but this study has shown that the Fe content in practice can be much higher.

However, Fe is present in its oxidic form, which is the form the cement industry strives for. The composition of the fine fraction (i.e., 62% consisting of valuable material for the cement industry) suggests that – depending on national legislation – applying this fraction in the cement industry as a substitute raw material could be a possibility. In this case, the present contaminants would also be introduced into the cement plant, which is why specific input limit values for secondary raw material still need to be fulfilled (BMLFUW Bundesministerium für Land- und Forstwirtschaft, Umwelt und Wasserwirtschaft, 2017). However, the average ash content of 71% indicates that the total organic carbon (TOC) present in the fraction may pose problems to the cement manufacturers. Furthermore, in several countries, the investigated original fine fraction <5 mm would not comply with the limit values for substitute raw materials concerning TOC (EC, 2013), Hg, or Pb (BMLFUW Bundesministerium für Land- und Forstwirtschaft, Umwelt und Wasserwirtschaft, 2017).

A combination of both pathways, i.e., removing Fe from the fine fraction for metal recycling and applying the residual fraction in the cement industry, could also be conceivable. The present study has demonstrated that it is possible to remove large parts of As, Co, Cr, Hg, and Ni together with the metal fraction. Despite the decreased concentrations, the residual non-magnetic fraction of the investigated waste stream still exceeds four of eight limit values of the Austrian WIO (As, Co, Hg, and Pb). Better results can likely be achieved by optimizing the particle size of the fraction that is treated by magnetic separation (e.g., original particle size <5 mm, or treating the whole fraction <10 mm). This could enable the production of residual fractions suitable for the cement industry. Even if the residual, non-magnetic fraction cannot be used in the cement industry, additional value may be generated by removing and recycling the magnetic fraction.

4. Conclusions

The particle size-dependent distribution of chemical elements contains valuable information for waste processors and SRF manufacturers. This study has demonstrated on a theoretical level that screening represents a possibility for improving SRF quality, but the considered parameters and local requirements on input waste quality are crucial. While the concentrations of most contaminants were decreased by removing the fine fraction, the increase of Cd, Sb, and Cl implies that a combination of screening and an NIR sorter to remove potential Cd, Sb, and Cl carriers (e.g., PVC and PET) could be a promising approach to decrease the concentrations of all SRF-relevant contaminants. In the present study the fine fraction <5 mm at the same time contained most contaminants and valuable raw materials for cement manufacturing. Especially the presence of Ca in the form of sulfates indicates, that besides biogenic carbon SRF may contain other chemical compounds that may contribute to reducing CO_2 emissions in the cement industry. The findings therefore indicate a potential conflict between resource utilization or conservation, respectively, and environmental protection, and imply that a genuine assessment of SRF quality has to take the final SRF utilization into account, as removing certain fractions might affect SRF co-incinerators differently. Concludingly, while only little attention was paid to the fine fractions in the past, paying more attention to this material stream in the future, including its proper characterization and treatment, could prove to be beneficial and open up new possibilities for recycling or material recovery.

Funding

Partial funding for this work was provided by: The Center of Competence for Recycling and Recovery of Waste 4.0 (acronym ReWaste4.0) (contract number 860 884) under the scope of the COMET – Competence Centers for Excellent Technologies – financially supported by BMK, BMDW, and the federal states of Styria, managed by the FFG.

CRediT authorship contribution statement

S.A. Viczek: Conceptualization, Methodology, Formal analysis, Investigation, Resources, Data curation, Writing – original draft, Writing – review & editing, Visualization, Project administration. **K. Khodier:** Methodology, Investigation, Writing – review & editing. **L. Kandlbauer:** Formal analysis, Investigation, Writing – original draft, Writing – review & editing, Visualization. **A. Aldrian:** Methodology, Resources, Writing – review & editing. **G. Redhammer:** Formal analysis, Investigation, Resources, Writing – original draft, Writing – review & editing, Visualization. **G. Tippelt:** Investigation, Formal analysis. **R. Sarc:** Conceptualization, Resources, Writing - review & editing, Supervision, Funding acquisition.

Declaration of competing interest

The authors declare that they have no known competing financial interests or personal relationships that could have appeared to influence the work reported in this paper.

Supplementary data

Supplementary data to this article can be found online at https://doi.org/10.1016/j.scitotenv.2021.145343.

References

Adam, J., Curtis, A., Sarc, R., 2018. Korngrößenspezifische Charakterisierung eines marktüblichen gemischten Gewerbemülls für die EBS Produktion. In: Pomberger, R., Adam, J., Aldrian, A., Curtis, A., Friedrich, K., Kranzinger, L., Küppers, B., Lorber,

K.E., Möllnitz, S., Neuhold, S., Nigl, T., Pfandl, K., Rutrecht, B., Sarc, R., Sattler, T., Schwarz, T., Sedlazeck, P., Viczek, S.A., Vollprecht, D., Weißenbach, T., Wellacher, M. (Eds.), Vorträge-Konferenzband zur 14. Recy & DepoTech-Konferenz, pp. 781–786.

ADEME (Agence de l'Environnement et de la Maîtrise de l'Energie), 2010. La composition des ordures ménagères et assimilées en France. ADEME, Angers.

Aldrian, A., Viczek, S.A., Pomberger, R., Sarc, R., 2020. Methods for identifying the material-recyclable share of SRF during co-processing in the cement industry. Methods X 7, 100837. https://doi.org/10.1016/j.mex.2020.100837.

ASI (Austrian Standards Institute), 2002. ÖNORM EN 13656 Characterization of waste – Microwave Assisted Digestion With Hydrofluoric (HF), Nitric (HNO3) and Hydrochloric (HCl) Acid Mixture for Subsequent Determination of Elements. Issued on 01/12/2002. Vienna. .

ASI (Austrian Standards Institute), 2007. ÖNORM EN 14346 Characterization of Waste - Calculation Of Dry Matter by Determination of Dry Residue or Water Content. Issued on 01/03/2007. Vienna. .

ASI (Austrian Standards Institute), 2011a. ÖNORM EN 15411 Solid Recovered Fuels – Methods for the Determination of the Content of Trace Elements (As, Ba, Be, Cd, Co, Cr, Cu, Hg, Mo, Mn, Ni, Pb, Sb, Se, Tl, V and Zn). Issued on 15/10/2011. Vienna. .

ASI (Austrian Standards Institute), 2011b. ÖNORM EN 15359 Solid Recovered Fuels - Specifications and Classes. Issued on 15/12/2011. Vienna. .

ASI (Austrian Standards Institute), 2016. ÖNORM EN 14582 Characterization of Waste — Halogen and Sulfur Content — Oxygen Combustion in Closed Systems and Determination Methods Issued 01/11/2016, Vienna.

ASI (Austrian Standards Institute), 2017. ÖNORM EN ISO 17294-2 Water quality - Application of Inductively Coupled Plasma Mass Spectrometry (ICP-MS) - Part 2: Determination of Selected Elements Including Uranium Isotopes Issued 15/01/2017, Vienna.

Beker, D., Cornelissen, A.A.J., 1999. Chemische analyse van huishoudelijk restafval: Resultaten 1994 en 1995.

Bharagava, R.N., 2017. Environmental Pollutants and their Bioremediation Approaches. CRC Press, Milton.

BMLFUW (Bundesministerium für Land- und Forstwirtschaft, Umwelt und Wasserwirtschaft), 2010. Verordnung über die Verbrennung von Abfällen (Abfallverbrennungsverordnung - AVV). BGBl. II Nr. 476/2010. BMLFUW, Vienna.

BMLFUW (Bundesministerium für Land- und Forstwirtschaft, Umwelt und Wasserwirtschaft), 2017. Technische Grundlagen für den Einsatz von Abfällen als Ersatzrohstoffe in Anlagen zur Zementerzeugung. BMLFUW, Vienna.

Cohen, J., 1988. Statistical Power Analysis for the Behavioral Sciences. 2nd ed. Taylor and Francis, Hoboken.

Curtis, A., Adam, J., Pomberger, R., Sarc, R., 2019. Grain size-related characterization of various non-hazardous municipal and commercial waste for solid recovered fuel (SRF) production. Detritus. Volume 07. https://doi.org/10.31025/2611-4135/2019.13847 September 2019(0):1.

DIN (Deutsches Institut für Normung), 2000. DIN 51900-1 Testing of Solid And Liquid Fuels - Determination of Gross Calorific Value by the Bomb Calorimeter and Calculation of Net Calorific Value - Part 1: Principles, Apparatus, Methods Issued 04/2000, Berlin.

DIN (Deutsches Institut für Normung), 2009. DIN EN ISO 10304-1 Water quality - Determination of Dissolved Anions by Liquid Chromatography of Ions - Part 1: Determination of Bromide, Chloride, Fluoride, Nitrate, Nitrite, Phosphate and Sulfate Issued 07/2009, Berlin.

DIN (German Institute for Standardization), 1997. DIN 51719 Testing of Solid Fuels – Solid Mineral Fuels – Determination of Ash Content. Issued 07/1997 Berlin.

DS (Danish Standards), 2013. DS 3077 Representative Sampling - Horizontal Standard. Danish Standards, Charlottenlund (03.120.30; 13.080.05) Issued 26/08/2013.

Dunnu, G., Maier, J., Hilber, T., Scheffknecht, G., 2009. Characterisation of large solid recovered fuel particles for direct co-firing in large PF power plants. Fuel 88 (12), 2403–2408. https://doi.org/10.1016/j.fuel.2009.03.004.

EC (European Commission), 2008a. Directive 2008/98/EC of the European Parliament and of the Council of 19 November 2008 on Waste and Repealing Certain Directives (Waste Framework Directive).

EC (European Commission), 2008b. Regulation (EC) No 1272/2008 of the European Parliament and the Council of December 16 2008 on Classification, Labelling and Packaging of Substances and Mixtures.

EC (European Commission), 2010. Directive 2010/75/EU of the European Parliament and of the Council of 24 November 2010 on Industrial Emissions (Integrated Pollution Prevention and Control).

EC (European Commission), 2013. Best Available Techniques (BAT) Reference Document for the Production of Cement, Lime and Magnesium Oxide.

EC (European Commission), 2018. Directive 2018/851 of the European Parliament and the Council of 30th May 2018 Amending Directive 2008/98/EC on Waste.

Flamme, S., Geiping, J., 2012. Quality standards and requirements for solid recovered fuels: a review. Waste Man Res 30 (4), 335–353. https://doi.org/10.1177/0734242X12440481.

Götze, R., Boldrin, A., Scheutz, C., Astrup, T.F., 2016a. Physico-chemical characterisation of material fractions in household waste: overview of data in literature. Waste Manag. 49, 3–14. https://doi.org/10.1016/j.wasman.2016.01.008.

Götze, R., Pivnenko, K., Boldrin, A., Scheutz, C., Astrup, T.F., 2016b. Physico-chemical characterisation of material fractions in residual and source-segregated household waste in Denmark. Waste Manag. 54, 13–26. https://doi.org/10.1016/j.wasman.2016.05.009.

Hilber, T., Maier, J., Scheffknecht, G., Agraniotis, M., Grammelis, P., Kakaras, E., et al., 2007. Advantages and possibilities of solid recovered fuel cocombustion in the European energy sector. J. Air Waste Manage. Assoc. 57 (10), 1178–1189. https://doi.org/10.3155/1047-3289.57.10.1178.

Holleman, A.F., Wiberg, E., Wiberg, N., 2007. Lehrbuch der anorganischen Chemie. 102nd ed. de Gruyter, Berlin.

ISSF (International Stainless Steel Forum), 2019. The Stainless Steel Family. http://www.worldstainless.org/Files/issf/non-image-files/PDF/TheStainlessSteelFamily.pdf. (Accessed 7 April 2019).

Janz, A. (2010): Schwermetalle aus Elektrogeräten und Batterien im kommunalen Restabfall. Potentiale, Mobilisierung und Freisetzung während der Deponierung. Dissertation, Technische Universitaet Dresden. The Editor is Forum für Abfallwirtschaft und Altlasten e.V, Pirna.

Khodier, K., Viczek, S.A., Curtis, A., Aldrian, A., O'Leary, P., Lehner, M., et al., 2020. Sampling and analysis of coarsely shredded mixed commercial waste. Part I: procedure, particle size and sorting analysis. Int. J. Environ. Sci. Technol. 17 (2), 959–972. https://doi.org/10.1007/s13762-019-02526-w.

Lagarec, K., Rancourt, D.G., 1997. Extended Voigt-based analytic lineshape method for determining N-dimensional correlated hyperfine parameter distributions in Mössbauer spectroscopy. Nucl. Instrum. Methods Phys. Res., Sect. B 129 (2), 266–280. https://doi.org/10.1016/s0168-583x(97)00284-x.

LfU Bayern (Bayerisches Landesamt für Umweltschutz), 2003. Zusammensetzung und Schadstoffgehalt von Siedlungsabfällen: Abschlussbericht.

LGL Bayern (Bayerisches Landesamt für Gesundheit und Lebensmittelsicherheit), 2012. Arbeit, Umwelt und Gesundheit aktuell: Quecksilber aus Energiesparlampen.

Lorber, K.E., Sarc, R., Aldrian, A., 2012. Design and quality assurance for solid recovered fuel. Waste Man Res 30 (4), 370–380. https://doi.org/10.1177/0734242X12440484.

Massart, D.L., Vandeginste, B.G.M., Buydens, L.M.C., de Jong, S., Lewi, P.J., Smeyers-Verbeke, J., 1997. Handbook of Chemometrics and Qualimetrics: Part A. Elsevier.

MathWorks, 2020a. Biplot. https://de.mathworks.com/help/stats/biplot.html. (Accessed 16 July 2020).

MathWorks, 2020b. pca. https://de.mathworks.com/help/stats/pca.html. (Accessed 16 July 2020).

MathWorks, 2020c. svd. https://de.mathworks.com/help/matlab/ref/double.svd.html. (Accessed 16 July 2020).

Möllnitz, S., Khodier, K., Pomberger, R., Sarc, R., 2020. Grain size dependent distribution of different plastic types in coarse shredded mixed commercial and municipal waste. Waste Manag. 103, 388–398. https://doi.org/10.1016/j.wasman.2019.12.037.

Nasrullah, M., Vainikka, P., Hannula, J., Hurme, M., 2015a. Elemental balance of SRF production process: solid recovered fuel produced from commercial and industrial waste. Fuel 145, 1–11. https://doi.org/10.1016/j.fuel.2014.12.071.

Nasrullah, M., Vainikka, P., Hannula, J., Hurme, M., Koskinen, J., 2015b. Elemental balance of SRF production process: solid recovered fuel produced from construction and demolition waste. Fuel 159, 280–288. https://doi.org/10.1016/j.fuel.2015.06.082.

Pieber, S., Ragossnig, A., Pomberger, R., Curtis, A., 2012. Biogenic carbon-enriched and pollutant depleted SRF from commercial and pretreated heterogeneous waste generated by NIR sensor-based sorting. Waste Man Res 30 (4), 381–391. https://doi.org/10.1177/0734242X12437567.

Pomberger, R., Aldrian, A., Sarc, R., 2015. Grenzwerte - Technische Sicht zur rechtlichen Notwendigkeit. In: Piska, C., Lindner, B. (Eds.), Abfallwirtschaftsrecht Jahrbuch 2015. NWV Neuer wissenschaftlicher Verlag, Wien, Graz, pp. 269–289.

Prochaska, M., Raber, G., Lorber, K.E., 2005. Herstellung von Ersatzbrennstoffen. Projekt-Endbericht. Montanuniversitaet Leoben.

Rancourt, D.G., Ping, J.Y., 1991. Voigt-based methods for arbitrary-shape static hyperfine parameter distributions in Mössbauer spectroscopy. Nucl. Instrum. Methods Phys. Res., Sect. B 58 (1), 85–97. https://doi.org/10.1016/0168-583x(91)95681-3.

Rugg, M., Hanna, N.K., 1992. Metals Concentrations in Compostable and Noncompostable Components of Municipal Solid Waste in Cape May County, New Jersey. Arlington, Virginia.

Sarc, R., 2015. Herstellung, Qualität und Qualitätssicherung von Ersatzbrennstoffen zur Erreichung der 100%-igen thermischen Substitution in der Zementindustrie.. Doctoral Thesis,. Montanuniversitaet Leoben.

Sarc, R., Lorber, K.E., Pomberger, R., Rogetzer, M., Sipple, E.M., 2014. Design, quality, and quality assurance of solid recovered fuels for the substitution of fossil feedstock in the cement industry. Waste Man Res 32 (7), 565–585. https://doi.org/10.1177/0734242X14536462.

Sarc, R., Seidler, I.M., Kandlbauer, L., Lorber, K.E., Pomberger, R., 2019. Design, quality and quality assurance of solid recovered fuels for the substitution of fossil feedstock in the cement industry – update 2019. Waste Man Res 37 (9), 885–897. https://doi.org/10.1177/0734242X19862600.

Swiss Federal Council, 2015. Verordnung über die Vermeidung und die Entsorgung von Abfällen.

Thiel, S., Thomé-Kozmiensky, K.J., 2012. Co-combustion of solid recovered fuels in coal-fired power plants. Waste Man Res 30 (4), 392–403. https://doi.org/10.1177/0734242X11427946.

Turner, A., 2019. Cadmium pigments in consumer products and their health risks. Sci. Total Environ. 657, 1409–1418. https://doi.org/10.1016/j.scitotenv.2018.12.096.

Turner, A., Filella, M., 2017. Field-portable-XRF reveals the ubiquity of antimony in plastic consumer products. Sci Total Environ 584–585, 982–989. https://doi.org/10.1016/j.scitotenv.2017.01.149.

US EPA (United States Environmental Protection Agency), 2019. Initial List of Hazardous Air Pollutants with Modifications. https://www.epa.gov/haps/initial-list-hazardous-air-pollutants-modifications. (Accessed 4 October 2019).

Viczek, S.A., Aldrian, A., Pomberger, R., Sarc, R., 2020a. Determination of the material-recyclable share of SRF during co-processing in the cement industry. Resources, Conservation and Recycling 156, 104696. https://doi.org/10.1016/j.resconrec.2020.104696.

Viczek, S.A., Aldrian, A., Pomberger, R., Sarc, R., 2020b. Origins and carriers of Sb, As, Cd, Cl, Cr, Co, Pb, Hg, and Ni in mixed solid waste – a literature-based evaluation. Waste Manag. 103, 87–112. https://doi.org/10.1016/j.wasman.2019.12.009.

Viczek, S.A., Kandlbauer, L., Khodier, K., Aldrian, A., Sarc, R., 2021. Sampling and analysis of coarsely shredded mixed commercial waste. Part II: particle size-dependent element determination (in submission).

Watanabe, N., Inoue, S., Ito, H., 1999. Antimony in municipal waste. Chemosphere 39 (10), 1689–1698. https://doi.org/10.1016/S0045-6535(99)00069-7.

Yan, J., Karlsson, A., Zou, Z., Dai, D., Edlund, U., 2020. Contamination of heavy metals and metalloids in biomass and waste fuels: comparative characterisation and trend estimation. Sci. Total Environ. 700, 134382. https://doi.org/10.1016/j.scitotenv.2019.134382.

Zhang, H., He, P.-J., Shao, L.-M., 2008. Implication of heavy metals distribution for a municipal solid waste management system — a case study in Shanghai. Sci. Total Environ. 402 (2–3), 257–267. https://doi.org/10.1016/j.scitotenv.2008.04.047.

3.6 Publication VI

Production of contaminant-depleted solid recovered fuel from mixed commercial waste for co-processing in the cement industry

S.A. Viczek, K.E. Lorber, R. Pomberger, R. Sarc

Fuel 294 (2021), 120414,
https://doi.org/10.1016/j.fuel.2021.120414

Author Contributions (CRediT Contributor Roles Taxonomy):

SV: Conceptualization, Methodology, Formal Analysis, Investigation, Data curation, Writing – original draft preparation, Writing – review and editing, Visualization, Project administration;

KL: Writing – review and editing, Supervision;

RP: Resources, Funding acquisition;

RS: Resources, Writing – review and editing, Supervision, Funding acquisition.

Graphical abstract:

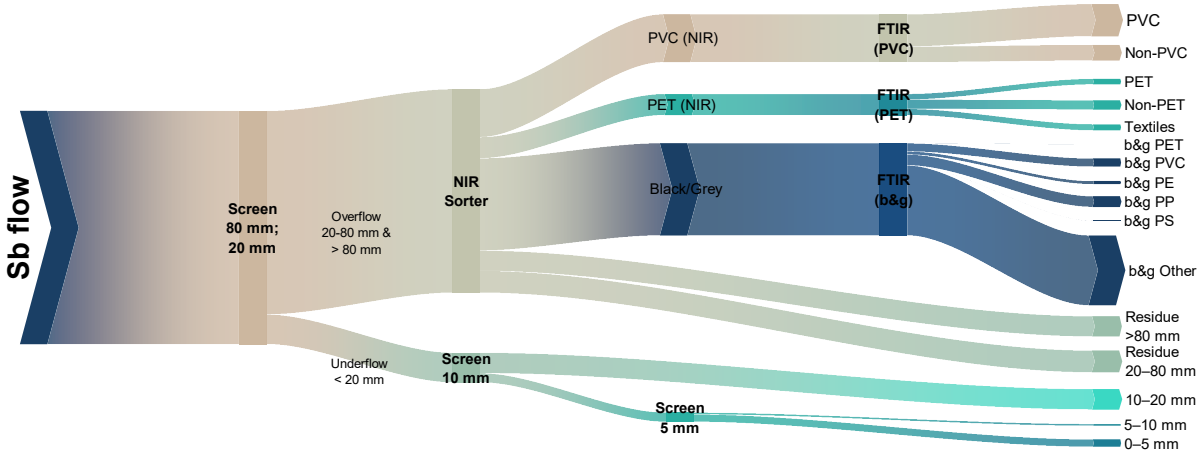

Fuel 294 (2021) 120414

Contents lists available at ScienceDirect

Fuel

journal homepage: www.elsevier.com/locate/fuel

Full Length Article

Production of contaminant-depleted solid recovered fuel from mixed commercial waste for co-processing in the cement industry

S.A. Viczek, K.E. Lorber, R. Pomberger, R. Sarc *

Chair of Waste Processing Technology and Waste Management, Department of Environmental and Energy Process Engineering, Montanuniversitaet Leoben, Franz-Josef-Strasse 18, Leoben 8700, Austria

ARTICLE INFO

Keywords:
Solid recovered fuel (SRF)
Heavy metals
Near-infrared sorting
Screening
Black plastics
Waste processing

ABSTRACT

Solid recovered fuels (SRF) have increasingly substituted primary fuels in the cement industry, even up to 100%. However, contaminants originating from the discarded consumer products are transferred into waste and SRF. With increasing amounts of SRF being utilized, closely monitoring contaminant concentrations – as is already state of the art in several countries and the cement industry – is gaining importance. SRF producers may need to take measures assuring that quality criteria are met, contaminant concentrations are kept at a low level, or to produce contaminant-depleted SRF. This work investigates and discusses the potential measures to reduce contaminant concentrations: removing the fine fractions, polyethylene terephthalate (PET), polyvinyl chloride (PVC), and black&grey materials. Five streams of mixed commercial waste were coarsely comminuted, screened, PET and PVC were removed using an industrial near-infrared sorter, and black&grey materials were manually removed and further sorted by fourier-transform infrared spectroscopy. Concentrations of Ag, Al, As, Ba, Ca, Cd, Cl, Co, Cr, Cu, Fe, Hg, K, Li, Mg, Mn, Mo, Na, Ni, P, Pb, Sb, Si, Sn, Sr, Ti, V, W, and Zn in the fractions are reported, and the effect of single and combined measures is presented. Results show that black&grey materials contain significant shares of the total Sb, Cl, and Co in the waste stream. Furthermore, the concentration of several contaminants is increased when only PET and PVC is removed. Removing the fine fraction together with PVC can lead to a concentration decrease of all investigated analytes, enabling the production of a contaminant-depleted SRF.

1. Introduction

In the past decades, the cement industry has increasingly substituted fossil fuels required for the energy-intensive clinker burning process with refuse-derived fuels (RDF). In some countries, thermal substitution rates (TSR) of >80% have already been reached routinely [1], and experiments have demonstrated that a TSR of 100% is technically possible when a mixture of selected RDF is applied [2].

However, the application of RDF and even SRF, which is a quality-assured subgroup of RDF that is only produced from non-hazardous, mainly mixed solid waste [3], is also linked to the introduction of additional inorganic contaminants, e.g., heavy metals and metalloids, into the cement kiln. These contaminants originate from consumer products ending up in the waste at the end of their life cycle [4] and may consequently become a part of the SRF. For this reason, strict compliance with limit values is obligatory for co-incineration plants in several countries. On the one hand, general limit values for exhaust gases restrict the release of contaminants into the environment, e.g., the EU Industrial Emissions Directive [5] or the US Clean air act [6]. On the other hand, specific limit values for SRF exist, mostly limiting the concentrations of the same elements that are subject to emission limit values. Examples include international standards [3], quality marks [7], or national legislation, for example, in Switzerland [8] or Austria [9]. These regulations do not only aim to limit the amount of contaminants released via flue gases but also to limit the transfer of these contaminants from waste into the product, the cement clinker [9].

It has to be noted that SRF in central Europe usually complies with the obligatory limit values [1,10]. Compared to hard coal, SRF typically features lower concentrations (mg/MJ) of, e.g., As, Co, and Hg, and may contain higher concentrations of Sb, Cr, and Ni [10]. Therefore the substitution of primary fuels with SRF may cause a concentration increase of some contaminants introduced into the clinker, while others decrease – assuming a constant quality of all other input materials. For this reason, closely monitoring contaminant concentrations in SRF is

* Corresponding author.
E-mail address: renato.sarc@unileoben.ac.at (R. Sarc).

https://doi.org/10.1016/j.fuel.2021.120414
Received 2 January 2021; Received in revised form 30 January 2021; Accepted 3 February 2021

necessary, and additional measures may be required to continuously keep SRF quality on a good, limit-value compliant level or to further reduce the amount of contaminants that are transferred into the cement clinker. Technical options to decrease contaminant concentrations in waste include limiting the permitted concentrations in products (as is the case for Cd in PVC, for example [11]). However, due to the long life cycle of several products, these measures take their time to reduce contaminant concentrations in the waste sector effectively. Another option that SRF producers can directly apply is to remove contaminants from the waste stream by introducing additional, adequate processing steps aiming at removing fractions that are known to carry significant amounts of the relevant contaminants.

1.1. Reduction of contaminant concentrations in mixed solid and commercial waste

Several studies have reported waste sorting analyses and chemical analyses of the sorted fractions (cf. reviews of Götze et al. [12] and Viczek et al. [4] and references therein). Others have balanced the element flows in the SRF production process from MSW [13], commercial and industrial waste [14], or construction and demolition waste [15]. However, only a few studies [16–18] have investigated how the targeted removal of contaminant-rich fractions affects SRF quality. Experimentswith mixed commercial waste (MCW) [17] have shown that several elements occur in higher concentrations in smaller grain size fractions, i.e., show a negative correlation between element concentration and particle size. This also applies to several contaminants relevant for SRF producers (e.g., As, Co, Cr, Hg, Ni, and Pb). Removing the fine fractions <5 mm or <10 mm by screening results in significant reductions of the elements showing this negative correlation, while the lower heating value (LHV) is increased. Therefore, the effects of screening are even more distinct when element concentrations are considered in mg/MJ, as required in EN 15,359 [3] or national legislation [9]. However, when the fine fraction is removed, an increase of Cd, Cl, and Sb concentrations may be observed. This is probably linked to the occurrence of these elements in plastics [4] and may be counteracted by removing prominent carriers of these elements by near-infrared (NIR) sorters. Pieber et al. [18], for example, report a reduction of Sb, Cl, and occasionally Cd by removing PET and PVC with an industrial NIR sorter.

A fraction that is not yet frequently removed from the waste stream but contains large amounts of contaminants such as Cl, Cd, Cr, Pb, and Sb [19] is black plastics. They are widespread among consumer products with different purposes, ranging from food packaging to clothing and garden tools [19]. Consequently, black plastics can make up significant shares (e.g., 12.4% [20]; 15% [19]) of the domestic plastic waste streams, mainly in the form of food trays and other single-use packaging made from polypropylene (PP) and crystalline polyethylene terephthalate (CPET) [19,20]. The issue with black materials in modern waste management arises from the primary pigment used to give plastics a black color, which is carbon black [21]. Although the addition of 0.5 – 2 wt% carbon black is usually sufficient to tint a polymer black [21,22], conventional industrial NIR sorters cannot identify and sort soot-blackened materials [20,23]. Soot-blackened plastics absorb most of the NIR radiation and cause a lack of information on material composition in the spectra [24,25]. For the same reason, the recognition and removal of grey plastics can be negatively affected, as well.

1.2. Aim of work

This work aims to find suitable measures to reduce the concentrations of all SRF-relevant contaminants in mixed commercial waste (MCW). For this purpose, it is the first scientific study applying an approach that combines the removal of the fine fraction by screening [16,17], the application of an industrial NIR sorter to remove PVC and PET [18], and, based on the report on black plastics of Turner [19], the manual removal of black and grey materials. The approach is applied to five MCW samples delivered to a waste processing plant on different days. The study quantifies the effect of these different measures and combinations thereof on element concentrations in the waste streams. Furthermore, the effect of technological improvements, e.g., the removal of certain black plastics or a more targeted removal of PVC, is assessed. Consequently, the study aims to give SRF manufacturers and SRF utilizing industries concrete indications on measures to take when facing high concentrations of certain chemical elements or contaminants, and to enable the production of a contaminant-depleted SRF.

2. Materials and methods

2.1. Samples and sample processing

Five separate deliveries of mixed commercial waste (masses between 7 and 16 metric tons) collected on different days in October 2019 in the area of Graz, Austria, were coarsely shredded using a mobile single-shaft coarse shredder (Terminator 5000 SD, F-type cutting unit, Komptech GmbH) operating with a closed cutting gap at 100% of the maximum shaft rotation speed, i.e., 31 rpm. The samples were taken from the falling waste stream after the shredder, cf. Fig. 1a. The waste stream was sampled by shifting the discharge conveyor belt from one side to the other and back (cf. Fig. 1b–d), thereby sampling the waste stream twice with a box (LWH (inner): 115 × 91.5 × 56.5 cm). This sampling step was carried out 27 times in time intervals of 60 s, i.e., 54 sample increments were taken and formed the composite sample. The shredding and sampling procedure was performed separately for each of the five deliveries, yielding a total of 5 composite samples (S01–S05) with masses between 92 and 240 kg that were kept separate for the further processing steps, cf. Fig. 2.

Samples S01 to S05 were screened using a batch drum screen (described in detail in [26]) to generate five particle size fractions: 0–5 mm, 5–10 mm, 10–20 mm, 20–80 mm, and > 80 mm. The fractions 20–80 mm, and > 80 mm were separately sorted using an industrial near-infrared (NIR) sorter (λ ca. 900–1700 nm). The waste was dosed manually from a feed conveyor belt and directed onto the NIR sorter's infeed conveyor belt to decrease the occupation density and to enhance the separation of single waste particles in the detection zone of the sorter. A multi-step approach was used for sorting: in the first step, PVC was sorted out and collected as a separate fraction. The residue was then reintroduced into the sorter, where PET was sorted out and separately collected. During both steps, black and grey materials were manually sorted out from the residue at the sorter's discharge conveyor belt. Because the particle size fractions 20–80 mm and > 80 mm were only generated to facilitate NIR sorting, these two particle size fractions of the same materials (PVC, PET, black/grey) were reunited.

Since industrial NIR sorters remove target particles with pressurized air, and because particles are usually not perfectly spatially separated on the conveyor belt (despite manually dosing the waste entering the conveyor belt), it is common that not all particles that are removed consist of the target material [27]. Furthermore, the identification algorithm may be set with the aim of removing as much of the PVC as possible (note: Cl is a technically limited parameter for SRF for the cement industry [28]), even if the spectrum of the particle does not exactly fit that of PVC, thereby accepting the co-ejection of other materials. For this reason, the fractions PVC and PET ejected by the NIR sorter, and also the manually removed black/grey materials were manually re-sorted using a lab scale Fourier-Transform infrared (FTIR) spectrometer (Cary 630, Agilent Technologies, diamond ATR unit). FTIR spectroscopy uses a broader spectral range for the identification of materials than industrial NIR sorters and may even identify soot-blackened polymers. However, because the ATR unit needs close contact to each waste particle to properly identify it, this technique cannot be applied for large scale sorting in a plant but is suitable for manual sorting in the laboratory. Using FTIR, fractions were assigned by mathematical comparison with spectra from databases and spectra of

Fig. 1. a: Experimental setup of the sampling process. The conveyor belt was moved from one side to the other, i.e., from the position depicted in b via c to position d, and back to the position depicted in b, thereby sampling the waste stream twice.

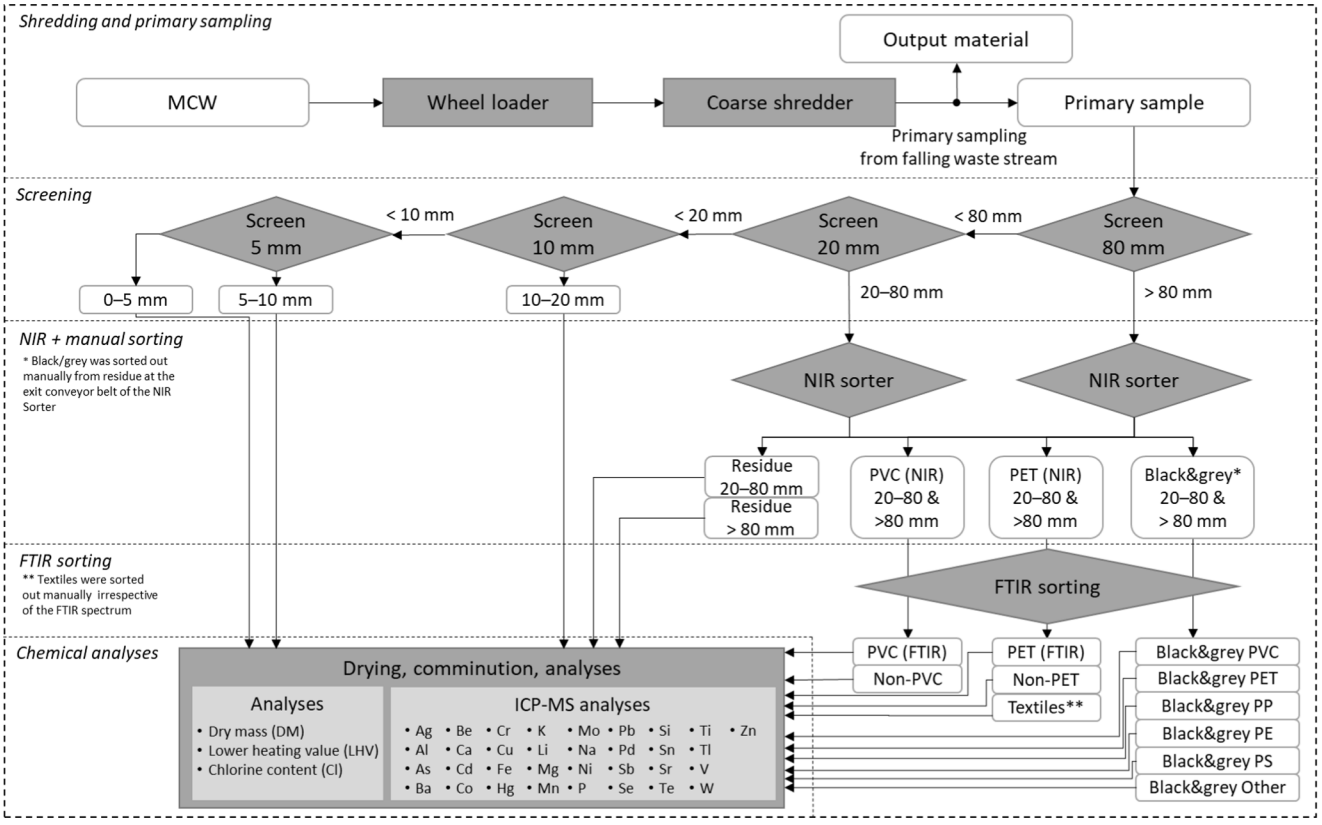

Fig. 2. Sampling and sample processing flowsheet.

black polypropylene (PP), polyethylene (PE), polystyrene (PS), glycol-modified polyethylene terephthalate (PET G), and PVC with defined carbon black contents of 0.5%, 1%, and 2%.

2.2. Chemical analyses

The final samples (fine fractions, residues, and fractions after FTIR sorting) were dried to constant mass at 105 °C , and the dry residue was determined according to EN 14,346 [29] (process A). The samples were

comminuted to a size <0.5 mm (plastics samples after FTIR sorting: <1 mm) using cutting mills and were homogenized and reduced in mass, where appropriate. Before comminution, hard impurities (e.g., visible stones, metal parts) were removed to avoid damaging the mills. Their weight was recorded, but they were not separately analyzed. To some extent, this approach mimics the processes the waste would undergo in typical SRF production plants (e.g., magnetic separators, wind sifters, heavy-material traps [1,10]), bringing the results close to those expected for the processed SRF sample. Results therefore refer to dry mass (DM) without hard impurities. For a more detailed discussion of this approach, cf. [4] and [30].

The concentrations of Ag, Al, As, Ba, Be, Ca, Cd, Co, Cr, Cu, Fe, Hg, K, Li, Mg, Mn, Mo, Na, Ni, P, Pb, Pd, Sb, Se, Si, Sn, Sr, Te, Ti, Tl, V, W, and Zn were determined by inductively coupled plasma mass spectrometry (ICP-MS; based on EN 15,411 [31] and EN ISO 17294-2 [32]) after microwave-assisted acid digestion (EN 13,656 [33]). The Cl content was determined by ion chromatography (EN ISO 10304-1 [34]) after calorimetric digestion (EN 14,582 [35]). Samples were analyzed as duplicates. The lower heating value (LHV) was calculated according to DIN 51900-1 [36].

2.3. Calculations

The overall concentrations in each waste stream before and after the removal of certain fractions, as well as the concentration in the fractions PET(NIR), PVC(NIR), and black&grey, were calculated from the concentrations (c_i, in mg/kg$_{DM}$) and masses (w_i, in kg$_{DM}$) of the individual screened, residual, and FTIR-sorted fractions as given in formula 1:

$$c_{mix} = \frac{\sum c_i * w_i}{\sum w_i} \quad (1)$$

Fractions with element concentrations (c) below the limit of quantification (L.O.Q.) were considered by assuming c = L.O.Q. While this may cause a slight overestimation of the elements' overall concentration in the waste stream, it also represents the worst-case scenario. The relative concentration change (Δc) in % was calculated according to formula 2, with c_1 being the concentration in the initial waste stream, and c_2 being the concentration after applying the investigated measures:

$$\Delta c = \frac{c_2 - c_1}{c_1} * 100 \quad (2)$$

The average concentrations given in this paper and the appendix represent the arithmetic means of the five concentrations observed for the five waste streams. Similarly, the average concentration change was calculated as the arithmetic mean of the five Δc values observed for the five waste streams.

3. Results and discussion

A comparison of the calculated overall element concentrations in the five waste samples with the literature evaluation of Götze et al. [12] for household waste shows that most element concentrations are located in the expected range, i.e., between the 25th and 75th percentile of the literature values (Fig. 3). All five samples show comparably low concentrations of Li and P. In contrast, concentrations of, e.g., Cl and Sb of all samples are located above the literature median, and sometimes even above the 90th percentile or maximum. These elements often occur in plastics, the abundance of which is also reflected by the LHV being located between the 75th and 90th percentile of literature values. Therefore, it is assumed that the investigated samples of MCW are richer in plastics than most household wastes considered in the literature review. This assumption is consistent with the study of Möllnitz et al. [37], which reports higher plastic contents in MCW than municipal solid waste (MSW).

The concentrations of Be, Pd, Se, Te, and Tl were below the L.O.Q. in most or all of the investigated fractions (Be, Se: <2.5 mg/kg$_{DM}$, Pd, Tl: <0.25 mg/kg$_{DM}$, Te < 0.5 mg/kg$_{DM}$).

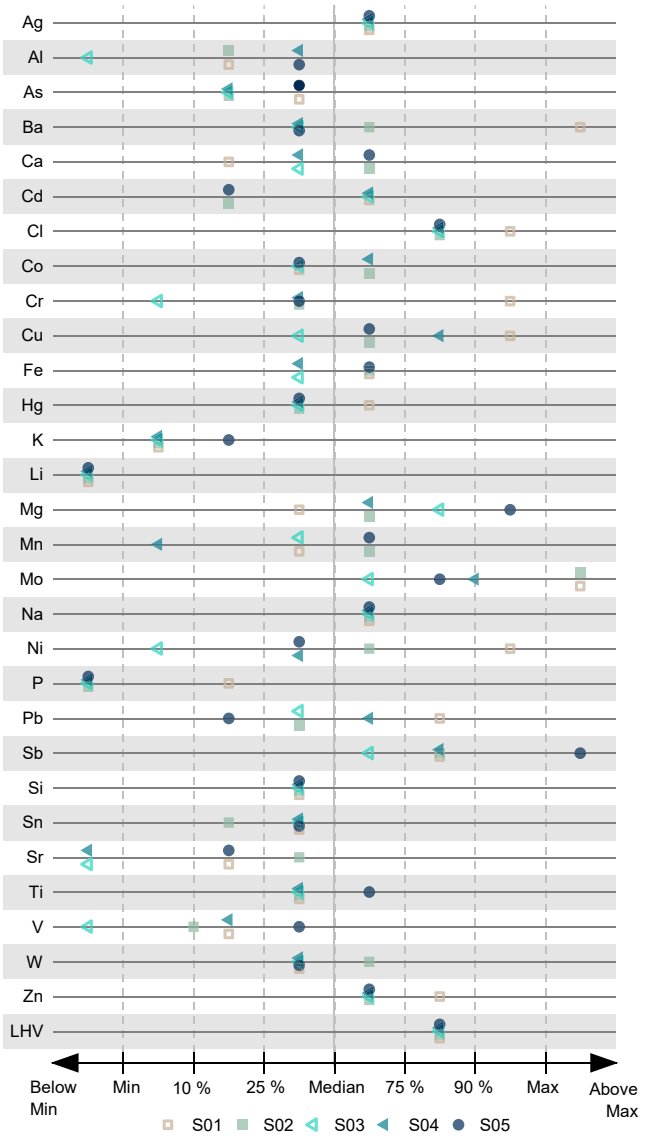

Fig. 3. Comparison of element concentrations in the five investigated MCW samples with the statistic evaluation of literature data from Götze et al. [12] for household waste.

3.1. Element flows

In the following section, the element-specific flows for As, Cd, Cl, Co, Cr, Hg, Ni, Pb, and Sb during the treatment of MCW (depicted in Fig. 4a–j) are discussed and compared with the respective mass flow. Concentrations and diagrams for all measured elements > L.O.Q. are given in the supplementary material (Appendix A).

3.1.1. Elements enriched in the fine fractions

The present investigations show that the fine fraction < 5 mm, on average amounting to 12.9% of the dry mass of the MCW samples, contains the largest shares of Cr and Ni (>40%, cf. Fig. 4) and significant amounts of As, Co, and Hg as well as several other elements (cf. Appendix A). The results are therefore consistent with the observations for the particle size-dependent element distribution [17], suggesting that screening is a suitable measure to decrease the concentrations of these elements in SRF.

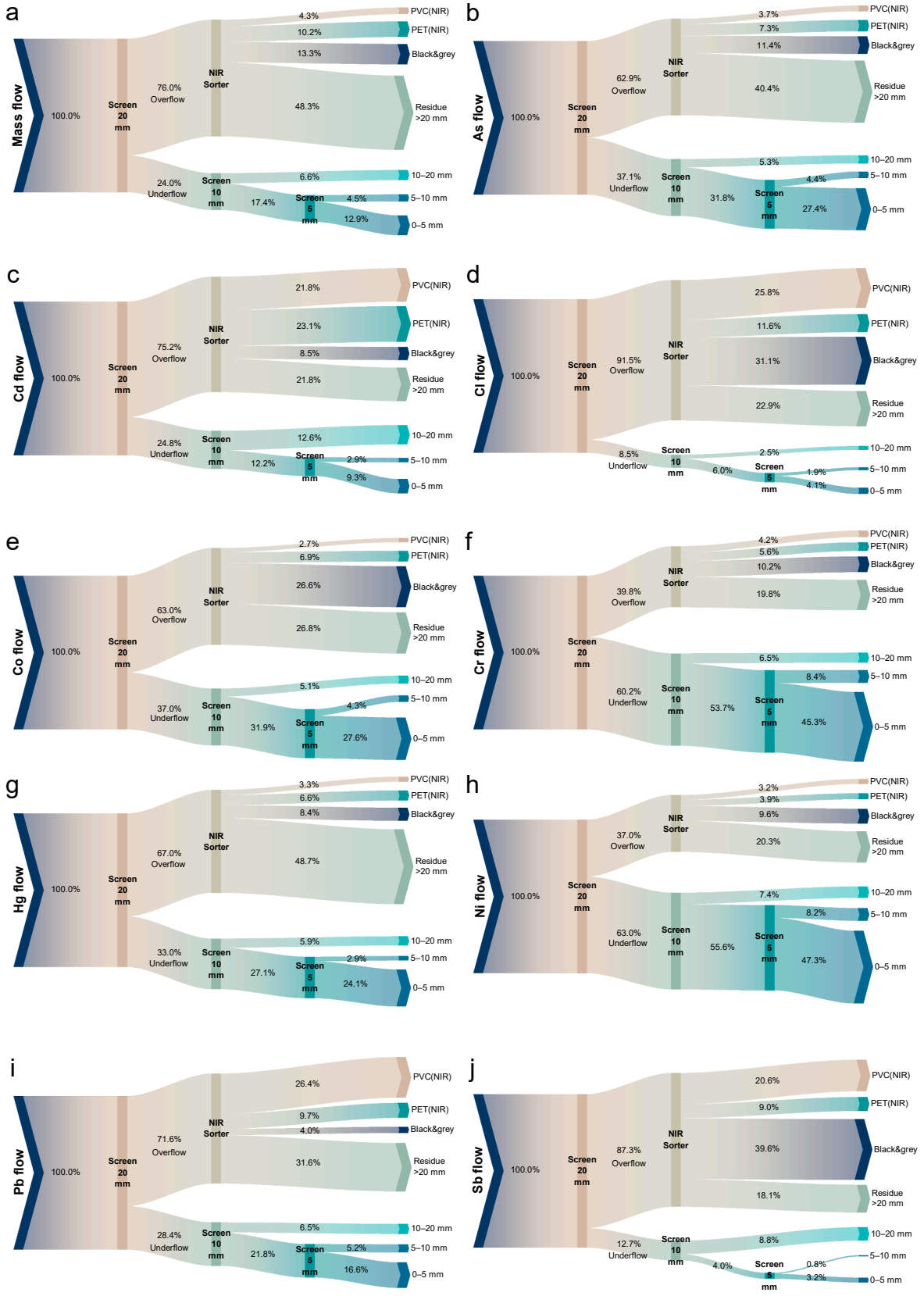

Fig. 4. a-j flow diagrams of the mass, As, Cd, Cl, Co, Cr, Hg, Ni, Pb, and Sb flows representing the arithmetic mean values of the five MCW samples S01–S05.

3.1.2. Elements enriched in the PVC and PET fractions (NIR sorted)

Despite PET being considered a prominent Sb carrier [cf. 4 and references therein] and making up approx. 10.2% of the dry mass of the investigated waste streams, the PET fraction removed by an NIR sorter only contains 9.0% of the total Sb. However, the PET(NIR) fraction, on average, contains the largest share of Cd (23.1%). This observation is caused by a high Cd concentration of 29 mg/kg_{DM} in the textile fraction of waste stream S04. In the literature, similar or even higher Cd concentrations are reported in black "clothing and accessories" [19]. Furthermore, mixed fractions containing textiles and leather, rubber, or shoes [4] may be linked to the use of Cd pigments, e.g., in textile dyes [38].

The second-largest share (21.8%) of Cd can be found in the PVC (NIR) fraction and likely originates from the (former) use of this element as a PVC stabilizer [39]. However, high Cd concentrations were detected in the "PVC" and the "non-PVC" fractions identified by FTIR. While the PVC (NIR) fraction amounts for 4.3% of the mass, it contains significant amounts of Pb (26.4%), Sb (20.6%), and Cl (25.8%). Pb is mainly present in single samples of the FTIR-assigned PVC fraction, likely due to its (former) use as a PVC stabilizer [39]. Sb concentrations in the PVC (FTIR) fractions of some waste samples suggest that flame-retarded PVC is present [39,40]. While Cl concentrations in the PVC(FTIR) fraction usually exceed those detected in the "non-PVC" fraction, i.e., the part of the PVC(NIR) fraction that was not identified as PVC by FTIR spectroscopy, Cl concentrations in the "non-PVC" fractions are high as well. Because of the larger mass share, the "non-PVC" fraction still carries an average of ~ 7.8% of the total Cl load, while about 18.1% of the Cl is located in the PVC(FTIR) fraction. Although a false negative identification of PVC with the FTIR spectrometer cannot be excluded, it is also possible that Cl carriers other than PVC are recognized and sorted out by the NIR sorter.

3.1.3. Elements enriched in black&grey materials

While black&grey (b&g) materials amount to 13.3% of the dry mass (DM), analyses revealed that this fraction contains about 31.1% of the total Cl, 26.6% of the total Co, and 39.6% of the total Sb present in the waste streams. The largest share of these elements in the b&g fraction is located in "b&g Other". This fraction comprised b&g materials that could not be assigned to the five plastics PET, PVC, PE, PP, and PS even with FTIR spectroscopy, and is the largest group of b&g materials (i.e., 71.5 mass-%) in this study. Materials in this group often consisted of composite materials, e.g., foam mats with thick silver-grey coatings. The average composition of the b&g fractions is depicted in Fig. 5.

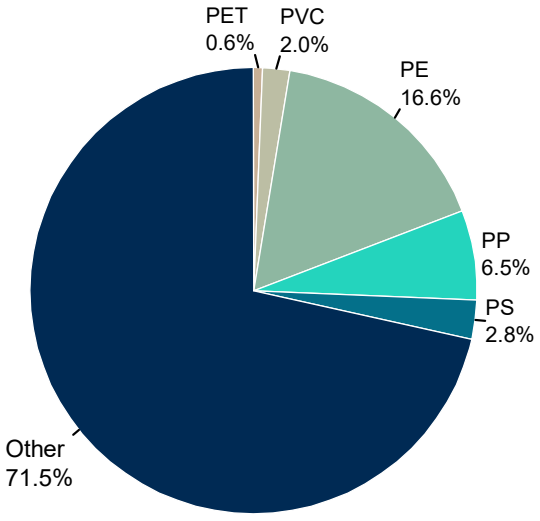

Fig. 5. Average composition (arithmetic mean value, n = 5) of the black & grey (b&g) fraction determined by FTIR Sorting.

3.2. Effects on SRF quality

The average relative concentration changes for 29 elements in the five investigated samples are given in Table 1 (concentration changes referring to mg/kg_{DM}) and Table 2 (referring to mg/MJ). For individual results for each sample, scenario, and element, refer to Appendix B. The calculated scenarios "single state-of-the-art process steps" only include technologies that are readily available for an industrial application and include steps that can be carried out simultaneously with one machine, e.g., the removal of PET and PVC in one step with an NIR sorter. Furthermore, combinations of these widely distributed, state-of-the-art technologies are evaluated. The last section presented in the tables, called "more targeted removal", however, represents the possible results after technologies with improved sorting abilities or after applying sorters for black plastics working in the mid-infrared range are applied more broadly.

3.2.1. Effect of screening

The observed effects of screening are largely consistent with the preceding investigations [17]: removing the fine fractions (0–5, 0–10, or 0–20 mm) decreases the concentrations of most elements except Cd, Cl, and Sb (Table 1) and increases the lower heating value (LHV), thereby enhancing the effect of screening when concentrations are considered in mg/MJ (Table 2). Considered in mg/MJ, also the Cd concentration is decreased.

3.2.2. Effect of NIR sorting

The calculations show that Cd, Cl, Pb, and Sb concentrations can be reduced by removing only PVC or PVC and PET with state-of-the-art industrial near-infrared sorters. The removal of PET alone has little influence, as it only reduces Cd (because of the textiles) and slightly decreases the Cl content. However, because the material that is removed often contains only low amounts of other SRF-relevant contaminants, but the reference mass [kg] or the LHV [MJ/kg] is decreased, the concentrations of several other elements in the waste stream increase (Table 1 and Table 2) if only PET and PVC are removed by NIR sorters, which is frequently the case in SRF production plants.

As pointed out in section 3.1.2, both the PVC and non-PVC fractions identified by FTIR spectroscopy contain large amounts of chlorine. Calculations show, that a more targeted removal of PVC by removing only the PVC(FTIR) fraction would not help to further reduce Cl concentrations. On the contrary, a more significant decrease of the Cl concentration may be achieved when the whole PVC(NIR) fraction is removed instead of the PVC(FTIR) fraction only.

This indicates the presence of unknown Cl carriers, which seems to be a particular issue for waste streams S01 and S05. In these samples, high Cl concentrations (2.9 and 1.3 $\%_{DM}$, respectively) in the residual fractions > 20 mm (after removing PVC, PET, and b&g materials) were observed, indicating that Cl is present in other fractions. Such unrecognized Cl carriers may include rubbers [14,41], (coated) wood, textiles, or composite materials, all of which are frequently present in waste [4,42]. This may also explain the comparably low relative concentration change for Cl of −20.1% achieved by these measures in waste stream S01. In the other waste streams, screening combined with the removal of PET, PVC and b&g materials resulted in much higher reductions of Cl concentrations (-43 to −79%). The Cl concentration in the residual fractions > 20 mm in samples S02, S03, and S04, was significantly lower than in samples S01 and S05, ranging from 0.44 to 0.58$\%_{DM}$. This concentration seems to be acceptable considering the estimate of Hoffmann et al. [43], who report that after a theoretical removal of all Cl bound in plastics (which they point out is not feasible in practice), the residual waste would still feature a minimum Cl content of 0.3$\%_{DM}$.

3.2.3. Effect of the removal of black&grey (b&g) materials

While prevalent industrial NIR sorters cannot recognize black materials, a sorting machine working in the range of visible light (VIS) or

Table 1
Calculated relative concentration change (in %, arithmetic mean values of the concentration changes observed for S01-S05 referring to mg/kg$_{DM}$), LHV change, and mass loss caused by removing particle size or material fractions. The highest reductions (or increases in the case of the LHV) for each of the three main sections are marked in bold.

	Removed fraction									Relative effect on parameter [%]																								
	0–5 mm	0–10 mm	0–20 mm	PET (NIR)	PVC (NIR)	B&g	PVC (FTIR)	B&g PVC	B&g Other	Mass	LHV	Ag	Al	As	Ba	Ca	Cd	Cl	Co	Cr	Cu	Fe	Hg	K	Li	Mg	Mn	Mo	Na	Ni	P	Pb	Sb	Si	Sn	Sr	Ti	V	W	Zn
Single state-of-the-art process steps	●									-12.9	*+8.4*	-25.0	-19.3	-16.4	-18.5	-13.1	*+4.0*	*+10.1*	-16.9	-37.3	-0.9	-40.3	**-12.6**	-25.2	**-13.2**	-29.8	-42.2	-31.6	-36.5	-39.7	-5.0	-4.3	*+11.4*	-34.6	-2.3	-29.8	**-7.7**	-24.9	-30.2	-10.7
		●								-17.4	*+10.1*	-32.0	**-20.4**	**-17.0**	-20.0	-13.3	*+6.0*	*+13.9*	-17.6	-44.2	-9.7	-45.2	-11.1	-29.2	-10.3	-31.6	-49.0	-46.4	-40.0	-46.5	-4.4	-5.2	*+16.9*	-39.2	-3.2	-34.5	-7.5	-28.0	-31.7	-13.6
			●							**-24.0**	*+11.5*	**-41.7**	-19.0	-16.2	**-21.5**	**-13.6**	-1.2	*+20.9*	**-17.7**	**-48.3**	**-48.9**	**-49.3**	-10.6	**-34.4**	-6.5	**-32.1**	**-53.8**	**-54.4**	**-56.2**	**-51.8**	-2.7	-5.9	*+16.1*	**-46.5**	-20.1	**-38.5**	-5.2	**-31.0**	**-35.2**	**-15.7**
				●						-10.2	-0.4	*+9.2*	*+5.6*	*+3.1*	*+5.2*	*+5.2*	-14.6	-1.7	*+3.6*	*+5.1*	*+7.4*	*+5.9*	*+4.0*	*+5.9*	*+3.8*	*+6.3*	*+6.8*	*+9.0*	*+6.6*	*+6.9*	*+3.7*	*+0.3*	*+1.2*	*+8.1*	*+8.3*	*+6.3*	-0.8	*+2.9*	*+10.2*	*+3.3*
					●					-4.3	-0.4	*+3.2*	*+0.3*	*+0.5*	-2.5	*+0.6*	-18.0	-22.5	*+1.6*	*+0.1*	-1.0	*+1.1*	*+1.0*	*+1.4*	*+0.5*	*+2.5*	*+2.3*	*+2.5*	*+2.4*	*+1.1*	-0.9	-23.0	-17.2	*+2.6*	*+0.4*	*+1.2*	-1.4	-0.6	*+3.8*	-3.4
						●				-13.3	-2.2	*+12.6*	-1.1	*+2.3*	*+8.4*	*+3.5*	*+5.8*	-20.8	-15.4	*+3.6*	-6.1	*+7.0*	*+5.7*	*+8.3*	*+2.7*	*+7.1*	*+9.5*	*+11.7*	*+9.0*	*+4.3*	**-5.6**	*+10.9*	**-30.0**	*+8.5*	*+4.6*	*+7.1*	*+0.2*	-6.2	*+14.0*	-6.8
				●	●					-14.4	-0.9	*+13.2*	*+6.3*	*+3.9*	*+2.7*	*+6.1*	**-35.5**	**-26.8**	*+5.6*	*+5.5*	*+6.7*	*+7.5*	*+5.3*	*+7.8*	*+4.5*	*+9.5*	*+9.7*	*+12.2*	*+9.6*	*+8.5*	*+2.9*	**-25.5**	-18.2	*+11.4*	*+9.3*	*+8.0*	-2.3	*+2.4*	*+14.9*	-0.3
Combinations of screening and state-of-the-art sorting	●			●						-23.1	*+9.1*	-17.6	-15.2	-15.0	-14.6	-8.8	-12.1	*+9.6*	-15.0	-36.2	*+7.6*	-38.6	-9.6	-21.6	-10.8	-26.2	-39.8	-25.3	-33.7	-36.8	-1.5	-4.5	*+14.4*	-29.8	*+7.1*	-26.4	-9.5	-24.8	-22.5	-7.9
		●		●						-27.5	*+11.0*	-25.1	-16.3	-15.7	-16.1	-8.9	-10.4	*+13.9*	-15.6	-43.9	-2.0	-44.0	-7.7	-26.0	-7.5	-28.1	-47.4	-41.6	-37.5	-44.3	-0.7	-5.4	*+20.9*	-34.7	*+6.7*	-31.6	-9.4	-28.3	-23.8	-11.1
			●	●						-34.1	*+12.7*	-35.7	-14.2	-14.4	-17.4	-8.7	-19.6	*+22.2*	-15.6	-48.6	-46.7	-48.6	-6.8	-31.7	-3.0	-28.3	-52.9	-50.6	-55.9	-50.3	*+1.8*	-6.0	*+20.6*	-42.7	-11.8	-35.8	-6.8	-31.7	-27.2	-13.2
	●				●					-17.2	*+8.4*	-22.7	-19.8	-16.5	-21.8	-13.2	-16.6	-15.4	-16.2	-39.0	-1.8	-41.2	**-12.0**	-25.0	**-13.5**	-28.6	-41.7	-30.3	-35.5	-40.6	-6.2	-30.8	-7.8	-33.5	-2.1	-29.9	-9.6	-27.1	-27.8	-14.7
		●			●					-21.6	*+10.1*	-30.0	-21.0	-17.1	-23.5	-13.5	-16.0	-13.1	-16.9	-46.2	-11.4	-46.4	-10.4	-29.2	-10.4	-30.5	-48.8	-45.8	-39.1	-47.7	-5.6	-33.2	-2.9	-38.2	-3.2	-34.9	-9.5	-30.5	-29.4	-17.9
			●		●					-28.2	*+11.7*	**-40.2**	-19.6	-16.2	**-25.2**	**-13.8**	-25.4	-7.9	-17.0	-50.9	-54.0	-51.0	-9.9	**-34.8**	-6.6	**-30.9**	**-53.9**	**-54.6**	**-56.4**	-53.7	-3.8	-35.9	-6.0	**-46.0**	**-21.3**	**-39.1**	-7.2	-33.8	**-33.2**	-20.5
	●			●	●					-27.3	*+9.0*	-14.6	-15.5	-15.1	-18.0	-8.7	-36.2	-19.4	-14.0	-38.0	*+7.3*	-39.4	-8.7	-21.3	-10.8	-24.6	-39.1	-23.4	-32.3	-37.6	-2.5	-34.7	-7.4	-28.2	*+8.0*	-26.3	-11.7	-27.3	-19.4	-12.2
		●		●	●					-31.8	*+11.1*	-22.4	-16.6	-15.7	-19.8	-8.7	-36.5	-16.9	-14.7	-46.2	-3.4	-45.2	-6.7	-25.9	-7.4	-26.5	-47.1	-40.6	-36.2	-45.6	-1.7	-37.6	-1.7	-33.3	*+7.5*	-31.9	-11.7	-31.2	-20.7	-15.7
			●	●	●					-38.4	*+12.9*	-33.6	-14.5	-14.3	-21.1	-8.6	-48.7	-10.9	-14.7	-51.6	-52.7	-50.4	-5.6	-32.1	-2.7	-26.6	-52.9	-50.5	-56.1	-52.4	*+0.9*	**-41.0**	-5.0	-41.8	-12.5	-36.3	-9.1	-35.1	-24.5	-18.3
	●					●				-26.2	*+7.3*	-14.7	-24.1	-16.8	-11.7	-11.3	*+11.6*	-12.3	-37.5	-40.3	-9.8	-39.2	-8.1	-20.0	-12.5	-27.0	-38.6	-24.0	-32.2	-42.2	-12.7	*+7.3*	-21.9	-30.8	*+2.5*	-26.7	-8.9	-37.1	-19.2	-20.6
		●				●				-30.7	*+9.2*	-22.3	-25.9	**-17.7**	-13.0	-11.5	*+14.5*	-9.0	-39.2	-48.6	-22.2	-45.0	-6.0	-24.4	-9.0	-29.1	-46.4	-40.9	-36.1	-50.5	-12.4	*+7.1*	-17.8	-36.1	*+1.4*	-32.1	-8.8	-41.8	-20.3	-24.6
			●			●				-37.3	*+10.9*	-32.9	-24.8	-16.3	-13.6	-11.3	*+6.8*	-3.2	-40.7	-53.8	-71.1	-49.7	-4.4	-30.4	-4.1	-29.4	-52.1	-50.0	-55.8	-57.2	-12.2	*+7.9*	-21.4	-44.5	-18.8	-36.4	-5.9	-46.6	-23.1	-29.1
	●				●	●				-30.4	*+7.2*	-11.4	-25.2	-16.8	-15.3	-11.2	-12.7	-43.8	-37.7	-42.7	-10.7	-40.1	-7.1	-19.5	-12.8	-25.3	-37.8	-22.1	-30.6	-43.4	**-14.9**	-23.0	-46.8	-29.2	*+3.2*	-26.6	-11.2	-40.1	-15.9	-26.2
		●				●				-34.9	*+9.2*	-19.3	**-27.1**	**-17.7**	-16.9	-11.4	-11.7	-42.8	-39.4	-51.5	-24.3	-46.3	-4.8	-24.2	-9.1	-27.5	-46.0	-39.9	-34.5	-52.2	-14.7	-25.2	-43.9	-34.6	*+2.0*	-32.4	-11.3	-45.3	-17.0	-30.8
			●			●				-41.5	*+11.0*	-30.5	-26.2	-16.0	-17.3	-11.2	-22.6	-40.0	-41.2	-57.6	-78.3	**-51.6**	-2.8	-30.6	-4.1	-27.7	-52.0	-49.9	-56.0	**-59.9**	**-14.9**	-27.0	-51.3	-43.6	-20.2	-36.9	-8.3	-50.9	-20.1	-36.4
	●			●		●				-36.4	*+7.9*	-4.0	-20.0	-15.0	-5.9	-5.9	-5.9	-16.6	-38.7	-39.5	-0.3	-37.0	-3.8	-14.8	-9.3	-22.3	-35.0	-15.2	-28.0	-39.1	-9.6	*+9.2*	-23.4	-24.4	*+15.0*	-22.1	-11.1	-38.8	-8.2	-19.0
		●		●		●				-40.8	*+10.2*	-12.1	-21.8	-15.9	-7.1	-5.7	-3.3	-13.0	-40.6	-49.1	-14.4	-43.6	-1.0	-19.6	-5.2	-24.3	-44.0	-34.1	-32.2	-48.5	-9.2	*+9.1*	-18.6	-30.0	*+14.7*	-28.1	-11.2	-44.4	-8.6	-23.6
			●	●		●				-47.4	*+12.3*	-23.5	-19.9	-13.5	-6.5	-4.7	-13.4	-6.3	-42.4	-55.3	-72.0	-48.8	*+1.9*	-26.1	*+1.0*	-24.1	-50.4	-44.2	-55.4	-56.2	-8.7	*+10.8*	-22.4	-39.3	-7.8	-32.5	-7.7	-50.4	-10.8	-28.8
	●			●	●	●				-40.6	*+7.8*	*+0.6*	-21.1	-14.8	-9.5	-5.4	-35.4	**-53.5**	-38.9	-42.1	-0.4	-37.8	-2.2	-13.9	-9.3	-20.0	-33.8	-12.2	-25.8	-40.2	-11.9	-26.2	-53.0	-22.0	*+17.0*	-21.6	-14.0	-42.5	-3.7	-25.4
		●		●	●	●				-45.1	*+10.2*	-7.9	-23.0	-15.8	-11.0	-5.2	-35.6	-52.9	-40.9	-52.5	-16.1	-44.8	*+0.9*	-19.0	-5.0	-22.1	-43.3	-32.3	-30.0	-50.3	-11.7	-28.9	-49.8	-27.8	*+16.7*	-28.0	**-14.2**	-48.8	-3.9	-30.7
			●	●	●	●				**-51.7**	*+12.4*	-19.8	-21.2	-12.8	-9.7	-3.9	**-50.1**	-50.6	**-43.2**	**-59.9**	**-81.0**	-50.7	*+4.4*	-26.1	*+1.6*	-21.5	-50.1	-43.7	-55.7	-59.4	-11.7	-30.8	**-59.2**	-37.7	-8.3	-32.7	-10.5	**-55.8**	-6.3	**-37.4**
More targeted removal							●	●		-1.3	*+0.1*	*+1.0*	*+0.8*	-0.7	-4.5	*+0.5*	-12.1	-21.1	*+0.8*	-0.8	*+0.8*	*+0.4*	*+0.4*	*+1.0*	*+0.7*	*+1.0*	*+0.9*	*+1.1*	*+1.0*	*+0.8*	*+0.1*	-20.8	-16.3	*+0.9*	-2.0	-0.6	-2.1	*+0.6*	*+1.2*	*+0.3*
	●						●	●		-14.2	*+8.6*	-24.3	-18.6	-17.5	-23.7	-12.7	-10.3	-14.2	-16.2	-38.6	0.0	-40.4	**-12.4**	-24.4	-12.7	-29.0	-41.7	-30.8	-36.0	-39.3	-5.0	-28.0	-7.1	-34.1	-4.8	-30.8	-10.1	-24.5	-29.3	-10.5
		●					●	●		-18.6	*+10.3*	-31.3	-19.8	-18.1	-25.5	-12.9	-9.5	-11.9	-16.9	-45.6	-8.9	-45.5	-10.9	-28.4	-9.6	-30.9	-48.5	-45.8	-39.5	-46.2	-4.4	-30.1	-2.4	-38.7	-6.0	-35.7	-10.1	-27.6	-30.8	-13.5
			●				●	●		-25.3	*+11.8*	**-41.1**	-18.2	-17.4	**-27.5**	-13.1	-18.3	-7.0	-16.9	-49.9	-48.7	-49.7	-10.3	-33.6	-5.8	**-31.3**	-53.4	-54.0	-55.8	-51.6	-2.6	-32.5	-5.3	**-46.1**	-23.5	**-39.7**	-7.9	-30.6	**-34.3**	-15.7
				●			●	●		-4.5	-0.4	*+3.4*	*+0.5*	*+0.5*	-2.4	*+0.7*	-17.8	-26.4	*+1.8*	*+0.3*	-0.8	*+1.2*	*+1.1*	*+1.6*	*+0.6*	*+2.7*	*+2.5*	*+2.8*	*+2.6*	*+1.2*	-0.7	-23.4	-20.7	*+2.7*	-0.6	*+1.2*	-1.9	*+0.6*	*+4.0*	-3.4
	●				●		●	●		-17.4	*+8.4*	-22.6	-19.7	-16.6	-21.7	-13.0	-16.3	-19.9	-16.0	-38.9	-1.5	-41.1	-11.9	-24.8	**-13.4**	-28.5	-41.6	-30.1	-35.4	-40.5	-6.0	-31.3	-11.6	-33.5	-3.2	-30.0	**-10.2**	-27.1	-27.6	-14.8
		●			●		●	●		-21.9	*+10.2*	-29.8	-20.9	-17.3	-23.4	-13.3	-15.7	-17.7	-16.7	-46.1	-11.1	-46.3	-10.3	-29.0	-10.3	-30.4	-48.7	-45.7	-39.0	-47.6	-5.4	-33.7	-6.9	-38.2	-4.3	-35.1	**-10.2**	-30.5	-29.3	-18.0
			●		●		●	●		-28.5	*+11.7*	-40.1	-19.5	-16.3	-25.1	**-13.6**	**-25.2**	-13.0	-16.9	-50.8	-54.0	-50.9	-9.8	**-34.7**	-6.5	-30.8	**-53.8**	**-54.4**	-56.3	-53.6	-3.5	**-36.5**	-10.3	-46.0	-22.8	-39.3	-7.9	-33.9	-33.1	-20.6
									●	-9.6	*+0.7*	*+8.9*	-3.5	*+1.2*	*+5.9*	*+1.9*	*+6.0*	-18.4	-16.7	*+0.7*	-9.5	*+2.9*	*+4.1*	*+5.1*	*+2.2*	*+4.4*	*+6.0*	*+8.0*	*+5.5*	*+1.7*	-8.0	*+8.5*	-22.1	*+5.4*	*+2.0*	*+4.4*	*+4.2*	-6.7	*+10.0*	-9.1
	●								●	-22.5	*+10.2*	-17.7	-26.0	-17.5	-14.0	-12.4	*+11.4*	-9.9	-37.9	-41.6	-13.8	-40.7	-9.4	-22.3	-12.4	-28.3	-40.4	-26.6	-34.6	-43.0	-15.2	*+4.9*	-13.5	-32.7	-0.5	-28.2	-3.8	-36.1	-22.0	-22.8
		●							●	-27.0	*+12.2*	-25.1	-27.7	-18.4	-15.4	-12.7	*+14.2*	-6.7	-39.5	-49.5	-25.7	-46.3	-7.5	-26.7	-9.0	-30.4	-47.9	-42.8	-38.4	-51.0	-15.1	*+4.5*	-9.4	-37.8	-1.7	-33.5	-3.5	-40.6	-23.2	-26.8
			●						●	-33.6	*+14.1*	-35.4	-26.9	-17.3	-16.5	-12.7	*+6.8*	-1.0	-40.9	-54.6	-71.8	-50.8	-6.2	-32.4	-4.3	-30.8	-53.5	-51.5	-56.9	-57.3	-15.3	*+5.0*	-12.3	-45.9	-20.8	-37.7	-0.2	-45.1	-26.0	-31.3
	●						●	●	●	-10.9	*+0.8*	*+10.1*	-2.6	*+0.4*	*+0.8*	*+2.4*	-7.7	-41.8	-16.2	-0.2	-8.8	*+4.3*	*+4.6*	*+6.3*	*+2.9*	*+5.5*	*+7.1*	*+9.3*	*+6.6*	*+2.5*	-8.0	-14.2	-40.4	*+6.4*	-0.3	*+3.8*	*+2.0*	-6.2	*+11.4*	-8.9
		●					●	●	●	-23.8	*+10.5*	-16.7	-25.3	-18.7	-20.1	-11.9	-4.8	-37.4	-37.6	-43.1	-13.1	-40.9	-9.1	-21.4	-11.8	-27.5	-39.8	-25.6	-33.9	-42.7	-15.3	-21.4	-34.7	-32.1	-3.4	-29.4	-6.5	-35.9	-20.9	-22.8
			●				●	●	●	-28.3	*+12.5*	-24.2	-27.1	**-19.7**	-22.0	-12.2	-3.7	-36.1	-39.1	-51.3	-25.1	-46.6	-7.2	-25.7	-8.2	-29.6	-47.5	-42.2	-37.8	-50.8	-15.2	-23.2	-31.5	-37.2	-4.9	-34.9	-6.2	-40.4	-22.0	-26.9
				●			●	●	●	-34.9	*+14.4*	-34.6	-26.2	-18.7	-23.6	-12.1	-13.2	-33.3	-40.6	-56.5	-72.1	-51.3	-5.8	-31.5	-3.4	-29.8	-53.0	-50.9	-56.5	-57.2	-15.3	-24.9	-37.4	-45.5	**-24.9**	-39.2	-3.2	-45.0	-24.7	-31.5
	●				●		●	●	●	-14.1	*+0.3*	*+13.0*	-3.3	*+1.8*	*+3.3*	*+2.8*	-14.0	**-48.6**	-15.4	*+0.9*	-10.5	*+5.5*	*+5.6*	*+7.2*	*+2.9*	*+7.6*	*+9.1*	*+11.4*	*+8.7*	*+3.2*	-9.5	-16.9	**-46.4**	*+8.6*	*+1.4*	*+5.9*	*+2.3*	-7.5	*+14.9*	-13.6
		●			●		●	●	●	-27.1	*+10.3*	-14.5	-27.0	-17.6	-17.5	-12.2	-11.6	-45.1	-37.9	-43.8	-14.7	-41.6	-8.4	-21.7	-12.6	-26.8	-39.6	-24.7	-33.1	-44.0	-17.3	-24.9	-41.2	-31.2	-1.4	-28.5	-6.4	-39.0	-18.9	-28.5
			●		●		●	●	●	-31.5	*+12.4*	-22.2	**-29.0**	-18.6	-19.3	-12.5	-10.7	-44.2	-39.6	-52.3	-27.7	-47.6	-6.3	-26.3	-9.0	-28.9	-47.6	-41.8	-37.0	-52.5	-17.3	-27.1	-38.2	-36.5	-2.8	-34.1	-6.2	-43.9	-20.0	-33.0
				●			●	●	●	**-38.1**	*+14.5*	-33.1	-28.3	-17.3	-20.3	-12.4	-21.0	-41.9	**-41.3**	**-58.1**	**-78.6**	**-52.7**	-4.8	-32.6	-4.2	-29.2	-53.4	-51.4	**-57.1**	**-59.7**	**-17.8**	-29.2	-44.9	-45.2	-24.0	-38.6	-2.9	**-49.0**	-23.1	**-38.5**
								●	●	-9.9	*+0.7*	*+9.1*	-3.4	*+1.7*	*+6.1*	*+2.0*	*+6.2*	-22.5	-16.6	*+0.9*	-9.2	*+6.1*	*+4.3*	*+5.4*	*+2.2*	*+4.6*	*+6.5*	*+8.3*	*+5.7*	*+1.9*	-7.9	*+8.2*	-25.8	*+5.5*	*+0.9*	*+4.4*	*+3.6*	-6.6	*+10.3*	-9.2
	●							●	●	-22.8	*+10.2*	-17.5	-25.9	-17.6	-13.8	-12.3	*+11.8*	-14.7	-37.8	-41.4	-13.5	-40.6	-9.3	-22.1	-12.3	-28.3	-40.2	-26.4	-34.4	-42.9	-15.0	*+4.5*	-17.7	-32.6	-1.7	-28.4	-4.5	-36.1	-21.8	-22.9
		●						●	●	-27.3	*+12.2*	-24.9	-27.7	-18.5	-15.3	-12.5	*+14.5*	-11.7	-39.4	-49.4	-25.4	-46.2	-7.4	-26.5	-8.9	-30.3	-47.8	-42.7	-38.3	-50.9	-15.0	*+4.1*	-13.7	-37.7	-3.0	-33.7	-4.1	-40.6	-23.0	-27.0
			●					●	●	-33.9	*+14.1*	-35.2	-26.8	-17.4	-16.3	-12.5	*+7.1*	-6.6	-40.9	-54.5	-71.7	-50.8	-6.1	-32.2	-4.2	-30.7	-53.3	-51.4	-56.8	-57.2	-15.1	*+4.5*	-17.0	-45.9	-22.4	-37.9	-1.0	-45.2	-25.8	-31.5

with a laser may be an option to remove black materials. According to the calculations for the investigated waste stream, this would, inter alia, result in a decrease of Co, Sb, and Cl, accompanied by a more pronounced increase of the concentrations of other SRF-relevant contaminants than for PVC removal.

3.2.4. Effect of combinations or a more targeted removal of contaminant carriers

As opposed to the application of only one single process step, i.e., screening, NIR sorting, or removing b&g materials, the combination of these measures seems to be a promising approach that allows SRF producers to reduce the concentrations of all investigated elements. Therefore, combined measures enable the production of a pollutant-depleted SRF and further limitation of contaminants that are introduced into the cement clinker via SRF. The simplest scenario causing a reduction of the concentrations of all investigated elements is screening combined with the removal of PVC with an industrial NIR sorter. For the investigated waste streams, being able to remove black PVC in addition to removing the PVC(NIR) fraction and the fine fraction(s) would result in the removal of 4–5% more Sb and Cl referring to the total content. However, it would not result in significant improvements for other elements, compared to the scenario of removing the fine fraction and PVC (NIR). Combining the removal of black PVC with screening and more targeted removal of PVC(FTIR) (i.e., as identified by FTIR spectroscopy) would not achieve significantly better results for most elements, see also section 3.1.2. The scenario showing the highest reductions for most elements, but also requiring the removal of a significantly higher amount of the waste stream's mass, is removing the fine fraction < 20 mm, the PVC(NIR) fraction, b&g PVC, and b&g Other. Additionally, this scenario would require technological improvements enabling the identification of b&g PVC and b&g Other on an industrial scale to become broadly available to SRF producers.

3.3. Relevance for the compliance with limit values

Currently, the main goal of taking measures to reduce the concentration of specific contaminants in waste presumably is to comply with limit values. As an example, Fig. 6a and b depict the compliance with Austrian limit values for SRF produced from the original waste stream without taking any measures, and the samples after theoretical screening at 20 mm and removal of PVC with an NIR sorter.

One of the best results concerning the relevant elements of the Austrian waste incineration ordinance (WIO) [9], i.e., As, Cd, Cr, Co, Hg, Ni, Pb, and Sb is achieved by removing the fraction 0–20 mm in addition to removing PVC with a state-of-the-art NIR sorter and removing black&grey plastics. Again, slightly better results are achieved when not the whole b&g fraction, but only "b&g PVC" and "b&g Other" are removed. With these measures (and a few other combinations, cf. Appendix B, section B.32), all relevant elements are likely to comply with the limit values. However, the desired maximum content of chlorine of 1%$_{DM}$ was only achieved for 3 of the 5 investigated MCW streams. This suggests that the removal of chlorine carriers needs further improvement, which possibly needs to be accompanied by a more thorough identification of potential chlorine carriers in the respective waste streams. However, the effects of the different screening and sorting combinations emphasize their practical relevance for SRF production.

3.4. Effects on the material-recyclable share of SRF

When SRF is co-processed in cement kilns, the ash that contains these elements is incorporated into the clinker. Thereby, SRF ash is substituting a small part of the raw materials required for cement clinker production [44,45]. A mixed recovery, i.e., a combination of energy and material recovery, is already recognized in some countries [44], e.g., Portugal [46,47]. For this reason, ash-forming elements that may be

Table 2
Calculated relative concentration change (in %, arithmetic mean values of the concentration changes observed for S01-S05 referring to mg/MJ), LHV change, and mass loss caused by removing particle size or material fractions. The highest reductions (or increases in the case of the LHV) for each of the three main sections are marked in bold.

	Removed fraction									Relative effect on parameter [%]																						
	0–5 mm	0–10 mm	0–20 mm	PET (NIR)	PVC (NIR)	B&g	PVC (FTIR)	B&g PVC	B&g Other	Mass	LHV	Ag	Al	As	Ba	Ca	Cd	Cl	Co	Cr	Cu	Fe	Hg	K	Li	Mg	Mn	Mo	Na	Ni	P	Pb	Sb	Si	Sn	Sr	Ti	V	W	Zn
Single state-of-the-art process steps										-12.9	*+8.4*	-30.8	-25.4	-22.9	-24.6	-19.8	-4.0	*+1.6*	-23.3	-42.1	-8.7	-44.8	-19.5	-30.9	**-20.0**	-35.1	-46.5	-36.8	-41.3	-44.3	-12.3	-11.7	*+2.7*	-39.6	-9.8	-35.1	-14.8	-30.8	-35.7	-17.4
	●									-17.4	*+10.1*	-38.1	**-27.5**	-24.6	-26.9	-21.2	-3.5	*+3.6*	-25.1	-49.2	-18.1	-49.9	-19.5	-35.5	-18.6	-37.7	-53.3	-51.2	-45.2	-51.3	**-13.0**	-13.9	*+6.0*	-44.6	-11.9	-40.3	**-15.8**	-34.7	-38.3	-21.2
		●								**-24.0**	*+11.5*	**-47.4**	-27.1	**-24.7**	**-29.2**	**-22.4**	-11.4	*+8.5*	**-26.0**	**-53.5**	**-54.8**	**-54.1**	**-20.1**	**-41.0**	-16.3	**-38.9**	**-58.3**	**-59.0**	**-60.4**	**-56.6**	-12.5	-15.4	*+3.7*	**-51.8**	**-28.3**	**-44.5**	-14.9	**-38.2**	**-42.1**	**-24.1**
			●							-10.2	-0.4	*+9.6*	*+6.1*	*+3.5*	*+5.6*	*+5.6*	-14.3	-1.3	*+4.0*	*+5.5*	*+7.9*	*+6.4*	*+4.4*	*+6.3*	*+4.2*	*+6.8*	*+7.2*	*+9.4*	*+7.0*	*+7.3*	*+4.1*	*+0.7*	*+1.6*	*+8.5*	*+8.8*	*+6.7*	-0.4	*+3.4*	*+10.6*	*+3.7*
				●						-4.3	-0.4	*+3.6*	*+0.7*	*+1.0*	-2.1	*+1.0*	-17.6	-22.1	*+2.0*	*+0.5*	-0.6	*+1.5*	*+1.4*	*+1.8*	*+0.9*	*+2.9*	*+2.7*	*+2.9*	*+2.9*	*+1.5*	-0.5	-22.6	-17.0	*+3.0*	*+0.8*	*+1.7*	-1.0	-0.3	*+4.2*	-3.0
					●					-13.3	-2.2	*+15.1*	*+1.1*	*+4.7*	*+10.8*	*+5.8*	*+8.1*	-19.1	-13.3	*+5.9*	-3.7	*+9.4*	*+8.0*	*+10.8*	*+5.0*	*+9.5*	*+12.0*	*+14.2*	*+11.5*	*+6.7*	-3.6	*+13.3*	**+28.4**	*+11.0*	*+7.0*	*+9.5*	*+2.4*	-4.0	*+16.6*	-4.8
				●	●					-14.4	-0.9	*+14.3*	*+7.2*	*+4.8*	*+3.7*	*+7.0*	**-34.6**	**-26.0**	*+6.6*	*+6.5*	*+7.7*	*+8.6*	*+6.2*	*+8.7*	*+5.5*	*+10.6*	*+10.8*	*+13.3*	*+10.7*	*+9.5*	*+3.8*	**-24.6**	-17.6	*+12.4*	*+10.3*	*+9.1*	-1.4	*+3.3*	*+16.0*	*+0.6*
Combinations of screening and state-of-the-art sorting	●			●						-23.1	*+9.1*	-24.4	-22.1	-22.0	-21.3	-16.3	-19.4	*+0.5*	-22.1	-41.5	-1.3	-43.5	-17.3	-28.1	-18.2	-32.3	-44.5	-31.4	-39.0	-42.0	-9.5	-12.4	*+4.7*	-35.6	-1.7	-32.4	-16.9	-31.1	-29.2	-15.2
		●		●						-27.5	*+11.0*	-32.5	-24.3	-23.9	-23.8	-17.8	-19.3	*+2.7*	-24.0	-49.4	-11.9	-49.2	-17.1	-33.1	-16.6	-35.1	-52.2	-47.3	-43.2	-49.8	-10.2	-14.8	*+8.6*	-41.0	-3.6	-38.1	-18.3	-35.5	-31.9	-19.4
			●	●						-34.1	*+12.7*	-42.6	-23.5	-23.8	-25.9	-18.8	-29.0	*+8.5*	-25.1	-54.3	-53.8	-54.0	-17.5	-39.2	-13.9	-36.2	-57.8	-56.0	-60.6	-55.7	-9.2	-16.5	*+6.2*	-48.9	-21.8	-42.7	-17.2	-39.6	-36.0	-22.5
	●				●					-17.2	*+8.4*	-28.7	-25.9	-23.0	-27.6	-19.8	-22.8	-21.9	-22.7	-43.8	-9.5	-45.6	-18.9	-30.8	**-20.2**	-34.0	-46.0	-35.7	-40.3	-45.1	-13.4	-36.4	-15.1	-38.6	-9.6	-35.2	-16.5	-32.8	-33.5	-21.1
		●			●					-21.6	*+10.1*	-36.4	-28.1	-24.8	-30.1	-21.3	-23.3	-20.9	-24.5	-51.2	-19.8	-51.1	-18.8	-35.6	-18.8	-36.7	-53.2	-50.7	-44.4	-52.5	-14.1	-39.7	-12.2	-43.8	-11.8	-40.7	-17.7	-36.9	-36.3	-25.1
			●		●					-28.2	*+11.7*	**-46.2**	-27.8	**-24.9**	**-32.6**	**-22.6**	-32.9	-17.3	-25.6	-56.0	-59.7	-55.7	**-19.5**	**-41.5**	-16.4	**-37.9**	**-58.5**	**-59.1**	-60.7	-58.4	-13.6	**-42.9**	-16.4	**-51.4**	**-29.4**	**-45.2**	-16.8	-40.8	**-40.5**	-28.5
	●			●	●					-27.3	*+9.0*	-21.6	-22.4	-22.0	-24.4	-16.2	-41.2	-25.9	-21.3	-43.1	-1.7	-44.3	-16.4	-27.8	-18.2	-30.9	-43.9	-29.7	-37.7	-42.8	-10.5	-40.3	-15.5	-34.1	-0.7	-32.3	-19.0	-33.5	-26.4	-19.1
		●		●	●					-31.8	*+11.1*	-30.1	-24.7	-24.0	-27.1	-17.7	-42.3	-24.9	-23.3	-51.6	-13.4	-50.4	-16.2	-33.1	-16.6	-33.8	-52.0	-46.4	-42.1	-51.0	-11.2	-44.2	-12.2	-39.8	-2.7	-38.4	-20.5	-38.2	-29.3	-23.6
			●	●	●					-38.4	*+12.9*	-40.8	-24.0	-23.9	-29.2	-18.8	-54.4	-20.8	-24.5	-57.1	-59.5	-55.6	-16.6	-39.7	-13.8	-34.9	-57.9	-56.0	**-61.0**	-57.8	-10.2	**-48.0**	-17.1	-48.2	-22.5	-43.3	-19.4	-42.7	-33.8	-27.2
	●					●				-26.2	*+7.3*	-20.5	-29.2	-22.3	-17.3	-17.3	*+4.2*	-18.4	-42.2	-44.3	-15.0	-43.2	-14.5	-25.4	-18.6	-31.9	-42.6	-29.1	-36.6	-46.0	-18.6	*0.0*	-27.0	-35.5	-4.2	-31.6	-14.9	-41.3	-25.1	-25.7
		●				●				-30.7	*+9.2*	-28.8	-31.8	-24.3	-19.6	-18.9	*+5.2*	-16.9	-44.9	-52.8	-27.4	-49.3	-14.2	-30.7	-16.9	-34.9	-50.6	-45.7	-41.0	-54.5	-19.8	-2.1	-24.5	-41.2	-6.6	-37.6	-16.3	-46.6	-27.7	-30.6
			●			●				-37.3	*+10.9*	-39.2	-31.8	-24.1	-21.2	-19.9	-3.5	-12.9	-47.1	-58.1	-73.5	-54.2	-14.1	-37.0	-13.8	-36.1	-56.4	-54.7	-59.9	-61.1	-20.7	-2.6	-29.1	-49.7	-26.6	-42.3	-14.9	-51.9	-31.5	-35.7
	●				●	●				-30.4	*+7.2*	-17.3	-30.1	-22.1	-20.4	-17.2	-17.9	-47.6	-42.2	-46.4	-15.7	-44.0	-13.4	-24.9	-18.7	-30.3	-41.7	-27.2	-35.0	-47.0	-20.7	-28.2	-50.5	-33.9	-3.2	-31.4	-17.1	-44.2	-22.0	-30.9
		●			●	●				-34.9	*+9.2*	-26.0	-33.0	-24.3	-23.0	-18.8	-18.1	-47.5	-45.1	-55.5	-29.3	-50.4	-12.9	-30.4	-17.0	-33.5	-50.2	-44.7	-39.5	-56.0	-22.0	-31.8	-48.8	-39.9	-5.7	-37.8	-18.5	-49.8	-24.7	-36.3
			●		●	●				-41.5	*+11.0*	-37.1	**-33.2**	-23.9	-24.4	-19.9	-29.3	-45.9	-47.7	-61.6	-80.2	**-55.9**	-12.7	-37.3	-13.8	-34.7	-56.4	-54.6	-60.1	**-63.6**	**-23.3**	-34.6	-56.6	-48.9	-27.6	-42.8	-17.1	-55.7	-28.9	-42.3
	●			●		●				-36.4	*+7.9*	-11.0	-25.7	-20.8	-12.0	-12.7	-12.8	-22.9	-43.6	-43.8	-6.0	-41.4	-10.9	-21.0	-15.9	-27.9	-39.4	-21.2	-32.9	-43.3	-16.2	*+1.1*	-28.7	-29.8	*+7.0*	-27.6	-17.5	-43.2	-15.6	-24.5
		●		●		●				-40.8	*+10.2*	-20.2	-28.6	-23.0	-14.4	-14.2	-12.2	-21.3	-46.8	-53.5	-20.3	-48.3	-10.3	-26.9	-14.0	-31.2	-48.6	-39.9	-37.7	-52.9	-17.5	-1.3	-25.8	-36.1	*+5.0*	-34.4	-19.1	-49.4	-18.2	-30.1
			●	●		●				-47.4	*+12.3*	-31.6	-28.1	-22.1	-15.1	-14.9	-23.2	-16.7	-49.6	-59.8	-74.6	-53.8	-9.6	-34.0	-10.1	-32.2	-55.2	-50.1	-60.0	-60.6	-18.4	-1.5	-30.9	-45.5	-17.7	-39.4	-17.4	-55.6	-22.0	-36.0
	●			●	●	●				-40.6	*+7.8*	-6.5	-26.6	-20.4	-14.8	-12.2	-39.2	-56.8	-43.7	-46.1	-5.7	-41.9	-9.2	-20.0	-15.8	-25.7	-38.1	-18.3	-30.6	-44.3	-18.3	-31.6	-56.5	-27.4	*+9.4*	-27.0	-20.0	-46.6	-11.3	-30.4
		●		●	●	●				-45.1	*+10.2*	-16.2	-29.7	-22.8	-17.4	-13.7	-40.2	**-57.2**	-47.1	-56.6	-21.7	-49.3	-8.4	-26.3	-13.7	-29.1	-47.8	-38.2	-35.5	-54.6	-19.9	-35.9	-54.8	-34.0	*+7.3*	-34.2	**-21.8**	-53.3	-14.1	-36.7
			●	●	●	●				**-51.7**	*+12.4*	-28.3	-29.5	-21.4	-17.5	-14.3	**-54.6**	-55.8	**-50.4**	**-64.1**	**-82.9**	-55.5	-7.2	-34.1	-9.6	-30.0	-54.9	-49.6	-60.4	**-63.6**	-21.3	-39.0	**-64.7**	-44.1	-17.8	-39.5	-20.0	**-60.5**	-18.4	**-43.9**
More targeted removal							●	●		-1.3	*+0.1*	*+0.9*	*+0.7*	-0.8	-4.5	*+0.4*	-12.2	-21.2	*+0.7*	-0.8	*+0.7*	*+0.5*	*+0.3*	*+0.9*	*+0.6*	*+0.9*	*+0.9*	*+1.0*	*+0.9*	*+0.7*	0.0	-20.8	-16.3	*+0.8*	-2.1	-0.6	-2.2	*+0.5*	*+1.1*	*+0.2*
	●						●	●		-14.2	*+8.6*	-30.2	-25.0	-24.0	-29.6	-19.6	-17.1	-21.0	-22.8	-43.5	-8.0	-45.0	-19.5	-30.3	-19.7	-34.6	-46.1	-36.2	-40.9	-44.1	-12.5	-33.9	-14.6	-39.3	-12.2	-36.2	-17.2	-30.6	-35.0	-17.4
		●					●	●		-18.6	*+10.3*	-37.6	-27.1	-25.8	-32.1	-21.0	-17.4	-20.0	-24.6	-50.8	-17.5	-50.2	-19.4	-34.9	-18.2	-37.2	-53.0	-50.9	-44.8	-51.2	-13.2	-37.0	-11.8	-44.3	-14.5	-41.5	**-18.4**	-34.5	-37.6	-21.3
			●				●	●		-25.3	*+11.8*	**-47.0**	-26.6	-26.0	**-34.7**	-22.1	-26.5	-16.6	-25.5	-55.1	-54.8	-54.5	**-20.0**	-40.4	-15.8	-38.3	-58.0	-58.6	-60.2	-56.5	-12.7	-39.9	-15.8	-51.6	-31.4	-45.8	-17.5	-38.0	**-41.4**	-24.2
	●					●		●		-4.5	-0.4	*+3.8*	*+0.9*	*+0.9*	-2.0	*+1.1*	-17.4	-26.0	*+2.2*	*+0.7*	-0.4	*+1.7*	*+1.5*	*+1.0*	*+1.0*	*+2.1*	*+2.9*	*+3.2*	*+3.1*	*+1.7*	-0.3	-23.0	-20.4	*+3.1*	-0.1	*+1.6*	**-1.5**	-8.2	*+4.5*	-3.1
		●				●		●		-17.4	*+8.4*	-28.5	-25.8	-23.1	-27.6	-19.7	-22.6	-26.0	-22.5	-43.7	-9.3	-45.6	-18.9	-30.6	-20.2	-34.0	-45.9	-35.5	-40.2	-45.1	-13.2	-36.8	-18.7	-38.6	-10.6	-35.4	-17.1	-32.8	-33.4	-21.2
			●			●		●		-21.9	*+10.2*	-36.2	-28.0	-24.9	-30.0	-21.2	-23.0	-25.2	-24.4	-51.2	-19.6	-51.0	-18.8	-35.4	-18.7	-36.7	-53.1	-50.6	-44.2	-52.4	-14.0	-40.2	-15.9	-43.8	-12.8	-40.8	**-18.4**	-37.0	-36.1	-25.3
				●		●		●		-28.5	*+11.7*	-46.0	-27.7	-25.0	-32.4	-22.5	**-32.7**	-21.9	-25.4	-55.9	-59.6	-55.6	-19.4	**-41.3**	-16.4	-37.9	-58.4	**-59.0**	-60.6	-58.3	-13.4	**-43.4**	-20.4	-51.4	-30.7	-45.3	-17.4	-40.9	-40.3	-28.6
									●	-9.6	*+0.7*	*+8.1*	-4.2	*+0.5*	*+5.2*	*+1.2*	*+5.2*	-18.9	-17.2	0.0	-10.1	*+3.2*	*+3.4*	*+4.4*	*+1.5*	*+3.7*	*+5.3*	*+7.3*	*+4.8*	*+1.0*	-8.6	*+7.8*	-22.7	*+4.7*	*+1.3*	*+3.7*	*+3.5*	-7.3	*+9.2*	-9.7
	●								●	-22.5	*+10.2*	-25.3	-32.7	-25.0	-21.7	-20.5	*+1.2*	-18.3	-44.0	-46.8	-21.3	-46.0	-18.0	-29.4	-20.5	-34.8	-45.7	-33.2	-40.5	-48.1	-23.0	-4.8	-21.3	-38.8	-9.6	-34.8	-12.6	-42.0	-29.4	-29.7
		●							●	-27.0	*+12.2*	-33.1	-35.3	-27.0	-24.1	-22.1	*+2.0*	-16.9	-46.5	-54.9	-32.8	-51.8	-17.8	-34.5	-19.0	-37.8	-53.3	-48.9	-44.8	-56.1	-24.3	-6.9	-18.9	-44.3	-12.0	-40.6	-13.8	-47.0	-32.0	-34.4
			●						●	-33.6	*+14.1*	-43.0	-35.6	-27.3	-26.3	-23.3	-6.3	-13.3	-48.8	-59.9	-74.8	-56.5	-18.1	-40.5	-16.3	**-39.0**	**-58.9**	-57.2	-61.9	-62.3	-25.6	-7.8	-23.0	**-52.3**	-30.4	-45.1	-12.4	-51.8	-35.5	-39.4
	●						●	●	●	-10.9	*+0.8*	*+9.2*	-3.4	-0.4	*+0.1*	*+1.7*	-8.4	-42.2	-16.8	-0.9	-9.5	*+3.6*	*+3.8*	*+5.5*	*+2.1*	*+4.7*	*+6.3*	*+8.4*	*+5.8*	*+1.7*	-8.7	-14.8	-40.9	*+5.6*	-1.1	*+3.0*	*+1.2*	-6.9	*+10.5*	-9.6
		●					●	●	●	-23.8	*+10.5*	-24.6	-32.2	-26.3	-27.4	-20.3	-13.5	-43.3	-43.8	-48.4	-20.8	-46.3	-17.9	-28.7	-20.2	-34.2	-45.3	-32.5	-40.0	-48.0	-23.3	-29.0	-40.7	-38.4	-12.3	-36.0	-15.3	-42.0	-28.5	-29.9
			●				●	●	●	-28.3	*+12.5*	-32.5	-34.9	-28.4	-30.1	-21.8	-13.7	-43.2	-46.4	-56.6	-32.4	-52.2	-17.8	-33.8	-18.6	-37.2	-53.0	-48.5	-44.4	-56.1	-24.6	-32.2	-39.0	-44.0	-14.9	-41.9	-16.5	-47.0	-31.1	-34.7
				●			●	●	●	-34.9	*+14.4*	-42.5	-35.1	**-28.7**	-32.7	-23.1	-23.5	-41.7	-48.6	-61.8	-75.1	-57.0	-18.0	-39.9	-15.8	-38.4	-58.6	-56.8	-61.7	-62.3	-25.9	-34.7	-45.3	-52.1	**-34.0**	**-46.7**	-15.3	-51.9	-34.6	-39.8
	●				●		●	●	●	-14.1	*+0.3*	*+12.7*	-3.7	*+1.5*	*+3.1*	*+2.5*	-14.1	-48.8	-15.5	*+0.6*	-10.6	*+5.2*	*+5.3*	*+6.9*	*+2.6*	*+7.3*	*+8.8*	*+11.1*	*+8.4*	*+2.9*	-9.8	-17.0	-46.6	*+8.3*	*+1.2*	*+5.7*	*+2.0*	-7.7	*+14.6*	-13.9
		●			●		●	●	●	-27.1	*+10.3*	-22.5	-33.7	-25.3	-25.0	-20.4	-19.6	-50.3	-44.1	-48.9	-22.2	-46.9	-17.1	-29.0	**-20.8**	-33.6	-45.0	-31.6	-39.2	-49.1	-25.0	-32.1	-46.7	-37.6	-10.3	-35.1	-15.1	-44.7	-26.6	-35.0
			●		●		●	●	●	-31.5	*+12.4*	-30.7	-36.5	-27.4	-27.7	-22.1	-19.9	**-50.4**	-46.8	-57.5	-34.8	-53.1	-16.9	-34.3	-19.2	-36.6	-53.0	-48.1	-43.6	-57.6	-26.5	-35.6	-45.0	-43.3	-13.0	-41.2	-16.4	-50.0	-29.3	-40.1
				●			●	●	●	**-38.1**	*+14.5*	-41.2	**-37.0**	-27.6	-29.9	**-23.4**	-30.5	-49.3	**-49.3**	**-63.2**	**-81.0**	**-58.2**	-17.1	-40.9	-16.4	-37.9	**-58.9**	-57.2	**-62.3**	**-64.5**	**-28.1**	-38.5	**-52.1**	-51.9	-33.2	-46.1	-15.0	**-55.4**	-33.2	**-46.0**
	●						●	●	●	-9.9	*+0.7*	*+8.4*	-4.0	*+0.4*	*+5.4*	*+1.3*	*+5.5*	-23.1	-17.1	*+0.2*	-9.8	*+3.4*	*+3.6*	*+4.7*	*+1.6*	*+3.9*	*+5.6*	*+7.5*	*+5.0*	*+1.2*	-8.5	*+7.4*	-26.3	*+4.8*	*+0.3*	*+3.7*	*+2.9*	-7.3	*+9.5*	-9.8
		●					●	●	●	-22.8	*+10.2*	-25.1	-32.6	-25.1	-21.6	-20.4	*+1.5*	-22.7	-43.9	-46.7	-21.0	-46.0	-17.9	-29.3	-20.5	-34.8	-45.6	-33.1	-40.4	-48.1	-22.9	-5.2	-25.2	-38.8	-10.7	-34.9	-13.3	-42.0	-29.2	-29.9
			●				●	●	●	-27.3	*+12.2*	-33.0	-35.3	-27.2	-24.0	-22.0	*+2.3*	-21.5	-46.5	-54.8	-32.5	-51.8	-17.8	-34.3	-19.0	-37.7	-53.2	-48.8	-44.7	-56.1	-24.2	-7.3	-22.9	-44.3	-13.1	-40.7	-14.4	-47.0	-31.8	-34.6
				●			●	●	●	-33.9	*+14.1*	-42.8	-35.5	-27.4	-26.1	-23.2	-6.0	-18.3	-48.7	-59.8	-74.8	-56.5	-18.0	-40.4	-16.2	**-39.0**	-58.8	-57.1	-61.9	-62.2	-25.5	-8.2	-27.2	**-52.3**	-31.8	-45.3	-13.1	-51.9	-35.3	-39.6

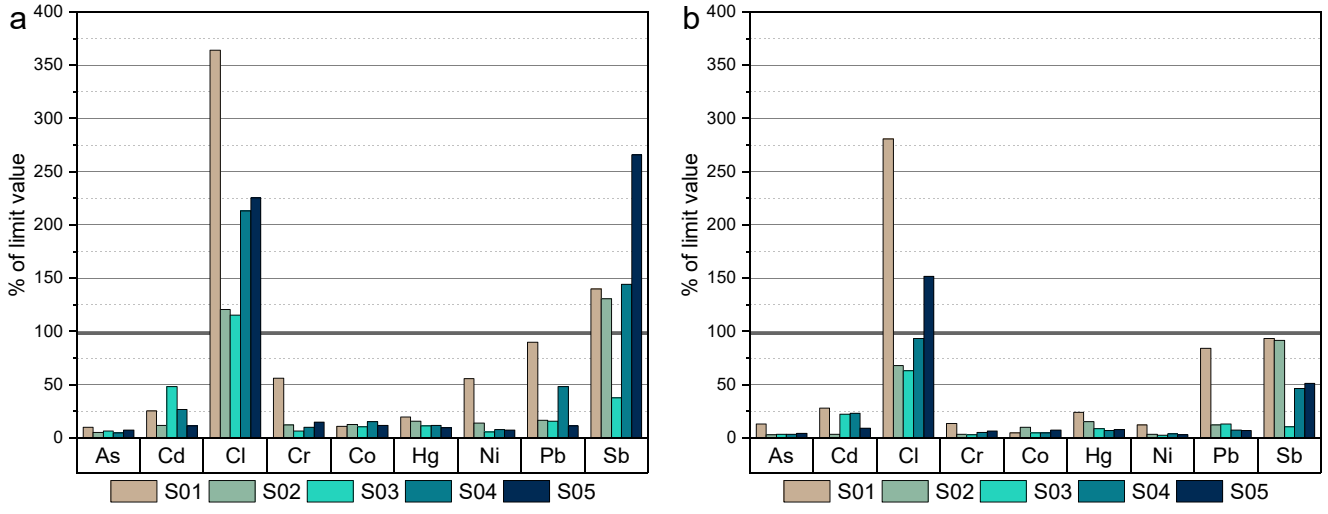

Fig. 6. Compliance of the MCW samples with the Austrian WIO limit values [9] and the desired maximum chlorine content of 1%$_{DM}$ of the a) original waste streams, and b) after removing both the fine fraction < 20 mm and the PVC(NIR) fraction.

considered as recycled in the cement industry, e.g., Al, Ca, Fe, Si, etc. [44], should be taken into account for the assessment of SRF quality as well. While the removed plastic fractions only contain minor amounts of Al, Ca, Fe, and Si, i.e., elements that are considered valuable raw materials for the cement industry (cf. Appendix A), the fine fractions were found to contain the largest share of these elements. If the fine fraction is removed before utilization of the SRF, not only contaminants but also a considerable share of valuable mineral constituents that could – from a technical perspective – be recycled on a material level is prevented from entering the kiln. Consequently, a decision has to be made on whether the fine fraction may be removed from the waste stream and treated separately or whether it should remain in the SRF, thereby introducing both contaminants and valuable materials into the cement kiln.

4. Conclusion

Despite the heterogeneity of the MCW streams reflected by different element concentrations and different compositions, a reduction of the

concentrations of all 29 investigated elements present at levels > L.O.Q. can theoretically be achieved by applying combinations of screening and sorting. However, it may not be necessary for SRF producers to reduce all of these elements. They may rather choose the suitable measures for the selected elements they need to target while considering the potential effects of the removal step on other relevant elements or contaminants and quality parameters. SRF producers that currently only remove PVC and PET with NIR sorters should consider the potential effects of this approach on the concentration of other heavy metals, especially if concentrations close to the required limit values are faced frequently. Depending on the purpose, e.g., reducing the amount of only some specific elements or producing a high-quality contaminant-depleted SRF, SRF producers need to choose the suitable measures. This will always involve finding a balance between the achieved reductions, the removed mass, and the LHV of the removed material. In this regard, a more targeted removal of contaminant carriers is expected to be beneficial, as less mass would be removed from the waste stream. After all, the removed materials need to be directed towards another suitable treatment option, which may not yet exist or be industrially established. For contaminant-rich fractions, however, conventional waste incineration legally and technically represents a feasible treatment possibility.

CRediT authorship contribution statement

S.A. Viczek: Conceptualization, Methodology, Formal analysis, Investigation, Data curation, Writing - original draft, Writing - review & editing, Visualization, Project administration. **K.E. Lorber:** Writing - review & editing, Supervision. **R. Pomberger:** Resources, Funding acquisition. **R. Sarc:** Resources, Writing - review & editing, Supervision, Funding acquisition.

Declaration of Competing Interest

The authors declare that they have no known competing financial interests or personal relationships that could have appeared to influence the work reported in this paper.

Supplementary data

Supplementary data to this article can be found online at https://doi.org/10.1016/j.fuel.2021.120414.

References

[1] Sarc R, Seidler IM, Kandlbauer L, Lorber KE, Pomberger R. Design, quality and quality assurance of solid recovered fuels for the substitution of fossil feedstock in the cement industry – update 2019. Waste Manage Res 2019;37(9):885–97. https://doi.org/10.1177/0734242X19862600.

[2] SarcHerstellung R. Qualität und Qualitätssicherung von Ersatzbrennstoffen zur Erreichung der 100%-igen thermischen Substitution in der Zementindustrie [Doctoral thesis Montanuniversitaet Leoben]; 2015.

[3] Austrian Standards Institute. ÖNORM EN 15359 Solid recovered fuels - Specifications and classes. Issued on 15/12/2011. Vienna; 2011.

[4] Viczek SA, Aldrian A, Pomberger R, Sarc R. Origins and carriers of Sb, As, Cd, Cl, Cr Co, Pb, Hg, and Ni in mixed solid waste – a literature-based evaluation. Waste Manage 2020;103:87–112. https://doi.org/10.1016/j.wasman.2019.12.009.

[5] European Commission. Directive 2010/75/EU of the European Parliament and of the Council of 24 November 2010 on industrial emissions (integrated pollution prevention and control); 2010.

[6] United States Environmental Protection Agency. Initial List of Hazardous Air Pollutants with Modifications; 2019; Available from: https://www.epa.gov/haps/initial-list-hazardous-air-pollutants-modifications [October 04, 2019].

[7] Flamme S, Gallenkemper B. Inhaltsstoffe von Sekundärbrennstoffen, Ableitung der Qualitätssicherung der Bundesgütegemeinschaft Sekundärbrennstoffe e. V. Muell und Abfall 2001;2:699–704.

[8] Swiss Federal Council. Verordnung über die Vermeidung und die Entsorgung von Abfällen; 2015.

[9] Bundesministerium für Land- und Forstwirtschaft, Umwelt und Wasserwirtschaft. Verordnung über die Verbrennung von Abfällen (Abfallverbrennungsverordnung – AVV). BGBl. II Nr. 476/2010, Wien; 2010.

[10] Sarc R, Lorber KE, Pomberger R, Rogetzer M, Sipple EM. Design, quality, and quality assurance of solid recovered fuels for the substitution of fossil feedstock in the cement industry. Waste Manage Res 2014;32(7):565–85. https://doi.org/10.1177/0734242X14536462.

[11] European Commission. Commission Regulation (EU) No 494/2011 of 20 May 2011 amending Regulation (EC) No 1907/2006 of the European Parliament and of the Council on the Registration, Evaluation, Authorisation and Restriction of Chemicals (REACH) as regards Annex XVII (Cadmium); 2011.

[12] Götze R, Boldrin A, Scheutz C, Astrup TF. Physico-chemical characterisation of material fractions in household waste: overview of data in literature. Waste Manage 2016;49:3–14. https://doi.org/10.1016/j.wasman.2016.01.008.

[13] Nasrullah M, Vainikka P, Hannula J, Hurme M, Oinas P. Elemental balance of SRF production process: Solid recovered fuel produced from municipal solid waste. Waste Manage Res 2016;34(1):38–46. https://doi.org/10.1177/0734242X15615697.

[14] Nasrullah M, Vainikka P, Hannula J, Hurme M. Elemental balance of SRF production process: solid recovered fuel produced from commercial and industrial waste. Fuel 2015;145:1–11. https://doi.org/10.1016/j.fuel.2014.12.071.

[15] Nasrullah M, Vainikka P, Hannula J, Hurme M, Koskinen J. Elemental balance of SRF production process: Solid recovered fuel produced from construction and demolition waste. Fuel 2015;159:280–8. https://doi.org/10.1016/j.fuel.2015.06.082.

[16] Curtis A, Adam J, Pomberger R, Sarc R. Grain size-related characterization of various non-hazardous municipal and commercial waste for solid recovered fuel (SRF) production. Detritus 2019;volume 07 – September 2019(0):1. https://doi.org/10.31025/2611-4135/2019.13847.

[17] Viczek SA, Khodier K, Kandlbauer L, Aldrian A, Redhammer G, Tippelt G et al. The particle size-dependent distribution of chemical elements in mixed commercial waste and implications for enhancing SRF quality. Sci Total Environ in press: 145343. https://doi.org/10.1016/j.scitotenv.2021.145343.

[18] Pieber S, Ragossnig A, Pomberger R, Curtis A. Biogenic carbon-enriched and pollutant depleted SRF from commercial and pretreated heterogeneous waste generated by NIR sensor-based sorting. Waste Manage Res 2012;30(4):381–91. https://doi.org/10.1177/0734242X12437567.

[19] Turner A. Black plastics: Linear and circular economies, hazardous additives and marine pollution. Environ Int 2018;117:308–18. https://doi.org/10.1016/j.envint.2018.04.036.

[20] Waste and Resources Action Programme. Commercial scale mixed plastics recycling: Final Report; 2009.

[21] Pfaff G. Inorganic Pigments. de Gruyter; 2017.

[22] Domininghaus H, Eyerer P, Elsner P, Hirth T. Kunststoffe: Eigenschaften und Anwendungen. Berlin Heidelberg: Springer; 2007.

[23] Küppers B, Hernández Parrodi JC, Garcia Lopez C, Pomberger R, Vollprecht D. Potential of sensor-based sorting in enhanced landfill mining. Detritus 2019; Volume 08 – December 2019(0):1. https://doi.org/10.31025/2611-4135/2019.13875.

[24] Rozenstein O, Puckrin E, Adamowski J. Development of a new approach based on midwave infrared spectroscopy for post-consumer black plastic waste sorting in the recycling industry. Waste Manage 2017;68:38–44. https://doi.org/10.1016/j.wasman.2017.07.023.

[25] Vrancken C, Longhurst PJ, Wagland ST. Critical review of real-time methods for solid waste characterisation: informing material recovery and fuel production. Waste Manage 2017;61:40–57. https://doi.org/10.1016/j.wasman.2017.01.019.

[26] Khodier K, Viczek SA, Curtis A, Aldrian A, O'Leary P, Lehner M, et al. Sampling and analysis of coarsely shredded mixed commercial waste. Part I: procedure, particle size and sorting analysis. Int J Environ Sci Technol 2020;17(2):959–72. https://doi.org/10.1007/s13762-019-02526-w.

[27] Küppers B, Seidler I, Koinig GR, Pomberger R, Vollprecht D. Influence of throughput rate and input composition on sensor-based sorting efficiency. Detritus 2020;9:59–67. https://doi.org/10.31025/2611-4135/2020.13906.

[28] Lorber KE, Sarc R, Aldrian A. Design and quality assurance for solid recovered fuel. Waste Manag Res 2012;30(4):370–80. https://doi.org/10.1177/0734242X12440484.

[29] Austrian Standards Institute. ÖNORM EN 14346 Characterization of waste - Calculation of dry matter by determination of dry residue or water content. Issued on 01/03/2007. Vienna; 2007.

[30] Viczek SA, Kandlbauer L, Khodier K, Aldrian A, Sarc R. Sampling and analysis of coarsely shredded mixed commercial waste. Part II: particle size-dependent element determination; in submission.

[31] Austrian Standards Institute. ÖNORM EN 15411 Solid recovered fuels – Methods for the determination of the content of trace elements (As, Ba, Be, Cd, Co, Cr, Cu, Hg, Mo, Mn, Ni, Pb, Sb, Se, Tl, V and Zn). Issued on 15/10/2011. Vienna; 2011.

[32] Austrian Standards Institute. ÖNORM EN ISO 17294-2 Water quality – Application of inductively coupled plasma mass spectrometry (ICP-MS) – Part 2: Determination of selected elements including uranium isotopes. Vienna; 2017.

[33] Austrian Standards Institute. ÖNORM EN 13656 Characterization of waste – Microwave assisted digestion with hydrofluoric (HF), nitric (HNO3) and hydrochloric (HCl) acid mixture for subsequent determination of elements. Issued on 01/12/2002. Vienna; 2002.

[34] Deutsches Institut für Normung. DIN EN ISO 10304-1 Water quality – Determination of dissolved anions by liquid chromatography of ions – Part 1: Determination of bromide, chloride, fluoride, nitrate, nitrite, phosphate and sulfate. Berlin; 2009.

[35] Austrian Standards Institute. ÖNORM EN 14582 Characterization of waste – Halogen and sulfur content – Oxygen combustion in closed systems and determination methods. Vienna; 2016.

[36] Deutsches Institut für Normung. DIN 51900-1 Testing of solid and liquid fuels – Determination of gross calorific value by the bomb calorimeter and calculation of net calorific value – Part 1: Principles, apparatus, methods. Berlin; 2000.
[37] Möllnitz S, Khodier K, Pomberger R, Sarc R. Grain size dependent distribution of different plastic types in coarse shredded mixed commercial and municipal waste. Waste Manage 2020;103:388–98. https://doi.org/10.1016/j.wasman.2019.12.037.
[38] Franklin Associates L. Characterization of products containing lead and cadmium in municipal solid waste in the United States, 1970–2000; 1989.
[39] Ranta-Korpi M, Vainikka P, Konttinen J, Saarimaa A, Rodriguez M. Ash forming elements in plastics and rubbers. The VTT publication series 2014;186.
[40] Belarra MA, Belategui I, Lavilla I, Anzano JM, Castillo JR. Screening of antimony in PVC by solid sampling-graphite furnace atomic absorption spectrometry. Talanta 1998;46(6):1265–72. https://doi.org/10.1016/S0039-9140(97)00390-1.
[41] Velis C, Wagland S, Longhurst P, Robson B, Sinfield K, Wise S, et al. Solid recovered fuel: influence of waste stream composition and processing on chlorine content and fuel quality. Environ Sci Technol 2012;46(3):1923–31. https://doi.org/10.1021/es2035653.
[42] Gerassimidou S, Velis CA, Williams PT, Castaldi MJ, Black L, Komilis D. Chlorine in waste-derived solid recovered fuel (SRF), co-combusted in cement kilns: a systematic review of sources, reactions, fate and implications. Crit Rev Environ Sci Technol 2020:1–47. https://doi.org/10.1080/10643389.2020.1717298.
[43] Hoffmann G, Schirmer M, Bilitewski B. Chlorstudie - Untersuchungen zu Hauptchlorträgern in verschiedenen Abfallströmen, Technische Universitaet Dresden; 2006.
[44] Viczek SA, Aldrian A, Pomberger R, Sarc R. Determination of the material-recyclable share of SRF during co-processing in the cement industry. Resour Conserv Recycl 2020;156:104696. https://doi.org/10.1016/j.resconrec.2020.104696.
[45] Aldrian A, Viczek SA, Pomberger R, Sarc R. Methods for identifying the material-recyclable share of SRF during co-processing in the cement industry. Methods X 2020;7:100837. https://doi.org/10.1016/j.mex.2020.100837.
[46] Assembleia da República Portugal. Regime geral da gestão de resíduos. Decreto-Lei n.° 178/2006 - Diário da República n.° 171/2006, Série I de 2006-09-05; 2006.
[47] Assembleia da República Portugal. Lei n.° 82-D/2014 Diário da República n.° 252/2014, 2° Suplemento, Série I de 2014-12-31; 2014.

3.7 Publication VII

Methods for identifying the material-recyclable share of SRF during co-processing in the cement industry

A. Aldrian, **S.A. Viczek**, R. Pomberger, R. Sarc

MethodsX 7 (2020), 100837,
https://doi.org/10.1016/j.mex.2020.100837

Author Contributions (CRediT Contributor Roles Taxonomy):

AA: Conceptualization, Methodology, Validation, Formal Analysis, Investigation, Data curation, Writing – original draft preparation, Visualization;

SV: Conceptualization, Methodology, Writing – review and editing, Visualization;

RP: Resources, Funding acquisition;

RS: Conceptualization, Methodology, Investigation, Data curation, Writing – review and editing, Project administration, Funding acquisition.

Graphical abstract:

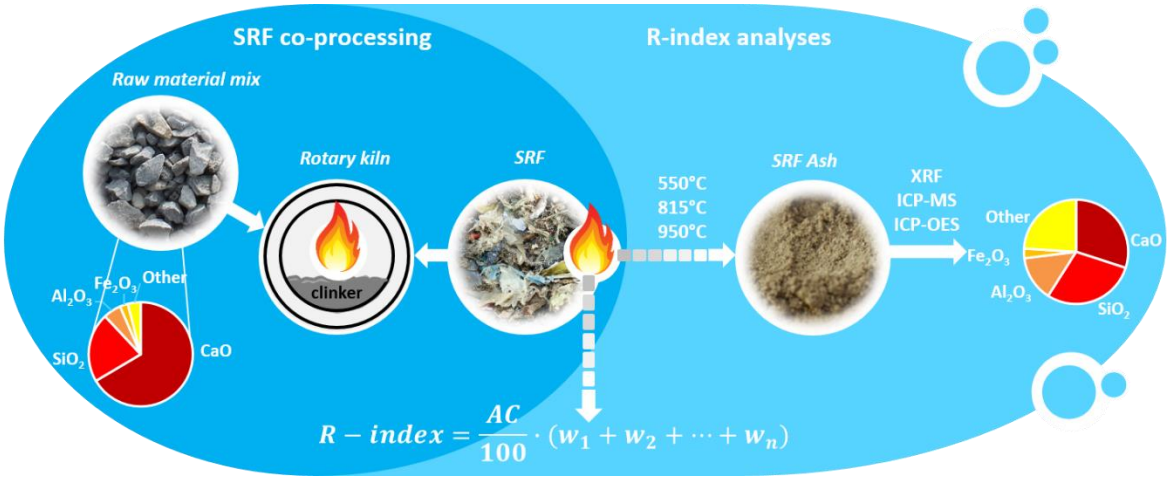

MethodsX 7 (2020) 100837

Contents lists available at ScienceDirect

MethodsX

journal homepage: www.elsevier.com/locate/mex

Method Article

Methods for identifying the material-recyclable share of SRF during co-processing in the cement industry

Alexia Aldrian, Sandra A. Viczek, Roland Pomberger, Renato Sarc*

Chair of Waste Processing Technology and Waste Management, Montanuniversitaet Leoben, Franz-Josef-Strasse 18, 8700 Leoben, Austria

A B S T R A C T

Solid Recovered Fuels (SRF) include non-combustible mineral components (e.g. $CaCO_3$, SiO_2, Al_2O_3) that are required as raw materials for producing clinker and are completely incorporated into the clinker during the thermal recovery of SRF. This paper discusses simple and practicable ways of finding the relative amount of SRF that may be utilised as raw material (given as the recycling index). For this purpose, the entire mineral content of SRF was determined as the ash content and its main components were identified using different analytical methods.

- A fusion melt of the previously incinerated sample with subsequent measuring using ICP-OES and XRF as well as a total digestion of the incinerated and non-incinerated sample with subsequent measuring using ICP-OES/ICP-MS were applied.
- The results showed a good agreement of all four analytical methods for the elementary oxides Al_2O_3, CaO, Fe_2O_3, SiO_2, TiO_2, P_2O_5 and MgO (relative deviation from 6.6 to 38.9%) and slightly higher deviations for K_2O, Na_2O and SO_3 (14.2–96.0%).
- It was also shown that different incineration temperatures (550 °C, 815 °C and 950 °C) have no effect on the result of the recycling index unless it is assumed that the recycling index equals the ash content.

A R T I C L E I N F O

Method name: R-Index

Keywords: Solid recovered fuel, Recycling, Ash content, Mineral matter, Main components, Methods, Cement industry

Article history: Received 12 January 2020; Accepted 17 February 2020; Available online 21 February 2020

DOI of original article: 10.1016/j.resconrec.2020.104696

* Corresponding author.

E-mail addresses: alexia.aldrian@unileoben.ac.at (A. Aldrian), sandra.viczek@unileoben.ac.at (S.A. Viczek), roland.pomberger@unileoben.ac.at (R. Pomberger), renato.sarc@unileoben.ac.at (R. Sarc).

https://doi.org/10.1016/j.mex.2020.100837

Specification Table

Subject Area:	Chemistry
More specific subject area:	*Environmental analytical chemistry*
Method name:	*R-Index*
Name and reference of original method:	–
Resource availability:	–

Introduction

Basic raw material components for making cement clinker in a cement plant include calcium oxide (CaO), silicon dioxide (SiO_2) and small amounts of aluminium oxide (Al_2O_3) and iron oxide (Fe_2O_3). Available raw materials include limestone, chalk, clay or limestone marl as well as quartz and feldspar, iron hydroxides or iron sulphides. Depending on the raw material deposits at the sites of cement plants, appropriate corrective substances may be required for ideal raw-material mixtures to compensate for missing ingredients. [1]

Cement plants use not only natural raw materials but also secondary raw materials or substitute raw materials. Just like natural raw materials, they contain the main ingredients required for producing cement clinker. There are many arguments for using secondary raw materials: first, natural resources and costs are saved. Moreover, waste that would otherwise have to be landfilled can be persuasively recycled, given that secondary raw materials must not contain any hazardous components that would impair the emissions of the cement plant or the composition of the clinker. [2,3]

Raw and secondary raw materials can be divided into the following groups by composition [3–5]:

- Ca Group: limestone, marl, chalk, lime sludge from drinking water and sewage treatment, aerated concrete granules, calcium chloride, calcium fluoride, industrial lime waste, carbide sludge, hydrated lime;
- Si Group: sand, foundry sands, silica and quartz waste, sand trap residues, chrome sand, microsilica;
- Fe Group: iron ore, roasted pyrite, contaminated ore, iron oxide/fly ash blends, mill scale, dusts from steel plants, red sludge, converter slag, tin slag;
- Al Group: residues from reprocessing salt slag, aluminium hydroxide, catalyst dust;
- Si-Al Group: clay, bentonites, kaolinites, coal processing residues;
- Si-Al-Ca Group: fly ash, granulated blast furnace slag, oil shale, trass, slag, crushed sand, bleaching earth, aluminium oxide sludge, paper residues, oil contaminated soils, natural stone processing residues.
- S Group: natural gypsum, natural anhydrite, gypsum from flue gas desulfurization;

Using SRF in the cement industry

Cement clinker production requires a high amount of thermal energy, mainly used for burning. The rather high energy consumption of cement clinker production is fulfilled by traditional fuels such as hard coal, lignite, petroleum coke and, to a lesser extent, petrol oil. Alternative fuels such as Refuse-Derived Fuels (RDF) are also applied. [1] These RDF include hazardous as well as non-hazardous waste like sewage sludge, waste wood, processed fractions of production, household and commercial waste, plastic waste, light shredder fractions, used tires, waste oil and used solvents. Solid Recovered Fuel (SRF) is a subgroup of RDF composed of non-hazardous sorted and mixed solid waste [6–9]. Two different types of SRF suitable for the use in the cement industry are basically present on the market, classified by their area of application [10,11]:

- SRF for secondary firing (SRF “secondary”): Lower heating value 12–18 MJ/kgOS (corresponding to class NCV 3 or 4 in EN 15,359), grain size $<$80 mm (used at calciner or kiln inlet) or $<$300 mm (used for hot disc combustion chamber), respectively.
- SRF for primary firing (SRF “primary”): Lower heating value 18–25 MJ/kgOS (corresponding to class NCV 1, 2, or 3 in EN 15,359), grain size $<$35 mm (used in primary firing of the rotary kiln of cement plants (main burner fuel)).

Table 1
Ash content of SRF from different sources (selection) (Abbreviations used: n/s.: not specified; MSW: Municipal solid waste; CW: Commercial waste; IW: Industrial waste; C&DW: Construction and demolition waste).

References	Ash content [wt%]	Incineration temperature	SRF origin
Bourtsalas et al. [13]	10.2–13.8	n/s	MSW
Gallardo et al. [14]	10.7	n/s	MSW
Hilber et al. [15]	7.9	n/s	Mixed waste of MSW and CW
Kara [16]	7.7	n/s	MSW
Kuna [17]	11.1–22.4 Mean: 16.3 ($n = 3$)	815 °C	MSW
Montané et al. [18]	18.2	550 °C	MSW
Nasrullah et al. [19]	12.5	550 °C	CW and IW
Nasrullah et al. [20]	9.0	550 °C	C&DW
Sarc et al. [8]	10.0–19.0 Mean: 14.3 ($n = 5$)	815 °C	SRF "primary"; Mixed waste of MSW and CW
Sarc et al. [8]	13.4 – 26.0 Mean: 17.8 ($n = 7$)	815 °C	SRF "secondary"; Mixed waste of MSW and CW
Sarc et al. [9]	6.3–23.4 Mean: 15.8 ($n = 13$)	815 °C	SRF "primary"; Mixed waste of MSW and CW
Sarc et al. [9]	12.3–30.6 Mean: 20.1 ($n = 12$)	815 °C	SRF "secondary"; Mixed waste of MSW and CW
Velis et al. [21]	17.3	550 °C	MSW
Wagland et al. [22]	11.1 (synthetic SRF) 16.2 (RDF)	n/s	Synthetic SRF: Paper, Pastic, Textile and Wood; RDF: MSW
Wu et al. [23]	12.9	n/s	n/s
Wu et al. [24]	5.7	n/s	n/s

The use of waste as substitute raw material or SRF in the cement industry is subject to specific European-based quality requirements defined in the BAT conclusions for the production of cement, lime and magnesium oxide of the European Union [12]. This includes ensuring constant quality as well as defined physical and chemical criteria (e. g. combustibility, reactivity, calorific value, chlorine content, sulphur content). Further aspects of the BAT conclusions concern the application of a quality assurance system for each waste load and control of the amount of relevant parameters such as relevant metals (e. g. cadmium, mercury).

Composition of SRF

SRF "primary" and SRF "secondary" consist primarily of plastics and of biogenic components. The main fractions are plastic (9.3–42.3 wt%), paper/cardboard/biogenic waste (5.3–25.6 wt%) and textiles (2.1–18.9 wt%). There is also a non-sortable fine fraction (<11.2 mm) (15.4–71.7 wt%) [8,9]. In addition to the combustible fraction, SRF also contain a non-combustible inorganic fraction. This is classified and indicated as ash content. Table 1 presents a selection of the ash contents of SRF samples of different origins given in references. Their range extends from 5.7 wt% to 30.6 wt%.

A typical composition of raw meal for the production of Portland cement is 77.36 wt% of $CaCO_3$, 13.73 wt% of SiO_2, 2.93 wt% of Al_2O_3, 1.84 wt% of Fe_2O_3, 1.83 wt% of MgO, 1.08 wt% of SO_3, 0.85 wt% of K_2O, 0.14 wt% of Na_2O, 0.02 wt% of P_2O_5, 0.15 wt% of TiO_2, 0.06 wt% of Cl and 0.01 wt% of ZnO [25]. All these ingredients are present in the ash residue of SRF. The non-flammable part of SRF is completely integrated into the clinker, i. e. individual components are used for clinker phase formation [1,26]

The chemical composition of the ash is a function of the quality of the SRF, i. e. of its input materials. It is also related to the combustion process and associated conditions (e. g. temperature, availability of oxygen, grain size of SRF used) [27]. Table 2 shows the compositions of SRF ash found in references. The list includes results analysed directly in the ash residues of the SRF.

While the mineralogical composition of coal and coal fly ash is quite well describable due to their natural origin [28–31], the mineral phases of SRF are much more complex and difficult to classify. This is explained by the fact that the main ingredients of SRF ash do not originate from natural

Table 2
Overview of the ash compositions of various SRF (abbreviations used: n/s.: not applicable; MSW: Municipal solid waste; CW: Commercial waste); Values in brackets were calculated from the total sulphur content in the original publication.

Elemental oxide [wt%]	Dunnu et al. [32]	Dunnu et al. [32]	Hilber et al. [15]	Kuna [17]	Pohl et al. [33]	Wagland et al. [22]	Wagland et al. [22]
Al_2O_3	11.18	16.18	13.68	12.0–17.3	10.47	4.3	9.5
CaO	25.41	21.80	25.77	20.4–24.5	40.13	60.4	18.5
Fe_2O_3	2.88	3.94	3.33	7.0–14.4	4.83	4.5	2.7
K_2O	2.34	2.82	2.02	1.1–1.8	0.78	0.1	1.9
MgO	3.68	2.59	2.43	2.3–2.8	3.23	1.2	2.0
Na_2O	4.18	4.80	5.27	2.4–3.8	2.20	0.3	3.3
P_2O_5	1.18	1.70	1.26	1.0–1.9	0.51	0.8	1.5
SO_3	4.50	2.50	1.34	3.6–11.9	(3.42)	(0.17)	(0.81)
SiO_2	38.12	36.07	26.52	33.4–35.7	23.87	7.5	48.1
TiO_2	2.33	1.31	2.28	1.6–2.4	2.68	8.1	1.8
SRF origin	MSW	Paper/plastic	MSW/CW	n/s	CW	Synthetic SRF: paper, plastic, textiles, wood	MSW
Determination method	XRF	XRF	n/s	ICP-OES	n/s	ICP-OES	ICP-OES

but rather from synthetic products, so that the theoretical range of present mineral phases may be accordingly broad [32]. There is evidence for not only the chemical composition, i.e. the content of Al_2O_3, Fe_2O_3, CaO, MgO and P_2O_5 or the ratio of SiO_2-Al_2O_3 significantly affecting the ash flow temperature but that the mineralogical composition has an impact, too [32]. For example, the melting (temperature difference between shrinkage temperature and flow temperature) of SRF ash occurs over a significantly shorter temperature range ('short slag') than in the case of hard coal ('long slag'). Nevertheless, the ash melting behaviour of SRF shows that SRF ash melts completely during clinker production in the rotary kiln, with flow temperatures in oxidising atmosphere given in sources as 1210 °C [32], 1210–1250 °C [17] and 1300 °C [33], respectively. From a technical point of view, this indicates that complete incorporation of ash into clinker leads to a certain amount of SRF not being thermally recovered but recycled.

Proposed analytical method for determining the recyclable fraction in SRF

The incombustible fraction of SRF is usually determined as the ash content. The SRF ash consists of a number of components (e. g. SiO_2, CaO, Fe_2O_3) contributing to the raw material content in clinker production. Individual components must be identified analytically. This recyclable fraction of SRF, given as the recycling index (or R-Index), is thus computed according to Formula 1 with w_1, w_2, ..., w_n being those mass fractions of elementary oxides that can be attributed to recycling. The R-Index refers to the dried sample (DM: dry mass).

$$R - Index = \frac{AC}{100} \cdot (w_1 + w_2 + \ldots + w_n) \quad (1)$$

With

R-Index Recycling-Index (recyclable fraction in SRF; the reference value is the dried sample) [$\%_{DM}$]
AC Ash content [$wt\%_{DM}$]
$w_{1, 2, \ldots, n}$ Mass fractions of elementary oxides that can be attributed to recycling [$wt\%_{DM}$]

Researched data based on literature references do not permit adequate estimations of the relative amount in SRF that would be attributable to recycling. First, Tables 1 and 2 clearly show that only few data from the references are available for both the ash content and the composition of SRF ashes. Second, quality and reliability of data are insufficient for all parameters due to the large differences between values given in the literature. Furthermore, different incineration temperatures used in determining the ash content (550 °C and 815 °C) and different methods (XRF, ICP-OES) for analysing the ash have been used in the references examined (cf. Tables 1 and 2), preventing direct compatibility of data.

As a first step, the methods for obtaining the fraction attributable to recycling have to be established to define standardised procedures. The objectives of this paper are therefore as follows:

- Investigating suitable methods for establishing the ash content and composition of SRF and comparing them.
- Developing a meaningful, methodical approach for finding the relevant main constituents of ash based on methodical research. Particular attention must be paid to simplicity and easy performance.
- Applying different analysis methods to obtain the ash composition and to compare the results.
- Evaluation of these methods for applicability and suitability.

The final purpose of this paper is to derive a distinct procedure including one or more methods to be used in future for obtaining the ash content and for ash analysis to identify the recyclable fraction of SRF so as to get reliable and representative results.

Materials and methods

Survey of relevant standardised methods for the SRF and fuel sector

There are already a number of standardised methods for the analysis of SRF and solid mineral fuels. They include analysis of ash content as well as of its main constituents and are based on international, European and national standards. They have been summarised and compared in Table 3. It clearly follows that while there are some similarities between the analysis of SRF and that of solid fuels, there are also profound differences. The different combustion temperatures applied to analyse the ash content are particularly apparent (550 °C for SRF vs. 815 °C for solid fuels), as are the various options for measuring the main elements. Methods for analysing the ash content and its main elements listed in Table 3 were drawn on for the series of test experiments carried out while compiling this paper.

Description and preparation of samples

Altogether, 80 real SRF samples were available for the series of experimental tests. Various samples were randomly selected for the test series from these 80 samples.

The SRF samples were provided by various SRF manufacturers and cement plants in four European countries (Austria, Slovenia, Croatia and Slovakia). The samples were taken by staff of the recycling plants or cement plants or by staff of the Chair of Waste Processing Technology and Waste Management, pursuant to the requirements of EN 15442 [43]. The samples all originated from the production years 2018 and 2019. A total of 50 samples of SRF “primary” and 30 samples of SRF “secondary” were available.

Pursuant to EN 14346 [44], original SRF samples were dried in a drying oven at 105 °C till mass constancy - note: comparable content and same requirement, i.e. 105 °C, as defined in ONR CEN/TS 15414-1 too [45] - and then comminuted to <0.5 mm using a fast-rotating cutting mill (Fritsch, Pulverisette 18 with cyclone) pursuant to the specifications of EN 15413 [46]. The samples were then again dried in a drying oven at 105 °C before incineration or melting.

In some cases, stored samples (already prepared to < 0.5 mm and dried) were provided by some companies. These samples were dried in a drying oven at 105 °C before incineration or melting.

Analytical methods for finding the main mineral components

A detailed representation of the individual processing stages is shown in Fig. 1 for all analytical methods used. The major element contents of the mineral substance were analysed for some randomly selected samples (Primary 2, 3, 4, 5, 6 and Secondary 17, 19, 20) for comparisons of all four analytical methods.

The methods applied are standard procedures, some of which having been modified. Incinerated residue was used for methods A, B and D, the dried and prepared sample was used for method C. The sample comminuted < 0.5 mm and dried at 105 °C was incinerated in a muffle furnace (Nabertherm L 9) at a temperature of (950 °C ± 25) °C for a period of 2 h, pursuant to the specifications of EN 196-2

Table 3
Overview on the analytical standard methods for SRF and solid fuels.

Parameters	Solid recovered fuels	Solid fuels
Scope of application	Solid recovered fuels	Solid mineral fuels (e. g. hard coal, coke, lignite, peat, charcoal and briquettes from these materials)
Ash content	**EN 15403** [34] Incineration of the sample at (250 ± 10) °C (60 min) and then at (550 ± 10) °C (120 min) in oxidizing atmosphere until the specified mass constancy is reached. **ISO/CD 21656** (currently under development)	**DIN 51719** [35] Incineration of the sample at (500 ± 10) °C (60 min) and then at (815 ± 10) °C (60 min) in oxidizing atmosphere until the mass remains constant. **ÖNORM G 1074** [36] Incineration of the sample at 500 °C and then at (815 ± 15) °C in oxidizing atmosphere until the mass remains constant. **ISO 1171** [37] Incineration of the sample at 500 °C (60 min) and then at (815 ± 10) °C (60 min) in oxidizing atmosphere until the mass remains constant.
Main components	**EN 15410** [38] Obtaining the mass fractions of the main components according to the following methods: 1) Measurement using e. g. ICP-OES or atomic absorption spectrometry after microwave digestion of the non-incinerated sample with hydrofluoric acid, nitric acid and hydrochloric acid. 2) Measurement using e. g. ICP-OES or atomic absorption spectrometry after digestion of the incinerated sample in a warm water bath with hydrofluoric acid, nitric acid and hydrochloric acid. 3) Measurement using e. g. ICP-OES or atomic absorption spectrometry after digestion of the non-incinerated sample in a furnace with hydrofluoric acid, nitric acid and perchloric acid. 4) Measurement using XRF, with pressed pellets or fused tablets being produced from the samples previously incinerated.	**DIN 51729–10** [39] Obtaining the mass fractions of the main components using XRF after fusion melt (with di-lithium tetraborate, lithium metaborate) of the sample previously incinerated at 950 °C to 1150 °C. **DIN 51729–11** [40] Obtaining the mass fractions of the main components by means of ICP-OES after fusion melt (e. g. with lithium metaborate) of the sample previously incinerated at 1050 °C and dissolution of the fused bead in diluted HCl solution. **DIN 51729–8** [41] Obtaining the sodium and potassium oxide contents by atomic absorption spectrometry or ICP-OES after digestion with hydrofluoric acid and hydrochloric acid of the sample previously incinerated at 1050 °C and dissolution of the fused bead in diluted hydrochloric acid solution. **ISO 13605** [42] Obtaining the mass fractions of the main components using XRF after fusion melt (with di-lithium tetraborate, lithium metaborate) of the sample previously incinerated at 815 °C.

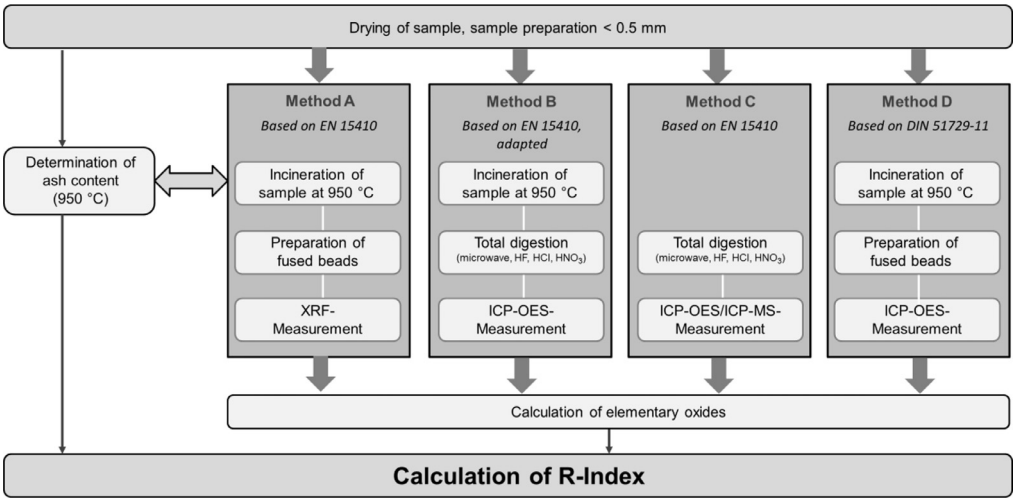

Fig. 1. Overview on the different analytical approaches for the determination of the R-Index.

[47]. EN 196-2 is a commonly used standard in the cement industry for the preparation of samples for XRF analyses.

The relative amounts of the main elements aluminium (Al), calcium (Ca), iron (Fe), potassium (K), magnesium (Mg), sodium (Na), phosphorus (P), sulphur (S), silicon (Si) and titanium (Ti) were obtained for all analytical methods since they were identified as main components in the SRF ashes by X-ray fluorescence analysis (see method A). Analysed samples also included the elements Cr, Mn, Ba, Sr, Cu and Zn in measurable concentrations. The relative amounts of these elements, however, were all very low for the investigated samples (Cr_2O_3 < 0.1 wt%, MnO < 0.2 wt%, BaO < 0.4 wt%, SrO < 0.06 wt%, Cu < 0.5 wt% Zn < 0.4 wt%). The contents of all other elements (e. g. V, Co, Ni, Cu, Zn, Pb) were below 0.05 wt%. For this reason, only the main elements were included in further measurements.

Method A: For measurements using X-ray fluorescence analysis (XRF), fused beads were made out of SRF samples incinerated at 950 °C. In each case, 1 g of sample was thoroughly mixed with 8 g of di-lithium tetraborate ($Li_2B_4O_7$, Sigma Aldrich) and melted in a platinum crucible (HD Elektronik und Elektrotechnik GmbH, Fusion Machine Type VAA2). The fused bead was then measured using XRF (PANalytical, Axios). The software GeoWSU was used for quantitative evaluation. This procedure is pursuant to Section 10.3 of EN 15410 [38]. Examinations were carried out in duplicate.

Method B: Samples incinerated at 950 °C were digested pursuant to EN 13656 (ASI, 2002) and the main elements subsequently measured using ICP-OES. 0.2 g of the incinerated samples were weighed and 6 ml of hydrochloric acid (HCl), 2 ml of nitric acid (HNO_3) and 2 ml of hydrofluoric acid (HF) added before heating the samples in a microwave oven (MLS, Ethos). Next, the HF was complexed with boric acid. The digestion solution was made up to a final volume of 50 ml with deionised water (< 0.055 µmS/cm) and measured using ICP-OES (Varian Vista-MPX CCD Simultaneous, Software: 4.1.0) at the following wavelengths: Al 308.215 nm; Ca 317.933 nm; Fe 238.204 nm; K 766.491 nm; Mg 279.553 nm; Na 589.592 nm; P 213.618 nm; S 180.669 nm; Si 251.611 nm; Ti 334.941 nm. The measured element contents were then converted into the respective oxides (Al_2O_3, CaO, Fe_2O_3, K_2O, MgO, Na_2O, P_2O_5, SO_3, SiO_2 und TiO_2) Examinations were carried out in duplicate. This approach corresponds in large parts to EN 15,410 (Section 9.1) but was slightly adapted.

Method C: This procedure corresponds to Section 9.1 for the identification of the main elements in SRF samples described in EN 15410 [38]. The dried sample, prepared to < 0.5 mm but not incinerated, was decomposed pursuant to EN 13656 [48]. 0.2 g were weighed and 6 ml of hydrochloric acid (HCl), 2 ml of nitric acid (HNO_3) and 2 ml of hydrofluoric acid (HF) were added before heating the

samples in a microwave oven (MLS, Ethos). Next, the HF was complexed with boric acid. The digestion solution was made up to a final volume of 50 ml with deionised water (< 0.055 µmS/cm). The main elements were then measured using ICP-OES and ICP-MS. The elements Al, Ca, K, Mg, Na, P, S, Si and Ti were measured using ICP-OES (Varian Vista-MPX CCD Simultaneous, Software: 4.1.0; see Method B) and the element Fe was measured using ICP-MS (Agilent, 7500ce; due to matrix effects in ICP-OES). The measured element contents were then converted into the respective oxides. Examinations were carried out in duplicate. In method C, oxide contents were obtained that are not related to the ash but to the dry original sample. Results were therefore compared with the relative ash content at 950 °C (cf. Table 6) of the respective sample so that they could be directly compared with the results of other methods.

Method D: The procedure complies with what is described in DIN 51729–11 [40] for identifying the main elements in solid fuels. 0.1 g of the incinerated samples were thoroughly mixed with 1 g of melting reagent (lithium metaborate, Sigma Aldrich) in a platinum crucible and melted in a muffle furnace (Nabertherm L 9) at 1050 °C for 20 min. The resulting fused bead was then cooled and dissolved in doses with a total of 80 ml of hydrochloric acid (c = 2 mol/l) while heating (at approx. 50 - 60 °C) and stirring (PTFE stirring bone). The solution was filled to a final volume of 250 ml with deionised water (< 0.055 µmS/cm). The digestion solutions were measured using ICP-OES (Varian Vista-MPX CCD Simultaneous, software: 4.1.0) at the wavelengths given for Method B. The measured element contents were again converted into the respective oxides. The limit of determination for the analysis procedure was 0.2 wt% for Al_2O_3, CaO, Fe_2O_3, K_2O, MgO, Na_2O, TiO_2 and 0.3 wt% for P_2O_5, SO_3 and SiO_2. All experimental tests were carried out once.

For method D, accuracy and precision of the analytical method applied to SRF were also measured since the standard has actually been developed for solid fuels and not solid recovered fuels. Regarding trueness, proficiency testing materials 1, 2 and 3 of the German supplier DCC (Delta Coal Control) from the years 2016, 2017 and 2018 were measured. To establish repeatability, four randomly selected SRF samples (Primary 21, 24 and 39 as well as Secondary 1) were each measured ten times using the previously described procedure. For the samples, ten separate experiments were carried out including the following steps: incineration, digestion and ICP-OES measurement under repeatable conditions (in each case the same experimenter, the same instruments).

Effects of incineration temperatures on the R-Index

For 22 selected SRF samples (Primary 1, 3, 4, 5, 6, 7, 19, 20, 22, 27, 32, 36, 40, 41, 44 and Secondary 17, 18, 19, 20, 21, 24, 28), effects of incineration temperatures on obtaining the R-Index was examined. These samples (< 0.5 mm and dried) were incinerated in a muffle furnace (Nabertherm L 9) at 950 °C for 2 h (see Section 2.3). They were also incinerated at 550 °C pursuant to EN 15403 (1 h 550 °C ± 10 °C) [34] and at 815 °C according to DIN 51719 (2 h at 500 °C ± 10 °C, then 1 h at 815 °C ± 10 °C) [35] using the muffle furnace. Ash residues obtained at different temperatures were examined for the main components following Method D.

All ash residues were also examined for their carbonate content (as TIC), identified using a Scheibler apparatus according to ÖNORM L 1084 [49]. In each case, diluted hydrochloric acid was added to the incinerated sample to digest the carbonates. The resulting carbon dioxide (CO_2) was measured using gas volumetry, taking air pressure and temperature into account.

Results and discussion

Trueness and precision of method D

The range of application provided in the standard DIN 51729–11 [40] is limited to solid fuels, SRF are not actually covered. Trueness and precision of the standardised procedure applied to SRF were therefore verified. The proficiency testing materials provider DCC (Delta Coal Control) provides interlaboratory comparison participants with various solid fuel samples, including SRF. Parameters analysed in the years 2016, 2017 and 2018 included the identification of the main components pursuant to EN 15410. A comparison of measurement results obtained using method D (incinerated

sample, fused beads, ICP-OES) with those of participants in the interlaboratory comparison (mean values after eliminating outliers, known as assigned values) [50–52] showed very good agreement. Table A1 (cf. Appendices) gives the results measured using method D for the selected elementary oxides for three proficiency testing materials including the calculated z-scores. Z-scores are a common evaluation tool for interlaboratory comparisons and are computed as follows:

$$z - Score = \frac{(Result - Assigned\ value)}{Variance} \quad (2)$$

A z-score of < 2 gives excellent agreement of the participant result with the assigned value. A z-score of 2–3 is satisfactory and a z-score of > 3 is not satisfactory. Results obtained from analysing proficiency testing materials using method D show z-scores < 2 and very good agreement with the assigned values (cf. Table A1).

Table 4 gives the repeatability results for four randomly selected SRF samples (Primary 21, 24 and 39 and Secondary 1) for Method D. The table includes results for all 10 samples of each material obtained under repeatable conditions (same experimenter, same instruments) as well as arithmetic mean, standard deviation and relative standard deviation (RSD).

EN 15410 [38] (Annex B) includes the characteristic process data for all elements except for sulphur. Accurate precision (the coefficient of variation of the precision) of the standard for SRF (made from municipal waste) is also given in Table 4.

The precision specified in EN 15410 [38] for SRF using method D is certainly achieved and in many cases undercut. The only exceptions are potassium and sodium, two samples of which showing slightly higher precision. But the results are only up to 16.6% and can therefore be regarded as satisfactory for a multistage analytical process.

Comparing the results of the four analytical methods applied to obtain the main mineral elements

Selected SRF samples (Primary 2, 3, 4, 5, 6 and Secondary 17, 19, 20) were analysed applying all four analytical methods (Method A, B, C and D). Figs. A1–A3 (cf. Appendices) show the results of the four analytical methods for all elementary oxides compared. Methods A, B and C were each carried out twice, with the duplicates matching perfectly (relative deviations <10%). The only exception is method C whose relative deviations between the duplicate analyses were partly >30%. Each of the results shown in the illustrations indicates the mean value of these duplicates.

The total of all measured and analysed elementary oxides for all four methods resulted in values between 80.5 and 99.2 wt%, with one exception (104.4% for Primary 6, Method C) (cf. Fig. A3). As an average (arithmetic mean), the following results for the total of all measured elements were obtained for the eight analysed samples:

- Method A: 91.9 wt%,
- Method B: 87.5 wt%,
- Method C: 90.1 wt% and
- Method D: 87.9 wt%.

Obviously the results obtained by RFA (Method A) tend to be slightly higher (the total of all measured elements was between 86.5 and 94.7 wt%). Theory suggests that the total of all elementary oxides should be close to 100 wt%, therefore the achieved values may be interpreted as satisfying when applying good laboratory practice. Deviations from 100 wt% may on the one hand be due to inherent measurement inaccuracies of the respective analytical method. On the other hand, note that not all components of the mineral content were identified because measurements were limited to elementary oxides identified as main constituents.

In Table 5, the highest and lowest results (minimum and maximum) of all four methods are shown for each elementary oxide and each sample analysed. Relative deviations (in %) between the highest and lowest results are also shown in this table, ranging from 6.6 to 96.0%. The relative deviations for the elementary oxides Al_2O_3, CaO, Fe_2O_3 and SiO_2 are <40% (6.6 to 38.9%). Basically this indicates a very good agreement between the various analytical methods. Although a relative deviation of about 40% between analytical methods may at first glance appear to be significant, note that each method

Table 4
Precision of the analytical approach for four SRFs (Primary 21, 39; Secondary 1, 24) in comparison with the relative standard deviation given in EN 15410.

Sample Identification	Al_2O_3 [wt%]	CaO [wt%]	Fe_2O_3 [wt%]	K_2O [wt%]	MgO [wt%]	Na_2O [wt%]	P_2O_5 [wt%]	SO_3 [wt%]	SiO_2 [wt%]	TiO_2 [wt%]	SUM [wt%]
RSD [%] ÖNORM EN 15410 [38]	**5/32**	**2/15**	**4/24**	**9/10**	**16/135**	**10**	**4/15**	**–**	**2/16**	**2/23**	**–**
Primary 21/1	43.4	20.6	1.0	0.3	1.0	0.4	0.2	2.6	10.8	2.0	82.4
Primary 21/2	43.7	21.5	1.0	0.3	1.1	0.4	0.3	3.2	10.4	2.1	83.9
Primary 21/3	41.0	26.5	1.1	0.2	1.1	0.4	0.3	3.8	11.1	2.3	87.7
Primary 21/4	41.0	23.4	1.4	0.3	1.1	0.4	0.3	3.7	11.1	2.1	84.7
Primary 21/5	39.0	25.1	1.0	0.2	1.2	0.3	0.3	3.2	10.0	2.3	82.5
Primary 21/6	39.3	22.6	1.1	0.2	1.1	0.4	0.3	3.2	10.0	2.3	80.5
Primary 21/7	42.5	21.5	1.2	0.2	1.1	0.4	0.3	3.0	10.8	2.1	83.1
Primary 21/8	41.6	24.5	1.1	0.2	1.1	0.4	0.2	3.8	11.2	2.1	86.1
Primary 21/9	43.3	21.4	1.2	0.3	1.1	0.5	0.3	3.9	10.5	2.2	84.6
Primary 21/10	41.8	22.9	1.0	0.3	1.1	0.4	0.3	3.6	10.1	2.2	83.8
Mean	**41.6**	**23.0**	**1.1**	**0.3**	**1.1**	**0.4**	**0.3**	**3.4**	**10.6**	**2.2**	**83.9**
Standard deviation	**1.6**	**1.9**	**0.1**	**0.0**	**0.0**	**0.1**	**0.0**	**0.4**	**0.5**	**0.1**	**2.0**
RSD [%]	**3.9**	**8.2**	**11.7**	**16.0**	**3.9**	**14.8**	**8.9**	**12.3**	**4.3**	**4.7**	**2.4**
Primary 39/1	28.0	27.0	2.6	0.8	2.3	1.2	0.8	2.6	27.0	6.4	98.8
Primary 39/2	29.3	28.5	2.1	0.7	1.9	0.9	0.4	2.3	27.2	6.4	99.7
Primary 39/3	32.2	26.9	2.7	0.9	1.7	0.7	0.5	1.9	25.2	6.4	99.1
Primary 39/4	29.1	30.2	3.3	1.0	1.8	0.9	0.5	2.3	24.0	6.8	100.0
Primary 39/5	25.0	29.2	2.5	0.8	1.8	1.0	0.6	2.7	26.0	5.4	95.0
Primary 39/6	29.0	26.1	2.0	0.6	1.8	1.0	0.5	1.7	25.2	5.5	93.3
Primary 39/7	27.1	25.3	3.2	0.7	1.7	0.9	0.5	1.5	24.5	5.6	91.1
Primary 39/8	29.8	27.2	2.2	0.9	1.9	1.1	0.5	2.0	26.2	5.6	97.4
Primary 39/9	30.0	24.7	2.2	1.0	1.7	1.0	0.4	1.7	26.4	6.0	95.2
Primary 39/10	27.5	26.6	2.3	0.8	1.8	1.1	0.5	2.1	25.7	5.6	93.9
Mean	**28.7**	**27.2**	**2.5**	**0.8**	**1.8**	**1.0**	**0.5**	**2.1**	**25.7**	**6.0**	**96.3**
Standard deviation	**1.9**	**1.7**	**0.5**	**0.1**	**0.2**	**0.1**	**0.1**	**0.4**	**1.0**	**0.5**	**3.1**
RSD [%]	**6.8**	**6.3**	**18.1**	**16.6**	**10.2**	**14.2**	**20.0**	**18.5**	**4.0**	**8.2**	**3.2**
Secondary 1/1	6.6	26.6	5.0	2.7	3.1	2.8	1.5	5.6	33.7	4.5	92.2
Secondary 1/2	6.9	26.9	4.9	2.6	3.2	2.5	1.6	5.6	33.2	5.0	92.5
Secondary 1/3	7.0	26.5	4.7	2.5	3.0	2.5	1.6	5.8	33.8	4.3	91.7
Secondary 1/4	6.6	27.2	4.4	2.6	3.0	2.1	1.6	6.6	32.4	4.7	91.0
Secondary 1/5	6.4	25.8	4.4	2.3	3.1	2.7	1.6	5.3	33.2	4.3	89.1
Secondary 1/6	6.6	26.5	4.6	2.6	3.0	2.5	1.5	6.6	33.1	4.4	91.2
Secondary 1/7	7.1	26.7	4.6	2.5	3.2	2.6	1.5	5.0	33.7	3.9	90.7
Secondary 1/8	6.6	27.3	6.4	2.5	3.1	2.2	1.5	5.3	32.0	4.5	91.5
Secondary 1/9	6.4	26.6	4.5	2.9	3.0	2.7	1.5	5.3	32.3	4.5	89.8
Secondary 1/10	6.3	25.7	4.9	2.5	3.0	2.2	1.5	7.1	32.8	4.1	90.1
Mean	**6.6**	**26.6**	**4.8**	**2.6**	**3.1**	**2.5**	**1.5**	**5.8**	**33.0**	**4.4**	**91.0**
Standard deviation	**0.3**	**0.5**	**0.6**	**0.1**	**0.1**	**0.2**	**0.1**	**0.7**	**0.6**	**0.3**	**1.1**
RSD [%]	**3.8**	**2.0**	**12.5**	**5.7**	**2.3**	**9.9**	**4.0**	**11.7**	**1.9**	**6.8**	**1.2**
Secondary 24/1	10.3	26.3	4.6	1.6	3.7	1.5	0.7	4.9	39.6	1.3	94.5
Secondary 24/2	11.5	24.9	4.8	1.8	3.6	1.7	0.6	4.3	39.6	1.1	93.8
Secondary 24/3	8.6	26.4	4.3	1.9	3.8	1.9	0.7	5.1	37.7	1.1	91.6
Secondary 24/4	9.4	23.3	5.2	1.9	3.5	1.9	0.7	4.4	40.9	1.3	92.6
Secondary 24/5	9.6	25.7	4.6	1.7	3.9	1.7	0.7	5.8	34.5	1.3	89.7
Secondary 24/6	9.5	27.9	5.2	1.9	3.9	1.7	0.7	4.7	37.6	1.3	94.4
Secondary 24/7	11.0	21.9	5.2	1.7	3.9	1.5	0.7	5.5	39.8	1.5	92.7
Secondary 24/8	11.1	20.0	4.6	2.3	3.5	2.2	0.6	4.0	43.9	1.2	93.3
Secondary 24/9	9.6	25.9	5.5	1.8	3.0	1.6	0.6	3.3	36.9	1.1	89.3
Secondary 24/10	11.6	21.1	4.5	2.2	3.7	1.8	0.6	5.0	42.0	1.3	93.6
Mean	**10.2**	**24.3**	**4.8**	**1.9**	**3.7**	**1.7**	**0.7**	**4.7**	**39.3**	**1.2**	**92.6**
Standard deviation	**1.0**	**2.6**	**0.4**	**0.2**	**0.3**	**0.2**	**0.1**	**0.7**	**2.7**	**0.1**	**1.8**
RSD [%]	**10.0**	**10.8**	**8.1**	**11.9**	**7.5**	**11.7**	**7.8**	**15.6**	**6.8**	**9.2**	**2.0**

Table 5
Minimum and maximum results as well as the relative deviation for all elemental oxides and analytical methods.

Sample Identification	Description of Result	Al_2O_3 [M.-%]	CaO [M.-%]	Fe_2O_3 [M.-%]	K_2O [M.-%]	MgO [M.-%]	Na_2O [M.-%]	P_2O_5 [M.-%]	SO_3 [M.-%]	SiO_2 [M.-%]	TiO_2 [M.-%]	SUM [M.-%]
Primary 2	Minimum result	7.4	28.1	2.8	1.1	2.7	0.6	0.5	3.9	25.0	3.5	82.7
	Maximum result	8.6	32.9	3.8	3.1	4.3	3.5	1.0	5.6	30.2	4.2	92.5
	Relative deviation between minimum and maximum [%]	14.2	14.7	26.3	64.7	37.3	83.3	51.6	30.2	17.2	17.3	10.7
Primary 3	Minimum result	8.3	22.7	2.1	0.8	2.4	3.3	0.3	1.7	37.5	0.8	84.4
	Maximum result	10.3	25.0	3.3	2.1	3.6	3.8	0.4	4.2	43.7	1.3	92.4
	Relative deviation between minimum and maximum [%]	19.2	9.4	34.7	61.6	33.5	14.2	28.3	58.1	14.0	38.4	8.7
Primary 4	Minimum result	6.3	20.7	2.3	1.1	2.4	1.9	0.3	3.0	42.1	0.7	85.4
	Maximum result	7.6	22.2	3.5	1.8	3.5	3.4	0.6	4.4	48.7	1.0	93.8
	Relative deviation between minimum and maximum [%]	17.0	6.6	33.9	40.2	32.7	43.6	49.9	30.9	13.5	32.8	8.9
Primary 6	Minimum result	9.6	27.7	1.8	2.8	1.8	2.3	1.0	0.5	22.0	1.1	83.8
	Maximum result	11.6	42.4	3.0	5.4	3.1	3.5	2.9	5.6	29.5	1.6	104.4
	Relative deviation between minimum and maximum [%]	17.2	34.7	38.9	48.6	42.5	33.5	65.4	91.1	25.4	32.4	19.7
Primary 7	Minimum result	6.5	28.5	2.4	2.3	1.5	2.8	1.0	1.1	28.3	0.9	80.5
	Maximum result	10.1	33.8	3.8	3.0	3.2	4.5	1.6	5.7	31.9	1.5	92.0
	Relative deviation between minimum and maximum [%]	35.9	15.7	37.6	24.3	53.3	38.3	36.9	80.7	11.3	41.2	12.5
Secondary 17	Minimum result	11.4	28.3	3.3	0.7	2.7	1.1	1.0	0.2	25.6	1.6	86.5
	Maximum result	14.0	36.9	4.3	3.1	3.6	4.9	1.7	4.2	28.4	2.1	94.9
	Relative deviation between minimum and maximum [%]	18.5	23.3	23.2	77.7	25.0	78.4	42.9	95.0	10.0	24.8	8.8
Secondary 19	Minimum result	15.0	18.7	3.0	1.5	2.5	2.4	0.8	0.2	33.2	0.9	84.3
	Maximum result	19.2	28.1	3.9	3.0	3.5	4.7	1.0	4.5	35.9	1.7	99.2
	Relative deviation between minimum and maximum [%]	21.7	33.5	23.8	48.7	29.4	48.8	17.0	96.0	7.6	47.9	15.0
Secondary 20	Minimum result	6.5	20.0	2.8	1.5	2.4	2.5	0.3	2.8	43.6	0.8	90.6
	Maximum result	8.3	22.2	3.9	2.4	3.3	4.5	0.6	4.4	57.7	1.1	97.8
	Relative deviation between minimum and maximum [%]	22.2	9.9	29.5	36.7	27.7	43.6	55.2	37.5	24.5	28.5	7.4

Table 6
Total inorganic carbon content (TIC) and ash content for different ash samples in relation to the incineration temperature.

Sample identification	TIC Ash residue 550 °C [wt%]	TIC Ash residue 815 °C [wt%]	TIC Ash residue 950 °C [wt%]	Ash content 550 °C [wt%]	Ash content 815 °C [wt%]	Ash content 950 °C [wt%]
Primary 1	3.1	0.3	0.1	12.3	11.0	11.5
Primary 3	4.4	0.2	0.2	15.8	12.6	11.6
Primary 4	3.3	0.6	0.4	25.5	23.4	18.3
Primary 5	4.0	0.3	0.4	22.1	19.4	17.3
Primary 6	4.5	0.7	0.6	26.3	19.4	16.7
Primary 7	4.0	0.7	0.5	22.2	18.6	17.6
Primary 19	4.3	0.7	< 0.1	17.5	16.0	16.1
Primary 20	2.7	0.6	0.4	25.3	24.3	23.1
Primary 22	3.9	0.5	0.3	14.9	12.7	12.8
Primary 27	5.5	0.5	0.4	36.0	29.4	29.4
Primary 32	4.1	0.6	0.4	9.7	8.5	8.5
Primary 36	3.8	0.2	0.1	29.1	21.1	21.0
Primary 40	1.7	0.2	< 0.1	9.8	9.0	9.0
Primary 41	2.1	0.7	0.5	9.9	9.0	8.9
Primary 44	4.0	0.5	0.4	27.5	23.4	24.0
Secondary 17	3.1	0.4	0.5	15.2	13.4	13.2
Secondary 18	2.0	0.1	0.1	19.9	16.2	15.8
Secondary 19	4.0	0.6	0.8	18.9	17.0	17.2
Secondary 20	3.3	0.2	0.2	31.7	30.6	30.2
Secondary 21	1.7	0.2	0.1	16.1	12.3	12.8
Secondary 24	1.7	0.3	0.3	32.9	28.9	27.2
Secondary 28	4.1	0.6	0.4	19.2	16.5	15.2

comprises a number of steps, all of which can be flawed. The emerging maximum error estimation is called extended inaccuracy in analytics. For method D, this extended inaccuracy has been assessed compliant with the EURACHEM/CITAC guidelines [53]: 32% Al_2O_3, 34% CaO, 45% Fe_2O_3, 45% K_2O, 32% MgO, 45% Na_2O, 40% P_2O_5, 50% SO_3, 29% SiO_2, 35% TiO_2. When comparing the four analytical methods, note that a certain dispersion may also result from potential inhomogeneity of the samples. Although all analysed samples derived from the same basic population (dried and prepared samples), they were incinerated, digested and measured independently of each other.

A slightly higher relative deviation of 24.8 to 65.4% between the analytical methods was observed for TiO_2, P_2O_5 and MgO. Even higher deviations between the different analytical methods were observed for K_2O, Na_2O and SO_3. Most of the deviations were well above 40%. For the SO_3 content, deviations between the four methods sometimes appear particularly significant. A possible explanation may be uncontrolled loss of sulphur, expressed as SO_2, during sample preparation for fused beads since especially for methods including melting digestions, the results tend to be lower. Note that methods B and D (melting digestion and total digestion from the ash) generally display better agreement than each of them vs. XRF (method A) and method C (total digestion from the dried sample). Method C is generally considered less suitable for identifying main elements than the other analytical procedures described although it is one of the methods proposed in EN 15410 [38]. This is explained by the fact that only about 0.2 g of the dried and prepared (and non-incinerated) sample is used for total digestion. But only approx. 9.8 to 31.7% does actually constitute mineral matter (ash content; cf. Table 6) and is hence relevant for analysis. In other words, the sample fraction of 0.2 g examined and analysed is once more reduced, down to approx. 0.02 to 0.06 g. With such small sample quantities, any inhomogeneity included in the sample may severely impact the analytical result. In case a sample already incinerated is used for digestion, the observed sample has a quantity of at least 0.2 g, reducing potential impacts of inhomogeneity. This clearly emerged from evaluating the duplicate runs of each analytical method. For method C, the relative deviations between the duplicates were sometimes > 30%, for all other methods, they were < 10%.

Effects of the incineration temperature on the R-index

The incineration temperature required for establishing the R-Index was an essential factor under discussion as the suggested approach was developed. 22 SRF samples (Primary 1, 3, 4, 5, 6, 7, 19, 20, 22, 27, 32, 36, 40, 41, 44 and Secondary 17, 18, 19, 20, 21, 24, 28) were incinerated at different temperatures, revealing distinct differences of the obtained ash content (see Table 6). The ash content obtained at 550 °C is much higher than any obtained at 815 °C or at 950 °C.

The EN 15403 [34] used for SRF stipulates an incineration temperature of 550 °C, however. This value is inappropriate for obtaining ash residue for subsequent digestion due to the following arguments:

- During a classical XRF investigation in cement manufacturing or geology, samples are incinerated before melting digestion, with incineration generally initiated at about 950 °C (cf. EN 196–2 [47]). Experimental procedures for XRF investigations (cf. Section 2.3) have shown that fused beads would repeatedly break or turn cloudy when residues incinerated from ashes at 550 °C were included. This has to be explained by the fact that e. g. carbonates may escape from the sample during melting expressed as CO_2 so that they are not integrated into the structure of the fusion agent. That is why higher incineration temperatures should be applied to the production of ash residues.
- The DIN 51729–11 standard [40], intended for testing ashes from solid fuels, stipulates an incineration temperature of 815 °C in compliance with the DIN 51719 standard [35].
- A further argument supporting incineration temperatures of at least 815 °C and higher for analysing the ash content and to provide ash residue for subsequent main-element analysis is found in the fact that temperatures of about 1450 °C prevail in the rotary kilns of cement plants. So much heat can only be achieved on a laboratory scale with special equipment (kilns) while incineration temperatures of 800 °C to 1000 °C can regularly be achieved using conventional muffle furnaces, mimicking real conditions sufficiently well.
- When ashes are chemically analysed, the discovered elemental mass fractions are commonly converted into oxide mass fractions of the highest oxidation state, adding up to a total value of approx. 100 wt%. If this is not the case, then presumably either other components are present as well or the analytical procedure was incorrect. Consider further that the conversion of element concentrations (e. g. of Al) into oxides (e.g. Al_2O_3) is based on the assumption that all measured elements are indeed present as oxides. But for SRF it can be assumed that some elements (e.g. Ca, Mg, Fe) will be present as carbonates (e.g. calcium carbonate $CaCO_3$, dolomite $CaMg(CO_3)_2$, siderite $FeCO_3$). Thus, $CaCO_3$ or $CaMg(CO_3)_2$ are not yet converted at an incineration temperature of 550 °C since the conversion into CaO does not initiate below approx. 800 °C. This means that only for incineration temperatures >800 °C, calcium etc. may be expected to be present as oxides with a high probability. Only incineration at suitably high temperatures helps making stoichiometric calculations of oxide contents accurate. If calcium would be given as calcium oxide though a part of it was expressed as carbonates, then the results would automatically be too low due to the much higher molar mass. The results of analysing the carbonate content (expressed as total inorganic carbon, TIC) (cf. Table 6) clearly show that residue incinerated at 550 °C still contains between 1.7 and 5.5 wt% of total inorganic carbon.

To compare the results for the 22 randomly selected SRF samples obtained at different incineration temperatures (550 °C, 815 °C and 915 °C), the R-Index was calculated using Formula 1 to directly relate to the respective ash content. At first, the total of all elementary oxides was used to calculate the R-index (cf. Fig. 2; above). Then, only a few selected elementary oxides (Al_2O_3, CaO, Fe_2O_3 and SiO_2) were used to calculate the R-index (Fig. 2; below). For the ash content, the values for different incineration temperatures given in Table 6 were used in calculations.

Fig. 2 and Table A2 (cf. Appendices) clearly reveal that for different incineration temperatures, the differences between calculated R-Indices are negligible. The relative differences between the highest and lowest values of a sample are found between 0.1 and 26.7% (for calculations based on the selected elementary oxides Al_2O_3, CaO, Fe_2O_3 und SiO_2) and between 4.6 and 26.0% (for calculations based on the total of all elementary oxides). This is because some elementary oxides are not yet present in the highest oxidation state when the incineration temperature is only 550 °C (say, Fe_2O_3, Al_2O_3), but

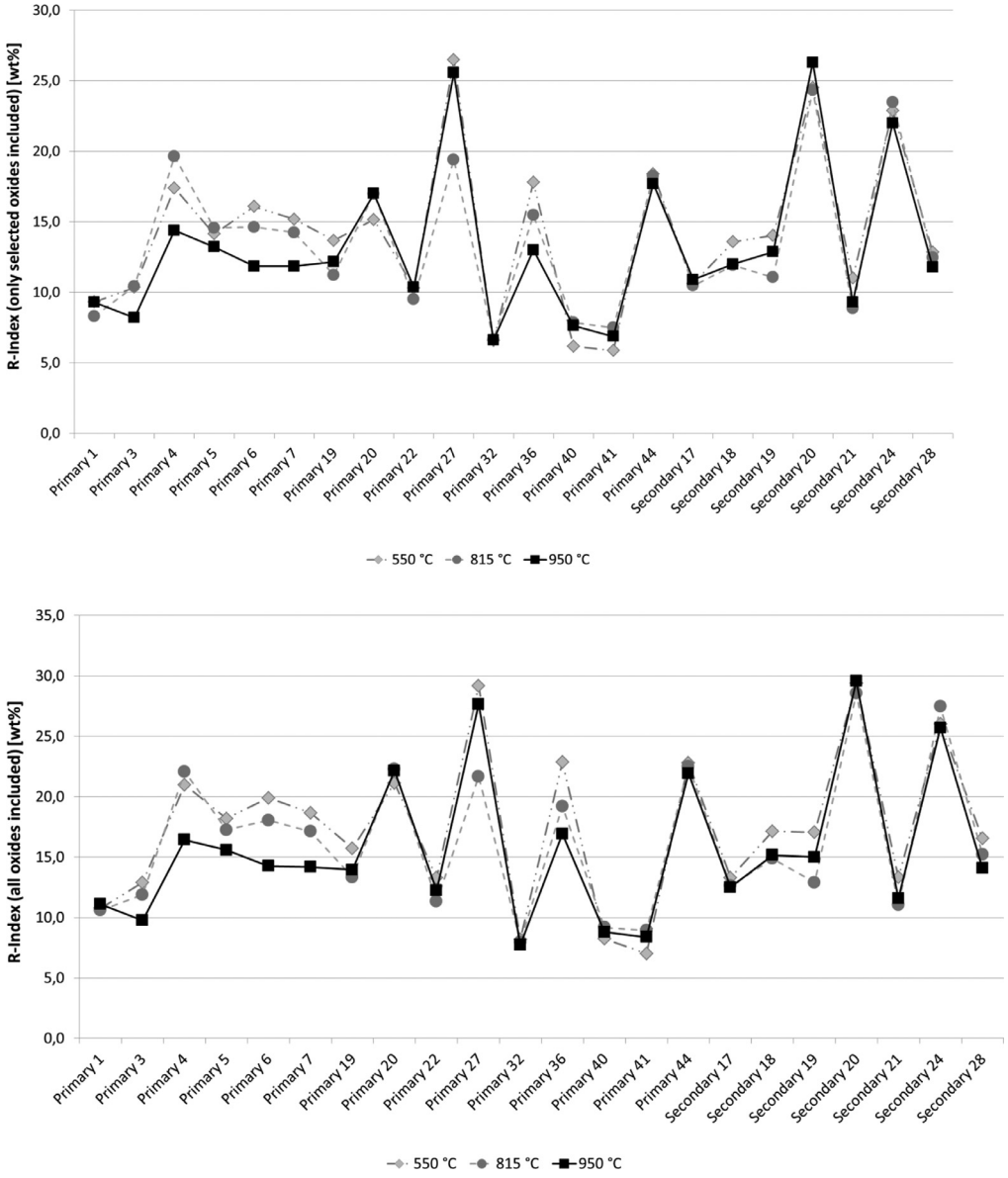

Fig. 2. Comparison of the R-Indices for randomly selected SRF samples at different incineration temperatures; including all measured elementary oxides (above) as well as selected elementary oxides Al_2O_3, CaO, Fe_2O_3, SiO_2 (below).

this is not taken into account when the elementary oxide content is computed. On the other hand, some elements contained in the samples are still present as carbonates after incineration at 550 °C, which as well is not included in the conversion to elementary oxides. Therefore, computations incline to produce too low results for the total of all or for selected elementary oxides obtained at 550 °C vs. those values obtained at 815 °C or 950 °C (cf. Table A2). Multiplying this value with the higher ash content obtained at 550 °C, however, the result almost matches that of the R-Index at 950 °C or 815 °C.

The results in Fig. 2 and Table A2 clearly show that, while much may speak in favour of incineration temperatures higher than 815 °C, the incineration temperature does not have a major effect on the final result for the R-Index for most samples when referring the sum of oxides on the respective ash content obtained by different temperatures.

Conclusions

Methods for finding the relative amount of recyclable SRF (known as the R-Index) have been presented in this paper. For this purpose, the total mineral content of SRF was classified as ash content and its main components were identified using various analytical methods. These methods are all based on available, though sometimes modified, standard methods. It was shown that all methods presented provide almost equivalent results (with the exception of Na_2O, K_2O and SO_3). Neither the type of digestion (melt digestion, total digestion), the measurement method for determining the main mineral components (XRF, ICP-OES/ICP-MS) nor the incineration temperature (550 °C, 815 °C or 950 °C) significantly affect the final result obtained for the R-Index.

Essentially it was shown that using an already incinerated sample (in contrast to the dried and prepared sample) for digestion is recommendable to identifying the main mineral components. This is because any inhomogeneity may severely impact the result due to the low initial weight during digestion, impairing the accuracy of the analytical method. Moreover, the ash content of the proposed procedure for determining the R-Index has to be identified anyway, providing ash residue for subsequent main element analysis as a by-product.

The methods presented in this paper are all easy to implement particularly in laboratories already performing SRF or fuel analysis. The methods do not require special equipment but the necessary steps can be managed using established equipment. While in laboratories for SRF or fuel analysis wet chemistry methods seem to be more convenient, the company laboratory of cement plants generally using XRF instruments for quality assurance of raw materials and products, may as well apply available methods and instruments for obtaining the R-Index.

Based on the experiences gained during the experimental part of this paper, methods D and A can certainly be recommended as the most practical and most suitable approaches for determining the main components in SRF. Both methods deliver reliable results. From a technical perspective it is also recommended to apply incineration temperatures $\geq$ 815 °C for the determination of the ash content or providing the ash residue to be analysed.

Method D was also applied for the experimental investigations on 80 SRF samples currently on the market in Austria, Croatia, Slovakia, and Slovenia in regards to the determination of the material-recyclable share presented in the work of Viczek et al. 2020 [11].

The analytical methods developed and introduced in this paper allow for reliably calculating the R-index. The methods were extensively validated and their applicability in practice was evaluated. The application of these methods ensures that the results obtained on an international, practical, and scientific level are comparable and equivalent. This is the precondition to make generally valid statements about the material-recyclable share of SRF when co-processed in the cement industry. Determining this material-recyclable share is of major importance for the cement industry, waste treatment companies, and governmental institutions.

Acknowledgements

Partial funding for this work was provided by: The Center of Competence for Recycling and Recovery of Waste 4.0 (acronym ReWaste4.0) (contract number 860 884) under the scope of the COMET – Competence Centers for Excellent Technologies – financially supported by BMVIT, BMDW, and the federal state of Styria, managed by the FFG. The research was organized in cooperation with FH Münster University of Applied Sciences, Germany (S. Flamme and S. Hams).

The authors would like to thank the Chair of General and Analytical Chemistry at the Montanuniversitaet Leoben for conducting the comparative measurements with XRF.

Declaration of Competing Interest

The Authors confirm that there are no conflicts of interest.

Appendix

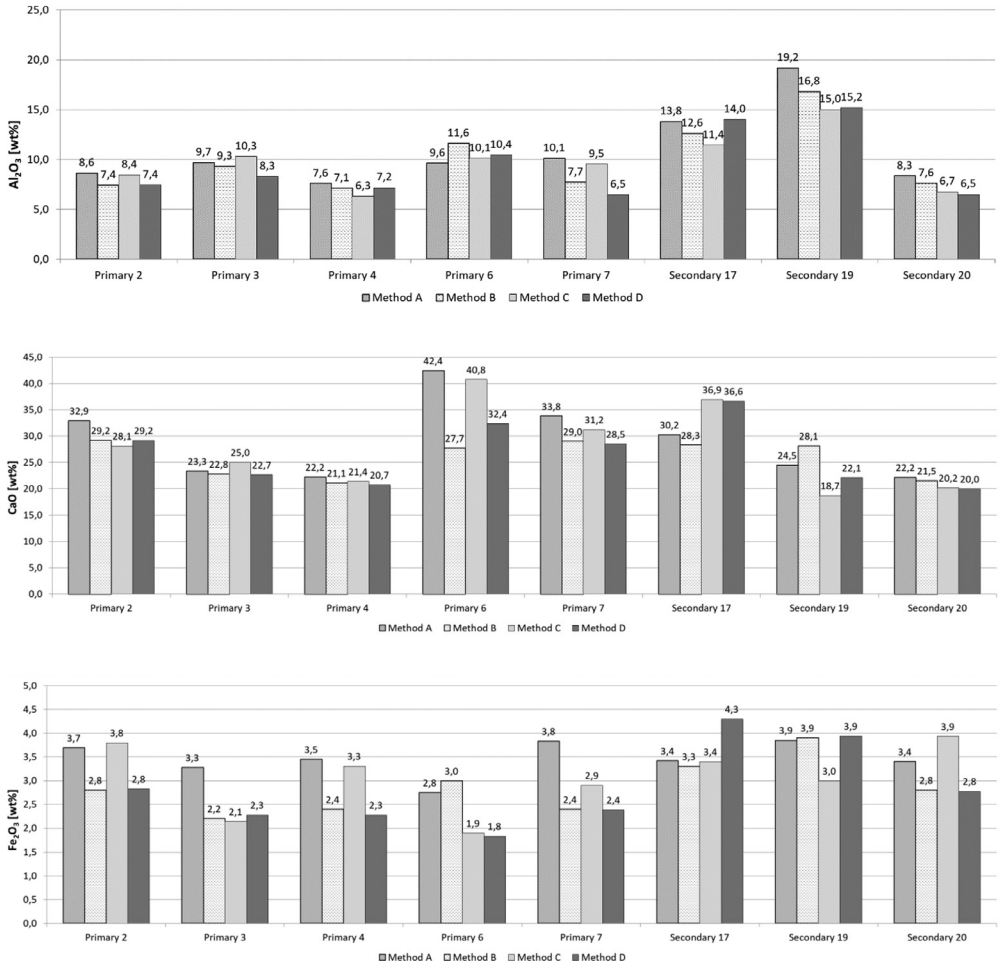

Fig. A1. Results for Al_2O_3, CaO and Fe_2O_3 and for all analytical methods for randomly selected samples.

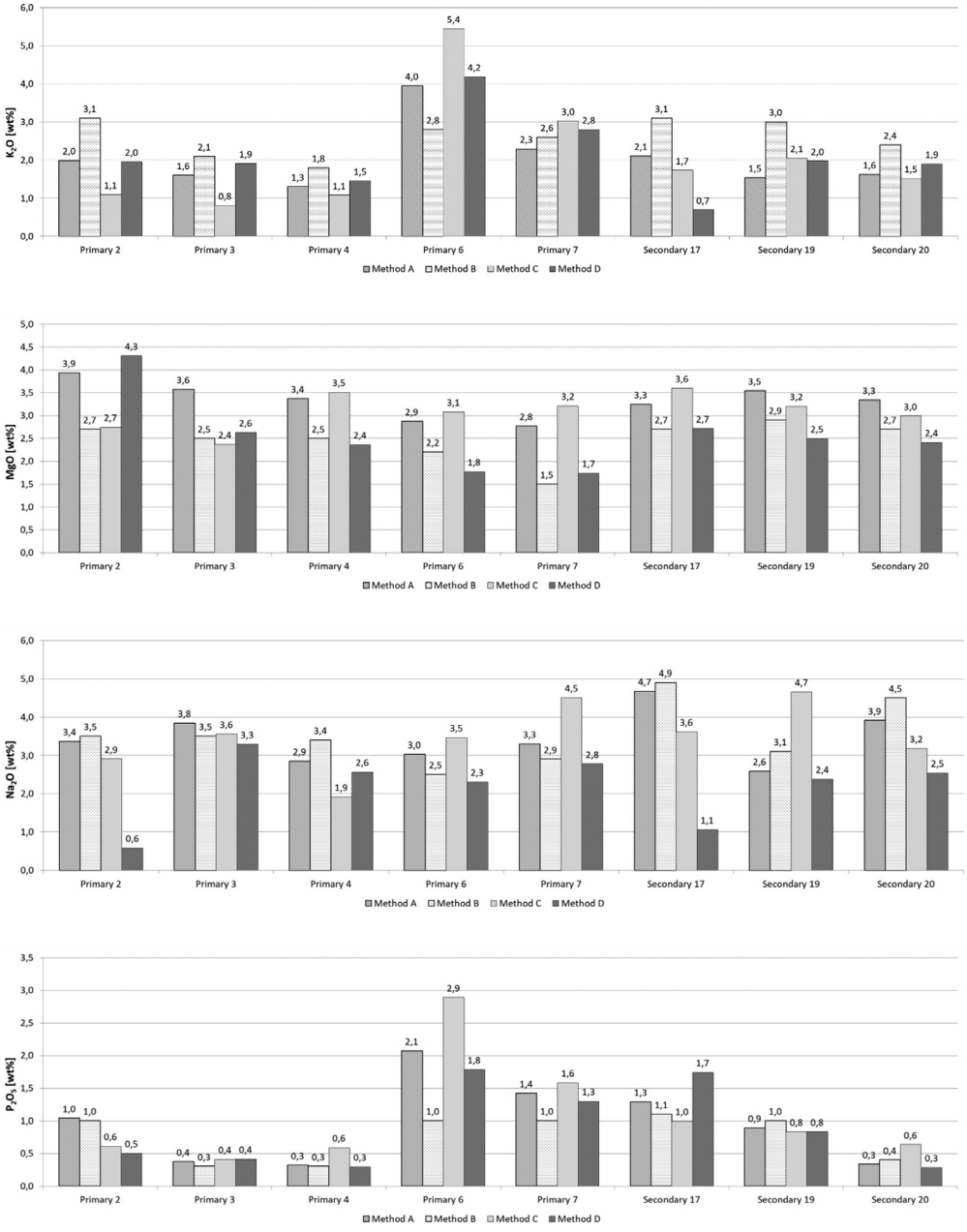

Fig. A2. Results for K_2O MgO, Na_2O and P_2O_5 and for all analytical methods for randomly selected samples.

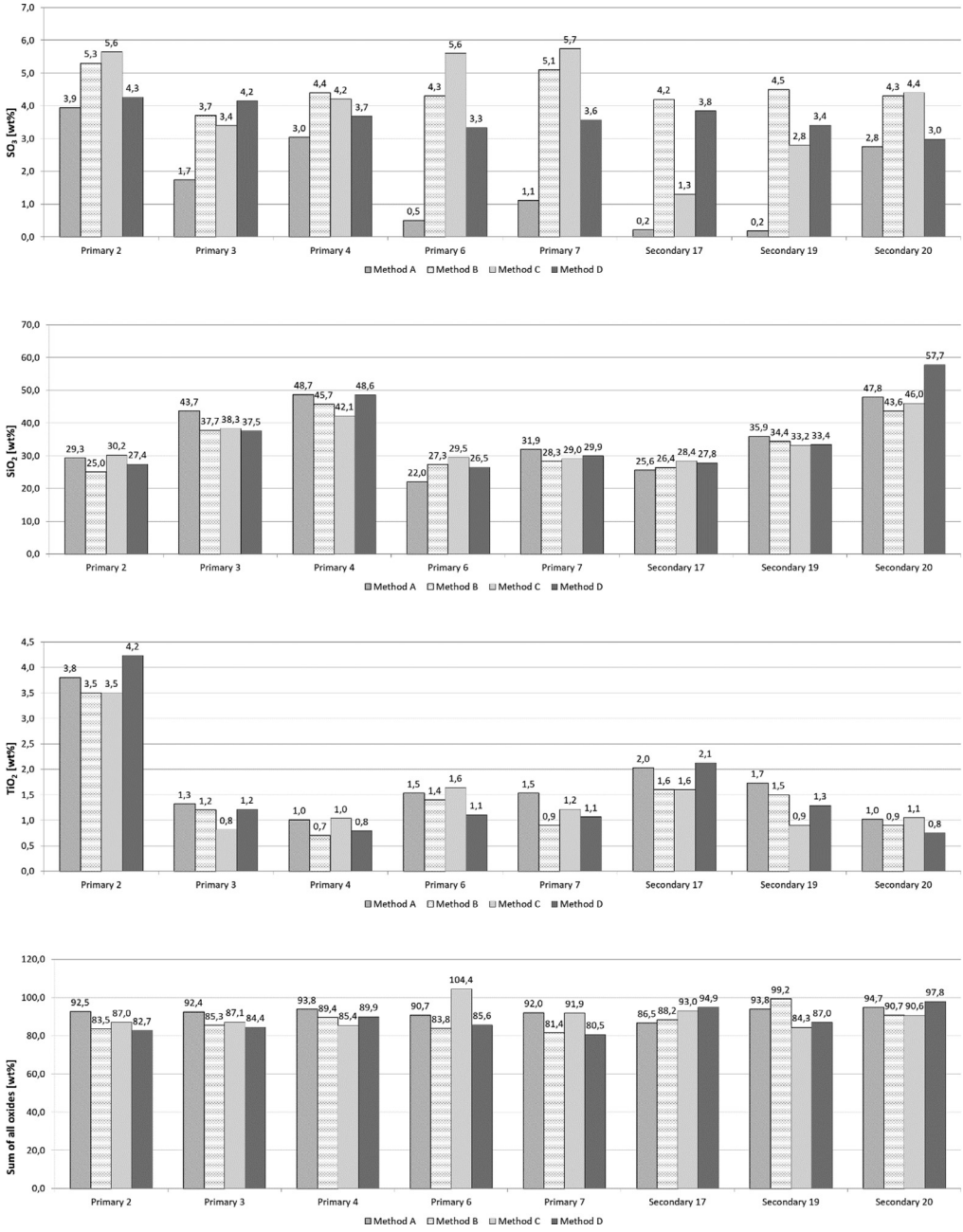

Fig. A3. Results for SO_3, SiO_2, TiO_2 and the sum of all measured oxides for all analytical methods for randomly selected samples.

Table A1
Results for the measured proficiency testing materials and the respective z-score.

Sample identification	Al_2O_3	CaO	Fe_2O_3	K_2O	MgO	Na_2O	P_2O_5	SO_3	SiO_2	TiO_2	SUM
Proficiency testing material 1 [wt%]	26.3	25.5	3.3	1.5	2.1	1.6	0.9	2.5	27.6	3.7	94.9
z-Score [-]	**0.24**	**−0.14**	**−0.04**	**0.79**	**0.33**	**−0.78**	**0.09**	**0.80**	**0.92**	**−0.62**	**–**
Proficiency testing material 2 [wt%]	26.4	25.7	3.0	1.5	2.5	2.9	1.0	2.6	20.0	3.4	89.1
z-Score [-]	**−0.15**	**−0.13**	**−0.52**	**1.24**	**0.53**	**−0.50**	**0.11**	**0.71**	**0.14**	**−0.91**	**–**
Proficiency testing material 3 [wt%]	29.5	27.6	3.1	1.3	1.9	2.3	1.0	2.4	25.1	4.1	98.3
z-Score [-]	**−0.25**	**0.60**	**−0.03**	**0.76**	**−0.26**	**−1.85**	**0.61**	**1.02**	**0.67**	**0.16**	**–**

Table A2
Results for the R indices of randomly selected SRF samples at different incineration temperatures and considering all elemental oxides and selected elemental oxides (Al_2O_3, CaO, Fe_2O_3, SiO_2).

Sample identification	R-Index (all elemental oxides included) [wt.%]			R-Index (only Al_2O_3, CaO, Fe_2O_3 and SiO_2 included) [wt.%]		
	550 °C	815 °C	915 °C	550 °C	815 °C	915 °C
Primary 1	10.8	10.6	11.1	9.3	8.3	9.3
Primary 3	12.9	11.9	9.8	10.4	10.4	8.2
Primary 4	21.0	22.1	16.4	17.4	19.6	14.4
Primary 5	18.2	17.2	15.6	14.1	14.6	13.2
Primary 6	19.9	18.0	14.3	16.1	14.6	11.9
Primary 7	18.7	17.1	14.2	15.2	14.2	11.8
Primary 19	15.7	13.3	14.0	13.7	11.2	12.1
Primary 20	21.1	22.3	22.1	15.2	17.0	17.0
Primary 22	13.3	11.3	12.2	10.3	9.5	10.4
Primary 27	29.2	21.7	27.7	26.5	19.4	25.6
Primary 32	8.2	8.0	7.7	6.6	6.6	6.6
Primary 36	22.9	19.2	16.9	17.8	15.5	13.0
Primary 40	8.2	9.2	8.8	6.2	7.9	7.6
Primary 41	7.0	8.9	8.4	5.9	7.5	6.9
Primary 44	22.8	22.5	21.9	18.4	18.2	17.7
Secondary 17	13.3	12.6	12.5	10.6	10.5	10.9
Secondary 18	17.1	14.9	15.2	13.6	11.9	12.0
Secondary 19	17.1	12.9	15.0	14.0	11.1	12.9
Secondary 20	29.4	28.6	29.6	24.5	24.3	26.3
Secondary 21	13.3	11.1	11.6	11.0	8.8	9.3
Secondary 24	26.0	27.5	25.7	22.9	23.5	22.0
Secondary 28	16.5	15.2	14.1	12.8	12.5	11.8

References

[1] Verein Deutscher Zementwerke e.V., Zement-Taschenbuch 2002, 50th ed., 2002.
[2] Bundesministerium für Land- und Forstwirtschaft, Umwelt und Wasserwirtschaft, Technische Grundlagen für den Einsatz von Abfällen als Ersatzrohstoffe in Anlagen zur Zementerzeugung, 2017 https://www.bmnt.gv.at/umwelt/abfall-ressourcen/behandlung-verwertung/ersatzrohstoffe.html.
[3] Verein Deutscher Zementwerke e.V., Technischer Bericht A-2015/0117-2 - Einsatz alternativer Rohstoffe im Zementherstellungsprozess - Hintergrundwissen, Technische Möglichkeiten und Handlungsempfehlungen, 2015 https://www.zement.at/downloads/downloads_2016/Einsatz_alternativer_Rohstoffe_im_Zementherstellungsprozess.pdf (accessed 10 February 2020).
[4] Bundesverband der Deutschen Zementindustrie, Verein Deutscher Zementwerke e.V., Zementrohstoffe in Deutschland: Geologie, Massenbilanz, Fallbeispiele, Bau und Technik, Düsseldorf, 2002.
[5] M. Schneider, M. Romer, M. Tschudin, H. Bolio, Sustainable cement production—present and future, Cement Concrete Res. 41 (2011) 642–650, doi:10.1016/j.cemconres.2011.03.019.
[6] K.E. Lorber, R. Sarc, A. Aldrian, Design and quality assurance for solid recovered fuel, Waste Manag. Res. 30 (2012) 370–380, doi:10.1177/0734242X12440484.
[7] R. Sarc, K.E. Lorber, Production, quality and quality assurance of refuse derived fuels (RDFs), Waste Manag. 33 (2013) 1825–1834, doi:10.1016/j.wasman.2013.05.004.

[8] R. Sarc, K.E. Lorber, R. Pomberger, M. Rogetzer, E.M. Sipple, quality Design, and quality assurance of solid recovered fuels for the substitution of fossil feedstock in the cement industry, Waste Manag. Res. 32 (2014) 565–585, doi:10.1177/0734242X14536462.
[9] R. Sarc, I.M. Seidler, L. Kandlbauer, K.E. Lorber, R. Pomberger, Design, quality and quality assurance of solid recovered fuels for the substitution of fossil feedstock in the cement industry – Update 2019, Waste Manag. Res. 37 (2019) 885–897, doi:10.1177/0734242X19862600.
[10] R. Sarc, Herstellung, Qualität und Qualitätssicherung von Ersatzbrennstoffen zur Erreichung der 100%-igen thermischen Substitution in der Zementindustrie, PhD Thesis, Montanuniversitaet Leoben, 2015.
[11] S.A. Viczek, A. Aldrian, R. Pomberger, R. Sarc, Determination of the material-recyclable share of SRF during co-processing in the cement industry, Resour. Conserv. Recycl. 156 (2020) 104696, doi:10.1016/j.resconrec.2020.104696.
[12] European Union, Commission Implementing Decision of 26 March 2013 Establishing the Best Available Techniques (BAT) Conclusions Under Directive 2010/75/EU of the European Parliament and of the Council on Industrial Emissions for the Production of Cement, Lime and Magnesium Oxide (notified under Document C (2013) 1728) (2013/163/EU), Official Journal of the European Union L100/1, 2013.
[13] A.C. Bourtsalas, J. Zhang, M.J. Castaldi, N.J. Themelis, Use of non-recycled plastics and paper as alternative fuel in cement production, J. Clean. Prod. 181 (2018) 8–16, doi:10.1016/j.jclepro.2018.01.214.
[14] A. Gallardo, M. Carlos, M.D. Bovea, F.J. Colomer, F. Albarrán, Analysis of refuse-derived fuel from the municipal solid waste reject fraction and its compliance with quality standards, J. Clean. Prod. 83 (2014) 118–125, doi:10.1016/j.jclepro.2014.07.085.
[15] T. Hilber, J. Maier, G. Scheffknecht, M. Agraniotis, P. Grammelis, E. Kakaras, T. Glorius, U. Becker, W. Derichs, H.-P. Schiffer, M. de Jong, L. Torri, Advantages and possibilities of solid recovered fuel cocombustion in the European energy sector, J. Air Waste Manage. Assoc. 57 (2007) 1178–1189, doi:10.3155/1047-3289.57.10.1178.
[16] M. Kara, Environmental and economic advantages associated with the use of RDF in cement kilns, Resour. Conserv. Recycl. 68 (2012) 21–28, doi:10.1016/j.resconrec.2012.06.011.
[17] M. Kuna, Analysis of thermal conversion of non-homogeneous solid recovered fuels (Master's Thesis), 2015 https://fenix.tecnico.ulisboa.pt/downloadFile/1126295043833896/Dissertation.pdf (accessed 9 August 2019).
[18] D. Montané, S. Abelló, X. Farriol, C. Berrueco, Volatilization characteristics of solid recovered fuels (SRFs), Fuel Process. Technol. 113 (2013) 90–96, doi:10.1016/j.fuproc.2013.03.026.
[19] M. Nasrullah, P. Vainikka, J. Hannula, M. Hurme, J. Kärki, Mass, energy and material balances of SRF production process. Part 1: SRF produced from commercial and industrial waste, Waste Manag. 34 (2014) 1398–1407, doi:10.1016/j.wasman.2014.03.011.
[20] M. Nasrullah, P. Vainikka, J. Hannula, M. Hurme, J. Kärki, Mass, energy and material balances of SRF production process. Part 2: SRF produced from construction and demolition waste, Waste Manag. 34 (2014) 2163–2170, doi:10.1016/j.wasman.2014.06.009.
[21] C. Velis, S. Wagland, P. Longhurst, B. Robson, K. Sinfield, S. Wise, S. Pollard, Solid recovered fuel: influence of waste stream composition and processing on chlorine content and fuel quality, Environ. Sci. Technol. 46 (2012) 1923–1931, doi:10.1021/es2035653.
[22] S.T. Wagland, P. Kilgallon, R. Coveney, A. Garg, R. Smith, P.J. Longhurst, S.J.T. Pollard, N. Simms, Comparison of coal/solid recovered fuel (SRF) with coal/refuse derived fuel (RDF) in a fluidised bed reactor, Waste Manag. 31 (2011) 1176–1183, doi:10.1016/j.wasman.2011.01.001.
[23] H. Wu, A.J. Pedersen, P. Glarborg, F.J. Frandsen, K. Dam-Johansen, B. Sander, Formation of fine particles in co-combustion of coal and solid recovered fuel in a pulverized coal-fired power station, Proc. Combust. Inst. 33 (2011) 2845–2852, doi:10.1016/j.proci.2010.06.125.
[24] H. Wu, P. Glarborg, F.J. Frandsen, K. Dam-Johansen, P.A. Jensen, B. Sander, Trace elements in co-combustion of solid recovered fuel and coal, Fuel Process. Technol. 105 (2013) 212–221, doi:10.1016/j.fuproc.2011.05.007.
[25] B. Hökfors, D. Boström, E. Viggh, R. Backman, On the phase chemistry of Portland cement clinker, Adv. Cement Res. 27 (2015) 50–60, doi:10.1680/adcr.13.00071.
[26] Waste & Resources Action Programme, A Classification Scheme to Define the Quality of Waste Derived Fuels, 2012 http://www.wrap.org.uk/sites/files/wrap/WDF_Classification_6P%20pdf.pdf.
[27] M. Beckmann, M. Pohl, D. Bernhardt, K. Gebauer, Criteria for solid recovered fuels as a substitute for fossil fuels—a review, Waste Manag. Res. 30 (2012) 354–369, doi:10.1177/0734242X12441237.
[28] C.B. Behr-Andres, S.D. McDowell, N.J. Hutzler, Quantitative mineral determinations of industrial coal ash, Air Waste 43 (1993) 1245–1251, doi:10.1080/1073161X.1993.10467202.
[29] M. Reinmöller, M. Klinger, M. Schreiner, H. Gutte, Relationship between ash fusion temperatures of ashes from hard coal, brown coal, and biomass and mineral phases under different atmospheres: a combined Factsage™ computational and network theoretical approach, Fuel 151 (2015) 118–123, doi:10.1016/j.fuel.2015.01.036.
[30] S.V. Vassilev, R. Menendez, Phase-mineral and chemical composition of coal fly ashes as a basis for their multicomponent utilization. 4. Characterization of heavy concentrates and improved fly ash residues, Fuel 84 (2005) 973–991, doi:10.1016/j.fuel.2004.11.021.
[31] S.V. Vassilev, R. Menendez, D. Alvarez, M. Diaz-Somoano, M.R. Martinez-Tarazona, Phase-mineral and chemical composition of coal fly ashes as a basis for their multicomponent utilization. 1. Characterization of feed coals and fly ashes☆, Fuel 82 (2003) 1793–1811, doi:10.1016/S0016-2361(03)00123-6.
[32] G. Dunnu, J. Maier, G. Scheffknecht, Ash fusibility and compositional data of solid recovered fuels, Fuel 89 (2010) 1534–1540, doi:10.1016/j.fuel.2009.09.008.
[33] M. Pohl, D. Bernhardt, M. Beckmann, W. Spiegel, Brennstoffcharakterisierung zur vorausschauenden bewertung des korrosionsrisikos, in: M. Born (Ed.), Dampferzeugerkorrosion 2011, SAXONIA Standortentwicklungs- und -verwaltungsgesellschaft mbH, Freiberg, 2011, pp. 67–83.
[34] Austrian Standards Institute, ÖNORM EN 15403 solid recovered fuels - Determination of ash content. Issued on 15/05/2011, Vienna, 2011.

[35] German Institute for Standardization, DIN 51719 testing of solid fuels – Solid mineral fuels – Determination of ash content. Issued 07/1997, 1997.
[36] Austrian Standards Institute, ÖNORM G 1074 testing of solid fuels – Determination of moisture, ash and volatile matters. Issued on 01/06/2004, Vienna, 2004.
[37] International Standard, ISO 1171 solid mineral fuels – Determination of ash. Issued 15/06/2010, Geneva, 2010.
[38] Austrian Standards Institute, ÖNORM EN 15410 solid recovered fuels – Methods for the determination of the content of major elements (Al, Ca, Fe, K, Mg, Na, P, Si, Ti). Issued on 15/12/2011, Vienna, 2011.
[39] German Institute for Standardization, DIN 51729-10 testing of solid fuels – Determination of chemical composition of fuel ash – Part 10: x-ray fluorescence analysis. Issued 04/2011, Berlin, 2011.
[40] German Institute for Standardization, DIN 51729-11 testing of solid fuels - Determination of chemical composition of fuel ash - Part 11: determination by inductively coupled plasma emission spectrometry (ICP-OES). Issued 11/1998, 1998.
[41] German Institute for Standardization, DIN 51729-8 testing of solid fuels – Determination of chemical composition of fuel ash – Part 8: determination of soda and potash (Na2O, K2O) contents. Issued 05/2001, Berlin, 2001.
[42] International Standard, ISO 13605 Solid Mineral Fuels – Major and Minor Elements in Coal Ash and Coke Ash – Wavelength Dispersive X-Ray Fluorescence Spectrometric Method, Final Draft, Geneva, 2018.
[43] Austrian Standards Institute, ÖNORM EN 15442 solid recovered fuels - Methods for sampling. Issued on 01/05/2011, Vienna, 2011.
[44] Austrian Standards Institute, ÖNORM EN 14346 characterization of waste - Calculation of dry matter by determination of dry residue or water content. Issued on 01/03/2007, Vienna, 2007.
[45] European Committee for Standardization, CEN/TS 15414-1 solid recovered fuels - Determination of moisture content using the oven dry method - Part 1: determination of total moisture by a reference method, 2010.
[46] Austrian Standards Institute, ÖNORM EN 15413 solid recovered fuels – Methods for the preparation of the test sample from the laboratory sample. Issued on 15/10/2011, Vienna, 2011.
[47] Austrian Standards Institute, ÖNORM EN 196-2 method of testing cement – Part 2: chemical analysis of cement. Issued on 01/10/2013, Vienna, 2013.
[48] Austrian Standards Institute, ÖNORM en 13656 characterization of waste – Microwave assisted digestion with hydrofluoric (HF), nitric (HNO3) and hydrochloric (HCl) acid mixture for subsequent determination of elements. Issued on 01/12/2002, Vienna, 2002.
[49] Austrian Standards Institute, ÖNORM L 1084 chemical analyses of soils – Determination of carbonate taking into account air pressure and temperature. Issued on 01/07/2016, Vienna, 2016.
[50] Delta Coal Control, DCC proficiency test analytic 2016, in: Evaluation final, #1014 Solid recovered fuels SRF., Germany, 2016.
[51] Delta Coal Control, DCC proficiency test analytic 2017, in: Draft 11/09/2017, #1014 Solid recovered fuels SRF., 2017.
[52] Delta Coal Control, DCC proficiency test analytic 2018, in: Evaluation final, #1014 Solid recovered fuels SRF, 2018.
[53] S.L.R. Ellison, A. Williams, EURACHEM/CITAC guide CG 4 quantifying uncertainty in analytical measurement, QUAM (2012) P1, 3rd edition, 2012 https://www.eurachem.org/images/stories/Guides/pdf/QUAM2012_P1.pdf.

3.8 Publication VIII

Determination of the material-recyclable share of SRF during co-processing in the cement industry

S.A. Viczek, A. Aldrian, R. Pomberger, R. Sarc

Resources, Conservation & Recycling 156 (2020), 104696,
https://doi.org/10.1016/j.resconrec.2020.104696

Author Contributions (CRediT Contributor Roles Taxonomy):

SV: Conceptualization, Methodology, Formal Analysis, Investigation, Data curation, Writing – original draft preparation, Writing – original draft preparation, Visualization;

AA: Conceptualization, Methodology, Investigation, Writing – review and editing;

RP: Resources, Funding acquisition;

RS: Conceptualization, Methodology, Investigation, Data curation, Writing – review and editing, Project administration, Funding acquisition.

Graphical abstract:

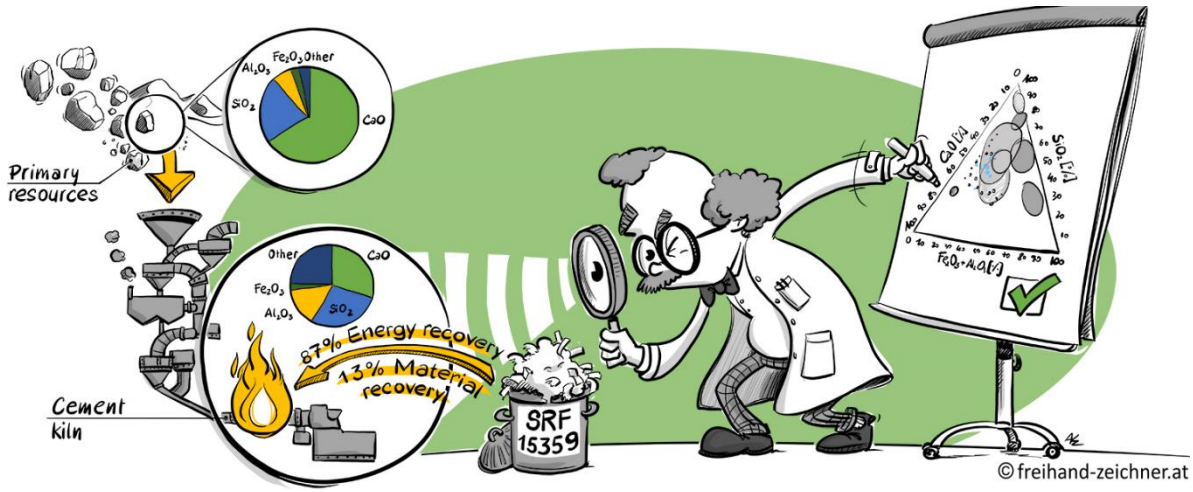

Resources, Conservation & Recycling 156 (2020) 104696

Contents lists available at ScienceDirect

Resources, Conservation & Recycling

journal homepage: www.elsevier.com/locate/resconrec

Full length article

Determination of the material-recyclable share of SRF during co-processing in the cement industry

S.A. Viczek, A. Aldrian, R. Pomberger, R. Sarc*

Chair of Waste Processing Technology and Waste Management, Montanuniversitaet Leoben, Leoben, Austria

ARTICLE INFO

Keywords:
Cement industry
Co-processing
Material recycling
Material recovery
Solid recovered fuel (SRF)

ABSTRACT

Solid recovered fuel (SRF according to EN 15359) is frequently used to substitute primary fuels required for the clinker burning process in the cement industry. Since the ash that is formed during the combustion of the SRF is directly incorporated into the product portland cement clinker, this process is also referred to as “co-processing”. While the use of SRF in cement plants is legally considered as energy recovery, the fact that mineral constituents are incorporated into the clinker implies that technically a certain share of SRF is recycled on a material level. The paper at hand aims at determining this share by analyzing 80 SRF samples representing SRF qualities that are currently available on the market in Austria, Croatia, Slovakia, and Slovenia. Results show that the SRF ashes on average consist of 76.8 % SiO_2, CaO, Al_2O_3 and Fe_2O_3, the main raw materials that are required for clinker production. Another 14.1 % consist of chemical compounds that are common clinker phases or frequently present in the primary raw materials used for clinker production. Different ways of calculating the recycling index, i.e. the share of SRF (referring to dry mass) that is used on a material level, are discussed, and recycling indices are found to range between 13.5 and 17.6 %. It is concluded that SRF ash represents a suitable secondary raw material for cement clinker manufacturing and that for the cement industry SRF-co-processing offers the possibility to contribute towards reaching the higher recycling rates specified by the European Union.

1. Introduction

The hydraulic binder cement is a crucial component for the manufacturing of mortar and concrete (Galvez-Martos and Schoenberger, 2014), the latter being one of the world’s most important manufactured materials (Huntzinger and Eatmon, 2009). For the production of cement clinker, raw materials providing the four main chemical components of cement clinker or precursors thereof are required, namely calcium oxide CaO, silicon dioxide SiO_2, aluminum oxide Al_2O_3, and iron(III) oxide Fe_2O_3 (cf. section 2.1). Besides raw materials, the manufacturing of cement also requires large amounts of energy (Galvez-Martos and Schoenberger, 2014). In modern rotary kiln plants, the production of 1 metric ton of cement clinker requires between 3.0 and 3.8 GJ of thermal energy (under optimal conditions and depending on the technology used). Wet or shaft kilns, in contrast, may require up to 5.8 GJ of thermal energy per ton clinker (European Cement Research Academy (ECRA), 2016). To provide this energy, cement plant operators use increasing amounts of alternative fuels, i.e. solid recovered fuels (SRF) and other refuse-derived fuels (RDF),[1] thereby substituting fossil fuels (European Commission (EC), 2013; Sarc et al., 2014, 2019b). In the European cement industry, the use of RDF is already state of the art (European Commission (EC), 2013), and high thermal substitution rates (i.e. the degree to which fossil fuels are replaced by RDF in cement plants) are achieved in some countries. Austria features the highest substitution rate worldwide (Sarc et al., 2019b) with more than 80 % of the thermal energy demand of the Austrian cement industry being covered by alternative fuels: 30 % are covered by RDF, e.g. old tires, used oil and solvents, etc. and 50 % are covered by SRF from plastic rich waste fractions of industrial, commercial, and municipal solid waste (MSW), corresponding to 358,580 tonnes of SRF (year 2018) (Mauschitz, 2019). Sarc (2015) has demonstrated that even 100 % of thermal substitution is technically feasible when different types of RDF are used for energy generation in the clinker production process. International studies report that the use of SRF or RDF in the

* Corresponding author.
E-mail addresses: sandra.viczek@unileoben.ac.at (S.A. Viczek), alexia.aldrian@unileoben.ac.at (A. Aldrian), roland.pomberger@unileoben.ac.at (R. Pomberger), renato.sarc@unileoben.ac.at (R. Sarc).

[1] SRF represent a subgroup of RDF. While RDF can be prepared of various non-hazardous and hazardous, liquid and solid waste materials (e.g. sewage sludge, waste wood, used solvents), the term SRF only refers to solid fuels made from non-hazardous mixed or sorted solid wastes, are furthermore quality assured, i.e. meet the criteria defined by EN 15359, and utilized for energy recovery.

https://doi.org/10.1016/j.resconrec.2020.104696
Received 9 October 2019; Received in revised form 17 December 2019; Accepted 6 January 2020

cement kiln offers environmental benefits, e.g. reducing landfilling (Kara, 2012; Reza et al., 2013), a high energy efficiency (Samolada and Zabaniotou, 2014), or a reduction of fossil CO_2 emissions as part of the carbon in SRF is of biogenic origin (Sarc et al., 2014, 2019b).

When SRF or other RDF are co-incinerated in the cement industry, this process is often also referred to as co-processing, a term that comprises industrial processes that simultaneously enable energy recovery and recycling of the mineral content of waste material and thereby allow for the replacement of both mineral resources and fossil fuels (Basel Convention, 2012; Lamas et al., 2013; Vodegel et al., 2018). Because the ash is directly incorporated into the product during the process, cement plant operators adapt the raw meal mix according to the fuels that are used (e.g. add more $CaCO_3$ to compensate for a lack of CaO in coal ash) (Locher, 2000).

SRF ashes are mainly composed of CaO, SiO_2, Al_2O_3, and Fe_2O_3 (the four main chemical components of cement clinker) and contain further compounds that typically occur in clinker (Dunnu et al., 2010; Hilber et al., 2007; Kuna, 2015; Pohl et al., 2011; Wagland et al., 2011) (cf. Section 2.1 for clinker composition and Section 2.2 for ash composition). This implies that SRF ashes can provide a certain proportion of the raw material that is required for the production of clinker. Similarly, several scientific publications have already examined the use of municipal solid waste incineration (MSWI) ashes as a mineral source for the manufacture of portland cement clinker (Ashraf et al., 2019; Clavier et al., 2019; Krammart and Tangtermsirikul, 2004; Lam et al., 2011; Saikia et al., 2007; Sarmiento et al., 2019), with the result that it is a suitable raw material for cement clinker production (compare Section 2.2).

Since SRF ash can provide raw materials for the production of cement clinker, and these minerals are incorporated into the clinker during co-processing of SRF, a certain proportion of the SRF that is co-processed in the cement industry can technically be considered as recycled on a material level. This also leads to the conclusion that - from a technical and material point of view - a certain proportion of cement clinker consists of recycled material. From the legal point of view, the use of SRF in the cement industry is currently merely considered as energy recovery, an R1 process ("*use principally as a fuel or other means to generate energy*") (European Commission (EC), 2008). In single countries, such as Hungary, France, or Portugal, mixed recovery, i.e. partial energy recovery and partial material recovery, is recognized for the co-processing of old tires or other RDF in the cement industry. In Hungary, the IPPC permit of single cement plants includes a mixed recovery of end-of-life-tires during co-incineration, with 85 % being recognized as energy recovery, and 15 % being recognized as material recovery (Lafarge, 2019), which is linked to the iron content of the tires (Országos Hulladékgazdálkodási Ügynökség (ÖHÜ), 2011). Also in France, mixed recovery of waste tires in the cement industry is reported, with 23.75 % of the tires being considered as material-recycled ("non-organic material recycling"), thus reducing the share of energy recovery (Aliapur, 2016, 2019; Collet, 2016). While in Hungary and France this mixed recovery is restricted to waste tires, Portugal adapted its general waste management scheme (Assembleia da República Portugal, 2006) that regulates the calculation of the waste management fee (taxa de gestão de resíduos, TGR) in 2014 (Assembleia da República Portugal, 2014) taking the results of a Portuguese study (Ribeiro et al., 2015) on the material recovery of alternative fuels in co-processing into account (CIMPOR, 2016). The altered regulations recognize mixed recovery by offering the possibility to decrease the TGR by the amount of material that is recovered, e.g. by being incorporated into the final product when the R1 process takes place in industrial process furnaces. The method of determination needs to be previously approved by the National waste authority (Autoridade Nacional de Resíduos, ANR) (Assembleia da República Portugal, 2014). The Portuguese cement industry reports that with this legislation material recycling indices of 14.0 % are achieved for different types of alternative fuels (CIMPOR, 2016).

As part of the European Union's Circular Economy Package (CEP), the European Parliament and Council agreed on a further stepwise increase of recycling targets for MSW that were written down in the amendment of directive 2008/98/EC (i.e. the waste framework directive (European Commission (EC), 2008)) in May 2018 (European Commission (EC), 2018b). In 2035, 65 % of MSW need to be recycled, with a derogation period of 5 years (i.e. 65 % in 2040) being offered for selected countries. Furthermore, by 2030 55 % of the total plastic packaging waste (which is of importance for SRF because the non-recyclable part is usually processed to SRF and utilized in the cement industry) shall be recycled (European Commission (EC), 2018a). These new targets make it an interesting option to acknowledge that mineral materials from SRF are incorporated into the product portland cement clinker, and to count this share e.g. towards the municipal waste recycling targets. This option was also considered by the European Parliament and Council in the very same amendment that set the recycling targets for municipal waste (European Commission (EC), 2018b):

> "The Commission shall assess co-processing technology that allows the incorporation of minerals in the co-incineration process of municipal waste. Where a reliable methodology can be found, as part of this review, the Commission shall consider whether such minerals may be counted towards recycling targets." (European Commission (EC), 2018b)

A different statement was part of a Commission implementing decision in June 2019 (European Commission (EC), 2019), where Article 3.7 specifically excludes counting the mineral part that is incorporated into cement clinker towards recycling:

> „Where municipal waste materials enter recovery operations whereby those materials are used principally as a fuel or other means to generate energy, the output of such operations that is subject to material recovery, such as the mineral fraction of incineration bottom ash or clinker resulting from co-incineration, shall not be included in the amount of municipal waste recycled with the exception of metals separated and recycled after incineration of municipal waste. Metals incorporated in the mineral output of the co-incineration process of municipal waste shall not be reported as recycled." (European Commission (EC), 2019)

Hence, co-processing is not yet recognized towards the recycling targets, but until 2028 - cf. Article 11(7) of the amended Waste Framework Directive 2018 (European Commission (EC), 2018b) - the European commission will review the targets and assess whether co-processing shall be acknowledged. At the moment, however, there is insufficient information on SRF-co-processing, the composition of SRF ash, the share of SRF ash that can be considered as recycled on a material level, and the contribution the cement industry could make towards reaching the EU recycling target. It also underlines that further international research on the topic is required in order to enable a discussion of what is and what is not counted towards the recycling target based on scientific data.

Aiming to fill this information gap by building up a database on the ash composition of a large variety of current real-market SRF samples and calculating possible recycling-indices (R-indices, i.e. the share of SRF that is recyclable on a material level), first of all different analytical methods based on European Standards (e.g. EN published by CEN) were tested and validated (Aldrian et al., 2020; Viczek et al., 2019a, b). The most suitable method was used to generate the results that are presented in this paper, which reports the ash composition and R-indices of 80 SRF samples from four European countries representing SRF qualities that are currently available on the market. Furthermore, the role of ash constituents and different ways of calculating the R-index are discussed.

2. Cement clinker manufacturing – raw material and SRF ash composition

2.1. Raw materials and cement clinker composition

For any of the 27 types of common cement that are defined in EN 197-1 (Austrian Standards Institute (ASI), 2011d) portland cement clinker is an important constituent that amounts for 5–100 % of the cement's mass, depending on the type of cement. Portland cement, which is the most common type of cement, consists of 95–100 % of portland cement clinker (Austrian Standards Institute (ASI), 2011d).

Raw materials used for clinker production have to provide the main chemical compounds required for the process, i.e. CaO, SiO_2, and smaller amounts of Al_2O_3 and Fe_2O_3 (Verein Deutscher Zementwerke e.V. (vdz), 2002). Primary resources in the form of raw rock types are commonly used, with limestone or chalk, clay, and marl being the most important raw materials. Sand, iron ores, and other correcting materials are added in order to achieve the desired bulk composition and to compensate for the lack of certain chemical components (Verein Deutscher Zementwerke e.V. (vdz), 2018). Apart from these raw rock types, secondary resources containing SiO_2, Al_2O_3, Fe_2O_3, and CaO or $CaCO_3$ can be used in the cement plant. A list of primary and secondary raw materials is given in Table 1.

Common portland cement clinkers consist of approximately 63–70 wt% CaO, 19–24 wt% SiO_2, 3–7 wt% Al_2O_3 and TiO_2, and 1–5 wt % Fe_2O_3 (Locher, 2000). For the production of portland cement clinker, the raw materials are milled, mixed to achieve the desired raw meal composition, and sintered at temperatures of about 1450 °C. Typical clinker phases and other constituents of portland cement clinker that are formed during the sintering process are given in Table 2.

2.2. SRF and MSWI ash composition in literature

To assess whether SRF is a suitable secondary raw material for cement clinker manufacturing, its ash composition needs to be taken into account. While the composition of MSWI ash has been researched by several publications (Ashraf et al., 2019; Gao et al., 2017; Garcia-Lodeiro et al., 2016; Pan et al., 2008; Saikia et al., 2007; Sarmiento et al., 2019), less data is available on the ash composition from SRF or RDF prepared from MSW (Dunnu et al., 2010; Hilber et al., 2007; Kuna, 2015; Pohl et al., 2011; Viczek et al., 2019a; Wagland et al., 2011). Table 3 lists SRF ash compositions reported in literature, and, for comparison, literature data on MSWI ashes are listed as well. MSWI ashes have already been proven to represent suitable raw materials for the cement industry that can be added for clinker production. Several studies successfully replaced different shares (up to 6 %) of raw materials with MSWI ashes (Clavier et al., 2019; Lam et al., 2011; Pan et al., 2008; Shih et al., 2003) without significant changes in clinker composition (Sarmiento et al., 2019). Other studies produced eco-cement with 50 % (Ampadu and Torii, 2001) or even exclusively from MSWI residues (Ashraf et al., 2019).

Table 3 shows that SRF ashes consist of the same main constituents as MSWI ashes and some even feature a similar composition. The main difference to SRF ashes is that MSWI ashes are incineration residues from a different process (i.e. MSW incineration) that can solely be processed as a raw material in the cement industry, while SRF ashes are formed directly in the kiln during the pyro-chemical clinker production process where SRF is used as a fuel, which means that energy and material recovery takes place during the same process.

There are no studies on the maximum share of SRF ash in the cement clinker, but the share is technically limited by the amount of energy required for clinker burning. Moreover, high thermal substitution rates of up to 80 % (50 % SRF and 30 % RDF) are already state of the art in some countries such as Austria (Sarc et al., 2019b), which means that in Austria approximately 1.5 mass-% of the clinker already consist of components derived from SRF ash without causing relevant issues (basis for calculation: thermal energy demand: 3.895 GJ/$t_{clinker}$, 50 % derived from SRF with a LHV of 19.38 MJ/kg (Mauschitz, 2019) and an ash content of 15.6 % (Sarc et al., 2019b)). As it is already practically applied, it can be assumed that similar to MSWI ash, SRF ash represents a suitable raw material for clinker production as well.

3. Materials and methods

Here, the collected and investigated SRF samples, the analysis methods applied and the calculation of the recycling-index (R-index) are described.

3.1. Samples

The paper at hand focuses on the analysis of SRF "secondary" and SRF "primary", both of which are used in the cement industry for the manufacturing of portland cement clinker (Sarc, 2015):

- SRF for secondary firing (SRF "secondary"): SRF with a lower heating value between 12 and 18 MJ/kg_{OS} (corresponding to class NCV 3 or 4 in EN 15359) suitable for the use in secondary firing (calciner, kiln inlet, or hot disc combustion chamber, etc.) in the kiln system of cement manufacturing plants. Grain sizes can range up to 80 mm when used in a calciner or at the kiln inlet and up to 300 mm

Table 1
Primary and alternative/secondary raw materials for the cement industry (Holleman et al., 2007; Locher, 2000; Scheffer et al., 2008; Scur, 2013; Verein Deutscher Zementwerke e.V. (vdz), 2002, 2018).

Primary raw material	Additional information	Major elements contained by primary raw material	Alternative/secondary raw material
Limestone, chalk	Consist of $CaCO_3$, which is transformed into CaO in the clinker burning process.	Ca	Lime mud, residues from lime burning, calcium fluoride
Marl	A natural mixture of $CaCO_3$ and clay.	Si, Ca, Al, Fe	Fly ash, ashes from the paper industry, bottom ash, slags, crushed concrete
Clay, bentonite, kaolinite	Clays represent a source for Al_2O_3 and SiO_2 and furthermore contain iron minerals such as FeOOH, FeS_2, FeO and Fe_2O_3, and feldspars, i.e. alumino-silicates that also contain Na_2O and K_2O.	Si, Al, Fe	Waste bentonite and fuller's earth
Sand, quartz sand	Represent a source for SiO_2 and is added when the SiO_2 content of the raw materials mixture is too low.	Si	Used foundry sand, contaminated soil
Iron ores	Source for Fe_2O_3. The addition might be required as a correcting material to achieve the desired bulk composition.	Fe	Materials from iron and steel industries, e.g roasted pyrite, contaminated ores, dust, mill scale, bauxite tailings (Fe and Al)
Gypsum or Anhydrite	Both represent a source for sulfate (SO_4^{2-}) in the form of $CaSO_4$. Small amounts of sulfate are added to bind alkali metals when the content of alkali metals in the raw materials mix is too high or the sulfate content is too low.	S	Gypsum from flue gas desulfurization

Table 2
Possible composition of cement clinkers and properties of clinker phases (Locher, 2000; Verein Deutscher Zementwerke e.V. (vdz), 2002).

Clinker phase/compound	Chemical formula	Content [mass %]	Additional information
Alite (tricalcium silicate)	3 CaO · SiO_2	45–85 %	Main phase giving cement its crucial properties.
Belite (dicalcium silicate)	2 CaO · SiO_2	0–32 %	Is formed when the clinker is not saturated with calcium oxide.
Calcium aluminoferrite	2 CaO · (Al_2O_3, Fe_2O_3)	4–16 %	Major part of Fe- and Al-oxides are bound in this phase.
Tricalcium aluminate	3 CaO · Al_2O_3	7–16 %	Form of Al-oxides that are not bound as calcium aluminoferrite.
Free CaO and free MgO	CaO	0.1–5.6 %	Free MgO originates from dolomite ($CaMg(CO_3)_2$), which is a constituent of many limestones, and clay, while free CaO can be a consequence of oversaturation of the system with Ca. High contents of MgO and CaO lead to problems due to expansion, which is why the content of MgO shall not exceed 5 % according to EN 197-1. The smaller the grain size of the cement, the larger the amount of free MgO and CaO that is acceptable.
(Periclase)	MgO	0.5–4.5 %	
Alkali sulfates	Na_2SO_4, K_2SO_4, (Na, K)$_2SO_4$, $K_2Ca_2(SO_4)_3$, K_2SO_4 · 2 $CaSO_4$	1–2 %	Are formed during the clinker burning process from a reaction between Na_2O and K_2O (originating from feldspars) and sulfate (originating from raw materials and fuels). Alkaline sulfates in cement alter the chemical reactivity with water.

for a hot disc combustion chamber.

- SRF for primary firing (SRF "primary"): SRF with a lower heating value between 18 and 25 MJ/kg_{OS} (corresponding to class NCV 1, 2, or 3 in EN 15359), and grain sizes below 30 (35) mm suitable for the use as a main burner fuel in the rotary kiln of cement manufacturing plants.

A total of 80 SRF samples consisting of 30 SRF "secondary" and 50 SRF "primary" samples from Austria, Croatia, Slovakia, and Slovenia were investigated in this study. The samples represent SRF qualities that are currently available on the market (production years 2018 and 2019) and are intended for the use in the cement industry. The samples comprised original samples as well as reference samples that were provided by various companies. All samples were either taken by employees of the chair of waste processing technology and waste management (Montanuniversitaet Leoben) or by employees of the cement plants or SRF production facilities under consideration of EN 15442 (Austrian Standards Institute (ASI), 2011a). The sampling method is described in detail in Lorber et al. (2012); Sarc et al. (2019b), and Sarc et al. (2019a). Samples were taken from the storage heap, conveyor belt or by using automatic sampling systems, if available on site. The minimum number of sampling increments was 6 per representative sample, the increment masses were calculated according to the formula given in EN 15442 (Austrian Standards Institute (ASI), 2011a) and typically ranged from 0.3–5 kg, depending on the grain size. Laboratory samples were prepared according to ÖNORM EN 15443 (Austrian Standards Institute (ASI), 2011c), test samples according to EN 15413 (Austrian Standards Institute (ASI), 2011b).

3.2. Chemical analyses

Different methods for the determination of ash composition as well as different ashing temperatures were tested and discussed in detail in Aldrian et al. (2020). The study found that ashing temperatures of 815 °C and 950 °C are suitable for the subsequent ash analysis, and that ICP-OES or XRF after a suitable sample preparation yield comparable results. The results presented in this paper were obtained as follows:

Original samples were dried to constant mass at 105 °C according to EN 14346 (Austrian Standards Institute (ASI), 2007)[2] and were comminuted to a grain size of < 0.5 mm using a cutting mill under consideration of EN 15413 (Austrian Standards Institute (ASI), 2011b). Before ashing and digestion the samples were redried at 105 °C.

Reference samples that were provided by various companies were already received in a dried and comminuted (< 0.5 mm) state. These samples were also redried at 105 °C before ashing and digestion.

[2] Note: comparable content and same requirement, i.e. 105 °C, as defined in ONR CEN/TS 15414-1 (European Committee for Standardization (CEN), 2010).

All samples were ashed at 950 °C (for a comparison of ashing temperatures please refer to Aldrian et al. (2020). Applying the method of DIN 51729-11 (for solid fuels) (German Institute for Standardization (DIN), 1998b), 0.1 g of the ash residue was fused with 1 g of lithium metaborate (Sigma Aldrich) in a platinum crucible and fused in a muffle oven (Nabertherm L 9) at 1050 °C for 20 min. The fused bead was allowed to cool down and subsequently dissolved by adding a total volume of 80 mL HCl (c = 2 mol/L) in portions, heating to 50–60 °C, and stirring (PTFE stirring bar). The digest solution was diluted with deionized water (< 0.055 µS/cm) to a volume of 250 mL and analyzed by ICP-OES (Varian Vista-MPX CCD Simultaneous, Software: 4.1.0) (German Institute for Standardization (DIN), 1998a) at the following wavelengths: Al 308.215 nm; Ca 317.933 nm; Fe 238.204 nm; K 766.491 nm; Mg 279.553 nm; Na 589.592 nm; P 213.618 nm; S 180.669 nm; Si 251.611 nm; Ti 334.941 nm. Assuming (for simplicity) that these elements are mainly present as oxides in the ash, the corresponding concentrations of the respective oxides (i.e. Al_2O_3, CaO, Fe_2O_3, K_2O, MgO, Na_2O, P_2O_5, SO_3, SiO_2, and TiO_2) were calculated. All measurements were performed as single measurements. The limits of detection (LOD) for the analysis method are given in Table 4.

3.3. Calculation of the recycling-index (R-index)

The R-index [$\%_{DM}$], i.e. the percentage share of SRF that can be considered as recycled on a material level, is calculated according to formula 1 (Aldrian et al., 2020). The R-index refers to the dried SRF sample.

$$R - index = \frac{AC}{100} \cdot (w_1 + w_2 + ... + w_n) \quad (1)$$

with

AC Ash content [$wt\%_{DM}$]

w_1, w_2, …, w_n mass share of selected element oxides in the ash [$wt\%_{DM}$]

4. Results and discussion

4.1. SRF ash composition

The average composition of the 30 SRF "secondary" (corresponding to class NCV 3 or 4 in EN 15359) and 50 SRF "primary" samples (corresponding to class NCV 1, 2, or 3 in EN 15359) is depicted in Fig. 1, detailed results are given in Table 4. Similar to the SRF ash composition reported in literature (compare Table 3), the main constituents of the analyzed ashes are CaO, SiO_2, Al_2O_3, and Fe_2O_3. Compositional differences between SRF "secondary" and "primary" ashes are rather small. For some oxides, the variability within each of the two groups is already quite high (Relative standard deviation (RSD) > 40

Table 3
Examples for the composition of SRF ash and MSWI ash reported in literature.

Sample and origin		Source	Composition [%]										Ash content [%]
			CaO	SiO_2	Al_2O_3	Fe_2O_3	SO_3	MgO	Na_2O	K_2O	TiO_2	P_2O_5	Sum of other analyzed constituents*	
SRF ash	MSW/CW	(Hilber et al., 2007)	25.77	26.52	13.68	3.33	1.34	2.43	5.27	2.02	2.28	1.26	0.05	7.93
	CW	(Pohl et al., 2011)	40.13	23.87	10.47	4.83	3.4**	3.23	2.20	0.78	2.68	0.51		12.25
	MSW	(Dunnu et al., 2010)	25.41	38.12	11.18	2.88	4.50	3.68	4.18	2.34	2.33	1.18	6.61	15.79
	Paper/plastic	(Dunnu et al., 2010)	21.80	36.07	16.18	3.94	2.50	2.59	4.80	2.82	1.31	1.70	7.71	24.82
	–	(Kuna, 2015)	20.4 - 24.5	33.4 - 35.7	12.0 - 17.3	7.0 - 14.4	3.6 - 11.9	2.3 - 2-8	1.8 - 3.8	1.1 - 1.8	1.6 - 2.4	1.0 - 1.9	0.5 - 0.9	11.1 - 22.4
	Synthetic SRF	(Wagland et al., 2011)	60.4	7.5	4.3	4.5	0.17**	1.2	0.3	0.1	8.1	0.8		11.1
	MSW	(Wagland et al., 2011)	18.5	48.1	9.5	2.7	0.8**	2	3.3	1.9	1.8	1.5		16.2
	MSW/CW	(Viczek et al., 2019a)	27.5	31.9	9.4	3.2	4.5	2.7	3.4	2.9	1.4	0.9		20
MSWI	Bottom ash	(Sarmiento et al., 2019)	16.2 - 37.6	33.4 - 50.6	5.39 - 11.6	2.64 - 11.1	0.97 - 3.84	1.52 - 2.07	2.22 - 5.13	0.61 - 1.02	0.69 - 1.39	0.87 - 2.22	0.87 - 1.88	
	Bottom ash	(Ashraf et al., 2019)	12.71 - 14.78	18.88 - 25.91	9.55 - 10.57	4.64 - 4.81	1.5**	1.75 - 1.81	1.53 - 2.09	0.88 - 1.16	1.87 - 2.17	1.44 - 1.46	25.73 - 27.025	
	Bottom ash	(Garcia-Lodeiro et al., 2016)	35.01	16.77	7.27	11.97	2.95	3.78	3.37 (Na_2O + K_2O)			2.45	2.9	
	Bottom ash	(Gao et al., 2017)	43.115	19.112	12.037	9.313	2.393	2.116	2.359	0.848	2.48	2.625	3.594	
	Bottom ash	(Pan et al., 2008)	50.39	13.44	1.26	8.84	1.79	2.26	12.66	1.78	2.36	3.19	9.68	
	Boiler ash	(Ashraf et al., 2019)	18.31 - 20.31	10.05 - 18.28	4.1 - 14.47	2.19 - 2.30	4.9 - 27.2**	1.57 - 6.73	8.83 - 12.66	2.21 - 6.52	1.69 - 1.76	1.4 - 3.50	5.72 - 6.30	
	Fly ash	(Pan et al., 2008)	45.42	13.60	0.92	3.83	6.27	3.16	4.16	3.85	3.12	1.72	13.22	
	Fly ash	(Sarmiento et al., 2019)	34.2 - 54.9	3.93 - 15.6	1.51 - 3.72	0.12 - 2.23	5.54 - 13.3	0.98 - 5.81	3.53 - 4.65	2.28 - 2.40	0.41 - 0.95	0.49 - 1.11	10.35 - 20.49	
	Fly ash	(Garcia-Lodeiro et al., 2016)	37.34	2.54	1.15	0.43	5.10	0.97	10.37 (Na_2O + K_2O)			0.52	13.8	
	Fly ash	(Saikia et al., 2007)	13.86	12.01	8.10	1.21	4.6**	2.62	17.19	7.41			23.51	
	Combined ash	(Sarmiento et al., 2019)	24.4 - 38.3	18.8 - 34.9	5.15 - 9.57	3.21 - 10.4	1.69 - 5.15	1.44 - 2.98	2.62 - 4.49	1.05 - 1.66	0.84 - 1.31	0.82 - 1.79	3.61 - 9.75	

MSW = Municipal solid waste; CW = Commercial waste; MSWI = Municipal solid waste incineration.
* Other constituents may include total C, Cl, BaO, Cr_2O_3, Mn_2O_3 or MnO, SrO, ZnO, etc.
** calculated from total S or SO_4^{2-}.

Table 4
Results from own investigations of ash composition, ash content, dry mass, heating value, and calculated R-index (4 main components) of SRF "secondary" and "primary".

Sample	Ash composition [wt%, 950 °C]																	
	CaO	SiO_2	Al_2O_3	Fe_2O_3	SO_3	MgO	Na_2O	K_2O	TiO_2	P_2O_5	Sum of all measured oxides	Sum CaO + SiO_2 + Al_2O_3 + Fe_2O_3	Ash 550 °C [$\%_{DM}$]	Ash 815 °C [$\%_{DM}$]	Ash 950 °C [$\%_{DM}$]	LHV [MJ/kg_{DM}]	Dry mass 105 °C [wt %]	R-Index (4 main components)
Secondary 1	26.6	33.7	6.6	5.0	5.6	3.1	2.8	2.7	4.5	1.5	92.2	71.9	16.4	15.7	15.6	23.8	76.7	11.2
Secondary 2	18.6	42.7	7.0	2.5	7.6	2.9	1.4	1.6	0.9	0.9	86.2	70.9	24.9	21.5	21.0	18.2	68.6	14.9
Secondary 3	22.1	38.1	11.2	3.0	6.7	3.0	1.9	1.7	1.8	0.9	90.2	74.4	16.6	13.4	14.0	18.0	69.7	10.4
Secondary 4	30.9	34.7	11.2	7.6	5.6	2.0	2.0	1.4	2.0	2.2	99.7	84.4	10.4	8.5	7.9	21.5	66.3	6.7
Secondary 5	21.8	36.4	10.4	3.3	6.4	3.0	1.9	1.5	2.2	1.8	88.9	72.0	15.1	12.9	12.5	18.5	66.1	9.0
Secondary 6	32.0	37.4	9.0	6.6	5.5	2.8	1.5	1.3	1.3	1.6	99.0	85.0	17.2	14.2	14.5	20.3	68.3	12.3
Secondary 7	22.9	35.9	13.1	2.1	5.6	2.3	2.4	2.0	2.2	1.0	89.4	74.0	12.1	11.0	10.4	23.1	74.8	7.7
Secondary 8	25.4	28.3	6.0	8.8	4.6	3.0	1.8	1.3	1.9	0.7	81.7	68.5	18.3	16.7	16.5	26.0	77.5	11.3
Secondary 9	26.5	26.5	11.6	3.5	6.8	2.8	1.0	1.1	0.9	0.5	81.2	68.2	28.5	21.6	21.3	16.8	80.5	14.5
Secondary 10	19.2	30.5	7.2	5.4	6.8	5.4	2.0	1.7	1.8	1.0	81.0	62.3	12.6	11.4	11.3	29.1	77.0	7.0
Secondary 11	22.0	31.5	12.1	12.1	7.5	3.3	0.6	0.5	2.9	0.5	93.1	77.7	17.0	13.2	12.1	21.6	83.0	9.4
Secondary 12	27.5	35.8	10.2	11.2	5.7	2.7	1.6	1.6	1.9	0.3	98.6	84.7	22.6	19.5	19.2	18.7	83.8	16.3
Secondary 13	20.7	38.0	9.8	3.5	9.2	2.9	2.3	1.8	1.4	0.8	90.3	72.0	19.4	16.1	16.3	21.6	86.8	11.7
Secondary 14	32.5	27.2	11.5	3.6	7.6	2.4	1.1	1.4	2.3	0.5	90.2	74.9	17.8	14.5	15.4	21.9	82.1	11.6
Secondary 15	23.6	36.5	12.2	6.9	8.8	2.5	1.4	1.4	2.4	0.6	96.4	79.1	21.7	18.4	18.4	19.7	74.2	14.6
Secondary 16	24.7	33.4	6.6	4.1	10.7	3.0	1.3	1.5	1.5	0.7	87.4	68.9	18.8	15.6	16.1	17.7	83.1	11.1
Secondary 17	36.6	27.8	14.0	4.3	3.8	2.7	1.1	0.7	2.1	1.7	94.9	82.7	15.2	13.4	13.2	22.1	79.4	10.9
Secondary 18	31.2	35.0	6.8	2.9	9.4	3.3	2.8	2.1	1.6	0.9	96.0	75.9	19.9	16.2	15.8	23.7	68.5	12.0
Secondary 19	22.1	33.4	15.2	3.9	3.4	2.5	2.4	2.0	1.3	0.8	87.0	74.6	18.9	17.0	17.2	20.4	65.0	12.9
Secondary 20	20.0	57.7	6.5	2.8	3.0	2.4	2.5	1.9	0.8	0.3	97.8	87.0	31.7	30.6	30.2	15.6	66.1	26.3
Secondary 21	33.2	27.1	7.3	5.1	6.6	3.5	1.9	1.7	3.5	0.7	90.6	72.7	16.1	12.3	12.8	29.1	74.7	9.3
Secondary 22	22.5	44.8	12.8	5.3	4.1	3.6	1.5	1.8	1.3	0.8	98.4	85.4	34.1	25.5	25.0	17.9	*	21.3
Secondary 23	27.9	36.1	11.7	5.6	5.8	3.8	1.9	1.9	1.2	0.6	96.4	81.3	29.3	27.8	27.0	17.5	*	22.0
Secondary 24	26.3	39.6	10.3	4.6	4.9	3.7	1.5	1.6	1.3	0.7	94.5	80.9	32.9	28.9	27.2	19.0	*	22.0
Secondary 25	27.5	42.0	12.4	6.4	3.5	3.3	1.9	1.7	2.0	0.8	101.6	88.3	25.3	24.6	24.1	19.3	*	21.3
Secondary 26	21.5	40.2	13.9	4.2	3.0	3.1	1.8	1.7	1.1	0.6	90.9	79.7	32.3	30.5	30.1	18.6	*	24.0
Secondary 27	25.0	41.8	16.0	4.9	3.5	4.0	1.4	1.6	1.5	0.6	100.4	87.7	25.9	23.4	23.2	19.7	*	20.4
Secondary 28	25.9	33.4	13.5	4.8	3.0	4.3	1.9	2.3	2.2	1.3	92.6	77.6	19.2	16.5	15.2	21.9	71.5	11.8
Secondary 29	26.4	35.0	13.9	5.0	4.6	3.5	1.4	1.8	1.9	1.0	94.4	80.2	19.6	16.9	16.2	21.5	74.8	13.0
Secondary 30	31.4	28.4	9.0	4.0	5.7	4.4	1.4	1.2	2.7	1.0	89.3	72.9	14.6	12.3	12.4	23.4	80.9	9.0
Primary 1	34.5	33.1	10.1	3.2	6.3	4.1	2.3	1.2	1.4	0.5	96.6	80.9	12.3	11.0	11.5	22.9	82.6	9.3
Primary 2	29.2	27.4	7.4	2.8	4.3	4.3	0.6	2.0	4.2	0.5	82.7	66.8	12.8	10.6	10.0	23.1	*	6.7
Primary 3	22.7	37.5	8.3	2.3	4.2	2.6	3.3	1.9	1.2	0.4	84.4	70.8	15.8	12.6	11.6	22.8	85.2	8.2
Primary 4	20.7	48.6	7.2	2.3	3.7	2.4	2.6	1.5	0.8	0.3	89.9	78.7	25.5	23.4	18.3	18.6	77.0	14.4
Primary 5	34.3	30.5	8.9	2.7	6.5	2.4	0.7	1.0	1.8	1.3	90.0	76.3	22.1	19.4	17.3	21.2	81.3	13.2
Primary 6	32.4	26.5	10.4	1.8	3.3	1.8	2.3	4.2	1.1	1.8	85.6	71.1	26.3	19.4	16.7	20.6	82.5	11.9
Primary 7	28.5	29.9	6.5	2.4	3.6	1.7	2.8	2.8	1.1	1.3	80.5	67.3	22.2	18.6	17.6	18.3	81.3	11.8
Primary 8	31.4	27.0	7.8	2.3	6.6	3.3	2.6	2.2	0.9	0.6	84.5	68.5	29.2	26.4	24.1	17.9	80.2	16.5
Primary 9	35.7	27.9	7.2	2.7	7.7	4.0	0.9	1.2	1.5	0.6	89.3	73.5	28.2	20.6	20.7	21.5	80.1	15.2
Primary 10	33.6	26.2	7.0	2.4	5.6	4.0	3.0	2.4	1.5	0.5	86.2	69.1	30.6	29.1	27.0	17.0	74.9	18.7
Primary 11	32.1	28.1	6.0	2.0	7.8	4.4	3.3	2.9	1.1	0.5	88.0	68.1	29.8	27.8	24.8	16.6	72.7	16.9
Primary 12	31.3	27.7	6.6	2.3	7.4	3.7	2.9	2.4	1.3	0.7	86.3	68.0	29.3	23.9	22.3	18.6	82.7	15.1
Primary 13	33.1	26.7	6.3	2.5	6.2	3.8	1.9	2.0	1.2	0.5	84.2	68.6	33.2	29.9	24.3	18.2	80.0	16.7
Primary 14	34.3	28.4	17.0	2.7	8.2	4.3	1.3	1.6	1.6	1.9	101.3	82.4	21.9	20.3	17.6	20.7	72.0	14.5
Primary 15	32.9	27.9	7.6	6.8	7.6	3.3	1.3	1.7	2.7	0.9	92.6	75.1	26.5	22.2	22.1	16.5	81.8	16.6
Primary 16	26.3	30.7	10.5	3.1	5.8	5.4	1.5	1.9	1.5	2.2	88.9	70.6	32.0	28.2	26.8	15.5	77.9	18.9
Primary 17	29.4	37.2	6.7	2.2	8.5	3.8	3.8	2.8	1.4	0.8	96.5	75.5	20.6	17.5	17.4	21.1	*	13.1
Primary 18	36.9	29.4	11.1	3.3	9.1	3.1	0.9	1.3	1.9	0.4	97.4	80.7	23.2	19.4	19.1	20.6	*	15.4
Primary 19	30.3	12.8	31.0	1.3	3.4	1.7	0.5	0.6	4.5	0.5	86.7	75.5	17.5	16.0	16.1	26.1	*	12.1
Primary 20	25.6	32.5	11.3	4.2	6.3	7.1	1.7	2.5	1.4	3.3	95.8	73.6	25.3	24.3	23.1	19.1	*	17.0

(*continued on next page*)

Table 4 (*continued*)

Sample	Ash composition [wt%, 950 °C]																	
	CaO	SiO_2	Al_2O_3	Fe_2O_3	SO_3	MgO	Na_2O	K_2O	TiO_2	P_2O_5	Sum of all measured oxides	Sum CaO + SiO_2 + Al_2O_3 + Fe_2O_3	Ash 550 °C [$\%_{DM}$]	Ash 815 °C [$\%_{DM}$]	Ash 950 °C [$\%_{DM}$]	LHV [MJ/kg_{DM}]	Dry mass 105 °C [wt %]	R-Index (4 main components)
Primary 21	20.6	10.8	43.4	1.0	2.6	1.0	0.4	0.3	2.0	0.2	82.4	75.7	16.2	12.7	12.7	24.8	*	9.6
Primary 22	36.4	29.1	13.2	2.3	6.0	3.0	1.4	1.6	2.0	0.6	95.7	81.0	14.9	12.7	12.8	23.1	*	10.4
Primary 23	31.5	33.0	9.7	2.9	6.5	3.1	1.1	1.2	2.0	0.4	91.3	77.0	23.7	20.9	20.6	20.7	*	15.9
Primary 24	37.4	32.4	7.8	2.5	6.1	3.3	1.7	1.6	1.1	0.6	94.3	80.0	20.5	18.0	17.8	20.4	*	14.2
Primary 25	26.4	20.0	34.2	1.4	4.0	1.2	0.5	0.7	3.3	0.4	92.1	82.0	17.8	14.5	14.6	25.6	*	12.0
Primary 26	37.1	35.5	9.5	2.6	6.5	3.1	1.0	1.3	2.0	0.5	99.1	84.7	20.5	18.8	17.9	23.0	*	15.2
Primary 27	32.5	30.3	23.2	0.9	3.6	0.7	0.4	0.4	2.0	0.1	94.1	86.9	36.0	29.4	29.4	21.1	*	25.6
Primary 28	28.1	34.9	8.1	4.6	4.8	3.0	1.2	1.2	2.3	0.3	88.7	75.8	25.6	21.4	21.5	21.5	72.9	16.3
Primary 29	36.4	32.6	10.8	2.6	0.6	0.3	1.0	1.2	1.9	0.5	88.0	82.4	20.2	17.0	16.4	22.5	90.9	13.5
Primary 30	33.3	18.5	35.9	1.4	4.0	1.9	0.7	0.9	4.2	0.3	101.0	89.0	17.7	14.9	14.3	25.9	83.0	12.7
Primary 31	32.3	25.1	17.6	3.4	4.1	2.4	1.5	1.2	4.1	1.5	93.2	78.4	9.3	8.0	8.1	29.4	*	6.4
Primary 32	29.5	24.3	21.1	2.9	3.2	2.2	1.1	1.2	4.4	1.2	91.0	77.8	9.7	8.5	8.5	27.4	*	6.6
Primary 33	25.7	28.1	30.2	2.0	2.3	1.6	1.8	1.7	3.0	1.2	97.5	86.0	12.0	11.4	11.4	25.7	*	9.8
Primary 34	21.3	33.4	26.0	2.1	2.0	1.5	3.0	2.5	2.6	1.0	95.3	82.7	14.8	13.3	13.0	24.5	*	10.8
Primary 35	32.0	29.1	11.6	3.3	4.8	2.4	1.8	1.7	1.8	1.1	89.6	76.0	15.6	15.2	13.4	22.7	*	10.2
Primary 36	22.2	31.1	5.7	2.9	9.2	5.4	0.9	1.0	1.4	0.8	80.6	61.9	29.1	21.1	21.0	15.7	84.7	13.0
Primary 37	24.4	39.6	6.5	2.6	6.4	2.6	2.2	2.0	0.8	0.6	87.7	73.1	33.4	30.8	28.7	15.8	79.1	21.0
Primary 38	26.0	21.9	31.7	2.4	2.7	2.1	1.0	1.3	4.8	0.8	94.6	81.9	9.9	8.3	8.6	28.6	*	7.0
Primary 39	27.0	27.0	28.0	2.6	2.6	2.3	1.2	0.8	6.4	0.8	98.8	84.6	11.6	10.5	10.2	27.5	*	8.6
Primary 40	23.5	25.4	31.4	4.5	2.3	2.2	1.3	1.6	4.9	0.7	97.8	84.8	9.8	9.0	9.0	31.0	*	7.6
Primary 41	25.4	23.5	23.9	4.4	2.0	2.3	1.0	10.3	0.6	0.8	94.1	77.1	9.9	9.0	8.9	29.9	*	6.9
Primary 42	31.4	29.3	23.4	2.0	2.5	1.8	1.6	1.4	2.3	1.1	96.6	86.1	10.6	9.4	9.3	26.4	*	8.0
Primary 43	27.5	20.8	32.5	2.1	2.7	2.6	0.8	0.7	1.6	0.9	92.3	83.0	8.5	7.1	7.2	31.9	*	6.0
Primary 44	35.8	29.8	5.6	2.7	8.6	5.1	0.9	1.0	1.4	0.7	91.5	73.8	27.5	23.4	24.0	16.5	85.4	17.7
Primary 45	34.6	29.5	6.5	2.4	10.0	4.3	1.1	1.1	1.6	0.9	91.9	73.0	26.2	23.3	20.8	18.5	88.0	15.2
Primary 46	32.1	33.2	7.4	2.1	8.2	3.6	1.3	1.3	1.4	0.6	91.1	74.8	30.2	25.9	26.1	17.1	88.4	19.5
Primary 47	33.8	27.1	7.6	2.2	10.7	3.7	1.5	1.5	1.4	0.5	90.1	70.7	28.6	25.9	25.8	16.9	90.6	18.3
Primary 48	41.0	20.5	8.7	7.1	5.8	2.5	1.0	0.6	2.9	1.3	91.4	77.4	11.2	9.6	9.3	21.3	94.0	7.2
Primary 49	23.6	40.6	12.7	2.2	6.5	4.3	2.0	1.8	2.3	0.5	96.4	79.0	23.2	19.6	18.8	21.8	90.6	14.9
Primary 50	21.1	39.9	10.6	2.3	7.6	4.0	2.2	1.3	2.4	0.3	91.6	73.9	31.3	29.6	29.0	19.2	91.2	21.4
Average Secondary	25.8	35.6	10.6	5.1	5.8	3.2	1.7	1.6	1.9	0.9	92.3	77.2	20.8	18.0	17.7	20.9	75.0	13.9
Std. dev. Secondary	4.6	6.5	2.9	2.3	2.0	0.7	0.5	0.4	0.8	0.5	5.6	6.7	6.5	6.1	5.9	3.3	6.6	5.4
RSD [%] Secondary	17.8	18.1	27.1	46.1	35.1	22.5	29.9	26.6	42.1	49.8	6.1	8.6	31.4	33.8	33.3	15.7	8.8	38.8
Min Secondary	18.6	26.5	6.0	2.1	3.0	2.0	0.6	0.5	0.8	0.3	81.0	62.3	10.4	8.5	7.9	15.6	65.0	6.7
Median Secondary	25.7	35.4	11.2	4.7	5.7	3.0	1.8	1.7	1.9	0.8	92.4	76.8	19.1	16.4	16.2	20.4	74.8	11.9
80^{th} percentile Secondary	31.1	39.9	13.3	6.5	7.6	3.7	2.2	1.9	2.3	1.2	98.1	84.6	27.2	24.0	23.7	23.3	82.1	20.9
Max Secondary	36.6	57.7	16.0	12.1	10.7	5.4	2.8	2.7	4.5	2.2	101.6	88.3	34.1	30.6	30.2	29.1	86.8	26.3
Average Primary	30.1	29.0	14.8	2.7	5.4	3.0	1.6	1.7	2.2	0.8	91.3	76.6	21.2	18.4	17.6	21.9	82.6	13.3
Std. dev. Primary	5.1	6.7	10.2	1.2	2.4	1.3	0.9	1.4	1.3	0.6	5.2	6.2	7.9	6.9	6.4	4.3	6.0	4.5
RSD [%] Primary	17.0	23.0	68.9	43.1	44.4	43.8	54.0	83.0	58.5	69.9	5.7	8.0	37.1	37.8	36.4	19.5	7.3	34.2
Min Primary	20.6	10.8	5.6	0.9	0.6	0.3	0.4	0.3	0.6	0.1	80.5	61.9	8.5	7.1	7.2	15.5	72.0	6.0
Median Primary	31.4	29.1	10.3	2.5	5.8	3.0	1.3	1.5	1.8	0.6	91.5	76.2	22.0	19.1	17.6	21.3	82.5	13.4
80^{th} percentile Primary	34.4	33.2	25.0	3.2	7.7	4.1	2.3	2.1	3.0	1.2	96.5	82.4	29.2	25.1	24.1	25.8	88.4	16.8
Max Primary	41.0	48.6	43.4	7.1	10.7	7.1	3.8	10.3	6.4	3.3	101.3	89.0	36.0	30.8	29.4	31.9	94.0	25.6
Average (all samples)	28.5	31.5	13.2	3.6	5.6	3.1	1.6	1.7	2.1	0.8	91.7	76.8	21.0	18.2	17.6	21.5	79.0	13.5
Std. dev. (all samples)	5.3	7.3	8.5	2.1	2.3	1.1	0.7	1.2	1.1	0.5	5.4	6.3	7.4	6.6	6.2	3.9	7.3	4.8

(*continued on next page*)

Table 4 (*continued*)

Sample	Ash composition [wt%, 950 °C]									Sum of all measured oxides	Sum CaO + SiO_2 + Al_2O_3 + Fe_2O_3	Ash 550 °C [$\%_{DM}$]	Ash 815 °C [$\%_{DM}$]	Ash 950 °C [$\%_{DM}$]	LHV [MJ/kg_{DM}]	Dry mass 105 °C [wt %]	R-Index (4 main components)
	CaO	SiO_2	Al_2O_3	Fe_2O_3	SO_3	MgO	Na_2O	K_2O	TiO_2	P_2O_5								
RSD [%] (all samples)	18.7	23.2	63.9	57.0	40.7	36.6	45.5	68.9	54.7	62.0	5.8	8.2	34.9	36.2	35.0	18.3	12.1	35.9
Min (all samples)	18.6	10.8	5.6	0.9	0.6	0.3	0.4	0.3	0.6	0.1	80.5	61.9	8.5	7.1	7.2	15.5	65.0	6.0
Median (all samples)	28.0	30.6	10.5	2.9	5.7	3.0	1.5	1.6	1.8	0.7	91.6	76.2	20.4	17.3	17.0	21.2	80.1	13.0
80^{th} percentile (all samples)	33.3	36.9	16.5	4.9	7.6	4.0	2.3	2.0	2.7	1.2	96.6	82.7	28.9	24.5	24.1	24.7	84.3	17.0
Max (all samples)	41.0	57.7	43.4	12.1	10.7	7.1	3.8	10.3	6.4	3.3	101.6	89.0	36.0	30.8	30.2	31.9	94.0	26.3
Limit of quantification	*0.2*	*0.3*	*0.2*	*0.2*	*0.3*	*0.2*	*0.2*	*0.2*	*0.2*	*0.3*								

* Reference samples, received in dry state.

%), and higher variabilities were mostly observed in ashes of SRF "primary", especially for Al_2O_3 and K_2O. However, it has to be taken into account that the number of samples for SRF "primary" was higher as well.

The numbers that are given in Fig. 1 and Table 4 were not normalized to 100 %. On average, summing up all analyzed oxides, 91.7 % of the ash content was recovered. Although theoretically the sum of all oxides should range close to 100 %, deviations from the total ash content can readily be explained by the measurement uncertainty and the fact that the analysis was limited to the 10 elements with the highest relevance. As the samples were ashed at 950 °C, carbonates are not expected to be present anymore (for more details, please refer to Aldrian et al. (2020)).

On average, 77.2 ± 6.7 $wt\%_{DM}$ of SRF "secondary" ash and 76.6 ± 6.2 $wt\%_{DM}$ of SRF "primary" ash consist of SiO_2, CaO, Al_2O_3, and Fe_2O_3, the four main chemical components that are considered as primary raw materials for the production of cement clinker (compare Section 2.1). This implies that similar to MSWI ash (compare Section 2.2), SRF ash can - to some degree - substitute these raw materials. Fig. 2 shows a comparison of the ratio of SiO_2, CaO, and Al_2O_3 + Fe_2O_3 of the 80 investigated SRF ashes with those of the ashes of other fuels (e.g. lignite coal) as well as alternative raw materials and cement clinker. Based on their composition, most of the 80 analyzed SRF ashes are located between cement clinker and lignite coal, often featuring a higher share of CaO which shifts them closer towards the SiO_2 : CaO : Al_2O_3 + Fe_2O_3 ratio that is desired for clinker. Other samples, especially SRF "primary" ashes, show a composition that is rather similar to sewage sludge, but some feature a higher share of Al_2O_3 + Fe_2O_3. Most samples, however, are located in the area between approx. 25–50 % CaO, 10–25 % Al_2O_3 + Fe_2O_3, and 35–55 % of SiO_2.

4.2. Calculation of R-indices

There are several possibilities to calculate the R-indices, which is why a discussion about the role of the different ash constituents in the cement industry is required. One option is to count only SiO_2, CaO, Al_2O_3, and Fe_2O_3 as recycled since they undoubtedly represent main raw materials for cement clinker. On average, these four compounds amount for 77.2 % (secondary) and 76.6 % (primary) of the SRF ash. Taking the ash content into account, in this case, the average R-index is 13.9 % (secondary) or 13.3 % (primary), and this percentage of the SRF that is co-processed could be considered as recycled.

As the ash analyses show, SRF ashes also constitute of other chemical compounds that are frequently present in natural raw materials or cement clinker phases and confer its specific properties to cement clinker. These minerals could be counted towards the R-index as well. Examples include MgO and TiO_2, both of which are minor constituents of portland cement clinker, Na_2O or K_2O which commonly occur in feldspars (compare Section 2.1), and SO_3 which is added to bind Na_2O or K_2O and form alkali sulfates. In contrast to feldspars, the results presented in this paper show that the SRF ash already provides all sulfur that is necessary to formally transform the alkali oxides present in the SRF ash into alkali sulfates (S: 0.69 mol/kg, Na: 0.51 mol/kg, K: 0.36 mol/kg, forming 0.26 mol/kg Na_2SO_4 and 0.18 mol/kg K_2SO_4). The excess sulfur could theoretically transform alkali metals originating from primary raw materials to sulfates. Counting these five oxides as well would increase the R-indices by 2.3 % (i.e. in total 16.2 % for secondary) or 2.6 % (i.e. in total 15.9 % for primary), respectively.

The possibility that leads to the highest R-indices is to set the R-index equal with the ash content, as reported by the European Cement Research Academy (ECRA) (2016). This approach is based on the fact that the whole ash, and not only specific minerals, are technically incorporated into the clinker. For the SRF samples that were investigated and are presented in this paper this would result in shares of 17.7 % (secondary) and 17.6 % (primary) of the SRF that can be considered as recycled on a material level. As these percentages also contain

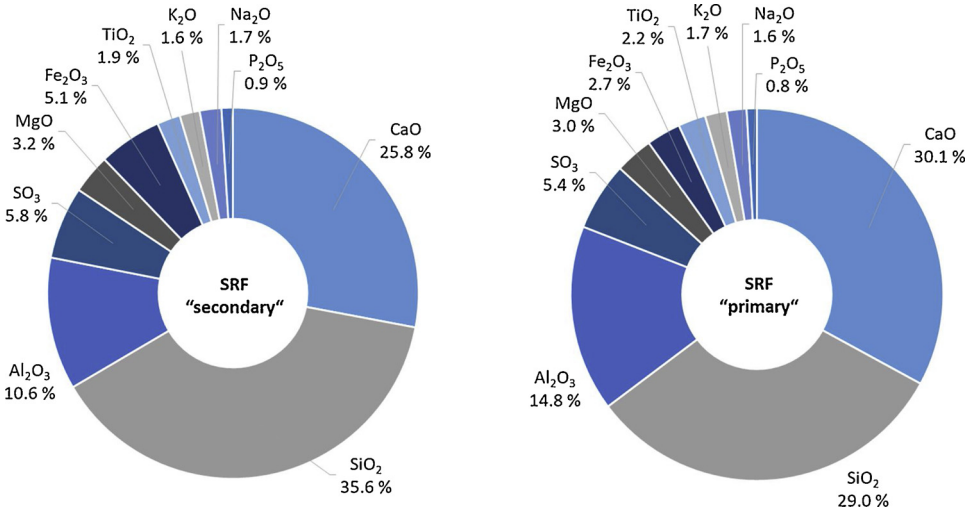

Fig. 1. Results from own investigations: Average ash composition (arithmetic means) of the SRF ashes of SRF for secondary firing ($n = 30$) and SRF for primary firing ($n = 50$) in mass percent dry mass ($wt\%_{DM}$); percentages are not normalized to 100 %.

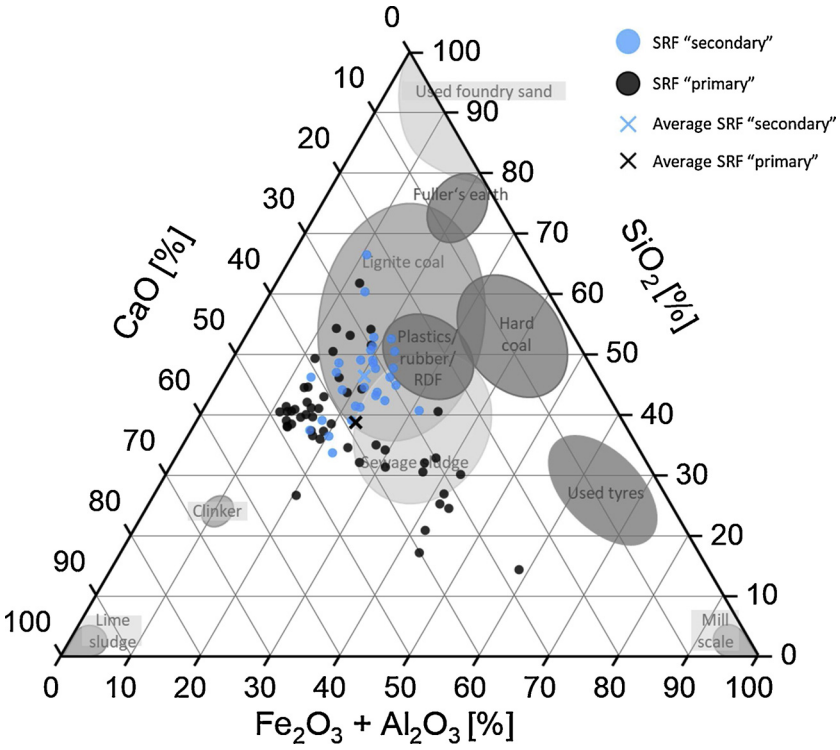

Fig. 2. Comparison of the SRF ash composition of 80 investigated SRF samples and their average values with other fuels and raw materials relevant to the cement industry. Ternary diagram reproduced from Verein Deutscher Zementwerke e.V. (vdz), 2019a and extended with results from own investigations on SRF ash composition.

significant amounts of oxygen, an important point of discussion in this regard is whether or not there is enough oxygen present in the initial SRF samples to formally oxidize all the analytes. Considering the average moisture content of the samples of 17.4 % (Table 3), the amount of inorganic carbon in the samples when ashed at lower temperatures (Aldrian et al., 2020), and the oxygen content of 17.8 % that was reported by Nasrullah et al. (2014) for SRF from commercial and industrial waste, it is very likely that formally there is enough oxygen present to form the oxides that are counted towards the R-index.

Hence, depending on the interpretation of the term "materials recycling" and the roles that are attributed to the ash constituents, possible average R-indices for the researched SRF samples can range anywhere between 13.3 % and 17.7 %.

4.3. Potential contribution of the cement industry towards recycling

The data obtained in the present investigations allows for the calculation of the potential contribution of the cement industry towards recycling and the EU recycling targets (e.g. for MSW). This contribution will differ depending on the thermal substitution rate, and the share of SRF that is used in the cement industry in every single country. With the new EU recycling targets, new calculation methods were introduced as well, and up to now there are only estimates about how these new calculations will influence the recycling quota in every single country in detail, but additional recycling will most likely be required to reach the targets (Obermeier and Lehmann, 2019).

Table 5 shows the cement industry's potential contribution towards recycling in Austria and Germany using three different ways to calculate the R-index to model 3 scenarios. In the case of Austria, the

Table 5
Potential contribution of the cement industry towards recycling in Austria and Germany with differently calculated R-indices.

Parameter	Austria	Germany
Total MSW generated [t/a] 2017	4,322,000 (Bundesministerium für Nachhaltigkeit und Tourismus, 2019)	51,790,000 (Statistisches Bundesamt Deutschland, 2019)
SRF used in cement plants [t/a] 2018	358,580 (Mauschitz, 2019)	2,256,000 (Verein Deutscher Zementwerke e.V. (vdz), 2019b)
Scenario 1:		
$R-index=\frac{AC}{100}\cdot(w_{SiO_2}+w_{CaO}+w_{Al_2O_3}+w_{Fe_2O_3})$	13.3	13.3
Contribution (recycled material) [t/a]	47,691	300,048
Contribution [% referring to total annual MSW generation]	1.10 %	0.58 %
Scenario 2:		
$R-index=\frac{AC}{100}\cdot(w_{SiO_2}+w_{CaO}+w_{Al_2O_3}+w_{Fe_2O_3}+w_{MgO}+w_{TiO_2}+w_{SO_3}+w_{Na_2O}+w_{K_2O})$	15.9	15.9
Contribution (recycled material) [t/a]	57,014	358,704
Contribution [% referring to total annual MSW generation]	1.32 %	0.69 %
Scenario 3:		
$R-index=AC$	17.4	17.4
Contribution (recycled material) [t/a]	62,393	392,544
Contribution [% referring to total annual MSW generation]	1.44 %	0.76 %

contribution ranges between 1.10 and 1.44 % of the total annual MSW generation. In Germany, the contribution is about half as large, ranging between 0.58 and 0.76 %. However, a major part of the SRF that is used in Germany is currently listed as originating from industrial and commercial waste (Verein Deutscher Zementwerke e.V. (vdz), 2019b). For Austria, no similar distinction for SRF exists, as it is simply referred to as “plastics waste” in the document listing the amounts of RDF that is used in the cement industry (Mauschitz, 2019). For this reason, the calculated contributions of the cement industry in Austria need to be split and attributed to the respective waste streams (i.e. packaging, MSW, commercial and industrial waste), and then could be counted towards the corresponding recycling targets (e.g. targets for plastic packaging, total packaging waste, or MSW). At the moment, the ratio of these waste types among the waste that is processed to SRF is not apparent in the current balances of SRF production plants or publicly available documents.

Furthermore, imports or exports have to be taken into account. Depending on their geographic SRF production plants also frequently process imported waste fractions from neighboring countries, or cement production plants might import SRF from neighboring countries.

5. Conclusions

The investigation of 80 SRF (according to EN 15359) samples representing currently available qualities in Austria, Croatia, Slovakia, and Slovenia revealed that SRF ashes (combusted at 950 °C) on average are composed of 76.8 % of SiO_2, CaO, Al_2O_3, and Fe_2O_3, all of which represent important raw materials for cement clinker manufacturing. Another 14.1 % of the ash consists of chemical compounds that are common clinker phases and/or frequently present in primary raw materials for clinker production. As the ash as a whole is incorporated into the product portland cement clinker, it is concluded that 76.8%–100% of the SRF ash can be considered as recycled on a material level, which on average corresponds to 13.5–17.6 % of the SRF (referring to dry mass).

Acknowledging the contribution the cement industry could make towards recycling could support EU countries in which SRF co-processing is state of the art in achieving the EU CEP recycling targets. In countries with rather small thermal substitution rates, the acknowledgment could lead to a shift of waste streams from landfilling or conventional waste incineration towards co-processing and thereby lead to environmental benefits with less intensive investments (de Beer et al., 2017). Although the method applied in this paper was primarily developed for SRF, after minor testing it could be transferred to other RDF (e.g. waste tires, different plastics that are not subject to other recycling processes, etc.) in the future.

However, in order to assign the contribution to the right recycling targets, i.e. MSW or plastic packaging waste, the origin of waste streams entering SRF production plants and their ratio in the output SRF needs to be taken into consideration. This very likely requires additional regulations and record-keeping.

Declaration of Competing Interest

The authors declare no conflict of interest.

Acknowledgments

Partial funding for this work was provided by: The Center of Competence for Recycling and Recovery of Waste 4.0 (acronym ReWaste4.0) (contract number 860 884) under the scope of the COMET – Competence Centers for Excellent Technologies – financially supported by BMVIT, BMDW, and the federal state of Styria, managed by the FFG.

References

Aldrian, A., Viczek, S.A., Pomberger, R., Sarc, R., 2020. Methods for identifying the material-recyclable share of SRF during co-processing in the cement industry. under review. Methods X.
Aliapur, 2016. Rapport d’activité 2015.
Aliapur, 2019. Rapport d’activité 2018.
Ampadu, K.O., Torii, K., 2001. Characterization of ecocement pastes and mortars produced from incinerated ashes. Cem. Concr. Res. 31 (3), 431–436.
Ashraf, M.S., Ghouleh, Z., Shao, Y., 2019. Production of eco-cement exclusively from municipal solid waste incineration residues. Resour. Conserv. Recycl. 149, 332–342.
Assembleia da República Portugal, 2006. Regime geral da gestão de resíduos. Decreto-Lei n.º 178/2006 - Diário da República n.º 171/2006, Série I de 2006-09-05.
Assembleia da República Portugal, 2014. Lei n.º 82-D/2014 Diário da República n.º 252/2014, 2º Suplemento, Série I de 2014-12-31.
Austrian Standards Institute (ASI), 2007. ÖNORM EN 14346 Characterization of waste - Calculation of dry matter by determination of dry residue or water content. Vienna. .
Austrian Standards Institute (ASI), 2011a. ÖNORM EN 15442 Solid recovered fuels - Methods for sampling. Vienna. .
Austrian Standards Institute (ASI), 2011b. ÖNORM EN 15413 Solid recovered fuels – Methods for the preparation of the test sample from the laboratory sample. Vienna. .
Austrian Standards Institute (ASI), 2011c. ÖNORM EN 15443 Solid recovered fuels – Methods for the preparation of the laboratory sample. Vienna. .
Austrian Standards Institute (ASI), 2011d. ÖNORM EN 197-1 Cement - Part 1: Composition, specifications and conformity criteria for common cements. Vienna. .
Basel Convention, 2012. Technical Guidelines on the Environmentally Sound Co-processing of Hazardous Wastes in Cement Kilns.
Bundesministerium für Nachhaltigkeit und Tourismus, 2019. Die Bestandsaufnahme der Abfallwirtschaft in Österreich: Statusbericht 2019.
CIMPOR, 2016. Declaração ambiental 2015. Centro de produção de Souselas.
Clavier, K.A., Watts, B., Liu, Y., Ferraro, C.C., Townsend, T.G., 2019. Risk and performance assessment of cement made using municipal solid waste incinerator bottom ash as a cement kiln feed. Resour. Conserv. Recycl. 146, 270–279.
Collet, P., 2016. Déchets pneumatiques: le recyclage progresse en 2015 grâce à la

valorisation mixte en cimenterie. Environn Tech.(359).
de Beer, J., Cihlar, J., Hensing, I., Zabeti, M., 2017. Status and Prospects of Co-processing of Waste in EU Cement Plants: Executive Summary.
Dunnu, G., Maier, J., Scheffknecht, G., 2010. Ash fusibility and compositional data of solid recovered fuels. Fuel 89 (7), 1534–1540.
European Cement Research Academy (ECRA), 2016. Technical Report A-2016/1039 Evaluation of the Energy Performance of Cement Kilns in the Context of Co-processing.
European Commission (EC), 2008. Directive 2008/98/EC of the European Parliament and of the Council of 19 November 2008 on Waste and Repealing Certain Directives (waste Framework Directive).
European Commission (EC), 2013. Best Available Techniques (BAT) Reference Document for the Production of Cement, Lime and Magnesium Oxide.
European Commission (EC), 2018a. Directive (EU) 2018/852 of the European Parliament and of the Council of 30 May 2018 Amending Directive 94/62/EC on Packaging and Packaging Waste.
European Commission (EC), 2018b. Directive 2018/851 of the European Parliament and the Council of 30th May 2018 Amending Directive 2008/98/EC on Waste.
European Commission (EC), 2019. Commission Implementing Decision (EU) 2019/1004 of 7 June 2019 Laying Down Rules for the Calculation, Verification and Reporting of Data on Waste in Accordance With Directive 2008/98/EC of the European Parliament and of the Council and Repealing Commission Implementing Decision C(2012) 2384 (notified Under Document C(2019) 4114).
European Committee for Standardization (CEN), 2010. CEN/TS 15414-1 Solid Recovered Fuels - Determination of Moisture Content Using the Oven Dry Method - Part 1: Determination of Total Moisture by a Reference Method.
Galvez-Martos, J.-L., Schoenberger, H., 2014. An analysis of the use of life cycle assessment for waste co-incineration in cement kilns. Resour. Conserv. Recycl. 86, 118–131.
Gao, X., Yuan, B., Yu, Q.L., Brouwers, H.J.H., 2017. Characterization and application of municipal solid waste incineration (MSWI) bottom ash and waste granite powder in alkali activated slag. J. Clean. Prod. 164, 410–419.
Garcia-Lodeiro, I., Carcelen-Taboada, V., Fernández-Jiménez, A., Palomo, A., 2016. Manufacture of hybrid cements with fly ash and bottom ash from a municipal solid waste incinerator. Constr. Build. Mater. 105, 218–226.
German Institute for Standardization (DIN), 1998a. DIN EN ISO 11885 Water Quality - Determination of 33 Elements by Inductively Coupled Plasma Atomic Emission Spectroscopy.
German Institute for Standardization (DIN), 1998b. DIN 51729-11 Testing of Solid Fuels - Determination of Chemical Composition of Fuel Ash - Part 11: Determination by Inductively Coupled Plasma Emission Spectrometry (ICP-OES).
Hilber, T., Maier, J., Scheffknecht, G., Agraniotis, M., Grammelis, P., Kakaras, E., et al., 2007. Advantages and possibilities of solid recovered fuel cocombustion in the European energy sector. J. Air Waste Manage. Assoc. 57 (10), 1178–1189.
Holleman, A.F., Wiberg, E., Wiberg, N., 2007. Lehrbuch Der Anorganischen Chemie, 102nd ed. de Gruyter, Berlin.
Huntzinger, D.N., Eatmon, T.D., 2009. A life-cycle assessment of Portland cement manufacturing: comparing the traditional process with alternative technologies. J. Clean. Prod. 17 (7), 668–675.
Kara, M., 2012. Environmental and economic advantages associated with the use of RDF in cement kilns. Resour. Conserv. Recycl. 68, 21–28.
Krammart, P., Tangtermsirikul, S., 2004. Properties of cement made by partially replacing cement raw materials with municipal solid waste ashes and calcium carbide waste. Constr. Build. Mater. 18 (8), 579–583.
Kuna, M., 2015. Analysis of Thermal Conversion of Non-homogeneous Solid Recovered Fuels (Master's Thesis). https://fenix.tecnico.ulisboa.pt/downloadFile/1126295043833896/Dissertation.pdf [August 09, 2019].
Lafarge, 2019. Personal Message on Mixed Recovery of End-of-life-tires in Hungary. IPPC Permit Available. Email, 20.09.2019. .
Lam, C.H.K., Barford, J.P., McKay, G., 2011. Utilization of municipal solid waste incineration ash in Portland cement clinker. Clean Technol. Environ. Policy 13 (4), 607–615.
de Queiroz Lamas, W., Palau, J.C.F., Rubens de Camargo, J., 2013. Waste materials co-processing in cement industry: ecological efficiency of waste reuse. Renewable Sustainable Energy Rev. 19, 200–207.
Locher, F.W., 2000. Zement: Grundlagen der Herstellung und Verwendung, 1st ed. Verlag Bau + Technik s.l.
Lorber, K.E., Sarc, R., Aldrian, A., 2012. Design and quality assurance for solid recovered fuel. Waste Manag. Res. 30 (4), 370–380.
Mauschitz, G., 2019. Emissionen aus Anlagen der österreichischen Zementindustrie: Berichtsjahr 2018.
Nasrullah, M., Vainikka, P., Hannula, J., Hurme, M., Kärki, J., 2014. Mass, energy and material balances of SRF production process. Part 1: SRF produced from commercial and industrial waste. Waste Manag. 34 (8), 1398–1407.
Obermeier, T., Lehmann, S., 2019. Recyclingquoten - Wo stehen Deutschland, Österreich und die Schweiz mit dem neuen Rechenverfahren im Blick auf die EU-Ziele? In: Thiel, S., Holm, O., Thomé-Kozmiensky, E., Goldmann, D., Friedrich, B. (Eds.), Recycling und Rohstoffe - Band 12. Thomé-Kozmiensky Verlag GmbH, Neuruppin, pp. 85–98.
Országos Hulladékgazdálkodási Ügynökség (ÖHÜ), 2011. Országos gyűjtési és hasznosítási terv –2012. év. http://www.szelektivinfo.hu/images/regi/ogyht_1.pdf [September 25, 2019].
Pan, J.R., Huang, C., Kuo, J.-J., Lin, S.-H., 2008. Recycling MSWI bottom and fly ash as raw materials for Portland cement. Waste Manag. 28 (7), 1113–1118.
Pohl, M., Bernhardt, D., Beckmann, M., Spiegel, W., 2011. Brennstoffcharakterisierung zur vorausschauenden Bewertung des Korrosionsrisikos. In: Born, M. (Ed.), Dampferzeugerkorrosion 2011. Freiberg: SAXONIA Standortentwicklungs- und -verwaltungsgesellschaft mbH, pp. 67–83.
Reza, B., Soltani, A., Ruparathna, R., Sadiq, R., Hewage, K., 2013. Environmental and economic aspects of production and utilization of RDF as alternative fuel in cement plants: a case study of Metro Vancouver Waste Management. Resour. Conserv. Recycl. 81, 105–114.
Ribeiro, P., Costa, I., Nazareth, P., 2015. Co-processing - Material Recovery of Alternative Fuels in the Cement Industry: Technical Summary (English Version).
Saikia, N., Kato, S., Kojima, T., 2007. Production of cement clinkers from municipal solid waste incineration (MSWI) fly ash. Waste Manag. 27 (9), 1178–1189.
Samolada, M.C., Zabaniotou, A.A., 2014. Energetic valorization of SRF in dedicated plants and cement kilns and guidelines for application in Greece and Cyprus. Resour. Conserv. Recycl. 83, 34–43.
Sarc, R., 2015. Herstellung, Qualität und Qualitätssicherung von Ersatzbrennstoffen zur Erreichung der 100%-igen thermischen Substitution in der Zementindustrie. Dissertation.
Sarc, R., Kandlbauer, L., Lorber, K.E., Pomberger, R., 2019a. Production and characterisation of SRF premium quality from municipal and commercial solid non-hazardous wastes in Austria, Croatia, Slovenia and Slovakia. Detritus 1 In Press.
Sarc, R., Lorber, K.E., Pomberger, R., Rogetzer, M., Sipple, E.M., 2014. Design, quality, and quality assurance of solid recovered fuels for the substitution of fossil feedstock in the cement industry. Waste Manag. Res. 32 (7), 565–585.
Sarc, R., Seidler, I.M., Kandlbauer, L., Lorber, K.E., Pomberger, R., 2019b. Design, Quality and Quality Assurance of Solid Recovered Fuels for the Substitution of Fossil Feedstock in the Cement Industry – Update 2019. Waste Manag. Res. 37 (9), 885–897.
Sarmiento, L.M., Clavier, K.A., Paris, J.M., Ferraro, C.C., Townsend, T.G., 2019. Critical examination of recycled municipal solid waste incineration ash as a mineral source for Portland cement manufacture – a case study. Resour. Conserv. Recycl. 148, 1–10.
Scheffer, F., Schachtschabel, P., Blume, H.-P., 2008. Lehrbuch Der Bodenkunde, 15th ed. Spektrum Akad. Verl, Heidelberg.
Scur, P., 2013. Mineralische Sekundärrohstoffe für die Verwertung in der Zementindustrie - Anforderungen an die Qualität. In: Thomé-Kozmiensky, K.J. (Ed.), Aschen, Schlacken, Stäube aus Abfallverbrennung und Metallurgie. TK Verlag Karl Thomé-Kozmiensky, Neuruppin.
Shih, P.-H., Chang, J.-E., Chiang, L.-C., 2003. Replacement of raw mix in cement production by municipal solid waste incineration ash. Cem. Concr. Res. 33 (11), 1831–1836.
Statistisches Bundesamt Deutschland, 2019. Abfallbilanz 2017. https://www.destatis.de/DE/Themen/Gesellschaft-Umwelt/Umwelt/Abfallwirtschaft/Tabellen/liste-abfallbilanz-kurzuebersicht.html [September 18, 2019].
Verein Deutscher Zementwerke e.V. (vdz), 2002. Zement-Taschenbuch 2002, 50th ed. .
Verein Deutscher Zementwerke e.V. (vdz), 2018. Environmental Data of the German Cement Industry 2017.
Verein Deutscher Zementwerke e.V. (vdz), 2019a. Personal Message on Ternary Diagram With Fuel Ash Composition. Email, 14.05.2019. .
Verein Deutscher Zementwerke e.V. (vdz), 2019b. Environmental Data of the German Cement Industry 2018.
Viczek, S.A., Aldrian, A., Pomberger, R., Sarc, R., 2019a. Analytical determination of recycling quota through SRF co-processing in the cement industry. In: Proceedings of the Heraklion 2019 7th International Confrerence on Sustainable Solid Waste Management. 26–29 June 2019. . Accessible Online: http://uest.ntua.gr/heraklion2019/proceedings/pdf/HERAKLION2019_Viczek_etal.pdf.
Viczek, S.A., Aldrian, A., Pomberger, R., Sarc, R., 2019b. Analytical Determination of the Material-recyclable Share of SRF Through Co-processing in the Cement Industry - Comparison of Ashing Temperatures. Proceedings of the 17th International Waste Management and Landfill Symposium. 30 Sept - 04 Oct 2019. Santa Margherita di Pula, Italy.
Vodegel, S., Davidovic, M., Ludewig, A., 2018. Differenzierung der energetischen Verwertung am Kriterium der Energieeffizienz. In: Thiel, S., Thomé-Kozmiensky, E., Quicker, P., Gosten, A. (Eds.), Energie aus Abfall: Band 15, pp. 761–768.
Wagland, S.T., Kilgallon, P., Coveney, R., Garg, A., Smith, R., Longhurst, P.J., et al., 2011. Comparison of coal/solid recovered fuel (SRF) with coal/refuse derived fuel (RDF) in a fluidised bed reactor. Waste Manag. 31 (6), 1176–1183.

4 SUMMARY AND DISCUSSION

Inorganic contaminants are present in several materials and products because heavy metals or metalloids are frequently applied in the industrial production of numerous consumer goods, see section 4.1. When these products reach the end of their life cycle, these contaminants end up in waste, for example, MSW or MCW, where they can become an issue for waste treatment options, including SRF co-processing. At the same time, ash forming elements added to various materials or products as fillers or pigments may represent valuable chemical compounds for the cement industry. Not all of the materials identified as contaminant carriers can readily be removed by technological means yet, but commonly applied technologies, e.g., Fe and non-Fe separators, NIR or other optical sorters, and mechanical screening may be suitable for removing contaminant carriers and reducing contaminant concentrations in the produced SRF, thereby improving SRF quality.

To improve SRF quality with respect to contaminants, the contaminant concentrations need to be determined first. This process may include some obstacles that require thorough consideration. For example, because of the common laboratory practice of removing hard impurities (e.g., stones, metal parts), only accounting for them in terms of weight, and assuming a concentration of zero, not all contaminant carriers may be reflected in the analytical results. The removal of hard impurities is required to avoid damage to the mills, and their amounts are often insufficient to be processed separately. For this reason, in the publications presented in this Thesis, hard impurities are removed, and their weight is recorded. They are not included in the analysis results, which always refer to dry mass (DM) without hard impurities. Since the analyzed samples are typically unprocessed waste samples, to some extent, this approach mimics the procedures during SRF production: metals and heavy items would be removed by magnetic separators or air classifiers (compare section 1.1), while parts that are too small to be sorted out remain in the waste, or the laboratory sample, respectively.

However, the first step required for chemical analyses is sampling. Because sensor-based continuous analysis methods are not yet applicable for all parameters of interest, conventional sampling is still unavoidable even in modern waste management. Especially for highly heterogeneous waste such as MCW, a reliable sampling procedure is crucial. For this reason, the relative sampling variability was determined for material fractions from sorting analyses and 30 chemical elements with a replication experiment, see section 4.2.

In the course of this replication experiment, the particle size-dependent distribution of 30 elements was investigated and revealed statistically significant correlations between particle size and element concentrations. Significant negative correlations were found for the majority of analytes, indicating a tendency to occur in higher concentrations in smaller particle size fractions and vice versa. For this reason, a notable reduction of contaminant concentrations in SRF can be achieved when the fine fraction is removed, see section 4.3. However, when the fine fraction <5 mm is removed, it means removing more than 15% of the waste stream's mass, and a formal increase of Cd, Cl, and Sb concentrations in the screen overflow may be observed. These elements frequently occur in plastics such as PET and PVC, which are

usually not part of the fine fraction due to their comminution behavior. This indicates that a combination of screening and removing potential Cl and Sb carriers by NIR sorting could be a promising approach, which was confirmed by follow-up experiments applying combinations of screening, NIR sorting, and the manual removal of black and grey colored materials. With a combination of these measures, the concentrations of all investigated chemical elements were reduced in the residual waste stream, which may subsequently be used as SRF.

Because ash constituting elements tend to occur in higher concentrations in smaller particle size fractions as well, the reduction of contaminants is accompanied by the removal of ash constituting elements. Then, these valuable chemical compounds for the cement industry cannot be incorporated into the cement clinker in the rotary kiln. The fact that the most significant share of these elements or element oxides in waste is located in the fine fraction is not the only reason why this fraction may be of interest for cement manufacturers; the presence of certain element species makes the fine fraction even more attractive. Analyses revealed that Ca is not only present as carbonates in the form of calcite ($CaCO_3$) and dolomite ($CaMg(CO_3)_2$), which is the same form that is present in the natural raw materials used by cement manufacturers (e.g., limestone, dolomite). During the thermal decomposition of calcium carbonates and their transformation into calcium oxide (CaO), CO_2 is formed. This calcination process is responsible for about 2/3 of a cement plants' CO_2 emissions (VDZ, 2020). When calcium or magnesium carbonates are present in SRF, they undergo the same transformation as in the raw meal, i.e., calcination, and CO_2 is freed. However, in the fine fraction of the investigated waste stream, a large share of calcium was present as sulfates, namely bassanite ($CaSO_4 \cdot 0.5H_2O$), gypsum ($CaSO_4 \cdot 2H_2O$), and anhydrite ($CaSO_4$). When these compounds are present in SRF and are combusted in the cement industry, Ca can substitute Ca from raw materials without the CO_2 emissions that would typically arise from the calcination process. The sulfate can then react with other compounds, as sulfate carriers are sometimes added to the raw meal mix to transfer alkali oxides into alkali sulfates. This implies that both the anion and the cation of calcium sulfates are used in the process and represent valuable materials to the cement industry. Furthermore, the findings indicate that – besides biogenic carbon (Lorber et al., 2012) – SRF may contain additional chemical compounds that may reduce CO_2 emissions of the cement industry. The presence of calcium sulfates in SRF may, though, strongly depend on the origin of the waste that enters the SRF production plant.

Assessing the role of the element oxides Al_2O_3, SiO_2, CaO, Fe_2O_3, MgO, TiO_2, Na_2O, K_2O, SO_3, and P_2O_5 in the cement clinker production process, and applying the developed analytical method for determining the SRF ash composition to 80 SRF samples and to sorted material fractions of SRF, supported the hypothesis that SRF ash consists of valuable raw materials for the cement industry. Especially fine or mixed material fractions extracted from SRF contribute to the R-index (see section 4.4), making the cement industry an attractive complementary recycling option to existing recycling processes.

If the European Commission decides to acknowledge the recycling of mineral constituents in the cement industry, the cement industry could help reach the EU recycling targets, especially in countries with high TSRs such as Austria. In countries where SRF co-processing is not

common yet, or TSRs are rather low, recognizing a mixed recovery could cause a shift of waste streams away from conventional waste incineration or landfilling towards co-processing. Such a shift is expected to result in an environmental benefit, while the investments remain relatively low compared to other options (de Beer et al., 2017). However, because the European Commission has defined recycling targets for different waste streams, e.g., MSW or plastics packaging waste, it is concluded that attention has to be paid to both the origin of the waste streams that are processed to SRF and their ratio in the final SRF. Consequently, additional regulations and record-keeping are probably required.

The summarized findings and discussions in the above paragraphs emphasize that the concentrations of ash constituents need to be considered together with the conventional parameters (e.g., LHV, heavy metals) in order to evaluate the quality of SRF intended for co-processing in the cement industry. In general, removing the fine fractions for the purpose of decreasing contaminant concentrations would decrease the ash content of the SRF, which indicates that the ratio between energy recovery and material recycling in SRF would probably be shifted towards energy recovery. The separate use of these fractions in the cement industry, e.g., as substitute raw materials, is likely obstructed by the high contaminant concentrations and the biogenic carbon content, the latter of which may cause emission problems due to incomplete combustion. However, because there is currently no treatment option for the fine fractions other than conventional waste incineration, the mineral content of these fractions cannot be recycled when the fractions are removed from the SRF. Consequently, a conflict of interest between resource utilization/conservation and environmental protection arises. Hence, a compromise between contaminant concentrations and valuable ash constituents in the produced SRF is the most viable solution.

4.1 Research Question 1

Which materials, products, or waste fractions do contaminants and ash constituents mainly occur in, why, and in which concentrations?

Contaminant carriers in waste include a large variety of different materials, products, or waste fractions, carrying different contaminants in different amounts. Despite the versatility of As, Cd, Cl, Co, Cr, Hg, Ni, and Pb carriers, some fractions stand out as carriers of a larger number of contaminants. Examples include inert materials, metals, plastics, composites, leather products, textiles, rubbers, electronic equipment, or batteries. Another remarkable contaminant-carrying fraction is the fine fraction, which was identified as a contaminant carrier for Cr, Co, Ni, and Pb, although different particle sizes defined these fractions in the reviewed studies. This observation may be linked to the presence of metal abrasions in fine waste fractions. In general, the investigated heavy metals and metalloids are frequently present in mixed municipal and commercial wastes because they are or formerly have been broadly applied for the industrial production of various consumer goods. Applications are discussed in detail in Publication I, which also lists expected contaminant concentrations.

The largest concentrations of the **ash-constituting elements** Al, Ca, K, Fe, Mg, Na, P, S, Si, and Ti, are naturally reported in materials with high ash contents, such as inert materials, metals, and glass. These fractions are typically removed from the waste stream during SRF production, provided that they are sufficiently large. However, small particles of these materials are likely to remain in the fine fraction of the SRF, which contributed the most considerable amounts of all element oxides except TiO_2, see Figure 5. The largest share of TiO_2 in SRF ash originates from plastics. TiO_2 and compounds of most of the investigated elements are broadly used as fillers or pigments in the plastics or pulp and paper industry and therefore are present in high concentrations in these materials as well. Due to the small ash content of most plastic types, plastics usually do not contribute much to the total amount of element oxides and the ash content. The results displayed for plastics in Figure 5 were obtained for a mixed, unwashed plastics fraction as present in SRF and are likely influenced by surface adhering particles (soil, dust). Concentrations are given in Publication II.

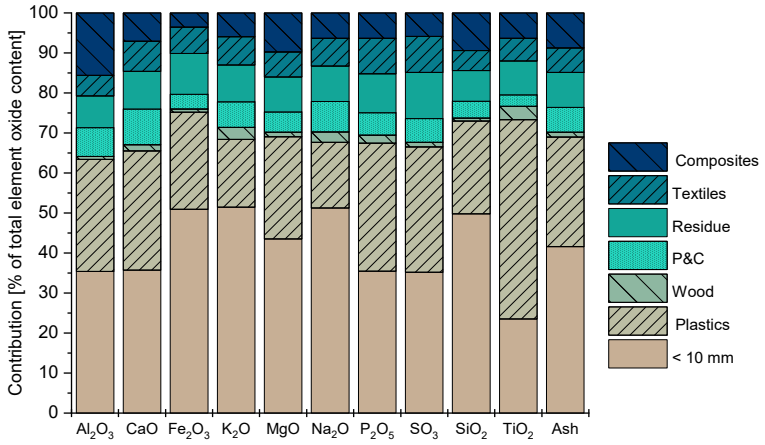

Figure 5: Average contribution (n=10) of different material classes to the total amount of element oxides in SRF ash (Viczek et al., 2021 in press). P&C = paper&cardboard.

4.2 Research Question 2

How reproducible or variable are analysis results with respect to material and/or chemical composition of mixed commercial waste (MCW)?

Regarding the **material composition**, the lowest RSVs were obtained for plastics 2D and 3D, but RSVs of up to 231% were observed for other materials. RSVs below the general consensus acceptance threshold of 20% were achieved for 37% of the material fractions >20 mm. A decrease of the RSV with increasing mass shares of the fractions was observed. This indicates that, as proposed by the TOS, larger primary sample masses are required to decrease the RSVs of material fractions with a small mass share.

Concerning the **chemical composition**, RSVs below the general consensus acceptance threshold of 20% were achieved for 39% of element-particle size class combinations but ranged up to 204%. Consequently, despite analytical sample preparation including subsampling, measurement uncertainties (MU), and the compositional heterogeneity coming into play more prominently in addition to the distributional heterogeneity, the RSVs were in the same range as those obtained for the material classes. The highest RSVs were observed for elements that are expected to be subject to high compositional heterogeneity due to their industrial applications, e.g., Cd, Pb, or Cu (Figure 6). Besides depending on the element, RSVs depended on the particle size and – similar to the RSVs for material classes in Publication III – on the mass of the particle size fraction in the sample. However, when the concentrations were aggregated and calculated for the original composite samples before screening, RSVs <20% were achieved for 57% of the analysis parameters. Because waste is usually sampled and analyzed as a whole and not separately in terms of particle sizes, it can be assumed that even better RSVs could be achieved when the waste mix is directly analyzed without separating it into fractions.

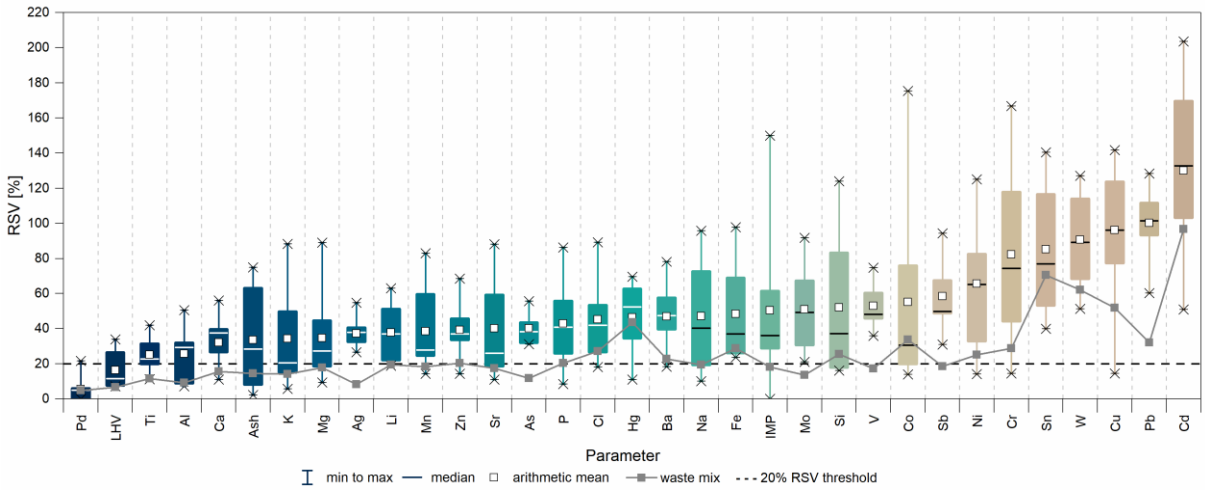

Figure 6: Relative sampling variabilities (RSVs) calculated for different analysis parameters in the different particle size classes illustrated as box plots. The solid grey line represents the RSVs calculated for the element concentrations in the whole waste mix (united particle size fractions). IMP = impurities. (Viczek et al., 2021 under review).

4.3 Research Question 3

How are the analytes distributed among different material or particle size fractions of mixed commercial waste (MCW), how can these fractions be removed, and how does their removal affect SRF quality?

Of the total 30 analyzed elements, 27 (Ag, Al, As, Ba, Ca, Co, Cr, Cu, Fe, Hg, K, Li, Mg, Mn, Mo, Na, Ni, P, Pd, Pb, Si, Sn, Sr, Ti, V, W, Zn) showed the tendency of occurring in higher concentrations in smaller particle size fractions (example in Figure 7). Cd mainly occurs in mid-sized particle size fractions, while Cl and Sb occur in higher concentrations in larger particle size fractions. Therefore, removing the fine fraction <5 mm or <10 mm results in concentration reductions (referring to mg/kg$_{DM}$) of 2.1% to 38% for many elements, including the ash constituents that represent valuable raw materials for the cement industry, see Figure 8. At the same time, a formal increase of Cd, Cl, and Sb concentrations by 10% to 17% is observed. When considered in mg/MJ, the reductions are even more pronounced while the simultaneous LHV increase attenuates the increase of Cd and Sb concentrations.

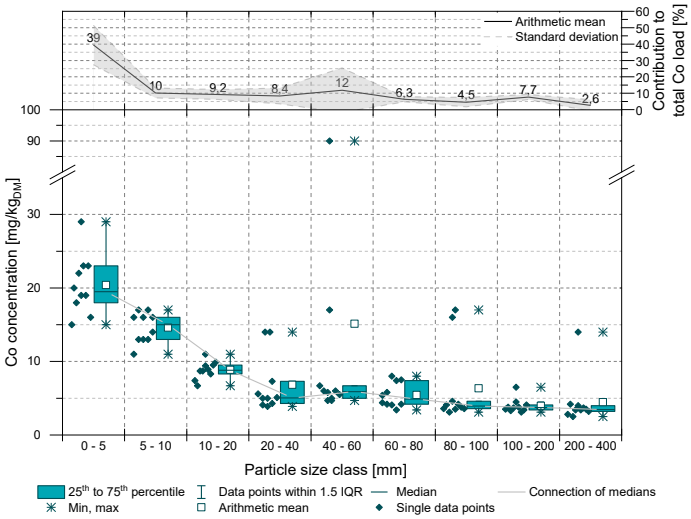

Figure 7: Particle size-dependent distribution of Cobalt (Co) in coarsely shredded mixed commercial waste and contribution of the particle size fractions to the total load of Co (Viczek et al., 2021a).

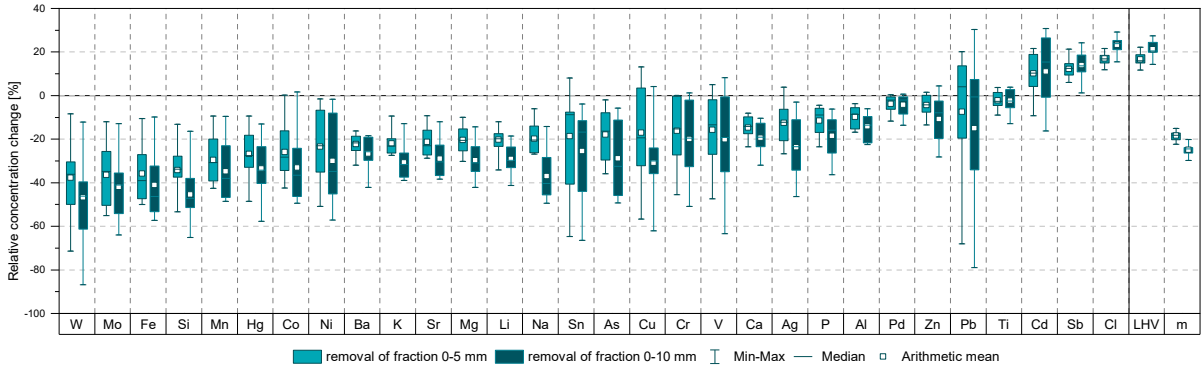

Figure 8: Relative concentration change (referring to mg/kg$_{DM}$) achieved by the removal of the fractions 0–5 mm or 0–10 mm, respectively (Viczek et al., 2021a)

When a combination of screening, the removal of PET and PVC (by NIR sorters), and the removal of black and grey colored materials (which would technically be feasible with technologies in the visible (VIS) range or lasers) is applied, a reduction of all investigated analytes can likely be achieved. An example of the distribution among the investigated particle size and material fractions is given in Figure 9. The highest concentrations of Cd, Cl, and Sb were observed in the fraction PVC, as was expected. However, the results also demonstrated that black and grey materials contain significant shares of Sb, Cl, and Co.

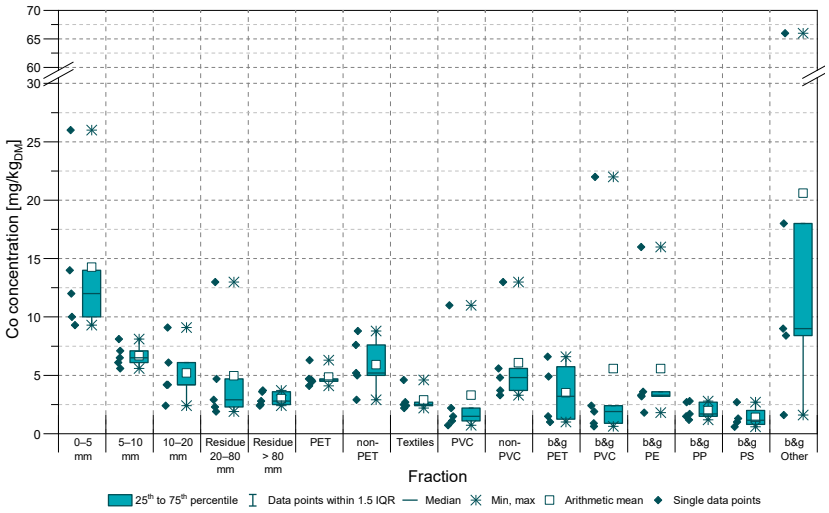

Figure 9: Cobalt (Co) concentrations in the fine fractions, sorted material fractions, and the sorting residue (Viczek et al., 2021b). B&g = black and grey colored materials.

It can be concluded that a significant reduction of the contaminant concentrations in SRF can be achieved with conventional aggregates that are already in use in state-of-the-art SRF production plants, namely screening and NIR sorting. However, while removing the fine fraction indeed leads to a reduction of contaminant concentrations, it is also accompanied by a reduction of the concentrations of valuable SRF ash constituents. The mineralogical characterization of the fine fractions has shown that they contain iron in its oxidic form, mainly as magnetite (Fe_3O_4) and wuestite (FeO). Furthermore, investigations demonstrated that Ca may not only be present in the form of calcite ($CaCO_3$) and dolomite ($CaMg(CO_3)_2$), the same form that is present in the natural raw materials used by cement manufacturers (e.g., limestone, dolomite), but also as sulfates, namely bassanite ($CaSO_4 \cdot 0.5H_2O$), gypsum ($CaSO_4 \cdot 2H_2O$), and anhydrite ($CaSO_4$), which makes the fine fraction an interesting fraction for cement manufacturers. Therefore, the fine fraction and the contained ash constituents need to be considered when measures for reducing contaminant concentrations are taken.

4.4 Research Question 4

What proportion of the SRF can be considered as recycled on a material level during co-processing in cement kilns, which are the main materials in SRF that are recycled, and what role could the cement industry take on in a circular economy?

Depending on the element oxides that are considered as recycled on a material level, the recycled share of the SRF (R-index, referring to dry mass) ranges from approx. 13.5% (considering Al_2O_3, CaO, Fe_2O_3, and SiO_2) to 17.6% (R-index = ash content). On average, 76.8% of the SRF ash consists of the four main chemical compounds required for cement clinker production, i.e., CaO, SiO_2, Al_2O_3, and Fe_2O_3. A comparison of SRF for primary and secondary firing is given in Figure 10.

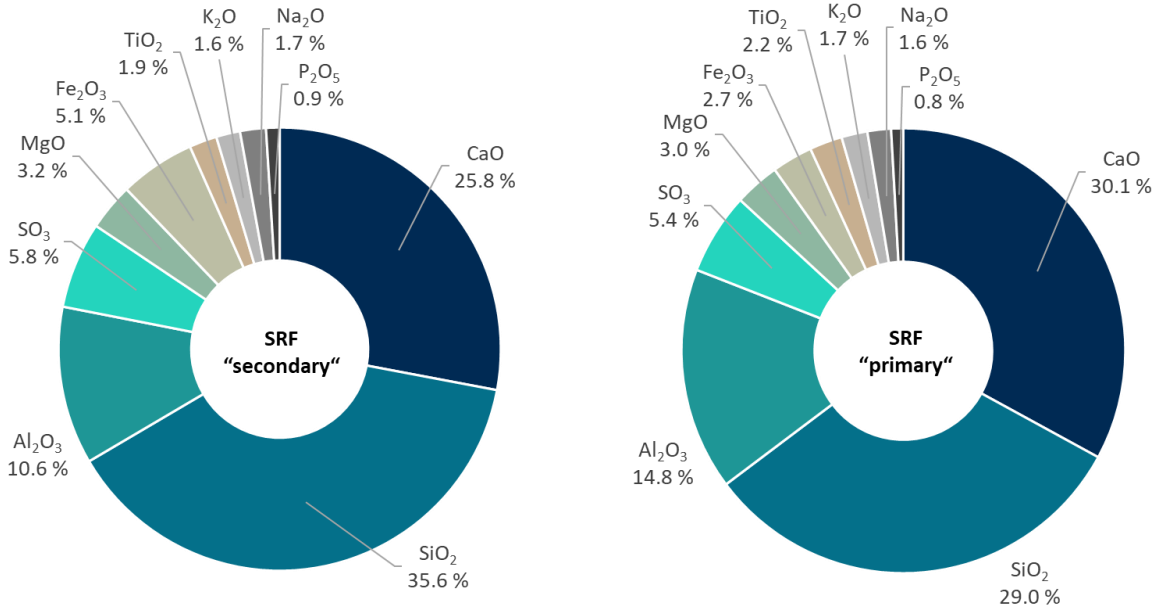

Figure 10: Average ash composition of ashes of SRF for secondary firing (*n = 30*) and SRF for primary firing (*n = 50*) in mass percent dry mass ($wt\%_{DM}$); percentages not normalized to 100% (Viczek et al., 2020a).

The analysis of defined materials and sorting fractions of SRF revealed that the fine fractions contribute most to the material-recyclable share of SRF because of their high ash content. For this fraction, also the highest material or waste fraction-specific R-indices were observed, followed by composites and the sorting residue (Figure 11). These analysis results emphasize that the materials that contribute most to the material-recyclable share of SRF are mixed fractions whose composition is often unknown and which are generally underexplored. Except for the composite material liquid packaging board (LPB), these material fractions are typically not subjected to other, established recycling processes. In the cement kiln, however, the mineral content of these materials is recycled, yet only from a technical point of view. For this reason, in a circular economy and with respect to material recycling, the cement industry represents a complementary recycling option to existing recycling processes. Besides SRF,

residues from existing recycling processes may be or already are recycled in the cement industry. These residues may include tire fluff from recycled old tires, reject materials from polymer or paper recycling, residues from primary sorting of mixed packaging waste, and similar fractions. In Austria, where co-processing of SRF and high thermal substitution rates are standard in cement plants, the mere acknowledgment of this mixed recovery could increase the overall recycling rate by approximately 1%, referring to the total annual MSW generation, without any additional investments being necessary.

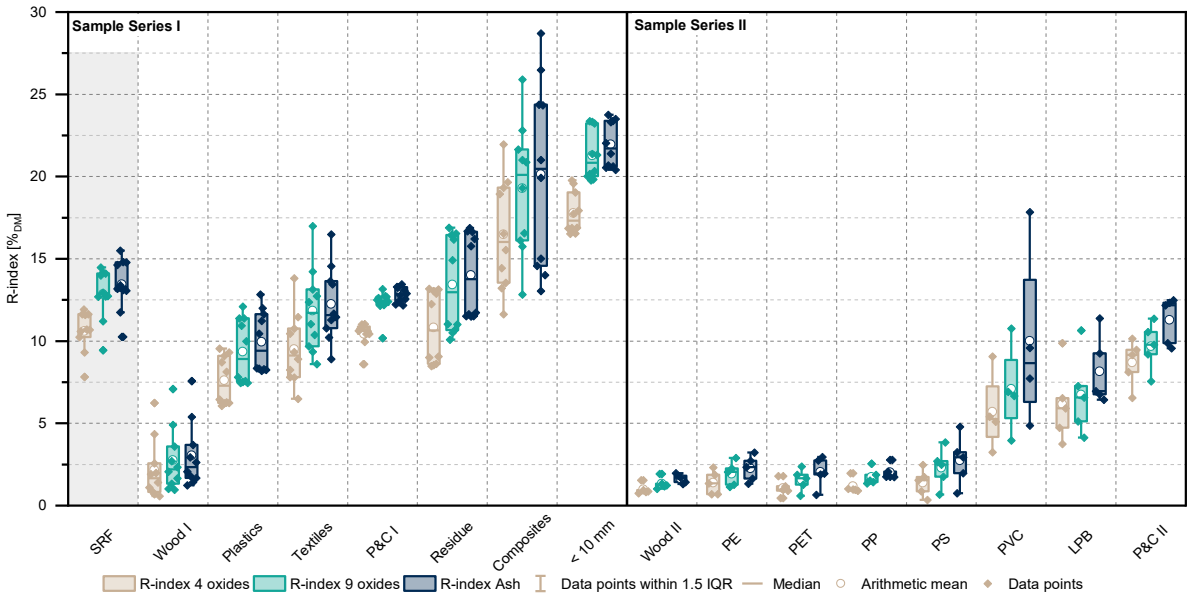

Figure 11: Calculated R-indices for sorted fractions of SRF and different materials. R-indices were calculated for three scenarios: “R-index 4 oxides”: Al_2O_3, CaO, Fe_2O_3, and SiO_2; “R-index 9 oxides”: Al_2O_3, CaO, Fe_2O_3, SiO_2, TiO_2, MgO, SO_3, Na_2O, and K_2O; and “R-index Ash”: R-index equals the ash content (Viczek et al., 2021 in press).

5 OUTLOOK AND FUTURE RESEARCH

The research carried out in the course of this doctoral Thesis indicates that further efforts are necessary and additional research may be conducted in the following four areas:

5.1 Better characterization of the fine fraction

The present Thesis demonstrates that the fine fractions have not gained enough attention from researchers yet, despite representing a general issue in waste management as it is unclear what is to be done with them. While these fractions can be treated by conventional waste incineration, the fine fractions of MCW may contain valuable materials that can either be recycled in the cement industry or could be subjected to other recycling options that are yet to be established for these fractions, e.g., metal recycling. Further research may investigate the composition of a broader range of samples, extend the scope to fine fractions of other waste streams, and search for possible alternative treatment methods for fine fractions. For example, methods to reduce the biogenic carbon and contaminant content could be investigated, making the fine fractions suitable for the use as a substitute raw material in the cement industry instead of using it as part of substitute fuels. Furthermore, methods removing contaminants that occur in metals, e.g., by magnetic separation, could be investigated together with the possibilities of recycling the removed metal fractions with metallurgical processes. If promising options are found, future research may also address the design of a suitable collection system that allows for collecting sufficiently large amounts of these fractions (which typically make up small shares of the waste) and direct these fractions to (possibly centralized) recycling sites. Concludingly, while the fine fractions have not received much attention in the past, paying more attention to this waste fraction in the future, including its proper characterization and treatment, could likely prove beneficial and open up new possibilities for material recovery.

5.2 Developing an international standard for the determination of the R-index

The cement industry has already proposed a potential position for co-processing in the waste hierarchy several years ago (Figure 12). The results presented in Publication VIII have scientifically determined the share of SRF that may be considered as recycled during co-processing (~13–18%, depending on the scenario; ~82–87% is subjected to energy recovery). The method and data provided by Publications VII and VIII have led to the proposal of a new work item concerning the R-index in the ISO and CEN committees. In February 2020, the ballot results with ISO member states voting in favor of the new work item were released, and the foundation for the preparation of an international standard was set. Currently, the working draft “ISO WD4349 Solid recovered fuels – Method for the determination of the Recycling Index” is elaborated in ISO/TC 300/WG 5 (ISO, 2020). CEN also approved the proposal, see CEN/TC 343 N 518 (BSI, 2020). The work is carried out under the Vienna Agreement under ISO lead.

The standard will be based on the two presented Publications VII and VIII, but the scope of the R-index calculation will be extended from SRF to a broader range of RDF. The elements that

are considered in the R-index are subject to discussion. As a result of this standardization process, an ISO EN standard is expected to be developed until February 2023. According to the CEN and CENELEC internal regulations, European Standards need to be adopted on a national level by member states, and any conflicting national standards must be withdrawn (CEN and CENELEC, 2018). Therefore, once this standard becomes effective, it may label co-processing a superior process to conventional energy recovery and entitle it to its own area in the waste hierarchy as a mixed recovery option between recycling and recovery.

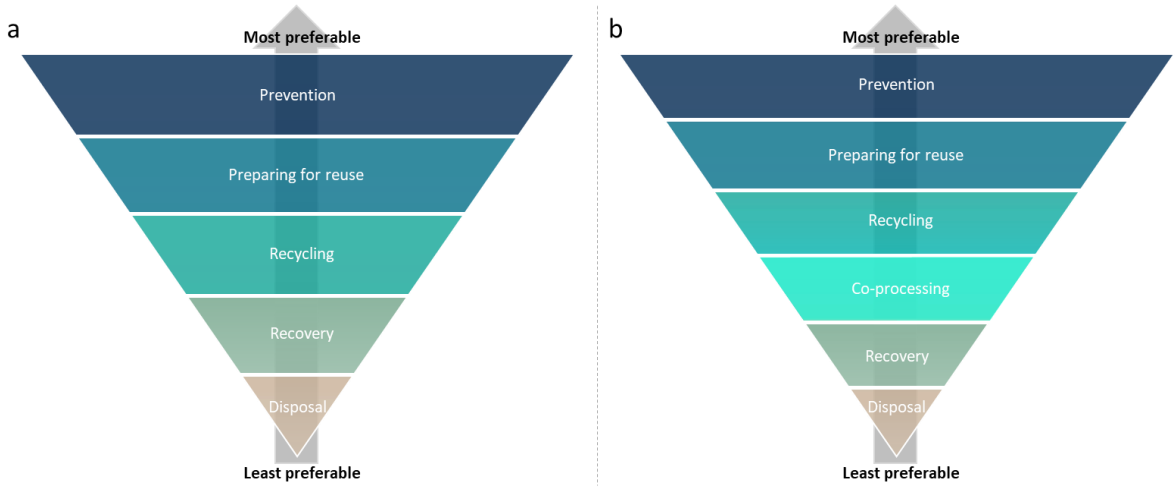

Figure 12: a) EU waste hierarchy (EC, 2008a) and b) proposed position for the integration of co-processing into the waste hierarchy according to Wehenpohl et al. (2006) and CSI (2014).

5.3 Resource conservation versus environmental and human health protection

Another topic that requires attention in the future is the role of contaminants, which are frequently part of products, in a circular economy. The importance of contaminants for processes currently considered R-operations, such as co-processing in the cement industry, has been discussed in this Thesis. However, as the cement industry rather represents a complementary recycling option, the share of materials directed towards specific material-recycling processes needs to be increased as well to meet the EU recycling targets. Despite the need for increased recycling, the transfer of contaminants from post-consumer products into new goods which may serve a different purpose has to be avoided. For this reason, contaminants also play a role in these recycling processes, which is, for example, demonstrated by the REACH regulations for Cd in PVC (EC, 2011).

Turner (2018) has already linked the occurrence of heavy metals in plastics for food contact to the poor sorting and subsequent recycling of waste electrical and electronic equipment. This emphasizes the need to closely monitor contaminants outside the SRF sector and to agree on criteria that regulate whether a product or waste can be recycled without risking the introduction of large amounts of contaminants into products with a higher risk of exposing consumers to these contaminants. While on the one hand, the degree of utilization of secondary resources, and thereby resource conservation needs to be facilitated according to the aims of sustainable

waste management, on the other hand, a decision needs to be made on what concentrations of contaminants can be tolerated, and research is required. Consequently, quality assured recycling is an essential topic for further waste management and circular economy developments.

5.4 Heavy metals in differently colored plastics

Heavy metals and metalloids are broadly applied as pigments in plastics and other materials. Depending on the pigment, this application may lead to high contaminant concentrations in plastics, see Publication I. Especially yellow, orange, and red hues are often achieved using such pigments. Therefore, certain colored plastics may pose a problem to SRF producers. This also implies that sorting these plastics with sensor-based techniques in the VIS range could be a possibility to remove contaminant-carrying plastics from the waste stream. Furthermore, a combination of VIS and NIR data could enable the removal of specifically colored plastic types, e.g., yellow PVC, if these materials often contained relevant contaminants. This could facilitate a more targeted removal of contaminant carriers without having to switch to element-selective techniques, which are not state of the art in modern SRF production plants yet. However, additional research is necessary to evaluate the distribution of heavy metals among differently colored plastics and to assess the impact of removing these materials.

REFERENCES

Achternbosch, M., Bräutigam, K.-R., Hartlieb, N., Kupsch, C., Richers, U., Stemmermann, P., 2003. Heavy Metals in Cement and Concrete Resulting from the Co-incineration of Wastes in Cement Kilns with Regard to the Legitimacy of Waste Utilisation.

Arancon, R.A.D., Lin, C.S.K., Chan, K.M., Kwan, T.H., Luque, R., 2013. Advances on waste valorization: new horizons for a more sustainable society. Energy Sci Eng 1, 53–71. https://doi.org/10.1002/ese3.9.

Ashraf, M.S., Ghouleh, Z., Shao, Y., 2019. Production of eco-cement exclusively from municipal solid waste incineration residues. Resour Conserv Recy 149, 332–342. https://doi.org/10.1016/j.resconrec.2019.06.018.

ASI (Austrian Standards Institute), 2011a. ÖNORM S 2127 - Basic characterization of waste heaps or from solid waste from containers and transport vehicles. Issued on 01/11/2011, Vienna.

ASI (Austrian Standards Institute), 2011b. ÖNORM EN 15359 Solid recovered fuels - Specifications and classes. Issued on 15/12/2011, Vienna.

Basel Convention, 2012. Technical guidelines on the environmentally sound co-processing of hazardous wastes in cement kilns.

BGS e.V., 2014. Sekundärbrennstoffe mit dem RAL-Gütezeichen 724.

BMLFUW (Bundesministerium für Land- und Forstwirtschaft, Umwelt und Wasserwirtschaft), 2010. Verordnung über die Verbrennung von Abfällen (Abfallverbrennungsverordnung - AVV), BGBl. II Nr. 476/2010, Wien.

BSI (British Standards Institution), 2020. CEN/TC 343 N 518 Solid recovered fuels – Method for the determination of the Recycling-Index. https://standardsdevelopment.bsigroup.com/projects/9019-03466#/section. Accessed 21 March 2021.

CEN (European Committee for Standardization), CENELEC (European Committee for Electrotecnical Standardization), 2018. Internal regulations Part 1.

Cipurkovic, A., Trumic, I., Hodžic, Z., Selimbašic, V., Djozic, A., 2014. Distribution of heavy metals in Portland cement production process. Adv Appl Sci Res 5, 252–259.

Clavier, K.A., Paris, J.M., Ferraro, C.C., Townsend, T.G., 2020. Opportunities and challenges associated with using municipal waste incineration ash as a raw ingredient in cement production – a review. Resour Conserv Recy 160, 104888. https://doi.org/10.1016/j.resconrec.2020.104888.

CSI (Cement Sustainability Initiative), 2014. Guidelines dor Co-Processing Fuels and Raw Materials in Cement Manufacturing.

Curtis, A., Adam, J., Pomberger, R., Sarc, R., 2019. Grain size-related characterization of various non-hazardous municipal and commercial waste for solid recovered fuel (SRF) production. Detritus 7, 55–67. https://doi.org/10.31025/2611-4135/2019.13847.

de Beer, J., Cihlar, J., Hensing, I., Zabeti, M., 2017. Status and prospects of co-processing of waste in EU cement plants: Executive summary.

DS (Danish Standards), 2013. DS 3077 Representative sampling - horizontal standard. Danish Standards, Charlottenlund 03.120.30; 13.080.05.

Dunnu, G., Maier, J., Scheffknecht, G., 2010. Ash fusibility and compositional data of solid recovered fuels. Fuel 89, 1534–1540. https://doi.org/10.1016/j.fuel.2009.09.008.

EC (European Commission), 2008a. Directive 2008/98/EC of the European Parliament and of the Council of 19 November 2008 on waste and repealing certain directives (waste framework directive).

EC (European Commission), 2008b. Regulation (EC) No 1272/2008 of the European Parliament and the Council of December 16 2008 on classification, labelling and packaging of substances and mixtures.

EC (European Commission), 2010. Directive 2010/75/EU of the European Parliament and of the Council of 24 November 2010 on industrial emissions (integrated pollution prevention and control).

EC (European Commission), 2011. Commission Regulation (EU) No 494/2011 of 20 May 2011 amending Regulation (EC) No 1907/2006 of the European Parliament and of the Council on the Registration, Evaluation, Authorisation and Restriction of Chemicals (REACH) as regards Annex XVII (Cadmium).

EC (European Commission), 2018. Directive (EU) 2018/851 of the European Parliament and of the Council of 30 May 2018 amending Directive 2008/98/EC on waste (Text with EEA relevance).

EC (European Commission), 2019. Commission Implementing Decision (EU) 2019/1004 of 7 June 2019 laying down rules for the calculation, verification and reporting of data on waste in accordance with Directive 2008/98/EC of the European Parliament and of the Council and repealing Commission Implementing Decision C(2012) 2384 (notified under document C(2019) 4114).

Esbensen, K.H., Wagner, C., 2014. Theory of sampling (TOS) versus measurement uncertainty (MU) – A call for integration. TrAC-Trend Anal Chem 57, 93–106. https://doi.org/10.1016/j.trac.2014.02.007.

Flamme, S., Geiping, J., 2012. Quality standards and requirements for solid recovered fuels: a review. Waste Manag Res 30, 335–353. https://doi.org/10.1177/0734242X12440481.

Gao, X., Yuan, B., Yu, Q.L., Brouwers, H.J.H., 2017. Characterization and application of municipal solid waste incineration (MSWI) bottom ash and waste granite powder in alkali activated slag. J Clean Prod 164, 410–419. https://doi.org/10.1016/j.jclepro.2017.06.218.

Garcia-Lodeiro, I., Carcelen-Taboada, V., Fernández-Jiménez, A., Palomo, A., 2016. Manufacture of hybrid cements with fly ash and bottom ash from a municipal solid waste incinerator. Constr Build Mater 105, 218–226. https://doi.org/10.1016/j.conbuildmat.2015.12.079.

GCCA (Global Cement and Concrete Association), 2021. Getting the Numbers Right. https://gccassociation.org/gnr/Excel/GNR%20-%20Totals_&_Averages%20-%20Light%20Report%202018.xls. Accessed 17 January 2021.

Gerassimidou, S., Velis, C.A., Williams, P.T., Castaldi, M.J., Black, L., Komilis, D., 2021. Chlorine in waste-derived solid recovered fuel (SRF), co-combusted in cement kilns: A systematic review of sources, reactions, fate and implications. Crit Rev Env Sci Tec 51(2), 140–186. https://doi.org/10.1080/10643389.2020.1717298.

Götze, R., Pivnenko, K., Boldrin, A., Scheutz, C., Astrup, T.F., 2016. Physico-chemical characterisation of material fractions in residual and source-segregated household waste in Denmark. Waste Manage 54, 13–26. https://doi.org/10.1016/j.wasman.2016.05.009.

Gy, P.M., 1995. Introduction to the theory of sampling I. Heterogeneity of a population of uncorrelated units. TrAC-Trend Anal Chem 14, 67–76. https://doi.org/10.1016/0165-9936(95)91474-7.

Hilber, T., Maier, J., Scheffknecht, G., Agraniotis, M., Grammelis, P., Kakaras, E., Glorius, T., Becker, U., Derichs, W., Schiffer, H.-P., Jong, M. de, Torri, L., 2007. Advantages and possibilities of solid recovered fuel cocombustion in the European energy sector. J Air Waste Manage 57, 1178–1189. https://doi.org/10.3155/1047-3289.57.10.1178.

ISO, 2020. ISO/WD 4349 Solid recovered fuels — Method for the determination of the Recycling-Index. https://www.iso.org/standard/79886.html. Accessed 21 March 2021.

Kabongo, J.D., 2013. Waste Valorization, in: Idowu, S.O., Capaldi, N. (Eds.), Encyclopedia of corporate social responsibility. Springer, Heidelberg, pp. 2701–2706.

Kaza, S., Yao, L.C., Bhada-Tata, P., van Woerden, F., 2018. What a Waste 2.0: A Global Snapshot of Solid Waste Management to 2050. Washington, DC: World Bank.

Krammart, P., Tangtermsirikul, S., 2004. Properties of cement made by partially replacing cement raw materials with municipal solid waste ashes and calcium carbide waste. Constr Build Mater 18, 579–583. https://doi.org/10.1016/j.conbuildmat.2004.04.014.

Kreindl, G., 2007. Schwermetallherkunft in den Inputfraktionen einer Alternativbrennstoffverwertungsanlage. Master's Thesis, Montanuniversitaet Leoben.

Kuna, M., 2015. Analysis of thermal conversion of non-homogeneous solid recovered fuels. Master's Thesis, Técnico Lisboa.

Lam, C.H.K., Barford, J.P., McKay, G., 2011. Utilization of municipal solid waste incineration ash in Portland cement clinker. Clean Technol Envir 13, 607–615. https://doi.org/10.1007/s10098-011-0367-z.

Lamas, W.d.Q., Palau, J.C.F., Camargo, J.R.d., 2013. Waste materials co-processing in cement industry: Ecological efficiency of waste reuse. Renew Sust Energ Rev 19, 200–207. https://doi.org/10.1016/j.rser.2012.11.015.

Lederer, J., Rechberger, H., Fellner, J., 2015. The utilization of MSWI fly ashes in cement production and its impact on heavy metal contents in cement, in: Proceedings Sardinia 2015, Fifteenth International Waste Management and Landfill Symposium, S. Margherita die Pula, Cagliari, Italy. 5-9 October 2015.

Lorber, K.E., Sarc, R., Aldrian, A., 2012. Design and quality assurance for solid recovered fuel. Waste Manag Res 30, 370–380. https://doi.org/10.1177/0734242X12440484.

Mauschitz, G., 2020. Emissionen aus Anlagen der österreichischen Zementindustrie. Berichtsjahr 2019.

Nasrullah, M., Vainikka, P., Hannula, J., Hurme, M., 2015. Elemental balance of SRF production process: Solid recovered fuel produced from commercial and industrial waste. Fuel 145, 1–11. https://doi.org/10.1016/j.fuel.2014.12.071.

Nasrullah, M., Vainikka, P., Hannula, J., Hurme, M., Oinas, P., 2016. Elemental balance of SRF production process: Solid recovered fuel produced from municipal solid waste. Waste Manag Res 34, 38–46. https://doi.org/10.1177/0734242X15615697.

Pan, J.R., Huang, C., Kuo, J.-J., Lin, S.-H., 2008. Recycling MSWI bottom and fly ash as raw materials for Portland cement. Waste Manage 28, 1113–1118. https://doi.org/10.1016/j.wasman.2007.04.009.

Pieber, S., Ragossnig, A., Pomberger, R., Curtis, A., 2012. Biogenic carbon-enriched and pollutant depleted SRF from commercial and pretreated heterogeneous waste generated

by NIR sensor-based sorting. Waste Manag Res 30, 381–391. https://doi.org/10.1177/0734242X12437567.

Pohl, M., Bernhardt, D., Beckmann, M., Spiegel, W., 2011. Brennstoffcharakterisierung zur vorausschauenden Bewertung des Korrosionsrisikos, in: Born, M. (Ed.), Dampferzeugerkorrosion 2011, Freiberg: SAXONIA Standortentwicklungs- und -verwaltungsgesellschaft mbH, pp. 67–83.

Pomberger, R., 2008. Entwicklung von Ersatzbrennstoff für das HOTDISC-Verfahren und Analyse der abfallwirtschaftlichen Relevanz. Doctoral Thesis, Montanuniversitaet Leoben.

Pomberger, R., 2020. Über theoretische, praktische und reale Recyclingfähigkeit. Österr Wasser- und Abfallw 72, 19–20. https://doi.org/10.1007/s00506-019-00648-6.

Pomberger, R., Aldrian, A., Sarc, R., 2015. Grenzwerte - Technische Sicht zur rechtlichen Notwendigkeit, in: Piska, C., Lindner, B. (Eds.), Abfallwirtschaftsrecht Jahrbuch 2015. NWV Neuer wissenschaftlicher Verlag, Wien, Graz, pp. 269–289.

Pomberger, R., Sarc, R., 2014. Use of Solid Recovered Fuels in the Cement Industry, in: Thomé-Kozmiensky, K.J., Thiel, S. (Eds.), Waste management. TK-Verl. Thomé-Kozmiensky, Neuruppin, pp. 417–488.

Rotter, S., 2002. Schwermetalle in Haushaltsabfällen. Potenzial, Verteilung und Steuerungsmöglichkeiten durch Aufbereitung. Doctoral Thesis, TU Dresden.

Saikia, N., Kato, S., Kojima, T., 2007. Production of cement clinkers from municipal solid waste incineration (MSWI) fly ash. Waste Manage 27, 1178–1189. https://doi.org/10.1016/j.wasman.2006.06.004.

Sarc, R., 2015. Herstellung, Qualität und Qualitätssicherung von Ersatzbrennstoffen zur Erreichung der 100%-igen thermischen Substitution in der Zementindustrie. Doctoral Thesis, Montanuniversitaet Leoben.

Sarc, R., Lorber, K.E., Pomberger, R., Rogetzer, M., Sipple, E.M., 2014. Design, quality, and quality assurance of solid recovered fuels for the substitution of fossil feedstock in the cement industry. Waste Manag Res 32, 565–585. https://doi.org/10.1177/0734242X14536462.

Sarc, R., Seidler, I.M., Kandlbauer, L., Lorber, K.E., Pomberger, R., 2019. Design, Quality and Quality Assurance of Solid Recovered Fuels for the Substitution of Fossil Feedstock in the Cement Industry – Update 2019. Waste Manag Res 37, 885–897. https://doi.org/10.1177/0734242X19862600.

Sarmiento, L.M., Clavier, K.A., Paris, J.M., Ferraro, C.C., Townsend, T.G., 2019. Critical examination of recycled municipal solid waste incineration ash as a mineral source for portland cement manufacture – A case study. Resour Conserv Recy 148, 1–10. https://doi.org/10.1016/j.resconrec.2019.05.002.

Swiss Federal Council, 2015. Verordnung über die Vermeidung und die Entsorgung von Abfällen.

Turner, A., 2018. Black plastics: Linear and circular economies, hazardous additives and marine pollution. Environment international 117, 308–318. https://doi.org/10.1016/j.envint.2018.04.036.

Turner, A., 2019. Cadmium pigments in consumer products and their health risks. Sci Total Environ 657, 1409–1418. https://doi.org/10.1016/j.scitotenv.2018.12.096.

Turner, A., Filella, M., 2017. Field-portable-XRF reveals the ubiquity of antimony in plastic consumer products. Sci Total Environ 584-585, 982–989. https://doi.org/10.1016/j.scitotenv.2017.01.149.

US EPA (United States Environmental Protection Agency), 2019. Initial List of Hazardous Air Pollutants with Modifications. https://www.epa.gov/haps/initial-list-hazardous-air-pollutants-modifications. Accessed 4 October 2019.

VDZ (Verein Deutscher Zementwerke e.V.), 2020. Dekarbonisierung von Zement und Beton - Minderungspfade und Handlungsstrategien.

Viczek, S.A., Aldrian, A., Pomberger, R., Sarc, R., 2020a. Determination of the material-recyclable share of SRF during co-processing in the cement industry. Resour Conserv Recy 156, 104696. https://doi.org/10.1016/j.resconrec.2020.104696.

Viczek, S.A., Aldrian, A., Pomberger, R., Sarc, R., 2020b. Origins and carriers of Sb, As, Cd, Cl, Cr, Co, Pb, Hg, and Ni in mixed solid waste – A literature-based evaluation. Waste Manage 103, 87–112. https://doi.org/10.1016/j.wasman.2019.12.009.

Viczek, S.A., Aldrian, A., Pomberger, R., Sarc, R., 2021 in press. Origins of major and minor ash constituents of SRF for co-processing in the cement industry. Waste Manage.

Viczek, S.A., Kandlbauer, L., Khodier, K., Aldrian, A., Sarc, R., 2021 under review. Sampling and analysis of coarsely shredded mixed commercial waste. Part II: particle size-dependent element determination.

Viczek, S.A., Khodier, K., Kandlbauer, L., Aldrian, A., Redhammer, G., Tippelt, G., Sarc, R., 2021a. The particle size-dependent distribution of chemical elements in mixed commercial waste and implications for enhancing SRF quality. Sci Total Environ 776, 145343. https://doi.org/10.1016/j.scitotenv.2021.145343.

Viczek, S.A., Lorber, K.E., Sarc, R., 2021b. Production of contaminant-depleted solid recovered fuel from mixed commercial waste for co-processing in the cement industry. Fuel 294, 120414. https://doi.org/10.1016/j.fuel.2021.120414.

Vodegel, S., Davidovic, M., Ludewig, A., 2018. Differenzierung der energetischen Verwertung am Kriterium der Energieeffizienz, in: Thiel, S., Thomé-Kozmiensky, E., Quicker, P., Gosten, A. (Eds.), Energie aus Abfall. Band 15, pp. 761–768.

Wagland, S.T., Kilgallon, P., Coveney, R., Garg, A., Smith, R., Longhurst, P.J., Pollard, S.J.T., Simms, N., 2011. Comparison of coal/solid recovered fuel (SRF) with coal/refuse derived fuel (RDF) in a fluidised bed reactor. Waste Manage 31, 1176–1183. https://doi.org/10.1016/j.wasman.2011.01.001.

Wehenpohl, G., Dubach, B., Degre, J.P., Mutz, D., 2006. Guidelines on co-processing waste materials in cement production. Basel: CH: Holcim Group, 14–27.

Yan, J., Karlsson, A., Zou, Z., Dai, D., Edlund, U., 2020. Contamination of heavy metals and metalloids in biomass and waste fuels: Comparative characterisation and trend estimation. Sci Total Environ 700, 134382. https://doi.org/10.1016/j.scitotenv.2019.134382.

Zeschmar-Lahl, B., 2003. Schadstoffanreicherung im Erzeugnis aufgrund des Einsatzes von Ersatzbrennstoffen in Zementwerken und Feuerungsanlagen - erforderliche Reglementierungen aus der Sicht des technischen Umweltschutzes. Doctoral Thesis, TU Berlin.

LIST OF ABBREVIATIONS

2D	2-dimensional (plastics)
3D	3-dimensional (plastics)
Ag	Silver
Al	Aluminum
Al_2O_3	Aluminum oxide (generic in the context of the R-index)
As	Arsenic
b&g	Black and grey (materials)
Ba	Barium
Be	Beryllium
Ca	Calcium
$CaCO_3$	Calcite, Calcium carbonate
$CaMg(CO_3)_2$	Dolomite
CaO	Calcium oxide (generic in the context of the R-index)
$CaSO_4$	Anhydrite
$CaSO_4 \cdot 0.5H_2O$	Bassanite
$CaSO_4 \cdot 2H_2O$	Gypsum
Cd	Cadmium
Cl	Chlorine
Co	Cobalt
Cr	Chromium
Cu	Copper
DM	Dry mass
Fe	Iron
FeO	Wuestite
Fe_2O_3	Iron(III) oxide (generic for iron oxides in the context of the R-index)
Fe_3O_4	Magnetite
FTIR	Fourier transform infrared (spectroscopy)
Hg	Mercury
ICP-MS	Inductively coupled plasma mass spectrometry
IMP	Impurities
K	Potassium
K_2O	Potassium oxide (generic in the context of the R-index)
LHV	Lower heating value
Li	Lithium
LPB	Liquid packaging board
MCW	Mixed commercial waste
Mg	Magnesium
MgO	Magnesium oxide (generic in the context of the R-index)
Mn	Manganese
Mo	Molybdenum
MSW	Municipal solid waste

MSWI	Municipal solid waste incineration
MU	Measurement uncertainty
Na	Sodium
Na_2O	Sodium oxide (generic in the context of the R-index)
Ni	Nickel
NIR	Near-infrared
P	Phosphorus
P_2O_5	Phosphorus pentoxide (generic in the context of the R-index)
P&C	Paper & cardboard
Pb	Lead
PE	Polyethylene
PET	Polyethylene terephthalate
PP	Polypropylene
PS	Polystyrene
PVC	Polyvinyl chloride
RAL	Quality mark in Germany; RAL Deutsches Institut für Gütesicherung und Kennzeichnung e.V.
RDF	Refuse-derived fuel
RSV	Relative sampling variability
R-index	Recycling index
S	Sulfur
SO_3	Sulfur trioxide (generic in the context of the R-index)
Sb	Antimony
Se	Selenium
Si	Silicon
SiO_2	Silicon dioxide (generic in the context of the R-index)
Sn	Tin
Sr	Strontium
SRF	Solid recovered fuel
Te	Tellurium
Ti	Titanium
TiO_2	Titanium dioxide (generic in the context of the R-index)
Tl	Thallium
TOS	Theory of sampling
TSR	Thermal substitution rate
V	Vanadium
VIS	Visible light spectrum
W	Tungsten
WIO	Waste incineration ordinance
XRD	X-ray diffraction
Zn	Zinc

SUPPLEMENTARY MATERIAL

The following documents are supplementary materials to the publications presented in this Thesis and were published online by the respective journals:

- Supplementary of **Publication II** "*Origins of major and minor ash constituents of solid recovered fuel for co-processing in the cement industry"*

- Supplementary of **Publication IV** "*Sampling and analysis of coarsely shredded mixed commercial waste. Part II: particle size-dependent element determination*"

- Supplementary of **Publication V** "*The particle size-dependent distribution of chemical elements in mixed commercial waste and implications for enhancing SRF quality*"

- Supplementary of **Publication VI** "*Production of contaminant-depleted solid recovered fuel from mixed commercial waste for co-processing in the cement industry"*

Publication II – Supplementary

Origins of major and minor ash constituents of solid recovered fuel for co-processing in the cement industry

S.A. Viczek, A. Aldrian, R. Pomberger, R. Sarc

Waste Management, accepted March 24, 2021

Content

1. Sample series I

1.1 Ash content and composition

Table S1: Ash content and composition of sorted material fractions (Part I)

SRF Sample No.	Sorted material fraction	Ash (815°C)	Al	Ca	Fe	K	Mg	Na	P	S	Si	Ti
		$\%_{DM}$	mg/kg_{DM}	mg/kg_{DM}	mg/kg_{DM}	mg/kg_{DM}	mg/kg_{DM}	mg/kg_{DM}	mg/kg_{DM}	mg/kg_{DM}	mg/kg_{DM}	mg/kg_{DM}
1	Sorting residue	16.64	54900	251000	50400	12000	27500	15000	2490	37400	120000	8660
2	Sorting residue	16.68	50500	242000	39500	14500	28100	18800	3060	47600	139000	10200
3	Sorting residue	11.53	54300	220000	47000	12900	22500	15900	3020	31600	142000	13200
4	Sorting residue	16.88	47300	244000	41200	15200	28700	20300	3000	39900	128000	10700
5	Sorting residue	15.78	50700	242000	49400	12200	27500	15300	2600	29000	127000	9280
6	Sorting residue	11.64	51300	217000	45500	12300	20700	14800	3010	19400	123000	12000
7	Sorting residue	11.74	49900	219000	45600	12400	22400	17600	3120	27800	143000	12900
8	Sorting residue	11.53	48800	213000	45500	13700	21700	15600	3150	33200	137000	12800
9	Sorting residue	16.22	53600	263000	44600	13500	28600	17400	2990	40100	131000	11400
10	Sorting residue	11.50	49100	212000	44300	14100	22000	16700	3180	29800	136000	12500
	Average: Sorting residue	**14.01**	**51040**	**232300**	**45300**	**13280**	**24970**	**16740**	**2962**	**33580**	**132600**	**11364**
	Std. dev.	**2.57**	**2508**	**18148**	**3297**	**1093**	**3336**	**1794**	**231**	**7940**	**7989**	**1596**
1	Wood	2.94	33400	168000	47300	29900	20800	46900	3190	29000	145000	21800
2	Wood	1.24	25300	195000	31100	65100	28000	67100	4830	37200	47100	34100
3	Wood	7.58	18200	450000	8800	4500	17100	6560	6110	14600	69000	20200
4	Wood	2.06	30000	263000	51500	42300	27300	42000	4810	28900	88600	54400
5	Wood	2.63	20300	377000	14400	8120	27200	15500	3130	22700	65100	20000
6	Wood	1.43	24900	163000	18100	29900	16300	42200	3310	16800	87700	14800
7	Wood	3.70	42300	153000	24100	48100	27800	57700	4220	21600	171000	25600
8	Wood	1.81	28200	132000	17700	38000	17400	47100	3830	21300	91300	49700
9	Wood	1.68	51000	196000	22400	59500	27900	67900	5780	28300	118000	33800
10	Wood	5.39	10800	478000	8650	8990	18400	4990	2080	16800	49900	7170
	Average: Wood	**3.05**	**28440**	**257500**	**24405**	**33441**	**22820**	**39795**	**4129**	**23720**	**93270**	**28157**
	Std. dev.	**2.02**	**11704**	**129652**	**14847**	**21336**	**5217**	**23278**	**1267**	**7053**	**40526**	**14965**
1	Composites	24.33	66800	217000	30000	6390	18400	8060	2730	19800	143000	7640
2	Composites	28.70	69900	148000	15700	2650	52000	7010	1450	17600	100000	5590
3	Composites	14.58	238000	131000	33600	14000	14500	48700	6430	13600	116000	6530
4	Composites	26.48	55400	197000	14500	10700	35200	12300	< 1300	20300	200000	6230
5	Composites	24.38	50700	228000	13500	7040	28800	10700	1480	19600	174000	5570
6	Composites	15.01	330000	179000	8200	4540	7960	6560	1740	10800	70200	8330
7	Composites	14.01	226000	199000	17800	12000	12500	22800	3170	16600	140000	7940
8	Composites	19.92	201000	54100	8350	10500	6560	8820	< 1300	8000	235000	17400
9	Composites	21.01	68500	165000	17800	7330	116000	9360	1460	20700	114000	14400
10	Composites	13.05	274000	189000	4790	4390	4000	8040	1890	22900	47900	7350
	Average: Composites	**20.15**	**158030**	**170710**	**16424**	**7954**	**29592**	**14235**	**2544**	**16990**	**134010**	**8698**
	Std. dev.	**5.72**	**106480**	**50599**	**9214**	**3698**	**33828**	**12988**	**1695**	**4779**	**57385**	**3974**
1	Textiles	11.46	33500	299000	50100	9580	25400	14000	2890	38500	105000	10300
2	Textiles	16.48	51400	187000	88700	17600	23900	19100	2530	36800	165000	8090
3	Textiles	11.68	43800	262000	35700	21800	29300	61400	10500	34600	140000	9550
4	Textiles	14.55	42900	313000	36500	11000	25500	10900	2240	41900	101000	9210
5	Textiles	13.64	38900	306000	40600	8600	24000	11000	2250	35800	96800	7300
6	Textiles	13.45	64600	250000	35000	20600	14900	16600	3590	32800	130000	13700
7	Textiles	10.79	43800	269000	50800	12700	26100	20500	5240	37200	109000	10500
8	Textiles	10.22	55500	188000	39200	26100	26000	22600	4030	24200	159000	11300
9	Textiles	8.92	45300	232000	33600	15100	27300	23100	4170	49000	126000	11700
10	Textiles	11.29	35100	264000	27000	5460	19800	6300	4050	27300	101000	13800
	Average: Textiles	**12.25**	**45480**	**257000**	**43720**	**14854**	**24220**	**20550**	**4149**	**35810**	**123280**	**10545**
	Std. dev.	**2.26**	**9475**	**44540**	**17380**	**6583**	**4104**	**15375**	**2434**	**6984**	**24901**	**2156**

Table S2: Ash content and composition of sorted material fractions (Part II)

SRF Sample No.	Sorted material fraction	Ash (815°C)	Al	Ca	Fe	K	Mg	Na	P	S	Si	Ti
		$\%_{DM}$	mg/kg_{DM}	mg/kg_{DM}	mg/kg_{DM}	mg/kg_{DM}	mg/kg_{DM}	mg/kg_{DM}	mg/kg_{DM}	mg/kg_{DM}	mg/kg_{DM}	mg/kg_{DM}
1	Plastics	12.00	44900	258000	41100	8910	31200	13800	2890	33400	119000	14900
2	Plastics	11.64	59000	260000	24100	6690	28000	10100	2650	30300	136000	20100
3	Plastics	8.36	68600	227000	31800	7460	21800	7890	3190	25600	131000	25200
4	Plastics	10.46	27600	236000	66800	5470	22700	6270	1870	36900	140000	20400
5	Plastics	11.23	59300	257000	31100	8790	26000	12900	2940	36100	122000	21100
6	Plastics	8.33	63600	228000	31200	7280	19600	8080	3430	30000	114000	24500
7	Plastics	8.26	64800	225000	35000	6630	20000	7760	3420	18600	125000	30200
8	Plastics	8.30	68000	225000	30500	8650	20300	8790	3450	23500	126000	24800
9	Plastics	12.83	46000	244000	21700	6910	26500	11300	3240	40400	133000	18600
10	Plastics	8.20	66800	228000	32900	8300	19400	8670	3460	24400	125000	25300
	Average: Plastics	**9.96**	**56860**	**238800**	**34620**	**7509**	**23550**	**9556**	**3054**	**29920**	**127100**	**22510**
	Std. dev.	**1.86**	**13320**	**14673**	**12504**	**1133**	**4120**	**2424**	**501**	**6892**	**7951**	**4331**
1	P&C	13.28	39600	258000	24800	9580	14800	19900	1340	20400	82400	3720
2	P&C	12.23	67500	336000	27000	13200	18300	23300	2020	21800	109000	7920
3	P&C	12.47	59400	300000	19700	13500	23900	35100	5930	27300	111000	3980
4	P&C	13.30	63800	286000	37900	15100	19400	21400	2170	24100	109000	4210
5	P&C	12.57	61000	303000	39400	15800	19700	24400	2020	25900	116000	6870
6	P&C	12.80	78400	333000	9530	11100	14400	14100	1580	18400	104000	5430
7	P&C	13.09	94600	279000	26100	11900	20200	19700	2210	17800	110000	7310
8	P&C	12.18	75900	332000	18800	9210	22500	18500	3430	23600	104000	6970
9	P&C	12.90	51900	356000	12900	15500	19500	23100	2150	28600	91000	4380
10	P&C	13.46	68500	343000	12100	13500	24700	17800	2820	28200	90400	4150
	Average: P&C	**12.83**	**66060**	**312600**	**22823**	**12839**	**19740**	**21730**	**2567**	**23610**	**102680**	**5494**
	Std. dev.	**0.46**	**15083**	**32001**	**10276**	**2349**	**3414**	**5597**	**1319**	**3938**	**10965**	**1612**
1	Fines < 10 mm	23.38	37200	175000	50100	13800	37000	39400	< 1300	16900	200000	3340
2	Fines < 10 mm	23.50	38600	170000	81500	12800	28100	18400	1710	18300	157000	6920
3	Fines < 10 mm	23.75	52100	175000	65300	17500	21100	36500	5460	14500	185000	6280
4	Fines < 10 mm	22.03	49900	171000	41200	17000	26000	19000	2210	22300	175000	6850
5	Fines < 10 mm	20.54	43900	187000	48100	16200	24500	17500	1910	25200	183000	6570
6	Fines < 10 mm	20.69	45200	191000	44000	15800	25200	16600	2030	25100	187000	7650
7	Fines < 10 mm	20.63	42000	188000	37100	15300	25400	17000	1780	25700	190000	7060
8	Fines < 10 mm	23.31	58300	180000	42700	16900	23200	33500	4610	18300	195000	6390
9	Fines < 10 mm	20.41	46700	208000	48900	15800	22500	16000	2100	26300	176000	7340
10	Fines < 10 mm	21.40	52000	199000	37900	17800	28200	17200	2080	26500	186000	7430
	Average: Fines < 10 mm	**21.96**	**46590**	**184400**	**49680**	**15890**	**26120**	**23110**	**2654**	**21910**	**183400**	**6583**
	Std. dev.	**1.40**	**6583**	**12545**	**13783**	**1594**	**4440**	**9359**	**1375**	**4496**	**12011**	**1224**

1.2 Results of sorting analyses

Table S3: Concentration factors ($c_{faction}/c_{mix}$) of As, Cd, Cl, Cr, Co, Fe, Hg, Ni, Pb, and Sb. MSW = Municipal solid waste, MCW = Mixed commercial waste, CIW = Commercial and industrial waste, SRF = Solid recovered fuel.

Fraction	Sample No.										Mean	Std.dev.
	1	2	3	4	5	6	7	8	9	10		
< 10 mm	34.2	36.2	21.8	22.5	23.6	12.2	36.6	23.7	22.7	23.3	25.7	7.7
Wood	7.6	13.5	2.4	15.0	10.8	4.0	2.9	2.9	9.4	2.3	7.0	5.0
Plastics	27.3	22.8	30.9	24.5	26.2	67.0	30.4	36.1	41.2	59.4	35.3	16.3
Paper&Cardboard	7.2	4.4	12.0	7.6	7.4	4.3	5.4	5.4	7.7	4.0	6.3	2.6
Sorting Residue	2.7	10.1	8.0	6.4	5.7	9.0	14.6	17.6	6.5	6.1	8.1	3.9
Textiles	8.9	7.1	14.7	8.4	9.1	2.0	6.2	4.2	6.0	2.6	6.7	3.8
Composite	3.6	2.7	7.1	13.7	14.3	1.5	1.0	6.9	2.6	1.8	5.5	5.0
Glass	1.8	0	0.5	0.9	0	0	1.5	0	0.2	0	0.4	0.6
Inert	3.0	2.2	2.2	0	0.8	0	0.1	0	0.5	0	0.9	1.2
Metals	3.6	1.0	0.5	0.9	2.0	0	1.3	3.1	3.4	0.5	1.6	1.3

2. Sample series II

Table S4: Ash content [$\%_{DM}$]and concentrations of elements in ash samples [mg/kg_{DM}] Part I. The amount of ash from PVC of SRF producer 2 was insufficient for analyses.

Material	SRF Producer	AG $\%_{DM}$	Li mg/kg_{DM}	Be mg/kg_{DM}	Na mg/kg_{DM}	Mg mg/kg_{DM}	Al mg/kg_{DM}	Si mg/kg_{DM}	P mg/kg_{DM}	S mg/kg_{DM}	K mg/kg_{DM}	Ca mg/kg_{DM}	Ti mg/kg_{DM}
PP	P1	2.79	30	< 2.5	2070	19900	13300	35000	860	10901	840	427000	84400
PP	P2	2.07	160	< 2.5	4310	28900	35100	63600	2690	6945	3870	197000	199000
PP	P3	1.74	180	< 2.5	3810	27300	28200	70100	1190	8846	5040	214000	105000
PP	P4	1.76	110	< 2.5	4270	16200	14900	28900	1700	14965	2300	324000	143000
PP	P5	1.76	35	< 2.5	1870	43400	11700	70400	4700	11738	1550	271000	83900
Average: PP		**2.02**	**103**	**< 2.5**	**3266**	**27140**	**20640**	**53600**	**2228**	**10679**	**2720**	**286600**	**123060**
Std. dev.		**0.45**	**69**	**-**	**1201**	**10483**	**10404**	**20066**	**1545**	**3035**	**1716**	**93077**	**48782**
LPB	P1	6.77	47	< 2.5	7880	6820	58200	55900	1400	11040	2160	225000	2680
LPB	P2	6.43	48	< 2.5	12300	5160	182000	49700	1460	11453	3730	197000	2520
LPB	P3	9.25	72	< 2.5	10600	7300	173000	53600	830	16771	5540	180000	2780
LPB	P4	6.96	66	< 2.5	20800	6130	208000	45000	2290	14800	6130	250000	7110
LPB	P5	11.39	15	< 2.5	140	15600	159000	49900	770	13295	550	317000	4630
Average: LPB		**8.16**	**50**	**< 2.5**	**10344**	**8202**	**156040**	**50820**	**1350**	**13472**	**3622**	**233800**	**3944**
Std. dev.		**2.12**	**22**	**-**	**7473**	**4213**	**57539**	**4169**	**613**	**2381**	**2321**	**53644**	**1967**
PE	P1	1.65	82	< 2.5	8500	10200	22700	63600	2160	18671	4040	159000	164000
PE	P2	2.33	110	< 2.5	8170	41700	59200	116000	2990	7456	3710	144000	120000
PE	P3	3.22	45	< 2.5	3760	15300	139000	64700	1230	15453	6810	217000	60000
PE	P4	1.34	280	< 2.5	11200	10900	34400	78700	7240	15176	5370	162000	157000
PE	P5	2.72	350	< 2.5	10600	21000	76500	106000	2150	21545	7640	198000	18800
Average: PE		**2.25**	**173**	**< 2.5**	**8446**	**19820**	**66360**	**85800**	**3154**	**15660**	**5514**	**176000**	**103960**
Std. dev.		**0.77**	**134**	**-**	**2927**	**12968**	**45712**	**24024**	**2367**	**5275**	**1706**	**30307**	**62968**
Wood	P1	1.82	830	< 2.5	46000	30200	27000	145000	1990	19623	28100	336000	11700
Wood	P2	1.98	280	< 2.5	36500	15100	14900	51600	3240	18259	13800	155000	3510
Wood	P3	1.43	310	< 2.5	61500	28400	29500	81300	4360	20205	40700	253000	11400
Wood	P4	1.32	180	< 2.5	49400	31600	24100	73500	3330	26182	29200	287000	26100
Wood	P5	1.71	240	< 2.5	33100	39500	25600	79300	6010	33551	21200	196000	4790
Average: Wood		**1.65**	**368**	**< 2.5**	**45300**	**28960**	**24220**	**86140**	**3786**	**23564**	**26600**	**245400**	**11500**
Std. dev.		**0.27**	**263**	**-**	**11247**	**8832**	**5576**	**34955**	**1501**	**6355**	**10010**	**71780**	**8973**
P&C	P1	12.18	15	< 2.5	1760	8650	85600	64700	1560	11372	260	316000	2950
P&C	P2	9.88	98	< 2.5	18500	13900	45900	76500	3410	15037	8480	284000	3520
P&C	P3	12.48	61	< 2.5	9130	14300	61900	95300	1520	15154	5210	304000	3960
P&C	P4	9.56	81	< 2.5	16900	13100	55400	72300	2380	20703	7060	411000	5170
P&C	P5	12.33	39	< 2.5	5390	20000	44000	70100	1780	19792	2640	408000	3060
Average: P&C		**11.29**	**59**	**< 2.5**	**10336**	**13990**	**58560**	**75780**	**2130**	**16411**	**4730**	**344600**	**3732**
Std. dev.		**1.44**	**33**	**-**	**7232**	**4048**	**16767**	**11712**	**794**	**3831**	**3319**	**60347**	**898**
PVC	P1	7.73	13	< 2.5	1090	7760	27400	35600	1720	14527	270	375000	91400
PVC	P2	8.72	-	-	-	-	-	-	-	-	-	-	-
PVC	P3	9.59	13	< 2.5	1630	15000	14000	45400	1290	9804	1670	312000	62200
PVC	P4	4.88	21	< 2.5	820	9010	10200	28800	2360	13255	730	413000	57500
PVC	P5	17.85	14	< 2.5	1230	7490	44000	15600	510	9605	510	277000	34100
Average: PVC		**9.75**	**15**	**< 2.5**	**1193**	**9815**	**23900**	**31350**	**1470**	**11797**	**795**	**344250**	**61300**
Std. dev.		**4.86**	**4**	**-**	**338**	**3520**	**15297**	**12517**	**776**	**2474**	**613**	**61196**	**23531**
PET	P1	0.65	210	< 2.5	18500	15900	94500	92200	5800	11748	8660	221000	71000
PET	P2	2.95	82	< 2.5	13400	18000	45800	138000	5240	8693	13200	135000	67700
PET	P3	2.75	300	6.0	4190	6500	44800	75100	1420	40695	21200	49700	121000
PET	P4	1.96	180	< 2.5	8000	14400	50300	71800	4420	12787	5770	212000	105000
PET	P5	1.89	74	< 2.5	7530	18900	37200	69500	16500	17699	4450	191000	38100
Average: PET		**2.04**	**169**	**3.2**	**10324**	**14740**	**54520**	**89320**	**6676**	**18324**	**10656**	**161740**	**80560**
Std. dev.		**0.91**	**94**	**1.6**	**5638**	**4932**	**22840**	**28636**	**5746**	**12918**	**6783**	**70996**	**32758**
PS	P1	1.98	220	< 2.5	7060	18600	19900	55000	3150	11171	4050	185000	225000
PS	P2	3.25	150	< 2.5	6690	20500	25400	69200	2550	8436	3210	188000	173000
PS	P3	4.79	65	< 2.5	2880	8660	35400	95500	3850	7548	6930	166000	146000
PS	P4	0.76	160	< 2.5	6890	8890	24800	51100	3240	13510	3520	201000	225000
PS	P5	2.93	120	< 2.5	6350	19300	22300	61000	2180	17786	4390	280000	99700
Average: PS		**2.74**	**143**	**< 2.5**	**5974**	**15190**	**25560**	**66360**	**2994**	**11690**	**4420**	**204000**	**173740**
Std. dev.		**1.50**	**57**	**-**	**1750**	**5896**	**5918**	**17662**	**648**	**4138**	**1476**	**44289**	**53636**

Table S5: Concentrations of elements in ash samples [mg/kg_{DM}] Part II. The amount of ash from PVC of SRF producer 2 was insufficient for analyses.

Material	SRF Producer	V mg/kg_{DM}	Cr mg/kg_{DM}	Mn mg/kg_{DM}	Fe mg/kg_{DM}	Co mg/kg_{DM}	Ni mg/kg_{DM}	Cu mg/kg_{DM}	Zn mg/kg_{DM}	As mg/kg_{DM}	Se mg/kg_{DM}	Sr mg/kg_{DM}	Mo mg/kg_{DM}
PP	P1	12	300	220	6910	26	70	280	5000	4.7	5.6	370	70
PP	P2	20	150	330	13100	27	110	460	2490	6.3	8.7	330	82
PP	P3	21	1730	360	11400	32	76	500	1820	7.5	5.5	390	48
PP	P4	10	130	460	5690	63	55	700	1770	5.1	6.7	280	27
PP	P5	23	350	260	8840	31	91	4020	1360	8.2	3.1	700	2.6
Average: PP		**17**	**532**	**326**	**9188**	**36**	**80**	**1192**	**2488**	**6.4**	**5.9**	**414**	**46**
Std. dev.		**6**	**676**	**93**	**3072**	**15**	**21**	**1588**	**1462**	**1.5**	**2.0**	**165**	**32**
LPB	P1	31	95	340	6120	16	57	240	360	2.7	< 2.5	890	3.7
LPB	P2	41	89	310	6630	21	56	270	400	< 2.5	< 2.5	1060	7.6
LPB	P3	48	110	370	8690	18	81	290	640	2.7	< 2.5	890	14
LPB	P4	45	82	730	6950	22	68	500	720	2.6	< 2.5	1150	5.4
LPB	P5	38	500	500	11400	35	380	310	480	5.2	< 2.5	470	7.1
Average: LPB		**41**	**175**	**450**	**7958**	**22**	**128**	**322**	**520**	**3.1**	**< 2.5**	**892**	**8**
Std. dev.		**7**	**182**	**172**	**2153**	**7**	**141**	**103**	**155**	**1.2**	**< 2.5**	**261**	**4**
PE	P1	30	13000	540	11800	50	210	1580	5500	5.4	5.7	360	< 0.25
PE	P2	34	180	390	11600	63	78	1710	4740	7.8	7.1	920	14
PE	P3	36	270	360	12200	25	140	460	1840	4.9	5.0	410	6.5
PE	P4	30	1100	1670	40100	140	920	2360	3470	9.7	7.4	550	55
PE	P5	100	510	1630	27900	39	160	890	3500	21	2.6	480	12
Average: PE		**46**	**3012**	**918**	**20720**	**63**	**302**	**1400**	**3810**	**9.8**	**5.6**	**544**	**18**
Std. dev.		**30**	**5595**	**672**	**12869**	**45**	**349**	**741**	**1398**	**6.6**	**1.9**	**222**	**22**
Wood	P1	31	270	2590	11000	38	130	1690	2400	240	< 2.5	1500	18
Wood	P2	24	590	1490	15200	79	180	550	9870	6.4	< 2.5	380	< 0.25
Wood	P3	71	470	5020	20100	680	190	800	3040	14	3.4	1040	22
Wood	P4	41	300	3880	15300	48	150	560	1940	9.0	3.1	2930	22
Wood	P5	64	630	6950	42400	76	260	1310	6660	55	17	840	45
Average: Wood		**46**	**452**	**3986**	**20800**	**184**	**182**	**982**	**4782**	**64.9**	**5.7**	**1338**	**21**
Std. dev.		**21**	**164**	**2124**	**12497**	**278**	**50**	**502**	**3399**	**99.9**	**6.3**	**977**	**16**
P&C	P1	32	98	400	6840	18	42	110	660	3.9	< 2.5	840	2.8
P&C	P2	29	170	540	11300	51	75	500	760	5.2	2.8	600	13
P&C	P3	29	120	490	9440	23	51	390	740	5.2	< 2.5	600	4.3
P&C	P4	30	130	1870	9720	28	57	600	4350	6.1	< 2.5	910	7.4
P&C	P5	34	280	640	13600	30	74	260	1060	6.2	< 2.5	760	8.2
Average: P&C		**31**	**160**	**788**	**10180**	**30**	**60**	**372**	**1514**	**5.3**	**2.6**	**742**	**7**
Std. dev.		**2**	**72**	**611**	**2493**	**13**	**14**	**194**	**1593**	**0.9**	**0.1**	**140**	**4**
PVC	P1	12	200	290	5490	13	42	180	4760	32	4.2	590	2.9
PVC	P2	-	-	-	-	-	-	-	-	-	-	-	-
PVC	P3	12	230	140	3340	11	29	100	1680	2.9	8.7	290	8.6
PVC	P4	8.9	330	380	5600	32	95	410	2940	5.2	5.8	710	4.9
PVC	P5	12	230	120	2750	11	49	160	2060	< 2.5	3.4	210	< 0.25
Average: PVC		**11**	**248**	**233**	**4295**	**17**	**54**	**213**	**2860**	**10.7**	**5.5**	**450**	**4**
Std. dev.		**2**	**57**	**124**	**1464**	**10**	**29**	**136**	**1372**	**14.3**	**2.3**	**238**	**4**
PET	P1	58	440	1750	27800	230	370	970	2940	9.7	3.6	430	12
PET	P2	58	220	840	27900	120	110	1070	1780	10	4.6	350	14
PET	P3	23	380	360	12700	100	260	240	980	3.9	4.3	950	12
PET	P4	34	230	1990	40300	160	200	3030	4990	14	3.7	440	37
PET	P5	59	1820	720	21100	310	190	790	1920	7.9	3.0	720	15
Average: PET		**46**	**618**	**1132**	**25960**	**184**	**226**	**1220**	**2522**	**9.1**	**3.8**	**578**	**18**
Std. dev.		**17**	**679**	**702**	**10152**	**86**	**97**	**1061**	**1546**	**3.7**	**0.6**	**251**	**11**
PS	P1	31	860	630	14800	42	140	700	6130	7.6	8.1	340	28
PS	P2	24	480	330	13000	61	150	1920	3920	7.2	9.0	520	20
PS	P3	25	140	200	8180	53	64	1030	2690	6.2	7.0	340	3.6
PS	P4	23	210	820	19500	48	160	8220	5030	6.5	7.9	320	8.2
PS	P5	56	710	540	20200	61	290	480	5590	8.5	5.3	350	23
Average: PS		**32**	**480**	**504**	**15136**	**53**	**161**	**2470**	**4672**	**7.2**	**7.5**	**374**	**17**
Std. dev.		**14**	**311**	**245**	**4943**	**8**	**82**	**3261**	**1378**	**0.9**	**1.4**	**82**	**10**

Table S6: Concentrations of elements in ash samples [mg/kg_{DM}] Part III. The amount of ash from PVC of SRF producer 2 was insufficient for analyses.

Material	SRF Producer	Pd mg/kg_{DM}	Ag mg/kg_{DM}	Cd mg/kg_{DM}	Sn mg/kg_{DM}	Sb mg/kg_{DM}	Te mg/kg_{DM}	Ba mg/kg_{DM}	W mg/kg_{DM}	Hg mg/kg_{DM}	Tl mg/kg_{DM}	Pb mg/kg_{DM}
PP	P1	0.29	1.9	2.1	14	190	< 0.50	6640	110	2.2	< 0.25	610
PP	P2	0.27	5.2	4.2	130	340	0.59	430	160	3.0	< 0.25	140
PP	P3	0.61	4.0	4.0	40	770	0.72	9420	19	0.54	< 0.25	1070
PP	P4	0.51	11	4.2	120	140	< 0.50	2660	30	0.69	< 0.25	78
PP	P5	4.0	1.3	150	82	1410	< 0.50	16800	32	0.69	< 0.25	960
Average: PP		**1.1**	**4.7**	**33**	**77**	**570**	**0.56**	**7190**	**70**	**1.4**	**< 0.25**	**572**
Std. dev.		**1.6**	**3.9**	**65**	**50**	**531**	**0.10**	**6400**	**62**	**1.1**	**-**	**456**
LPB	P1	0.53	1.8	3.6	43	39	1.2	240	12	0.35	< 0.25	58
LPB	P2	0.61	1.7	1.2	43	56	0.56	190	67	1.7	< 0.25	39
LPB	P3	0.49	3.3	2.7	20	48	< 0.50	560	34	0.89	< 0.25	86
LPB	P4	0.68	5.9	2.1	11	74	10	230	3.6	< 0.25	< 0.25	100
LPB	P5	0.42	0.58	1.0	160	83	< 0.50	260	13	0.33	< 0.25	74
Average: LPB		**0.5**	**2.7**	**2**	**55**	**60**	**2.55**	**296**	**26**	**0.7**	**< 0.25**	**71**
Std. dev.		**0.1**	**2.1**	**1**	**60**	**18**	**4.17**	**150**	**26**	**0.6**	**-**	**24**
PE	P1	0.63	3.3	6.5	37	500	1.4	58700	24	1.0	< 0.25	200
PE	P2	0.75	4.9	2.4	40	140	1.5	1530	190	4.1	< 0.25	120
PE	P3	0.40	1.8	14	53	1150	< 0.50	8670	26	0.64	< 0.25	140
PE	P4	0.65	11	8.2	260	600	2.0	11500	53	2.7	< 0.25	290
PE	P5	21	6.1	4.1	110	150	0.63	1840	99	2.3	< 0.25	560
Average: PE		**4.7**	**5.4**	**7**	**100**	**508**	**1.21**	**16448**	**78**	**2.1**	**< 0.25**	**262**
Std. dev.		**9.1**	**3.5**	**4**	**94**	**414**	**0.63**	**24011**	**69**	**1.4**	**-**	**179**
Wood	P1	1.2	7.5	8.5	120	260	1.8	4530	7.6	0.31	< 0.25	1380
Wood	P2	0.36	4.7	19	31	89	1.2	5180	61	1.8	< 0.25	160
Wood	P3	0.93	13	17	70	130	0.71	1400	54	1.3	< 0.25	360
Wood	P4	1.8	9.0	9.5	120	230	3.3	12100	8.0	0.49	< 0.25	290
Wood	P5	5.7	3.7	9.2	130	120	1.1	4670	110	2.3	< 0.25	200
Average: Wood		**2.0**	**7.6**	**13**	**94**	**166**	**1.62**	**5576**	**48**	**1.2**	**< 0.25**	**478**
Std. dev.		**2.1**	**3.7**	**5**	**42**	**75**	**1.02**	**3939**	**43**	**0.8**	**-**	**510**
P&C	P1	0.59	0.92	2.0	95	51	< 0.50	200	15	0.40	< 0.25	66
P&C	P2	0.44	4.4	2.0	49	46	< 0.50	510	43	1.1	< 0.25	76
P&C	P3	0.49	3.5	2.0	58	63	< 0.50	590	11	0.33	< 0.25	110
P&C	P4	0.61	6.9	5.8	26	160	2.3	2940	16	0.35	< 0.25	170
P&C	P5	2.4	0.60	1.7	31	52	0.70	640	130	2.7	< 0.25	110
Average: P&C		**0.9**	**3.3**	**3**	**52**	**74**	**0.90**	**976**	**43**	**1.0**	**< 0.25**	**106**
Std. dev.		**0.8**	**2.6**	**2**	**27**	**48**	**0.79**	**1111**	**50**	**1.0**	**-**	**41**
PVC	P1	0.48	0.55	7.2	4900	20	< 0.50	18600	9.2	< 0.25	< 0.25	590
PVC	P2	-	-	-	-	-	-	-	-	-	-	-
PVC	P3	< 0.25	1.3	25	1270	500	< 0.50	2540	5.1	< 0.25	< 0.25	420
PVC	P4	0.52	3.3	15	1250	600	< 0.50	16100	5.0	< 0.25	< 0.25	380
PVC	P5	1.4	2.9	1.7	1810	37	< 0.50	820	6.4	< 0.25	< 0.25	540
Average: PVC		**0.7**	**2.0**	**12**	**2308**	**289**	**< 0.50**	**9515**	**6**	**< 0.25**	**< 0.25**	**483**
Std. dev.		**0.5**	**1.3**	**10**	**1748**	**304**	**-**	**9132**	**2**	**-**	**-**	**99**
PET	P1	0.68	40	13	160	13900	0.99	4210	34	1.4	< 0.25	310
PET	P2	0.56	7.4	4.6	82	8940	1.7	8160	64	1.6	< 0.25	180
PET	P3	0.49	5.4	4.2	280	3750	0.57	14300	30	0.89	1.8	120
PET	P4	0.58	15	43	220	22600	< 0.50	2570	17	0.50	< 0.25	260
PET	P5	14	5.2	4.3	120	10300	1.8	2950	99	2.0	< 0.25	2130
Average: PET		**3.3**	**14.6**	**14**	**172**	**11898**	**1.11**	**6438**	**49**	**1.3**	**0.6**	**600**
Std. dev.		**6.0**	**14.7**	**17**	**79**	**7004**	**0.61**	**4921**	**33**	**0.6**	**0.7**	**858**
PS	P1	0.39	5.5	3.7	110	4420	1.5	8130	60	1.4	< 0.25	110
PS	P2	0.61	2.7	3.9	45	110	0.87	2510	140	2.9	< 0.25	180
PS	P3	0.50	5.7	450	36	240	< 0.50	1480	12	0.30	0.26	160
PS	P4	2.2	4.9	6.1	220	280	< 0.50	6100	23	0.68	< 0.25	220
PS	P5	7.6	1.7	4.4	74	130	0.59	4740	49	1.1	< 0.25	480
Average: PS		**2.3**	**4.1**	**94**	**97**	**1036**	**0.79**	**4592**	**57**	**1.3**	**0.3**	**230**
Std. dev.		**3.1**	**1.8**	**199**	**75**	**1893**	**0.42**	**2685**	**50**	**1.0**	**0.0**	**145**

3. Thermogravimetric analysis of SRF (exemplary)

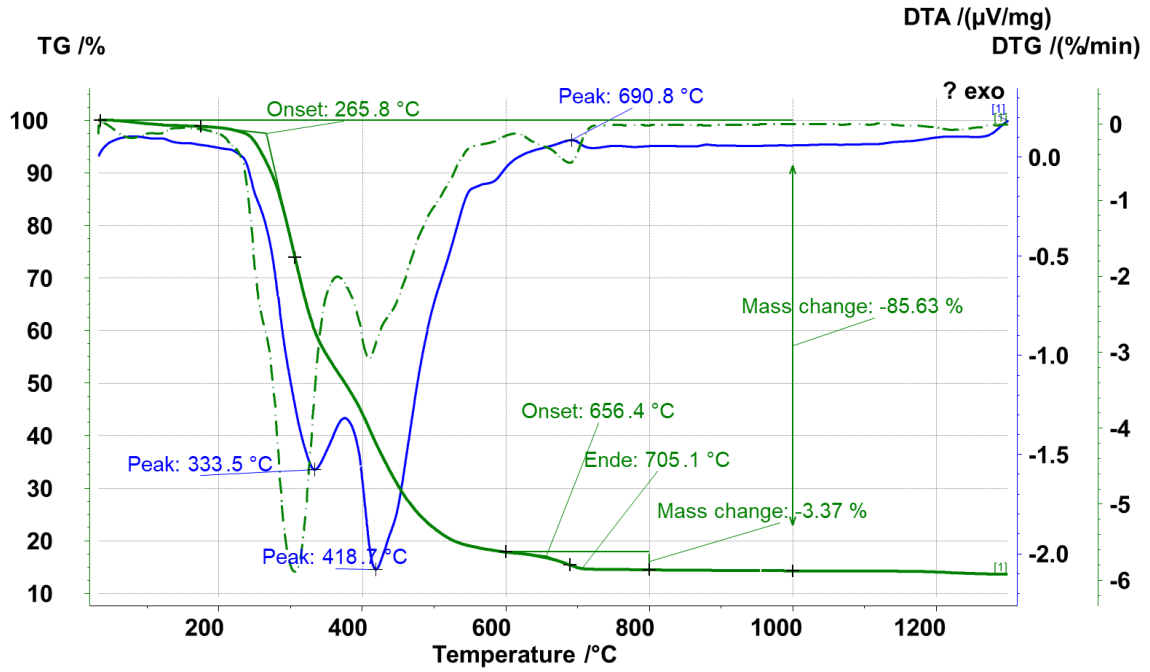

Figure S1: Thermogravimetric analysis (green line), derivative (DTG; green dash-dotted line), and differential scanning calorimetry (DSC; blue line) of SRF sample No. 1 under air atmosphere (Kittinger, 2020).

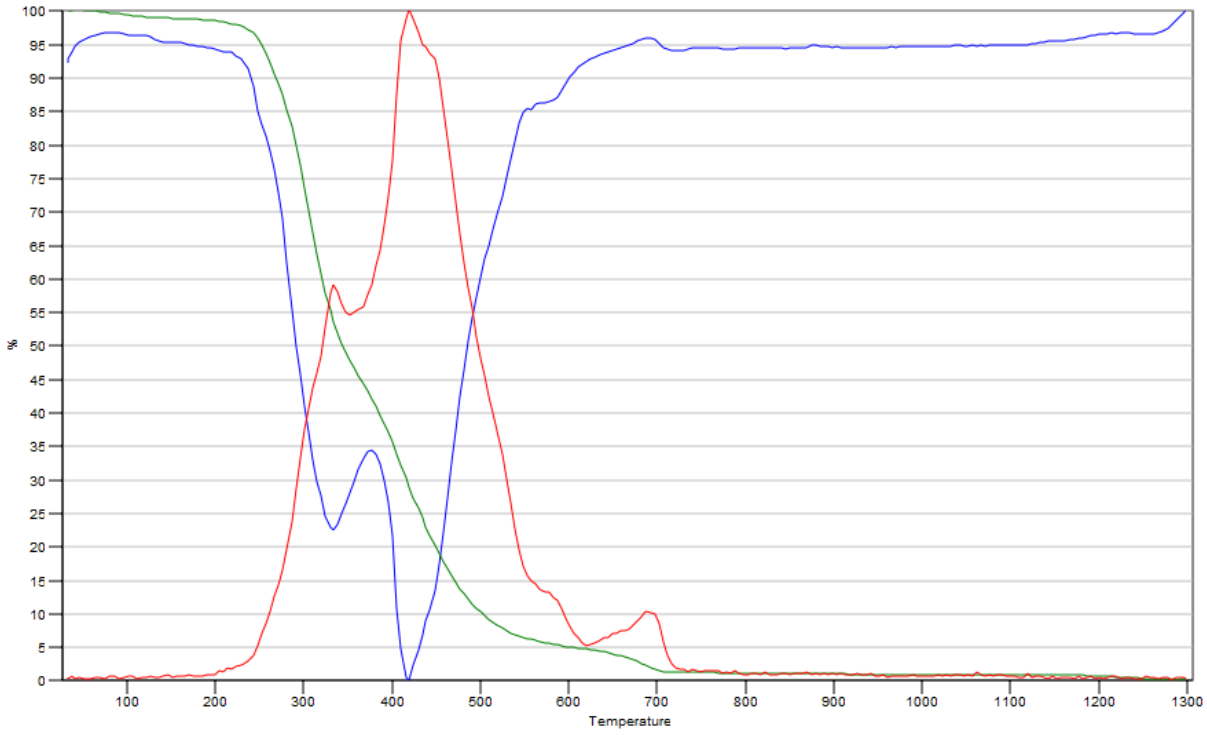

Figure S2: STA with thermogravimetry (TG, green line), differential scanning calorimetry (DSC; blue line), and CO_2 development (red line) of SRF sample No. 1 under air atmosphere. All curves are normalized to 100 % (Kittinger, 2020).

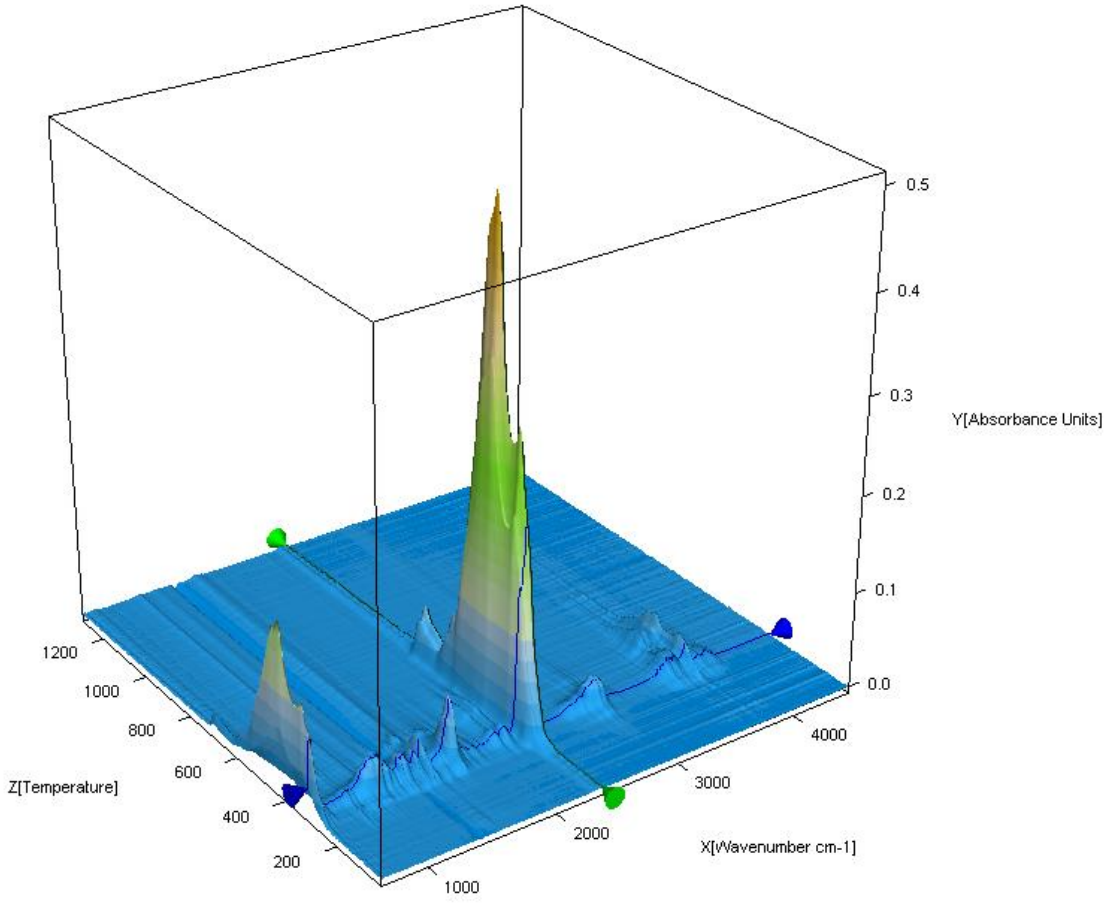

Figure S3: Overview of the detectable gases and the temperature (z-axis) with wave number (x-axis) and absorbance (y-axis) of SRF samples No. 1 (Kittinger, 2020).

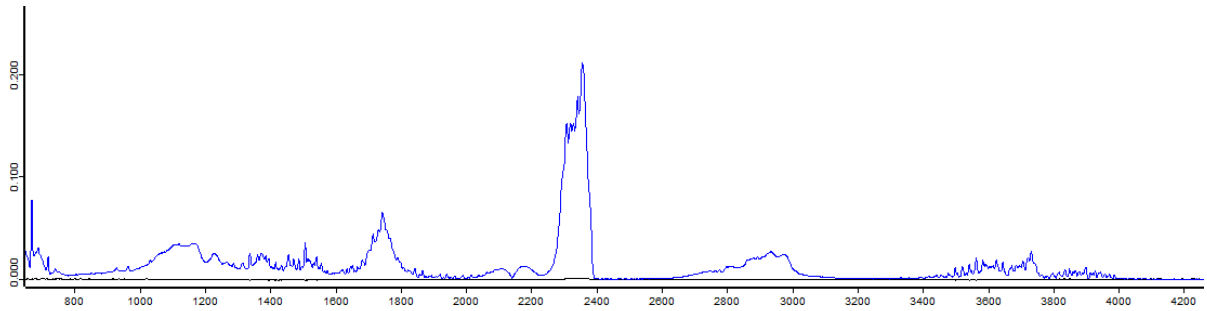

Figure S4: FTIR spectrum of SRF sample No. 1 at 306°C (Kittinger, 2020).

References

Kittinger, F. (2020): Internal report thermogravimetric analysis.

Publication IV – Supplementary

Sampling and analysis of coarsely shredded mixed commercial waste. Part II: particle size-dependent element determination

S.A. Viczek, L. Kandlbauer, K. Khodier, A. Aldrian, R. Sarc

Submitted to journal: January 04, 2021
Status on March 24, 2021: Under review since January 13, 2021

Content

Appendix A - RSV and GEE

Table A.1 RSV values [%] of element concentrations referring to dry mass without hard impurities. Max = 203.5 (Cd; 60–80 mm), Min = 0 (Impurities, 0–5 mm), Mean = 51.1 %, Median = 41.4 %. 58 values (20 %) with RSV < 20 % (petrol blue), 117 values (39 %) 20 % ≤ RSV < 50 % (light blue), 122 values (41 %) with RSV > 50 % (grey).

	0–5 mm	5–10 mm	10–20 mm	20–40 mm	40–60 mm	60–80 mm	80–100 mm	100–200 mm	200–400 mm
Ag	33.0	37.9	37.8	41.6	26.4	32.5	40.5	29.1	54.7
Al	8.9	7.6	7.1	29.3	30.4	31.8	50.5	23.9	40.1
As	32.1	43.4	31.3	52.9	34.2	31.0	55.6	38.3	41.7
Ba	18.3	22.3	39.7	57.4	47.3	62.1	78.1	55.6	40.6
Ca	11.0	11.4	26.7	41.4	39.4	37.5	55.9	27.3	37.7
Cd	50.8	103.4	74.7	143.4	172.7	203.5	119.1	132.7	169.6
Cl	21.2	26.7	18.1	41.8	41.0	43.7	53.2	72.3	89.2
Co	19.9	14.1	13.9	57.1	175.4	30.6	84.6	24.6	75.8
Cr	30.8	14.4	150.6	74.3	44.2	117.7	66.3	75.7	166.7
Cu	77.4	135.5	72.8	141.8	96.2	82.3	123.6	14.5	122.2
Fe	37.0	26.2	24.1	68.8	72.4	54.1	97.9	23.6	30.7
Hg	69.6	43.7	56.0	64.6	62.5	22.6	52.4	34.6	10.9
K	5.6	12.0	15.1	49.6	54.5	19.7	88.3	20.6	42.0
Li	18.8	24.6	22.1	51.2	51.0	48.8	62.8	22.1	36.9
Mg	9.3	16.4	27.3	44.5	52.6	18.7	89.1	30.0	23.7
Mn	24.7	14.3	15.4	61.1	59.4	33.9	83.1	26.4	27.7
Mo	27.1	30.7	39.3	67.2	74.3	21.1	91.8	49.3	56.2
Na	10.0	19.3	14.9	72.4	80.7	37.9	95.9	40.3	51.8
Ni	33.0	14.1	125.1	65.2	49.4	119.9	82.5	23.4	77.2
P	8.4	14.4	25.9	86.3	40.7	43.0	79.3	31.8	55.7
Pb	118.2	111.5	80.9	60.3	99.8	93.4	128.4	108.8	101.5
Pd	21.7	11.2	0.0	5.8	5.0	0.0	5.0	0.0	0.0
Sb	38.1	30.8	49.7	63.4	67.3	94.4	83.3	48.8	49.2
Si	18.0	16.1	17.0	83.2	105.6	37.1	124.0	38.6	27.7
Sn	140.4	76.8	55.5	39.8	116.4	51.3	93.6	53.1	139.4
Sr	12.8	10.9	22.0	58.0	64.5	25.9	88.2	18.6	59.1
Ti	11.1	18.1	22.7	20.9	25.5	41.8	19.9	34.8	31.3
V	48.1	50.9	60.2	39.0	35.9	48.0	45.9	74.6	72.6
W	84.5	68.4	127.1	115.9	98.8	51.2	114.0	89.3	66.4
Zn	14.2	68.4	24.9	36.9	34.9	33.6	45.5	44.2	49.1
Ash	2.2	8.3	8.0	63.0	68.2	28.4	74.9	13.1	35.0
Impurities	0.0	61.3	35.9	69.4	28.6	29.3	49.1	28.9	149.9
LHV	11.5	7.4	7.2	31.0	26.3	8.1	33.8	7.7	13.9

RSV < 20 %	20 % ≤ RSV < 50 %	RSV ≥ 50 %

Table A.2 RSV values [%] of element concentrations referring to dry mass including hard impurities. Max = 204.2 % (Cd; 60–80 mm), Min = 2.2 % (Ash, 0–5 mm), Mean = 52.3 %, Median = 43.1 %. 55 values (19 %) with RSV < 20 % (petrol blue), 110 values (38 %) with 20 % ≤ RSV < 50 % (light blue), 123 values (43 %) with RSV > 50 % (grey).

	0–5 mm	5–10 mm	10–20 mm	20–40 mm	40–60 mm	60–80 mm	80–100 mm	100–200 mm	200–400 mm
Ag	33.0	39.3	36.9	40.8	27.0	36.0	41.6	29.5	60.1
Al	8.9	8.0	8.5	31.9	27.9	34.4	54.9	22.7	45.4
As	32.1	44.2	33.1	52.6	34.7	31.7	59.7	37.8	46.1
Ba	18.3	22.7	39.3	58.5	49.5	59.0	82.5	52.1	40.5
Ca	11.0	11.9	27.0	40.5	42.1	35.8	60.4	28.5	42.8
Cd	50.8	103.2	75.7	145.3	166.8	204.2	119.6	134.4	171.8
Cl	21.2	28.4	23.3	44.7	43.4	44.2	50.5	74.7	88.2
Co	19.9	14.8	13.2	55.5	167.1	29.8	88.7	24.4	80.8
Cr	30.8	15.8	150.3	72.7	46.8	118.2	68.6	76.1	173.4
Cu	77.4	135.5	72.6	144.6	92.2	86.5	124.3	16.3	125.9
Fe	37.0	26.1	25.4	67.8	74.9	54.2	101.6	25.4	36.6
Hg	69.6	44.9	64.4	68.5	66.9	20.3	56.1	38.5	18.3
K	5.6	12.2	11.5	48.2	57.5	19.1	92.2	21.6	46.3
Li	18.8	24.9	21.3	49.9	55.8	48.5	67.5	22.9	41.3
Mg	9.3	15.9	28.2	43.2	54.8	20.7	92.8	29.0	29.9
Mn	24.7	14.6	16.6	59.6	61.7	36.2	87.0	26.3	34.2
Mo	27.1	30.8	39.9	65.8	76.9	19.2	94.7	52.2	60.1
Na	10.0	19.6	14.5	70.2	83.3	40.9	99.8	41.6	54.6
Ni	33.0	13.9	124.9	63.6	50.8	119.3	86.1	25.3	81.7
P	8.4	14.2	23.8	93.6	43.0	42.7	84.2	32.3	59.8
Pb	118.2	110.0	79.5	63.3	101.3	89.6	125.7	109.4	103.6
Pd	21.7	11.9	6.0	11.7	8.5	5.4	11.9	4.1	12.6
Sb	38.1	31.4	51.0	52.9	70.9	94.5	80.2	48.3	50.9
Si	18.0	15.7	15.5	80.7	108.4	38.0	126.5	38.7	33.3
Sn	140.4	76.9	54.7	40.8	117.5	52.5	97.7	50.5	141.7
Sr	12.8	10.1	22.8	58.3	66.9	27.4	92.0	16.5	64.6
Ti	11.1	17.1	21.9	25.3	26.3	38.8	25.9	33.1	36.8
V	48.1	51.8	60.9	40.6	35.2	48.4	48.9	74.5	77.4
W	84.5	69.6	136.5	121.3	102.5	50.9	115.9	92.2	71.3
Zn	14.2	69.5	22.6	34.1	30.7	33.5	48.0	44.9	53.1
Ash	2.2	9.3	9.5	65.2	72.7	25.7	76.3	13.1	44.7
LHV	11.5	7.0	9.8	33.6	26.9	9.0	35.0	9.8	18.6

RSV < 20 %	20 % ≤ RSV < 50 %	RSV ≥ 50 %

Table A.3 RSV values [%] of element concentrations referring to original mass including hard impurities. Max = 201.7 % (Cd; 60–80 mm), Min = 3.9 % (Ash, 0–5 mm), Mean = 52.4 %, Median = 43.2 %. 54 values (19 %) with RSV < 20 % (petrol blue), 110 values (38 %) with 20 % ≤ RSV < 50 % (light blue), 124 values (43 %) with RSV > 50 % (grey). Note: the water content was not determined directly, but after sample processing (screening, sorting) and storage in between.

	0–5 mm	5–10 mm	10–20 mm	20–40 mm	40–60 mm	60–80 mm	80–100 mm	100–200 mm	200–400 mm
Ag	32.3	39.7	39.0	39.7	30.5	35.0	40.9	31.0	59.2
Al	8.7	8.4	9.0	31.2	29.8	31.1	54.2	22.2	45.1
As	32.7	44.6	32.1	50.4	37.9	28.3	57.4	36.3	45.6
Ba	17.6	23.7	39.6	55.3	51.7	60.6	79.5	50.1	39.2
Ca	12.4	13.2	26.8	37.4	46.4	36.0	61.2	29.9	42.9
Cd	51.0	103.4	75.1	146.1	166.3	201.7	120.8	134.4	172.9
Cl	20.9	28.4	21.5	47.0	38.9	44.0	51.2	74.9	88.3
Co	21.5	14.8	15.3	51.9	165.0	28.4	88.5	23.5	80.2
Cr	32.5	16.8	153.5	67.9	48.9	118.8	69.0	75.6	175.0
Cu	80.0	135.5	72.0	150.7	90.1	83.1	121.0	17.7	124.5
Fe	38.8	27.4	24.8	63.8	81.4	52.3	101.0	25.7	36.4
Hg	67.8	43.8	60.1	64.5	64.8	25.8	55.3	39.0	18.8
K	6.1	13.1	12.1	44.2	62.1	16.9	91.7	21.4	46.4
Li	19.7	25.6	20.6	49.2	57.9	53.8	67.7	24.4	41.6
Mg	9.1	15.6	28.2	39.3	60.2	17.4	92.6	27.4	29.8
Mn	26.3	15.7	16.4	54.7	67.8	33.5	86.6	24.6	33.6
Mo	27.8	30.0	41.6	60.7	83.2	20.1	93.4	52.4	60.8
Na	9.6	19.4	14.4	66.1	89.8	37.2	99.3	41.1	54.8
Ni	34.7	13.9	128.3	59.9	54.2	119.7	85.6	25.6	81.1
P	7.5	14.7	24.4	96.7	43.6	42.3	85.5	30.7	59.4
Pb	118.5	109.3	80.7	66.5	107.3	91.7	120.5	111.6	103.2
Pd	21.5	13.2	5.3	12.9	11.5	5.8	11.4	7.0	13.6
Sb	39.6	31.8	50.2	55.5	66.9	94.3	81.0	49.0	52.2
Si	18.4	15.5	14.6	75.6	116.1	33.7	125.2	36.9	33.3
Sn	140.1	78.7	54.8	41.8	126.4	51.4	97.4	47.9	140.8
Sr	12.4	10.1	23.0	57.9	73.2	22.7	91.7	16.0	64.1
Ti	10.4	16.9	24.3	27.1	23.5	40.6	24.2	28.6	37.4
V	48.1	52.1	62.1	41.3	32.6	46.6	45.2	73.6	76.8
W	82.5	68.0	130.8	116.3	107.5	50.7	114.3	92.5	70.9
Zn	15.5	71.3	23.3	31.7	31.4	33.1	46.8	46.2	53.1
Ash	3.9	10.8	9.7	62.3	79.2	23.7	78.6	15.5	45.2
LHV	9.5	7.8	10.0	34.2	26.4	11.5	34.8	10.9	19.5

RSV < 20 %	20 % ≤ RSV < 50 %	RSV ≥ 50 %

Table A.4 RSV values [%] of element concentrations referring to mg/MJ. Max = 219.5 % (Si; 40–60 mm), Min = 7.2 % (Pd, 10–20 mm mm), Mean = 72.6 %, Median = 55.8 %. 36 values (13 %) with RSV < 20 % (petrol blue), 96 values (33 %) with 20 % ≤ RSV < 50 % (light blue), 156 values (54 %) with RSV > 50 % (grey).

	0–5 mm	5–10 mm	10–20 mm	20–40 mm	40–60 mm	60–80 mm	80–100 mm	100–200 mm	200–400 mm
Ag	30.0	39.7	40.2	98.9	79.2	31.3	106.7	32.9	77.5
Al	14.7	12.4	11.0	73.7	99.2	35.4	129.1	25.7	56.0
As	40.2	47.8	32.7	109.9	125.2	34.1	135.3	37.5	56.1
Ba	14.9	26.1	42.7	93.5	143.3	63.5	144.4	56.3	44.2
Ca	20.2	13.9	28.2	100.4	131.2	42.1	127.4	29.7	57.3
Cd	48.1	107.8	79.6	136.6	166.2	197.0	95.8	133.6	165.1
Cl	22.3	29.0	14.2	26.2	30.9	37.1	37.7	73.3	98.0
Co	31.0	17.7	16.8	119.1	158.5	31.5	157.9	24.7	103.8
Cr	42.5	17.3	152.2	135.8	140.9	112.3	116.7	77.1	167.2
Cu	77.4	135.5	72.8	141.8	96.2	82.3	123.6	14.5	122.2
Fe	49.3	24.3	27.3	127.9	184.8	59.2	168.3	20.7	48.2
Hg	65.6	46.9	53.0	80.1	149.3	19.5	133.5	35.5	27.7
K	12.8	15.2	17.7	113.0	163.3	24.3	161.8	18.0	56.3
Li	26.1	25.1	20.0	106.7	131.0	47.4	137.0	23.6	42.4
Mg	13.8	20.6	34.0	107.2	160.8	22.6	161.8	31.9	38.9
Mn	36.2	15.6	19.8	124.4	170.6	39.0	158.4	24.0	42.3
Mo	35.3	32.2	42.2	130.6	189.7	23.9	169.6	50.1	66.2
Na	13.2	24.1	21.0	134.1	195.3	40.8	168.2	37.3	65.8
Ni	44.7	13.3	126.7	125.4	143.1	111.0	158.3	22.2	104.8
P	9.4	13.8	30.3	89.5	130.6	38.5	145.3	30.0	75.6
Pb	118.2	110.2	83.3	65.2	187.2	95.1	146.2	115.9	119.7
Pd	27.2	13.7	7.2	55.5	83.8	7.7	80.8	7.3	15.6
Sb	47.7	35.2	54.3	47.2	60.7	97.7	69.5	45.1	41.7
Si	19.7	20.8	22.6	144.6	219.5	42.1	192.2	33.7	36.7
Sn	140.4	76.8	55.5	39.8	116.4	51.3	93.6	53.1	139.4
Sr	15.0	11.2	28.6	108.4	178.7	31.0	161.3	21.2	84.6
Ti	10.9	21.8	23.0	53.8	80.6	42.5	92.7	35.0	38.8
V	52.7	53.1	58.7	64.1	71.6	49.5	105.5	73.0	88.7
W	78.2	71.7	123.1	101.4	203.7	52.6	191.7	82.9	82.1
Zn	22.0	66.9	28.9	92.3	90.3	37.1	90.4	48.9	66.6
Ash	9.3	14.0	8.5	102.5	156.7	35.4	125.2	14.4	53.0
Impurities	12.0	60.3	35.9	84.1	64.4	30.4	68.1	31.0	150.1

RSV < 20 %	20 % ≤ RSV < 50 %	RSV ≥ 50 %

Table A.5 RSV values [%] of element concentrations referring to the mass share [%] of the element with respect to the primary sample [DM without hard impurities]. Max = 210.4 % (Cd) Min = 6.5 % (Pd), Mean = 58.1 %, Median = 50.2 %. 32 parameters (12 %) with RSV < 20 % (petrol blue), 102 parameters (38 %) with 20 % ≤ RSV < 50 % (light blue), 136 parameters (50 %) with RSV > 50 % (grey)

	0–5 mm	5–10 mm	10–20 mm	20–40 mm	40–60 mm	60–80 mm	80–100 mm	100–200 mm	200–400 mm
Ag	33.1	46.2	41.3	45.0	29.5	35.9	41.3	39.9	89.0
Al	13.5	14.3	15.7	31.5	34.1	29.3	52.9	31.6	67.3
As	37.9	45.2	40.3	54.9	40.5	29.8	57.8	39.3	65.9
Ba	14.1	15.4	40.4	51.8	53.5	65.7	79.7	57.6	55.0
Ca	20.6	12.0	25.4	44.7	44.7	33.2	58.9	30.2	69.6
Cd	50.5	99.0	85.1	139.6	173.6	210.4	122.8	135.1	166.6
Cl	24.3	33.0	21.0	45.6	40.2	48.6	54.2	75.4	106.1
Co	28.8	17.6	20.7	59.5	175.6	30.4	87.0	21.5	114.9
Cr	40.9	22.0	151.5	75.9	50.7	122.7	68.2	76.7	190.3
Cu	86.8	131.5	60.0	140.8	99.4	77.6	127.9	20.1	112.0
Fe	45.3	22.9	28.6	69.6	80.9	46.4	100.4	27.9	60.4
Hg	66.4	46.3	57.8	71.5	67.7	26.3	55.3	38.9	43.2
K	14.0	13.8	15.9	51.9	62.3	17.7	90.8	24.1	74.0
Li	25.7	28.2	17.0	55.2	55.3	45.7	64.7	23.5	61.5
Mg	13.5	12.3	42.2	48.3	59.9	15.9	91.7	25.5	53.3
Mn	32.8	13.9	23.2	62.0	67.7	28.5	85.9	27.3	54.4
Mo	33.8	36.1	43.8	67.9	83.4	24.3	95.3	51.6	78.0
Na	12.1	20.5	24.5	74.7	89.8	36.1	99.0	43.2	73.9
Ni	43.2	20.4	126.6	67.4	51.6	126.6	85.2	27.9	114.7
P	11.6	19.1	33.9	83.8	46.7	46.4	81.0	28.0	87.1
Pb	118.1	115.3	81.3	62.8	104.3	96.5	118.1	119.6	135.4
Pd	25.1	15.8	14.5	14.8	11.6	6.5	10.6	11.8	34.9
Sb	43.4	23.8	55.7	56.6	67.8	94.2	82.8	52.3	58.8
Si	21.7	15.9	23.2	84.5	115.6	33.7	128.2	41.0	54.4
Sn	143.3	67.8	61.3	48.6	115.8	54.2	95.9	47.7	164.8
Sr	16.9	15.9	35.7	60.1	73.3	22.2	90.7	18.0	96.9
Ti	10.3	15.2	26.3	24.0	25.7	45.8	23.6	28.7	54.8
V	51.2	52.8	67.2	42.1	37.2	47.8	44.2	74.7	99.6
W	80.7	69.6	125.5	125.4	106.9	50.0	119.1	94.3	92.3
Zn	22.6	71.2	28.5	38.3	37.6	31.7	46.5	55.9	77.5

RSV < 20 %	20 % ≤ RSV < 50 %	RSV ≥ 50 %

Table A.6 RSV values [%] of overall element concentrations in the waste mix referring to mg/kg_{DM} and mg/MJ. For mg/kg_{DM}: Max = 96.8 % (Cd) Min = 2.7 % (dry matter), Mean = 24.6 %, Median = 18.4 %. 20 parameters (57 %) with RSV < 20 % (petrol blue), 11 parameters (31 %) with 20 % ≤ RSV < 50 % (light blue), 4 parameters (11 %) with RSV > 50 % (grey). For mg/MJ: Max = 102.2 % (Cd) Min = 7.7 % (Pd), Mean = 29.8 %, Median = 24.7 %. 9 parameters (30 %) with RSV < 20 % (petrol blue), 18 parameters (60 %) with 20 % ≤ RSV < 50 % (light blue), 3 parameters (10 %) with RSV > 50 % (grey).

	mg/kg_{DM}	mg/MJ
Ag	8.2	12.8
Al	9.1	16.1
As	11.7	14.3
Ba	22.7	29.0
Ca	15.5	19.2
Cd	96.8	102.2
Cl	27.1	23.0
Co	33.7	39.3
Cr	28.7	31.2
Cu	51.7	48.5
Fe	28.7	30.2
Hg	43.6	39.7
K	14.1	21.5
Li	19.3	21.5
Mg	17.8	24.9
Mn	18.4	22.4
Mo	13.5	15.1
Na	19.4	26.4
Ni	25.1	28.9
P	20.3	25.1
Pb	32.1	35.1
Pd	4.7	7.7
Sb	18.4	16.4
Si	25.5	33.1
Sn	70.3	76.1
Sr	17.4	24.4
Ti	11.6	12.1
V	17.1	14.8
W	62.0	58.9
Zn	20.3	23.8
Ash	14.4	
Impurities	18.2	
LHV	6.5	
Dry matter	2.7	
Water content	14.3	

RSV < 20 %
20 % ≤ RSV < 50 %
RSV ≥ 50 %

Appendix B - Element-material and LHV-material correlations

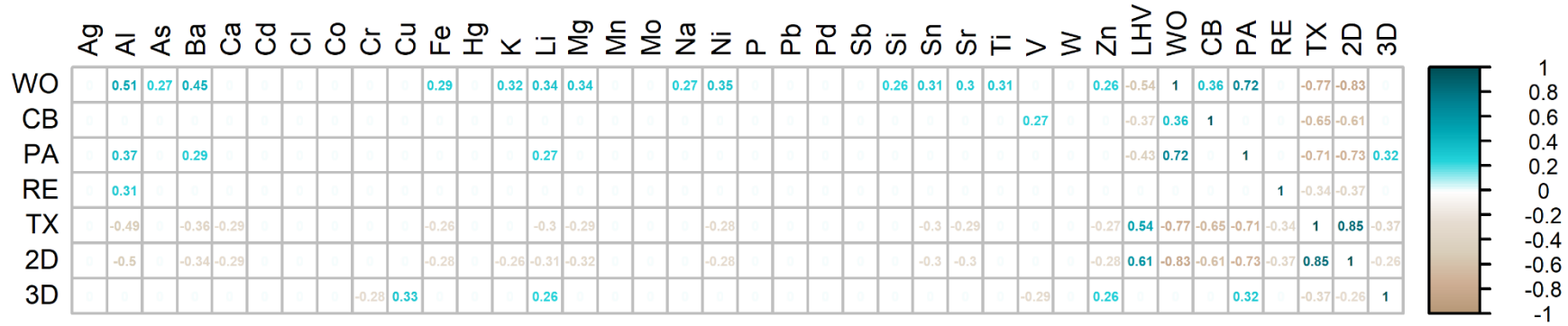

Figure B.1: Pearson correlation coefficients for statistically significant ($p < 0.05$) positive (petrol blue) and negative (beige) correlations of chemical analysis parameters and sorting analyses for particle size classes >20mm, see Appendix E

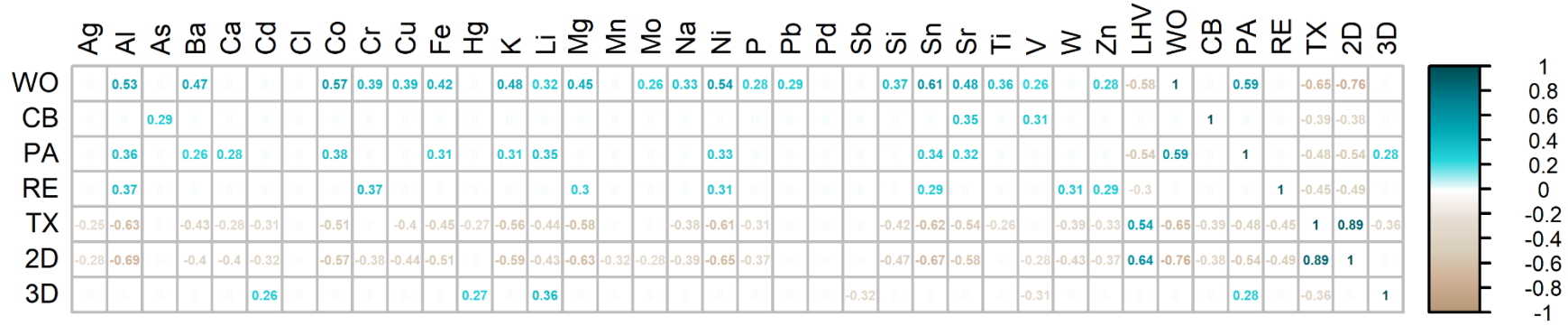

Figure B.2: Spearman correlation coefficients for statistically significant ($p < 0.05$) positive (petrol blue) and negative (beige) correlations of chemical analysis parameters and sorting analyses for particle size classes >20mm, see Appendix E

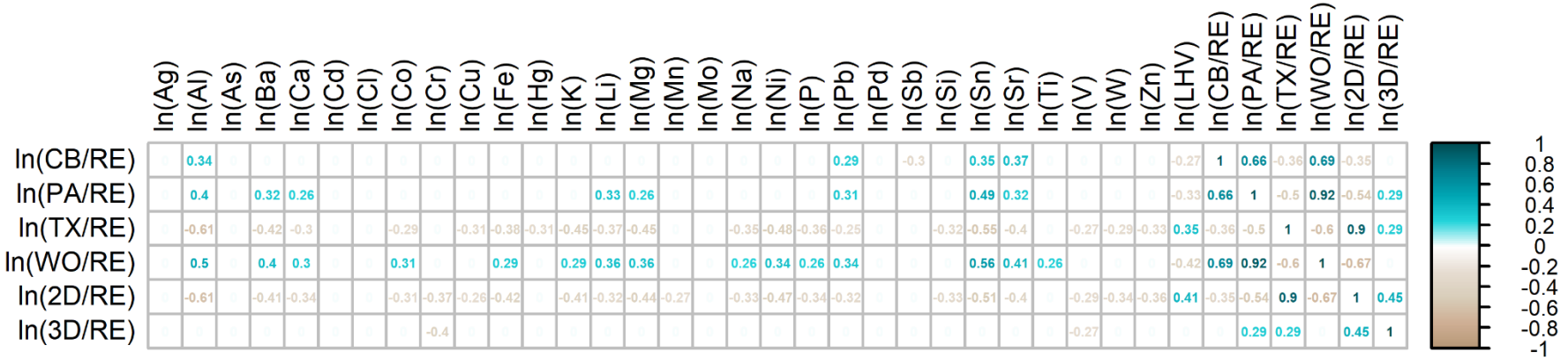

Figure B.3: Pearson correlation coefficients for statistically significant ($p < 0.05$) positive (petrol blue) and negative (beige) correlations of chemical analysis parameters and log-ratios (reference fraction: residual) from sorting analyses for particle size classes >20mm, see Appendix E

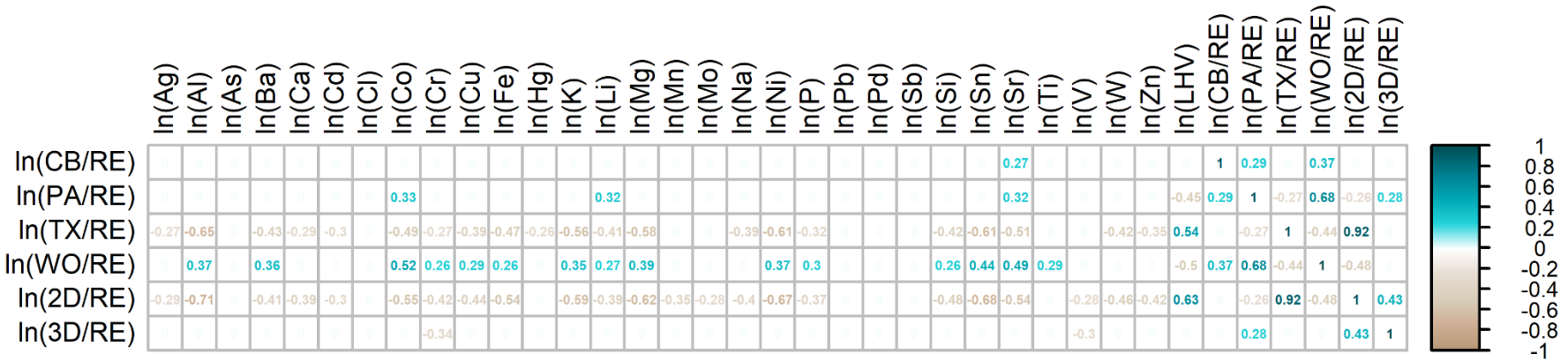

Figure B.4: Spearman correlation coefficients for statistically significant ($p < 0.05$) positive (petrol blue) and negative (beige) correlations of chemical analysis parameters and log-ratios (reference fraction: residual) from sorting analyses for particle size classes >20mm, see Appendix E

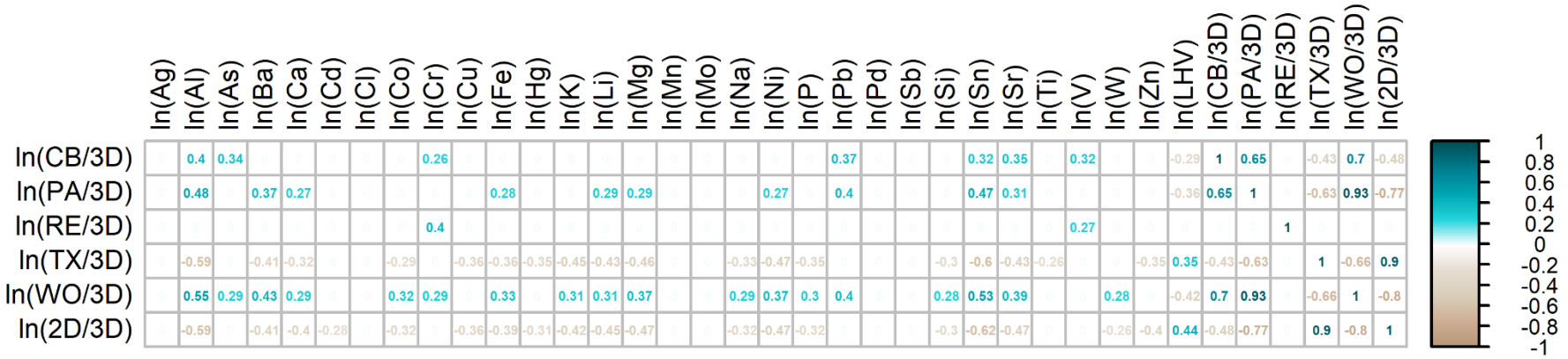

Figure B.5: Pearson correlation coefficients for statistically significant ($p < 0.05$) positive (petrol blue) and negative (beige) correlations of chemical analysis parameters and log-ratios (reference fraction: 3D plastics) from sorting analyses for particle size classes >20mm, see Appendix E

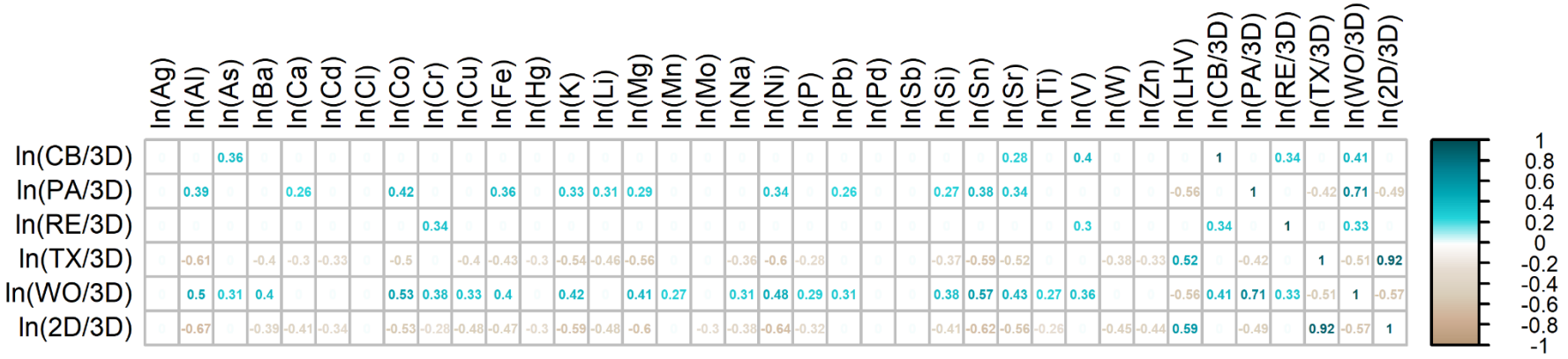

Figure B.6: Spearman correlation coefficients for statistically significant ($p < 0.05$) positive (petrol blue) and negative (beige) correlations of chemical analysis parameters and log-ratios (reference fraction: 3D plastics) from sorting analyses for particle size classes >20mm, see Appendix E

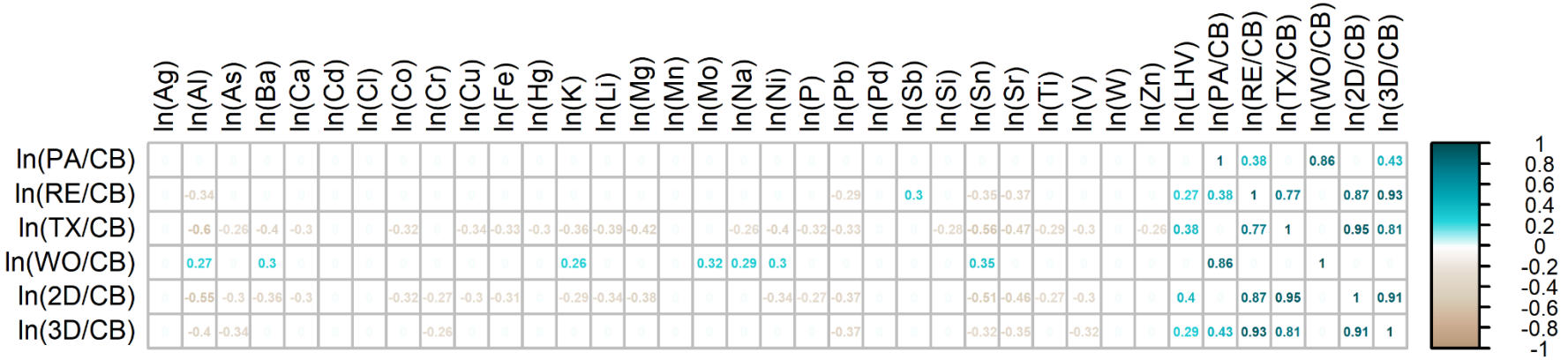

Figure B.7: Pearson correlation coefficients for statistically significant ($p < 0.05$) positive (petrol blue) and negative (beige) correlations of chemical analysis parameters and log-ratios (reference fraction: cardboard) from sorting analyses for particle size classes >20mm, see Appendix E

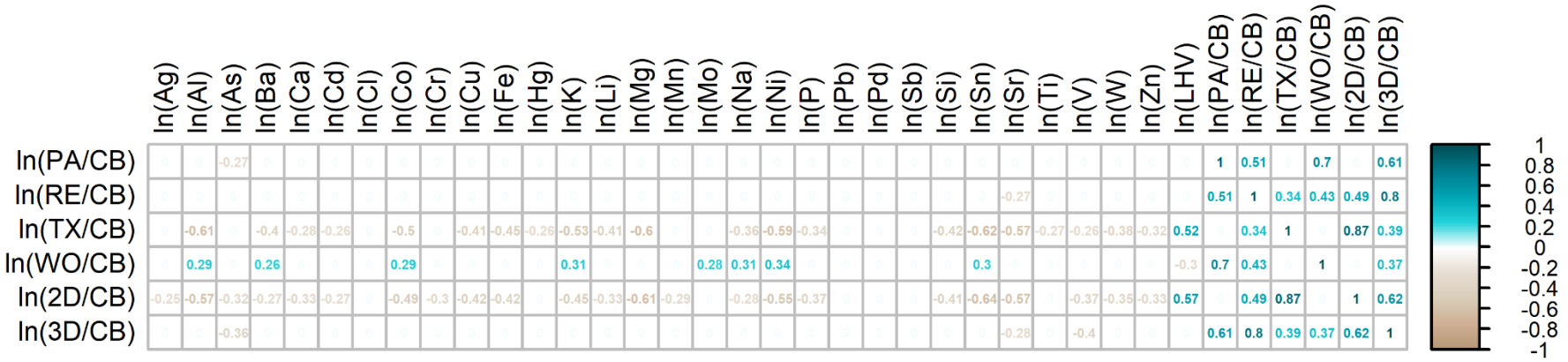

Figure B.8: Spearman correlation coefficients for statistically significant ($p < 0.05$) positive (petrol blue) and negative (beige) correlations of chemical analysis parameters and log-ratios (reference fraction: cardboard) from sorting analyses for particle size classes >20mm, see Appendix E

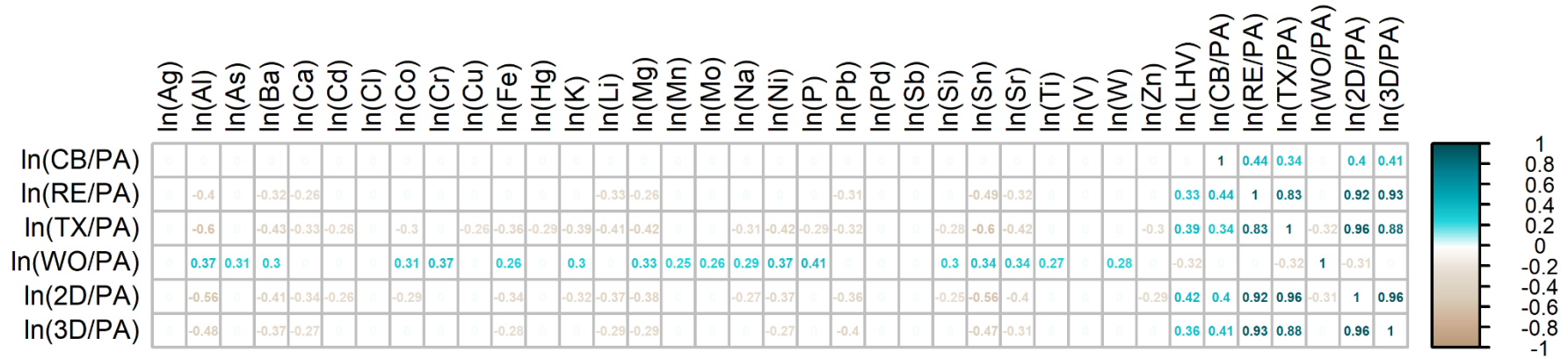

Figure B.9: Pearson correlation coefficients for statistically significant ($p < 0.05$) positive (petrol blue) and negative (beige) correlations of chemical analysis parameters and log-ratios (reference fraction: paper) from sorting analyses for particle size classes >20mm, see Appendix E

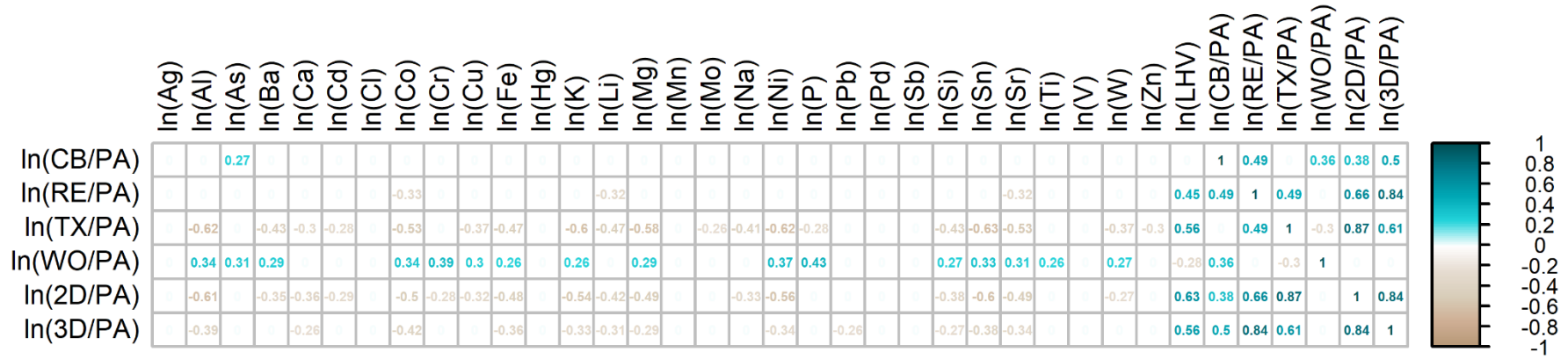

Figure B.10: Spearman correlation coefficients for statistically significant ($p < 0.05$) positive (petrol blue) and negative (beige) correlations of chemical analysis parameters and log-ratios (reference fraction: paper) from sorting analyses for particle size classes >20mm, see Appendix E

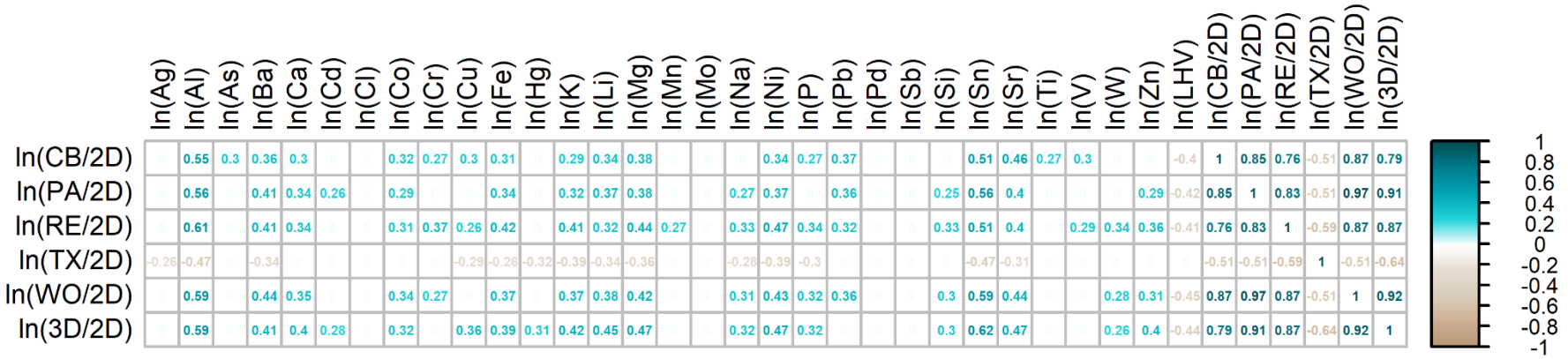

Figure B.11: Pearson correlation coefficients for statistically significant ($p < 0.05$) positive (petrol blue) and negative (beige) correlations of chemical analysis parameters and log-ratios (reference fraction: 2D plastics) from sorting analyses for particle size classes >20mm, see Appendix E

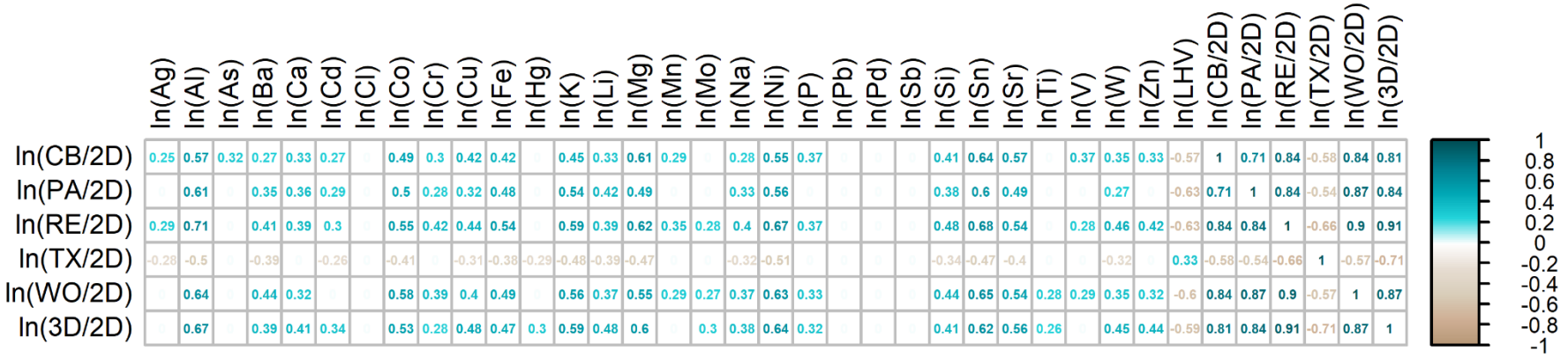

Figure B.12: Spearman correlation coefficients for statistically significant ($p < 0.05$) positive (petrol blue) and negative (beige) correlations of chemical analysis parameters and log-ratios (reference fraction: 2D plastics) from sorting analyses for particle size classes >20mm, see Appendix E

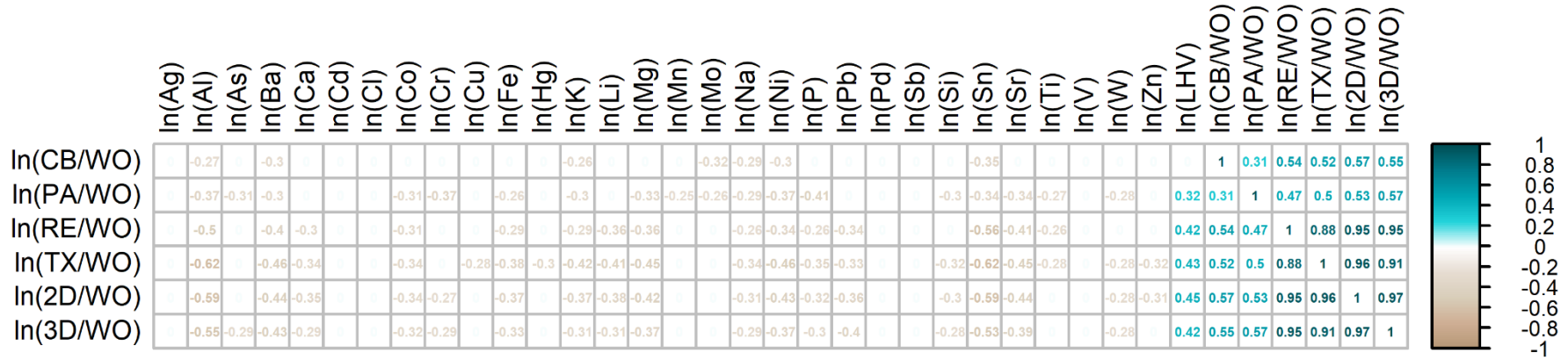

Figure B.13: Pearson correlation coefficients for statistically significant ($p < 0.05$) positive (petrol blue) and negative (beige) correlations of chemical analysis parameters and log-ratios (reference fraction: wood) from sorting analyses for particle size classes >20mm, see Appendix E

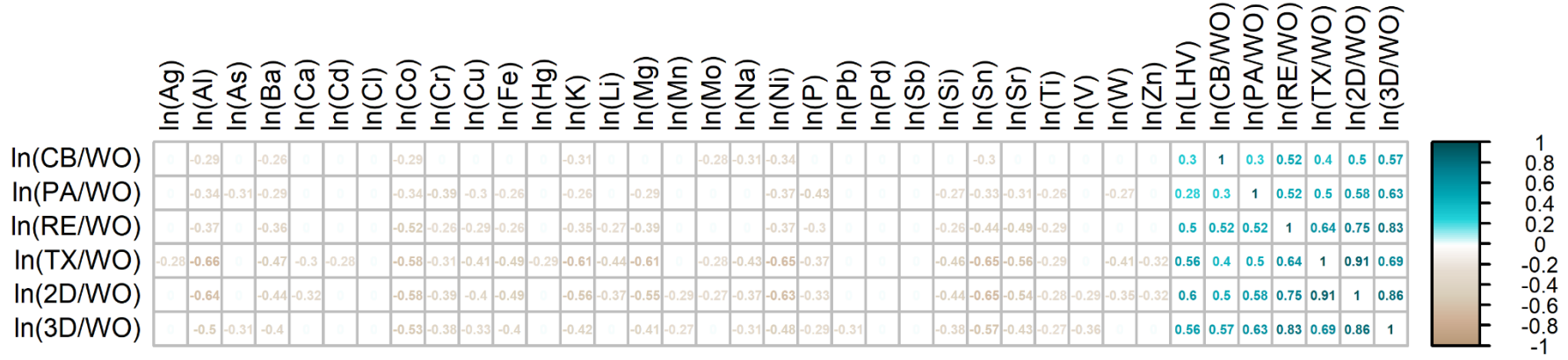

Figure B.14: Spearman correlation coefficients for statistically significant ($p < 0.05$) positive (petrol blue) and negative (beige) correlations of chemical analysis parameters and log-ratios (reference fraction: wood) from sorting analyses for particle size classes >20mm, see Appendix E

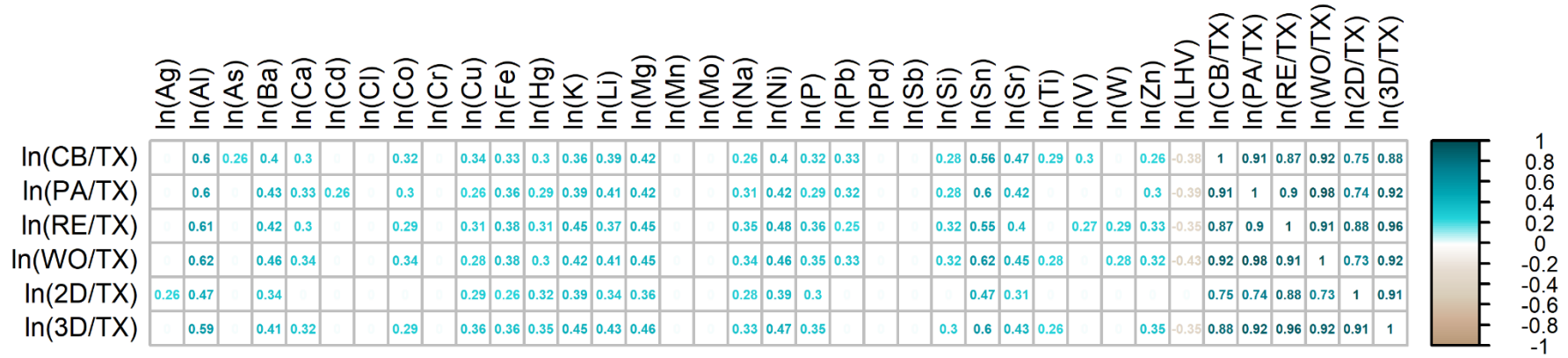

Figure B.15: Pearson correlation coefficients for statistically significant ($p < 0.05$) positive (petrol blue) and negative (beige) correlations of chemical analysis parameters and log-ratios (reference fraction: textiles) from sorting analyses for particle size classes >20mm, see Appendix E

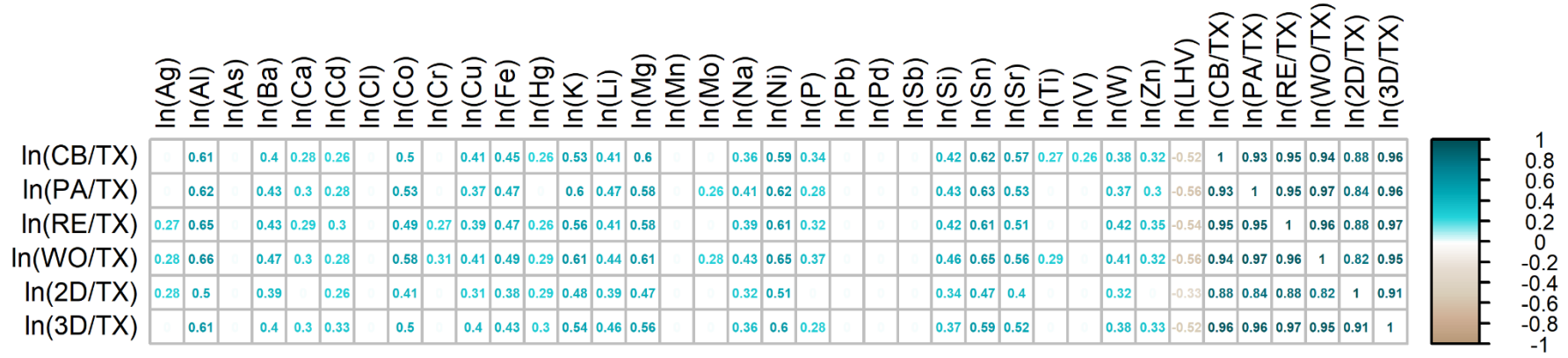

Figure B.16: Spearman correlation coefficients for statistically significant ($p < 0.05$) positive (petrol blue) and negative (beige) correlations of chemical analysis parameters and log-ratios (reference fraction: textiles) from sorting analyses for particle size classes >20mm, see Appendix E

Appendix C - Information for regression model

Table C.1: Number of available datasets for the building of the regression models (outliers already removed)

Element	20–40mm	40–60mm	60–80mm	80–100mm	100–200mm	200–400mm
Ag	9	10	10	10	9	8
Al	10	9	10	10	10	10
As	10	10	8	10	10	10
Ba	10	9	9	10	10	10
Ca	10	9	9	10	10	9
Cd	7	7	7	8	7	7
Cl	10	10	8	9	7	9
Co	8	8	10	8	9	9
Cr	8	9	8	10	7	6
Cu	8	8	9	7	10	7
Fe	8	8	9	8	10	9
Hg	9	7	7	7	7	8
K	8	9	10	8	10	8
Li	9	8	9	8	10	9
Mg	8	9	10	8	9	9
Mn	8	9	10	8	10	10
Mo	9	9	10	8	10	10
Na	8	7	10	8	8	10
Ni	8	8	8	8	10	9
P	9	10	9	8	10	9
Pb	10	8	9	8	9	8
Sb	7	10	8	8	9	10
Si	8	9	10	8	9	10
Sn	10	7	9	6	10	8
Sr	7	9	10	8	10	9
Ti	10	10	9	10	9	10
V	9	9	10	10	10	10
W	9	8	10	8	9	10
Zn	10	10	10	10	9	9
LHV	8	9	10	8	7	9

Table C.2: Number of considered factors/dimensions for the regression models

Element	number of considered dimensions[1]
Ag	2
Al	2
As	1
Ba	1
Ca	1
Cd	1
Cl	1
Co	1
Cr	2
Cu	2
Fe	1
Hg	2
K	2
Li	2
Mg	2
Mn	1
Mo	1
Na	2
Ni	2
P	2
Pb	1
Sb	2
Si	1
Sn	3
Sr	1
Ti	1
V	1
W	2
Zn	2
LHV	3

[1] Calculated over cross validation with the criteria of the smallest resulting predicted residual sum of squares (PRESS)

C.1 Ag

Table C.3: Regression coefficients for silver (Ag)

Particle size class [mm]	k0	k_CB	k_PA	k_RE	k_TX	k_WO	k_2D
20–40	2.02	-0.20	-0.71	-0.09	0.61	-0.54	-0.30
40–60	6.14	-0.53	0.05	0.02	0.88	0.07	1.67
60–80	0.05	0.31	-0.44	0.37	-0.53	0.33	0.20
80–100	1.37	-0.13	0.12	-0.46	0.26	-0.01	-0.10
100–200	1.10	-0.26	-0.02	0.18	0.27	-0.02	-0.20
200–400	0.58	-0.01	-0.08	-0.08	0.00	-0.02	0.06

C.2 Al

Table C.4: Regression coefficients for aluminium (Al)

Particle size class [mm]	k0	k_CB	k_PA	k_RE	k_TX	k_WO	k_2D
20–40	24069.63	-3994.15	-1879.95	2167.54	4864.87	-990.46	-1559.84
40–60	17207.31	1281.59	-4057.32	4843.83	3294.38	-4123.18	1245.41
60–80	3610.18	-544.74	2443.54	2466.98	-3591.04	-765.79	-784.13
80–100	5755.58	-1064.64	-2884.16	-3714.70	4041.14	3731.29	-6804.91
100–200	8291.87	-153.13	1103.91	1281.06	-645.70	468.02	318.81
200–400	5803.60	664.92	-210.62	-1336.36	-63.94	-47.78	66.21

C.3 As

Table C.5: Regression coefficients for arsenic (As)

Particle size class [mm]	k0	k_CB	k_PA	k_RE	k_TX	k_WO	k_2D
20–40	-0.79	2.75	-4.00	-0.22	-0.61	-0.71	-0.49
40–60	11.32	2.39	-2.28	0.52	2.39	-0.54	0.41
60–80	5.37	-0.67	0.26	0.38	-1.08	-1.45	0.14
80–100	11.36	0.92	0.32	0.48	1.56	2.61	-0.05
100–200	8.33	0.55	0.81	0.66	1.00	0.70	0.44
200–400	7.42	0.70	0.05	0.07	-0.09	0.09	0.02

C.4 Ba

Table C.6: Regression coefficients for barium (Ba)

Particle size class [mm]	k0	k_CB	k_PA	k_RE	k_TX	k_WO	k_2D
20–40	-59.75	-458.92	-223.24	-474.97	-85.23	-98.72	-88.08
40–60	916.88	60.89	57.14	89.76	142.78	-8.38	-36.18
60–80	392.56	26.21	50.28	28.40	-80.97	93.13	65.26
80–100	1181.52	87.87	39.74	31.20	134.11	350.63	6.85
100–200	591.55	-22.84	75.60	59.05	22.28	43.65	55.34
200–400	481.59	39.62	15.65	2.82	-13.26	7.35	-7.40

C.5 Ca

Table C.7: Regression coefficients for calcium (Ca)

Particle size class [mm]	k0	k_CB	k_PA	k_RE	k_TX	k_WO	k_2D
20–40	72297.36	19342.39	-30151.06	7266.95	13015.74	7738.74	-11196.56
40–60	111010.64	9794.07	17892.19	28457.73	11201.31	-3023.99	10719.31
60–80	55891.99	-8728.85	7300.57	-8793.16	6062.18	-14952.34	-5689.83
80–100	105235.34	2635.08	8008.33	-2145.86	19840.52	7922.04	-3697.88
100–200	28938.52	-3388.34	-7809.03	-5853.82	215.73	-5590.83	-2800.44
200–400	32847.46	-2337.12	-34.04	-95.42	-106.11	148.61	390.95

C.6 Cd

Table C.8: Regression coefficients for cadmium (Cd)

Particle size class [mm]	k0	k_CB	k_PA	k_RE	k_TX	k_WO	k_2D
20–40	-0.67	-0.20	-0.17	-0.14	-0.26	-0.15	-0.08
40–60	1.83	0.26	-0.05	-0.07	0.54	-0.07	-0.18
60–80	2.10	-0.31	-0.14	-0.25	0.78	0.01	0.10
80–100	-0.62	-0.52	-0.96	0.06	-0.02	-0.57	-0.03
100–200	0.28	-0.09	0.00	-0.09	-0.19	-0.07	-0.06
200–400	0.25	0	0	0	0	0	0

C.7 Cl

Table C.9: Regression coefficients for chlorine (Cl)

Particle size class [mm]	k0	k_CB	k_PA	k_RE	k_TX	k_WO	k_2D
20–40	5844.30	1947.39	4571.25	3609.29	-2773.72	1978.66	50.53
40–60	10853.93	5237.68	8392.27	1452.25	-3507.53	5944.71	1227.97
60–80	12408.90	900.61	1976.57	543.35	448.83	2406.36	537.78
80–100	545.30	-297.57	-295.81	168.05	-3682.19	-468.57	-175.18
100–200	4718.50	-664.25	-2372.93	-2157.59	599.95	943.47	-1259.84
200–400	35365.29	39.69	5419.93	2664.94	-6273.38	86.17	-3650.58

C.8 Co

Table C.10: Regression coefficients for cobalt (Co)

Particle size class [mm]	k0	k_CB	k_PA	k_RE	k_TX	k_WO	k_2D
20–40	6.84	-1.16	1.02	0.70	0.32	-0.14	-0.07
40–60	8.07	0.29	0.61	0.13	0.62	0.84	0.24
60–80	3.26	-0.05	-0.23	0.98	-1.68	-1.03	0.80
80–100	3.42	0.00	-0.40	-0.03	-0.05	0.15	0.02
100–200	4.55	-0.12	0.30	0.00	0.16	0.17	0.06
200–400	2.90	0.17	-0.17	-0.12	-0.02	-0.06	0.08

C.9 Cr

Table C.11: Regression coefficients for chromium (Cr)

Particle size class [mm]	k0	k_CB	k_PA	k_RE	k_TX	k_WO	k_2D
20–40	-80.01	-36.13	9.28	78.86	-39.72	-36.12	-1.92
40–60	-76.99	5.86	23.79	92.85	-21.23	47.23	-95.01
60–80	233.35	-4.84	52.13	136.17	59.33	-28.06	8.83
80–100	305.79	90.96	-34.77	20.72	56.85	78.20	32.35
100–200	43.03	2.68	3.10	4.90	-0.30	1.89	-1.59
200–400[2]	-	-	-	-	-	-	-

[2] The particle size class 200–400mm was excluded in the regression models, because too little values were present, after removing the outliers

C.10 Cu

Table C.12: Regression coefficients for copper (Cu)

Particle size class [mm]	k0	k_CB	k_PA	k_RE	k_TX	k_WO	k_2D
20–40	2011.20	16.07	-465.29	-205.56	541.46	-456.23	303.86
40–60	139.41	-49.20	-165.79	41.26	53.99	-63.78	7.39
60–80	7.96	-1.41	40.46	32.53	-58.26	-24.06	-15.16
80–100	41.87	0.24	-13.70	-30.88	-20.06	48.14	-12.34
100–200	59.13	-0.99	-4.36	5.31	3.29	0.47	-1.53
200–400	33.63	-2.68	-1.31	-2.34	2.32	0.67	1.13

C.11 Fe

Table C.13: Regression coefficients for iron (Fe)

Particle size class [mm]	k0	k_CB	k_PA	k_RE	k_TX	k_WO	k_2D
20–40	74129.17	-3422.45	9367.47	11172.43	10387.35	294.78	1753.45
40–60	31864.00	4386.08	2477.43	2163.40	3242.15	2079.69	180.04
60–80	18218.87	-447.04	7313.82	1884.38	-5030.23	2094.31	1483.01
80–100	13895.68	-344.89	-2027.06	-552.68	468.42	-2090.86	678.32
100–200	17069.89	302.82	84.77	1076.91	1592.90	502.36	609.99
200–400	10214.52	-359.96	-459.06	-1047.89	-479.18	-431.63	143.79

C.12 Hg

Table C.14: Regression coefficients for mercury (Hg)

Particle size class [mm]	k0	k_CB	k_PA	k_RE	k_TX	k_WO	k_2D
20–40	-0.7	0.1	-0.03	-0.15	-0.23	0.21	-0.21
40–60[3]	0.25	0	0	0	0	0	0
60–80[4]	0.25	0	0	0	0	0	0
80–100[5]	0.25	0	0	0	0	0	0
100–200[6]	0.25	0	0	0	0	0	0
200–400[7]	0.25	0	0	0	0	0	0

[3] All considered values for the regression model were the value for LOQ
[4] All considered values for the regression model were the value for LOQ
[5] All considered values for the regression model were the value for LOQ
[6] All considered values for the regression model were the value for LOQ
[7] All considered values for the regression model were the value for LOQ

C.13 K

Table C.15: Regression coefficients for potassium (K)

Particle size class [mm]	k0	k_CB	k_PA	k_RE	k_TX	k_WO	k_2D
20–40	1496.86	-338.17	141.51	536.35	-155.94	-180.94	41.61
40–60	1550.28	19.63	862.48	441.93	-346.48	575.90	3.83
60–80	1644.25	-599.09	520.90	-9.42	-242.35	-209.23	252.37
80–100	1177.28	-70.03	-109.45	-175.33	184.88	49.37	-122.63
100–200	1301.42	-41.16	54.94	239.77	-51.41	16.74	132.75
200–400	568.55	14.85	-69.40	-129.95	-5.20	-77.52	-20.60

C.14 Li

Table C.16: Regression coefficients for lithium (Li)

Particle size class [mm]	k0	k_CB	k_PA	k_RE	k_TX	k_WO	k_2D
20–40	-12.12	2.74	0.83	0.11	0.99	-3.57	-12.04
40–60	4.67	0.37	1.45	1.94	-0.23	0.92	0.10
60–80	5.97	-2.85	2.24	0.04	0.72	-2.47	-0.24
80–100	3.37	-0.15	0.65	-0.50	0.11	-0.56	-0.27
100–200	2.27	-0.21	-0.05	0.04	-0.38	-0.63	0.31
200–400	-0.23	0.25	-0.50	-0.60	-0.12	-0.49	-0.06

C.15 Mg

Table C.17: Regression coefficients for magnesium (Mg)

Particle size class [mm]	k0	k_CB	k_PA	k_RE	k_TX	k_WO	k_2D
20–40	4852.82	985.00	-739.57	301.09	409.32	0.22	237.32
40–60	1924.87	131.32	268.20	2383.20	-335.82	-2342.88	-178.93
60–80	2970.02	-469.72	597.22	401.60	-440.92	-67.48	524.71
80–100	1899.92	-4.23	-582.45	-221.66	30.42	533.10	47.24
100–200	2072.49	257.08	140.07	325.92	-102.14	-75.30	198.73
200–400	1135.63	26.76	-123.32	-222.67	-67.78	-135.46	-27.07

C.16 Mn

Table C.18: Regression coefficients for manganese (Mn)

Particle size class [mm]	k0	k_CB	k_PA	k_RE	k_TX	k_WO	k_2D
20–40	746.57	-19.11	69.99	87.04	93.84	0.86	18.60
40–60	524.81	67.45	16.52	18.37	76.09	13.83	2.54
60–80	115.98	-5.53	151.31	83.95	-153.75	-62.87	-41.76
80–100	279.35	5.43	-25.23	6.36	23.54	23.02	9.90
100–200	320.56	19.03	10.74	33.57	29.18	17.45	21.28
200–400	308.53	28.53	-6.20	-11.79	-6.79	-5.41	-2.08

C.17 Mo

Table C.19: Regression coefficients for molybdenum (Mo)

Particle size class [mm]	k0	k_CB	k_PA	k_RE	k_TX	k_WO	k_2D
20–40	-18.69	-8.94	-11.36	1.65	-3.18	-4.99	-4.66
40–60	8.18	-2.55	-0.35	-2.05	-1.86	0.22	-1.03
60–80	12.70	2.91	0.42	-0.34	0.61	1.84	-1.05
80–100	15.08	-1.34	0.21	-1.17	2.82	0.31	0.29
100–200	10.85	-2.60	-1.36	-0.29	4.50	-2.25	2.33
200–400	11.94	-1.19	0.07	-0.11	-0.41	0.27	0.25

C.18 Na

Table C.20: Regression coefficients for sodium (Na)

Particle size class [mm]	k0	k_CB	k_PA	k_RE	k_TX	k_WO	k_2D
20–40	-997.29	-252.61	-1037.80	1414.00	-761.24	-2006.78	363.99
40–60	1602.52	-374.24	83.90	-199.78	-151.57	-96.12	-325.35
60–80	1130.91	-759.85	926.09	91.34	-1409.92	604.25	179.45
80–100	1327.98	322.97	-394.55	72.67	-516.26	822.83	-149.37
100–200	2742.37	50.31	404.59	493.37	52.76	135.64	314.19
200–400	6177.54	-38.06	246.37	-690.02	342.03	871.47	-211.39

C.19 Ni

Table C.21: Regression coefficients for nickel (Ni)

Particle size class [mm]	k0	k_CB	k_PA	k_RE	k_TX	k_WO	k_2D
20–40	-27.22	-21.85	-0.28	39.79	-12.90	-15.64	-6.08
40–60	23.63	8.06	6.20	-11.10	-5.11	15.10	-4.62
60–80	17.99	7.44	7.24	3.85	-6.35	-1.12	-2.07
80–100	20.05	-3.64	-5.31	-2.35	2.29	-1.40	0.84
100–200	17.74	-1.73	-1.27	2.47	2.48	-2.04	0.99
200–400	5.31	-0.80	-2.38	-2.45	-0.58	-0.46	2.30

C.20 P

Table C.22: Regression coefficients for phosphorus (P)

Particle size class [mm]	k0	k_CB	k_PA	k_RE	k_TX	k_WO	k_2D
20–40	-173.13	139.34	-348.74	-50.15	-37.69	-93.64	-26.44
40–60	131.37	199.99	-393.77	217.44	16.75	-85.36	99.13
60–80	241.24	23.93	-74.43	253.26	-99.54	-82.59	177.35
80–100	173.00	24.14	-97.57	38.56	2.92	76.87	-6.88
100–200	327.26	12.79	26.80	-17.71	52.62	22.36	26.90
200–400	478.19	-11.49	29.98	-1.02	7.85	45.65	-20.83

C.21 Pb

Table C.23: Regression coefficients for lead (Pb)

Particle size class [mm]	k0	k_CB	k_PA	k_RE	k_TX	k_WO	k_2D
20–40	-148.49	5.89	-52.54	-30.43	-49.27	-30.12	-3.94
40–60	199.31	75.57	105.55	205.83	-22.57	72.21	31.17
60–80	141.38	59.42	-56.81	-23.77	16.14	100.93	20.97
80–100	279.32	-1.75	113.15	2.19	-21.30	85.35	-15.35
100–200	148.37	-2.63	-8.53	55.41	92.31	-108.65	103.27
200–400	69.74	4.63	0.99	6.25	6.08	6.00	3.47

C.22 Sb

Table C.24: Regression coefficients for antimony (Sb)

Particle size class [mm]	k0	k_CB	k_PA	k_RE	k_TX	k_WO	k_2D
20–40	-19.80	1.43	4.24	6.13	-15.85	0.21	3.00
40–60	89.69	11.57	59.80	82.19	-10.69	11.84	20.35
60–80	9.35	56.27	-16.56	5.58	5.13	14.06	-16.42
80–100	30.34	-9.61	5.11	-2.30	14.43	-7.84	-6.49
100–200	33.75	-3.76	-3.02	7.79	8.29	3.94	-4.11
200–400	80.14	-9.26	12.80	-15.48	-30.08	1.35	37.50

C.23 Si

Table C.25: Regression coefficients for silicon (Si)

Particle size class [mm]	k0	k_CB	k_PA	k_RE	k_TX	k_WO	k_2D
20–40	32262.08	-3752.12	1793.55	3196.78	2038.78	-3019.11	877.67
40–60	30452.36	3092.33	257.33	524.37	2674.10	880.65	56.88
60–80	10882.35	1107.42	8830.03	2084.87	-8707.38	-2357.71	-1253.88
80–100	14382.50	295.83	-4772.40	769.16	1172.24	2635.90	91.46
100–200	21115.22	1550.38	1158.44	2372.37	2323.14	1286.91	1790.25
200–400	18379.13	1361.91	-338.51	-1069.10	-187.28	-223.93	116.27

C.24 Sn

Table C.26: Regression coefficients for tin (Sn)

Particle size class [mm]	k0	k_CB	k_PA	k_RE	k_TX	k_WO	k_2D
20–40	-8.91	27.19	-11.88	76.64	-6.67	55.36	-75.10
40–60	35.68	18.43	-47.42	8.79	-6.82	-32.71	-27.11
60–80	26.58	3.72	-23.16	-5.83	-64.23	42.69	43.41
80–100[8]	-	-	-	-	-	-	-
100–200	18.09	9.67	9.72	4.38	-13.52	-16.59	17.22
200–400	13.33	-0.46	-1.20	-16.17	7.90	1.27	-3.39

[8] The particle size class 80–100mm was excluded in the regression models, because too little values were present, after removing the outliers

C.25 Sr

Table C.27: Regression coefficients for strontium (Sr)

Particle size class [mm]	k0	k_CB	k_PA	k_RE	k_TX	k_WO	k_2D
20–40	250.64	-8.94	6.75	-42.26	31.15	22.96	10.86
40–60	155.91	10.59	-7.90	2.96	22.16	-2.81	-3.10
60–80	117.19	-7.77	51.04	7.48	-12.49	-4.29	-1.57
80–100	80.14	-1.01	-11.13	0.50	7.03	2.93	-0.65
100–200	85.70	9.10	0.38	-13.17	2.40	1.88	-4.34
200–400	71.05	3.86	-0.14	-0.10	-0.05	0.14	0.10

C.26 Ti

Table C.28: Regression coefficients for titanium (Ti)

Particle size class [mm]	k0	k_CB	k_PA	k_RE	k_TX	k_WO	k_2D
20–40	194.53	42.69	-435.77	-311.43	-391.03	-253.54	21.96
40–60	587.47	-239.28	-205.57	553.44	-519.03	-248.31	-141.98
60–80	3260.80	273.24	-347.38	-128.20	652.09	566.51	226.74
80–100	1917.32	92.90	-114.78	-307.62	38.99	377.99	-228.39
100–200	1651.28	-245.85	114.51	-199.40	-89.66	-78.96	-7.23
200–400	1673.77	216.88	-114.35	-35.95	25.51	-52.86	11.46

C.27 V

Table C.29: Regression coefficients for vanadium (V)

Particle size class [mm]	k0	k_CB	k_PA	k_RE	k_TX	k_WO	k_2D
20–40	17.26	1.67	0.41	1.67	1.26	-0.25	0.51
40–60	20.46	2.51	-0.04	-0.88	1.89	1.49	0.29
60–80	2.69	6.36	1.46	3.41	-7.05	2.83	0.29
80–100	11.00	1.38	-3.65	1.57	1.70	3.26	0.44
100–200	16.07	1.50	2.28	1.85	2.85	1.83	1.15
200–400	15.50	2.43	0.05	-0.12	-0.32	0.15	-0.02

C.28 W

Table C.30: Regression coefficients for tungsten (W)

Particle size class [mm]	k0	k_CB	k_PA	k_RE	k_TX	k_WO	k_2D
20–40	120.46	10.94	-44.91	-11.89	31.44	7.76	-8.73
40–60	18.94	19.74	-30.33	9.81	11.29	-45.32	-6.29
60–80	13.92	-8.33	-24.88	6.79	3.66	-12.31	2.71
80–100	-0.14	2.99	-25.81	2.86	1.27	1.66	-1.17
100–200	62.60	-17.14	15.00	1.07	10.47	-0.03	4.09
200–400	82.85	1.82	7.68	1.94	-2.03	6.91	-2.95

C.29 Zn

Table C.31: Regression coefficients for zinc (Zn)

Particle size class [mm]	k0	k_CB	k_PA	k_RE	k_TX	k_WO	k_2D
20–40	935.79	-124.11	-303.42	-122.76	298.88	-59.30	-82.58
40–60	662.98	-56.78	-188.78	-86.11	260.81	-198.16	-210.82
60–80	235.39	-39.14	158.09	42.39	-73.81	-242.13	-84.78
80–100	39.46	85.44	-211.03	4.98	-36.14	73.48	-89.75
100–200	387.00	-4.20	77.59	32.06	-9.66	23.35	16.64
200–400	-39.42	-18.58	-32.00	-35.43	-8.98	-39.08	-26.41

C.30 LHV

Table C.32: Regression coefficients for the lower heating value (LHV)

Particle size class [mm]	k0	k_CB	k_PA	k_RE	k_TX	k_WO	k_2D
20–40	11860.31	16.22	1113.49	-1613.44	-1642.91	147.83	-1972.09
40–60	10025.98	1671.18	-1987.35	-2385.84	-2369.86	1047.78	-1146.08
60–80	18501.00	-547.52	-5396.81	517.19	454.12	1585.98	2528.51
80–100	19163.10	1073.48	-1091.36	82.81	-322.44	597.45	-442.97
100–200	22415.17	-93.91	-360.65	-68.33	-20.72	875.12	401.61
200–400	34017.56	117.60	666.70	-2381.47	-3303.06	1051.54	2712.35

Appendix D - Results from prediction models – Box plots[9]

D.1 Ag

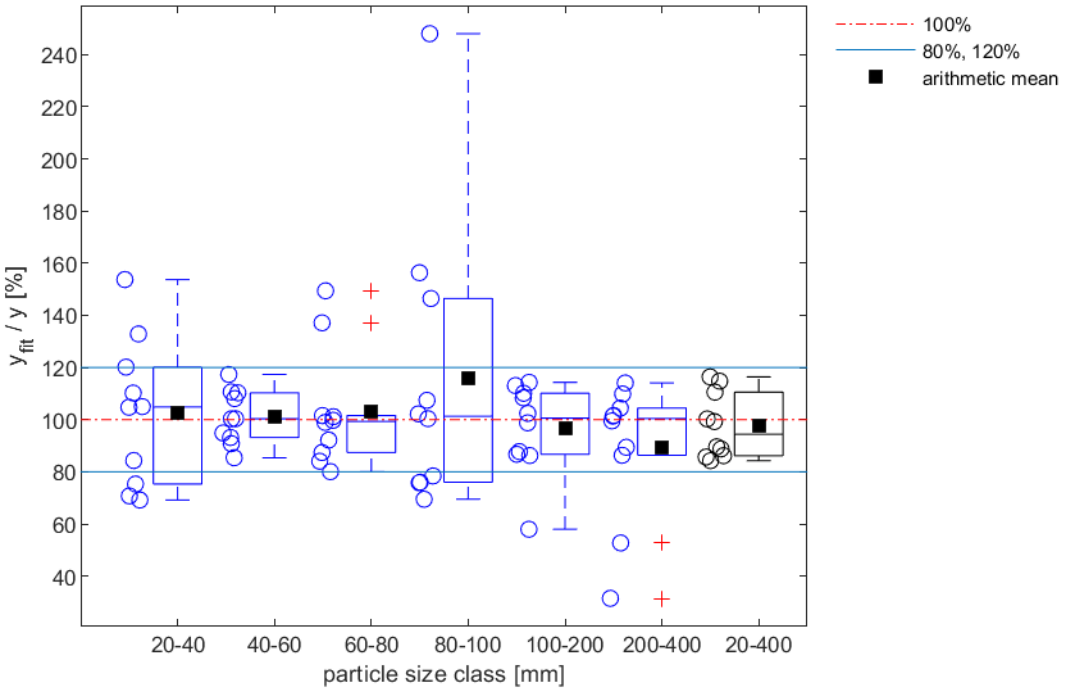

Figure D.1: Box plot of silver (Ag) for the results of the prediction models in different particle size classes, as well as the material mix in the particle size classes >20mm

Table D.1: Ratios of the predicted values y_{fit} through the regression models and the original values y [in %] for silver (Ag)

Sample No.	20–40mm	40–60mm	60–80mm	80–100mm	100–200mm	200–400mm	20–400mm
1	113.1	107.4	99.3	84.2	88.9	64.3	98.2
2	85.9	91.6	104.7	85.0	92.4	102.3	91.6
3	69.4	92.7	85.8	73.1	110.8	99.5	86.8
4	129.5	102.8	82.7	99.6	100.8	34.7	87.7
5	109.8	111.4	106.7	99.9	63.4	102.3	89.8
6	144.9	95.1	120.3	123.0	98.7	102.3	113.2
7	92.0	113.3	129.9	116.4	112.7	100.9	110.9
8	80.0	84.8	113.4	124.6	91.7	95.1	93.3
9	90.0	104.2	99.3	243.9	99.4	108.6	111.0
10	118.6	106.8	78.7	71.6	109.7	90.9	98.8

[9] For the box plots, the boxes in the diagrams show the range from the 25th (lower quartile) to the 75th (upper quartile) percentile of the values, while the horizontal line inside the box defines the median. The whiskers, which are the extending vertical lines from the boxes, indicate variability outside the upper and lower quartile and consider a range for data points within 1.5 interquartile range. Outliers are marked with a '+'-symbol and additionally the mean of each box plot, as well as the individual data points are plotted.

D.2 Al

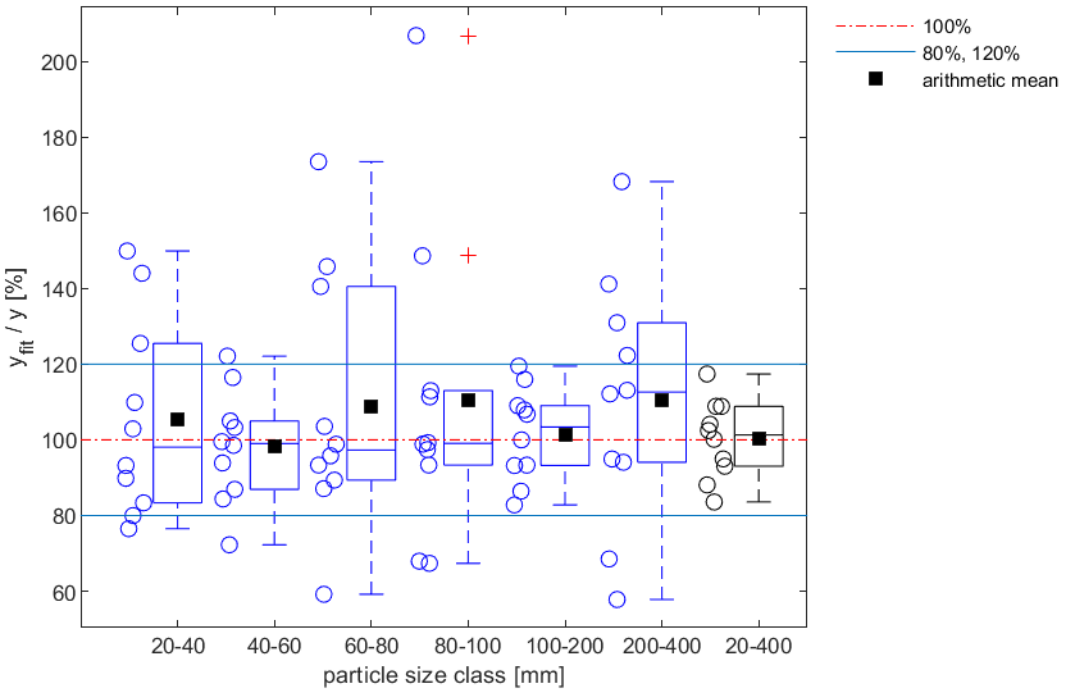

Figure D.2: Box plot of aluminium (Al) for the results of the prediction models in different particle size classes, as well as the material mix in the particle size classes >20mm

Table D.2: Ratios of the predicted values y_{fit} through the regression models and the original values y [in %] for aluminium (Al)

Sample No.	20–40mm	40–60mm	60–80mm	80–100mm	100–200mm	200–400mm	20–400mm
1	80.0	72.3	140.5	67.4	100.0	112.1	83.6
2	93.2	84.4	93.3	67.9	107.9	57.8	88.1
3	76.5	116.5	98.8	206.9	109.0	94.9	104.1
4	144.0	105.0	59.2	111.4	93.2	68.5	95.0
5	149.9	103.3	87.1	99.3	86.4	113.1	102.4
6	125.5	86.9	103.6	93.3	119.5	131.0	108.8
7	109.9	98.5	145.8	97.4	106.8	122.3	108.9
8	83.3	99.5	95.8	98.9	93.3	94.1	93.0
9	89.8	93.9	173.5	148.6	116.0	141.2	117.4
10	102.9	122.1	89.4	113.0	82.8	168.3	100.2

D.3 As

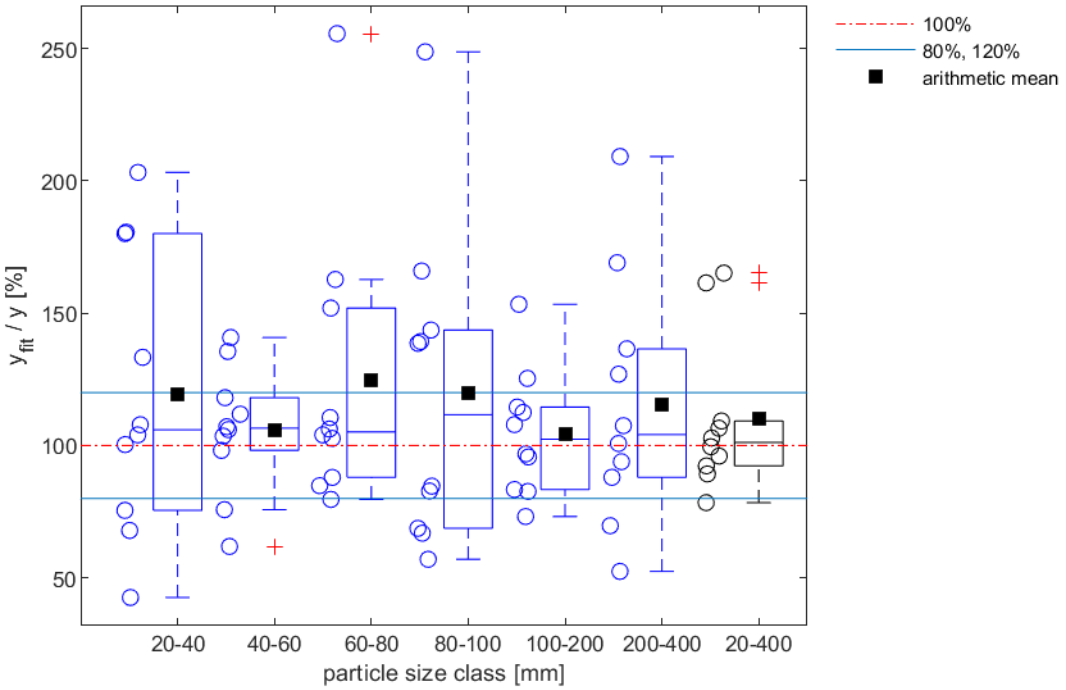

Figure D.3: Box plot of arsenic (As) for the results of the prediction models in different particle size classes, as well as the material mix in the particle size classes >20mm

Table D.3: Ratios of the predicted values y_{fit} through the regression models and the original values y [in %] for arsenic (As)

Sample No.	20–40mm	40–60mm	60–80mm	80–100mm	100–200mm	200–400mm	20–400mm
1	203.2	107.1	88.0	68.7	73.2	100.8	96.0
2	75.5	61.9	106.2	66.9	95.7	52.4	78.4
3	67.9	98.2	104.0	138.6	114.5	107.5	99.5
4	100.4	111.8	79.6	82.8	96.8	69.7	92.3
5	180.6	75.8	84.8	84.7	83.4	93.9	89.3
6	107.9	103.6	110.6	165.9	82.7	127.0	109.3
7	104.0	106.0	151.9	57.0	107.9	88.0	106.5
8	42.6	118.1	102.7	139.3	112.5	136.5	102.8
9	133.3	140.8	162.7	248.7	153.4	209.2	165.1
10	180.1	135.5	255.6	143.6	125.4	169.0	161.4

D.4 Ba

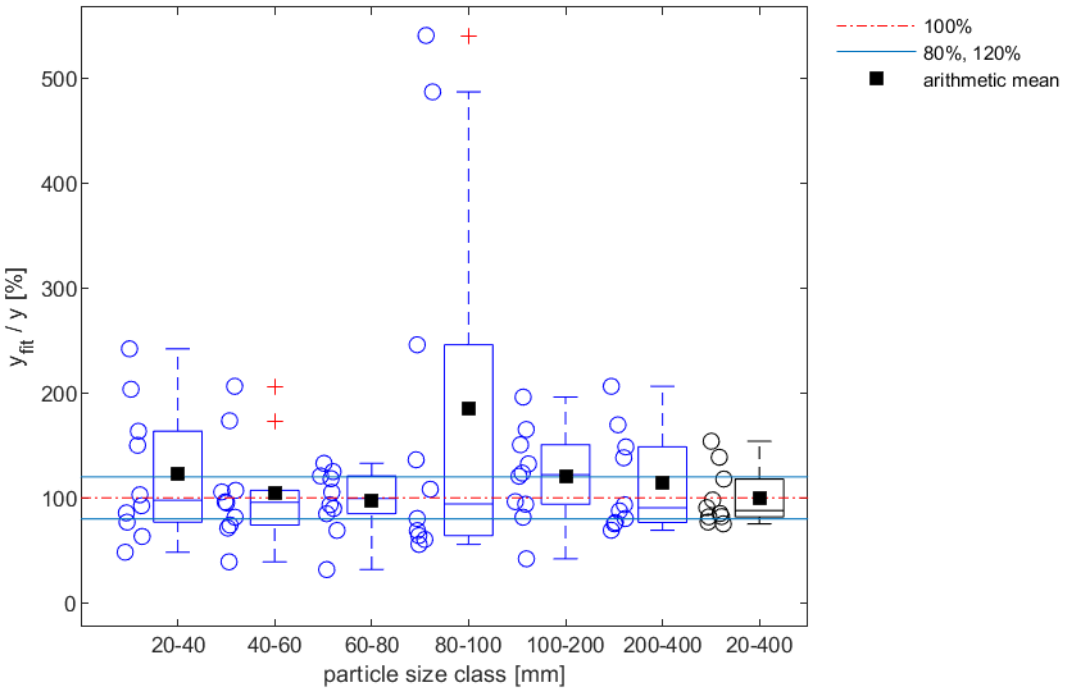

Figure D.4: Box plot of barium (Ba) for the results of the prediction models in different particle size classes, as well as the material mix in the particle size classes >20mm

Table D.4: Ratios of the predicted values y_{fit} through the regression models and the original values y [in %] for barium (Ba)

Sample No.	20–40mm	40–60mm	60–80mm	80–100mm	100–200mm	200–400mm	20–400mm
1	48.2	107.2	120.9	68.8	165.2	87.6	90.7
2	92.5	39.1	89.8	64.1	120.6	80.3	75.3
3	63.2	206.3	132.9	245.9	123.6	148.6	117.9
4	102.9	81.5	93.5	60.3	81.5	93.5	82.2
5	85.7	74.1	69.0	55.7	96.4	76.6	77.0
6	242.0	105.6	84.9	486.9	196.1	169.6	154.0
7	203.5	71.3	105.3	80.3	94.0	138.2	98.0
8	150.1	173.5	125.0	136.3	150.6	69.2	138.7
9	76.9	95.2	31.7	540.6	132.4	206.3	81.9
10	163.5	96.2	118.3	108.2	41.9	75.3	85.1

D.5 Ca

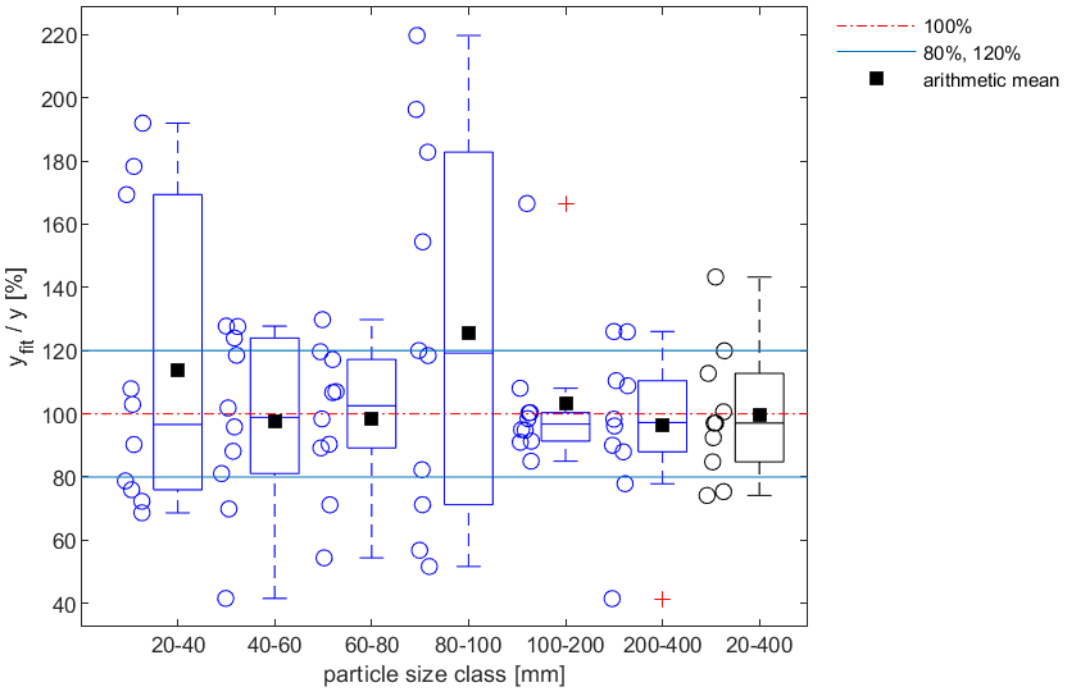

Figure D.5: Box plot of calcium (Ca) for the results of the prediction models in different particle size classes, as well as the material mix in the particle size classes >20mm

Table D.5: Ratios of the predicted values y_{fit} through the regression models and the original values y [in %] for calcium (Ca)

Sample No.	20–40mm	40–60mm	60–80mm	80–100mm	100–200mm	200–400mm	20–400mm
1	103.0	127.8	107.0	56.8	108.1	96.1	97.0
2	78.8	41.6	119.6	71.3	94.8	126.0	74.2
3	68.7	124.0	106.7	219.7	100.4	98.3	100.6
4	191.9	127.6	117.2	182.8	98.5	41.5	119.9
5	90.3	101.9	90.4	120.0	95.0	108.9	97.1
6	178.3	118.5	98.4	196.3	166.5	125.9	143.3
7	107.9	95.9	71.2	51.7	91.0	77.9	84.8
8	72.3	81.1	54.4	82.3	85.0	88.0	75.4
9	76.0	88.2	89.2	118.4	91.4	90.1	92.4
10	169.3	69.9	129.8	154.4	100.3	110.5	112.8

D.6 Cd

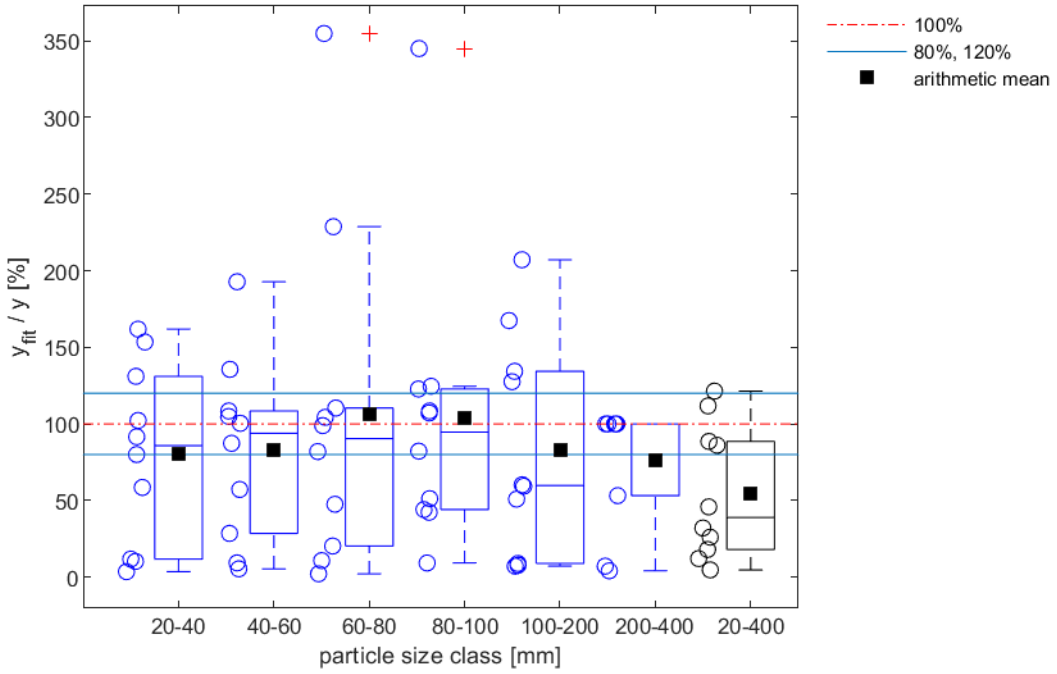

Figure D.6: Box plot of cadmium (Cd) for the results of the prediction models in different particle size classes, as well as the material mix in the particle size classes >20mm

Table D.6: Ratios of the predicted values y_{fit} through the regression models and the original values y [in %] for cadmium (Cd)

Sample No.	20–40mm	40–60mm	60–80mm	80–100mm	100–200mm	200–400mm	20–400mm
1	102.3	5.4	2.1	51.2	7.7	100.0	4.7
2	131.1	104.9	104.3	44.1	167.5	100.0	111.7
3	91.6	87.3	98.9	108.5	50.9	100.0	88.6
4	153.5	100.4	354.9	107.1	59.3	7.1	86.1
5	161.9	57.2	110.4	82.2	7.2	100.0	26.0
6	58.5	192.8	228.8	124.6	127.5	100.0	121.4
7	10.2	28.5	47.5	42.3	8.9	4.1	18.0
8	3.5	9.3	10.8	345.1	134.3	100.0	12.1
9	11.7	135.6	81.9	9.2	207.2	53.2	32.1
10	80.0	108.4	20.3	122.8	60.2	100.0	45.8

D.7 Cl

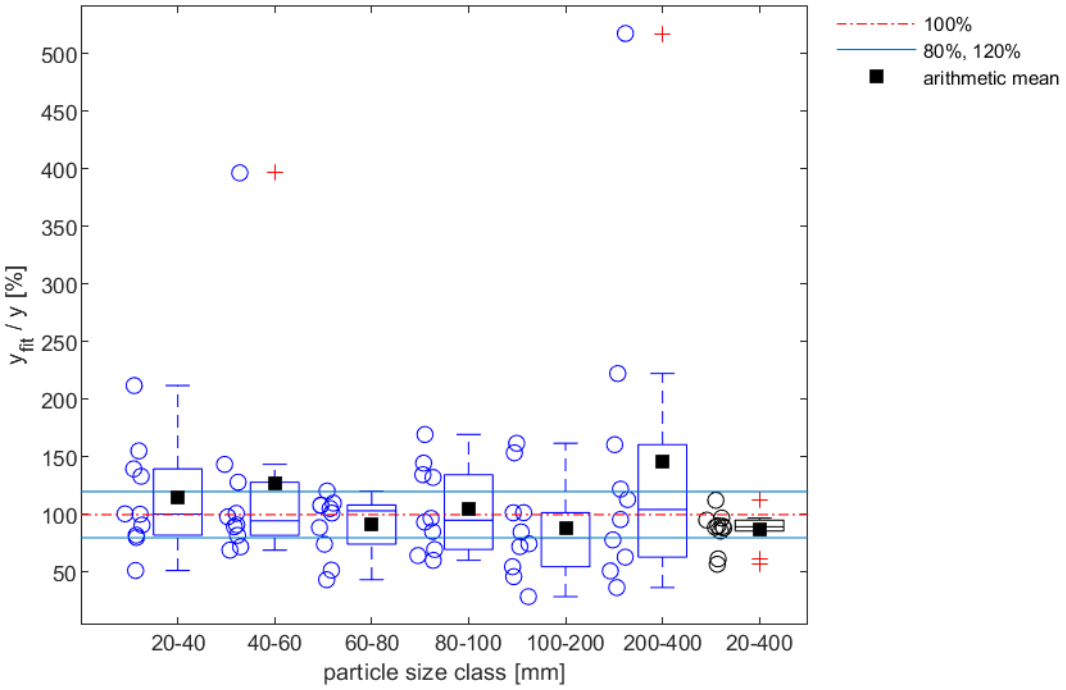

Figure D.7: Box plot of chlorine (Cl) for the results of the prediction models in different particle size classes, as well as the material mix in the particle size classes >20mm

Table D.7: Ratios of the predicted values y_{fit} through the regression models and the original values y [in %] for chlorine (Cl)

Sample No.	20–40mm	40–60mm	60–80mm	80–100mm	100–200mm	200–400mm	20–400mm
1	100.7	91.2	51.9	169.5	153.6	517.3	95.3
2	155.3	396.4	43.6	144.7	72.3	122.1	85.8
3	212.0	98.1	120.5	69.8	101.7	113.1	112.4
4	139.7	89.4	105.3	96.8	85.0	51.1	89.2
5	90.9	69.2	88.8	93.5	101.6	95.8	88.5
6	82.2	82.1	74.4	85.4	161.9	160.7	90.3
7	80.2	101.1	110.0	64.5	28.9	63.2	61.7
8	133.3	143.6	101.4	134.6	54.8	78.1	89.9
9	100.4	128.2	107.9	60.4	74.7	222.4	97.1
10	51.6	72.1	108.3	132.3	46.2	36.8	57.0

D.8 Co

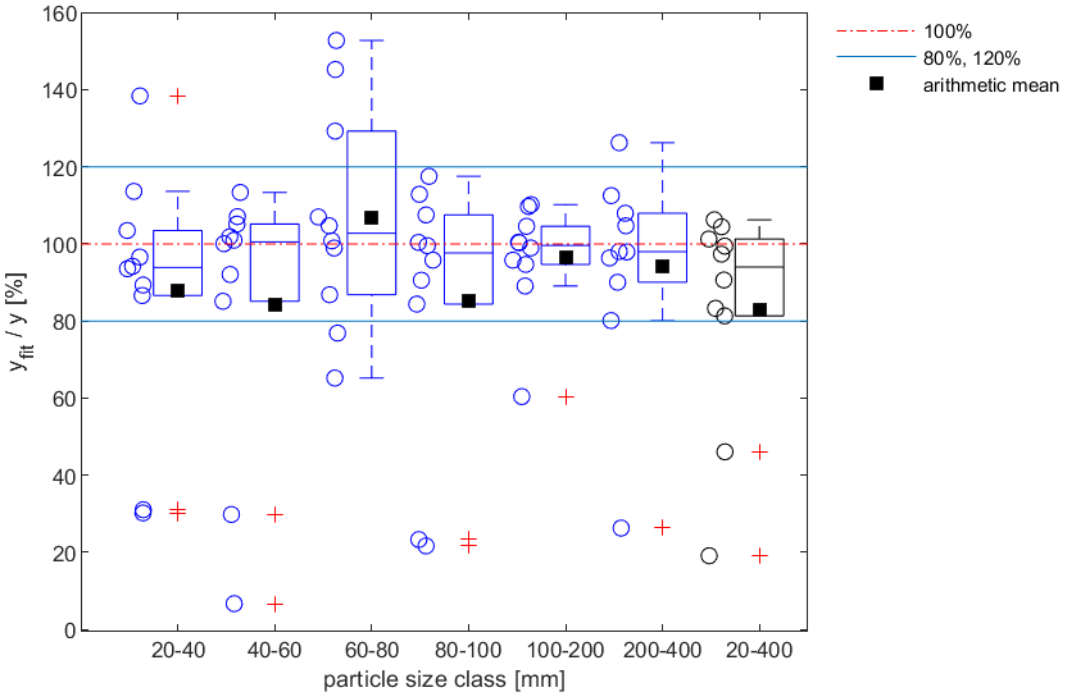

Figure D.8: Box plot of cobalt (Co) for the results of the prediction models in different particle size classes, as well as the material mix in the particle size classes >20mm

Table D.8: Ratios of the predicted values y_{fit} through the regression models and the original values y [in %] for cobalt (Co)

Sample No.	20–40mm	40–60mm	60–80mm	80–100mm	100–200mm	200–400mm	20–400mm
1	93.6	6.7	65.2	21.7	60.4	96.4	19.1
2	31.1	29.8	104.7	23.3	94.7	90.1	46.1
3	30.2	113.4	152.8	112.9	110.2	108.0	81.3
4	113.6	101.0	100.8	84.4	100.5	26.3	83.3
5	138.4	105.2	86.8	95.8	109.7	126.3	104.5
6	103.5	92.1	98.9	117.5	104.6	104.7	101.3
7	94.2	101.9	145.2	107.5	99.0	80.1	106.3
8	86.6	107.1	76.9	90.6	95.8	97.9	90.7
9	96.6	85.1	107.0	100.4	100.3	112.5	97.4
10	89.3	100.1	129.3	99.6	89.1	98.0	99.4

D.9 Cr

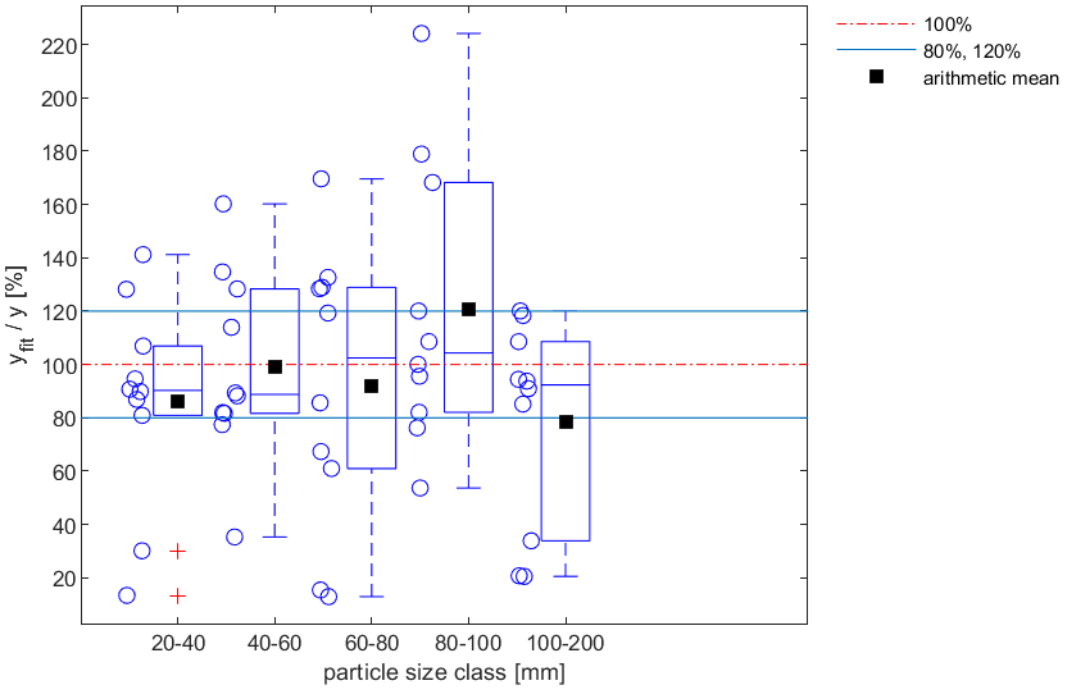

Figure D.9: Box plot of chromium (Cr) for the results of the prediction models in different particle size classes (the particle size class 200–400mm was excluded in the regression models, because too little values were present, after removing the outliers)

Table D.9: Ratios of the predicted values y_{fit} through the regression models and the original values y [in %] for chromium (Cr)

Sample No.	20–40mm	40–60mm	60–80mm	80–100mm	100–200mm	200–400mm	20–400mm
1	89.8	134.7	13.0	76.3	90.9	-	-
2	30.1	35.3	85.6	100.1	94.4	-	-
3	13.4	77.5	15.4	120.1	118.4	-	-
4	80.9	82.0	67.4	82.1	33.9	-	-
5	86.9	113.9	61.0	224.1	85.2	-	-
6	128.2	160.2	132.7	178.9	108.6	-	-
7	90.7	88.2	128.9	95.6	20.5	-	-
8	94.6	128.3	119.3	53.7	20.8	-	-
9	141.2	89.3	169.6	168.2	93.8	-	-
10	106.9	81.7	128.4	108.6	120.1	-	-

D.10 Cu

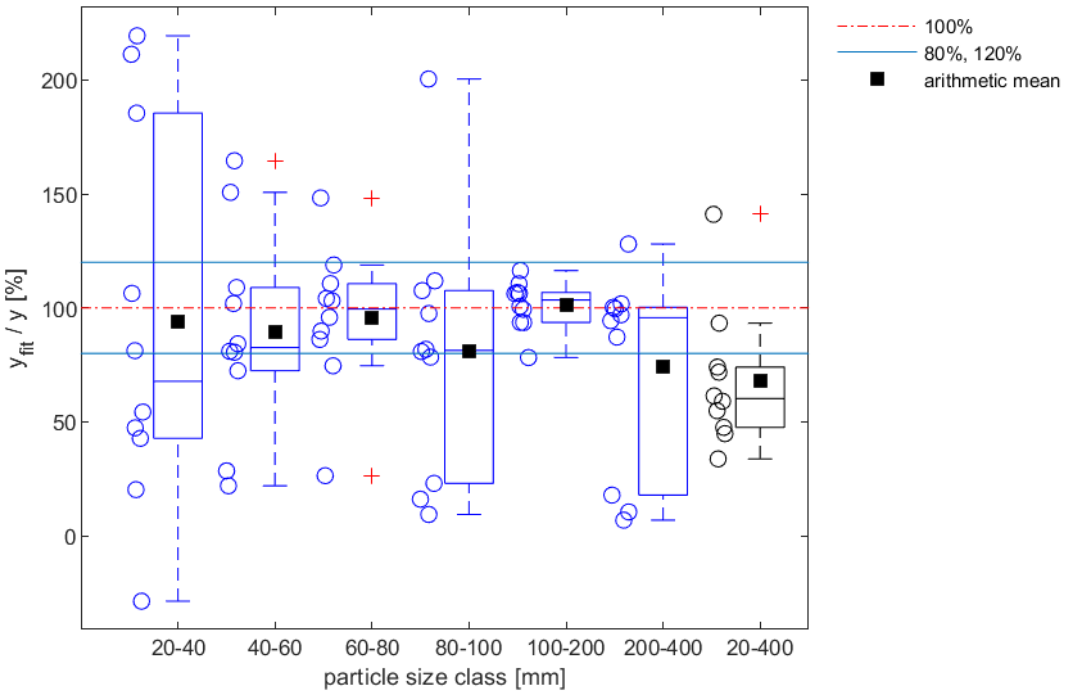

Figure D.10: Box plot of copper (Cu) for the results of the prediction models in different particle size classes, as well as the material mix in the particle size classes >20mm

Table D.10: Ratios of the predicted values y_{fit} through the regression models and the original values y [in %] for copper (Cu)

Sample No.	20–40mm	40–60mm	60–80mm	80–100mm	100–200mm	200–400mm	20–400mm
1	219.4	150.7	103.1	23.0	106.3	6.8	93.3
2	106.4	80.5	95.9	9.3	78.2	87.2	61.4
3	42.7	108.9	104.1	111.9	110.5	96.9	59.0
4	81.2	21.9	86.1	78.4	106.7	17.8	54.9
5	211.3	164.6	118.8	107.6	106.3	94.4	141.0
6	54.3	80.9	26.4	200.4	100.7	10.4	44.8
7	-28.7	72.4	110.6	16.0	99.3	99.6	47.6
8	47.3	84.2	74.6	80.8	93.6	101.8	74.0
9	185.5	28.5	148.2	97.5	93.6	128.0	71.8
10	20.2	101.9	89.8	81.8	116.4	100.2	33.7

D.11 Fe

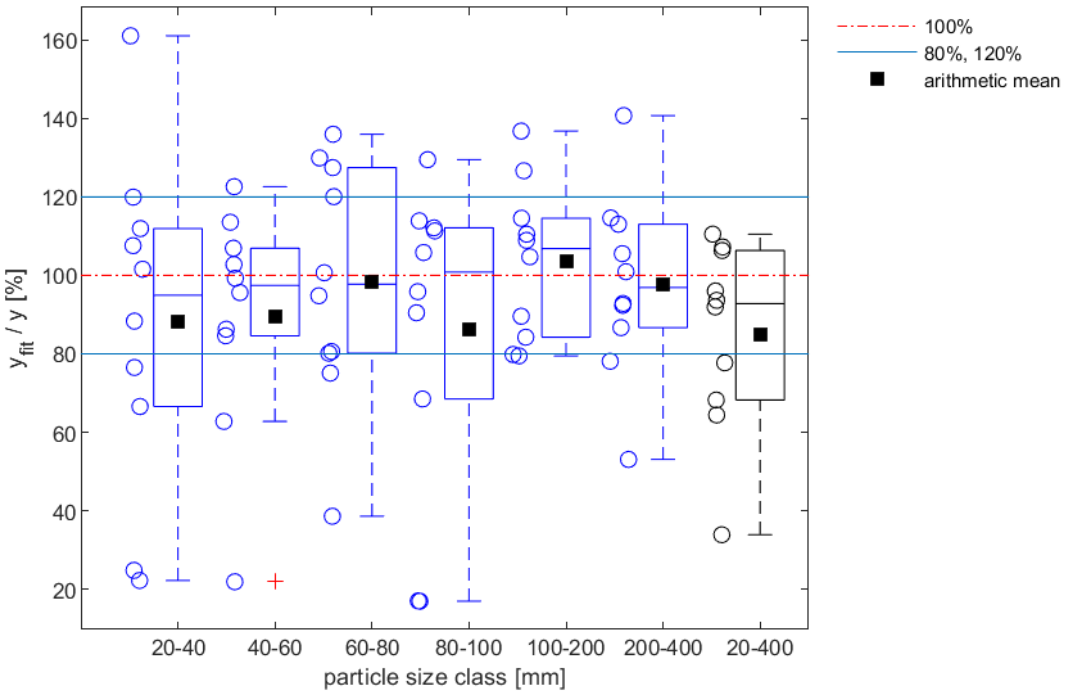

Figure D.11: Box plot of iron (Fe) for the results of the prediction models in different particle size classes, as well as the material mix in the particle size classes >20mm

Table D.11: Ratios of the predicted values y_{fit} through the regression models and the original values y [in %] for iron (Fe)

Sample No.	20–40mm	40–60mm	60–80mm	80–100mm	100–200mm	200–400mm	20–400mm
1	101.6	122.6	136.0	17.0	126.7	78.1	77.7
2	22.2	21.9	94.8	16.9	79.5	92.4	33.9
3	24.8	102.8	130.0	113.9	114.6	101.0	68.2
4	107.6	95.6	80.6	90.5	108.9	53.1	92.0
5	120.0	84.6	75.1	95.9	104.8	114.6	96.0
6	161.1	99.3	80.1	129.5	110.5	113.1	110.5
7	88.3	86.3	127.5	112.1	79.8	86.7	93.6
8	76.5	62.8	38.6	68.5	84.2	92.8	64.4
9	111.9	106.9	120.1	105.8	89.6	140.8	107.2
10	66.6	113.6	100.7	111.3	136.8	105.5	106.3

D.12 Hg

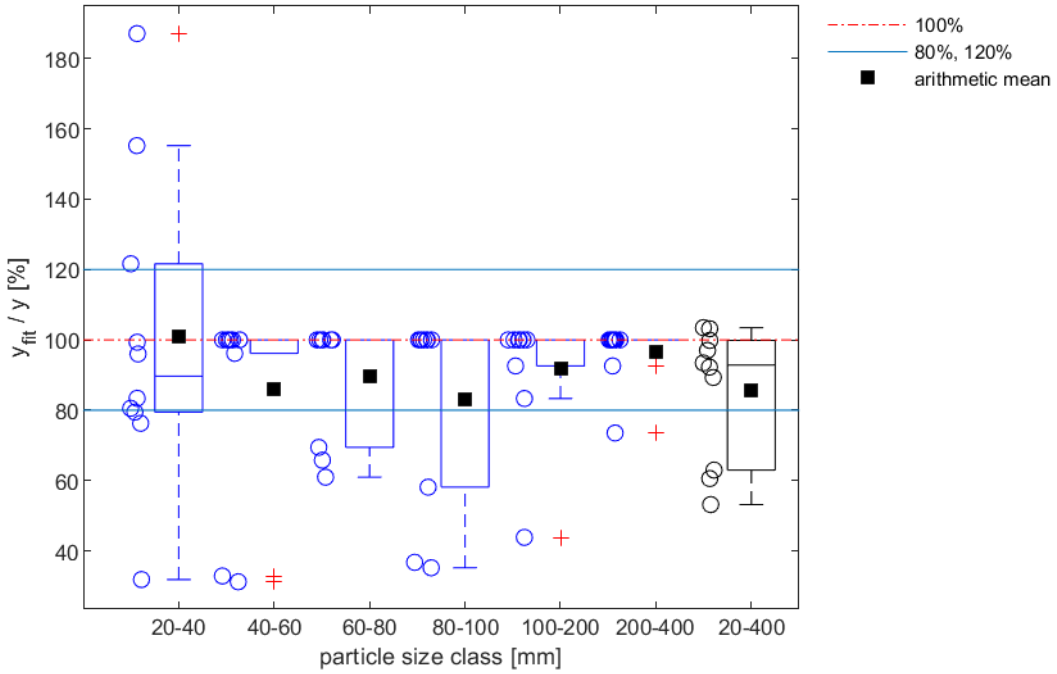

Figure D.12: Box plot of mercury (Hg) for the results of the prediction models in different particle size classes, as well as the material mix in the particle size classes >20mm

Table D.12: Ratios of the predicted values y_{fit} through the regression models and the original values y [in %] for mercury (Hg)

Sample No.	20–40mm	40–60mm	60–80mm	80–100mm	100–200mm	200–400mm	20–400mm
1	155.2	100.0	100.0	36.8	100.0	100.0	92.2
2	83.4	32.9	69.4	35.2	92.6	100.0	60.6
3	80.5	100.0	100.0	100.0	100.0	100.0	93.4
4	31.9	100.0	100.0	100.0	100.0	73.5	63.0
5	121.6	100.0	100.0	100.0	100.0	100.0	103.5
6	99.3	100.0	100.0	100.0	100.0	100.0	99.8
7	96.0	31.3	61.0	58.1	43.9	92.6	53.2
8	79.5	100.0	100.0	100.0	100.0	100.0	97.0
9	76.3	96.2	100.0	100.0	83.3	100.0	89.3
10	187.1	100.0	65.8	100.0	100.0	100.0	103.2

D.13 K

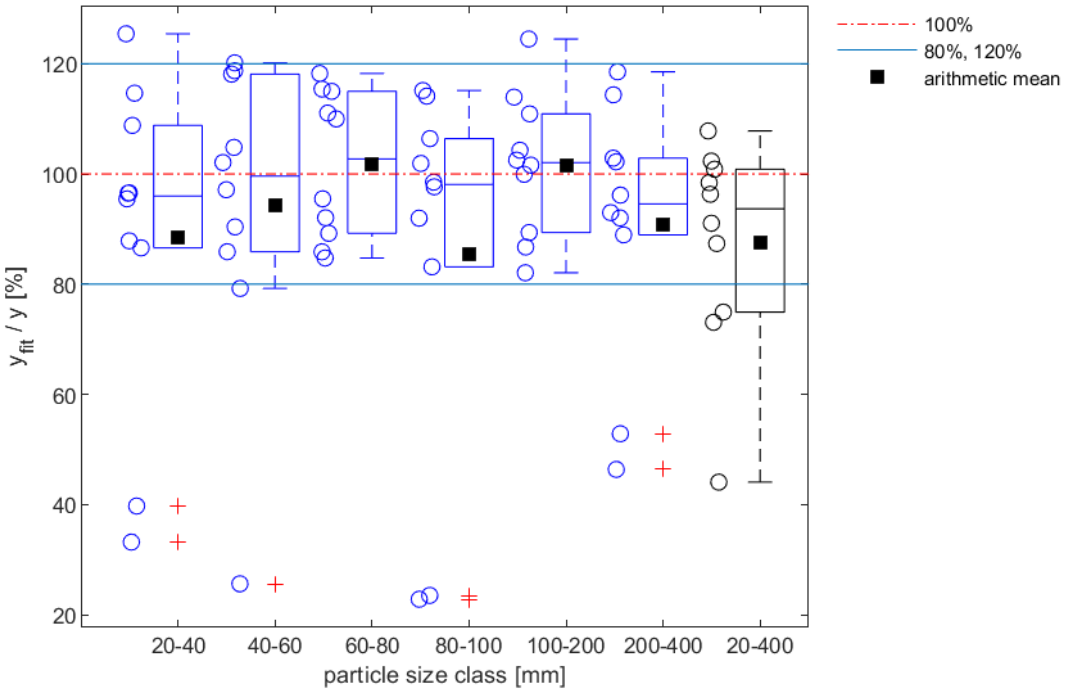

Figure D.13: Box plot of potassium (K) for the results of the prediction models in different particle size classes, as well as the material mix in the particle size classes >20mm

Table D.13: Ratios of the predicted values y_{fit} through the regression models and the original values y [in %] for potassium (K)

Sample No.	20–40mm	40–60mm	60–80mm	80–100mm	100–200mm	200–400mm	20–400mm
1	86.6	118.1	115.4	22.8	124.5	92.0	74.9
2	39.7	25.6	92.0	23.5	89.4	88.9	44.1
3	33.2	104.8	118.2	115.1	104.3	102.9	73.1
4	114.7	79.2	89.2	83.1	99.9	46.4	87.4
5	108.8	97.1	84.7	106.4	110.9	114.4	100.9
6	125.4	120.2	85.9	114.1	101.6	102.2	107.8
7	96.6	85.9	95.5	92.0	86.7	118.5	91.0
8	95.5	118.7	110.0	97.7	102.5	52.9	98.4
9	96.5	90.4	115.0	101.9	82.1	93.0	96.3
10	87.9	102.1	111.0	98.5	113.9	96.2	102.3

D.14 Li

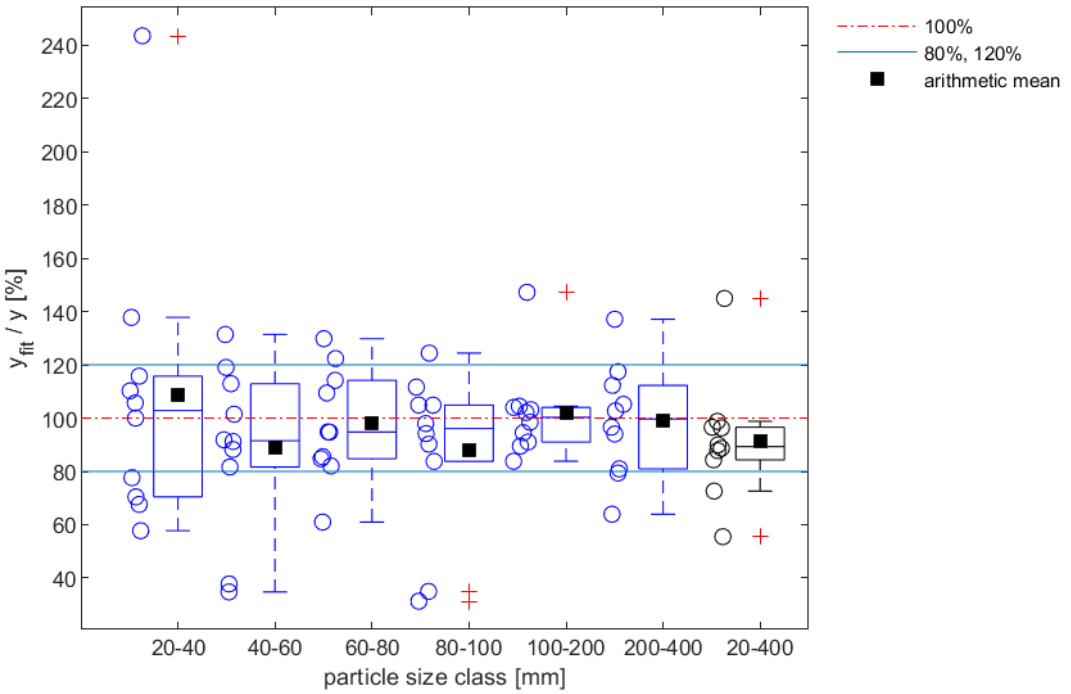

Figure D.14: Box plot of lithium (Li) for the results of the prediction models in different particle size classes, as well as the material mix in the particle size classes >20mm

Table D.14: Ratios of the predicted values y_{fit} through the regression models and the original values y [in %] for lithium (Li)

Sample No.	20–40mm	40–60mm	60–80mm	80–100mm	100–200mm	200–400mm	20–400mm
1	137.8	101.5	84.8	31.3	103.2	112.3	84.3
2	57.7	34.8	94.9	35.0	89.5	94.0	55.5
3	70.4	131.4	114.2	104.9	83.8	96.6	90.0
4	105.7	81.7	122.4	97.9	104.5	79.4	98.8
5	243.5	112.9	129.8	124.4	147.2	137.1	144.9
6	110.3	91.9	85.5	104.9	91.0	102.7	96.6
7	115.7	91.2	94.7	83.8	94.5	117.4	96.3
8	67.6	119.0	82.0	94.2	102.1	63.9	88.7
9	77.6	37.8	109.4	90.2	98.5	81.0	72.6
10	100.0	88.2	61.0	111.6	104.0	105.2	87.8

D.15 Mg

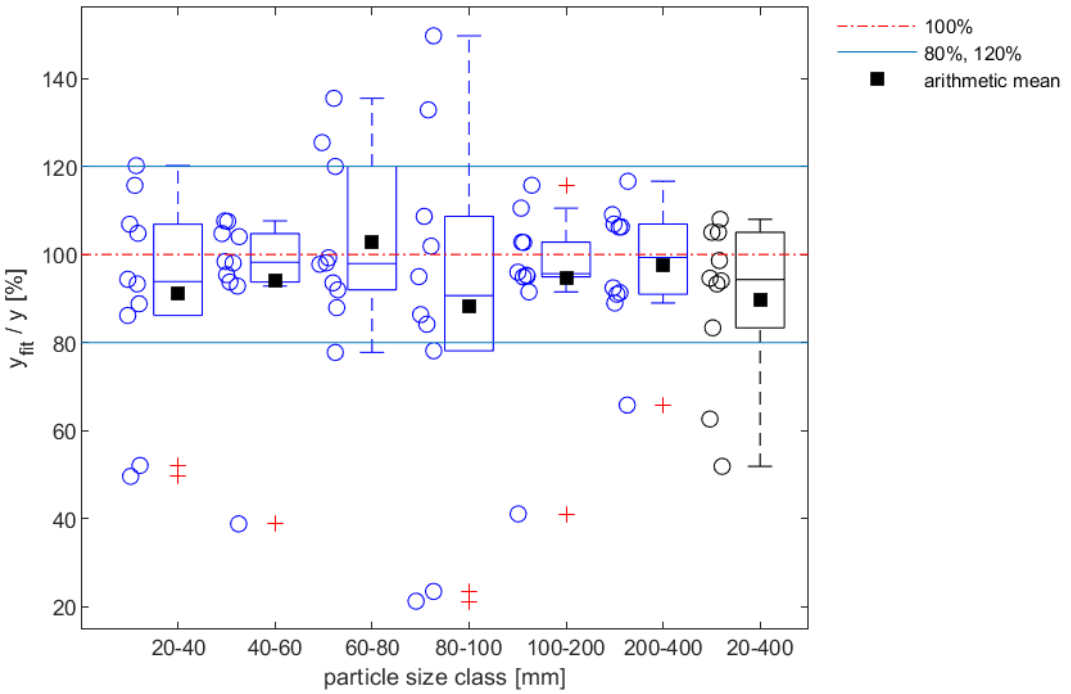

Figure D.15: Box plot of magnesium (Mg) for the results of the prediction models in different particle size classes, as well as the material mix in the particle size classes >20mm

Table D.15: Ratios of the predicted values y_{fit} through the regression models and the original values y [in %] for magnesium (Mg)

Sample No.	20–40mm	40–60mm	60–80mm	80–100mm	100–200mm	200–400mm	20–400mm
1	86.2	104.1	93.6	21.3	41.1	92.4	62.7
2	52.1	38.9	97.8	23.5	94.9	109.0	51.9
3	49.6	92.8	120.0	132.8	115.7	106.3	83.4
4	115.7	95.4	87.9	78.2	95.3	65.8	93.3
5	94.4	98.1	92.0	95.0	91.5	116.6	94.6
6	120.2	104.7	77.8	149.6	110.5	106.9	105.0
7	106.9	93.8	135.5	101.9	102.8	106.2	105.0
8	93.3	107.5	99.3	84.2	102.7	91.0	98.6
9	104.8	107.6	125.4	108.7	96.0	91.3	108.0
10	88.8	98.4	98.1	86.4	95.1	89.0	94.0

D.16 Mn

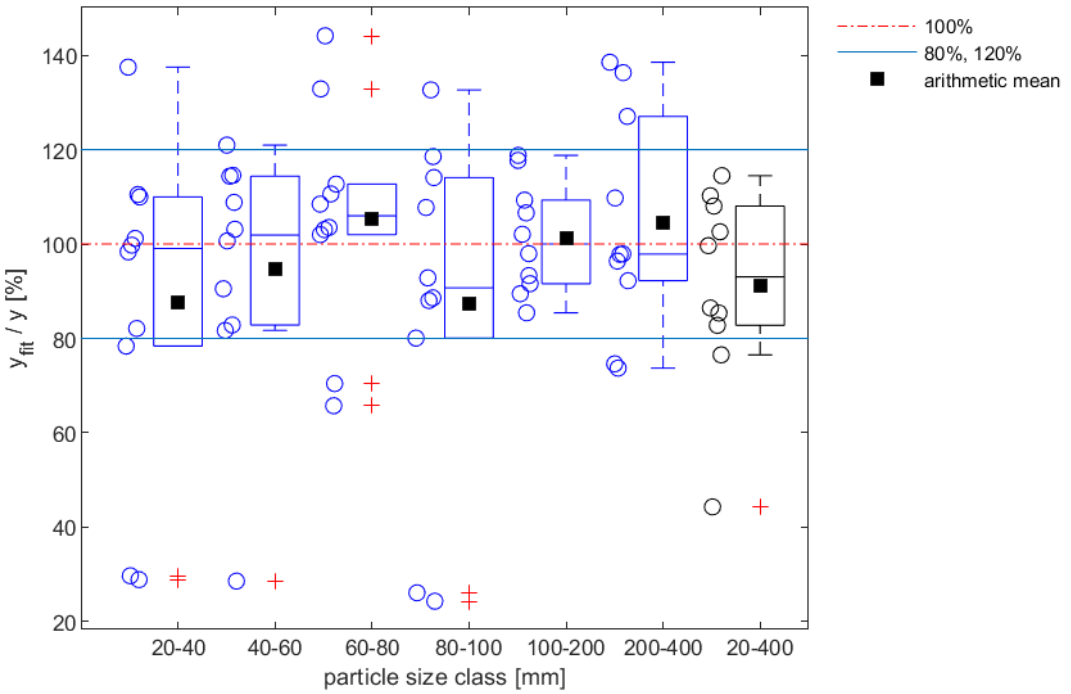

Figure D.16: Box plot of manganese (Mn) for the results of the prediction models in different particle size classes, as well as the material mix in the particle size classes >20mm

Table D.16: Ratios of the predicted values y_{fit} through the regression models and the original values y [in %] for manganese (Mn)

Sample No.	20–40mm	40–60mm	60–80mm	80–100mm	100–200mm	200–400mm	20–400mm
1	101.2	121.0	110.6	24.3	117.7	97.9	82.8
2	29.7	28.6	102.0	26.1	85.4	73.7	44.3
3	28.9	81.7	108.5	114.1	118.8	136.3	76.5
4	98.3	100.7	65.7	80.1	91.6	74.6	86.5
5	110.5	90.5	112.7	88.0	98.0	138.5	102.6
6	137.5	114.6	103.5	132.6	89.5	97.8	110.2
7	99.8	103.1	132.9	107.7	102.1	109.7	108.0
8	82.1	82.8	70.4	88.6	106.6	92.2	85.4
9	110.0	114.4	144.1	118.5	93.3	127.0	114.5
10	78.4	108.8	103.0	92.8	109.3	96.4	99.7

D.17 Mo

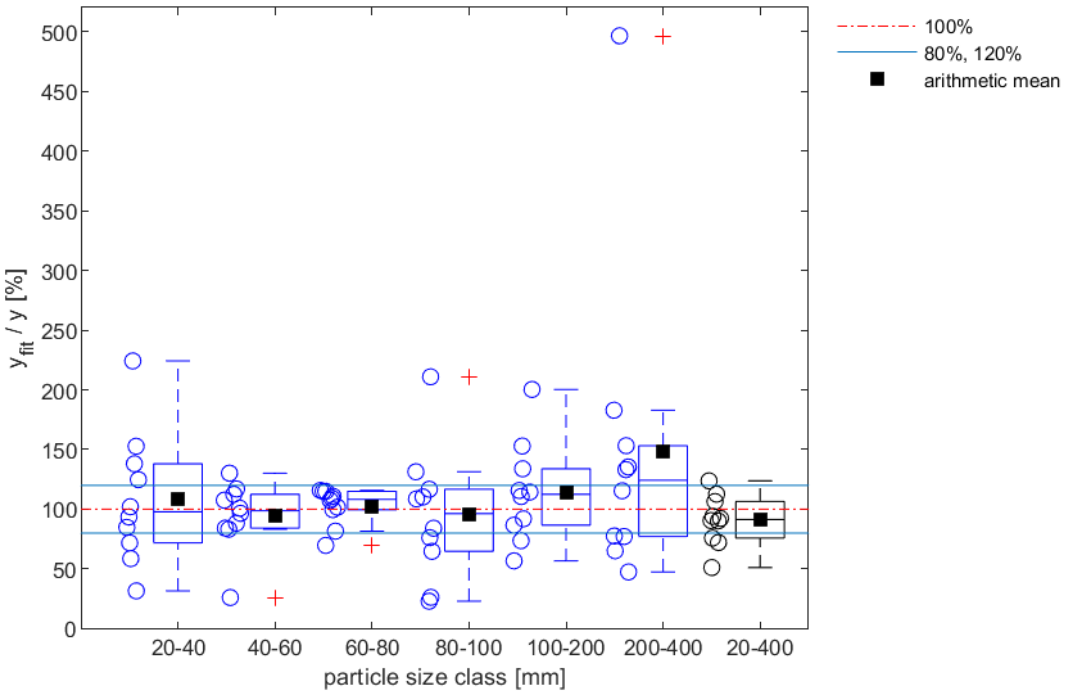

Figure D.17: Box plot of molybdenum (Mo) for the results of the prediction models in different particle size classes, as well as the material mix in the particle size classes >20mm

Table D.17: Ratios of the predicted values y_{fit} through the regression models and the original values y [in %] for molybdenum (Mo)

Sample No.	20–40mm	40–60mm	60–80mm	80–100mm	100–200mm	200–400mm	20–400mm
1	152.7	130.2	110.9	26.2	200.3	115.4	90.2
2	71.8	26.0	115.0	22.9	92.0	182.9	51.1
3	31.6	83.2	99.6	131.4	133.9	133.2	72.1
4	124.7	88.3	101.7	64.7	115.7	47.5	92.3
5	93.5	112.5	81.6	84.1	73.6	153.2	90.5
6	84.8	117.0	115.8	210.9	152.9	496.6	123.8
7	102.1	100.8	69.7	108.7	56.7	65.2	75.8
8	58.6	96.5	115.0	110.3	114.4	77.1	94.0
9	224.2	84.2	109.1	116.7	86.7	77.6	106.5
10	138.0	107.6	107.5	76.2	110.6	135.4	112.6

D.18 Na

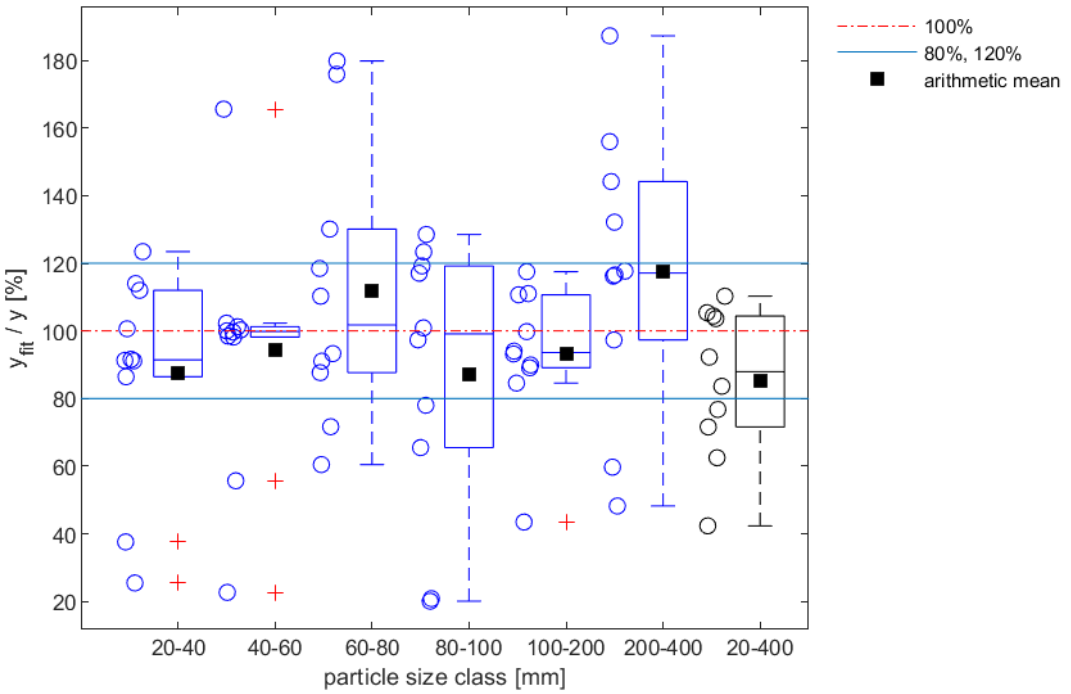

Figure D.18: Box plot of sodium (Na) for the results of the prediction models in different particle size classes, as well as the material mix in the particle size classes >20mm

Table D.18: Ratios of the predicted values y_{fit} through the regression models and the original values y [in %] for sodium (Na)

Sample No.	20–40mm	40–60mm	60–80mm	80–100mm	100–200mm	200–400mm	20–400mm
1	86.5	102.3	179.8	20.9	110.7	132.2	71.6
2	37.6	22.7	87.7	20.1	93.2	117.7	42.4
3	25.5	98.2	110.3	97.4	84.6	144.2	62.5
4	112.0	100.0	60.5	78.0	99.8	48.2	83.6
5	123.4	101.2	91.1	119.2	117.5	187.2	110.3
6	100.6	100.3	71.7	128.5	89.1	97.3	92.3
7	114.0	55.7	130.1	100.9	43.5	156.0	76.8
8	91.1	98.5	118.5	123.4	94.0	116.2	103.6
9	91.3	99.7	175.9	117.1	89.9	59.7	105.4
10	91.6	165.6	93.3	65.5	111.0	116.6	104.4

D.19 Ni

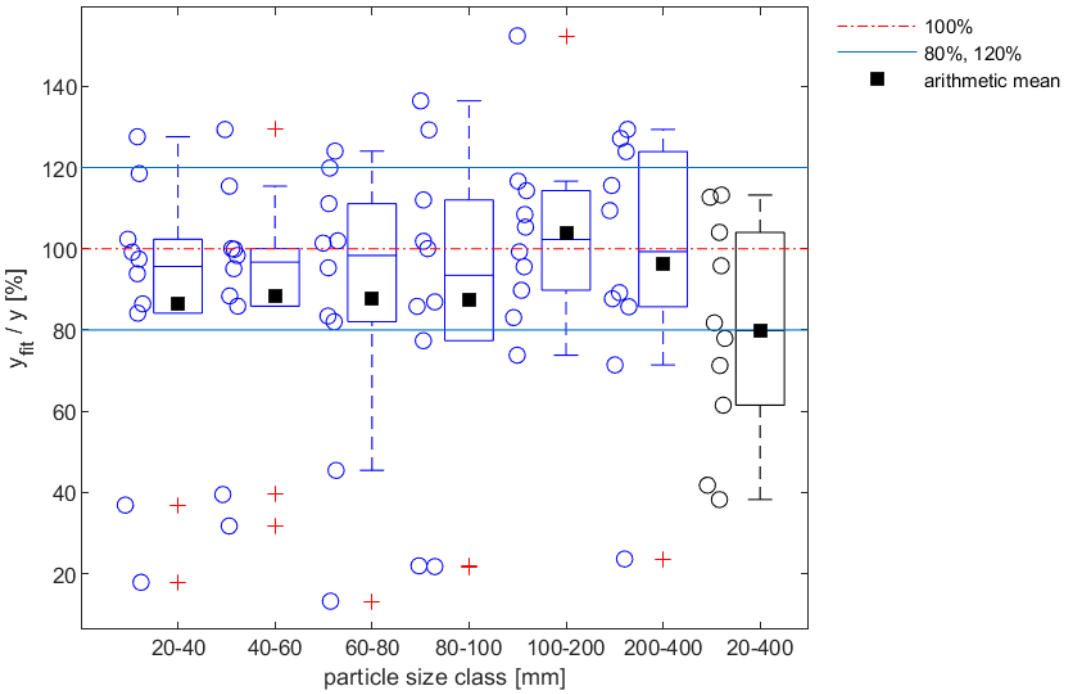

Figure D.19: Box plot of nickel (Ni) for the results of the prediction models in different particle size classes, as well as the material mix in the particle size classes >20mm

Table D.19: Ratios of the predicted values y_{fit} through the regression models and the original values y [in %] for nickel (Ni)

Sample No.	20–40mm	40–60mm	60–80mm	80–100mm	100–200mm	200–400mm	20–400mm
1	93.9	129.4	13.2	21.7	116.6	87.7	38.2
2	36.9	31.7	102.0	21.9	73.8	127.1	41.8
3	17.9	85.9	111.1	136.4	114.3	109.4	61.5
4	86.4	98.3	83.4	77.4	108.4	23.6	77.9
5	84.1	39.5	82.0	85.8	95.6	123.9	71.3
6	118.5	115.4	101.4	129.3	105.3	129.4	113.2
7	97.4	100.0	95.3	112.0	83.1	85.7	95.8
8	99.2	88.4	45.4	86.9	99.2	89.2	81.8
9	127.6	99.9	119.9	101.8	89.8	71.4	104.0
10	102.3	95.1	124.0	100.0	152.4	115.6	112.7

D.20 P

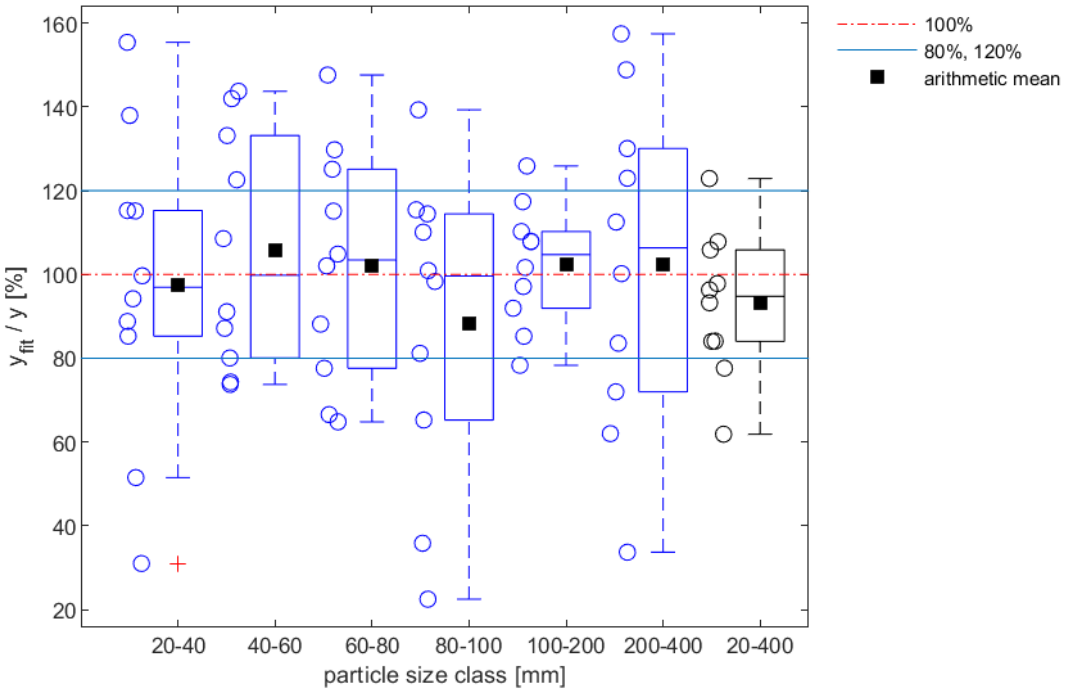

Figure D-20: Box plot of phosphorus (P) for the results of the prediction models in different particle size classes, as well as the material mix in the particle size classes >20mm

Table D.20: Ratios of the predicted values y_{fit} through the regression models and the original values y [in %] for phosphorus (P)

Sample No.	20–40mm	40–60mm	60–80mm	80–100mm	100–200mm	200–400mm	20–400mm
1	94.2	122.6	104.9	22.5	107.9	72.0	84.1
2	99.7	80.1	66.6	35.8	97.1	100.2	77.6
3	85.3	108.6	125.1	98.3	125.9	123.0	105.9
4	138.0	91.1	64.8	81.2	85.3	33.7	84.0
5	115.3	87.2	77.6	100.9	91.9	157.4	93.2
6	155.4	133.2	102.1	114.5	110.2	112.5	122.9
7	31.0	73.8	147.6	110.1	101.7	148.8	61.9
8	51.5	142.0	115.1	139.3	117.4	83.6	107.8
9	115.2	74.3	129.8	115.4	78.3	130.1	97.8
10	88.8	143.7	88.1	65.3	107.8	62.0	96.3

D.21 Pb

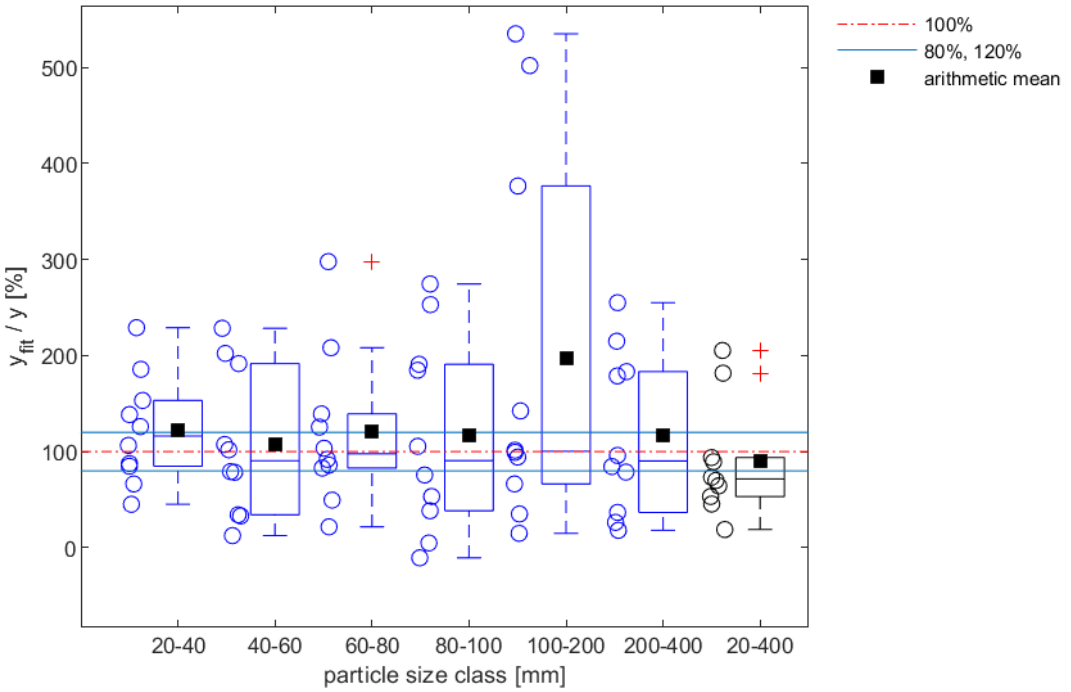

Figure D.21: Box plot of lead (Pb) for the results of the prediction models in different particle size classes, as well as the material mix in the particle size classes >20mm

Table D.21: Ratios of the predicted values y_{fit} through the regression models and the original values y [in %] for lead (Pb)

Sample No.	20–40mm	40–60mm	60–80mm	80–100mm	100–200mm	200–400mm	20–400mm
1	185.6	228.4	139.3	253.0	142.4	183.3	181.7
2	138.6	12.6	82.9	38.4	101.5	36.7	45.5
3	126.1	191.6	125.5	274.5	376.5	84.4	205.3
4	84.8	78.5	208.1	105.5	94.4	18.1	93.8
5	153.3	202.2	103.5	4.9	14.9	26.4	18.9
6	45.2	101.9	85.9	75.7	534.9	96.1	89.5
7	106.5	79.2	49.5	-10.5	35.1	78.7	53.3
8	87.5	33.1	297.8	184.7	99.3	255.1	73.3
9	229.0	107.4	21.7	53.3	501.8	178.8	64.4
10	66.4	34.3	92.0	190.9	66.4	214.9	70.0

D.22 Sb

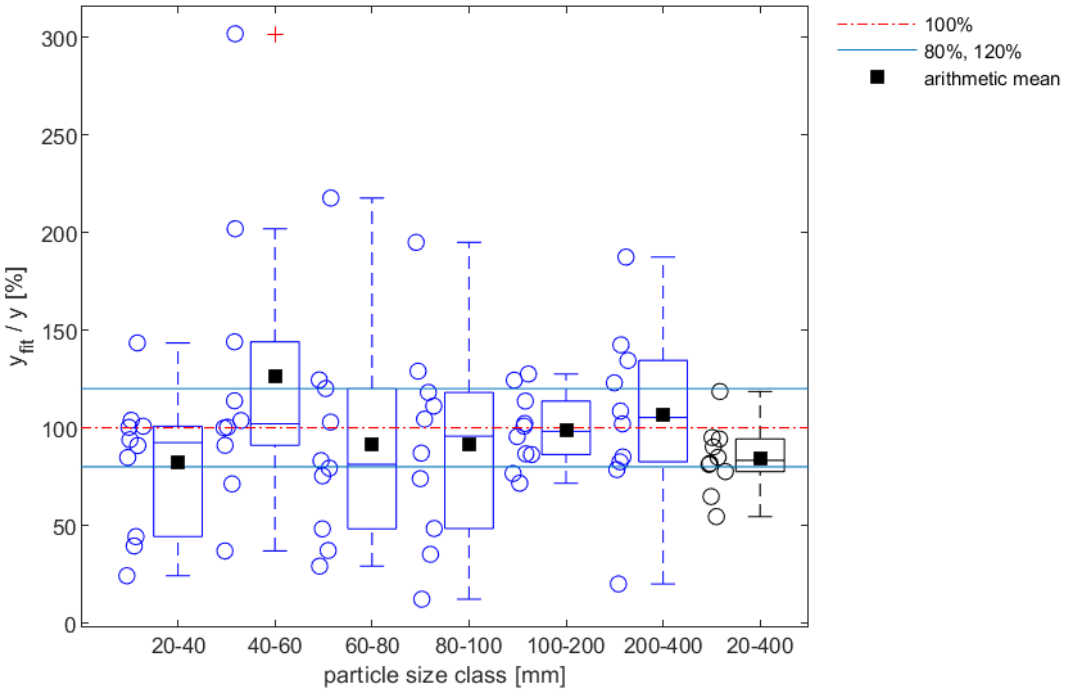

Figure D.22: Box plot of antimony (Sb) for the results of the prediction models in different particle size classes, as well as the material mix in the particle size classes >20mm

Table D.22: Ratios of the predicted values y_{fit} through the regression models and the original values y [in %] for antimony (Sb)

Sample No.	20–40mm	40–60mm	60–80mm	80–100mm	100–200mm	200–400mm	20–400mm
1	93.9	100.3	79.3	129.0	100.8	134.4	95.0
2	90.9	201.9	217.6	194.9	86.6	102.0	118.6
3	143.4	144.0	124.5	87.0	71.6	20.0	94.3
4	84.8	71.3	102.9	12.2	102.2	187.4	81.7
5	24.2	301.7	120.1	118.1	127.5	82.6	81.2
6	39.5	113.8	29.1	48.4	76.6	108.5	54.5
7	100.8	91.0	37.2	111.1	124.4	85.1	77.5
8	103.8	99.9	48.2	104.4	86.3	78.6	90.2
9	44.3	103.7	83.2	73.9	113.7	123.0	84.8
10	100.2	36.9	75.4	35.2	95.5	142.4	64.7

D.23 Si

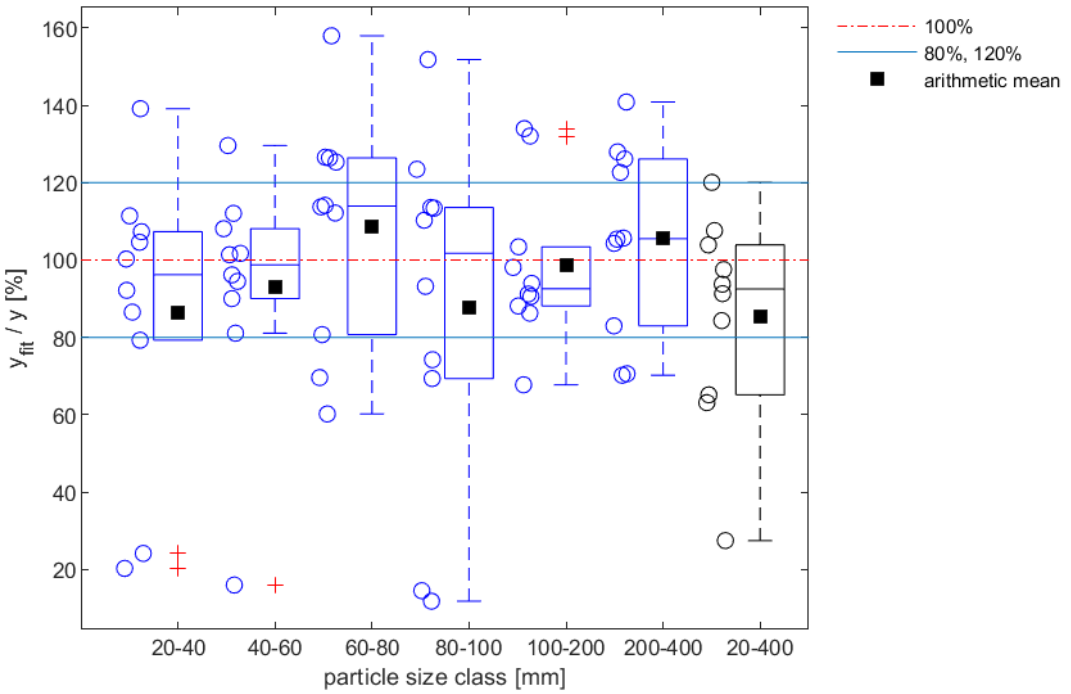

Figure D.23: Box plot of silicon (Si) for the results of the prediction models in different particle size classes, as well as the material mix in the particle size classes >20mm

Table D.23: Ratios of the predicted values y_{fit} through the regression models and the original values y [in %] for silicon (Si)

Sample No.	20–40mm	40–60mm	60–80mm	80–100mm	100–200mm	200–400mm	20–400mm
1	92.2	96.2	126.4	14.6	98.1	105.7	65.2
2	24.2	16.0	112.2	11.8	67.8	70.2	27.5
3	20.3	101.4	126.6	113.6	103.4	122.6	63.1
4	104.6	94.5	60.2	69.4	90.6	83.0	84.3
5	139.1	81.1	69.6	93.2	94.0	126.1	91.3
6	107.3	101.7	80.7	151.8	88.1	104.3	97.5
7	100.3	90.0	157.9	113.4	91.2	105.4	103.9
8	86.5	129.6	114.1	110.3	132.0	70.6	107.6
9	111.4	108.1	125.3	123.4	134.0	140.8	120.1
10	79.3	112.1	113.7	74.2	86.3	127.9	93.7

D.24 Sn

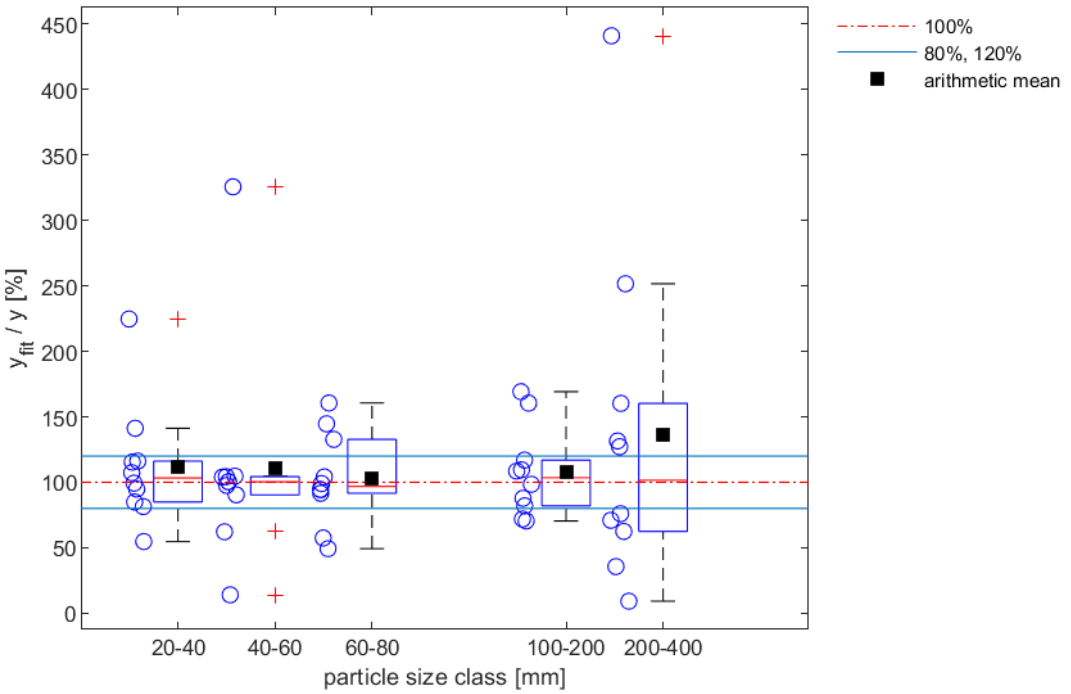

Figure D.24: Box plot of tin (Sn) for the results of the prediction models in different particle size classes (the particle size class 80–100mm was excluded in the regression models, because too little values were present, after removing the outliers)

Table D.24: Ratios of the predicted values y_{fit} through the regression models and the original values y [in %] for tin (Sn)

Sample No.	20–40mm	40–60mm	60–80mm	80–100mm	100–200mm	200–400mm	20–400mm
1	81.4	100.3	49.3	-	71.9	160.3	-
2	141.2	62.2	99.0	-	116.9	251.7	-
3	84.9	325.8	132.8	-	160.5	131.6	-
4	224.8	97.6	94.3	-	87.7	9.1	-
5	99.3	104.0	104.1	-	108.6	441.2	-
6	94.8	90.4	57.4	-	109.5	35.6	-
7	116.2	104.3	160.6	-	169.2	127.2	-
8	115.4	14.0	94.6	-	98.5	70.9	-
9	107.3	104.7	144.7	-	82.0	62.4	-
10	54.7	100.5	91.6	-	70.4	75.9	-

D.25 Sr

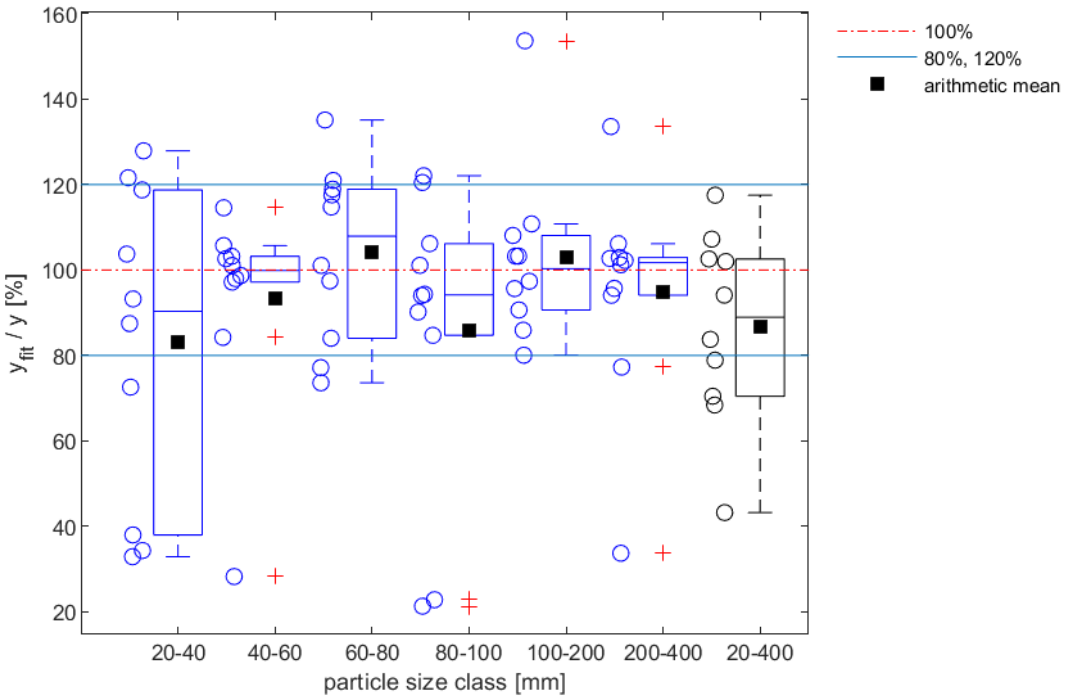

Figure D.25: Box plot of strontium (Sr) for the results of the prediction models in different particle size classes, as well as the material mix in the particle size classes >20mm

Table D.25: Ratios of the predicted values y_{fit} through the regression models and the original values y [in %] for strontium (Sr)

Sample No.	20–40mm	40–60mm	60–80mm	80–100mm	100–200mm	200–400mm	20–400mm
1	72.6	97.2	117.6	21.3	90.6	94.1	70.5
2	34.4	28.3	101.1	22.8	103.2	77.3	43.3
3	38.0	101.1	118.9	120.5	108.1	102.7	78.9
4	121.6	98.0	77.2	84.7	85.9	33.7	83.8
5	118.7	103.2	73.6	94.3	95.6	102.2	94.1
6	127.9	98.7	84.0	122.1	103.3	95.7	102.0
7	93.2	102.6	135.1	101.1	153.6	106.2	117.5
8	103.7	105.7	114.7	90.2	97.4	101.2	102.6
9	87.5	114.6	120.9	94.0	110.8	133.6	107.2
10	32.9	84.2	97.4	106.2	80.1	102.9	68.4

D.26 Ti

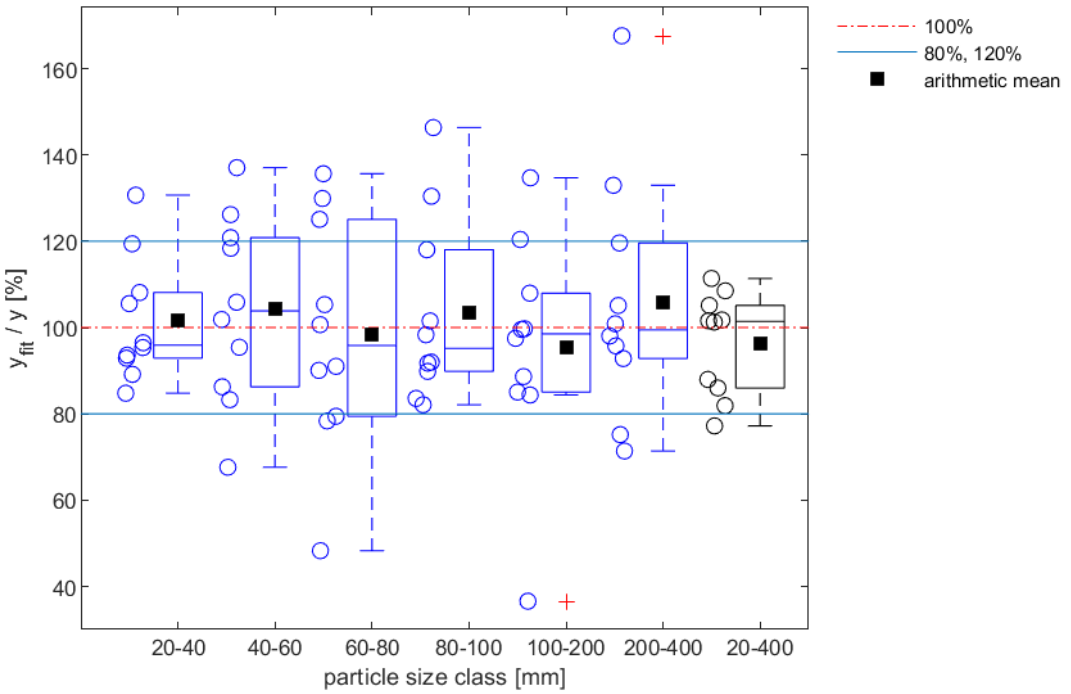

Figure D.26: Box plot of titanium (Ti) for the results of the prediction models in different particle size classes, as well as the material mix in the particle size classes >20mm

Table D.26: Ratios of the predicted values y_{fit} through the regression models and the original values y [in %] for titanium (Ti)

Sample No.	20–40mm	40–60mm	60–80mm	80–100mm	100–200mm	200–400mm	20–400mm
1	108.1	95.4	91.0	91.7	120.4	133.0	101.8
2	119.4	101.9	100.7	83.6	99.6	98.0	101.3
3	105.5	126.2	135.6	146.3	85.0	95.8	111.4
4	89.2	83.3	125.1	92.0	36.6	92.8	77.2
5	92.9	120.8	78.4	101.5	108.0	167.6	101.6
6	93.6	105.9	90.1	130.4	134.7	75.2	105.1
7	95.4	67.6	79.4	82.1	88.6	105.1	81.9
8	96.5	137.0	129.9	89.8	99.7	100.9	108.5
9	130.7	118.4	48.3	118.0	97.5	119.6	86.0
10	84.8	86.3	105.3	98.3	84.4	71.4	88.0

D.27 V

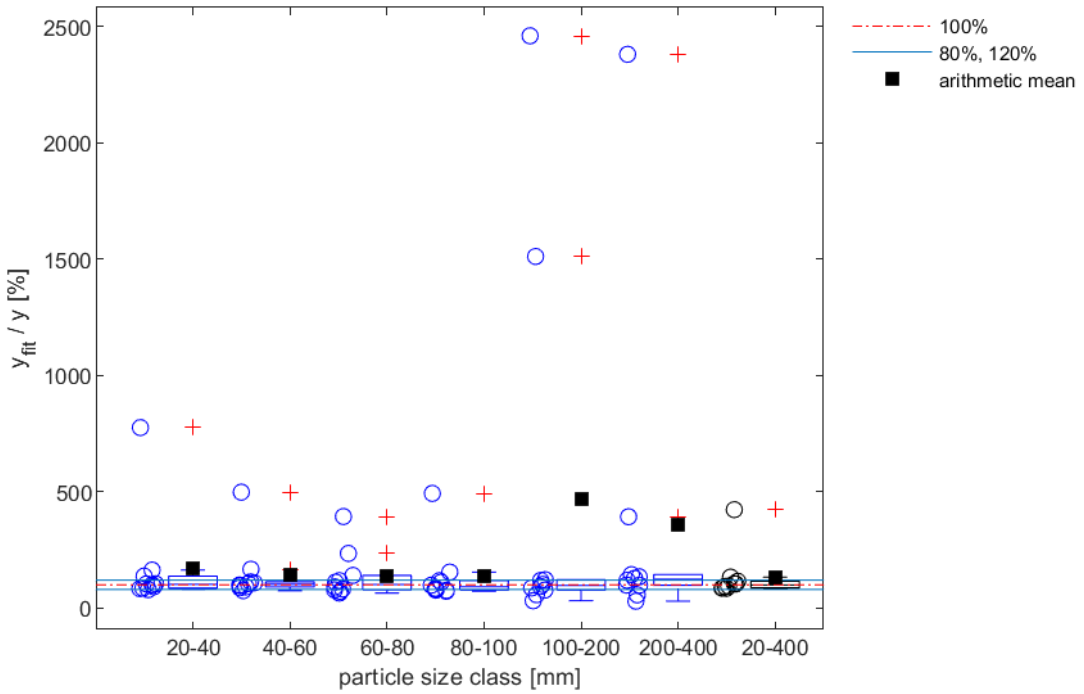

(A)

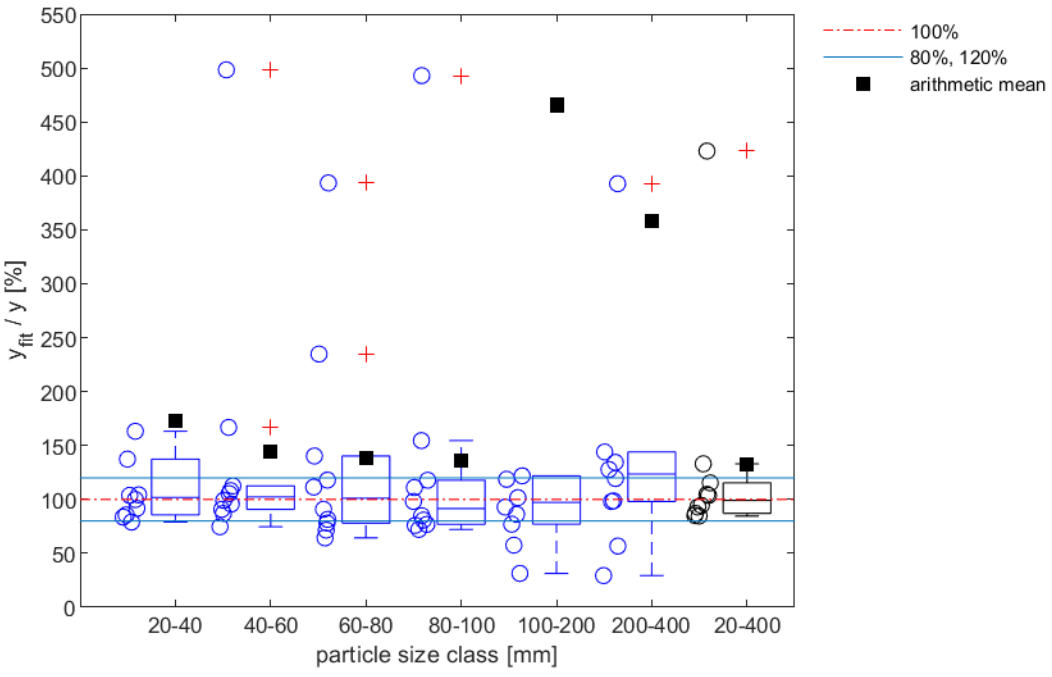

(B)

Figure D.27: A: Box plot of vanadium (V) for the results of the prediction models in different particle size classes, as well as the material mix in the particle size classes >20mm; B: Detailed Box plot of vanadium (V) for the results of the prediction models in different particle size classes, as well as the material mix in the particle size classes >20mm for better visualization

Table D.27: Ratios of the predicted values y_{fit} through the regression models and the original values y [in %] for vanadium (V)

Sample No.	20–40mm	40–60mm	60–80mm	80–100mm	100–200mm	200–400mm	20–400mm
1	137.4	87.0	81.5	76.9	57.6	98.1	84.6
2	103.8	112.5	111.4	84.9	86.1	29.4	94.5
3	104.2	90.8	140.3	117.8	121.9	134.4	115.3
4	83.6	99.1	71.5	80.8	101.7	56.8	85.1
5	776.0	74.7	64.4	76.0	77.1	119.4	87.1
6	85.7	105.4	90.8	154.5	31.4	127.7	93.0
7	99.9	95.7	117.9	98.2	118.7	144.0	104.7
8	91.7	166.8	78.0	111.0	92.9	98.7	103.7
9	163.2	498.3	393.5	493.0	2460.9	2381.2	423.0
10	79.0	108.1	234.8	72.2	1511.8	392.7	133.0

D.28 W

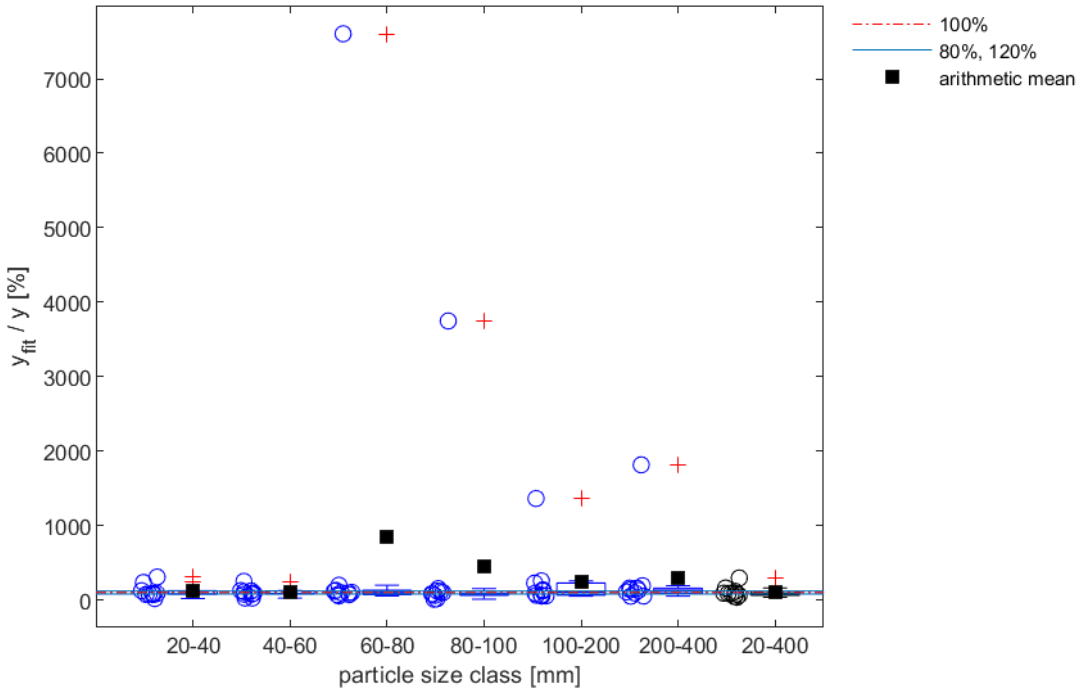

(A)

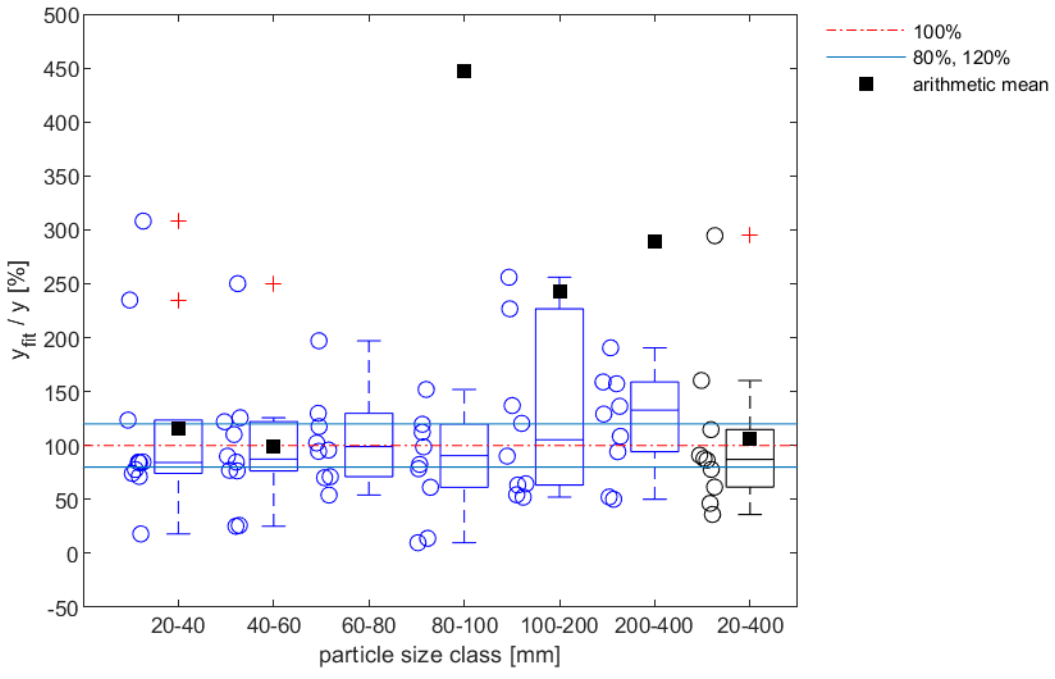

(B)

Figure D.28: A: Box plot of tungsten (W) for the results of the prediction models in different particle size classes, as well as the material mix in the particle size classes >20mm; B: Detailed Box plot of tungsten (W) for the results of the prediction models in different particle size classes, as well as the material mix in the particle size classes >20mm for better visualization

Table D.28: Ratios of the predicted values y_{fit} through the regression models and the original values y [in %] for tungsten (W)

Sample No.	20–40mm	40–60mm	60–80mm	80–100mm	100–200mm	200–400mm	20–400mm
1	123.6	84.6	129.9	13.9	226.7	94.2	91.0
2	84.6	25.9	102.3	9.8	63.4	52.3	46.4
3	77.7	90.1	70.2	119.7	90.2	129.2	86.4
4	18.0	110.2	54.0	61.2	120.5	50.2	36.1
5	83.9	77.0	71.1	112.3	52.1	136.4	77.9
6	308.1	76.5	7605.2	3747.7	1362.4	1814.7	294.5
7	84.7	25.1	94.6	98.7	64.5	190.6	61.5
8	74.2	122.1	95.8	78.4	54.3	157.3	87.8
9	71.3	250.1	197.1	152.0	137.0	158.9	114.7
10	234.9	125.7	117.6	82.4	256.0	108.5	160.3

D.29 Zn

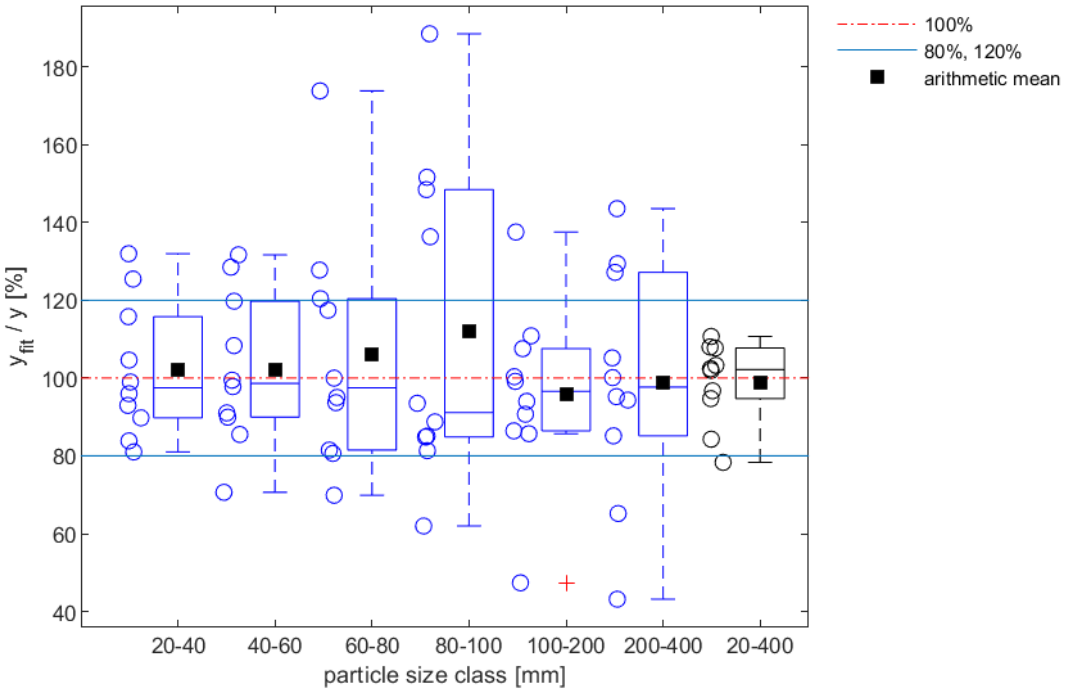

Figure D.29: Box plot of zinc (Zn) for the results of the prediction models in different particle size classes, as well as the material mix in the particle size classes >20mm

Table D.29: Ratios of the predicted values y_{fit} through the regression models and the original values y [in %] for zinc (Zn)

Sample No.	20–40mm	40–60mm	60–80mm	80–100mm	100–200mm	200–400mm	20–400mm
1	132.0	97.8	81.5	62.0	107.6	85.1	94.7
2	99.0	99.5	117.4	81.3	90.7	95.2	96.7
3	81.0	131.7	93.7	136.3	110.9	94.4	103.3
4	104.6	91.0	69.9	85.1	94.0	43.2	84.3
5	89.8	90.0	80.6	148.4	47.4	127.2	78.3
6	115.8	70.6	127.8	151.6	85.7	100.1	102.4
7	83.9	85.5	173.8	84.8	99.2	129.4	101.9
8	93.0	119.8	120.4	93.5	86.4	143.5	108.0
9	96.0	128.5	100.0	188.5	100.3	105.2	110.7
10	125.4	108.3	95.0	88.7	137.5	65.2	107.7

D.30 LHV

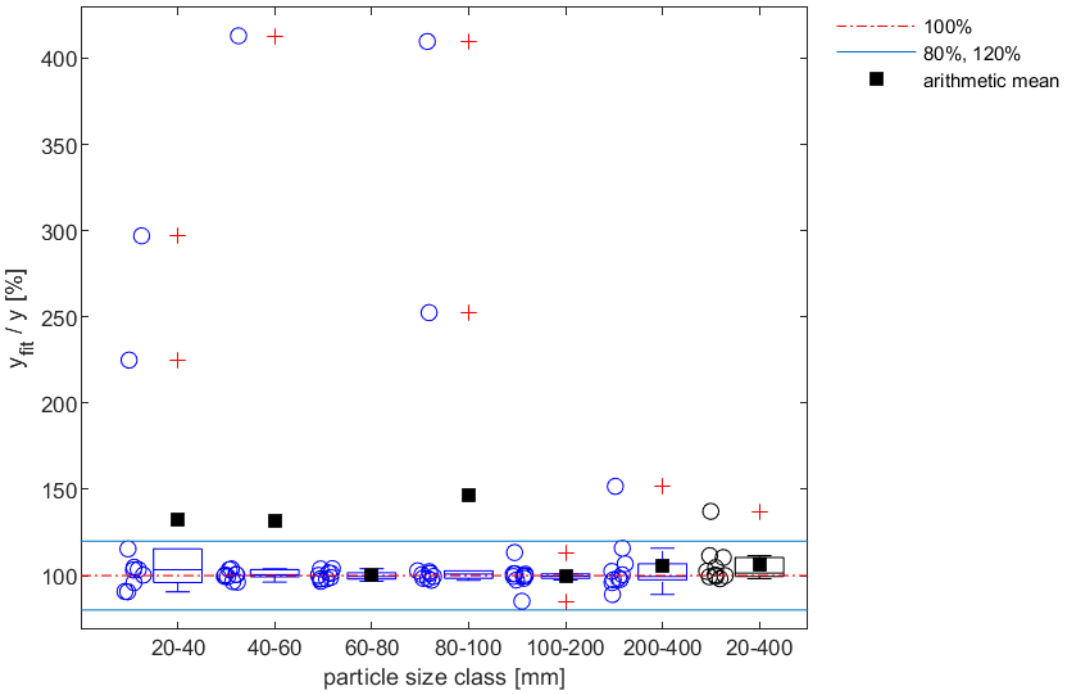

Figure D.30: Box plot of the lower heating value (LHV) for the results of the prediction models in different particle size classes, as well as the material mix in the particle size classes >20mm

Table D.30: Ratios of the predicted values y_{fit} through the regression models and the original values y [in %] for the lower heating value (LHV)

Sample No.	20–40mm	40–60mm	60–80mm	80–100mm	100–200mm	200–400mm	20–400mm
1	115.5	103.9	97.9	252.5	100.8	106.8	111.6
2	224.9	413.0	100.1	409.7	85.1	115.9	137.2
3	297.0	96.5	98.0	100.6	97.4	97.5	110.5
4	90.8	99.6	101.3	99.5	99.6	151.7	102.5
5	96.0	100.4	104.0	102.8	113.4	102.4	104.6
6	90.6	103.4	101.6	102.3	99.8	100.4	99.3
7	100.3	100.7	103.8	98.3	98.4	97.7	100.0
8	103.5	96.2	98.9	97.2	101.0	89.0	98.2
9	104.8	100.5	96.7	98.4	99.5	95.9	99.5
10	103.3	99.3	98.2	101.2	101.0	98.5	100.4

Appendix E - Detailed results of sorting analyses of Part I

Table E.1: Detailed results of sorting analysis of composite sample No. 1

Particle size class [mm]	Metal	Wood	Paper	Card-board	Plastics 2D	Plastics 3D	Inert	Textile	Residue
20–40	10.30%	11.94%	5.71%	22.11%	2.93%	14.38%	13.72%	0.58%	18.32%
40–60	6.91%	13.82%	5.79%	27.06%	4.60%	14.61%	7.79%	1.70%	17.72%
60–80	12.97%	16.33%	5.82%	19.70%	5.11%	15.41%	4.66%	3.28%	16.72%
80–100	8.92%	14.95%	10.44%	17.14%	5.87%	20.33%	0.00%	6.00%	16.35%
100–200	1.63%	6.05%	8.19%	29.32%	8.65%	19.08%	9.28%	13.31%	4.48%
200–400	0.78%	0.00%	0.00%	24.95%	26.88%	17.61%	0.00%	15.05%	14.74%

Table E.2: Detailed results of sorting analysis of composite sample No. 2

Particle size class [mm]	Metal	Wood	Paper	Card-board	Plastics 2D	Plastics 3D	Inert	Textile	Residue
20–40	4.22%	12.74%	3.95%	17.06%	3.42%	22.91%	14.35%	0.57%	20.77%
40–60	7.56%	14.10%	5.39%	20.78%	4.92%	18.59%	6.58%	1.14%	20.95%
60–80	9.62%	18.52%	5.62%	15.01%	7.39%	17.95%	4.46%	2.63%	18.80%
80–100	10.89%	16.53%	8.66%	16.14%	7.17%	17.97%	0.00%	7.22%	15.40%
100–200	11.78%	8.77%	11.53%	16.42%	10.45%	15.17%	0.00%	9.39%	16.48%
200–400	0.00%	0.00%	0.00%	0.21%	27.28%	16.90%	0.00%	44.35%	11.26%

Table E.3: Detailed results of sorting analysis of composite sample No. 3

Particle size class [mm]	Metal	Wood	Paper	Card-board	Plastics 2D	Plastics 3D	Inert	Textile	Residue
20–40	3.77%	12.72%	5.71%	24.36%	3.58%	20.36%	13.12%	0.64%	15.73%
40–60	5.25%	18.26%	6.20%	25.19%	4.13%	16.21%	9.33%	1.06%	14.37%
60–80	3.87%	15.67%	9.28%	24.16%	4.64%	18.62%	2.20%	2.03%	19.54%
80–100	12.91%	13.32%	4.17%	17.18%	6.96%	16.50%	0.00%	7.97%	21.00%
100–200	2.78%	8.37%	3.57%	26.40%	10.97%	11.62%	0.00%	15.50%	20.78%
200–400	2.06%	0.00%	0.17%	9.57%	22.79%	7.80%	0.00%	30.93%	26.68%

Table E.4: Detailed results of sorting analysis of composite sample No. 4

Particle size class [mm]	Metal	Wood	Paper	Card-board	Plastics 2D	Plastics 3D	Inert	Textile	Residue
20–40	4.84%	10.95%	6.55%	23.09%	4.70%	19.75%	14.44%	0.65%	15.02%
40–60	14.30%	14.49%	7.05%	22.63%	2.99%	16.65%	3.84%	2.27%	15.79%
60–80	5.75%	21.69%	9.01%	16.33%	5.57%	17.03%	0.64%	5.56%	18.42%
80–100	5.79%	19.90%	7.67%	19.02%	6.97%	20.42%	0.00%	3.28%	16.96%
100–200	5.08%	2.20%	2.68%	31.99%	20.08%	9.92%	0.00%	11.28%	16.78%
200–400	0.00%	0.00%	0.00%	8.85%	28.71%	22.62%	0.00%	21.34%	18.48%

Table E.5: Detailed results of sorting analysis of composite sample No. 5

Particle size class [mm]	Metal	Wood	Paper	Card-board	Plastics 2D	Plastics 3D	Inert	Textile	Residue
20–40	6.07%	11.86%	7.44%	10.41%	3.10%	18.26%	23.82%	0.61%	18.43%
40–60	3.86%	12.22%	8.85%	18.14%	4.43%	18.87%	14.03%	0.83%	18.77%
60–80	7.85%	11.22%	8.70%	16.63%	6.35%	20.84%	6.33%	2.87%	19.22%
80–100	1.44%	11.19%	5.09%	15.50%	9.91%	26.72%	1.44%	4.65%	24.05%
100–200	12.49%	5.26%	3.15%	27.95%	7.87%	14.65%	3.62%	5.04%	19.97%
200–400	0.00%	0.00%	1.42%	2.33%	19.36%	21.00%	0.00%	17.82%	38.07%

Table E.6: Detailed results of sorting analysis of composite sample No. 6

Particle size class [mm]	Metal	Wood	Paper	Card-board	Plastics 2D	Plastics 3D	Inert	Textile	Residue
20–40	5.23%	12.60%	7.37%	16.92%	2.71%	16.72%	17.48%	0.50%	20.46%
40–60	6.86%	18.18%	8.16%	18.76%	4.11%	16.40%	10.08%	0.76%	16.70%
60–80	5.56%	17.54%	10.16%	19.58%	5.41%	18.67%	2.80%	3.23%	17.04%
80–100	15.90%	11.28%	11.63%	16.92%	6.85%	19.29%	0.00%	1.83%	16.31%
100–200	5.43%	3.21%	4.27%	33.73%	11.76%	23.13%	1.06%	2.29%	15.12%
200–400	0.12%	0.15%	0.20%	3.82%	30.21%	23.33%	0.00%	33.76%	8.41%

Table E.7: Detailed results of sorting analysis of composite sample No. 7

Particle size class [mm]	Metal	Wood	Paper	Card-board	Plastics 2D	Plastics 3D	Inert	Textile	Residue
20–40	4.93%	11.43%	5.27%	23.63%	3.29%	17.95%	16.32%	0.26%	16.93%
40–60	6.08%	15.17%	7.96%	24.13%	3.88%	13.71%	5.30%	0.98%	22.78%
60–80	11.15%	15.59%	7.09%	17.55%	5.04%	17.65%	6.65%	4.04%	15.24%
80–100	3.06%	6.08%	3.71%	17.43%	7.16%	27.35%	12.67%	3.13%	19.40%
100–200	7.66%	4.23%	8.64%	16.41%	16.59%	26.52%	0.61%	9.82%	9.50%
200–400	1.69%	0.33%	0.26%	0.00%	43.27%	17.75%	0.00%	20.99%	15.72%

Table E.8: Detailed results of sorting analysis of composite sample No. 8

Particle size class [mm]	Metal	Wood	Paper	Card-board	Plastics 2D	Plastics 3D	Inert	Textile	Residue
20–40	4.57%	9.89%	10.42%	10.30%	3.44%	17.37%	17.33%	0.61%	26.08%
40–60	8.06%	12.59%	8.98%	22.23%	4.23%	15.59%	5.17%	1.40%	21.76%
60–80	8.44%	12.80%	10.70%	13.75%	5.88%	19.29%	4.34%	3.68%	21.11%
80–100	8.95%	9.20%	8.91%	18.72%	10.05%	21.97%	0.00%	5.51%	16.69%
100–200	5.56%	2.26%	1.33%	30.67%	10.87%	17.74%	2.05%	12.48%	17.05%
200–400	0.40%	0.00%	0.00%	1.29%	35.14%	19.17%	0.00%	34.18%	9.82%

Table E.9: Detailed results of sorting analysis of composite sample No. 9

Particle size class [mm]	Metal	Wood	Paper	Card-board	Plastics 2D	Plastics 3D	Inert	Textile	Residue
20–40	7.30%	13.96%	9.72%	10.64%	3.97%	22.98%	17.69%	0.46%	13.28%
40–60	3.65%	19.93%	9.53%	16.96%	5.08%	18.27%	8.28%	1.18%	17.11%
60–80	9.73%	17.40%	10.67%	12.57%	6.03%	16.89%	5.60%	4.58%	16.52%
80–100	3.97%	14.87%	12.50%	14.41%	6.77%	21.41%	0.00%	8.91%	17.16%
100–200	5.24%	7.10%	2.23%	32.95%	11.38%	20.24%	0.00%	11.48%	9.38%
200–400	8.32%	0.00%	0.00%	0.00%	25.88%	15.59%	0.00%	32.60%	17.61%

Table E.10: Detailed results of sorting analysis of composite sample No. 10

Particle size class [mm]	Metal	Wood	Paper	Card-board	Plastics 2D	Plastics 3D	Inert	Textile	Residue
20–40	5.50%	9.88%	5.27%	14.30%	4.14%	22.90%	22.67%	0.44%	14.90%
40–60	6.86%	12.27%	6.30%	14.85%	4.22%	19.18%	14.56%	0.93%	20.83%
60–80	7.55%	11.53%	6.80%	15.89%	6.42%	24.13%	4.15%	5.64%	17.88%
80–100	15.94%	5.74%	10.69%	11.42%	8.08%	21.68%	9.63%	4.66%	12.16%
100–200	0.83%	6.54%	6.99%	20.38%	14.32%	26.71%	4.68%	5.95%	13.62%
200–400	5.96%	0.00%	0.00%	0.00%	20.51%	19.64%	0.00%	32.72%	21.17%

Publication V – Supplementary

The particle size-dependent distribution of chemical elements in mixed commercial waste and implications for enhancing SRF quality

S.A. Viczek, K. Khodier, L. Kandlbauer, A. Aldrian, G. Redhammer, G. Tippelt, R. Sarc

Science of the total environment 776 (2021), 145343,
https://doi.org/10.1016/j.scitotenv.2021.145343

Content

Appendix A - Comparison with data in literature

Table A.1: Reported concentrations of As, Cd, Cl, Cr, Co, Fe, Hg, Ni, Pb, and Sb in the fine fractions (c_{fine}) in comparison to the concentration in the waste mix (c_{mix}) of various studies. Values marked with * refer to wet mass. MSW = Municipal solid waste, MCW = Mixed commercial waste, CIW = Commercial and industrial waste, SRF = Solid recovered fuel.

		As [mg/kg$_{DM}$]	Cd [mg/kg$_{DM}$]	Cl [mg/kg$_{DM}$]	Cr [mg/kg$_{DM}$]	Co [mg/kg$_{DM}$]	Fe [mg/kg$_{DM}$]	Hg [mg/kg$_{DM}$]	Ni [mg/kg$_{DM}$]	Pb [mg/kg$_{DM}$]	Sb [mg/kg$_{DM}$]
Rugg und Hanna (1992) **(MSW)**	waste mix	3.3	4.5		377			5.8	34	152	
	fines, n.def.	4.3	2		24			0.31	30	462	
Beker und Cornelissen (1999) Data 1994 **(MSW)**	waste mix	<5	4.8	4940	111	3.4	34400	0.1	67	141	23
	< 3 mm	<5	< 0.1	1817	270	1.2	9833	0.2	127	583	< 0.5
	3-8 mm	<5	< 0.1	2838	176.7	3.5	16333	0.2	70	543	< 0.5
	8-20mm	<5	< 0.1	4517	363.3	< 0.5	6167	0.3	163	397	< 0.5
Beker und Cornelissen (1999) Data 1995 **(MSW)**	waste mix	<5	2.2		88	6.7	36000	0.1	59	77	12
	< 3 mm	<5	0.7		450	7	8600	0.5	280	220	0.7
	3-8 mm	<5	0.6		280	42	9900	0.9	550	110	3.8
	8-20mm	<5	0.7		240	4	5500	0.7	170	89	2.6
Watanabe et al. (1999) Plant 2 **(MSW)**	All combust.										135.5
	< 5 mm										479.6
Watanabe et al. (1999) Plant 7 **(MSW)**	All combust.										110
	< 5 mm										7.2
LfU Bayern (2003) **(MSW)**	waste mix	9.0*	9.6		336			0.191	38	208	
	< 10 mm	27.7	2.4		279		17870	0.394	26.5	131	
	10 - 40 mm	10.9	4.3		90		7570	0.11	16.8	83	
ADEME (2010) **(MSW)**	waste mix	2.52	1.29	2878	87			0.1	20		
	< 8 mm	1.07	1.17	4093	86			0.039	44		
Nasrullah et al. (2015) **(CIW)**	waste mix	5.0	1.2	6000	290	2.4	4399	0.1	22	90	7.2
	< 10 mm	9.8	1.0	4000	190	12	12000	0.3	94	235	31
Sarc (2015) **(SRF)**	Waste mix	7.4	11.6	10880	99	38		0.4	40	362	157
	< 6.3 mm	13.6	6.3	9160	218	67		0.8	87	730	80
Curtis et al. (2019) waste stream 1 **(MCW)**	waste mix	< 2.5	1.00	11339	52	4.9		< 0.25	22	55	37
	0 - 20 mm	< 2.5	0.57	12493	41	3.2		< 0.25	22	34	14
	20 - 40 mm	< 2.5	0.25	12567	11	1.0		< 0.25	6	46	15
	40 - 65 mm	< 2.5	0.93	7757	8	1.3		< 0.25	6	12	17
	> 65 mm	< 2.5	1.43	11573	81	7.8		< 0.25	31	76	56
Curtis et al. (2019) waste stream 2 **(MCW)**	waste mix	3.2	0.59	8983	92	21		1.26	39	80	35
	0 - 20 mm	4.1	0.56	5738	145	50		2.80	71	81	20
	20 - 40 mm	5.6	0.94	9555	87	22		1.41	50	39	22
	40 - 65 mm	3.7	1.40	6245	94	26		1.32	54	39	18
	> 65 mm	< 2.5	0.37	10008	79	12		0.82	25	88	42
Curtis et al. (2019) waste stream 3 **(MCW)**	waste mix	2.6	1.70	9626	235	6.4		0.72	74	244	85
	0 - 20 mm	< 2.5	0.56	6270	266	9.3		0.34	88	226	32
	20 - 40 mm	3.4	0.27	4333	130	7.5		0.36	53	1080	57
	40 - 65 mm	< 2.5	0.25	5937	202	4.8		0.31	85	228	9
	> 65 mm	< 2.5	2.43	12017	251	6.1		0.87	73	167	116
Curtis et al. (2019) waste stream 4 **(MCW)**	waste mix	8.1	1.78	26462	106	11.7		0.86	53	84	32
	0 - 20 mm	5.3	0.35	9000	115	11.5		0.76	51	81	13
	20 - 40 mm	3.9	0.25	43900	16	2.9		0.26	12	41	20
	40 - 65 mm	< 2.5	0.37	37450	19	3.8		< 0.25	9	186	37
	> 65 mm	10.3	2.68	25650	133	14.4		1.08	67	71	37
This study **(MCW)**	mix	9	2.60	8328	155	10	44321	0.58	63	242	32
	< 5 mm	16	0.78	1948	245	20	113550	1.34	123	348	15
	5 - 10 mm	18	1.62	3762	182	15	52550	0.86	91	459.1	30
	10 - 20 mm	7	1.73	8339	194	9	40330	0.52	97	111.2	33
	20 - 40 mm	7	3.70	9268	117	7	34380	0.50	55	109.6	43
	40 - 60 mm	7	3.69	12148	110	15	30310	0.36	50	277	50
	60 - 80 mm	6	5.87	10917	179	5	21560	0.29	44	153.9	39
	80 - 100 mm	7	1.56	7348	147	6	30370	0.36	39	333.4	29
	100 - 200 mm	5	2.62	10982	69	4	14716	0.29	19	247.2	27
	200 - 400 mm	5	1.18	12211	129	4	15520	0.26	24	64.6	53

Legend: $c_{fine} \leq 0.5 * c_{mix}$ | $c_{fine} < c_{mix}$ | $c_{fine} > c_{mix}$ | $c_{fine} \geq 2 * c_{mix}$

Table A.2: Concentration factors ($c_{faction}/c_{mix}$) of As, Cd, Cl, Cr, Co, Fe, Hg, Ni, Pb, and Sb. MSW = Municipal solid waste, MCW = Mixed commercial waste, CIW = Commercial and industrial waste, SRF = Solid recovered fuel.

		As [mg/kg$_{DM}$]	Cd [mg/kg$_{DM}$]	Cl [mg/kg$_{DM}$]	Cr [mg/kg$_{DM}$]	Co [mg/kg$_{DM}$]	Fe [mg/kg$_{DM}$]	Hg [mg/kg$_{DM}$]	Ni [mg/kg$_{DM}$]	Pb [mg/kg$_{DM}$]	Sb [mg/kg$_{DM}$]
Rugg und Hanna (1992) **(MSW)**	fines, n. def.	1.3	0.4		0.1			0.1	0.9	3.0	
Beker und Cornelissen (1999) Data 1994 **(MSW)**	< 3 mm	1.0	0.0	0.4	2.4	0.4	0.3	2.0	1.9	4.1	0.0
	3-8 mm	1.0	0.0	0.6	1.6	1.0	0.5	2.0	1.0	3.9	0.0
	8-20mm	1.0	0.0	0.9	3.3	0.1	0.2	3.0	2.4	2.8	0.0
Beker und Cornelissen (1999) Data 1995 **(MSW)**	< 3 mm	1.0	0.3		5.1	1.0	0.2	5.0	4.7	2.9	0.1
	3-8 mm	1.0	0.3		3.2	6.3	0.3	9.0	9.3	1.4	0.3
	8-20mm	1.0	0.3		2.7	0.6	0.2	7.0	2.9	1.2	0.2
Watanabe et al. (1999) Plant 2 **(MSW)**	< 5 mm										3.5
Watanabe et al. (1999) Plant 7 **(MSW)**	< 5 mm										0.1
LfU Bayern (2003) **(MSW)**	< 10 mm	3.1	0.3		0.8			2.1	0.7	0.6	
	10 - 40 mm	1.2	0.4		0.3			0.6	0.4	0.4	
ADEME (2010) **(MSW)**	< 8 mm	0.4	0.9	1.4	1.0			0.4	2.2		
Nasrullah et al. (2015) **(CIW)**	< 10 mm	2.0	0.8	0.7	0.7	5.0	2.7	3.0	4.3	2.6	4.3
Sarc (2015) **(SRF)**	< 6.3 mm	1.8	0.5	0.8	2.2	1.8		2.0	2.2	2.0	0.5
Curtis et al. (2019) waste stream 1 **(MCW)**	0 - 20 mm	1.0	0.6	1.1	0.8	0.7		1.0	1.0	0.6	0.4
	20 - 40 mm	1.0	0.2	1.1	0.2	0.2		1.0	0.3	0.8	0.4
	40 - 65 mm	1.0	0.9	0.7	0.2	0.3		1.0	0.3	0.2	0.5
	> 65 mm	1.0	1.4	1.0	1.6	1.6		1.0	1.4	1.4	1.5
Curtis et al. (2019) waste stream 2 **(MCW)**	0 - 20 mm	1.3	0.9	0.6	1.6	2.4		2.2	1.8	1.0	0.6
	20 - 40 mm	1.7	1.6	1.1	1.0	1.1		1.1	1.3	0.5	0.6
	40 - 65 mm	1.2	2.4	0.7	1.0	1.2		1.0	1.4	0.5	0.5
	> 65 mm	0.8	0.6	1.1	0.9	0.6		0.6	0.7	1.1	1.2
Curtis et al. (2019) waste stream 3 **(MCW)**	0 - 20 mm	1.0	0.3	0.7	1.1	1.5		0.5	1.2	0.9	0.4
	20 - 40 mm	1.3	0.2	0.5	0.6	1.2		0.5	0.7	4.4	0.7
	40 - 65 mm	1.0	0.1	0.6	0.9	0.7		0.4	1.2	0.9	0.1
	> 65 mm	1.0	1.4	1.2	1.1	1.0		1.2	1.0	0.7	1.4
Curtis et al. (2019) waste stream 4 **(MCW)**	0 - 20 mm	0.6	0.2	0.3	1.1	1.0		0.9	1.0	1.0	0.4
	20 - 40 mm	0.5	0.1	1.7	0.2	0.2		0.3	0.2	0.5	0.6
	40 - 65 mm	0.3	0.2	1.4	0.2	0.3		0.3	0.2	2.2	1.2
	> 65 mm	1.3	1.5	1.0	1.3	1.2		1.3	1.3	0.8	1.2
This study **(MCW)**	< 5 mm	1.8	0.3	0.2	1.6	2	2.6	2.3	1.9	1.4	0.5
	5 - 10 mm	2.0	0.6	0.5	1.2	1.4	1.2	1.5	1.4	1.9	0.9
	10 - 20 mm	0.8	0.7	1.0	1.2	0.9	0.9	0.9	1.5	0.5	1.0
	20 - 40 mm	0.7	1.4	1.1	0.8	0.7	0.8	0.9	0.9	0.5	1.3
	40 - 60 mm	0.8	1.4	1.5	0.7	1.5	0.7	0.6	0.8	1.1	1.6
	60 - 80 mm	0.7	2.3	1.3	1.2	0.5	0.5	0.5	0.7	0.6	1.2
	80 - 100 mm	0.8	0.6	0.9	0.9	0.6	0.7	0.6	0.6	1.4	0.9
	100 - 200 mm	0.6	1.0	1.3	0.4	0.4	0.3	0.5	0.3	1.0	0.8
	200 - 400 mm	0.6	0.5	1.5	0.8	0.4	0.4	0.5	0.4	0.3	1.6

Legend

$c_{fine} \leq 0.5 * c_{mix}$	$c_{fine} < c_{mix}$	$c_{fine} > c_{mix}$	$c_{fine} \geq 2 * c_{mix}$

Appendix B - Results for the concentration of analytes/parameters in particle size classes

B.1. Ag

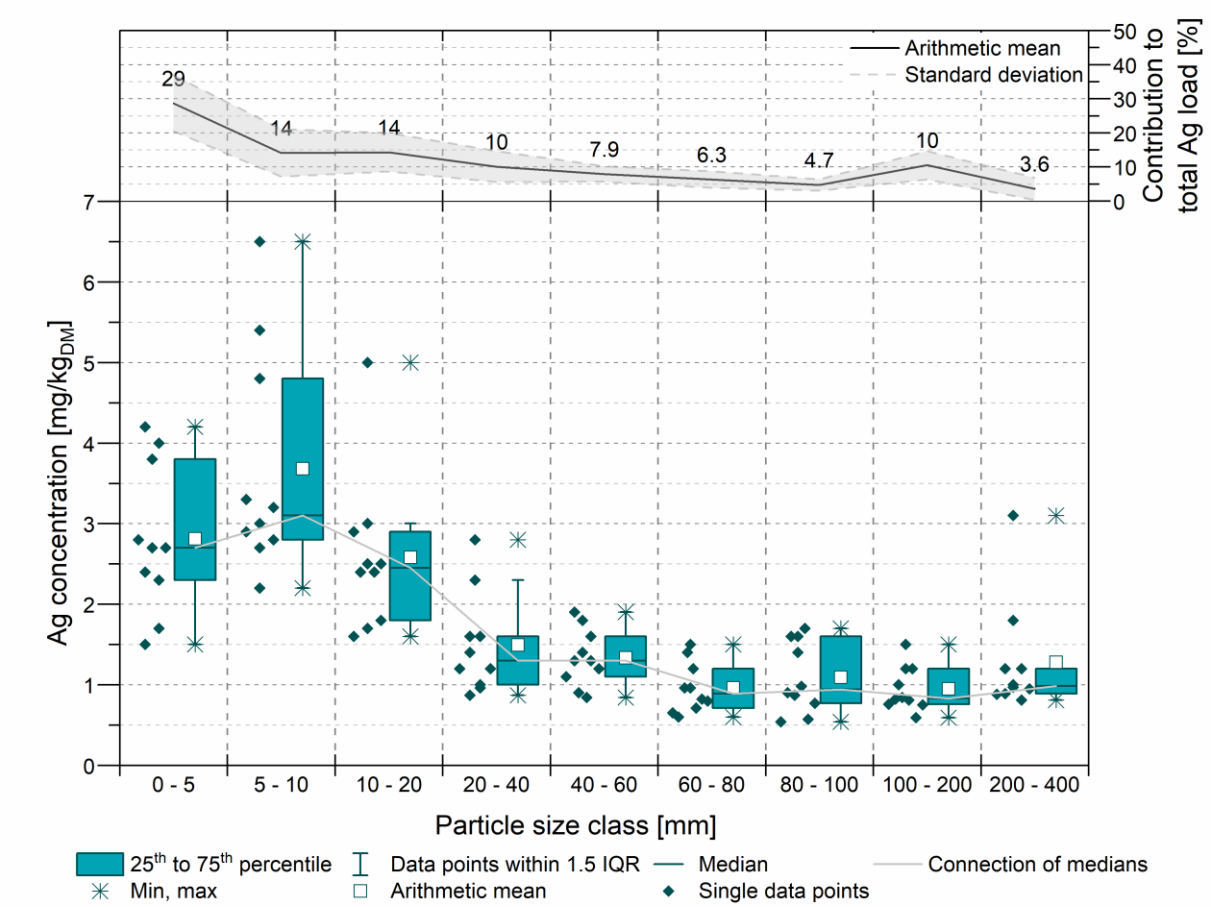

Figure B.1: Below: Box plot of silver (Ag) concentrations in different particle size classes in mg/kg referring to dry mass without hard impurities. Above: Contribution of the particle size fractions (average ± standard deviation) to the total content of Ag

Table B.1: Silver (Ag) concentrations in mg/kg referring to dry mass without hard impurities. LOQ = 0.25 mg/kg

Composite sample	0 - 5 mm	5 - 10 mm	10 - 20 mm	20 - 40 mm	40 - 60 mm	60 - 80 mm	80 - 100 mm	100 - 200 mm	200 - 400 mm
1	3.8	2.7	3.0	1.0	1.8	1.2	1.6	0.81	1.8
2	2.7	2.9	2.4	2.8	1.4	1.4	1.6	1.2	1.0
3	1.7	2.2	1.7	2.3	1.3	1.5	1.0	1.0	0.89
4	2.3	2.8	2.5	1.0	1.3	1.0	1.4	0.8	3.1
5	1.5	3.0	5.0	1.4	0.84	1.0	0.87	1.5	0.81
6	2.8	6.5	1.6	0.87	1.1	0.71	0.57	0.59	1.0
7	4.0	4.8	1.8	1.2	1.2	0.60	0.90	0.82	1.2
8	2.7	3.3	2.4	1.6	1.9	0.82	0.77	1.2	1.2
9	2.4	5.4	2.9	1.2	1.6	0.65	0.54	0.75	0.88
10	4.2	3.2	2.5	1.6	0.90	0.80	1.7	0.76	0.95

B.2. Al

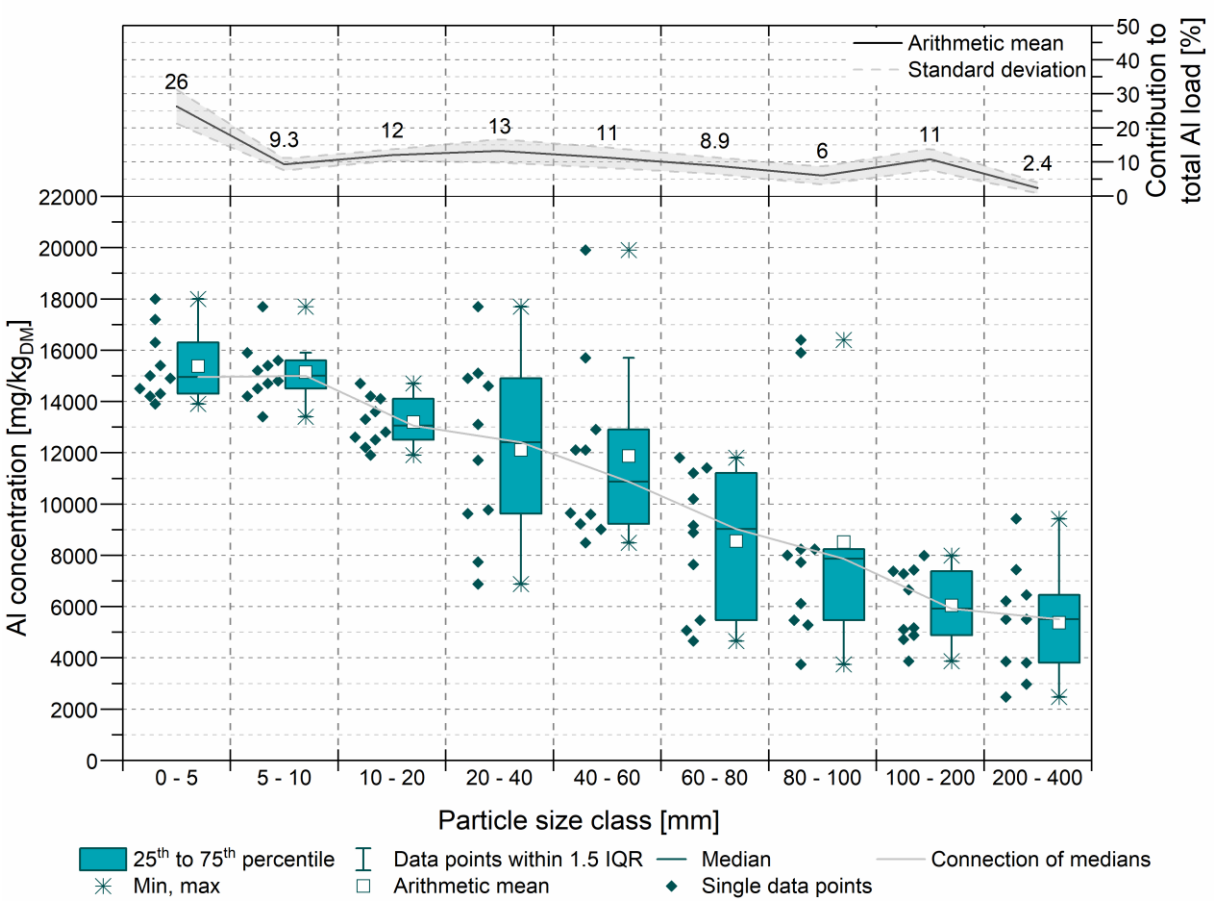

Figure B.2: Below: Box plot of aluminum (Al) concentrations in different particle size classes in mg/kg referring to dry mass without hard impurities. Above: Contribution of the grain size fractions (average ± standard deviation) to the total content of Al

Table B.2: Aluminum (Al) concentrations in mg/kg referring to dry mass without hard impurities. LOQ = 2.5 mg/kg

Composite sample	0 - 5 mm	5 - 10 mm	10 - 20 mm	20 - 40 mm	40 - 60 mm	60 - 80 mm	80 - 100 mm	100 - 200 mm	200 - 400 mm
1	14300	15400	14200	14600	19900	5460	16400	4880	6450
2	16300	15200	13600	14900	15700	9160	15900	7430	7440
3	15400	15600	12500	15100	8490	11200	5280	6650	5500
4	14200	14700	12200	7740	12100	11800	8230	7270	9420
5	14900	15900	14700	9770	9600	11400	8000	7990	3800
6	18000	14500	13300	9620	9220	8880	3740	5170	5500
7	17200	14800	12800	6870	12100	5070	8240	5100	3850
8	14500	13400	11900	17700	12900	10200	6110	4720	6220
9	15000	14200	14100	13100	9010	4650	7720	3870	2970
10	13900	17700	12600	11700	9640	7640	5460	7370	2470

B.3. As

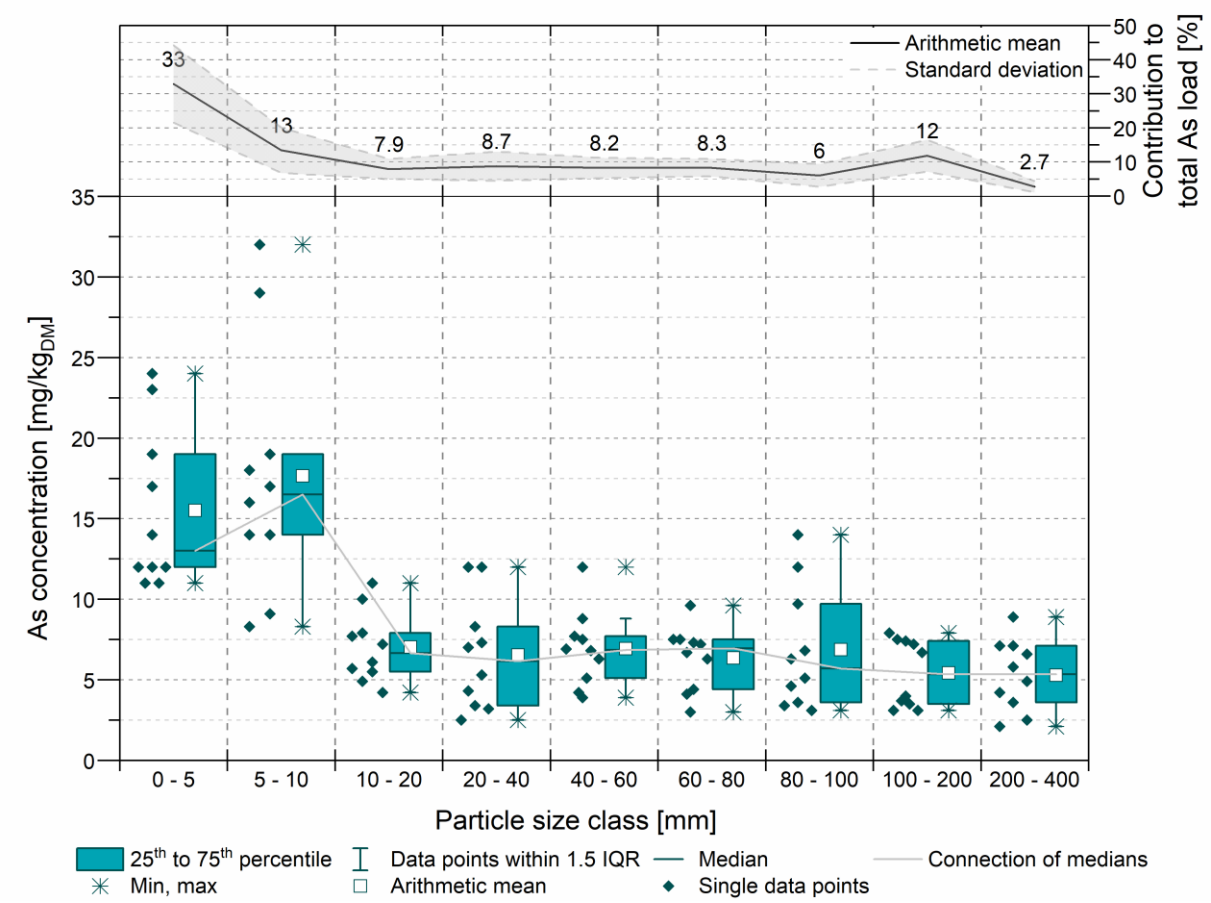

Figure B.3: Below: Box plot of arsenic (As) concentrations in different particle size classes in mg/kg referring to dry mass without hard impurities. Above: Contribution of the grain size fractions (average ± standard deviation) to the total content of As

Table B.3: Arsenic (As) concentrations in mg/kg referring to dry mass without hard impurities. LOQ = 2.5 mg/kg

Composite sample	0 - 5 mm	5 - 10 mm	10 - 20 mm	20 - 40 mm	40 - 60 mm	60 - 80 mm	80 - 100 mm	100 - 200 mm	200 - 400 mm
1	11	9.1	5.5	3.4	8.8	7.3	12	7.4	7.1
2	11	17	6.1	12	12	6.7	14	7.5	7.1
3	12	14	4.9	12	7.5	7.2	6.8	7.2	6.6
4	12	8.3	11	7.3	7.7	7.5	9.7	7.9	8.9
5	12	16	4.2	< 2.5	6.8	9.6	6.3	6.7	5.8
6	19	29	7.9	5.3	5.1	6.3	3.6	3.5	4.2
7	23	19	7.2	8.3	6.9	4.4	5.1	3.7	4.9
8	24	18	10	7.0	6.3	7.5	4.6	4.0	3.6
9	17	14	7.7	3.2	3.9	4.1	3.4	3.1	2.1
10	14	32	5.7	4.3	4.2	3.0	3.1	3.1	< 2.5

B.4. Ba

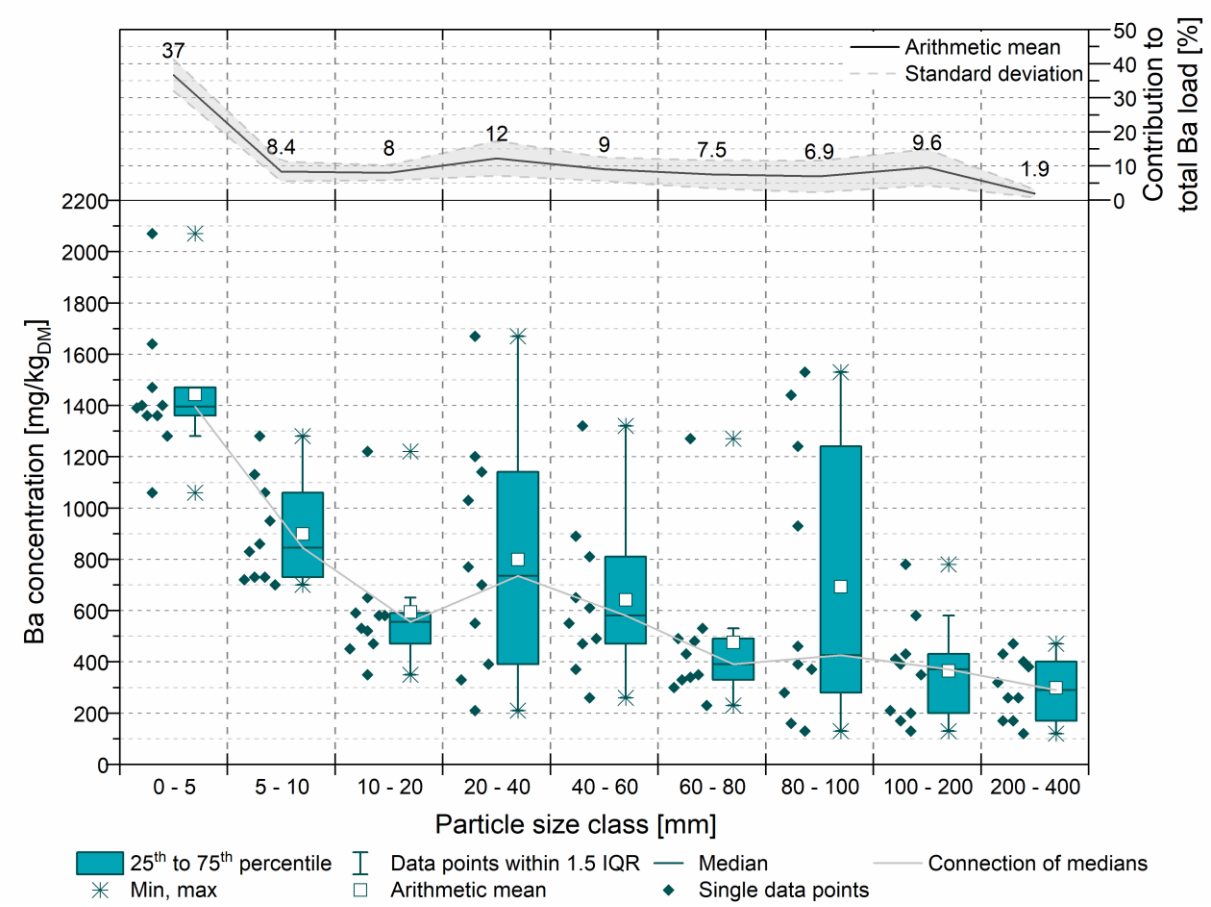

Figure B.4: Below: Box plot of barium (Ba) concentrations in different particle size classes in mg/kg referring to dry mass without hard impurities. Above: Contribution of the grain size fractions (average ± standard deviation) to the total content of Ba

Table B.4: Barium (Ba) concentrations in mg/kg referring to dry mass without hard impurities. LOQ = 0.50 mg/kg

Composite sample	0 - 5 mm	5 - 10 mm	10 - 20 mm	20 - 40 mm	40 - 60 mm	60 - 80 mm	80 - 100 mm	100 - 200 mm	200 - 400 mm
1	1360	860	520	550	610	340	1240	200	470
2	2070	1280	1220	1140	1320	480	1530	430	260
3	1360	830	530	1200	260	330	390	410	260
4	1640	730	470	700	810	430	1440	580	380
5	1470	730	650	1030	650	530	930	390	430
6	1060	1060	590	210	470	490	130	130	170
7	1400	700	580	330	890	350	280	350	170
8	1280	1130	450	390	370	300	460	170	400
9	1390	720	580	1670	550	1270	160	210	120
10	1400	950	350	770	490	230	370	780	320

B.5. Ca

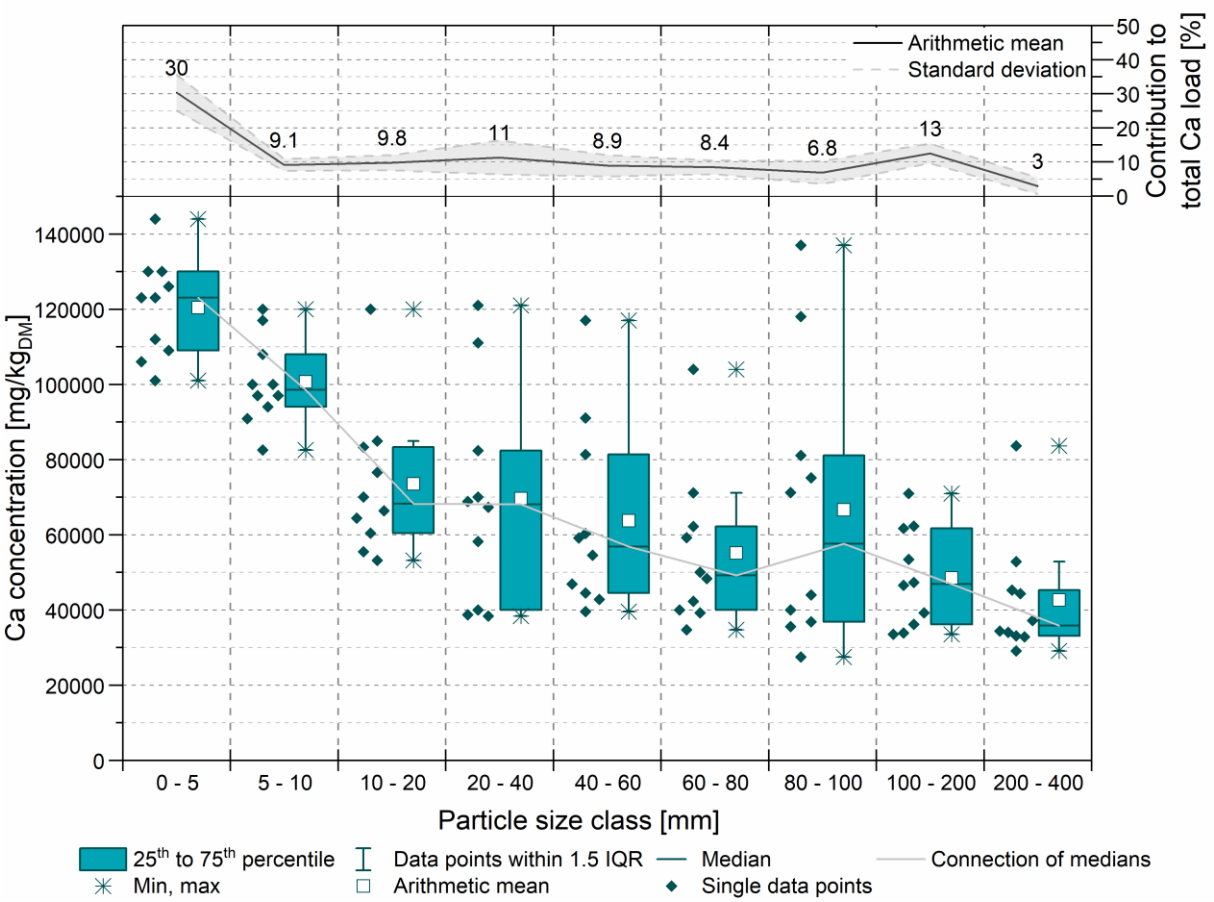

Figure B.5: Below: Box plot of calcium (Ca) concentrations in different particle size classes in mg/kg referring to dry mass without hard impurities. Above: Contribution of the grain size fractions (average ± standard deviation) to the total content of Ca.

Table B.5: Calcium (Ca) concentrations in mg/kg referring to dry mass without hard impurities. LOQ = 50 mg/kg

Composite sample	0 - 5 mm	5 - 10 mm	10 - 20 mm	20 - 40 mm	40 - 60 mm	60 - 80 mm	80 - 100 mm	100 - 200 mm	200 - 400 mm
1	130000	108000	84900	82400	54500	39200	137000	47300	33100
2	123000	100000	76600	111000	117000	34700	118000	36200	34000
3	101000	94000	53200	121000	39600	42300	36800	33900	32800
4	112000	82500	70000	38400	44500	40000	35600	39200	83600
5	144000	97000	83300	67300	46900	62200	44000	46500	34400
6	123000	97000	60400	40000	42800	50000	27500	33500	29100
7	106000	90900	64400	68800	81300	71100	75100	62300	52800
8	130000	120000	120000	70000	91000	104000	81100	71000	44300
9	126000	100000	66400	58200	59100	59200	71200	61700	45300
10	109000	117000	55500	38700	60300	48300	40000	53400	37200

B.6. Cd

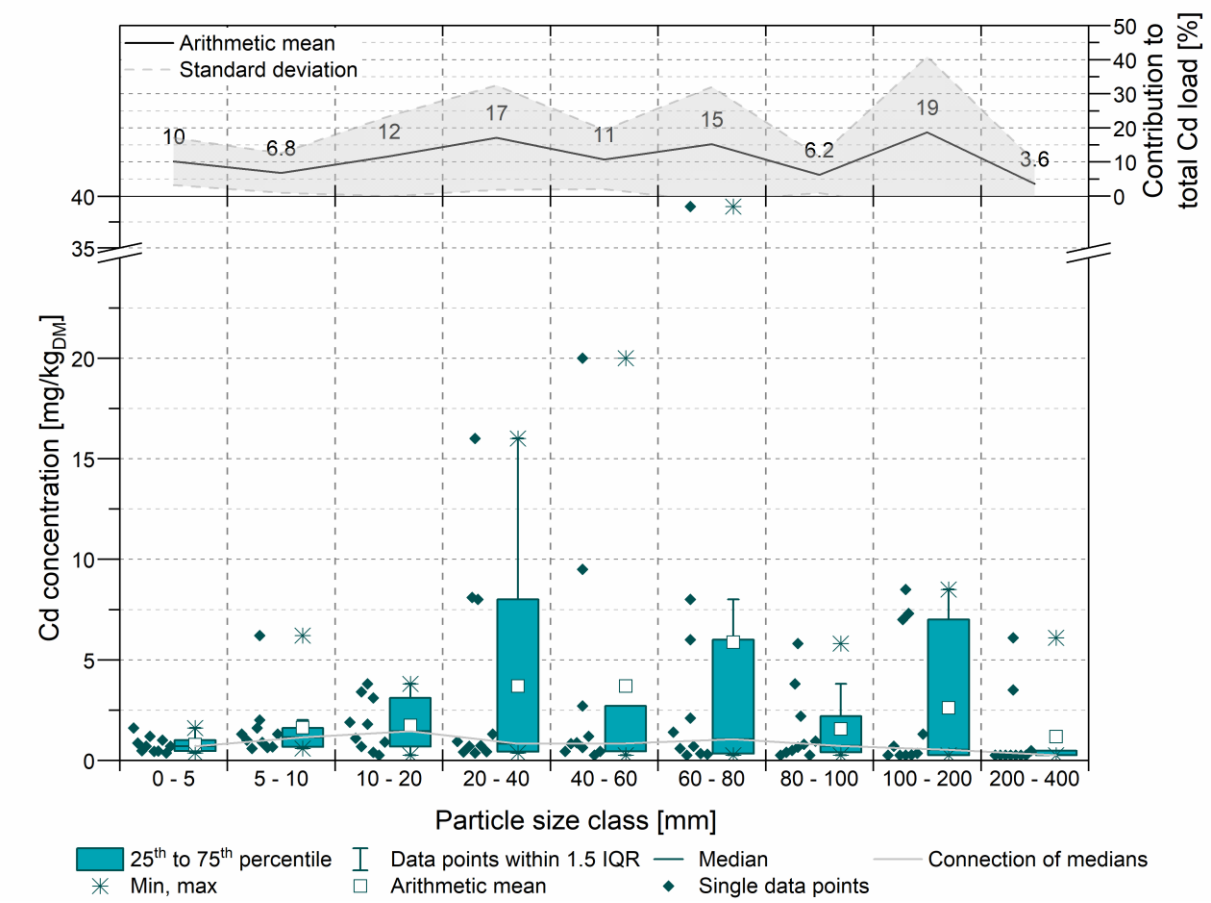

Figure B.6: Below: Box plot of cadmium (Cd) concentrations in different particle size classes in mg/kg referring to dry mass without hard impurities. Above: Contribution of the grain size fractions (average ± standard deviation) to the total content of Cd

Table B.6: Cadmium (Cd) concentrations in mg/kg referring to dry mass without hard impurities. LOQ = 0.25 mg/kg

Composite sample	0 - 5 mm	5 - 10 mm	10 - 20 mm	20 - 40 mm	40 - 60 mm	60 - 80 mm	80 - 100 mm	100 - 200 mm	200 - 400 mm
1	0.44	0.89	3.8	0.36	20	39	0.65	7.3	< 0.25
2	1.2	1.6	1.8	0.70	0.64	0.70	0.50	< 0.25	< 0.25
3	0.46	0.63	0.68	0.73	0.88	< 0.25	0.79	< 0.25	< 0.25
4	0.70	0.59	3.4	0.41	1.2	0.34	0.40	0.27	3.5
5	1.0	0.67	0.40	0.43	0.82	0.59	2.2	7.0	< 0.25
6	0.47	1.0	1.1	0.94	< 0.25	0.31	< 0.25	0.70	< 0.25
7	0.36	1.3	0.25	8.0	2.7	2.1	5.8	8.5	6.1
8	0.86	1.3	3.1	16	9.5	8.0	< 0.25	0.35	< 0.25
9	0.70	2.0	1.9	8.1	0.44	1.4	3.8	< 0.25	0.47
10	1.6	6.2	0.91	1.3	0.45	6.0	0.96	1.3	< 0.25

B.7. Cl

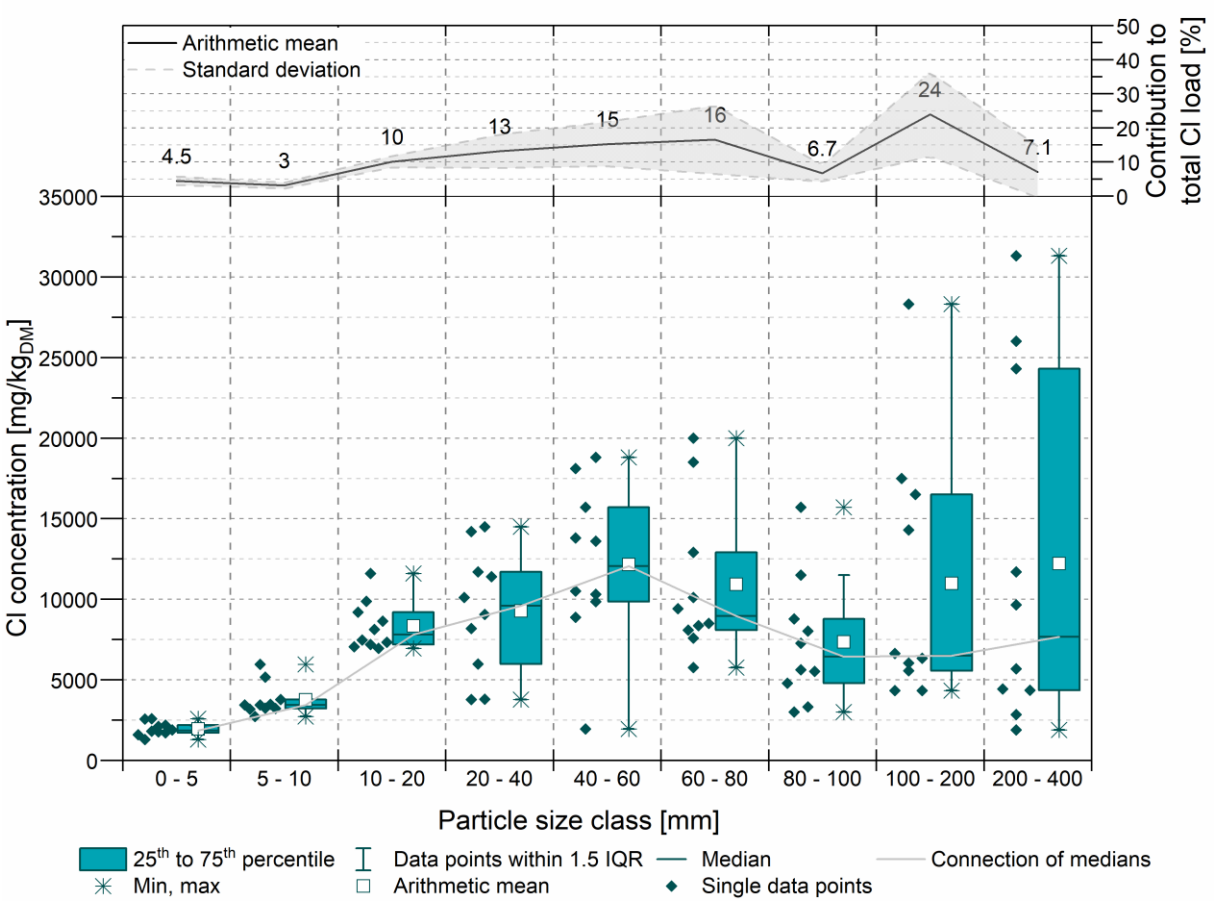

Figure B.7: Below: Box plot of chlorine (Cl) concentrations in different particle size classes in mg/kg referring to dry mass without hard impurities. Above: Contribution of the particle size fractions (average ± standard deviation) to the total content of Cl

Table B.7: Chlorine (Cl) concentrations in mg/kg referring to dry mass without hard impurities. LOQ = 100 mg/kg

Composite sample	0 - 5 mm	5 - 10 mm	10 - 20 mm	20 - 40 mm	40 - 60 mm	60 - 80 mm	80 - 100 mm	100 - 200 mm	200 - 400 mm
1	1760	3230	7190	11700	13600	18500	3310	6030	2840
2	2110	3440	8120	3790	1950	20000	2990	6640	5670
3	1800	3480	7470	3780	13800	7580	5610	5560	4420
4	1710	2720	6940	5970	10300	10100	8020	4330	26000
5	2580	5170	7050	10100	15700	8350	8770	6340	24300
6	2190	3220	9860	14500	18800	12900	11500	4320	1890
7	2560	5960	11600	14200	18100	8080	15700	28300	11700
8	1300	3180	7320	9060	9850	8500	4790	16500	9650
9	1890	3780	8640	8180	10500	9410	7270	14300	4340
10	1580	3440	9200	11400	8880	5750	5520	17500	31300

B.8. Co

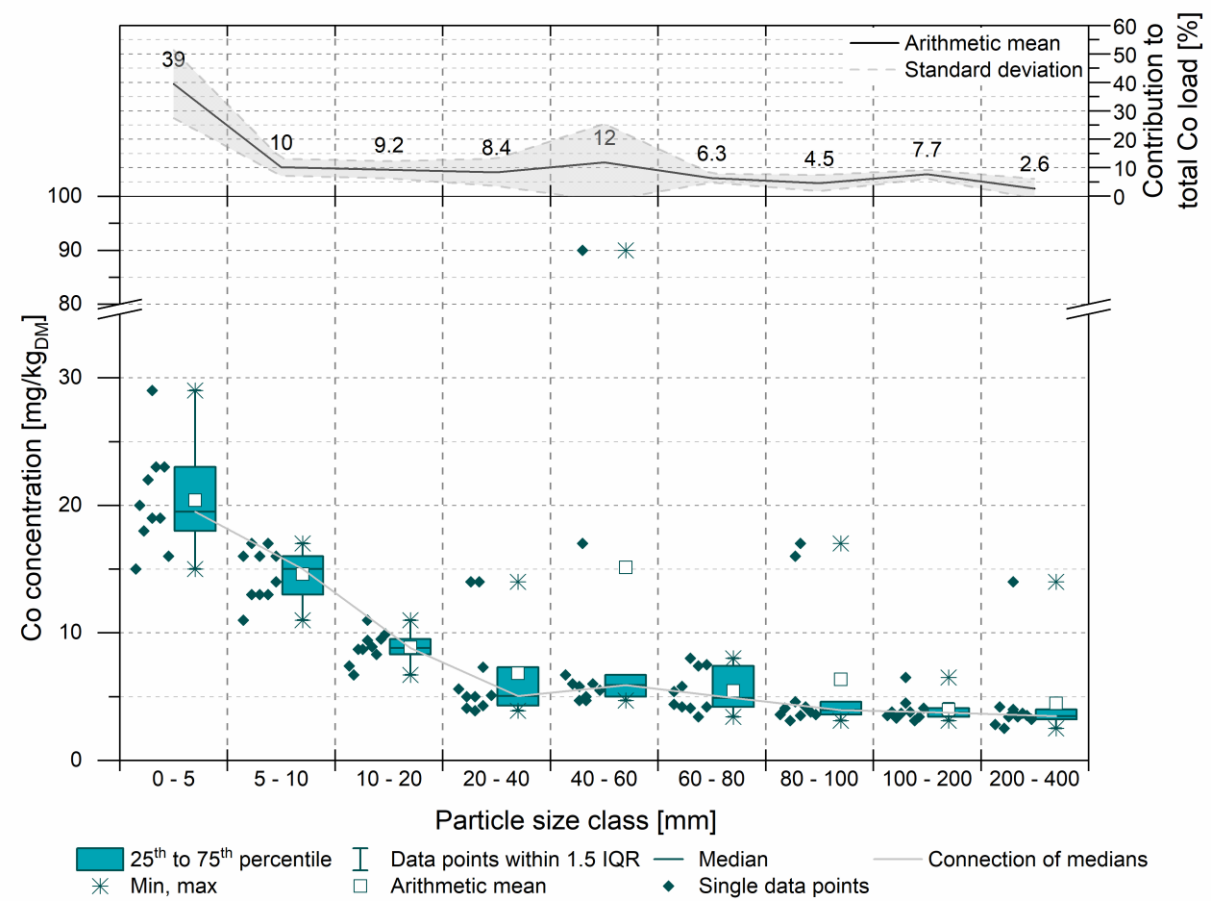

Figure B.8: Below: Box plot of cobalt (Co) concentrations in different particle size classes in mg/kg referring to dry mass without hard impurities. Above: Contribution of the particle size fractions (average ± standard deviation) to the total content of Co

Table B.8: Cobalt (Co) concentrations in mg/kg referring to dry mass without hard impurities. LOQ = 0.25 mg/kg

Composite sample	0 - 5 mm	5 - 10 mm	10 - 20 mm	20 - 40 mm	40 - 60 mm	60 - 80 mm	80 - 100 mm	100 - 200 mm	200 - 400 mm
1	19	16	9.4	5.0	90	8.0	17	6.5	4.0
2	18	13	8.7	14	17	5.8	16	4.5	3.4
3	19	13	8.9	14	5.0	4.1	3.5	3.7	3.4
4	15	13	8.7	3.9	5.8	4.2	4.6	3.8	14
5	16	11	11	4.1	4.7	7.4	4.2	3.3	2.5
6	23	17	8.3	5.0	6.0	5.4	3.1	3.1	3.7
7	22	17	6.7	4.3	6.0	3.4	3.8	3.8	4.2
8	29	16	9.5	7.3	5.5	7.5	4.1	3.4	3.5
9	23	14	7.4	5.6	6.7	4.4	3.6	3.5	2.8
10	20	16	9.9	5.1	4.7	4.2	3.6	4.1	3.2

B.9. Cr

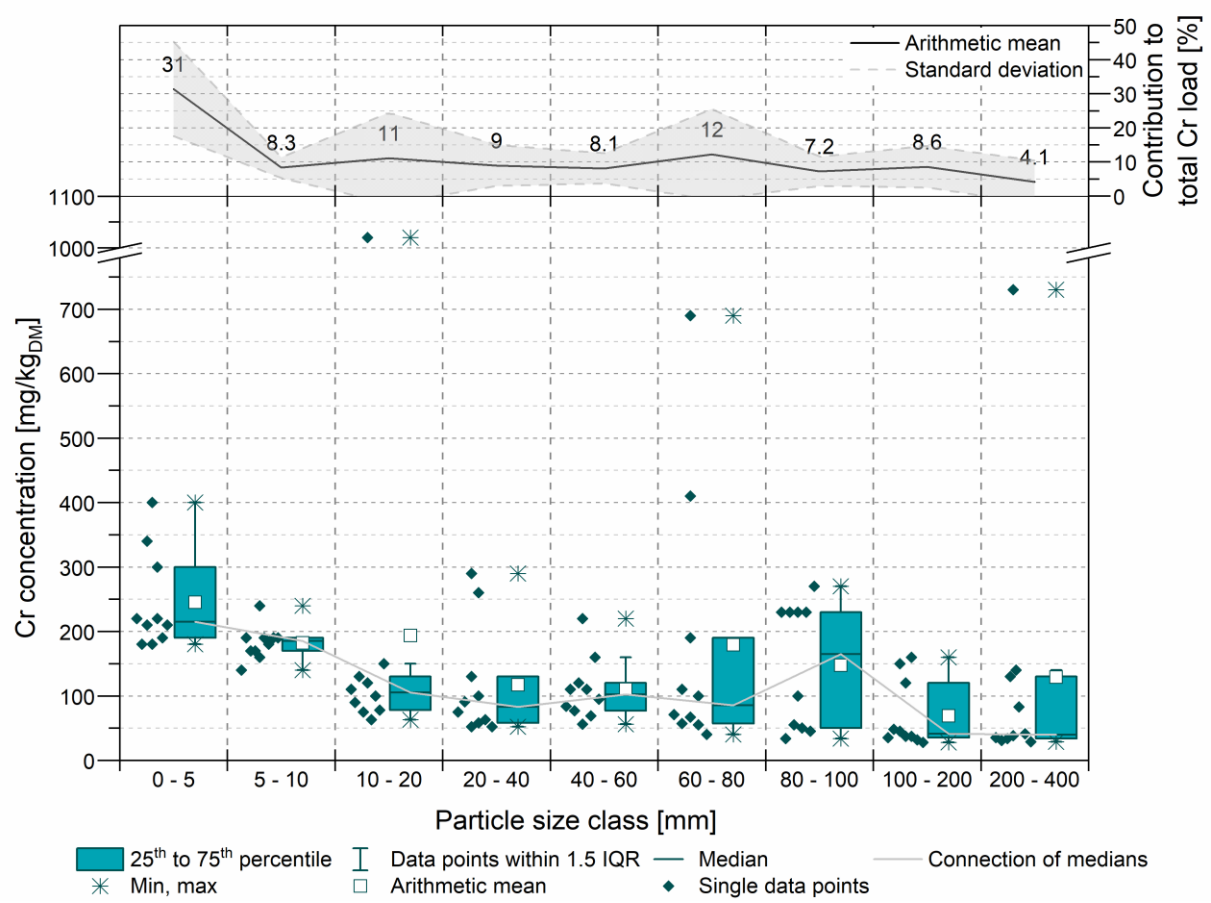

Figure B.9: Below: Box plot of chromium (Cr) concentrations in different particle size classes in mg/kg referring to dry mass without hard impurities. Above: Contribution of the grain size fractions (average ± standard deviation) to the total content of Cr

Table B.9: Chromium (Cr) concentrations in mg/kg referring to dry mass without hard impurities. LOQ = 0.50 mg/kg

Composite sample	0 - 5 mm	5 - 10 mm	10 - 20 mm	20 - 40 mm	40 - 60 mm	60 - 80 mm	80 - 100 mm	100 - 200 mm	200 - 400 mm
1	180	160	120	58	56	690	230	37	38
2	180	170	130	260	220	67	230	45	34
3	220	190	100	290	110	410	230	37	730
4	210	170	110	52	120	190	230	120	140
5	210	240	1020	100	77	110	50	48	83
6	220	180	63	63	69	57	55	32	31
7	300	190	75	91	160	55	45	150	41
8	400	190	150	130	84	100	270	160	35
9	340	140	78	52	95	71	100	35	29
10	190	190	90	75	110	40	34	28	130

B.10. Cu

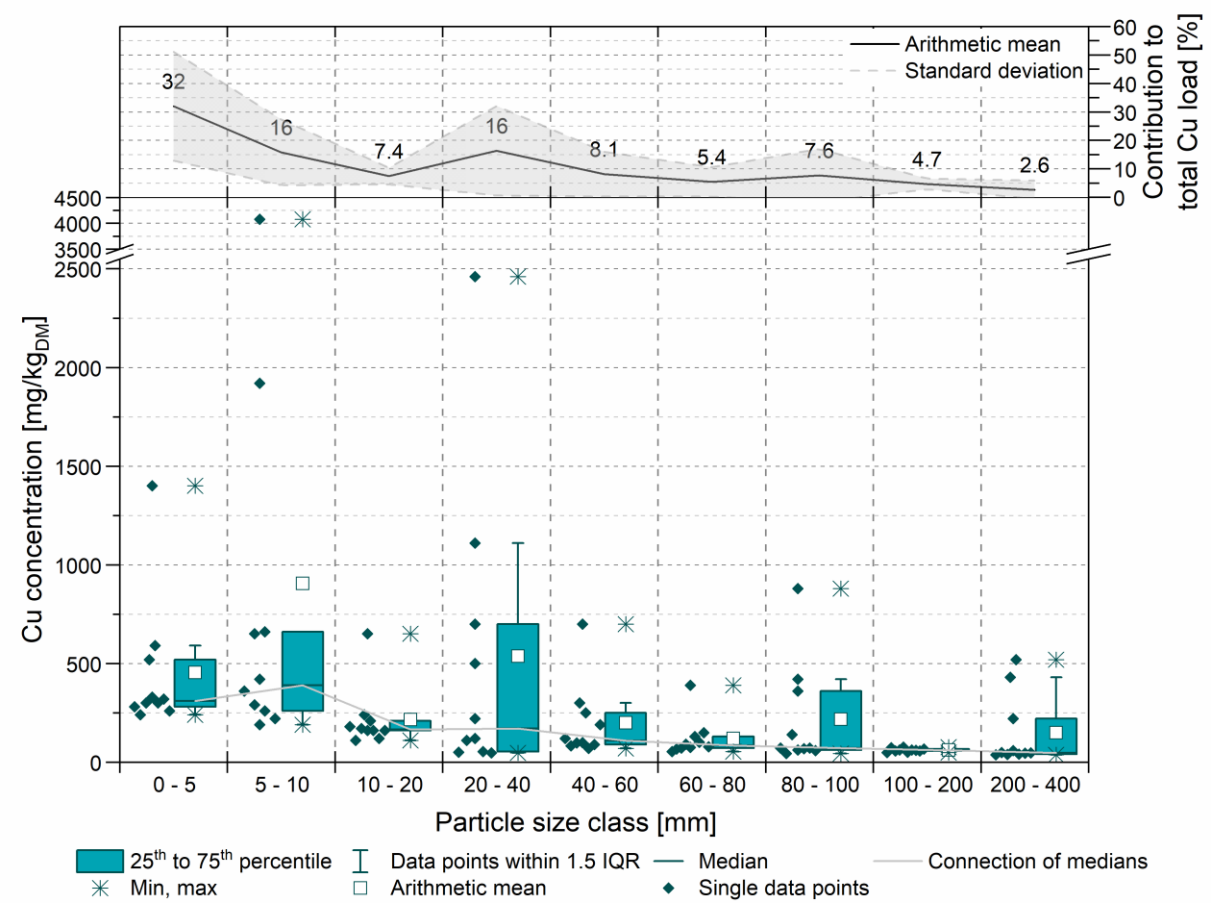

Figure B.10: Below: Box plot of copper (Cu) concentrations in different particle size classes in mg/kg referring to dry mass without hard impurities. Above: Contribution of the grain size fractions (average ± standard deviation) to the total content of Cu

Table B.10: Copper (Cu) concentrations in mg/kg referring to dry mass without hard impurities. LOQ = 0.50 mg/kg

Composite sample	0 - 5 mm	5 - 10 mm	10 - 20 mm	20 - 40 mm	40 - 60 mm	60 - 80 mm	80 - 100 mm	100 - 200 mm	200 - 400 mm
1	330	260	160	120	99	74	360	51	520
2	300	660	210	500	250	91	880	76	59
3	300	1920	170	1110	98	130	61	61	39
4	240	290	240	700	700	71	140	61	220
5	590	650	160	110	70	100	68	60	41
6	520	220	110	54	82	390	44	56	430
7	320	190	120	51	89	67	420	56	48
8	1400	420	650	220	120	150	72	73	46
9	280	360	180	47	300	54	72	67	37
10	260	4080	160	2460	190	78	59	49	47

B.11. Fe

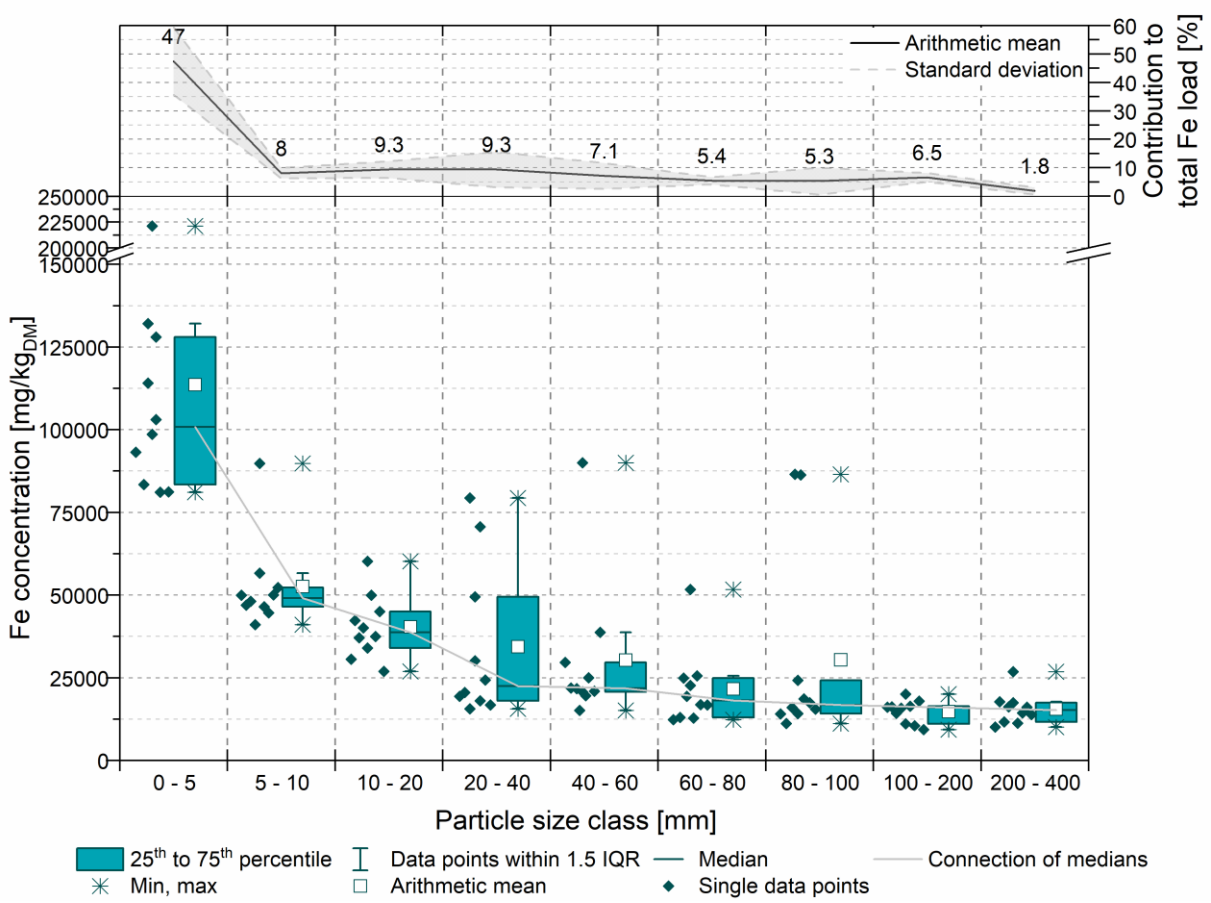

Figure B.11: Below: Box plot of iron (Fe) concentrations in different particle size classes in mg/kg referring to dry mass without hard impurities. Above: Contribution of the grain size fractions (average ± standard deviation) to the total content of Fe

Table B.11: Iron (Fe) concentrations in mg/kg referring to dry mass without hard impurities. LOQ = 2.5 mg/kg

Composite sample	0 - 5 mm	5 - 10 mm	10 - 20 mm	20 - 40 mm	40 - 60 mm	60 - 80 mm	80 - 100 mm	100 - 200 mm	200 - 400 mm
1	98600	56600	49900	30100	20700	12800	86300	11000	17400
2	83400	41000	40000	70600	90000	19300	86500	20000	16200
3	81100	46400	34000	79300	21700	16800	14100	15800	11200
4	93200	48100	45000	20500	25000	22600	16000	16300	26800
5	103000	44600	42300	24300	21900	24900	18600	14200	11600
6	128000	46900	37000	18000	20900	25500	11100	10400	14300
7	132000	50000	37400	15600	29600	13000	17400	16200	17700
8	221000	89800	60200	49400	38700	51700	24200	17900	16100
9	114000	49900	30600	16700	19500	16700	14000	16100	10100
10	81200	52200	26900	19300	15100	12300	15500	9260	13800

B.12. Hg

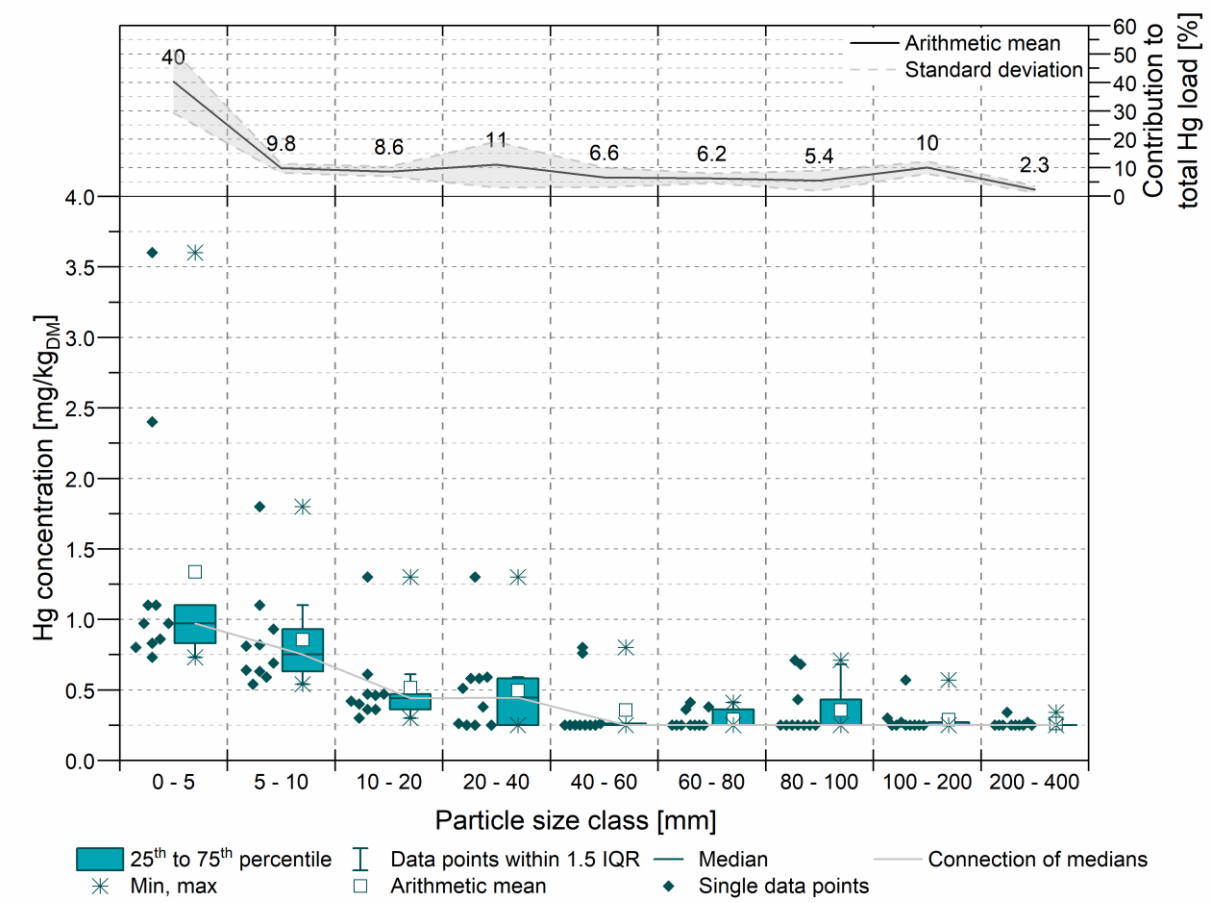

Figure B.12: Below: Box plot of mercury (Hg) concentrations in different particle size classes in mg/kg referring to dry mass without hard impurities. Above: Contribution of the particle size fractions (average ± standard deviation) to the total content of Hg.

Table B.12: Mercury (Hg) concentrations in mg/kg referring to dry mass without hard impurities. LOQ = 0.25 mg/kg

Composite sample	0 - 5 mm	5 - 10 mm	10 - 20 mm	20 - 40 mm	40 - 60 mm	60 - 80 mm	80 - 100 mm	100 - 200 mm	200 - 400 mm
1	0.73	0.59	0.36	< 0.25	0.25	< 0.25	0.68	< 0.25	< 0.25
2	0.83	0.82	0.47	0.58	0.76	0.36	0.71	0.27	< 0.25
3	0.97	0.54	0.40	0.58	< 0.25	< 0.25	< 0.25	< 0.25	< 0.25
4	0.86	0.81	0.30	1.3	< 0.25	< 0.25	< 0.25	< 0.25	0.34
5	0.80	0.63	0.46	0.25	< 0.25	< 0.25	< 0.25	< 0.25	< 0.25
6	2.4	1.1	0.61	0.38	< 0.25	< 0.25	< 0.25	< 0.25	< 0.25
7	3.6	1.8	1.3	0.59	0.80	0.41	0.43	0.57	0.27
8	0.97	0.93	0.42	0.26	< 0.25	< 0.25	< 0.25	< 0.25	< 0.25
9	1.1	0.64	0.36	0.51	0.26	< 0.25	< 0.25	0.30	< 0.25
10	1.1	0.69	0.47	< 0.25	< 0.25	0.38	< 0.25	< 0.25	< 0.25

B.13. K

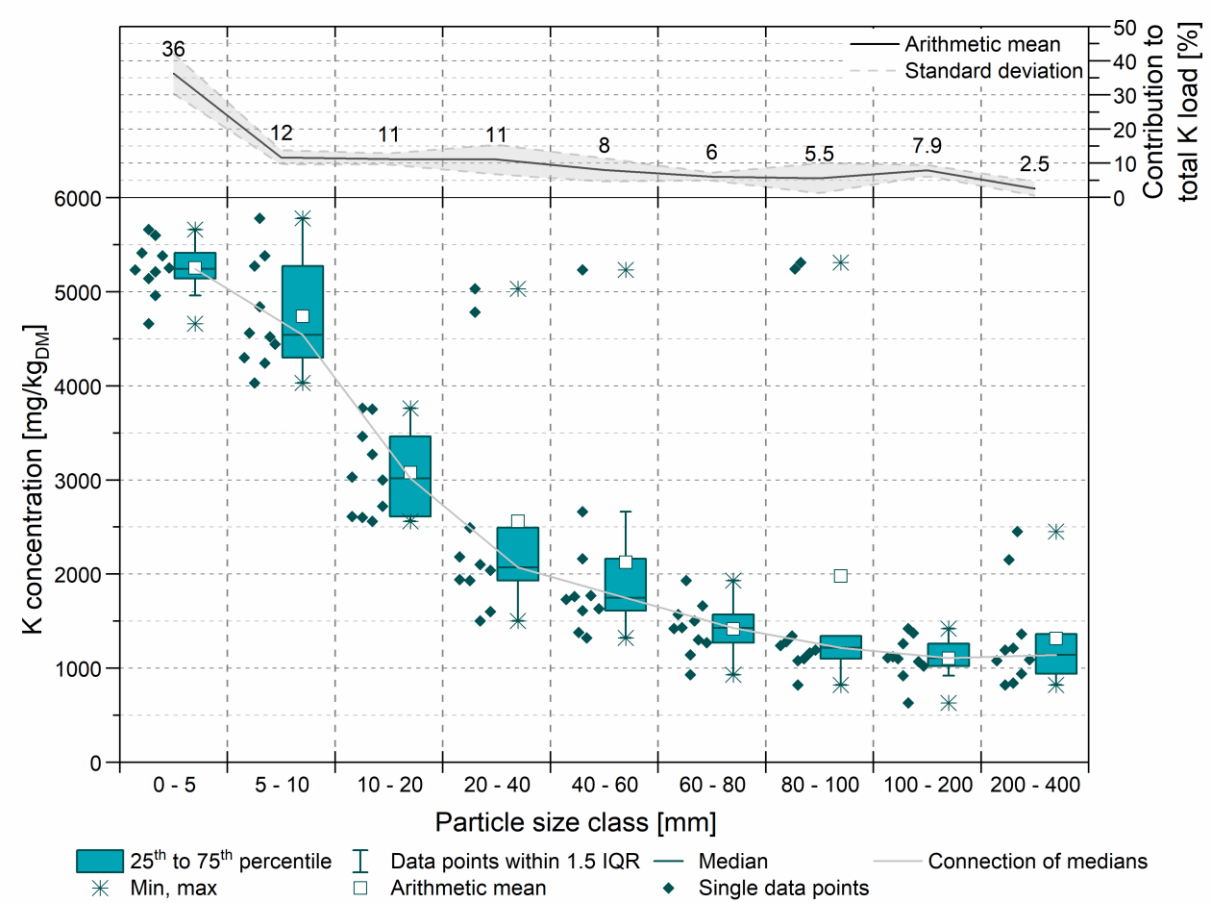

Figure B.13: Below: Box plot of potassium (K) concentrations in different particle size classes in mg/kg referring to dry mass without hard impurities. Above: Contribution of the grain size fractions (average ± standard deviation) to the total content of K

Table B.13: Potassium (K) concentrations in mg/kg referring to dry mass without hard impurities. LOQ = 2.5 mg/kg

Composite sample	0 - 5 mm	5 - 10 mm	10 - 20 mm	20 - 40 mm	40 - 60 mm	60 - 80 mm	80 - 100 mm	100 - 200 mm	200 - 400 mm
1	4960	4240	3270	2100	1320	930	5310	630	1210
2	5600	5380	3750	4780	5230	1500	5240	1420	1190
3	5210	4840	3460	5030	1610	1140	1080	1260	840
4	5140	4030	2560	1500	1760	1430	1340	1370	2450
5	5380	4440	3000	1930	1770	1930	1100	1100	820
6	5410	4560	2600	1600	1730	1660	820	1070	1360
7	5250	4300	2720	1940	2660	1300	1280	1120	940
8	4660	4520	2610	2490	1630	1570	1160	1020	2150
9	5660	5270	3760	2040	2160	1420	1240	1110	1080
10	5230	5780	3030	2180	1380	1270	1190	920	1090

B.14. Li

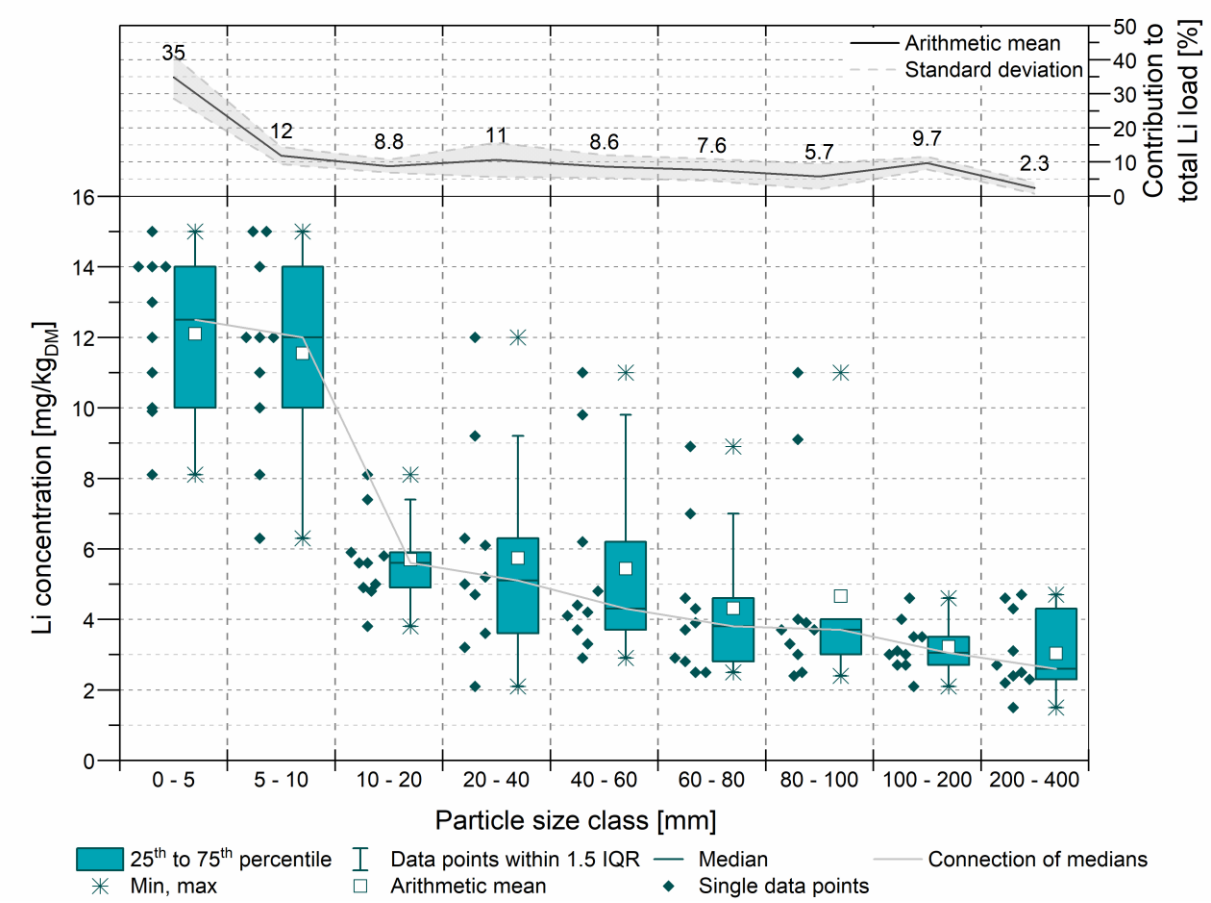

Figure B.14: Below: Box plot of lithium (Li) concentrations in different particle size classes in mg/kg referring to dry mass without hard impurities. Above: Contribution of the grain size fractions (average ± standard deviation) to the total content of Li

Table B.14: Lithium (Li) concentrations in mg/kg referring to dry mass without hard impurities. LOQ = 0.50 mg/kg

Composite sample	0 - 5 mm	5 - 10 mm	10 - 20 mm	20 - 40 mm	40 - 60 mm	60 - 80 mm	80 - 100 mm	100 - 200 mm	200 - 400 mm
1	9.9	8.1	5.6	3.6	4.2	2.5	11	2.7	3.1
2	14	12	5.6	12	9.8	2.8	9.1	3.0	2.4
3	10	12	4.8	9.2	2.9	2.5	2.5	2.7	2.2
4	8.1	10	5.0	3.2	4.4	2.9	3.0	3.1	4.3
5	11	6.3	3.8	2.1	3.3	3.9	2.4	2.1	1.5
6	14	15	5.9	6.1	4.8	4.3	3.3	4.6	4.6
7	14	11	5.8	4.7	6.2	3.7	3.9	4.0	2.5
8	13	14	7.4	6.3	4.1	7.0	3.7	3.5	4.7
9	15	15	8.1	5.2	11	4.6	4.0	3.0	2.7
10	12	12	4.9	5.0	3.7	8.9	3.7	3.5	2.3

B.15. Mg

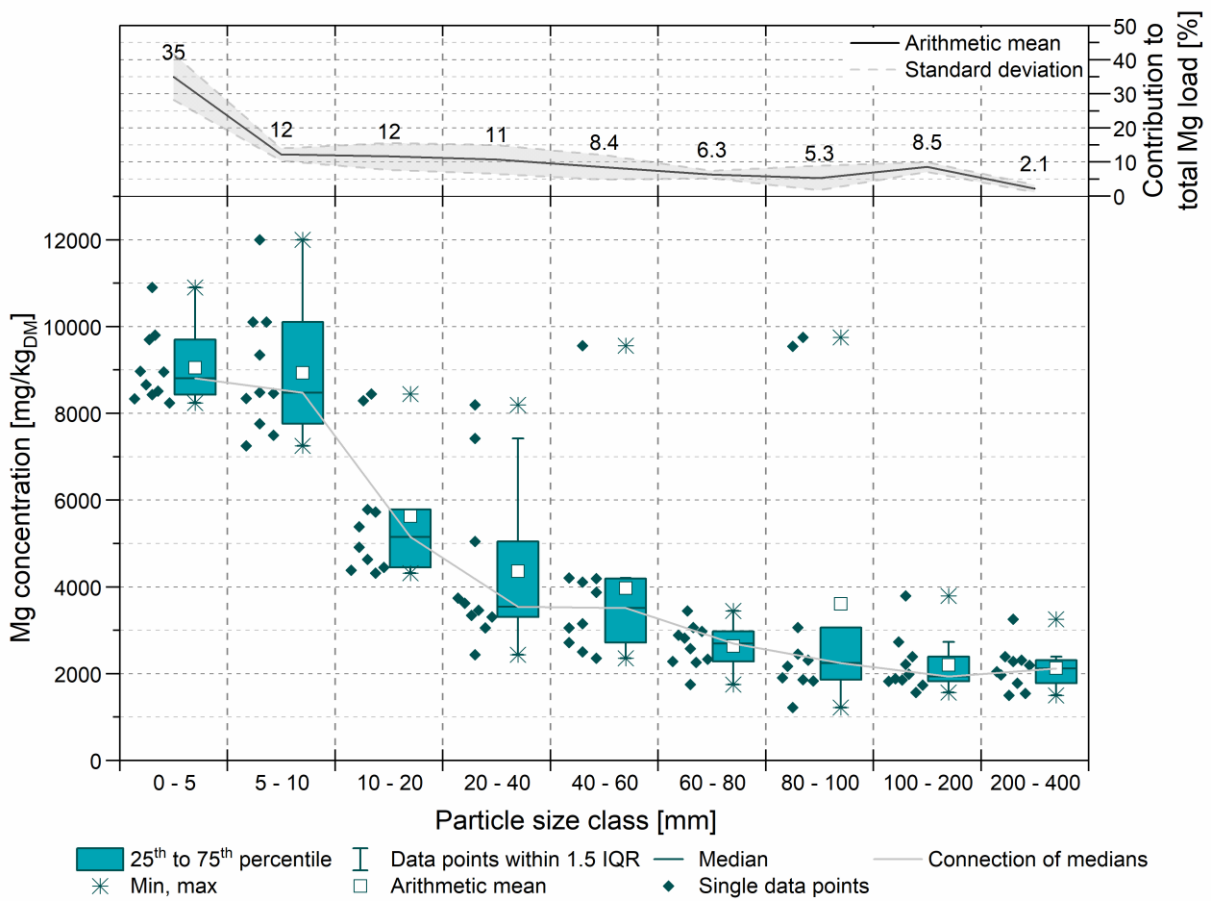

Figure B.15: Below: Box plot of magnesium (Mg) concentrations in different particle size classes in mg/kg referring to dry mass without hard impurities. Above: Contribution of the grain size fractions (average ± standard deviation) to the total content of Mg

Table B.15: Magnesium (Mg) concentrations in mg/kg referring to dry mass without hard impurities. LOQ = 0.50 mg/kg

Composite sample	0 - 5 mm	5 - 10 mm	10 - 20 mm	20 - 40 mm	40 - 60 mm	60 - 80 mm	80 - 100 mm	100 - 200 mm	200 - 400 mm
1	10900	12000	8440	5040	3150	2570	9750	3790	2280
2	9800	10100	5780	7420	9560	2820	9540	2210	1780
3	8430	9340	4630	8190	2500	2260	1860	1980	1500
4	8660	7760	8290	3460	3050	2880	3060	2730	3250
5	8510	7250	4910	3340	4110	3060	2450	2390	1540
6	9700	8480	4310	3050	2710	3440	1220	1850	2390
7	8970	8340	4380	3620	4200	1750	2170	1560	1970
8	8950	8460	5380	3300	3870	2970	2310	1880	2310
9	8330	7490	4450	2430	2350	2280	1830	1730	2040
10	8240	10100	5720	3740	4190	2330	1900	1820	2190

B.16. Mn

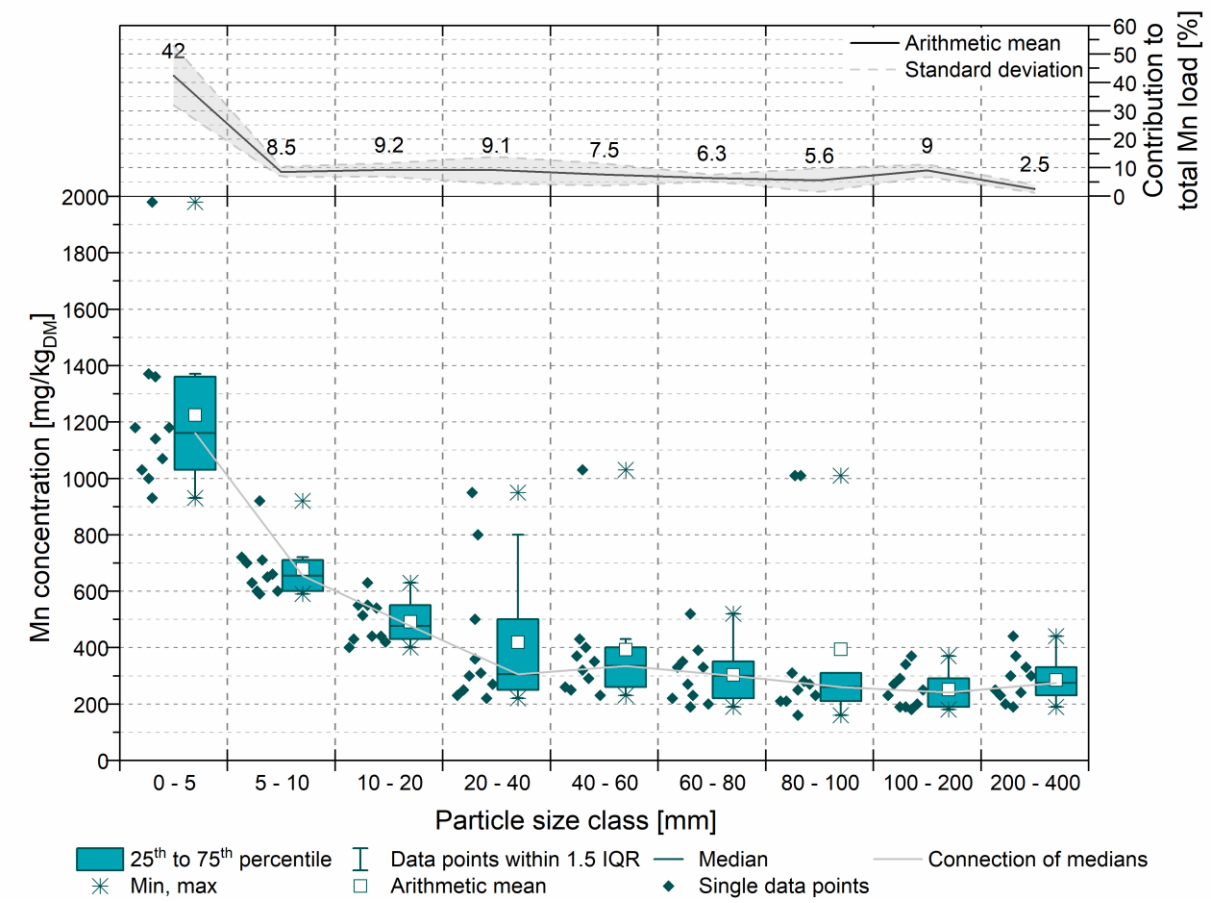

Figure B.16: Below: Box plot of manganese (Mn) concentrations in different particle size classes in mg/kg referring to dry mass without hard impurities. Above: Contribution of the grain size fractions (average ± standard deviation) to the total content of Mn

Table B.16: Manganese (Mn) concentrations in mg/kg referring to dry mass without hard impurities. LOQ = 0.50 mg/kg

Composite sample	0 - 5 mm	5 - 10 mm	10 - 20 mm	20 - 40 mm	40 - 60 mm	60 - 80 mm	80 - 100 mm	100 - 200 mm	200 - 400 mm
1	1140	710	550	360	320	230	1010	190	370
2	1000	600	514	800	1030	270	1010	340	300
3	1070	650	440	950	400	390	250	290	240
4	1030	590	550	300	370	350	310	370	440
5	1180	630	540	310	290	330	280	270	200
6	1360	660	430	250	250	330	160	200	330
7	1370	700	440	220	350	190	210	190	230
8	1980	920	630	500	430	520	270	230	300
9	1180	600	400	230	260	200	210	250	190
10	930	720	420	270	230	220	230	180	250

B.17. Mo

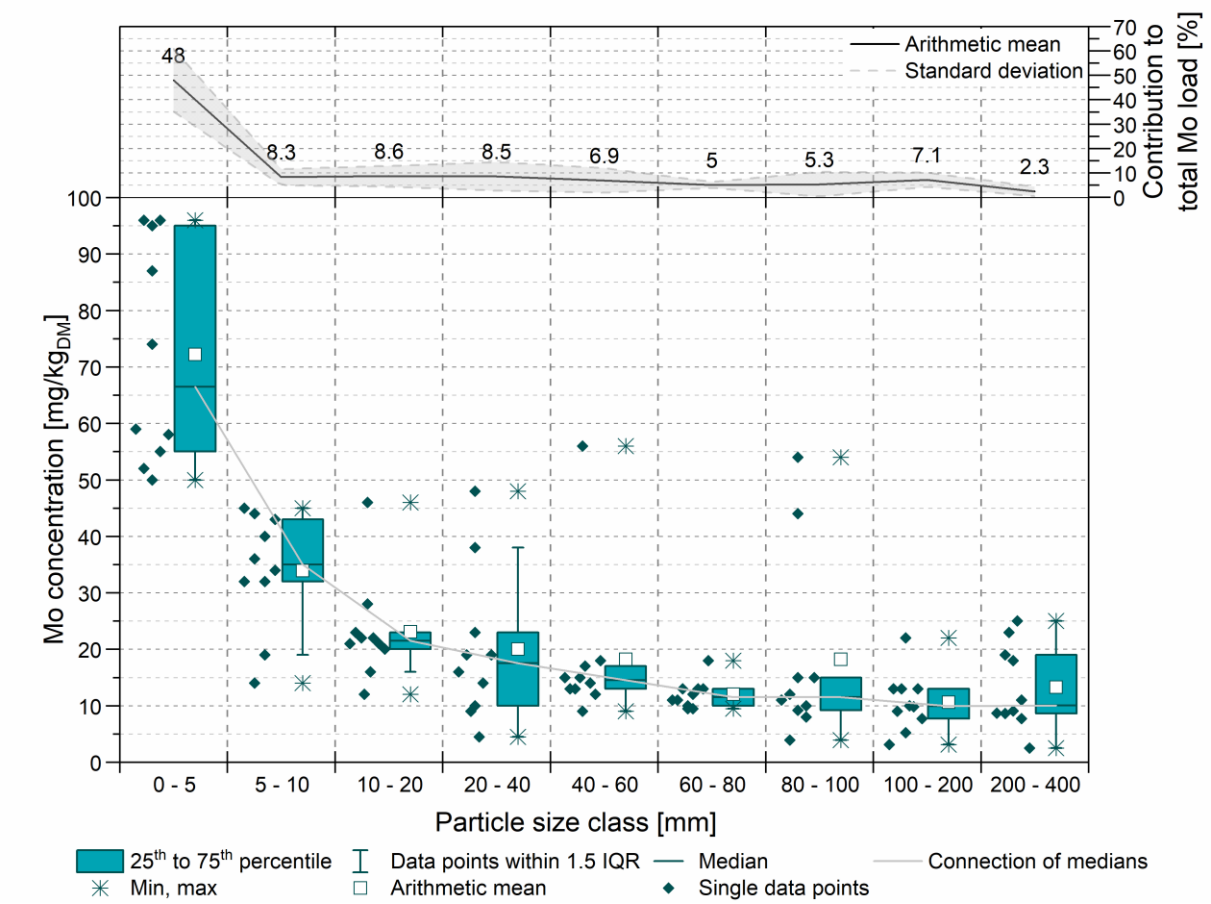

Figure B.17: Below: Box plot of molybdenum (Mo) concentrations in different particle size classes in mg/kg referring to dry mass without hard impurities. Above: Contribution of the grain size fractions (average ± standard deviation) to the total content of Mo

Table B.17: Molybdenum (Mo) concentrations in mg/kg referring to dry mass without hard impurities. LOQ = 0.25 mg/kg

Composite sample	0 - 5 mm	5 - 10 mm	10 - 20 mm	20 - 40 mm	40 - 60 mm	60 - 80 mm	80 - 100 mm	100 - 200 mm	200 - 400 mm
1	50	40	28	4.5	9.0	12	44	5.2	9.1
2	52	32	22	38	56	10	54	10	8.6
3	55	36	16	48	17	13	9.2	9.0	7.7
4	59	44	22	10	15	13	15	13	25
5	58	34	46	19	14	13	12	9.8	8.7
6	95	43	23	14	13	11	3.9	3.1	2.5
7	96	45	21	16	12	18	8.0	22	23
8	96	32	21	23	13	9.5	10	13	18
9	87	19	12	9.0	18	11	11	13	19
10	74	14	20	19	15	9.5	15	7.7	11

B.18. Na

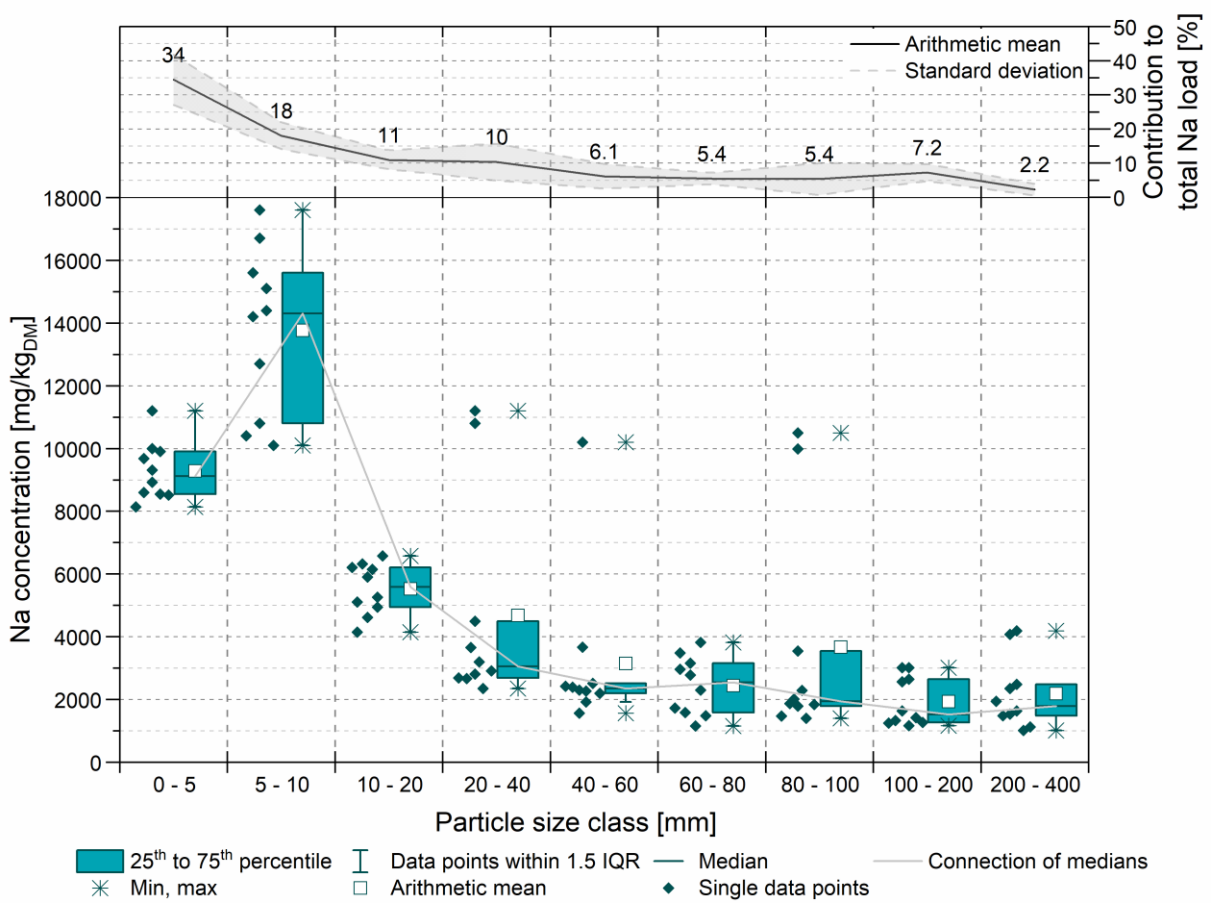

Figure B.18: Below: Box plot of sodium (Na) concentrations in different particle size classes in mg/kg referring to dry mass without hard impurities. Above: Contribution of the grain size fractions (average ± standard deviation) to the total content of Na

Table B.18: Sodium (Na) concentrations in mg/kg referring to dry mass without hard impurities. LOQ = 5 mg/kg

Composite sample	0 - 5 mm	5 - 10 mm	10 - 20 mm	20 - 40 mm	40 - 60 mm	60 - 80 mm	80 - 100 mm	100 - 200 mm	200 - 400 mm
1	8920	10800	6150	2810	1920	1150	9990	1160	1630
2	10000	16700	6320	10800	10200	3150	10500	2640	2480
3	9310	17600	6580	11200	2270	2780	2290	3010	1530
4	8600	10400	6210	2660	2300	3480	3540	2560	4190
5	8550	14400	5900	2350	2510	2960	1790	1630	1010
6	11200	15100	5110	2690	2390	3820	1870	1420	1480
7	9680	15600	4610	3200	3670	1580	2010	3010	1120
8	8140	10100	5260	3660	2200	2300	1400	1330	2350
9	8510	12700	4150	2910	2420	1480	1470	1270	4070
10	9900	14200	4940	4490	1560	1730	1840	1250	1940

B.19. Ni

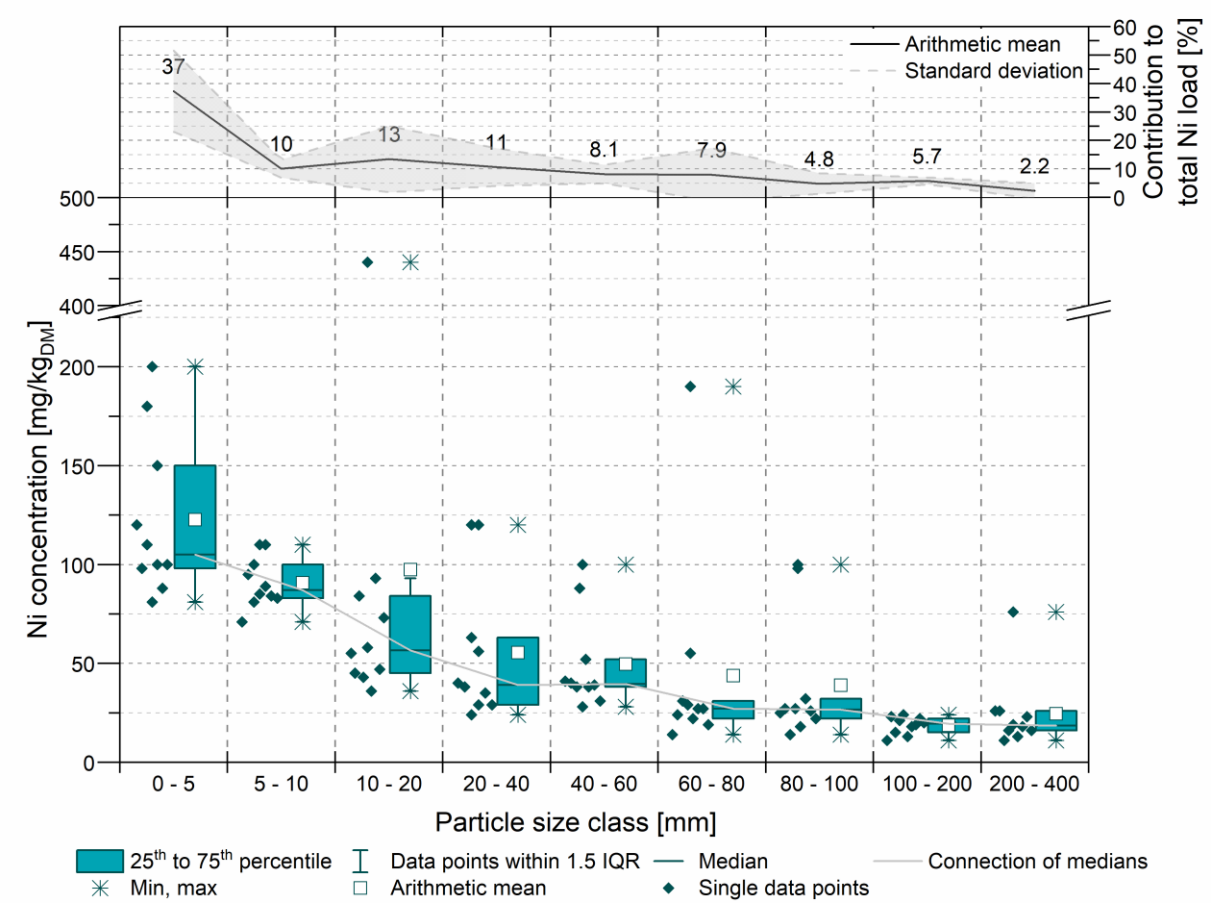

Figure B.19: Below: Box plot of nickel (Ni) concentrations in different particle size classes in mg/kg referring to dry mass without hard impurities. Above: Contribution of the grain size fractions (average ± standard deviation) to the total content of Ni

Table B.19: Nickel (Ni) concentrations in mg/kg referring to dry mass without hard impurities. LOQ = 0.50 mg/kg

Composite sample	0 - 5 mm	5 - 10 mm	10 - 20 mm	20 - 40 mm	40 - 60 mm	60 - 80 mm	80 - 100 mm	100 - 200 mm	200 - 400 mm
1	81	85	58	29	28	190	98	13	19
2	98	81	84	120	100	22	100	24	16
3	100	89	93	120	52	29	18	18	13
4	110	110	55	24	38	27	27	21	76
5	100	95	440	56	88	31	32	19	11
6	120	84	36	35	38	27	14	15	18
7	150	100	43	38	40	24	26	22	26
8	200	110	73	63	39	55	27	23	23
9	180	71	47	29	41	19	22	20	26
10	88	83	45	40	31	14	25	11	16

B.20. P

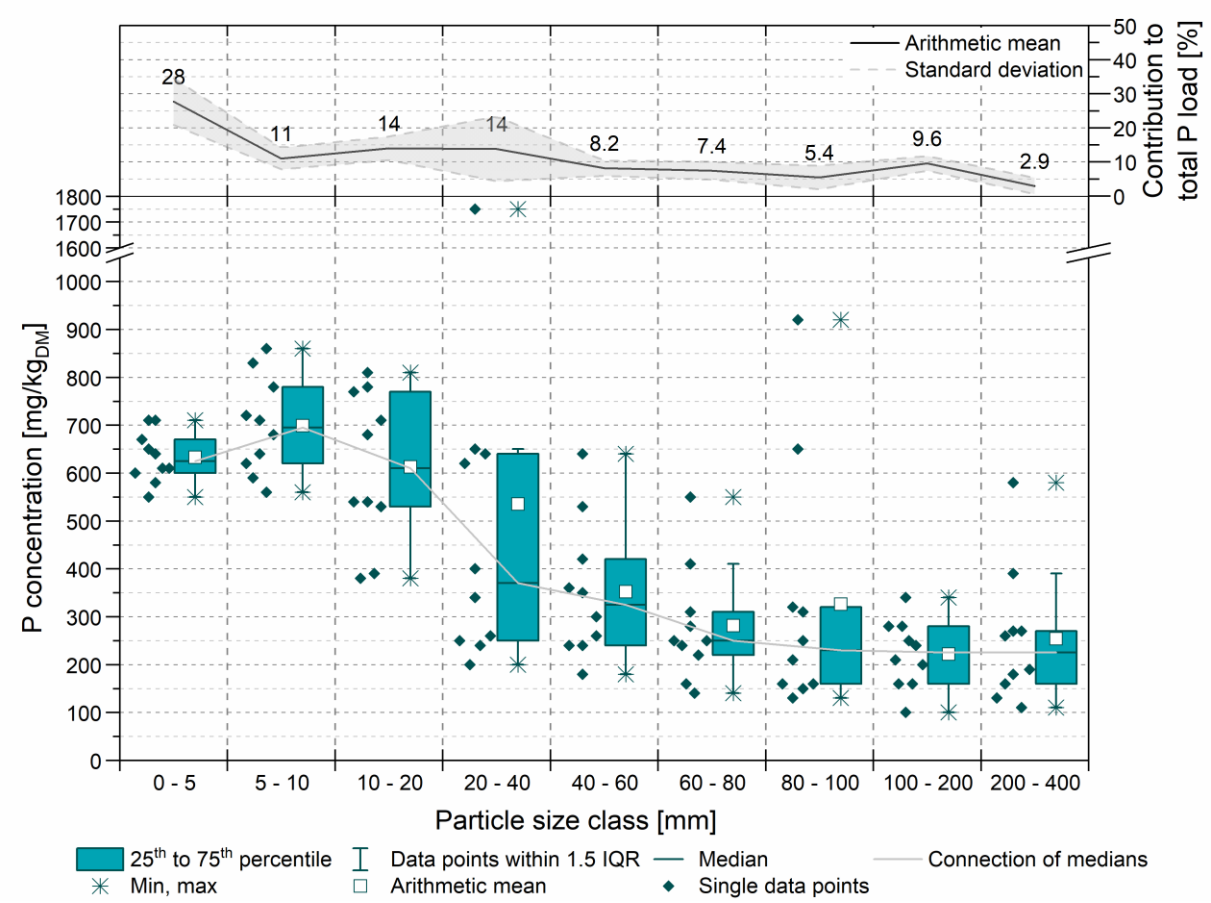

Figure B.20: Below: Box plot of phosphorus (P) concentrations in different particle size classes in mg/kg referring to dry mass without hard impurities. Above: Contribution of the grain size fractions (average ± standard deviation) to the total content of P

Table B.20: Phosphorus (P) concentrations in mg/kg referring to dry mass without hard impurities. LOQ = 2.5 mg/kg

Composite sample	0 - 5 mm	5 - 10 mm	10 - 20 mm	20 - 40 mm	40 - 60 mm	60 - 80 mm	80 - 100 mm	100 - 200 mm	200 - 400 mm
1	710	860	680	400	420	280	920	250	270
2	710	710	810	650	640	550	650	280	260
3	580	560	780	620	350	240	310	240	180
4	640	720	770	340	360	310	320	340	580
5	650	640	540	240	300	410	250	210	160
6	610	620	390	200	180	220	150	100	110
7	670	590	380	1750	530	140	210	200	130
8	550	680	540	260	240	250	130	160	270
9	610	830	530	250	240	160	160	280	190
10	600	780	710	640	260	250	160	160	390

B.21. Pb

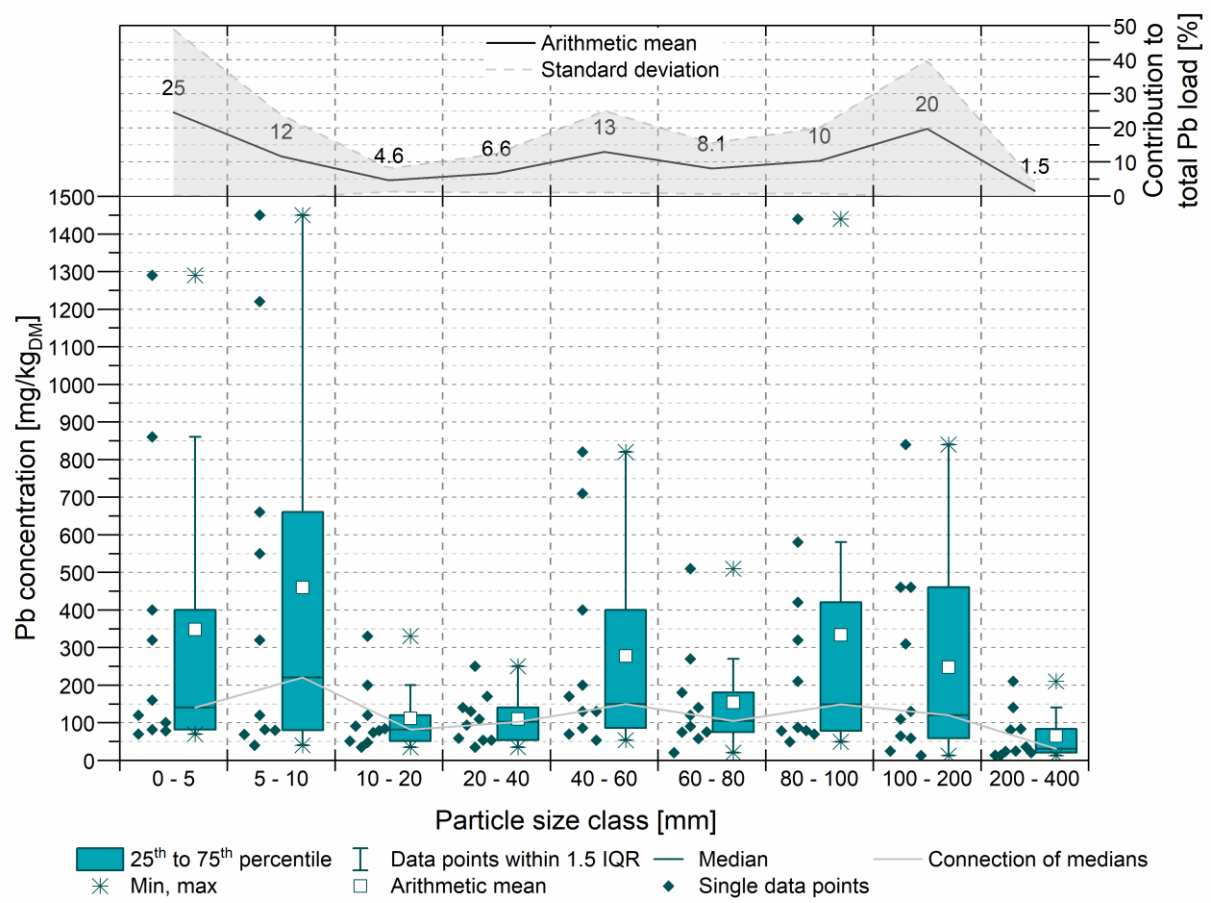

Figure B.21: Below: Box plot of lead (Pb) concentrations in different particle size classes in mg/kg referring to dry mass without hard impurities. Above: Contribution of the grain size fractions (average ± standard deviation) to the total content of Pb

Table B.21: Lead (Pb) concentrations in mg/kg referring to dry mass without hard impurities. LOQ = 0.25 mg/kg

Composite sample	0 - 5 mm	5 - 10 mm	10 - 20 mm	20 - 40 mm	40 - 60 mm	60 - 80 mm	80 - 100 mm	100 - 200 mm	200 - 400 mm
1	860	82	48	35	86	120	88	59	25
2	160	320	330	110	820	180	580	130	81
3	1290	1450	120	94	70	90	49	65	83
4	82	40	35	130	130	75	210	460	210
5	70	80	74	54	54	58	1440	840	140
6	120	120	91	170	170	140	320	13	24
7	320	69	79	140	400	270	79	460	36
8	100	660	51	59	710	20	78	310	13
9	78	1220	84	54	130	510	420	25	20
10	400	550	200	250	200	76	70	110	14

B.22. Pd - most values below L.O.Q.

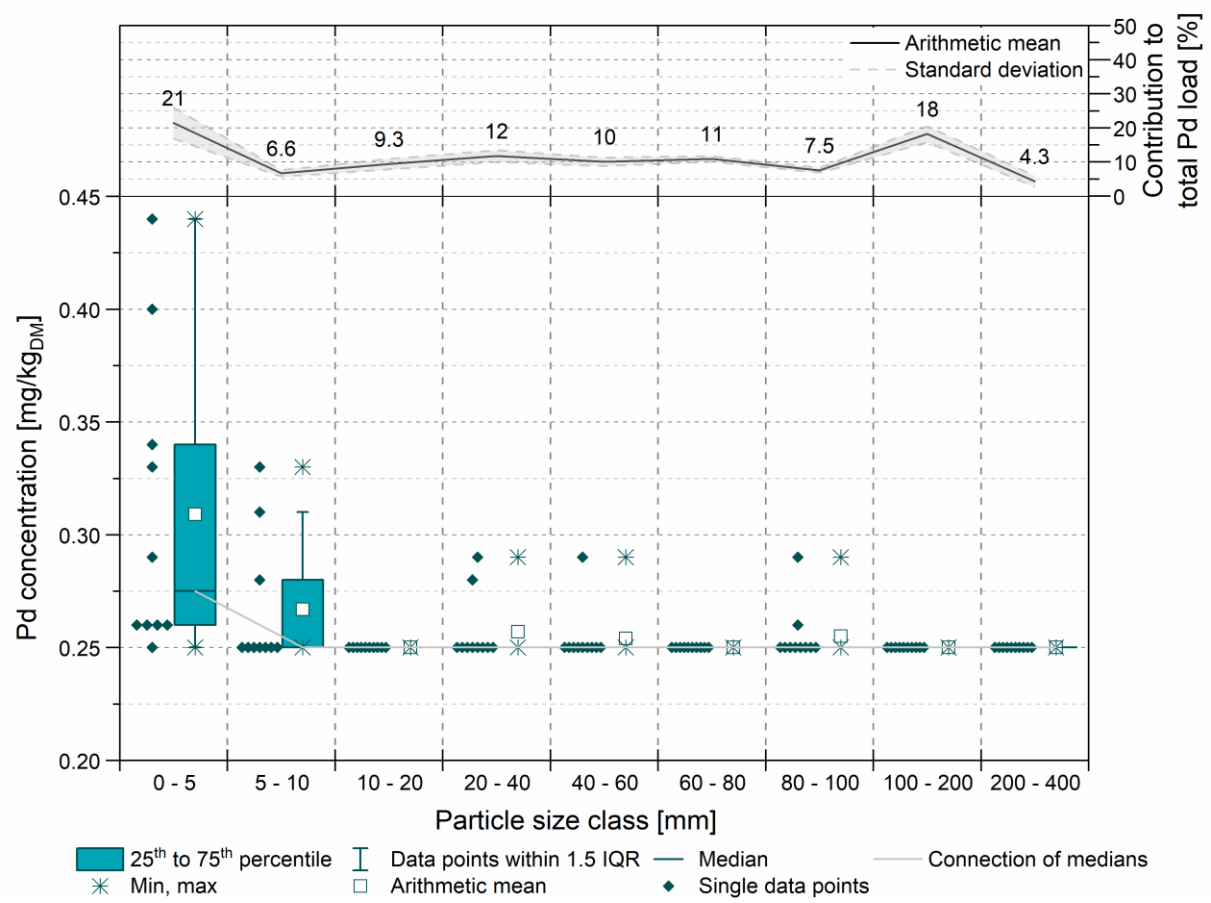

Figure B.22: Below: Box plot of palladium (Pd) concentrations in different particle size classes in mg/kg referring to dry mass without hard impurities. Above: Contribution of the grain size fractions (average ± standard deviation) to the total content of Pd

Table B.22: Palladium (Pd) concentrations in mg/kg referring to dry mass without hard impurities. LOQ = 0.25 mg/kg

Composite sample	0 - 5 mm	5 - 10 mm	10 - 20 mm	20 - 40 mm	40 - 60 mm	60 - 80 mm	80 - 100 mm	100 - 200 mm	200 - 400 mm
1	0.33	< 0.25	< 0.25	< 0.25	< 0.25	< 0.25	0.26	< 0.25	< 0.25
2	0.26	< 0.25	< 0.25	0.29	0.29	< 0.25	0.29	< 0.25	< 0.25
3	0.26	< 0.25	< 0.25	< 0.25	< 0.25	< 0.25	< 0.25	< 0.25	< 0.25
4	0.26	< 0.25	< 0.25	< 0.25	< 0.25	< 0.25	< 0.25	< 0.25	< 0.25
5	0.26	< 0.25	< 0.25	< 0.25	< 0.25	< 0.25	< 0.25	< 0.25	< 0.25
6	0.44	0.31	< 0.25	< 0.25	< 0.25	< 0.25	< 0.25	< 0.25	< 0.25
7	0.40	< 0.25	< 0.25	< 0.25	< 0.25	< 0.25	< 0.25	< 0.25	< 0.25
8	0.34	0.33	< 0.25	< 0.25	< 0.25	< 0.25	< 0.25	< 0.25	< 0.25
9	0.29	< 0.25	< 0.25	< 0.25	< 0.25	< 0.25	< 0.25	< 0.25	< 0.25
10	< 0.25	0.28	< 0.25	0.28	< 0.25	< 0.25	< 0.25	< 0.25	< 0.25

B.23. Sb

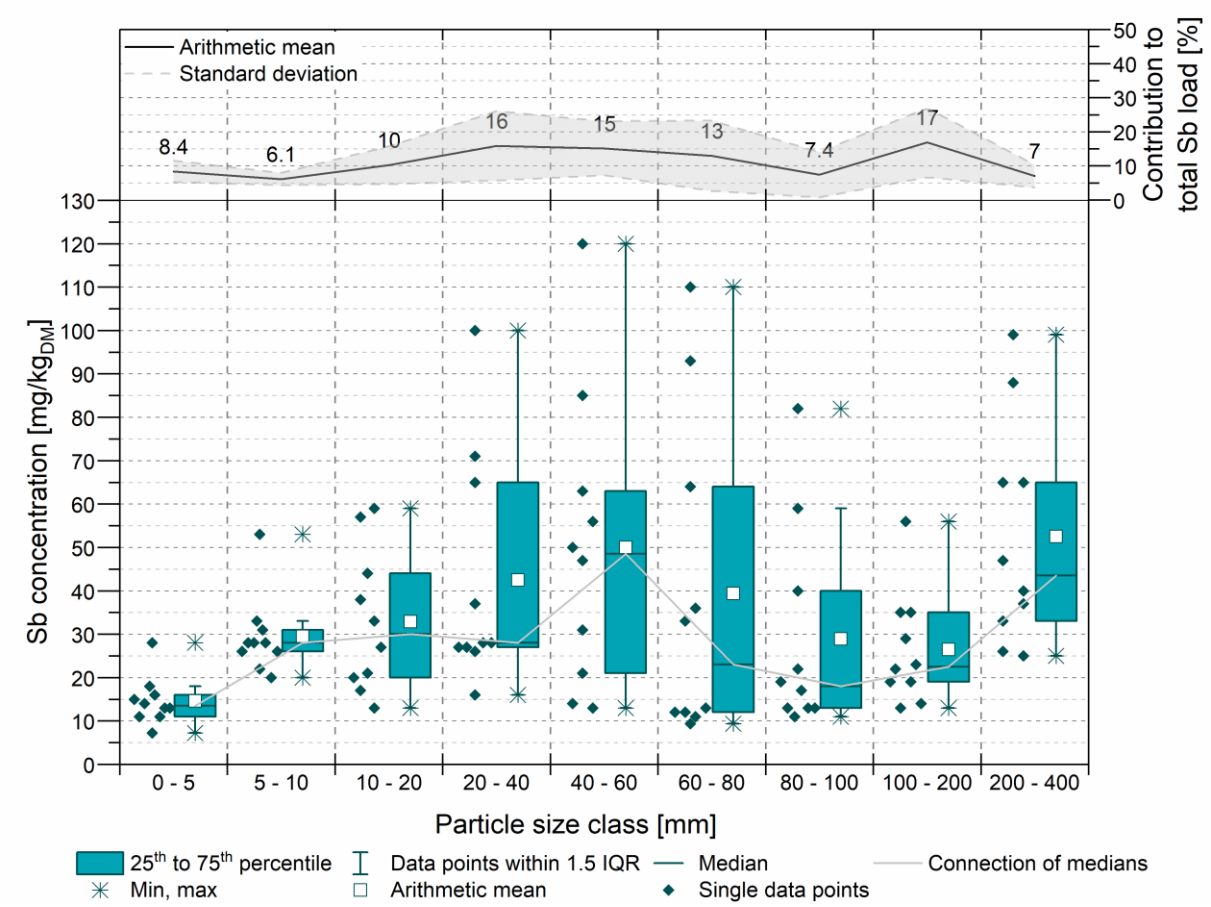

Figure B.23: Below: Box plot of antimony (Sb) concentrations in different particle size classes in mg/kg referring to dry mass without hard impurities. Above: Contribution of the grain size fractions (average ± standard deviation) to the total content of Sb

Table B.23: Antimony (Sb) concentrations in mg/kg referring to dry mass without hard impurities. LOQ = 0.25 mg/kg

Composite sample	0 - 5 mm	5 - 10 mm	10 - 20 mm	20 - 40 mm	40 - 60 mm	60 - 80 mm	80 - 100 mm	100 - 200 mm	200 - 400 mm
1	16	31	59	26	56	64	17	19	37
2	18	53	57	27	13	11	11	35	65
3	11	22	21	16	21	36	22	56	25
4	14	28	33	28	31	33	59	29	26
5	13	28	13	100	14	9.4	13	22	65
6	11	33	20	71	50	110	13	13	40
7	13	28	44	37	120	93	13	14	99
8	28	20	38	27	85	12	19	35	88
9	7.2	26	27	65	47	13	40	23	47
10	15	26	17	28	63	12	82	19	33

B.24. Si

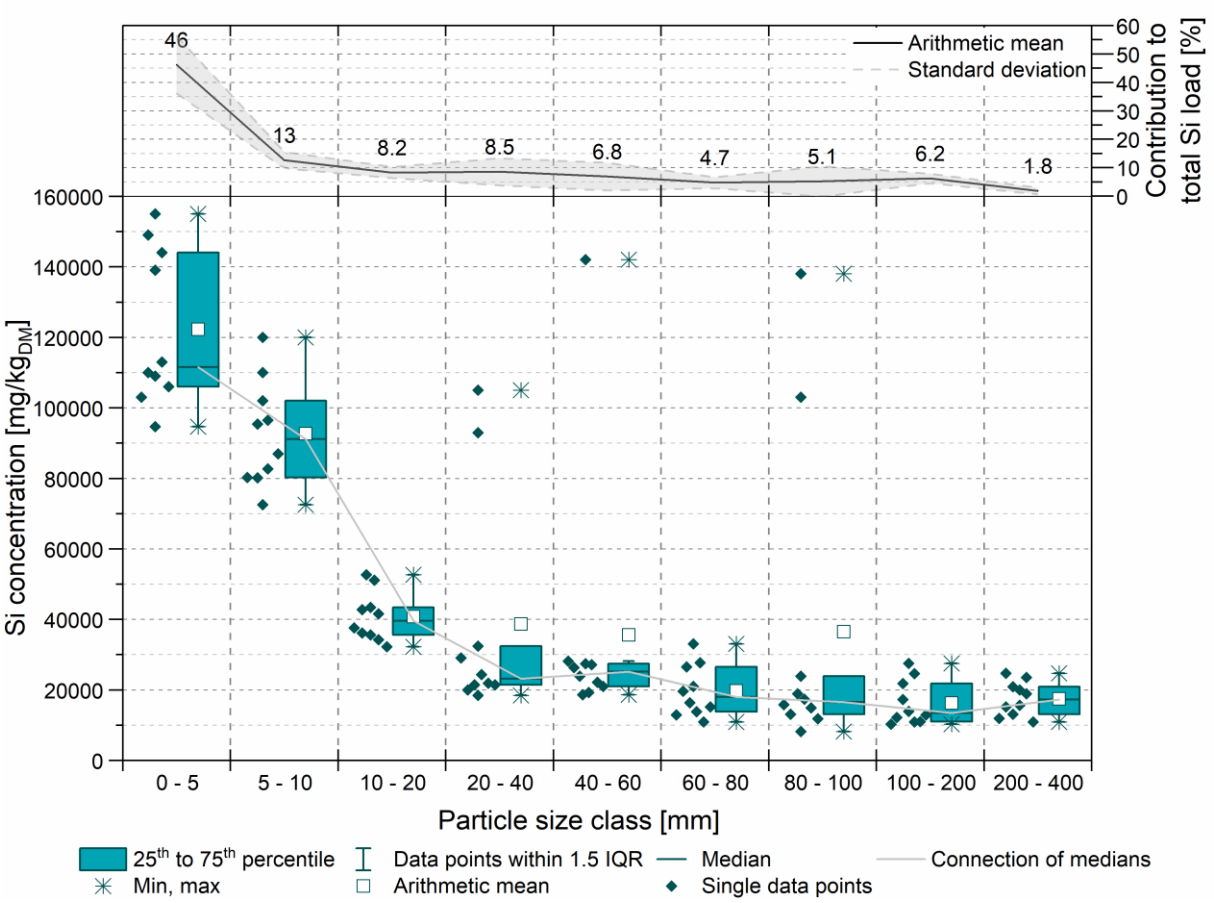

Figure B.24: Below: Box plot of silicon (Si) concentrations in different particle size classes in mg/kg referring to dry mass without hard impurities. Above: Contribution of the grain size fractions (average ± standard deviation) to the total content of Si

Table B.24: Silicon (Si) concentrations in mg/kg referring to dry mass without hard impurities. LOQ = 2.5 mg/kg

Composite sample	0 - 5 mm	5 - 10 mm	10 - 20 mm	20 - 40 mm	40 - 60 mm	60 - 80 mm	80 - 100 mm	100 - 200 mm	200 - 400 mm
1	109000	82700	43400	24300	27400	13800	103000	13900	20000
2	139000	110000	51100	92900	142000	16300	138000	27500	20900
3	155000	120000	52600	105000	23900	21000	17300	21800	15600
4	113000	80100	42700	21400	27100	26500	23900	24600	23500
5	103000	96500	41600	18400	26300	33000	18900	17200	13100
6	110000	86900	35600	21900	22100	27700	8140	10900	18900
7	106000	95400	36100	20000	28100	10900	14900	12200	15200
8	94700	72500	34200	32400	19200	19600	13100	11000	24700
9	144000	80200	37600	21400	21000	15200	11800	10300	10900
10	149000	102000	32200	29000	18600	12900	15800	12900	11900

B.25. Sn

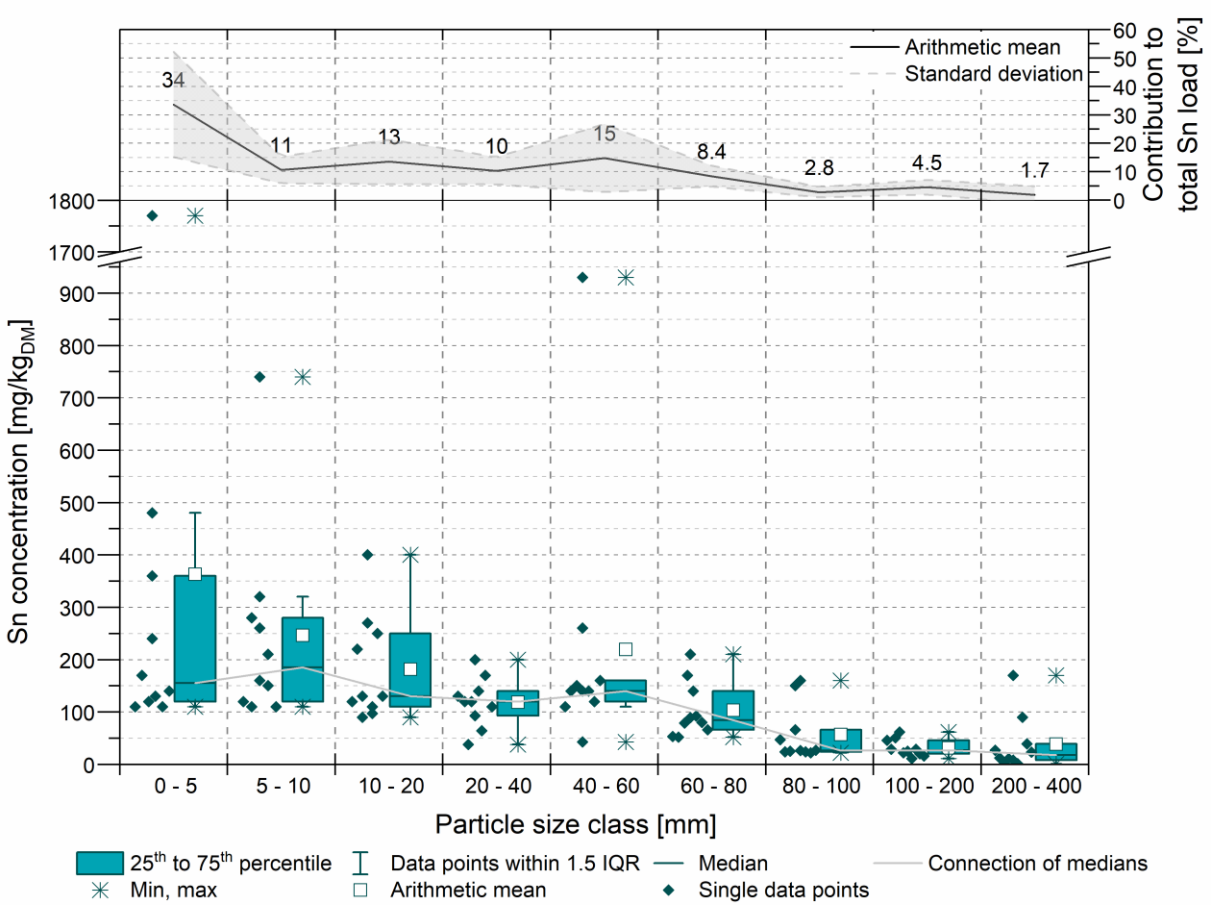

Figure B.25: Below: Box plot of tin (Sn) concentrations in different particle size classes in mg/kg referring to dry mass without hard impurities. Above: Contribution of the grain size fractions (average ± standard deviation) to the total content of Sn

Table B.25: Tin (Sn) concentrations in mg/kg referring to dry mass without hard impurities. LOQ = 0.50 mg/kg

Composite sample	0 - 5 mm	5 - 10 mm	10 - 20 mm	20 - 40 mm	40 - 60 mm	60 - 80 mm	80 - 100 mm	100 - 200 mm	200 - 400 mm
1	1770	260	270	200	140	210	160	25	8.2
2	240	280	400	93	260	140	150	22	11
3	130	210	220	140	43	89	26	11	1.3
4	120	160	250	38	150	79	66	62	170
5	110	110	110	120	140	92	24	29	0.50
6	170	150	130	170	140	170	25	51	90
7	360	120	130	120	120	52	22	20	12
8	140	740	97	110	930	80	24	29	39
9	110	110	120	64	110	53	27	16	27
10	480	320	90	130	160	66	47	46	23

B.26. Sr

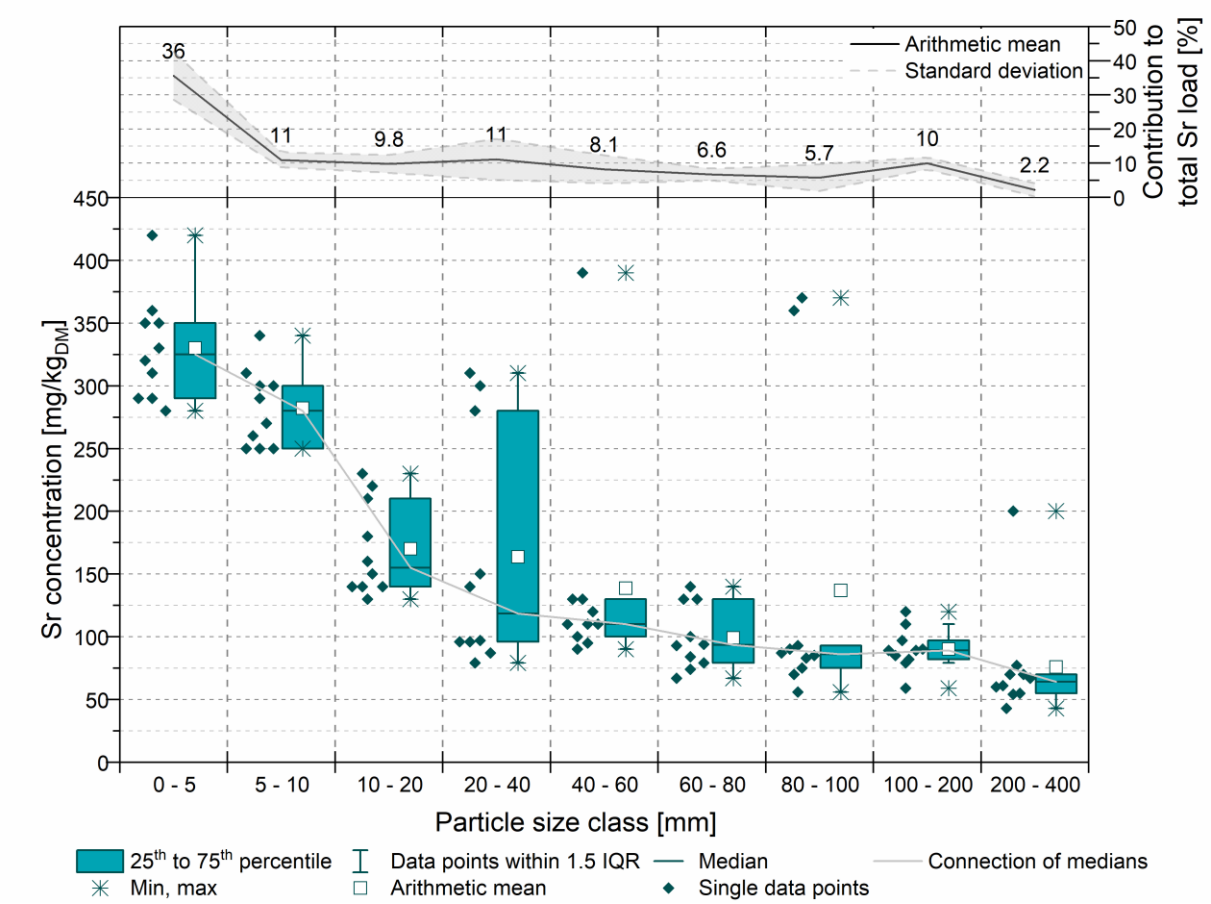

Figure B.26: Below: Box plot of strontium (Sr) concentrations in different particle size classes in mg/kg referring to dry mass without hard impurities. Above: Contribution of the grain size fractions (average ± standard deviation) to the total content of Sr

Table B.26: Strontium (Sr) concentrations in mg/kg referring to dry mass without hard impurities. LOQ = 0.25 mg/kg

Composite sample	0 - 5 mm	5 - 10 mm	10 - 20 mm	20 - 40 mm	40 - 60 mm	60 - 80 mm	80 - 100 mm	100 - 200 mm	200 - 400 mm
1	420	300	220	150	130	74	370	120	77
2	350	310	210	280	390	84	360	82	70
3	290	250	150	300	110	93	75	79	70
4	350	340	230	97	130	130	93	97	200
5	360	250	180	96	95	140	90	89	61
6	330	270	140	79	100	130	56	85	67
7	310	250	140	87	110	67	83	59	54
8	290	300	140	96	110	100	87	90	60
9	320	260	130	140	90	94	85	89	43
10	280	290	160	310	120	79	70	110	55

B.27. Ti

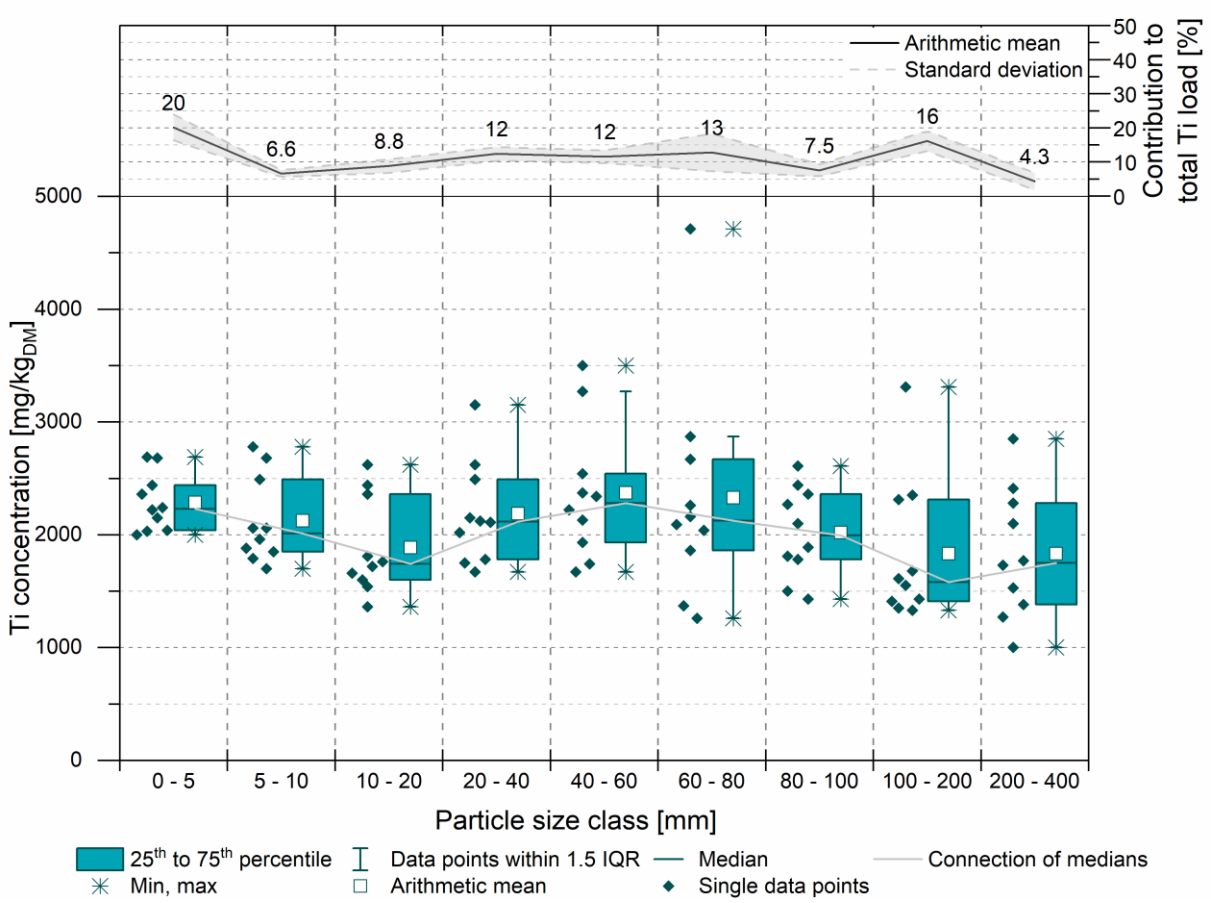

Figure B.27: Below: Box plot of titanium (Ti) concentrations in different particle size classes in mg/kg referring to dry mass without hard impurities. Above: Contribution of the particle size fractions (average ± standard deviation) to the total content of Ti

Table B.27: Titanium (Ti) concentrations in mg/kg referring to dry mass without hard impurities. LOQ = 0.25 mg/kg

Composite sample	0 - 5 mm	5 - 10 mm	10 - 20 mm	20 - 40 mm	40 - 60 mm	60 - 80 mm	80 - 100 mm	100 - 200 mm	200 - 400 mm
1	2220	2060	1810	1670	2130	2670	2360	1550	1770
2	2680	2490	2360	2120	2540	2160	2610	1680	1380
3	2690	2680	1720	2150	1740	1260	1430	1410	2410
4	2440	2060	1600	2490	2370	2090	2440	3310	2280
5	2360	1960.0	2440	2110	2220	2040	1890	1330	1000
6	2150	1700	1360	2020	2340	2260	1500	1350	2850
7	2240	1790	1760	2620	3500	2870	2270	2350	1530
8	2030	1880	1660	1750	1670	1370	2100	1430	1730
9	2040	1850	1540	1780	1930	4710	1780	1610	1270
10	2000	2780	2620	3150	3270	1860	1810	2310	2100

B.28. V

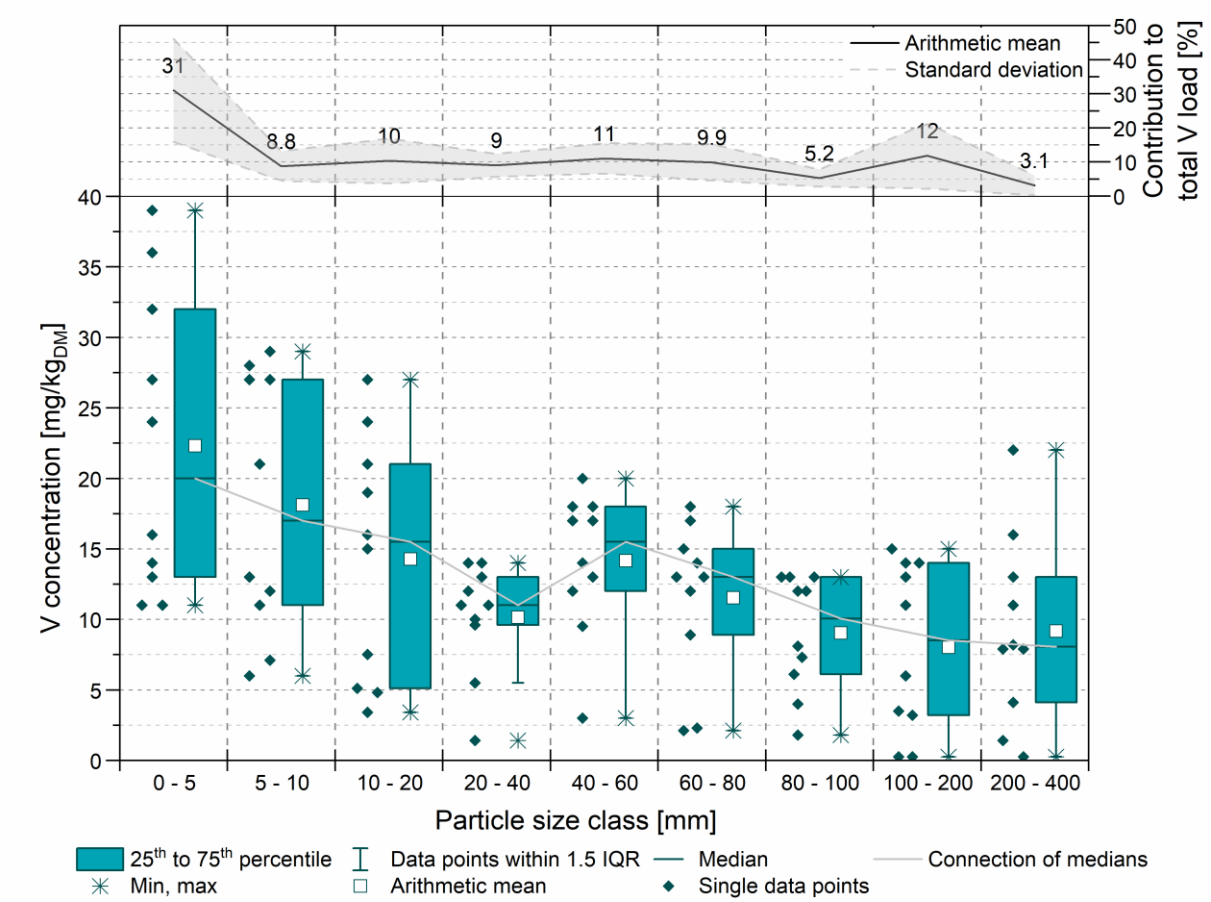

Figure B.28: Below: Box plot of vanadium (V) concentrations in different particle size classes in mg/kg referring to dry mass without hard impurities. Above: Contribution of the grain size fractions (average ± standard deviation) to the total content of V

Table B.28: Vanadium (V) concentrations in mg/kg referring to dry mass without hard impurities. LOQ = 0.25 mg/kg

Composite sample	0 - 5 mm	5 - 10 mm	10 - 20 mm	20 - 40 mm	40 - 60 mm	60 - 80 mm	80 - 100 mm	100 - 200 mm	200 - 400 mm
1	11	7.1	3.4	10	20	17	12	14	16
2	16	12	4.8	10	13	12	13	15	13
3	14	13	7.5	11	18	13	12	13	11
4	11	11	24	14	17	14	13	14	22
5	13	6.0	5.1	1.4	18	18	13	11	7.9
6	36	29	21	14	14	15	4.0	3.2	7.9
7	39	28	15	11	17	8.9	8.1	3.5	4.1
8	32	27	19	13	9.5	13	7.3	6.0	8.2
9	27	21	16	5.5	3.0	2.3	1.8	< 0.25	< 0.25
10	24	27	27	12	12	2.1	6.1	< 0.25	1.4

B.29. W

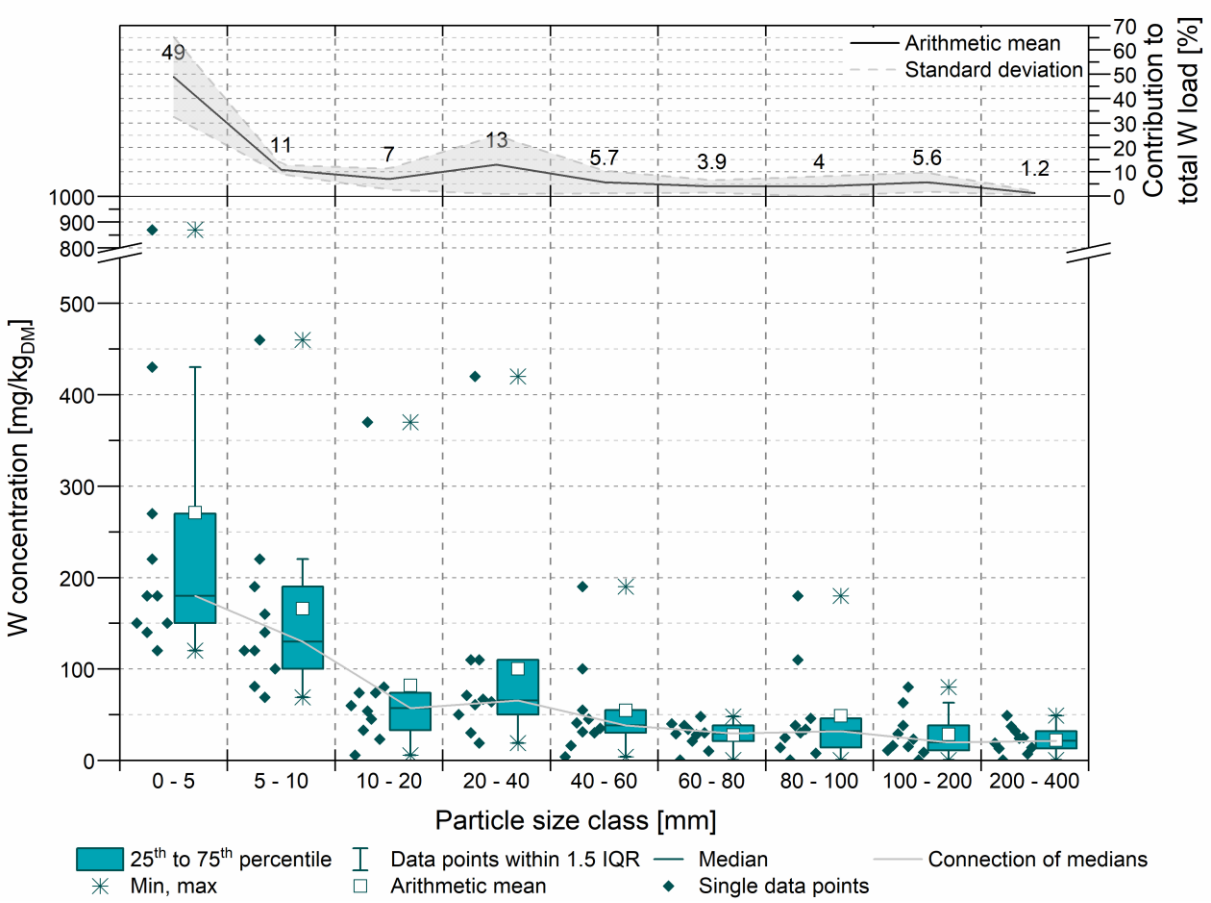

Figure B.29: Below: Box plot of tungsten (W) concentrations in different particle size classes in mg/kg referring to dry mass without hard impurities. Above: Contribution of the grain size fractions (average ± standard deviation) to the total content of W

Table B.29: Tungsten (W) concentrations in mg/kg referring to dry mass without hard impurities. LOQ = 0.25 mg/kg

Composite sample	0 - 5 mm	5 - 10 mm	10 - 20 mm	20 - 40 mm	40 - 60 mm	60 - 80 mm	80 - 100 mm	100 - 200 mm	200 - 400 mm
1	180	140	54	61	55	21	110	15	32
2	220	220	74	110	190	34	180	80	37
3	270	120	45	110	31	28	30	38	24
4	180	160	74	420	41	38	38	23	49
5	150	100	33	71	45	48	34	29	25
6	430	190	60	19	16	< 0.25	< 0.25	< 0.25	< 0.25
7	870	460	370	67	100	30	46	63	6.9
8	120	120	23	50	30	29	25	16	13
9	140	69	5.6	64	3.9	10	7.6	8.8	14
10	150	81	80	30	35	40	14	11	19

B.30. Zn

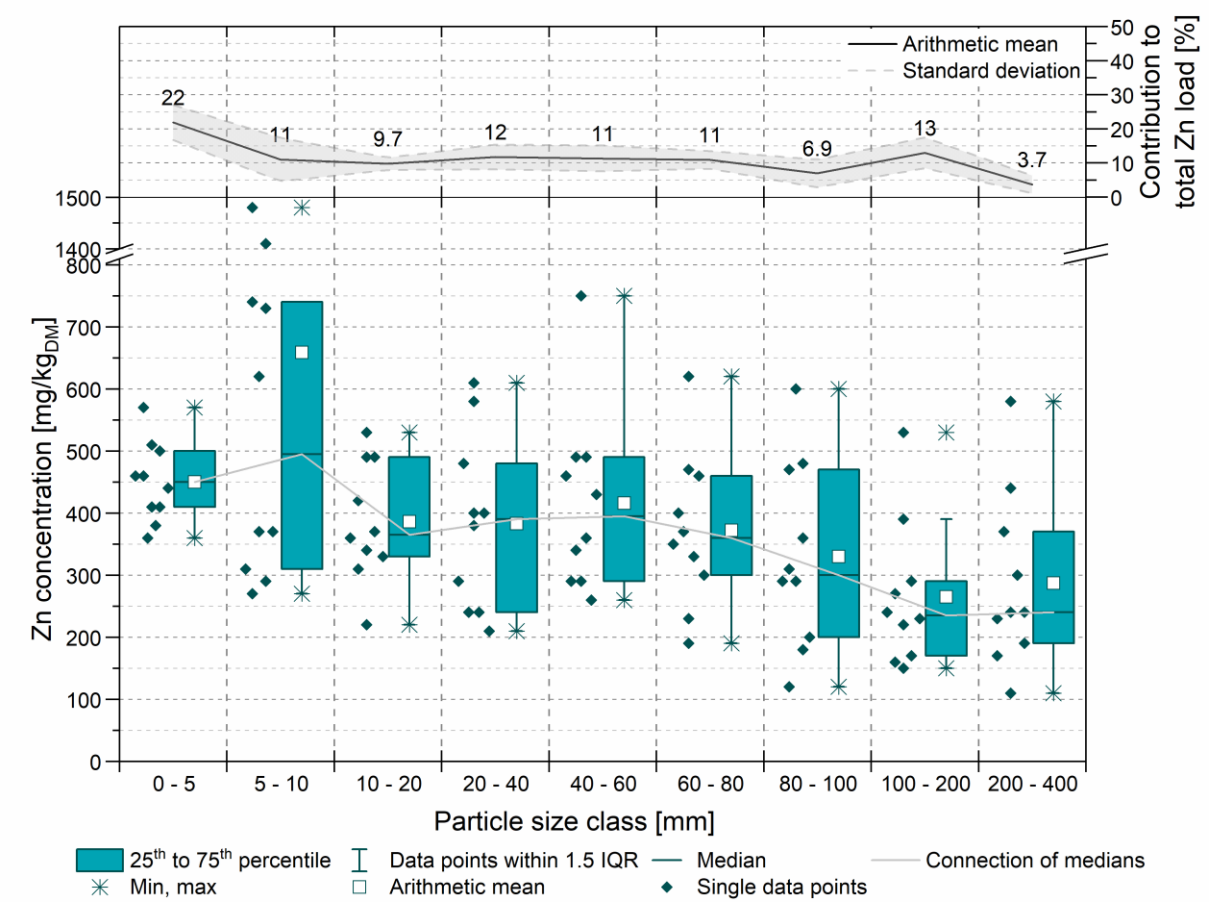

Figure B.30: Below: Box plot of zinc (Zn) concentrations in different particle size classes in mg/kg referring to dry mass without hard impurities. Above: Contribution of the grain size fractions (average ± standard deviation) to the total content of Zn

Table B.30: Zinc (Zn) concentrations in mg/kg referring to dry mass without hard impurities. LOQ = 2.5 mg/kg

Composite sample	0 - 5 mm	5 - 10 mm	10 - 20 mm	20 - 40 mm	40 - 60 mm	60 - 80 mm	80 - 100 mm	100 - 200 mm	200 - 400 mm
1	380	290	340	240	490	330	480	220	240
2	510	370	530	610	490	230	360	390	300
3	360	730	490	580	290	470	310	270	110
4	410	270	420	400	750	370	470	290	580
5	570	1410	490	480	430	620	290	530	170
6	460	740	310	240	360	300	180	240	370
7	410	310	220	210	290	190	600	230	230
8	460	1480	370	290	340	400	290	150	190
9	500	620	360	380	260	350	120	160	240
10	440	370	330	400	460	460	200	170	440

B.31. Hard impurities

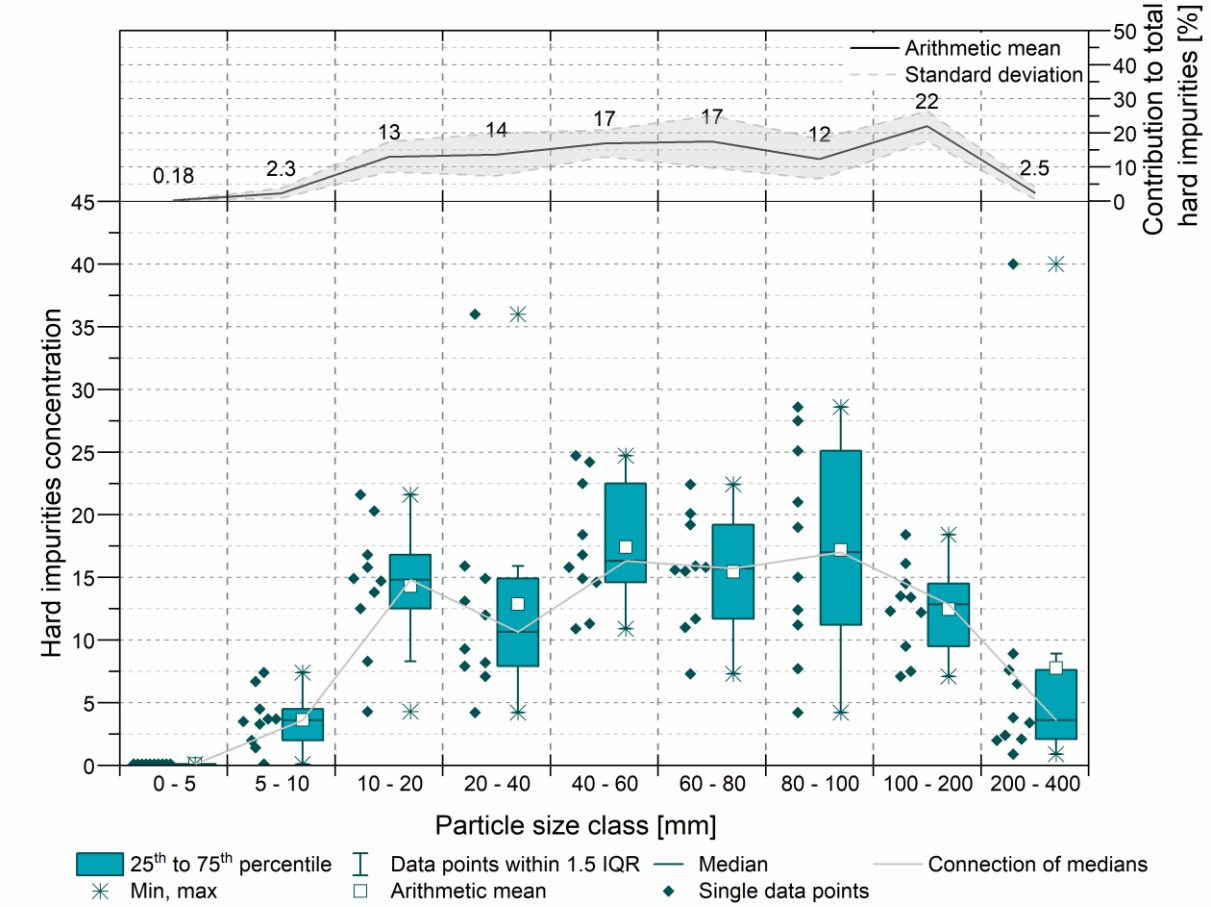

Figure B.31: Below: Box plot of the mass share of hard impurities in % referring to dry mass that were removed from different particle size classes during sample preparation. Above: Contribution of the grain size fractions (average ± standard deviation) to the total content of hard impurities

Table B.31: Mass share of hard impurities in % referring to dry mass

Composite sample	0 - 5 mm	5 - 10 mm	10 - 20 mm	20 - 40 mm	40 - 60 mm	60 - 80 mm	80 - 100 mm	100 - 200 mm	200 - 400 mm
1	< 0.1	4.5	13.8	12.0	24.2	15.9	11.2	13.4	0.9
2	< 0.1	3.3	15.8	14.9	14.9	15.5	15.0	9.5	3.8
3	< 0.1	7.4	20.3	15.9	15.8	7.3	25.1	13.5	2.4
4	< 0.1	6.7	12.5	8.2	22.5	11.7	7.7	16.1	2.1
5	< 0.1	< 0.1	14.9	36.0	18.4	20.1	19.0	12.2	40.0
6	< 0.1	1.4	8.3	13.1	14.6	11	27.5	12.3	2.0
7	< 0.1	2.0	4.3	4.2	11.3	22.4	21	7.5	3.4
8	< 0.1	3.7	14.7	7.1	16.8	15.8	12.4	14.5	6.5
9	< 0.1	3.5	21.6	7.9	10.9	19.2	4.2	7.1	7.6
10	< 0.1	3.7	16.8	9.3	24.7	15.6	28.6	18.4	8.9

B.32. LHV

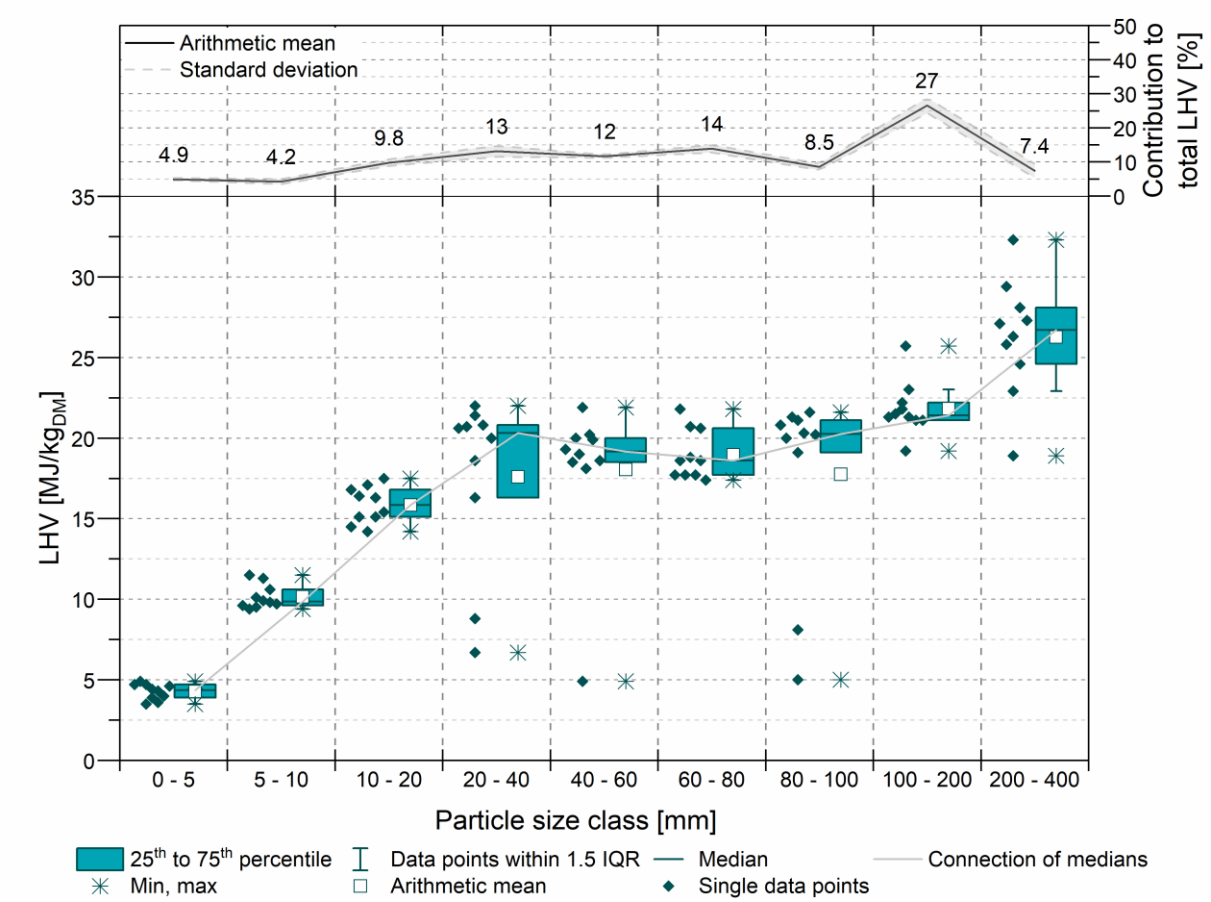

Figure B.32: Below: Box plot of the lower heating value (LHV) in different particle size classes in kJ/kg referring to dry mass without hard impurities. Above: Contribution of the grain size fractions (average ± standard deviation) to the total LHV

Table B.32: Lower heating value (LHV) in kJ/kg referring to dry mass without hard impurities

Composite sample	0 - 5 mm	5 - 10 mm	10 - 20 mm	20 - 40 mm	40 - 60 mm	60 - 80 mm	80 - 100 mm	100 - 200 mm	200 - 400 mm
1	4400	9900	14200	16300	18100	20700	8100	21300	28100
2	4700	9500	15100	8800	4900	21800	5000	25700	22900
3	4300	9800	15100	6700	21900	17700	21100	23000	24600
4	4900	11300	14500	21400	19000	18800	21300	21800	18900
5	4000	10100	15400	20700	20000	17700	20300	19200	26300
6	3900	9400	17100	22000	19900	17400	20000	21100	27100
7	4700	9700	16400	20800	18500	18600	21600	21500	29400
8	3500	10600	16300	18600	18600	17700	20800	21100	32300
9	3600	11500	16800	20600	19300	18600	20200	22200	27300
10	4600	9600	17500	20000	20200	20600	19100	21300	25800

B.33. Ash content

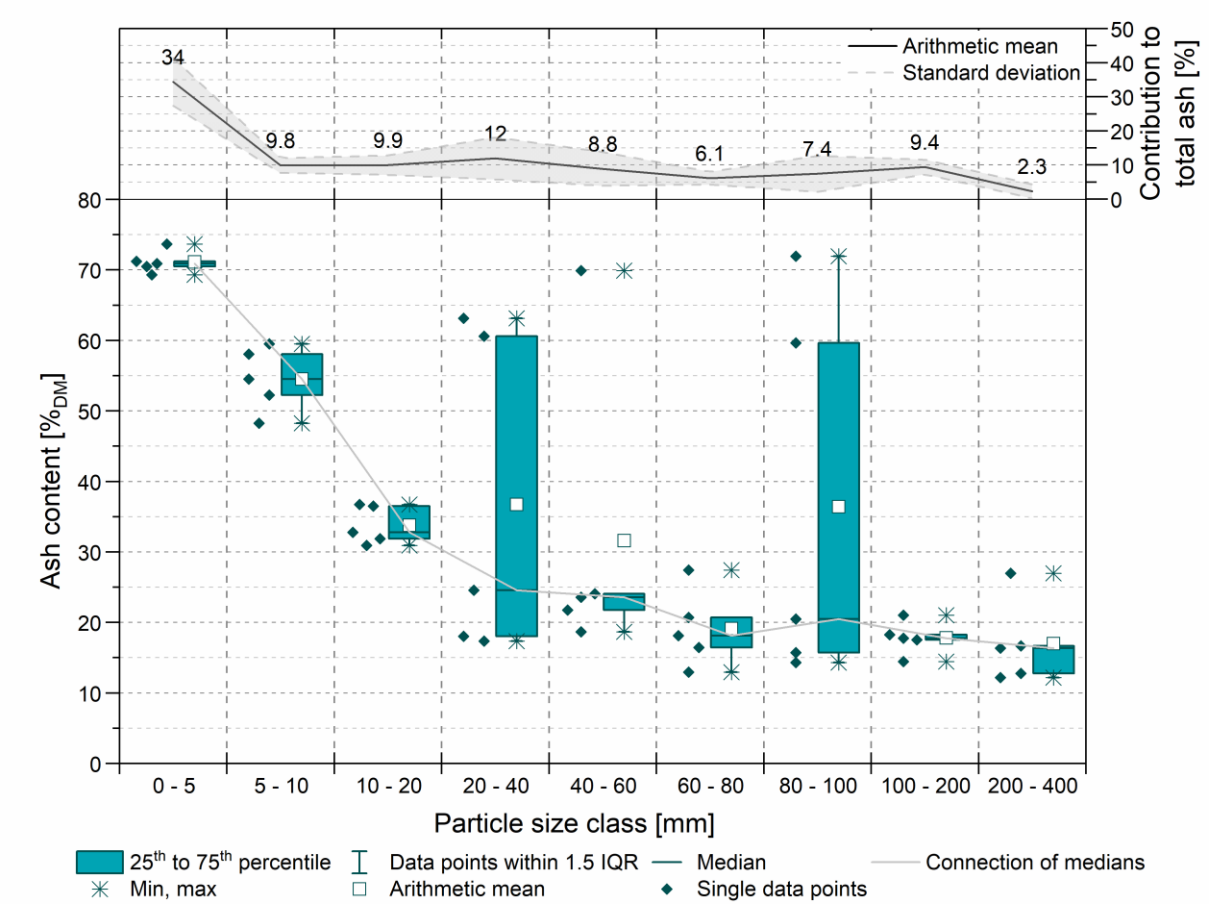

Figure B.33: Below: Box plot of the Ash content (AC) of different particle size classes in % referring to dry mass without hard impurities. Above: Contribution of the grain size fractions (average ± standard deviation) to the total ash

Table B.33: Ash content in % referring to dry mass without hard impurities

Composite sample	0 - 5 mm	5 - 10 mm	10 - 20 mm	20 - 40 mm	40 - 60 mm	60 - 80 mm	80 - 100 mm	100 - 200 mm	200 - 400 mm
1	70.9	52.2	30.9	24.5	23.5	13.0	59.6	14.4	16.7
2	70.5	59.5	36.5	60.6	69.9	16.4	71.9	17.7	16.3
3	73.6	58.0	32.7	63.1	18.6	18.1	14.3	21.0	12.7
4	69.3	48.2	36.7	17.4	21.7	20.7	20.5	18.3	26.9
5	71.2	54.5	31.9	18.0	24.1	27.4	15.7	17.5	12.1

B.34. Dry matter

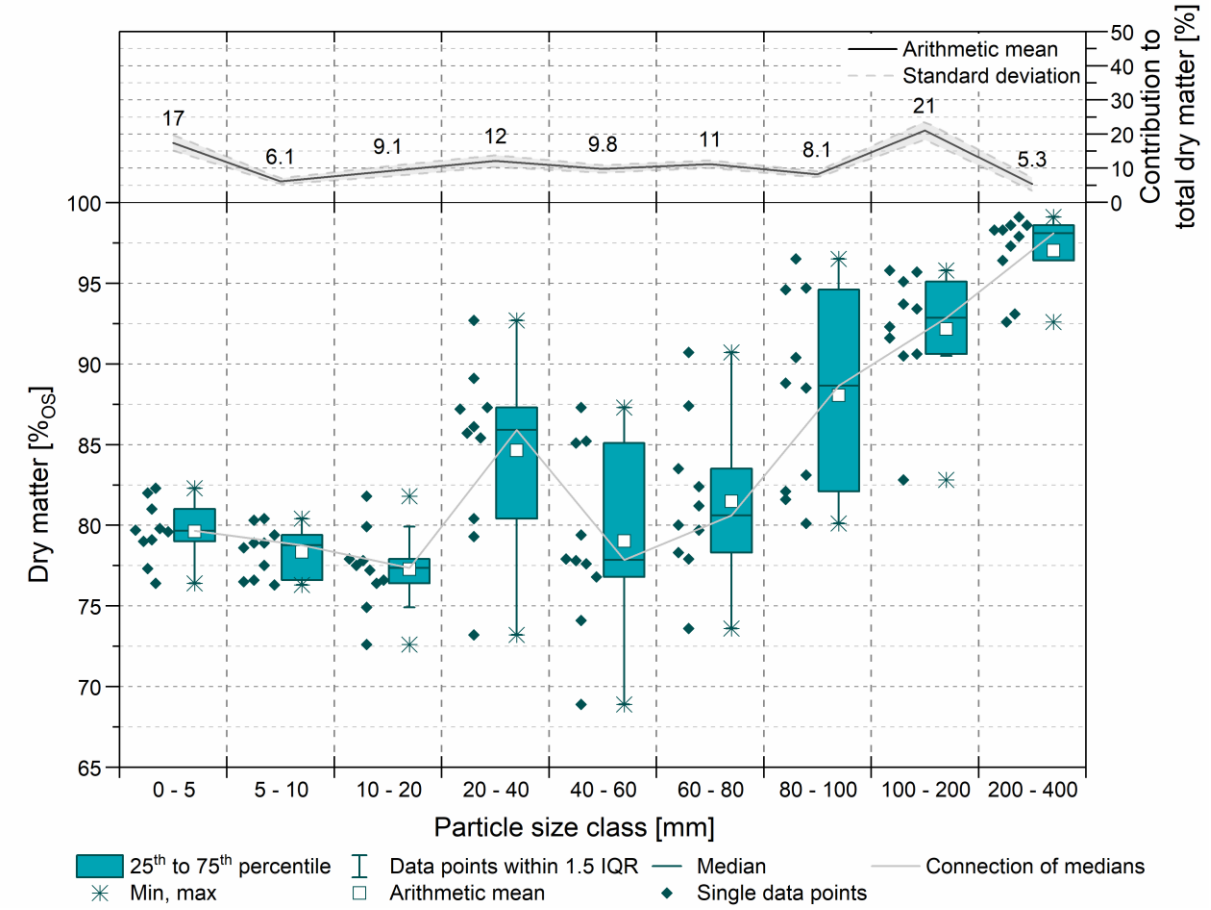

Figure B.34: Below: Box plot of the content of dry matter (including hard impurities) in different particle size classes in % referring to original substance (OS). Note, that the dry matter or water content was not determined directly after the samples were taken. Some water has very likely evaporated during sample processing on site (screening, reduction of sample mass, sorting analysis, storage in closed bins and buckets with lids or sealed plastic bags). Above: Contribution of the grain size fractions (average ± standard deviation) to the total dry matter.

Table B.34: Dry matter (including hard impurities) in % referring to original mass

Composite sample	0 - 5 mm	5 - 10 mm	10 - 20 mm	20 - 40 mm	40 - 60 mm	60 - 80 mm	80 - 100 mm	100 - 200 mm	200 - 400 mm
1	79.1	77.5	77.2	85.4	77.6	81.2	90.4	90.5	93.1
2	79.0	78.9	77.8	86.1	85.2	82.4	83.1	91.6	97.3
3	79.8	76.6	74.9	73.2	77.8	79.7	82.1	93.7	98.6
4	76.4	76.3	76.4	79.3	76.8	73.6	80.1	82.8	96.4
5	81.0	80.4	79.9	92.7	77.9	78.3	81.6	95.1	92.6
6	79.7	78.9	77.5	87.2	74.1	77.9	96.5	95.8	98.3
7	77.3	76.5	72.6	87.3	68.9	87.4	88.5	92.3	99.1
8	82.3	80.3	76.6	85.7	87.3	80.0	94.7	93.4	98.3
9	82.0	79.4	77.9	80.4	79.4	83.5	88.8	95.7	98.6
10	79.6	78.6	81.8	89.1	85.1	90.7	94.6	90.6	97.9

B.35. Water content

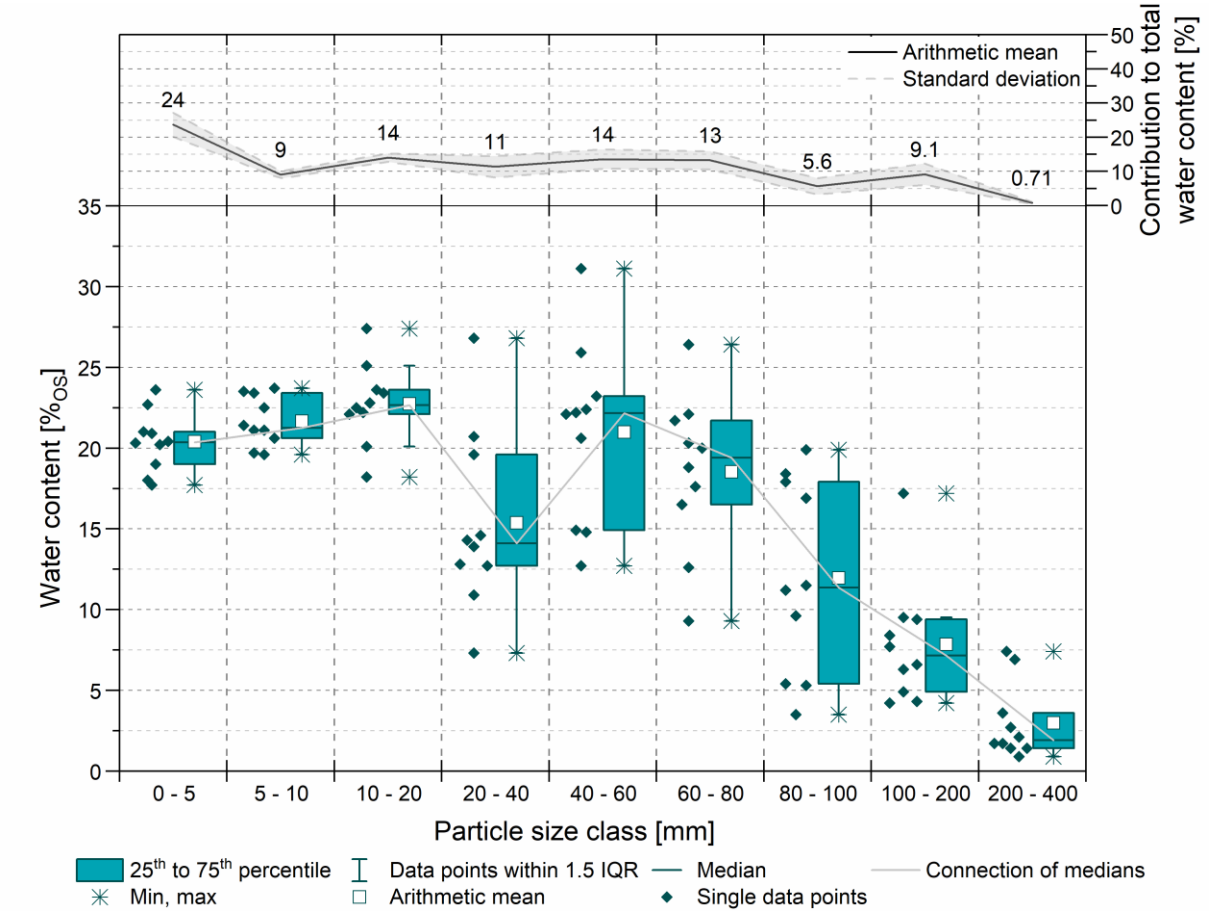

Figure B.35: Below: Box plot of the water content in different particle size classes in % referring to original substance (OS) including hard impurities. Note, that the water content was not determined directly after the samples were taken. Some water has very likely evaporated during sample processing on site (screening, reduction of sample mass, sorting analysis, storage in closed bins and buckets with lids or sealed plastic bags). Above: Contribution of the grain size fractions (average ± standard deviation) to the total water content.

Table B.35: Water content in % referring to original mass including hard impurities

Composite sample	0 - 5 mm	5 - 10 mm	10 - 20 mm	20 - 40 mm	40 - 60 mm	60 - 80 mm	80 - 100 mm	100 - 200 mm	200 - 400 mm
1	20.9	22.5	22.8	14.6	22.4	18.8	9.6	9.5	6.9
2	21.0	21.1	22.2	13.9	14.8	17.6	16.9	8.4	2.7
3	20.2	23.4	25.1	26.8	22.2	20.3	17.9	6.3	1.4
4	23.6	23.7	23.6	20.7	23.2	26.4	19.9	17.2	3.6
5	19.0	19.6	20.1	7.3	22.1	21.7	18.4	4.9	7.4
6	20.3	21.1	22.5	12.8	25.9	22.1	3.5	4.2	1.7
7	22.7	23.5	27.4	12.7	31.1	12.6	11.5	7.7	0.9
8	17.7	19.7	23.4	14.3	12.7	20.0	5.3	6.6	1.7
9	18.0	20.6	22.1	19.6	20.6	16.5	11.2	4.3	1.4
10	20.4	21.4	18.2	10.9	14.9	9.3	5.4	9.4	2.1

B.36. Masses of particle size classes

Table B.36: Masses of particle size fractions in kg referring to dry mass without hard impurities

Composite sample	0 - 5 mm	5 - 10 mm	10 - 20 mm	20 - 40 mm	40 - 60 mm	60 - 80 mm	80 - 100 mm	100 - 200 mm	200 - 400 mm
1	31.0	10.3	18.8	24.2	17.6	20.3	12.9	27.6	3.8
2	26.3	8.7	16.9	22.9	20.0	21.5	14.4	36.0	7.0
3	27.7	9.6	13.7	17.5	17.7	18.1	10.5	30.8	9.7
4	27.0	13.5	22.9	23.7	19.4	19.4	13.6	27.5	12.4
5	34.3	12.9	16.8	17.4	14.8	18.8	11.5	39.1	3.8
6	36.3	14.5	19.8	25.5	19.4	21.4	15.5	36.7	9.2
7	27.7	10.7	16.0	18.5	17.0	19.6	12.7	32.3	6.2
8	45.1	12.7	17.5	23.7	22.5	22.4	19.0	43.3	13.6
9	40.6	13.4	14.6	18.2	19.0	21.8	15.3	31.1	7.6
10	33.2	11.3	18.2	22.2	17.7	20.7	14.1	37.0	9.5

Table B.37: Masses of particle size fractions in kg referring to original substance (OS) including hard impurities

Composite sample	0 - 5 mm	5 - 10 mm	10 - 20 mm	20 - 40 mm	40 - 60 mm	60 - 80 mm	80 - 100 mm	100 - 200 mm	200 - 400 mm
1	39.2	13.9	28.2	32.2	29.9	29.8	16.0	35.2	4.1
2	33.4	11.4	25.7	31.3	27.6	30.9	20.3	43.4	7.4
3	34.7	13.5	23.0	28.4	27.0	24.4	17.1	38.0	10.1
4	35.3	19.0	34.2	32.5	32.6	29.9	18.4	39.6	13.1
5	42.4	16.0	24.6	29.3	23.2	30.0	17.4	46.8	6.8
6	45.6	18.7	27.9	33.6	30.7	30.9	22.2	43.7	9.6
7	35.8	14.2	23.1	22.2	27.8	28.8	18.2	37.9	6.5
8	54.9	16.5	26.8	29.7	31.0	33.3	22.9	54.3	14.8
9	49.5	17.4	23.9	24.5	26.9	32.4	18.0	35.0	8.3
10	41.8	14.9	26.7	27.4	27.7	27.0	20.9	50.0	10.6

Appendix C - Correlations

C.1. Element-particle size and parameter-particle size correlations

a

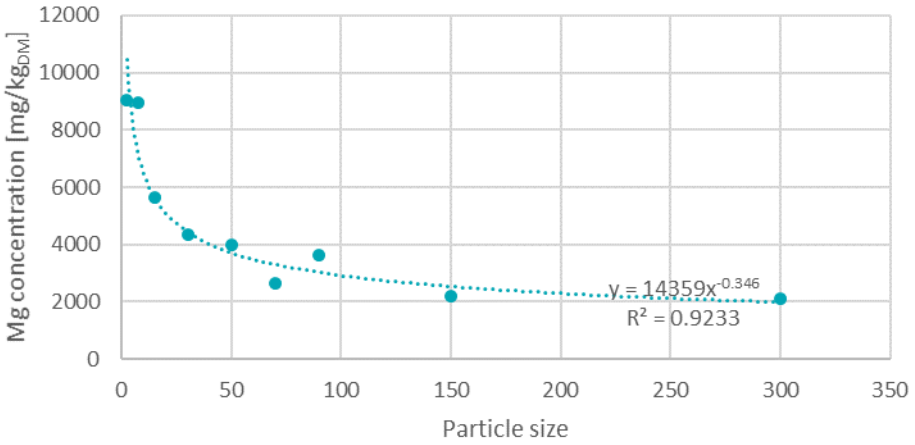

b

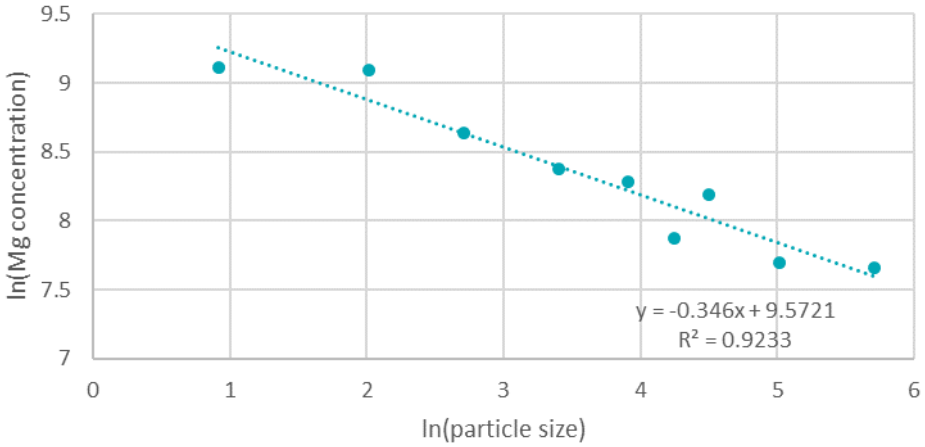

c

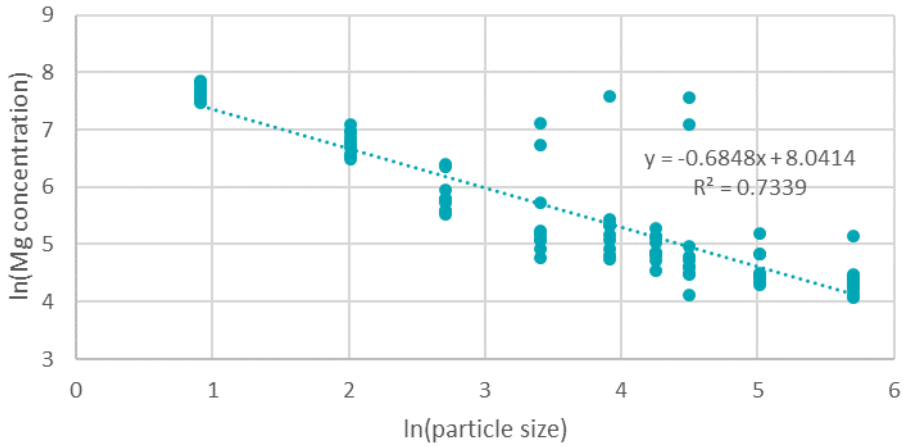

Figure C.1: Correlations of particle size and element concentration at the example of Mg. a) Logarithmic correlation between mean Mg concentrations and particle size (mean value of class, e.g. 300 mm for class 200 - 400 mm); b) Linear correlation between ln(Mg concentrations) vs. ln(particle size) for mean Mg concentrations; c) linear correlation of ln(Mg concentrations) vs. ln(particle size) for all 90 data points.

Table C.1: Results for statistical analyses of the analyte concentration [mg/kg$_{DM}$; ash and impurities in %, LHV in kJ/kg] - particle size correlation: Significantly different ($p < 0.05$) mean values according to one-way ANOVA, Correlations, Pearson and Spearman correlation coefficients, R^2, and p-values.

Element	Mean values significantly different	p	Regression analysis of whole population, n = 90, Pearson					Regression analysis of whole population, n = 90, Spearman				
			Correlation ln(x) vs. ln(GS)	Significant	Pearson r	R^2	p	Correlation ln(x) vs. ln(GS)	Significant	Spearman ρ	R^2	p
Ag	Yes	1.91E-14	Yes, negative	Yes	-0.71	0.50	5.27E-15	Yes, negative	Yes	-0.70	0.50	9.27E-15
Al	Yes	2.62E-16	Yes, negative	Yes	-0.76	0.57	5.68E-18	Yes, negative	Yes	-0.79	0.63	8.94E-21
As	Yes	1.02E-12	Yes, negative	Yes	-0.64	0.41	9.18E-12	Yes, negative	Yes	-0.60	0.36	5.78E-10
Ba	Yes	6.60E-11	Yes, negative	Yes	-0.67	0.45	5.75E-13	Yes, negative	Yes	-0.66	0.44	1.20E-12
Ca	Yes	1.21E-11	Yes, negative	Yes	-0.71	0.51	3.08E-15	Yes, negative	Yes	-0.69	0.47	6.91E-14
Cd	No	4.35E-01	No	No	-0.07	0.00	5.37E-01	Yes, negative	Yes	-0.22	0.05	3.65E-02
Cl	Yes	1.33E-04	**Yes, positive**	Yes	0.56	0.31	1.03E-08	**Yes, positive**	Yes	0.43	0.19	2.15E-05
Co	Yes	7.67E-04	Yes, negative	Yes	-0.75	0.56	2.59E-17	Yes, negative	Yes	-0.80	0.63	5.87E-21
Cr	No	2.91E-01	Yes, negative	Yes	-0.49	0.24	9.55E-07	Yes, negative	Yes	-0.50	0.25	3.94E-07
Cu	Yes	1.02E-02	Yes, negative	Yes	-0.58	0.33	3.07E-09	Yes, negative	Yes	-0.62	0.39	5.21E-11
Fe	Yes	2.58E-16	Yes, negative	Yes	-0.81	0.65	5.26E-22	Yes, negative	Yes	-0.79	0.62	3.25E-20
Hg	Yes	1.48E-08	Yes, negative	Yes	-0.76	0.58	3.92E-18	Yes, negative	Yes	-0.74	0.54	1.23E-16
K	Yes	1.85E-20	Yes, negative	Yes	-0.83	0.69	3.12E-24	Yes, negative	Yes	-0.83	0.69	6.14E-24
Li	Yes	2.46E-17	Yes, negative	Yes	-0.78	0.60	2.94E-19	Yes, negative	Yes	-0.76	0.58	2.03E-18
Mg	Yes	2.34E-19	Yes, negative	Yes	-0.83	0.69	5.12E-24	Yes, negative	Yes	-0.83	0.68	1.23E-23
Mn	Yes	4.86E-18	Yes, negative	Yes	-0.77	0.60	4.21E-19	Yes, negative	Yes	-0.72	0.52	9.18E-16
Mo	Yes	4.39E-19	Yes, negative	Yes	-0.73	0.53	4.54E-16	Yes, negative	Yes	-0.69	0.47	8.69E-14
Na	Yes	1.13E-22	Yes, negative	Yes	-0.78	0.61	1.21E-19	Yes, negative	Yes	-0.75	0.57	1.20E-17
Ni	Yes	4.63E-05	Yes, negative	Yes	-0.75	0.57	8.96E-18	Yes, negative	Yes	-0.79	0.62	2.59E-20
P	Yes	6.13E-08	Yes, negative	Yes	-0.69	0.47	7.54E-14	Yes, negative	Yes	-0.70	0.49	1.85E-14
Pb	No	5.87E-02	Yes, negative	Yes	-0.27	0.08	8.89E-03	Yes, negative	Yes	-0.21	0.05	4.29E-02
Pd	Yes	1.31E-05	Yes, negative	Yes	-0.48	0.23	1.75E-06	Yes, negative	Yes	-0.48	0.23	1.98E-06
Sb	No	1.38E-02	**Yes, positive**	Yes	0.30	0.09	4.06E-03	**Yes, positive**	Yes	0.22	0.05	3.46E-02
Si	Yes	1.34E-17	Yes, negative	Yes	-0.80	0.65	1.35E-21	Yes, negative	Yes	-0.78	0.61	1.19E-19
Sn	Yes	6.59E-03	Yes, negative	Yes	-0.66	0.44	1.05E-12	Yes, negative	Yes	-0.71	0.50	8.04E-15
Sr	Yes	6.68E-15	Yes, negative	Yes	-0.80	0.64	4.46E-21	Yes, negative	Yes	-0.78	0.61	6.78E-20
Ti	No	1.88E-01	Yes, negative	Yes	-0.22	0.05	3.56E-02	Yes, negative	Yes	-0.23	0.06	2.58E-02
V	Yes	1.21E-04	Yes, negative	Yes	-0.42	0.18	3.65E-05	Yes, negative	Yes	-0.42	0.17	4.43E-05
W	Yes	2.65E-06	Yes, negative	Yes	-0.60	0.36	5.21E-10	Yes, negative	Yes	-0.70	0.50	9.68E-15
Zn	Yes	1.13E-03	Yes, negative	Yes	-0.46	0.21	6.56E-06	Yes, negative	Yes	-0.46	0.21	5.74E-06
Ash	Yes	4.71E-06	Yes, negative	Yes	-0.76	0.57	1.91E-09	Yes, negative	Yes	-0.73	0.53	1.63E-08
Impurities	Yes	1.06E-08	**Yes, positive**	Yes	0.63	0.40	2.94E-11	**Yes, positive**	Yes	0.35	0.12	7.69E-04
LHV	Yes	1.05E-22	**Yes, positive**	Yes	0.81	0.66	3.83E-22	**Yes, positive**	Yes	0.83	0.69	6.14E-24

Legend: Strong correlation, r ≥ 0.5 or r ≤ -0.5 | Moderate correlation, r ≥ 0.3 or r ≤ -0.3 | Weak correlation, r ≥ 0.1 or r ≤ -0.1 | No correlation 0.1 > r > -0.1

Table C.2: Results for statistical analyses of the analyte concentration [mg/MJ] - particle size correlation: Correlations, Pearson correlation coefficients, R^2 and p-values for linear regression analysis for all samples (n = 90)

	Regression analysis of whole population, n = 90, Pearson					Regression analysis of whole population, n = 90, Spearman				
Element	Correlation ln(x) vs. ln(GS)	Significant	Pearson r	R^2	p	Correlation ln(x) vs. ln(GS)	Significant	Spearman ρ	R^2	p
Ag	Yes, negative	Yes	-0.85	0.72	5.72E-26	Yes, negative	Yes	-0.81	0.66	2.65E-22
Al	Yes, negative	Yes	-0.86	0.74	2.60E-27	Yes, negative	Yes	-0.86	0.73	7.15E-27
As	Yes, negative	Yes	-0.78	0.61	1.02E-19	Yes, negative	Yes	-0.71	0.50	6.72E-15
Ba	Yes, negative	Yes	-0.79	0.63	1.89E-20	Yes, negative	Yes	-0.77	0.59	8.19E-19
Ca	Yes, negative	Yes	-0.81	0.65	6.27E-22	Yes, negative	Yes	-0.78	0.60	2.34E-19
Cd	Yes, negative	Yes	-0.41	0.17	5.30E-05	Yes, negative	Yes	-0.43	0.19	1.97E-05
Cl	No	No	-0.09	0.01	3.84E-01	No	No	-0.08	0.01	4.76E-01
Co	Yes, negative	Yes	-0.82	0.67	1.14E-22	Yes, negative	Yes	-0.83	0.69	4.71E-24
Cr	Yes, negative	Yes	-0.70	0.49	1.10E-14	Yes, negative	Yes	-0.65	0.42	5.32E-12
Cu	Yes, negative	Yes	-0.73	0.53	3.77E-16	Yes, negative	Yes	-0.73	0.54	2.43E-16
Fe	Yes, negative	Yes	-0.83	0.69	4.43E-24	Yes, negative	Yes	-0.84	0.70	5.12E-25
Hg	Yes, negative	Yes	-0.83	0.69	2.32E-24	Yes, negative	Yes	-0.84	0.70	1.04E-24
K	Yes, negative	Yes	-0.86	0.73	5.02E-27	Yes, negative	Yes	-0.87	0.76	5.47E-29
Li	Yes, negative	Yes	-0.84	0.70	1.05E-24	Yes, negative	Yes	-0.82	0.67	5.11E-23
Mg	Yes, negative	Yes	-0.86	0.73	4.96E-27	Yes, negative	Yes	-0.86	0.74	7.85E-28
Mn	Yes, negative	Yes	-0.81	0.66	3.07E-22	Yes, negative	Yes	-0.79	0.63	9.00E-21
Mo	Yes, negative	Yes	-0.80	0.64	5.54E-21	Yes, negative	Yes	-0.77	0.59	8.78E-19
Na	Yes, negative	Yes	-0.84	0.70	7.06E-25	Yes, negative	Yes	-0.82	0.67	1.06E-22
Ni	Yes, negative	Yes	-0.83	0.69	2.93E-24	Yes, negative	Yes	-0.84	0.70	5.45E-25
P	Yes, negative	Yes	-0.83	0.69	8.20E-24	Yes, negative	Yes	-0.80	0.65	1.51E-21
Pb	Yes, negative	Yes	-0.55	0.30	2.26E-08	Yes, negative	Yes	-0.47	0.22	2.71E-06
Pd	Yes, negative	Yes	-0.80	0.64	2.84E-21	Yes, negative	Yes	-0.83	0.69	4.51E-24
Sb	Yes, negative	Yes	-0.41	0.17	5.82E-05	Yes, negative	Yes	-0.44	0.19	1.73E-05
Si	Yes, negative	Yes	-0.83	0.69	5.63E-24	Yes, negative	Yes	-0.82	0.67	3.81E-23
Sn	Yes, negative	Yes	-0.79	0.63	1.16E-20	Yes, negative	Yes	-0.82	0.68	2.02E-23
Sr	Yes, negative	Yes	-0.83	0.69	2.83E-24	Yes, negative	Yes	-0.82	0.67	5.81E-23
Ti	Yes, negative	Yes	-0.76	0.58	2.56E-18	Yes, negative	Yes	-0.72	0.52	1.52E-15
V	Yes, negative	Yes	-0.67	0.45	5.95E-13	Yes, negative	Yes	-0.67	0.45	3.28E-13
W	Yes, negative	Yes	-0.72	0.51	1.98E-15	Yes, negative	Yes	-0.75	0.56	1.59E-17
Zn	Yes, negative	Yes	-0.77	0.59	8.23E-19	Yes, negative	Yes	-0.74	0.55	9.45E-17

Legend:	Strong correlation	Moderate correlation	Weak correlation	No correlation
	r ≥ 0.5 or r ≤ -0.5	r ≥ 0.3 or r ≤ -0.3	r ≥ 0.1 or r ≤ -0.1	0.1 > r > -0.1

C.2. Element-element and element-LHV correlations

Figure C.2: Statistically significant ($p < 0.05$) positive (petrol blue) and negative (beige) element-element and element-LHV correlations in all 90 samples. The size of the circles is proportional to the strength of the linear correlation. The numbers in the plot represent Pearson (left) and Spearman (right) correlation coefficients

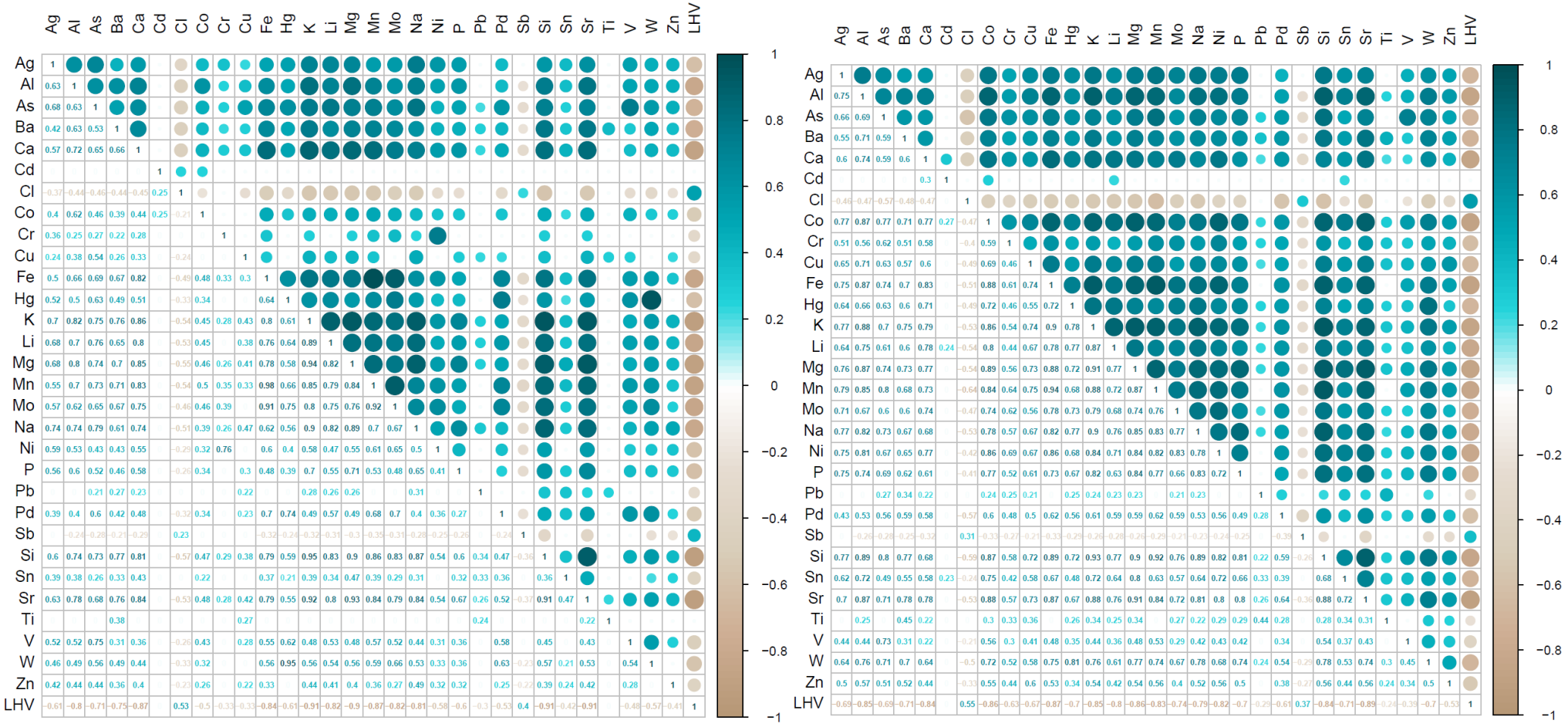

Figure C.3: Statistically significant ($p < 0.05$) positive (petrol blue) and negative (beige) element-element and element-LHV correlations for 5 of 10 representative samples, for which the ash content was determined. The size of the circles is proportional to the strength of the linear correlation. The numbers in the plot represent Pearson (left) and Spearman (right) correlation coefficients

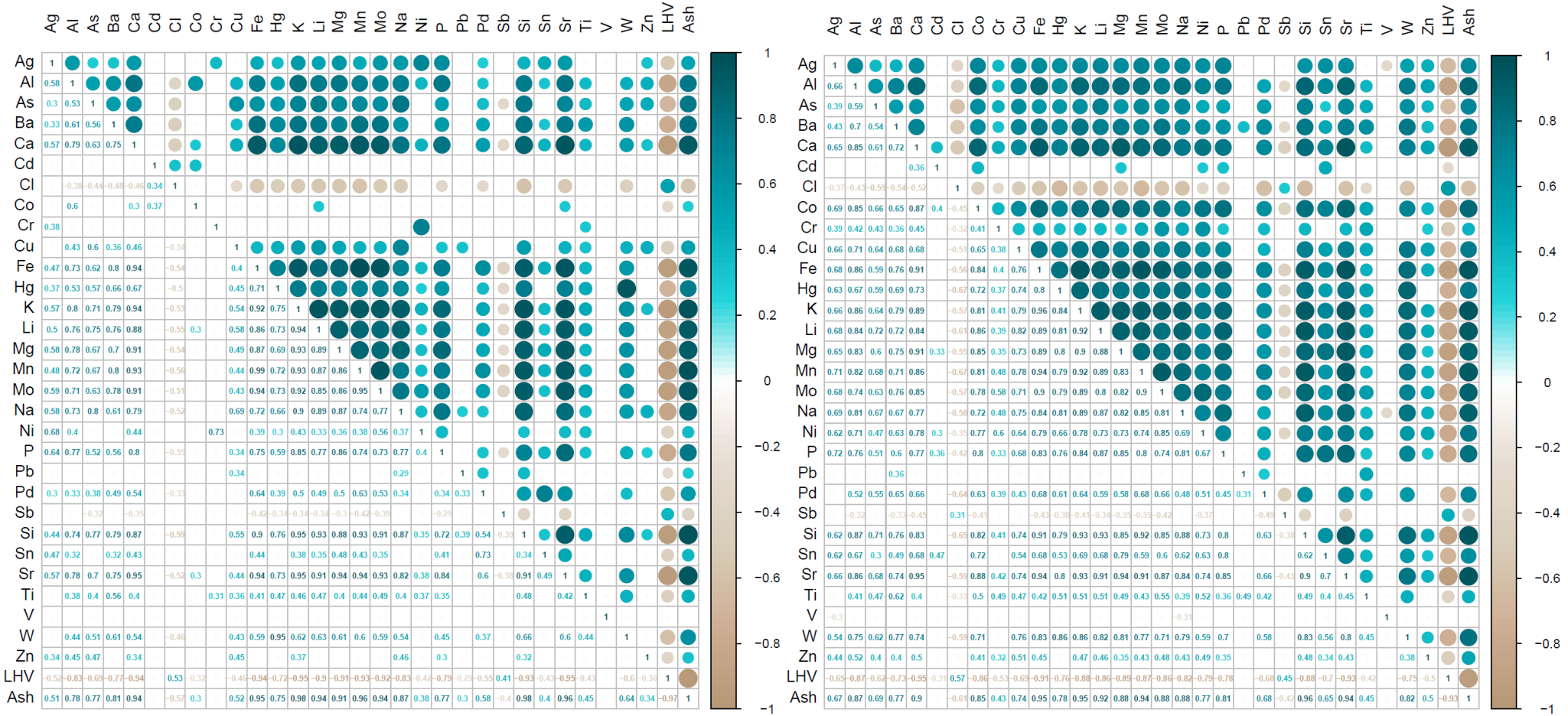

Figure C.4: Statistically significant ($p < 0.05$) positive (petrol blue) and negative (beige) element-element and element-LHV correlations for small fractions < 20 mm. The size of the circles is proportional to the strength of the linear correlation. The numbers in the plot represent Pearson (left) and Spearman (right) correlation coefficients

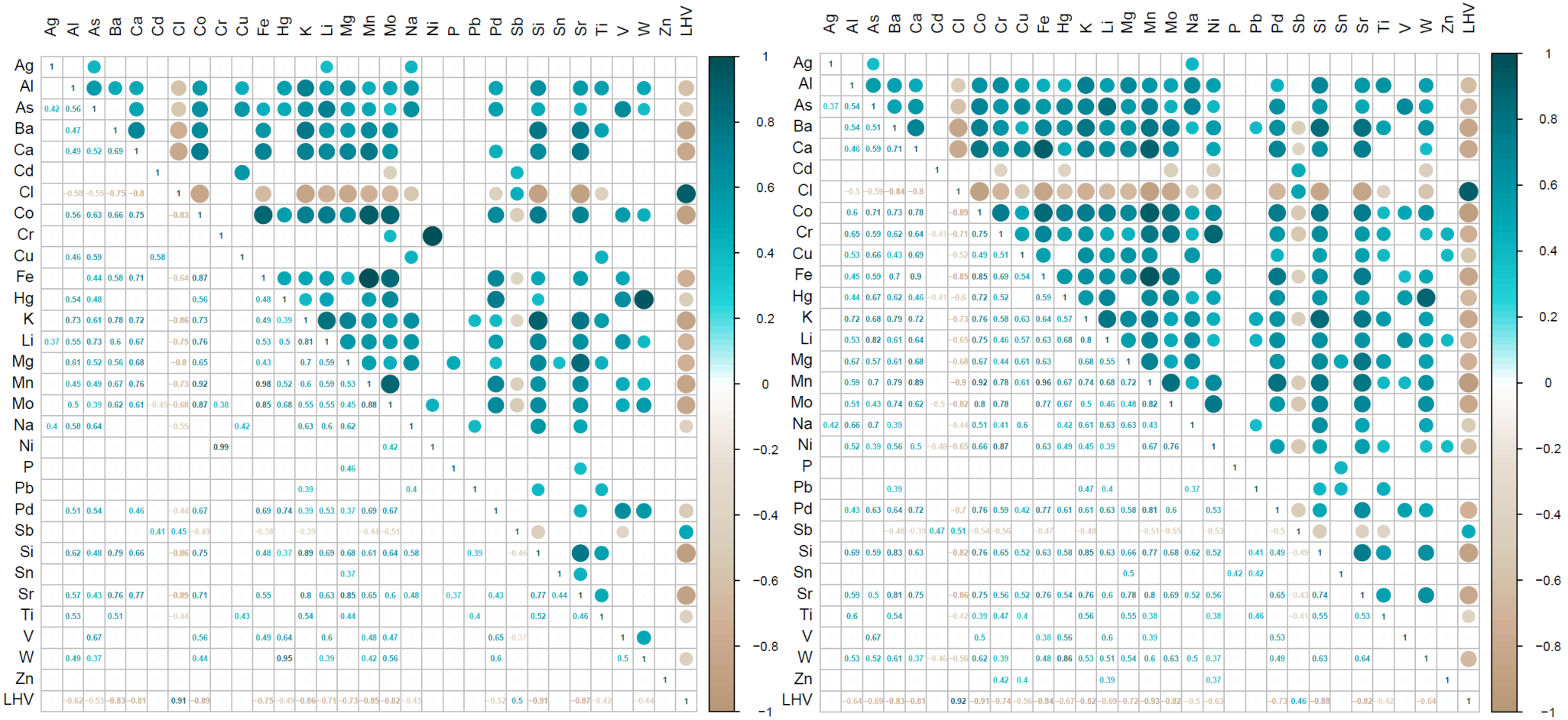

Figure C.5: Statistically significant ($p < 0.05$) positive (petrol blue) and negative (beige) element-element correlations in the fractions < 5 mm after magnetic separation. The size of the circles is proportional to the strength of the linear correlation. The numbers in the plot represent Pearson (left) and Spearman (right) correlation coefficients. Note, that correlations might not indicate elements occurring together in the same material, but rather which elements are transferred into the same fraction by magnetic separation

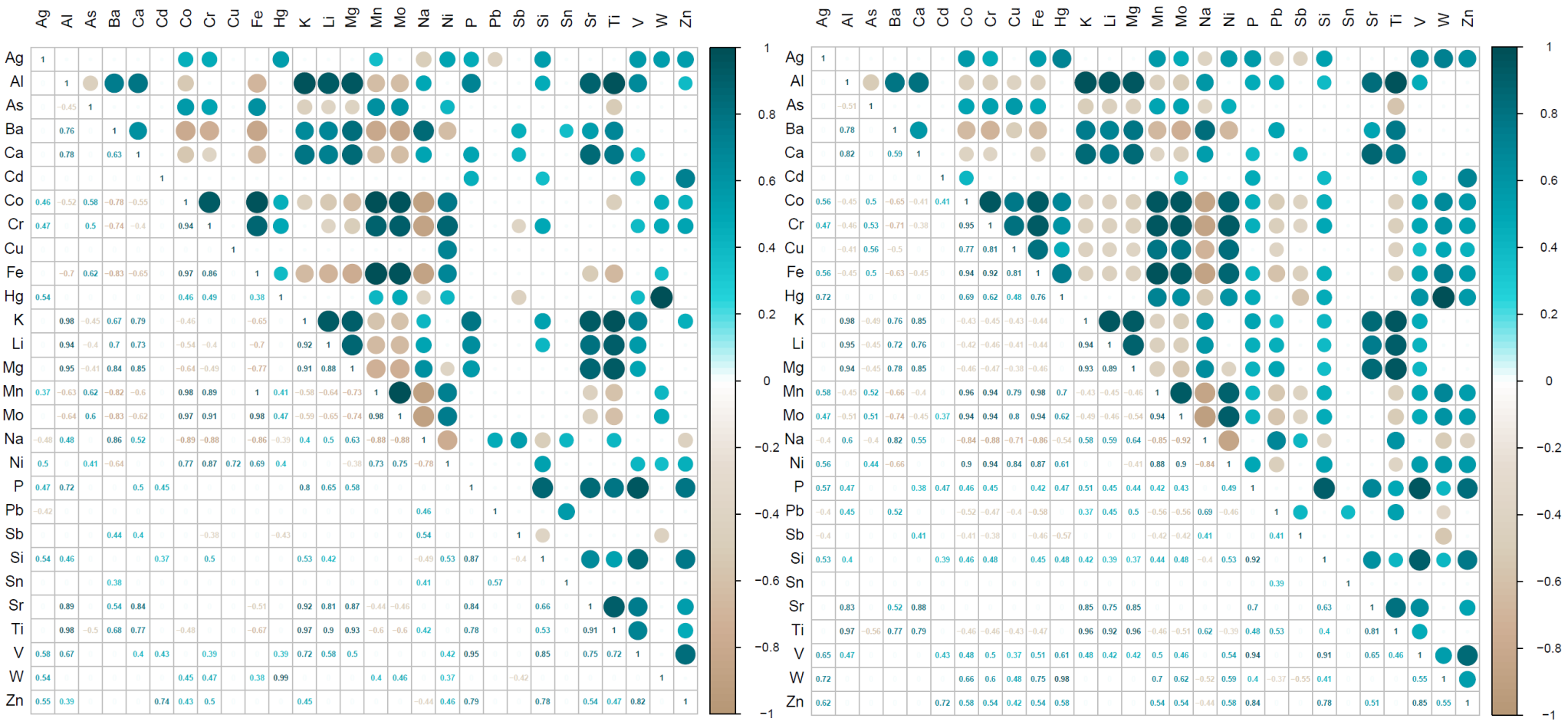

Appendix D - Effect of removing particle size classes

D.1. Overall concentrations in the original waste mix

Table D.1: Calculated average concentration, standard deviation and median values of the 30 analytes in the original waste mix. Note, that the overall Pd concentration is likely overestimated as values below the L.O.Q. (0.25 mg/kg$_{DM}$) were considered in the calculations with 0.25 mg/kg$_{DM}$.

Element, Unit		Average	Standard deviation	Median
Ag	mg/kg$_{DM}$	1.8	0.15	1.8
Al	mg/kg$_{DM}$	10900	990	10800
As	mg/kg$_{DM}$	8.8	1.0	8.9
Ba	mg/kg$_{DM}$	730	170	700
Ca	mg/kg$_{DM}$	73800	11500	76800
Cd	mg/kg$_{DM}$	2.6	2.5	1.9
Cl	%$_{DM}$	0.83	0.26	0.79
Co	mg/kg$_{DM}$	10	3.4	8.9
Cr	mg/kg$_{DM}$	160	45	150
Cu	mg/kg$_{DM}$	300	15	260
Fe	mg/kg$_{DM}$	44300	12700	41400
Hg	mg/kg$_{DM}$	0.58	0.25	0.49
K	mg/kg$_{DM}$	2700	380	2560
Li	mg/kg$_{DM}$	6.4	1.2	6.5
Mg	mg/kg$_{DM}$	4850	860	4540
Mn	mg/kg$_{DM}$	540	100	510
Mo	mg/kg$_{DM}$	28	3.7	27
Na	mg/kg$_{DM}$	5080	990	4790
Ni	mg/kg$_{DM}$	63	16	63
P	mg/kg$_{DM}$	440	89	420
Pb	mg/kg$_{DM}$	240	78	230
Pd	mg/kg$_{DM}$	0.26	0.01	0.26
Sb	mg/kg$_{DM}$	32	6	29
Si	mg/kg$_{DM}$	50000	12700	46600
Sn	mg/kg$_{DM}$	160	110	120
Sr	mg/kg$_{DM}$	170	30	170
Ti	mg/kg$_{DM}$	2110	240	2080
V	mg/kg$_{DM}$	13	2.3	13
W	mg/kg$_{DM}$	99	62	84
Zn	mg/kg$_{DM}$	390	79	370
LHV	kJ/kg$_{DM}$	15800	1000	16100

D.2. Concentrations of As, Cd, Cl, Co, Cr, Hg, Ni, Pb, and Sb in screen underflow and overflow after a single screening step and comparison with limit values

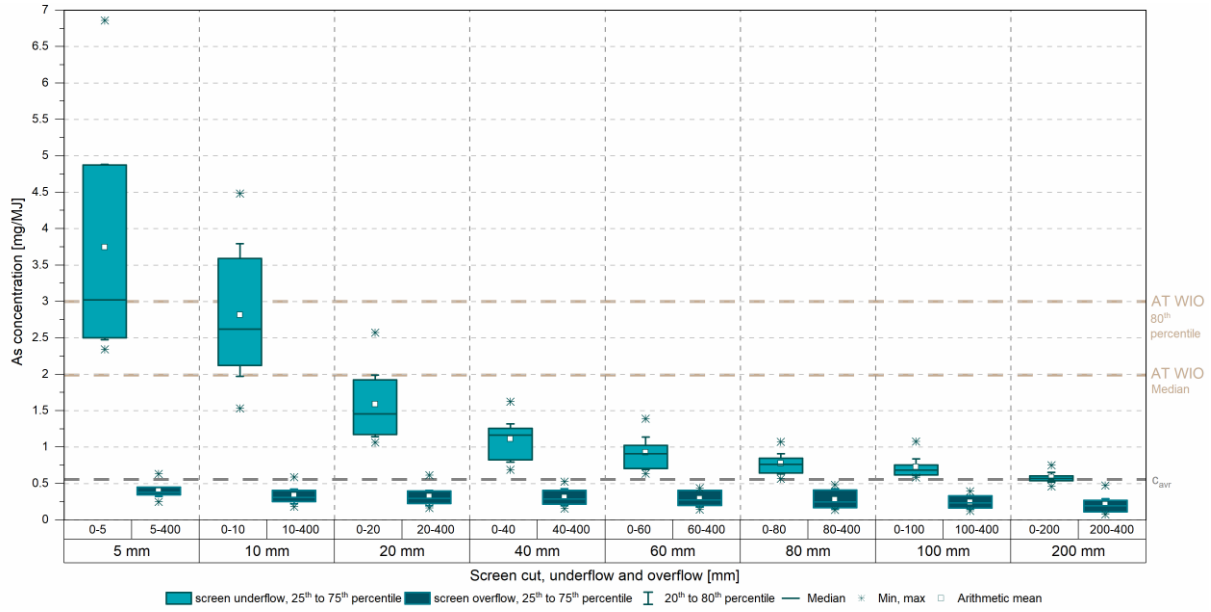

Figure D.1: Calculated As concentrations [mg/MJ] in screen overflow and underflow after a single screening step and comparison with limit values from the Austrian waste incineration ordinance (AT WIO) (BMLFUW, 2010)

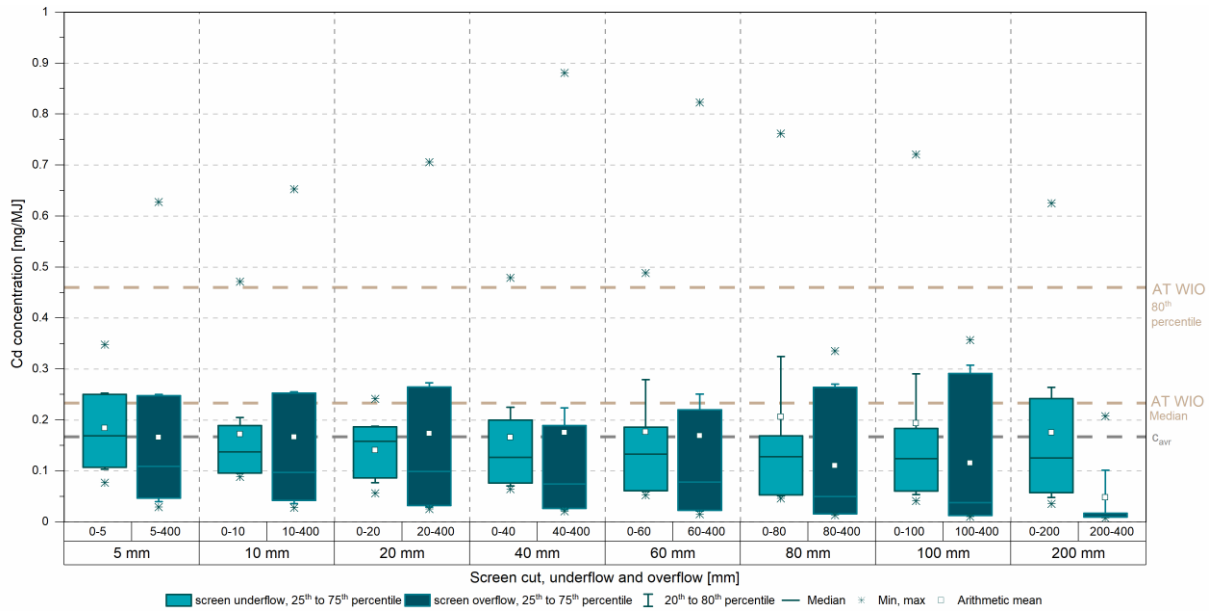

Figure D.2: Calculated Cd concentrations [mg/MJ] in screen overflow and underflow after a single screening step and comparison with limit values from the Austrian waste incineration ordinance (AT WIO) (BMLFUW, 2010)

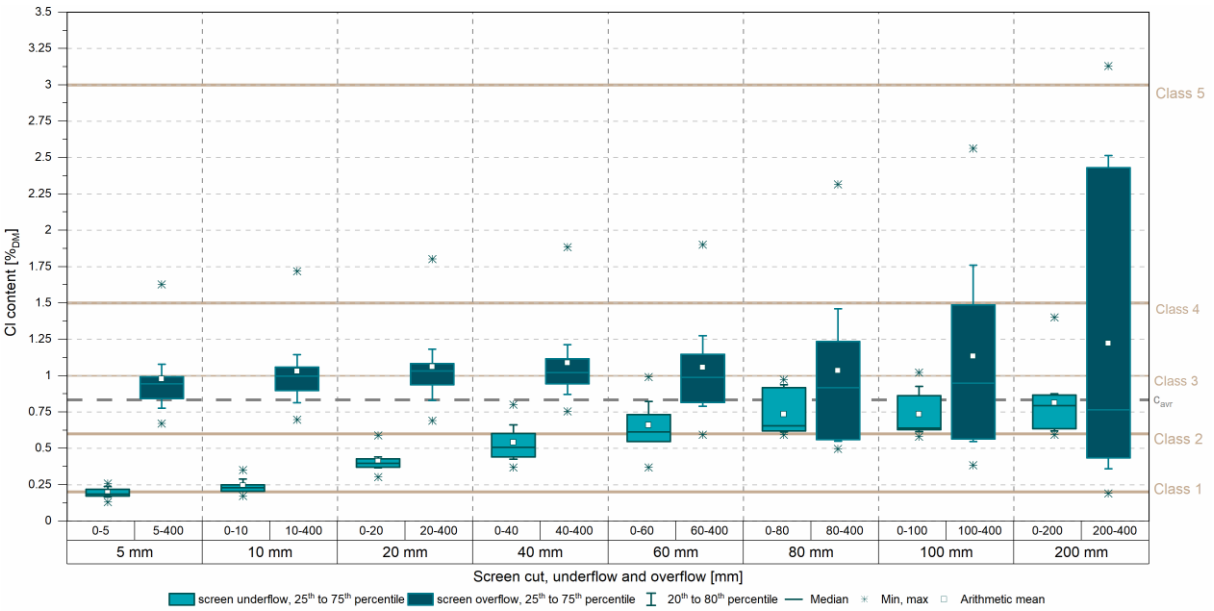

Figure D.3: Calculated Cl contents [%DM] in screen overflow and underflow after a single screening step and comparison with limit values for the classes listed in EN 15359 (ASI, 2011)

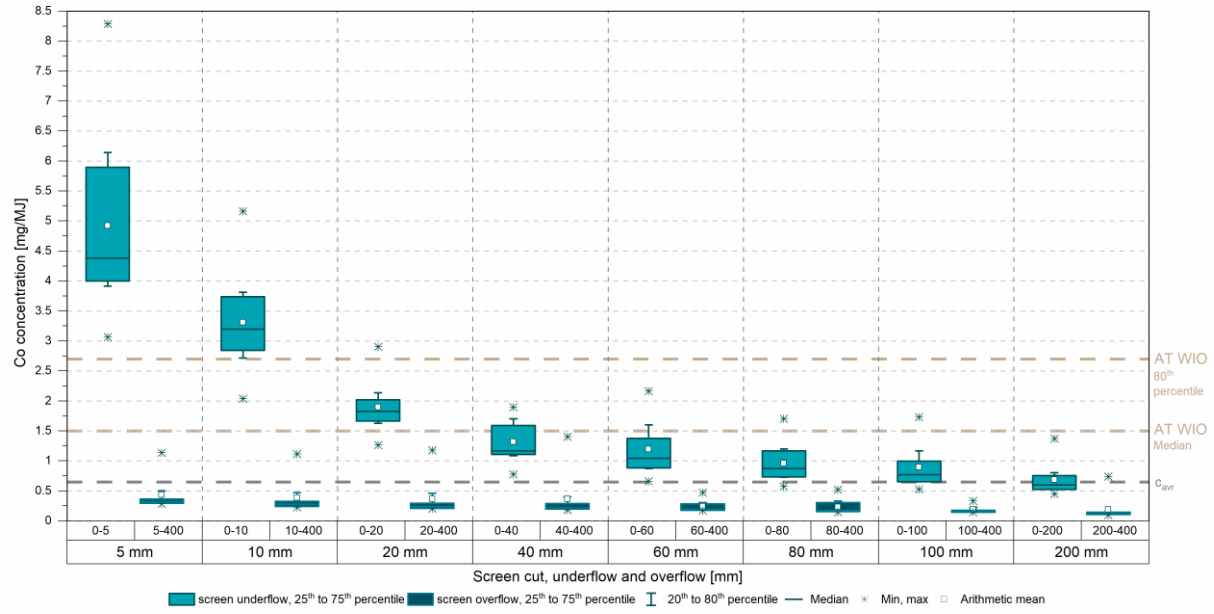

Figure D.4: Calculated Co concentrations [mg/MJ] in screen overflow and underflow after a single screening step and comparison with limit values from the Austrian waste incineration ordinance (AT WIO) (BMLFUW, 2010)

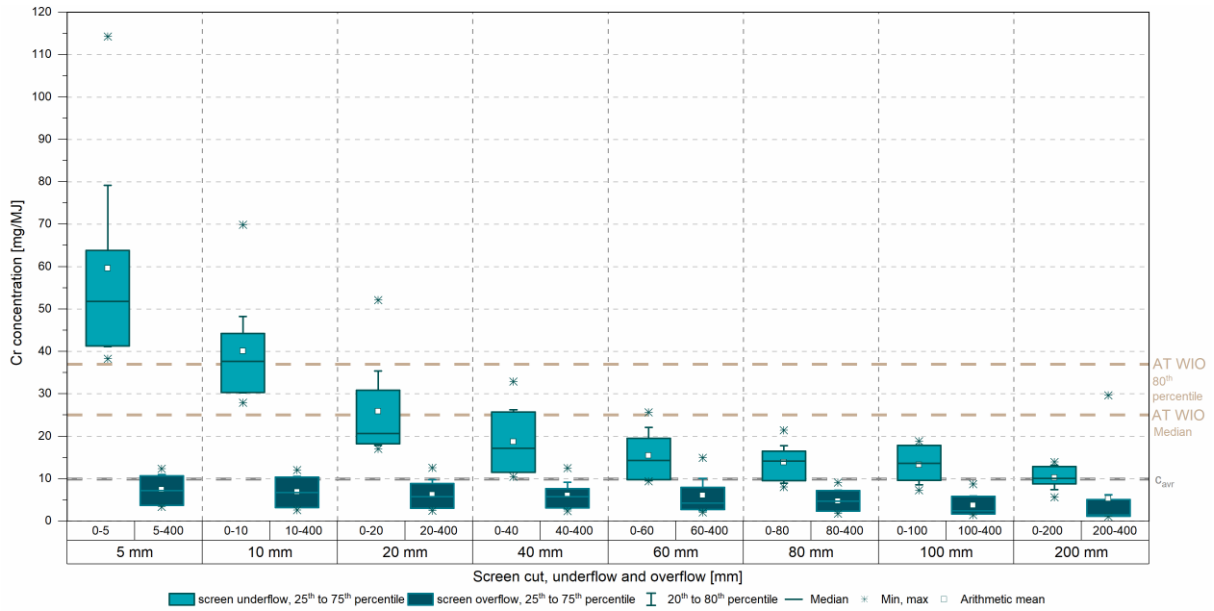

Figure D.5: Calculated Cr concentrations [mg/MJ] in screen overflow and underflow after a single screening step and comparison with limit values from the Austrian waste incineration ordinance (AT WIO) (BMLFUW, 2010)

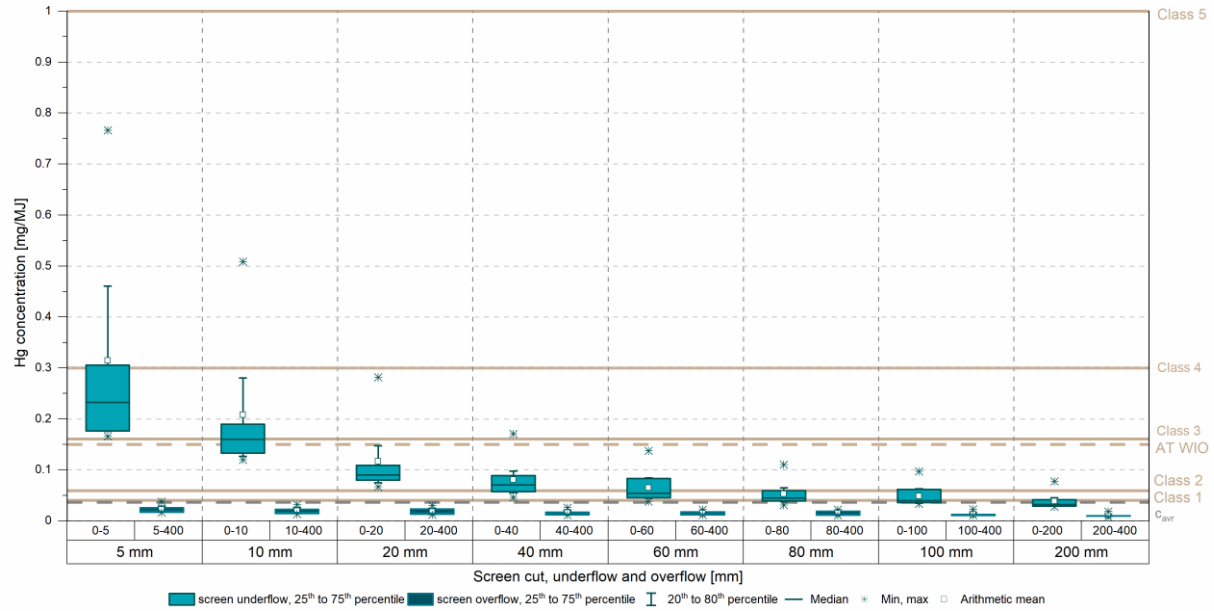

Figure D.6: Calculated Hg concentrations [mg/MJ] in screen overflow and underflow after a single screening step and comparison with the 80th percentile limit values from EN 15359 (ASI, 2011) and the Austrian waste incineration ordinance (AT WIO) (BMLFUW, 2010)

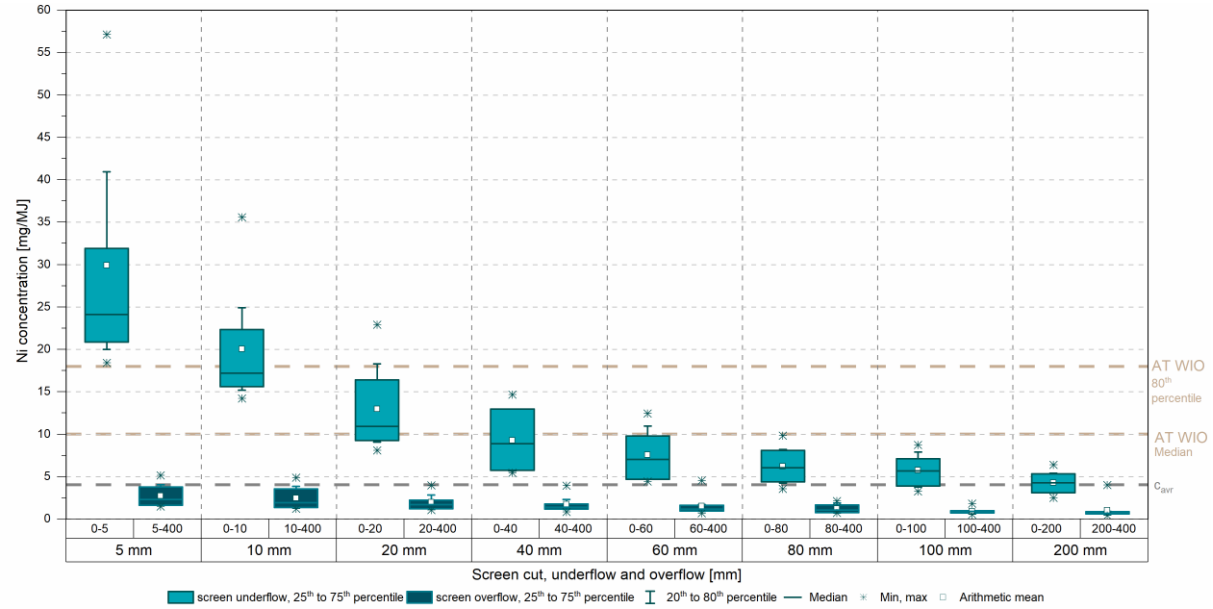

Figure D.7: Calculated Ni concentrations [mg/MJ] in screen overflow and underflow after a single screening step and comparison with limit values from the Austrian waste incineration ordinance (AT WIO) (BMLFUW, 2010)

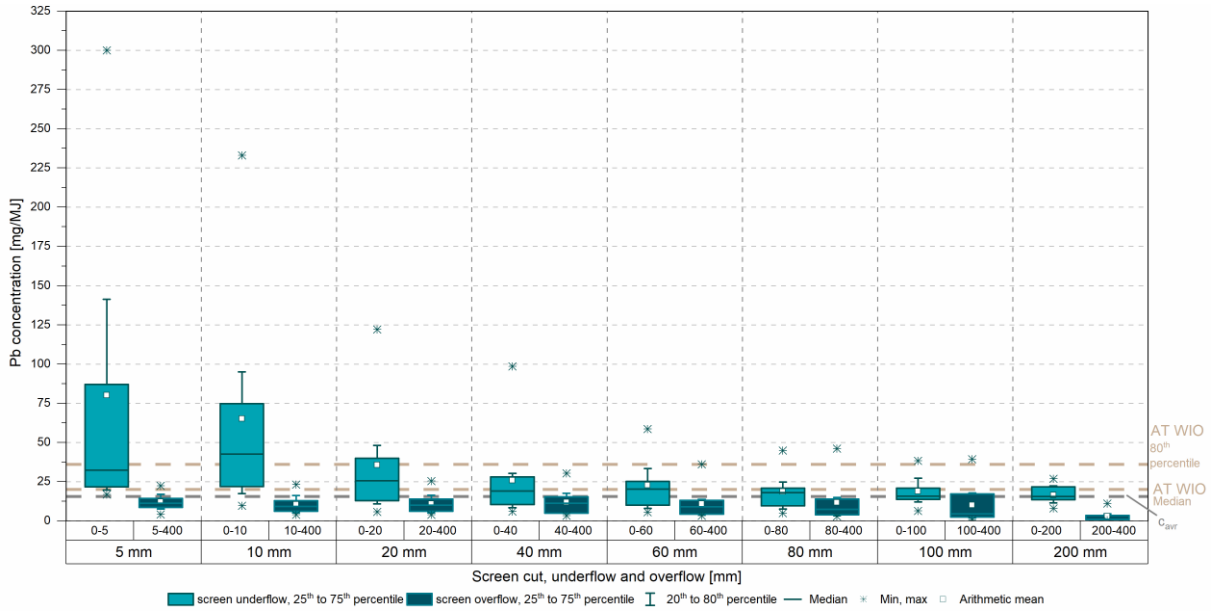

Figure D.8: Calculated Pb concentrations [mg/MJ] in screen overflow and underflow after a single screening step and comparison with limit values from the Austrian waste incineration ordinance (AT WIO) (BMLFUW, 2010)

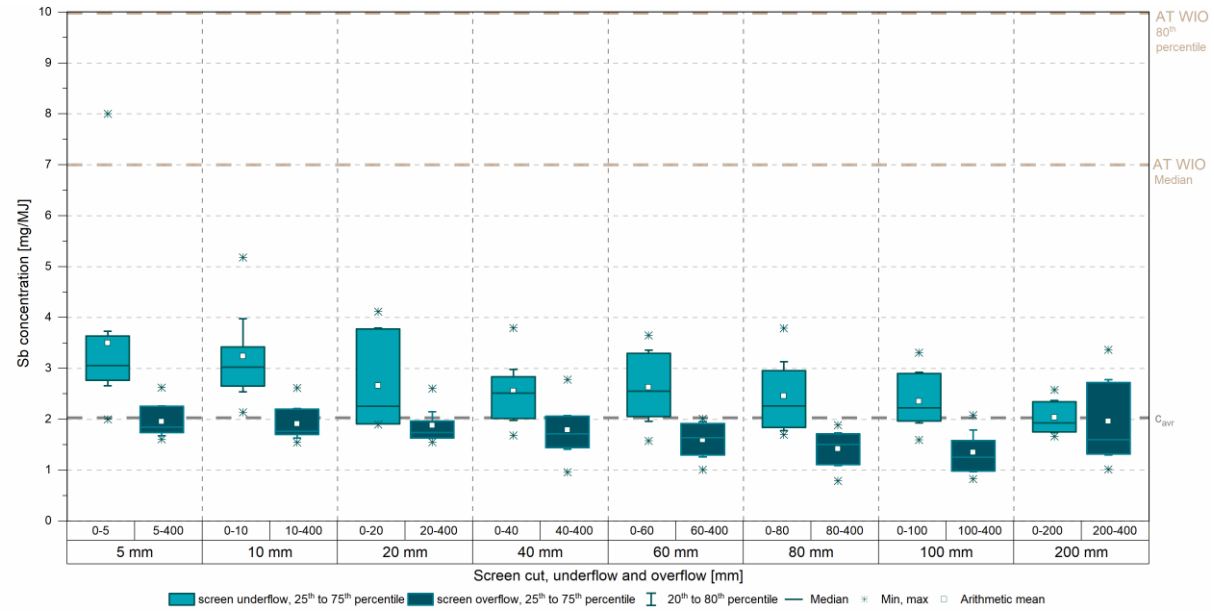

Figure D.9: Calculated Sb concentrations [mg/MJ] in screen overflow and underflow after a single screening step and comparison with limit values from the Austrian waste incineration ordinance (AT WIO) (BMLFUW, 2010)

D.3. Average element concentrations, ash content and LHV of screen underflow and overflow after a single screening step

Table D.2: Calculated average (n=10) element concentration, ash content and LHV of screen underflow and overflow after a single screening step at 5, 10, 20, 40, 60, 80, 100 or 200 mm

Element, unit		5 mm		10 mm		20 mm		40 mm		60 mm		80 mm		100 mm		200 mm		Original
		0-5	5-400	0-10	10-400	0-20	20-400	0-40	40-400	0-60	60-400	0-80	80-400	0-100	100-400	0-200	200-400	0-400
Ag	mg/kg_{DM}	2.8	1.5	3.0	1.3	2.9	1.2	2.5	1.1	2.3	1.0	2.1	1.1	2.0	1.0	1.8	1.3	**1.8**
Al	mg/kg_{DM}	15400	9830	15300	9360	14700	8780	14000	8070	13600	7120	12800	6670	12300	5970	11096	5362	**10900**
As	mg/kg_{DM}	16	7.2	16	6.3	14	6.2	12	6.1	11	5.9	10	5.8	9.8	5.4	8.9	5.3	**8.8**
Ba	mg/kg_{DM}	1440	570	1300	550	1100	540	1010	490	950	450	870	440	850	350	750	300	**730**
Ca	mg/kg_{DM}	120000	63300	115000	60000	103000	57900	94900	55300	89400	53300	83600	53100	81900	48000	75100	42700	**73800**
Cd	mg/kg_{DM}	0.78	3.0	0.99	3.2	1.2	3.4	1.8	3.4	2.1	3.4	2.7	2.3	2.6	2.5	2.6	1.2	**2.6**
Cl	mg/kg_{DM}	1950	9770	2430	10300	4100	10600	5400	10900	6600	10600	7340	10300	7340	11300	8110	12200	**8330**
Co	mg/kg_{DM}	20	7.8	19	7.1	16	6.9	14	7.1	14	4.9	13	4.8	12	4.2	10	4.5	**10**
Cr	mg/kg_{DM}	250	130	230	130	220	120	200	120	180	120	180	100	180	84	160	130	**160**
Cu	mg/kg_{DM}	450	260	570	200	470	200	500	130	440	110	390	110	370	77	310	150	**300**
Fe	mg/kg_{DM}	114000	28200	97600	26100	82100	23800	70400	21600	63200	19500	56200	19100	53500	15000	45700	15500	**44300**
Hg	mg/kg_{DM}	1.3	0.41	1.2	0.37	1.0	0.35	0.88	0.31	0.79	0.30	0.70	0.31	0.67	0.29	0.59	0.26	**0.58**
K	mg/kg_{DM}	5250	2120	5100	1890	4530	1710	4040	1530	3700	1380	3310	1380	3170	1160	2760	1310	**2700**
Li	mg/kg_{DM}	12	5.1	12	4.6	10	4.4	9.1	4.1	8.4	3.8	7.7	3.6	7.4	3.2	6.6	3.0	**6.4**
Mg	mg/kg_{DM}	9050	3900	9000	3460	8070	3110	7130	2840	6570	2580	5900	2580	5670	2210	4970	2130	**4850**
Mn	mg/kg_{DM}	1220	380	1080	350	920	330	800	310	720	290	650	300	630	260	550	290	**540**
Mo	mg/kg_{DM}	72	18	62	16	51	15	44	14	39	13	35	13	33	11	28	13	**28**
Na	mg/kg_{DM}	9280	4130	10500	3280	9070	2940	7970	2570	7100	2430	6310	2460	6040	2000	5210	2180	**5080**
Ni	mg/kg_{DM}	120	50	110	50	110	40	97	34	88	31	81	25	77	20	65	24	**63**
P	mg/kg_{DM}	630	390	650	360	640	320	620	280	570	260	520	260	500	230	440	250	**440**
Pb	mg/kg_{DM}	350	220	370	200	300	210	250	230	260	220	240	250	250	220	250	65	**240**
Pd	mg/kg_{DM}	0.31	0.25	0.30	0.25	0.28	0.25	0.28	0.25	0.27	0.25	0.27	0.25	0.27	0.25	0.26	0.25	**0.26**
Sb	mg/kg_{DM}	15	36	19	37	23	37	27	36	31	33	33	30	32	31	31	53	**32**
Si	mg/kg_{DM}	122000	33600	115000	28400	93700	26500	79900	24000	72000	21100	63100	21900	60400	16500	51500	17500	**50000**
Sn	mg/kg_{DM}	360	120	330	110	290	94	240	88	240	58	220	40	200	34	170	38	**160**
Sr	mg/kg_{DM}	330	140	320	120	280	120	250	110	230	100	210	100	200	89	180	76	**170**
Ti	mg/kg_{DM}	2290	2070	2240	2070	2140	2100	2150	2080	2190	2010	2210	1890	2190	1830	2120	1830	**2110**
V	mg/kg_{DM}	22	11	21	11	19	10	17	10	17	9.3	16	8.5	15	8.4	14	9.2	**13**
W	mg/kg_{DM}	270	62	240	53	200	48	170	36	150	32	130	33	120	28	100	22	**99**
Zn	mg/kg_{DM}	450	370	500	350	470	340	450	330	440	310	430	290	420	280	390	290	**390**
Ash	$\%_{DM}$	71	29	66	27	57	26	52	24	48	22	43	23	42	18	37	17	**37**
LHV	kJ/kg_{DM}	4260	18500	5800	19200	8620	19700	10800	20200	12100	20700	13300	21300	13700	22600	15400	26300	**15800**

D.4. Percentage distribution of analytes in screen underflow and overflow after a single screening step

Table D.3: Calculated percentage of each parameter ending up in screen underflow and overflow after a single screening step at 5, 10, 20, 40, 60, 80, 100 or 200 mm

Element, unit	5 mm		10 mm		20 mm		40 mm		60 mm		80 mm		100 mm		200 mm		Original
	0-5	5-400	0-10	10-400	0-20	20-400	0-40	40-400	0-60	60-400	0-80	80-400	0-100	100-400	0-200	200-400	0-400
Ag %	29	71	43	57	57	43	67	33	75	25	81	19	86	14	96	4	**100**
Al %	26	74	35	65	47	53	61	39	72	28	81	19	87	13	98	2	**100**
As %	33	67	47	53	55	45	64	36	72	28	80	20	86	14	97	3	**100**
Ba %	36	64	44	56	52	48	65	35	74	26	81	19	89	11	98	2	**100**
Ca %	30	70	39	61	49	51	60	40	69	31	77	23	85	15	97	3	**100**
Cd %	6	94	10	90	17	83	33	67	48	52	75	25	79	21	98	2	**100**
Cl %	4	96	7	93	17	83	30	70	45	55	60	40	67	33	93	7	**100**
Co %	38	62	48	52	56	44	64	36	79	21	85	15	90	10	98	2	**100**
Cr %	30	70	38	62	50	50	59	41	66	34	79	21	87	13	96	4	**100**
Cu %	30	70	49	51	56	44	77	23	84	16	89	11	94	6	98	2	**100**
Fe %	49	51	56	44	65	35	74	26	81	19	87	13	92	8	98	2	**100**
Hg %	42	58	52	48	61	39	71	29	78	22	83	17	88	12	98	2	**100**
K %	36	64	47	53	58	42	70	30	78	22	84	16	90	10	97	3	**100**
Li %	35	65	47	53	55	45	66	34	75	25	82	18	88	12	98	2	**100**
Mg %	34	66	46	54	58	42	69	31	77	23	84	16	89	11	98	2	**100**
Mn %	43	57	51	49	60	40	69	31	77	23	83	17	89	11	97	3	**100**
Mo %	49	51	57	43	65	35	74	26	81	19	85	15	90	10	98	2	**100**
Na %	34	66	51	49	62	38	73	27	80	20	85	15	91	9	98	2	**100**
Ni %	37	63	47	53	61	39	72	28	80	20	88	12	92	8	98	2	**100**
P %	27	73	38	62	52	48	66	34	74	26	82	18	87	13	97	3	**100**
Pb %	25	75	37	63	42	58	47	53	60	40	68	32	78	22	99	1	**100**
Pd %	22	78	28	72	38	62	49	51	59	41	70	30	78	22	96	4	**100**
Sb %	9	91	14	86	24	76	40	60	56	44	70	30	77	23	93	7	**100**
Si %	45	55	57	43	65	35	74	26	82	18	86	14	92	8	98	2	**100**
Sn %	40	60	50	50	61	39	70	30	85	15	92	8	95	5	99	1	**100**
Sr %	35	65	46	54	56	44	67	33	75	25	82	18	88	12	98	2	**100**
Ti %	20	80	26	74	35	65	47	53	59	41	72	28	79	21	96	4	**100**
V %	31	69	41	59	51	49	61	39	71	29	81	19	86	14	97	3	**100**
W %	49	51	60	40	68	32	80	20	86	14	90	10	93	7	99	1	**100**
Zn %	22	78	33	67	43	57	55	45	66	34	77	23	83	17	96	4	**100**
Ash %	34	66	43	57	53	47	65	35	75	25	81	19	89	11	98	2	**100**
LHV %	5	95	9	91	19	81	32	68	44	56	57	43	66	34	92	8	**100**

Appendix E - Characterization of the fraction < 5 mm

E.1. Average concentrations in fractions after magnetic separation

Table E.1: Average element concentrations (n = 10) in the magnetic and non-magnetic fractions, distribution [%] among the three fractions (normalized to 100%), and average recovery of the element in comparison to the initial concentration in the fine fraction < 5 mm (see Appendix B)

Element	Average concentration [mg/kg$_{DM}$]			Distribution among fractions [%]			Recovery [%]
	Magnetic I	Magnetic II	Non-magnetic	Magnetic I	Magnetic II	Non-magnetic	
Ag	3.5	3.2	1.7	35	15	50	88
Al	12100	24400	17700	18	15	67	110
As	12	7.1	8.9	30	9	62	65
Ba	640	1560	1790	11	11	78	102
Ca	71300	107000	96700	20	13	68	75
Cd	0.96	1.1	0.62	32	14	54	105
Co	38	17	10	53	11	36	88
Cr	470	260	92	56	15	30	87
Cu	620	660	290	34	23	43	119
Fe	349000	40600	12200	87	5	8	91
Hg	2.0	1.6	0.82	43	14	43	93
K	3820	7360	5060	19	16	65	94
Li	8	15	11	18	14	68	94
Mg	5950	11500	9720	17	14	70	98
Mn	3270	910	460	67	8	25	100
Mo	120	26	4.4	84	8	8	53
Na	1080	6120	11300	3	8	89	88
Ni	290	180	33	62	18	19	97
P	700	1180	470	29	21	50	94
Pb	97	140	340	10	6	84	130
Pd	0.34	0.64	0.44	19	16	65	147
Sb	11	11	17	19	8	73	110
Si	313000	421000	146000	37	20	42	184
Sn	110	97	530	9	3	88	169
Sr	260	440	300	22	15	63	90
Ti	1300	3050	1930	17	17	66	82
V	36	52	23	30	19	51	162
W	190	150	80	46	13	41	49
Zn	670	780	380	34	17	49	111

E.2. Element concentrations in fractions for all composite samples

Table E.2: Element concentrations in fraction "Magnetic I"

Element, Unit		Composite Sample No.									
		1	2	3	4	5	6	7	8	9	10
Ag	mg/kg_{DM}	< 2.5	2.6	< 2.5	2.5	< 2.5	5.8	3.6	2.8	3.6	3.5
Al	mg/kg_{DM}	11200	11900	12300	12800	12300	14700	11800	9480	12200	12200
As	mg/kg_{DM}	9.6	11	12	14	11	10	13	11	13	11
Ba	mg/kg_{DM}	510	760	560	640	560	740	630	560	650	770
Ca	mg/kg_{DM}	80000	71700	72500	81200	84700	85700	59400	54700	62200	60900
Cd	mg/kg_{DM}	0.58	1.3	0.86	0.87	0.77	0.51	0.62	1.4	0.63	2.1
Co	mg/kg_{DM}	35	36	38	34	34	35	42	40	43	42
Cr	mg/kg_{DM}	400	460	560	410	420	420	640	420	460	480
Cu	mg/kg_{DM}	580	700	570	530	610	590	670	770	560	600
Fe	mg/kg_{DM}	344000	361000	338000	306000	330000	278000	386000	408000	373000	365000
Hg	mg/kg_{DM}	1.3	1.4	1.4	1.3	1.1	2.7	4.8	1.4	2.6	2.2
K	mg/kg_{DM}	3580	4010	3900	4240	3990	4710	3490	2660	3940	3670
Li	mg/kg_{DM}	7.1	7.4	8.3	8.7	7.8	9.0	7.3	6.6	8.0	7.7
Mg	mg/kg_{DM}	7120	6530	6520	6060	5660	6990	5030	4440	5550	5620
Mn	mg/kg_{DM}	3200	3320	3150	3040	3050	2710	3530	3690	3500	3470
Mo	mg/kg_{DM}	110	120	110	110	110	100	180	150	120	120
Na	mg/kg_{DM}	1370	1190	1890	790	810	1850	490	710	880	800
Ni	mg/kg_{DM}	230	260	300	260	260	320	400	290	290	280
P	mg/kg_{DM}	740	790	720	770	680	790	660	480	650	680
Pb	mg/kg_{DM}	56	94	340	91	51	67	91	55	54	66
Pd	mg/kg_{DM}	0.42	0.35	0.32	0.42	0.34	0.39	0.26	0.27	0.31	0.27
Sb	mg/kg_{DM}	8.9	12	12	16	12	10	11	13	10	9.2
Si	mg/kg_{DM}	329000	332000	313000	321000	298000	335000	299000	295000	313000	296000
Sn	mg/kg_{DM}	100	110	100	100	84	92	130	120	110	110
Sr	mg/kg_{DM}	300	250	240	310	260	310	210	190	250	240
Ti	mg/kg_{DM}	1250	1450	1520	1360	1250	1430	1240	940	1200	1340
V	mg/kg_{DM}	35	37	37	39	36	38	40	31	34	36
W	mg/kg_{DM}	100	140	120	96	110	260	460	170	230	230
Zn	mg/kg_{DM}	500	720	650	710	660	700	580	700	640	860
Mass share of fraction	$\%_{DM}$ referring to sum of the 3 fractions	25%	20%	20%	24%	22%	29%	27%	45%	24%	17%

Table E.3: Element concentrations in fraction "Magnetic II"

Element, Unit		Composite Sample No.									
		1	2	3	4	5	6	7	8	9	10
Ag	mg/kg_{DM}	< 2.5	2.8	3.1	3.0	< 2.5	2.7	3.7	4.7	4.1	3.3
Al	mg/kg_{DM}	21800	26300	23400	24200	24100	12600	28900	25600	27700	28900
As	mg/kg_{DM}	6.9	7.9	7.6	9.0	7.8	3.5	6.6	7.3	7.8	6.3
Ba	mg/kg_{DM}	1290	1790	1190	1410	1400	770	1940	1890	1960	2000
Ca	mg/kg_{DM}	125000	117000	111000	116000	134000	61600	100000	99300	108000	103000
Cd	mg/kg_{DM}	0.67	2.5	0.91	1.0	1.5	0.31	0.63	0.83	0.72	1.7
Co	mg/kg_{DM}	16	18	20	18	16	9.4	17	16	20	22
Cr	mg/kg_{DM}	260	240	390	360	250	140	240	210	210	340
Cu	mg/kg_{DM}	290	340	300	3410	400	210	400	550	370	360
Fe	mg/kg_{DM}	36500	40900	39300	41600	39800	22300	48500	45300	45200	46200
Hg	mg/kg_{DM}	0.94	1.3	1.3	1.1	1.0	1.1	4.7	1.6	1.5	1.6
K	mg/kg_{DM}	6470	8340	7350	7580	7690	4120	8060	6600	8800	8560
Li	mg/kg_{DM}	13	15	15	15	15	7.6	17	16	18	16
Mg	mg/kg_{DM}	11900	12900	10700	11500	11300	6030	12000	12000	12500	14300
Mn	mg/kg_{DM}	750	960	1000	990	900	490	1070	930	970	1010
Mo	mg/kg_{DM}	22	25	36	30	30	16	27	24	24	21
Na	mg/kg_{DM}	4500	6980	6480	5330	6930	3110	6990	5950	6940	7940
Ni	mg/kg_{DM}	140	120	210	540	140	71	130	160	110	160
P	mg/kg_{DM}	1120	1400	1140	1250	1220	630	1270	980	1300	1500
Pb	mg/kg_{DM}	97	150	490	110	75	41	110	98	84	110
Pd	mg/kg_{DM}	0.73	0.73	0.59	1.1	0.64	0.30	0.55	0.54	0.58	0.62
Sb	mg/kg_{DM}	13	13	12	13	13	4.7	8.1	15	7.6	11
Si	mg/kg_{DM}	548000	460000	468000	464000	413000	200000	463000	412000	416000	369000
Sn	mg/kg_{DM}	110	110	97	96	83	39	160	73	88	110
Sr	mg/kg_{DM}	500	500	410	460	460	230	420	400	490	490
Ti	mg/kg_{DM}	2830	3530	3160	3000	2910	1550	3440	3050	3170	3790
V	mg/kg_{DM}	41	57	50	55	50	27	61	53	56	69
W	mg/kg_{DM}	72	110	120	88	88	100	440	170	150	160
Zn	mg/kg_{DM}	670	1230	830	730	720	380	690	850	720	980
Mass share of fraction	$\%_{DM}$ referring to sum of the 3 fractions	12%	12%	11%	13%	12%	10%	10%	8%	9%	8%

Table E.4: Element concentrations in fraction "Non-magnetic"

Element, Unit		Composite Sample No.									
		1	2	3	4	5	6	7	8	9	10
Ag	mg/kg_{DM}	1.3	1.3	0.84	1.3	2.7	3.1	1.8	1.7	1.7	1.5
Al	mg/kg_{DM}	17400	17800	16100	17900	17700	18000	19400	21000	16100	15400
As	mg/kg_{DM}	8.4	8.4	6.7	11	12	6.8	9.4	14	5.2	7.5
Ba	mg/kg_{DM}	1660	2270	1310	1980	1660	1720	2200	2160	1580	1330
Ca	mg/kg_{DM}	113000	92500	73400	91400	117000	115000	98800	117000	75700	73200
Cd	mg/kg_{DM}	0.37	0.71	0.59	0.44	0.84	0.84	0.43	0.38	< 0.25	1.3
Co	mg/kg_{DM}	12	11	8.3	10	10	10	9.0	8.4	7.7	9.1
Cr	mg/kg_{DM}	85	100	90	110	96	95	84	120	72	68
Cu	mg/kg_{DM}	420	490	330	350	160	260	140	530	90	130
Fe	mg/kg_{DM}	12300	12300	10800	12900	12600	12300	14500	14400	10100	10100
Hg	mg/kg_{DM}	0.40	0.88	0.39	0.56	0.46	0.86	2.7	0.71	0.49	0.71
K	mg/kg_{DM}	4530	4940	4660	5230	5460	5410	5680	5450	4790	4430
Li	mg/kg_{DM}	11	9.7	13	14	14	10	11	11	9.1	11
Mg	mg/kg_{DM}	10300	9880	7990	10600	9460	10400	9890	12400	8160	8120
Mn	mg/kg_{DM}	510	440	370	420	650	480	450	510	380	370
Mo	mg/kg_{DM}	4.0	5.8	4.2	7.1	5.8	3.5	3.6	3.3	2.9	3.6
Na	mg/kg_{DM}	10600	10500	11100	11800	10800	12800	12100	12700	10200	10700
Ni	mg/kg_{DM}	28	35	28	41	32	66	27	29	21	22
P	mg/kg_{DM}	570	590	420	520	510	480	470	350	340	410
Pb	mg/kg_{DM}	450	140	950	210	68	280	140	910	120	150
Pd	mg/kg_{DM}	0.54	0.51	0.34	0.81	0.42	0.43	0.38	0.45	0.29	0.27
Sb	mg/kg_{DM}	21	19	9.4	20	19	21	12	20	14	13
Si	mg/kg_{DM}	135000	150000	148000	160000	148000	141000	151000	151000	104000	174000
Sn	mg/kg_{DM}	370	72	230	140	51	96	1370	2560	78	310
Sr	mg/kg_{DM}	330	340	230	300	300	340	290	350	240	230
Ti	mg/kg_{DM}	1720	2070	1880	1920	1810	2240	2100	2260	1640	1690
V	mg/kg_{DM}	24	26	21	23	24	25	27	27	16	16
W	mg/kg_{DM}	33	79	37	51	41	81	280	77	49	70
Zn	mg/kg_{DM}	360	510	270	330	440	450	520	290	220	380
LHV	MJ/kg_{DM}	4670	5270	3930	4890	3310	3910	3700	2720	2990	3920
Mass share of fraction	$\%_{DM}$ referring to sum of the 3 fractions	64%	68%	69%	63%	66%	61%	63%	46%	67%	75%

E.3. XRD patterns

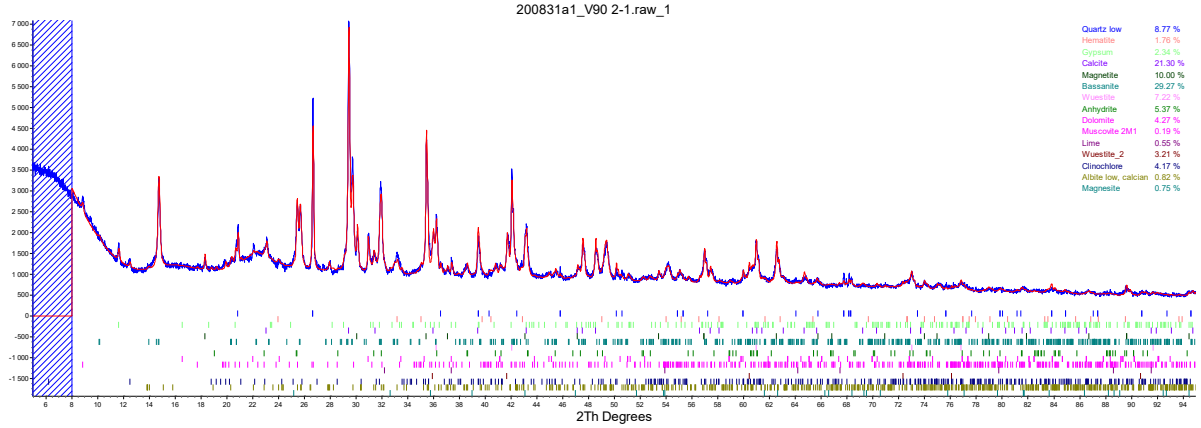

Figure E.1: XRD pattern of Magnetic Fraction I of composite sample 1

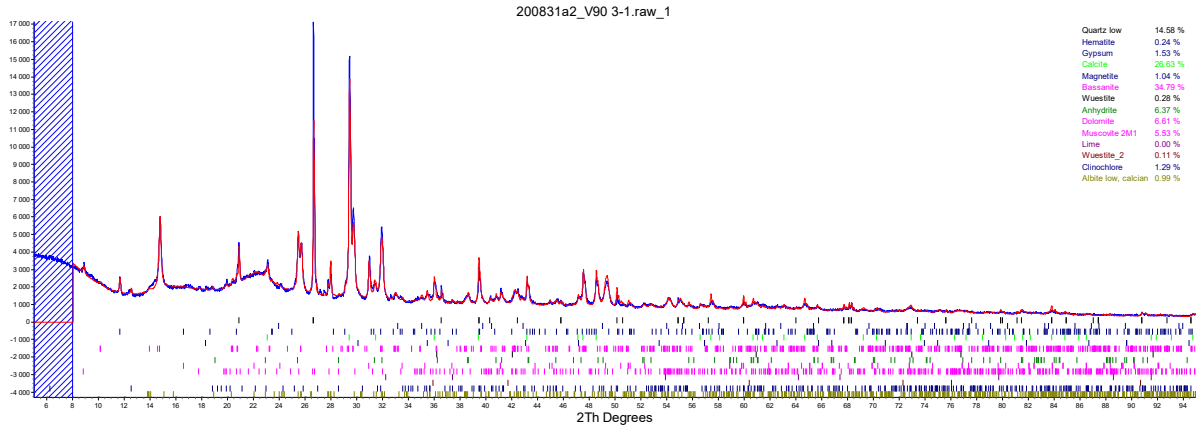

Figure E.2: XRD pattern of Magnetic Fraction II of composite sample 1

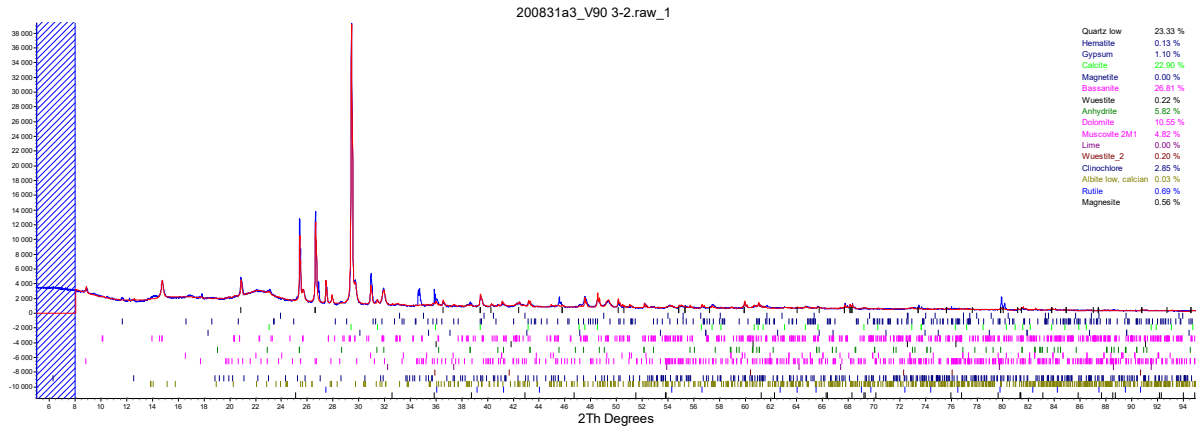

Figure E.3: XRD pattern of the non-magnetic fraction of composite sample 1

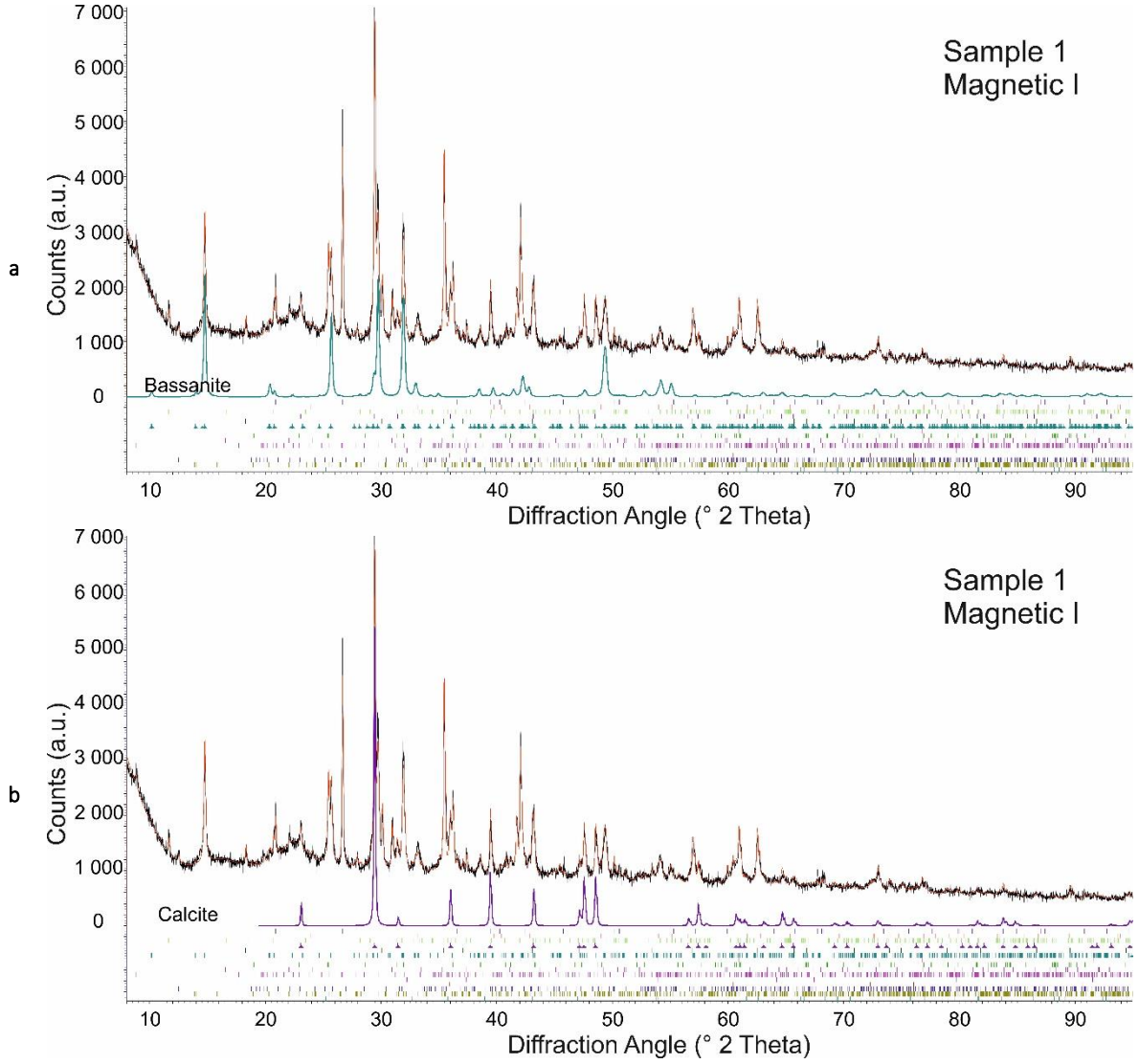

Figure E.4: XRD pattern of the non-magnetic fraction of composite sample 1 and calculated patterns for a) bassanite and b) calcite

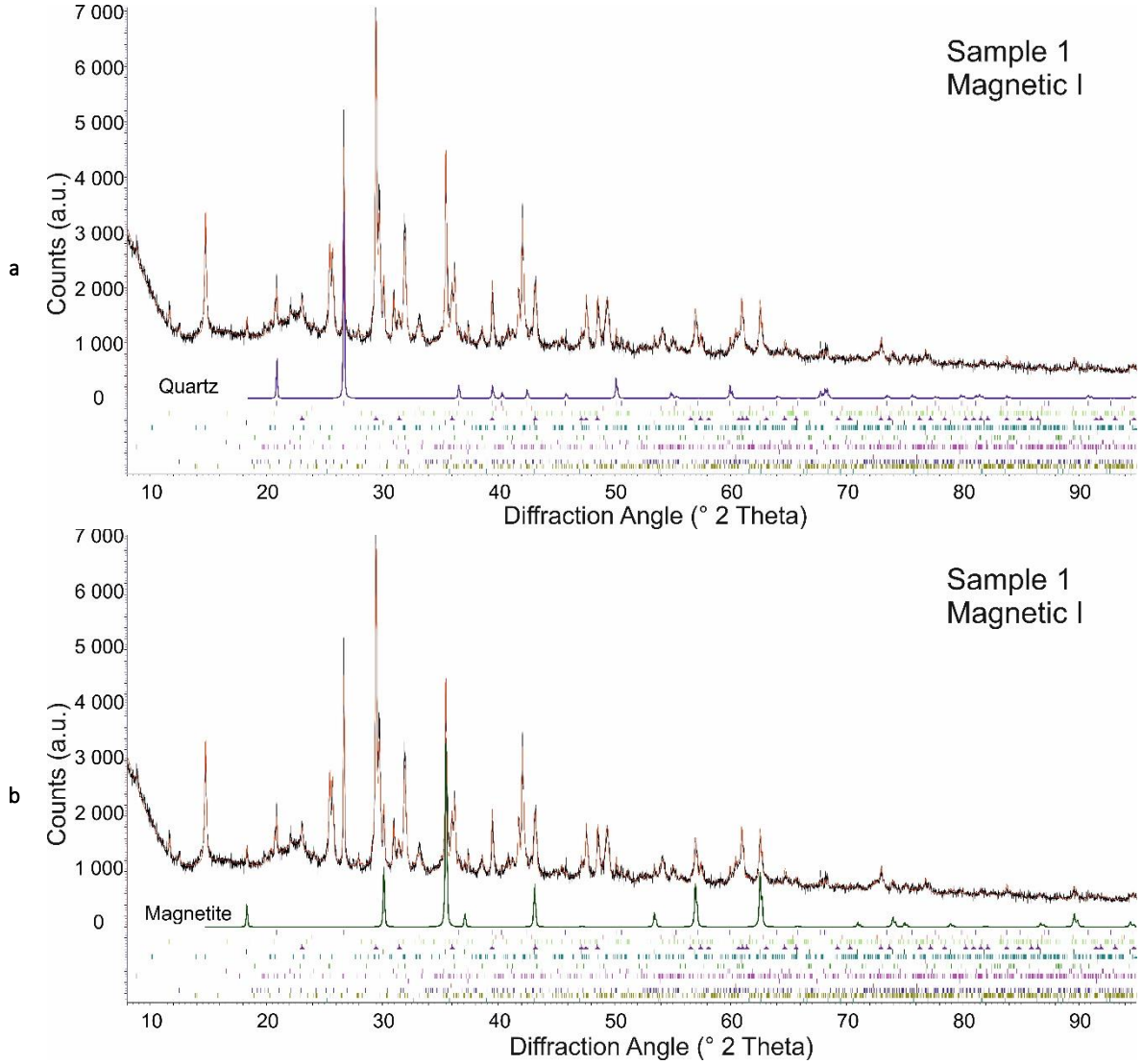

Figure E.5: XRD pattern of the non-magnetic fraction of composite sample 1 and calculated patterns for a) quartz and b) magnetite

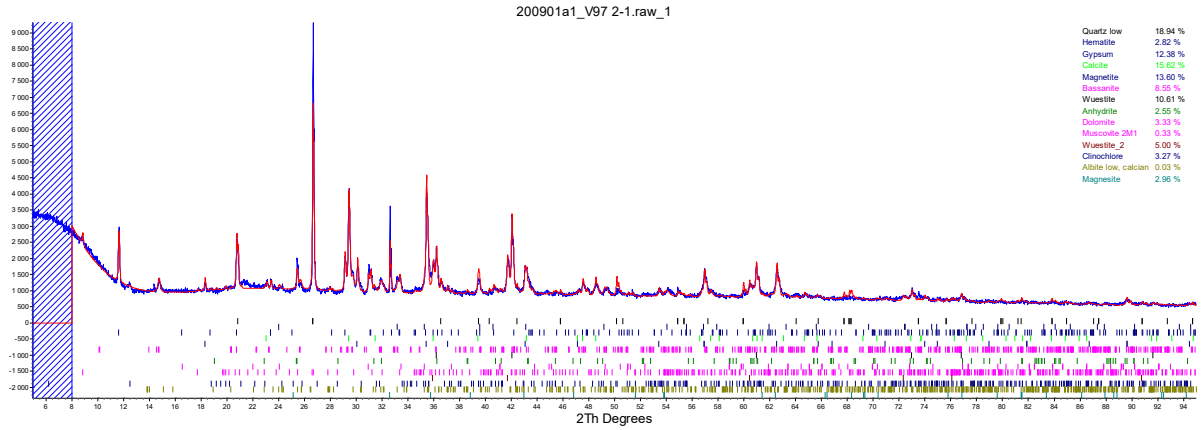

Figure E.6: XRD pattern of Magnetic Fraction I of composite sample 8

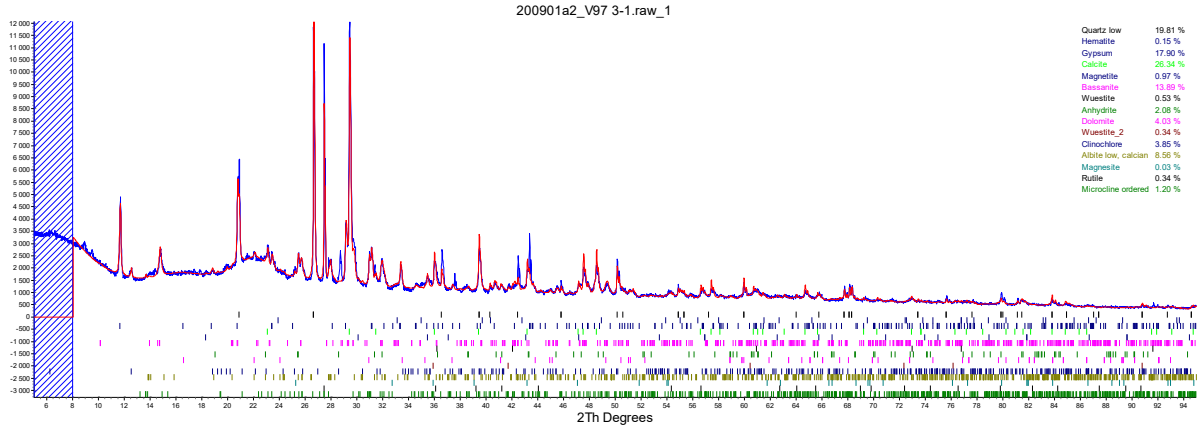

Figure E.7: XRD pattern of Magnetic Fraction II of composite sample 8

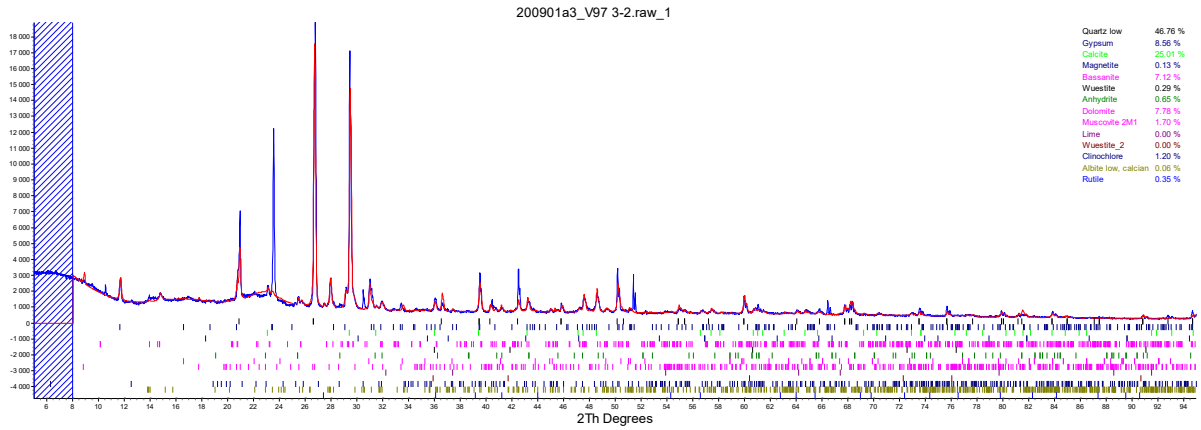

Figure E.8: XRD pattern of the non-magnetic fraction of composite sample 8

E.4. Mössbauer spectroscopy

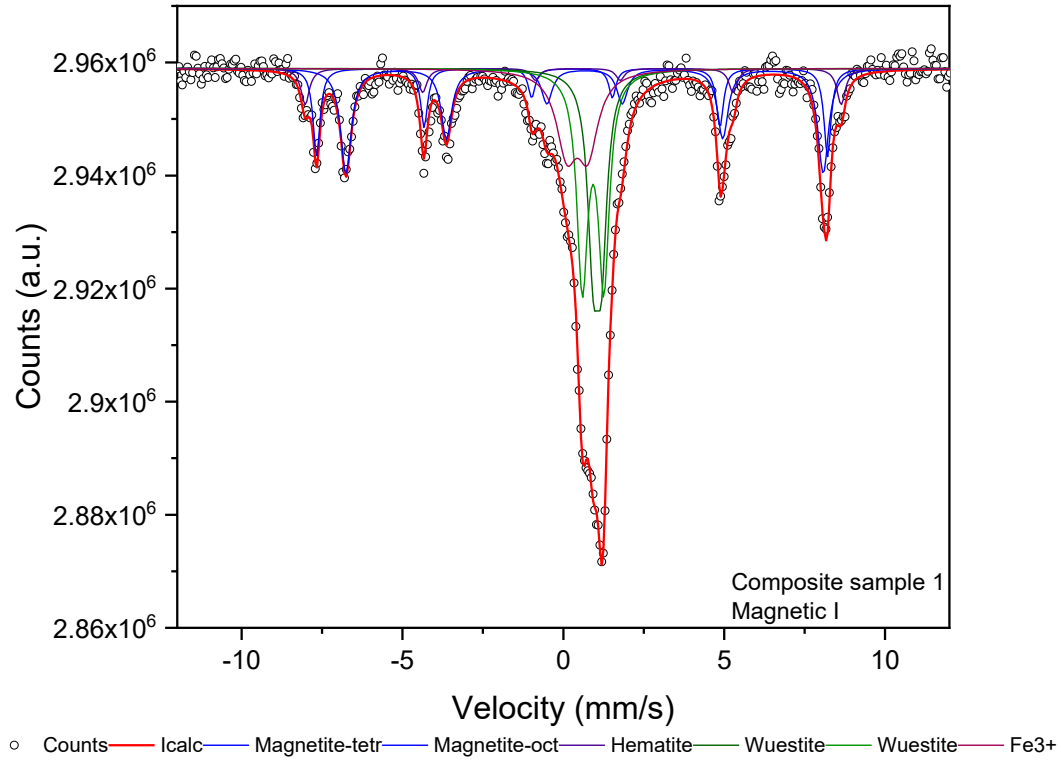

Figure E.9: Mössbauer Spectrum of Magnetic Fraction I of Composite Sample 1

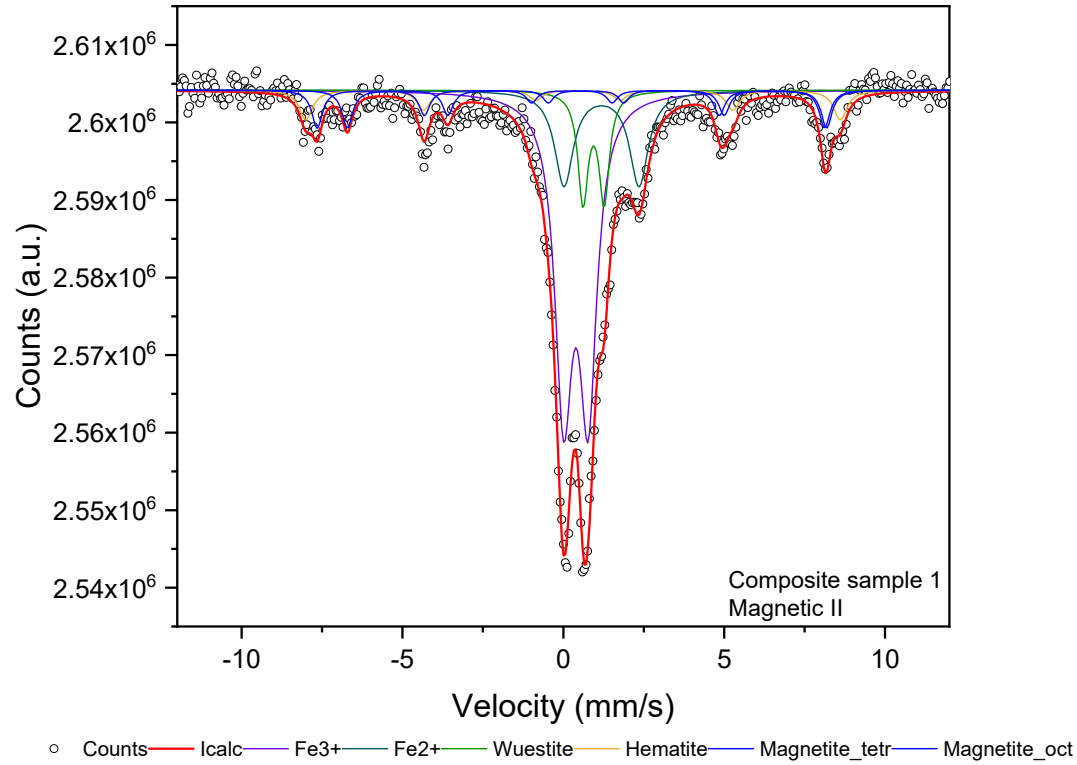

Figure E.10: Mössbauer Spectrum of Magnetic Fraction II of Composite Sample 1

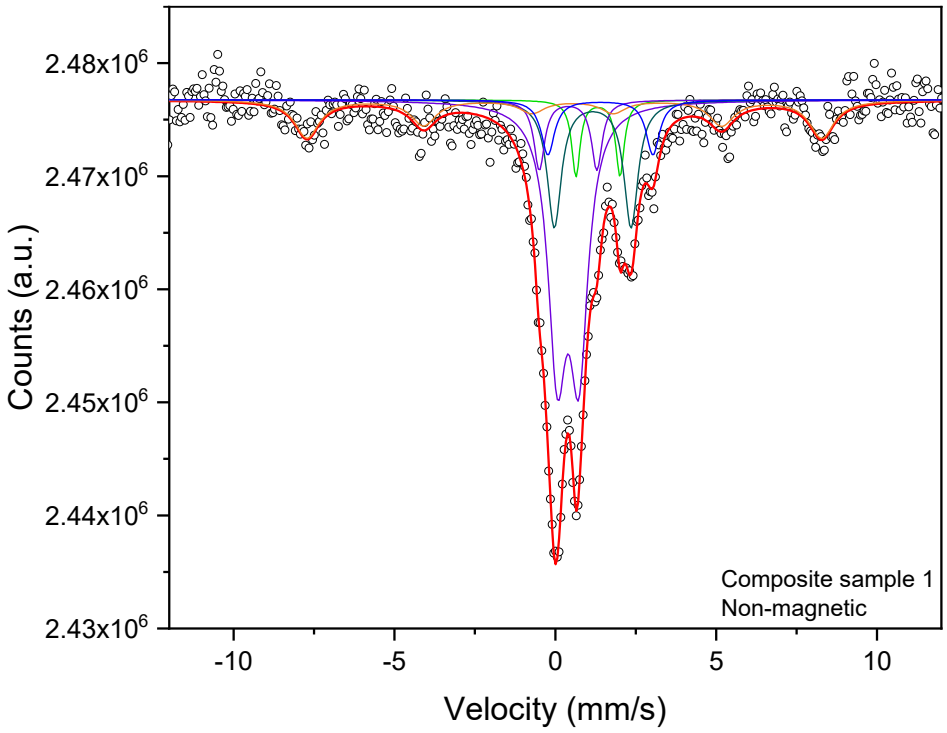

Figure E.11: Mössbauer Spectrum of the non-magnetic Fraction I of Composite Sample 1

Table E.5 Mössbauer data of Composite Sample 1.

	IS	H	QS	FWHM	Area	Assigment	
Magnetic I	0.271(12)	493(1)	0	0.131(11)	12.5(8)	Fe^{3+}	Magnetite
	0.660(13)	460(1)	0	0.202(12)	23.0(8)	$Fe^{2.5+}$	Magnetite
	0.379(13)	517(2)	-0.148(6)	0.157(13)	6.2(8)	Fe^{3+}	Hematite
	1.057(9)	--	0.257(18)	0.205(18)	18.7(8)	Fe^{2+}	Wuestite
	0.925(8)	--	0.669(14)	0.206(8)	23.5(5)	Fe^{2+}	Wuestite
	0.433(3)	--	0.652(5)	0.386(14)	16.1(7)	Fe^{3+}	Chlorite
Magnetic II	0.267(14)	491(2)	0	0.201(13)	5.1(9)	Fe^{3+}	Magnetite
	0.705(12)	460(2)	0	0.199(11	10.2(9)	$Fe^{2.5+}$	Hematite
	0.384(14)	515(2)	-0.162(8)	0.251(12)	7.5(8)	Fe^{3+}	Hematite
	0.941(8)	--	0.658(11)	0.192(12)	10.6(6)	Fe^{2+}	Wuestite
	1.187(14)	--	2.331(5)	0.351(9)	16.7(9)	Fe^{2+}	Mica?
	0.389(11)	--	0.763(11)	0.326(9)	50.0(9)	Fe^{3+}	Chlorite
Non-magnetic	0.396(16)	--	0.673(13)	0.345(12)	44.0(9)	Fe^{3+}	?
	0.397(13)	--	1.790(8)	0.202(9)	7.2(9)	Fe^{3+}	?
	0.411(9)	496(4)	-0.16(3)	0.46(1)	18(2)	Fe^{3+}	Hematite
	1.226(9)	--	1.369(17)	0.157(13)	6.2(9)	Fe^{2+}	?
	1.162(13)	--	2.385(12)	0.265(15)	17.3(9)	Fe^{2+}	Mica?
	1.401(15)	--	3.26(1)	0.251(14)	7.1(9)	Fe^{2+}	?

Appendix F - Visualization of element flows

Figure F.1: Average Ag flows (n=10) in MCW after screening and magnetic separation of the fine fraction

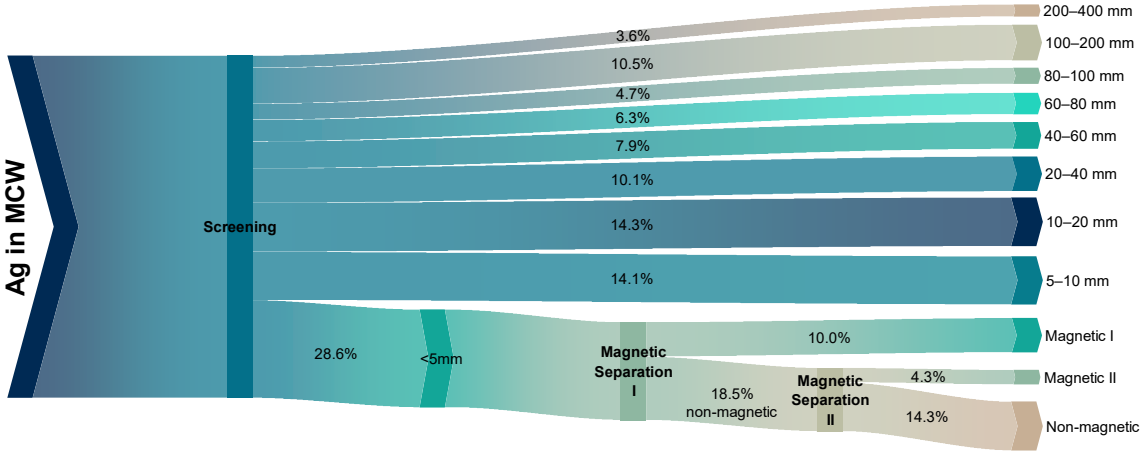

Figure F.2: Average Al flows (n=10) in MCW after screening and magnetic separation of the fine fraction

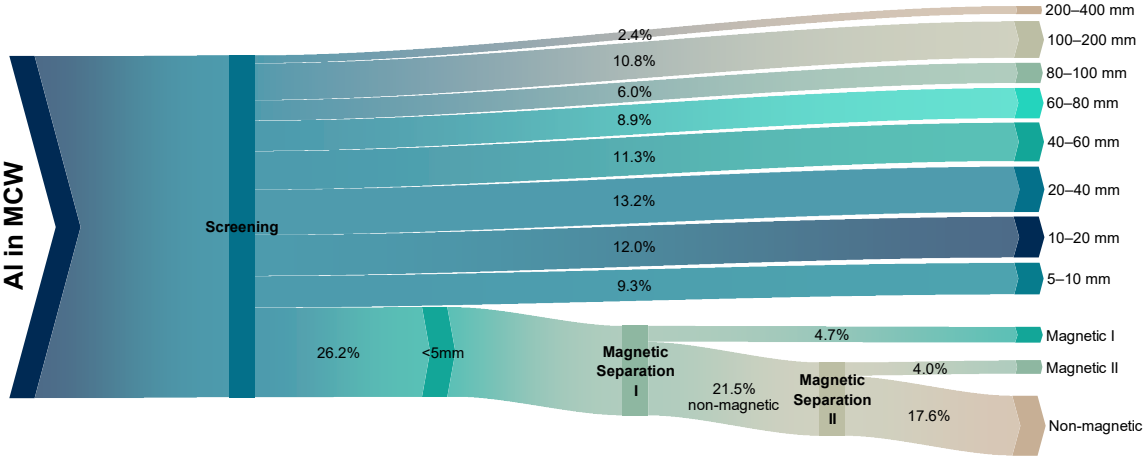

Figure F.3: Average As flows (n=10) in MCW after screening and magnetic separation of the fine fraction

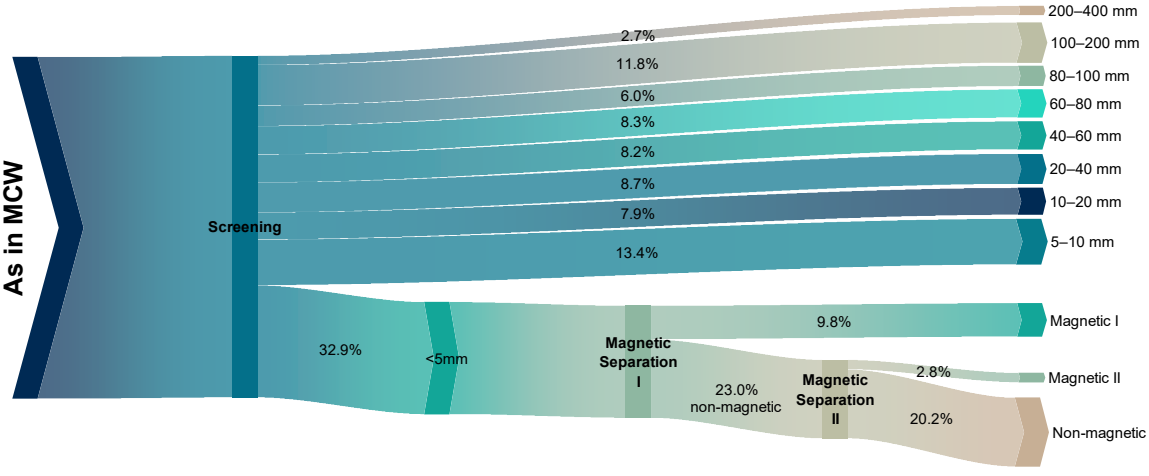

Figure F.4: Average Ba flows (n=10) in MCW after screening and magnetic separation of the fine fraction

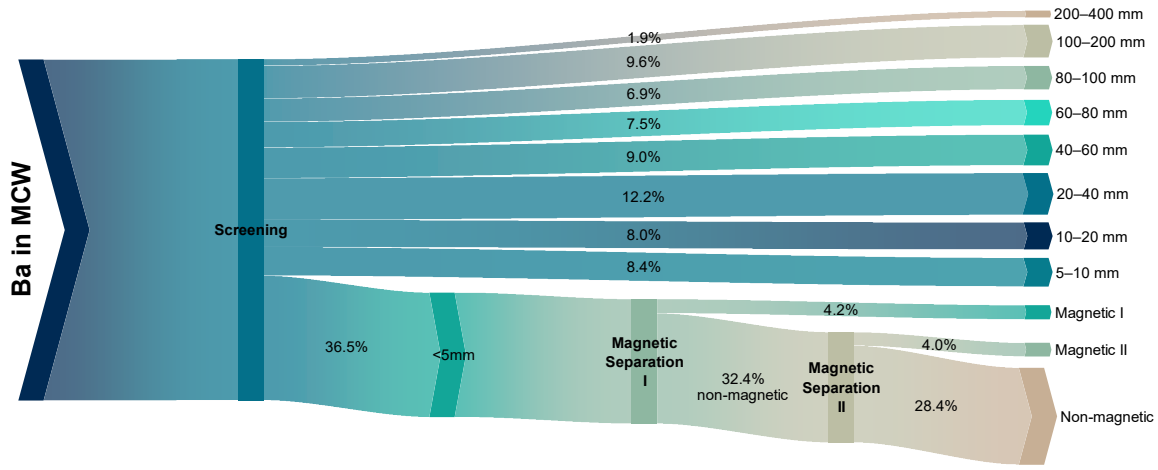

Figure F.5: Average Ca flows (n=10) in MCW after screening and magnetic separation of the fine fraction

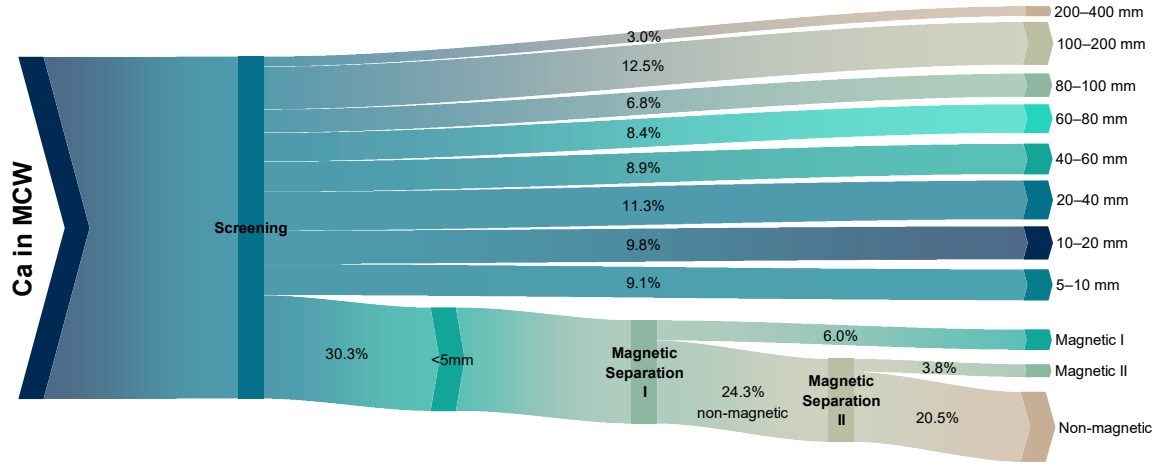

Figure F.6: Average Cd flows (n=10) in MCW after screening and magnetic separation of the fine fraction

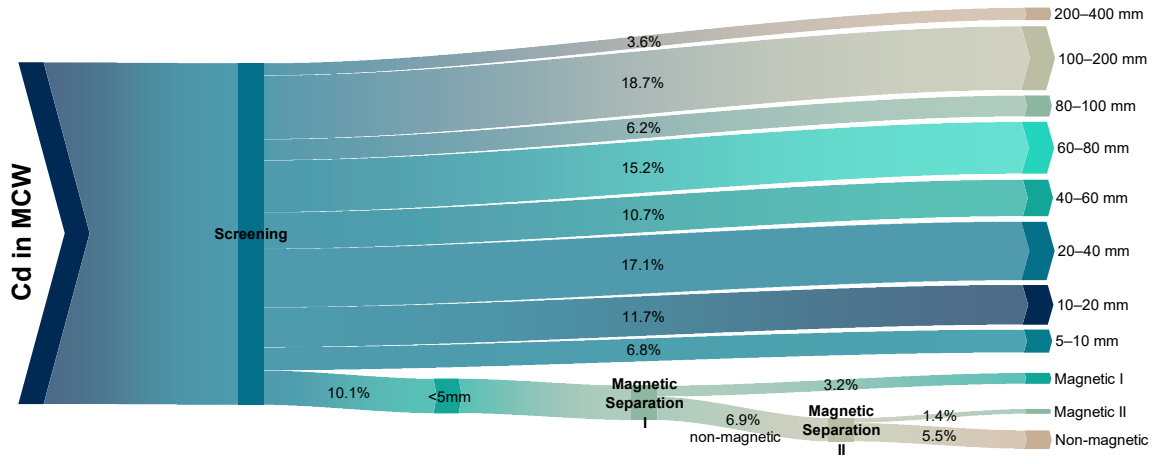

Figure F.7: Average Cl flows (n=10) in MCW after screening. Due to the small share of Cl in the fraction <5 mm, the Cl content after magnetic separation was not determined.

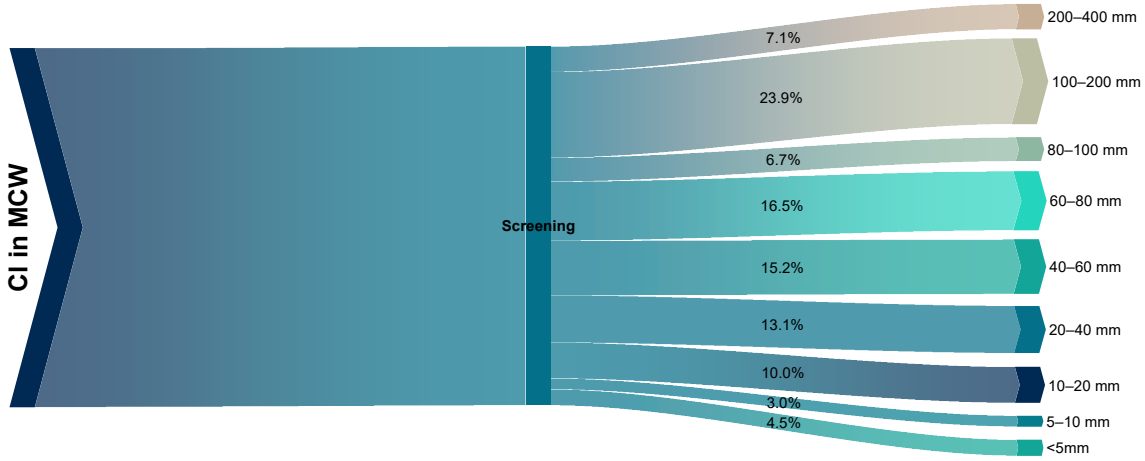

Figure F.8: Average Co flows (n=10) in MCW after screening and magnetic separation of the fine fraction

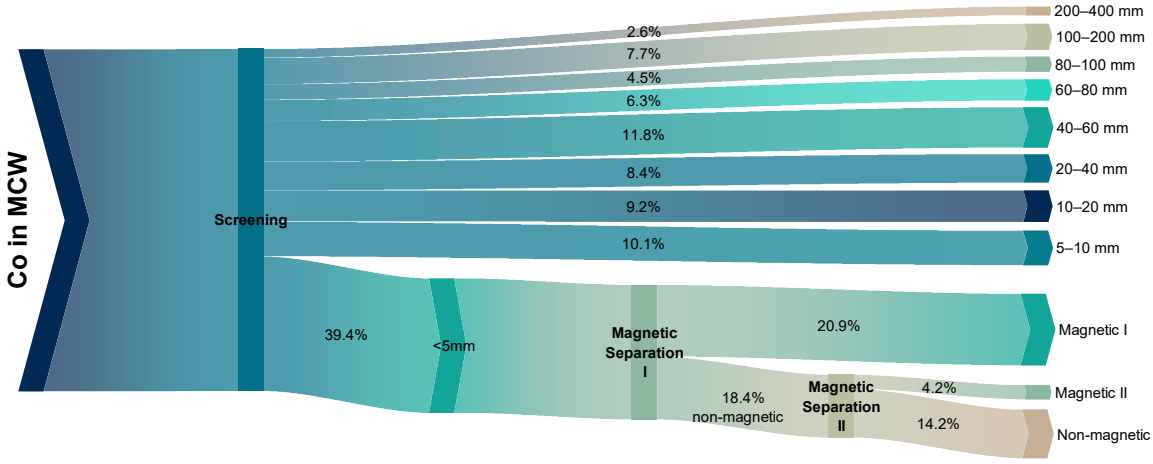

Figure F.9: Average Cr flows (n=10) in MCW after screening and magnetic separation of the fine fraction

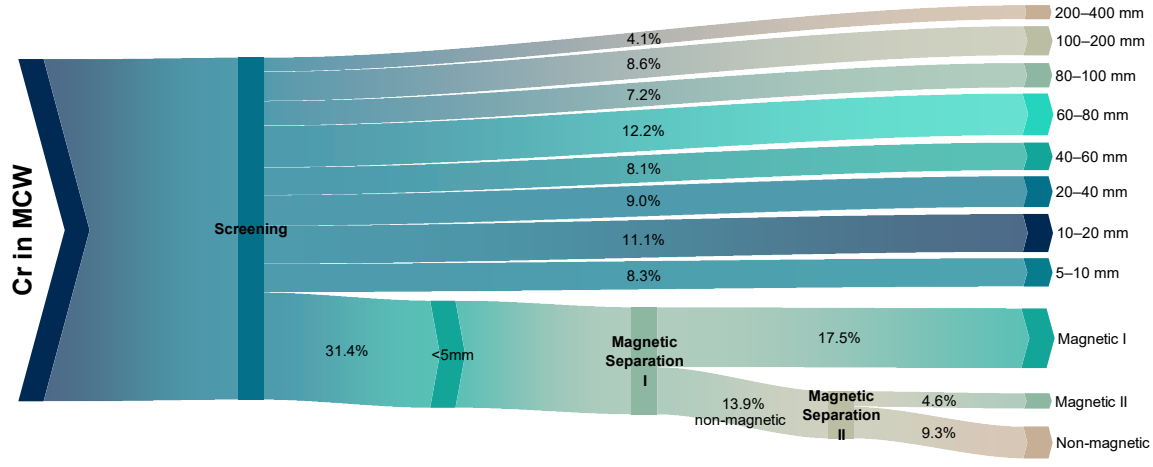

Figure F.10: Average Cu flows (n=10) in MCW after screening and magnetic separation of the fine fraction

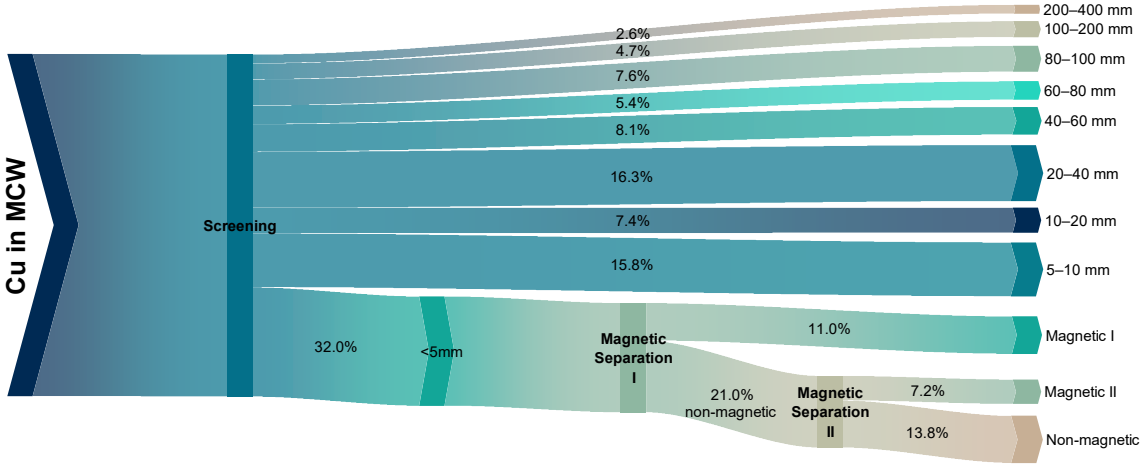

Figure F.11: Average Fe flows (n=10) in MCW after screening and magnetic separation of the fine fraction

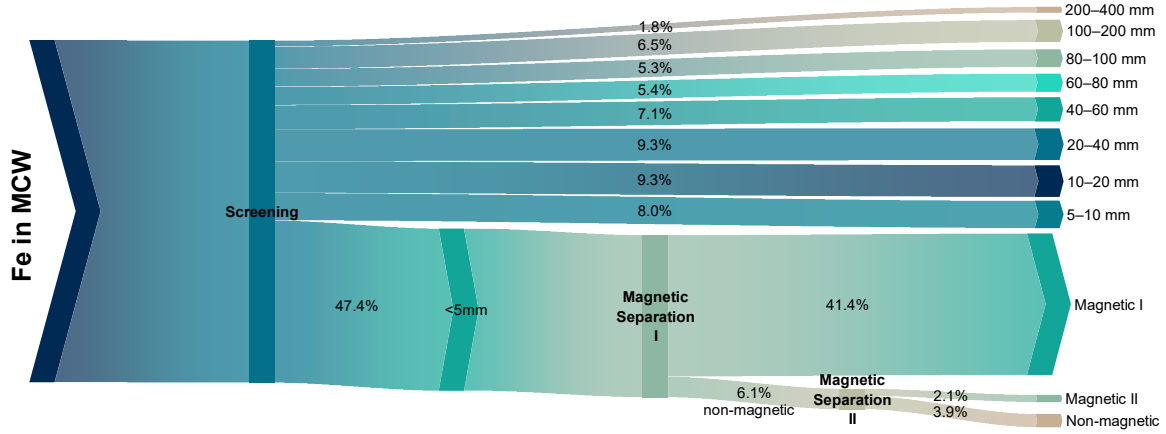

Figure F.12: Average Hg flows (n=10) in MCW after screening and magnetic separation of the fine fraction

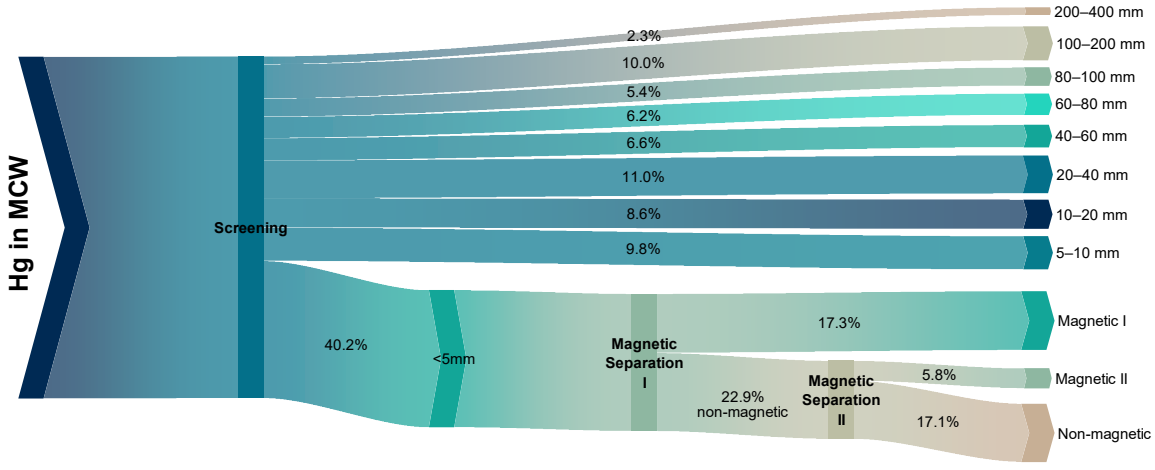

Figure F.13: Average K flows (n=10) in MCW after screening and magnetic separation of the fine fraction

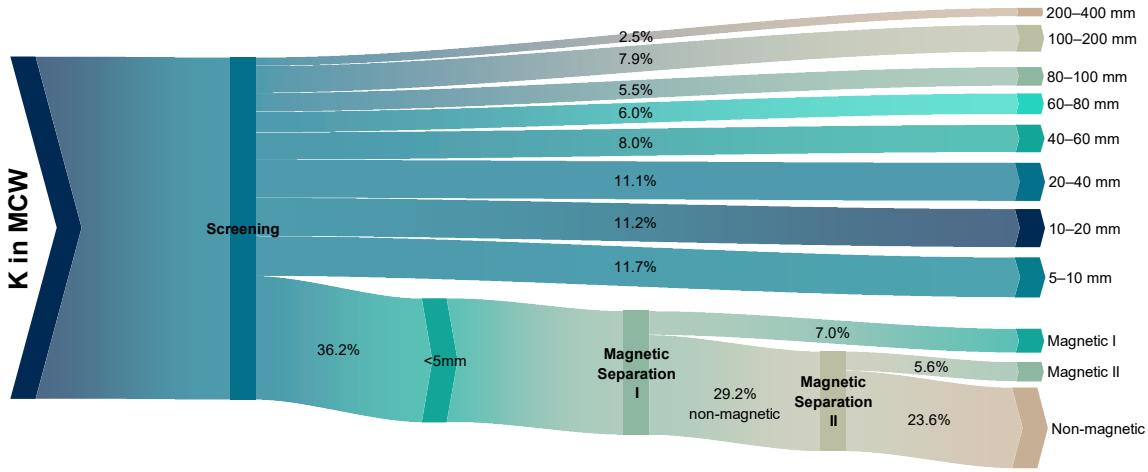

Figure F.14: Average Li flows (n=10) in MCW after screening and magnetic separation of the fine fraction

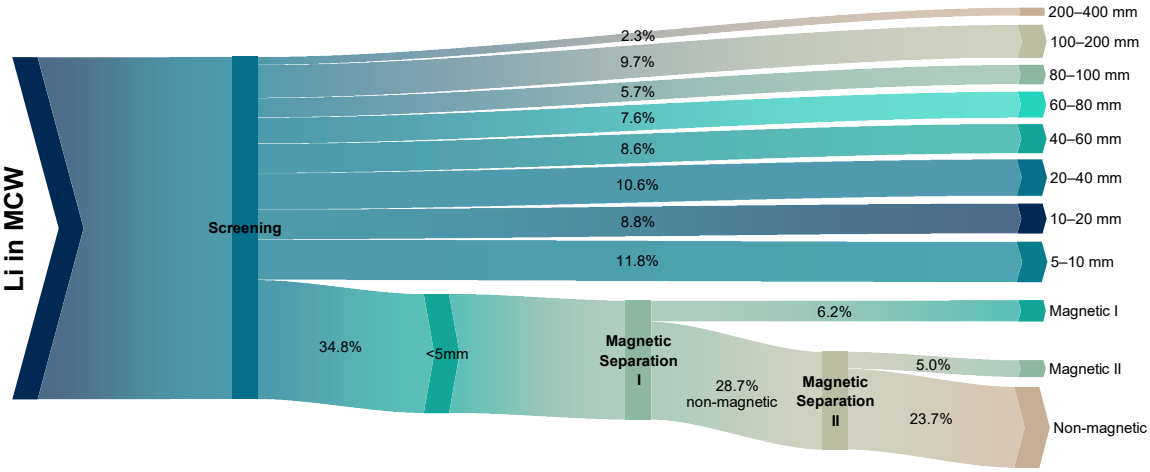

Figure F.15: Average Mg flows (n=10) in MCW after screening and magnetic separation of the fine fraction

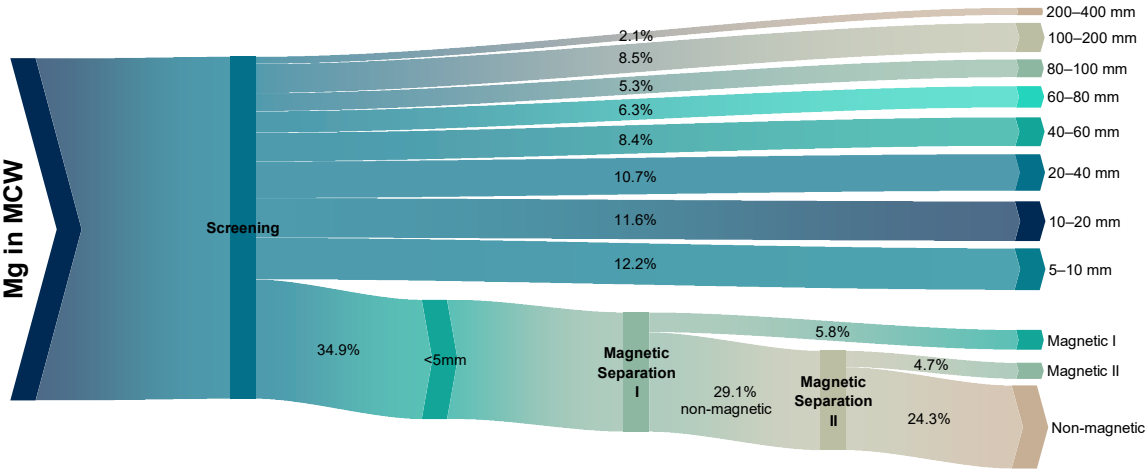

Figure F.16: Average Mn flows (n=10) in MCW after screening and magnetic separation of the fine fraction

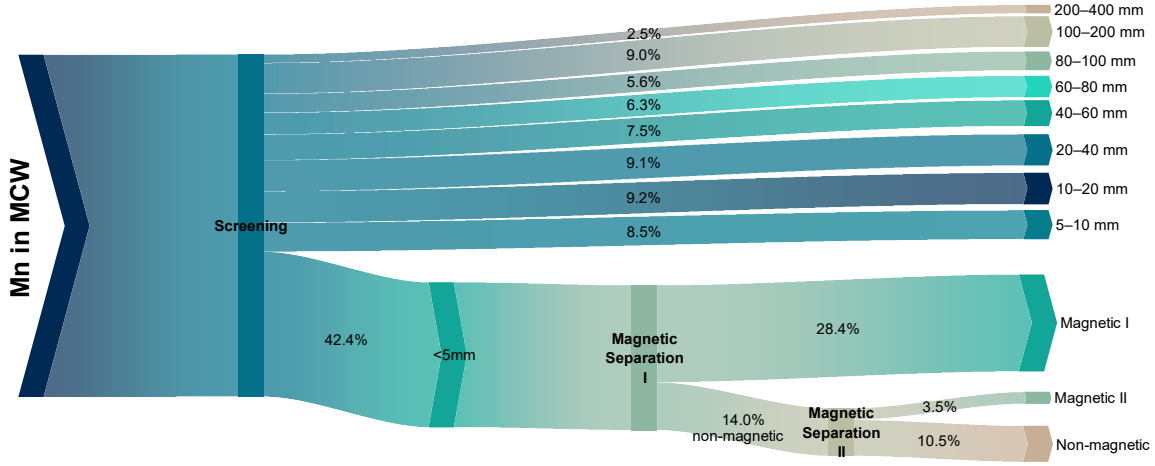

Figure F.17: Average Mo flows (n=10) in MCW after screening and magnetic separation of the fine fraction

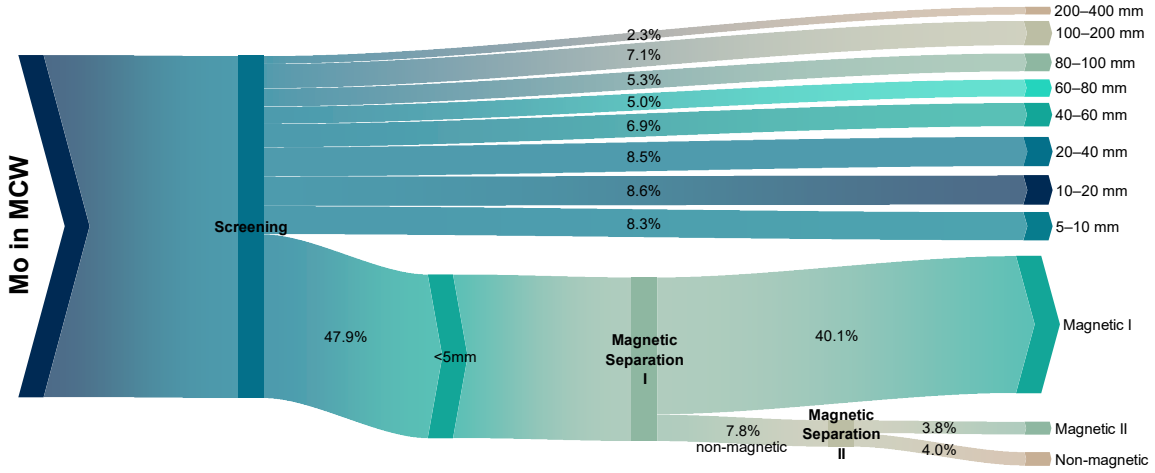

Figure F.18: Average Na flows (n=10) in MCW after screening and magnetic separation of the fine fraction

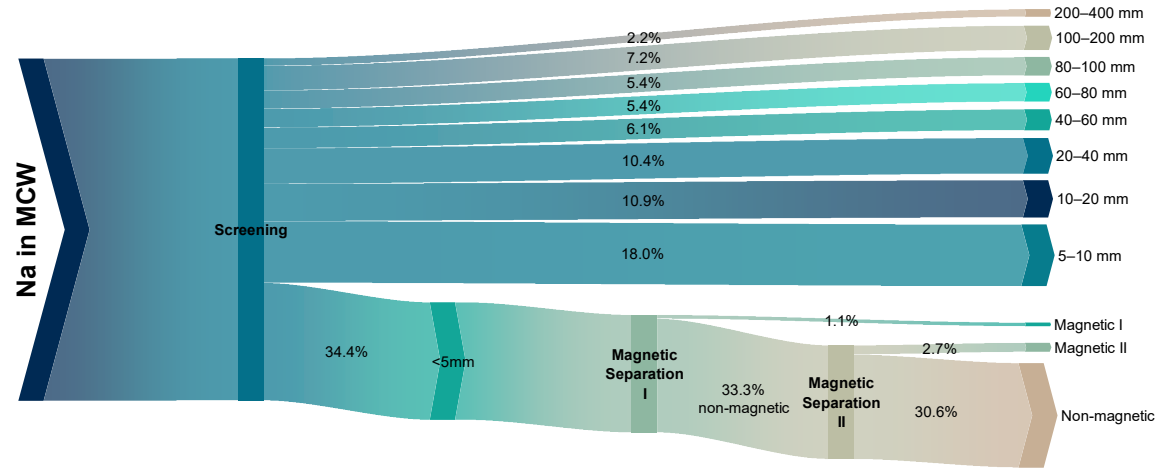

Figure F.19: Average Ni flows (n=10) in MCW after screening and magnetic separation of the fine fraction

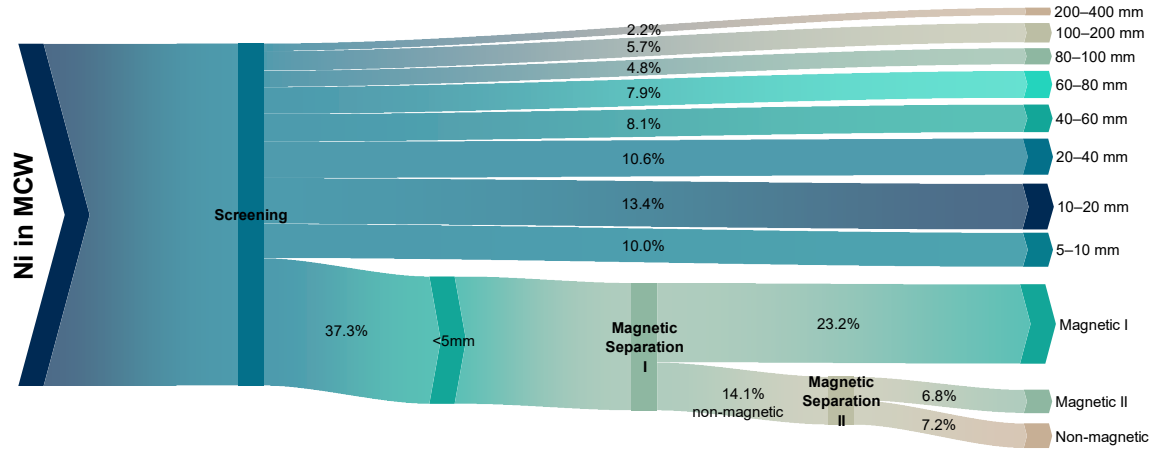

Figure F.20: Average P flows (n=10) in MCW after screening and magnetic separation of the fine fraction

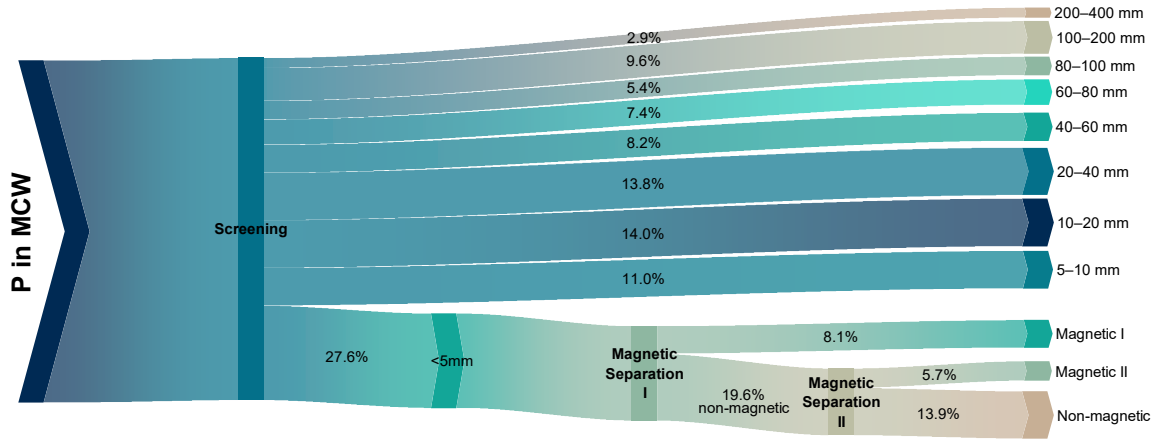

Figure F.21: Average Pb flows (n=10) in MCW after screening and magnetic separation of the fine fraction

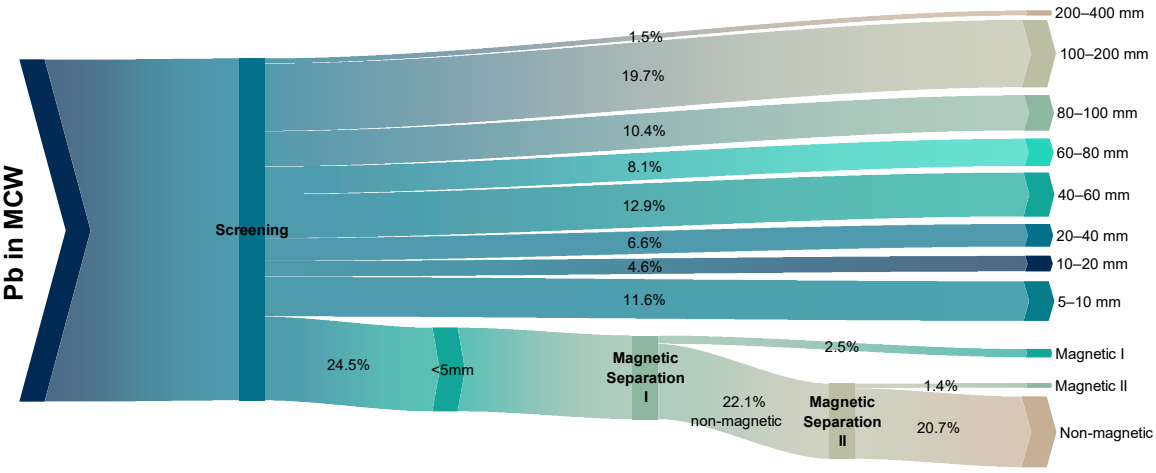

Figure F.22: Average Pd flows (n=10) in MCW after screening and magnetic separation of the fine fraction.

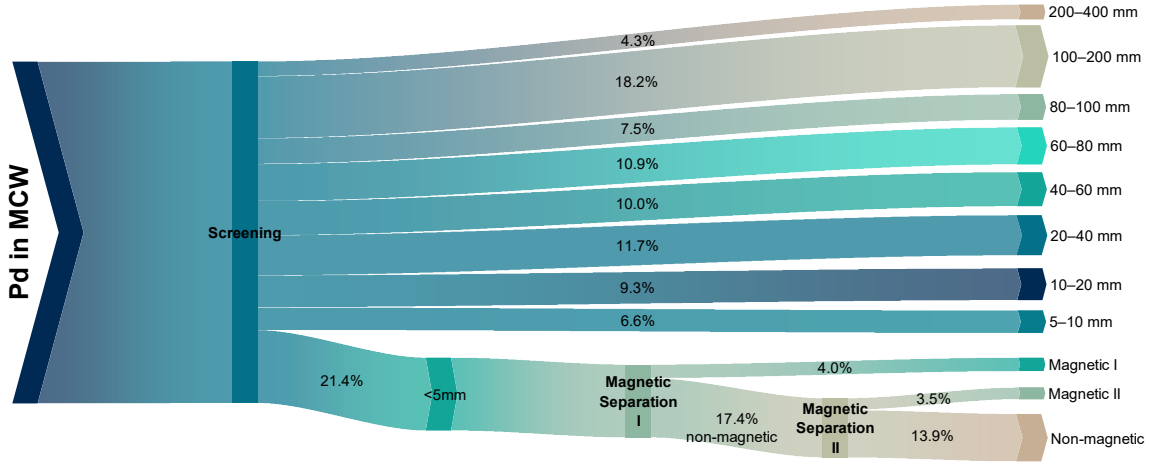

Figure F.23: Average Sb flows (n=10) in MCW after screening and magnetic separation of the fine fraction

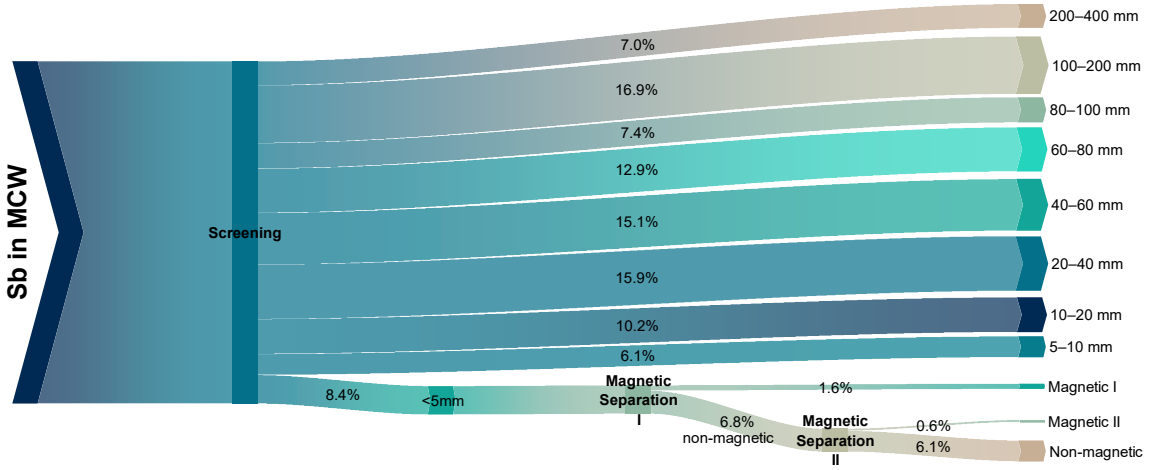

Figure F.24: Average Si flows (n=10) in MCW after screening and magnetic separation of the fine fraction

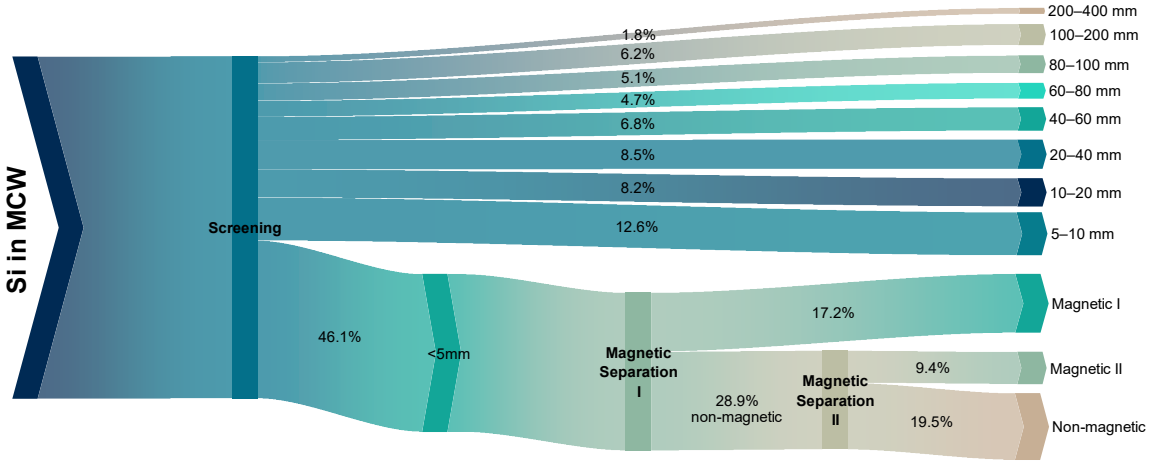

Figure F.25: Average Sn flows (n=10) in MCW after screening and magnetic separation of the fine fraction

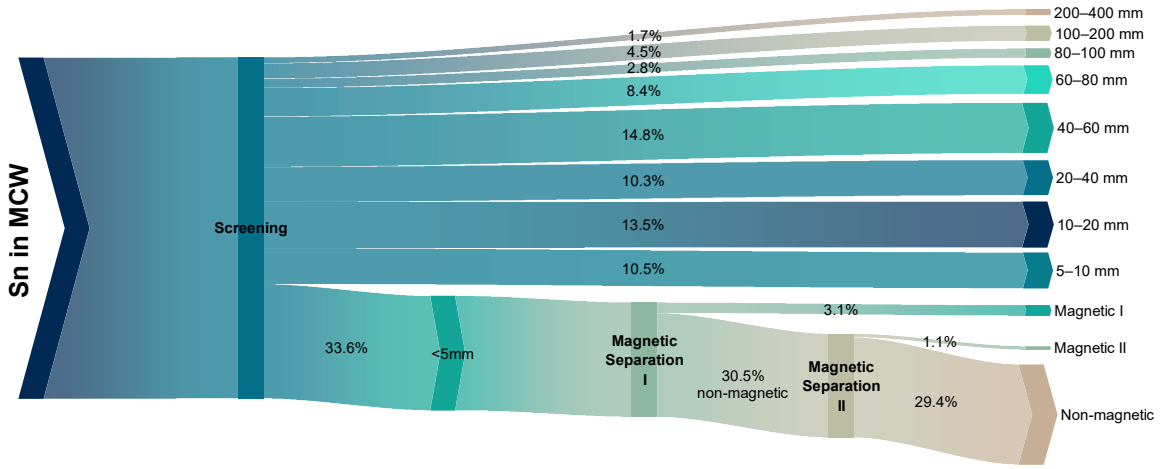

Figure F.26: Average Sr flows (n=10) in MCW after screening and magnetic separation of the fine fraction

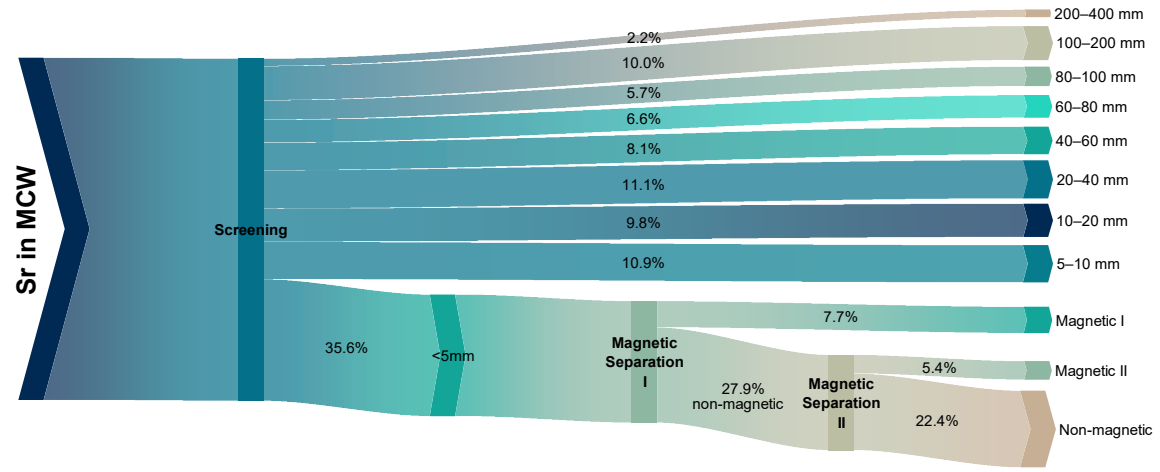

Figure F.27: Average Ti flows (n=10) in MCW after screening and magnetic separation of the fine fraction

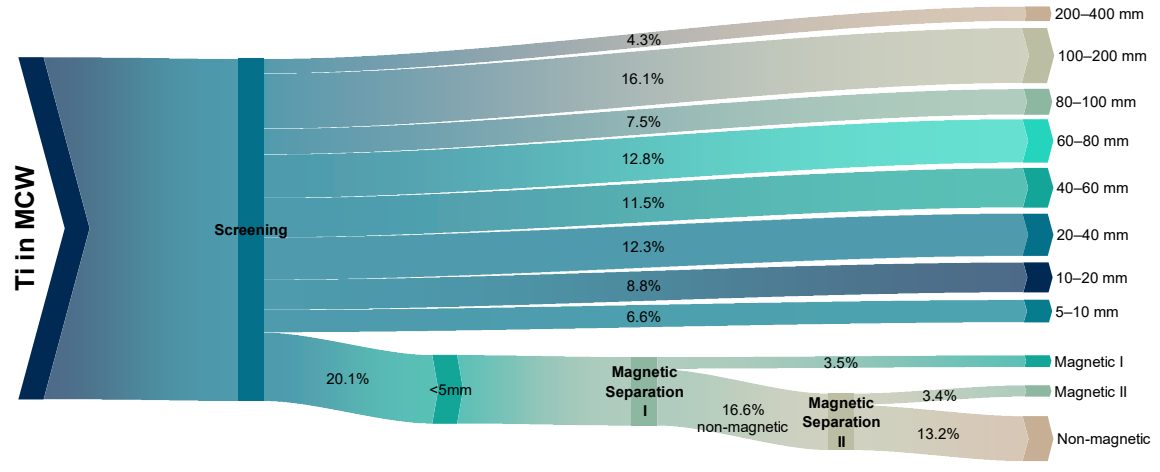

Figure F.28: Average V flows (n=10) in MCW after screening and magnetic separation of the fine fraction

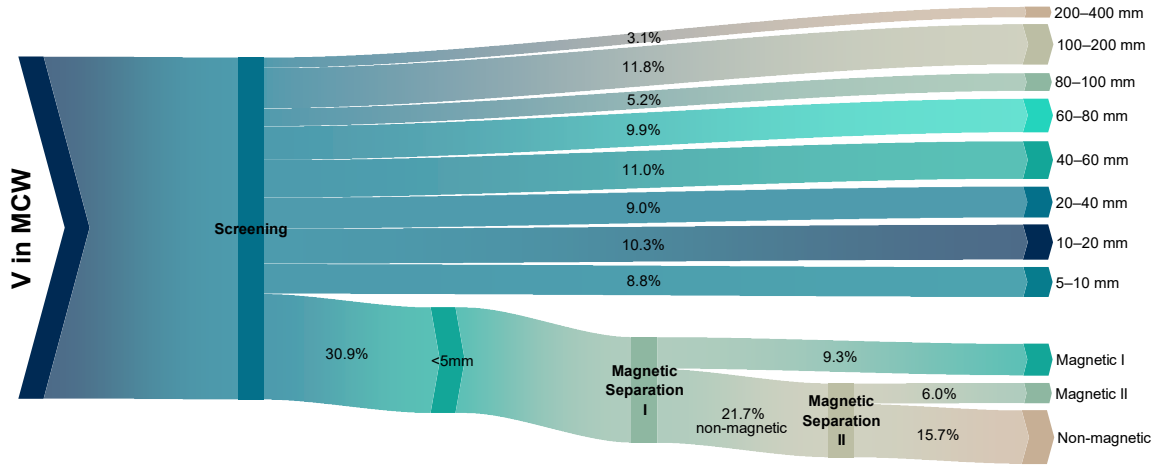

Figure F.29: Average W flows (n=10) in MCW after screening and magnetic separation of the fine fraction

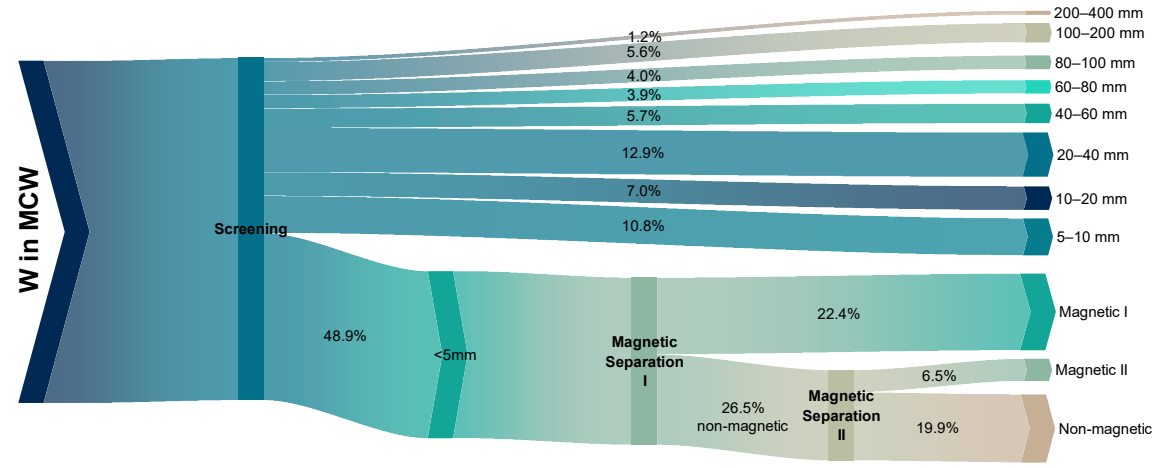

Figure F.30: Average Zn flows (n=10) in MCW after screening and magnetic separation of the fine fraction

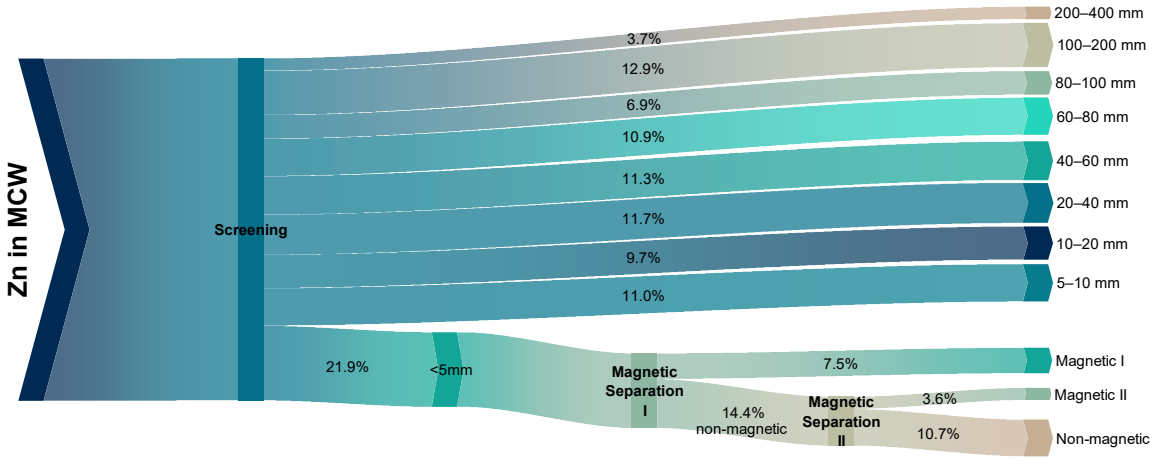

Figure F.31: Average mass flows (n=10; referring to dry mass without hard impurities) of MCW after screening and magnetic separation of the fine fraction

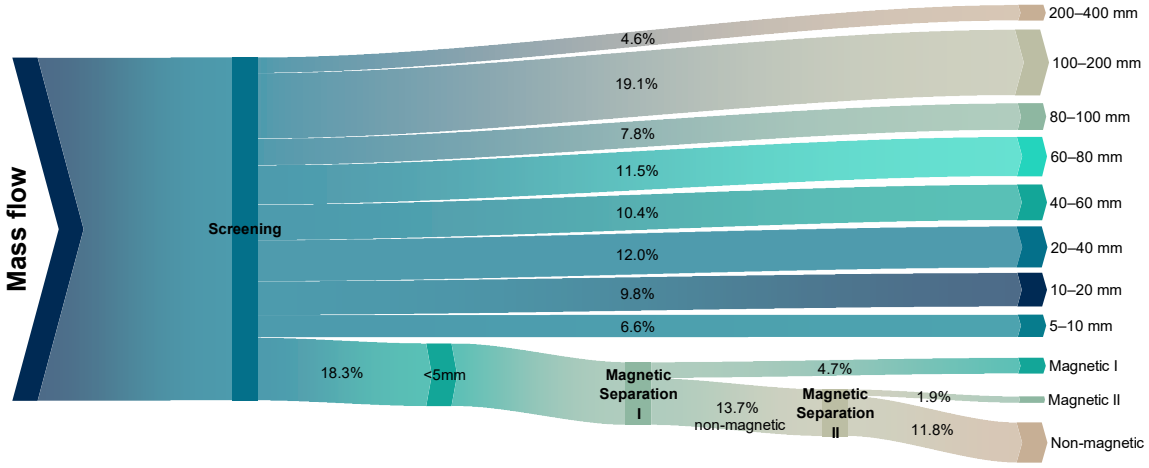

References

ADEME (Agence de l'Environnement et de la Maîtrise de l'Energie), 2010. La composition des ordures ménagères et assimilées en France. ADEME, Angers.

ASI (Austrian Standards Institute), 2011. ÖNORM EN 15359 Solid recovered fuels - Specifications and classes. Issued on 15/12/2011, Vienna.

Beker, D., Cornelissen, A.A.J., 1999. Chemische analyse van huishoudelijk restafval: Resultaten 1994 en 1995.

BMLFUW (Bundesministerium für Land- und Forstwirtschaft, Umwelt und Wasserwirtschaft), 2010. Verordnung über die Verbrennung von Abfällen (Abfallverbrennungsverordnung - AVV), BGBl. II Nr. 476/2010, Wien.

Curtis, A., Adam, J., Pomberger, R., Sarc, R., 2019. Grain size-related characterization of various non-hazardous municipal and commercial waste for solid recovered fuel (SRF) production. Detritus Volume 07 - September 2019 (0), 1. 10.31025/2611-4135/2019.13847.

LfU Bayern (Bayerisches Landesamt für Umweltschutz), 2003. Zusammensetzung und Schadstoffgehalt von Siedlungsabfällen: Abschlussbericht.

Nasrullah, M., Vainikka, P., Hannula, J., Hurme, M., 2015. Elemental balance of SRF production process: Solid recovered fuel produced from commercial and industrial waste. Fuel 145, 1–11. 10.1016/j.fuel.2014.12.071.

Rugg, M., Hanna, N.K., 1992. Metals concentrations in compostable and noncompostable components of municipal solid waste in Cape May County, New Jersey. Second United States Conference on Municipal Solid Waste Management, 2 June 1992, Arlington, Virginia.

Sarc, R., 2015. Herstellung, Qualität und Qualitätssicherung von Ersatzbrennstoffen zur Erreichung der 100%-igen thermischen Substitution in der Zementindustrie. Doctoral Thesis.

Watanabe, N., Inoue, S., Ito, H., 1999. Antimony in municipal waste. Chemosphere 39 (10), 1689–1698. 10.1016/S0045-6535(99)00069-7.

Publication VI – Supplementary

Production of contaminant-depleted solid recovered fuel from mixed commercial waste for co-processing in the cement industry

S.A. Viczek, K.E. Lorber, R. Pomberger, R. Sarc

Fuel 294 (2021), 120414
https://doi.org/10.1016/j.fuel.2021.120414

Content

Appendix A - Analyte concentrations in fractions

A.1. Masses of fractions

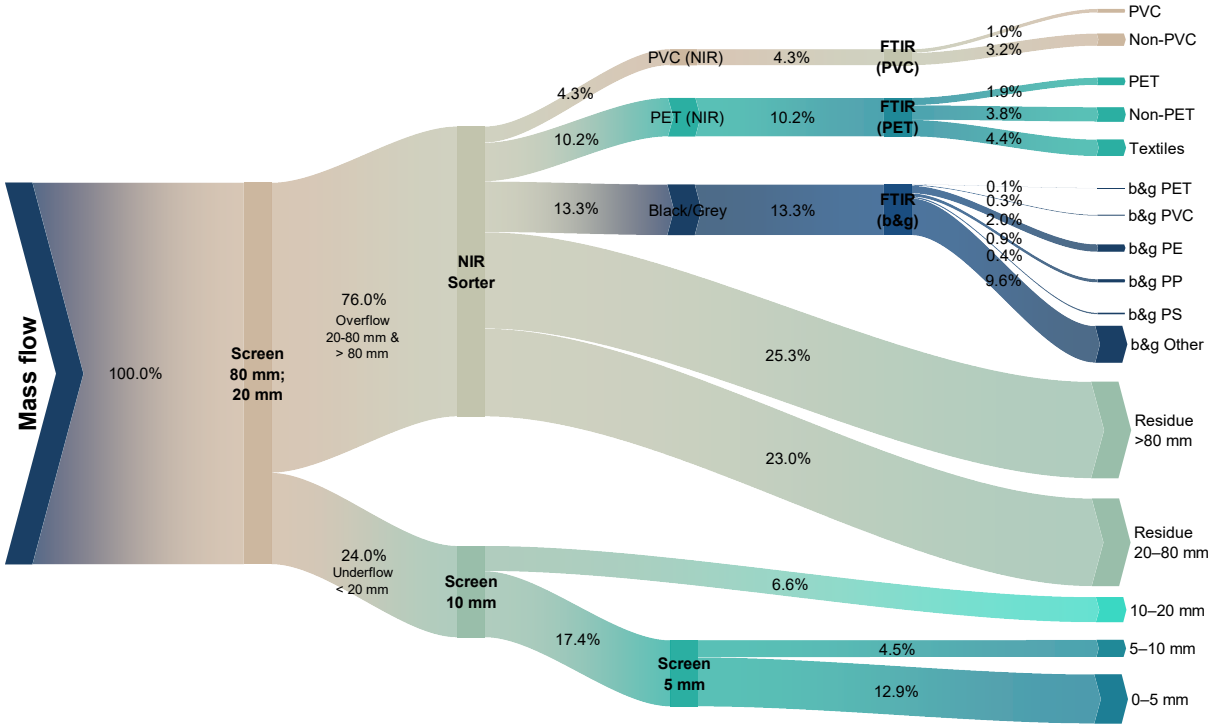

Figure A.1: Diagram of mass flows representing the arithmetic mean values of the five MCW samples S01–S05. B&g = black and grey fractions.

Table A.1: Mass share of each fraction in % referring to dry mass without hard impurities

Fraction		Composite sample					Mean	Std. Dev.	Rel. Std. Dev [%]
		S01	S02	S03	S04	S05			
Screen	0–5 mm	13.50	18.25	8.54	10.71	13.50	12.90	3.64	28
	5–10 mm	4.22	8.64	3.12	2.94	3.45	4.47	2.38	53
	10–20 mm	11.35	6.93	4.44	4.98	5.40	6.62	2.80	42
NIR Residue	20–80 mm	19.50	22.55	21.78	27.21	24.04	23.02	2.86	12
	> 80 mm	20.09	22.53	31.61	27.91	24.30	25.29	4.54	18
NIR PET Fraction	PET	5.26	0.96	0.97	1.58	0.94	1.94	1.87	97
	Non-PET	2.49	3.89	5.41	4.02	3.38	3.84	1.06	28
	Textile	2.14	2.83	5.23	4.76	6.92	4.38	1.92	44
NIR PVC Fraction	PVC	0.50	1.15	0.71	1.89	0.80	1.01	0.55	54
	Non-PVC	5.11	0.99	1.13	2.50	6.49	3.24	2.46	76
Black & Grey Fraction	PET	0.31	0.03	0	0.04	0.06	0.09	0.12	139
	PVC	0.36	0.09	0.20	0.61	0.02	0.26	0.24	91
	PE	1.49	1.13	0.96	2.22	4.16	1.99	1.31	66
	PP	1.28	0.93	1.25	0.68	0.31	0.89	0.41	46
	PS	1.71	0.19	0.16	0	0.08	0.43	0.72	169
	Other	10.70	8.91	14.49	7.95	6.14	9.64	3.17	33

A.2. LHV

a

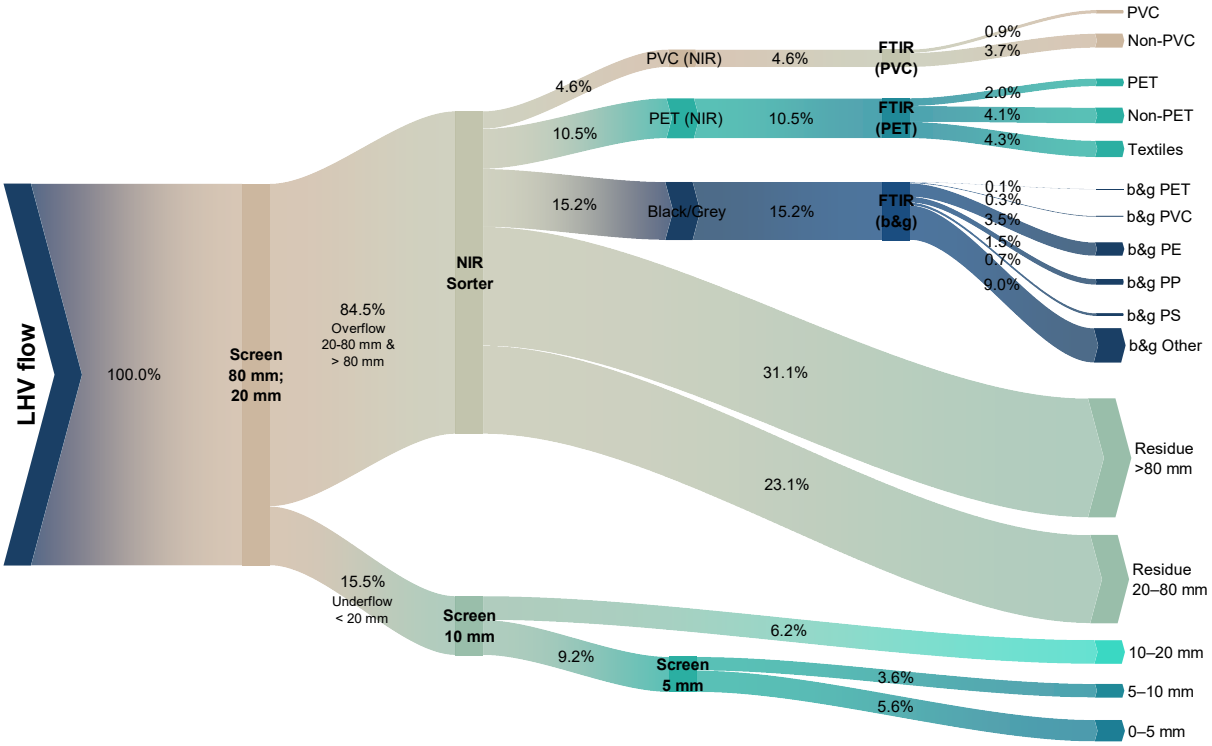

b

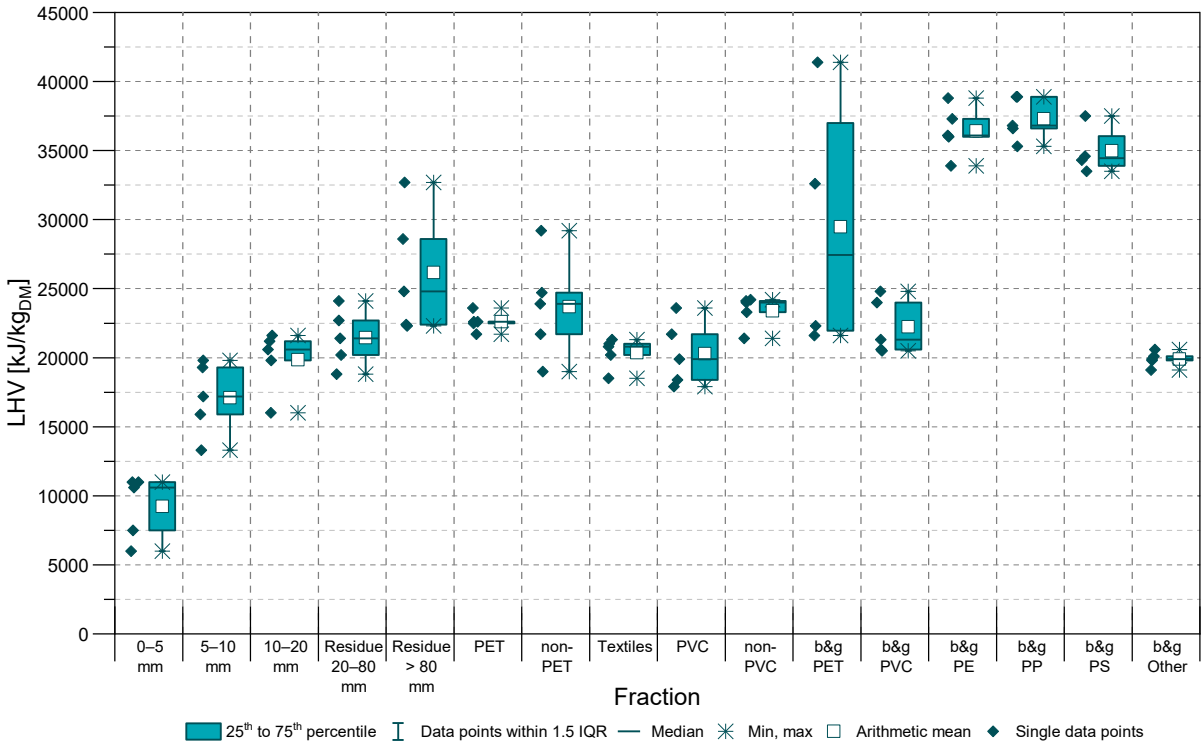

Figure A.2: a) Diagram of LHV flows representing the arithmetic mean values of the five MCW samples S01–S05. B&g = black and grey fractions. b) Box plot of LHVs in different particle size classes and sorted fractions in kJ/kg referring to dry mass without hard impurities

Table A.2: Lower heating value (LHV) in kJ/kg referring to dry mass without hard impurities

Fraction		Composite sample					Mean	Std. Dev.	Rel. Std. Dev [%]
		S01	S02	S03	S04	S05			
Screen	0–5 mm	11000	10600	7500	11000	6000	9200	2300	25
	5–10 mm	19800	17200	15900	19300	13300	17100	2600	15
	10–20 mm	21200	21600	19800	20600	16000	19800	2300	11
NIR Residue	20–80 mm	24100	22700	21400	18800	20200	21400	2100	10
	> 80 mm	22300	32700	24800	28600	22400	26200	4500	17
NIR PET Fraction	PET	22500	22600	23600	21700	22600	22600	680	3
	Non-PET	29200	21700	19000	23900	24700	23700	380	16
	Textile	21000	18500	20200	21300	20800	20400	1100	5
NIR PVC Fraction	PVC	21700	19900	23600	18400	17900	20300	2400	12
	Non-PVC	24100	24200	21400	24000	23300	23400	1200	5
Black & Grey Fraction	PET	22300	32600	-	21600	41400	29500	9400	32
	PVC	24000	21300	24800	20600	20500	22200	2000	9
	PE	36000	37300	33900	38800	36100	36400	1800	5
	PP	36600	35300	36800	38900	38900	37300	1600	4
	PS	37500	34600	34300	-	33500	35000	1700	5
	Other	19900	20600	19800	20100	19100	19900	540	3
Overall	kJ/kg	21500	22100	21000	22000	19400	21200	1100	5

A.3. Ag

a

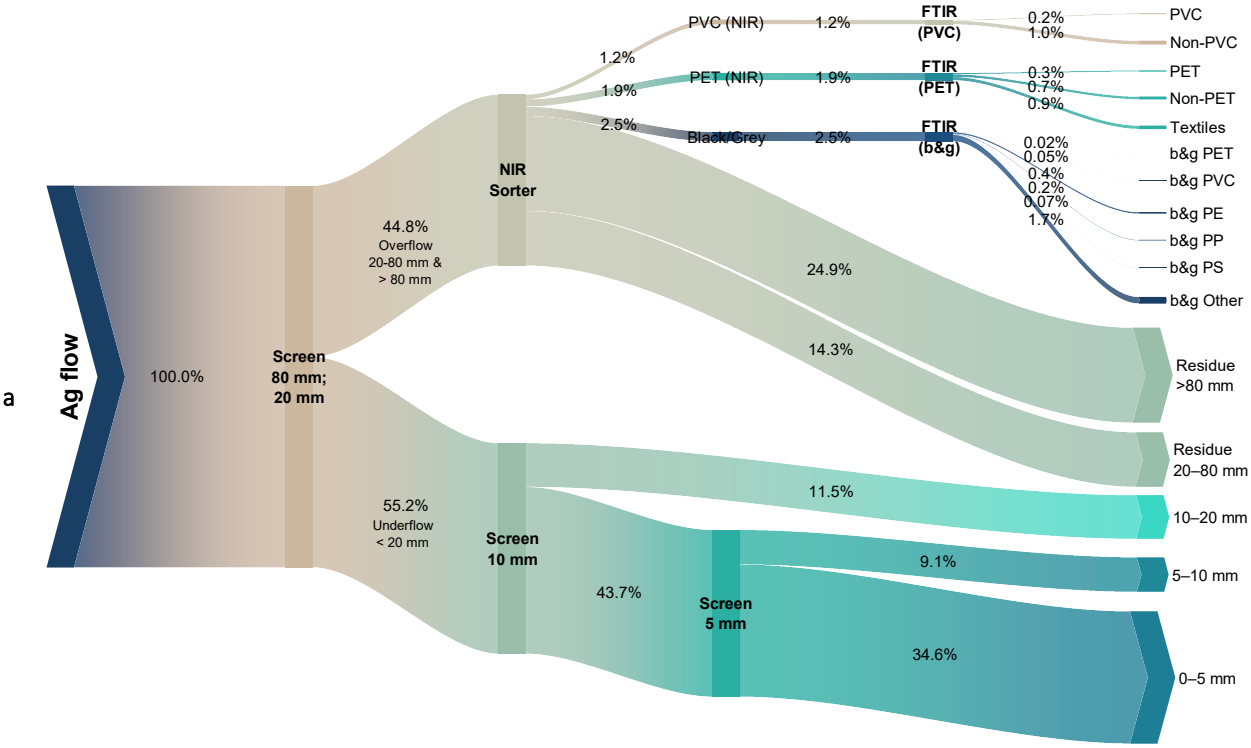

b

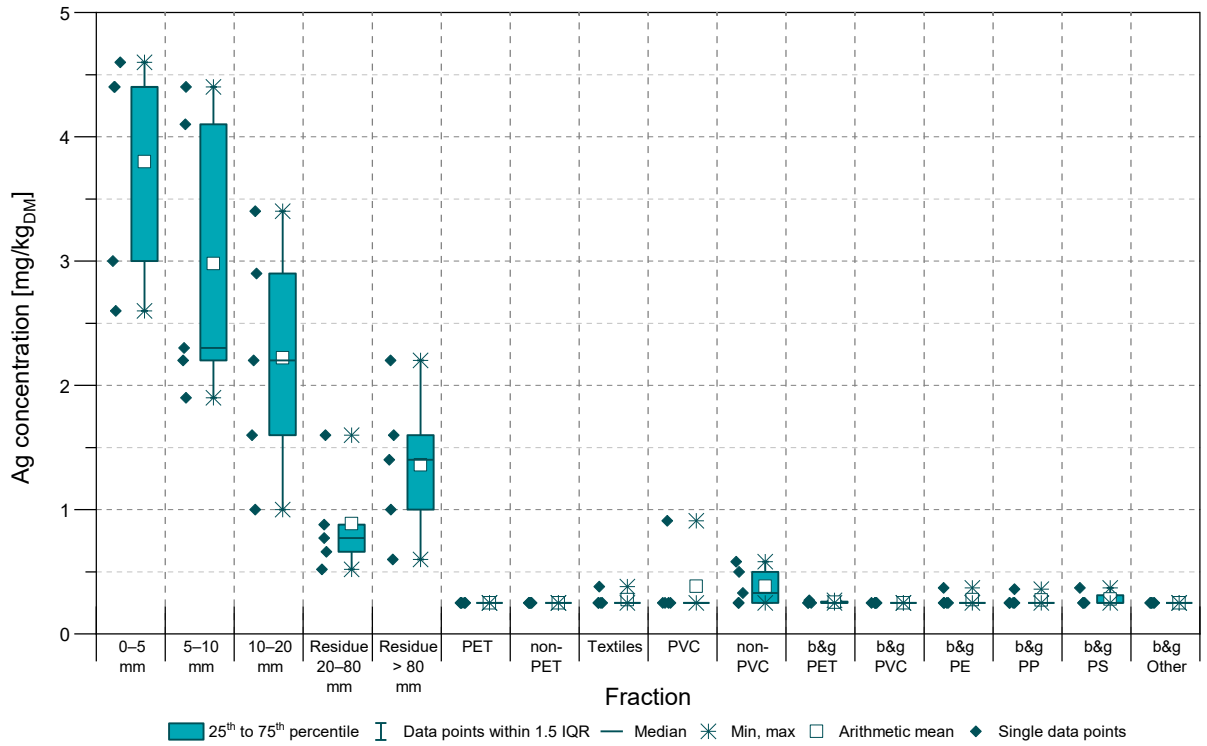

Figure A.3: a) Diagram of silver (Ag) flows representing the arithmetic mean values of the five MCW samples S01–S05. B&g = black and grey fractions. b) Box plot of Ag concentrations in different particle size classes and sorted fractions in mg/kg referring to dry mass without hard impurities

Table A.3: Silver (Ag) concentrations in mg/kg (unless stated otherwise) referring to dry mass without hard impurities. LOQ = 0.25 mg/kg

Fraction		Composite sample					Mean	Std. Dev.	Rel. Std. Dev [%]
		S01	S02	S03	S04	S05			
Screen	0–5 mm	4.4	2.6	4.4	4.6	3.0	3.8	0.93	24
	5–10 mm	4.4	1.9	2.2	4.1	2.3	3.0	1.2	39
	10–20 mm	2.2	2.9	1.0	1.6	3.4	2.2	0.97	43
NIR Residue	20–80 mm	0.88	0.77	1.6	0.52	0.66	0.89	0.42	47
	> 80 mm	1.6	1.0	2.2	1.4	0.60	1.4	0.61	45
NIR PET Fraction	PET	0.25	< 0.25	< 0.25	< 0.25	< 0.25	0.25	0	0
	Non-PET	< 0.25	< 0.25	< 0.25	< 0.25	< 0.25	0.25	0	0
	Textile	0.38	< 0.25	< 0.25	< 0.25	< 0.25	0.28	0.06	21
NIR PVC Fraction	PVC	< 0.25	< 0.25	0.91	< 0.25	< 0.25	0.38	0.30	77
	Non-PVC	< 0.25	0.33	0.58	< 0.25	0.50	0.38	0.15	39
Black & Grey Fraction	PET	0.27	< 0.25	-	< 0.25	< 0.25	0.26	0.01	4
	PVC	< 0.25	< 0.25	< 0.25	< 0.25	< 0.25	0.25	0	0
	PE	< 0.25	< 0.25	< 0.25	0.37	< 0.25	0.27	0.05	19
	PP	< 0.25	0.36	< 0.25	< 0.25	< 0.25	0.27	0.05	18
	PS	< 0.25	< 0.25	0.37	-	< 0.25	0.28	0.06	21
	Other	< 0.25	< 0.25	< 0.25	< 0.25	< 0.25	0.25	0	0
Overall	mg/kg	1.6	1.3	1.6	1.3	1.1	1.37	0.24	17
	mg/MJ	0.07	0.06	0.08	0.06	0.05	0.06	0.01	16

A.4. Al

a

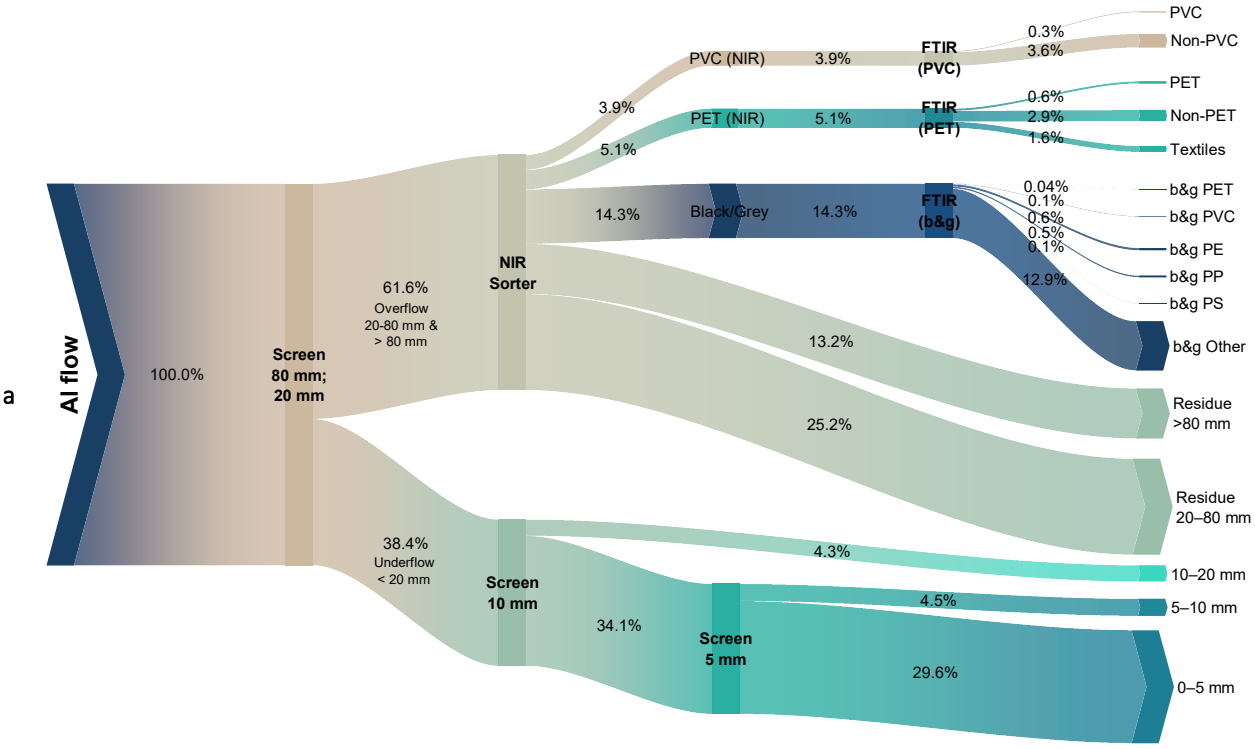

b

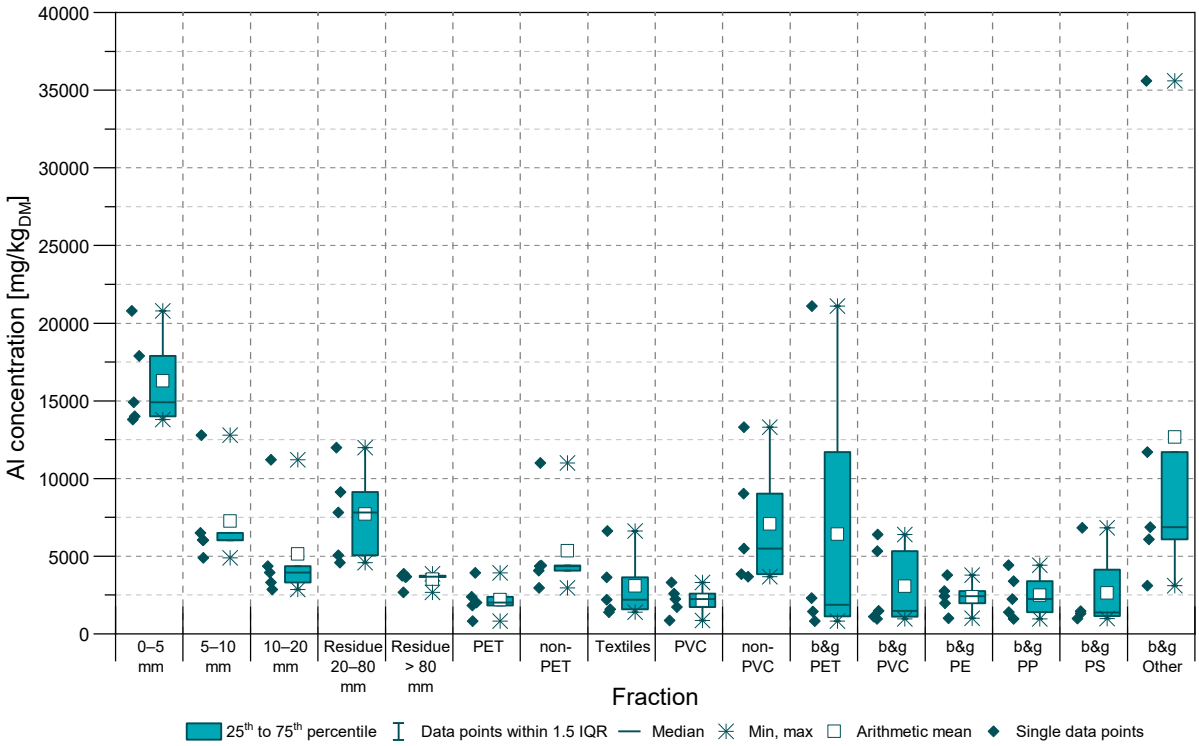

Figure A.4: a) Diagram of aluminum (Al) flows representing the arithmetic mean values of the five MCW samples S01–S05. B&g = black and grey fractions. b) Box plot of Al concentrations in different particle size classes and sorted fractions in mg/kg referring to dry mass without hard impurities

Table A.4: Aluminum (Al) concentrations in mg/kg referring to dry mass without hard impurities. LOQ = 2.5 mg/kg

Fraction		Composite sample					Mean	Std. Dev.	Rel. Std. Dev [%]
		S01	S02	S03	S04	S05			
Screen	0–5 mm	13800	14000	14900	17900	20800	16300	3010	19
	5–10 mm	4900	6020	6490	6040	12800	7250	3160	44
	10–20 mm	3950	2860	3320	4370	11200	5140	3440	67
NIR Residue	20–80 mm	7820	5050	4580	12000	9140	7720	3060	40
	> 80 mm	3690	3860	2680	3740	3660	3530	480	14
NIR PET Fraction	PET	1840	820	2380	3920	2020	2200	1120	51
	Non-PET	4350	2960	4400	4070	11000	5360	3210	60
	Textile	6620	2200	1400	1590	3650	3090	2160	70
NIR PVC Fraction	PVC	870	1730	2590	2240	3320	2150	920	43
	Non-PVC	9020	3690	3850	5490	13300	7070	4090	58
Black & Grey Fraction	PET	1440	21100	-	2310	820	6420	9810	153
	PVC	1120	5330	970	6390	1480	3060	2590	85
	PE	1970	1000	3790	2420	2760	2390	1030	43
	PP	1400	3390	4430	2250	970	2490	1430	57
	PS	1310	1450	980	-	6830	2640	2800	106
	Other	11700	6860	3110	6080	35600	12700	13200	104
Overall	mg/kg	6930	6190	4410	7690	10800	7200	2340	33
	mg/MJ	320	280	210	350	560	340	130	38

A.5. As

a

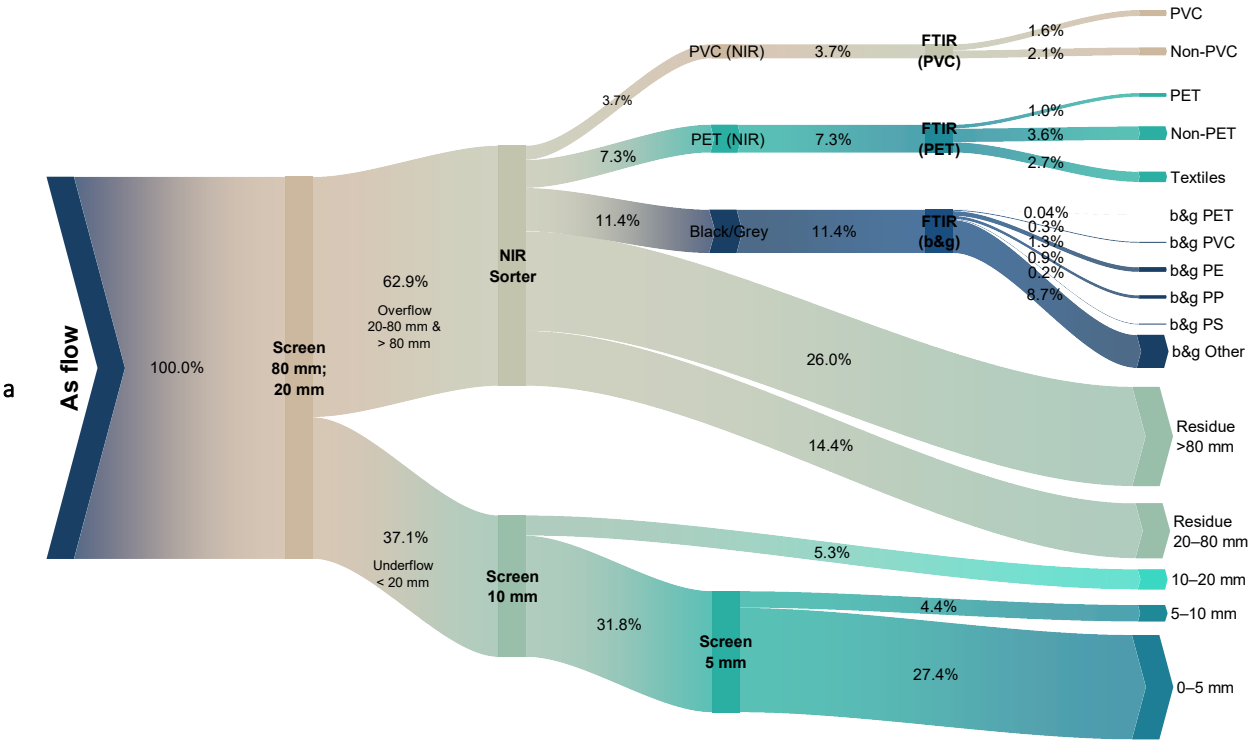

b

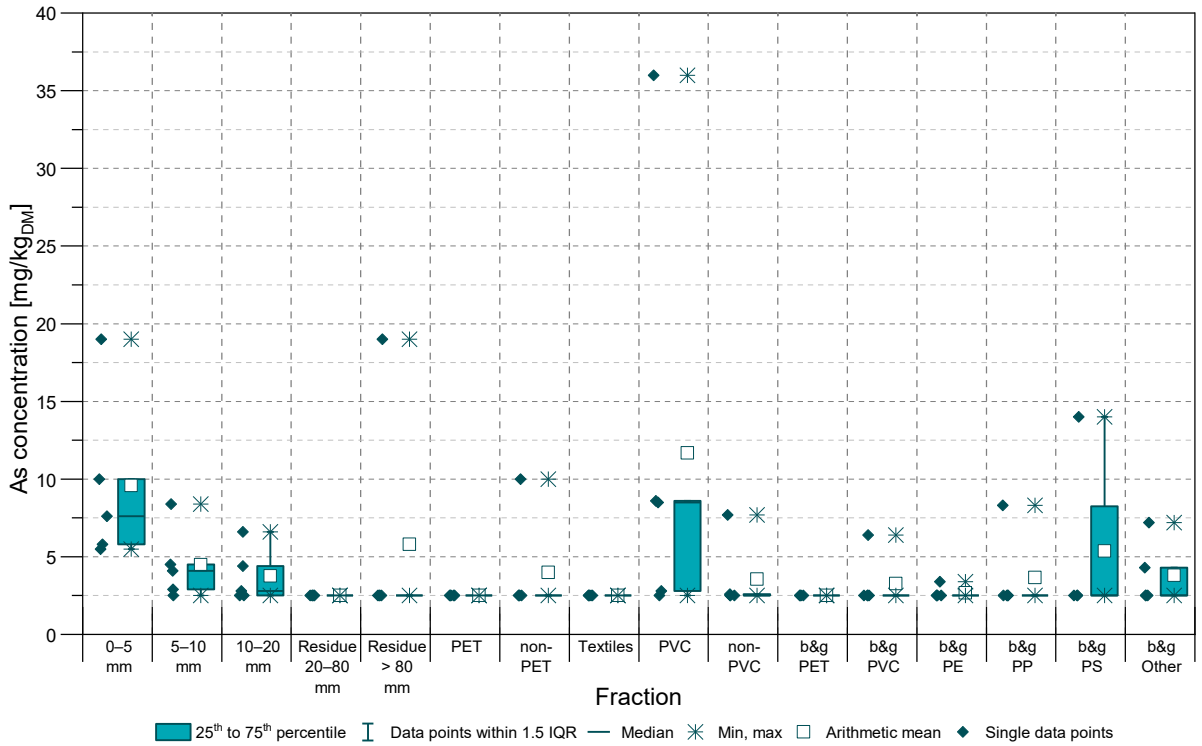

Figure A.5: a) Diagram of arsenic (As) flows representing the arithmetic mean values of the five MCW samples S01–S05. B&g = black and grey fractions. b) Box plot of As concentrations in different particle size classes and sorted fractions in mg/kg referring to dry mass without hard impurities

Table A.5: Arsenic (As) concentrations in mg/kg referring to dry mass without hard impurities. LOQ = 2.5 mg/kg

Fraction		Composite sample					Mean	Std. Dev.	Rel. Std. Dev [%]
		S01	S02	S03	S04	S05			
Screen	0–5 mm	5.5	5.8	19	7.6	10	9.6	5.6	58
	5–10 mm	2.9	< 2.5	4.5	4.1	8.4	4.5	2.3	52
	10–20 mm	2.8	< 2.5	4.4	< 2.5	6.6	3.8	1.8	47
NIR Residue	20–80 mm	< 2.5	< 2.5	< 2.5	< 2.5	< 2.5	2.5	0	0
	> 80 mm	19	< 2.5	< 2.5	< 2.5	< 2.5	5.8	7.4	127
NIR PET Fraction	PET	< 2.5	< 2.5	< 2.5	< 2.5	< 2.5	2.5	0.0	0
	Non-PET	< 2.5	< 2.5	< 2.5	< 2.5	10	4.0	3.4	84
	Textile	< 2.5	< 2.5	< 2.5	< 2.5	< 2.5	2.5	0	0
NIR PVC Fraction	PVC	36	2.8	8.5	< 2.5	8.6	12	14	119
	Non-PVC	2.6	< 2.5	7.7	< 2.5	< 2.5	3.6	2.3	65
Black & Grey Fraction	PET	< 2.5	< 2.5	-	< 2.5	< 2.5	2.5	0	0
	PVC	< 2.5	< 2.5	< 2.5	6.4	< 2.5	3.3	1.7	53
	PE	< 2.5	< 2.5	3.4	< 2.5	< 2.5	2.7	0.40	15
	PP	< 2.5	< 2.5	8.3	< 2.5	< 2.5	3.7	2.6	71
	PS	< 2.5	< 2.5	< 2.5	-	14	5.4	5.8	107
	Other	< 2.5	7.2	< 2.5	< 2.5	4.3	3.8	2.1	54
Overall	mg/kg	6.4	3.5	4.2	3.1	4.4	4.3	1.3	30
	mg/MJ	0.30	0.16	0.20	0.14	0.22	0.21	0.06	30

A.6. Ba

a

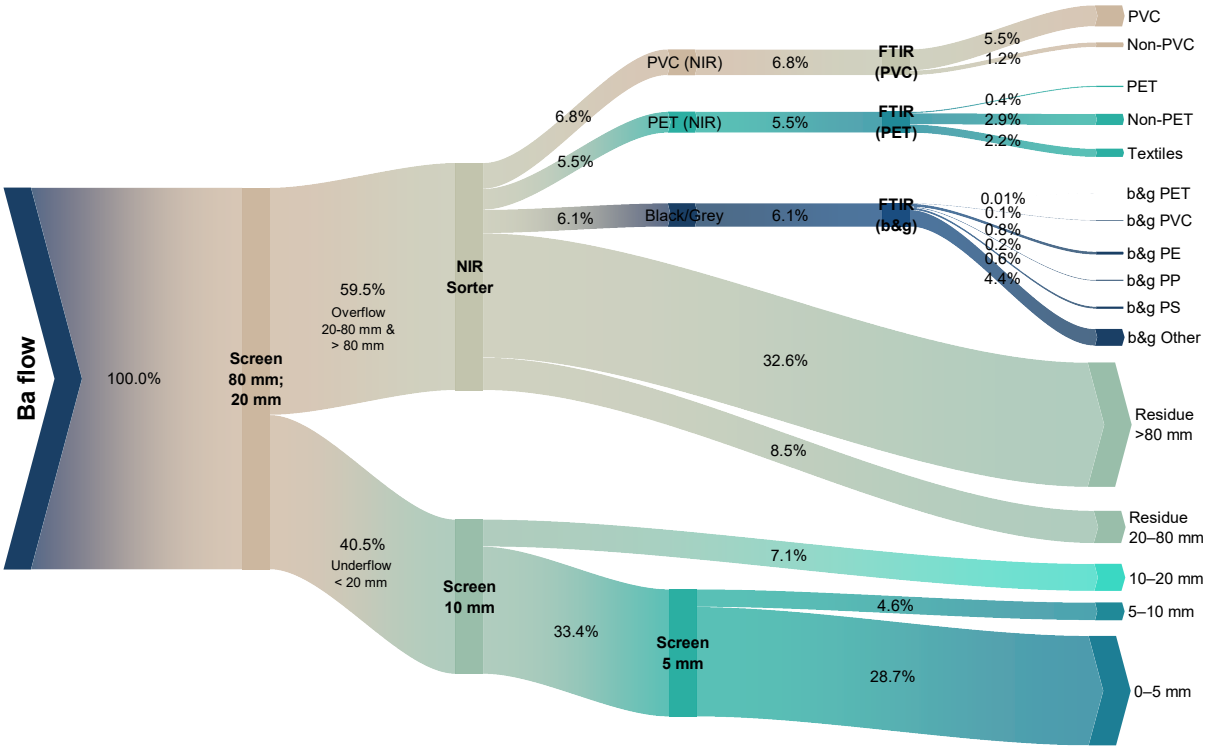

b

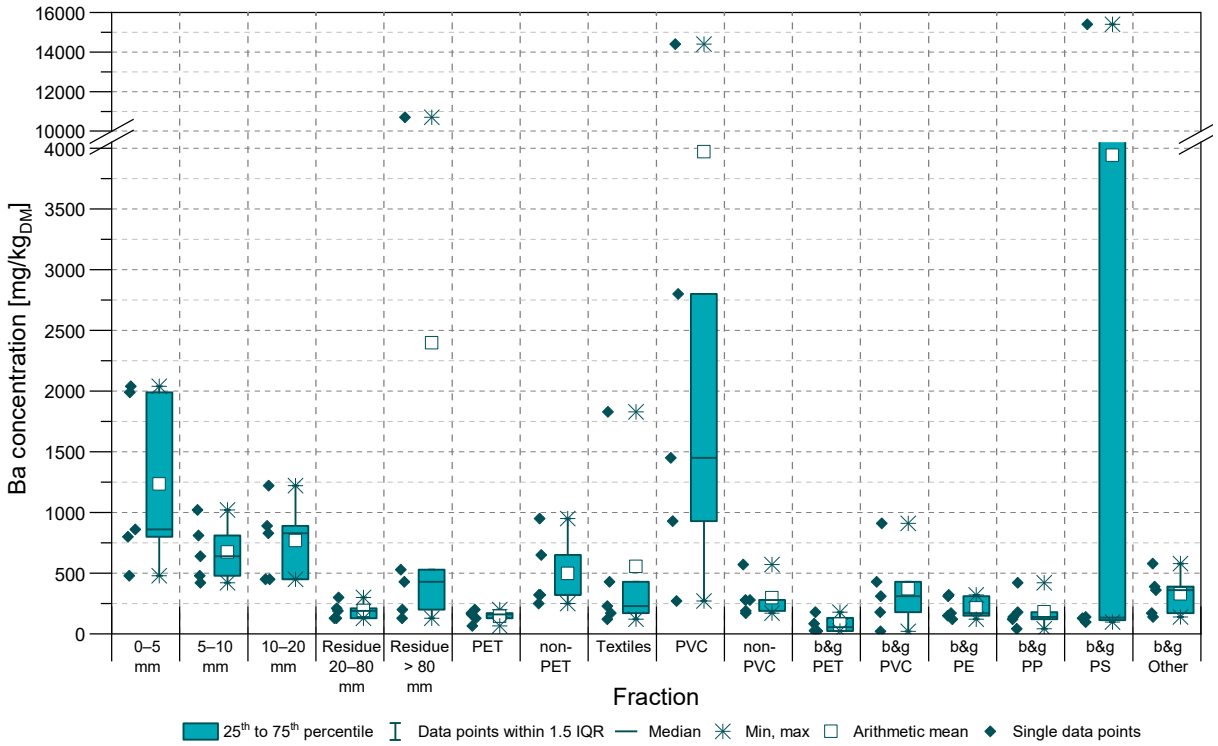

Figure A.6: a) Diagram of barium (Ba) flows representing the arithmetic mean values of the five MCW samples S01–S05. B&g = black and grey fractions. b) Box plot of Ba concentrations in different particle size classes and sorted fractions in mg/kg referring to dry mass without hard impurities

Table A.6: Barium (Ba) concentrations in mg/kg referring to dry mass without hard impurities. LOQ = 0.50 mg/kg

Fraction		Composite sample					Mean	Std. Dev.	Rel. Std. Dev [%]
		S01	S02	S03	S04	S05			
Screen	0–5 mm	480	2040	1990	860	800	1230	730	59
	5–10 mm	640	420	1020	480	810	670	250	36
	10–20 mm	890	450	1220	450	830	770	330	42
NIR Residue	20–80 mm	130	210	190	130	300	190	70	37
	> 80 mm	10700	200	130	530	430	2400	4640	194
NIR PET Fraction	PET	160	67	170	200	130	150	50	35
	Non-PET	950	320	650	250	320	500	300	60
	Textile	1830	230	430	170	120	560	720	130
NIR PVC Fraction	PVC	1450	2800	14400	270	930	3970	5900	149
	Non-PVC	280	280	570	170	190	300	160	54
Black & Grey Fraction	PET	180	25	-	85	23	78	74	94
	PVC	430	20	180	310	910	370	340	91
	PE	320	120	170	310	150	210	94	44
	PP	140	420	120	43	180	180	140	79
	PS	140	97	130	-	15400	3940	7640	194
	Other	580	360	140	390	170	330	180	55
Overall	mg/kg	2530	620	530	380	430	900	920	102
	mg/MJ	120	28	25	17	22	42	42	101

A.7. Ca

a

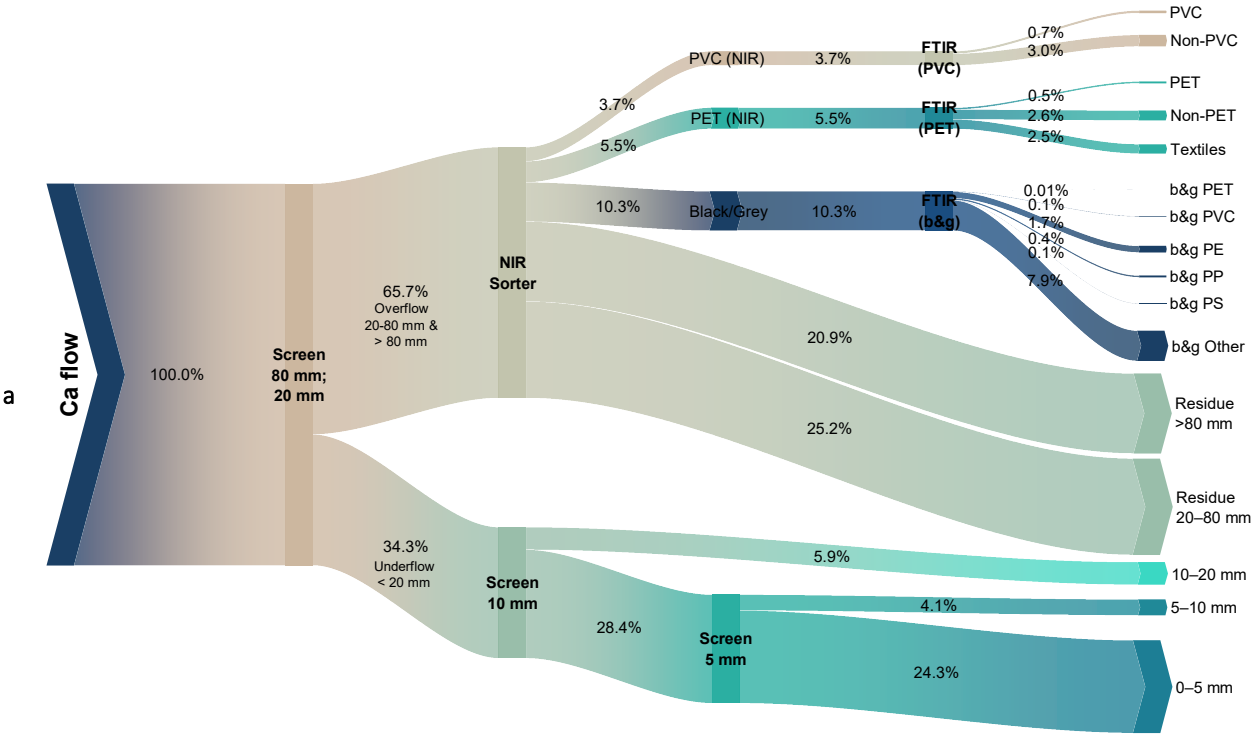

b

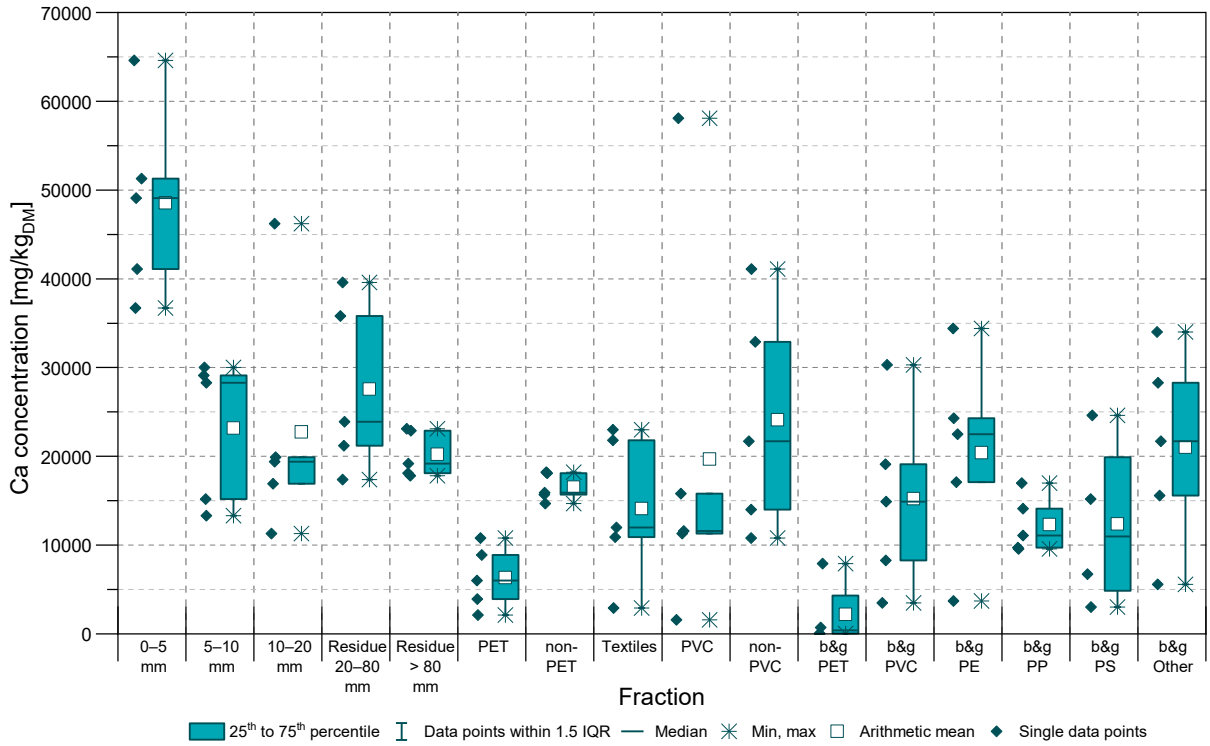

Figure A.7: a) Diagram of calcium (Ca) flows representing the arithmetic mean values of the five MCW samples S01–S05. B&g = black and grey fractions. b) Box plot of Ca concentrations in different particle size classes and sorted fractions in mg/kg referring to dry mass without hard impurities

Table A.7: Calcium (Ca) concentrations in mg/kg referring to dry mass without hard impurities. LOQ = 50 mg/kg

Fraction		Composite sample					Mean	Std. Dev.	Rel. Std. Dev [%]
		S01	S02	S03	S04	S05			
Screen	0–5 mm	36700	41100	49100	51300	64600	48600	10700	22
	5–10 mm	13300	28300	29100	15200	30000	23200	8200	35
	10–20 mm	16900	19900	19400	11300	46200	22700	13600	60
NIR Residue	20–80 mm	17400	39600	21200	35800	23900	27600	9620	35
	> 80 mm	22900	19200	18100	23100	17800	20200	2590	13
NIR PET Fraction	PET	3920	2110	6000	10800	8880	6340	3540	56
	Non-PET	14700	15900	18100	15700	18200	16500	1560	9
	Textile	2900	21800	10900	12000	23000	14100	8350	59
NIR PVC Fraction	PVC	1580	11600	15800	11300	58100	19700	22100	112
	Non-PVC	10800	32900	21700	14000	41100	24100	12800	53
Black & Grey Fraction	PET	720	< 50	-	< 50	7900	2180	3830	176
	PVC	3480	8280	19100	14900	30300	15200	10400	68
	PE	24300	22500	17100	3720	34400	20400	11200	55
	PP	9590	14100	9710	17000	11100	12300	3200	26
	PS	3020	15200	6730	-	24600	12400	9600	78
	Other	5570	21700	28300	15600	34000	21000	11100	53
Overall	mg/kg	17800	28600	22700	26200	31300	25300	5290	21
	mg/MJ	830	1290	1090	1190	1610	1200	290	24

A.8. Cd

a

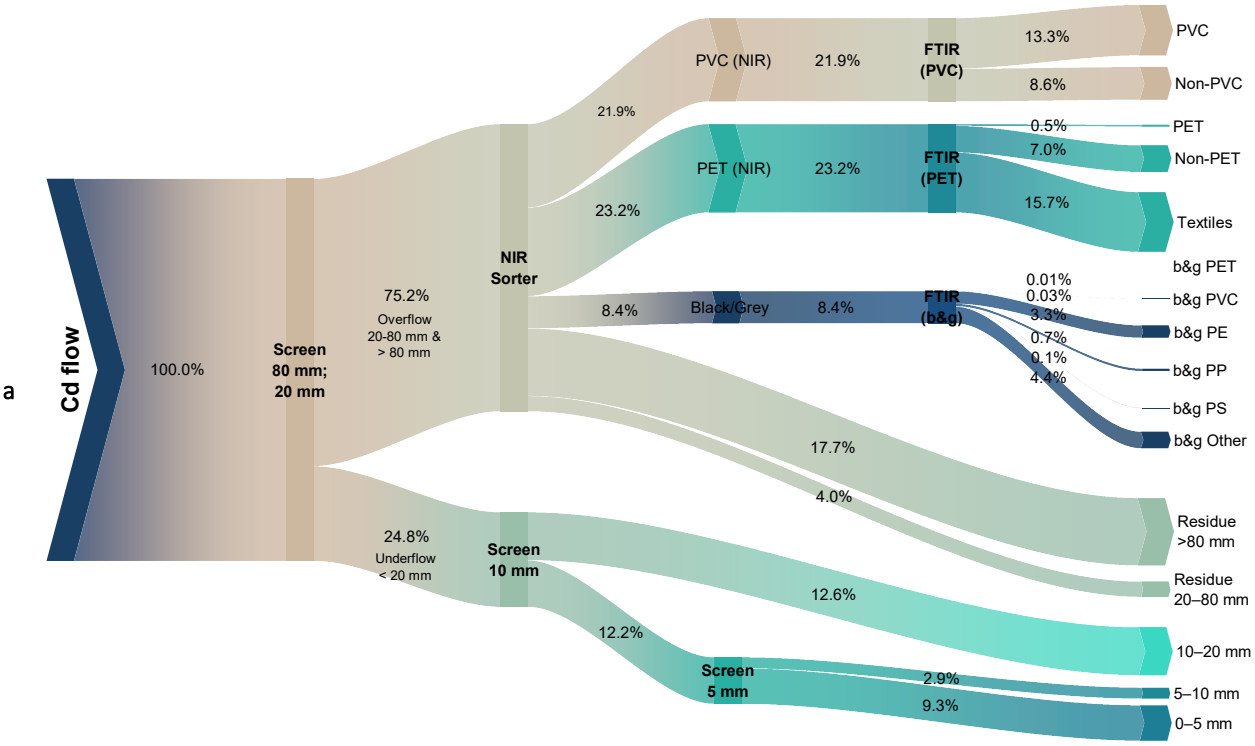

b

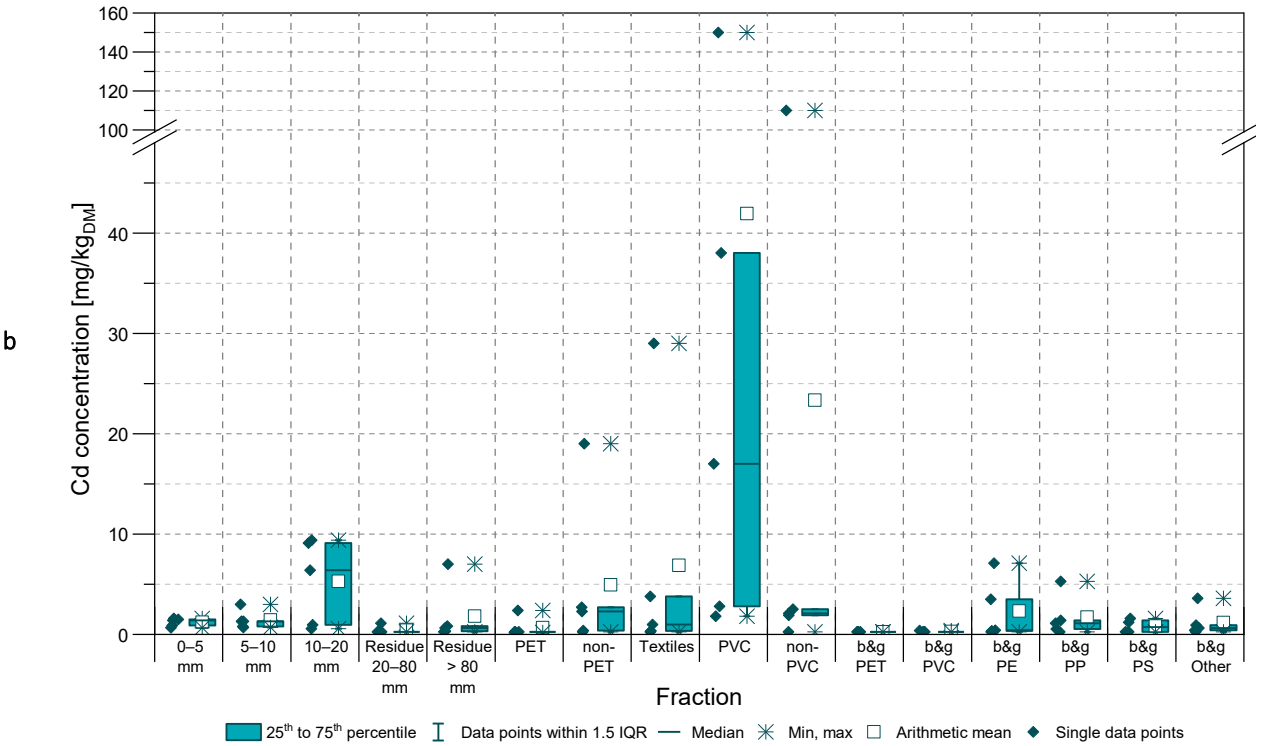

Figure A.8: a) Diagram of cadmium (Cd) flows representing the arithmetic mean values of the five MCW samples S01–S05. B&g = black and grey fractions. b) Box plot of Cd concentrations in different particle size classes and sorted fractions in mg/kg referring to dry mass without hard impurities

Table A.8: Cadmium (Cd) concentrations in mg/kg referring to dry mass without hard impurities. LOQ = 0.25 mg/kg

Fraction		Composite sample					Mean	Std. Dev.	Rel. Std. Dev [%]
		S01	S02	S03	S04	S05			
Screen	0–5 mm	0.90	1.6	1.4	1.5	0.66	1.2	0.41	34
	5–10 mm	1.3	0.71	3.0	0.79	1.3	1.4	0.93	65
	10–20 mm	6.4	0.94	9.4	9.1	0.56	5.3	4.3	81
NIR Residue	20–80 mm	< 0.25	0.25	1.1	< 0.25	< 0.25	0.42	0.38	91
	> 80 mm	7	0.32	0.65	< 0.25	0.84	1.8	2.9	161
NIR PET Fraction	PET	< 0.25	< 0.25	0.20	2.4	< 0.25	0.67	0.97	144
	Non-PET	< 0.25	2.3	19	2.7	0.37	4.9	7.9	161
	Textile	0.35	< 0.25	1.0	29	3.8	6.9	12	181
NIR PVC Fraction	PVC	17	38	150	2.8	1.8	42	62	148
	Non-PVC	< 0.25	2.5	110	2.1	1.9	23	48	207
Black & Grey Fraction	PET	< 0.25	< 0.25	-	< 0.25	< 0.25	0.25	0.00	0
	PVC	0.39	< 0.25	0.27	< 0.25	0.27	0.29	0.06	21
	PE	0.34	0.41	7.1	< 0.25	3.5	2.3	3.0	129
	PP	0.53	1.4	1.1	< 0.25	5.3	1.7	2.1	120
	PS	0.25	1.2	< 0.25	-	1.6	0.83	0.68	83
	Other	< 0.25	0.65	0.92	3.6	0.42	1.2	1.4	118
Overall	mg/kg	2.5	1.2	4.7	2.7	1.0	2.4	1.5	61
	mg/MJ	0.12	0.05	0.22	0.12	0.05	0.11	0.07	61

A.9. Cl

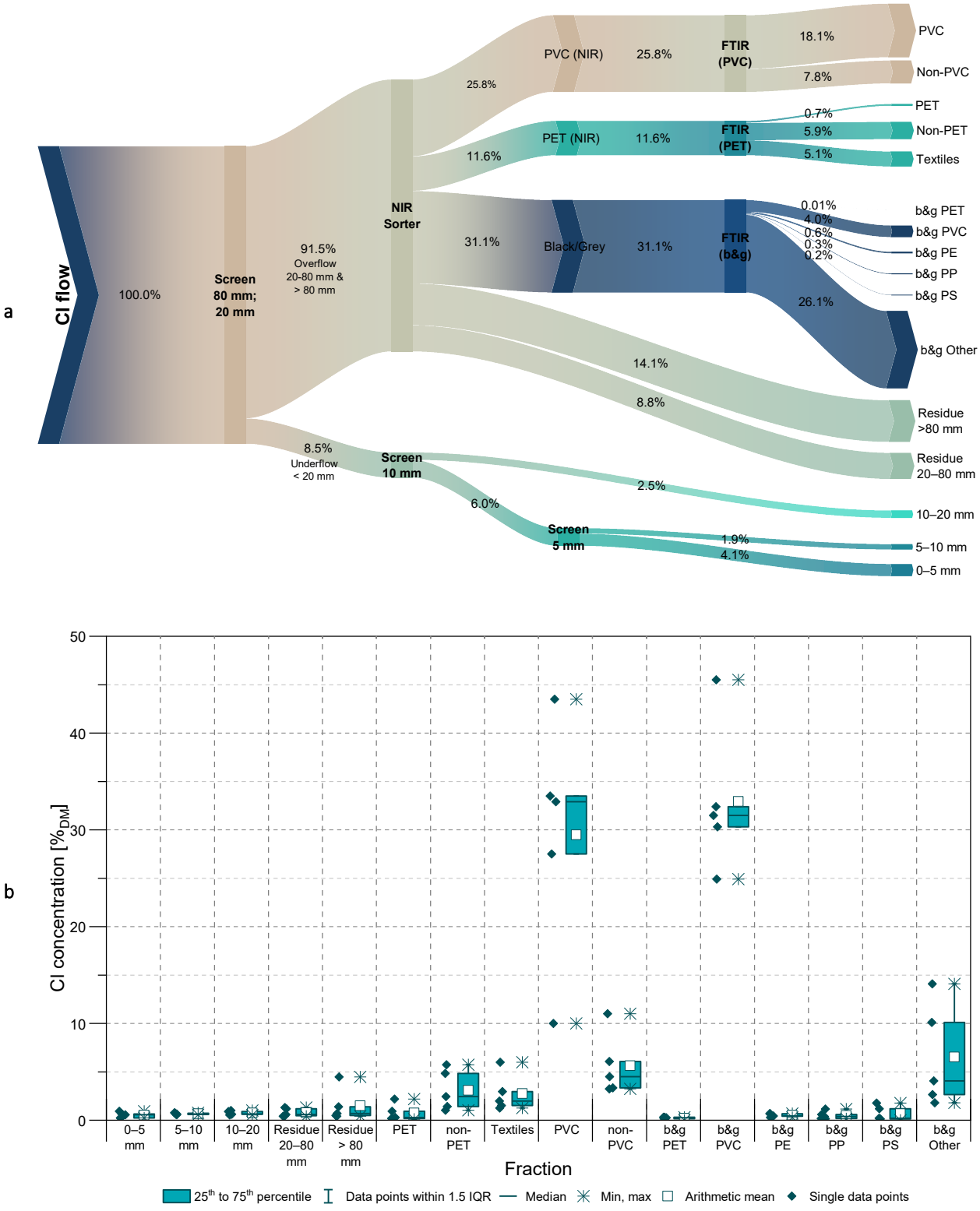

Figure A.9: a) Diagram of chlorine (Cl) flows representing the arithmetic mean values of the five MCW samples S01–S05. B&g = black and grey fractions. b) Box plot of Cl concentrations in different particle size classes and sorted fractions in mg/kg referring to dry mass without hard impurities

Table A.9: Chlorine (Cl) concentrations in mg/kg referring to dry mass without hard impurities. LOQ = 100 mg/kg

Fraction		Composite sample					Mean	Std. Dev.	Rel. Std. Dev [%]
		S01	S02	S03	S04	S05			
Screen	0–5 mm	2430	6410	2380	5680	9180	5210	2880	55
	5–10 mm	5580	6480	7700	5820	7320	6580	920	14
	10–20 mm	5410	6110	10000	9030	6380	7390	2010	27
NIR Residue	20–80 mm	13000	4560	5830	4040	11700	7830	4210	54
	> 80 mm	44700	7060	4040	4780	14000	14900	17100	115
NIR PET Fraction	PET	9380	1110	1810	21800	2760	7370	8710	118
	Non-PET	24300	10400	14100	48300	57300	30900	20900	68
	Textile	59900	19900	15100	29600	12500	27400	19300	70
NIR PVC Fraction	PVC	335000	329000	100000	435000	275000	295000	123000	42
	Non-PVC	60700	33300	110000	32500	45000	56300	32100	57
Black & Grey Fraction	PET	3110	1530	-	3090	2660	2600	740	29
	PVC	315000	455000	324000	249000	303000	329000	76100	23
	PE	2920	4360	4240	6630	6960	5020	1720	34
	PP	5920	11600	1920	3980	1430	4970	4110	83
	PS	11900	2050	17800	-	1400	8290	7960	96
	Other	141000	18000	26500	40500	101000	65400	53300	81
Overall	mg/kg	36400	12000	11500	21300	22600	20800	10100	49
	mg/MJ	1690	540	550	970	1160	980	480	49

A.10. Co

a

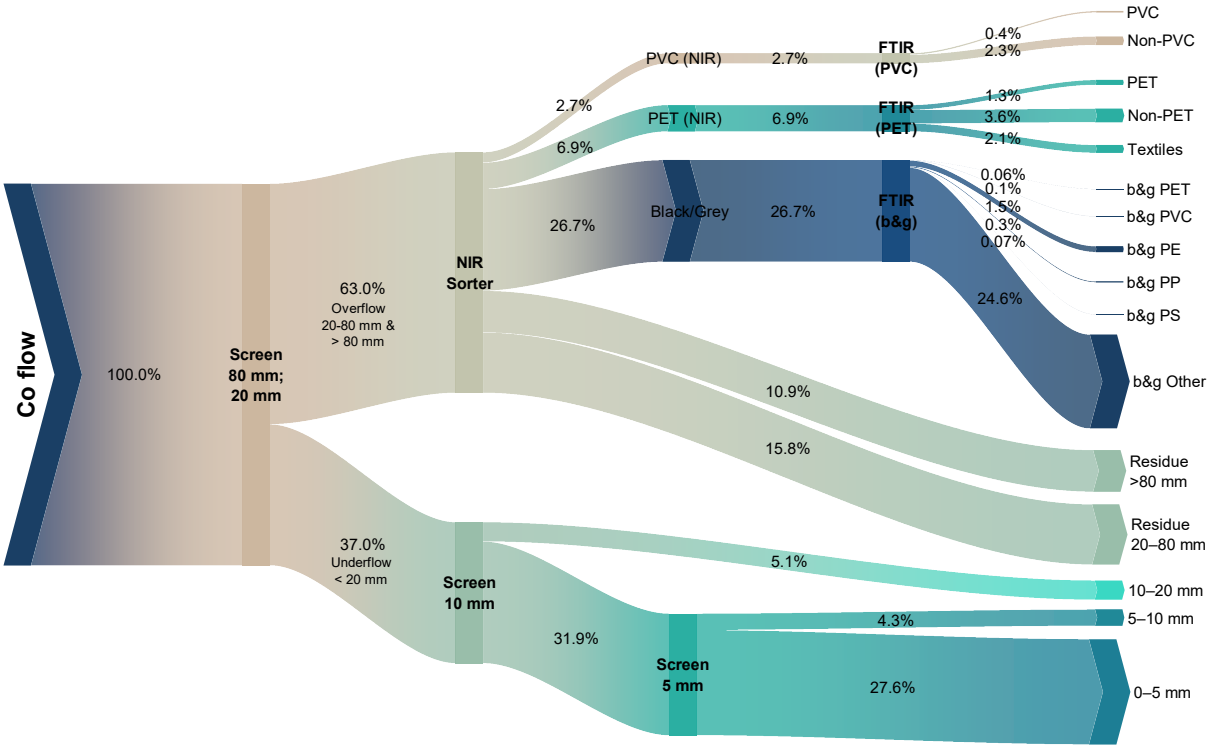

b

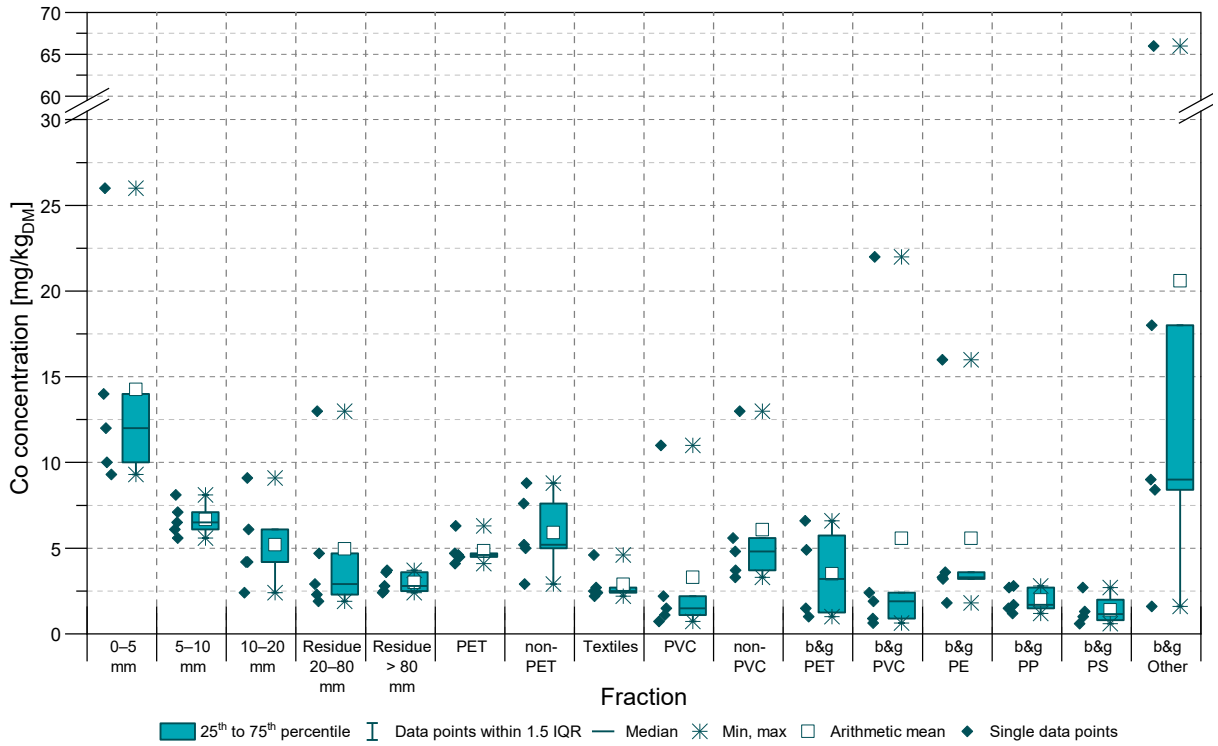

Figure A.10: a) Diagram of cobalt (Co) flows representing the arithmetic mean values of the five MCW samples S01–S05. B&g = black and grey fractions. b) Box plot of Co concentrations in different particle size classes and sorted fractions in mg/kg referring to dry mass without hard impurities

Table A.10: Cobalt (Co) concentrations in mg/kg referring to dry mass without hard impurities. LOQ = 0.25 mg/kg

Fraction		Composite sample					Mean	Std. Dev.	Rel. Std. Dev [%]
		S01	S02	S03	S04	S05			
Screen	0–5 mm	26	10	12	9.3	14	14	6.8	48
	5–10 mm	5.6	7.1	6.1	6.5	8.1	6.7	0.97	14
	10–20 mm	4.2	6.1	4.2	2.4	9.1	5.2	2.5	49
NIR Residue	20–80 mm	2.3	13	1.9	2.9	4.7	5.0	4.6	93
	> 80 mm	3.7	2.8	2.5	2.4	3.6	3.0	0.61	20
NIR PET Fraction	PET	4.1	6.3	4.7	4.6	4.5	4.8	0.85	18
	Non-PET	2.9	5.2	8.8	7.6	5	5.9	2.3	39
	Textile	2.2	2.5	2.7	2.4	4.60	2.9	0.98	34
NIR PVC Fraction	PVC	0.72	1.5	2.2	1.1	11	3.3	4.3	131
	Non-PVC	4.8	13	5.6	3.3	3.7	6.1	4.0	65
Black & Grey Fraction	PET	4.9	1.5		6.6	1	3.5	2.7	77
	PVC	2.4	0.64	0.89	1.9	22	5.6	9.2	166
	PE	3.2	1.8	3.6	16	3.3	5.6	5.9	105
	PP	2.7	2.8	1.5	1.2	1.7	2.0	0.73	37
	PS	1.0	2.7	0.59		1.3	1.4	0.92	66
	Other	1.6	8.4	18	66	9	21	26	126
Overall	mg/kg	6.3	7.7	6.0	9.0	6.2	7.0	1.3	18
	mg/MJ	0.29	0.35	0.29	0.41	0.32	0.33	0.05	15

A.11. Cr

a

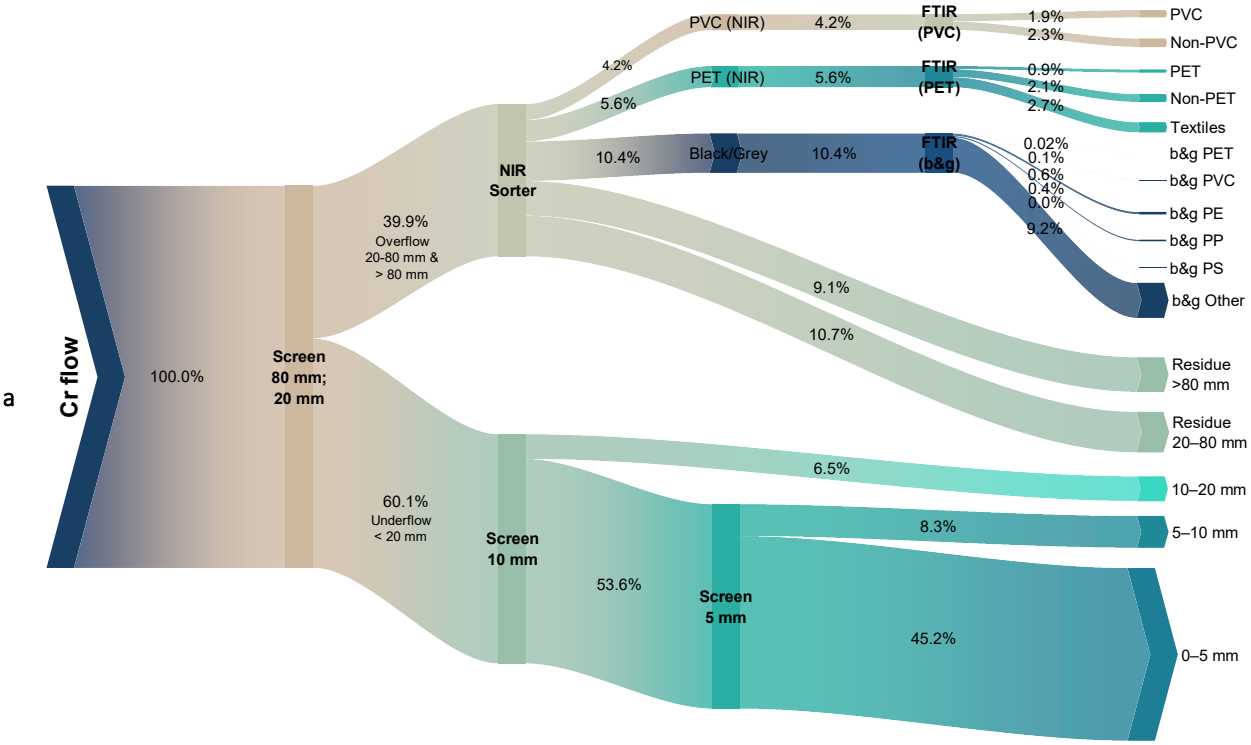

b

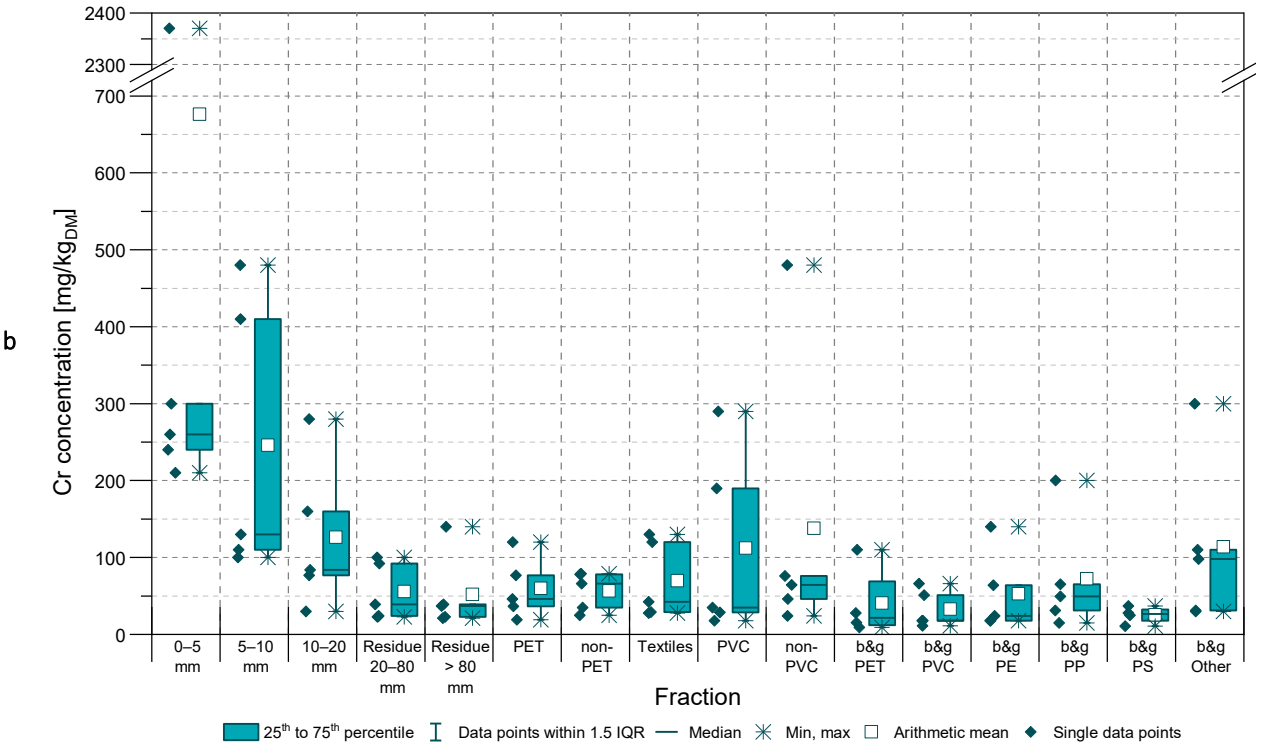

Figure A.11: a) Diagram of chromium (Cr) flows representing the arithmetic mean values of the five MCW samples S01–S05. B&g = black and grey fractions. b) Box plot of Cr concentrations in different particle size classes and sorted fractions in mg/kg referring to dry mass without hard impurities

Table A.11: Chromium (Cr) concentrations in mg/kg referring to dry mass without hard impurities. LOQ = 0.50 mg/kg

Fraction		Composite sample					Mean	Std. Dev.	Rel. Std. Dev [%]
		S01	S02	S03	S04	S05			
Screen	0–5 mm	2370	300	260	210	240	680	950	140
	5–10 mm	410	130	100	480	110	250	180	75
	10–20 mm	160	84	77	30	280	130	98	77
NIR Residue	20–80 mm	100	23	24	39	92	56	38	67
	> 80 mm	140	39	21	37	23	52	50	96
NIR PET Fraction	PET	120	37	46	77	19	60	40	67
	Non-PET	79	78	35	25	66	57	25	44
	Textile	130	42	29	120	28	70	51	73
NIR PVC Fraction	PVC	35	29	190	290	18	110	120	109
	Non-PVC	480	64	76	24	46	140	190	139
Black & Grey Fraction	PET	110	15	-	28	9.1	41	47	115
	PVC	66	11	18	18	51	33	24	74
	PE	140	24	64	18	18	53	52	99
	PP	200	49	31	15	65	72	74	103
	PS	37	28	11	-	25	25	11	43
	Other	30	98	31	110	300	110	110	97
Overall	mg/kg	450	100	52	82	110	160	160	104
	mg/MJ	21	4.6	2.5	3.7	5.5	7.4	7.6	102

A.12. Cu

a

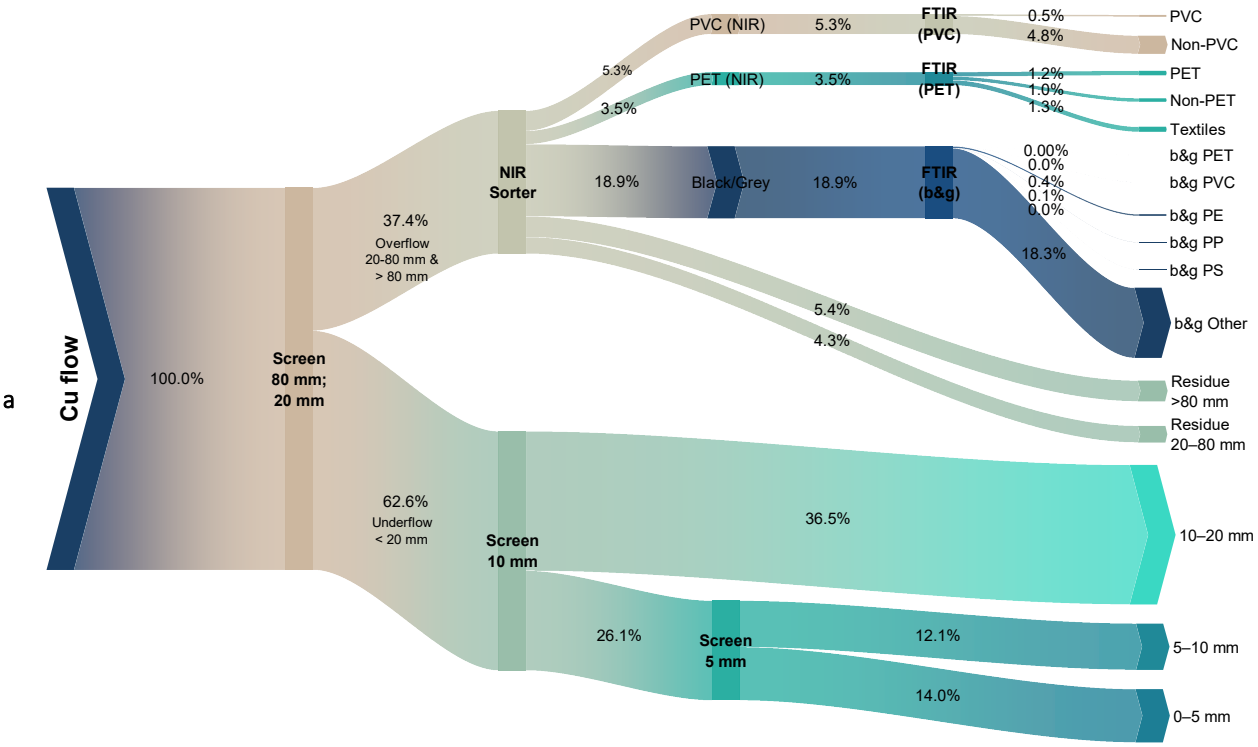

b

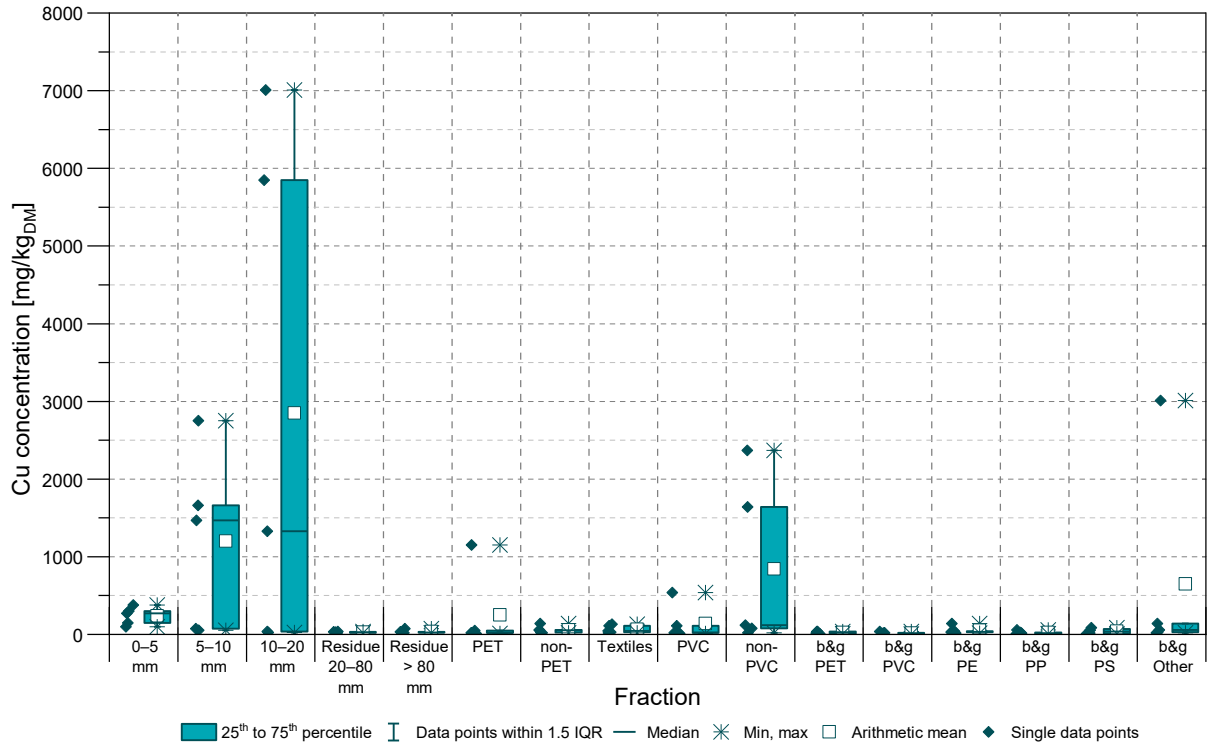

Figure A.12: a) Diagram of copper (Cu) flows representing the arithmetic mean values of the five MCW samples S01–S05. B&g = black and grey fractions. b) Box plot of Cu concentrations in different particle size classes and sorted fractions in mg/kg referring to dry mass without hard impurities

Table A.12: Copper (Cu) concentrations in mg/kg referring to dry mass without hard impurities. LOQ = 0.50 mg/kg

Fraction		Composite sample					Mean	Std. Dev.	Rel. Std. Dev [%]
		S01	S02	S03	S04	S05			
Screen	0–5 mm	270	300	150	380	98	240	110	48
	5–10 mm	2750	55	76	1660	1470	1200	1150	95
	10–20 mm	7010	23	38	5850	1330	2850	3340	117
NIR Residue	20–80 mm	29	19	22	33	36	28	7.2	26
	> 80 mm	74	25	23	33	21	35	22	63
NIR PET Fraction	PET	1150	19	20	50	11	250	500	201
	Non-PET	140	52	21	59	25	59	49	81
	Textile	110	46	28	130	19	67	51	75
NIR PVC Fraction	PVC	540	12	110	24	19	140	230	161
	Non-PVC	2370	77	120	1640	19	850	1090	129
Black & Grey Fraction	PET	39	39	-	17	10	26	15	57
	PVC	39	2.3	12	15	19	17	14	77
	PE	140	16	41	33	28	52	50	97
	PP	59	10	6.8	23	16	23	21	92
	PS	55	15	9.1	-	85	41	36	87
	Other	140	3010	28	59	21	650	1320	202
Overall	mg/kg	1180	340	38	460	160	430	450	103
	mg/MJ	55	16	1.8	21	8.0	20	21	102

A.13. Fe

a

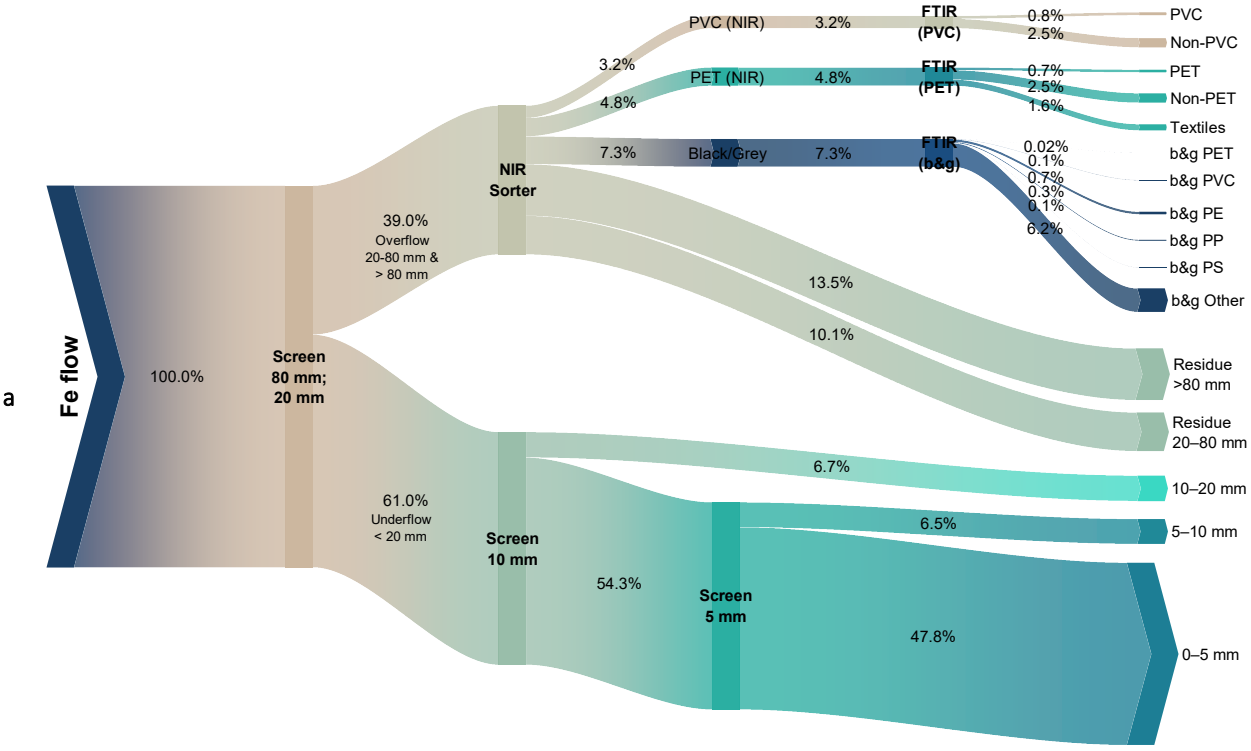

b

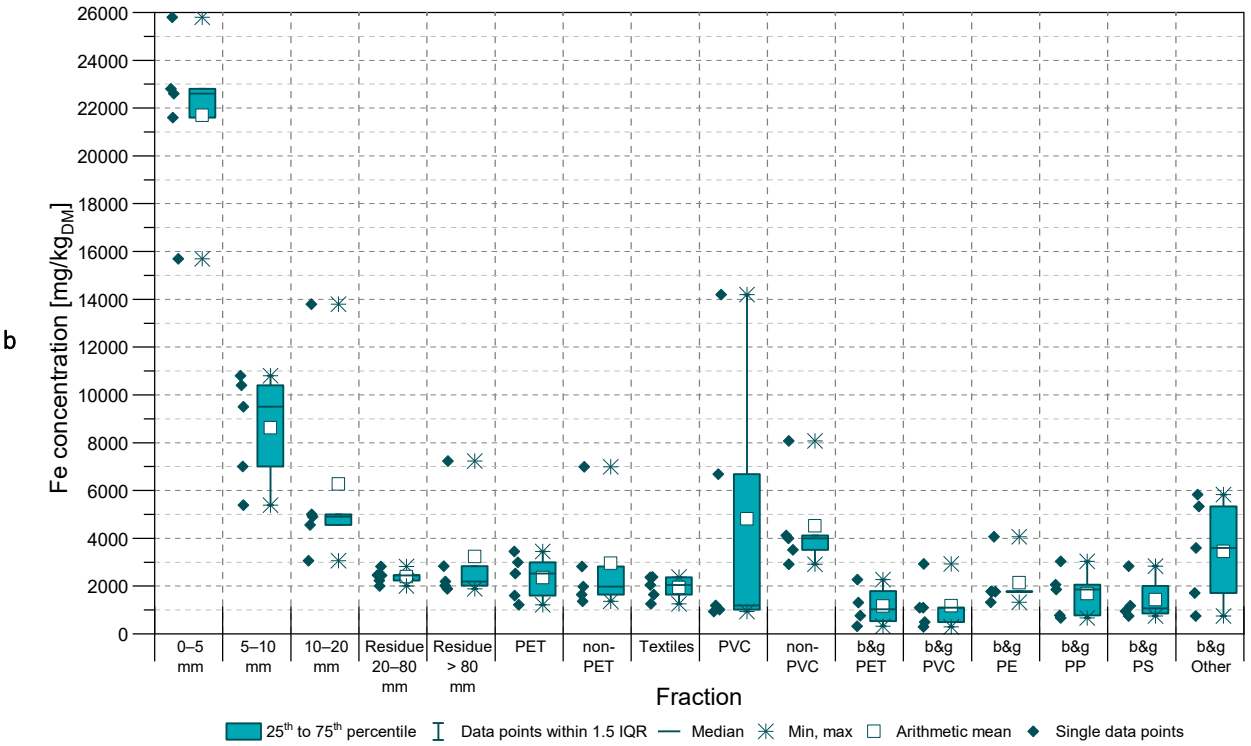

Figure A.13: a) Diagram of iron (Fe) flows representing the arithmetic mean values of the five MCW samples S01–S05. B&g = black and grey fractions. b) Box plot of Fe concentrations in different particle size classes and sorted fractions in mg/kg referring to dry mass without hard impurities

Table A.13: Iron (Fe) concentrations in mg/kg referring to dry mass without hard impurities. LOQ = 2.5 mg/kg

Fraction		Composite sample					Mean	Std. Dev.	Rel. Std. Dev [%]
		S01	S02	S03	S04	S05			
Screen	0–5 mm	25800	22600	21600	15700	22800	21700	3700	17
	5–10 mm	5390	9510	10800	7000	10400	8620	2330	27
	10–20 mm	4560	4900	5000	3060	13800	6260	4280	68
NIR Residue	20–80 mm	2230	2010	2820	2460	2440	2390	300	13
	> 80 mm	7230	2190	2020	2830	1880	3230	2270	70
NIR PET Fraction	PET	1610	2520	3450	3000	1210	2360	940	40
	Non-PET	1360	2820	6990	1640	1980	2960	2320	78
	Textile	1260	2370	2380	1640	2050	1940	490	25
NIR PVC Fraction	PVC	940	14200	6690	1010	1190	4810	5790	121
	Non-PVC	4000	3520	4120	8070	2910	4520	2040	45
Black & Grey Fraction	PET	1310	2270	-	320	760	1170	840	72
	PVC	1090	290	1100	2930	500	1180	1040	88
	PE	1770	1760	4060	1780	1330	2140	1090	51
	PP	1860	3030	2060	770	670	1680	980	58
	PS	750	2830	950	-	1180	1430	950	67
	Other	750	5330	3600	5830	1710	3440	2210	64
Overall	mg/kg	6620	7160	4880	4440	5810	5780	1140	20
	mg/MJ	310	320	230	200	300	270	53	19

A.14. Hg

a

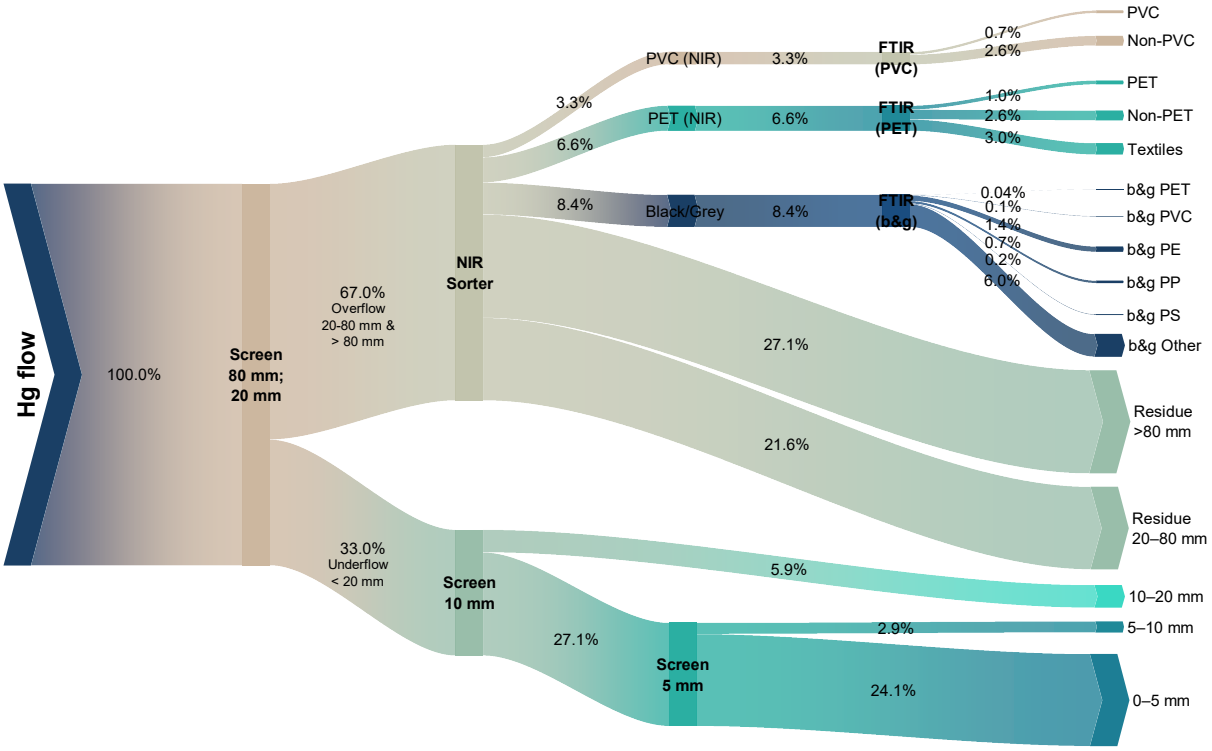

b

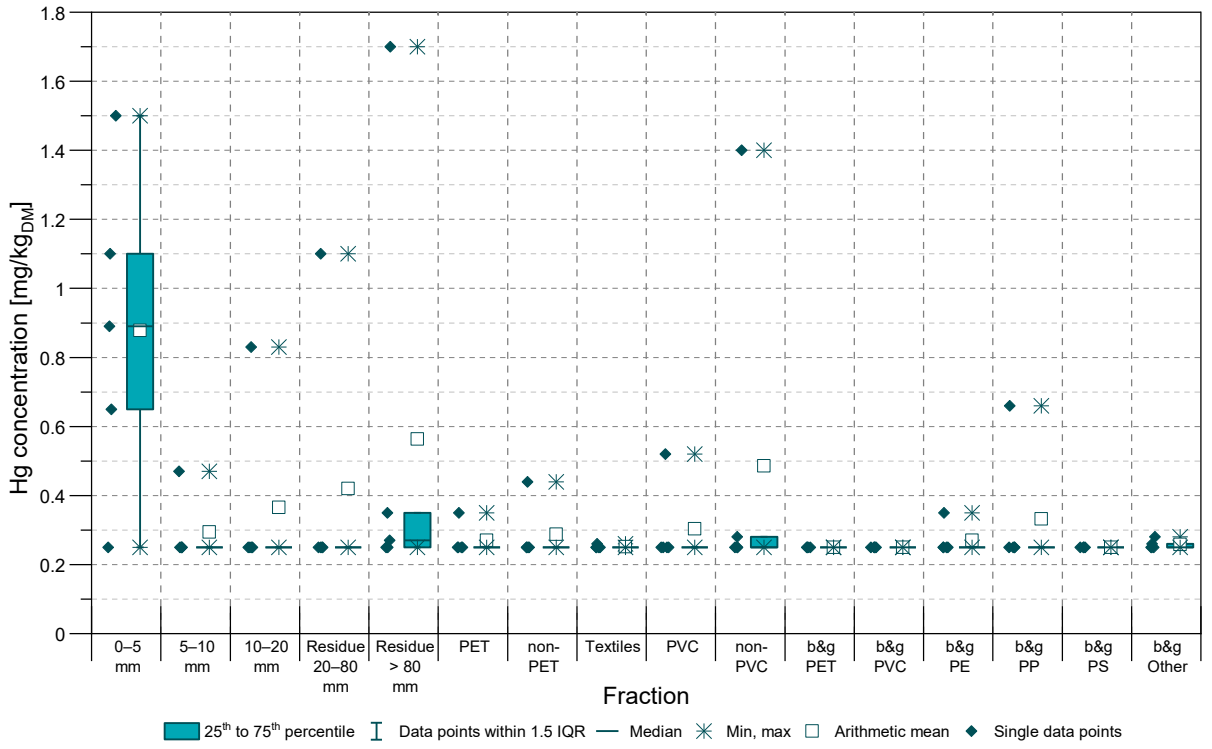

Figure A.14: a) Diagram of mercury (Hg) flows representing the arithmetic mean values of the five MCW samples S01–S05. B&g = black and grey fractions. b) Box plot of Hg concentrations in different particle size classes and sorted fractions in mg/kg referring to dry mass without hard impurities

Table A.14: Mercury (Hg) concentrations in mg/kg referring to dry mass without hard impurities. LOQ = 0.25 mg/kg

Fraction		Composite sample					Mean	Std. Dev.	Rel. Std. Dev [%]
		S01	S02	S03	S04	S05			
Screen	0–5 mm	0.89	0.65	1.1	1.5	< 0.25	0.88	0.47	54
	5–10 mm	< 0.25	< 0.25	0.47	< 0.25	< 0.25	0.29	0.10	33
	10–20 mm	< 0.25	< 0.25	< 0.25	< 0.25	0.83	0.37	0.26	71
NIR Residue	20–80 mm	< 0.25	1.1	< 0.25	< 0.25	< 0.25	0.42	0.38	91
	> 80 mm	1.7	< 0.25	0.35	< 0.25	0.27	0.56	0.64	113
NIR PET Fraction	PET	< 0.25	0.35	< 0.25	< 0.25	< 0.25	0.27	0.04	17
	Non-PET	0.44	< 0.25	< 0.25	< 0.25	< 0.25	0.29	0.08	30
	Textile	0.26	< 0.25	< 0.25	< 0.25	< 0.25	0.25	< 0.01	2
NIR PVC Fraction	PVC	< 0.25	< 0.25	0.52	< 0.25	< 0.25	0.30	0.12	40
	Non-PVC	0.28	1.4	< 0.25	< 0.25	< 0.25	0.49	0.51	105
Black & Grey Fraction	PET	< 0.25	< 0.25	-	< 0.25	< 0.25	0.25	0	0
	PVC	< 0.25	< 0.25	< 0.25	< 0.25	< 0.25	0.25	0	0
	PE	0.35	< 0.25	< 0.25	0.25	< 0.25	0.27	0.04	17
	PP	0.66	< 0.25	< 0.25	< 0.25	< 0.25	0.33	0.18	55
	PS	< 0.25	< 0.25	< 0.25	-	< 0.25	0.25	0	0
	Other	< 0.25	0.28	0.26	< 0.25	< 0.25	0.26	0.01	5
Overall	mg/kg	0.64	0.53	0.36	0.38	0.29	0.44	0.14	32
	mg/MJ	0.030	0.024	0.017	0.017	0.015	0.021	0.006	30

A.15. K

a

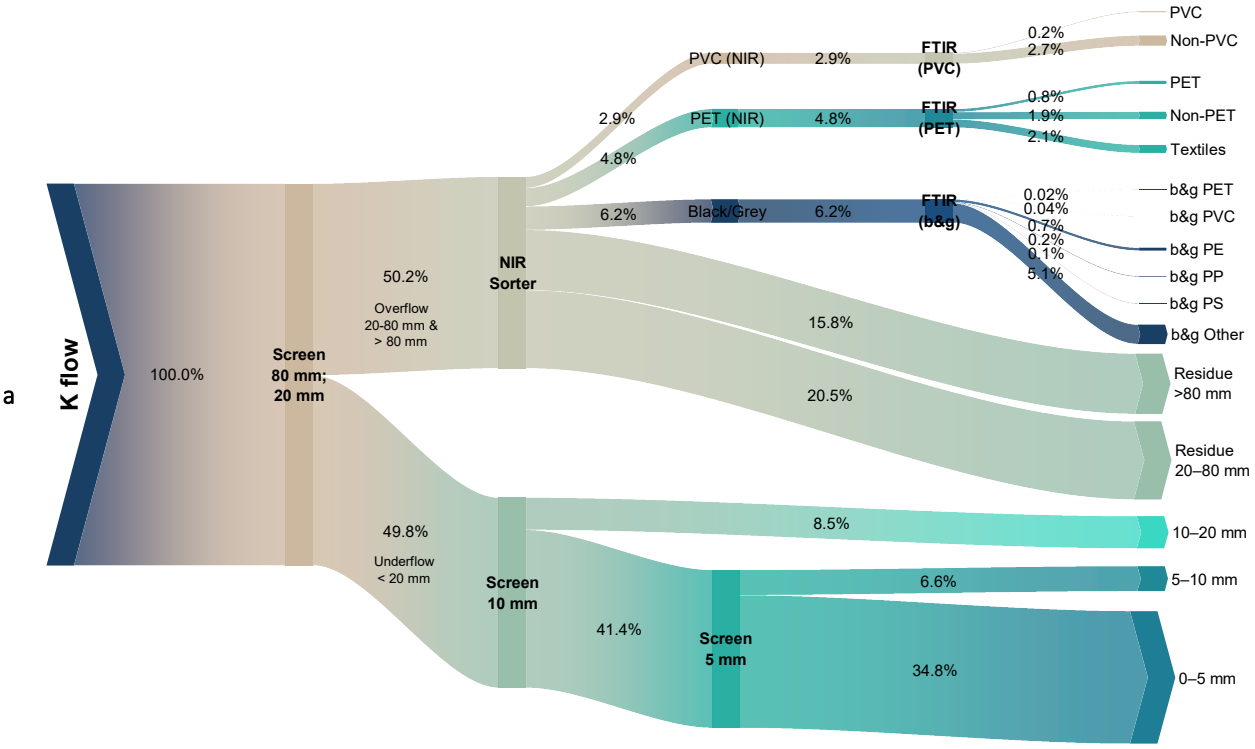

b

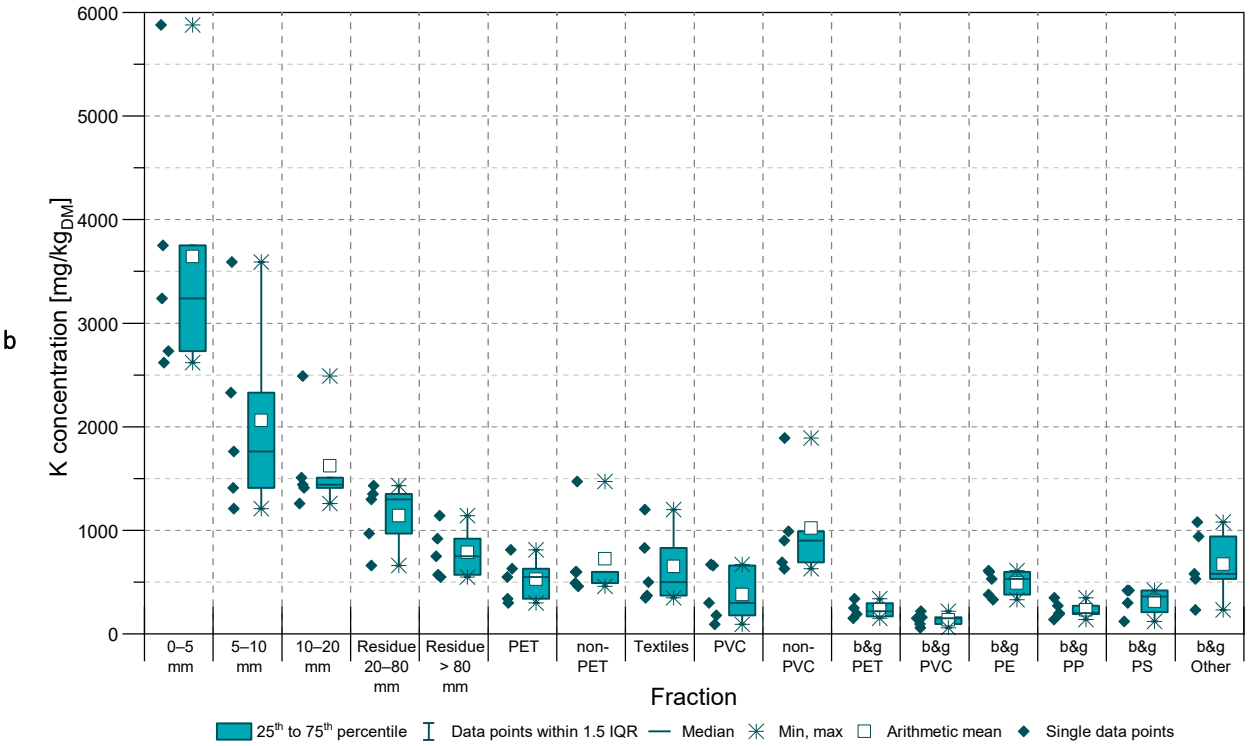

Figure A.15: a) Diagram of potassium (K) flows representing the arithmetic mean values of the five MCW samples S01–S05. B&g = black and grey fractions. b) Box plot of K concentrations in different particle size classes and sorted fractions in mg/kg referring to dry mass without hard impurities

Table A.15: Potassium (K) concentrations in mg/kg referring to dry mass without hard impurities. LOQ = 2.5 mg/kg

Fraction		Composite sample					Mean	Std. Dev.	Rel. Std. Dev [%]
		S01	S02	S03	S04	S05			
Screen	0–5 mm	3240	2620	3750	2730	5880	3640	1330	36
	5–10 mm	1210	1760	2330	1410	3590	2060	960	46
	10–20 mm	1510	1410	1440	1260	2490	1620	490	30
NIR Residue	20–80 mm	660	1300	1350	970	1430	1140	320	28
	> 80 mm	550	570	920	750	1140	790	250	32
NIR PET Fraction	PET	340	300	550	810	630	530	210	40
	Non-PET	600	600	460	490	1470	720	420	58
	Textile	350	830	370	500	1200	650	360	56
NIR PVC Fraction	PVC	300	180	660	94	670	380	270	71
	Non-PVC	900	990	690	630	1890	1020	510	50
Black & Grey Fraction	PET	340	250	-	150	190	230	80	36
	PVC	150	59	96	220	160	140	60	45
	PE	600	330	530	380	610	490	130	26
	PP	350	200	140	270	190	230	80	35
	PS	300	420	120	-	420	320	140	45
	Other	230	940	530	1080	580	670	340	51
Overall	mg/kg	1030	1300	1190	1040	2000	1310	400	31
	mg/MJ	48	59	57	47	100	63	23	37

A.16. Li

a

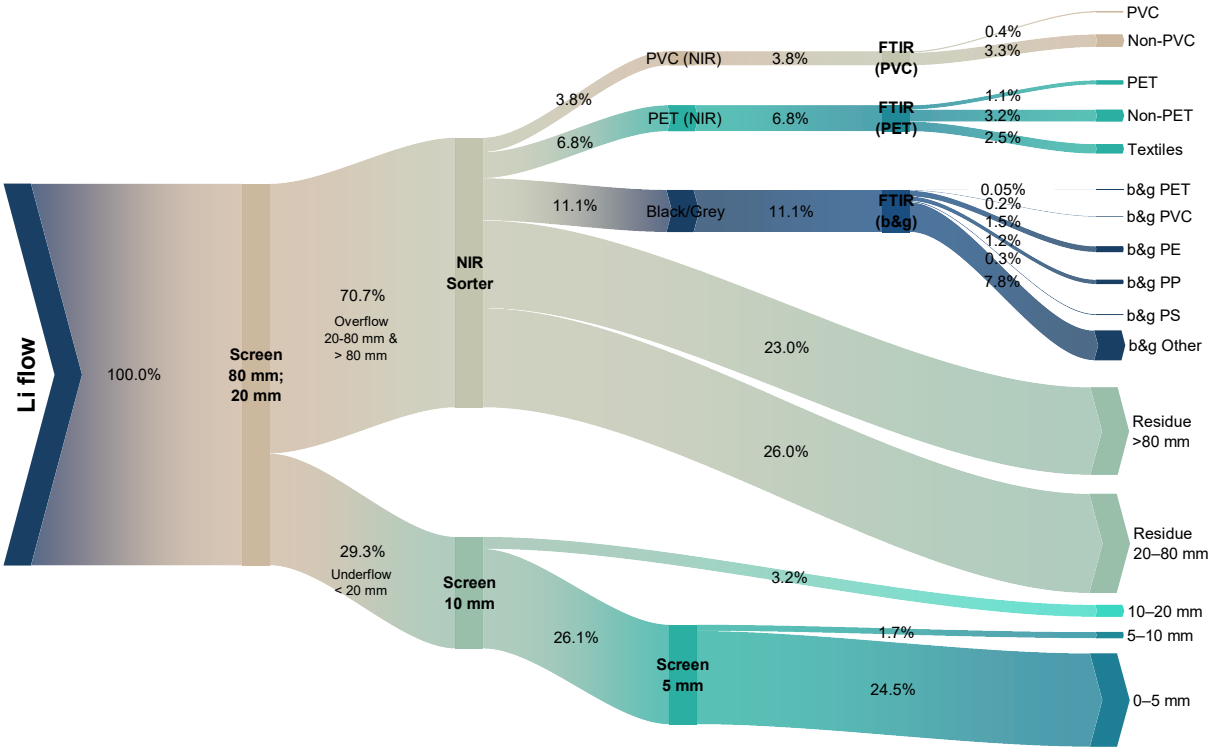

b

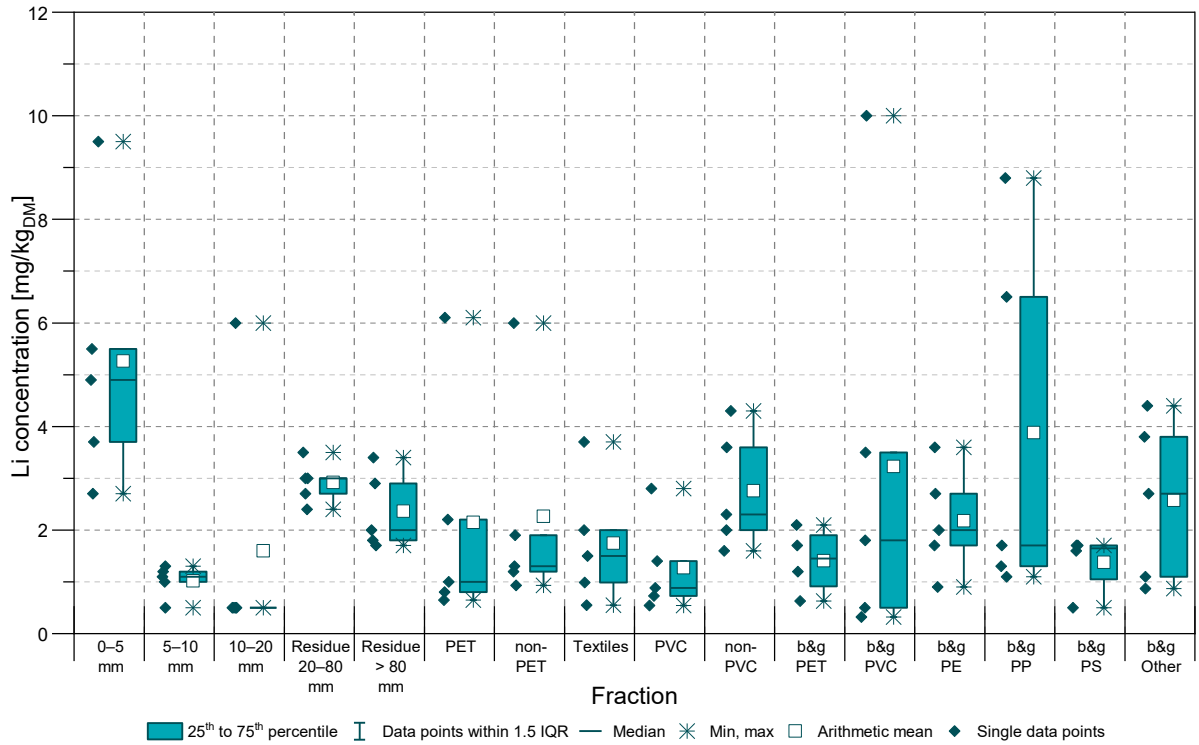

Figure A.16: a) Diagram of lithium (Li) flows representing the arithmetic mean values of the five MCW samples S01–S05. B&g = black and grey fractions. b) Box plot of Li concentrations in different particle size classes and sorted fractions in mg/kg referring to dry mass without hard impurities

Table A.16: Lithium (Li) concentrations in mg/kg referring to dry mass without hard impurities. LOQ = 0.50 mg/kg.

Fraction		Composite sample					Mean	Std. Dev.	Rel. Std. Dev [%]
		S01	S02	S03	S04	S05			
Screen	0–5 mm	5.5	3.7	2.7	9.5	4.9	5.3	2.6	50
	5–10 mm	1.3	< 0.5	1.1	1	1.2	1.0	0.31	31
	10–20 mm	< 0.5	< 0.5	< 0.5	< 0.5	6	1.6	2.5	154
NIR Residue	20–80 mm	2.7	3	2.4	3.5	3	2.9	0.41	14
	> 80 mm	1.7	3.4	1.8	2	2.9	2.4	0.75	32
NIR PET Fraction	PET	0.8	6.1	0.65	2.2	1	2.2	2.3	107
	Non-PET	1.3	6	0.93	1.2	1.9	2.3	2.1	93
	Textile	0.99	3.7	0.55	1.5	2	1.7	1.2	70
NIR PVC Fraction	PVC	0.54	1.4	0.73	0.88	2.8	1.3	0.91	72
	Non-PVC	2.3	4.3	1.6	2	3.6	2.8	1.1	41
Black & Grey Fraction	PET	1.2	1.7	-	2.1	0.63	1.4	0.64	45
	PVC	0.32	1.8	< 0.5	3.5	10	3.2	4.0	124
	PE	2.7	2	0.9	3.6	1.7	2.2	1.0	47
	PP	1.7	6.5	1.3	8.8	1.1	3.9	3.5	91
	PS	1.7	1.6	< 0.5	-	1.7	1.4	0.59	43
	Other	1.1	2.7	0.87	4.4	3.8	2.6	1.6	61
Overall	mg/kg	2.2	3.0	1.6	3.3	3.2	2.7	0.73	28
	mg/MJ	0.10	0.13	0.08	0.15	0.17	0.13	0.04	29

A.17. Mg

a

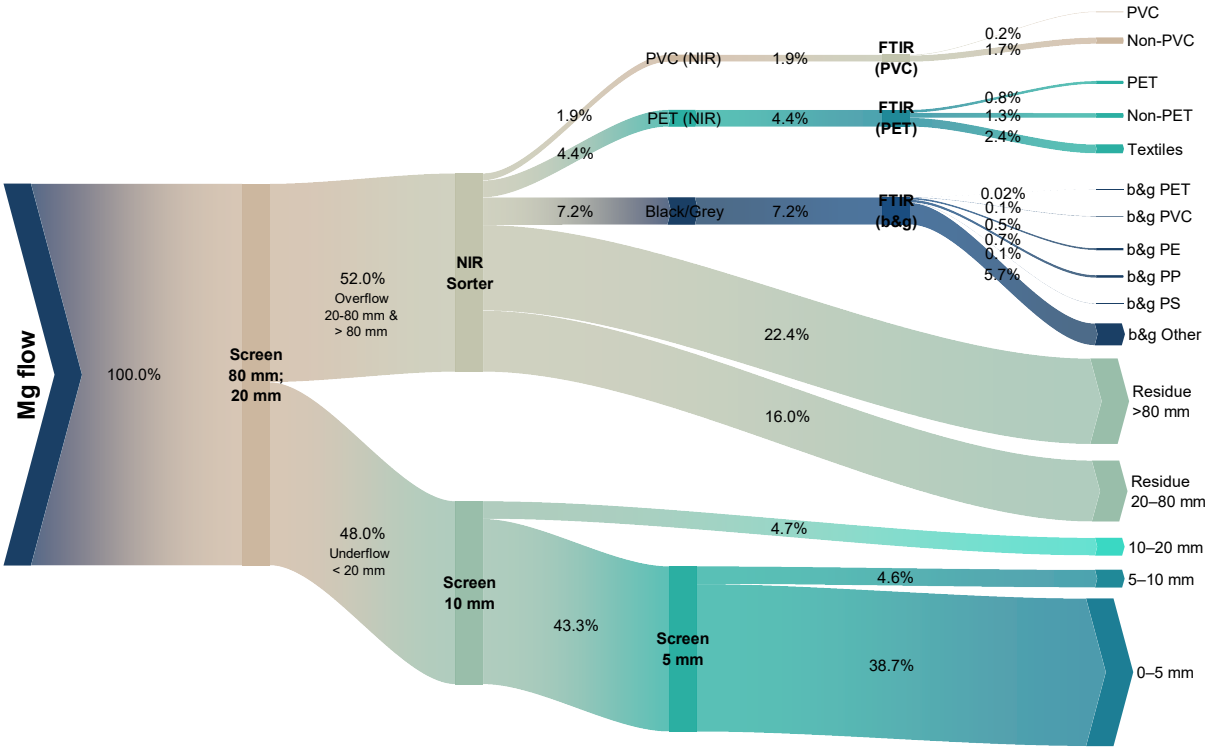

b

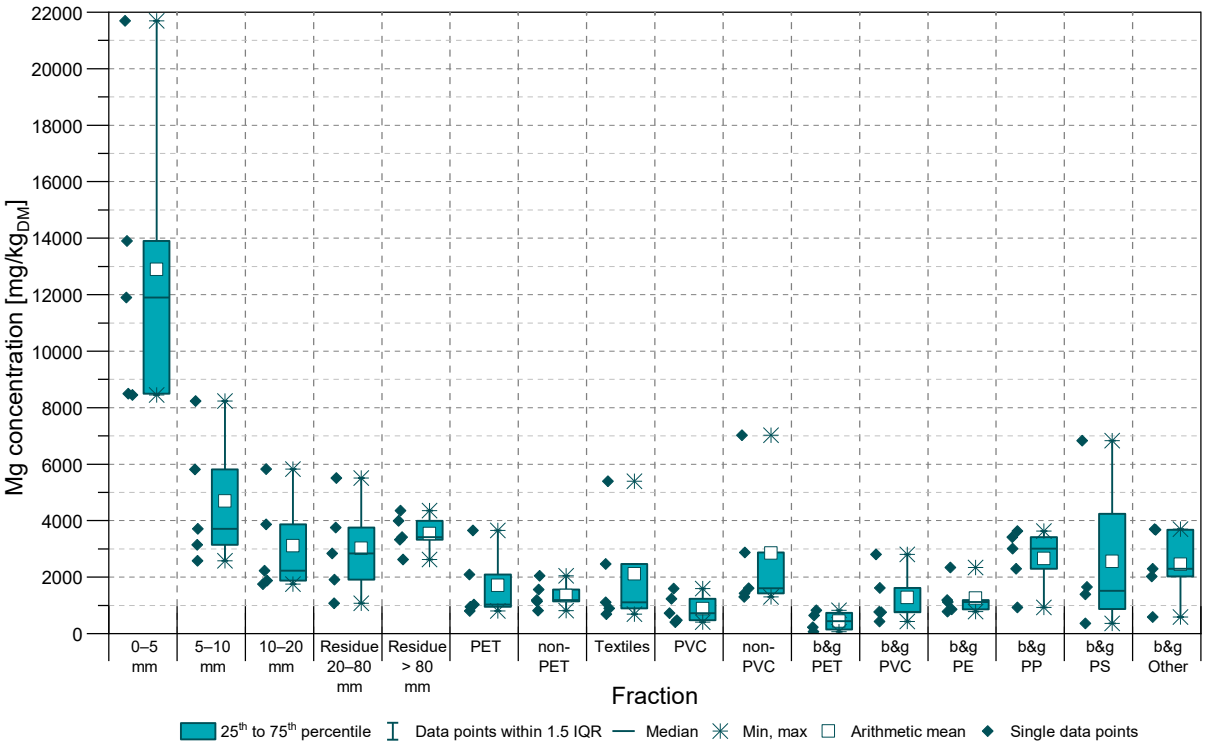

Figure A.17: a) Diagram of magnesium (Mg) flows representing the arithmetic mean values of the five MCW samples S01–S05. B&g = black and grey fractions. b) Box plot of Mg concentrations in different particle size classes and sorted fractions in mg/kg referring to dry mass without hard impurities

Table A.17: Magnesium (Mg) concentrations in mg/kg referring to dry mass without hard impurities. LOQ = 0.50 mg/kg

Fraction		Composite sample					Mean	Std. Dev.	Rel. Std. Dev [%]
		S01	S02	S03	S04	S05			
Screen	0–5 mm	11900	8500	13900	8450	21700	12900	5450	42
	5–10 mm	2580	3710	5810	3150	8240	4700	2330	50
	10–20 mm	2230	1880	3870	1750	5830	3110	1740	56
NIR Residue	20–80 mm	1080	1910	3760	2840	5510	3020	1720	57
	> 80 mm	2620	4360	3320	3990	3420	3540	670	19
NIR PET Fraction	PET	800	950	2090	3650	1030	1700	1200	71
	Non-PET	810	1140	2050	1190	1560	1350	470	35
	Textile	690	1110	5400	890	2470	2110	1970	93
NIR PVC Fraction	PVC	720	480	1590	410	1230	890	510	57
	Non-PVC	1300	1610	7020	1430	2870	2850	2420	85
Black & Grey Fraction	PET	650	63	-	230	830	440	360	81
	PVC	2800	430	770	1620	760	1280	960	75
	PE	1120	860	2340	780	1190	1260	630	50
	PP	3010	3630	3420	2300	930	2660	1090	41
	PS	360	1390	6830	-	1650	2560	2900	113
	Other	590	3680	2300	3700	2030	2460	1300	53
Overall	mg/kg	2990	3900	4320	3500	6290	4200	1270	30
	mg/MJ	140	180	210	160	320	200	73	36

A.18. Mn

a

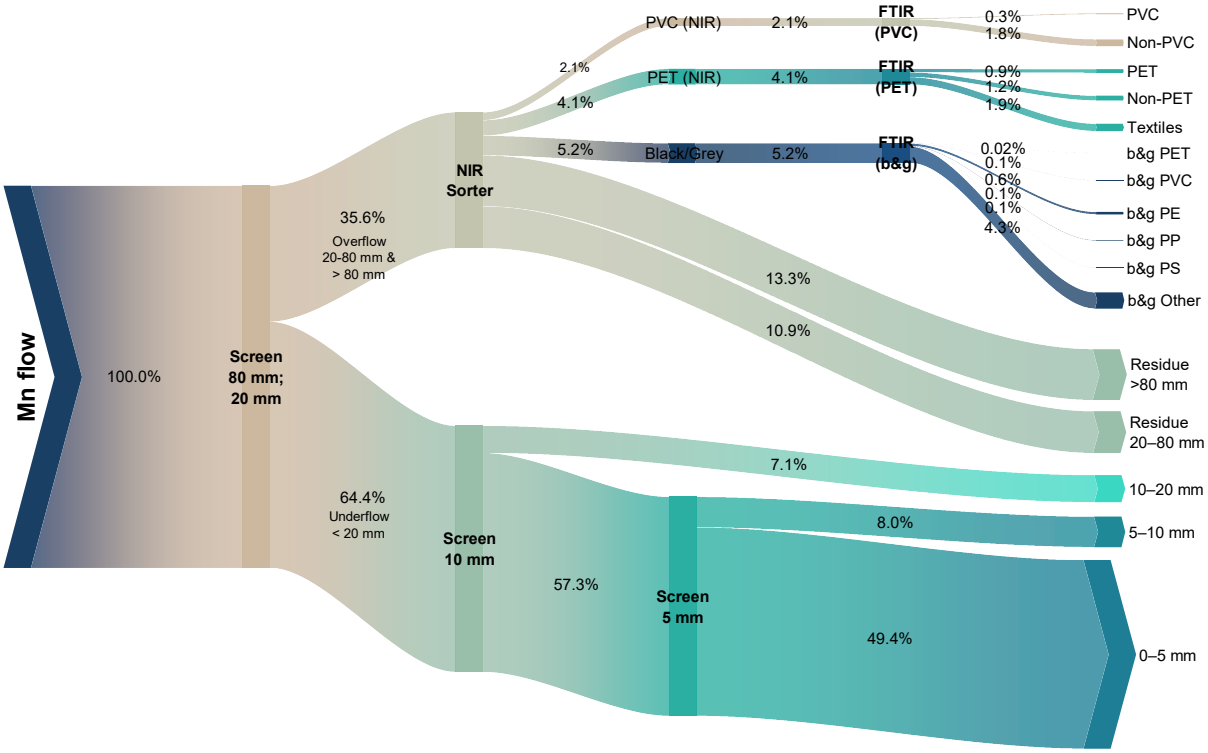

b

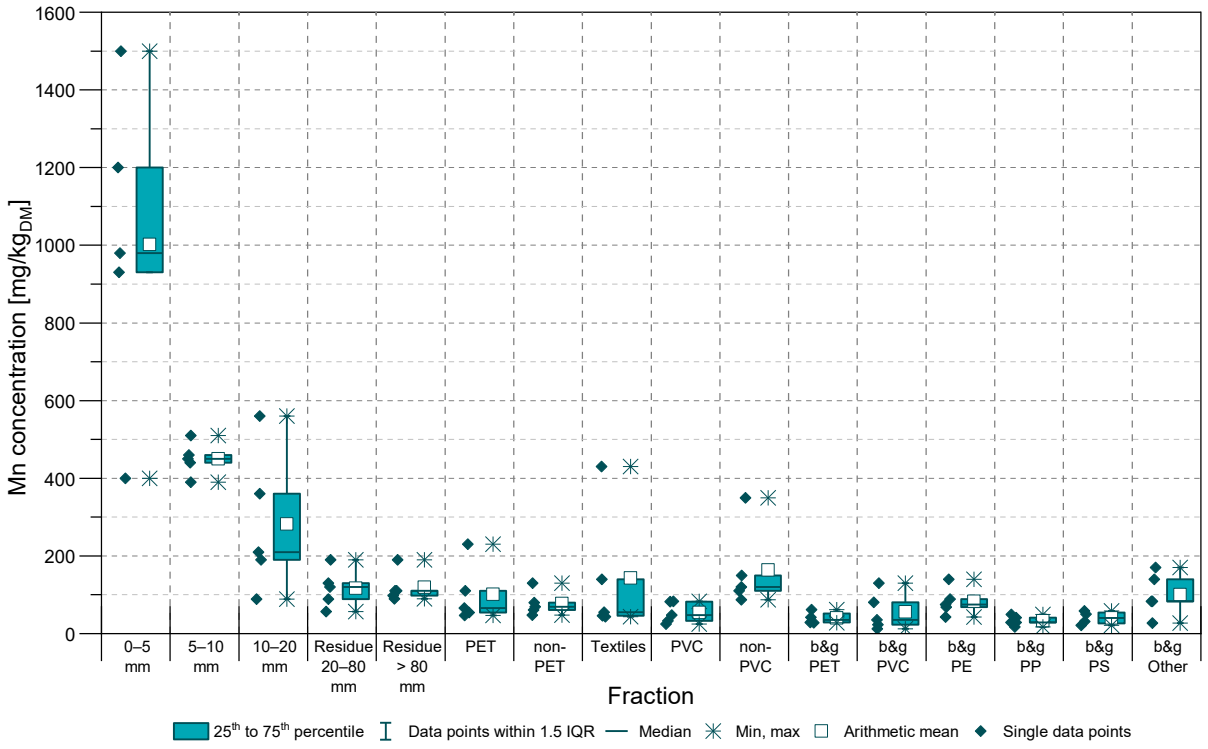

Figure A.18: a) Diagram of manganese (Mn) flows representing the arithmetic mean values of the five MCW samples S01–S05. B&g = black and grey fractions. b) Box plot of Mn concentrations in different particle size classes and sorted fractions in mg/kg referring to dry mass without hard impurities

Table A.18: Manganese (Mn) concentrations in mg/kg referring to dry mass without hard impurities. LOQ = 0.50 mg/kg

Fraction		Composite sample					Mean	Std. Dev.	Rel. Std. Dev [%]
		S01	S02	S03	S04	S05			
Screen	0–5 mm	930	1500	980	400	1200	1000	410	40
	5–10 mm	390	510	450	440	460	450	40	10
	10–20 mm	210	190	560	89	360	280	180	65
NIR Residue	20–80 mm	89	130	120	57	190	120	50	42
	> 80 mm	190	110	90	98	110	120	40	34
NIR PET Fraction	PET	47	110	66	230	54	100	76	75
	Non-PET	61	130	69	48	80	78	32	41
	Textile	46	430	55	44	140	140	170	116
NIR PVC Fraction	PVC	25	83	82	48	33	54	27	50
	Non-PVC	120	350	110	87	150	160	110	65
Black & Grey Fraction	PET	62	42	-	29	28	40	16	39
	PVC	81	12	35	23	130	56	49	87
	PE	68	89	140	43	75	83	36	43
	PP	49	41	29	17	29	33	12	37
	PS	31	58	21	-	50	40	17	42
	Other	27	170	83	140	83	100	56	55
Overall	mg/kg	240	420	200	130	300	260	110	44
	mg/MJ	11	19	9.5	5.7	15	12	5.2	43

A.19. Mo

a

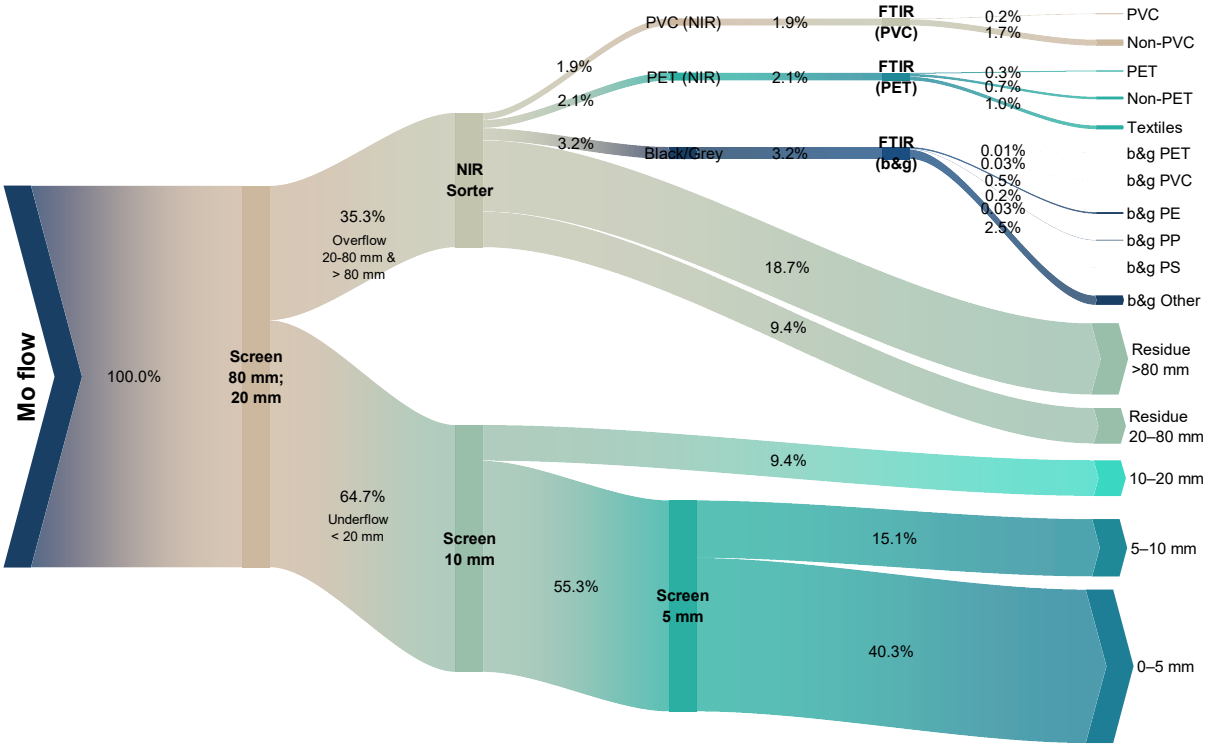

b

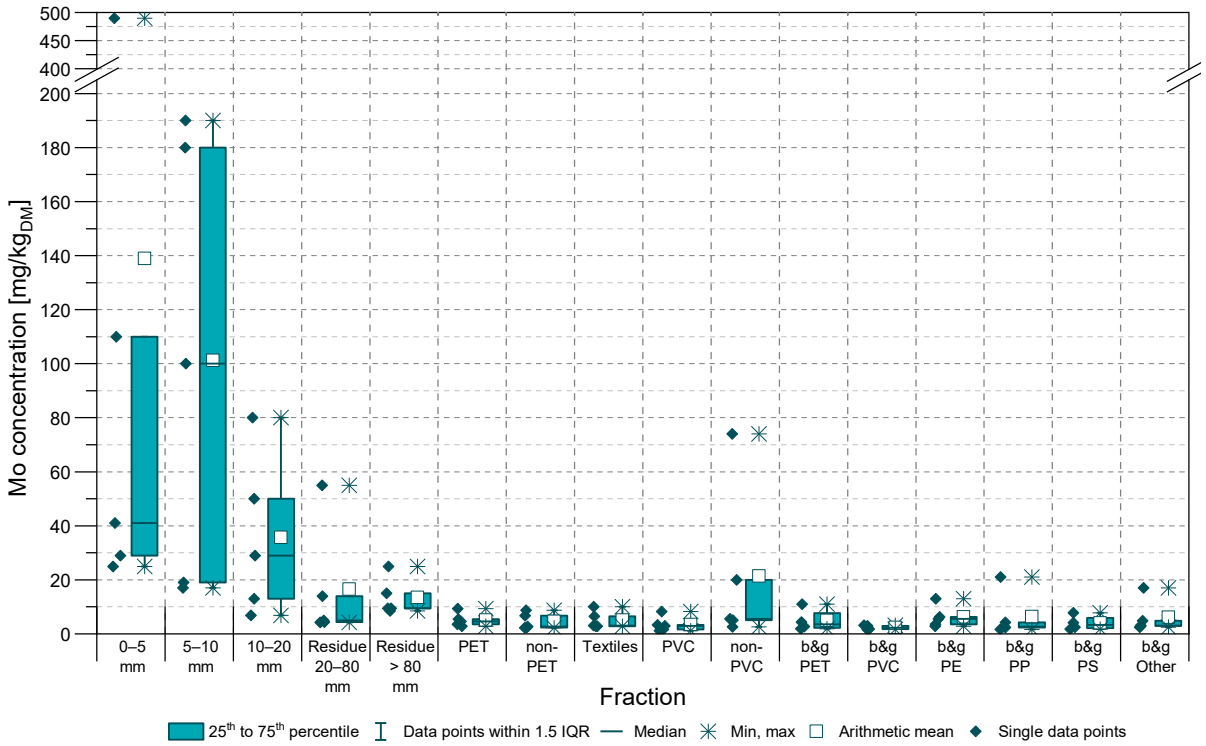

Figure A.19: a) Diagram of molybdenum (Mo) flows representing the arithmetic mean values of the five MCW samples S01–S05. B&g = black and grey fractions. b) Box plot of Mo concentrations in different particle size classes and sorted fractions in mg/kg referring to dry mass without hard impurities

Table A.19: Molybdenum (Mo) concentrations in mg/kg referring to dry mass without hard impurities. LOQ = 0.25 mg/kg

Fraction		Composite sample					Mean	Std. Dev.	Rel. Std. Dev [%]
		S01	S02	S03	S04	S05			
Screen	0–5 mm	490	110	41	29	25	140	200	143
	5–10 mm	190	100	17	180	19	100	84	83
	10–20 mm	80	29	13	6.8	50	36	30	83
NIR Residue	20–80 mm	55	14	5.0	4.2	4.4	17	22	133
	> 80 mm	9.5	25	9.5	15	8.5	14	6.9	51
NIR PET Fraction	PET	9.4	5.4	3.5	4.6	2.8	5.1	2.6	50
	Non-PET	8.7	6.7	2.7	2.3	2.4	4.6	3.0	65
	Textile	6.5	10	2.8	2.8	3.1	5.0	3.2	63
NIR PVC Fraction	PVC	3.3	2.9	8.3	1.6	1.2	3.5	2.8	82
	Non-PVC	74	20	5.5	2.6	5.1	21	30	141
Black & Grey Fraction	PET	11	4.4	-	1.9	2.7	5.0	4.1	83
	PVC	3.2	2.9	1.7	2.3	1.8	2.4	0.66	28
	PE	13	6.3	5.5	3.5	2.8	6.2	4.0	65
	PP	21	4.2	1.7	2.7	2.4	6.4	8.2	128
	PS	4.1	7.8	1.8	-	2.5	4.1	2.7	66
	Other	3.1	17	3.0	4.9	2.5	6.1	6.2	101
Overall	mg/kg	100	42	10	15	11	36	39	109
	mg/MJ	4.7	1.9	0.46	0.68	0.56	1.7	1.8	108

A.20. Na

a

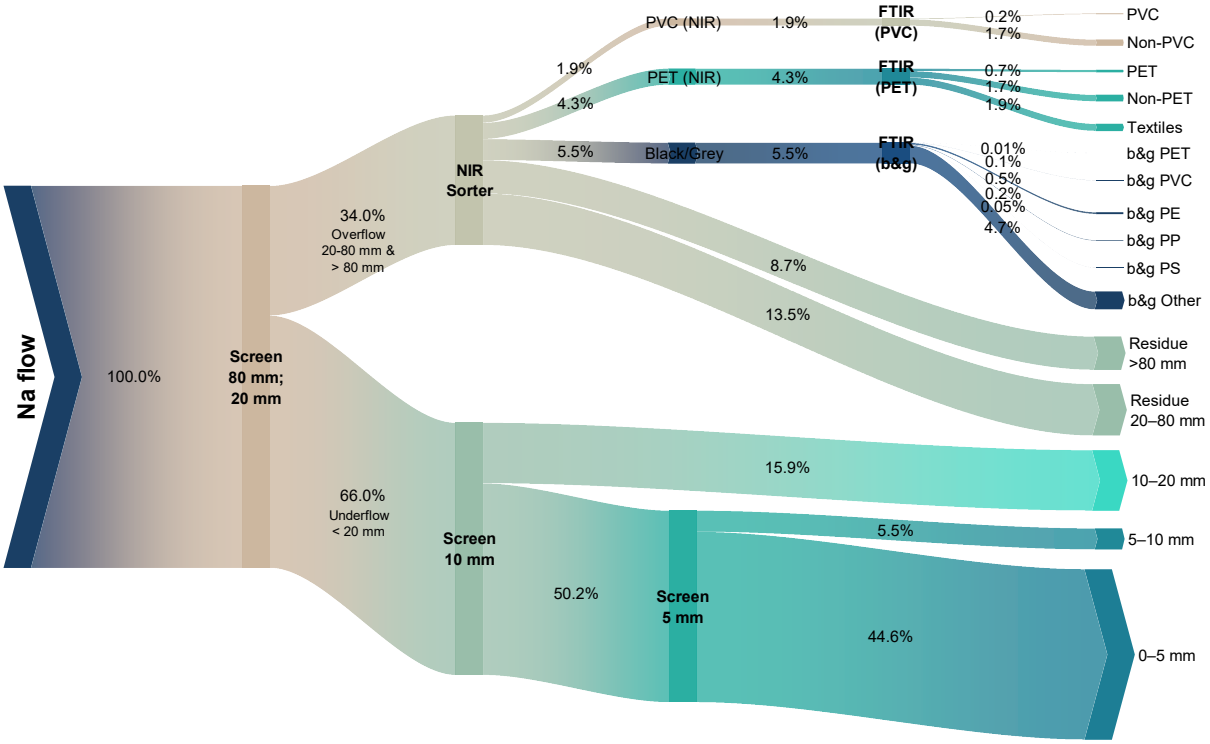

b

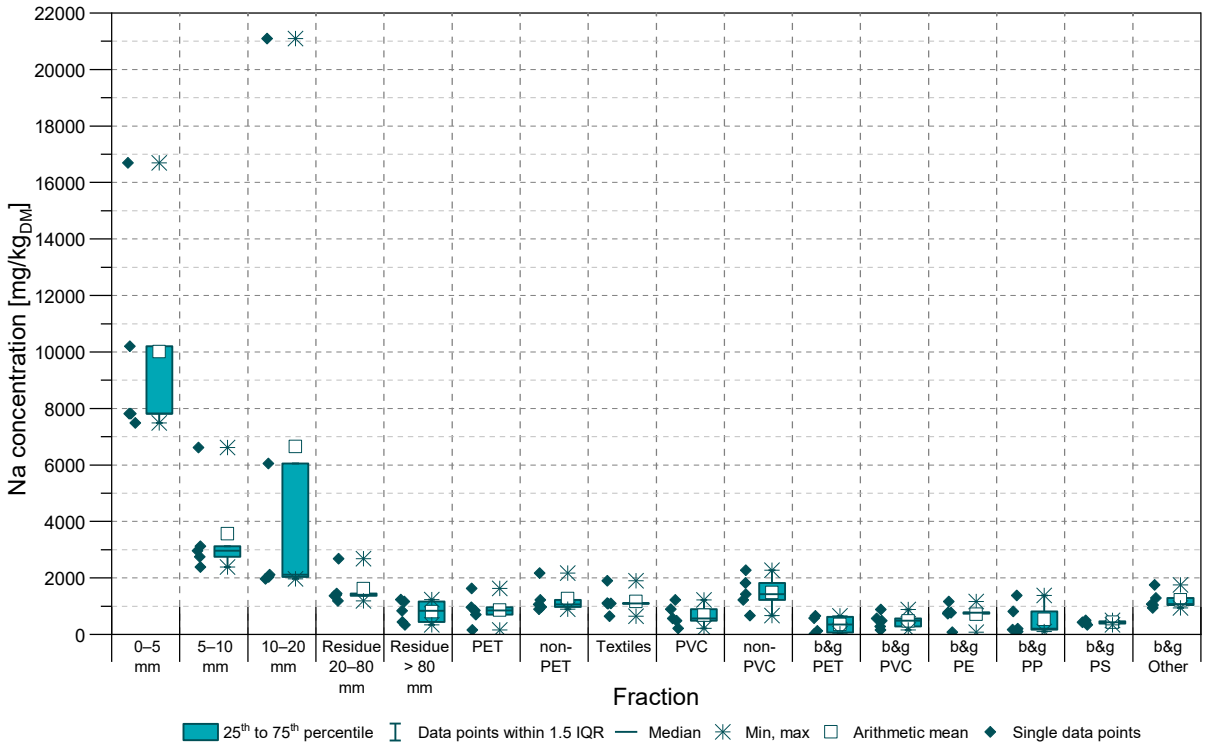

Figure A.20: a) Diagram of sodium (Na) flows representing the arithmetic mean values of the five MCW samples S01–S05. B&g = black and grey fractions. b) Box plot of Na concentrations in different particle size classes and sorted fractions in mg/kg referring to dry mass without hard impurities

Table A.20: Sodium (Na) concentrations in mg/kg referring to dry mass without hard impurities. LOQ = 5 mg/kg

Fraction		Composite sample					Mean	Std. Dev.	Rel. Std. Dev [%]
		S01	S02	S03	S04	S05			
Screen	0–5 mm	7820	7820	10200	7490	16700	10000	3900	39
	5–10 mm	2390	3120	2960	2750	6620	3570	1730	48
	10–20 mm	21100	2110	2040	1970	6050	6650	8260	124
NIR Residue	20–80 mm	1400	1450	1190	1370	2680	1620	600	37
	> 80 mm	340	440	840	1230	1170	800	410	51
NIR PET Fraction	PET	1630	160	960	850	700	860	530	61
	Non-PET	2170	890	970	1060	1220	1260	520	41
	Textile	1090	1110	650	1100	1900	1170	450	39
NIR PVC Fraction	PVC	890	210	1220	490	570	680	390	58
	Non-PVC	1820	670	1220	1420	2270	1480	610	41
Black & Grey Fraction	PET	660	23	-	580	120	350	320	93
	PVC	570	160	280	880	490	480	280	59
	PE	1170	80	770	780	740	710	390	56
	PP	820	97	170	1380	200	530	560	104
	PS	430	500	430	-	340	430	66	15
	Other	940	1290	1040	1750	1080	1220	320	26
Overall	mg/kg	4290	2460	1860	2020	4170	2960	1180	40
	mg/MJ	200	110	89	92	210	141	61	43

A.21. Ni

a

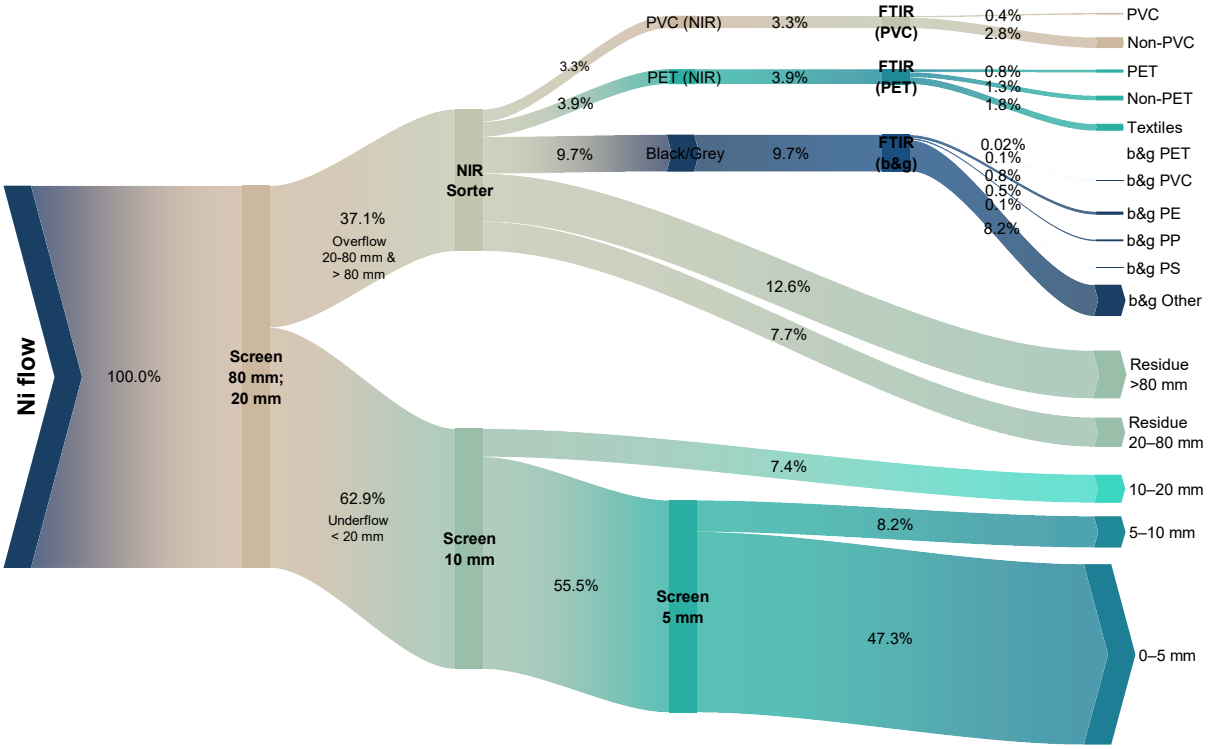

b

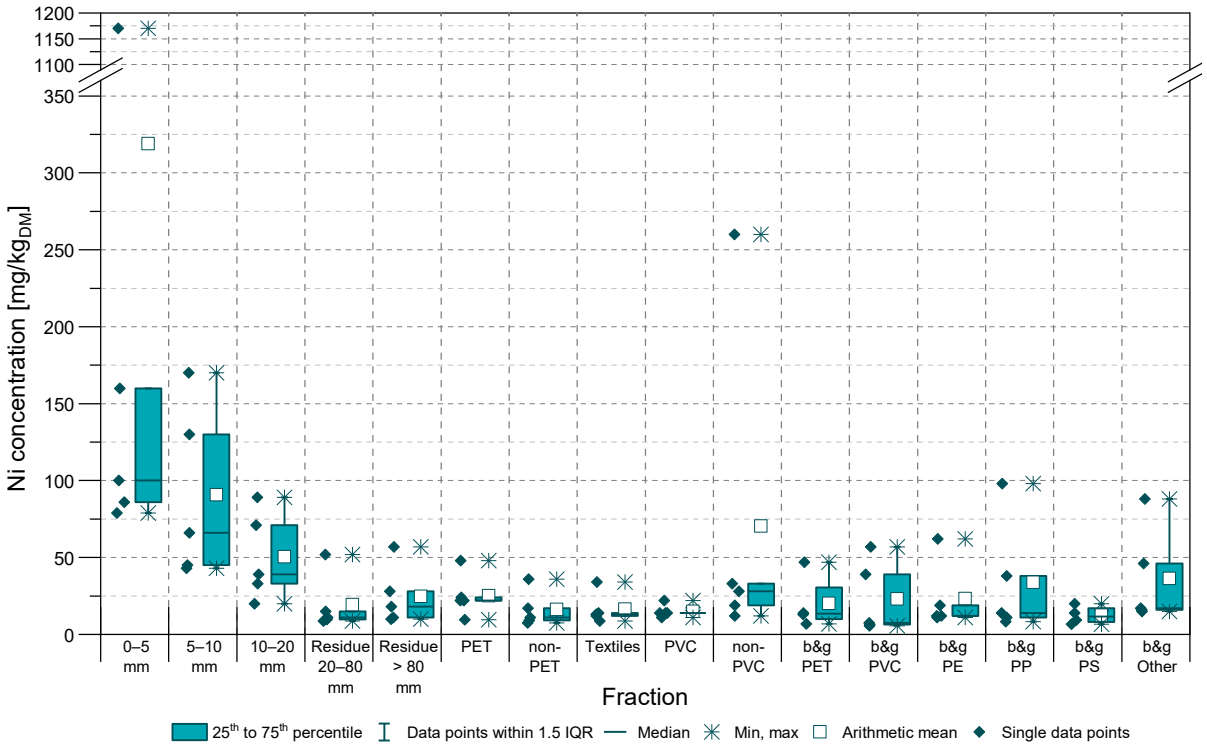

Figure A.21: a) Diagram of nickel (Ni) flows representing the arithmetic mean values of the five MCW samples S01–S05. B&g = black and grey fractions. b) Box plot of Ni concentrations in different particle size classes and sorted fractions in mg/kg referring to dry mass without hard impurities

Table A.21: Nickel (Ni) concentrations in mg/kg referring to dry mass without hard impurities. LOQ = 0.50 mg/kg

Fraction		Composite sample					Mean	Std. Dev.	Rel. Std. Dev [%]
		S01	S02	S03	S04	S05			
Screen	0–5 mm	1170	160	100	86	79	320	480	149
	5–10 mm	130	66	43	170	45	91	57	62
	10–20 mm	71	39	33	20	89	50	29	57
NIR Residue	20–80 mm	52	15	9.8	8.7	11	19	18	96
	> 80 mm	57	18	10	28	11	25	19	78
NIR PET Fraction	PET	48	24	22	22	9.5	25	14	56
	Non-PET	36	17	11	7.4	9.2	16	12	72
	Textile	34	12	14	8.8	13	16	10	61
NIR PVC Fraction	PVC	14	14	22	14	11	15	4.1	27
	Non-PVC	260	28	33	12	19	70	110	151
Black & Grey Fraction	PET	47	14	-	13	6.8	20	18	90
	PVC	39	5.7	7.4	6.4	57	23	24	102
	PE	62	12	19	11	12	23	22	95
	PP	98	38	14	8.4	11	34	38	111
	PS	20	14	6.6	-	9.4	13	5.9	47
	Other	16	88	15	46	17	36	32	87
Overall	mg/kg	220	55	21	31	27	70	82	118
	mg/MJ	10	2.5	1.0	1.4	1.4	3.3	3.8	117

A.22. P

a

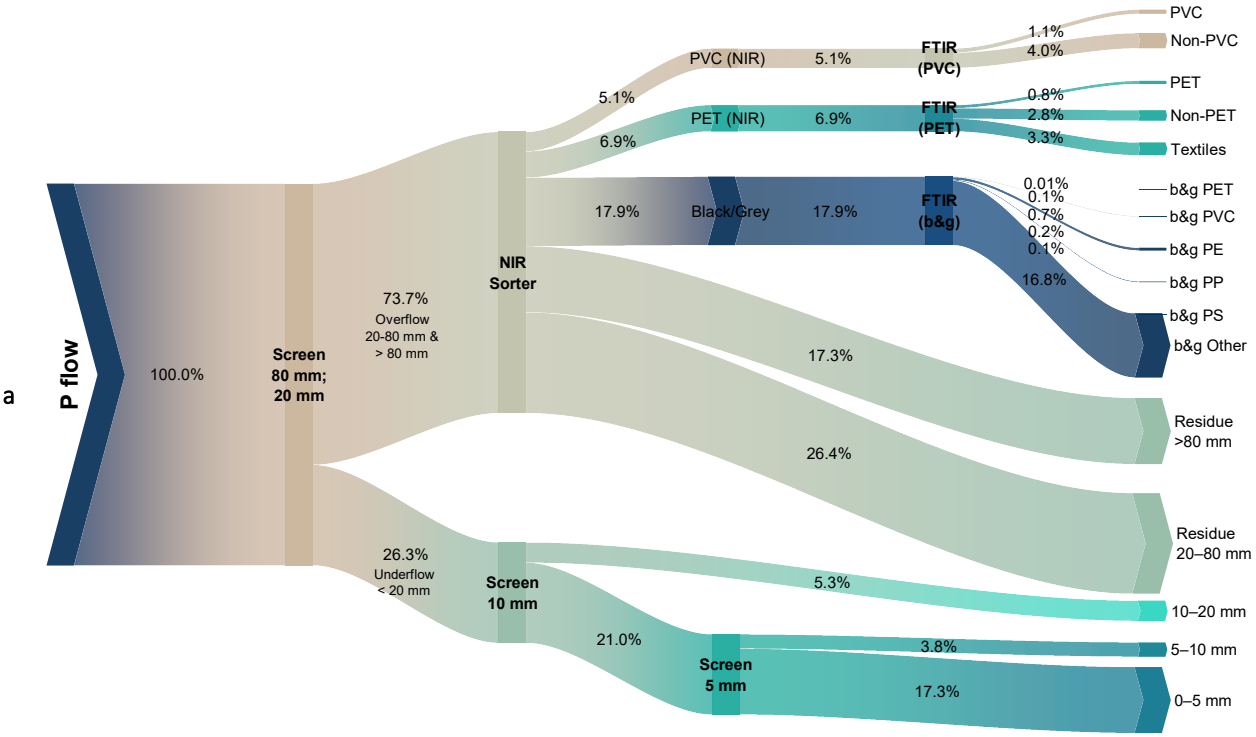

b

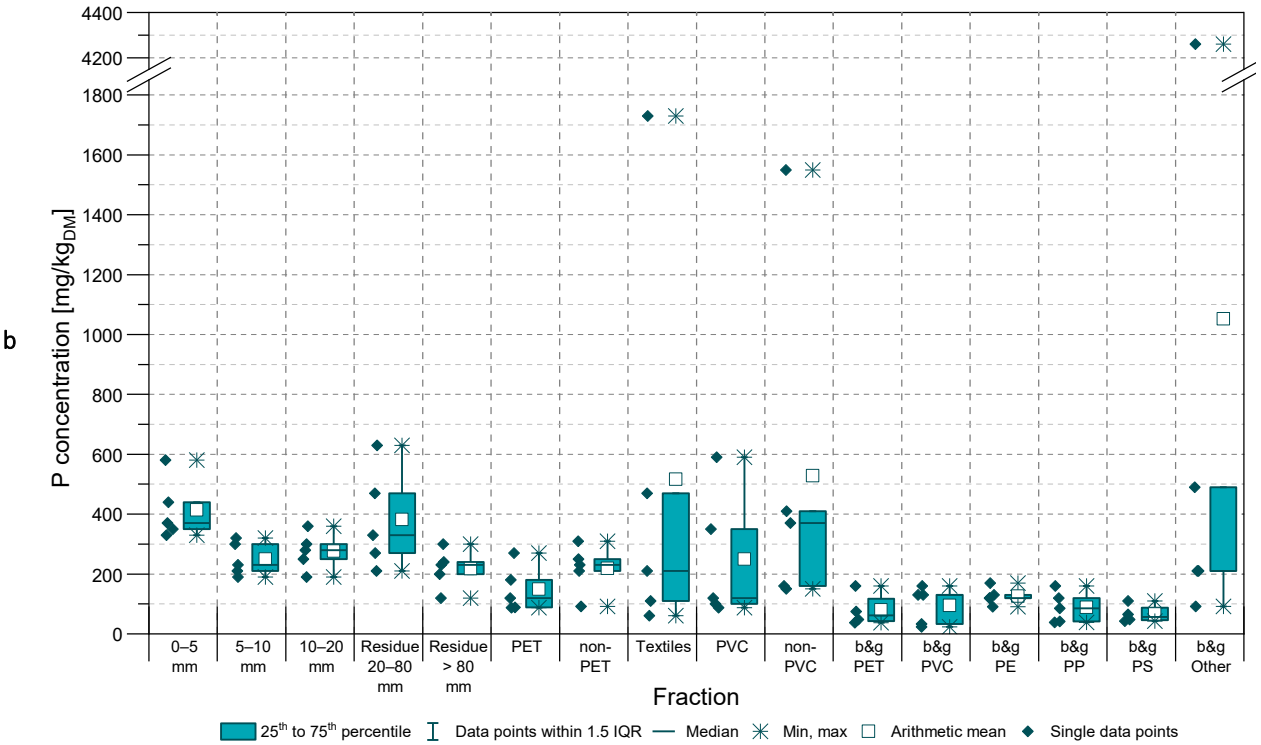

Figure A.22: a) Diagram of phosphorus (P) flows representing the arithmetic mean values of the five MCW samples S01–S05. B&g = black and grey fractions. b) Box plot of P concentrations in different particle size classes and sorted fractions in mg/kg referring to dry mass without hard impurities

Table A.22: Phosphorus (P) concentrations in mg/kg referring to dry mass without hard impurities. LOQ = 2.5 mg/kg

Fraction		Composite sample					Mean	Std. Dev.	Rel. Std. Dev [%]
		S01	S02	S03	S04	S05			
Screen	0–5 mm	330	440	370	350	580	410	100	25
	5–10 mm	190	230	300	210	320	250	57	23
	10–20 mm	280	360	190	250	300	280	63	23
NIR Residue	20–80 mm	470	270	210	330	630	380	170	44
	> 80 mm	240	230	120	200	300	220	66	30
NIR PET Fraction	PET	180	88	120	270	89	150	77	52
	Non-PET	210	250	92	310	230	220	80	37
	Textile	1730	470	61	110	210	520	700	135
NIR PVC Fraction	PVC	350	88	100	590	120	250	220	88
	Non-PVC	1550	370	160	150	410	530	590	111
Black & Grey Fraction	PET	75	160	-	37	48	80	56	70
	PVC	130	24	33	160	130	95	62	65
	PE	170	130	91	120	120	130	28	23
	PP	160	85	38	120	42	89	52	58
	PS	65	110	43	-	48	67	30	46
	Other	4260	210	92	210	490	1050	1800	171
Overall	mg/kg	820	290	160	260	420	390	260	66
	mg/MJ	38	13	7.6	12	21	18	12	66

A.23. Pb

a

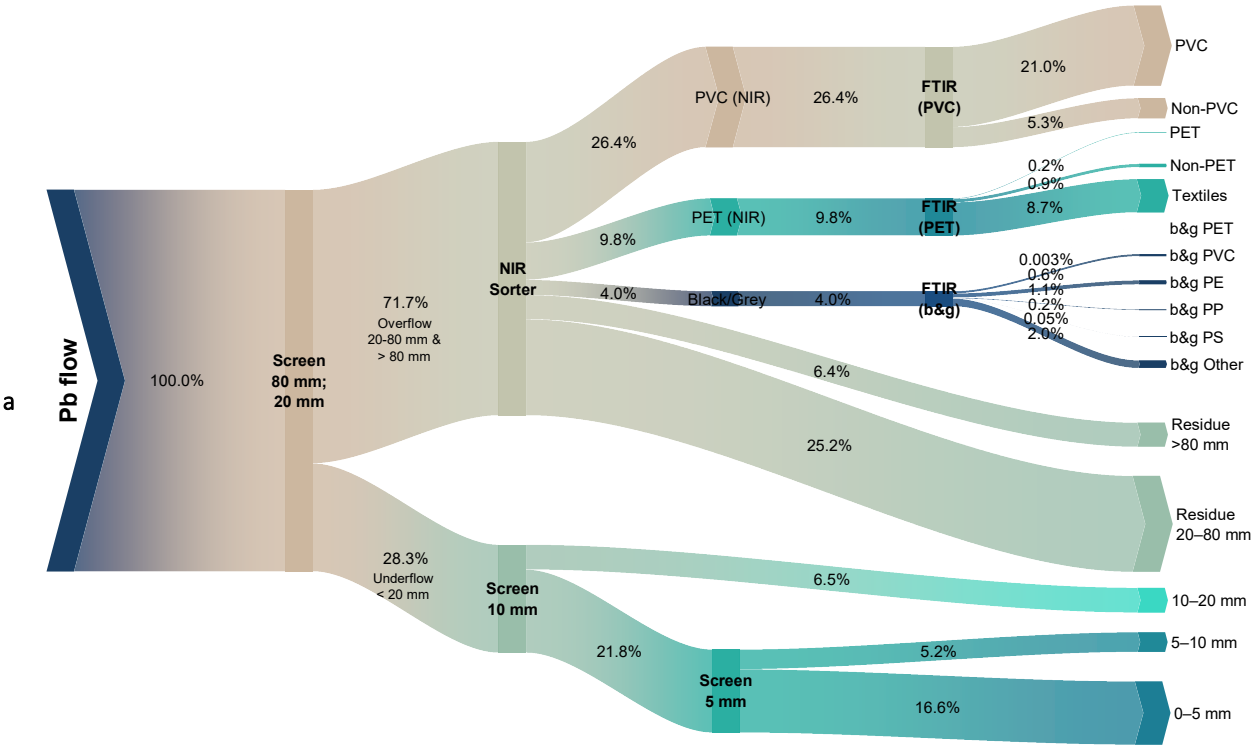

b

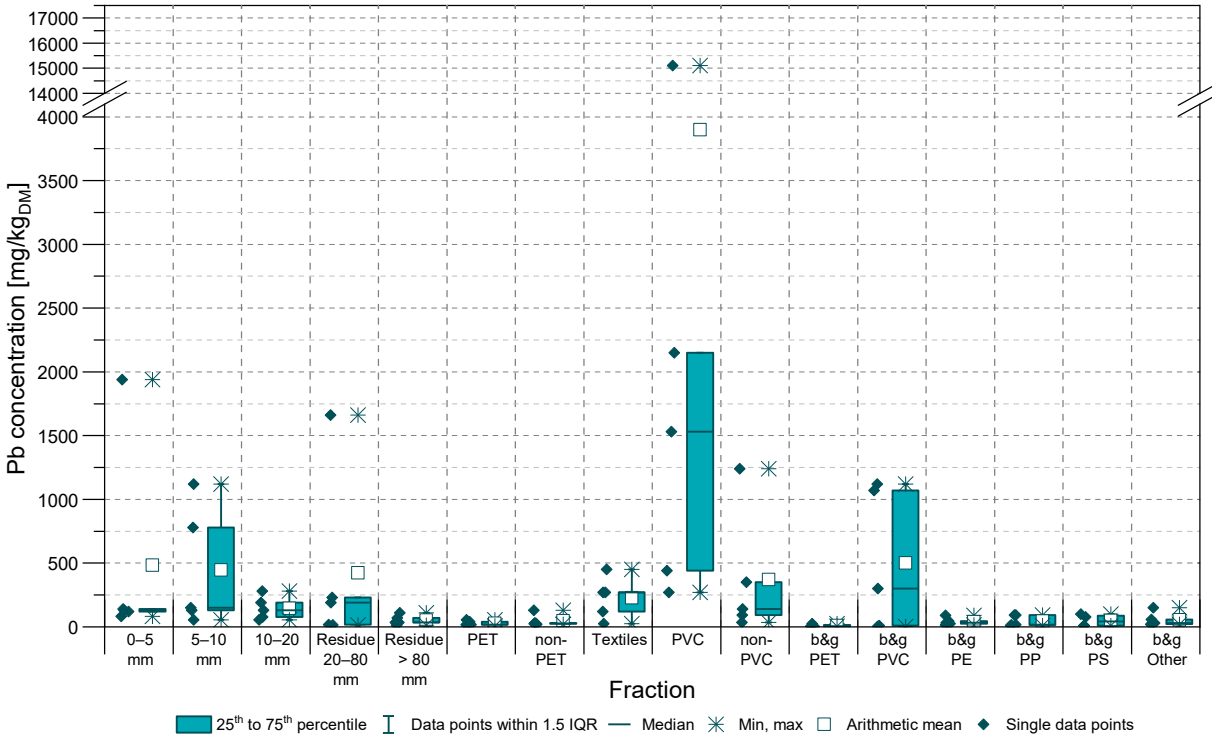

Figure A.23 a) Lead (Pb) flows diagram representing the arithmetic mean values of the five MCW samples S01–S05; b) Box plot of Pb concentrations in different particle size classes and sorted fractions in mg/kg referring to dry mass without hard impurities

Table A.23: Lead (Pb) concentrations in mg/kg referring to dry mass without hard impurities. LOQ = 0.25 mg/kg

Fraction		Composite sample					Mean	Std. Dev.	Rel. Std. Dev [%]
		S01	S02	S03	S04	S05			
Screen	0–5 mm	1940	130	140	120	83	480	820	169
	5–10 mm	1120	54	150	780	130	450	480	107
	10–20 mm	190	130	77	55	280	150	91	62
NIR Residue	20–80 mm	1660	190	230	17	14	420	700	166
	> 80 mm	110	70	13	35	35	53	38	72
NIR PET Fraction	PET	54	8.6	18	39	17	27	19	68
	Non-PET	31	26	20	130	28	47	46	99
	Textile	26	120	270	450	270	230	160	71
NIR PVC Fraction	PVC	440	2150	1530	15100	270	3900	6310	162
	Non-PVC	34	350	1240	92	140	370	500	135
Black & Grey Fraction	PET	26	5.6	-	4.0	4.2	10	11	108
	PVC	1070	2.7	1120	300	9.1	500	560	111
	PE	32	24	44	15	90	41	29	72
	PP	16	92	11	93	18	46	43	92
	PS	9.5	9.3	100	-	77	49	47	95
	Other	57	31	22	150	19	56	55	98
Overall	mg/kg	700	130	120	380	79	280	260	92
	mg/MJ	32	6.0	5.7	17	4.1	13	12	91

A.24. Sb

a

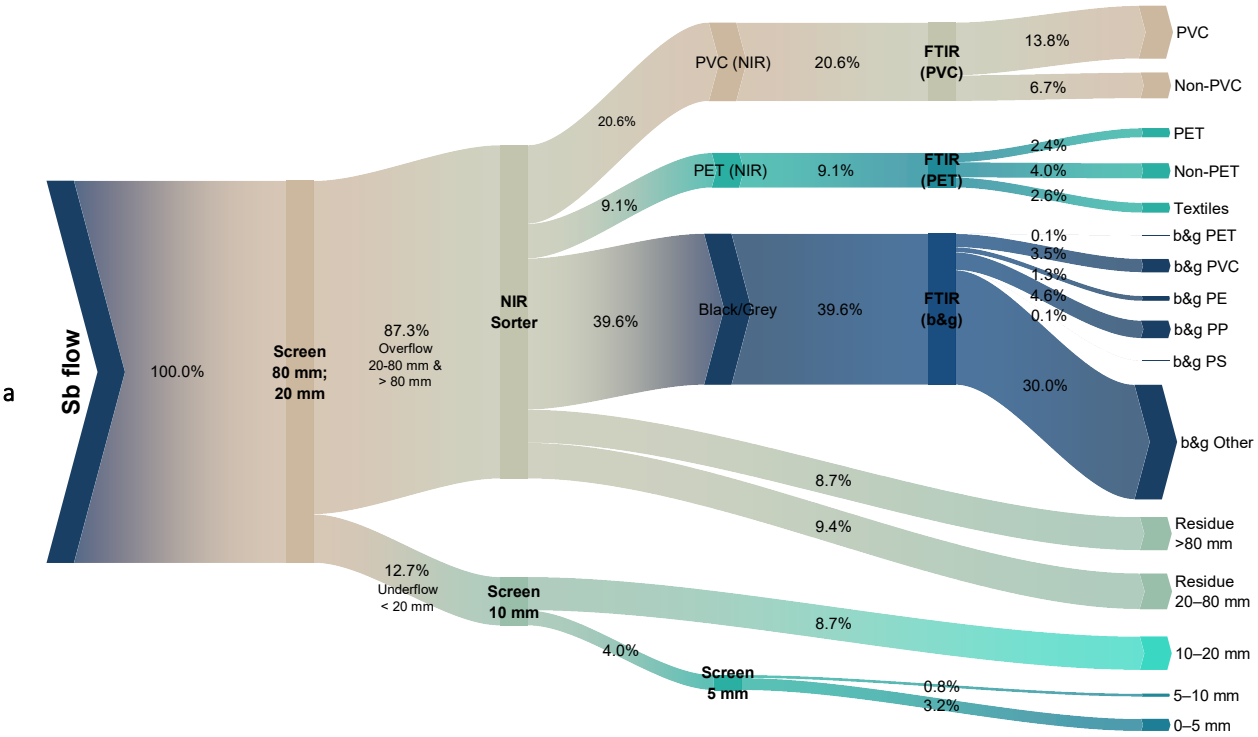

b

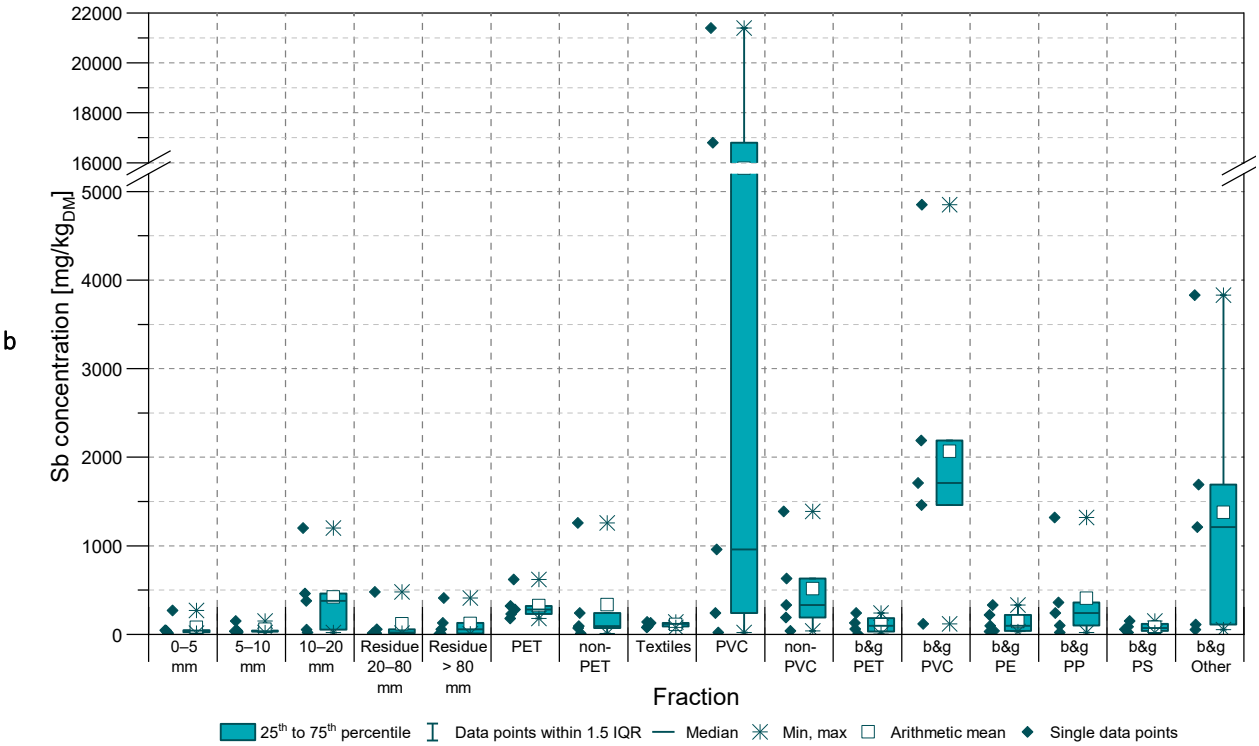

Figure A.24: a) Diagram of antimony (Sb) flows representing the arithmetic mean values of the five MCW samples S01–S05. B&g = black and grey fractions. b) Box plot of Sb concentrations in different particle size classes and sorted fractions in mg/kg referring to dry mass without hard impurities

Table A.24: Antimony (Sb) concentrations in mg/kg referring to dry mass without hard impurities. LOQ = 0.25 mg/kg

Fraction		Composite sample					Mean	Std. Dev.	Rel. Std. Dev [%]
		S01	S02	S03	S04	S05			
Screen	0–5 mm	43	13	26	270	47	80	110	134
	5–10 mm	31	22	37	44	150	57	53	93
	10–20 mm	460	23	54	1200	380	420	480	112
NIR Residue	20–80 mm	23	480	15	13	56	120	200	173
	> 80 mm	410	59	12	6.1	130	120	170	136
NIR PET Fraction	PET	320	230	180	620	280	330	170	53
	Non-PET	94	72	11	1260	240	340	520	156
	Textile	90	81	120	130	140	110	26	23
NIR PVC Fraction	PVC	21400	20	240	960	16800	7880	10400	132
	Non-PVC	190	38	1390	330	630	520	540	104
Black & Grey Fraction	PET	240	63	-	130	4	110	100	93
	PVC	1710	1460	2190	4850	120	2070	1740	84
	PE	99	41	330	31	220	140	130	89
	PP	240	100	1320	360	23	410	530	129
	PS	22	86	59	-	150	79	54	68
	Other	53	1690	110	1210	3830	1380	1540	112
Overall	mg/kg	300	290	79	320	520	300	160	52
	mg/MJ	14	13	3.8	14	27	14	8.1	57

A.25. Si

a

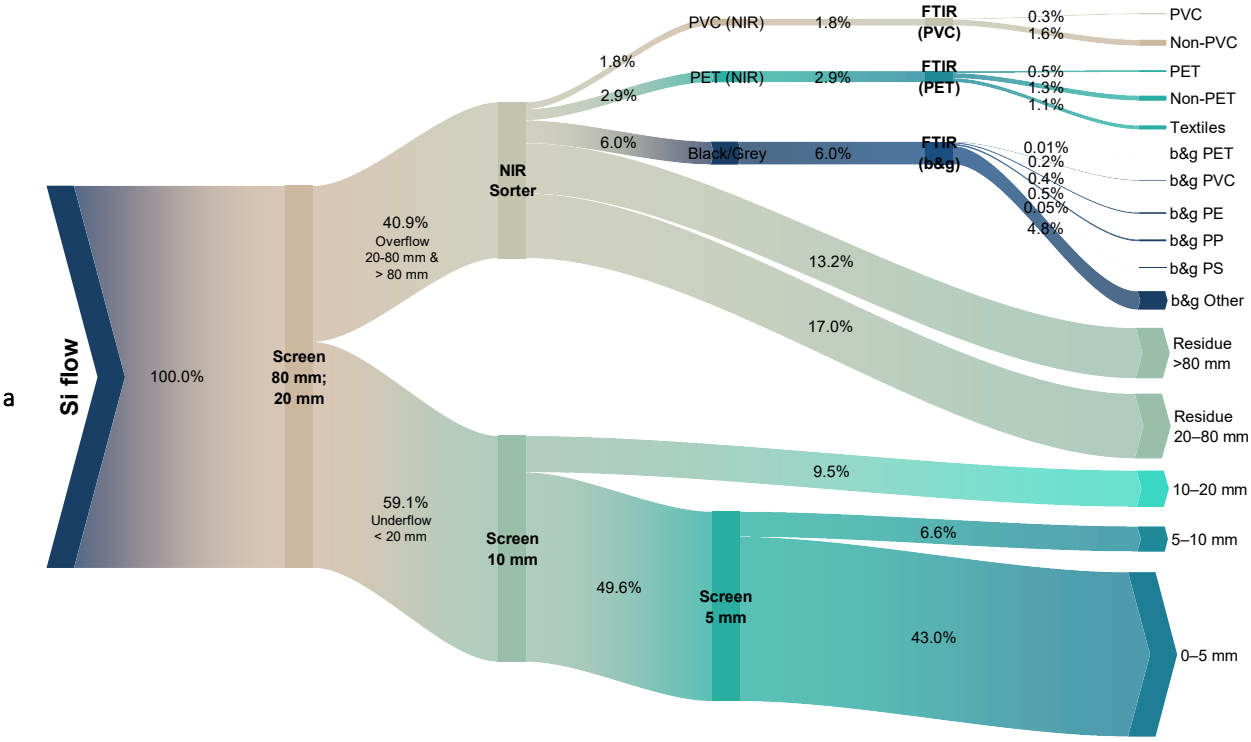

b

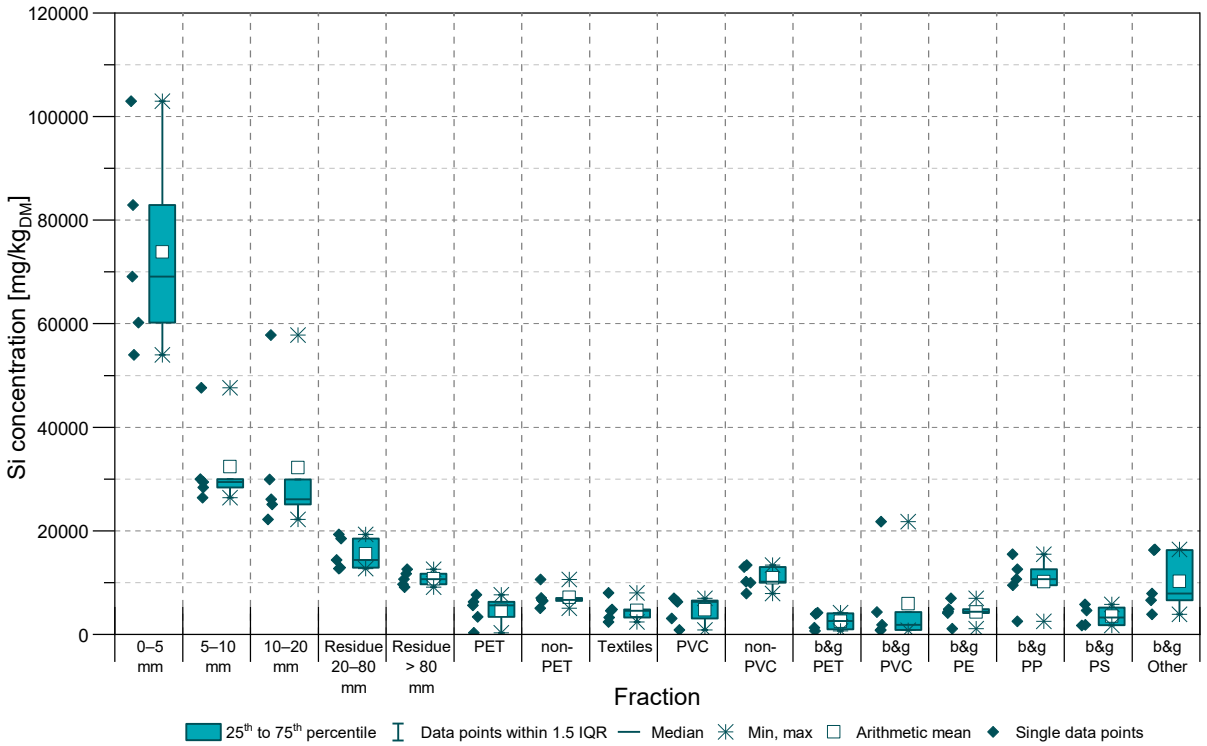

Figure A.25: a) Diagram of silicon (Si) flows representing the arithmetic mean values of the five MCW samples S01–S05. B&g = black and grey fractions. b) Box plot of Si concentrations in different particle size classes and sorted fractions in mg/kg referring to dry mass without hard impurities

Table A.25: Silicon (Si) concentrations in mg/kg referring to dry mass without hard impurities. LOQ = 2.5 mg/kg. Note: Mineral wool was present in sample S05 and may have caused the higher Si values in the fine and residual fractions.

Fraction		Composite sample					Mean	Std. Dev.	Rel. Std. Dev [%]
		S01	S02	S03	S04	S05			
Screen	0–5 mm	69100	54000	82900	60200	103000	73800	19600	27
	5–10 mm	28400	29400	30000	26400	47600	32400	8630	27
	10–20 mm	29900	25100	26100	22200	57800	32200	14600	45
NIR Residue	20–80 mm	19300	12700	12900	14400	18500	15600	3130	20
	> 80 mm	12600	9130	10700	9680	11700	10800	1420	13
NIR PET Fraction	PET	6270	330	5600	7635	3410	4650	2860	61
	Non-PET	7030	10600	6470	5055	6670	7170	2060	29
	Textile	3240	2420	4570	4820	8020	4610	2140	46
NIR PVC Fraction	PVC	3090	890	6570	6300	6960	4760	2660	56
	Non-PVC	10200	9990	13000	7910	13400	10900	2290	21
Black & Grey Fraction	PET	3930	690	-	1310	4190	2530	1790	71
	PVC	4300	850	790	21800	1850	5920	8990	152
	PE	4900	1130	6970	4390	4110	4300	2100	49
	PP	9520	12600	15500	10700	2540	10200	4830	47
	PS	1870	5770	1730	-	4650	3500	2020	58
	Other	3910	16400	7900	16300	6620	10200	5770	56
Overall	mg/kg	22000	21300	17600	17400	28300	21300	4420	21
	mg/MJ	1020	960	840	790	1460	1010	260	26

A.26. Sn

a

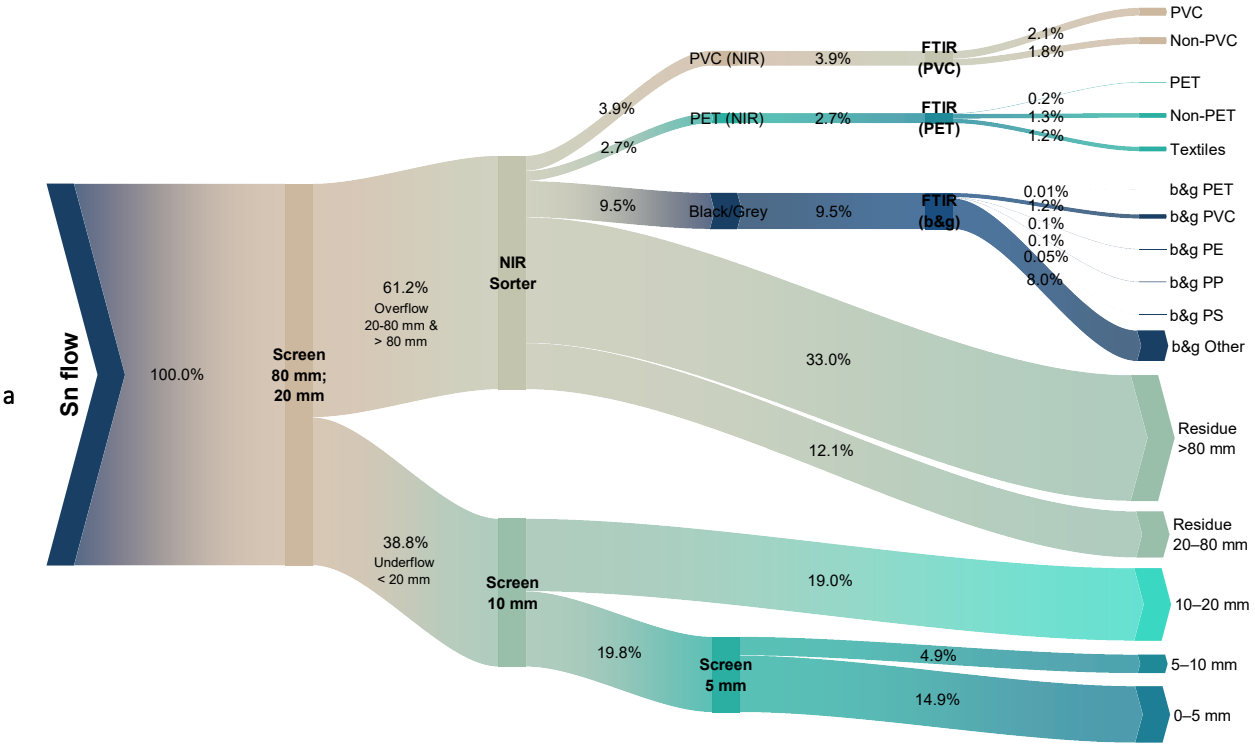

b

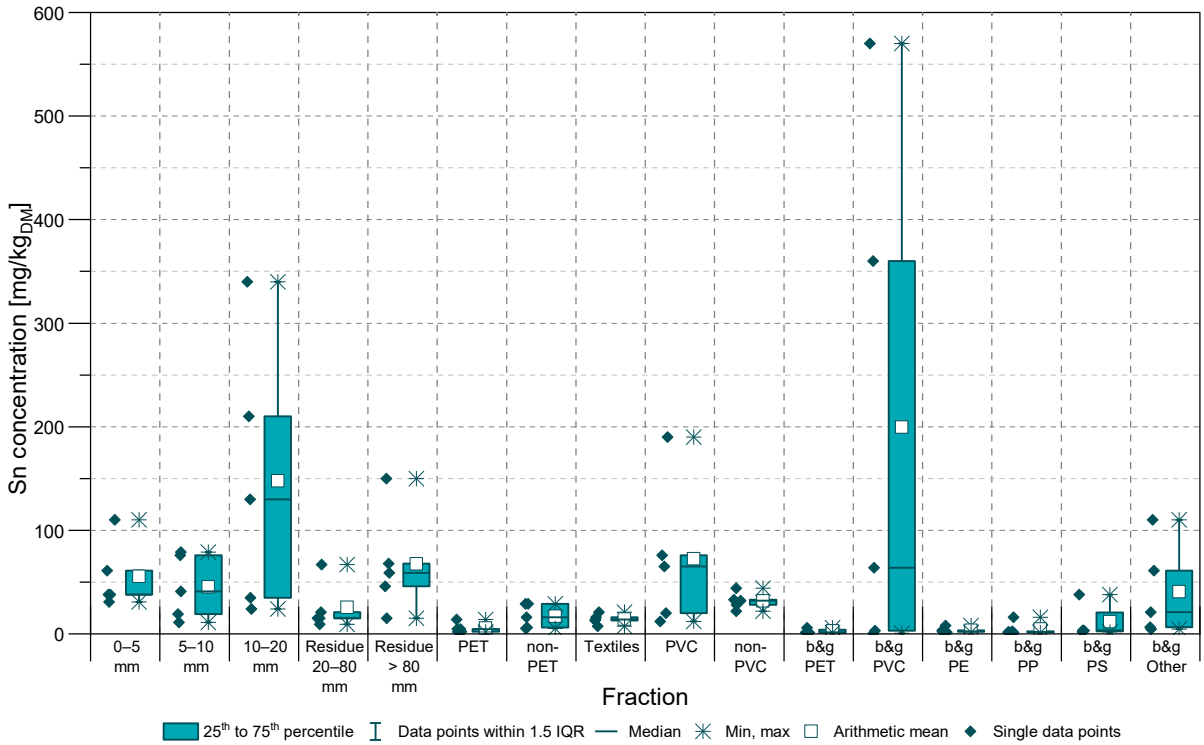

Figure A.26 : a) Diagram of tin (Sn) flows representing the arithmetic mean values of the five MCW samples S01–S05. B&g = black and grey fractions. b) Box plot of Sn concentrations in different particle size classes and sorted fractions in mg/kg referring to dry mass without hard impurities

Table A.26: Tin (Sn) concentrations in mg/kg referring to dry mass without hard impurities. LOQ = 0.50 mg/kg

Fraction		Composite sample					Mean	Std. Dev.	Rel. Std. Dev [%]
		S01	S02	S03	S04	S05			
Screen	0–5 mm	38	38	31	110	61	56	32	58
	5–10 mm	79	41	19	76	11	45	31	70
	10–20 mm	210	24	35	340	130	150	130	89
NIR Residue	20–80 mm	9.4	15	21	15	67	25	24	93
	> 80 mm	59	15	150	46	68	68	50	74
NIR PET Fraction	PET	4.5	1.7	14	4.7	2.2	5.4	5.0	92
	Non-PET	16	5.2	29	29	6.3	17	12	68
	Textile	16	13	7.3	21	14	14	5.0	35
NIR PVC Fraction	PVC	12	190	65	20	76	73	71	98
	Non-PVC	22	32	33	44	28	32	8	25
Black & Grey Fraction	PET	5.9	2.0	-	1.3	1.3	2.6	2.2	84
	PVC	570	< 0.50	360	64	3.2	200	260	128
	PE	2.3	1.5	7.9	2.5	3.3	3.5	2.5	73
	PP	1.9	16	1.4	2.5	1.2	4.6	6.4	139
	PS	3.5	1.7	38	-	3.2	12	18	152
	Other	21	61	4.6	110	6.5	40	43	111
Overall	mg/kg	53	28	61	61	52	51	14	27
	mg/MJ	2.4	1.2	2.9	2.8	2.7	2.4	0.67	28

A.27. Sr

a

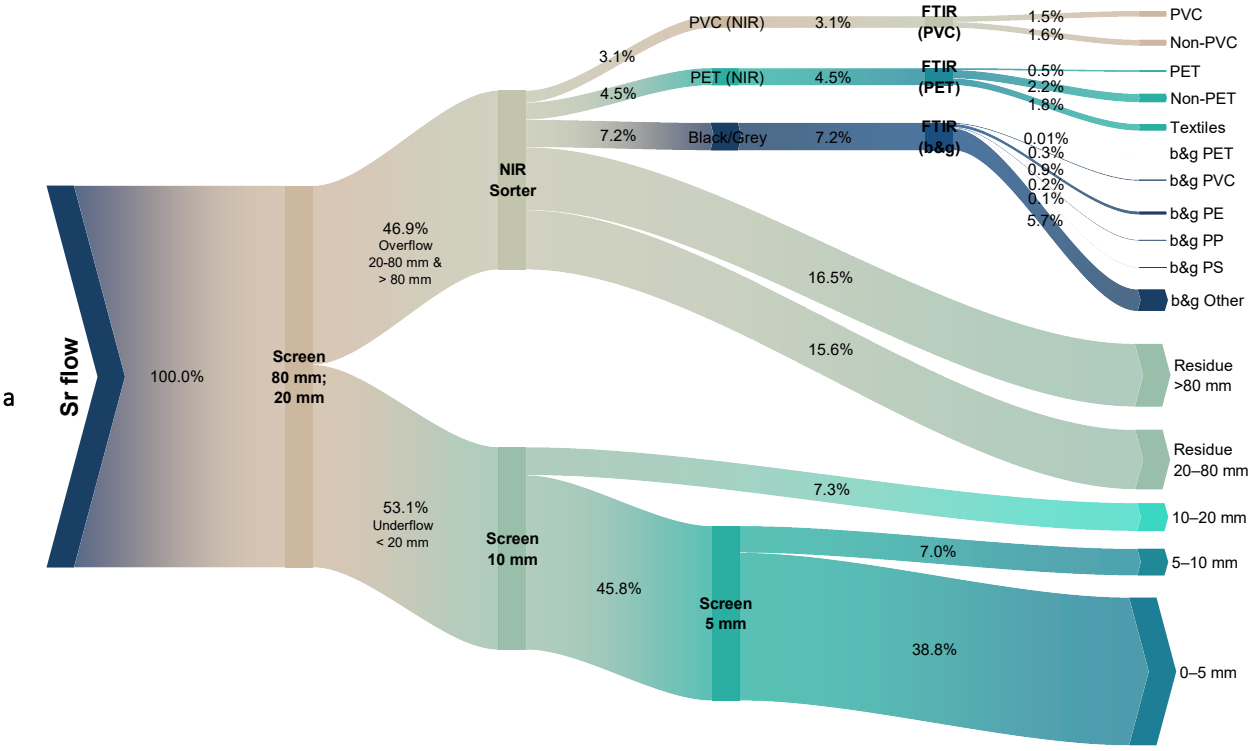

b

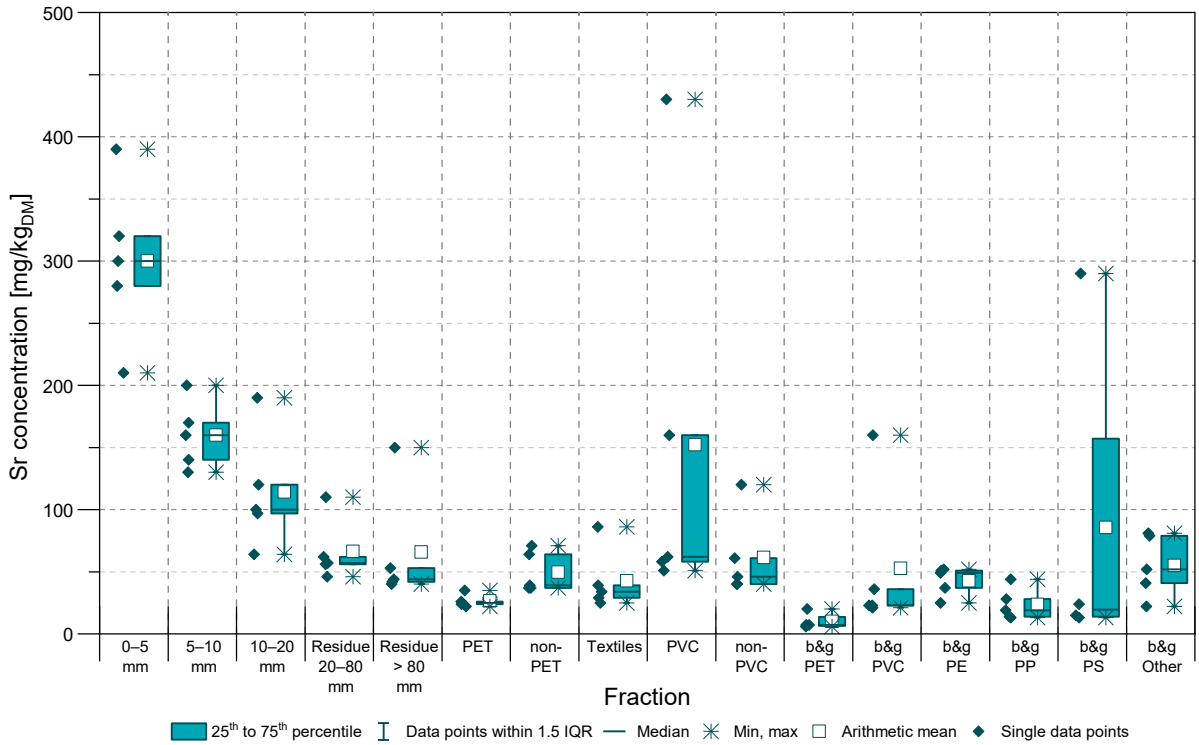

Figure A.27: a) Diagram of strontium (Sr) flows representing the arithmetic mean values of the five MCW samples S01–S05. B&g = black and grey fractions. b) Box plot of Sr concentrations in different particle size classes and sorted fractions in mg/kg referring to dry mass without hard impurities

Table A.27: Strontium (Sr) concentrations in mg/kg referring to dry mass without hard impurities. LOQ = 0.25 mg/kg

Fraction		Composite sample					Mean	Std. Dev.	Rel. Std. Dev [%]
		S01	S02	S03	S04	S05			
Screen	0–5 mm	280	320	300	210	390	300	65	22
	5–10 mm	140	170	160	130	200	160	27	17
	10–20 mm	100	120	97	64	190	110	47	41
NIR Residue	20–80 mm	56	110	46	62	57	66	25	38
	> 80 mm	150	42	40	53	44	66	47	72
NIR PET Fraction	PET	24	25	26	35	22	26	5.0	19
	Non-PET	39	64	71	37	37	50	17	33
	Textile	29	86	25	34	39	43	25	58
NIR PVC Fraction	PVC	58	160	430	62	51	152	160	106
	Non-PVC	40	120	61	40	46	61	34	55
Black & Grey Fraction	PET	20	7.1	-	5.9	7.1	10	6.7	67
	PVC	23	21	23	160	36	53	60	115
	PE	51	37	52	25	49	43	12	27
	PP	28	44	19	14	13	24	13	54
	PS	13	24	15	-	290	86	140	160
	Other	22	79	52	81	41	55	25	46
Overall	mg/kg	110	130	75	75	110	99	24	24
	mg/MJ	4.9	6.0	3.6	3.4	5.5	4.7	1.1	24

A.28. Ti

a

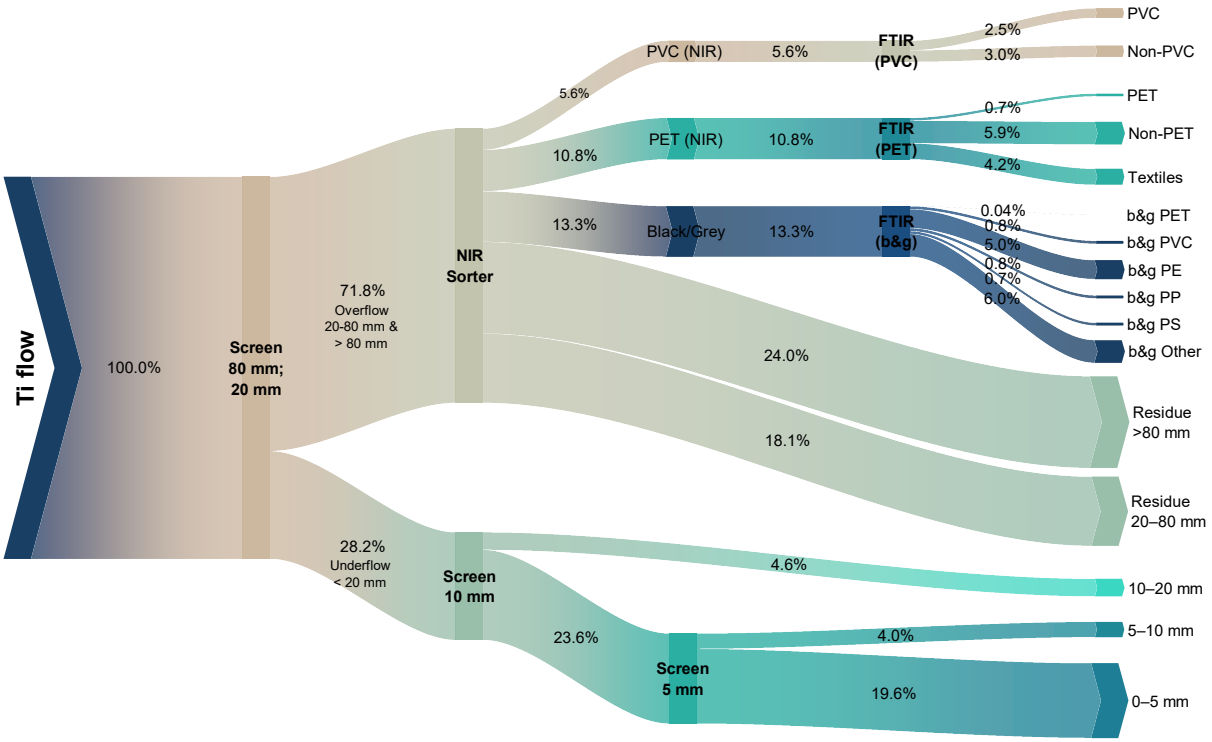

b

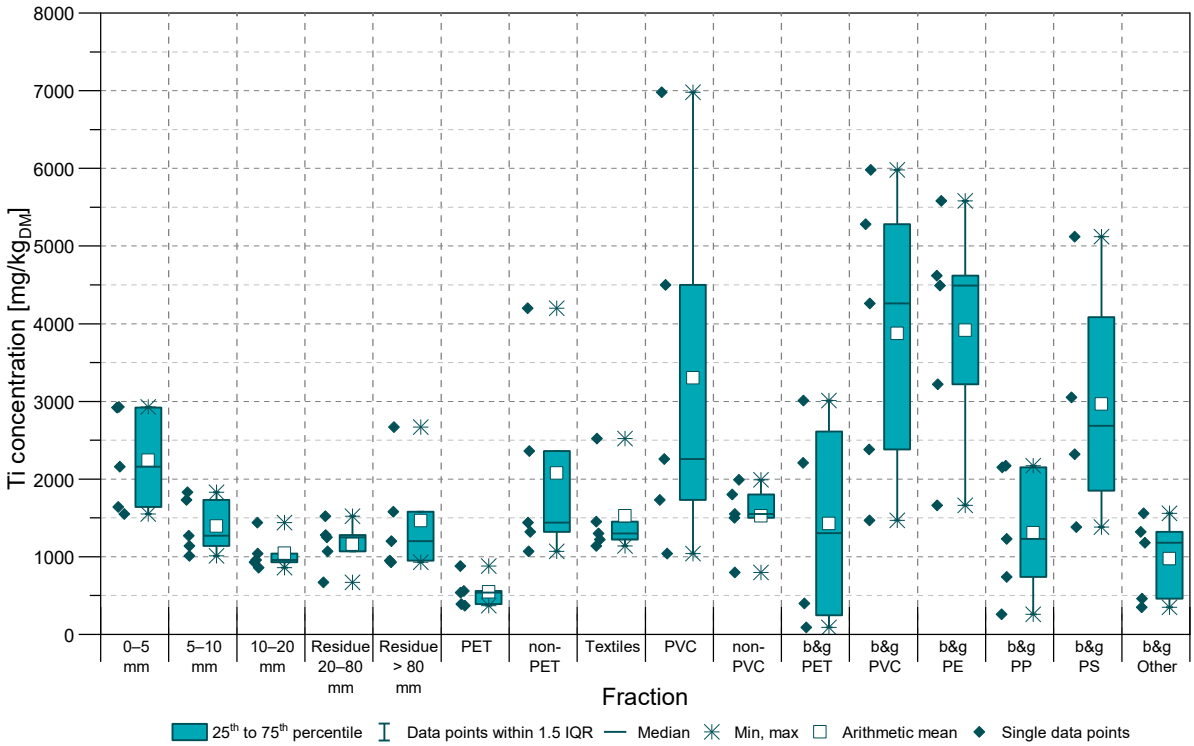

Figure A.28: a) Diagram of titanium (Ti) flows representing the arithmetic mean values of the five MCW samples S01–S05. B&g = black and grey fractions. b) Box plot of Ti concentrations in different particle size classes and sorted fractions in mg/kg referring to dry mass without hard impurities

Table A.28: Titanium (Ti) concentrations in mg/kg referring to dry mass without hard impurities. LOQ = 0.25 mg/kg

Fraction		Composite sample					Mean	Std. Dev.	Rel. Std. Dev [%]
		S01	S02	S03	S04	S05			
Screen	0–5 mm	1640	2160	2930	1550	2920	2240	670	30
	5–10 mm	1140	1010	1730	1270	1830	1400	360	26
	10–20 mm	960	860	1040	930	1440	1050	230	22
NIR Residue	20–80 mm	1520	1280	1250	670	1070	1160	320	27
	> 80 mm	2670	1200	930	950	1580	1470	720	49
NIR PET Fraction	PET	540	390	880	560	370	550	200	37
	Non-PET	1070	1440	1320	4200	2360	2080	1280	62
	Textile	2520	1450	1300	1220	1140	1530	570	37
NIR PVC Fraction	PVC	1730	1040	2260	4500	6980	3300	2430	74
	Non-PVC	1500	1990	1800	800	1550	1530	450	30
Black & Grey Fraction	PET	400	3010	-	2210	90	1430	1410	99
	PVC	5280	1470	2380	4260	5980	3870	1910	49
	PE	3220	5580	4490	1660	4620	3910	1510	39
	PP	2150	740	260	2170	1230	1310	850	65
	PS	2320	5120	3050	-	1380	2970	1590	54
	Other	350	1180	460	1560	1320	970	540	55
Overall	mg/kg	1580	1420	1220	1240	1770	1450	230	16
	mg/MJ	73	64	58	56	91	69	14	21

A.29. V

a

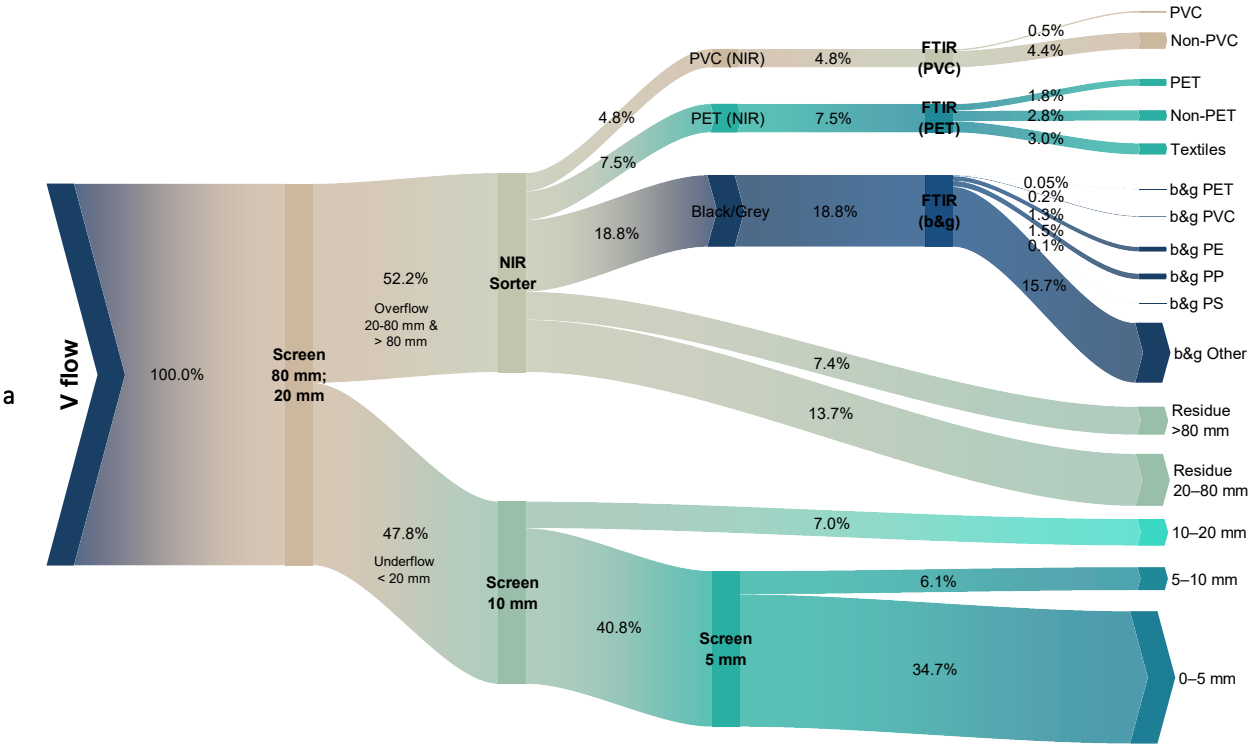

b

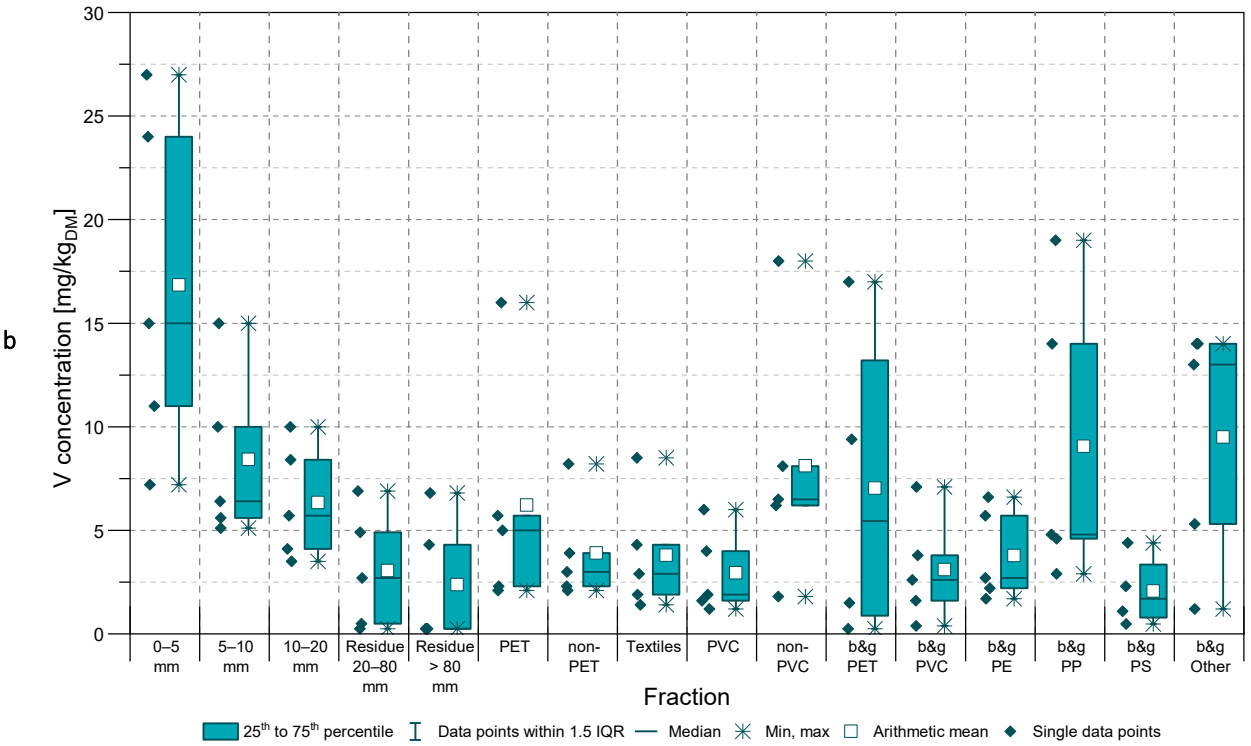

Figure A.29: a) Diagram of vanadium (V) flows representing the arithmetic mean values of the five MCW samples S01–S05. B&g = black and grey fractions. b) Box plot of V concentrations in different particle size classes and sorted fractions in mg/kg referring to dry mass without hard impurities

Table A.29: Vanadium (V) concentrations in mg/kg referring to dry mass without hard impurities. LOQ = 0.25 mg/kg

Fraction		Composite sample					Mean	Std. Dev.	Rel. Std. Dev [%]
		S01	S02	S03	S04	S05			
Screen	0–5 mm	24	7.2	15	11	27	17	8.4	50
	5–10 mm	5.6	5.1	10	6.4	15	8.4	4.1	49
	10–20 mm	5.7	3.5	8.4	4.1	10	6.3	2.8	44
NIR Residue	20–80 mm	< 0.25	4.9	0.49	6.9	2.7	3.0	2.9	94
	> 80 mm	6.8	< 0.25	< 0.25	< 0.25	4.3	2.4	3.0	128
NIR PET Fraction	PET	2.1	2.3	5.7	16	5.0	6.2	5.7	92
	Non-PET	2.1	3.0	3.9	2.3	8.2	3.9	2.5	64
	Textile	1.9	4.3	2.9	1.4	8.5	3.8	2.9	75
NIR PVC Fraction	PVC	1.6	1.2	4.0	1.9	6.0	2.9	2.0	69
	Non-PVC	6.5	8.1	6.2	1.8	18	8.1	6.0	74
Black & Grey Fraction	PET	1.5	17	-	< 0.25	9.4	7.0	7.8	111
	PVC	2.6	0.39	1.6	7.1	3.8	3.1	2.6	83
	PE	1.7	2.2	6.6	2.7	5.7	3.8	2.2	59
	PP	14	2.9	4.8	19	4.6	9.1	7.1	78
	PS	0.48	2.3	1.1	-	4.4	2.1	1.7	83
	Other	1.2	14	5.3	14	13	9.5	5.9	62
Overall	mg/kg	6.4	4.8	3.6	5.4	9.6	6.0	2.3	38
	mg/MJ	0.30	0.22	0.17	0.24	0.49	0.28	0.13	44

A.30. W

a

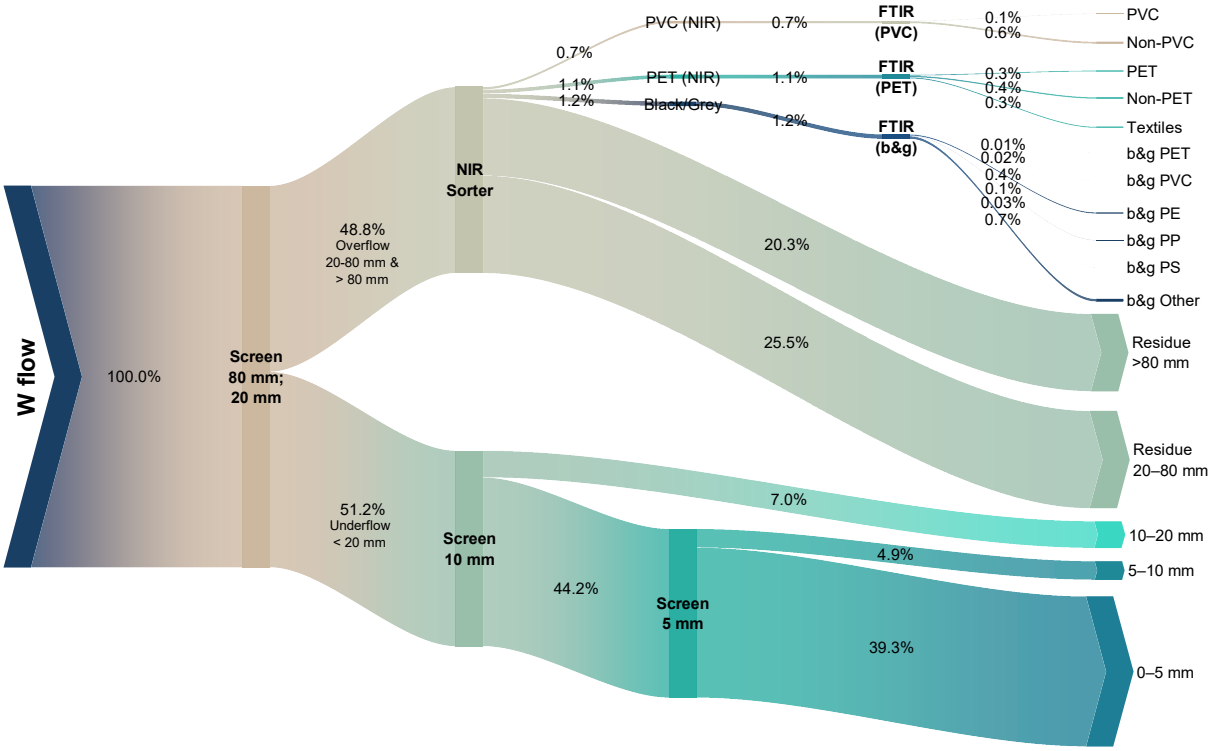

b

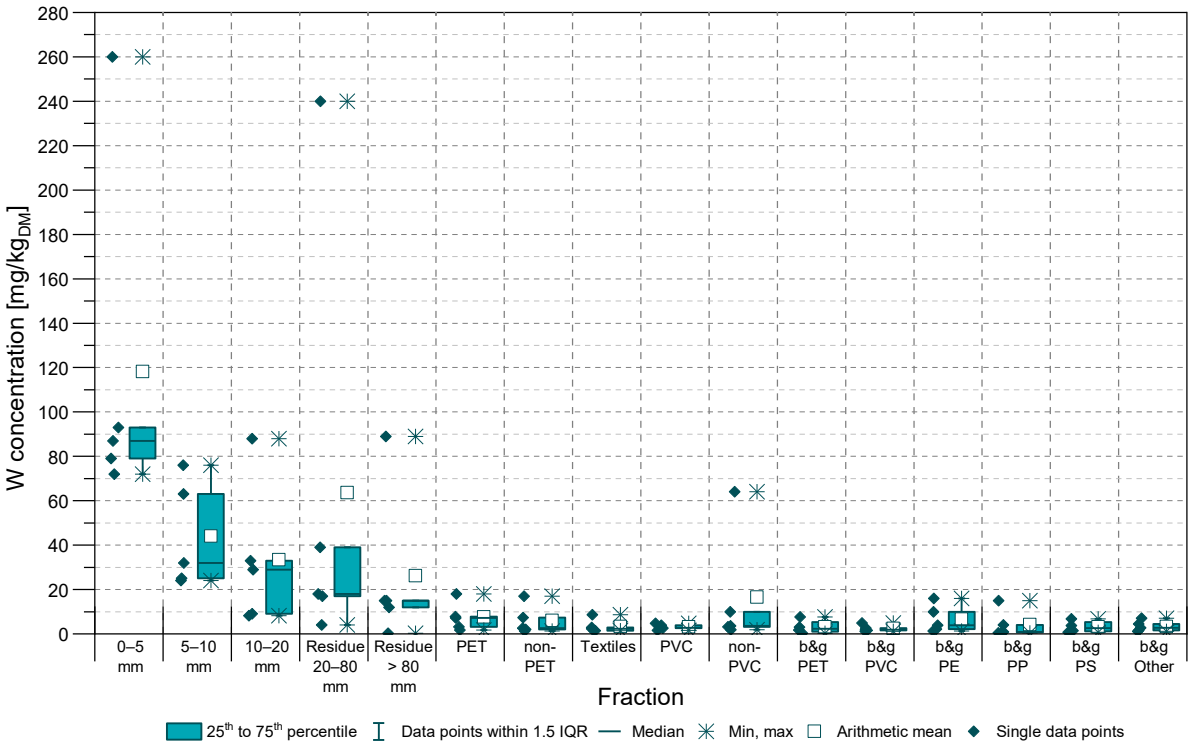

Figure A.30: a) Diagram of tungsten (W) flows representing the arithmetic mean values of the five MCW samples S01–S05. B&g = black and grey fractions. b) Box plot of W concentrations in different particle size classes and sorted fractions in mg/kg referring to dry mass without hard impurities

Table A.30: Tungsten (W) concentrations in mg/kg referring to dry mass without hard impurities. LOQ = 0.25 mg/kg

Fraction		Composite sample					Mean	Std. Dev.	Rel. Std. Dev [%]
		S01	S02	S03	S04	S05			
Screen	0–5 mm	260	72	87	93	79	120	80	67
	5–10 mm	63	32	24	76	25	44	24	54
	10–20 mm	33	29	9	8.2	88	33	33	97
NIR Residue	20–80 mm	39	240	4	18	17	64	99	156
	> 80 mm	12	15	89	15	< 0.25	26	36	136
NIR PET Fraction	PET	7.2	18	7.8	3.2	1.7	7.6	6.4	84
	Non-PET	17	7.4	2.0	2.6	1.3	6.1	6.6	108
	Textile	8.7	2.9	1.5	1.5	2.3	3.4	3.0	90
NIR PVC Fraction	PVC	4.7	2.6	2.8	3.9	1.6	3.1	1.2	39
	Non-PVC	10	64	3.2	3.6	1.8	17	27	162
Black & Grey Fraction	PET	7.7	3.0	-	1.7	< 0.25	3.2	3.2	102
	PVC	4.9	1.8	1.1	2.6	1.6	2.4	1.5	62
	PE	16	3.9	2.1	9.9	1.3	6.6	6.2	94
	PP	15	4.1	0.45	0.68	0.8	4.2	6.2	148
	PS	3.8	6.8	0.76	-	1.4	3.2	2.7	86
	Other	4.5	7.0	1.6	2.7	1.1	3.4	2.4	71
Overall	mg/kg	54	77	38	23	21	43	24	55
	mg/MJ	2.5	3.5	1.8	1.0	1.1	2.0	1.0	52

A.31. Zn

a

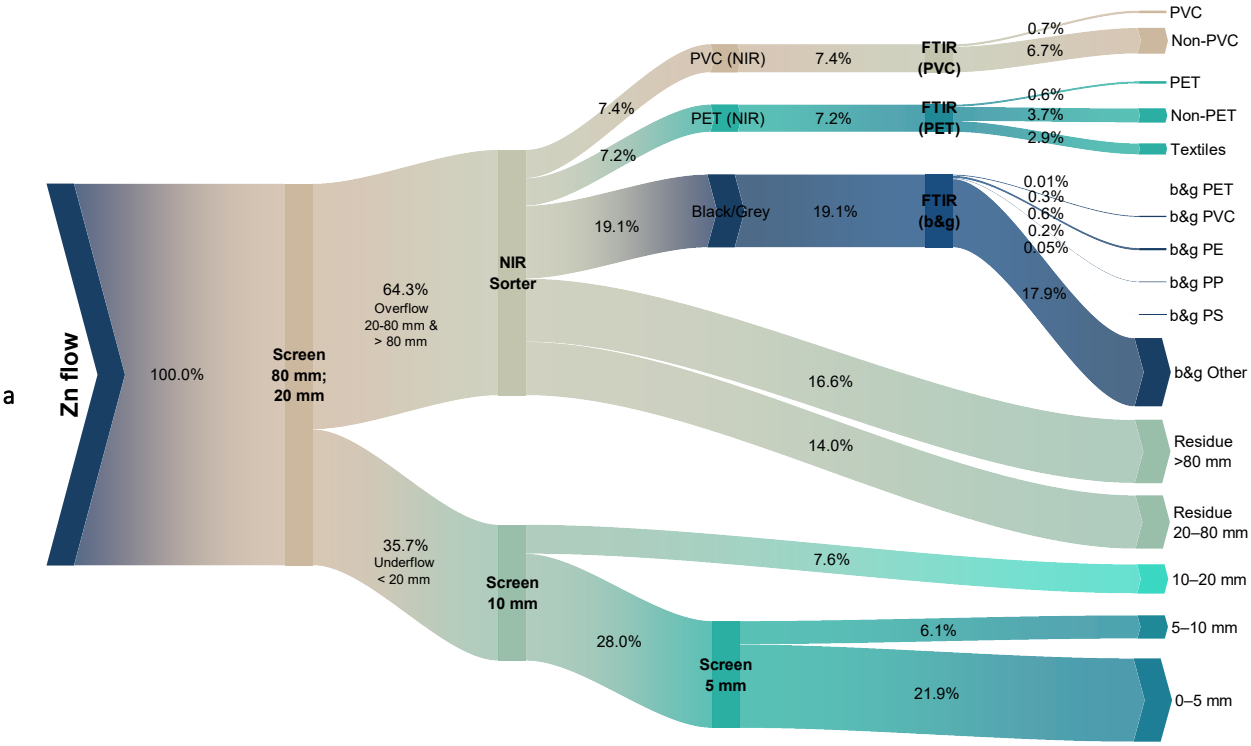

b

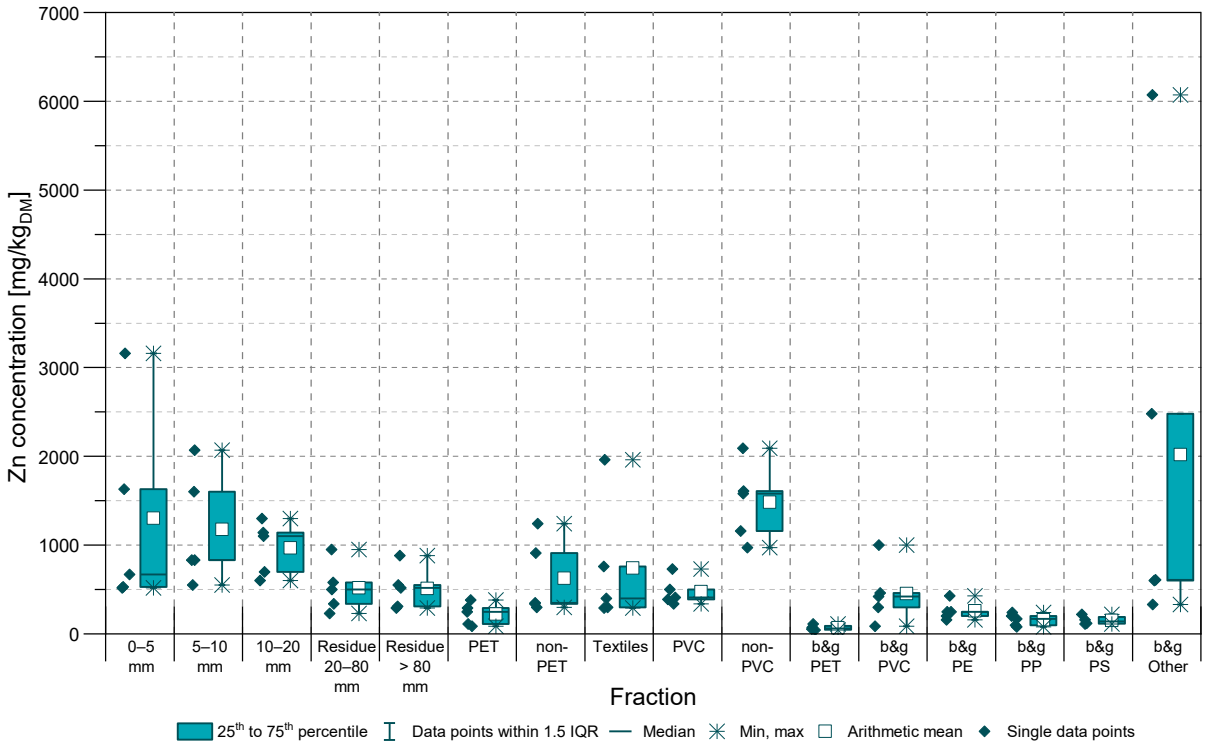

Figure A.31: a) Diagram of zinc (Zn) flows representing the arithmetic mean values of the five MCW samples S01–S05. B&g = black and grey fractions. b) Box plot of Zn concentrations in different particle size classes and sorted fractions in mg/kg referring to dry mass without hard impurities

Table A.31: Zinc (Zn) concentrations in mg/kg referring to dry mass without hard impurities. LOQ = 2.5 mg/kg

Fraction		Composite sample					Mean	Std. Dev.	Rel. Std. Dev [%]
		S01	S02	S03	S04	S05			
Screen	0–5 mm	530	3160	1630	670	520	1300	1140	87
	5–10 mm	2070	830	830	1600	550	1180	630	54
	10–20 mm	1300	700	1100	600	1140	970	300	31
NIR Residue	20–80 mm	950	500	580	230	340	520	280	53
	> 80 mm	520	550	310	290	880	510	240	47
NIR PET Fraction	PET	290	110	250	380	85	220	120	56
	Non-PET	910	350	1240	340	300	630	430	68
	Textile	1960	760	400	300	290	740	710	95
NIR PVC Fraction	PVC	390	410	730	340	500	470	150	33
	Non-PVC	2090	970	1160	1580	1610	1480	440	29
Black & Grey Fraction	PET	110	71	-	53	42	69	30	43
	PVC	88	420	300	1000	460	450	340	75
	PE	250	250	430	160	200	260	100	40
	PP	240	170	200	98	78	160	68	43
	PS	110	160	220	-	120	150	50	33
	Other	6070	610	330	600	2480	2020	2420	120
Overall	mg/kg	1440	1040	600	430	750	850	400	47
	mg/MJ	67	47	29	20	38	40	18	45

A.32. Hard impurities

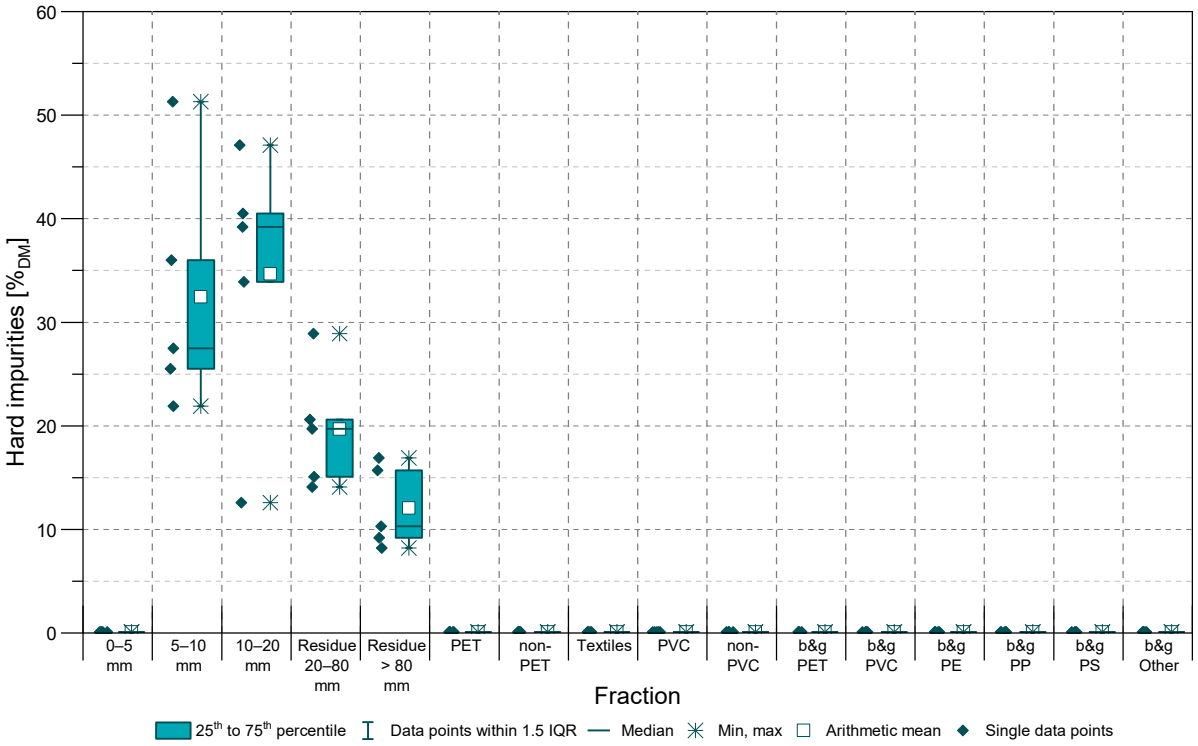

Figure A.32: Box plot of hard impurities in different particle size classes and sorted fractions in mass-% referring to dry mass without hard impurities

Table A.32: Mass share of hard impurities in % referring to dry mass

Fraction		Composite sample					Mean	Std. Dev.	Rel. Std. Dev [%]
		S01	S02	S03	S04	S05			
Screen	0–5 mm	< 0.1	< 0.1	< 0.1	< 0.1	< 0.1	0.10	0.00	0
	5–10 mm	27.5	21.9	25.5	51.3	36.0	32.4	11.8	36
	10–20 mm	12.6	33.9	40.5	47.1	39.2	34.7	13.2	38
NIR Residue	20–80 mm	14.1	19.7	28.9	20.6	15.1	19.7	5.9	30
	> 80 mm	8.2	9.2	16.9	15.7	10.3	12.1	4.0	33
NIR PET Fraction	PET	< 0.1	< 0.1	< 0.1	< 0.1	< 0.1	0.1	0	0
	Non-PET	< 0.1	< 0.1	< 0.1	< 0.1	< 0.1	0.1	0	0
	Textile	< 0.1	< 0.1	< 0.1	< 0.1	< 0.1	0.1	0	0
NIR PVC Fraction	PVC	< 0.1	< 0.1	< 0.1	< 0.1	< 0.1	0.1	0	0
	Non-PVC	< 0.1	< 0.1	< 0.1	< 0.1	< 0.1	0.1	0	0
Black & Grey Fraction	PET	< 0.1	< 0.1	-	< 0.1	< 0.1	0.1	0	0
	PVC	< 0.1	< 0.1	< 0.1	< 0.1	< 0.1	0.1	0	0
	PE	< 0.1	< 0.1	< 0.1	< 0.1	< 0.1	0.1	0	0
	PP	< 0.1	< 0.1	< 0.1	< 0.1	< 0.1	0.1	0	0
	PS	< 0.1	< 0.1	< 0.1	-	< 0.1	0.1	0	0
	Other	< 0.1	< 0.1	< 0.1	< 0.1	< 0.1	0.1	0	0
Overall	%DM	7.0	10.8	14.3	13.9	9.5	11.1	3.0	27

Appendix B - Effect of removing particle size classes

B.1. Mass

Table B.1 Relative mass loss in % caused by the removal of different material or particle size fractions referring dry mass without hard impurities

	Removed fractions	Mass loss [%]					
		S01	S02	S03	S04	S05	Avr
Single process steps	0–5 mm	-13.5	-18.2	-8.5	-10.7	-13.5	-12.9
	0–10 mm	-17.7	-26.9	-11.7	-13.6	-16.9	-17.4
	0–20 mm	-29.1	-33.8	-16.1	-18.6	-22.3	-24.0
	PET (NIR)	-9.9	-7.7	-11.6	-10.4	-11.2	-10.2
	PVC (NIR)	-5.6	-2.1	-1.8	-4.4	-7.3	-4.3
	b&g	-15.8	-11.3	-17.1	-11.5	-10.8	-13.3
	PET + PVC (NIR)	-15.5	-9.8	-13.4	-14.7	-18.5	-14.4
Combinations of Screening and state-of-the-art NIR sorting or manual removal of black materials	0–5 mm + PET (NIR)	-23.4	-25.9	-20.1	-21.1	-24.7	-23.1
	0–10 mm + PET (NIR)	-27.6	-34.6	-23.3	-24.0	-28.2	-27.5
	0–20 mm + PET (NIR)	-39.0	-41.5	-27.7	-29.0	-33.6	-34.1
	0–5 mm + PVC (NIR)	-19.1	-20.4	-10.4	-15.1	-20.8	-17.2
	0–10 mm + PVC (NIR)	-23.3	-29.0	-13.5	-18.0	-24.2	-21.6
	0–20 mm + PVC (NIR)	-34.7	-36.0	-17.9	-23.0	-29.6	-28.2
	0–5 mm + PET (NIR) + PVC (NIR)	-29.0	-28.1	-22.0	-25.5	-32.0	-27.3
	0–10 mm + PET (NIR) + PVC (NIR)	-33.2	-36.7	-25.1	-28.4	-35.5	-31.8
	0–20 mm + PET (NIR) + PVC (NIR)	-44.6	-43.6	-29.5	-33.4	-40.9	-38.4
	0–5 mm + b&g	-29.3	-29.5	-25.6	-22.2	-24.3	-26.2
	0–10 mm + b&g	-33.6	-38.2	-28.7	-25.2	-27.7	-30.7
	0–20 mm + b&g	-44.9	-45.1	-33.2	-30.1	-33.1	-37.3
	0–5 mm + b&g + PVC (NIR)	-35.0	-31.7	-27.4	-26.6	-31.6	-30.4
	0–10 mm + b&g + PVC (NIR)	-39.2	-40.3	-30.6	-29.6	-35.0	-34.9
	0–20 mm + b&g + PVC (NIR)	-50.5	-47.2	-35.0	-34.5	-40.4	-41.5
	0–5 mm + b&g + PET (NIR)	-39.2	-37.2	-37.2	-32.6	-35.5	-36.4
	0–10 mm + b&g + PET (NIR)	-43.5	-45.9	-40.3	-35.5	-39.0	-40.8
	0–20 mm + b&g + PET (NIR)	-54.8	-52.8	-44.8	-40.5	-44.4	-47.4

More targeted removal	0–5 mm + b&g + PET (NIR) + PVC (NIR)	-44.8	-39.4	-39.0	-37.0	-42.8	**-40.6**
	0–10 mm + b&g + PET (NIR) + PVC (NIR)	-49.1	-48.0	-42.2	-39.9	-46.3	**-45.1**
	0–20 mm + b&g + PET (NIR) + PVC (NIR)	-60.4	-54.9	-46.6	-44.9	-51.7	**-51.7**
	PVC (FTIR) + b&g PVC	-0.9	-1.2	-0.9	-2.5	-0.8	**-1.3**
	0–5 mm + PVC (FTIR) + b&g PVC	-14.4	-19.5	-9.5	-13.2	-14.3	**-14.2**
	0–10 mm + PVC (FTIR) + b&g PVC	-18.6	-28.1	-12.6	-16.2	-17.8	**-18.6**
	0–20 mm + PVC (FTIR) + b&g PVC	-29.9	-35.1	-17.0	-21.1	-23.2	**-25.3**
	PVC (NIR) + b&g PVC	-6.0	-2.2	-2.0	-5.0	-7.3	**-4.5**
	0–5 mm + PVC (NIR) + b&g PVC	-19.5	-20.5	-10.6	-15.7	-20.8	**-17.4**
	0–10 mm + PVC (NIR) + b&g PVC	-23.7	-29.1	-13.7	-18.7	-24.3	**-21.9**
	0–20 mm + PVC (NIR) + b&g PVC	-35.0	-36.0	-18.2	-23.6	-29.7	**-28.5**
	PET (FTIR) + Textiles + b&g PET	-7.7	-3.8	-6.2	-6.4	-7.9	**-6.4**
	0–5 mm + PET (FTIR) + Textiles + b&g PET	-21.2	-22.1	-14.7	-17.1	-21.4	**-19.3**
	0–10 mm + PET (FTIR) + Textiles + b&g PET	-25.4	-30.7	-17.9	-20.0	-24.9	**-23.8**
	0–20 mm + PET (FTIR) + Textiles + b&g PET	-36.8	-37.6	-22.3	-25.0	-30.3	**-30.4**
	b&g Other	-10.7	-8.9	-14.5	-8.0	-6.1	**-9.6**
	0–5 mm + b&g Other	-24.2	-27.2	-23.0	-18.7	-19.6	**-22.5**
	0–10 mm + b&g Other	-28.4	-35.8	-26.2	-21.6	-23.1	**-27.0**
	0–20 mm + b&g Other	-39.8	-42.7	-30.6	-26.6	-28.5	**-33.6**
	PVC (FTIR) + b&g PVC + b&g Other	-11.6	-10.2	-15.4	-10.5	-7.0	**-10.9**
	0–5 mm + PVC (FTIR) + b&g PVC + b&g Other	-25.1	-28.4	-23.9	-21.2	-20.5	**-23.8**
	0–10 mm + PVC (FTIR) + b&g PVC + b&g Other	-29.3	-37.0	-27.1	-24.1	-23.9	**-28.3**
	0–20 mm + PVC (FTIR) + b&g PVC + b&g Other	-40.6	-44.0	-31.5	-29.1	-29.3	**-34.9**
	PVC (NIR) + b&g PVC + b&g Other	-16.7	-11.1	-16.5	-13.0	-13.5	**-14.1**
	0–5 mm + PVC (NIR) + b&g PVC + b&g Other	-30.2	-29.4	-25.1	-23.7	-27.0	**-27.1**
	0–10 mm + PVC (NIR) + b&g PVC + b&g Other	-34.4	-38.0	-28.2	-26.6	-30.4	**-31.5**
	0–20 mm + PVC (NIR) + b&g PVC + b&g Other	-45.7	-45.0	-32.6	-31.6	-35.8	**-38.1**
	b&g Other + b&g PVC	-11.1	-9.0	-14.7	-8.6	-6.2	**-9.9**
	0–5 mm + b&g Other + b&g PVC	-24.6	-27.3	-23.2	-19.3	-19.7	**-22.8**
	0–10 mm + b&g Other + b&g PVC	-28.8	-35.9	-26.4	-22.2	-23.1	**-27.3**
	0–20 mm + b&g Other + b&g PVC	-40.1	-42.8	-30.8	-27.2	-28.5	**-33.9**

B.2. LHV

Table B.2: LHV and relative change (in %) of LHV after the removal of different material or particle size fractions referring to dry mass without hard impurities

	Removed fractions	LHV after removal	LHV					
			S01	S02	S03	S04	S05	Avr
Single process steps	0–5 mm	kJ/kg	23179	24711	22258	23311	21524	**22997**
		ΔLHV	7.6	11.6	6.0	6.0	10.8	8.4
	0–10 mm	kJ/kg	23352	25598	22483	23448	21865	**23349**
		ΔLHV	8.4	15.6	7.1	6.6	12.5	10.1
	0–20 mm	kJ/kg	23696	26017	22625	23622	22273	**23647**
		ΔLHV	10.0	17.5	7.8	7.4	14.6	11.5
	PET (NIR)	kJ/kg	21280	22261	21138	21949	19086	**21143**
		ΔLHV	-1.2	0.6	0.7	-0.2	-1.8	-0.4
	PVC (NIR)	kJ/kg	21395	22141	20974	22011	19170	**21138**
		ΔLHV	-0.6	0.0	-0.1	0.1	-1.3	-0.4
	b&g	kJ/kg	20920	21930	20783	21621	18577	**20766**
		ΔLHV	-2.9	-0.9	-1.0	-1.7	-4.4	-2.2
	PET + PVC (NIR)	kJ/kg	21106	22270	21114	21968	18762	**21044**
		ΔLHV	-2.0	0.6	0.6	-0.1	-3.4	-0.9
Combinations of Screening and state-of-the-art NIR sorting or manual removal of black materials	0–5 mm + PET (NIR)	kJ/kg	23091	25134	22597	23435	21434	**23138**
		ΔLHV	7.2	13.5	7.6	6.6	10.3	9.1
	0–10 mm + PET (NIR)	kJ/kg	23283	26182	22870	23595	21825	**23551**
		ΔLHV	8.1	18.3	8.9	7.3	12.3	11.0
	0–20 mm + PET (NIR)	kJ/kg	23670	26725	23058	23805	22298	**23911**
		ΔLHV	9.9	20.7	9.8	8.2	14.8	12.7
	0–5 mm + PVC (NIR)	kJ/kg	23130	24787	22258	23400	21415	**22998**
		ΔLHV	7.4	12.0	6.0	6.4	10.2	8.4
	0–10 mm + PVC (NIR)	kJ/kg	23313	25710	22488	23547	21784	**23368**
		ΔLHV	8.3	16.1	7.1	7.1	12.1	10.1
	0–20 mm + PVC (NIR)	kJ/kg	23680	26155	22633	23738	22228	**23687**
		ΔLHV	10.0	18.2	7.8	7.9	14.4	11.7
	0–5 mm + PET (NIR) + PVC (NIR)	kJ/kg	23028	25231	22605	23543	21297	23141
		ΔLHV	6.9	14.0	7.7	7.0	9.6	9.0
	0–10 mm + PET (NIR) + PVC (NIR)	kJ/kg	23232	26327	22885	23717	21725	23577
		ΔLHV	7.9	18.9	9.0	7.8	11.8	11.1
	0–20 mm + PET (NIR) + PVC (NIR)	kJ/kg	23648	26908	23080	23951	22248	23967
		ΔLHV	9.8	21.6	9.9	8.9	14.5	12.9
	0–5 mm + b&g	kJ/kg	22815	24864	22309	23083	20819	**22778**
		ΔLHV	5.9	12.3	6.2	5.0	7.2	7.3
	0–10 mm + b&g	kJ/kg	23007	25934	22590	23232	21178	**23188**
		ΔLHV	6.8	17.2	7.6	5.6	9.0	9.2
	0–20 mm + b&g	kJ/kg	23379	26482	22775	23420	21596	**23530**
		ΔLHV	8.6	19.6	8.5	6.5	11.2	10.9
	0–5 mm + b&g + PVC (NIR)	kJ/kg	22723	24957	22310	23172	20618	**22756**
		ΔLHV	5.5	12.7	6.3	5.4	6.1	7.2
	0–10 mm + b&g + PVC (NIR)	kJ/kg	22926	26080	22599	23334	21006	**23189**
		ΔLHV	6.5	17.8	7.6	6.1	8.1	9.2
	0–20 mm + b&g + PVC (NIR)	kJ/kg	23322	26668	22790	23542	21460	**23556**
		ΔLHV	8.3	20.5	8.5	7.0	10.5	11.0
	0–5 mm + b&g + PET (NIR)	kJ/kg	22645	25382	22749	23193	20592	**22912**
		ΔLHV	5.2	14.7	8.3	5.5	6.0	7.9
	0–10 mm + b&g + PET (NIR)	kJ/kg	22858	26687	23108	23370	21004	**23405**
		ΔLHV	6.1	20.6	10.1	6.3	8.1	10.2
	0–20 mm + b&g + PET (NIR)	kJ/kg	23274	27434	23374	23602	21490	**23835**
		ΔLHV	8.1	23.9	11.3	7.3	10.6	12.3
	0–5 mm + b&g + PET (NIR) + PVC (NIR)	kJ/kg	22519	25506	22764	23304	20322	**22883**
		ΔLHV	4.6	15.2	8.4	6.0	4.6	7.8
	0–10 mm + b&g + PET (NIR) + PVC (NIR)	kJ/kg	22744	26885	23135	23500	20773	**23407**
		ΔLHV	5.6	21.5	10.2	6.9	6.9	10.2
	0–20 mm + b&g + PET (NIR) + PVC (NIR)	kJ/kg	23187	27697	23413	23762	21306	**23873**
		ΔLHV	7.7	25.1	11.5	8.0	9.7	12.4

More targeted removal	PVC (FTIR) + b&g PVC	kJ/kg	21525	22163	20971	22071	19440	**21234**
		ΔLHV	0.0	0.1	-0.1	0.4	0.1	0.1
	0–5 mm + PVC (FTIR) + b&g PVC	kJ/kg	23184	24784	22242	23437	21558	**23041**
		ΔLHV	7.7	12.0	5.9	6.6	11.0	8.6
	0–10 mm + PVC (FTIR) + b&g PVC	kJ/kg	23359	25695	22468	23582	21904	**23402**
		ΔLHV	8.5	16.1	7.0	7.2	12.7	10.3
	0–20 mm + PVC (FTIR) + b&g PVC	kJ/kg	23709	26132	22611	23771	22319	**23708**
		ΔLHV	10.1	18.1	7.7	8.1	14.9	11.8
	PVC (NIR) + b&g PVC	kJ/kg	21385	22142	20966	22020	19169	**21137**
		ΔLHV	-0.7	0.0	-0.1	0.1	-1.3	-0.4
	0–5 mm + PVC (NIR) + b&g PVC	kJ/kg	23126	24791	22252	23421	21415	**23001**
		ΔLHV	7.4	12.0	6.0	6.5	10.2	8.4
	0–10 mm + PVC (NIR) + b&g PVC	kJ/kg	23310	25716	22482	23569	21784	**23372**
		ΔLHV	8.2	16.2	7.1	7.2	12.1	10.2
	0–20 mm + PVC (NIR) + b&g PVC	kJ/kg	23678	26162	22628	23763	22228	**23692**
		ΔLHV	10.0	18.2	7.8	8.0	14.4	11.7
	PET (FTIR) + Textiles + b&g PET	kJ/kg	21490	22235	21015	22033	19277	**21210**
		ΔLHV	-0.2	0.4	0.1	0.2	-0.8	-0.1
	0–5 mm + PET (FTIR) + Textiles + b&g PET	kJ/kg	23287	24960	22369	23458	21558	**23126**
		ΔLHV	8.1	12.8	6.5	6.7	11.0	9.0
	0–10 mm + PET (FTIR) + Textiles + b&g PET	kJ/kg	23484	25927	22615	23611	21937	**23515**
		ΔLHV	9.1	17.1	7.7	7.4	12.9	10.8
	0–20 mm + PET (FTIR) + Textiles + b&g PET	kJ/kg	23894	26408	22776	23811	22397	**23857**
		ΔLHV	11.0	19.3	8.5	8.3	15.3	12.5
	b&g Other	kJ/kg	21731	22286	21200	22156	19449	**21365**
		ΔLHV	0.9	0.7	1.0	0.7	0.1	0.7
	0–5 mm + b&g Other	kJ/kg	23642	25214	22721	23625	21709	**23382**
		ΔLHV	9.8	13.9	8.2	7.4	11.7	10.2
	0–10 mm + b&g Other	kJ/kg	23868	26292	23009	23788	22086	**23809**
		ΔLHV	10.8	18.8	9.6	8.2	13.7	12.2
	0–20 mm + b&g Other	kJ/kg	24371	26860	23215	24004	22545	**24199**
		ΔLHV	13.2	21.3	10.6	9.1	16.0	14.1
	PVC (FTIR) + b&g PVC + b&g Other	kJ/kg	21722	22318	21171	22246	19462	**21384**
		ΔLHV	0.9	0.8	0.8	1.2	0.2	0.8
	0–5 mm + PVC (FTIR) + b&g PVC + b&g Other	kJ/kg	23653	25305	22707	23774	21747	**23437**
		ΔLHV	9.8	14.3	8.1	8.1	11.9	10.5
	0–10 mm + PVC (FTIR) + b&g PVC + b&g Other	kJ/kg	23883	26416	22998	23947	22130	**23875**
		ΔLHV	10.9	19.3	9.5	8.9	13.9	12.5
	0–20 mm + PVC (FTIR) + b&g PVC + b&g Other	kJ/kg	24396	27012	23206	24182	22598	**24279**
		ΔLHV	13.3	22.0	10.5	10.0	16.3	14.4
	PVC (NIR) + b&g PVC + b&g Other	kJ/kg	21576	22297	21168	22196	19174	**21282**
		ΔLHV	0.2	0.7	0.8	0.9	-1.3	0.3
	0–5 mm + PVC (NIR) + b&g PVC + b&g Other	kJ/kg	23620	25320	22727	23767	21609	**23409**
		ΔLHV	9.7	14.4	8.2	8.1	11.2	10.3
	0–10 mm + PVC (NIR) + b&g PVC + b&g Other	kJ/kg	23866	26452	23024	23945	22021	**23862**
		ΔLHV	10.8	19.5	9.7	8.9	13.3	12.4
	0–20 mm + PVC (NIR) + b&g PVC + b&g Other	kJ/kg	24423	27063	23236	24189	22528	**24288**
		ΔLHV	13.4	22.3	10.7	10.0	16.0	14.5
	b&g Other + b&g PVC	kJ/kg	21722	22287	21191	22167	19449	**21363**
		ΔLHV	0.9	0.7	0.9	0.8	0.1	0.7
	0–5 mm + b&g Other + b&g PVC	kJ/kg	23640	25219	22715	23648	21709	**23386**
		ΔLHV	9.8	13.9	8.2	7.5	11.7	10.2
	0–10 mm + b&g Other + b&g PVC	kJ/kg	23868	26299	23004	23813	22086	**23814**
		ΔLHV	10.8	18.8	9.6	8.3	13.7	12.2
	0–20 mm + b&g Other + b&g PVC	kJ/kg	24373	26869	23210	24033	22546	**24206**
		ΔLHV	13.2	21.4	10.5	9.3	16.1	14.1

B.3. Ag

Table B.3: Relative concentration change (Δc, in %) of Ag caused by the removal of different material or particle size fractions referring to mg/kg and mg/MJ, both calculated for dry mass without hard impurities

	Removed fractions	Conc. after removal	mg/kg$_{DM}$ S01	S02	S03	S04	S05	Avr	mg/MJ S01	S02	S03	S04	S05	Avr
Single process steps	0–5 mm	c	1.17	1.00	1.36	0.90	0.76	**1.04**	0.05	0.04	0.06	0.04	0.04	**0.05**
		Δc [%]	-27.2	-22.6	-16.1	-30.7	-28.5	**-25.0**	-32.4	-30.6	-20.8	-34.6	-35.5	**-30.8**
	0–10 mm	c	1.00	0.90	1.33	0.79	0.70	**0.94**	0.04	0.03	0.06	0.03	0.03	**0.04**
		Δc [%]	-37.6	-30.8	-17.9	-39.1	-34.5	**-32.0**	-42.4	-40.1	-23.3	-42.9	-41.8	**-38.1**
	0–20 mm	c	0.81	0.69	1.35	0.74	0.51	**0.82**	0.03	0.03	0.06	0.03	0.02	**0.03**
		Δc [%]	-49.5	-47.0	-16.8	-42.9	-52.2	**-41.7**	-54.1	-54.9	-22.8	-46.9	-58.3	**-47.4**
	PET (NIR)	c	1.75	1.38	1.80	1.41	1.16	**1.50**	0.08	0.06	0.09	0.06	0.06	**0.07**
		Δc [%]	9.1	6.7	11.1	9.3	9.7	**9.2**	10.4	6.1	10.4	9.5	11.6	**9.6**
	PVC (NIR)	c	1.68	1.32	1.63	1.34	1.11	**1.42**	0.08	0.06	0.08	0.06	0.06	**0.07**
		Δc [%]	5.0	1.7	1.1	3.7	4.4	**3.2**	5.7	1.7	1.2	3.6	5.8	**3.6**
	b&g	c	1.86	1.42	1.90	1.43	1.16	**1.55**	0.09	0.06	0.09	0.07	0.06	**0.07**
		Δc [%]	15.9	10.2	17.4	10.3	9.2	**12.6**	19.3	11.2	18.6	12.2	14.2	**15.1**
	PET + PVC (NIR)	c	1.85	1.41	1.82	1.47	1.23	**1.56**	0.09	0.06	0.09	0.07	0.07	**0.07**
		Δc [%]	15.3	8.7	12.5	13.9	15.5	**13.2**	17.6	8.1	11.9	14.1	19.6	**14.3**
Combinations of Screening and state-of-the-art NIR sorting or manual removal of black materials	0–5 mm + PET (NIR)	c	1.28	1.08	1.52	0.98	0.84	**1.14**	0.06	0.04	0.07	0.04	0.04	**0.05**
		Δc [%]	-20.1	-16.5	-6.1	-24.1	-21.3	**-17.6**	-25.4	-26.5	-12.8	-28.8	-28.7	**-24.4**
	0–10 mm + PET (NIR)	c	1.10	0.97	1.49	0.86	0.77	**1.04**	0.05	0.04	0.07	0.04	0.04	**0.04**
		Δc [%]	-31.4	-24.9	-7.8	-33.4	-27.9	**-25.1**	-36.5	-36.5	-15.4	-38.0	-35.9	**-32.5**
	0–20 mm + PET (NIR)	c	0.90	0.74	1.52	0.81	0.55	**0.90**	0.04	0.03	0.07	0.03	0.02	**0.04**
		Δc [%]	-44.1	-42.6	-6.0	-37.4	-48.1	**-35.7**	-49.2	-52.4	-14.4	-42.2	-54.8	**-42.6**
	0–5 mm + PVC (NIR)	c	1.23	1.02	1.37	0.93	0.79	**1.07**	0.05	0.04	0.06	0.04	0.04	**0.05**
		Δc [%]	-23.2	-21.1	-15.2	-28.1	-26.0	**-22.7**	-28.5	-29.5	-20.0	-32.4	-32.9	**-28.7**
	0–10 mm + PVC (NIR)	c	1.06	0.91	1.34	0.82	0.72	**0.97**	0.05	0.04	0.06	0.03	0.03	**0.04**
		Δc [%]	-34.1	-29.4	-17.1	-36.9	-32.5	**-30.0**	-39.2	-39.2	-22.6	-41.0	-39.8	**-36.4**
	0–20 mm + PVC (NIR)	c	0.86	0.70	1.36	0.77	0.51	**0.84**	0.04	0.03	0.06	0.03	0.02	**0.04**
		Δc [%]	-46.5	-46.0	-15.9	-40.8	-51.9	**-40.2**	-51.4	-54.3	-22.0	-45.1	-57.9	**-46.2**
	0–5 mm + PET (NIR) + PVC (NIR)	c	1.36	1.10	1.54	1.02	0.87	**1.18**	0.06	0.04	0.07	0.04	0.04	**0.05**
		Δc [%]	-15.0	-14.7	-4.9	-20.8	-17.7	**-14.6**	-20.5	-25.2	-11.7	-26.0	-24.9	**-21.6**
	0–10 mm + PET (NIR) + PVC (NIR)	c	1.17	0.99	1.51	0.90	0.80	**1.07**	0.05	0.04	0.07	0.04	0.04	**0.05**
		Δc [%]	-26.9	-23.1	-6.6	-30.5	-24.8	**-22.4**	-32.3	-35.4	-14.3	-35.6	-32.8	**-30.1**
	0–20 mm + PET (NIR) + PVC (NIR)	c	0.96	0.76	1.54	0.85	0.56	**0.93**	0.04	0.03	0.07	0.04	0.03	**0.04**
		Δc [%]	-40.1	-41.3	-4.7	-34.6	-47.2	**-33.6**	-45.4	-51.7	-13.3	-39.9	-53.9	**-40.8**
	0–5 mm + b&g	c	1.37	1.12	1.61	0.99	0.83	**1.19**	0.06	0.05	0.07	0.04	0.04	**0.05**
		Δc [%]	-14.4	-13.4	-0.4	-23.5	-21.7	**-14.7**	-19.2	-22.9	-6.2	-27.1	-26.9	**-20.5**
	0–10 mm + b&g	c	1.18	1.01	1.59	0.87	0.76	**1.08**	0.05	0.04	0.07	0.04	0.04	**0.05**
		Δc [%]	-26.4	-21.8	-2.0	-33.0	-28.3	**-22.3**	-31.1	-33.3	-8.9	-36.5	-34.2	**-28.8**
	0–20 mm + b&g	c	0.97	0.77	1.62	0.81	0.55	**0.95**	0.04	0.03	0.07	0.03	0.03	**0.04**
		Δc [%]	-39.5	-40.2	0.4	-37.0	-48.3	**-32.9**	-44.3	-50.0	-7.4	-40.9	-53.5	**-39.2**
	0–5 mm + b&g + PVC (NIR)	c	1.47	1.15	1.63	1.03	0.87	**1.23**	0.06	0.05	0.07	0.04	0.04	**0.05**
		Δc [%]	-8.4	-11.4	1.0	-20.1	-18.1	**-11.4**	-13.1	-21.4	-4.9	-24.2	-22.8	**-17.3**
	0–10 mm + b&g + PVC (NIR)	c	1.27	1.04	1.61	0.91	0.79	**1.12**	0.06	0.04	0.07	0.04	0.04	**0.05**
		Δc [%]	-21.0	-19.8	-0.5	-30.0	-25.2	**-19.3**	-25.8	-31.9	-7.6	-34.0	-30.8	**-26.0**
	0–20 mm + b&g + PVC (NIR)	c	1.05	0.79	1.65	0.85	0.56	**0.98**	0.05	0.03	0.07	0.04	0.03	**0.04**
		Δc [%]	-34.4	-38.7	2.0	-34.1	-47.4	**-30.5**	-39.4	-49.1	-6.0	-38.4	-52.4	**-37.1**
	0–5 mm + b&g + PET (NIR)	c	1.55	1.23	1.86	1.10	0.93	**1.34**	0.07	0.05	0.08	0.05	0.05	**0.06**
		Δc [%]	-3.3	-5.1	15.2	-14.7	-12.1	**-4.0**	-8.0	-17.3	6.3	-19.2	-17.1	**-11.0**
	0–10 mm + b&g + PET (NIR)	c	1.34	1.12	1.85	0.97	0.86	**1.23**	0.06	0.04	0.08	0.04	0.04	**0.05**
		Δc [%]	-16.6	-13.4	14.1	-25.3	-19.4	**-12.1**	-21.4	-28.2	3.7	-29.7	-25.4	**-20.2**
	0–20 mm + b&g + PET (NIR)	c	1.12	0.86	1.91	0.91	0.61	**1.08**	0.05	0.03	0.08	0.04	0.03	**0.05**
		Δc [%]	-30.0	-33.7	18.3	-29.4	-42.6	**-23.5**	-35.3	-46.5	6.3	-34.2	-48.1	**-31.6**
	0–5 mm + b&g + PET (NIR) + PVC (NIR)	c	1.68	1.26	1.90	1.16	0.99	**1.40**	0.07	0.05	0.08	0.05	0.05	**0.06**
		Δc [%]	5.0	-2.6	17.3	-10.2	-6.6	**0.6**	0.4	-15.4	8.2	-15.2	-10.7	**-6.5**
	0–10 mm + b&g + PET (NIR) + PVC (NIR)	c	1.46	1.15	1.88	1.02	0.91	**1.28**	0.06	0.04	0.08	0.04	0.04	**0.06**
		Δc [%]	-9.1	-10.8	16.3	-21.3	-14.5	**-7.9**	-13.9	-26.5	5.6	-26.3	-20.0	**-16.2**
	0–20 mm + b&g + PET (NIR) + PVC (NIR)	c	1.25	0.88	1.96	0.97	0.63	**1.14**	0.05	0.03	0.08	0.04	0.03	**0.05**
		Δc [%]	-22.3	-31.6	20.9	-25.3	-40.7	**-19.8**	-27.9	-45.3	8.4	-30.9	-45.9	**-28.3**

More targeted removal	PVC (FTIR) + b&g PVC	c	1.62	1.31	1.63	1.32	1.07	**1.39**	0.08	0.06	0.08	0.06	0.05	**0.07**
		Δc [%]	0.7	1.0	0.5	2.1	0.6	1.0	0.8	0.9	0.6	1.7	0.6	0.9
	0–5 mm + PVC (FTIR) + b&g PVC	c	1.18	1.01	1.36	0.92	0.76	**1.05**	0.05	0.04	0.06	0.04	0.04	**0.05**
		Δc [%]	-26.6	-21.7	-15.7	-29.2	-28.0	**-24.3**	-31.9	-30.0	-20.4	-33.6	-35.1	**-30.2**
	0–10 mm + PVC (FTIR) + b&g PVC	c	1.01	0.91	1.33	0.80	0.70	**0.95**	0.04	0.04	0.06	0.03	0.03	**0.04**
		Δc [%]	-37.1	-29.9	-17.5	-37.9	-34.1	**-31.3**	-42.0	-39.6	-22.9	-42.0	-41.5	**-37.6**
	0–20 mm + PVC (FTIR) + b&g PVC	c	0.82	0.69	1.35	0.75	0.51	**0.83**	0.03	0.03	0.06	0.03	0.02	**0.04**
		Δc [%]	-49.1	-46.4	-16.4	-41.7	-52.0	**-41.1**	-53.8	-54.6	-22.4	-46.1	-58.2	**-47.0**
	PVC (NIR) + b&g PVC	c	1.69	1.32	1.64	1.35	1.11	**1.42**	0.08	0.06	0.08	0.06	0.06	**0.07**
		Δc [%]	5.4	1.8	1.2	4.2	4.4	3.4	6.1	1.7	1.4	4.1	5.8	3.8
	0–5 mm + PVC (NIR) + b&g PVC	c	1.24	1.02	1.37	0.94	0.79	**1.07**	0.05	0.04	0.06	0.04	0.04	**0.05**
		Δc [%]	-23.0	-21.0	-15.1	-27.7	-26.0	**-22.6**	-28.3	-29.5	-19.9	-32.1	-32.9	**-28.5**
	0–10 mm + PVC (NIR) + b&g PVC	c	1.06	0.91	1.34	0.82	0.72	**0.97**	0.05	0.04	0.06	0.03	0.03	**0.04**
		Δc [%]	-33.9	-29.3	-16.9	-36.5	-32.5	**-29.8**	-38.9	-39.1	-22.4	-40.8	-39.8	**-36.2**
	0–20 mm + PVC (NIR) + b&g PVC	c	0.86	0.70	1.36	0.77	0.51	**0.84**	0.04	0.03	0.06	0.03	0.02	**0.04**
		Δc [%]	-46.3	-45.9	-15.8	-40.5	-51.9	**-40.1**	-51.2	-54.3	-21.8	-44.9	-57.9	**-46.0**
	PET (FTIR) + Textiles + b&g PET	c	1.71	1.33	1.71	1.36	1.13	**1.45**	0.08	0.06	0.08	0.06	0.06	**0.07**
		Δc [%]	6.9	3.2	5.6	5.5	6.6	5.5	7.1	2.7	5.5	5.3	7.4	5.6
	0–5 mm + PET (FTIR) + Textiles + b&g PET	c	1.25	1.04	1.44	0.95	0.81	**1.10**	0.05	0.04	0.06	0.04	0.04	**0.05**
		Δc [%]	-21.8	-19.7	-11.1	-26.8	-23.6	**-20.6**	-27.7	-28.8	-16.5	-31.4	-31.2	**-27.1**
	0–10 mm + PET (FTIR) + Textiles + b&g PET	c	1.08	0.93	1.41	0.83	0.74	**1.00**	0.05	0.04	0.06	0.04	0.03	**0.04**
		Δc [%]	-33.0	-28.0	-12.9	-35.8	-30.1	**-27.9**	-38.5	-38.5	-19.1	-40.2	-38.1	**-34.9**
	0–20 mm + PET (FTIR) + Textiles + b&g PET	c	0.87	0.71	1.43	0.78	0.54	**0.87**	0.04	0.03	0.06	0.03	0.02	**0.04**
		Δc [%]	-45.5	-44.9	-11.4	-39.7	-49.5	**-38.2**	-50.9	-53.9	-18.4	-44.3	-56.2	**-44.7**
	b&g Other	c	1.77	1.40	1.85	1.38	1.12	**1.50**	0.08	0.06	0.09	0.06	0.06	**0.07**
		Δc [%]	10.1	7.9	14.3	7.0	5.0	8.9	9.1	7.2	13.2	6.2	4.9	8.1
	0–5 mm + b&g Other	c	1.30	1.09	1.57	0.96	0.80	**1.14**	0.05	0.04	0.07	0.04	0.04	**0.05**
		Δc [%]	-19.1	-15.5	-3.2	-25.8	-24.8	**-17.7**	-26.3	-25.8	-10.5	-30.9	-32.7	**-25.3**
	0–10 mm + b&g Other	c	1.11	0.98	1.54	0.84	0.73	**1.04**	0.05	0.04	0.07	0.04	0.03	**0.04**
		Δc [%]	-30.6	-23.8	-4.8	-34.9	-31.2	**-25.1**	-37.3	-35.9	-13.2	-39.8	-39.4	**-33.1**
	0–20 mm + b&g Other	c	0.91	0.75	1.57	0.79	0.53	**0.91**	0.04	0.03	0.07	0.03	0.02	**0.04**
		Δc [%]	-43.3	-41.8	-2.7	-38.9	-50.1	**-35.4**	-49.9	-52.0	-12.0	-44.0	-57.0	**-43.0**
	PVC (FTIR) + b&g PVC + b&g Other	c	1.78	1.41	1.86	1.42	1.12	**1.52**	0.08	0.06	0.09	0.06	0.06	**0.07**
		Δc [%]	11.0	9.1	15.0	9.4	5.7	10.1	10.1	8.2	14.1	8.2	5.5	9.2
	0–5 mm + PVC (FTIR) + b&g PVC + b&g Other	c	1.31	1.11	1.58	0.98	0.80	**1.16**	0.06	0.04	0.07	0.04	0.04	**0.05**
		Δc [%]	-18.4	-14.3	-2.6	-24.0	-24.3	**-16.7**	-25.7	-25.1	-9.9	-29.7	-32.4	**-24.6**
	0–10 mm + PVC (FTIR) + b&g PVC + b&g Other	c	1.12	1.00	1.55	0.86	0.74	**1.05**	0.05	0.04	0.07	0.04	0.03	**0.04**
		Δc [%]	-29.9	-22.7	-4.2	-33.4	-30.7	**-24.2**	-36.8	-35.2	-12.6	-38.8	-39.1	**-32.5**
	0–20 mm + PVC (FTIR) + b&g PVC + b&g Other	c	0.92	0.76	1.58	0.81	0.53	**0.92**	0.04	0.03	0.07	0.03	0.02	**0.04**
		Δc [%]	-42.7	-40.9	-2.0	-37.4	-49.8	**-34.6**	-49.4	-51.6	-11.4	-43.1	-56.9	**-42.5**
	PVC (NIR) + b&g PVC + b&g Other	c	1.87	1.42	1.88	1.45	1.17	**1.56**	0.09	0.06	0.09	0.07	0.06	**0.07**
		Δc [%]	16.9	10.0	16.1	12.0	10.1	13.0	16.7	9.3	15.2	11.0	11.6	12.7
	0–5 mm + PVC (NIR) + b&g PVC + b&g Other	c	1.39	1.12	1.59	1.01	0.83	**1.19**	0.06	0.04	0.07	0.04	0.04	**0.05**
		Δc [%]	-13.6	-13.5	-1.7	-22.2	-21.7	**-14.5**	-21.2	-24.4	-9.1	-28.0	-29.6	**-22.5**
	0–10 mm + PVC (NIR) + b&g PVC + b&g Other	c	1.19	1.01	1.56	0.88	0.76	**1.08**	0.05	0.04	0.07	0.04	0.03	**0.05**
		Δc [%]	-25.7	-21.9	-3.3	-31.8	-28.6	**-22.2**	-32.9	-34.6	-11.8	-37.3	-37.0	**-30.7**
	0–20 mm + PVC (NIR) + b&g PVC + b&g Other	c	0.98	0.77	1.60	0.83	0.54	**0.94**	0.04	0.03	0.07	0.03	0.02	**0.04**
		Δc [%]	-38.8	-40.3	-1.0	-35.8	-49.5	**-33.1**	-46.0	-51.2	-10.5	-41.6	-56.5	**-41.2**
	b&g Other + b&g PVC	c	1.77	1.40	1.85	1.39	1.12	**1.51**	0.08	0.06	0.09	0.06	0.06	**0.07**
		Δc [%]	10.5	8.0	14.6	7.6	5.0	9.1	9.5	7.2	13.5	6.7	4.9	8.4
	0–5 mm + b&g Other + b&g PVC	c	1.30	1.09	1.57	0.97	0.80	**1.15**	0.06	0.04	0.07	0.04	0.04	**0.05**
		Δc [%]	-18.8	-15.4	-3.0	-25.4	-24.8	**-17.5**	-26.1	-25.7	-10.3	-30.6	-32.7	**-25.1**
	0–10 mm + b&g Other + b&g PVC	c	1.12	0.99	1.54	0.85	0.73	**1.05**	0.05	0.04	0.07	0.04	0.03	**0.04**
		Δc [%]	-30.3	-23.8	-4.6	-34.5	-31.1	**-24.9**	-37.1	-35.8	-12.9	-39.5	-39.4	**-33.0**
	0–20 mm + b&g Other + b&g PVC	c	0.91	0.75	1.58	0.80	0.53	**0.91**	0.04	0.03	0.07	0.03	0.02	**0.04**
		Δc [%]	-43.1	-41.7	-2.5	-38.5	-50.1	**-35.2**	-49.7	-52.0	-11.8	-43.7	-57.0	**-42.8**

B.4. Al

Table B.4: Relative concentration change (Δc, in %) of Al caused by the removal of different material or particle size fractions referring to mg/kg and mg/MJ, both calculated for dry mass without hard impurities

	Removed fractions	Conc. after removal	mg/kg$_{DM}$ S01	S02	S03	S04	S05	Avr	mg/MJ S01	S02	S03	S04	S05	Avr
Single process steps	0–5 mm	c	5854	4448	3430	6470	9221	**5885**	253	180	154	278	428	**259**
		Δc [%]	-15.5	-28.2	-22.2	-15.9	-14.5	**-19.3**	-21.5	-35.6	-26.6	-20.7	-22.8	**-25.4**
	0–10 mm	c	5903	4262	3322	6485	9073	**5809**	253	166	148	277	415	**252**
		Δc [%]	-14.8	-31.2	-24.7	-15.7	-15.9	**-20.4**	-21.4	-40.5	-29.7	-20.9	-25.3	**-27.5**
	0–20 mm	c	6215	4409	3322	6614	8925	**5897**	262	169	147	280	401	**252**
		Δc [%]	-10.3	-28.8	-24.7	-14.0	-17.2	**-19.0**	-18.5	-39.4	-30.1	-20.0	-27.8	**-27.1**
	PET (NIR)	c	7302	6506	4611	8247	11426	**7618**	343	292	218	376	599	**366**
		Δc [%]	5.4	5.1	4.6	7.2	5.9	**5.6**	6.7	4.5	3.9	7.4	7.8	**6.1**
	PVC (NIR)	c	6845	6269	4429	7860	10672	**7215**	320	283	211	357	557	**346**
		Δc [%]	-1.2	1.3	0.4	2.1	-1.0	**0.3**	-0.5	1.2	0.6	2.1	0.3	**0.7**
	b&g	c	6650	6225	4659	8025	9498	**7012**	318	284	224	371	511	**342**
		Δc [%]	-4.0	0.6	5.6	4.3	-11.9	**-1.1**	-1.2	1.5	6.7	6.1	-7.9	**1.1**
	PET + PVC (NIR)	c	7236	6597	4637	8461	11356	**7657**	343	296	220	385	605	**370**
		Δc [%]	4.5	6.6	5.2	10.0	5.3	**6.3**	6.6	5.9	4.6	10.1	9.0	**7.2**
Combinations of Screening and state-of-the-art NIR sorting or manual removal of black materials	0–5 mm + PET (NIR)	c	6157	4659	3510	6937	9744	**6201**	267	185	155	296	455	**272**
		Δc [%]	-11.1	-24.7	-20.4	-9.8	-9.6	**-15.2**	-17.1	-33.7	-26.0	-15.4	-18.1	**-22.1**
	0–10 mm + PET (NIR)	c	6230	4479	3388	6972	9597	**6133**	268	171	148	295	440	**264**
		Δc [%]	-10.1	-27.6	-23.2	-9.4	-11.0	**-16.3**	-16.8	-38.8	-29.5	-15.5	-20.8	**-24.3**
	0–20 mm + PET (NIR)	c	6654	4671	3393	7155	9467	**6268**	281	175	147	301	425	**266**
		Δc [%]	-3.9	-24.5	-23.1	-7.0	-12.2	**-14.2**	-12.6	-37.5	-29.9	-14.1	-23.5	**-23.5**
	0–5 mm + PVC (NIR)	c	5685	4496	3431	6593	8946	**5830**	246	181	154	282	418	**256**
		Δc [%]	-17.9	-27.4	-22.2	-14.3	-17.0	**-19.8**	-23.6	-35.1	-26.6	-19.5	-24.7	**-25.9**
	0–10 mm + PVC (NIR)	c	5728	4311	3321	6613	8771	**5749**	246	168	148	281	403	**249**
		Δc [%]	-17.3	-30.4	-24.7	-14.1	-18.7	**-21.0**	-23.6	-40.0	-29.7	-19.7	-27.5	**-28.1**
	0–20 mm + PVC (NIR)	c	6036	4468	3321	6758	8584	**5834**	255	171	147	285	386	**249**
		Δc [%]	-12.9	-27.8	-24.7	-12.2	-20.4	**-19.6**	-20.7	-38.9	-30.1	-18.6	-30.4	**-27.8**
	0–5 mm + PET (NIR) + PVC (NIR)	c	5988	4719	3513	7105	9480	**6161**	260	187	155	302	445	**270**
		Δc [%]	-13.6	-23.8	-20.3	-7.7	-12.1	**-15.5**	-19.2	-33.1	-26.0	-13.7	-19.8	**-22.4**
	0–10 mm + PET (NIR) + PVC (NIR)	c	6057	4542	3389	7149	9302	**6088**	261	173	148	301	428	**262**
		Δc [%]	-12.6	-26.6	-23.2	-7.1	-13.7	**-16.6**	-18.9	-38.3	-29.5	-13.8	-22.9	**-24.7**
	0–20 mm + PET (NIR) + PVC (NIR)	c	6488	4749	3393	7356	9129	**6223**	274	176	147	307	410	**263**
		Δc [%]	-6.3	-23.3	-23.1	-4.4	-15.4	**-14.5**	-14.7	-36.9	-30.0	-12.2	-26.1	**-24.0**
	0–5 mm + b&g	c	5284	4212	3483	6666	7483	**5426**	232	169	156	289	359	**241**
		Δc [%]	-23.7	-32.0	-21.0	-13.4	-30.6	**-24.1**	-28.0	-39.4	-25.7	-17.5	-35.3	**-29.2**
	0–10 mm + b&g	c	5309	3959	3351	6690	7229	**5308**	231	153	148	288	341	**232**
		Δc [%]	-23.4	-36.0	-24.0	-13.0	-33.0	**-25.9**	-28.3	-45.4	-29.4	-17.7	-38.5	**-31.8**
	0–20 mm + b&g	c	5588	4098	3353	6856	6909	**5361**	239	155	147	293	320	**231**
		Δc [%]	-19.3	-33.8	-24.0	-10.9	-35.9	**-24.8**	-25.7	-44.7	-29.9	-16.3	-42.4	**-31.8**
	0–5 mm + b&g + PVC (NIR)	c	5024	4261	3486	6820	6980	**5314**	221	171	156	294	339	**236**
		Δc [%]	-27.5	-31.2	-21.0	-11.4	-35.3	**-25.2**	-31.3	-38.9	-25.6	-15.9	-39.0	**-30.1**
	0–10 mm + b&g + PVC (NIR)	c	5033	4007	3350	6852	6671	**5183**	220	154	148	294	318	**227**
		Δc [%]	-27.3	-35.3	-24.0	-10.9	-38.1	**-27.1**	-31.7	-45.1	-29.4	-16.1	-42.8	**-33.0**
	0–20 mm + b&g + PVC (NIR)	c	5281	4158	3353	7041	6261	**5219**	226	156	147	299	292	**224**
		Δc [%]	-23.8	-32.8	-24.0	-8.5	-41.9	**-26.2**	-29.6	-44.3	-30.0	-14.5	-47.4	**-33.2**
	0–5 mm + b&g + PET (NIR)	c	5573	4432	3594	7243	7790	**5727**	246	175	158	312	378	**254**
		Δc [%]	-19.5	-28.4	-18.5	-5.9	-27.8	**-20.0**	-23.5	-37.6	-24.8	-10.7	-31.9	**-25.7**
	0–10 mm + b&g + PET (NIR)	c	5624	4179	3442	7298	7507	**5610**	246	157	149	312	357	**244**
		Δc [%]	-18.8	-32.5	-21.9	-5.2	-30.4	**-21.8**	-23.5	-44.0	-29.1	-10.7	-35.6	**-28.6**
	0–20 mm + b&g + PET (NIR)	c	6044	4373	3452	7543	7148	**5712**	260	159	148	320	333	**244**
		Δc [%]	-12.7	-29.4	-21.7	-2.0	-33.7	**-19.9**	-19.3	-43.0	-29.7	-8.7	-40.1	**-28.1**
	0–5 mm + b&g + PET (NIR) + PVC (NIR)	c	5296	4496	3601	7462	7227	**5616**	235	176	158	320	356	**249**
		Δc [%]	-23.5	-27.4	-18.3	-3.0	-33.0	**-21.1**	-26.9	-37.0	-24.7	-8.5	-35.9	**-26.6**
	0–10 mm + b&g + PET (NIR) + PVC (NIR)	c	5329	4243	3445	7532	6869	**5484**	234	158	149	320	331	**238**
		Δc [%]	-23.1	-31.5	-21.9	-2.1	-36.3	**-23.0**	-27.2	-43.6	-29.1	-8.4	-40.4	**-29.7**
	0–20 mm + b&g + PET (NIR) + PVC (NIR)	c	5724	4455	3455	7818	6386	**5568**	247	161	148	329	300	**237**
		Δc [%]	-17.4	-28.0	-21.6	1.6	-40.8	**-21.2**	-23.2	-42.5	-29.7	-6.0	-46.0	**-29.5**

More targeted removal	PVC (FTIR) + b&g PVC	c	6978	6244	4430	7808	10847	**7261**	324	282	211	354	558	**346**
		Δc [%]	0.7	0.9	0.5	1.5	0.6	0.8	0.8	0.7	0.6	1.1	0.5	0.7
	0–5 mm + PVC (FTIR) + b&g PVC	c	5903	4486	3442	6563	9278	**5934**	255	181	155	280	430	**260**
		Δc [%]	-14.8	-27.5	-21.9	-14.7	-14.0	**-18.6**	-20.8	-35.3	-26.3	-20.0	-22.5	**-25.0**
	0–10 mm + PVC (FTIR) + b&g PVC	c	5955	4301	3333	6581	9131	**5860**	255	167	148	279	417	**253**
		Δc [%]	-14.0	-30.5	-24.4	-14.5	-15.3	**-19.8**	-20.7	-40.1	-29.4	-20.2	-24.9	**-27.1**
	0–20 mm + PVC (FTIR) + b&g PVC	c	6279	4455	3334	6721	8985	**5955**	265	170	147	283	403	**254**
		Δc [%]	-9.3	-28.0	-24.4	-12.7	-16.7	**-18.2**	-17.7	-39.0	-29.8	-19.2	-27.5	**-26.6**
	PVC (NIR) + b&g PVC	c	6867	6270	4437	7869	10675	**7223**	321	283	212	357	557	**346**
		Δc [%]	-0.9	1.3	0.6	2.3	-1.0	0.5	-0.2	1.2	0.8	2.1	0.3	0.9
	0–5 mm + PVC (NIR) + b&g PVC	c	5705	4495	3437	6595	8949	**5836**	247	181	154	282	418	**256**
		Δc [%]	-17.6	-27.4	-22.1	-14.3	-17.0	**-19.7**	-23.3	-35.2	-26.5	-19.5	-24.7	**-25.8**
	0–10 mm + PVC (NIR) + b&g PVC	c	5749	4310	3326	6615	8773	**5755**	247	168	148	281	403	**249**
		Δc [%]	-17.0	-30.4	-24.6	-14.0	-18.6	**-20.9**	-23.3	-40.1	-29.6	-19.8	-27.4	**-28.0**
	0–20 mm + PVC (NIR) + b&g PVC	c	6064	4467	3327	6761	8587	**5841**	256	171	147	285	386	**249**
		Δc [%]	-12.5	-27.8	-24.6	-12.1	-20.4	**-19.5**	-20.4	-39.0	-30.0	-18.7	-30.4	**-27.7**
	PET (FTIR) + Textiles + b&g PET	c	7242	6358	4598	8071	11417	**7537**	337	286	219	366	592	**360**
		Δc [%]	4.5	2.7	4.3	4.9	5.9	4.5	4.8	2.2	4.2	4.7	6.7	4.5
	0–5 mm + PET (FTIR) + Textiles + b&g PET	c	6118	4568	3566	6801	9805	**6172**	263	183	159	290	455	**270**
		Δc [%]	-11.7	-26.2	-19.1	-11.6	-9.1	**-15.5**	-18.3	-34.6	-24.1	-17.1	-18.1	**-22.4**
	0–10 mm + PET (FTIR) + Textiles + b&g PET	c	6187	4387	3455	6829	9668	**6105**	263	169	153	289	441	**263**
		Δc [%]	-10.7	-29.1	-21.7	-11.2	-10.4	**-16.6**	-18.1	-39.5	-27.3	-17.3	-20.6	**-24.6**
	0–20 mm + PET (FTIR) + Textiles + b&g PET	c	6589	4557	3463	6992	9549	**6230**	276	173	152	294	426	**264**
		Δc [%]	-4.9	-26.4	-21.5	-9.1	-11.5	**-14.7**	-14.3	-38.3	-27.6	-16.1	-23.2	**-23.9**
	b&g Other	c	6354	6125	4630	7834	9161	**6821**	292	275	218	354	471	**322**
		Δc [%]	-8.3	-1.1	5.0	1.8	-15.1	**-3.5**	-9.1	-1.7	4.0	1.1	-15.1	**-4.2**
	0–5 mm + b&g Other	c	5029	4153	3490	6508	7205	**5277**	213	165	154	275	332	**228**
		Δc [%]	-27.4	-32.9	-20.9	-15.4	-33.2	**-26.0**	-33.9	-41.1	-26.9	-21.3	-40.2	**-32.7**
	0–10 mm + b&g Other	c	5036	3901	3363	6526	6955	**5156**	211	148	146	274	315	**219**
		Δc [%]	-27.3	-37.0	-23.7	-15.2	-35.5	**-27.7**	-34.4	-46.9	-30.4	-21.6	-43.3	**-35.3**
	0–20 mm + b&g Other	c	5241	4027	3366	6672	6634	**5188**	215	150	145	278	294	**216**
		Δc [%]	-24.3	-34.9	-23.7	-13.3	-38.5	**-26.9**	-33.1	-46.4	-31.0	-20.5	-47.0	**-35.6**
	PVC (FTIR) + b&g PVC + b&g Other	c	6407	6183	4656	7961	9213	**6884**	295	277	220	358	473	**325**
		Δc [%]	-7.5	-0.1	5.6	3.5	-14.6	**-2.6**	-8.3	-0.9	4.7	2.3	-14.7	**-3.4**
	0–5 mm + PVC (FTIR) + b&g PVC + b&g Other	c	5075	4190	3505	6611	7246	**5326**	215	166	154	278	333	**229**
		Δc [%]	-26.7	-32.3	-20.5	-14.1	-32.8	**-25.3**	-33.3	-40.8	-26.5	-20.5	-40.0	**-32.2**
	0–10 mm + PVC (FTIR) + b&g PVC + b&g Other	c	5085	3939	3377	6634	6994	**5206**	213	149	147	277	316	**220**
		Δc [%]	-26.6	-36.4	-23.4	-13.8	-35.1	**-27.1**	-33.8	-46.7	-30.1	-20.8	-43.1	**-34.9**
	0–20 mm + PVC (FTIR) + b&g PVC + b&g Other	c	5302	4072	3381	6793	6673	**5244**	217	151	146	281	295	**218**
		Δc [%]	-23.5	-34.2	-23.3	-11.7	-38.1	**-26.2**	-32.4	-46.1	-30.6	-19.7	-46.8	**-35.1**
	PVC (NIR) + b&g PVC + b&g Other	c	6246	6210	4667	8033	8907	**6812**	290	279	220	362	465	**323**
		Δc [%]	-9.8	0.3	5.8	4.4	-17.4	**-3.3**	-10.0	-0.4	5.0	3.4	-16.3	**-3.7**
	0–5 mm + PVC (NIR) + b&g PVC + b&g Other	c	4786	4197	3500	6648	6708	**5168**	203	166	154	280	310	**223**
		Δc [%]	-30.9	-32.2	-20.6	-13.6	-37.8	**-27.0**	-37.0	-40.7	-26.7	-20.0	-44.1	**-33.7**
	0–10 mm + PVC (NIR) + b&g PVC + b&g Other	c	4779	3943	3370	6673	6406	**5034**	200	149	146	279	291	**213**
		Δc [%]	-31.0	-36.3	-23.6	-13.3	-40.6	**-29.0**	-37.7	-46.7	-30.3	-20.4	-47.6	**-36.5**
	0–20 mm + PVC (NIR) + b&g PVC + b&g Other	c	4952	4079	3373	6840	6003	**5050**	203	151	145	283	266	**210**
		Δc [%]	-28.5	-34.1	-23.5	-11.1	-44.3	**-28.3**	-37.0	-46.1	-30.9	-19.2	-52.0	**-37.0**
	b&g Other + b&g PVC	c	6376	6126	4639	7843	9163	**6829**	294	275	219	354	471	**322**
		Δc [%]	-8.0	-1.0	5.2	1.9	-15.0	**-3.4**	-8.7	-1.7	4.2	1.1	-15.1	**-4.0**
	0–5 mm + b&g Other + b&g PVC	c	5047	4151	3497	6509	7207	**5282**	214	165	154	275	332	**228**
		Δc [%]	-27.1	-32.9	-20.7	-15.4	-33.2	**-25.9**	-33.6	-41.1	-26.7	-21.3	-40.2	**-32.6**
	0–10 mm + b&g Other + b&g PVC	c	5056	3899	3370	6527	6956	**5162**	212	148	146	274	315	**219**
		Δc [%]	-27.0	-37.0	-23.6	-15.2	-35.5	**-27.7**	-34.1	-47.0	-30.3	-21.7	-43.3	**-35.3**
	0–20 mm + b&g Other + b&g PVC	c	5265	4025	3373	6675	6636	**5195**	216	150	145	278	294	**217**
		Δc [%]	-24.0	-35.0	-23.5	-13.3	-38.5	**-26.8**	-32.8	-46.4	-30.8	-20.6	-47.0	**-35.5**

B.5. As

Table B.5: Relative concentration change (Δc, in %) of As caused by the removal of different material or particle size fractions referring to mg/kg and mg/MJ, both calculated for dry mass without hard impurities

	Removed fractions	Conc. after removal	mg/kg$_{DM}$ S01	S02	S03	S04	S05	Avr	mg/MJ S01	S02	S03	S04	S05	Avr
Single process steps	0–5 mm	c	6.6	3.0	2.9	2.6	3.5	**3.7**	0.28	0.12	0.13	0.11	0.16	**0.16**
		Δc [%]	2.3	-14.4	-32.5	-17.2	-20.2	**-16.4**	-5.0	-23.3	-36.4	-21.9	-28.0	**-22.9**
	0–10 mm	c	6.8	3.1	2.8	2.5	3.3	**3.7**	0.29	0.12	0.12	0.11	0.15	**0.16**
		Δc [%]	5.2	-12.7	-33.9	-18.9	-24.9	**-17.0**	-3.0	-24.5	-38.3	-23.9	-33.3	**-24.6**
	0–20 mm	c	7.4	3.1	2.7	2.5	3.0	**3.8**	0.31	0.12	0.12	0.11	0.14	**0.16**
		Δc [%]	15.1	-11.0	-35.9	-18.9	-30.2	**-16.2**	4.6	-24.2	-40.5	-24.5	-39.1	**-24.7**
	PET (NIR)	c	6.9	3.6	4.5	3.2	4.3	**4.5**	0.32	0.16	0.21	0.15	0.23	**0.21**
		Δc [%]	6.7	2.4	5.4	2.3	-1.1	**3.1**	8.0	1.8	4.7	2.5	0.6	**3.5**
	PVC (NIR)	c	6.5	3.5	4.2	3.1	4.5	**4.4**	0.30	0.16	0.20	0.14	0.23	**0.21**
		Δc [%]	0.8	0.5	-1.7	0.9	2.1	**0.5**	1.5	0.5	-1.6	0.8	3.5	**1.0**
	b&g	c	7.2	3.2	4.5	3.2	4.4	**4.5**	0.34	0.15	0.22	0.15	0.24	**0.22**
		Δc [%]	11.5	-9.7	6.1	1.7	2.1	**2.3**	14.8	-8.9	7.2	3.5	6.8	**4.7**
	PET + PVC (NIR)	c	7.0	3.6	4.4	3.2	4.4	**4.5**	0.33	0.16	0.21	0.15	0.24	**0.22**
		Δc [%]	8.1	3.1	3.6	3.4	1.2	**3.9**	10.3	2.4	3.0	3.5	4.8	**4.8**
Combinations of Screening and state-of-the-art NIR sorting or manual removal of black materials	0–5 mm + PET (NIR)	c	7.1	3.1	2.9	2.6	3.3	**3.8**	0.31	0.12	0.13	0.11	0.15	**0.16**
		Δc [%]	10.5	-12.9	-31.3	-16.9	-24.6	**-15.0**	3.0	-23.3	-36.2	-22.0	-31.6	**-22.0**
	0–10 mm + PET (NIR)	c	7.4	3.1	2.8	2.5	3.0	**3.8**	0.32	0.12	0.12	0.11	0.14	**0.16**
		Δc [%]	14.3	-10.8	-32.8	-18.8	-30.2	**-15.7**	5.7	-24.5	-38.3	-24.3	-37.9	**-23.9**
	0–20 mm + PET (NIR)	c	8.2	3.2	2.8	2.5	2.8	**3.9**	0.35	0.12	0.12	0.11	0.12	**0.16**
		Δc [%]	27.5	-8.6	-35.1	-18.7	-36.8	**-14.4**	16.0	-24.3	-40.9	-24.9	-45.0	**-23.8**
	0–5 mm + PVC (NIR)	c	6.7	3.0	2.8	2.6	3.5	**3.7**	0.29	0.12	0.12	0.11	0.16	**0.16**
		Δc [%]	3.4	-14.1	-35.0	-17.1	-19.5	**-16.5**	-3.7	-23.3	-38.7	-22.1	-27.0	**-23.0**
	0–10 mm + PVC (NIR)	c	6.9	3.1	2.7	2.5	3.3	**3.7**	0.29	0.12	0.12	0.11	0.15	**0.16**
		Δc [%]	6.6	-12.3	-36.5	-18.9	-24.7	**-17.1**	-1.5	-24.5	-40.7	-24.2	-32.8	**-24.8**
	0–20 mm + PVC (NIR)	c	7.6	3.2	2.6	2.5	3.0	**3.8**	0.32	0.12	0.11	0.11	0.14	**0.16**
		Δc [%]	17.6	-10.5	-38.7	-18.8	-30.5	**-16.2**	6.9	-24.3	-43.1	-24.8	-39.2	**-24.9**
	0–5 mm + PET (NIR) + PVC (NIR)	c	7.2	3.1	2.8	2.6	3.3	**3.8**	0.31	0.12	0.12	0.11	0.15	**0.17**
		Δc [%]	12.4	-12.5	-34.1	-16.7	-24.3	**-15.1**	5.1	-23.3	-38.8	-22.2	-30.9	**-22.0**
	0–10 mm + PET (NIR) + PVC (NIR)	c	7.5	3.2	2.7	2.5	3.0	**3.8**	0.32	0.12	0.12	0.11	0.14	**0.16**
		Δc [%]	16.6	-10.3	-35.8	-18.7	-30.5	**-15.7**	8.1	-24.6	-41.1	-24.6	-37.9	**-24.0**
	0–20 mm + PET (NIR) + PVC (NIR)	c	8.5	3.2	2.6	2.5	2.7	**3.9**	0.36	0.12	0.11	0.11	0.12	**0.16**
		Δc [%]	31.6	-8.0	-38.3	-18.6	-38.0	**-14.3**	19.9	-24.3	-43.9	-25.3	-45.9	**-23.9**
	0–5 mm + b&g	c	7.5	2.5	2.8	2.6	3.5	**3.8**	0.33	0.10	0.13	0.11	0.17	**0.17**
		Δc [%]	16.5	-28.9	-33.2	-17.9	-20.6	**-16.8**	10.0	-36.7	-37.1	-21.7	-25.9	**-22.3**
	0–10 mm + b&g	c	7.8	2.5	2.8	2.5	3.2	**3.8**	0.34	0.10	0.12	0.11	0.15	**0.16**
		Δc [%]	21.1	-28.9	-34.9	-19.8	-26.0	**-17.7**	13.3	-39.3	-39.5	-24.1	-32.1	**-24.3**
	0–20 mm + b&g	c	8.8	2.5	2.7	2.5	3.0	**3.9**	0.38	0.09	0.12	0.11	0.14	**0.17**
		Δc [%]	37.0	-28.9	-37.5	-19.8	-32.3	**-16.3**	26.2	-40.6	-42.3	-24.7	-39.1	**-24.1**
	0–5 mm + b&g + PVC (NIR)	c	7.7	2.5	2.7	2.6	3.5	**3.8**	0.34	0.10	0.12	0.11	0.17	**0.17**
		Δc [%]	19.1	-29.1	-36.2	-17.7	-19.9	**-16.8**	12.9	-37.1	-40.0	-21.9	-24.5	**-22.1**
	0–10 mm + b&g + PVC (NIR)	c	8.0	2.5	2.6	2.5	3.2	**3.8**	0.35	0.10	0.12	0.11	0.15	**0.16**
		Δc [%]	24.3	-29.1	-38.2	-19.8	-25.9	**-17.7**	16.7	-39.8	-42.5	-24.4	-31.4	**-24.3**
	0–20 mm + b&g + PVC (NIR)	c	9.2	2.5	2.5	2.5	2.9	**3.9**	0.39	0.09	0.11	0.11	0.14	**0.17**
		Δc [%]	42.8	-29.1	-41.0	-19.8	-32.9	**-16.0**	31.9	-41.1	-45.7	-25.1	-39.2	**-23.9**
	0–5 mm + b&g + PET (NIR)	c	8.3	2.5	2.9	2.6	3.2	**3.9**	0.37	0.10	0.13	0.11	0.16	**0.17**
		Δc [%]	29.2	-28.9	-31.7	-17.6	-25.8	**-15.0**	22.8	-38.0	-37.0	-21.8	-30.0	**-20.8**
	0–10 mm + b&g + PET (NIR)	c	8.7	2.5	2.8	2.5	2.9	**3.9**	0.38	0.09	0.12	0.11	0.14	**0.17**
		Δc [%]	35.4	-28.9	-33.7	-19.8	-32.5	**-15.9**	27.6	-41.0	-39.7	-24.5	-37.6	**-23.0**
	0–20 mm + b&g + PET (NIR)	c	10.2	2.5	2.7	2.5	2.6	**4.1**	0.44	0.09	0.11	0.11	0.12	**0.17**
		Δc [%]	58.5	-28.9	-36.7	-19.8	-40.6	**-13.5**	46.7	-42.6	-43.1	-25.3	-46.3	**-22.1**
	0–5 mm + b&g + PET (NIR) + PVC (NIR)	c	8.6	2.5	2.7	2.6	3.2	**3.9**	0.38	0.10	0.12	0.11	0.16	**0.17**
		Δc [%]	33.5	-29.1	-35.3	-17.4	-25.6	**-14.8**	27.7	-38.4	-40.4	-22.1	-28.9	**-20.4**
	0–10 mm + b&g + PET (NIR) + PVC (NIR)	c	9.1	2.5	2.6	2.5	2.9	**3.9**	0.40	0.09	0.11	0.11	0.14	**0.17**
		Δc [%]	40.9	-29.1	-37.6	-19.8	-33.2	**-15.8**	33.4	-41.6	-43.4	-24.9	-37.5	**-22.8**
	0–20 mm + b&g + PET (NIR) + PVC (NIR)	c	10.9	2.5	2.5	2.5	2.5	**4.2**	0.47	0.09	0.11	0.11	0.12	**0.18**
		Δc [%]	68.8	-29.1	-41.0	-19.8	-42.6	**-12.8**	56.7	-43.3	-47.1	-25.8	-47.7	**-21.4**

More targeted removal	PVC (FTIR) + b&g PVC	c	6.3	3.5	4.2	3.1	4.3	**4.3**	0.29	0.16	0.20	0.14	0.22	**0.20**
		Δc [%]	-2.1	0.3	-0.6	-0.3	-0.8	**-0.7**	-2.0	0.1	-0.5	-0.6	-0.8	**-0.8**
	0–5 mm + PVC (FTIR) + b&g PVC	c	6.4	3.0	2.8	2.6	3.4	**3.7**	0.28	0.12	0.13	0.11	0.16	**0.16**
		Δc [%]	-0.1	-14.3	-33.5	-18.1	-21.3	**-17.5**	-7.2	-23.5	-37.3	-23.1	-29.1	**-24.0**
	0–10 mm + PVC (FTIR) + b&g PVC	c	6.6	3.1	2.8	2.5	3.2	**3.6**	0.28	0.12	0.12	0.11	0.15	**0.16**
		Δc [%]	2.7	-12.5	-35.0	-19.8	-26.1	**-18.1**	-5.3	-24.6	-39.2	-25.2	-34.4	**-25.8**
	0–20 mm + PVC (FTIR) + b&g PVC	c	7.2	3.1	2.7	2.5	3.0	**3.7**	0.31	0.12	0.12	0.11	0.13	**0.16**
		Δc [%]	12.3	-10.8	-37.0	-19.8	-31.5	**-17.4**	2.0	-24.4	-41.5	-25.8	-40.4	**-26.0**
	PVC (NIR) + b&g PVC	c	6.5	3.5	4.2	3.1	4.5	**4.4**	0.30	0.16	0.20	0.14	0.23	**0.21**
		Δc [%]	1.1	0.6	-1.6	0.2	2.2	**0.5**	1.8	0.5	-1.4	0.1	3.5	**0.9**
	0–5 mm + PVC (NIR) + b&g PVC	c	6.7	3.0	2.8	2.6	3.5	**3.7**	0.29	0.12	0.12	0.11	0.16	**0.16**
		Δc [%]	3.7	-14.1	-35.0	-18.0	-19.5	**-16.6**	-3.5	-23.3	-38.7	-23.0	-27.0	**-23.1**
	0–10 mm + PVC (NIR) + b&g PVC	c	6.9	3.1	2.7	2.5	3.3	**3.7**	0.30	0.12	0.12	0.11	0.15	**0.16**
		Δc [%]	6.9	-12.3	-36.5	-19.8	-24.6	**-17.3**	-1.2	-24.5	-40.7	-25.2	-32.8	**-24.9**
	0–20 mm + PVC (NIR) + b&g PVC	c	7.6	3.2	2.6	2.5	3.0	**3.8**	0.32	0.12	0.11	0.11	0.14	**0.16**
		Δc [%]	18.0	-10.5	-38.7	-19.8	-30.5	**-16.3**	7.3	-24.3	-43.1	-25.8	-39.2	**-25.0**
	PET (FTIR) + Textiles + b&g PET	c	6.8	3.6	4.4	3.2	4.5	**4.5**	0.32	0.16	0.21	0.14	0.23	**0.21**
		Δc [%]	5.1	1.2	2.7	1.3	3.7	**2.8**	5.3	0.7	2.6	1.2	4.5	**2.9**
	0–5 mm + PET (FTIR) + Textiles + b&g PET	c	7.0	3.0	2.9	2.6	3.6	**3.8**	0.30	0.12	0.13	0.11	0.17	**0.17**
		Δc [%]	8.5	-13.7	-31.9	-17.1	-17.9	**-14.4**	0.3	-23.5	-36.1	-22.2	-26.0	**-21.5**
	0–10 mm + PET (FTIR) + Textiles + b&g PET	c	7.2	3.1	2.8	2.5	3.4	**3.8**	0.31	0.12	0.12	0.11	0.15	**0.16**
		Δc [%]	12.1	-11.8	-33.4	-18.8	-23.0	**-15.0**	2.8	-24.7	-38.1	-24.4	-31.8	**-23.3**
	0–20 mm + PET (FTIR) + Textiles + b&g PET	c	8.0	3.2	2.7	2.5	3.1	**3.9**	0.34	0.12	0.12	0.11	0.14	**0.16**
		Δc [%]	24.4	-9.9	-35.5	-18.8	-28.8	**-13.7**	12.1	-24.4	-40.5	-25.0	-38.2	**-23.2**
	b&g Other	c	6.9	3.2	4.5	3.2	4.4	**4.4**	0.32	0.14	0.21	0.14	0.22	**0.21**
		Δc [%]	7.3	-10.2	6.9	1.7	0.1	**1.2**	6.4	-10.8	5.9	1.0	0.0	**0.5**
	0–5 mm + b&g Other	c	7.2	2.5	2.9	2.6	3.4	**3.7**	0.30	0.10	0.13	0.11	0.16	**0.16**
		Δc [%]	11.2	-28.9	-30.9	-17.0	-21.6	**-17.5**	1.3	-37.6	-36.2	-22.7	-29.9	**-25.0**
	0–10 mm + b&g Other	c	7.4	2.5	2.9	2.5	3.2	**3.7**	0.31	0.10	0.12	0.11	0.14	**0.16**
		Δc [%]	15.2	-28.9	-32.5	-18.8	-26.8	**-18.4**	3.9	-40.2	-38.4	-24.9	-35.6	**-27.0**
	0–20 mm + b&g Other	c	8.3	2.5	2.8	2.5	2.9	**3.8**	0.34	0.09	0.12	0.11	0.13	**0.16**
		Δc [%]	28.7	-28.9	-34.8	-18.8	-32.7	**-17.3**	13.7	-41.4	-41.0	-25.6	-42.0	**-27.3**
	PVC (FTIR) + b&g PVC + b&g Other	c	6.8	3.2	4.5	3.2	4.3	**4.4**	0.31	0.14	0.21	0.14	0.22	**0.21**
		Δc [%]	5.1	-10.1	6.3	1.5	-0.7	**0.4**	4.2	-10.8	5.4	0.3	-0.9	**-0.4**
	0–5 mm + PVC (FTIR) + b&g PVC + b&g Other	c	7.0	2.5	2.9	2.6	3.4	**3.7**	0.30	0.10	0.13	0.11	0.15	**0.16**
		Δc [%]	8.6	-29.1	-32.1	-17.9	-22.8	**-18.7**	-1.1	-38.0	-37.2	-24.0	-31.1	**-26.3**
	0–10 mm + PVC (FTIR) + b&g PVC + b&g Other	c	7.2	2.5	2.8	2.5	3.1	**3.6**	0.30	0.09	0.12	0.10	0.14	**0.15**
		Δc [%]	12.4	-29.1	-33.8	-19.8	-28.1	**-19.7**	1.4	-40.6	-39.5	-26.3	-36.8	**-28.4**
	0–20 mm + PVC (FTIR) + b&g PVC + b&g Other	c	8.1	2.5	2.7	2.5	2.9	**3.7**	0.33	0.09	0.12	0.10	0.13	**0.15**
		Δc [%]	25.6	-29.1	-36.2	-19.8	-34.1	**-18.7**	10.9	-41.9	-42.3	-27.1	-43.4	**-28.7**
	PVC (NIR) + b&g PVC + b&g Other	c	7.0	3.2	4.5	3.2	4.5	**4.5**	0.33	0.14	0.21	0.14	0.23	**0.21**
		Δc [%]	9.0	-9.8	5.3	2.1	2.4	**1.8**	8.8	-10.5	4.4	1.1	3.8	**1.5**
	0–5 mm + PVC (NIR) + b&g PVC + b&g Other	c	7.3	2.5	2.8	2.6	3.4	**3.7**	0.31	0.10	0.12	0.11	0.16	**0.16**
		Δc [%]	13.6	-29.1	-33.8	-17.8	-21.1	**-17.6**	3.6	-38.0	-38.9	-24.0	-29.0	**-25.3**
	0–10 mm + PVC (NIR) + b&g PVC + b&g Other	c	7.6	2.5	2.7	2.5	3.2	**3.7**	0.32	0.09	0.12	0.10	0.15	**0.16**
		Δc [%]	18.0	-29.1	-35.6	-19.8	-26.7	**-18.6**	6.5	-40.6	-41.2	-26.3	-35.3	**-27.4**
	0–20 mm + PVC (NIR) + b&g PVC + b&g Other	c	8.6	2.5	2.6	2.5	2.9	**3.8**	0.35	0.09	0.11	0.10	0.13	**0.16**
		Δc [%]	33.6	-29.1	-38.2	-19.8	-33.3	**-17.3**	17.8	-42.0	-44.1	-27.1	-42.5	**-27.6**
	b&g Other + b&g PVC	c	6.9	3.2	4.5	3.1	4.4	**4.4**	0.32	0.14	0.21	0.14	0.22	**0.21**
		Δc [%]	7.6	-10.2	7.1	1.0	0.1	**1.1**	6.7	-10.8	6.1	0.2	0.0	**0.4**
	0–5 mm + b&g Other + b&g PVC	c	7.2	2.5	2.9	2.6	3.4	**3.7**	0.30	0.10	0.13	0.11	0.16	**0.16**
		Δc [%]	11.6	-28.9	-30.9	-17.9	-21.6	**-17.6**	1.7	-37.6	-36.1	-23.7	-29.9	**-25.1**
	0–10 mm + b&g Other + b&g PVC	c	7.4	2.5	2.9	2.5	3.2	**3.7**	0.31	0.10	0.12	0.10	0.14	**0.16**
		Δc [%]	15.5	-28.9	-32.5	-19.8	-26.8	**-18.5**	4.2	-40.2	-38.4	-25.9	-35.6	**-27.2**
	0–20 mm + b&g Other + b&g PVC	c	8.3	2.5	2.8	2.5	2.9	**3.8**	0.34	0.09	0.12	0.10	0.13	**0.16**
		Δc [%]	29.2	-28.9	-34.8	-19.8	-32.7	**-17.4**	14.1	-41.4	-41.0	-26.6	-42.0	**-27.4**

B.6. Ba

Table B.6: Relative concentration change (Δc, in %) of Ba caused by the removal of different material or particle size fractions referring to mg/kg and mg/MJ, both calculated for dry mass without hard impurities

	Removed fractions	Conc. after removal	mg/kg$_{DM}$ S01	S02	S03	S04	S05	Avr	mg/MJ S01	S02	S03	S04	S05	Avr
Single process steps	0–5 mm	c	2854	308	394	325	368	**850**	123	12	18	14	17	**37**
		Δc [%]	12.6	-50.6	-25.7	-15.0	-13.7	**-18.5**	4.7	-55.8	-29.9	-19.8	-22.1	**-24.6**
	0–10 mm	c	2968	295	371	320	350	**861**	127	12	17	14	16	**37**
		Δc [%]	17.1	-52.7	-29.9	-16.3	-18.0	**-20.0**	8.0	-59.1	-34.5	-21.5	-27.1	**-26.9**
	0–20 mm	c	3300	279	327	312	317	**907**	139	11	14	13	14	**38**
		Δc [%]	30.2	-55.3	-38.4	-18.4	-25.8	**-21.5**	18.4	-62.0	-42.8	-24.0	-35.3	**-29.2**
	PET (NIR)	c	2732	655	532	403	458	**956**	128	29	25	18	24	**45**
		Δc [%]	7.9	4.9	0.5	5.3	7.3	**5.2**	9.1	4.3	-0.2	5.6	9.2	**5.6**
	PVC (NIR)	c	2661	602	430	390	439	**904**	124	27	20	18	23	**43**
		Δc [%]	5.0	-3.5	-18.9	2.0	2.9	**-2.5**	5.7	-3.6	-18.8	2.0	4.3	**-2.1**
	b&g	c	2924	661	610	387	445	**1006**	140	30	29	18	24	**48**
		Δc [%]	15.4	5.9	15.1	1.2	4.4	**8.4**	18.8	6.9	16.3	2.9	9.2	**10.8**
	PET + PVC (NIR)	c	2888	632	419	413	474	**965**	137	28	20	19	25	**46**
		Δc [%]	14.0	1.2	-21.0	7.9	11.2	**2.7**	16.3	0.6	-21.4	8.0	15.2	**3.7**
Combinations of Screening and state-of-the-art NIR sorting or manual removal of black materials	0–5 mm + PET (NIR)	c	3129	314	377	341	396	**911**	136	12	17	15	18	**40**
		Δc [%]	23.5	-49.7	-28.9	-10.9	-7.1	**-14.6**	15.2	-55.7	-34.0	-16.3	-15.8	**-21.3**
	0–10 mm + PET (NIR)	c	3275	300	350	336	376	**927**	141	11	15	14	17	**40**
		Δc [%]	29.2	-52.0	-33.9	-12.3	-11.8	**-16.1**	19.5	-59.4	-39.3	-18.2	-21.5	**-23.8**
	0–20 mm + PET (NIR)	c	3718	282	297	328	339	**993**	157	11	13	14	15	**42**
		Δc [%]	46.7	-54.8	-44.0	-14.4	-20.4	**-17.4**	33.5	-62.6	-49.0	-20.9	-30.7	**-25.9**
	0–5 mm + PVC (NIR)	c	3025	273	281	331	377	**857**	131	11	13	14	18	**37**
		Δc [%]	19.4	-56.3	-47.0	-13.4	-11.6	**-21.8**	11.2	-61.0	-50.0	-18.6	-19.8	**-27.6**
	0–10 mm + PVC (NIR)	c	3157	255	254	326	358	**870**	135	10	11	14	16	**37**
		Δc [%]	24.6	-59.2	-52.0	-14.8	-16.2	**-23.5**	15.1	-64.9	-55.2	-20.5	-25.2	**-30.1**
	0–20 mm + PVC (NIR)	c	3550	234	202	318	321	**925**	150	9	9	13	14	**39**
		Δc [%]	40.1	-62.6	-61.9	-16.9	-24.7	**-25.2**	27.4	-68.3	-64.6	-23.0	-34.2	**-32.6**
	0–5 mm + PET (NIR) + PVC (NIR)	c	3346	274	247	349	410	**925**	145	11	11	15	19	**40**
		Δc [%]	32.1	-56.0	-53.4	-8.9	-4.0	**-18.0**	23.5	-61.4	-56.7	-14.9	-12.4	**-24.4**
	0–10 mm + PET (NIR) + PVC (NIR)	c	3517	255	215	343	388	**944**	151	10	9	14	18	**41**
		Δc [%]	38.8	-59.2	-59.5	-10.3	-9.0	**-19.8**	28.7	-65.7	-62.9	-16.8	-18.6	**-27.1**
	0–20 mm + PET (NIR) + PVC (NIR)	c	4055	231	151	335	348	**1024**	171	9	7	14	16	**43**
		Δc [%]	60.1	-63.1	-71.5	-12.4	-18.4	**-21.1**	45.8	-69.6	-74.1	-19.5	-28.8	**-29.2**
	0–5 mm + b&g	c	3391	304	452	322	382	**970**	149	12	20	14	18	**43**
		Δc [%]	33.8	-51.2	-14.8	-15.9	-10.4	**-11.7**	26.3	-56.6	-19.8	-19.8	-16.4	**-17.3**
	0–10 mm + b&g	c	3565	288	427	316	362	**992**	155	11	19	14	17	**43**
		Δc [%]	40.7	-53.8	-19.5	-17.5	-15.2	**-13.0**	31.7	-60.6	-25.2	-21.9	-22.2	**-19.6**
	0–20 mm + b&g	c	4116	268	374	306	324	**1078**	176	10	16	13	15	**46**
		Δc [%]	62.5	-57.1	-29.4	-20.0	-24.0	**-13.6**	49.7	-64.1	-34.9	-24.9	-31.7	**-21.2**
	0–5 mm + b&g + PVC (NIR)	c	3650	263	314	329	394	**990**	161	11	14	14	19	**44**
		Δc [%]	44.1	-57.9	-40.8	-14.2	-7.6	**-15.3**	36.5	-62.7	-44.2	-18.5	-12.9	**-20.4**
	0–10 mm + b&g + PVC (NIR)	c	3859	240	282	322	372	**1015**	168	9	12	14	18	**44**
		Δc [%]	52.3	-61.6	-46.8	-15.8	-12.8	**-16.9**	43.1	-67.4	-50.5	-20.6	-19.3	**-23.0**
	0–20 mm + b&g + PVC (NIR)	c	4540	212	218	312	331	**1123**	195	8	10	13	15	**48**
		Δc [%]	79.2	-66.0	-58.9	-18.3	-22.5	**-17.3**	65.5	-71.8	-62.1	-23.7	-29.8	**-24.4**
	0–5 mm + b&g + PET (NIR)	c	3825	310	441	340	417	**1067**	169	12	19	15	20	**47**
		Δc [%]	51.0	-50.3	-16.9	-11.2	-2.2	**-5.9**	43.6	-56.6	-23.3	-15.8	-7.7	**-12.0**
	0–10 mm + b&g + PET (NIR)	c	4063	293	410	333	395	**1099**	178	11	18	14	19	**48**
		Δc [%]	60.4	-53.1	-22.6	-12.9	-7.4	**-7.1**	51.1	-61.1	-29.6	-18.0	-14.3	**-14.4**
	0–20 mm + b&g + PET (NIR)	c	4859	270	345	324	353	**1230**	209	10	15	14	16	**53**
		Δc [%]	91.8	-56.8	-34.9	-15.4	-17.3	**-6.5**	77.5	-65.1	-41.5	-21.2	-25.2	**-15.1**
	0–5 mm + b&g + PET (NIR) + PVC (NIR)	c	4175	264	277	349	436	**1100**	185	10	12	15	21	**49**
		Δc [%]	64.8	-57.8	-47.8	-8.9	2.2	**-9.5**	57.6	-63.4	-51.9	-14.0	-2.3	**-14.8**
	0–10 mm + b&g + PET (NIR) + PVC (NIR)	c	4468	238	236	342	412	**1139**	196	9	10	15	20	**50**
		Δc [%]	76.4	-61.9	-55.4	-10.6	-3.4	**-11.0**	67.0	-68.7	-59.5	-16.3	-9.7	**-17.4**
	0–20 mm + b&g + PET (NIR) + PVC (NIR)	c	5493	205	154	333	365	**1310**	237	7	7	14	17	**56**
		Δc [%]	116.8	-67.2	-70.9	-13.1	-14.4	**-9.7**	101.4	-73.8	-73.9	-19.6	-21.9	**-17.5**

More targeted removal	PVC (FTIR) + b&g PVC	c	2547	600	432	385	422	**877**	118	27	21	17	22	**41**
		Δc [%]	0.5	-4.0	-18.5	0.7	-1.0	**-4.5**	0.6	-4.1	-18.4	0.3	-1.0	**-4.5**
	0–5 mm + PVC (FTIR) + b&g PVC	c	2872	273	285	327	363	**824**	124	11	13	14	17	**36**
		Δc [%]	13.4	-56.3	-46.3	-14.6	-14.9	**-23.7**	5.3	-60.9	-49.3	-19.9	-23.3	**-29.6**
	0–10 mm + PVC (FTIR) + b&g PVC	c	2988	255	259	321	344	**833**	128	10	12	14	16	**36**
		Δc [%]	17.9	-59.1	-51.2	-16.0	-19.3	**-25.5**	8.7	-64.8	-54.4	-21.7	-28.4	**-32.1**
	0–20 mm + PVC (FTIR) + b&g PVC	c	3328	235	207	313	310	**879**	140	9	9	13	14	**37**
		Δc [%]	31.3	-62.4	-60.9	-18.1	-27.3	**-27.5**	19.3	-68.2	-63.7	-24.3	-36.7	**-34.7**
	PVC (NIR) + b&g PVC	c	2670	603	430	391	439	**906**	125	27	21	18	23	**43**
		Δc [%]	5.4	-3.5	-18.8	2.2	2.8	**-2.4**	6.1	-3.5	-18.7	2.0	4.2	**-2.0**
	0–5 mm + PVC (NIR) + b&g PVC	c	3037	273	281	331	377	**860**	131	11	13	14	18	**37**
		Δc [%]	19.9	-56.3	-46.9	-13.4	-11.6	**-21.7**	11.6	-61.0	-49.9	-18.7	-19.8	**-27.6**
	0–10 mm + PVC (NIR) + b&g PVC	c	3170	255	254	326	357	**872**	136	10	11	14	16	**37**
		Δc [%]	25.1	-59.2	-52.0	-14.8	-16.2	**-23.4**	15.6	-64.8	-55.2	-20.5	-25.3	**-30.0**
	0–20 mm + PVC (NIR) + b&g PVC	c	3568	234	202	318	321	**928**	151	9	9	13	14	**39**
		Δc [%]	40.8	-62.5	-61.9	-16.9	-24.7	**-25.1**	28.1	-68.3	-64.6	-23.1	-34.2	**-32.4**
	PET (FTIR) + Textiles + b&g PET	c	2693	642	539	397	453	**945**	125	29	26	18	23	**44**
		Δc [%]	6.3	2.8	1.7	3.7	6.2	**4.1**	6.5	2.3	1.7	3.5	7.0	**4.2**
	0–5 mm + PET (FTIR) + Textiles + b&g PET	c	3072	314	394	337	393	**902**	132	13	18	14	18	**39**
		Δc [%]	21.3	-49.7	-25.7	-12.0	-7.8	**-14.8**	12.1	-55.4	-30.2	-17.5	-16.9	**-21.6**
	0–10 mm + PET (FTIR) + Textiles + b&g PET	c	3210	301	370	332	374	**917**	137	12	16	14	17	**39**
		Δc [%]	26.7	-51.8	-30.2	-13.3	-12.3	**-16.2**	16.2	-58.8	-35.2	-19.3	-22.3	**-23.9**
	0–20 mm + PET (FTIR) + Textiles + b&g PET	c	3626	285	321	324	339	**979**	152	11	14	14	15	**41**
		Δc [%]	43.1	-54.4	-39.3	-15.4	-20.6	**-17.3**	29.0	-61.8	-44.1	-21.9	-31.1	**-26.0**
	b&g Other	c	2768	650	596	382	443	**968**	127	29	28	17	23	**45**
		Δc [%]	9.2	4.1	12.5	-0.2	3.9	**5.9**	8.3	3.4	11.4	-0.9	3.8	**5.2**
	0–5 mm + b&g Other	c	3175	302	441	319	383	**924**	134	12	19	14	18	**39**
		Δc [%]	25.3	-51.6	-16.7	-16.6	-10.1	**-14.0**	14.2	-57.5	-23.0	-22.4	-19.6	**-21.7**
	0–10 mm + b&g Other	c	3325	286	417	313	364	**941**	139	11	18	13	16	**40**
		Δc [%]	31.2	-54.2	-21.3	-18.2	-14.6	**-15.4**	18.4	-61.4	-28.2	-24.4	-24.9	**-24.1**
	0–20 mm + b&g Other	c	3783	266	365	304	329	**1010**	155	10	16	13	15	**42**
		Δc [%]	49.3	-57.3	-31.0	-20.6	-22.8	**-16.5**	31.9	-64.8	-37.6	-27.3	-33.5	**-26.3**
	PVC (FTIR) + b&g PVC + b&g Other	c	2785	623	482	385	439	**943**	128	28	23	17	23	**44**
		Δc [%]	9.9	-0.2	-9.1	0.6	2.9	**0.8**	9.0	-1.0	-9.8	-0.6	2.7	**0.1**
	0–5 mm + PVC (FTIR) + b&g PVC + b&g Other	c	3200	262	312	320	378	**894**	135	10	14	13	17	**38**
		Δc [%]	26.3	-58.0	-41.1	-16.3	-11.4	**-20.1**	15.0	-63.3	-45.5	-22.6	-20.9	**-27.4**
	0–10 mm + PVC (FTIR) + b&g PVC + b&g Other	c	3353	241	282	314	358	**909**	140	9	12	13	16	**38**
		Δc [%]	32.3	-61.5	-46.8	-17.9	-16.0	**-22.0**	19.3	-67.7	-51.4	-24.6	-26.3	**-30.1**
	0–20 mm + PVC (FTIR) + b&g PVC + b&g Other	c	3823	215	221	305	322	**977**	157	8	10	13	14	**40**
		Δc [%]	50.9	-65.6	-58.3	-20.4	-24.5	**-23.6**	33.2	-71.8	-62.2	-27.6	-35.1	**-32.7**
	PVC (NIR) + b&g PVC + b&g Other	c	2938	627	481	391	458	**979**	136	28	23	18	24	**46**
		Δc [%]	16.0	0.4	-9.3	2.2	7.3	**3.3**	15.8	-0.3	-10.1	1.3	8.7	**3.1**
	0–5 mm + PVC (NIR) + b&g PVC + b&g Other	c	3413	262	308	325	394	**941**	145	10	14	14	18	**40**
		Δc [%]	34.7	-58.1	-41.8	-15.0	-7.5	**-17.5**	22.8	-63.3	-46.2	-21.3	-16.9	**-25.0**
	0–10 mm + PVC (NIR) + b&g PVC + b&g Other	c	3592	240	278	319	374	**960**	151	9	12	13	17	**40**
		Δc [%]	41.8	-61.6	-47.6	-16.6	-12.3	**-19.3**	27.9	-67.8	-52.2	-23.4	-22.7	**-27.7**
	0–20 mm + PVC (NIR) + b&g PVC + b&g Other	c	4157	213	215	310	336	**1046**	170	8	9	13	15	**43**
		Δc [%]	64.1	-65.8	-59.4	-19.1	-21.3	**-20.3**	44.7	-72.0	-63.3	-26.5	-32.2	**-29.9**
	b&g Other + b&g PVC	c	2777	651	597	383	443	**970**	128	29	28	17	23	**45**
		Δc [%]	9.6	4.2	12.7	0.0	3.9	**6.1**	8.7	3.5	11.6	-0.8	3.8	**5.4**
	0–5 mm + b&g Other + b&g PVC	c	3188	302	442	319	383	**927**	135	12	19	13	18	**39**
		Δc [%]	25.8	-51.6	-16.6	-16.6	-10.2	**-13.8**	14.6	-57.5	-22.9	-22.4	-19.6	**-21.6**
	0–10 mm + b&g Other + b&g PVC	c	3339	287	418	313	364	**944**	140	11	18	13	16	**40**
		Δc [%]	31.8	-54.1	-21.2	-18.2	-14.6	**-15.3**	18.9	-61.4	-28.1	-24.4	-24.9	**-24.0**
	0–20 mm + b&g Other + b&g PVC	c	3803	267	366	304	329	**1014**	156	10	16	13	15	**42**
		Δc [%]	50.1	-57.3	-30.9	-20.6	-22.9	**-16.3**	32.6	-64.8	-37.5	-27.4	-33.6	**-26.1**

B.7. Ca

Table B.7: Relative concentration change (Δc, in %) of Ca caused by the removal of different material or particle size fractions referring to mg/kg and mg/MJ, both calculated for dry mass without hard impurities

	Removed fractions	Conc. after removal	mg/kg$_{DM}$						mg/MJ					
			S01	S02	S03	S04	S05	Avr	S01	S02	S03	S04	S05	Avr
Single process steps	0–5 mm	c	14813	25870	20237	23140	26136	**22039**	639	1047	909	993	1214	**960**
		Δc [%]	-16.6	-9.7	-10.9	-11.5	-16.6	**-13.1**	-22.5	-19.1	-15.9	-16.5	-24.7	**-19.8**
	0–10 mm	c	14890	25582	19924	23411	25976	**21957**	638	999	886	998	1188	**942**
		Δc [%]	-16.2	-10.7	-12.2	-10.5	-17.1	**-13.3**	-22.7	-22.8	-18.0	-16.0	-26.3	**-21.2**
	0–20 mm	c	14569	26178	19952	24153	24569	**21884**	615	1006	882	1022	1103	**926**
		Δc [%]	-18.0	-8.6	-12.1	-7.7	-21.6	**-13.6**	-25.5	-22.3	-18.4	-14.0	-31.6	**-22.4**
	PET (NIR)	c	19013	29673	23865	27646	32717	**26583**	893	1333	1129	1260	1714	**1266**
		Δc [%]	7.0	3.6	5.1	5.7	4.4	**5.2**	8.3	3.0	4.4	5.9	6.3	**5.6**
	PVC (NIR)	c	18230	28807	22765	26767	30416	**25397**	852	1301	1085	1216	1587	**1208**
		Δc [%]	2.6	0.6	0.3	2.3	-2.9	**0.6**	3.3	0.5	0.4	2.3	-1.6	**1.0**
	b&g	c	19750	29637	22027	27830	31095	**26068**	944	1351	1060	1287	1674	**1263**
		Δc [%]	11.2	3.4	-3.0	6.4	-0.7	**3.5**	14.4	4.4	-2.0	8.2	3.8	**5.8**
	PET + PVC (NIR)	c	19612	29869	23959	28408	31801	**26730**	929	1341	1135	1293	1695	**1279**
		Δc [%]	10.4	4.3	5.5	8.6	1.5	**6.1**	12.6	3.6	4.9	8.7	5.1	**7.0**
Combinations of Screening and state-of-the-art NIR sorting or manual removal of black materials	0–5 mm + PET (NIR)	c	15897	26858	21165	24437	26996	**23071**	688	1069	937	1043	1260	**999**
		Δc [%]	-10.5	-6.3	-6.8	-6.6	-13.8	**-8.8**	-16.6	-17.4	-13.4	-12.3	-21.9	**-16.3**
	0–10 mm + PET (NIR)	c	16048	26667	20842	24795	26852	**23041**	689	1019	911	1051	1230	**980**
		Δc [%]	-9.7	-6.9	-8.2	-5.2	-14.3	**-8.9**	-16.5	-21.3	-15.7	-11.6	-23.7	**-17.8**
	0–20 mm + PET (NIR)	c	15890	27469	20931	25742	25279	**23062**	671	1028	908	1081	1134	**964**
		Δc [%]	-10.6	-4.1	-7.8	-1.6	-19.3	**-8.7**	-18.6	-20.6	-16.0	-9.1	-29.7	**-18.8**
	0–5 mm + PVC (NIR)	c	15148	25989	20254	23673	24589	**21930**	655	1048	910	1012	1148	**955**
		Δc [%]	-14.7	-9.3	-10.8	-9.5	-21.5	**-13.2**	-20.6	-19.0	-15.8	-14.9	-28.8	**-19.8**
	0–10 mm + PVC (NIR)	c	15249	25708	19934	23977	24343	**21842**	654	1000	886	1018	1117	**935**
		Δc [%]	-14.2	-10.3	-12.2	-8.3	-22.3	**-13.5**	-20.7	-22.7	-18.0	-14.4	-30.7	**-21.3**
	0–20 mm + PVC (NIR)	c	14963	26336	19963	24798	22665	**21745**	632	1007	882	1045	1020	**917**
		Δc [%]	-15.8	-8.1	-12.1	-5.2	-27.7	**-13.8**	-23.4	-22.2	-18.4	-12.2	-36.8	**-22.6**
	0–5 mm + PET (NIR) + PVC (NIR)	c	16364	27019	21206	25120	25286	**22999**	711	1071	938	1067	1187	**995**
		Δc [%]	-7.9	-5.7	-6.6	-4.0	-19.3	**-8.7**	-13.9	-17.3	-13.2	-10.3	-26.4	**-16.2**
	0–10 mm + PET (NIR) + PVC (NIR)	c	16558	26845	20877	25527	25034	**22968**	713	1020	912	1076	1152	**975**
		Δc [%]	-6.8	-6.3	-8.0	-2.4	-20.1	**-8.7**	-13.6	-21.2	-15.6	-9.5	-28.5	**-17.7**
	0–20 mm + PET (NIR) + PVC (NIR)	c	16487	27699	20970	26591	23100	**22970**	697	1029	909	1110	1038	**957**
		Δc [%]	-7.2	-3.3	-7.6	1.7	-26.3	**-8.6**	-15.5	-20.5	-16.0	-6.6	-35.6	**-18.8**
	0–5 mm + b&g	c	16512	26668	18917	24598	25121	**22363**	724	1073	848	1066	1207	**983**
		Δc [%]	-7.1	-6.9	-16.7	-6.0	-19.8	**-11.3**	-12.3	-17.1	-21.6	-10.4	-25.2	**-17.3**
	0–10 mm + b&g	c	16716	26440	18471	24967	24888	**22297**	727	1020	818	1075	1175	**963**
		Δc [%]	-5.9	-7.7	-18.6	-4.5	-20.6	**-11.5**	-11.9	-21.2	-24.4	-9.6	-27.1	**-18.9**
	0–20 mm + b&g	c	16678	27266	18409	25942	23167	**22293**	713	1030	808	1108	1073	**946**
		Δc [%]	-6.1	-4.8	-18.9	-0.8	-26.1	**-11.3**	-13.5	-20.4	-25.2	-6.9	-33.5	**-19.9**
	0–5 mm + b&g + PVC (NIR)	c	17075	26832	18904	25301	23222	**22267**	751	1075	847	1092	1126	**978**
		Δc [%]	-3.9	-6.3	-16.7	-3.3	-25.9	**-11.2**	-8.9	-16.9	-21.6	-8.2	-30.2	**-17.2**
	0–10 mm + b&g + PVC (NIR)	c	17337	26620	18446	25723	22863	**22198**	756	1021	816	1102	1088	**957**
		Δc [%]	-2.4	-7.1	-18.8	-1.7	-27.0	**-11.4**	-8.3	-21.1	-24.5	-7.3	-32.5	**-18.8**
	0–20 mm + b&g + PVC (NIR)	c	17438	27503	18380	26821	20748	**22178**	748	1031	807	1139	967	**938**
		Δc [%]	-1.9	-4.0	-19.0	2.5	-33.8	**-11.2**	-9.4	-20.3	-25.4	-4.2	-40.0	**-19.9**
	0–5 mm + b&g + PET (NIR)	c	18155	27932	19854	26340	25948	**23646**	802	1100	873	1136	1260	**1034**
		Δc [%]	2.2	-2.5	-12.6	0.7	-17.2	**-5.9**	-2.8	-15.0	-19.3	-4.5	-21.9	**-12.7**
	0–10 mm + b&g + PET (NIR)	c	18518	27873	19369	26848	25719	**23666**	810	1044	838	1149	1225	**1013**
		Δc [%]	4.2	-2.7	-14.7	2.6	-17.9	**-5.7**	-1.8	-19.3	-22.5	-3.4	-24.1	**-14.2**
	0–20 mm + b&g + PET (NIR)	c	18924	29044	19367	28150	23731	**23843**	813	1059	829	1193	1104	**999**
		Δc [%]	6.5	1.4	-14.7	7.6	-24.3	**-4.7**	-1.4	-18.2	-23.4	0.3	-31.5	**-14.9**
	0–5 mm + b&g + PET (NIR) + PVC (NIR)	c	18987	28161	19866	27280	23782	**23615**	843	1104	873	1171	1170	**1032**
		Δc [%]	6.9	-1.7	-12.5	4.3	-24.1	**-5.4**	2.2	-14.7	-19.3	-1.6	-27.4	**-12.2**
	0–10 mm + b&g + PET (NIR) + PVC (NIR)	c	19458	28138	19367	27871	23383	**23643**	856	1047	837	1186	1126	**1010**
		Δc [%]	9.5	-1.8	-14.7	6.6	-25.4	**-5.2**	3.7	-19.1	-22.6	-0.3	-30.2	**-13.7**
	0–20 mm + b&g + PET (NIR) + PVC (NIR)	c	20191	29405	19365	29369	20834	**23833**	871	1062	827	1236	978	**995**
		Δc [%]	13.6	2.6	-14.7	12.3	-33.5	**-3.9**	5.5	-18.0	-23.5	3.9	-39.4	**-14.3**

More targeted removal	PVC (FTIR) + b&g PVC	c	17900	28867	22760	26514	31115	**25431**	832	1302	1085	1201	1601	**1204**
		Δc [%]	0.7	0.8	0.2	1.4	-0.7	**0.5**	0.8	0.6	0.4	1.0	-0.7	**0.4**
	0–5 mm + PVC (FTIR) + b&g PVC	c	14937	26094	20275	23456	25838	**22120**	644	1053	912	1001	1199	**962**
		Δc [%]	-15.9	-8.9	-10.7	-10.3	-17.5	**-12.7**	-21.9	-18.7	-15.7	-15.8	-25.7	**-19.6**
	0–10 mm + PVC (FTIR) + b&g PVC	c	15022	25828	19959	23746	25663	**22044**	643	1005	888	1007	1172	**943**
		Δc [%]	-15.5	-9.8	-12.1	-9.2	-18.1	**-12.9**	-22.1	-22.3	-17.8	-15.3	-27.3	**-21.0**
	0–20 mm + PVC (FTIR) + b&g PVC	c	14718	26461	19989	24532	24220	**21984**	621	1013	884	1032	1085	**927**
		Δc [%]	-17.2	-7.6	-12.0	-6.2	-22.7	**-13.1**	-24.8	-21.8	-18.2	-13.2	-32.7	**-22.1**
	PVC (NIR) + b&g PVC	c	18286	28826	22772	26844	30416	**25429**	855	1302	1086	1219	1587	**1210**
		Δc [%]	2.9	0.6	0.3	2.6	-2.9	**0.7**	3.6	0.6	0.5	2.5	-1.6	**1.1**
	0–5 mm + PVC (NIR) + b&g PVC	c	15200	26009	20257	23737	24587	**21958**	657	1049	910	1014	1148	**956**
		Δc [%]	-14.5	-9.2	-10.8	-9.2	-21.5	**-13.0**	-20.3	-18.9	-15.8	-14.8	-28.8	**-19.7**
	0–10 mm + PVC (NIR) + b&g PVC	c	15305	25730	19936	24045	24341	**21871**	657	1001	887	1020	1117	**936**
		Δc [%]	-13.9	-10.2	-12.2	-8.1	-22.3	**-13.3**	-20.4	-22.7	-18.0	-14.2	-30.7	**-21.2**
	0–20 mm + PVC (NIR) + b&g PVC	c	15026	26362	19965	24877	22663	**21779**	635	1008	882	1047	1020	**918**
		Δc [%]	-15.4	-8.0	-12.1	-4.9	-27.7	**-13.6**	-23.1	-22.1	-18.4	-12.0	-36.8	**-22.5**
	PET (FTIR) + Textiles + b&g PET	c	18957	29125	23533	27147	32201	**26193**	882	1310	1120	1232	1670	**1243**
		Δc [%]	6.7	1.7	3.7	3.8	2.8	**3.7**	6.9	1.2	3.6	3.6	3.6	**3.8**
	0–5 mm + PET (FTIR) + Textiles + b&g PET	c	15918	26321	20971	24027	26634	**22774**	684	1055	937	1024	1235	**987**
		Δc [%]	-10.4	-8.1	-7.6	-8.1	-15.0	**-9.9**	-17.1	-18.5	-13.3	-13.9	-23.4	**-17.2**
	0–10 mm + PET (FTIR) + Textiles + b&g PET	c	16066	26074	20662	24352	26479	**22726**	684	1006	914	1031	1207	**968**
		Δc [%]	-9.6	-9.0	-9.0	-6.9	-15.5	**-10.0**	-17.1	-22.3	-15.5	-13.3	-25.1	**-18.7**
	0–20 mm + PET (FTIR) + Textiles + b&g PET	c	15916	26760	20734	25219	24952	**22716**	666	1013	910	1059	1114	**953**
		Δc [%]	-10.4	-6.6	-8.7	-3.6	-20.4	**-9.9**	-19.3	-21.7	-15.8	-10.9	-30.9	**-19.7**
	b&g Other	c	19229	29329	21755	27068	31155	**25707**	885	1316	1026	1222	1602	**1210**
		Δc [%]	8.2	2.4	-4.2	3.5	-0.6	**1.9**	7.3	1.7	-5.1	2.7	-0.7	**1.2**
	0–5 mm + b&g Other	c	16118	26380	18720	23878	25535	**22126**	682	1046	824	1011	1176	**948**
		Δc [%]	-9.3	-7.9	-17.5	-8.7	-18.5	**-12.4**	-17.4	-19.2	-23.8	-15.0	-27.1	**-20.5**
	0–10 mm + b&g Other	c	16284	26122	18281	24203	25335	**22045**	682	994	794	1017	1147	**927**
		Δc [%]	-8.3	-8.8	-19.5	-7.5	-19.1	**-12.7**	-17.3	-23.2	-26.5	-14.4	-28.9	**-22.1**
	0–20 mm + b&g Other	c	16168	26875	18209	25079	23759	**22018**	663	1001	784	1045	1054	**909**
		Δc [%]	-9.0	-6.2	-19.8	-4.1	-24.2	**-12.7**	-19.6	-22.7	-27.5	-12.2	-34.7	**-23.3**
	PVC (FTIR) + b&g PVC + b&g Other	c	19392	29578	21811	27484	30924	**25838**	893	1325	1030	1235	1589	**1215**
		Δc [%]	9.1	3.2	-3.9	5.1	-1.3	**2.4**	8.2	2.4	-4.7	3.9	-1.5	**1.7**
	0–5 mm + PVC (FTIR) + b&g PVC + b&g Other	c	16275	26641	18746	24249	25208	**22224**	688	1053	826	1020	1159	**949**
		Δc [%]	-8.4	-7.0	-17.4	-7.3	-19.5	**-11.9**	-16.6	-18.7	-23.6	-14.2	-28.1	**-20.3**
	0–10 mm + PVC (FTIR) + b&g PVC + b&g Other	c	16452	26413	18302	24599	24991	**22152**	689	1000	796	1027	1129	**928**
		Δc [%]	-7.4	-7.8	-19.4	-6.0	-20.2	**-12.2**	-16.5	-22.7	-26.4	-13.6	-30.0	**-21.8**
	0–20 mm + PVC (FTIR) + b&g PVC + b&g Other	c	16367	27219	18231	25534	23370	**22144**	671	1008	786	1056	1034	**911**
		Δc [%]	-7.9	-5.0	-19.7	-2.4	-25.4	**-12.1**	-18.7	-22.1	-27.3	-11.2	-35.9	**-23.1**
	PVC (NIR) + b&g PVC + b&g Other	c	19920	29541	21813	27872	30161	**25861**	923	1325	1030	1256	1573	**1221**
		Δc [%]	12.1	3.1	-3.9	6.6	-3.7	**2.8**	11.9	2.4	-4.7	5.6	-2.5	**2.5**
	0–5 mm + PVC (NIR) + b&g PVC + b&g Other	c	16676	26553	18701	24585	23796	**22062**	706	1049	823	1034	1101	**943**
		Δc [%]	-6.1	-7.3	-17.6	-6.0	-24.0	**-12.2**	-14.4	-19.0	-23.9	-13.0	-31.7	**-20.4**
	0–10 mm + PVC (NIR) + b&g PVC + b&g Other	c	16893	26310	18249	24961	23489	**21980**	708	995	793	1042	1067	**921**
		Δc [%]	-4.9	-8.2	-19.6	-4.6	-25.0	**-12.5**	-14.2	-23.1	-26.7	-12.4	-33.9	**-22.1**
	0–20 mm + PVC (NIR) + b&g PVC + b&g Other	c	16891	27117	18173	25956	21578	**21943**	692	1002	782	1073	958	**901**
		Δc [%]	-4.9	-5.3	-20.0	-0.8	-31.1	**-12.4**	-16.2	-22.6	-27.7	-9.8	-40.6	**-23.4**
	b&g Other + b&g PVC	c	19293	29350	21762	27150	31155	**25742**	888	1317	1027	1225	1602	**1212**
		Δc [%]	8.6	2.4	-4.1	3.8	-0.6	**2.0**	7.7	1.8	-5.0	3.0	-0.7	**1.3**
	0–5 mm + b&g Other + b&g PVC	c	16178	26402	18719	23946	25534	**22156**	684	1047	824	1013	1176	**949**
		Δc [%]	-8.9	-7.8	-17.5	-8.4	-18.5	**-12.3**	-17.1	-19.1	-23.8	-14.9	-27.1	**-20.4**
	0–10 mm + b&g Other + b&g PVC	c	16349	26147	18278	24277	25333	**22077**	685	994	795	1019	1147	**928**
		Δc [%]	-8.0	-8.7	-19.5	-7.2	-19.1	**-12.5**	-17.0	-23.2	-26.5	-14.3	-28.9	**-22.0**
	0–20 mm + b&g Other + b&g PVC	c	16244	26904	18206	25165	23757	**22055**	666	1001	784	1047	1054	**911**
		Δc [%]	-8.6	-6.1	-19.8	-3.8	-24.2	**-12.5**	-19.2	-22.6	-27.5	-12.0	-34.7	**-23.2**

B.8. Cd

Table B.8: Relative concentration change (Δc, in %) of Cd caused by the removal of different material or particle size fractions referring to mg/kg and mg/MJ, both calculated for dry mass without hard impurities

	Removed fractions	Conc. after removal	mg/kg$_{DM}$ S01	S02	S03	S04	S05	Avr	mg/MJ S01	S02	S03	S04	S05	Avr
Single process steps	0–5 mm	c	2.8	1.1	5.0	2.8	1.1	**2.6**	0.12	0.04	0.22	0.12	0.05	**0.11**
		Δc [%]	10.0	-7.8	6.5	5.3	5.6	**4.0**	2.2	-17.4	0.5	-0.6	-4.6	**-4.0**
	0–10 mm	c	2.9	1.1	5.1	2.9	1.1	**2.6**	0.12	0.04	0.22	0.12	0.05	**0.11**
		Δc [%]	13.1	-4.0	8.0	7.9	4.8	**6.0**	4.3	-16.9	0.9	1.2	-6.9	**-3.5**
	0–20 mm	c	2.3	1.2	4.8	2.5	1.1	**2.4**	0.10	0.04	0.21	0.11	0.05	**0.10**
		Δc [%]	-9.4	-2.2	3.1	-6.1	8.3	**-1.2**	-17.6	-16.8	-4.3	-12.6	-5.5	**-11.4**
	PET (NIR)	c	2.8	1.2	4.1	1.3	0.9	**2.0**	0.13	0.05	0.19	0.06	0.04	**0.10**
		Δc [%]	9.8	-0.7	-13.0	-51.4	-17.6	**-14.6**	11.1	-1.3	-13.6	-51.3	-16.2	**-14.3**
	PVC (NIR)	c	2.6	0.7	2.4	2.7	1.0	**1.9**	0.12	0.03	0.12	0.12	0.05	**0.09**
		Δc [%]	1.9	-37.6	-48.3	0.5	-6.5	**-18.0**	2.5	-37.7	-48.2	0.4	-5.2	**-17.6**
	b&g	c	2.9	1.2	5.4	2.7	0.9	**2.6**	0.14	0.06	0.26	0.13	0.05	**0.13**
		Δc [%]	16.7	5.3	15.0	0.7	-8.5	**5.8**	20.1	6.3	16.2	2.4	-4.3	**8.1**
	PET + PVC (NIR)	c	2.8	0.7	1.5	1.3	0.8	**1.4**	0.13	0.03	0.07	0.06	0.04	**0.07**
		Δc [%]	12.5	-41.6	-68.1	-53.5	-26.6	**-35.5**	14.8	-41.9	-68.3	-53.5	-24.0	**-34.6**
Combinations of Screening and state-of-the-art NIR sorting or manual removal of black materials	0–5 mm + PET (NIR)	c	3.1	1.1	4.4	1.3	0.9	**2.1**	0.13	0.04	0.19	0.05	0.04	**0.09**
		Δc [%]	22.9	-9.5	-6.9	-52.4	-14.3	**-12.1**	14.6	-20.3	-13.5	-55.3	-22.3	**-19.4**
	0–10 mm + PET (NIR)	c	3.2	1.1	4.4	1.3	0.9	**2.2**	0.14	0.04	0.19	0.06	0.04	**0.09**
		Δc [%]	27.0	-5.4	-5.8	-51.7	-16.2	**-10.4**	17.5	-20.0	-13.5	-55.0	-25.4	**-19.3**
	0–20 mm + PET (NIR)	c	2.6	1.1	4.1	0.8	0.9	**1.9**	0.11	0.04	0.18	0.03	0.04	**0.08**
		Δc [%]	3.6	-3.6	-12.3	-71.9	-13.8	**-19.6**	-5.8	-20.1	-20.2	-74.1	-24.9	**-29.0**
	0–5 mm + PVC (NIR)	c	2.9	0.5	2.5	2.9	1.0	**2.0**	0.12	0.02	0.11	0.12	0.05	**0.09**
		Δc [%]	12.9	-54.3	-46.2	6.2	-1.5	**-16.6**	5.1	-59.2	-49.3	-0.2	-10.6	**-22.8**
	0–10 mm + PVC (NIR)	c	2.9	0.5	2.5	2.9	1.0	**2.0**	0.13	0.02	0.11	0.12	0.05	**0.09**
		Δc [%]	16.3	-56.0	-46.6	8.9	-2.7	**-16.0**	7.4	-62.1	-50.1	1.8	-13.2	**-23.3**
	0–20 mm + PVC (NIR)	c	2.3	0.5	2.1	2.5	1.0	**1.7**	0.10	0.02	0.09	0.11	0.05	**0.07**
		Δc [%]	-7.5	-59.8	-54.6	-5.8	0.6	**-25.4**	-15.9	-66.0	-57.9	-12.7	-12.1	**-32.9**
	0–5 mm + PET (NIR) + PVC (NIR)	c	3.2	0.5	1.5	1.2	0.8	**1.4**	0.14	0.02	0.07	0.05	0.04	**0.06**
		Δc [%]	27.1	-61.0	-67.9	-54.8	-24.7	**-36.2**	18.9	-65.8	-70.2	-57.8	-31.3	**-41.2**
	0–10 mm + PET (NIR) + PVC (NIR)	c	3.3	0.4	1.4	1.2	0.7	**1.4**	0.14	0.02	0.06	0.05	0.03	**0.06**
		Δc [%]	31.9	-63.8	-69.2	-54.2	-27.4	**-36.5**	22.3	-69.6	-71.7	-57.5	-35.1	**-42.3**
	0–20 mm + PET (NIR) + PVC (NIR)	c	2.7	0.4	0.9	0.6	0.8	**1.1**	0.11	0.01	0.04	0.03	0.03	**0.05**
		Δc [%]	7.1	-69.1	-79.9	-75.9	-25.8	**-48.7**	-2.5	-74.6	-81.7	-77.9	-35.2	**-54.4**
	0–5 mm + b&g	c	3.3	1.2	5.8	2.9	1.0	**2.8**	0.15	0.05	0.26	0.13	0.05	**0.13**
		Δc [%]	32.2	-2.4	24.8	6.9	-3.5	**11.6**	24.8	-13.1	17.4	1.8	-10.0	**4.2**
	0–10 mm + b&g	c	3.5	1.2	6.0	3.0	1.0	**2.9**	0.15	0.05	0.26	0.13	0.05	**0.13**
		Δc [%]	37.3	2.9	27.4	9.9	-4.9	**14.5**	28.5	-12.2	18.4	4.1	-12.8	**5.2**
	0–20 mm + b&g	c	2.9	1.3	5.7	2.5	1.0	**2.7**	0.12	0.05	0.25	0.11	0.05	**0.12**
		Δc [%]	13.5	5.9	22.5	-6.3	-1.6	**6.8**	4.5	-11.5	13.0	-12.0	-11.5	**-3.5**
	0–5 mm + b&g + PVC (NIR)	c	3.5	0.5	2.8	2.9	0.9	**2.1**	0.15	0.02	0.13	0.13	0.04	**0.09**
		Δc [%]	37.7	-56.3	-39.9	8.0	-12.7	**-12.7**	30.5	-61.3	-43.5	2.5	-17.8	**-17.9**
	0–10 mm + b&g + PVC (NIR)	c	3.6	0.5	2.8	3.0	0.9	**2.2**	0.16	0.02	0.12	0.13	0.04	**0.09**
		Δc [%]	43.7	-58.7	-40.1	11.2	-14.8	**-11.7**	35.0	-64.9	-44.4	4.8	-21.2	**-18.1**
	0–20 mm + b&g + PVC (NIR)	c	3.0	0.4	2.3	2.5	0.9	**1.8**	0.13	0.02	0.10	0.11	0.04	**0.08**
		Δc [%]	18.5	-63.7	-49.8	-5.9	-11.9	**-22.6**	9.5	-69.8	-53.7	-12.1	-20.3	**-29.3**
	0–5 mm + b&g + PET (NIR)	c	3.8	1.1	5.2	1.1	0.7	**2.4**	0.17	0.05	0.23	0.05	0.04	**0.10**
		Δc [%]	52.0	-3.7	11.0	-60.5	-28.4	**-5.9**	44.5	-16.0	2.4	-62.5	-32.5	**-12.8**
	0–10 mm + b&g + PET (NIR)	c	4.0	1.2	5.3	1.1	0.7	**2.5**	0.18	0.05	0.23	0.05	0.03	**0.11**
		Δc [%]	59.5	2.1	13.4	-60.0	-31.5	**-3.3**	50.2	-15.3	3.1	-62.4	-36.6	**-12.2**
	0–20 mm + b&g + PET (NIR)	c	3.4	1.3	5.0	0.4	0.7	**2.2**	0.15	0.05	0.21	0.02	0.03	**0.09**
		Δc [%]	35.9	5.5	6.4	-84.9	-30.1	**-13.4**	25.8	-14.9	-4.4	-85.9	-36.8	**-23.2**
	0–5 mm + b&g + PET (NIR) + PVC (NIR)	c	4.1	0.4	1.6	1.0	0.6	**1.5**	0.18	0.02	0.07	0.04	0.03	**0.07**
		Δc [%]	60.4	-64.6	-66.4	-63.9	-42.6	**-35.4**	53.4	-69.3	-69.1	-65.9	-45.1	**-39.2**
	0–10 mm + b&g + PET (NIR) + PVC (NIR)	c	4.3	0.4	1.5	1.0	0.5	**1.5**	0.19	0.01	0.06	0.04	0.03	**0.07**
		Δc [%]	69.5	-68.6	-68.1	-63.6	-47.0	**-35.6**	60.5	-74.2	-71.1	-65.9	-50.4	**-40.2**
	0–20 mm + b&g + PET (NIR) + PVC (NIR)	c	3.7	0.3	0.8	0.3	0.5	**1.1**	0.16	0.01	0.04	0.01	0.03	**0.05**
		Δc [%]	45.4	-76.0	-82.2	-90.7	-47.1	**-50.1**	35.1	-80.8	-84.0	-91.4	-51.8	**-54.6**

More targeted removal	PVC (FTIR) + b&g PVC	c	2.5	0.8	3.6	2.7	1.0	**2.1**	0.11	0.03	0.17	0.12	0.05	**0.10**
		Δc [%]	-2.6	-36.1	-22.0	0.5	-0.6	**-12.1**	-2.5	-36.2	-21.9	0.1	-0.6	**-12.2**
	0–5 mm + PVC (FTIR) + b&g PVC	c	2.7	0.6	3.9	2.9	1.1	**2.2**	0.12	0.02	0.17	0.12	0.05	**0.10**
		Δc [%]	7.2	-52.2	-17.4	6.0	5.0	**-10.3**	-0.4	-57.3	-22.0	-0.5	-5.4	**-17.1**
	0–10 mm + PVC (FTIR) + b&g PVC	c	2.8	0.5	3.9	2.9	1.1	**2.2**	0.12	0.02	0.17	0.12	0.05	**0.10**
		Δc [%]	10.1	-53.7	-16.8	8.7	4.2	**-9.5**	1.5	-60.1	-22.2	1.4	-7.6	**-17.4**
	0–20 mm + PVC (FTIR) + b&g PVC	c	2.2	0.5	3.6	2.5	1.1	**2.0**	0.09	0.02	0.16	0.11	0.05	**0.09**
		Δc [%]	-13.1	-57.2	-23.1	-5.7	7.7	**-18.3**	-21.1	-63.7	-28.6	-12.7	-6.3	**-26.5**
	PVC (NIR) + b&g PVC	c	2.6	0.7	2.4	2.7	1.0	**1.9**	0.12	0.03	0.12	0.12	0.05	**0.09**
		Δc [%]	2.2	-37.6	-48.2	1.1	-6.5	**-17.8**	2.9	-37.6	-48.1	1.0	-5.2	**-17.4**
	0–5 mm + PVC (NIR) + b&g PVC	c	2.9	0.5	2.5	2.9	1.0	**2.0**	0.12	0.02	0.11	0.12	0.05	**0.09**
		Δc [%]	13.4	-54.2	-46.1	6.9	-1.4	**-16.3**	5.6	-59.1	-49.1	0.4	-10.6	**-22.6**
	0–10 mm + PVC (NIR) + b&g PVC	c	3.0	0.5	2.5	3.0	1.0	**2.0**	0.13	0.02	0.11	0.13	0.05	**0.09**
		Δc [%]	16.8	-55.9	-46.5	9.7	-2.7	**-15.7**	7.9	-62.1	-50.0	2.4	-13.2	**-23.0**
	0–20 mm + PVC (NIR) + b&g PVC	c	2.3	0.5	2.1	2.6	1.0	**1.7**	0.10	0.02	0.09	0.11	0.05	**0.07**
		Δc [%]	-7.1	-59.8	-54.5	-5.1	0.6	**-25.2**	-15.5	-66.0	-57.8	-12.2	-12.0	**-32.7**
	PET (FTIR) + Textiles + b&g PET	c	2.7	1.2	4.9	1.4	0.8	**2.2**	0.13	0.06	0.23	0.06	0.04	**0.10**
		Δc [%]	7.4	3.1	5.4	-49.2	-19.3	**-10.5**	7.7	2.7	5.3	-49.3	-18.7	**-10.5**
	0–5 mm + PET (FTIR) + Textiles + b&g PET	c	3.0	1.1	5.3	1.4	0.9	**2.3**	0.13	0.05	0.24	0.06	0.04	**0.10**
		Δc [%]	19.7	-4.3	12.9	-49.8	-16.4	**-7.6**	10.7	-15.1	6.0	-53.0	-24.7	**-15.2**
	0–10 mm + PET (FTIR) + Textiles + b&g PET	c	3.1	1.2	5.4	1.4	0.8	**2.4**	0.13	0.05	0.24	0.06	0.04	**0.10**
		Δc [%]	23.6	0.2	14.8	-49.1	-18.4	**-5.8**	13.3	-14.5	6.6	-52.6	-27.7	**-15.0**
	0–20 mm + PET (FTIR) + Textiles + b&g PET	c	2.5	1.2	5.1	0.9	0.9	**2.1**	0.11	0.05	0.23	0.04	0.04	**0.09**
		Δc [%]	0.3	2.5	9.8	-68.1	-16.2	**-14.3**	-9.6	-14.1	1.3	-70.5	-27.3	**-24.0**
	b&g Other	c	2.8	1.2	5.3	2.6	1.1	**2.6**	0.13	0.06	0.25	0.12	0.06	**0.12**
		Δc [%]	10.8	4.4	13.6	-2.9	3.9	**6.0**	9.8	3.7	12.5	-3.6	3.8	**5.2**
	0–5 mm + b&g Other	c	3.1	1.1	5.7	2.8	1.1	**2.8**	0.13	0.05	0.25	0.12	0.05	**0.12**
		Δc [%]	24.2	-3.2	22.9	2.6	10.6	**11.4**	13.1	-15.0	13.6	-4.5	-1.0	**1.2**
	0–10 mm + b&g Other	c	3.2	1.2	5.9	2.8	1.1	**2.9**	0.14	0.05	0.25	0.12	0.05	**0.12**
		Δc [%]	28.5	1.8	25.4	5.4	9.9	**14.2**	15.9	-14.3	14.4	-2.6	-3.3	**2.0**
	0–20 mm + b&g Other	c	2.7	1.2	5.6	2.4	1.2	**2.6**	0.11	0.05	0.24	0.10	0.05	**0.11**
		Δc [%]	5.0	4.5	20.5	-10.4	14.1	**6.8**	-7.2	-13.9	9.0	-17.9	-1.6	**-6.3**
	PVC (FTIR) + b&g PVC + b&g Other	c	2.7	0.8	4.1	2.6	1.1	**2.3**	0.13	0.03	0.19	0.12	0.05	**0.11**
		Δc [%]	8.0	-35.2	-12.0	-2.4	3.3	**-7.7**	7.1	-35.8	-12.7	-3.5	3.1	**-8.4**
	0–5 mm + PVC (FTIR) + b&g PVC + b&g Other	c	3.1	0.6	4.4	2.8	1.1	**2.4**	0.13	0.02	0.19	0.12	0.05	**0.10**
		Δc [%]	21.1	-53.1	-5.4	3.3	10.0	**-4.8**	10.2	-59.0	-12.6	-4.4	-1.7	**-13.5**
	0–10 mm + PVC (FTIR) + b&g PVC + b&g Other	c	3.2	0.5	4.5	2.9	1.1	**2.4**	0.13	0.02	0.19	0.12	0.05	**0.10**
		Δc [%]	25.2	-54.9	-4.1	6.2	9.3	**-3.7**	12.9	-62.2	-12.5	-2.5	-4.1	**-13.7**
	0–20 mm + PVC (FTIR) + b&g PVC + b&g Other	c	2.5	0.5	4.2	2.4	1.2	**2.2**	0.10	0.02	0.18	0.10	0.05	**0.09**
		Δc [%]	0.8	-59.1	-11.0	-10.0	13.5	**-13.2**	-11.1	-66.5	-19.4	-18.2	-2.4	**-23.5**
	PVC (NIR) + b&g PVC + b&g Other	c	2.9	0.7	2.7	2.7	1.0	**2.0**	0.13	0.03	0.13	0.12	0.05	**0.09**
		Δc [%]	14.0	-36.8	-42.6	-1.8	-2.7	**-14.0**	13.8	-37.3	-43.1	-2.7	-1.5	**-14.1**
	0–5 mm + PVC (NIR) + b&g PVC + b&g Other	c	3.3	0.5	2.8	2.8	1.1	**2.1**	0.14	0.02	0.12	0.12	0.05	**0.09**
		Δc [%]	29.2	-55.4	-39.5	4.1	3.4	**-11.6**	17.8	-61.0	-44.1	-3.6	-7.0	**-19.6**
	0–10 mm + PVC (NIR) + b&g PVC + b&g Other	c	3.4	0.5	2.8	2.9	1.1	**2.1**	0.14	0.02	0.12	0.12	0.05	**0.09**
		Δc [%]	34.2	-57.5	-39.7	7.1	2.3	**-10.7**	21.1	-64.4	-45.0	-1.6	-9.7	**-19.9**
	0–20 mm + PVC (NIR) + b&g PVC + b&g Other	c	2.8	0.4	2.4	2.4	1.1	**1.8**	0.11	0.02	0.10	0.10	0.05	**0.08**
		Δc [%]	9.3	-62.1	-48.9	-9.6	6.4	**-21.0**	-3.6	-69.0	-53.9	-17.8	-8.3	**-30.5**
	b&g Other + b&g PVC	c	2.8	1.2	5.3	2.6	1.1	**2.6**	0.13	0.06	0.25	0.12	0.06	**0.12**
		Δc [%]	11.2	4.5	13.9	-2.3	3.9	**6.2**	10.2	3.8	12.8	-3.1	3.8	**5.5**
	0–5 mm + b&g Other + b&g PVC	c	3.2	1.1	5.8	2.8	1.1	**2.8**	0.13	0.05	0.25	0.12	0.05	**0.12**
		Δc [%]	24.7	-3.1	23.2	3.3	10.6	**11.8**	13.6	-14.9	13.9	-3.9	-1.0	**1.5**
	0–10 mm + b&g Other + b&g PVC	c	3.3	1.2	5.9	2.9	1.1	**2.9**	0.14	0.05	0.26	0.12	0.05	**0.12**
		Δc [%]	29.0	1.9	25.7	6.1	10.0	**14.5**	16.4	-14.2	14.7	-2.0	-3.3	**2.3**
	0–20 mm + b&g Other + b&g PVC	c	2.7	1.2	5.7	2.4	1.2	**2.6**	0.11	0.05	0.24	0.10	0.05	**0.11**
		Δc [%]	5.5	4.6	20.9	-9.7	14.2	**7.1**	-6.8	-13.8	9.4	-17.4	-1.6	**-6.0**

B.9. Cl

Table B.9: Relative concentration change (Δc, in %) of Cl caused by the removal of different material or particle size fractions referring to mg/kg and mg/MJ, both calculated for dry mass without hard impurities

	Removed fractions	Conc. after removal	mg/kg$_{DM}$						mg/MJ					
			S01	S02	S03	S04	S05	Avr	S01	S02	S03	S04	S05	Avr
Single process steps	0–5 mm	c	41699	13305	12403	23174	24650	**23046**	1799	538	557	994	1145	**1007**
		Δc [%]	14.6	10.4	7.4	8.8	9.3	10.1	6.4	-1.1	1.3	2.6	-1.4	1.6
	0–10 mm	c	43552	14111	12569	23764	25369	**23873**	1865	551	559	1013	1160	**1030**
		Δc [%]	19.7	17.1	8.9	11.6	12.4	13.9	10.3	1.3	1.7	4.6	-0.1	3.6
	0–20 mm	c	49652	14949	12705	24667	26690	**25733**	2095	575	562	1044	1198	**1095**
		Δc [%]	36.4	24.1	10.0	15.8	18.3	20.9	24.0	5.6	2.1	7.8	3.2	8.5
	PET (NIR)	c	37751	11989	11287	19641	22233	**20580**	1774	539	534	895	1165	**981**
		Δc [%]	3.7	-0.5	-2.3	-7.8	-1.5	-1.7	5.0	-1.0	-2.9	-7.6	0.3	-1.3
	PVC (NIR)	c	33509	8101	9777	12846	18824	**16611**	1566	366	466	584	982	**793**
		Δc [%]	-7.9	-32.8	-15.3	-39.7	-16.6	-22.5	-7.3	-32.8	-15.2	-39.7	-15.4	-22.1
	b&g	c	23577	11126	8384	18503	17919	**15902**	1127	507	403	856	965	**772**
		Δc [%]	-35.2	-7.6	-27.4	-13.1	-20.6	-20.8	-33.3	-6.8	-26.6	-11.6	-16.9	-19.1
	PET + PVC (NIR)	c	34614	7705	9274	10075	17951	**15924**	1640	346	439	459	957	**768**
		Δc [%]	-4.9	-36.0	-19.7	-52.7	-20.4	-26.8	-3.0	-36.4	-20.1	-52.6	-17.6	-26.0
Combinations of Screening and state-of-the-art NIR sorting or manual removal of black materials	0–5 mm + PET (NIR)	c	43974	13364	12239	21535	24575	**23138**	1904	532	542	919	1147	**1009**
		Δc [%]	20.8	10.9	6.0	1.1	8.9	9.6	12.7	-2.3	-1.5	-5.1	-1.3	0.5
	0–10 mm + PET (NIR)	c	46213	14273	12424	22143	25404	**24091**	1985	545	543	938	1164	**1035**
		Δc [%]	27.0	18.5	7.6	4.0	12.6	13.9	17.4	0.2	-1.2	-3.1	0.2	2.7
	0–20 mm + PET (NIR)	c	53796	15240	12573	23063	26951	**26325**	2273	570	545	969	1209	**1113**
		Δc [%]	47.8	26.5	8.9	8.3	19.5	22.2	34.5	4.8	-0.8	0.0	4.1	8.5
	0–5 mm + PVC (NIR)	c	38695	8488	10482	13750	20468	**18377**	1673	342	471	588	956	**806**
		Δc [%]	6.3	-29.5	-9.2	-35.4	-9.3	-15.4	-1.0	-37.1	-14.4	-39.3	-17.7	-21.9
	0–10 mm + PVC (NIR)	c	40519	8733	10582	14034	21066	**18987**	1738	340	471	596	967	**822**
		Δc [%]	11.3	-27.5	-8.4	-34.1	-6.6	-13.1	2.8	-37.6	-14.4	-38.5	-16.7	-20.9
	0–20 mm + PVC (NIR)	c	46616	9016	10614	14358	22194	**20560**	1969	345	469	605	998	**877**
		Δc [%]	28.1	-25.2	-8.1	-32.6	-1.6	-7.9	16.5	-36.7	-14.7	-37.5	-14.0	-17.3
	0–5 mm + PET (NIR) + PVC (NIR)	c	40732	8034	10029	10706	19694	**17839**	1769	318	444	455	925	**782**
		Δc [%]	11.9	-33.3	-13.1	-49.7	-12.7	-19.4	4.7	-41.5	-19.3	-53.0	-20.4	-25.9
	0–10 mm + PET (NIR) + PVC (NIR)	c	42954	8246	10126	10907	20355	**18518**	1849	313	442	460	937	**800**
		Δc [%]	18.0	-31.6	-12.3	-48.8	-9.8	-16.9	9.4	-42.4	-19.5	-52.5	-19.3	-24.9
	0–20 mm + PET (NIR) + PVC (NIR)	c	50637	8508	10134	11047	21631	**20392**	2141	316	439	461	972	**866**
		Δc [%]	39.1	-29.4	-12.2	-48.1	-4.1	-10.9	26.7	-41.9	-20.2	-52.4	-16.3	-20.8
	0–5 mm + b&g	c	27617	12347	9074	20269	19477	**17757**	1210	497	407	878	936	**785**
		Δc [%]	-24.1	2.5	-21.4	-4.8	-13.7	-12.3	-28.4	-8.8	-26.0	-9.3	-19.4	-18.4
	0–10 mm + b&g	c	29017	13166	9134	20837	20057	**18442**	1261	508	404	897	947	**803**
		Δc [%]	-20.3	9.3	-20.9	-2.2	-11.1	-9.0	-25.4	-6.7	-26.5	-7.4	-18.4	-16.9
	0–20 mm + b&g	c	33879	14057	9076	21679	21161	**19971**	1449	531	399	926	980	**857**
		Δc [%]	-6.9	16.7	-21.4	1.8	-6.2	-3.2	-14.3	-2.5	-27.5	-4.4	-15.6	-12.9
	0–5 mm + b&g + PVC (NIR)	c	22667	6704	6617	9193	14086	**11853**	998	269	297	397	683	**529**
		Δc [%]	-37.7	-44.3	-42.7	-56.8	-37.6	-43.8	-41.0	-50.6	-46.1	-59.0	-41.2	-47.6
	0–10 mm + b&g + PVC (NIR)	c	23853	6737	6568	9334	14445	**12187**	1040	258	291	400	688	**535**
		Δc [%]	-34.5	-44.1	-43.1	-56.2	-36.0	-42.8	-38.4	-52.5	-47.1	-58.7	-40.8	-47.5
	0–20 mm + b&g + PVC (NIR)	c	28082	6819	6333	9357	15176	**13153**	1204	256	278	397	707	**568**
		Δc [%]	-22.8	-43.4	-45.2	-56.1	-32.7	-40.0	-28.8	-53.0	-49.5	-59.0	-39.1	-45.9
	0–5 mm + b&g + PET (NIR)	c	28195	12299	8251	17905	18488	**17027**	1245	485	363	772	898	**752**
		Δc [%]	-22.5	2.1	-28.5	-15.9	-18.1	-16.6	-26.3	-11.0	-34.0	-20.3	-22.7	-22.9
	0–10 mm + b&g + PET (NIR)	c	29883	13227	8280	18456	19119	**17793**	1307	496	358	790	910	**772**
		Δc [%]	-17.9	9.8	-28.3	-13.4	-15.3	-13.0	-22.7	-8.9	-34.8	-18.5	-21.6	-21.3
	0–20 mm + b&g + PET (NIR)	c	36025	14272	8142	19245	20355	**19608**	1548	520	348	815	947	**836**
		Δc [%]	-1.0	18.5	-29.5	-9.6	-9.8	-6.3	-8.4	-4.4	-36.7	-15.8	-18.4	-16.7
	0–5 mm + b&g + PET (NIR) + PVC (NIR)	c	22416	5939	5302	4845	11911	**10083**	995	233	233	208	586	**451**
		Δc [%]	-38.4	-50.7	-54.1	-77.3	-47.2	-53.5	-41.1	-57.2	-57.6	-78.5	-49.5	-56.8
	0–10 mm + b&g + PET (NIR) + PVC (NIR)	c	23812	5849	5172	4797	12205	**10367**	1047	218	224	204	588	**456**
		Δc [%]	-34.6	-51.4	-55.2	-77.5	-45.9	-52.9	-38.1	-60.0	-59.3	-78.9	-49.4	-57.2
	0–20 mm + b&g + PET (NIR) + PVC (NIR)	c	29085	5809	4770	4415	12856	**11387**	1254	210	204	186	603	**491**
		Δc [%]	-20.1	-51.8	-58.7	-79.3	-43.0	-50.6	-25.8	-61.5	-62.9	-80.8	-48.0	-55.8

More targeted removal	PVC (FTIR) + b&g PVC	c	33889	7943	10273	11862	20466	**16887**	1574	358	490	537	1053	**803**
		Δc [%]	-6.9	-34.1	-11.0	-44.3	-9.3	**-21.1**	-6.9	-34.1	-10.9	-44.5	-9.3	**-21.2**
	0–5 mm + PVC (FTIR) + b&g PVC	c	38847	8291	11018	12624	22245	**18605**	1676	335	495	539	1032	**815**
		Δc [%]	6.7	-31.2	-4.6	-40.7	-1.4	**-14.2**	-0.9	-38.5	-9.9	-44.4	-11.1	**-21.0**
	0–10 mm + PVC (FTIR) + b&g PVC	c	40572	8509	11136	12863	22871	**19190**	1737	331	496	545	1044	**831**
		Δc [%]	11.5	-29.4	-3.6	-39.6	1.4	**-11.9**	2.8	-39.2	-9.9	-43.7	-10.1	**-20.0**
	0–20 mm + PVC (FTIR) + b&g PVC	c	46264	8765	11197	13105	24030	**20672**	1951	335	495	551	1077	**882**
		Δc [%]	27.1	-27.2	-3.0	-38.5	6.5	**-7.0**	15.5	-38.4	-10.0	-43.1	-7.3	**-16.6**
	PVC (NIR) + b&g PVC	c	32431	7688	9122	11318	18748	**15862**	1517	347	435	514	978	**758**
		Δc [%]	-10.9	-36.2	-21.0	-46.9	-16.9	**-26.4**	-10.3	-36.2	-20.9	-46.9	-15.8	**-26.0**
	0–5 mm + PVC (NIR) + b&g PVC	c	37460	7981	9767	12034	20380	**17524**	1620	322	439	514	952	**769**
		Δc [%]	2.9	-33.7	-15.4	-43.5	-9.7	**-19.9**	-4.2	-40.8	-20.2	-46.9	-18.1	**-26.0**
	0–10 mm + PVC (NIR) + b&g PVC	c	39223	8164	9841	12259	20974	**18092**	1683	317	438	520	963	**784**
		Δc [%]	7.8	-32.2	-14.8	-42.4	-7.0	**-17.7**	-0.4	-41.7	-20.4	-46.3	-17.1	**-25.2**
	0–20 mm + PVC (NIR) + b&g PVC	c	45128	8387	9833	12470	22095	**19582**	1906	321	435	525	994	**836**
		Δc [%]	24.0	-30.4	-14.8	-41.5	-2.1	**-13.0**	12.8	-41.1	-21.0	-45.8	-14.4	**-21.9**
	PET (FTIR) + Textiles + b&g PET	c	37503	11928	11449	20879	23534	**21059**	1745	536	545	948	1221	**999**
		Δc [%]	3.0	-1.0	-0.8	-2.0	4.3	**0.7**	3.3	-1.4	-0.9	-2.2	5.1	**0.8**
	0–5 mm + PET (FTIR) + Textiles + b&g PET	c	43512	13220	12357	22842	26000	**23586**	1869	530	552	974	1206	**1026**
		Δc [%]	19.5	9.7	7.0	7.2	15.2	**11.8**	10.6	-2.7	0.5	0.5	3.9	**2.5**
	0–10 mm + PET (FTIR) + Textiles + b&g PET	c	45659	14061	12535	23468	26858	**24516**	1944	542	554	994	1224	**1052**
		Δc [%]	25.4	16.7	8.6	10.2	19.0	**16.0**	15.0	-0.4	0.8	2.6	5.4	**4.7**
	0–20 mm + PET (FTIR) + Textiles + b&g PET	c	52880	14944	12680	24427	28444	**26675**	2213	566	557	1026	1270	**1126**
		Δc [%]	45.3	24.0	9.8	14.7	26.1	**24.0**	30.9	4.0	1.2	5.9	9.4	**10.3**
	b&g Other	c	23861	11464	9013	19641	17430	**16282**	1098	514	425	886	896	**764**
		Δc [%]	-34.4	-4.8	-21.9	-7.8	-22.7	**-18.4**	-35.0	-5.5	-22.7	-8.5	-22.8	**-18.9**
	0–5 mm + b&g Other	c	27678	12731	9750	21479	18816	**18091**	1171	505	429	909	867	**776**
		Δc [%]	-24.0	5.7	-15.6	0.8	-16.6	**-9.9**	-30.7	-7.2	-22.0	-6.1	-25.4	**-18.3**
	0–10 mm + b&g Other	c	28981	13572	9836	22066	19331	**18757**	1214	516	428	928	875	**792**
		Δc [%]	-20.4	12.7	-14.8	3.6	-14.3	**-6.7**	-28.2	-5.2	-22.3	-4.2	-24.6	**-16.9**
	0–20 mm + b&g Other	c	33421	14475	9826	22951	20309	**20196**	1371	539	423	956	901	**838**
		Δc [%]	-8.2	20.2	-14.9	7.8	-10.0	**-1.0**	-18.9	-1.0	-23.0	-1.3	-22.4	**-13.3**
	PVC (FTIR) + b&g PVC + b&g Other	c	20927	6946	7494	9318	15151	**11967**	963	311	354	419	778	**565**
		Δc [%]	-42.5	-42.3	-35.1	-56.3	-32.8	**-41.8**	-43.0	-42.8	-35.6	-56.8	-33.0	**-42.2**
	0–5 mm + PVC (FTIR) + b&g PVC + b&g Other	c	24258	7082	8069	9812	16165	**13077**	1026	280	355	413	743	**563**
		Δc [%]	-33.4	-41.2	-30.1	-53.9	-28.4	**-37.4**	-39.3	-48.6	-35.4	-57.4	-36.0	**-43.3**
	0–10 mm + PVC (FTIR) + b&g PVC + b&g Other	c	25373	7165	8085	9967	16566	**13431**	1062	271	352	416	749	**570**
		Δc [%]	-30.3	-40.5	-30.0	-53.2	-26.6	**-36.1**	-37.1	-50.2	-36.1	-57.0	-35.5	**-43.2**
	0–20 mm + PVC (FTIR) + b&g PVC + b&g Other	c	29188	7295	7960	10032	17344	**14364**	1196	270	343	415	767	**598**
		Δc [%]	-19.8	-39.4	-31.1	-52.9	-23.1	**-33.3**	-29.2	-50.4	-37.6	-57.2	-33.9	**-41.7**
	PVC (NIR) + b&g PVC + b&g Other	c	18487	6653	6107	8651	12913	**10562**	857	298	288	390	673	**501**
		Δc [%]	-49.2	-44.8	-47.1	-59.4	-42.8	**-48.6**	-49.3	-45.2	-47.5	-59.8	-42.0	**-48.8**
	0–5 mm + PVC (NIR) + b&g PVC + b&g Other	c	21590	6716	6532	9068	13603	**11502**	914	265	287	382	629	**496**
		Δc [%]	-40.7	-44.2	-43.4	-57.4	-39.7	**-45.1**	-45.9	-51.3	-47.7	-60.6	-45.8	**-50.3**
	0–10 mm + PVC (NIR) + b&g PVC + b&g Other	c	22621	6749	6481	9198	13914	**11793**	948	255	281	384	632	**500**
		Δc [%]	-37.9	-44.0	-43.9	-56.8	-38.3	**-44.2**	-43.9	-53.1	-48.8	-60.3	-45.6	**-50.4**
	0–20 mm + PVC (NIR) + b&g PVC + b&g Other	c	26219	6830	6249	9211	14548	**12611**	1074	252	269	381	646	**524**
		Δc [%]	-28.0	-43.3	-45.9	-56.8	-35.5	**-41.9**	-36.5	-53.6	-51.1	-60.7	-44.4	**-49.3**
	b&g Other + b&g PVC	c	22683	11024	8260	18099	17354	**15484**	1044	495	390	816	892	**727**
		Δc [%]	-37.7	-8.5	-28.5	-15.0	-23.1	**-22.5**	-38.2	-9.1	-29.1	-15.7	-23.2	**-23.1**
	0–5 mm + b&g Other + b&g PVC	c	26306	12182	8915	19747	18728	**17176**	1113	483	392	835	863	**737**
		Δc [%]	-27.7	1.1	-22.8	-7.3	-17.0	**-14.7**	-34.2	-11.2	-28.6	-13.8	-25.7	**-22.7**
	0–10 mm + b&g Other + b&g PVC	c	27535	12950	8966	20273	19240	**17793**	1154	492	390	851	871	**752**
		Δc [%]	-24.4	7.5	-22.3	-4.8	-14.7	**-11.7**	-31.7	-9.5	-29.1	-12.1	-25.0	**-21.5**
	0–20 mm + b&g Other + b&g PVC	c	31727	13779	8900	21043	20211	**19132**	1302	513	383	876	896	**794**
		Δc [%]	-12.8	14.4	-22.9	-1.2	-10.4	**-6.6**	-23.0	-5.8	-30.3	-9.6	-22.8	**-18.3**

B.10. Co

Table B.10: Relative concentration change (Δc, in %) of Co caused by the removal of different material or particle size fractions referring to mg/kg and mg/MJ, both calculated for dry mass without hard impurities

	Removed fractions	Conc. after removal	mg/kg$_{DM}$ S01	S02	S03	S04	S05	Avr	mg/MJ S01	S02	S03	S04	S05	Avr
Single process steps	0–5 mm	c	3.2	7.2	5.5	9.0	5.0	**6.0**	0.14	0.29	0.24	0.38	0.23	**0.26**
		Δc [%]	-48.9	-6.7	-9.3	-0.4	-19.5	**-16.9**	-52.5	-16.4	-14.4	-6.0	-27.3	**-23.3**
	0–10 mm	c	3.1	7.2	5.4	9.0	4.9	**5.9**	0.13	0.28	0.24	0.39	0.22	**0.25**
		Δc [%]	-50.8	-6.5	-9.7	0.5	-21.6	**-17.6**	-54.6	-19.2	-15.7	-5.7	-30.3	**-25.1**
	0–20 mm	c	2.9	7.3	5.5	9.4	4.6	**6.0**	0.12	0.28	0.24	0.40	0.21	**0.25**
		Δc [%]	-53.6	-5.0	-8.6	5.0	-26.3	**-17.7**	-57.9	-19.2	-15.2	-2.2	-35.7	**-26.0**
	PET (NIR)	c	6.6	8.0	6.1	9.5	6.4	**7.3**	0.31	0.36	0.29	0.43	0.34	**0.34**
		Δc [%]	5.1	3.6	0.7	5.4	3.1	**3.6**	6.3	3.1	0.0	5.6	4.9	**4.0**
	PVC (NIR)	c	6.4	7.7	6.0	9.3	6.4	**7.2**	0.30	0.35	0.29	0.42	0.33	**0.34**
		Δc [%]	1.8	0.3	0.5	3.4	2.2	**1.6**	2.4	0.2	0.6	3.3	3.6	**2.0**
	b&g	c	7.1	7.8	4.0	3.8	6.2	**5.8**	0.34	0.35	0.19	0.18	0.33	**0.28**
		Δc [%]	13.3	1.0	-32.9	-57.7	-0.6	**-15.4**	16.6	1.9	-32.2	-57.0	4.0	**-13.3**
	PET + PVC (NIR)	c	6.8	8.0	6.1	9.8	6.6	**7.5**	0.32	0.36	0.29	0.45	0.35	**0.35**
		Δc [%]	7.4	4.0	1.3	9.5	5.8	**5.6**	9.5	3.4	0.7	9.6	9.6	**6.6**
Combinations of Screening and state-of-the-art NIR sorting or manual removal of black materials	0–5 mm + PET (NIR)	c	3.2	7.5	5.4	9.5	5.1	**6.1**	0.14	0.30	0.24	0.41	0.24	**0.26**
		Δc [%]	-49.2	-2.8	-9.9	5.7	-18.8	**-15.0**	-52.6	-14.4	-16.3	-0.8	-26.4	**-22.1**
	0–10 mm + PET (NIR)	c	3.1	7.5	5.4	9.6	4.9	**6.1**	0.13	0.29	0.24	0.41	0.23	**0.26**
		Δc [%]	-51.5	-2.2	-10.4	7.0	-21.1	**-15.6**	-55.1	-17.3	-17.7	-0.3	-29.8	**-24.0**
	0–20 mm + PET (NIR)	c	2.8	7.7	5.5	10.1	4.6	**6.1**	0.12	0.29	0.24	0.43	0.20	**0.26**
		Δc [%]	-54.8	0.1	-9.2	12.6	-26.6	**-15.6**	-58.9	-17.1	-17.3	4.1	-36.0	**-25.1**
	0–5 mm + PVC (NIR)	c	3.1	7.2	5.5	9.3	5.1	**6.0**	0.14	0.29	0.25	0.40	0.24	**0.26**
		Δc [%]	-50.2	-6.5	-8.9	3.4	-18.7	**-16.2**	-53.7	-16.5	-14.1	-2.8	-26.3	**-22.7**
	0–10 mm + PVC (NIR)	c	3.0	7.2	5.5	9.4	4.9	**6.0**	0.13	0.28	0.24	0.40	0.23	**0.26**
		Δc [%]	-52.4	-6.4	-9.3	4.5	-21.0	**-16.9**	-56.0	-19.4	-15.3	-2.4	-29.5	**-24.5**
	0–20 mm + PVC (NIR)	c	2.8	7.3	5.5	9.8	4.6	**6.0**	0.12	0.28	0.24	0.41	0.21	**0.25**
		Δc [%]	-55.7	-4.8	-8.2	9.5	-26.1	**-17.0**	-59.7	-19.4	-14.8	1.5	-35.4	**-25.6**
	0–5 mm + PET (NIR) + PVC (NIR)	c	3.1	7.5	5.4	9.9	5.1	**6.2**	0.13	0.30	0.24	0.42	0.24	**0.27**
		Δc [%]	-50.8	-2.6	-9.5	10.4	-17.8	**-14.0**	-54.0	-14.5	-15.9	3.1	-25.0	**-21.3**
	0–10 mm + PET (NIR) + PVC (NIR)	c	2.9	7.6	5.4	10.1	5.0	**6.2**	0.13	0.29	0.24	0.42	0.23	**0.26**
		Δc [%]	-53.3	-1.8	-9.9	12.0	-20.4	**-14.7**	-56.7	-17.5	-17.4	3.8	-28.8	**-23.3**
	0–20 mm + PET (NIR) + PVC (NIR)	c	2.7	7.7	5.5	10.6	4.6	**6.2**	0.11	0.29	0.24	0.44	0.21	**0.26**
		Δc [%]	-57.4	0.5	-8.7	18.3	-26.4	**-14.7**	-61.2	-17.3	-16.9	8.7	-35.8	**-24.5**
	0–5 mm + b&g	c	3.5	7.2	3.1	3.0	4.8	**4.3**	0.15	0.29	0.14	0.13	0.23	**0.19**
		Δc [%]	-44.0	-6.5	-48.1	-66.2	-22.9	**-37.5**	-47.2	-16.7	-51.1	-67.8	-28.1	**-42.2**
	0–10 mm + b&g	c	3.4	7.2	3.0	2.9	4.6	**4.2**	0.15	0.28	0.13	0.13	0.22	**0.18**
		Δc [%]	-46.1	-6.3	-50.2	-67.7	-25.5	**-39.2**	-49.6	-20.0	-53.7	-69.4	-31.6	**-44.9**
	0–20 mm + b&g	c	3.2	7.4	2.9	2.9	4.3	**4.1**	0.14	0.28	0.13	0.13	0.20	**0.17**
		Δc [%]	-48.8	-4.4	-51.6	-67.3	-31.2	**-40.7**	-52.8	-20.1	-55.4	-69.3	-38.2	**-47.1**
	0–5 mm + b&g + PVC (NIR)	c	3.4	7.2	3.1	3.1	4.8	**4.3**	0.15	0.29	0.14	0.13	0.23	**0.19**
		Δc [%]	-45.3	-6.3	-48.6	-65.7	-22.4	**-37.7**	-48.1	-16.9	-51.6	-67.5	-26.9	**-42.2**
	0–10 mm + b&g + PVC (NIR)	c	3.3	7.2	3.0	2.9	4.7	**4.2**	0.14	0.28	0.13	0.13	0.22	**0.18**
		Δc [%]	-47.7	-6.1	-50.8	-67.3	-25.2	**-39.4**	-50.8	-20.3	-54.3	-69.2	-30.8	**-45.1**
	0–20 mm + b&g + PVC (NIR)	c	3.1	7.4	2.9	3.0	4.3	**4.1**	0.13	0.28	0.13	0.13	0.20	**0.17**
		Δc [%]	-51.0	-4.1	-52.2	-66.8	-31.7	**-41.2**	-54.7	-20.4	-56.0	-69.0	-38.1	**-47.7**
	0–5 mm + b&g + PET (NIR)	c	3.5	7.6	2.6	2.8	4.8	**4.3**	0.16	0.30	0.12	0.12	0.23	**0.18**
		Δc [%]	-43.7	-1.9	-56.0	-69.1	-22.7	**-38.7**	-46.4	-14.5	-59.4	-70.7	-27.1	**-43.6**
	0–10 mm + b&g + PET (NIR)	c	3.4	7.6	2.5	2.6	4.6	**4.1**	0.15	0.29	0.11	0.11	0.22	**0.17**
		Δc [%]	-46.1	-1.0	-59.0	-71.0	-25.7	**-40.6**	-49.2	-17.9	-62.8	-72.7	-31.3	**-46.8**
	0–20 mm + b&g + PET (NIR)	c	3.2	7.9	2.3	2.6	4.2	**4.0**	0.14	0.29	0.10	0.11	0.20	**0.17**
		Δc [%]	-49.3	1.9	-61.4	-70.8	-32.6	**-42.4**	-53.1	-17.7	-65.3	-72.8	-39.1	**-49.6**
	0–5 mm + b&g + PET (NIR) + PVC (NIR)	c	3.5	7.6	2.6	2.8	4.9	**4.3**	0.15	0.30	0.11	0.12	0.24	**0.18**
		Δc [%]	-45.1	-1.6	-56.8	-68.8	-22.0	**-38.9**	-47.5	-14.6	-60.2	-70.5	-25.5	**-43.7**
	0–10 mm + b&g + PET (NIR) + PVC (NIR)	c	3.3	7.7	2.4	2.6	4.6	**4.1**	0.14	0.29	0.10	0.11	0.22	**0.17**
		Δc [%]	-47.9	-0.5	-60.0	-70.8	-25.4	**-40.9**	-50.7	-18.1	-63.7	-72.7	-30.2	**-47.1**
	0–20 mm + b&g + PET (NIR) + PVC (NIR)	c	3.0	7.9	2.3	2.6	4.1	**4.0**	0.13	0.29	0.10	0.11	0.19	**0.16**
		Δc [%]	-52.2	2.6	-62.5	-70.6	-33.4	**-43.2**	-55.6	-18.0	-66.4	-72.7	-39.3	**-50.4**

More targeted removal	PVC (FTIR) + b&g PVC	c	6.3	7.8	6.0	9.2	6.2	**7.1**	0.29	0.35	0.29	0.42	0.32	**0.33**
		Δc [%]	0.7	1.0	0.6	2.2	-0.7	0.8	0.7	0.9	0.8	1.8	-0.7	0.7
	0–5 mm + PVC (FTIR) + b&g PVC	c	3.2	7.3	5.5	9.2	5.0	**6.0**	0.14	0.29	0.25	0.39	0.23	**0.26**
		Δc [%]	-48.6	-5.5	-8.7	2.0	-20.5	**-16.2**	-52.2	-15.6	-13.8	-4.3	-28.3	**-22.8**
	0–10 mm + PVC (FTIR) + b&g PVC	c	3.1	7.3	5.5	9.3	4.8	**6.0**	0.13	0.28	0.24	0.39	0.22	**0.25**
		Δc [%]	-50.5	-5.2	-9.1	3.1	-22.6	**-16.9**	-54.4	-18.4	-15.0	-3.9	-31.3	**-24.6**
	0–20 mm + PVC (FTIR) + b&g PVC	c	2.9	7.4	5.5	9.7	4.5	**6.0**	0.12	0.28	0.24	0.41	0.20	**0.25**
		Δc [%]	-53.3	-3.6	-8.0	7.9	-27.4	**-16.9**	-57.6	-18.3	-14.5	-0.2	-36.8	**-25.5**
	PVC (NIR) + b&g PVC	c	6.4	7.7	6.1	9.3	6.4	**7.2**	0.30	0.35	0.29	0.42	0.33	**0.34**
		Δc [%]	2.0	0.3	0.7	3.9	2.1	1.8	2.7	0.3	0.9	3.8	3.5	2.2
	0–5 mm + PVC (NIR) + b&g PVC	c	3.1	7.2	5.5	9.3	5.1	**6.0**	0.14	0.29	0.25	0.40	0.24	**0.26**
		Δc [%]	-50.2	-6.4	-8.7	4.0	-18.8	**-16.0**	-53.6	-16.4	-13.9	-2.4	-26.3	**-22.5**
	0–10 mm + PVC (NIR) + b&g PVC	c	3.0	7.2	5.5	9.4	4.9	**6.0**	0.13	0.28	0.24	0.40	0.23	**0.26**
		Δc [%]	-52.3	-6.3	-9.1	5.1	-21.0	**-16.7**	-56.0	-19.3	-15.1	-1.9	-29.6	**-24.4**
	0–20 mm + PVC (NIR) + b&g PVC	c	2.8	7.3	5.5	9.9	4.6	**6.0**	0.12	0.28	0.24	0.42	0.21	**0.25**
		Δc [%]	-55.7	-4.7	-8.0	10.2	-26.2	**-16.9**	-59.7	-19.3	-14.6	2.0	-35.5	**-25.4**
	PET (FTIR) + Textiles + b&g PET	c	6.5	7.9	6.2	9.4	6.4	**7.3**	0.30	0.35	0.30	0.43	0.33	**0.34**
		Δc [%]	3.6	2.2	3.3	4.6	2.3	3.2	3.8	1.7	3.2	4.4	3.1	3.2
	0–5 mm + PET (FTIR) + Textiles + b&g PET	c	3.2	7.4	5.6	9.4	5.1	**6.1**	0.14	0.30	0.25	0.40	0.23	**0.26**
		Δc [%]	-49.5	-4.3	-6.4	4.7	-18.8	**-14.8**	-53.3	-15.1	-12.1	-1.8	-26.8	**-21.8**
	0–10 mm + PET (FTIR) + Textiles + b&g PET	c	3.0	7.4	5.6	9.5	4.9	**6.1**	0.13	0.29	0.25	0.40	0.22	**0.26**
		Δc [%]	-51.7	-3.8	-6.7	5.9	-21.0	**-15.4**	-55.7	-17.9	-13.3	-1.4	-30.0	**-23.7**
	0–20 mm + PET (FTIR) + Textiles + b&g PET	c	2.8	7.6	5.7	10.0	4.6	**6.1**	0.12	0.29	0.25	0.42	0.21	**0.26**
		Δc [%]	-55.0	-1.9	-5.3	11.2	-26.2	**-15.5**	-59.4	-17.8	-12.7	2.7	-36.0	**-24.6**
	b&g Other	c	6.9	7.6	4.0	4.1	6.0	**5.7**	0.32	0.34	0.19	0.18	0.31	**0.27**
		Δc [%]	8.9	-0.9	-33.8	-54.8	-2.9	**-16.7**	8.0	-1.6	-34.4	-55.1	-3.0	**-17.2**
	0–5 mm + b&g Other	c	3.4	7.0	3.1	3.4	4.7	**4.3**	0.15	0.28	0.14	0.14	0.22	**0.18**
		Δc [%]	-45.2	-8.6	-48.6	-62.5	-24.4	**-37.9**	-50.1	-19.7	-52.5	-65.1	-32.3	**-44.0**
	0–10 mm + b&g Other	c	3.3	7.0	3.0	3.3	4.6	**4.2**	0.14	0.27	0.13	0.14	0.21	**0.18**
		Δc [%]	-47.3	-8.7	-50.7	-63.8	-26.8	**-39.5**	-52.4	-23.1	-55.0	-66.5	-35.6	**-46.5**
	0–20 mm + b&g Other	c	3.2	7.1	2.9	3.3	4.2	**4.1**	0.13	0.27	0.12	0.14	0.19	**0.17**
		Δc [%]	-49.9	-7.2	-52.0	-63.1	-32.3	**-40.9**	-55.7	-23.5	-56.6	-66.2	-41.7	**-48.8**
	PVC (FTIR) + b&g PVC + b&g Other	c	6.9	7.7	4.0	4.1	6.0	**5.8**	0.32	0.35	0.19	0.19	0.31	**0.27**
		Δc [%]	9.8	0.2	-33.4	-54.0	-3.7	**-16.2**	8.8	-0.6	-34.0	-54.5	-3.8	**-16.8**
	0–5 mm + PVC (FTIR) + b&g PVC + b&g Other	c	3.5	7.1	3.1	3.4	4.6	**4.4**	0.15	0.28	0.14	0.14	0.21	**0.18**
		Δc [%]	-44.9	-7.3	-48.4	-61.8	-25.5	**-37.6**	-49.8	-18.9	-52.2	-64.6	-33.4	**-43.8**
	0–10 mm + PVC (FTIR) + b&g PVC + b&g Other	c	3.3	7.1	3.0	3.3	4.5	**4.3**	0.14	0.27	0.13	0.14	0.20	**0.18**
		Δc [%]	-46.9	-7.2	-50.5	-63.1	-28.0	**-39.1**	-52.1	-22.3	-54.8	-66.1	-36.8	**-46.4**
	0–20 mm + PVC (FTIR) + b&g PVC + b&g Other	c	3.2	7.3	2.9	3.4	4.1	**4.2**	0.13	0.27	0.12	0.14	0.18	**0.17**
		Δc [%]	-49.5	-5.6	-51.8	-62.4	-33.7	**-40.6**	-55.4	-22.6	-56.4	-65.8	-43.0	**-48.6**
	PVC (NIR) + b&g PVC + b&g Other	c	7.0	7.7	4.0	4.2	6.2	**5.8**	0.33	0.34	0.19	0.19	0.32	**0.27**
		Δc [%]	11.8	-0.5	-33.8	-53.7	-0.9	**-15.4**	11.6	-1.3	-34.3	-54.1	0.4	**-15.5**
	0–5 mm + PVC (NIR) + b&g PVC + b&g Other	c	3.4	7.1	3.1	3.4	4.7	**4.3**	0.14	0.28	0.13	0.14	0.22	**0.18**
		Δc [%]	-46.4	-8.4	-49.0	-61.7	-24.1	**-37.9**	-51.2	-19.9	-52.9	-64.6	-31.8	**-44.1**
	0–10 mm + PVC (NIR) + b&g PVC + b&g Other	c	3.2	7.1	2.9	3.3	4.6	**4.2**	0.14	0.27	0.13	0.14	0.21	**0.17**
		Δc [%]	-48.7	-8.4	-51.2	-63.1	-26.8	**-39.6**	-53.7	-23.4	-55.5	-66.1	-35.4	**-46.8**
	0–20 mm + PVC (NIR) + b&g PVC + b&g Other	c	3.0	7.2	2.9	3.4	4.2	**4.1**	0.12	0.27	0.12	0.14	0.19	**0.17**
		Δc [%]	-51.9	-6.9	-52.6	-62.3	-33.0	**-41.3**	-57.6	-23.8	-57.1	-65.7	-42.2	**-49.3**
	b&g Other + b&g PVC	c	6.9	7.6	4.0	4.1	6.0	**5.7**	0.32	0.34	0.19	0.18	0.31	**0.27**
		Δc [%]	9.2	-0.8	-33.7	-54.6	-3.0	**-16.6**	8.3	-1.5	-34.3	-55.0	-3.1	**-17.1**
	0–5 mm + b&g Other + b&g PVC	c	3.5	7.1	3.1	3.4	4.7	**4.3**	0.15	0.28	0.14	0.14	0.22	**0.18**
		Δc [%]	-45.2	-8.5	-48.5	-62.4	-24.5	**-37.8**	-50.1	-19.7	-52.4	-65.0	-32.4	**-43.9**
	0–10 mm + b&g Other + b&g PVC	c	3.3	7.0	3.0	3.3	4.5	**4.2**	0.14	0.27	0.13	0.14	0.21	**0.18**
		Δc [%]	-47.2	-8.6	-50.6	-63.7	-26.9	**-39.4**	-52.4	-23.0	-54.9	-66.4	-35.7	**-46.5**
	0–20 mm + b&g Other + b&g PVC	c	3.2	7.2	2.9	3.3	4.2	**4.1**	0.13	0.27	0.12	0.14	0.19	**0.17**
		Δc [%]	-49.8	-7.1	-51.9	-63.0	-32.4	**-40.9**	-55.7	-23.4	-56.5	-66.2	-41.8	**-48.7**

B.11. Cr

Table B.11: Relative concentration change (Δc, in %) of Cr caused by the removal of different material or particle size fractions referring to mg/kg and mg/MJ, both calculated for dry mass without hard impurities

	Removed fractions	Conc. after removal	mg/kg$_{DM}$ S01	S02	S03	S04	S05	Avr	mg/MJ S01	S02	S03	S04	S05	Avr
Single process steps	0–5 mm	c	148	56	33	67	85	**78**	6.4	2.3	1.5	2.9	3.9	**3.4**
		Δc [%]	-67.0	-44.1	-37.2	-18.6	-19.8	**-37.3**	-69.3	-49.9	-40.7	-23.2	-27.6	**-42.1**
	0–10 mm	c	134	48	30	53	84	**70**	5.8	1.9	1.4	2.3	3.8	**3.0**
		Δc [%]	-70.0	-52.7	-41.7	-35.6	-20.7	**-44.2**	-72.3	-59.1	-45.6	-39.6	-29.6	**-49.2**
	0–20 mm	c	130	44	28	54	70	**65**	5.5	1.7	1.2	2.3	3.2	**2.8**
		Δc [%]	-70.9	-56.5	-46.4	-33.9	-33.6	**-48.3**	-73.5	-63.0	-50.3	-38.5	-42.1	**-53.5**
	PET (NIR)	c	485	104	55	83	114	**168**	22.8	4.7	2.6	3.8	6.0	**8.0**
		Δc [%]	8.2	3.4	4.8	0.8	8.0	**5.1**	9.5	2.8	4.1	1.0	10.0	**5.5**
	PVC (NIR)	c	448	102	51	80	111	**158**	21.0	4.6	2.4	3.6	5.8	**7.5**
		Δc [%]	0.1	1.2	-2.4	-3.1	4.7	**0.1**	0.8	1.2	-2.3	-3.2	6.1	**0.5**
	b&g	c	521	103	56	83	97	**172**	24.9	4.7	2.7	3.8	5.2	**8.3**
		Δc [%]	16.4	2.1	7.8	0.2	-8.5	**3.6**	19.8	3.0	8.9	1.9	-4.3	**5.9**
	PET + PVC (NIR)	c	488	106	53	80	121	**170**	23.1	4.7	2.5	3.7	6.4	**8.1**
		Δc [%]	8.9	4.8	2.1	-2.6	14.1	**5.5**	11.1	4.2	1.6	-2.5	18.1	**6.5**
Combinations of Screening and state-of-the-art NIR sorting or manual removal of black materials	0–5 mm + PET (NIR)	c	153	56	33	66	92	**80**	6.6	2.2	1.4	2.8	4.3	**3.5**
		Δc [%]	-65.9	-44.4	-37.3	-20.1	-13.2	**-36.2**	-68.2	-51.1	-41.7	-25.0	-21.4	**-41.5**
	0–10 mm + PET (NIR)	c	138	46	30	50	91	**71**	5.9	1.8	1.3	2.1	4.2	**3.1**
		Δc [%]	-69.3	-54.1	-42.5	-39.5	-14.0	**-43.9**	-71.6	-61.2	-47.2	-43.6	-23.5	**-49.4**
	0–20 mm + PET (NIR)	c	133	42	27	51	76	**66**	5.6	1.6	1.2	2.2	3.4	**2.8**
		Δc [%]	-70.2	-58.5	-48.0	-37.8	-28.6	**-48.6**	-72.9	-65.6	-52.7	-42.6	-37.8	**-54.3**
	0–5 mm + PVC (NIR)	c	128	57	31	63	89	**74**	5.5	2.3	1.4	2.7	4.1	**3.2**
		Δc [%]	-71.5	-43.8	-40.6	-23.0	-16.1	**-39.0**	-73.5	-49.8	-43.9	-27.7	-23.9	**-43.8**
	0–10 mm + PVC (NIR)	c	112	48	29	48	88	**65**	4.8	1.9	1.3	2.1	4.0	**2.8**
		Δc [%]	-75.0	-52.6	-45.4	-41.2	-17.0	**-46.2**	-76.9	-59.2	-49.0	-45.1	-26.0	**-51.2**
	0–20 mm + PVC (NIR)	c	104	44	26	50	73	**59**	4.4	1.7	1.1	2.1	3.3	**2.5**
		Δc [%]	-76.8	-56.5	-50.4	-39.7	-30.9	**-50.9**	-78.9	-63.2	-54.0	-44.2	-39.6	**-56.0**
	0–5 mm + PET (NIR) + PVC (NIR)	c	130	56	31	62	97	**75**	5.6	2.2	1.4	2.6	4.6	**3.3**
		Δc [%]	-71.0	-44.1	-41.2	-25.3	-8.3	**-38.0**	-72.9	-51.0	-45.4	-30.2	-16.3	**-43.1**
	0–10 mm + PET (NIR) + PVC (NIR)	c	112	46	28	44	96	**65**	4.8	1.8	1.2	1.9	4.4	**2.8**
		Δc [%]	-75.0	-54.1	-46.7	-46.1	-8.9	**-46.2**	-76.8	-61.4	-51.1	-50.0	-18.6	**-51.6**
	0–20 mm + PET (NIR) + PVC (NIR)	c	102	42	25	45	80	**59**	4.3	1.5	1.1	1.9	3.6	**2.5**
		Δc [%]	-77.2	-58.6	-52.7	-44.8	-24.7	**-51.6**	-79.2	-66.0	-56.9	-49.3	-34.3	**-57.1**
	0–5 mm + b&g	c	168	52	33	65	71	**78**	7.4	2.1	1.5	2.8	3.4	**3.4**
		Δc [%]	-62.4	-48.5	-37.0	-21.1	-32.5	**-40.3**	-64.5	-54.2	-40.7	-24.9	-37.1	**-44.3**
	0–10 mm + b&g	c	153	41	30	49	70	**68**	6.6	1.6	1.3	2.1	3.3	**3.0**
		Δc [%]	-65.9	-59.4	-42.7	-40.9	-34.3	**-48.6**	-68.1	-65.3	-46.7	-44.1	-39.7	**-52.8**
	0–20 mm + b&g	c	151	36	27	50	53	**63**	6.5	1.3	1.2	2.1	2.4	**2.7**
		Δc [%]	-66.2	-64.7	-48.7	-39.3	-50.3	**-53.8**	-68.9	-70.5	-52.7	-43.0	-55.3	**-58.1**
	0–5 mm + b&g + PVC (NIR)	c	145	52	31	61	74	**73**	6.4	2.1	1.4	2.6	3.6	**3.2**
		Δc [%]	-67.7	-48.3	-41.2	-26.5	-29.7	**-42.7**	-69.4	-54.2	-44.7	-30.2	-33.7	**-46.4**
	0–10 mm + b&g + PVC (NIR)	c	126	41	28	43	73	**62**	5.5	1.6	1.2	1.8	3.5	**2.7**
		Δc [%]	-71.8	-59.5	-47.2	-47.7	-31.5	**-51.5**	-73.5	-65.6	-51.0	-50.7	-36.6	**-55.5**
	0–20 mm + b&g + PVC (NIR)	c	119	35	24	44	54	**55**	5.1	1.3	1.1	1.9	2.5	**2.4**
		Δc [%]	-73.5	-65.1	-53.7	-46.5	-49.2	**-57.6**	-75.5	-71.0	-57.3	-50.0	-54.0	**-61.6**
	0–5 mm + b&g + PET (NIR)	c	177	51	33	63	77	**80**	7.8	2.0	1.4	2.7	3.7	**3.6**
		Δc [%]	-60.4	-49.5	-37.1	-23.3	-27.1	**-39.5**	-62.3	-55.9	-42.0	-27.3	-31.3	**-43.8**
	0–10 mm + b&g + PET (NIR)	c	160	38	29	44	75	**69**	7.0	1.4	1.3	1.9	3.6	**3.0**
		Δc [%]	-64.3	-62.0	-43.9	-46.4	-28.9	**-49.1**	-66.3	-68.5	-49.0	-49.5	-34.2	**-53.5**
	0–20 mm + b&g + PET (NIR)	c	160	32	25	45	55	**64**	6.9	1.2	1.1	1.9	2.6	**2.7**
		Δc [%]	-64.3	-68.6	-51.2	-44.9	-47.7	**-55.3**	-66.9	-74.7	-56.2	-48.7	-52.7	**-59.8**
	0–5 mm + b&g + PET (NIR) + PVC (NIR)	c	151	51	30	58	82	**74**	6.7	2.0	1.3	2.5	4.0	**3.3**
		Δc [%]	-66.4	-49.3	-42.2	-29.6	-23.0	**-42.1**	-67.8	-56.0	-46.7	-33.6	-26.4	**-46.1**
	0–10 mm + b&g + PET (NIR) + PVC (NIR)	c	129	38	26	37	80	**62**	5.7	1.4	1.1	1.6	3.8	**2.7**
		Δc [%]	-71.2	-62.3	-49.4	-54.7	-24.8	**-52.5**	-72.7	-68.9	-54.1	-57.6	-29.6	**-56.6**
	0–20 mm + b&g + PET (NIR) + PVC (NIR)	c	120	31	22	38	57	**54**	5.2	1.1	0.9	1.6	2.7	**2.3**
		Δc [%]	-73.1	-69.3	-57.4	-53.9	-45.9	**-59.9**	-75.1	-75.4	-61.8	-57.3	-50.7	**-64.1**

More targeted removal	PVC (FTIR) + b&g PVC	c	451	102	51	79	107	**158**	21.0	4.6	2.4	3.6	5.5	**7.4**
		Δc [%]	0.8	0.9	-1.7	-4.4	0.7	**-0.8**	0.8	0.8	-1.6	-4.7	0.6	**-0.8**
	0–5 mm + PVC (FTIR) + b&g PVC	c	149	57	32	63	86	**77**	6.4	2.3	1.4	2.7	4.0	**3.4**
		Δc [%]	-66.8	-43.6	-39.5	-24.0	-19.2	**-38.6**	-69.1	-49.7	-42.8	-28.7	-27.2	**-43.5**
	0–10 mm + PVC (FTIR) + b&g PVC	c	135	48	29	48	85	**69**	5.8	1.9	1.3	2.0	3.9	**3.0**
		Δc [%]	-69.8	-52.4	-44.1	-41.8	-20.1	**-45.6**	-72.1	-59.0	-47.8	-45.7	-29.2	**-50.8**
	0–20 mm + PVC (FTIR) + b&g PVC	c	131	44	27	49	71	**64**	5.5	1.7	1.2	2.1	3.2	**2.7**
		Δc [%]	-70.7	-56.2	-49.0	-40.4	-33.1	**-49.9**	-73.4	-62.9	-52.7	-44.9	-41.8	**-55.1**
	PVC (NIR) + b&g PVC	c	450	102	51	80	111	**159**	21.0	4.6	2.4	3.6	5.8	**7.5**
		Δc [%]	0.4	1.3	-2.3	-2.6	4.7	**0.3**	1.1	1.3	-2.1	-2.8	6.1	**0.7**
	0–5 mm + PVC (NIR) + b&g PVC	c	128	57	31	64	89	**74**	5.5	2.3	1.4	2.7	4.1	**3.2**
		Δc [%]	-71.4	-43.7	-40.5	-22.6	-16.1	**-38.9**	-73.4	-49.8	-43.9	-27.4	-23.9	**-43.7**
	0–10 mm + PVC (NIR) + b&g PVC	c	112	48	29	49	88	**65**	4.8	1.9	1.3	2.1	4.0	**2.8**
		Δc [%]	-74.9	-52.6	-45.3	-40.9	-17.0	**-46.1**	-76.8	-59.2	-48.9	-44.8	-26.0	**-51.2**
	0–20 mm + PVC (NIR) + b&g PVC	c	104	44	26	50	73	**59**	4.4	1.7	1.1	2.1	3.3	**2.5**
		Δc [%]	-76.8	-56.5	-50.3	-39.4	-30.9	**-50.8**	-78.9	-63.2	-53.9	-43.9	-39.6	**-55.9**
	PET (FTIR) + Textiles + b&g PET	c	475	103	54	81	113	**165**	22.1	4.6	2.5	3.7	5.8	**7.8**
		Δc [%]	6.1	2.4	2.6	-2.2	6.4	**3.1**	6.3	1.9	2.5	-2.4	7.3	**3.1**
	0–5 mm + PET (FTIR) + Textiles + b&g PET	c	150	57	33	64	91	**79**	6.5	2.3	1.5	2.7	4.2	**3.4**
		Δc [%]	-66.4	-43.3	-37.0	-22.5	-14.2	**-36.7**	-68.9	-49.7	-40.9	-27.3	-22.7	**-41.9**
	0–10 mm + PET (FTIR) + Textiles + b&g PET	c	136	48	30	49	90	**71**	5.8	1.9	1.3	2.1	4.1	**3.0**
		Δc [%]	-69.7	-52.3	-41.9	-41.0	-15.0	**-44.0**	-72.2	-59.3	-46.0	-45.1	-24.8	**-49.5**
	0–20 mm + PET (FTIR) + Textiles + b&g PET	c	131	44	28	50	75	**66**	5.5	1.7	1.2	2.1	3.4	**2.8**
		Δc [%]	-70.7	-56.3	-47.0	-39.5	-28.9	**-48.5**	-73.6	-63.3	-51.1	-44.1	-38.4	**-54.1**
	b&g Other	c	498	101	56	80	93	**166**	22.9	4.5	2.6	3.6	4.8	**7.7**
		Δc [%]	11.2	0.3	6.9	-2.9	-12.0	**0.7**	10.2	-0.4	5.9	-3.6	-12.1	**0.0**
	0–5 mm + b&g Other	c	165	51	33	63	69	**76**	7.0	2.0	1.5	2.7	3.2	**3.3**
		Δc [%]	-63.3	-49.1	-36.5	-23.7	-35.3	**-41.6**	-66.5	-55.3	-41.3	-28.9	-42.1	**-46.8**
	0–10 mm + b&g Other	c	150	41	30	47	67	**67**	6.3	1.5	1.3	2.0	3.0	**2.8**
		Δc [%]	-66.5	-59.6	-41.9	-42.6	-37.0	**-49.5**	-69.8	-66.0	-47.0	-47.0	-44.6	**-54.9**
	0–20 mm + b&g Other	c	148	35	27	48	51	**62**	6.1	1.3	1.2	2.0	2.2	**2.6**
		Δc [%]	-66.9	-64.8	-47.6	-41.2	-52.2	**-54.6**	-70.8	-71.0	-52.6	-46.1	-58.8	**-59.9**
	PVC (FTIR) + b&g PVC + b&g Other	c	502	102	55	76	94	**166**	23.1	4.6	2.6	3.4	4.8	**7.7**
		Δc [%]	12.2	1.3	4.9	-7.7	-11.4	**-0.2**	11.2	0.5	4.1	-8.8	-11.5	**-0.9**
	0–5 mm + PVC (FTIR) + b&g PVC + b&g Other	c	166	52	32	58	69	**75**	7.0	2.0	1.4	2.4	3.2	**3.2**
		Δc [%]	-63.0	-48.7	-39.2	-29.8	-34.8	**-43.1**	-66.3	-55.1	-43.8	-35.1	-41.7	**-48.4**
	0–10 mm + PVC (FTIR) + b&g PVC + b&g Other	c	151	41	29	41	67	**66**	6.3	1.6	1.3	1.7	3.0	**2.8**
		Δc [%]	-66.2	-59.4	-44.8	-49.7	-36.5	**-51.3**	-69.5	-65.9	-49.6	-53.8	-44.3	**-56.6**
	0–20 mm + PVC (FTIR) + b&g PVC + b&g Other	c	150	36	26	42	51	**61**	6.1	1.3	1.1	1.7	2.3	**2.5**
		Δc [%]	-66.6	-64.6	-50.8	-48.7	-51.9	**-56.5**	-70.5	-71.0	-55.5	-53.3	-58.6	**-61.8**
	PVC (NIR) + b&g PVC + b&g Other	c	504	103	55	78	97	**167**	23.3	4.6	2.6	3.5	5.1	**7.8**
		Δc [%]	12.5	1.7	4.4	-5.9	-8.0	**0.9**	12.2	1.0	3.5	-6.8	-6.8	**0.6**
	0–5 mm + PVC (NIR) + b&g PVC + b&g Other	c	143	52	31	59	71	**71**	6.0	2.0	1.4	2.5	3.3	**3.0**
		Δc [%]	-68.1	-48.9	-40.5	-28.5	-32.9	**-43.8**	-70.9	-55.3	-45.0	-33.8	-39.6	**-48.9**
	0–10 mm + PVC (NIR) + b&g PVC + b&g Other	c	126	41	28	42	69	**61**	5.3	1.5	1.2	1.8	3.1	**2.6**
		Δc [%]	-71.9	-59.7	-46.2	-49.0	-34.7	**-52.3**	-74.7	-66.3	-51.0	-53.1	-42.4	**-57.5**
	0–20 mm + PVC (NIR) + b&g PVC + b&g Other	c	118	35	25	43	51	**55**	4.9	1.3	1.1	1.8	2.3	**2.3**
		Δc [%]	-73.5	-65.1	-52.4	-47.9	-51.4	**-58.1**	-76.7	-71.5	-57.0	-52.6	-58.1	**-63.2**
	b&g Other + b&g PVC	c	500	101	56	80	93	**166**	23.0	4.5	2.6	3.6	4.8	**7.7**
		Δc [%]	11.6	0.4	7.1	-2.4	-12.0	**0.9**	10.6	-0.3	6.1	-3.2	-12.1	**0.2**
	0–5 mm + b&g Other + b&g PVC	c	165	51	33	63	69	**76**	7.0	2.0	1.5	2.7	3.2	**3.3**
		Δc [%]	-63.2	-49.1	-36.4	-23.2	-35.3	**-41.4**	-66.4	-55.3	-41.2	-28.6	-42.1	**-46.7**
	0–10 mm + b&g Other + b&g PVC	c	150	41	30	47	67	**67**	6.3	1.5	1.3	2.0	3.0	**2.8**
		Δc [%]	-66.4	-59.6	-41.9	-42.4	-37.0	**-49.4**	-69.7	-66.0	-46.9	-46.8	-44.6	**-54.8**
	0–20 mm + b&g Other + b&g PVC	c	149	36	27	49	51	**62**	6.1	1.3	1.2	2.0	2.2	**2.6**
		Δc [%]	-66.8	-64.8	-47.6	-40.9	-52.2	**-54.5**	-70.7	-71.0	-52.6	-45.9	-58.8	**-59.8**

B.12. Cu

Table B.12: Relative concentration change (Δc, in %) of Cu caused by the removal of different material or particle size fractions referring to mg/kg and mg/MJ, both calculated for dry mass without hard impurities

	Removed fractions	Conc. after removal	mg/kg$_{DM}$ S01	S02	S03	S04	S05	Avr	mg/MJ S01	S02	S03	S04	S05	Avr
Single process steps	0–5 mm	c	1319	354	28	465	165	**466**	57	14	1	20	8	**20**
		Δc [%]	12.0	2.9	-27.1	2.0	5.8	**-0.9**	4.1	-7.9	-31.2	-3.8	-4.5	**-8.7**
	0–10 mm	c	1246	389	26	424	111	**439**	53	15	1	18	5	**19**
		Δc [%]	5.8	13.1	-31.5	-6.9	-29.0	**-9.7**	-2.4	-2.2	-36.1	-12.7	-36.9	**-18.1**
	0–20 mm	c	324	428	26	92	26	**179**	14	16	1	4	1	**7**
		Δc [%]	-72.5	24.3	-33.1	-79.9	-83.5	**-48.9**	-75.0	5.7	-37.9	-81.2	-85.6	**-54.8**
	PET (NIR)	c	1233	369	40	498	173	**463**	58	17	2	23	9	**22**
		Δc [%]	4.7	7.2	4.9	9.3	11.0	**7.4**	6.0	6.6	4.2	9.5	13.0	**7.9**
	PVC (NIR)	c	1116	351	37	433	166	**421**	52	16	2	20	9	**20**
		Δc [%]	-5.2	1.9	-3.8	-4.9	6.9	**-1.0**	-4.6	1.9	-3.7	-5.0	8.3	**-0.6**
	b&g	c	1377	85	41	509	172	**437**	66	4	2	24	9	**21**
		Δc [%]	16.9	-75.3	6.2	11.6	10.2	**-6.1**	20.3	-75.1	7.3	13.5	15.3	**-3.7**
	PET + PVC (NIR)	c	1168	377	39	475	187	**449**	55	17	2	22	10	**21**
		Δc [%]	-0.8	9.5	0.7	4.2	19.9	**6.7**	1.2	8.8	0.2	4.3	24.1	**7.7**
Combinations of Screening and state-of-the-art NIR sorting or manual removal of black materials	0–5 mm + PET (NIR)	c	1403	386	29	514	186	**504**	61	15	1	22	9	**22**
		Δc [%]	19.1	12.2	-25.6	12.8	19.7	**7.6**	11.1	-1.2	-30.9	5.8	8.5	**-1.3**
	0–10 mm + PET (NIR)	c	1324	430	27	470	125	**475**	57	16	1	20	6	**20**
		Δc [%]	12.5	24.8	-30.6	3.0	-19.9	**-2.0**	4.0	5.6	-36.3	-4.0	-28.7	**-11.9**
	0–20 mm + PET (NIR)	c	268	478	26	92	27	**178**	11	18	1	4	1	**7**
		Δc [%]	-77.3	38.9	-32.5	-79.8	-82.9	**-46.7**	-79.3	15.0	-38.5	-81.3	-85.1	**-53.8**
	0–5 mm + PVC (NIR)	c	1258	362	26	440	178	**453**	54	15	1	19	8	**19**
		Δc [%]	6.8	5.3	-31.8	-3.5	14.4	**-1.8**	-0.6	-6.0	-35.7	-9.3	3.8	**-9.5**
	0–10 mm + PVC (NIR)	c	1175	400	24	396	119	**423**	50	16	1	17	5	**18**
		Δc [%]	-0.2	16.2	-36.5	-13.1	-23.4	**-11.4**	-7.8	0.0	-40.7	-18.8	-31.7	**-19.8**
	0–20 mm + PVC (NIR)	c	162	440	24	43	26	**139**	7	17	1	2	1	**6**
		Δc [%]	-86.2	28.0	-38.4	-90.5	-83.0	**-54.0**	-87.5	8.3	-42.9	-91.2	-85.2	**-59.7**
	0–5 mm + PET (NIR) + PVC (NIR)	c	1339	396	27	489	204	**491**	58	16	1	21	10	**21**
		Δc [%]	13.7	15.1	-31.0	7.2	31.2	**7.3**	6.4	1.0	-35.9	0.1	19.7	**-1.7**
	0–10 mm + PET (NIR) + PVC (NIR)	c	1250	443	24	440	137	**459**	54	17	1	19	6	**19**
		Δc [%]	6.2	28.7	-36.4	-3.4	-12.3	**-3.4**	-1.6	8.2	-41.6	-10.4	-21.5	**-13.4**
	0–20 mm + PET (NIR) + PVC (NIR)	c	71	494	24	36	28	**131**	3	18	1	1	1	**5**
		Δc [%]	-93.9	43.7	-38.6	-92.1	-82.3	**-52.7**	-94.5	18.2	-44.1	-92.8	-84.5	**-59.5**
	0–5 mm + b&g	c	1588	29	28	526	185	**471**	70	1	1	23	9	**21**
		Δc [%]	34.9	-91.5	-26.4	15.5	18.7	**-9.8**	27.3	-92.4	-30.7	10.0	10.7	**-15.0**
	0–10 mm + b&g	c	1514	26	26	482	123	**434**	66	1	1	21	6	**19**
		Δc [%]	28.6	-92.5	-31.8	5.7	-20.7	**-22.2**	20.4	-93.6	-36.6	0.1	-27.3	**-27.4**
	0–20 mm + b&g	c	382	26	25	99	26	**112**	16	1	1	4	1	**5**
		Δc [%]	-67.5	-92.4	-33.9	-78.3	-83.3	**-71.1**	-70.1	-93.7	-39.0	-79.6	-85.0	**-73.5**
	0–5 mm + b&g + PVC (NIR)	c	1535	29	26	501	202	**459**	68	1	1	22	10	**20**
		Δc [%]	30.3	-91.6	-32.2	10.0	30.0	**-10.7**	23.5	-92.5	-36.2	4.4	22.5	**-15.7**
	0–10 mm + b&g + PVC (NIR)	c	1450	25	24	453	135	**417**	63	1	1	19	6	**18**
		Δc [%]	23.2	-92.7	-38.0	-0.6	-13.2	**-24.3**	15.7	-93.8	-42.4	-6.3	-19.7	**-29.3**
	0–20 mm + b&g + PVC (NIR)	c	176	25	23	42	27	**59**	8	1	1	2	1	**3**
		Δc [%]	-85.1	-92.6	-40.5	-90.8	-82.7	**-78.3**	-86.2	-93.9	-45.2	-91.4	-84.4	**-80.2**
	0–5 mm + b&g + PET (NIR)	c	1737	27	29	593	213	**520**	77	1	1	26	10	**23**
		Δc [%]	47.5	-92.1	-24.4	30.2	37.1	**-0.3**	40.3	-93.1	-30.2	23.4	29.3	**-6.0**
	0–10 mm + b&g + PET (NIR)	c	1662	23	27	545	142	**480**	73	1	1	23	7	**21**
		Δc [%]	41.1	-93.3	-30.8	19.5	-8.5	**-14.4**	33.0	-94.5	-37.1	12.5	-15.4	**-20.3**
	0–20 mm + b&g + PET (NIR)	c	319	23	26	100	27	**99**	14	1	1	4	1	**4**
		Δc [%]	-72.9	-93.3	-33.1	-78.0	-82.5	**-72.0**	-74.9	-94.6	-39.9	-79.5	-84.2	**-74.6**
	0–5 mm + b&g + PET (NIR) + PVC (NIR)	c	1689	27	26	569	238	**510**	75	1	1	24	12	**23**
		Δc [%]	43.5	-92.2	-31.2	24.8	53.0	**-0.4**	37.2	-93.2	-36.5	17.8	46.3	**-5.7**
	0–10 mm + b&g + PET (NIR) + PVC (NIR)	c	1602	22	24	515	159	**464**	70	1	1	22	8	**20**
		Δc [%]	36.0	-93.6	-38.1	13.1	2.3	**-16.1**	28.8	-94.7	-43.9	5.8	-4.4	**-21.7**
	0–20 mm + b&g + PET (NIR) + PVC (NIR)	c	52	22	23	33	28	**32**	2	1	1	1	1	**1**
		Δc [%]	-95.6	-93.6	-41.2	-92.8	-81.7	**-81.0**	-95.9	-94.9	-47.3	-93.3	-83.3	**-82.9**

More targeted removal	PVC (FTIR) + b&g PVC	c	1185	348	38	467	157	**439**	55	16	2	21	8	**20**
		Δc [%]	0.6	1.2	-1.2	2.4	0.7	**0.8**	0.7	1.1	-1.1	2.1	0.7	**0.7**
	0–5 mm + PVC (FTIR) + b&g PVC	c	1329	359	27	478	166	**472**	57	14	1	20	8	**20**
		Δc [%]	12.9	4.4	-28.7	4.8	6.7	**0.0**	4.8	-6.8	-32.7	-1.7	-3.9	**-8.0**
	0–10 mm + PVC (FTIR) + b&g PVC	c	1255	396	26	436	111	**445**	54	15	1	18	5	**19**
		Δc [%]	6.6	15.0	-33.2	-4.3	-28.4	**-8.9**	-1.7	-0.9	-37.6	-10.8	-36.5	**-17.5**
	0–20 mm + PVC (FTIR) + b&g PVC	c	324	435	25	94	26	**181**	14	17	1	4	1	**7**
		Δc [%]	-72.5	26.6	-34.9	-79.4	-83.4	**-48.7**	-75.0	7.2	-39.6	-80.9	-85.6	**-54.8**
	PVC (NIR) + b&g PVC	c	1120	351	37	436	167	**422**	52	16	2	20	9	**20**
		Δc [%]	-4.8	2.0	-3.6	-4.3	6.9	**-0.8**	-4.2	2.0	-3.5	-4.5	8.4	**-0.4**
	0–5 mm + PVC (NIR) + b&g PVC	c	1263	363	26	443	178	**455**	55	15	1	19	8	**20**
		Δc [%]	7.3	5.4	-31.7	-2.8	14.4	**-1.5**	-0.1	-5.9	-35.6	-8.7	3.8	**-9.3**
	0–10 mm + PVC (NIR) + b&g PVC	c	1181	400	24	399	119	**425**	51	16	1	17	5	**18**
		Δc [%]	0.3	16.3	-36.4	-12.4	-23.3	**-11.1**	-7.4	0.1	-40.6	-18.3	-31.6	**-19.6**
	0–20 mm + PVC (NIR) + b&g PVC	c	163	441	24	43	26	**139**	7	17	1	2	1	**6**
		Δc [%]	-86.2	28.2	-38.3	-90.5	-83.0	**-54.0**	-87.4	8.5	-42.8	-91.2	-85.2	**-59.6**
	PET (FTIR) + Textiles + b&g PET	c	1208	356	39	479	168	**450**	56	16	2	22	9	**21**
		Δc [%]	2.6	3.5	2.0	5.2	7.6	**4.2**	2.8	3.1	1.9	5.0	8.5	**4.2**
	0–5 mm + PET (FTIR) + Textiles + b&g PET	c	1368	369	28	492	180	**487**	59	15	1	21	8	**21**
		Δc [%]	16.2	7.3	-26.9	8.0	15.3	**4.0**	7.5	-4.8	-31.4	1.2	3.9	**-4.7**
	0–10 mm + PET (FTIR) + Textiles + b&g PET	c	1290	408	26	449	120	**459**	55	16	1	19	5	**19**
		Δc [%]	9.6	18.7	-31.6	-1.4	-22.7	**-5.5**	0.5	1.4	-36.5	-8.2	-31.6	**-14.9**
	0–20 mm + PET (FTIR) + Textiles + b&g PET	c	264	451	26	90	27	**172**	11	17	1	4	1	**7**
		Δc [%]	-77.6	31.2	-33.4	-80.2	-82.9	**-48.6**	-79.8	10.0	-38.6	-81.7	-85.2	**-55.1**
	b&g Other	c	1302	83	40	490	165	**416**	60	4	2	22	8	**19**
		Δc [%]	10.6	-75.8	4.6	7.5	5.7	**-9.5**	9.6	-76.0	3.6	6.7	5.5	**-10.1**
	0–5 mm + b&g Other	c	1486	29	28	505	176	**445**	63	1	1	21	8	**19**
		Δc [%]	26.2	-91.6	-27.1	10.7	12.8	**-13.8**	14.9	-92.6	-32.6	3.1	1.0	**-21.3**
	0–10 mm + b&g Other	c	1411	25	26	461	118	**408**	59	1	1	19	5	**17**
		Δc [%]	19.8	-92.6	-32.4	1.2	-24.4	**-25.7**	8.1	-93.8	-38.3	-6.4	-33.5	**-32.8**
	0–20 mm + b&g Other	c	356	26	25	95	26	**106**	15	1	1	4	1	**4**
		Δc [%]	-69.7	-92.6	-34.4	-79.1	-83.2	**-71.8**	-73.2	-93.9	-40.7	-80.8	-85.5	**-74.8**
	PVC (FTIR) + b&g PVC + b&g Other	c	1311	84	40	503	166	**421**	60	4	2	23	9	**19**
		Δc [%]	11.4	-75.5	3.3	10.4	6.5	**-8.8**	10.4	-75.7	2.4	9.1	6.3	**-9.5**
	0–5 mm + PVC (FTIR) + b&g PVC + b&g Other	c	1499	29	27	520	177	**450**	63	1	1	22	8	**19**
		Δc [%]	27.3	-91.5	-29.0	14.1	13.9	**-13.1**	15.9	-92.6	-34.3	5.5	1.7	**-20.8**
	0–10 mm + PVC (FTIR) + b&g PVC + b&g Other	c	1424	26	25	476	119	**414**	60	1	1	20	5	**17**
		Δc [%]	20.9	-92.6	-34.4	4.4	-23.7	**-25.1**	9.1	-93.8	-40.1	-4.1	-33.1	**-32.4**
	0–20 mm + PVC (FTIR) + b&g PVC + b&g Other	c	357	26	24	98	26	**106**	15	1	1	4	1	**4**
		Δc [%]	-69.7	-92.5	-36.6	-78.5	-83.2	**-72.1**	-73.2	-93.8	-42.6	-80.5	-85.5	**-75.1**
	PVC (NIR) + b&g PVC + b&g Other	c	1246	84	39	470	177	**403**	58	4	2	21	9	**19**
		Δc [%]	5.8	-75.5	0.4	3.2	13.6	**-10.5**	5.6	-75.7	-0.4	2.3	15.1	**-10.6**
	0–5 mm + PVC (NIR) + b&g PVC + b&g Other	c	1435	28	26	483	191	**433**	61	1	1	20	9	**18**
		Δc [%]	21.9	-91.7	-32.6	6.0	22.9	**-14.7**	11.1	-92.8	-37.7	-1.9	10.5	**-22.2**
	0–10 mm + PVC (NIR) + b&g PVC + b&g Other	c	1350	25	24	436	128	**393**	57	1	1	18	6	**17**
		Δc [%]	14.7	-92.8	-38.3	-4.3	-17.8	**-27.7**	3.5	-94.0	-43.7	-12.1	-27.5	**-34.8**
	0–20 mm + PVC (NIR) + b&g PVC + b&g Other	c	167	25	23	42	27	**57**	7	1	1	2	1	**2**
		Δc [%]	-85.8	-92.7	-40.7	-90.9	-82.7	**-78.6**	-87.5	-94.1	-46.4	-91.7	-85.1	**-81.0**
	b&g Other + b&g PVC	c	1307	83	40	493	165	**418**	60	4	2	22	8	**19**
		Δc [%]	11.0	-75.8	4.8	8.2	5.7	**-9.2**	10.0	-76.0	3.8	7.4	5.6	**-9.8**
	0–5 mm + b&g Other + b&g PVC	c	1493	29	28	508	176	**447**	63	1	1	21	8	**19**
		Δc [%]	26.8	-91.6	-27.0	11.5	12.9	**-13.5**	15.5	-92.6	-32.5	3.7	1.0	**-21.0**
	0–10 mm + b&g Other + b&g PVC	c	1418	25	26	465	118	**410**	59	1	1	20	5	**17**
		Δc [%]	20.4	-92.6	-32.3	2.0	-24.4	**-25.4**	8.7	-93.8	-38.2	-5.8	-33.5	**-32.5**
	0–20 mm + b&g Other + b&g PVC	c	358	26	25	96	26	**106**	15	1	1	4	1	**4**
		Δc [%]	-69.6	-92.6	-34.3	-78.9	-83.2	**-71.7**	-73.1	-93.9	-40.6	-80.7	-85.5	**-74.8**

B.13. Fe

Table B.13: Relative concentration change (Δc, in %) of Fe caused by the removal of different material or particle size fractions referring to mg/kg and mg/MJ, both calculated for dry mass without hard impurities

	Removed fractions	Conc. after removal	mg/kg$_{DM}$						mg/MJ					
			S01	S02	S03	S04	S05	Avr	S01	S02	S03	S04	S05	Avr
Single process steps	0–5 mm	c	3628	3714	3315	3087	3156	**3380**	157	150	149	132	147	**147**
		Δc [%]	-45.2	-48.1	-32.0	-30.4	-45.7	**-40.3**	-49.1	-53.5	-35.9	-34.4	-51.0	**-44.8**
	0–10 mm	c	3537	3030	3050	2953	2855	**3085**	151	118	136	126	131	**132**
		Δc [%]	-46.6	-57.7	-37.5	-33.4	-50.8	**-45.2**	-50.7	-63.4	-41.6	-37.6	-56.3	**-49.9**
	0–20 mm	c	3374	2834	2947	2947	2094	**2839**	142	109	130	125	94	**120**
		Δc [%]	-49.0	-60.4	-39.6	-33.6	-63.9	**-49.3**	-53.7	-66.3	-43.9	-38.2	-68.6	**-54.1**
	PET (NIR)	c	7186	7539	4911	4737	6296	**6134**	338	339	232	216	330	**291**
		Δc [%]	8.5	5.3	0.7	6.7	8.4	**5.9**	9.8	4.7	0.0	7.0	10.3	**6.4**
	PVC (NIR)	c	6793	7115	4873	4410	6051	**5848**	317	321	232	200	316	**277**
		Δc [%]	2.6	-0.6	-0.1	-0.6	4.2	**1.1**	3.3	-0.7	0.0	-0.7	5.6	**1.5**
	b&g	c	7688	7475	5169	4420	6326	**6216**	367	341	249	204	341	**300**
		Δc [%]	16.1	4.4	6.0	-0.4	8.9	**7.0**	19.5	5.4	7.1	1.3	13.9	**9.4**
	PET + PVC (NIR)	c	7415	7498	4907	4721	6615	**6231**	351	337	232	215	353	**298**
		Δc [%]	12.0	4.7	0.6	6.4	13.9	**7.5**	14.3	4.1	0.1	6.5	17.9	**8.6**
Combinations of Screening and state-of-the-art NIR sorting or manual removal of black materials	0–5 mm + PET (NIR)	c	3906	3828	3126	3249	3335	**3489**	169	152	138	139	156	**151**
		Δc [%]	-41.0	-46.5	-35.9	-26.8	-42.6	**-38.6**	-45.0	-52.9	-40.4	-31.3	-48.0	**-43.5**
	0–10 mm + PET (NIR)	c	3819	3078	2813	3104	2996	**3162**	164	118	123	132	137	**135**
		Δc [%]	-42.3	-57.0	-42.3	-30.0	-48.4	**-44.0**	-46.6	-63.7	-47.0	-34.8	-54.1	**-49.2**
	0–20 mm + PET (NIR)	c	3682	2862	2679	3107	2117	**2889**	156	107	116	131	95	**121**
		Δc [%]	-44.4	-60.0	-45.1	-30.0	-63.6	**-48.6**	-49.4	-66.9	-50.0	-35.3	-68.2	**-54.0**
	0–5 mm + PVC (NIR)	c	3621	3565	3278	2986	3196	**3329**	157	144	147	128	149	**145**
		Δc [%]	-45.3	-50.2	-32.8	-32.7	-45.0	**-41.2**	-49.1	-55.5	-36.6	-36.8	-50.1	**-45.6**
	0–10 mm + PVC (NIR)	c	3523	2841	3007	2842	2868	**3016**	151	111	134	121	132	**130**
		Δc [%]	-46.8	-60.3	-38.4	-36.0	-50.6	**-46.4**	-50.8	-65.8	-42.4	-40.2	-56.0	**-51.1**
	0–20 mm + PVC (NIR)	c	3343	2619	2899	2828	2029	**2743**	141	100	128	119	91	**116**
		Δc [%]	-49.5	-63.4	-40.6	-36.3	-65.1	**-51.0**	-54.1	-69.0	-44.9	-41.0	-69.5	**-55.7**
	0–5 mm + PET (NIR) + PVC (NIR)	c	3920	3666	3079	3144	3400	**3442**	170	145	136	134	160	**149**
		Δc [%]	-40.8	-48.8	-36.9	-29.1	-41.5	**-39.4**	-44.6	-55.1	-41.4	-33.8	-46.6	**-44.3**
	0–10 mm + PET (NIR) + PVC (NIR)	c	3827	2869	2757	2986	3026	**3093**	165	109	120	126	139	**132**
		Δc [%]	-42.2	-59.9	-43.5	-32.7	-47.9	**-45.2**	-46.4	-66.3	-48.1	-37.6	-53.4	**-50.4**
	0–20 mm + PET (NIR) + PVC (NIR)	c	3677	2619	2616	2980	2042	**2787**	155	97	113	124	92	**116**
		Δc [%]	-44.5	-63.4	-46.4	-32.8	-64.8	**-50.4**	-49.4	-69.9	-51.2	-38.3	-69.3	**-55.6**
	0–5 mm + b&g	c	4227	3558	3282	2867	3389	**3465**	185	143	147	124	163	**152**
		Δc [%]	-36.1	-50.3	-32.7	-35.4	-41.7	**-39.2**	-39.7	-55.8	-36.7	-38.5	-45.6	**-43.2**
	0–10 mm + b&g	c	4154	2726	2953	2704	3054	**3118**	181	105	131	116	144	**135**
		Δc [%]	-37.3	-61.9	-39.5	-39.1	-47.4	**-45.0**	-41.3	-67.5	-43.7	-42.3	-51.8	**-49.3**
	0–20 mm + b&g	c	4070	2452	2817	2679	2186	**2841**	174	93	124	114	101	**121**
		Δc [%]	-38.5	-65.8	-42.3	-39.6	-62.4	**-49.7**	-43.4	-71.4	-46.8	-43.3	-66.1	**-54.2**
	0–5 mm + b&g + PVC (NIR)	c	4270	3379	3236	2737	3460	**3416**	188	135	145	118	168	**151**
		Δc [%]	-35.5	-52.8	-33.6	-38.3	-40.4	**-40.1**	-38.9	-58.2	-37.6	-41.5	-43.9	**-44.0**
	0–10 mm + b&g + PVC (NIR)	c	4193	2492	2896	2559	3091	**3046**	183	96	128	110	147	**133**
		Δc [%]	-36.7	-65.2	-40.6	-42.3	-46.8	**-46.3**	-40.5	-70.5	-44.8	-45.6	-50.8	**-50.4**
	0–20 mm + b&g + PVC (NIR)	c	4108	2175	2752	2521	2121	**2735**	176	82	121	107	99	**117**
		Δc [%]	-37.9	-69.6	-43.6	-43.2	-63.5	**-51.6**	-42.7	-74.8	-48.0	-46.9	-66.9	**-55.9**
	0–5 mm + b&g + PET (NIR)	c	4676	3673	3036	3023	3638	**3609**	206	145	133	130	177	**158**
		Δc [%]	-29.4	-48.7	-37.8	-31.9	-37.4	**-37.0**	-32.8	-55.3	-42.6	-35.4	-40.9	**-41.4**
	0–10 mm + b&g + PET (NIR)	c	4622	2742	2629	2842	3256	**3218**	202	103	114	122	155	**139**
		Δc [%]	-30.2	-61.7	-46.1	-36.0	-43.9	**-43.6**	-34.2	-68.2	-51.0	-39.7	-48.1	**-48.3**
	0–20 mm + b&g + PET (NIR)	c	4638	2425	2438	2823	2232	**2911**	199	88	104	120	104	**123**
		Δc [%]	-29.9	-66.1	-50.0	-36.4	-61.6	**-48.8**	-35.2	-72.7	-55.1	-40.7	-65.3	**-53.8**
	0–5 mm + b&g + PET (NIR) + PVC (NIR)	c	4772	3475	2973	2883	3755	**3572**	212	136	131	124	185	**157**
		Δc [%]	-27.9	-51.5	-39.0	-35.0	-35.4	**-37.8**	-31.1	-57.9	-43.8	-38.7	-38.2	**-41.9**
	0–10 mm + b&g + PET (NIR) + PVC (NIR)	c	4721	2473	2550	2682	3328	**3151**	208	92	110	114	160	**137**
		Δc [%]	-28.7	-65.5	-47.7	-39.6	-42.7	**-44.8**	-32.5	-71.6	-52.5	-43.4	-46.4	**-49.3**
	0–20 mm + b&g + PET (NIR) + PVC (NIR)	c	4767	2100	2346	2647	2159	**2804**	206	76	100	111	101	**119**
		Δc [%]	-28.0	-70.7	-51.9	-40.3	-62.8	**-50.7**	-33.1	-76.6	-56.9	-44.8	-66.1	**-55.5**

More targeted removal	PVC (FTIR) + b&g PVC	c	6669	7085	4872	4513	5847	**5797**	310	320	232	204	301	**273**
		Δc [%]	0.7	-1.1	-0.1	1.7	0.7	0.4	0.8	-1.2	0.0	1.3	0.6	0.3
	0–5 mm + PVC (FTIR) + b&g PVC	c	3654	3568	3294	3133	3175	**3365**	158	144	148	134	147	**146**
		Δc [%]	-44.8	-50.2	-32.5	-29.4	-45.3	**-40.4**	-48.7	-55.5	-36.2	-33.7	-50.7	**-45.0**
	0–10 mm + PVC (FTIR) + b&g PVC	c	3564	2854	3025	2997	2872	**3063**	153	111	135	127	131	**131**
		Δc [%]	-46.2	-60.1	-38.0	-32.5	-50.6	**-45.5**	-50.4	-65.7	-42.0	-37.0	-56.1	**-50.2**
	0–20 mm + PVC (FTIR) + b&g PVC	c	3403	2636	2920	2993	2104	**2811**	144	101	129	126	94	**119**
		Δc [%]	-48.6	-63.2	-40.1	-32.5	-63.8	**-49.7**	-53.3	-68.8	-44.4	-37.6	-68.5	**-54.5**
	PVC (NIR) + b&g PVC	c	6814	7121	4881	4420	6052	**5858**	319	322	233	201	316	**278**
		Δc [%]	2.9	-0.6	0.1	-0.4	4.2	1.2	3.6	-0.6	0.2	-0.5	5.6	1.7
	0–5 mm + PVC (NIR) + b&g PVC	c	3632	3569	3283	2986	3197	**3333**	157	144	148	128	149	**145**
		Δc [%]	-45.1	-50.2	-32.7	-32.7	-45.0	**-41.1**	-48.9	-55.5	-36.5	-36.8	-50.1	**-45.6**
	0–10 mm + PVC (NIR) + b&g PVC	c	3535	2845	3011	2841	2869	**3020**	152	111	134	121	132	**130**
		Δc [%]	-46.6	-60.3	-38.3	-36.0	-50.6	**-46.3**	-50.7	-65.8	-42.3	-40.3	-56.0	**-51.0**
	0–20 mm + PVC (NIR) + b&g PVC	c	3356	2622	2903	2827	2030	**2747**	142	100	128	119	91	**116**
		Δc [%]	-49.3	-63.4	-40.5	-36.3	-65.1	**-50.9**	-53.9	-69.0	-44.8	-41.0	-69.5	**-55.6**
	PET (FTIR) + Textiles + b&g PET	c	7048	7350	5031	4606	6141	**6035**	328	331	239	209	319	**285**
		Δc [%]	6.5	2.6	3.2	3.8	5.7	4.4	6.7	2.2	3.1	3.6	6.6	4.4
	0–5 mm + PET (FTIR) + Textiles + b&g PET	c	3836	3778	3371	3173	3279	**3487**	165	151	151	135	152	**151**
		Δc [%]	-42.1	-47.2	-30.9	-28.5	-43.6	**-38.4**	-46.4	-53.2	-35.1	-33.0	-49.1	**-43.4**
	0–10 mm + PET (FTIR) + Textiles + b&g PET	c	3748	3064	3088	3032	2952	**3177**	160	118	137	128	135	**135**
		Δc [%]	-43.4	-57.2	-36.7	-31.7	-49.2	**-43.6**	-48.1	-63.5	-41.2	-36.4	-55.0	**-48.8**
	0–20 mm + PET (FTIR) + Textiles + b&g PET	c	3602	2860	2979	3030	2112	**2917**	151	108	131	127	94	**122**
		Δc [%]	-45.6	-60.1	-38.9	-31.7	-63.6	**-48.0**	-51.0	-66.5	-43.7	-36.9	-68.5	**-53.3**
	b&g Other	c	7324	7340	5094	4317	6076	**6030**	337	329	240	195	312	**283**
		Δc [%]	10.6	2.5	4.4	-2.7	4.6	3.9	9.6	1.8	3.4	-3.4	4.5	3.2
	0–5 mm + b&g Other	c	4034	3516	3261	2818	3266	**3379**	171	139	144	119	150	**145**
		Δc [%]	-39.1	-50.9	-33.1	-36.5	-43.8	**-40.7**	-44.5	-56.9	-38.2	-40.9	-49.7	**-46.0**
	0–10 mm + b&g Other	c	3954	2710	2942	2662	2947	**3043**	166	103	128	112	133	**128**
		Δc [%]	-40.3	-62.2	-39.7	-40.0	-49.3	**-46.3**	-46.1	-68.1	-44.9	-44.5	-55.4	**-51.8**
	0–20 mm + b&g Other	c	3840	2445	2811	2635	2127	**2771**	158	91	121	110	94	**115**
		Δc [%]	-42.0	-65.9	-42.4	-40.6	-63.4	**-50.8**	-48.7	-71.9	-47.9	-45.6	-68.4	**-56.5**
	PVC (FTIR) + b&g PVC + b&g Other	c	7386	7259	5090	4396	6120	**6050**	340	325	240	198	314	**284**
		Δc [%]	11.6	1.4	4.4	-0.9	5.4	4.3	10.6	0.5	3.5	-2.1	5.2	3.6
	0–5 mm + PVC (FTIR) + b&g PVC + b&g Other	c	4069	3349	3235	2861	3288	**3360**	172	132	142	120	151	**144**
		Δc [%]	-38.5	-53.2	-33.7	-35.5	-43.4	**-40.9**	-44.0	-59.1	-38.7	-40.4	-49.4	**-46.3**
	0–10 mm + PVC (FTIR) + b&g PVC + b&g Other	c	3990	2503	2911	2700	2966	**3014**	167	95	127	113	134	**127**
		Δc [%]	-39.7	-65.0	-40.3	-39.1	-48.9	**-46.6**	-45.7	-70.7	-45.5	-44.1	-55.2	**-52.2**
	0–20 mm + PVC (FTIR) + b&g PVC + b&g Other	c	3881	2207	2776	2675	2138	**2735**	159	82	120	111	95	**113**
		Δc [%]	-41.4	-69.2	-43.1	-39.7	-63.2	**-51.3**	-48.3	-74.7	-48.5	-45.2	-68.4	**-57.0**
	PVC (NIR) + b&g PVC + b&g Other	c	7593	7300	5103	4291	6360	**6130**	352	327	241	193	332	**289**
		Δc [%]	14.7	2.0	4.6	-3.3	9.5	5.5	14.5	1.2	3.8	-4.2	11.0	5.2
	0–5 mm + PVC (NIR) + b&g PVC + b&g Other	c	4074	3346	3222	2690	3322	**3331**	172	132	142	113	154	**143**
		Δc [%]	-38.5	-53.3	-33.9	-39.4	-42.8	**-41.6**	-43.9	-59.1	-39.0	-43.9	-48.6	**-46.9**
	0–10 mm + PVC (NIR) + b&g PVC + b&g Other	c	3989	2487	2892	2517	2971	**2971**	167	94	126	105	135	**125**
		Δc [%]	-39.7	-65.3	-40.7	-43.3	-48.8	**-47.6**	-45.6	-70.9	-45.9	-47.9	-54.9	**-53.1**
	0–20 mm + PVC (NIR) + b&g PVC + b&g Other	c	3870	2183	2753	2478	2060	**2669**	158	81	118	102	91	**110**
		Δc [%]	-41.6	-69.5	-43.5	-44.2	-64.5	**-52.7**	-48.5	-75.1	-49.0	-49.2	-69.4	**-58.2**
	b&g Other + b&g PVC	c	7350	7347	5103	4326	6078	**6041**	338	330	241	195	313	**283**
		Δc [%]	11.0	2.6	4.6	-2.5	4.6	4.1	10.1	1.9	3.7	-3.3	4.5	3.4
	0–5 mm + b&g Other + b&g PVC	c	4048	3521	3267	2818	3267	**3384**	171	140	144	119	151	**145**
		Δc [%]	-38.9	-50.8	-33.0	-36.5	-43.7	**-40.6**	-44.3	-56.8	-38.1	-40.9	-49.7	**-46.0**
	0–10 mm + b&g Other + b&g PVC	c	3969	2714	2948	2659	2947	**3047**	166	103	128	112	133	**129**
		Δc [%]	-40.1	-62.1	-39.6	-40.1	-49.3	**-46.2**	-45.9	-68.1	-44.8	-44.6	-55.4	**-51.8**
	0–20 mm + b&g Other + b&g PVC	c	3857	2449	2816	2632	2128	**2776**	158	91	121	110	94	**115**
		Δc [%]	-41.8	-65.8	-42.3	-40.7	-63.4	**-50.8**	-48.5	-71.8	-47.8	-45.7	-68.4	**-56.5**

B.14. Hg

Table B.14: Relative concentration change (Δc, in %) of Hg caused by the removal of different material or particle size fractions referring to mg/kg and mg/MJ, both calculated for dry mass without hard impurities

	Removed fractions	Conc. after removal	mg/kg$_{DM}$						mg/MJ					
			S01	S02	S03	S04	S05	Avr	S01	S02	S03	S04	S05	Avr
Single process steps	0–5 mm	c	0.60	0.50	0.30	0.25	0.29	**0.39**	0.026	0.020	0.013	0.011	0.014	**0.017**
		Δc [%]	-6.1	-5.1	-18.9	-34.9	2.0	**-12.6**	-12.7	-15.0	-23.5	-38.6	-8.0	**-19.5**
	0–10 mm	c	0.62	0.53	0.29	0.25	0.29	**0.40**	0.027	0.021	0.013	0.011	0.013	**0.017**
		Δc [%]	-3.2	0.6	-20.5	-34.9	2.6	**-11.1**	-10.8	-13.0	-25.8	-38.9	-8.9	**-19.5**
	0–20 mm	c	0.68	0.56	0.29	0.25	0.26	**0.41**	0.029	0.022	0.013	0.011	0.012	**0.017**
		Δc [%]	6.0	6.2	-20.0	-34.9	-10.5	**-10.6**	-3.7	-9.7	-25.7	-39.4	-21.9	**-20.1**
	PET (NIR)	c	0.68	0.55	0.38	0.40	0.29	**0.46**	0.032	0.025	0.018	0.018	0.015	**0.022**
		Δc [%]	5.8	4.2	4.1	4.0	1.6	**4.0**	7.1	3.6	3.4	4.2	3.4	**4.4**
	PVC (NIR)	c	0.66	0.52	0.36	0.39	0.29	**0.45**	0.031	0.024	0.017	0.018	0.015	**0.021**
		Δc [%]	3.4	-1.0	0.1	1.6	1.0	**1.0**	4.0	-1.1	0.2	1.5	2.4	**1.4**
	b&g	c	0.71	0.56	0.39	0.40	0.29	**0.47**	0.034	0.026	0.019	0.019	0.016	**0.022**
		Δc [%]	10.2	6.1	6.0	4.5	1.5	**5.7**	13.5	7.1	7.1	6.3	6.2	**8.0**
	PET + PVC (NIR)	c	0.70	0.55	0.38	0.41	0.29	**0.47**	0.033	0.025	0.018	0.019	0.016	**0.022**
		Δc [%]	10.0	3.2	4.3	6.0	2.9	**5.3**	12.2	2.6	3.7	6.2	6.5	**6.2**
Combinations of Screening and state-of-the-art NIR sorting or manual removal of black materials	0–5 mm + PET (NIR)	c	0.64	0.53	0.30	0.25	0.30	**0.40**	0.028	0.021	0.013	0.011	0.014	**0.017**
		Δc [%]	0.0	-0.4	-17.0	-34.9	4.2	**-9.6**	-6.7	-12.3	-22.9	-38.9	-5.6	**-17.3**
	0–10 mm + PET (NIR)	c	0.66	0.56	0.30	0.25	0.30	**0.41**	0.029	0.022	0.013	0.011	0.014	**0.017**
		Δc [%]	3.6	6.6	-18.9	-34.9	5.0	**-7.7**	-4.2	-9.9	-25.5	-39.3	-6.6	**-17.1**
	0–20 mm + PET (NIR)	c	0.74	0.60	0.30	0.25	0.26	**0.43**	0.031	0.023	0.013	0.011	0.012	**0.018**
		Δc [%]	15.6	13.6	-18.1	-34.9	-10.1	**-6.8**	5.1	-5.9	-25.5	-39.8	-21.7	**-17.5**
	0–5 mm + PVC (NIR)	c	0.62	0.50	0.29	0.25	0.30	**0.39**	0.027	0.020	0.013	0.011	0.014	**0.017**
		Δc [%]	-2.6	-6.5	-19.2	-34.9	3.3	**-12.0**	-9.3	-16.5	-23.8	-38.8	-6.3	**-18.9**
	0–10 mm + PVC (NIR)	c	0.65	0.53	0.29	0.25	0.30	**0.40**	0.028	0.020	0.013	0.011	0.014	**0.017**
		Δc [%]	0.7	-0.8	-20.9	-34.9	4.0	**-10.4**	-7.0	-14.6	-26.2	-39.2	-7.2	**-18.8**
	0–20 mm + PVC (NIR)	c	0.71	0.55	0.29	0.25	0.26	**0.41**	0.030	0.021	0.013	0.011	0.012	**0.017**
		Δc [%]	11.4	4.8	-20.4	-34.9	-10.2	**-9.9**	1.3	-11.3	-26.1	-39.7	-21.5	**-19.5**
	0–5 mm + PET (NIR) + PVC (NIR)	c	0.67	0.52	0.30	0.25	0.30	**0.41**	0.029	0.021	0.013	0.011	0.014	**0.018**
		Δc [%]	4.5	-1.8	-17.4	-34.9	6.0	**-8.7**	-2.3	-13.8	-23.2	-39.2	-3.3	**-16.4**
	0–10 mm + PET (NIR) + PVC (NIR)	c	0.70	0.56	0.29	0.25	0.31	**0.42**	0.030	0.021	0.013	0.011	0.014	**0.018**
		Δc [%]	8.6	5.2	-19.3	-34.9	7.0	**-6.7**	0.7	-11.6	-26.0	-39.6	-4.4	**-16.2**
	0–20 mm + PET (NIR) + PVC (NIR)	c	0.79	0.59	0.30	0.25	0.26	**0.44**	0.033	0.022	0.013	0.010	0.012	**0.018**
		Δc [%]	22.9	12.3	-18.5	-34.9	-9.8	**-5.6**	11.9	-7.6	-25.9	-40.2	-21.2	**-16.6**
	0–5 mm + b&g	c	0.67	0.54	0.30	0.25	0.30	**0.41**	0.029	0.022	0.014	0.011	0.014	**0.018**
		Δc [%]	4.8	1.9	-16.5	-34.9	4.1	**-8.1**	-1.1	-9.3	-21.4	-37.9	-2.9	**-14.5**
	0–10 mm + b&g	c	0.70	0.58	0.30	0.25	0.30	**0.43**	0.030	0.022	0.013	0.011	0.014	**0.018**
		Δc [%]	8.9	9.5	-18.5	-34.9	4.9	**-6.0**	2.0	-6.6	-24.2	-38.3	-3.8	**-14.2**
	0–20 mm + b&g	c	0.79	0.62	0.30	0.25	0.26	**0.44**	0.034	0.023	0.013	0.011	0.012	**0.019**
		Δc [%]	23.3	17.3	-17.6	-34.9	-10.1	**-4.4**	13.6	-1.9	-24.1	-38.8	-19.1	**-14.1**
	0–5 mm + b&g + PVC (NIR)	c	0.71	0.53	0.30	0.25	0.30	**0.42**	0.031	0.021	0.014	0.011	0.015	**0.018**
		Δc [%]	10.1	0.4	-16.9	-34.9	5.8	**-7.1**	4.3	-10.9	-21.7	-38.2	-0.3	**-13.4**
	0–10 mm + b&g + PVC (NIR)	c	0.74	0.57	0.30	0.25	0.31	**0.43**	0.032	0.022	0.013	0.011	0.015	**0.018**
		Δc [%]	15.0	8.1	-18.9	-34.9	6.8	**-4.8**	8.0	-8.2	-24.7	-38.6	-1.2	**-12.9**
	0–20 mm + b&g + PVC (NIR)	c	0.85	0.62	0.30	0.25	0.26	**0.45**	0.036	0.023	0.013	0.011	0.012	**0.019**
		Δc [%]	32.4	16.1	-18.1	-34.9	-9.8	**-2.8**	22.3	-3.6	-24.5	-39.2	-18.3	**-12.7**
	0–5 mm + b&g + PET (NIR)	c	0.73	0.57	0.31	0.25	0.31	**0.44**	0.032	0.023	0.014	0.011	0.015	**0.019**
		Δc [%]	14.2	8.3	-13.8	-34.9	7.0	**-3.8**	8.6	-5.6	-20.4	-38.2	0.9	**-10.9**
	0–10 mm + b&g + PET (NIR)	c	0.77	0.62	0.31	0.25	0.31	**0.45**	0.034	0.023	0.013	0.011	0.015	**0.019**
		Δc [%]	19.8	18.0	-16.0	-34.9	8.1	**-1.0**	12.9	-2.1	-23.7	-38.7	0.0	**-10.3**
	0–20 mm + b&g + PET (NIR)	c	0.90	0.68	0.31	0.25	0.26	**0.48**	0.039	0.025	0.013	0.011	0.012	**0.020**
		Δc [%]	40.1	28.4	-14.8	-34.9	-9.6	**1.9**	29.6	3.6	-23.4	-39.3	-18.3	**-9.6**
	0–5 mm + b&g + PET (NIR) + PVC (NIR)	c	0.78	0.57	0.31	0.25	0.31	**0.44**	0.035	0.022	0.014	0.011	0.015	**0.019**
		Δc [%]	21.4	6.9	-14.1	-34.9	9.5	**-2.2**	16.1	-7.2	-20.8	-38.5	4.6	**-9.2**
	0–10 mm + b&g + PET (NIR) + PVC (NIR)	c	0.82	0.62	0.30	0.25	0.32	**0.46**	0.036	0.023	0.013	0.011	0.015	**0.020**
		Δc [%]	28.2	16.8	-16.4	-34.9	10.9	**0.9**	21.4	-3.8	-24.1	-39.0	3.7	**-8.4**
	0–20 mm + b&g + PET (NIR) + PVC (NIR)	c	0.99	0.68	0.31	0.25	0.26	**0.50**	0.043	0.024	0.013	0.011	0.012	**0.021**
		Δc [%]	53.8	27.5	-15.2	-34.9	-9.1	**4.4**	42.8	1.9	-23.9	-39.7	-17.1	**-7.2**

More targeted removal	PVC (FTIR) + b&g PVC	c	0.64	0.53	0.36	0.39	0.29	**0.44**	0.030	0.024	0.017	0.018	0.015	**0.021**
		Δc [%]	0.5	0.7	-0.2	0.9	0.1	0.4	0.6	0.5	-0.1	0.5	0.0	0.3
	0–5 mm + PVC (FTIR) + b&g PVC	c	0.61	0.51	0.29	0.25	0.29	**0.39**	0.026	0.020	0.013	0.011	0.014	**0.017**
		Δc [%]	-5.5	-4.3	-19.3	-34.9	2.1	-12.4	-12.2	-14.6	-23.8	-38.9	-8.0	-19.5
	0–10 mm + PVC (FTIR) + b&g PVC	c	0.62	0.54	0.29	0.25	0.29	**0.40**	0.027	0.021	0.013	0.011	0.013	**0.017**
		Δc [%]	-2.6	1.5	-21.0	-34.9	2.7	-10.9	-10.2	-12.6	-26.2	-39.3	-8.9	-19.4
	0–20 mm + PVC (FTIR) + b&g PVC	c	0.68	0.57	0.29	0.25	0.26	**0.41**	0.029	0.022	0.013	0.011	0.011	**0.017**
		Δc [%]	6.8	7.3	-20.5	-34.9	-10.4	-10.3	-3.0	-9.1	-26.2	-39.7	-22.0	-20.0
	PVC (NIR) + b&g PVC	c	0.66	0.52	0.36	0.39	0.29	**0.45**	0.031	0.024	0.017	0.018	0.015	**0.021**
		Δc [%]	3.6	-1.0	0.1	1.8	1.0	1.1	4.3	-1.0	0.3	1.7	2.4	1.5
	0–5 mm + PVC (NIR) + b&g PVC	c	0.63	0.50	0.29	0.25	0.30	**0.39**	0.027	0.020	0.013	0.011	0.014	**0.017**
		Δc [%]	-2.3	-6.4	-19.2	-34.9	3.3	-11.9	-9.0	-16.4	-23.7	-38.8	-6.3	-18.9
	0–10 mm + PVC (NIR) + b&g PVC	c	0.65	0.53	0.29	0.25	0.30	**0.40**	0.028	0.020	0.013	0.011	0.014	**0.017**
		Δc [%]	1.0	-0.8	-20.9	-34.9	4.0	-10.3	-6.7	-14.6	-26.1	-39.2	-7.2	-18.8
	0–20 mm + PVC (NIR) + b&g PVC	c	0.72	0.56	0.29	0.25	0.26	**0.41**	0.030	0.021	0.013	0.011	0.012	**0.017**
		Δc [%]	11.8	4.9	-20.3	-34.9	-10.2	-9.8	1.7	-11.3	-26.1	-39.7	-21.5	-19.4
	PET (FTIR) + Textiles + b&g PET	c	0.67	0.54	0.37	0.39	0.29	**0.45**	0.031	0.024	0.018	0.018	0.015	**0.021**
		Δc [%]	5.1	1.9	2.1	2.4	1.1	2.5	5.3	1.5	2.0	2.2	1.9	2.6
	0–5 mm + PET (FTIR) + Textiles + b&g PET	c	0.64	0.51	0.30	0.25	0.30	**0.40**	0.027	0.021	0.013	0.011	0.014	**0.017**
		Δc [%]	-0.7	-3.0	-17.9	-34.9	3.4	-10.6	-8.2	-13.9	-23.0	-38.9	-6.8	-18.2
	0–10 mm + PET (FTIR) + Textiles + b&g PET	c	0.66	0.55	0.29	0.25	0.30	**0.41**	0.028	0.021	0.013	0.011	0.014	**0.017**
		Δc [%]	2.7	3.2	-19.7	-34.9	4.2	-8.9	-5.8	-11.9	-25.5	-39.3	-7.7	-18.0
	0–20 mm + PET (FTIR) + Textiles + b&g PET	c	0.73	0.58	0.30	0.25	0.26	**0.42**	0.031	0.022	0.013	0.010	0.011	**0.017**
		Δc [%]	14.1	9.5	-19.1	-34.9	-10.2	-8.1	2.8	-8.2	-25.4	-39.8	-22.1	-18.5
	b&g Other	c	0.69	0.55	0.38	0.40	0.29	**0.46**	0.032	0.025	0.018	0.018	0.015	**0.021**
		Δc [%]	7.3	4.6	4.9	3.0	0.8	4.1	6.3	3.9	3.9	2.3	0.7	3.4
	0–5 mm + b&g Other	c	0.65	0.53	0.30	0.25	0.30	**0.41**	0.028	0.021	0.013	0.011	0.014	**0.017**
		Δc [%]	1.7	0.1	-17.0	-34.9	3.1	-9.4	-7.4	-12.1	-23.3	-39.4	-7.7	-18.0
	0–10 mm + b&g Other	c	0.68	0.57	0.30	0.25	0.30	**0.42**	0.028	0.022	0.013	0.011	0.013	**0.017**
		Δc [%]	5.4	7.2	-19.0	-34.9	3.8	-7.5	-4.9	-9.8	-26.0	-39.8	-8.7	-17.8
	0–20 mm + b&g Other	c	0.76	0.61	0.30	0.25	0.26	**0.43**	0.031	0.023	0.013	0.010	0.011	**0.018**
		Δc [%]	17.9	14.4	-18.2	-34.9	-10.3	-6.2	4.2	-5.7	-26.0	-40.3	-22.7	-18.1
	PVC (FTIR) + b&g PVC + b&g Other	c	0.69	0.56	0.38	0.40	0.29	**0.46**	0.032	0.025	0.018	0.018	0.015	**0.022**
		Δc [%]	8.0	5.4	4.6	4.1	0.9	4.6	7.0	4.5	3.8	2.9	0.8	3.8
	0–5 mm + PVC (FTIR) + b&g PVC + b&g Other	c	0.66	0.53	0.30	0.25	0.30	**0.41**	0.028	0.021	0.013	0.011	0.014	**0.017**
		Δc [%]	2.4	1.0	-17.5	-34.9	3.3	-9.1	-6.8	-11.7	-23.7	-39.8	-7.8	-17.9
	0–10 mm + PVC (FTIR) + b&g PVC + b&g Other	c	0.68	0.57	0.29	0.25	0.30	**0.42**	0.028	0.022	0.013	0.010	0.013	**0.017**
		Δc [%]	6.2	8.4	-19.5	-34.9	4.0	-7.2	-4.2	-9.2	-26.5	-40.2	-8.7	-17.8
	0–20 mm + PVC (FTIR) + b&g PVC + b&g Other	c	0.76	0.61	0.30	0.25	0.26	**0.44**	0.031	0.023	0.013	0.010	0.011	**0.018**
		Δc [%]	19.0	15.9	-18.7	-34.9	-10.2	-5.8	5.1	-5.0	-26.5	-40.8	-22.8	-18.0
	PVC (NIR) + b&g PVC + b&g Other	c	0.72	0.55	0.38	0.40	0.29	**0.47**	0.033	0.025	0.018	0.018	0.015	**0.022**
		Δc [%]	11.9	3.6	5.1	5.2	2.0	5.6	11.7	2.9	4.3	4.2	3.3	5.3
	0–5 mm + PVC (NIR) + b&g PVC + b&g Other	c	0.68	0.52	0.30	0.25	0.30	**0.41**	0.029	0.021	0.013	0.011	0.014	**0.017**
		Δc [%]	6.7	-1.3	-17.3	-34.9	4.7	-8.4	-2.7	-13.7	-23.6	-39.7	-5.9	-17.1
	0–10 mm + PVC (NIR) + b&g PVC + b&g Other	c	0.71	0.56	0.29	0.25	0.30	**0.42**	0.030	0.021	0.013	0.010	0.014	**0.018**
		Δc [%]	11.1	5.9	-19.3	-34.9	5.5	-6.3	0.2	-11.4	-26.4	-40.2	-6.9	-16.9
	0–20 mm + PVC (NIR) + b&g PVC + b&g Other	c	0.81	0.60	0.30	0.25	0.26	**0.44**	0.033	0.022	0.013	0.010	0.011	**0.018**
		Δc [%]	26.1	13.3	-18.5	-34.9	-10.0	-4.8	11.2	-7.3	-26.4	-40.8	-22.4	-17.1
	b&g Other + b&g PVC	c	0.69	0.55	0.38	0.40	0.29	**0.46**	0.032	0.025	0.018	0.018	0.015	**0.021**
		Δc [%]	7.6	4.7	4.9	3.3	0.8	4.3	6.7	4.0	4.0	2.5	0.7	3.6
	0–5 mm + b&g Other + b&g PVC	c	0.65	0.53	0.30	0.25	0.30	**0.41**	0.028	0.021	0.013	0.011	0.014	**0.017**
		Δc [%]	2.0	0.1	-17.0	-34.9	3.1	-9.3	-7.1	-12.1	-23.2	-39.4	-7.7	-17.9
	0–10 mm + b&g Other + b&g PVC	c	0.68	0.57	0.30	0.25	0.30	**0.42**	0.028	0.022	0.013	0.010	0.013	**0.017**
		Δc [%]	5.7	7.3	-18.9	-34.9	3.8	-7.4	-4.6	-9.7	-26.0	-39.9	-8.7	-17.8
	0–20 mm + b&g Other + b&g PVC	c	0.76	0.61	0.30	0.25	0.26	**0.43**	0.031	0.023	0.013	0.010	0.011	**0.018**
		Δc [%]	18.4	14.6	-18.1	-34.9	-10.3	-6.1	4.6	-5.6	-25.9	-40.4	-22.7	-18.0

B.15. K

Table B.15: Relative concentration change (Δc, in %) of K caused by the removal of different material or particle size fractions referring to mg/kg and mg/MJ, both calculated for dry mass without hard impurities

	Removed fractions	Conc. after removal	mg/kg$_{DM}$ S01	S02	S03	S04	S05	Avr	mg/MJ S01	S02	S03	S04	S05	Avr
Single process steps	0–5 mm	c	687	1007	949	839	1396	**975**	30	41	43	36	65	**43**
		Δc [%]	-33.4	-22.6	-20.1	-19.5	-30.2	**-25.2**	-38.1	-30.7	-24.7	-24.0	-37.0	**-30.9**
	0–10 mm	c	660	918	900	819	1305	**920**	28	36	40	35	60	**40**
		Δc [%]	-36.0	-29.5	-24.3	-21.3	-34.8	**-29.2**	-41.0	-39.0	-29.3	-26.2	-42.1	**-35.5**
	0–20 mm	c	524	866	871	792	1223	**855**	22	33	39	34	55	**36**
		Δc [%]	-49.2	-33.4	-26.7	-23.9	-38.9	**-34.4**	-53.8	-43.4	-31.9	-29.2	-46.7	**-41.0**
	PET (NIR)	c	1100	1356	1288	1099	2099	**1388**	52	61	61	50	110	**67**
		Δc [%]	6.6	4.2	8.4	5.5	4.9	**5.9**	7.9	3.6	7.7	5.7	6.7	**6.3**
	PVC (NIR)	c	1042	1318	1198	1071	2021	**1330**	49	60	57	49	105	**64**
		Δc [%]	1.1	1.3	0.8	2.8	1.0	**1.4**	1.7	1.2	0.9	2.7	2.3	**1.8**
	b&g	c	1173	1365	1331	1066	2174	**1422**	56	62	64	49	117	**70**
		Δc [%]	13.7	4.9	12.0	2.4	8.6	**8.3**	17.0	5.9	13.2	4.2	13.6	**10.8**
	PET + PVC (NIR)	c	1117	1375	1301	1135	2130	**1411**	53	62	62	52	114	**68**
		Δc [%]	8.3	5.6	9.5	9.0	6.4	**7.8**	10.5	5.0	8.9	9.1	10.2	**8.7**
Combinations of Screening and state-of-the-art NIR sorting or manual removal of black materials	0–5 mm + PET (NIR)	c	723	1044	1024	877	1421	**1018**	31	42	45	37	66	**44**
		Δc [%]	-29.9	-19.8	-13.8	-15.7	-29.0	**-21.6**	-34.6	-29.3	-19.9	-20.9	-35.7	**-28.1**
	0–10 mm + PET (NIR)	c	694	950	971	857	1317	**958**	30	36	42	36	60	**41**
		Δc [%]	-32.7	-27.0	-18.2	-17.7	-34.2	**-26.0**	-37.7	-38.3	-24.9	-23.3	-41.5	**-33.1**
	0–20 mm + PET (NIR)	c	543	895	942	828	1221	**886**	23	33	41	35	55	**37**
		Δc [%]	-47.4	-31.2	-20.7	-20.4	-39.0	**-31.7**	-52.1	-43.0	-27.8	-26.5	-46.9	**-39.2**
	0–5 mm + PVC (NIR)	c	676	1019	954	861	1363	**975**	29	41	43	37	64	**43**
		Δc [%]	-34.5	-21.7	-19.7	-17.3	-31.9	**-25.0**	-39.0	-30.1	-24.2	-22.2	-38.2	**-30.8**
	0–10 mm + PVC (NIR)	c	646	929	905	842	1262	**917**	28	36	40	36	58	**40**
		Δc [%]	-37.3	-28.6	-23.9	-19.2	-37.0	**-29.2**	-42.1	-38.5	-28.9	-24.5	-43.8	**-35.6**
	0–20 mm + PVC (NIR)	c	496	877	876	815	1168	**846**	21	34	39	34	53	**36**
		Δc [%]	-51.9	-32.6	-26.3	-21.8	-41.7	**-34.8**	-56.2	-43.0	-31.6	-27.5	-49.0	**-41.5**
	0–5 mm + PET (NIR) + PVC (NIR)	c	713	1059	1033	905	1385	**1019**	31	42	46	38	65	**44**
		Δc [%]	-30.9	-18.6	-13.1	-13.0	-30.8	**-21.3**	-35.3	-28.6	-19.3	-18.8	-36.9	**-27.8**
	0–10 mm + PET (NIR) + PVC (NIR)	c	682	963	978	885	1267	**955**	29	37	43	37	58	**41**
		Δc [%]	-33.9	-26.0	-17.6	-15.0	-36.7	**-25.9**	-38.7	-37.8	-24.4	-21.2	-43.4	**-33.1**
	0–20 mm + PET (NIR) + PVC (NIR)	c	512	908	949	857	1155	**876**	22	34	41	36	52	**37**
		Δc [%]	-50.3	-30.2	-20.1	-17.7	-42.3	**-32.1**	-54.8	-42.6	-27.3	-24.4	-49.6	**-39.7**
	0–5 mm + b&g	c	778	1040	1053	837	1513	**1044**	34	42	47	36	73	**46**
		Δc [%]	-24.6	-20.1	-11.3	-19.6	-24.4	**-20.0**	-28.8	-28.8	-16.5	-23.4	-29.5	**-25.4**
	0–10 mm + b&g	c	750	939	997	815	1414	**983**	33	36	44	35	67	**43**
		Δc [%]	-27.3	-27.8	-16.0	-21.7	-29.4	**-24.4**	-31.9	-38.4	-22.0	-25.9	-35.2	**-30.7**
	0–20 mm + b&g	c	594	880	968	783	1327	**910**	25	33	43	33	61	**39**
		Δc [%]	-42.5	-32.4	-18.5	-24.8	-33.7	**-30.4**	-47.0	-43.5	-24.9	-29.4	-40.4	**-37.0**
	0–5 mm + b&g + PVC (NIR)	c	772	1055	1063	863	1487	**1048**	34	42	48	37	72	**47**
		Δc [%]	-25.2	-18.9	-10.5	-17.1	-25.7	**-19.5**	-29.1	-28.1	-15.8	-21.3	-30.0	**-24.9**
	0–10 mm + b&g + PVC (NIR)	c	741	953	1006	841	1376	**983**	32	37	45	36	65	**43**
		Δc [%]	-28.1	-26.7	-15.3	-19.3	-31.3	**-24.2**	-32.5	-37.8	-21.3	-23.9	-36.4	**-30.4**
	0–20 mm + b&g + PVC (NIR)	c	565	893	976	809	1275	**904**	24	33	43	34	59	**39**
		Δc [%]	-45.2	-31.4	-17.8	-22.3	-36.3	**-30.6**	-49.4	-43.0	-24.3	-27.4	-42.4	**-37.3**
	0–5 mm + b&g + PET (NIR)	c	838	1088	1169	882	1562	**1108**	37	43	51	38	76	**49**
		Δc [%]	-18.8	-16.4	-1.6	-15.2	-22.0	**-14.8**	-22.8	-27.1	-9.2	-19.6	-26.4	**-21.0**
	0–10 mm + b&g + PET (NIR)	c	810	981	1108	858	1447	**1041**	35	37	48	37	69	**45**
		Δc [%]	-21.5	-24.6	-6.7	-17.6	-27.7	**-19.6**	-26.0	-37.5	-15.2	-22.4	-33.1	**-26.9**
	0–20 mm + b&g + PET (NIR)	c	634	918	1082	825	1346	**961**	27	33	46	35	63	**41**
		Δc [%]	-38.5	-29.5	-9.0	-20.8	-32.8	**-26.1**	-43.1	-43.1	-18.2	-26.2	-39.2	**-34.0**
	0–5 mm + b&g + PET (NIR) + PVC (NIR)	c	837	1107	1184	916	1537	**1116**	37	43	52	39	76	**50**
		Δc [%]	-18.9	-14.9	-0.4	-12.0	-23.2	**-13.9**	-22.4	-26.2	-8.1	-17.0	-26.6	**-20.0**
	0–10 mm + b&g + PET (NIR) + PVC (NIR)	c	806	998	1122	892	1405	**1045**	35	37	48	38	68	**45**
		Δc [%]	-21.9	-23.3	-5.6	-14.3	-29.8	**-19.0**	-26.0	-36.8	-14.3	-19.8	-34.3	**-26.3**
	0–20 mm + b&g + PET (NIR) + PVC (NIR)	c	604	935	1095	859	1284	**956**	26	34	47	36	60	**41**
		Δc [%]	-41.4	-28.1	-7.8	-17.5	-35.8	**-26.1**	-45.6	-42.6	-17.3	-23.7	-41.5	**-34.1**

More targeted removal	PVC (FTIR) + b&g PVC	c	1038	1316	1194	1065	2013	**1325**	48	59	57	48	104	**63**
		Δc [%]	0.7	1.1	0.5	2.3	0.6	1.0	0.7	1.0	0.6	1.9	0.5	0.9
	0–5 mm + PVC (FTIR) + b&g PVC	c	691	1020	953	859	1403	**985**	30	41	43	37	65	**43**
		Δc [%]	-33.0	-21.6	-19.8	-17.5	-29.9	-24.4	-37.7	-30.0	-24.3	-22.6	-36.8	-30.3
	0–10 mm + PVC (FTIR) + b&g PVC	c	664	931	904	840	1312	**930**	28	36	40	36	60	**40**
		Δc [%]	-35.6	-28.5	-23.9	-19.3	-34.5	-28.4	-40.6	-38.4	-28.9	-24.8	-41.9	-34.9
	0–20 mm + PVC (FTIR) + b&g PVC	c	528	880	875	813	1229	**865**	22	34	39	34	55	**37**
		Δc [%]	-48.9	-32.4	-26.4	-21.9	-38.6	-33.6	-53.5	-42.7	-31.6	-27.7	-46.6	-40.4
	PVC (NIR) + b&g PVC	c	1046	1319	1200	1076	2021	**1332**	49	60	57	49	105	**64**
		Δc [%]	1.4	1.3	1.0	3.4	1.0	1.6	2.1	1.3	1.1	3.2	2.3	2.0
	0–5 mm + PVC (NIR) + b&g PVC	c	678	1020	956	866	1364	**977**	29	41	43	37	64	**43**
		Δc [%]	-34.3	-21.6	-19.5	-16.8	-31.9	-24.8	-38.8	-30.0	-24.1	-21.9	-38.2	-30.6
	0–10 mm + PVC (NIR) + b&g PVC	c	649	930	906	846	1262	**919**	28	36	40	36	58	**40**
		Δc [%]	-37.1	-28.5	-23.7	-18.7	-36.9	-29.0	-41.9	-38.5	-28.7	-24.2	-43.8	-35.4
	0–20 mm + PVC (NIR) + b&g PVC	c	498	878	877	819	1168	**848**	21	34	39	34	53	**36**
		Δc [%]	-51.7	-32.5	-26.1	-21.3	-41.7	-34.7	-56.1	-42.9	-31.5	-27.2	-49.0	-41.3
	PET (FTIR) + Textiles + b&g PET	c	1089	1326	1240	1073	2077	**1361**	51	60	59	49	108	**65**
		Δc [%]	5.6	1.9	4.4	3.1	3.8	3.7	5.8	1.4	4.3	2.9	4.6	3.8
	0–5 mm + PET (FTIR) + Textiles + b&g PET	c	720	1022	989	859	1424	**1003**	31	41	44	37	66	**44**
		Δc [%]	-30.2	-21.4	-16.8	-17.5	-28.9	-22.9	-35.4	-30.3	-21.9	-22.7	-35.9	-29.2
	0–10 mm + PET (FTIR) + Textiles + b&g PET	c	693	930	938	839	1324	**945**	29	36	41	36	60	**41**
		Δc [%]	-32.8	-28.5	-21.1	-19.4	-33.8	-27.1	-38.4	-39.0	-26.7	-25.0	-41.4	-34.1
	0–20 mm + PET (FTIR) + Textiles + b&g PET	c	546	877	909	811	1234	**875**	23	33	40	34	55	**37**
		Δc [%]	-47.1	-32.6	-23.5	-22.1	-38.3	-32.7	-52.3	-43.5	-29.5	-28.1	-46.5	-40.0
	b&g Other	c	1128	1337	1299	1038	2095	**1379**	52	60	61	47	108	**66**
		Δc [%]	9.3	2.7	9.4	-0.3	4.6	5.1	8.3	2.0	8.3	-1.1	4.5	4.4
	0–5 mm + b&g Other	c	751	1015	1027	815	1459	**1014**	32	40	45	34	67	**44**
		Δc [%]	-27.2	-22.0	-13.5	-21.7	-27.1	-22.3	-33.7	-31.5	-20.1	-27.1	-34.8	-29.4
	0–10 mm + b&g Other	c	724	915	972	793	1363	**953**	30	35	42	33	62	**40**
		Δc [%]	-29.8	-29.7	-18.2	-23.9	-31.9	-26.7	-36.6	-40.8	-25.3	-29.6	-40.1	-34.5
	0–20 mm + b&g Other	c	576	855	942	761	1278	**883**	24	32	41	32	57	**37**
		Δc [%]	-44.1	-34.3	-20.7	-26.9	-36.1	-32.4	-50.6	-45.9	-28.2	-33.0	-45.0	-40.5
	PVC (FTIR) + b&g PVC + b&g Other	c	1136	1353	1308	1063	2107	**1393**	52	61	62	48	108	**66**
		Δc [%]	10.1	4.0	10.1	2.1	5.3	6.3	9.2	3.1	9.2	1.0	5.1	5.5
	0–5 mm + PVC (FTIR) + b&g PVC + b&g Other	c	757	1030	1033	837	1467	**1025**	32	41	46	35	67	**44**
		Δc [%]	-26.6	-20.9	-13.0	-19.6	-26.7	-21.4	-33.2	-30.8	-19.6	-25.6	-34.5	-28.7
	0–10 mm + PVC (FTIR) + b&g PVC + b&g Other	c	730	930	978	815	1371	**965**	31	35	43	34	62	**41**
		Δc [%]	-29.2	-28.6	-17.7	-21.8	-31.5	-25.7	-36.2	-40.1	-24.9	-28.1	-39.9	-33.8
	0–20 mm + PVC (FTIR) + b&g PVC + b&g Other	c	581	870	948	783	1285	**894**	24	32	41	32	57	**37**
		Δc [%]	-43.7	-33.1	-20.2	-24.8	-35.8	-31.5	-50.3	-45.2	-27.8	-31.6	-44.8	-39.9
	PVC (NIR) + b&g PVC + b&g Other	c	1151	1357	1316	1076	2124	**1405**	53	61	62	48	111	**67**
		Δc [%]	11.6	4.3	10.8	3.3	6.1	7.2	11.3	3.5	9.9	2.4	7.5	6.9
	0–5 mm + PVC (NIR) + b&g PVC + b&g Other	c	747	1030	1039	844	1429	**1018**	32	41	46	35	66	**44**
		Δc [%]	-27.6	-20.8	-12.6	-19.0	-28.6	-21.7	-34.0	-30.8	-19.2	-25.0	-35.8	-29.0
	0–10 mm + PVC (NIR) + b&g PVC + b&g Other	c	717	929	982	821	1322	**954**	30	35	43	34	60	**40**
		Δc [%]	-30.5	-28.6	-17.3	-21.1	-33.9	-26.3	-37.3	-40.3	-24.6	-27.6	-41.7	-34.3
	0–20 mm + PVC (NIR) + b&g PVC + b&g Other	c	551	868	952	789	1224	**877**	23	32	41	33	54	**37**
		Δc [%]	-46.6	-33.3	-19.9	-24.2	-38.8	-32.6	-52.9	-45.4	-27.6	-31.1	-47.3	-40.9
	b&g Other + b&g PVC	c	1132	1338	1302	1043	2095	**1382**	52	60	61	47	108	**66**
		Δc [%]	9.7	2.8	9.6	0.2	4.7	5.4	8.8	2.1	8.6	-0.6	4.6	4.7
	0–5 mm + b&g Other + b&g PVC	c	754	1016	1030	820	1459	**1016**	32	40	45	35	67	**44**
		Δc [%]	-26.9	-21.9	-13.3	-21.3	-27.1	-22.1	-33.4	-31.4	-19.9	-26.8	-34.8	-29.3
	0–10 mm + b&g Other + b&g PVC	c	727	916	975	797	1364	**956**	30	35	42	33	62	**41**
		Δc [%]	-29.5	-29.6	-17.9	-23.4	-31.9	-26.5	-36.4	-40.7	-25.1	-29.3	-40.1	-34.3
	0–20 mm + b&g Other + b&g PVC	c	579	856	945	766	1279	**885**	24	32	41	32	57	**37**
		Δc [%]	-43.9	-34.2	-20.5	-26.5	-36.1	-32.2	-50.4	-45.8	-28.0	-32.7	-45.0	-40.4

B.16. Li

Table B.16: Relative concentration change (Δc, in %) of Li caused by the removal of different material or particle size fractions referring to mg/kg and mg/MJ, both calculated for dry mass without hard impurities

	Removed fractions	Conc. after removal	mg/kg$_{DM}$ S01	S02	S03	S04	S05	Avr	mg/MJ S01	S02	S03	S04	S05	Avr
Single process steps	0–5 mm	c	1.6	2.8	1.5	2.6	3.0	**2.3**	0.07	0.11	0.07	0.11	0.14	**0.10**
		Δc [%]	-24.3	-5.4	-6.0	-22.4	-8.1	**-13.2**	-29.7	-15.3	-11.4	-26.8	-17.0	**-20.0**
	0–10 mm	c	1.6	3.1	1.6	2.6	3.0	**2.4**	0.07	0.12	0.07	0.11	0.14	**0.10**
		Δc [%]	-23.5	3.8	-5.1	-20.8	-5.8	**-10.3**	-29.5	-10.2	-11.4	-25.7	-16.3	**-18.6**
	0–20 mm	c	1.8	3.4	1.6	2.8	2.8	**2.5**	0.08	0.13	0.07	0.12	0.13	**0.10**
		Δc [%]	-15.0	12.9	-1.7	-16.8	-12.1	**-6.5**	-22.7	-3.9	-8.7	-22.6	-23.4	**-16.3**
	PET (NIR)	c	2.3	2.8	1.8	3.5	3.4	**2.8**	0.11	0.13	0.08	0.16	0.18	**0.13**
		Δc [%]	6.0	-6.1	7.2	6.4	5.3	**3.8**	7.3	-6.6	6.5	6.6	7.2	**4.2**
	PVC (NIR)	c	2.2	3.0	1.6	3.4	3.2	**2.7**	0.10	0.13	0.08	0.15	0.17	**0.13**
		Δc [%]	0.0	0.2	0.4	2.5	-0.7	**0.5**	0.7	0.2	0.5	2.4	0.7	**0.9**
	b&g	c	2.3	3.0	1.8	3.2	3.3	**2.7**	0.11	0.14	0.09	0.15	0.18	**0.13**
		Δc [%]	7.0	0.3	9.3	-4.5	1.3	**2.7**	10.2	1.2	10.5	-2.8	5.9	**5.0**
	PET + PVC (NIR)	c	2.3	2.8	1.8	3.6	3.4	**2.8**	0.11	0.13	0.08	0.17	0.18	**0.13**
		Δc [%]	6.5	-6.1	7.9	9.5	5.0	**4.5**	8.6	-6.6	7.3	9.6	8.7	**5.5**
Combinations of Screening and state-of-the-art NIR sorting or manual removal of black materials	0–5 mm + PET (NIR)	c	1.7	2.6	1.7	2.7	3.1	**2.4**	0.07	0.10	0.07	0.12	0.15	**0.10**
		Δc [%]	-20.3	-13.6	1.1	-18.1	-3.0	**-10.8**	-25.7	-23.9	-6.1	-23.1	-12.1	**-18.2**
	0–10 mm + PET (NIR)	c	1.7	2.8	1.7	2.8	3.2	**2.5**	0.07	0.11	0.07	0.12	0.15	**0.10**
		Δc [%]	-19.2	-4.4	2.5	-16.1	-0.2	**-7.5**	-25.3	-19.2	-5.9	-21.8	-11.1	**-16.6**
	0–20 mm + PET (NIR)	c	2.0	3.1	1.8	2.9	3.0	**2.6**	0.08	0.12	0.08	0.12	0.13	**0.11**
		Δc [%]	-8.5	5.0	6.9	-11.3	-7.1	**-3.0**	-16.7	-13.1	-2.6	-18.0	-19.1	**-13.9**
	0–5 mm + PVC (NIR)	c	1.6	2.8	1.5	2.6	2.9	**2.3**	0.07	0.11	0.07	0.11	0.14	**0.10**
		Δc [%]	-25.9	-5.3	-5.7	-20.7	-9.6	**-13.5**	-31.1	-15.4	-11.0	-25.5	-18.0	**-20.2**
	0–10 mm + PVC (NIR)	c	1.6	3.1	1.6	2.7	3.0	**2.4**	0.07	0.12	0.07	0.11	0.14	**0.10**
		Δc [%]	-25.2	4.2	-4.7	-19.0	-7.2	**-10.4**	-30.9	-10.3	-11.0	-24.3	-17.2	**-18.8**
	0–20 mm + PVC (NIR)	c	1.8	3.4	1.6	2.8	2.8	**2.5**	0.08	0.13	0.07	0.12	0.12	**0.10**
		Δc [%]	-16.2	13.6	-1.2	-14.7	-14.3	**-6.6**	-23.8	-3.8	-8.3	-21.0	-25.1	**-16.4**
	0–5 mm + PET (NIR) + PVC (NIR)	c	1.7	2.6	1.7	2.8	3.1	**2.4**	0.07	0.10	0.07	0.12	0.15	**0.10**
		Δc [%]	-21.9	-13.7	1.7	-16.0	-4.3	**-10.8**	-27.0	-24.3	-5.6	-21.5	-12.7	**-18.2**
	0–10 mm + PET (NIR) + PVC (NIR)	c	1.7	2.9	1.7	2.9	3.2	**2.5**	0.07	0.11	0.07	0.12	0.15	**0.10**
		Δc [%]	-20.8	-4.2	3.1	-13.8	-1.2	**-7.4**	-26.6	-19.5	-5.4	-20.0	-11.6	**-16.6**
	0–20 mm + PET (NIR) + PVC (NIR)	c	2.0	3.1	1.8	3.0	2.9	**2.6**	0.08	0.12	0.08	0.13	0.13	**0.11**
		Δc [%]	-9.3	5.5	7.7	-8.4	-9.1	**-2.7**	-17.4	-13.2	-2.0	-15.9	-20.6	**-13.8**
	0–5 mm + b&g	c	1.7	2.8	1.7	2.3	3.0	**2.3**	0.07	0.11	0.08	0.10	0.14	**0.10**
		Δc [%]	-21.4	-5.9	3.0	-30.8	-7.7	**-12.5**	-25.8	-16.2	-3.1	-34.0	-13.9	**-18.6**
	0–10 mm + b&g	c	1.7	3.1	1.7	2.3	3.1	**2.4**	0.07	0.12	0.08	0.10	0.14	**0.10**
		Δc [%]	-20.2	4.9	4.6	-29.2	-5.1	**-9.0**	-25.3	-10.5	-2.8	-33.0	-12.9	**-16.9**
	0–20 mm + b&g	c	2.0	3.5	1.8	2.5	2.8	**2.5**	0.08	0.13	0.08	0.11	0.13	**0.11**
		Δc [%]	-8.5	16.0	9.5	-25.2	-12.4	**-4.1**	-15.8	-3.0	0.9	-29.8	-21.2	**-13.8**
	0–5 mm + b&g + PVC (NIR)	c	1.7	2.8	1.7	2.3	2.9	**2.3**	0.07	0.11	0.08	0.10	0.14	**0.10**
		Δc [%]	-23.2	-5.8	3.7	-29.4	-9.4	**-12.8**	-27.2	-16.5	-2.4	-32.9	-14.7	**-18.7**
	0–10 mm + b&g + PVC (NIR)	c	1.7	3.1	1.7	2.4	3.0	**2.4**	0.07	0.12	0.08	0.10	0.14	**0.10**
		Δc [%]	-22.0	5.4	5.3	-27.7	-6.6	**-9.1**	-26.8	-10.6	-2.2	-31.8	-13.6	**-17.0**
	0–20 mm + b&g + PVC (NIR)	c	1.9	3.5	1.8	2.5	2.7	**2.5**	0.08	0.13	0.08	0.11	0.13	**0.11**
		Δc [%]	-9.5	17.0	10.4	-23.3	-15.0	**-4.1**	-16.4	-2.9	1.7	-28.4	-23.0	**-13.8**
	0–5 mm + b&g + PET (NIR)	c	1.8	2.5	1.9	2.4	3.2	**2.4**	0.08	0.10	0.08	0.10	0.15	**0.10**
		Δc [%]	-15.9	-15.6	13.7	-27.0	-1.8	**-9.3**	-20.0	-26.4	5.0	-30.8	-7.3	**-15.9**
	0–10 mm + b&g + PET (NIR)	c	1.8	2.8	1.9	2.5	3.3	**2.5**	0.08	0.11	0.08	0.11	0.16	**0.11**
		Δc [%]	-14.1	-4.8	16.2	-25.1	1.7	**-5.2**	-19.1	-21.1	5.6	-29.5	-6.0	**-14.0**
	0–20 mm + b&g + PET (NIR)	c	2.2	3.2	2.0	2.7	3.0	**2.6**	0.09	0.12	0.09	0.11	0.14	**0.11**
		Δc [%]	1.6	6.7	23.1	-20.1	-6.5	**1.0**	-6.0	-13.9	10.6	-25.5	-15.4	**-10.1**
	0–5 mm + b&g + PET (NIR) + PVC (NIR)	c	1.8	2.5	1.9	2.5	3.1	**2.4**	0.08	0.10	0.08	0.11	0.15	**0.10**
		Δc [%]	-17.4	-15.9	14.8	-25.1	-3.1	**-9.3**	-21.1	-27.0	5.9	-29.3	-7.4	**-15.8**
	0–10 mm + b&g + PET (NIR) + PVC (NIR)	c	1.8	2.8	1.9	2.6	3.3	**2.5**	0.08	0.11	0.08	0.11	0.16	**0.11**
		Δc [%]	-15.6	-4.7	17.4	-22.9	0.7	**-5.0**	-20.1	-21.5	6.6	-27.9	-5.8	**-13.7**
	0–20 mm + b&g + PET (NIR) + PVC (NIR)	c	2.2	3.2	2.0	2.7	2.9	**2.6**	0.09	0.12	0.09	0.12	0.14	**0.11**
		Δc [%]	1.9	7.4	24.7	-17.3	-8.8	**1.6**	-5.4	-14.2	11.8	-23.5	-16.8	**-9.6**

More targeted removal	PVC (FTIR) + b&g PVC	c	2.2	3.0	1.6	3.4	3.2	**2.7**	0.10	0.14	0.08	0.15	0.17	**0.13**
		Δc [%]	0.7	0.7	0.5	1.4	0.1	**0.7**	0.7	0.5	0.7	1.0	0.0	**0.6**
	0–5 mm + PVC (FTIR) + b&g PVC	c	1.6	2.8	1.6	2.6	3.0	**2.3**	0.07	0.11	0.07	0.11	0.14	**0.10**
		Δc [%]	-23.7	-4.7	-5.5	-21.5	-8.1	**-12.7**	-29.2	-14.9	-10.8	-26.3	-17.1	**-19.7**
	0–10 mm + PVC (FTIR) + b&g PVC	c	1.7	3.1	1.6	2.7	3.0	**2.4**	0.07	0.12	0.07	0.11	0.14	**0.10**
		Δc [%]	-22.9	4.8	-4.5	-19.8	-5.8	**-9.6**	-28.9	-9.7	-10.8	-25.2	-16.4	**-18.2**
	0–20 mm + PVC (FTIR) + b&g PVC	c	1.8	3.4	1.6	2.8	2.8	**2.5**	0.08	0.13	0.07	0.12	0.13	**0.10**
		Δc [%]	-14.2	14.2	-1.0	-15.6	-12.2	**-5.8**	-22.1	-3.3	-8.1	-22.0	-23.6	**-15.8**
	PVC (NIR) + b&g PVC	c	2.2	3.0	1.6	3.4	3.2	**2.7**	0.10	0.13	0.08	0.15	0.17	**0.13**
		Δc [%]	0.3	0.2	0.6	2.5	-0.7	**0.6**	1.0	0.2	0.7	2.3	0.6	**1.0**
	0–5 mm + PVC (NIR) + b&g PVC	c	1.6	2.8	1.5	2.6	2.9	**2.3**	0.07	0.11	0.07	0.11	0.14	**0.10**
		Δc [%]	-25.7	-5.3	-5.5	-20.9	-9.7	**-13.4**	-30.8	-15.4	-10.9	-25.7	-18.0	**-20.2**
	0–10 mm + PVC (NIR) + b&g PVC	c	1.6	3.1	1.6	2.7	3.0	**2.4**	0.07	0.12	0.07	0.11	0.14	**0.10**
		Δc [%]	-24.9	4.2	-4.6	-19.2	-7.2	**-10.3**	-30.6	-10.3	-10.9	-24.6	-17.3	**-18.7**
	0–20 mm + PVC (NIR) + b&g PVC	c	1.8	3.4	1.6	2.8	2.8	**2.5**	0.08	0.13	0.07	0.12	0.12	**0.10**
		Δc [%]	-15.9	13.7	-1.0	-14.9	-14.4	**-6.5**	-23.5	-3.8	-8.2	-21.2	-25.2	**-16.4**
	PET (FTIR) + Textiles + b&g PET	c	2.3	2.9	1.7	3.4	3.3	**2.7**	0.11	0.13	0.08	0.16	0.17	**0.13**
		Δc [%]	5.0	-1.7	4.3	3.4	3.6	**2.9**	5.2	-2.2	4.2	3.2	4.4	**3.0**
	0–5 mm + PET (FTIR) + Textiles + b&g PET	c	1.7	2.7	1.6	2.6	3.1	**2.4**	0.07	0.11	0.07	0.11	0.14	**0.10**
		Δc [%]	-20.8	-7.8	-1.7	-20.3	-4.6	**-11.1**	-26.8	-18.2	-7.7	-25.3	-14.0	**-18.4**
	0–10 mm + PET (FTIR) + Textiles + b&g PET	c	1.7	3.0	1.6	2.7	3.2	**2.5**	0.07	0.12	0.07	0.11	0.14	**0.10**
		Δc [%]	-19.8	1.6	-0.5	-18.5	-1.9	**-7.8**	-26.4	-13.3	-7.6	-24.1	-13.2	**-16.9**
	0–20 mm + PET (FTIR) + Textiles + b&g PET	c	1.9	3.3	1.7	2.8	3.0	**2.6**	0.08	0.13	0.07	0.12	0.13	**0.11**
		Δc [%]	-9.5	11.0	3.4	-14.1	-8.7	**-3.6**	-18.5	-7.0	-4.7	-20.6	-20.8	**-14.3**
	b&g Other	c	2.3	3.0	1.8	3.2	3.2	**2.7**	0.10	0.13	0.08	0.15	0.16	**0.13**
		Δc [%]	5.9	0.9	8.0	-2.8	-1.1	**2.2**	4.9	0.2	6.9	-3.5	-1.3	**1.5**
	0–5 mm + b&g Other	c	1.7	2.8	1.7	2.4	2.9	**2.3**	0.07	0.11	0.07	0.10	0.13	**0.10**
		Δc [%]	-20.8	-4.9	1.7	-27.8	-10.0	**-12.4**	-27.9	-16.5	-6.0	-32.8	-19.5	**-20.5**
	0–10 mm + b&g Other	c	1.7	3.1	1.7	2.4	3.0	**2.4**	0.07	0.12	0.07	0.10	0.14	**0.10**
		Δc [%]	-19.7	5.6	3.1	-26.2	-7.6	**-9.0**	-27.6	-11.1	-5.9	-31.8	-18.8	**-19.0**
	0–20 mm + b&g Other	c	2.0	3.5	1.8	2.6	2.8	**2.5**	0.08	0.13	0.08	0.11	0.12	**0.10**
		Δc [%]	-9.0	16.4	7.8	-22.2	-14.7	**-4.3**	-19.6	-4.1	-2.5	-28.7	-26.5	**-16.3**
	PVC (FTIR) + b&g PVC + b&g Other	c	2.3	3.0	1.8	3.3	3.2	**2.7**	0.11	0.14	0.08	0.15	0.16	**0.13**
		Δc [%]	6.7	1.7	8.7	-1.4	-1.1	**2.9**	5.8	0.8	7.8	-2.5	-1.3	**2.1**
	0–5 mm + PVC (FTIR) + b&g PVC + b&g Other	c	1.7	2.9	1.7	2.4	2.9	**2.3**	0.07	0.11	0.07	0.10	0.13	**0.10**
		Δc [%]	-20.1	-4.1	2.4	-26.9	-10.0	**-11.8**	-27.3	-16.1	-5.3	-32.4	-19.6	**-20.2**
	0–10 mm + PVC (FTIR) + b&g PVC + b&g Other	c	1.7	3.2	1.7	2.5	3.0	**2.4**	0.07	0.12	0.07	0.10	0.13	**0.10**
		Δc [%]	-19.0	6.8	3.9	-25.3	-7.6	**-8.2**	-27.0	-10.5	-5.1	-31.4	-18.9	**-18.6**
	0–20 mm + PVC (FTIR) + b&g PVC + b&g Other	c	2.0	3.5	1.8	2.6	2.8	**2.5**	0.08	0.13	0.08	0.11	0.12	**0.10**
		Δc [%]	-7.9	17.9	8.7	-21.1	-14.8	**-3.4**	-18.7	-3.4	-1.7	-28.2	-26.7	**-15.8**
	PVC (NIR) + b&g PVC + b&g Other	c	2.3	3.0	1.8	3.3	3.2	**2.7**	0.11	0.14	0.08	0.15	0.17	**0.13**
		Δc [%]	6.7	1.2	8.8	-0.3	-2.0	**2.9**	6.5	0.4	7.9	-1.2	-0.7	**2.6**
	0–5 mm + PVC (NIR) + b&g PVC + b&g Other	c	1.7	2.8	1.7	2.4	2.8	**2.3**	0.07	0.11	0.07	0.10	0.13	**0.10**
		Δc [%]	-22.1	-4.8	2.5	-26.5	-11.9	**-12.6**	-29.0	-16.7	-5.3	-32.0	-20.8	**-20.8**
	0–10 mm + PVC (NIR) + b&g PVC + b&g Other	c	1.7	3.2	1.7	2.5	2.9	**2.4**	0.07	0.12	0.07	0.10	0.13	**0.10**
		Δc [%]	-21.0	6.2	4.0	-24.8	-9.4	**-9.0**	-28.7	-11.2	-5.2	-30.9	-20.1	**-19.2**
	0–20 mm + PVC (NIR) + b&g PVC + b&g Other	c	2.0	3.5	1.8	2.6	2.7	**2.5**	0.08	0.13	0.08	0.11	0.12	**0.10**
		Δc [%]	-9.3	17.4	8.9	-20.4	-17.4	**-4.2**	-20.1	-4.0	-1.6	-27.6	-28.8	**-16.4**
	b&g Other + b&g PVC	c	2.3	3.0	1.8	3.2	3.2	**2.7**	0.11	0.13	0.08	0.15	0.16	**0.13**
		Δc [%]	6.2	1.0	8.1	-2.9	-1.2	**2.2**	5.3	0.3	7.1	-3.6	-1.3	**1.6**
	0–5 mm + b&g Other + b&g PVC	c	1.7	2.8	1.7	2.4	2.9	**2.3**	0.07	0.11	0.07	0.10	0.13	**0.10**
		Δc [%]	-20.5	-4.9	1.9	-28.0	-10.1	**-12.3**	-27.6	-16.5	-5.8	-33.1	-19.5	**-20.5**
	0–10 mm + b&g Other + b&g PVC	c	1.7	3.1	1.7	2.4	3.0	**2.4**	0.07	0.12	0.07	0.10	0.14	**0.10**
		Δc [%]	-19.4	5.7	3.3	-26.4	-7.7	**-8.9**	-27.3	-11.0	-5.7	-32.1	-18.8	**-19.0**
	0–20 mm + b&g Other + b&g PVC	c	2.0	3.5	1.8	2.6	2.8	**2.5**	0.08	0.13	0.08	0.11	0.12	**0.10**
		Δc [%]	-8.5	16.5	8.0	-22.4	-14.8	**-4.2**	-19.2	-4.0	-2.3	-29.0	-26.5	**-16.2**

B.17. Mg

Table B.17: Relative concentration change (Δc, in %) of Mg caused by the removal of different material or particle size fractions referring to mg/kg and mg/MJ, both calculated for dry mass without hard impurities

	Removed fractions	Conc. after removal	mg/kg$_{DM}$ S01	S02	S03	S04	S05	Avr	mg/MJ S01	S02	S03	S04	S05	Avr
Single process steps	0–5 mm	c	1598	2868	3430	2906	3888	**2938**	69	116	154	125	181	**129**
		Δc [%]	-46.5	-26.4	-20.7	-17.0	-38.2	**-29.8**	-50.3	-34.1	-25.2	-21.7	-44.2	**-35.1**
	0–10 mm	c	1548	2768	3346	2897	3708	**2853**	66	108	149	124	170	**123**
		Δc [%]	-48.2	-28.9	-22.6	-17.2	-41.1	**-31.6**	-52.2	-38.6	-27.7	-22.3	-47.7	**-37.7**
	0–20 mm	c	1439	2861	3318	2968	3560	**2829**	61	110	147	126	160	**121**
		Δc [%]	-51.9	-26.6	-23.3	-15.2	-43.4	**-32.1**	-56.3	-37.5	-28.8	-21.0	-50.7	**-38.9**
	PET (NIR)	c	3231	4128	4424	3739	6827	**4470**	152	185	209	170	358	**215**
		Δc [%]	8.1	6.0	2.3	6.8	8.5	**6.3**	9.4	5.4	1.6	7.0	10.4	**6.8**
	PVC (NIR)	c	3092	3959	4313	3615	6576	**4311**	145	179	206	164	343	**207**
		Δc [%]	3.5	1.6	-0.3	3.3	4.5	**2.5**	4.1	1.6	-0.2	3.2	5.9	**2.9**
	b&g	c	3389	3969	4718	3574	6853	**4501**	162	181	227	165	369	**221**
		Δc [%]	13.4	1.9	9.1	2.1	8.9	**7.1**	16.7	2.8	10.2	3.9	13.9	**9.5**
	PET + PVC (NIR)	c	3363	4202	4413	3880	7197	**4611**	159	189	209	177	384	**223**
		Δc [%]	12.5	7.9	2.1	10.9	14.4	**9.5**	14.8	7.2	1.5	11.0	18.4	**10.6**
Combinations of Screening and state-of-the-art NIR sorting or manual removal of black materials	0–5 mm + PET (NIR)	c	1704	3051	3410	3100	4159	**3085**	74	121	151	132	194	**134**
		Δc [%]	-43.0	-21.7	-21.1	-11.4	-33.9	**-26.2**	-46.8	-31.0	-26.7	-16.9	-40.1	**-32.3**
	0–10 mm + PET (NIR)	c	1653	2964	3313	3098	3963	**2998**	71	113	145	131	182	**128**
		Δc [%]	-44.7	-23.9	-23.4	-11.5	-37.0	**-28.1**	-48.8	-35.7	-29.7	-17.5	-43.9	**-35.1**
	0–20 mm + PET (NIR)	c	1546	3092	3278	3192	3811	**2984**	65	116	142	134	171	**126**
		Δc [%]	-48.3	-20.6	-24.2	-8.8	-39.4	**-28.3**	-52.9	-34.3	-31.0	-15.7	-47.2	**-36.2**
	0–5 mm + PVC (NIR)	c	1622	2918	3399	3005	3998	**2988**	70	118	153	128	187	**131**
		Δc [%]	-45.7	-25.1	-21.4	-14.1	-36.5	**-28.6**	-49.5	-33.1	-25.9	-19.3	-42.4	**-34.0**
	0–10 mm + PVC (NIR)	c	1570	2821	3312	3000	3805	**2902**	67	110	147	127	175	**125**
		Δc [%]	-47.5	-27.6	-23.4	-14.3	-39.5	**-30.5**	-51.5	-37.6	-28.5	-19.9	-46.1	**-36.7**
	0–20 mm + PVC (NIR)	c	1455	2923	3282	3080	3650	**2878**	61	112	145	130	164	**122**
		Δc [%]	-51.3	-25.0	-24.1	-12.0	-42.0	**-30.9**	-55.7	-36.5	-29.6	-18.4	-49.3	**-37.9**
	0–5 mm + PET (NIR) + PVC (NIR)	c	1740	3112	3375	3224	4316	**3153**	76	123	149	137	203	**138**
		Δc [%]	-41.8	-20.1	-22.0	-7.9	-31.4	**-24.6**	-45.6	-29.9	-27.5	-13.9	-37.4	**-30.9**
	0–10 mm + PET (NIR) + PVC (NIR)	c	1687	3030	3273	3227	4107	**3065**	73	115	143	136	189	**131**
		Δc [%]	-43.6	-22.2	-24.3	-7.8	-34.7	**-26.5**	-47.7	-34.6	-30.6	-14.5	-41.6	**-33.8**
	0–20 mm + PET (NIR) + PVC (NIR)	c	1576	3171	3235	3337	3949	**3054**	67	118	140	139	178	**128**
		Δc [%]	-47.3	-18.6	-25.2	-4.6	-37.2	**-26.6**	-52.0	-33.0	-31.9	-12.4	-45.2	**-34.9**
	0–5 mm + b&g	c	1763	2795	3664	2902	4205	**3066**	77	112	164	126	202	**136**
		Δc [%]	-41.0	-28.2	-15.3	-17.1	-33.2	**-27.0**	-44.3	-36.1	-20.3	-21.0	-37.6	**-31.9**
	0–10 mm + b&g	c	1711	2668	3570	2892	4013	**2971**	74	103	158	125	189	**130**
		Δc [%]	-42.7	-31.5	-17.4	-17.3	-36.2	**-29.1**	-46.4	-41.5	-23.3	-21.8	-41.5	**-34.9**
	0–20 mm + b&g	c	1605	2767	3550	2974	3866	**2952**	69	104	156	127	179	**127**
		Δc [%]	-46.3	-29.0	-17.9	-15.0	-38.6	**-29.4**	-50.5	-40.6	-24.3	-20.2	-44.7	**-36.1**
	0–5 mm + b&g + PVC (NIR)	c	1808	2852	3632	3016	4367	**3135**	80	114	163	130	212	**140**
		Δc [%]	-39.5	-26.8	-16.0	-13.8	-30.6	**-25.3**	-42.7	-35.1	-21.0	-18.2	-34.6	**-30.3**
	0–10 mm + b&g + PVC (NIR)	c	1754	2727	3534	3011	4161	**3037**	77	105	156	129	198	**133**
		Δc [%]	-41.3	-30.0	-18.3	-14.0	-33.9	**-27.5**	-44.9	-40.6	-24.1	-18.9	-38.8	**-33.5**
	0–20 mm + b&g + PVC (NIR)	c	1645	2839	3511	3107	4010	**3022**	71	106	154	132	187	**130**
		Δc [%]	-45.0	-27.1	-18.8	-11.2	-36.3	**-27.7**	-49.2	-39.5	-25.2	-17.1	-42.3	**-34.7**
	0–5 mm + b&g + PET (NIR)	c	1924	3002	3683	3129	4577	**3263**	85	118	162	135	222	**144**
		Δc [%]	-35.6	-22.9	-14.8	-10.6	-27.3	**-22.3**	-38.8	-32.8	-21.4	-15.2	-31.4	**-27.9**
	0–10 mm + b&g + PET (NIR)	c	1875	2890	3571	3128	4370	**3167**	82	108	155	134	208	**137**
		Δc [%]	-37.3	-25.8	-17.4	-10.6	-30.6	**-24.3**	-40.9	-38.5	-25.0	-15.9	-35.8	**-31.2**
	0–20 mm + b&g + PET (NIR)	c	1785	3038	3547	3243	4228	**3168**	77	111	152	137	197	**135**
		Δc [%]	-40.3	-22.0	-18.0	-7.3	-32.8	**-24.1**	-44.7	-37.1	-26.3	-13.6	-39.3	**-32.2**
	0–5 mm + b&g + PET (NIR) + PVC (NIR)	c	1992	3073	3645	3277	4817	**3361**	88	120	160	141	237	**149**
		Δc [%]	-33.3	-21.1	-15.7	-6.3	-23.5	**-20.0**	-36.3	-31.5	-22.3	-11.6	-26.8	**-25.7**
	0–10 mm + b&g + PET (NIR) + PVC (NIR)	c	1943	2967	3528	3284	4597	**3264**	85	110	152	140	221	**142**
		Δc [%]	-35.0	-23.8	-18.4	-6.2	-26.9	**-22.1**	-38.4	-37.3	-26.0	-12.2	-31.7	**-29.1**
	0–20 mm + b&g + PET (NIR) + PVC (NIR)	c	1861	3134	3500	3422	4460	**3275**	80	113	149	144	209	**139**
		Δc [%]	-37.7	-19.5	-19.1	-2.2	-29.1	**-21.5**	-42.2	-35.7	-27.4	-9.5	-35.4	**-30.0**

More targeted removal	PVC (FTIR) + b&g PVC	c	3001	3939	4351	3571	6335	**4239**	139	178	207	162	326	**202**
		Δc [%]	0.4	1.1	0.6	2.0	0.7	**1.0**	0.4	1.0	0.7	1.7	0.6	**0.9**
	0–5 mm + PVC (FTIR) + b&g PVC	c	1598	2905	3450	2969	3914	**2967**	69	117	155	127	182	**130**
		Δc [%]	-46.5	-25.4	-20.2	-15.2	-37.8	**-29.0**	-50.3	-33.4	-24.7	-20.4	-44.0	**-34.6**
	0–10 mm + PVC (FTIR) + b&g PVC	c	1547	2808	3366	2963	3733	**2883**	66	109	150	126	170	**124**
		Δc [%]	-48.2	-27.9	-22.2	-15.3	-40.7	**-30.9**	-52.3	-37.9	-27.3	-21.0	-47.4	**-37.2**
	0–20 mm + PVC (FTIR) + b&g PVC	c	1437	2907	3339	3039	3585	**2861**	61	111	148	128	161	**122**
		Δc [%]	-51.9	-25.4	-22.8	-13.1	-43.0	**-31.3**	-56.3	-36.8	-28.3	-19.6	-50.4	**-38.3**
	PVC (NIR) + b&g PVC	c	3093	3962	4320	3628	6578	**4316**	145	179	206	165	343	**208**
		Δc [%]	3.5	1.7	-0.1	3.7	4.5	**2.7**	4.2	1.7	0.1	3.5	5.9	**3.1**
	0–5 mm + PVC (NIR) + b&g PVC	c	1617	2921	3405	3015	3999	**2991**	70	118	153	129	187	**131**
		Δc [%]	-45.9	-25.0	-21.3	-13.9	-36.4	**-28.5**	-49.6	-33.1	-25.7	-19.1	-42.3	**-34.0**
	0–10 mm + PVC (NIR) + b&g PVC	c	1564	2824	3318	3010	3806	**2905**	67	110	148	128	175	**125**
		Δc [%]	-47.7	-27.5	-23.3	-14.0	-39.5	**-30.4**	-51.7	-37.6	-28.3	-19.7	-46.1	**-36.7**
	0–20 mm + PVC (NIR) + b&g PVC	c	1448	2927	3288	3092	3651	**2881**	61	112	145	130	164	**123**
		Δc [%]	-51.6	-24.9	-24.0	-11.6	-42.0	**-30.8**	-55.9	-36.4	-29.4	-18.2	-49.3	**-37.9**
	PET (FTIR) + Textiles + b&g PET	c	3175	4008	4287	3631	6638	**4348**	148	180	204	165	344	**208**
		Δc [%]	6.2	2.9	-0.9	3.8	5.5	**3.5**	6.4	2.4	-0.9	3.6	6.3	**3.6**
	0–5 mm + PET (FTIR) + Textiles + b&g PET	c	1680	2956	3324	3009	4050	**3004**	72	118	149	128	188	**131**
		Δc [%]	-43.8	-24.1	-23.1	-14.0	-35.6	**-28.1**	-48.0	-32.7	-27.8	-19.4	-42.0	**-34.0**
	0–10 mm + PET (FTIR) + Textiles + b&g PET	c	1629	2862	3230	3003	3858	**2916**	69	110	143	127	176	**125**
		Δc [%]	-45.5	-26.5	-25.3	-14.2	-38.7	**-30.0**	-50.0	-37.3	-30.7	-20.1	-45.7	**-36.7**
	0–20 mm + PET (FTIR) + Textiles + b&g PET	c	1521	2972	3193	3087	3705	**2895**	64	113	140	130	165	**122**
		Δc [%]	-49.1	-23.7	-26.2	-11.8	-41.1	**-30.4**	-54.1	-36.1	-31.9	-18.5	-48.9	**-37.9**
	b&g Other	c	3276	3917	4667	3482	6572	**4383**	151	176	220	157	338	**208**
		Δc [%]	9.6	0.5	7.9	-0.5	4.4	**4.4**	8.6	-0.1	6.9	-1.2	4.3	**3.7**
	0–5 mm + b&g Other	c	1741	2768	3642	2828	4030	**3002**	74	110	160	120	186	**130**
		Δc [%]	-41.8	-28.9	-15.8	-19.2	-36.0	**-28.3**	-47.0	-37.6	-22.2	-24.8	-42.7	**-34.8**
	0–10 mm + b&g Other	c	1691	2642	3551	2816	3842	**2908**	71	100	154	118	174	**124**
		Δc [%]	-43.4	-32.2	-17.9	-19.5	-39.0	**-30.4**	-49.0	-42.9	-25.1	-25.6	-46.3	**-37.8**
	0–20 mm + b&g Other	c	1590	2734	3530	2888	3691	**2887**	65	102	152	120	164	**121**
		Δc [%]	-46.8	-29.8	-18.4	-17.5	-41.3	**-30.8**	-53.0	-42.2	-26.2	-24.4	-49.5	**-39.0**
	PVC (FTIR) + b&g PVC + b&g Other	c	3293	3964	4702	3560	6619	**4428**	152	178	222	160	340	**210**
		Δc [%]	10.2	1.8	8.7	1.7	5.2	**5.5**	9.2	0.9	7.8	0.6	5.0	**4.7**
	0–5 mm + PVC (FTIR) + b&g PVC + b&g Other	c	1742	2808	3669	2895	4059	**3035**	74	111	162	122	187	**131**
		Δc [%]	-41.7	-27.9	-15.2	-17.3	-35.5	**-27.5**	-46.9	-36.9	-21.5	-23.5	-42.4	**-34.2**
	0–10 mm + PVC (FTIR) + b&g PVC + b&g Other	c	1692	2684	3577	2886	3870	**2942**	71	102	156	120	175	**125**
		Δc [%]	-43.4	-31.1	-17.3	-17.5	-38.5	**-29.6**	-48.9	-42.3	-24.5	-24.3	-46.0	**-37.2**
	0–20 mm + PVC (FTIR) + b&g PVC + b&g Other	c	1590	2784	3558	2965	3720	**2923**	65	103	153	123	165	**122**
		Δc [%]	-46.8	-28.5	-17.7	-15.3	-40.9	**-29.8**	-53.1	-41.4	-25.5	-22.9	-49.2	**-38.4**
	PVC (NIR) + b&g PVC + b&g Other	c	3415	3990	4671	3621	6900	**4520**	158	179	221	163	360	**216**
		Δc [%]	14.3	2.4	8.0	3.5	9.6	**7.6**	14.0	1.7	7.1	2.5	11.1	**7.3**
	0–5 mm + PVC (NIR) + b&g PVC + b&g Other	c	1775	2825	3619	2943	4165	**3065**	75	112	159	124	193	**133**
		Δc [%]	-40.6	-27.5	-16.3	-15.9	-33.8	**-26.8**	-45.9	-36.6	-22.7	-22.2	-40.5	**-33.6**
	0–10 mm + PVC (NIR) + b&g PVC + b&g Other	c	1723	2701	3523	2935	3963	**2969**	72	102	153	123	180	**126**
		Δc [%]	-42.4	-30.7	-18.5	-16.1	-37.0	**-28.9**	-48.0	-42.0	-25.7	-23.0	-44.4	**-36.6**
	0–20 mm + PVC (NIR) + b&g PVC + b&g Other	c	1617	2805	3500	3021	3806	**2950**	66	104	151	125	169	**123**
		Δc [%]	-45.9	-28.0	-19.1	-13.7	-39.5	**-29.2**	-52.3	-41.1	-26.9	-21.5	-47.8	**-37.9**
	b&g Other + b&g PVC	c	3278	3920	4677	3495	6574	**4389**	151	176	221	158	338	**209**
		Δc [%]	9.7	0.6	8.1	-0.1	4.5	**4.6**	8.7	-0.1	7.2	-0.9	4.3	**3.9**
	0–5 mm + b&g Other + b&g PVC	c	1736	2771	3650	2837	4031	**3005**	73	110	161	120	186	**130**
		Δc [%]	-41.9	-28.9	-15.6	-18.9	-35.9	**-28.3**	-47.1	-37.6	-22.0	-24.6	-42.7	**-34.8**
	0–10 mm + b&g Other + b&g PVC	c	1685	2645	3558	2825	3843	**2911**	71	101	155	119	174	**124**
		Δc [%]	-43.6	-32.1	-17.7	-19.3	-38.9	**-30.3**	-49.1	-42.9	-24.9	-25.4	-46.3	**-37.7**
	0–20 mm + b&g Other + b&g PVC	c	1582	2737	3538	2899	3692	**2890**	65	102	152	121	164	**121**
		Δc [%]	-47.1	-29.7	-18.2	-17.2	-41.3	**-30.7**	-53.2	-42.1	-26.0	-24.2	-49.4	**-39.0**

B.18. Mn

Table B.18: Relative concentration change (Δc, in %) of Mn caused by the removal of different material or particle size fractions referring to mg/kg and mg/MJ, both calculated for dry mass without hard impurities

	Removed fractions	Conc. after removal	mg/kg$_{DM}$ S01	S02	S03	S04	S05	Avr	mg/MJ S01	S02	S03	S04	S05	Avr
Single process steps	0–5 mm	c	130	184	127	93	161	**139**	5.6	7.5	5.7	4.0	7.5	**6.1**
		Δc [%]	-45.3	-56.6	-36.4	-26.0	-46.6	**-42.2**	-49.2	-61.1	-40.0	-30.2	-51.8	**-46.5**
	0–10 mm	c	117	146	116	82	148	**122**	5.0	5.7	5.2	3.5	6.8	**5.2**
		Δc [%]	-50.9	-65.6	-42.1	-35.4	-50.7	**-49.0**	-54.8	-70.3	-45.9	-39.4	-56.2	**-53.3**
	0–20 mm	c	102	141	92	81	134	**110**	4.3	5.4	4.1	3.4	6.0	**4.6**
		Δc [%]	-57.2	-66.7	-53.9	-35.8	-55.6	**-53.8**	-61.1	-71.7	-57.2	-40.2	-61.3	**-58.3**
	PET (NIR)	c	259	440	218	132	325	**275**	12.2	19.8	10.3	6.0	17.0	**13.1**
		Δc [%]	8.7	3.7	9.0	4.8	7.8	**6.8**	10.0	3.1	8.3	5.0	9.8	**7.2**
	PVC (NIR)	c	246	429	202	129	314	**264**	11.5	19.4	9.6	5.8	16.4	**12.5**
		Δc [%]	3.2	1.1	0.9	2.0	4.3	**2.3**	3.8	1.1	1.1	1.9	5.7	**2.7**
	b&g	c	276	460	225	129	328	**283**	13.2	21.0	10.8	5.9	17.7	**13.7**
		Δc [%]	16.1	8.3	12.2	1.9	9.0	**9.5**	19.5	9.3	13.4	3.7	13.9	**12.0**
	PET + PVC (NIR)	c	269	445	221	135	341	**282**	12.7	20.0	10.5	6.2	18.2	**13.5**
		Δc [%]	12.8	5.0	10.3	7.3	13.4	**9.7**	15.0	4.3	9.7	7.4	17.4	**10.8**
Combinations of Screening and state-of-the-art NIR sorting or manual removal of black materials	0–5 mm + PET (NIR)	c	140	179	137	96	168	**144**	6.1	7.1	6.1	4.1	7.8	**6.2**
		Δc [%]	-41.0	-57.9	-31.7	-24.0	-44.3	**-39.8**	-45.0	-62.9	-36.5	-28.7	-49.5	**-44.5**
	0–10 mm + PET (NIR)	c	126	135	124	83	154	**124**	5.4	5.2	5.4	3.5	7.0	**5.3**
		Δc [%]	-47.1	-68.2	-38.1	-34.6	-49.0	**-47.4**	-51.1	-73.1	-43.1	-39.0	-54.6	**-52.2**
	0–20 mm + PET (NIR)	c	110	129	97	82	137	**111**	4.7	4.8	4.2	3.4	6.1	**4.7**
		Δc [%]	-53.7	-69.7	-51.5	-34.9	-54.6	**-52.9**	-57.9	-74.9	-55.8	-39.9	-60.4	**-57.8**
	0–5 mm + PVC (NIR)	c	131	184	128	95	163	**140**	5.7	7.4	5.7	4.0	7.6	**6.1**
		Δc [%]	-44.8	-56.7	-36.1	-25.1	-45.9	**-41.7**	-48.6	-61.3	-39.7	-29.6	-50.9	**-46.0**
	0–10 mm + PVC (NIR)	c	117	144	116	82	149	**122**	5.0	5.6	5.2	3.5	6.9	**5.2**
		Δc [%]	-50.8	-66.1	-41.9	-34.9	-50.4	**-48.8**	-54.5	-70.8	-45.8	-39.2	-55.8	**-53.2**
	0–20 mm + PVC (NIR)	c	101	139	92	82	133	**109**	4.3	5.3	4.1	3.4	6.0	**4.6**
		Δc [%]	-57.5	-67.2	-53.9	-35.3	-55.8	**-53.9**	-61.4	-72.3	-57.3	-40.0	-61.3	**-58.5**
	0–5 mm + PET (NIR) + PVC (NIR)	c	143	178	138	97	171	**145**	6.2	7.1	6.1	4.1	8.0	**6.3**
		Δc [%]	-40.1	-58.1	-31.3	-22.8	-43.3	**-39.1**	-43.9	-63.2	-36.1	-27.9	-48.2	**-43.9**
	0–10 mm + PET (NIR) + PVC (NIR)	c	127	133	125	83	155	**125**	5.5	5.0	5.4	3.5	7.2	**5.3**
		Δc [%]	-46.6	-68.8	-37.8	-34.0	-48.4	**-47.1**	-50.5	-73.7	-42.9	-38.8	-53.8	**-52.0**
	0–20 mm + PET (NIR) + PVC (NIR)	c	110	126	97	83	137	**110**	4.7	4.7	4.2	3.5	6.1	**4.6**
		Δc [%]	-53.7	-70.4	-51.5	-34.3	-54.6	**-52.9**	-57.9	-75.7	-55.9	-39.7	-60.3	**-57.9**
	0–5 mm + b&g	c	152	190	138	91	172	**149**	6.6	7.6	6.2	4.0	8.3	**6.5**
		Δc [%]	-36.4	-55.2	-31.1	-27.7	-42.7	**-38.6**	-39.9	-60.1	-35.2	-31.1	-46.5	**-42.6**
	0–10 mm + b&g	c	136	146	124	78	159	**128**	5.9	5.6	5.5	3.3	7.5	**5.6**
		Δc [%]	-42.7	-65.7	-37.9	-38.5	-47.3	**-46.4**	-46.4	-70.7	-42.3	-41.8	-51.6	**-50.6**
	0–20 mm + b&g	c	121	140	95	77	143	**115**	5.2	5.3	4.2	3.3	6.6	**4.9**
		Δc [%]	-49.1	-67.0	-52.4	-39.2	-52.7	**-52.1**	-53.1	-72.4	-56.1	-42.9	-57.4	**-56.4**
	0–5 mm + b&g + PVC (NIR)	c	155	190	139	92	176	**150**	6.8	7.6	6.2	4.0	8.5	**6.6**
		Δc [%]	-34.9	-55.3	-30.6	-26.7	-41.4	**-37.8**	-38.3	-60.4	-34.7	-30.4	-44.8	**-41.7**
	0–10 mm + b&g + PVC (NIR)	c	139	143	125	78	161	**129**	6.0	5.5	5.5	3.3	7.7	**5.6**
		Δc [%]	-41.8	-66.2	-37.6	-38.2	-46.5	**-46.0**	-45.3	-71.3	-42.0	-41.7	-50.5	**-50.2**
	0–20 mm + b&g + PVC (NIR)	c	122	137	95	77	143	**115**	5.2	5.1	4.2	3.3	6.7	**4.9**
		Δc [%]	-48.7	-67.7	-52.5	-38.8	-52.4	**-52.0**	-52.6	-73.2	-56.2	-42.9	-56.9	**-56.4**
	0–5 mm + b&g + PET (NIR)	c	168	184	152	94	183	**156**	7.4	7.3	6.7	4.0	8.9	**6.9**
		Δc [%]	-29.5	-56.6	-24.1	-25.6	-39.4	**-35.0**	-32.9	-62.1	-30.0	-29.4	-42.8	**-39.4**
	0–10 mm + b&g + PET (NIR)	c	151	132	136	78	167	**133**	6.6	5.0	5.9	3.3	7.9	**5.8**
		Δc [%]	-36.4	-68.8	-31.9	-38.1	-44.6	**-44.0**	-40.1	-74.1	-38.2	-41.7	-48.7	**-48.6**
	0–20 mm + b&g + PET (NIR)	c	137	124	102	77	148	**118**	5.9	4.5	4.4	3.3	6.9	**5.0**
		Δc [%]	-42.6	-70.8	-49.0	-38.8	-50.8	**-50.4**	-46.9	-76.4	-54.2	-43.0	-55.5	**-55.2**
	0–5 mm + b&g + PET (NIR) + PVC (NIR)	c	174	184	153	96	188	**159**	7.7	7.2	6.7	4.1	9.3	**7.0**
		Δc [%]	-27.1	-56.8	-23.3	-24.3	-37.4	**-33.8**	-30.2	-62.5	-29.3	-28.5	-40.2	**-38.1**
	0–10 mm + b&g + PET (NIR) + PVC (NIR)	c	156	129	137	79	171	**134**	6.8	4.8	5.9	3.3	8.2	**5.8**
		Δc [%]	-34.6	-69.5	-31.4	-37.6	-43.2	**-43.3**	-38.1	-74.9	-37.7	-41.6	-46.9	**-47.8**
	0–20 mm + b&g + PET (NIR) + PVC (NIR)	c	140	120	102	78	150	**118**	6.0	4.3	4.4	3.3	7.0	**5.0**
		Δc [%]	-41.1	-71.7	-48.9	-38.4	-50.2	**-50.1**	-45.3	-77.4	-54.2	-43.0	-54.6	**-54.9**

More targeted removal	PVC (FTIR) + b&g PVC	c	240	429	201	128	303	**260**	11.1	19.3	9.6	5.8	15.6	**12.3**
		Δc [%]	0.7	1.0	0.6	1.7	0.7	0.9	0.7	0.9	0.7	1.4	0.7	0.9
	0–5 mm + PVC (FTIR) + b&g PVC	c	131	186	128	95	162	**140**	5.6	7.5	5.7	4.0	7.5	**6.1**
		Δc [%]	-45.0	-56.2	-36.1	-24.9	-46.2	**-41.7**	-48.9	-60.9	-39.7	-29.5	-51.5	**-46.1**
	0–10 mm + PVC (FTIR) + b&g PVC	c	118	147	116	83	149	**123**	5.0	5.7	5.2	3.5	6.8	**5.3**
		Δc [%]	-50.6	-65.4	-41.9	-34.5	-50.4	**-48.5**	-54.5	-70.2	-45.7	-38.9	-56.0	**-53.0**
	0–20 mm + PVC (FTIR) + b&g PVC	c	103	142	93	82	135	**111**	4.3	5.5	4.1	3.5	6.0	**4.7**
		Δc [%]	-56.9	-66.4	-53.7	-34.8	-55.3	**-53.4**	-60.9	-71.6	-57.0	-39.6	-61.1	**-58.0**
	PVC (NIR) + b&g PVC	c	246	430	202	129	314	**264**	11.5	19.4	9.7	5.9	16.4	**12.6**
		Δc [%]	3.4	1.2	1.1	2.6	4.3	2.5	4.1	1.2	1.3	2.4	5.7	2.9
	0–5 mm + PVC (NIR) + b&g PVC	c	132	184	128	95	163	**140**	5.7	7.4	5.8	4.1	7.6	**6.1**
		Δc [%]	-44.7	-56.7	-36.0	-24.7	-45.9	**-41.6**	-48.5	-61.3	-39.6	-29.3	-50.9	**-45.9**
	0–10 mm + PVC (NIR) + b&g PVC	c	117	144	116	83	149	**122**	5.0	5.6	5.2	3.5	6.9	**5.2**
		Δc [%]	-50.7	-66.0	-41.8	-34.6	-50.4	**-48.7**	-54.5	-70.8	-45.7	-38.9	-55.8	**-53.1**
	0–20 mm + PVC (NIR) + b&g PVC	c	101	139	92	82	133	**110**	4.3	5.3	4.1	3.5	6.0	**4.6**
		Δc [%]	-57.5	-67.2	-53.9	-34.9	-55.8	**-53.8**	-61.3	-72.2	-57.2	-39.7	-61.3	**-58.4**
	PET (FTIR) + Textiles + b&g PET	c	254	428	210	129	316	**267**	11.8	19.2	10.0	5.8	16.4	**12.6**
		Δc [%]	6.7	0.7	4.7	2.0	4.9	3.8	6.9	0.3	4.6	1.8	5.7	3.9
	0–5 mm + PET (FTIR) + Textiles + b&g PET	c	138	176	132	94	164	**141**	5.9	7.1	5.9	4.0	7.6	**6.1**
		Δc [%]	-41.9	-58.4	-33.8	-25.8	-45.5	**-41.1**	-46.3	-63.1	-37.9	-30.5	-50.9	**-45.7**
	0–10 mm + PET (FTIR) + Textiles + b&g PET	c	124	135	120	81	150	**122**	5.3	5.2	5.3	3.4	6.9	**5.2**
		Δc [%]	-47.9	-68.2	-39.9	-35.9	-50.1	**-48.4**	-52.2	-72.9	-44.2	-40.3	-55.8	**-53.1**
	0–20 mm + PET (FTIR) + Textiles + b&g PET	c	109	129	95	80	134	**109**	4.5	4.9	4.2	3.4	6.0	**4.6**
		Δc [%]	-54.4	-69.7	-52.4	-36.4	-55.5	**-53.7**	-58.9	-74.6	-56.1	-41.2	-61.4	**-58.4**
	b&g Other	c	263	449	220	125	315	**275**	12.1	20.2	10.4	5.6	16.2	**12.9**
		Δc [%]	10.6	5.9	9.9	-0.9	4.7	6.0	9.6	5.2	8.9	-1.7	4.6	5.3
	0–5 mm + b&g Other	c	145	186	136	89	167	**144**	6.1	7.4	6.0	3.8	7.7	**6.2**
		Δc [%]	-39.2	-56.2	-32.2	-29.7	-44.6	**-40.4**	-44.6	-61.5	-37.4	-34.5	-50.5	**-45.7**
	0–10 mm + b&g Other	c	130	143	122	76	153	**125**	5.5	5.4	5.3	3.2	7.0	**5.3**
		Δc [%]	-45.3	-66.4	-38.9	-40.1	-49.0	**-47.9**	-50.6	-71.7	-44.2	-44.6	-55.1	**-53.3**
	0–20 mm + b&g Other	c	115	137	94	75	138	**112**	4.7	5.1	4.1	3.1	6.1	**4.6**
		Δc [%]	-51.6	-67.8	-52.9	-40.8	-54.2	**-53.5**	-57.2	-73.4	-57.4	-45.8	-60.5	**-58.9**
	PVC (FTIR) + b&g PVC + b&g Other	c	266	454	222	127	318	**277**	12.2	20.4	10.5	5.7	16.3	**13.0**
		Δc [%]	11.5	7.1	10.7	0.9	5.6	7.1	10.5	6.2	9.8	-0.3	5.4	6.3
	0–5 mm + PVC (FTIR) + b&g PVC + b&g Other	c	146	188	136	90	168	**146**	6.2	7.4	6.0	3.8	7.7	**6.2**
		Δc [%]	-38.8	-55.7	-31.8	-28.5	-44.2	**-39.8**	-44.2	-61.3	-37.0	-33.8	-50.1	**-45.3**
	0–10 mm + PVC (FTIR) + b&g PVC + b&g Other	c	131	144	123	77	155	**126**	5.5	5.4	5.3	3.2	7.0	**5.3**
		Δc [%]	-44.9	-66.1	-38.6	-39.2	-48.6	**-47.5**	-50.3	-71.6	-43.9	-44.2	-54.9	**-53.0**
	0–20 mm + PVC (FTIR) + b&g PVC + b&g Other	c	116	138	95	76	139	**113**	4.8	5.1	4.1	3.1	6.2	**4.6**
		Δc [%]	-51.2	-67.5	-52.7	-39.9	-53.8	**-53.0**	-56.9	-73.3	-57.2	-45.3	-60.3	**-58.6**
	PVC (NIR) + b&g PVC + b&g Other	c	274	456	223	128	330	**282**	12.7	20.4	10.5	5.8	17.2	**13.3**
		Δc [%]	15.3	7.3	11.5	1.8	9.7	9.1	15.0	6.6	10.6	0.9	11.2	8.8
	0–5 mm + PVC (NIR) + b&g PVC + b&g Other	c	148	186	137	90	170	**146**	6.3	7.3	6.0	3.8	7.8	**6.3**
		Δc [%]	-38.0	-56.2	-31.6	-28.4	-43.7	**-39.6**	-43.4	-61.7	-36.9	-33.7	-49.3	**-45.0**
	0–10 mm + PVC (NIR) + b&g PVC + b&g Other	c	132	141	123	76	155	**125**	5.5	5.3	5.3	3.2	7.0	**5.3**
		Δc [%]	-44.5	-66.9	-38.5	-39.5	-48.4	**-47.6**	-49.9	-72.3	-43.9	-44.4	-54.5	**-53.0**
	0–20 mm + PVC (NIR) + b&g PVC + b&g Other	c	116	134	94	75	138	**112**	4.7	5.0	4.1	3.1	6.1	**4.6**
		Δc [%]	-51.4	-68.4	-52.9	-40.2	-54.2	**-53.4**	-57.1	-74.1	-57.4	-45.6	-60.5	**-58.9**
	b&g Other + b&g PVC	c	264	450	220	126	315	**275**	12.2	20.2	10.4	5.7	16.2	**12.9**
		Δc [%]	10.9	6.0	10.1	-0.4	4.8	6.3	10.0	5.2	9.1	-1.2	4.6	5.6
	0–5 mm + b&g Other + b&g PVC	c	145	186	136	89	167	**145**	6.1	7.4	6.0	3.8	7.7	**6.2**
		Δc [%]	-39.1	-56.1	-32.1	-29.3	-44.6	**-40.2**	-44.5	-61.5	-37.2	-34.2	-50.5	**-45.6**
	0–10 mm + b&g Other + b&g PVC	c	131	143	123	76	154	**125**	5.5	5.4	5.3	3.2	7.0	**5.3**
		Δc [%]	-45.2	-66.4	-38.8	-39.8	-49.0	**-47.8**	-50.6	-71.7	-44.1	-44.4	-55.1	**-53.2**
	0–20 mm + b&g Other + b&g PVC	c	115	137	94	75	138	**112**	4.7	5.1	4.1	3.1	6.1	**4.6**
		Δc [%]	-51.5	-67.7	-52.8	-40.5	-54.2	**-53.3**	-57.2	-73.4	-57.3	-45.5	-60.5	**-58.8**

B.19. Mo

Table B.19: Relative concentration change (Δc, in %) of Mo caused by the removal of different material or particle size fractions referring to mg/kg and mg/MJ, both calculated for dry mass without hard impurities

	Removed fractions	Conc. after removal	mg/kg$_{DM}$ S01	S02	S03	S04	S05	Avr	mg/MJ S01	S02	S03	S04	S05	Avr
Single process steps	0–5 mm	c	41	27	7	13	9	19	1.76	1.08	0.30	0.57	0.40	0.82
		Δc [%]	-59.8	-36.2	-30.3	-11.3	-20.5	**-31.6**	-62.6	-42.8	-34.2	-16.3	-28.3	**-36.8**
	0–10 mm	c	33	18	6	8	8	15	1.42	0.71	0.28	0.32	0.37	0.62
		Δc [%]	-67.3	-56.8	-34.0	-49.2	-24.5	**-46.4**	-69.9	-62.6	-38.4	-52.4	-32.9	**-51.2**
	0–20 mm	c	26	17	6	8	5	12	1.08	0.65	0.27	0.32	0.24	0.51
		Δc [%]	-74.7	-59.5	-37.7	-48.9	-51.5	**-54.4**	-77.0	-65.5	-42.2	-52.4	-57.7	**-59.0**
	PET (NIR)	c	112	45	11	16	12	39	5.25	2.01	0.50	0.75	0.62	1.82
		Δc [%]	10.0	6.8	9.3	9.3	9.3	9.0	11.4	6.2	8.6	9.5	11.3	9.4
	PVC (NIR)	c	103	43	10	16	11	37	4.83	1.93	0.46	0.71	0.59	1.70
		Δc [%]	2.0	1.6	0.6	3.9	4.5	2.5	2.6	1.6	0.7	3.8	5.9	2.9
	b&g	c	119	45	11	16	12	41	5.71	2.07	0.53	0.76	0.63	1.94
		Δc [%]	17.8	8.3	14.1	9.2	9.2	11.7	21.2	9.3	15.3	11.1	14.2	14.2
	PET + PVC (NIR)	c	115	46	11	17	12	40	5.43	2.05	0.50	0.78	0.66	1.88
		Δc [%]	12.9	8.7	10.2	14.2	15.2	12.2	15.2	8.1	9.6	14.3	19.3	13.3
Combinations of Screening and state-of-the-art NIR sorting or manual removal of black materials	0–5 mm + PET (NIR)	c	45	29	7	15	9	21	1.95	1.14	0.32	0.62	0.44	0.90
		Δc [%]	-55.7	-31.5	-24.4	-2.1	-12.6	**-25.3**	-58.7	-39.6	-29.7	-8.2	-20.8	**-31.4**
	0–10 mm + PET (NIR)	c	36	19	7	8	9	16	1.57	0.74	0.30	0.35	0.41	0.67
		Δc [%]	-64.0	-53.9	-28.5	-44.9	-16.9	**-41.6**	-66.7	-61.0	-34.3	-48.6	-26.0	**-47.3**
	0–20 mm + PET (NIR)	c	28	18	7	8	6	13	1.20	0.68	0.28	0.35	0.25	0.55
		Δc [%]	-72.0	-56.6	-32.3	-44.2	-47.8	**-50.6**	-74.5	-64.0	-38.4	-48.5	-54.5	**-56.0**
	0–5 mm + PVC (NIR)	c	39	27	7	14	9	19	1.68	1.10	0.30	0.59	0.42	0.82
		Δc [%]	-61.6	-35.1	-30.3	-7.4	-17.2	**-30.3**	-64.3	-42.1	-34.2	-13.0	-24.9	**-35.7**
	0–10 mm + PVC (NIR)	c	31	18	6	8	8	14	1.31	0.71	0.28	0.34	0.39	0.61
		Δc [%]	-69.8	-56.2	-34.1	-47.3	-21.4	**-45.8**	-72.1	-62.3	-38.5	-50.7	-29.9	**-50.7**
	0–20 mm + PVC (NIR)	c	22	17	6	8	5	12	0.93	0.66	0.27	0.34	0.24	0.49
		Δc [%]	-78.3	-59.0	-37.8	-46.8	-50.9	**-54.6**	-80.2	-65.3	-42.3	-50.7	-57.1	**-59.1**
	0–5 mm + PET (NIR) + PVC (NIR)	c	43	29	7	15	10	**21**	1.87	1.16	0.32	0.65	0.47	**0.90**
		Δc [%]	-57.5	-30.2	-24.2	2.8	-7.9	**-23.4**	-60.2	-38.8	-29.6	-4.0	-16.0	**-29.7**
	0–10 mm + PET (NIR) + PVC (NIR)	c	34	20	7	9	9	**16**	1.46	0.75	0.30	0.36	0.44	**0.66**
		Δc [%]	-66.6	-53.2	-28.4	-42.4	-12.4	**-40.6**	-69.0	-60.6	-34.3	-46.6	-21.6	**-46.4**
	0–20 mm + PET (NIR) + PVC (NIR)	c	24	19	7	9	6	**13**	1.03	0.69	0.28	0.37	0.26	**0.53**
		Δc [%]	-75.9	-55.9	-32.3	-41.5	-46.7	**-50.5**	-78.1	-63.7	-38.5	-46.3	-53.4	**-56.0**
	0–5 mm + b&g	c	49	29	8	15	9	22	2.13	1.16	0.34	0.63	0.45	0.94
		Δc [%]	-52.0	-31.5	-21.5	-2.4	-12.7	**-24.0**	-54.7	-39.0	-26.1	-7.0	-18.5	**-29.1**
	0–10 mm + b&g	c	40	19	7	8	9	17	1.72	0.72	0.32	0.35	0.42	0.71
		Δc [%]	-60.9	-55.2	-25.7	-45.9	-16.9	**-40.9**	-63.4	-61.8	-31.0	-48.7	-23.8	**-45.7**
	0–20 mm + b&g	c	31	18	7	8	6	14	1.34	0.66	0.30	0.35	0.26	0.58
		Δc [%]	-69.1	-58.3	-29.7	-45.2	-47.6	**-50.0**	-71.5	-65.1	-35.2	-48.6	-52.8	**-54.7**
	0–5 mm + b&g + PVC (NIR)	c	47	29	8	15	10	22	2.07	1.17	0.34	0.66	0.48	0.95
		Δc [%]	-53.6	-30.2	-21.2	2.5	-8.0	**-22.1**	-56.1	-38.1	-25.8	-2.7	-13.3	**-27.2**
	0–10 mm + b&g + PVC (NIR)	c	37	19	7	8	9	16	1.62	0.73	0.32	0.36	0.45	0.70
		Δc [%]	-63.4	-54.5	-25.6	-43.4	-12.4	**-39.9**	-65.7	-61.4	-30.8	-46.6	-19.0	**-44.7**
	0–20 mm + b&g + PVC (NIR)	c	27	18	7	9	6	13	1.17	0.67	0.30	0.37	0.27	0.55
		Δc [%]	-73.1	-57.6	-29.7	-42.5	-46.5	**-49.9**	-75.2	-64.8	-35.2	-46.3	-51.5	**-54.6**
	0–5 mm + b&g + PET (NIR)	c	55	31	8	16	11	24	2.44	1.23	0.37	0.71	0.51	1.05
		Δc [%]	-45.6	-25.4	-12.3	9.6	-2.1	**-15.2**	-48.3	-34.9	-19.1	3.9	-7.6	**-21.2**
	0–10 mm + b&g + PET (NIR)	c	45	20	8	9	10	19	1.97	0.76	0.35	0.38	0.48	0.79
		Δc [%]	-55.5	-51.5	-16.9	-40.3	-6.5	**-34.1**	-58.1	-59.8	-24.5	-43.8	-13.5	**-39.9**
	0–20 mm + b&g + PET (NIR)	c	36	19	8	9	6	16	1.56	0.70	0.33	0.39	0.29	0.65
		Δc [%]	-64.2	-54.5	-21.1	-39.1	-42.3	**-44.2**	-66.8	-63.3	-29.1	-43.2	-47.9	**-50.1**
	0–5 mm + b&g + PET (NIR) + PVC (NIR)	c	54	32	9	17	11	25	2.39	1.26	0.37	0.75	0.56	1.07
		Δc [%]	-46.9	-23.7	-11.7	16.2	4.9	**-12.2**	-49.2	-33.7	-18.6	9.7	0.3	**-18.3**
	0–10 mm + b&g + PET (NIR) + PVC (NIR)	c	43	21	8	9	11	18	1.87	0.77	0.35	0.40	0.52	0.78
		Δc [%]	-58.0	-50.5	-16.5	-37.0	0.3	**-32.3**	-60.2	-59.3	-24.2	-41.0	-6.2	**-38.2**
	0–20 mm + b&g + PET (NIR) + PVC (NIR)	c	32	19	8	10	6	15	1.38	0.70	0.33	0.41	0.30	0.62
		Δc [%]	-68.5	-53.6	-20.7	-35.4	-40.2	**-43.7**	-70.8	-62.9	-28.9	-40.2	-45.4	**-49.6**

More targeted removal	PVC (FTIR) + b&g PVC	c	102	42	10	15	11	36	4.75	1.92	0.46	0.69	0.56	1.68
		Δc [%]	0.8	1.2	0.3	2.3	0.7	1.1	0.9	1.0	0.4	1.9	0.7	1.0
	0–5 mm + PVC (FTIR) + b&g PVC	c	41	27	7	14	9	19	1.78	1.10	0.30	0.58	0.40	0.83
		Δc [%]	-59.4	-35.3	-30.3	-9.0	-19.9	-30.8	-62.3	-42.2	-34.2	-14.6	-27.8	-36.2
	0–10 mm + PVC (FTIR) + b&g PVC	c	33	18	6	8	8	15	1.43	0.72	0.28	0.33	0.38	0.63
		Δc [%]	-67.0	-56.1	-34.1	-48.0	-23.9	-45.8	-69.6	-62.2	-38.4	-51.5	-32.5	-50.9
	0–20 mm + PVC (FTIR) + b&g PVC	c	26	17	6	8	5	12	1.09	0.66	0.27	0.33	0.24	0.52
		Δc [%]	-74.4	-58.8	-37.8	-47.6	-51.1	-54.0	-76.8	-65.1	-42.2	-51.5	-57.4	-58.6
	PVC (NIR) + b&g PVC	c	104	43	10	16	11	37	4.85	1.93	0.46	0.71	0.59	1.71
		Δc [%]	2.4	1.7	0.8	4.5	4.5	2.8	3.1	1.7	0.9	4.4	5.9	3.2
	0–5 mm + PVC (NIR) + b&g PVC	c	39	27	7	14	9	19	1.69	1.10	0.30	0.59	0.42	0.82
		Δc [%]	-61.5	-35.1	-30.1	-6.9	-17.2	-30.1	-64.1	-42.0	-34.1	-12.5	-24.9	-35.5
	0–10 mm + PVC (NIR) + b&g PVC	c	31	18	6	8	8	14	1.32	0.72	0.28	0.34	0.39	0.61
		Δc [%]	-69.7	-56.2	-34.0	-47.0	-21.4	-45.7	-72.0	-62.3	-38.3	-50.5	-29.9	-50.6
	0–20 mm + PVC (NIR) + b&g PVC	c	22	17	6	8	5	12	0.94	0.66	0.27	0.34	0.24	0.49
		Δc [%]	-78.2	-58.9	-37.7	-46.5	-50.9	-54.4	-80.1	-65.3	-42.2	-50.5	-57.1	-59.0
	PET (FTIR) + Textiles + b&g PET	c	109	43	10	16	11	38	5.08	1.95	0.48	0.72	0.59	1.76
		Δc [%]	7.6	3.1	4.6	5.3	6.2	5.4	7.9	2.7	4.5	5.1	7.0	5.4
	0–5 mm + PET (FTIR) + Textiles + b&g PET	c	44	28	7	14	9	20	1.89	1.11	0.31	0.60	0.42	0.87
		Δc [%]	-56.7	-34.1	-27.4	-6.1	-15.4	-27.9	-59.9	-41.5	-31.9	-12.0	-23.7	-33.8
	0–10 mm + PET (FTIR) + Textiles + b&g PET	c	36	19	7	8	9	16	1.52	0.72	0.29	0.34	0.40	0.65
		Δc [%]	-64.8	-55.5	-31.3	-46.9	-19.6	-43.6	-67.8	-62.0	-36.3	-50.5	-28.8	-49.1
	0–20 mm + PET (FTIR) + Textiles + b&g PET	c	28	18	6	8	5	13	1.16	0.66	0.28	0.34	0.24	0.54
		Δc [%]	-72.7	-58.3	-35.1	-46.4	-49.2	-52.3	-75.4	-65.0	-40.2	-50.5	-55.9	-57.4
	b&g Other	c	113	44	11	16	11	39	5.21	1.99	0.51	0.71	0.58	1.80
		Δc [%]	11.6	5.8	11.7	5.8	5.0	8.0	10.6	5.1	10.6	5.0	4.9	7.3
	0–5 mm + b&g Other	c	46	28	7	14	9	21	1.95	1.11	0.33	0.60	0.42	0.88
		Δc [%]	-54.5	-33.3	-23.0	-5.8	-16.2	-26.6	-58.6	-41.5	-28.8	-12.3	-25.0	-33.2
	0–10 mm + b&g Other	c	38	18	7	8	9	16	1.58	0.70	0.31	0.33	0.39	0.66
		Δc [%]	-62.9	-56.4	-27.2	-47.4	-20.4	-42.8	-66.5	-63.3	-33.6	-51.3	-29.9	-48.9
	0–20 mm + b&g Other	c	30	17	7	8	5	13	1.22	0.63	0.29	0.33	0.24	0.54
		Δc [%]	-70.8	-59.5	-31.1	-46.9	-49.3	-51.5	-74.2	-66.6	-37.7	-51.3	-56.3	-57.2
	PVC (FTIR) + b&g PVC + b&g Other	c	114	45	11	16	11	40	5.26	2.02	0.51	0.73	0.59	1.82
		Δc [%]	12.7	7.2	12.1	8.4	5.9	9.3	11.7	6.3	11.2	7.2	5.7	8.4
	0–5 mm + PVC (FTIR) + b&g PVC + b&g Other	c	47	28	7	14	9	21	1.97	1.12	0.33	0.61	0.42	0.89
		Δc [%]	-54.0	-32.3	-22.9	-3.2	-15.5	-25.6	-58.2	-40.8	-28.7	-10.4	-24.5	-32.5
	0–10 mm + PVC (FTIR) + b&g PVC + b&g Other	c	38	19	7	8	9	16	1.59	0.70	0.31	0.34	0.39	0.67
		Δc [%]	-62.5	-55.7	-27.2	-46.0	-19.6	-42.2	-66.2	-62.8	-33.5	-50.4	-29.4	-48.5
	0–20 mm + PVC (FTIR) + b&g PVC + b&g Other	c	30	17	7	8	6	14	1.23	0.64	0.29	0.34	0.24	0.55
		Δc [%]	-70.4	-58.7	-31.2	-45.4	-48.9	-50.9	-73.9	-66.2	-37.7	-50.4	-56.0	-56.8
	PVC (NIR) + b&g PVC + b&g Other	c	117	45	11	17	12	40	5.41	2.03	0.52	0.75	0.62	1.87
		Δc [%]	15.1	7.9	12.9	11.1	10.3	11.4	14.9	7.1	12.0	10.0	11.7	11.1
	0–5 mm + PVC (NIR) + b&g PVC + b&g Other	c	45	29	7	15	9	21	1.89	1.13	0.33	0.63	0.44	0.88
		Δc [%]	-56.0	-32.0	-22.6	-0.6	-12.2	-24.7	-59.9	-40.5	-28.5	-8.0	-21.0	-31.6
	0–10 mm + PVC (NIR) + b&g PVC + b&g Other	c	35	19	7	8	9	16	1.48	0.70	0.31	0.34	0.41	0.65
		Δc [%]	-65.2	-55.7	-26.9	-44.8	-16.5	-41.8	-68.6	-62.9	-33.3	-49.3	-26.4	-48.1
	0–20 mm + PVC (NIR) + b&g PVC + b&g Other	c	26	17	7	8	6	13	1.06	0.64	0.29	0.35	0.25	0.52
		Δc [%]	-74.5	-58.8	-31.0	-44.1	-48.5	-51.4	-77.5	-66.3	-37.6	-49.2	-55.6	-57.2
	b&g Other + b&g PVC	c	114	44	11	16	11	39	5.23	2.00	0.51	0.72	0.58	1.81
		Δc [%]	12.1	5.9	11.9	6.4	5.1	8.3	11.1	5.2	10.9	5.6	4.9	7.5
	0–5 mm + b&g Other + b&g PVC	c	46	28	7	14	9	21	1.96	1.11	0.33	0.60	0.42	0.88
		Δc [%]	-54.3	-33.2	-22.8	-5.2	-16.2	-26.4	-58.4	-41.4	-28.7	-11.8	-25.0	-33.1
	0–10 mm + b&g Other + b&g PVC	c	38	18	7	8	9	16	1.58	0.70	0.31	0.33	0.39	0.66
		Δc [%]	-62.7	-56.3	-27.0	-47.1	-20.3	-42.7	-66.4	-63.2	-33.4	-51.1	-29.9	-48.8
	0–20 mm + b&g Other + b&g PVC	c	30	17	7	8	5	13	1.22	0.63	0.29	0.33	0.24	0.54
		Δc [%]	-70.6	-59.4	-31.0	-46.6	-49.3	-51.4	-74.0	-66.6	-37.6	-51.1	-56.3	-57.1

B.20. Na

Table B.20: Relative concentration change (Δc, in %) of Na caused by the removal of different material or particle size fractions referring to mg/kg and mg/MJ, both calculated for dry mass without hard impurities

	Removed fractions	Conc. after removal	mg/kg$_{DM}$ S01	S02	S03	S04	S05	Avr	mg/MJ S01	S02	S03	S04	S05	Avr
Single process steps	0–5 mm	c	3742	1268	1080	1366	2212	**1933**	161	51	49	59	103	**85**
		Δc [%]	-12.8	-48.5	-41.9	-32.4	-46.9	**-36.5**	-19.0	-53.9	-45.2	-36.3	-52.1	**-41.3**
	0–10 mm	c	3811	1049	1013	1319	2029	**1844**	163	41	45	56	93	**80**
		Δc [%]	-11.2	-57.4	-45.5	-34.8	-51.3	**-40.0**	-18.1	-63.2	-49.1	-38.8	-56.8	**-45.2**
	0–20 mm	c	1046	938	959	1279	1749	**1194**	44	36	42	54	79	**51**
		Δc [%]	-75.6	-61.9	-48.4	-36.7	-58.0	**-56.2**	-77.9	-67.6	-52.1	-41.1	-63.4	**-60.4**
	PET (NIR)	c	4582	2595	1994	2134	4494	**3160**	215	117	94	97	235	**152**
		Δc [%]	6.8	5.4	7.3	5.6	7.8	**6.6**	8.0	4.8	6.6	5.8	9.7	**7.0**
	PVC (NIR)	c	4444	2508	1871	2068	4332	**3044**	208	113	89	94	226	**146**
		Δc [%]	3.5	1.8	0.6	2.3	3.9	**2.4**	4.2	1.8	0.8	2.2	5.3	**2.9**
	b&g	c	4934	2644	2047	2091	4561	**3255**	236	121	98	97	246	**159**
		Δc [%]	15.0	7.3	10.1	3.4	9.4	**9.0**	18.3	8.3	11.2	5.2	14.5	**11.5**
	PET + PVC (NIR)	c	4771	2647	2011	2192	4709	**3266**	226	119	95	100	251	**158**
		Δc [%]	11.2	7.4	8.2	8.4	13.0	**9.6**	13.4	6.8	7.6	8.5	17.0	**10.7**
Combinations of Screening and state-of-the-art NIR sorting or manual removal of black materials	0–5 mm + PET (NIR)	c	4012	1308	1117	1408	2304	**2030**	174	52	49	60	107	**89**
		Δc [%]	-6.5	-46.9	-39.9	-30.4	-44.7	**-33.7**	-12.8	-53.2	-44.2	-34.6	-49.9	**-39.0**
	0–10 mm + PET (NIR)	c	4106	1069	1042	1356	2097	**1934**	176	41	46	57	96	**83**
		Δc [%]	-4.3	-56.6	-44.0	-32.9	-49.7	**-37.5**	-11.5	-63.3	-48.6	-37.5	-55.2	**-43.2**
	0–20 mm + PET (NIR)	c	948	945	980	1313	1775	**1192**	40	35	43	55	80	**51**
		Δc [%]	-77.9	-61.6	-47.3	-35.1	-57.4	**-55.9**	-79.9	-68.2	-52.0	-40.0	-62.9	**-60.6**
	0–5 mm + PVC (NIR)	c	3880	1290	1077	1384	2223	**1971**	168	52	48	59	104	**86**
		Δc [%]	-9.6	-47.6	-42.1	-31.6	-46.7	**-35.5**	-15.8	-53.2	-45.4	-35.7	-51.6	**-40.3**
	0–10 mm + PVC (NIR)	c	3963	1068	1009	1335	2023	**1879**	185	41	45	58	97	**85**
		Δc [%]	-7.7	-56.7	-45.7	-34.0	-51.5	**-39.1**	-7.0	-62.8	-48.8	-36.9	-55.0	**-42.1**
	0–20 mm + PVC (NIR)	c	986	955	953	1294	1714	**1180**	42	37	42	54	77	**50**
		Δc [%]	-77.0	-61.2	-48.7	-36.0	-58.9	**-56.4**	-79.1	-67.2	-52.4	-40.7	-64.0	**-60.7**
	0–5 mm + PET (NIR) + PVC (NIR)	c	4191	1334	1114	1431	2327	**2080**	182	53	49	61	109	**91**
		Δc [%]	-2.3	-45.8	-40.1	-29.2	-44.2	**-32.3**	-8.7	-52.5	-44.3	-33.9	-49.1	**-37.7**
	0–10 mm + PET (NIR) + PVC (NIR)	c	4305	1091	1037	1377	2098	**1981**	182	53	49	61	109	**91**
		Δc [%]	0.3	-55.7	-44.2	-31.9	-49.7	**-36.2**	-8.7	-52.5	-44.3	-33.9	-49.1	**-37.7**
	0–20 mm + PET (NIR) + PVC (NIR)	c	868	965	974	1332	1737	**1175**	37	36	42	56	78	**50**
		Δc [%]	-79.8	-60.8	-47.6	-34.1	-58.3	**-56.1**	-81.6	-67.8	-52.3	-39.5	-63.6	**-61.0**
	0–5 mm + b&g	c	4383	1303	1110	1348	2397	**2108**	192	52	50	58	115	**94**
		Δc [%]	2.1	-47.1	-40.3	-33.3	-42.5	**-32.2**	-3.6	-52.9	-43.8	-36.5	-46.3	**-36.6**
	0–10 mm + b&g	c	4509	1050	1029	1292	2195	**2015**	196	40	46	56	104	**88**
		Δc [%]	5.1	-57.4	-44.6	-36.1	-47.3	**-36.1**	-1.7	-63.6	-48.5	-39.5	-51.7	**-41.0**
	0–20 mm + b&g	c	1093	916	962	1244	1884	**1220**	47	35	42	53	87	**53**
		Δc [%]	-74.5	-62.8	-48.3	-38.5	-54.8	**-55.8**	-76.6	-68.9	-52.3	-42.2	-59.3	**-59.9**
	0–5 mm + b&g + PVC (NIR)	c	4611	1331	1107	1367	2430	**2169**	203	53	50	59	118	**97**
		Δc [%]	7.4	-46.0	-40.4	-32.4	-41.7	**-30.6**	1.8	-52.1	-43.9	-35.8	-45.1	**-35.0**
	0–10 mm + b&g + PVC (NIR)	c	4765	1072	1024	1309	2208	**2076**	208	41	45	56	105	**91**
		Δc [%]	11.0	-56.5	-44.9	-35.2	-47.0	**-34.5**	4.3	-63.1	-48.8	-39.0	-51.0	**-39.5**
	0–20 mm + b&g + PVC (NIR)	c	1019	936	955	1259	1860	**1206**	44	35	42	53	87	**52**
		Δc [%]	-76.2	-62.0	-48.6	-37.7	-55.4	**-56.0**	-78.1	-68.5	-52.7	-41.8	-59.6	**-60.1**
	0–5 mm + b&g + PET (NIR)	c	4827	1355	1163	1394	2537	**2255**	213	53	51	60	123	**100**
		Δc [%]	12.5	-45.0	-37.4	-31.1	-39.1	**-28.0**	7.0	-52.0	-42.3	-34.6	-42.6	**-32.9**
	0–10 mm + b&g + PET (NIR)	c	5009	1074	1069	1332	2306	**2158**	219	40	46	57	110	**94**
		Δc [%]	16.7	-56.4	-42.5	-34.1	-44.7	**-32.2**	10.0	-63.8	-47.8	-38.0	-48.8	**-37.7**
	0–20 mm + b&g + PET (NIR)	c	971	922	991	1279	1942	**1221**	42	34	42	54	90	**52**
		Δc [%]	-77.4	-62.6	-46.7	-36.8	-53.4	**-55.4**	-79.1	-69.8	-52.1	-41.1	-57.9	**-60.0**
	0–5 mm + b&g + PET (NIR) + PVC (NIR)	c	5142	1388	1161	1420	2594	**2341**	228	54	51	61	128	**104**
		Δc [%]	19.8	-43.7	-37.5	-29.8	-37.8	**-25.8**	14.6	-51.1	-42.4	-33.7	-40.5	**-30.6**
	0–10 mm + b&g + PET (NIR) + PVC (NIR)	c	5370	1100	1064	1355	2336	**2245**	236	41	46	58	112	**99**
		Δc [%]	25.1	-55.3	-42.8	-33.0	-44.0	**-30.0**	18.5	-63.2	-48.0	-37.3	-47.6	**-35.5**
	0–20 mm + b&g + PET (NIR) + PVC (NIR)	c	862	945	983	1299	1921	**1202**	37	34	42	55	90	**52**
		Δc [%]	-79.9	-61.6	-47.1	-35.7	-53.9	**-55.7**	-81.3	-69.3	-52.6	-40.5	-58.0	**-60.4**

More targeted removal	PVC (FTIR) + b&g PVC	c	4323	2492	1867	2059	4198	**2987**	201	112	89	93	216	**142**
		Δc [%]	0.7	1.2	0.4	1.8	0.7	**1.0**	0.8	1.0	0.5	1.5	0.7	**0.9**
	0–5 mm + PVC (FTIR) + b&g PVC	c	3771	1284	1080	1388	2227	**1950**	163	52	49	59	103	**85**
		Δc [%]	-12.1	-47.9	-41.9	-31.3	-46.6	**-36.0**	-18.4	-53.4	-45.1	-35.6	-51.8	**-40.9**
	0–10 mm + PVC (FTIR) + b&g PVC	c	3843	1063	1013	1341	2043	**1861**	165	41	45	57	93	**80**
		Δc [%]	-10.5	-56.8	-45.5	-33.7	-51.0	**-39.5**	-17.5	-62.8	-49.1	-38.2	-56.5	**-44.8**
	0–20 mm + PVC (FTIR) + b&g PVC	c	1049	952	958	1301	1762	**1204**	44	36	42	55	79	**51**
		Δc [%]	-75.6	-61.4	-48.5	-35.7	-57.7	**-55.8**	-77.8	-67.3	-52.1	-40.5	-63.2	**-60.2**
	PVC (NIR) + b&g PVC	c	4459	2510	1874	2075	4333	**3050**	208	113	89	94	226	**146**
		Δc [%]	3.9	1.9	0.8	2.7	4.0	**2.6**	4.6	1.9	1.0	2.5	5.4	**3.1**
	0–5 mm + PVC (NIR) + b&g PVC	c	3895	1292	1079	1388	2224	**1975**	168	52	48	59	104	**86**
		Δc [%]	-9.2	-47.6	-42.0	-31.4	-46.6	**-35.4**	-15.5	-53.2	-45.3	-35.6	-51.6	**-40.2**
	0–10 mm + PVC (NIR) + b&g PVC	c	3979	1069	1010	1338	2024	**1884**	171	42	45	57	93	**81**
		Δc [%]	-7.3	-56.6	-45.6	-33.8	-51.4	**-39.0**	-14.4	-62.6	-49.2	-38.2	-56.7	**-44.2**
	0–20 mm + PVC (NIR) + b&g PVC	c	989	956	955	1297	1715	**1182**	42	37	42	55	77	**50**
		Δc [%]	-77.0	-61.2	-48.6	-35.8	-58.9	**-56.3**	-79.1	-67.2	-52.4	-40.6	-64.0	**-60.6**
	PET (FTIR) + Textiles + b&g PET	c	4530	2527	1935	2089	4377	**3092**	211	114	92	95	227	**148**
		Δc [%]	5.5	2.6	4.1	3.3	5.0	**4.1**	5.8	2.1	4.0	3.1	5.8	**4.2**
	0–5 mm + PET (FTIR) + Textiles + b&g PET	c	3966	1288	1107	1391	2259	**2002**	170	52	50	59	105	**87**
		Δc [%]	-7.6	-47.7	-40.4	-31.2	-45.8	**-34.5**	-14.5	-53.6	-44.1	-35.5	-51.2	**-39.8**
	0–10 mm + PET (FTIR) + Textiles + b&g PET	c	4056	1059	1037	1342	2059	**1910**	173	41	46	57	94	**82**
		Δc [%]	-5.5	-57.0	-44.2	-33.6	-50.6	**-38.2**	-13.4	-63.3	-48.2	-38.2	-56.3	**-43.9**
	0–20 mm + PET (FTIR) + Textiles + b&g PET	c	997	942	979	1300	1750	**1194**	42	36	43	55	78	**51**
		Δc [%]	-76.8	-61.7	-47.3	-35.7	-58.0	**-55.9**	-79.1	-67.9	-51.4	-40.6	-63.6	**-60.5**
	b&g Other	c	4694	2578	1998	2045	4370	**3137**	216	116	94	92	225	**149**
		Δc [%]	9.4	4.7	7.5	1.2	4.8	**5.5**	8.4	4.0	6.4	0.4	4.7	**4.8**
	0–5 mm + b&g Other	c	4137	1265	1087	1328	2298	**2023**	175	50	48	56	106	**87**
		Δc [%]	-3.6	-48.7	-41.5	-34.3	-44.9	**-34.6**	-12.2	-54.9	-46.0	-38.8	-50.7	**-40.5**
	0–10 mm + b&g Other	c	4240	1015	1008	1275	2104	**1929**	178	39	44	54	95	**82**
		Δc [%]	-1.2	-58.8	-45.8	-36.9	-49.5	**-38.4**	-10.9	-65.3	-50.5	-41.7	-55.6	**-44.8**
	0–20 mm + b&g Other	c	1064	883	942	1228	1806	**1185**	44	33	41	51	80	**50**
		Δc [%]	-75.2	-64.2	-49.3	-39.3	-56.7	**-56.9**	-78.1	-70.5	-54.2	-44.4	-62.7	**-61.9**
	PVC (FTIR) + b&g PVC + b&g Other	c	4732	2611	2008	2086	4403	**3168**	218	117	95	94	226	**150**
		Δc [%]	10.2	6.0	8.0	3.2	5.7	**6.6**	9.3	5.1	7.1	2.0	5.5	**5.8**
	0–5 mm + PVC (FTIR) + b&g PVC + b&g Other	c	4176	1283	1088	1352	2316	**2043**	177	51	48	57	106	**88**
		Δc [%]	-2.7	-47.9	-41.5	-33.1	-44.4	**-33.9**	-11.4	-54.4	-45.9	-38.1	-50.4	**-40.0**
	0–10 mm + PVC (FTIR) + b&g PVC + b&g Other	c	4282	1031	1008	1298	2121	**1948**	179	39	44	54	96	**82**
		Δc [%]	-0.2	-58.1	-45.8	-35.8	-49.1	**-37.8**	-10.0	-64.9	-50.5	-41.0	-55.3	**-44.4**
	0–20 mm + PVC (FTIR) + b&g PVC + b&g Other	c	1069	898	941	1251	1821	**1196**	44	33	41	52	81	**50**
		Δc [%]	-75.1	-63.5	-49.4	-38.1	-56.3	**-56.5**	-78.0	-70.1	-54.2	-43.7	-62.4	**-61.7**
	PVC (NIR) + b&g PVC + b&g Other	c	4911	2633	2019	2105	4563	**3246**	228	118	95	95	238	**155**
		Δc [%]	14.4	6.9	8.6	4.1	9.5	**8.7**	14.2	6.1	7.7	3.2	10.9	**8.4**
	0–5 mm + PVC (NIR) + b&g PVC + b&g Other	c	4348	1292	1086	1350	2320	**2079**	184	51	48	57	107	**89**
		Δc [%]	1.3	-47.6	-41.6	-33.2	-44.3	**-33.1**	-7.6	-54.2	-46.0	-38.2	-50.0	**-39.2**
	0–10 mm + PVC (NIR) + b&g PVC + b&g Other	c	4474	1037	1004	1294	2107	**1983**	187	39	44	54	96	**84**
		Δc [%]	4.2	-57.9	-46.0	-36.0	-49.4	**-37.0**	-5.9	-64.8	-50.7	-41.2	-55.4	**-43.6**
	0–20 mm + PVC (NIR) + b&g PVC + b&g Other	c	998	902	936	1244	1775	**1171**	41	33	40	51	79	**49**
		Δc [%]	-76.7	-63.4	-49.6	-38.5	-57.4	**-57.1**	-79.5	-70.1	-54.5	-44.0	-63.3	**-62.3**
	b&g Other + b&g PVC	c	4711	2581	2002	2053	4371	**3143**	217	116	94	93	225	**149**
		Δc [%]	9.7	4.8	7.7	1.5	4.9	**5.7**	8.8	4.0	6.7	0.8	4.8	**5.0**
	0–5 mm + b&g Other + b&g PVC	c	4154	1266	1089	1332	2299	**2028**	176	50	48	56	106	**87**
		Δc [%]	-3.2	-48.6	-41.4	-34.1	-44.8	**-34.4**	-11.8	-54.9	-45.8	-38.7	-50.6	**-40.4**
	0–10 mm + b&g Other + b&g PVC	c	4259	1017	1010	1278	2105	**1934**	178	39	44	54	95	**82**
		Δc [%]	-0.8	-58.7	-45.7	-36.8	-49.5	**-38.3**	-10.5	-65.3	-50.4	-41.6	-55.6	**-44.7**
	0–20 mm + b&g Other + b&g PVC	c	1067	884	944	1231	1807	**1187**	44	33	41	51	80	**50**
		Δc [%]	-75.1	-64.1	-49.2	-39.1	-56.6	**-56.8**	-78.0	-70.4	-54.1	-44.3	-62.6	**-61.9**

B.21. Ni

Table B.21: Relative concentration change (Δc, in %) of Ni caused by the removal of different material or particle size fractions referring to mg/kg and mg/MJ, both calculated for dry mass without hard impurities

	Removed fractions	Conc. after removal	mg/kg$_{DM}$						mg/MJ					
			S01	S02	S03	S04	S05	Avr	S01	S02	S03	S04	S05	Avr
Single process steps	0–5 mm	c	66	32	14	24	18	**31**	2.9	1.3	0.6	1.0	0.9	**1.3**
		Δc [%]	-69.3	-42.5	-34.6	-21.3	-30.8	**-39.7**	-71.5	-48.5	-38.3	-25.7	-37.5	**-44.3**
	0–10 mm	c	63	28	13	19	17	**28**	2.7	1.1	0.6	0.8	0.8	**1.2**
		Δc [%]	-70.8	-49.9	-39.4	-37.2	-35.0	**-46.5**	-73.1	-56.7	-43.4	-41.1	-42.2	**-51.3**
	0–20 mm	c	61	26	12	19	12	**26**	2.6	1.0	0.5	0.8	0.6	**1.1**
		Δc [%]	-71.4	-52.1	-44.4	-37.3	-53.7	**-51.8**	-74.0	-59.2	-48.4	-41.7	-59.7	**-56.6**
	PET (NIR)	c	234	58	22	33	28	**75**	11.0	2.6	1.1	1.5	1.5	**3.5**
		Δc [%]	8.8	5.9	4.9	7.7	7.2	**6.9**	10.1	5.3	4.2	7.9	9.1	**7.3**
	PVC (NIR)	c	214	56	21	32	27	**70**	10.0	2.5	1.0	1.4	1.4	**3.3**
		Δc [%]	-0.6	1.4	-0.7	2.7	2.5	**1.1**	0.0	1.3	-0.5	2.6	3.9	**1.5**
	b&g	c	250	53	23	31	28	**77**	12.0	2.4	1.1	1.4	1.5	**3.7**
		Δc [%]	16.3	-4.4	6.1	-1.6	5.3	**4.3**	19.8	-3.5	7.2	0.1	10.1	**6.7**
	PET + PVC (NIR)	c	234	59	22	34	29	**76**	11.1	2.7	1.1	1.6	1.6	**3.6**
		Δc [%]	8.7	7.5	4.3	11.1	10.6	**8.5**	10.9	6.9	3.7	11.3	14.6	**9.5**
Combinations of Screening and state-of-the-art NIR sorting or manual removal of black materials	0–5 mm + PET (NIR)	c	69	33	14	26	19	**32**	3.0	1.3	0.6	1.1	0.9	**1.4**
		Δc [%]	-67.8	-39.6	-34.1	-15.3	-27.0	**-36.8**	-70.0	-46.8	-38.8	-20.5	-33.8	**-42.0**
	0–10 mm + PET (NIR)	c	66	29	13	21	18	**29**	2.8	1.1	0.6	0.9	0.8	**1.2**
		Δc [%]	-69.5	-47.4	-39.7	-33.2	-31.6	**-44.3**	-71.8	-55.5	-44.6	-37.7	-39.1	**-49.8**
	0–20 mm + PET (NIR)	c	65	28	12	21	12	**27**	2.7	1.0	0.5	0.9	0.6	**1.1**
		Δc [%]	-69.9	-49.6	-45.5	-33.0	-53.3	**-50.3**	-72.7	-58.2	-50.4	-38.1	-59.3	**-55.7**
	0–5 mm + PVC (NIR)	c	54	32	14	25	18	**29**	2.3	1.3	0.6	1.1	0.9	**1.2**
		Δc [%]	-74.8	-42.0	-36.0	-19.3	-30.7	**-40.6**	-76.6	-48.2	-39.6	-24.2	-37.1	**-45.1**
	0–10 mm + PVC (NIR)	c	50	28	13	20	17	**25**	2.1	1.1	0.6	0.8	0.8	**1.1**
		Δc [%]	-76.8	-49.5	-41.0	-36.1	-35.3	**-47.7**	-78.5	-56.5	-44.9	-40.3	-42.3	**-52.5**
	0–20 mm + PVC (NIR)	c	46	27	11	20	12	**23**	2.0	1.0	0.5	0.8	0.5	**1.0**
		Δc [%]	-78.5	-51.7	-46.2	-36.1	-56.0	**-53.7**	-80.4	-59.1	-50.1	-40.8	-61.6	**-58.4**
	0–5 mm + PET (NIR) + PVC (NIR)	c	56	34	14	27	20	**30**	2.4	1.3	0.6	1.1	0.9	**1.3**
		Δc [%]	-74.0	-38.9	-35.8	-12.7	-26.5	**-37.6**	-75.7	-46.4	-40.3	-18.5	-32.9	**-42.8**
	0–10 mm + PET (NIR) + PVC (NIR)	c	51	29	12	21	18	**26**	2.2	1.1	0.5	0.9	0.8	**1.1**
		Δc [%]	-76.2	-46.9	-41.5	-31.6	-31.6	**-45.6**	-78.0	-55.4	-46.3	-36.6	-38.8	**-51.0**
	0–20 mm + PET (NIR) + PVC (NIR)	c	47	28	11	21	12	**24**	2.0	1.0	0.5	0.9	0.5	**1.0**
		Δc [%]	-78.1	-49.1	-47.6	-31.4	-55.9	**-52.4**	-80.1	-58.1	-52.3	-37.0	-61.5	**-57.8**
	0–5 mm + b&g	c	75	25	14	23	19	**31**	3.3	1.0	0.6	1.0	0.9	**1.4**
		Δc [%]	-65.4	-54.9	-35.7	-26.2	-28.9	**-42.2**	-67.3	-59.8	-39.5	-29.7	-33.7	**-46.0**
	0–10 mm + b&g	c	71	19	12	17	18	**27**	3.1	0.7	0.5	0.7	0.8	**1.2**
		Δc [%]	-67.0	-65.3	-41.8	-44.8	-33.6	**-50.5**	-69.1	-70.4	-45.9	-47.8	-39.1	**-54.5**
	0–20 mm + b&g	c	71	17	11	17	12	**25**	3.0	0.6	0.5	0.7	0.5	**1.1**
		Δc [%]	-67.0	-69.9	-48.2	-45.5	-55.3	**-57.2**	-69.6	-74.8	-52.3	-48.8	-59.8	**-61.1**
	0–5 mm + b&g + PVC (NIR)	c	60	25	13	23	19	**28**	2.7	1.0	0.6	1.0	0.9	**1.2**
		Δc [%]	-71.9	-54.6	-37.5	-24.3	-28.6	**-43.4**	-73.4	-59.8	-41.2	-28.1	-32.7	**-47.0**
	0–10 mm + b&g + PVC (NIR)	c	56	19	12	17	18	**24**	2.4	0.7	0.5	0.7	0.8	**1.1**
		Δc [%]	-74.2	-65.4	-43.8	-44.0	-33.8	**-52.2**	-75.7	-70.6	-47.8	-47.2	-38.8	**-56.0**
	0–20 mm + b&g + PVC (NIR)	c	52	16	11	17	11	**21**	2.2	0.6	0.5	0.7	0.5	**0.9**
		Δc [%]	-75.8	-70.2	-50.6	-44.6	-58.2	**-59.9**	-77.7	-75.2	-54.5	-48.3	-62.2	**-63.6**
	0–5 mm + b&g + PET (NIR)	c	80	26	14	25	20	**33**	3.5	1.0	0.6	1.1	1.0	**1.4**
		Δc [%]	-62.9	-52.9	-35.4	-20.0	-24.1	**-39.1**	-64.7	-58.9	-40.3	-24.1	-28.4	**-43.3**
	0–10 mm + b&g + PET (NIR)	c	76	20	12	18	19	**29**	3.3	0.7	0.5	0.8	0.9	**1.3**
		Δc [%]	-64.6	-64.5	-42.6	-41.3	-29.4	**-48.5**	-66.7	-70.6	-47.8	-44.8	-34.7	**-52.9**
	0–20 mm + b&g + PET (NIR)	c	77	17	11	18	12	**27**	3.3	0.6	0.5	0.8	0.6	**1.1**
		Δc [%]	-64.0	-69.7	-50.4	-41.8	-55.1	**-56.2**	-66.7	-75.6	-55.5	-45.8	-59.4	**-60.6**
	0–5 mm + b&g + PET (NIR) + PVC (NIR)	c	64	26	13	26	20	**30**	2.8	1.0	0.6	1.1	1.0	**1.3**
		Δc [%]	-70.4	-52.6	-37.5	-17.3	-23.2	**-40.2**	-71.7	-58.8	-42.3	-21.9	-26.5	**-44.3**
	0–10 mm + b&g + PET (NIR) + PVC (NIR)	c	58	19	12	19	19	**25**	2.6	0.7	0.5	0.8	0.9	**1.1**
		Δc [%]	-72.9	-64.6	-45.0	-40.0	-29.1	**-50.3**	-74.4	-70.9	-50.1	-43.9	-33.7	**-54.6**
	0–20 mm + b&g + PET (NIR) + PVC (NIR)	c	55	16	10	18	11	**22**	2.4	0.6	0.4	0.8	0.5	**0.9**
		Δc [%]	-74.6	-70.0	-53.4	-40.4	-58.6	**-59.4**	-76.5	-76.1	-58.2	-44.9	-62.2	**-63.6**

More targeted removal	PVC (FTIR) + b&g PVC	c	217	56	21	32	27	**70**	10.1	2.5	1.0	1.4	1.4	**3.3**
		Δc [%]	0.8	1.0	0.1	1.6	0.4	0.8	0.8	0.8	0.2	1.2	0.4	0.7
	0–5 mm + PVC (FTIR) + b&g PVC	c	66	32	14	25	18	**31**	2.9	1.3	0.6	1.1	0.9	**1.3**
		Δc [%]	-69.1	-42.0	-34.8	-20.1	-30.6	**-39.3**	-71.3	-48.2	-38.4	-25.0	-37.4	**-44.1**
	0–10 mm + PVC (FTIR) + b&g PVC	c	63	28	13	20	17	**28**	2.7	1.1	0.6	0.8	0.8	**1.2**
		Δc [%]	-70.6	-49.4	-39.7	-36.5	-34.8	**-46.2**	-72.9	-56.4	-43.6	-40.8	-42.2	**-51.2**
	0–20 mm + PVC (FTIR) + b&g PVC	c	62	27	12	20	12	**26**	2.6	1.0	0.5	0.8	0.6	**1.1**
		Δc [%]	-71.2	-51.6	-44.8	-36.6	-53.7	**-51.6**	-73.8	-59.0	-48.7	-41.3	-59.7	**-56.5**
	PVC (NIR) + b&g PVC	c	214	56	21	32	27	**70**	10.0	2.5	1.0	1.5	1.4	**3.3**
		Δc [%]	-0.3	1.5	-0.5	3.2	2.5	1.3	0.4	1.4	-0.4	3.1	3.8	1.7
	0–5 mm + PVC (NIR) + b&g PVC	c	54	32	14	25	18	**29**	2.3	1.3	0.6	1.1	0.9	**1.2**
		Δc [%]	-74.8	-41.9	-35.9	-18.9	-30.8	**-40.5**	-76.5	-48.1	-39.6	-23.8	-37.2	**-45.1**
	0–10 mm + PVC (NIR) + b&g PVC	c	50	28	13	20	17	**26**	2.1	1.1	0.6	0.8	0.8	**1.1**
		Δc [%]	-76.7	-49.5	-40.9	-35.8	-35.3	**-47.6**	-78.5	-56.5	-44.8	-40.1	-42.3	**-52.4**
	0–20 mm + PVC (NIR) + b&g PVC	c	46	27	11	20	12	**23**	2.0	1.0	0.5	0.8	0.5	**1.0**
		Δc [%]	-78.4	-51.6	-46.2	-35.8	-56.1	**-53.6**	-80.4	-59.1	-50.0	-40.6	-61.6	**-58.3**
	PET (FTIR) + Textiles + b&g PET	c	229	57	22	32	28	**74**	10.7	2.5	1.0	1.5	1.4	**3.4**
		Δc [%]	6.6	2.9	1.9	4.2	4.5	4.0	6.9	2.4	1.8	4.0	5.4	4.1
	0–5 mm + PET (FTIR) + Textiles + b&g PET	c	68	32	14	25	19	**32**	2.9	1.3	0.6	1.1	0.9	**1.4**
		Δc [%]	-68.3	-41.0	-35.0	-18.2	-28.6	**-38.2**	-70.7	-47.7	-39.0	-23.3	-35.6	**-43.3**
	0–10 mm + PET (FTIR) + Textiles + b&g PET	c	65	28	13	20	18	**29**	2.8	1.1	0.6	0.8	0.8	**1.2**
		Δc [%]	-69.9	-48.6	-40.2	-35.3	-33.1	**-45.4**	-72.4	-56.1	-44.5	-39.8	-40.7	**-50.7**
	0–20 mm + PET (FTIR) + Textiles + b&g PET	c	64	27	12	20	12	**27**	2.7	1.0	0.5	0.8	0.5	**1.1**
		Δc [%]	-70.4	-50.8	-45.7	-35.3	-53.8	**-51.2**	-73.3	-58.8	-49.9	-40.3	-60.0	**-56.5**
	b&g Other	c	239	52	22	30	27	**74**	11.0	2.3	1.1	1.3	1.4	**3.4**
		Δc [%]	11.1	-5.8	5.0	-4.2	2.4	1.7	10.1	-6.5	4.0	-4.9	2.2	1.0
	0–5 mm + b&g Other	c	73	25	14	22	18	**30**	3.1	1.0	0.6	0.9	0.9	**1.3**
		Δc [%]	-66.0	-55.0	-35.5	-28.1	-30.4	**-43.0**	-69.0	-60.5	-40.4	-33.0	-37.7	**-48.1**
	0–10 mm + b&g Other	c	70	19	12	17	17	**27**	2.9	0.7	0.5	0.7	0.8	**1.1**
		Δc [%]	-67.5	-65.1	-41.4	-45.9	-34.9	**-51.0**	-70.7	-70.6	-46.5	-50.0	-42.7	**-56.1**
	0–20 mm + b&g Other	c	70	17	11	17	12	**25**	2.9	0.6	0.5	0.7	0.5	**1.0**
		Δc [%]	-67.7	-69.5	-47.5	-46.6	-55.3	**-57.3**	-71.4	-74.8	-52.5	-51.1	-61.5	**-62.3**
	PVC (FTIR) + b&g PVC + b&g Other	c	241	52	22	30	27	**75**	11.1	2.3	1.1	1.4	1.4	**3.5**
		Δc [%]	12.1	-4.9	5.2	-2.6	2.8	2.5	11.1	-5.7	4.3	-3.7	2.7	1.7
	0–5 mm + PVC (FTIR) + b&g PVC + b&g Other	c	74	25	14	23	19	**31**	3.1	1.0	0.6	1.0	0.9	**1.3**
		Δc [%]	-65.7	-54.7	-35.8	-27.0	-30.2	**-42.7**	-68.8	-60.4	-40.6	-32.5	-37.6	**-48.0**
	0–10 mm + PVC (FTIR) + b&g PVC + b&g Other	c	70	19	12	17	17	**27**	2.9	0.7	0.5	0.7	0.8	**1.1**
		Δc [%]	-67.3	-64.9	-41.7	-45.4	-34.7	**-50.8**	-70.5	-70.6	-46.8	-49.9	-42.7	**-56.1**
	0–20 mm + PVC (FTIR) + b&g PVC + b&g Other	c	70	17	11	17	12	**25**	2.9	0.6	0.5	0.7	0.5	**1.0**
		Δc [%]	-67.4	-69.3	-48.0	-46.1	-55.3	**-57.2**	-71.2	-74.9	-53.0	-51.0	-61.6	**-62.3**
	PVC (NIR) + b&g PVC + b&g Other	c	240	53	22	31	28	**75**	11.1	2.4	1.1	1.4	1.5	**3.5**
		Δc [%]	11.5	-4.4	4.5	-0.9	5.2	3.2	11.3	-5.1	3.7	-1.8	6.6	2.9
	0–5 mm + PVC (NIR) + b&g PVC + b&g Other	c	60	25	13	23	19	**28**	2.5	1.0	0.6	1.0	0.9	**1.2**
		Δc [%]	-72.1	-54.8	-37.2	-25.9	-30.3	**-44.0**	-74.5	-60.5	-42.0	-31.4	-37.4	**-49.1**
	0–10 mm + PVC (NIR) + b&g PVC + b&g Other	c	56	19	12	17	17	**24**	2.3	0.7	0.5	0.7	0.8	**1.0**
		Δc [%]	-74.2	-65.2	-43.2	-44.9	-35.3	**-52.5**	-76.7	-70.8	-48.2	-49.4	-42.9	**-57.6**
	0–20 mm + PVC (NIR) + b&g PVC + b&g Other	c	52	17	11	17	11	**22**	2.1	0.6	0.5	0.7	0.5	**0.9**
		Δc [%]	-75.7	-69.7	-49.7	-45.6	-58.0	**-59.7**	-78.5	-75.2	-54.6	-50.5	-63.8	**-64.5**
	b&g Other + b&g PVC	c	240	52	22	30	27	**74**	11.0	2.3	1.1	1.3	1.4	**3.4**
		Δc [%]	11.5	-5.8	5.2	-3.7	2.3	1.9	10.5	-6.4	4.2	-4.4	2.2	1.2
	0–5 mm + b&g Other + b&g PVC	c	73	25	14	22	18	**31**	3.1	1.0	0.6	0.9	0.9	**1.3**
		Δc [%]	-65.9	-55.0	-35.5	-27.7	-30.5	**-42.9**	-69.0	-60.5	-40.3	-32.7	-37.8	**-48.1**
	0–10 mm + b&g Other + b&g PVC	c	70	19	12	17	17	**27**	2.9	0.7	0.5	0.7	0.8	**1.1**
		Δc [%]	-67.5	-65.1	-41.3	-45.7	-34.9	**-50.9**	-70.7	-70.6	-46.4	-49.8	-42.8	**-56.1**
	0–20 mm + b&g Other + b&g PVC	c	70	17	11	17	12	**25**	2.9	0.6	0.5	0.7	0.5	**1.0**
		Δc [%]	-67.6	-69.4	-47.5	-46.3	-55.3	**-57.2**	-71.3	-74.8	-52.5	-50.9	-61.5	**-62.2**

B.22. P

Table B.22: Relative concentration change (Δc, in %) of P caused by the removal of different material or particle size fractions referring to mg/kg and mg/MJ, both calculated for dry mass without hard impurities

	Removed fractions	Conc. after removal	mg/kg$_{DM}$						mg/MJ					
			S01	S02	S03	S04	S05	Avr	S01	S02	S03	S04	S05	Avr
Single process steps	0–5 mm	c	896	254	140	249	390	**386**	39	10	6	11	18	**17**
		Δc [%]	9.3	-11.8	-12.3	-4.2	-6.2	**-5.0**	1.6	-21.0	-17.3	-9.6	-15.3	**-12.3**
	0–10 mm	c	932	256	134	250	393	**393**	40	10	6	11	18	**17**
		Δc [%]	13.7	-10.9	-15.8	-3.7	-5.5	**-4.4**	4.9	-22.9	-21.4	-9.6	-16.0	**-13.0**
	0–20 mm	c	1036	246	132	250	400	**413**	44	9	6	11	18	**18**
		Δc [%]	26.5	-14.6	-17.7	-3.7	-3.9	**-2.7**	14.9	-27.4	-23.6	-10.3	-16.2	**-12.5**
	PET (NIR)	c	852	286	170	265	443	**403**	40	13	8	12	23	**19**
		Δc [%]	4.0	-0.7	6.5	2.1	6.4	**3.7**	5.2	-1.2	5.8	2.3	8.3	**4.1**
	PVC (NIR)	c	782	289	160	256	419	**381**	37	13	8	12	22	**18**
		Δc [%]	-4.5	0.5	0.3	-1.4	0.7	**-0.9**	-3.9	0.5	0.4	-1.5	2.1	**-0.5**
	b&g	c	424	300	175	270	427	**319**	20	14	8	12	23	**16**
		Δc [%]	-48.2	4.4	9.4	3.8	2.6	**-5.6**	-46.7	5.4	10.5	5.6	7.3	**-3.6**
	PET + PVC (NIR)	c	812	287	171	261	448	**396**	38	13	8	12	24	**19**
		Δc [%]	-0.8	-0.1	7.0	0.7	7.8	**2.9**	1.2	-0.7	6.4	0.8	11.6	**3.8**
Combinations of Screening and state-of-the-art NIR sorting or manual removal of black materials	0–5 mm + PET (NIR)	c	944	248	149	254	418	**402**	41	10	7	11	19	**18**
		Δc [%]	15.2	-13.9	-6.9	-2.3	0.5	**-1.5**	7.4	-24.2	-13.5	-8.3	-8.9	**-9.5**
	0–10 mm + PET (NIR)	c	988	250	143	255	423	**412**	42	10	6	11	19	**18**
		Δc [%]	20.6	-13.1	-10.7	-1.7	1.6	**-0.7**	11.5	-26.5	-18.0	-8.3	-9.6	**-10.2**
	0–20 mm + PET (NIR)	c	1119	237	140	256	433	**437**	47	9	6	11	19	**18**
		Δc [%]	36.6	-17.6	-12.5	-1.5	4.0	**1.8**	24.3	-31.8	-20.4	-9.0	-9.4	**-9.2**
	0–5 mm + PVC (NIR)	c	858	255	140	244	391	**378**	37	10	6	10	18	**16**
		Δc [%]	4.7	-11.5	-12.3	-6.0	-5.9	**-6.2**	-2.5	-21.0	-17.2	-11.6	-14.6	**-13.4**
	0–10 mm + PVC (NIR)	c	894	258	134	245	395	**385**	38	10	6	10	18	**17**
		Δc [%]	9.2	-10.5	-15.9	-5.5	-5.1	**-5.6**	0.8	-22.9	-21.4	-11.7	-15.4	**-14.1**
	0–20 mm + PVC (NIR)	c	1001	246	131	245	402	**405**	42	9	6	10	18	**17**
		Δc [%]	22.2	-14.3	-17.8	-5.6	-3.4	**-3.8**	11.1	-27.5	-23.7	-12.5	-15.5	**-13.6**
	0–5 mm + PET (NIR) + PVC (NIR)	c	904	249	149	249	422	**395**	39	10	7	11	20	**17**
		Δc [%]	10.4	-13.6	-6.7	-4.2	1.5	**-2.5**	3.2	-24.2	-13.3	-10.5	-7.4	**-10.5**
	0–10 mm + PET (NIR) + PVC (NIR)	c	949	251	143	250	428	**404**	41	10	6	11	20	**17**
		Δc [%]	15.9	-12.7	-10.6	-3.6	2.8	**-1.7**	7.4	-26.6	-18.0	-10.6	-8.1	**-11.2**
	0–20 mm + PET (NIR) + PVC (NIR)	c	1086	238	140	250	439	**431**	46	9	6	10	20	**18**
		Δc [%]	32.6	-17.4	-12.5	-3.6	5.6	**0.9**	20.7	-32.0	-20.4	-11.5	-7.8	**-10.2**
	0–5 mm + b&g	c	442	264	152	259	399	**303**	19	11	7	11	19	**13**
		Δc [%]	-46.0	-8.2	-4.6	-0.5	-4.0	**-12.7**	-49.1	-18.3	-10.2	-5.2	-10.4	**-18.6**
	0–10 mm + b&g	c	458	269	146	260	403	**307**	20	10	6	11	19	**13**
		Δc [%]	-44.1	-6.5	-8.7	0.3	-3.1	**-12.4**	-47.7	-20.2	-15.1	-5.1	-11.1	**-19.8**
	0–20 mm + b&g	c	495	257	143	261	411	**313**	21	10	6	11	19	**13**
		Δc [%]	-39.6	-10.5	-10.5	0.6	-1.1	**-12.2**	-44.4	-25.2	-17.5	-5.6	-11.0	**-20.7**
	0–5 mm + b&g + PVC (NIR)	c	356	265	153	254	401	**286**	16	11	7	11	19	**13**
		Δc [%]	-56.6	-7.7	-4.4	-2.3	-3.5	**-14.9**	-58.9	-18.1	-10.0	-7.3	-9.0	**-20.7**
	0–10 mm + b&g + PVC (NIR)	c	367	271	146	256	406	**289**	16	10	6	11	19	**13**
		Δc [%]	-55.2	-5.9	-8.5	-1.6	-2.4	**-14.7**	-57.9	-20.1	-15.0	-7.3	-9.8	**-22.0**
	0–20 mm + b&g + PVC (NIR)	c	387	259	143	256	415	**292**	17	10	6	11	19	**13**
		Δc [%]	-52.7	-10.0	-10.4	-1.5	-0.1	**-14.9**	-56.4	-25.3	-17.5	-7.9	-9.6	**-23.3**
	0–5 mm + b&g + PET (NIR)	c	429	258	166	266	433	**310**	19	10	7	11	21	**14**
		Δc [%]	-47.6	-10.2	3.7	2.3	4.1	**-9.6**	-50.2	-21.7	-4.3	-3.0	-1.8	**-16.2**
	0–10 mm + b&g + PET (NIR)	c	447	263	159	268	439	**315**	20	10	7	11	21	**14**
		Δc [%]	-45.5	-8.6	-0.7	3.3	5.6	**-9.2**	-48.6	-24.2	-9.8	-2.8	-2.3	**-17.5**
	0–20 mm + b&g + PET (NIR)	c	489	249	156	270	453	**323**	21	9	7	11	21	**14**
		Δc [%]	-40.4	-13.6	-2.3	3.8	8.9	**-8.7**	-44.8	-30.3	-12.2	-3.2	-1.6	**-18.4**
	0–5 mm + b&g + PET (NIR) + PVC (NIR)	c	326	260	166	261	440	**290**	14	10	7	11	22	**13**
		Δc [%]	-60.2	-9.7	4.2	0.3	5.8	**-11.9**	-62.0	-21.6	-3.9	-5.3	1.1	**-18.3**
	0–10 mm + b&g + PET (NIR) + PVC (NIR)	c	337	265	159	263	448	**294**	15	10	7	11	22	**13**
		Δc [%]	-58.9	-8.0	-0.3	1.3	7.6	**-11.7**	-61.1	-24.2	-9.5	-5.2	0.7	**-19.9**
	0–20 mm + b&g + PET (NIR) + PVC (NIR)	c	353	250	157	264	464	**298**	15	9	7	11	22	**13**
		Δc [%]	-56.9	-13.1	-1.9	1.7	11.6	**-11.7**	-59.9	-30.5	-12.0	-5.9	1.7	**-21.3**

More targeted removal	PVC (FTIR) + b&g PVC	c	824	290	160	254	418	**389**	38	13	8	12	22	**18**
		Δc [%]	0.6	0.9	0.4	-2.2	0.6	**0.1**	0.6	0.8	0.6	-2.6	0.5	**0.0**
	0–5 mm + PVC (FTIR) + b&g PVC	c	902	256	141	242	393	**387**	39	10	6	10	18	**17**
		Δc [%]	10.1	-10.9	-11.9	-6.8	-5.5	**-5.0**	2.3	-20.4	-16.9	-12.5	-14.9	**-12.5**
	0–10 mm + PVC (FTIR) + b&g PVC	c	939	259	135	243	396	**394**	40	10	6	10	18	**17**
		Δc [%]	14.6	-9.8	-15.5	-6.3	-4.8	**-4.4**	5.7	-22.3	-21.0	-12.7	-15.6	**-13.2**
	0–20 mm + PVC (FTIR) + b&g PVC	c	1046	249	132	243	403	**414**	44	10	6	10	18	**18**
		Δc [%]	27.6	-13.6	-17.4	-6.5	-3.2	**-2.6**	15.9	-26.8	-23.3	-13.5	-15.7	**-12.7**
	PVC (NIR) + b&g PVC	c	785	289	160	257	419	**382**	37	13	8	12	22	**18**
		Δc [%]	-4.2	0.6	0.4	-1.2	0.7	**-0.7**	-3.6	0.6	0.6	-1.3	2.1	**-0.3**
	0–5 mm + PVC (NIR) + b&g PVC	c	861	255	140	245	392	**378**	37	10	6	10	18	**17**
		Δc [%]	5.1	-11.4	-12.1	-5.7	-5.9	**-6.0**	-2.2	-20.9	-17.1	-11.5	-14.6	**-13.2**
	0–10 mm + PVC (NIR) + b&g PVC	c	898	258	135	246	395	**386**	39	10	6	10	18	**17**
		Δc [%]	9.6	-10.4	-15.7	-5.2	-5.1	**-5.4**	1.3	-22.8	-21.3	-11.6	-15.4	**-14.0**
	0–20 mm + PVC (NIR) + b&g PVC	c	1006	247	132	246	402	**406**	42	9	6	10	18	**17**
		Δc [%]	22.8	-14.2	-17.6	-5.3	-3.3	**-3.5**	11.7	-27.4	-23.5	-12.4	-15.5	**-13.4**
	PET (FTIR) + Textiles + b&g PET	c	837	284	166	267	435	**398**	39	13	8	12	23	**19**
		Δc [%]	2.2	-1.2	3.7	2.9	4.6	**2.4**	2.4	-1.6	3.6	2.7	5.4	**2.5**
	0–5 mm + PET (FTIR) + Textiles + b&g PET	c	924	248	145	257	410	**397**	40	10	6	11	19	**17**
		Δc [%]	12.8	-13.8	-9.1	-1.2	-1.4	**-2.6**	4.3	-23.6	-14.7	-7.4	-11.1	**-10.5**
	0–10 mm + PET (FTIR) + Textiles + b&g PET	c	965	250	139	258	414	**405**	41	10	6	11	19	**17**
		Δc [%]	17.8	-13.1	-12.8	-0.6	-0.4	**-1.8**	8.1	-25.8	-19.0	-7.4	-11.8	**-11.2**
	0–20 mm + PET (FTIR) + Textiles + b&g PET	c	1088	238	136	259	423	**429**	46	9	6	11	19	**18**
		Δc [%]	32.9	-17.3	-14.6	-0.3	1.7	**0.5**	19.7	-30.7	-21.3	-8.0	-11.8	**-10.4**
	b&g Other	c	407	295	171	264	411	**310**	19	13	8	12	21	**15**
		Δc [%]	-50.3	2.6	7.2	1.7	-1.2	**-8.0**	-50.8	1.9	6.2	0.9	-1.3	**-8.6**
	0–5 mm + b&g Other	c	421	259	149	253	383	**293**	18	10	7	11	18	**13**
		Δc [%]	-48.7	-10.0	-6.6	-2.7	-8.0	**-15.2**	-53.2	-21.0	-13.7	-9.4	-17.7	**-23.0**
	0–10 mm + b&g Other	c	434	263	143	254	386	**296**	18	10	6	11	17	**13**
		Δc [%]	-47.0	-8.6	-10.6	-2.1	-7.3	**-15.1**	-52.2	-23.1	-18.4	-9.5	-18.5	**-24.3**
	0–20 mm + b&g Other	c	463	251	140	255	392	**300**	19	9	6	11	17	**12**
		Δc [%]	-43.5	-12.7	-12.5	-2.0	-5.8	**-15.3**	-50.0	-28.1	-20.9	-10.2	-18.8	**-25.6**
	PVC (FTIR) + b&g PVC + b&g Other	c	408	298	172	258	414	**310**	19	13	8	12	21	**15**
		Δc [%]	-50.2	3.7	7.8	-0.7	-0.5	**-8.0**	-50.6	2.8	6.9	-1.8	-0.7	**-8.7**
	0–5 mm + PVC (FTIR) + b&g PVC + b&g Other	c	422	262	150	245	385	**293**	18	10	7	10	18	**13**
		Δc [%]	-48.4	-8.9	-6.1	-5.5	-7.3	**-15.3**	-53.1	-20.3	-13.2	-12.6	-17.2	**-23.3**
	0–10 mm + PVC (FTIR) + b&g PVC + b&g Other	c	436	266	144	247	388	**296**	18	10	6	10	18	**12**
		Δc [%]	-46.7	-7.4	-10.2	-5.0	-6.6	**-15.2**	-52.0	-22.4	-18.0	-12.8	-18.0	**-24.6**
	0–20 mm + PVC (FTIR) + b&g PVC + b&g Other	c	466	255	140	246	395	**301**	19	9	6	10	17	**12**
		Δc [%]	-43.1	-11.4	-12.1	-5.1	-5.0	**-15.3**	-49.8	-27.4	-20.4	-13.7	-18.3	**-25.9**
	PVC (NIR) + b&g PVC + b&g Other	c	338	297	172	261	414	**297**	16	13	8	12	22	**14**
		Δc [%]	-58.7	3.4	7.9	0.5	-0.5	**-9.5**	-58.8	2.6	7.0	-0.4	0.8	**-9.8**
	0–5 mm + PVC (NIR) + b&g PVC + b&g Other	c	340	260	150	248	383	**276**	14	10	7	10	18	**12**
		Δc [%]	-58.5	-9.4	-6.2	-4.3	-7.9	**-17.3**	-62.2	-20.8	-13.4	-11.5	-17.2	**-25.0**
	0–10 mm + PVC (NIR) + b&g PVC + b&g Other	c	349	265	143	250	386	**279**	15	10	6	10	18	**12**
		Δc [%]	-57.3	-8.0	-10.3	-3.7	-7.1	**-17.3**	-61.5	-23.0	-18.2	-11.6	-18.0	**-26.5**
	0–20 mm + PVC (NIR) + b&g PVC + b&g Other	c	364	253	140	250	394	**280**	15	9	6	10	17	**12**
		Δc [%]	-55.6	-12.1	-12.3	-3.7	-5.4	**-17.8**	-60.8	-28.1	-20.7	-12.5	-18.4	**-28.1**
	b&g Other + b&g PVC	c	408	295	172	265	411	**310**	19	13	8	12	21	**15**
		Δc [%]	-50.2	2.7	7.4	1.9	-1.1	**-7.9**	-50.6	2.0	6.4	1.1	-1.3	**-8.5**
	0–5 mm + b&g Other + b&g PVC	c	422	259	149	253	383	**293**	18	10	7	11	18	**13**
		Δc [%]	-48.5	-9.9	-6.4	-2.4	-8.0	**-15.0**	-53.1	-20.9	-13.5	-9.3	-17.6	**-22.9**
	0–10 mm + b&g Other + b&g PVC	c	436	263	143	255	386	**297**	18	10	6	11	17	**13**
		Δc [%]	-46.8	-8.5	-10.4	-1.8	-7.3	**-15.0**	-52.0	-23.0	-18.2	-9.3	-18.5	**-24.2**
	0–20 mm + b&g Other + b&g PVC	c	465	251	140	255	392	**301**	19	9	6	11	17	**12**
		Δc [%]	-43.2	-12.6	-12.3	-1.7	-5.7	**-15.1**	-49.8	-28.0	-20.7	-10.0	-18.8	**-25.5**

B.23. Pb

Table B.23: Relative concentration change (Δc, in %) of Pb caused by the removal of different material or particle size fractions referring to mg/kg and mg/MJ, both calculated for dry mass without hard impurities

	Removed fractions	Conc. after removal	mg/kg$_{DM}$ S01	S02	S03	S04	S05	Avr	mg/MJ S01	S02	S03	S04	S05	Avr
Single process steps	0–5 mm	c	501	133	119	413	78	**249**	22	5	5	18	4	**11**
		Δc [%]	-27.9	0.4	-1.5	8.2	-0.8	**-4.3**	-33.0	-10.0	-7.1	2.1	-10.5	**-11.7**
	0–10 mm	c	470	143	118	401	76	**241**	20	6	5	17	3	**10**
		Δc [%]	-32.5	7.5	-2.4	5.0	-3.6	**-5.2**	-37.7	-7.0	-8.9	-1.6	-14.3	**-13.9**
	0–20 mm	c	514	144	120	422	62	**252**	22	6	5	18	3	**11**
		Δc [%]	-26.1	8.5	-0.6	10.5	-21.6	**-5.9**	-32.8	-7.7	-7.8	2.9	-31.6	**-15.4**
	PET (NIR)	c	767	139	119	396	66	**297**	36	6	6	18	3	**14**
		Δc [%]	10.3	4.7	-1.3	3.6	-15.7	**0.3**	11.6	4.1	-1.9	3.8	-14.2	**0.7**
	PVC (NIR)	c	733	107	98	99	73	**222**	34	5	5	5	4	**10**
		Δc [%]	5.3	-19.6	-19.1	-74.0	-7.5	**-23.0**	6.0	-19.6	-19.0	-74.0	-6.3	**-22.6**
	b&g	c	814	145	138	415	83	**319**	39	7	7	19	4	**15**
		Δc [%]	17.0	9.4	14.4	8.7	4.9	**10.9**	20.4	10.4	15.6	10.5	9.7	**13.3**
	PET + PVC (NIR)	c	813	111	93	79	59	**231**	39	5	4	4	3	**11**
		Δc [%]	17.0	-16.5	-23.0	-79.2	-25.6	**-25.5**	19.3	-17.0	-23.4	-79.2	-23.0	**-24.6**
Combinations of Screening and state-of-the-art NIR sorting or manual removal of black materials	0–5 mm + PET (NIR)	c	561	141	117	433	63	**263**	24	6	5	18	3	**11**
		Δc [%]	-19.4	6.3	-3.1	13.4	-19.4	**-4.5**	-24.8	-6.4	-10.0	6.4	-27.0	**-12.4**
	0–10 mm + PET (NIR)	c	528	152	116	420	60	**255**	23	6	5	18	3	**11**
		Δc [%]	-24.1	15.0	-4.3	9.9	-23.5	**-5.4**	-29.8	-2.8	-12.1	2.4	-31.9	**-14.8**
	0–20 mm + PET (NIR)	c	591	155	118	445	42	**270**	25	6	5	19	2	**11**
		Δc [%]	-15.1	17.0	-2.3	16.6	-46.2	**-6.0**	-22.7	-3.1	-11.0	7.7	-53.1	**-16.5**
	0–5 mm + PVC (NIR)	c	531	101	94	97	71	**179**	23	4	4	4	3	**8**
		Δc [%]	-23.6	-23.6	-22.4	-74.7	-9.7	**-30.8**	-28.9	-31.8	-26.8	-76.2	-18.1	**-36.4**
	0–10 mm + PVC (NIR)	c	499	107	92	72	68	**168**	21	4	4	3	3	**7**
		Δc [%]	-28.3	-19.2	-24.1	-81.1	-13.1	**-33.2**	-33.8	-30.5	-29.2	-82.4	-22.5	**-39.7**
	0–20 mm + PVC (NIR)	c	552	105	92	73	52	**175**	23	4	4	3	2	**7**
		Δc [%]	-20.6	-21.1	-23.5	-80.8	-33.8	**-35.9**	-27.8	-33.2	-29.0	-82.2	-42.1	**-42.9**
	0–5 mm + PET (NIR) + PVC (NIR)	c	599	106	88	74	54	**184**	26	4	4	3	3	**8**
		Δc [%]	-13.8	-20.1	-27.2	-80.8	-31.8	**-34.7**	-19.4	-29.9	-32.4	-82.0	-37.8	**-40.3**
	0–10 mm + PET (NIR) + PVC (NIR)	c	566	113	85	45	50	**172**	24	4	4	2	2	**7**
		Δc [%]	-18.6	-14.8	-29.4	-88.3	-37.0	**-37.6**	-24.5	-28.4	-35.2	-89.2	-43.6	**-44.2**
	0–20 mm + PET (NIR) + PVC (NIR)	c	643	111	86	44	29	**182**	27	4	4	2	1	**8**
		Δc [%]	-7.5	-16.4	-28.9	-88.6	-63.7	**-41.0**	-15.8	-31.2	-35.4	-89.5	-68.3	**-48.0**
	0–5 mm + b&g	c	598	149	138	456	83	**285**	26	6	6	20	4	**12**
		Δc [%]	-14.0	12.3	14.2	19.3	4.8	**7.3**	-18.8	0.0	7.5	13.7	-2.2	**0.0**
	0–10 mm + b&g	c	565	162	137	443	80	**278**	25	6	6	19	4	**12**
		Δc [%]	-18.7	22.3	13.8	16.0	2.0	**7.1**	-23.9	4.4	5.7	9.8	-6.5	**-2.1**
	0–20 mm + b&g	c	642	166	141	471	64	**297**	27	6	6	20	3	**13**
		Δc [%]	-7.6	25.4	17.1	23.2	-18.5	**7.9**	-14.9	4.8	7.9	15.7	-26.7	**-2.6**
	0–5 mm + b&g + PVC (NIR)	c	644	112	107	92	75	**206**	28	5	5	4	4	**9**
		Δc [%]	-7.4	-15.3	-11.3	-76.0	-4.9	**-23.0**	-12.3	-24.9	-16.5	-77.2	-10.3	**-28.2**
	0–10 mm + b&g + PVC (NIR)	c	611	121	105	63	72	**194**	27	5	5	3	3	**8**
		Δc [%]	-12.2	-8.9	-12.9	-83.5	-8.6	**-25.2**	-17.5	-22.7	-19.0	-84.5	-15.4	**-31.8**
	0–20 mm + b&g + PVC (NIR)	c	707	120	107	64	53	**210**	30	4	5	3	2	**9**
		Δc [%]	1.7	-9.8	-11.3	-83.4	-32.5	**-27.0**	-6.1	-25.2	-18.3	-84.4	-38.9	**-34.6**
	0–5 mm + b&g + PET (NIR)	c	689	160	139	485	66	**308**	30	6	6	21	3	**13**
		Δc [%]	-1.0	20.7	15.0	27.0	-15.9	**9.2**	-5.8	5.3	6.1	20.5	-20.6	**1.1**
	0–10 mm + b&g + PET (NIR)	c	657	177	138	472	63	**301**	29	7	6	20	3	**13**
		Δc [%]	-5.6	33.5	14.5	23.5	-20.5	**9.1**	-11.0	10.7	4.1	16.2	-26.4	**-1.3**
	0–20 mm + b&g + PET (NIR)	c	774	184	143	507	42	**330**	33	7	6	21	2	**14**
		Δc [%]	11.3	38.7	18.6	32.6	-47.3	**10.8**	2.9	11.9	6.5	23.6	-52.3	**-1.5**
	0–5 mm + b&g + PET (NIR) + PVC (NIR)	c	752	119	102	64	55	**218**	33	5	4	3	3	**10**
		Δc [%]	8.1	-10.1	-15.3	-83.4	-30.1	**-26.2**	3.4	-22.0	-21.9	-84.3	-33.2	**-31.6**
	0–10 mm + b&g + PET (NIR) + PVC (NIR)	c	721	130	100	29	50	**206**	32	5	4	1	2	**9**
		Δc [%]	3.7	-2.0	-17.4	-92.5	-36.2	**-28.9**	-1.8	-19.3	-25.0	-93.0	-40.4	**-35.9**
	0–20 mm + b&g + PET (NIR) + PVC (NIR)	c	874	130	102	26	25	**231**	38	5	4	1	1	**10**
		Δc [%]	25.6	-2.0	-15.9	-93.2	-68.8	**-30.8**	16.6	-21.7	-24.5	-93.7	-71.6	**-39.0**

More targeted removal	PVC (FTIR) + b&g PVC	c	695	109	109	98	77	**218**	32	5	5	4	4	**10**
		Δc [%]	0.0	-17.7	-10.0	-74.4	-1.9	**-20.8**	0.0	-17.8	-9.9	-74.5	-2.0	**-20.8**
	0–5 mm + PVC (FTIR) + b&g PVC	c	499	105	106	95	76	**176**	22	4	5	4	4	**8**
		Δc [%]	-28.2	-21.2	-12.5	-75.1	-3.1	**-28.0**	-33.3	-29.6	-17.4	-76.6	-12.7	**-33.9**
	0–10 mm + PVC (FTIR) + b&g PVC	c	467	111	104	71	74	**165**	20	4	5	3	3	**7**
		Δc [%]	-32.8	-16.6	-13.8	-81.4	-5.9	**-30.1**	-38.1	-28.2	-19.5	-82.7	-16.6	**-37.0**
	0–20 mm + PVC (FTIR) + b&g PVC	c	512	109	105	72	60	**172**	22	4	5	3	3	**7**
		Δc [%]	-26.4	-18.2	-12.6	-81.1	-24.3	**-32.5**	-33.1	-30.7	-18.8	-82.5	-34.1	**-39.9**
	PVC (NIR) + b&g PVC	c	731	107	96	98	73	**221**	34	5	5	4	4	**10**
		Δc [%]	5.2	-19.5	-20.8	-74.4	-7.5	**-23.4**	5.9	-19.5	-20.7	-74.4	-6.3	**-23.0**
	0–5 mm + PVC (NIR) + b&g PVC	c	529	101	91	95	71	**178**	23	4	4	4	3	**8**
		Δc [%]	-24.0	-23.5	-24.4	-75.1	-9.7	**-31.3**	-29.2	-31.7	-28.6	-76.6	-18.1	**-36.8**
	0–10 mm + PVC (NIR) + b&g PVC	c	496	107	89	70	68	**166**	21	4	4	3	3	**7**
		Δc [%]	-28.7	-19.1	-26.1	-81.6	-13.1	**-33.7**	-34.1	-30.4	-31.0	-82.8	-22.5	**-40.2**
	0–20 mm + PVC (NIR) + b&g PVC	c	550	105	90	71	52	**174**	23	4	4	3	2	**7**
		Δc [%]	-21.0	-21.0	-25.6	-81.3	-33.7	**-36.5**	-28.1	-33.2	-31.0	-82.7	-42.1	**-43.4**
	PET (FTIR) + Textiles + b&g PET	c	750	134	113	385	65	**289**	35	6	5	17	3	**13**
		Δc [%]	7.8	1.2	-6.0	0.7	-17.4	**-2.7**	8.0	0.8	-6.1	0.5	-16.8	**-2.7**
	0–5 mm + PET (FTIR) + Textiles + b&g PET	c	546	135	111	419	62	**255**	23	5	5	18	3	**11**
		Δc [%]	-21.5	2.0	-8.2	9.6	-21.3	**-7.9**	-27.4	-9.5	-13.9	2.8	-29.1	**-15.4**
	0–10 mm + PET (FTIR) + Textiles + b&g PET	c	513	145	109	405	59	**246**	22	6	5	17	3	**10**
		Δc [%]	-26.2	9.6	-9.5	6.1	-25.3	**-9.0**	-32.3	-6.4	-15.9	-1.1	-33.8	**-17.9**
	0–20 mm + PET (FTIR) + Textiles + b&g PET	c	571	147	111	429	42	**260**	24	6	5	18	2	**11**
		Δc [%]	-17.8	10.9	-7.9	12.2	-47.0	**-9.9**	-25.9	-7.0	-15.1	3.7	-54.1	**-19.7**
	b&g Other	c	772	143	137	402	83	**307**	36	6	6	18	4	**14**
		Δc [%]	11.0	7.5	13.9	5.2	5.0	**8.5**	10.0	6.8	12.8	4.5	4.8	**7.8**
	0–5 mm + b&g Other	c	564	146	137	439	83	**274**	24	6	6	19	4	**12**
		Δc [%]	-18.9	9.9	13.6	15.0	4.9	**4.9**	-26.1	-3.5	5.0	7.0	-6.1	**-4.8**
	0–10 mm + b&g Other	c	531	158	137	426	80	**267**	22	6	6	18	4	**11**
		Δc [%]	-23.6	19.2	13.2	11.6	2.2	**4.5**	-31.1	0.3	3.3	3.2	-10.1	**-6.9**
	0–20 mm + b&g Other	c	596	161	140	452	65	**283**	24	6	6	19	3	**12**
		Δc [%]	-14.4	21.7	16.3	18.2	-16.9	**5.0**	-24.3	0.3	5.2	8.3	-28.4	**-7.8**
	PVC (FTIR) + b&g PVC + b&g Other	c	773	117	123	93	81	**237**	36	5	6	4	4	**11**
		Δc [%]	11.1	-11.8	2.3	-75.6	3.0	**-14.2**	10.1	-12.5	1.4	-75.9	2.8	**-14.8**
	0–5 mm + PVC (FTIR) + b&g PVC + b&g Other	c	562	114	122	90	81	**194**	24	4	5	4	4	**8**
		Δc [%]	-19.1	-14.3	0.7	-76.6	2.5	**-21.4**	-26.4	-25.0	-6.9	-78.3	-8.4	**-29.0**
	0–10 mm + PVC (FTIR) + b&g PVC + b&g Other	c	529	122	120	63	79	**183**	22	5	5	3	4	**8**
		Δc [%]	-23.9	-8.1	-0.3	-83.6	-0.3	**-23.2**	-31.4	-23.0	-9.0	-84.9	-12.5	**-32.2**
	0–20 mm + PVC (FTIR) + b&g PVC + b&g Other	c	594	121	123	63	63	**193**	24	4	5	3	3	**8**
		Δc [%]	-14.6	-8.9	2.0	-83.4	-19.8	**-24.9**	-24.6	-25.3	-7.7	-84.9	-31.1	**-34.7**
	PVC (NIR) + b&g PVC + b&g Other	c	818	114	108	93	77	**242**	38	5	5	4	4	**11**
		Δc [%]	17.6	-13.8	-10.3	-75.6	-2.7	**-16.9**	17.4	-14.4	-11.0	-75.8	-1.4	**-17.0**
	0–5 mm + PVC (NIR) + b&g PVC + b&g Other	c	601	110	105	89	75	**196**	25	4	5	4	3	**8**
		Δc [%]	-13.6	-16.8	-13.3	-76.6	-4.1	**-24.9**	-21.2	-27.3	-19.9	-78.3	-13.8	**-32.1**
	0–10 mm + PVC (NIR) + b&g PVC + b&g Other	c	568	118	103	62	73	**185**	24	4	4	3	3	**8**
		Δc [%]	-18.4	-10.9	-14.9	-83.8	-7.6	**-27.1**	-26.3	-25.4	-22.4	-85.1	-18.5	**-35.6**
	0–20 mm + PVC (NIR) + b&g PVC + b&g Other	c	647	117	104	62	55	**197**	26	4	4	3	2	**8**
		Δc [%]	-7.0	-12.0	-13.5	-83.7	-29.7	**-29.2**	-18.0	-28.0	-21.8	-85.2	-39.4	**-38.5**
	b&g Other + b&g PVC	c	771	143	135	403	83	**307**	35	6	6	18	4	**14**
		Δc [%]	10.8	7.6	11.9	5.4	5.0	**8.2**	9.9	6.9	10.9	4.6	4.9	**7.4**
	0–5 mm + b&g Other + b&g PVC	c	562	146	134	440	83	**273**	24	6	6	19	4	**12**
		Δc [%]	-19.2	10.0	11.4	15.2	4.9	**4.5**	-26.4	-3.4	3.0	7.2	-6.1	**-5.2**
	0–10 mm + b&g Other + b&g PVC	c	529	158	134	427	80	**266**	22	6	6	18	4	**11**
		Δc [%]	-24.0	19.3	10.9	11.9	2.2	**4.1**	-31.4	0.5	1.2	3.3	-10.1	**-7.3**
	0–20 mm + b&g Other + b&g PVC	c	593	162	137	453	65	**282**	24	6	6	19	3	**12**
		Δc [%]	-14.8	21.9	13.9	18.6	-16.9	**4.5**	-24.7	0.5	3.1	8.5	-28.4	**-8.2**

B.24. Sb

Table B.24: Relative concentration change (Δc, in %) of Sb caused by the removal of different material or particle size fractions referring to mg/kg and mg/MJ, both calculated for dry mass without hard impurities

	Removed fractions	Conc. after removal	mg/kg$_{DM}$ S01	S02	S03	S04	S05	Avr	mg/MJ S01	S02	S03	S04	S05	Avr
Single process steps	0–5 mm	c	341	350	84	323	590	**338**	15	14	4	14	27	**15**
		Δc [%]	13.4	21.3	6.3	1.8	14.2	11.4	5.3	8.7	0.2	-4.0	3.1	2.7
	0–10 mm	c	357	389	86	333	608	**355**	15	15	4	14	28	**15**
		Δc [%]	18.7	34.7	8.4	4.8	17.7	16.9	9.4	16.5	1.2	-1.7	4.6	6.0
	0–20 mm	c	341	428	87	280	624	**352**	14	16	4	12	28	**15**
		Δc [%]	13.2	48.0	10.5	-11.9	20.8	16.1	2.9	25.9	2.5	-18.0	5.4	3.7
	PET (NIR)	c	310	305	80	280	559	**307**	15	14	4	13	29	**15**
		Δc [%]	3.2	5.6	0.8	-11.9	8.2	1.2	4.4	5.0	0.1	-11.7	10.1	1.6
	PVC (NIR)	c	196	295	63	304	369	**245**	9	13	3	14	19	**12**
		Δc [%]	-34.9	2.0	-20.6	-4.1	-28.6	-17.2	-34.5	1.9	-20.5	-4.2	-27.6	-17.0
	b&g	c	337	153	47	213	305	**211**	16	7	2	10	16	**10**
		Δc [%]	11.9	-47.2	-40.8	-33.0	-41.0	-30.0	15.2	-46.7	-40.1	-31.8	-38.3	-28.4
	PET + PVC (NIR)	c	194	312	61	263	395	**245**	9	14	3	12	21	**12**
		Δc [%]	-35.6	7.9	-22.5	-17.1	-23.6	-18.2	-34.3	7.2	-22.9	-17.0	-20.9	-17.6
Combinations of Screening and state-of-the-art NIR sorting or manual removal of black materials	0–5 mm + PET (NIR)	c	358	377	85	281	651	**350**	15	15	4	12	30	**15**
		Δc [%]	18.9	30.5	8.1	-11.4	26.0	14.4	10.8	14.9	0.4	-16.9	14.2	4.7
	0–10 mm + PET (NIR)	c	377	424	87	290	675	**371**	16	16	4	12	31	**16**
		Δc [%]	25.2	46.7	10.6	-8.5	30.6	20.9	15.8	24.0	1.5	-14.7	16.3	8.6
	0–20 mm + PET (NIR)	c	361	471	89	227	699	**369**	15	18	4	10	31	**16**
		Δc [%]	20.0	63.2	13.2	-28.6	35.3	20.6	9.2	35.1	3.1	-34.1	17.9	6.2
	0–5 mm + PVC (NIR)	c	221	359	66	309	424	**276**	10	14	3	13	20	**12**
		Δc [%]	-26.5	24.3	-16.1	-2.7	-18.0	-7.8	-31.5	11.0	-20.9	-8.6	-25.6	-15.1
	0–10 mm + PVC (NIR)	c	232	400	67	318	436	**291**	10	16	3	14	20	**12**
		Δc [%]	-23.0	38.5	-14.8	0.3	-15.5	-2.9	-28.9	19.3	-20.4	-6.4	-24.7	-12.2
	0–20 mm + PVC (NIR)	c	192	441	68	261	441	**281**	8	17	3	11	20	**12**
		Δc [%]	-36.2	52.6	-13.9	-17.7	-14.7	-6.0	-42.0	29.2	-20.1	-23.8	-25.5	-16.4
	0–5 mm + PET (NIR) + PVC (NIR)	c	222	387	65	262	464	**280**	10	15	3	11	22	**12**
		Δc [%]	-26.1	34.1	-17.6	-17.4	-10.2	-7.4	-30.9	17.6	-23.5	-22.8	-18.1	-15.5
	0–10 mm + PET (NIR) + PVC (NIR)	c	234	437	66	271	481	**298**	10	17	3	11	22	**13**
		Δc [%]	-22.1	51.3	-16.1	-14.5	-7.0	-1.7	-27.8	27.2	-23.0	-20.7	-16.8	-12.2
	0–20 mm + PET (NIR) + PVC (NIR)	c	188	488	67	202	490	**287**	8	18	3	8	22	**12**
		Δc [%]	-37.4	69.0	-15.1	-36.4	-5.2	-5.0	-43.0	39.0	-22.8	-41.6	-17.2	-17.1
	0–5 mm + b&g	c	393	189	49	205	351	**237**	17	8	2	9	17	**11**
		Δc [%]	30.6	-34.7	-37.7	-35.5	-32.1	-21.9	23.2	-41.9	-41.4	-38.5	-36.6	-27.0
	0–10 mm + b&g	c	416	212	50	211	361	**250**	18	8	2	9	17	**11**
		Δc [%]	38.2	-26.6	-37.1	-33.5	-30.2	-17.8	29.4	-37.4	-41.5	-37.0	-36.0	-24.5
	0–20 mm + b&g	c	407	236	49	141	359	**238**	17	9	2	6	17	**10**
		Δc [%]	35.2	-18.4	-37.4	-55.7	-30.5	-21.4	24.5	-31.8	-42.3	-58.4	-37.5	-29.1
	0–5 mm + b&g + PVC (NIR)	c	248	194	26	181	133	**157**	11	8	1	8	6	**7**
		Δc [%]	-17.5	-33.0	-66.5	-42.9	-74.2	-46.8	-21.8	-40.5	-68.5	-45.8	-75.7	-50.5
	0–10 mm + b&g + PVC (NIR)	c	263	218	26	187	132	**165**	11	8	1	8	6	**7**
		Δc [%]	-12.5	-24.4	-67.1	-41.1	-74.4	-43.9	-17.8	-35.8	-69.4	-44.5	-76.3	-48.8
	0–20 mm + b&g + PVC (NIR)	c	218	244	24	110	110	**141**	9	9	1	5	5	**6**
		Δc [%]	-27.5	-15.5	-69.5	-65.4	-78.7	-51.3	-33.0	-29.8	-71.9	-67.7	-80.7	-56.6
	0–5 mm + b&g + PET (NIR)	c	422	200	45	137	380	**237**	19	8	2	6	18	**11**
		Δc [%]	40.3	-30.7	-43.6	-56.7	-26.4	-23.4	33.4	-39.6	-47.9	-58.9	-30.5	-28.7
	0–10 mm + b&g + PET (NIR)	c	451	229	45	142	393	**252**	20	9	2	6	19	**11**
		Δc [%]	50.0	-20.9	-43.1	-55.4	-23.8	-18.6	41.3	-34.4	-48.3	-58.0	-29.6	-25.8
	0–20 mm + b&g + PET (NIR)	c	449	259	44	53	395	**240**	19	9	2	2	18	**10**
		Δc [%]	49.3	-10.4	-44.0	-83.3	-23.6	-22.4	38.1	-27.7	-49.7	-84.4	-30.9	-30.9
	0–5 mm + b&g + PET (NIR) + PVC (NIR)	c	254	206	17	105	124	**141**	11	8	1	5	6	**6**
		Δc [%]	-15.4	-28.6	-78.0	-66.9	-76.1	-53.0	-19.1	-38.1	-79.7	-68.7	-77.1	-56.5
	0–10 mm + b&g + PET (NIR) + PVC (NIR)	c	273	237	16	108	122	**151**	12	9	1	5	6	**6**
		Δc [%]	-9.3	-18.0	-79.3	-65.9	-76.4	-49.8	-14.1	-32.5	-81.2	-68.1	-77.9	-54.8
	0–20 mm + b&g + PET (NIR) + PVC (NIR)	c	219	270	13	10	93	**121**	9	10	1	0	4	**5**
		Δc [%]	-27.1	-6.7	-83.3	-97.0	-82.0	-59.2	-32.3	-25.4	-85.0	-97.2	-83.6	-64.7

More targeted removal	PVC (FTIR) + b&g PVC	c	190	291	74	276	386	**243**	9	13	4	13	20	**12**
		Δc [%]	-36.9	0.7	-6.9	-12.9	-25.3	**-16.3**	-36.8	0.6	-6.8	-13.2	-25.3	**-16.3**
	0–5 mm + PVC (FTIR) + b&g PVC	c	213	354	78	277	440	**272**	9	14	4	12	20	**12**
		Δc [%]	-29.2	22.5	-1.3	-12.7	-14.9	**-7.1**	-34.2	9.4	-6.8	-18.0	-23.3	**-14.6**
	0–10 mm + PVC (FTIR) + b&g PVC	c	223	394	80	285	452	**287**	10	15	4	12	21	**12**
		Δc [%]	-26.0	36.3	0.6	-10.1	-12.6	**-2.4**	-31.8	17.4	-6.0	-16.1	-22.5	**-11.8**
	0–20 mm + PVC (FTIR) + b&g PVC	c	184	433	81	228	457	**277**	8	17	4	10	20	**12**
		Δc [%]	-38.8	50.0	2.3	-28.3	-11.6	**-5.3**	-44.4	27.1	-5.0	-33.7	-23.0	**-15.8**
	PVC (NIR) + b&g PVC	c	190	293	58	275	369	**237**	9	13	3	12	19	**11**
		Δc [%]	-36.9	1.6	-26.2	-13.4	-28.6	**-20.7**	-36.4	1.6	-26.0	-13.5	-27.6	**-20.4**
	0–5 mm + PVC (NIR) + b&g PVC	c	215	358	61	276	424	**267**	9	14	3	12	20	**12**
		Δc [%]	-28.7	23.9	-22.2	-13.2	-17.9	**-11.6**	-33.6	10.6	-26.6	-18.5	-25.6	**-18.7**
	0–10 mm + PVC (NIR) + b&g PVC	c	225	399	62	284	436	**281**	10	16	3	12	20	**12**
		Δc [%]	-25.3	38.0	-21.1	-10.5	-15.5	**-6.9**	-31.0	18.8	-26.3	-16.5	-24.7	**-15.9**
	0–20 mm + PVC (NIR) + b&g PVC	c	184	439	63	224	441	**270**	8	17	3	9	20	**11**
		Δc [%]	-39.0	52.1	-20.5	-29.3	-14.7	**-10.3**	-44.5	28.7	-26.3	-34.6	-25.4	**-20.4**
	PET (FTIR) + Textiles + b&g PET	c	305	296	76	322	548	**309**	14	13	4	15	28	**15**
		Δc [%]	1.3	2.3	-4.2	1.4	6.0	**1.4**	1.5	1.9	-4.3	1.2	6.8	**1.4**
	0–5 mm + PET (FTIR) + Textiles + b&g PET	c	350	362	81	329	634	**351**	15	14	4	14	29	**15**
		Δc [%]	16.2	25.3	2.1	3.5	22.7	**14.0**	7.5	11.1	-4.2	-2.9	10.6	**4.4**
	0–10 mm + PET (FTIR) + Textiles + b&g PET	c	368	404	82	339	656	**370**	16	16	4	14	30	**16**
		Δc [%]	22.2	39.9	4.2	6.8	27.0	**20.0**	12.1	19.5	-3.2	-0.5	12.4	**8.1**
	0–20 mm + PET (FTIR) + Textiles + b&g PET	c	351	447	84	282	677	**368**	15	17	4	12	30	**15**
		Δc [%]	16.7	54.6	6.3	-11.2	31.1	**19.5**	5.2	29.6	-2.0	-18.0	13.7	**5.7**
	b&g Other	c	331	152	74	240	300	**219**	15	7	3	11	15	**10**
		Δc [%]	9.9	-47.5	-6.6	-24.3	-42.0	**-22.1**	8.9	-47.8	-7.5	-24.9	-42.0	**-22.7**
	0–5 mm + b&g Other	c	382	186	79	236	342	**245**	16	7	3	10	16	**11**
		Δc [%]	26.9	-35.4	0.1	-25.5	-33.7	**-13.5**	15.6	-43.3	-7.5	-30.7	-40.7	**-21.3**
	0–10 mm + b&g Other	c	402	209	81	244	351	**257**	17	8	4	10	16	**11**
		Δc [%]	33.8	-27.8	2.3	-23.2	-32.1	**-9.4**	20.7	-39.2	-6.6	-29.0	-40.2	**-18.9**
	0–20 mm + b&g Other	c	392	231	83	179	349	**247**	16	9	4	7	15	**10**
		Δc [%]	30.2	-20.0	4.5	-43.7	-32.5	**-12.3**	15.0	-34.1	-5.5	-48.4	-41.8	**-23.0**
	PVC (FTIR) + b&g PVC + b&g Other	c	206	152	67	194	159	**156**	10	7	3	9	8	**7**
		Δc [%]	-31.4	-47.3	-14.8	-39.0	-69.3	**-40.4**	-32.0	-47.8	-15.5	-39.7	-69.3	**-40.9**
	0–5 mm + PVC (FTIR) + b&g PVC + b&g Other	c	236	188	72	183	178	**171**	10	7	3	8	8	**7**
		Δc [%]	-21.6	-35.1	-9.0	-42.3	-65.6	**-34.7**	-28.6	-43.2	-15.8	-46.6	-69.3	**-40.7**
	0–10 mm + PVC (FTIR) + b&g PVC + b&g Other	c	248	210	73	189	179	**180**	10	8	3	8	8	**8**
		Δc [%]	-17.5	-27.2	-7.1	-40.6	-65.3	**-31.5**	-25.6	-39.0	-15.2	-45.5	-69.6	**-39.0**
	0–20 mm + PVC (FTIR) + b&g PVC + b&g Other	c	208	233	75	117	164	**159**	9	9	3	5	7	**6**
		Δc [%]	-31.0	-19.2	-5.5	-63.0	-68.3	**-37.4**	-39.1	-33.8	-14.5	-66.3	-72.8	**-45.3**
	PVC (NIR) + b&g PVC + b&g Other	c	207	153	49	190	123	**145**	10	7	2	9	6	**7**
		Δc [%]	-31.0	-46.9	-37.5	-40.3	-76.1	**-46.4**	-31.2	-47.3	-38.0	-40.8	-75.8	**-46.6**
	0–5 mm + PVC (NIR) + b&g PVC + b&g Other	c	239	190	52	178	138	**159**	10	7	2	8	6	**7**
		Δc [%]	-20.5	-34.3	-34.1	-43.8	-73.4	**-41.2**	-27.5	-42.6	-39.1	-48.0	-76.1	**-46.7**
	0–10 mm + PVC (NIR) + b&g PVC + b&g Other	c	253	213	53	184	137	**168**	11	8	2	8	6	**7**
		Δc [%]	-16.0	-26.3	-33.3	-42.1	-73.5	**-38.2**	-24.2	-38.3	-39.2	-46.8	-76.6	**-45.0**
	0–20 mm + PVC (NIR) + b&g PVC + b&g Other	c	209	237	53	110	117	**145**	9	9	2	5	5	**6**
		Δc [%]	-30.4	-18.0	-33.4	-65.4	-77.4	**-44.9**	-38.6	-32.9	-39.8	-68.6	-80.5	**-52.1**
	b&g Other + b&g PVC	c	325	150	69	209	300	**211**	15	7	3	9	15	**10**
		Δc [%]	8.0	-47.9	-13.0	-34.1	-41.9	**-25.8**	7.1	-48.3	-13.8	-34.6	-42.0	**-26.3**
	0–5 mm + b&g Other + b&g PVC	c	375	185	74	201	342	**236**	16	7	3	9	16	**10**
		Δc [%]	24.8	-36.0	-7.0	-36.6	-33.7	**-17.7**	13.7	-43.8	-14.0	-41.0	-40.7	**-25.2**
	0–10 mm + b&g Other + b&g PVC	c	396	207	75	207	351	**247**	17	8	3	9	16	**10**
		Δc [%]	31.6	-28.4	-5.1	-34.7	-32.1	**-13.7**	18.7	-39.7	-13.3	-39.7	-40.2	**-22.9**
	0–20 mm + b&g Other + b&g PVC	c	384	229	76	139	349	**235**	16	9	3	6	15	**10**
		Δc [%]	27.5	-20.7	-3.3	-56.1	-32.5	**-17.0**	12.7	-34.6	-12.6	-59.8	-41.8	**-27.2**

B.25. Si

Table B.25: Relative concentration change (Δc, in %) of Si caused by the removal of different material or particle size fractions referring to mg/kg and mg/MJ, both calculated for dry mass without hard impurities

	Removed fractions	Conc. after removal	mg/kg$_{DM}$ S01	S02	S03	S04	S05	Avr	mg/MJ S01	S02	S03	S04	S05	Avr
Single process steps	0–5 mm	c	14647	13939	11519	12289	16629	**13805**	632	564	518	527	773	**603**
		Δc [%]	-33.4	-34.4	-34.6	-29.5	-41.2	**-34.6**	-38.1	-41.2	-38.3	-33.4	-46.9	**-39.6**
	0–10 mm	c	13942	12113	10865	11808	15343	**12814**	597	473	483	504	702	**552**
		Δc [%]	-36.6	-43.0	-38.3	-32.2	-45.8	**-39.2**	-41.6	-50.7	-42.4	-36.4	-51.8	**-44.6**
	0–20 mm	c	11389	10753	10059	11172	12390	**11153**	481	413	445	473	556	**474**
		Δc [%]	-48.2	-49.4	-42.9	-35.9	-56.2	**-46.5**	-52.9	-56.9	-47.0	-40.3	-61.8	**-51.8**
	PET (NIR)	c	23774	22495	19202	18814	30958	**23049**	1117	1011	908	857	1622	**1103**
		Δc [%]	8.1	5.9	9.0	8.0	9.4	**8.1**	9.4	5.3	8.3	8.2	11.4	**8.5**
	PVC (NIR)	c	22736	21603	17750	17888	29516	**21899**	1063	976	846	813	1540	**1047**
		Δc [%]	3.4	1.7	0.8	2.7	4.3	**2.6**	4.0	1.6	0.9	2.6	5.7	**3.0**
	b&g	c	25340	22145	19542	17877	31044	**23190**	1211	1010	940	827	1671	**1132**
		Δc [%]	15.2	4.2	10.9	2.6	9.7	**8.5**	18.6	5.2	12.1	4.4	14.8	**11.0**
	PET + PVC (NIR)	c	24717	22908	19386	19411	32591	**23803**	1171	1029	918	884	1737	**1148**
		Δc [%]	12.4	7.8	10.0	11.4	15.2	**11.4**	14.6	7.2	9.4	11.6	19.3	**12.4**
Combinations of Screening and state-of-the-art NIR sorting or manual removal of black materials	0–5 mm + PET (NIR)	c	15788	14733	12387	13200	18033	**14828**	684	586	548	563	841	**645**
		Δc [%]	-28.2	-30.7	-29.7	-24.2	-36.3	**-29.8**	-33.1	-38.9	-34.7	-28.9	-42.2	**-35.6**
	0–10 mm + PET (NIR)	c	15053	12796	11670	12689	16614	**13764**	647	489	510	538	761	**589**
		Δc [%]	-31.6	-39.8	-33.8	-27.2	-41.3	**-34.7**	-36.7	-49.1	-39.2	-32.1	-47.7	**-41.0**
	0–20 mm + PET (NIR)	c	12293	11339	10783	12022	13264	**11940**	519	424	468	505	595	**502**
		Δc [%]	-44.1	-46.6	-38.8	-31.0	-53.1	**-42.7**	-49.2	-55.8	-44.3	-36.2	-59.2	**-48.9**
	0–5 mm + PVC (NIR)	c	14999	14177	11540	12551	16991	**14051**	648	572	518	536	793	**614**
		Δc [%]	-31.8	-33.3	-34.5	-28.0	-39.9	**-33.5**	-36.5	-40.4	-38.2	-32.3	-45.5	**-38.6**
	0–10 mm + PVC (NIR)	c	14261	12325	10873	12054	15597	**13022**	612	479	483	512	716	**561**
		Δc [%]	-35.2	-42.0	-38.3	-30.8	-44.9	**-38.2**	-40.1	-50.1	-42.4	-35.4	-50.8	**-43.8**
	0–20 mm + PVC (NIR)	c	11545	10942	10048	11397	12359	**11258**	488	418	444	480	556	**477**
		Δc [%]	-47.5	-48.5	-43.0	-34.6	-56.3	**-46.0**	-52.3	-56.4	-47.1	-39.4	-61.8	**-51.4**
	0–5 mm + PET (NIR) + PVC (NIR)	c	16279	15019	12431	13552	18605	**15177**	707	595	550	576	874	**660**
		Δc [%]	-26.0	-29.3	-29.4	-22.2	-34.2	**-28.2**	-30.8	-38.0	-34.5	-27.3	-40.0	**-34.1**
	0–10 mm + PET (NIR) + PVC (NIR)	c	15513	13057	11698	13024	17056	**14070**	668	496	511	549	785	**602**
		Δc [%]	-29.5	-38.6	-33.6	-25.2	-39.7	**-33.3**	-34.6	-48.3	-39.1	-30.7	-46.1	**-39.8**
	0–20 mm + PET (NIR) + PVC (NIR)	c	12569	11576	10790	12338	13334	**12121**	532	430	468	515	599	**509**
		Δc [%]	-42.9	-45.5	-38.8	-29.2	-52.9	**-41.8**	-48.0	-55.2	-44.3	-35.0	-58.8	**-48.2**
	0–5 mm + b&g	c	16980	13896	12266	12049	18214	**14681**	744	559	550	522	875	**650**
		Δc [%]	-22.8	-34.6	-30.4	-30.8	-35.6	**-30.8**	-27.1	-41.8	-34.5	-34.1	-39.9	**-35.5**
	0–10 mm + b&g	c	16254	11730	11488	11485	16812	**13554**	706	452	509	494	794	**591**
		Δc [%]	-26.1	-44.8	-34.8	-34.1	-40.6	**-36.1**	-30.8	-52.9	-39.4	-37.6	-45.5	**-41.2**
	0–20 mm + b&g	c	13444	10042	10517	10721	13502	**11645**	575	379	462	458	625	**500**
		Δc [%]	-38.9	-52.7	-40.3	-38.5	-52.3	**-44.5**	-43.7	-60.5	-45.0	-42.2	-57.1	**-49.7**
	0–5 mm + b&g + PVC (NIR)	c	17619	14172	12310	12338	18801	**15048**	775	568	552	532	912	**668**
		Δc [%]	-19.9	-33.3	-30.1	-29.2	-33.5	**-29.2**	-24.1	-40.9	-34.2	-32.8	-37.4	**-33.9**
	0–10 mm + b&g + PVC (NIR)	c	16871	11968	11514	11751	17273	**13875**	736	459	509	504	822	**606**
		Δc [%]	-23.3	-43.7	-34.6	-32.5	-38.9	**-34.6**	-28.0	-52.2	-39.3	-36.4	-43.5	**-39.9**
	0–20 mm + b&g + PVC (NIR)	c	13883	10243	10517	10955	13600	**11840**	595	384	461	465	634	**508**
		Δc [%]	-36.9	-51.8	-40.3	-37.1	-51.9	**-43.6**	-41.7	-60.0	-45.0	-41.2	-56.5	**-48.9**
	0–5 mm + b&g + PET (NIR)	c	18798	14826	13508	13079	20129	**16068**	830	584	594	564	978	**710**
		Δc [%]	-14.5	-30.2	-23.3	-24.9	-28.8	**-24.4**	-18.7	-39.2	-29.2	-28.8	-32.9	**-29.8**
	0–10 mm + b&g + PET (NIR)	c	18081	12501	12644	12471	18577	**14855**	791	468	547	534	884	**645**
		Δc [%]	-17.8	-41.2	-28.2	-28.4	-34.3	**-30.0**	-22.6	-51.2	-34.8	-32.6	-39.3	**-36.1**
	0–20 mm + b&g + PET (NIR)	c	15115	10652	11562	11657	14770	**12751**	649	388	495	494	687	**543**
		Δc [%]	-31.3	-49.9	-34.4	-33.1	-47.8	**-39.3**	-36.4	-59.6	-41.0	-37.6	-52.8	**-45.5**
	0–5 mm + b&g + PET (NIR) + PVC (NIR)	c	19736	15170	13598	13487	21076	**16613**	876	595	597	579	1037	**737**
		Δc [%]	-10.3	-28.6	-22.8	-22.6	-25.5	**-22.0**	-14.2	-38.0	-28.8	-26.9	-28.8	**-27.4**
	0–10 mm + b&g + PET (NIR) + PVC (NIR)	c	19018	12806	12712	12855	19374	**15353**	836	476	549	547	933	**668**
		Δc [%]	-13.5	-39.7	-27.8	-26.2	-31.5	**-27.8**	-18.1	-50.4	-34.5	-30.9	-35.9	**-34.0**
	0–20 mm + b&g + PET (NIR) + PVC (NIR)	c	15900	10916	11598	12010	15082	**13101**	686	394	495	505	708	**558**
		Δc [%]	-27.7	-48.6	-34.2	-31.1	-46.7	**-37.7**	-32.9	-58.9	-41.0	-36.2	-51.4	**-44.1**

More targeted removal	PVC (FTIR) + b&g PVC	c	22157	21506	17731	17607	28468	**21494**	1029	970	846	798	1464	**1021**
		Δc [%]	0.7	1.2	0.6	1.1	0.6	**0.9**	0.8	1.1	0.8	0.7	0.6	**0.8**
	0–5 mm + PVC (FTIR) + b&g PVC	c	14758	14141	11582	12351	16723	**13911**	637	571	521	527	776	**606**
		Δc [%]	-32.9	-33.5	-34.3	-29.1	-40.9	**-34.1**	-37.7	-40.6	-37.9	-33.5	-46.7	**-39.3**
	0–10 mm + PVC (FTIR) + b&g PVC	c	14050	12307	10924	11859	15428	**12914**	601	479	486	503	704	**555**
		Δc [%]	-36.1	-42.1	-38.0	-31.9	-45.5	**-38.7**	-41.1	-50.1	-42.1	-36.5	-51.6	**-44.3**
	0–20 mm + PVC (FTIR) + b&g PVC	c	11484	10942	10111	11205	12450	**11239**	484	419	447	471	558	**476**
		Δc [%]	-47.8	-48.5	-42.6	-35.7	-56.0	**-46.1**	-52.6	-56.4	-46.7	-40.5	-61.7	**-51.6**
	PVC (NIR) + b&g PVC	c	22807	21623	17786	17862	29523	**21920**	1066	977	848	811	1540	**1049**
		Δc [%]	3.7	1.8	1.0	2.5	4.4	**2.7**	4.4	1.7	1.1	2.4	5.8	**3.1**
	0–5 mm + PVC (NIR) + b&g PVC	c	15047	14192	11564	12483	16995	**14056**	651	572	520	533	794	**614**
		Δc [%]	-31.6	-33.2	-34.4	-28.3	-39.9	**-33.5**	-36.3	-40.4	-38.1	-32.7	-45.5	**-38.6**
	0–10 mm + PVC (NIR) + b&g PVC	c	14308	12340	10896	11980	15602	**13025**	614	480	485	508	716	**561**
		Δc [%]	-35.0	-41.9	-38.2	-31.2	-44.9	**-38.2**	-39.9	-50.0	-42.2	-35.8	-50.8	**-43.8**
	0–20 mm + PVC (NIR) + b&g PVC	c	11586	10957	10071	11313	12362	**11258**	489	419	445	476	556	**477**
		Δc [%]	-47.3	-48.4	-42.8	-35.1	-56.3	**-46.0**	-52.1	-56.4	-47.0	-39.9	-61.8	**-51.4**
	PET (FTIR) + Textiles + b&g PET	c	23388	22021	18468	18232	30086	**22439**	1088	990	879	827	1561	**1069**
		Δc [%]	6.3	3.6	4.8	4.7	6.3	**5.2**	6.5	3.2	4.7	4.5	7.2	**5.2**
	0–5 mm + PET (FTIR) + Textiles + b&g PET	c	15558	14531	12012	12812	17556	**14494**	668	582	537	546	814	**630**
		Δc [%]	-29.3	-31.6	-31.8	-26.5	-37.9	**-31.4**	-34.6	-39.4	-36.0	-31.0	-44.1	**-37.0**
	0–10 mm + PET (FTIR) + Textiles + b&g PET	c	14831	12678	11328	12312	16177	**13465**	632	489	501	521	737	**576**
		Δc [%]	-32.6	-40.3	-35.7	-29.3	-42.8	**-36.2**	-38.2	-49.1	-40.3	-34.2	-49.4	**-42.2**
	0–20 mm + PET (FTIR) + Textiles + b&g PET	c	12127	11297	10483	11655	12953	**11703**	508	428	460	489	578	**493**
		Δc [%]	-44.9	-46.8	-40.5	-33.1	-54.2	**-43.9**	-50.3	-55.4	-45.1	-38.2	-60.3	**-49.9**
	b&g Other	c	24165	21725	19264	17516	29708	**22476**	1112	975	909	791	1527	**1063**
		Δc [%]	9.9	2.2	9.3	0.6	5.0	**5.4**	8.9	1.5	8.3	-0.2	4.9	**4.7**
	0–5 mm + b&g Other	c	16163	13638	12200	11896	17394	**14258**	684	541	537	504	801	**613**
		Δc [%]	-26.5	-35.8	-30.7	-31.7	-38.5	**-32.7**	-33.1	-43.7	-36.0	-36.4	-45.0	**-38.8**
	0–10 mm + b&g Other	c	15441	11518	11447	11352	16039	**13160**	647	438	498	477	726	**557**
		Δc [%]	-29.8	-45.8	-35.0	-34.8	-43.3	**-37.8**	-36.7	-54.4	-40.7	-39.7	-50.1	**-44.3**
	0–20 mm + b&g Other	c	12718	9874	10509	10616	12886	**11321**	522	368	453	442	572	**471**
		Δc [%]	-42.2	-53.5	-40.3	-39.1	-54.5	**-45.9**	-48.9	-61.7	-46.0	-44.2	-60.8	**-52.3**
	PVC (FTIR) + b&g PVC + b&g Other	c	24365	22013	19415	17723	29910	**22685**	1122	986	917	797	1537	**1072**
		Δc [%]	10.8	3.6	10.2	1.7	5.7	**6.4**	9.8	2.7	9.3	0.6	5.5	**5.6**
	0–5 mm + PVC (FTIR) + b&g PVC + b&g Other	c	16307	13860	12283	11953	17503	**14381**	689	548	541	503	805	**617**
		Δc [%]	-25.9	-34.8	-30.3	-31.4	-38.1	**-32.1**	-32.5	-42.9	-35.5	-36.5	-44.7	**-38.4**
	0–10 mm + PVC (FTIR) + b&g PVC + b&g Other	c	15585	11728	11524	11393	16139	**13274**	653	444	501	476	729	**561**
		Δc [%]	-29.2	-44.8	-34.6	-34.6	-43.0	**-37.2**	-36.1	-53.8	-40.3	-39.9	-49.9	**-44.0**
	0–20 mm + PVC (FTIR) + b&g PVC + b&g Other	c	12850	10074	10579	10634	12956	**11419**	527	373	456	440	573	**474**
		Δc [%]	-41.6	-52.6	-40.0	-39.0	-54.2	**-45.5**	-48.4	-61.2	-45.7	-44.5	-60.6	**-52.1**
	PVC (NIR) + b&g PVC + b&g Other	c	25234	22146	19501	18005	31148	**23207**	1170	993	921	811	1624	**1104**
		Δc [%]	14.7	4.2	10.7	3.4	10.1	**8.6**	14.5	3.5	9.8	2.4	11.6	**8.3**
	0–5 mm + PVC (NIR) + b&g PVC + b&g Other	c	16754	13914	12273	12086	17867	**14579**	709	550	540	509	827	**627**
		Δc [%]	-23.8	-34.5	-30.3	-30.6	-36.8	**-31.2**	-30.6	-42.8	-35.6	-35.8	-43.2	**-37.6**
	0–10 mm + PVC (NIR) + b&g PVC + b&g Other	c	16005	11756	11501	11512	16394	**13434**	671	444	500	481	744	**568**
		Δc [%]	-27.2	-44.7	-34.7	-33.9	-42.0	**-36.5**	-34.3	-53.7	-40.5	-39.3	-48.9	**-43.3**
	0–20 mm + PVC (NIR) + b&g PVC + b&g Other	c	13099	10075	10538	10734	12912	**11472**	536	372	454	444	573	**476**
		Δc [%]	-40.5	-52.6	-40.2	-38.4	-54.4	**-45.2**	-47.5	-61.2	-45.9	-44.0	-60.6	**-51.9**
	b&g Other + b&g PVC	c	24246	21746	19308	17488	29715	**22501**	1116	976	911	789	1528	**1064**
		Δc [%]	10.2	2.3	9.6	0.4	5.0	**5.5**	9.3	1.6	8.6	-0.4	4.9	**4.8**
	0–5 mm + b&g Other + b&g PVC	c	16220	13654	12231	11821	17399	**14265**	686	541	538	500	801	**613**
		Δc [%]	-26.3	-35.7	-30.6	-32.1	-38.5	**-32.6**	-32.8	-43.6	-35.8	-36.9	-45.0	**-38.8**
	0–10 mm + b&g Other + b&g PVC	c	15498	11533	11477	11270	16044	**13164**	649	439	499	473	726	**557**
		Δc [%]	-29.5	-45.7	-34.9	-35.3	-43.3	**-37.7**	-36.4	-54.3	-40.5	-40.2	-50.1	**-44.3**
	0–20 mm + b&g Other + b&g PVC	c	12769	9889	10538	10522	12890	**11321**	524	368	454	438	572	**471**
		Δc [%]	-42.0	-53.5	-40.2	-39.6	-54.4	**-45.9**	-48.7	-61.7	-45.9	-44.7	-60.7	**-52.3**

B.26. Sn

Table B.26: Relative concentration change (Δc, in %) of Sn caused by the removal of different material or particle size fractions referring to mg/kg and mg/MJ, both calculated for dry mass without hard impurities

	Removed fractions	Conc. after removal	mg/kg$_{DM}$ S01	S02	S03	S04	S05	Avr	mg/MJ S01	S02	S03	S04	S05	Avr
Single process steps	0–5 mm	c	55	25	64	55	51	**50**	2.4	1.0	2.9	2.4	2.4	**2.2**
		Δc [%]	4.3	-8.4	4.6	-9.7	-2.5	**-2.3**	-3.1	-18.0	-1.3	-14.8	-12.0	**-9.8**
	0–10 mm	c	54	23	66	54	53	**50**	2.3	0.9	2.9	2.3	2.4	**2.2**
		Δc [%]	2.0	-15.1	7.2	-10.9	0.6	**-3.2**	-6.0	-26.6	0.1	-16.4	-10.6	**-11.9**
	0–20 mm	c	29	23	67	37	47	**41**	1.2	0.9	3.0	1.6	2.1	**1.8**
		Δc [%]	-45.6	-15.4	9.9	-39.7	-9.6	**-20.1**	-50.6	-28.0	2.0	-43.8	-21.2	**-28.3**
	PET (NIR)	c	57	29	67	65	58	**55**	2.7	1.3	3.2	3.0	3.0	**2.6**
		Δc [%]	8.9	6.0	9.3	7.4	10.1	**8.3**	10.2	5.4	8.5	7.7	12.1	**8.8**
	PVC (NIR)	c	54	26	62	62	54	**52**	2.5	1.2	2.9	2.8	2.8	**2.5**
		Δc [%]	3.6	-7.1	0.5	2.0	2.9	**0.4**	4.2	-7.1	0.6	2.0	4.3	**0.8**
	b&g	c	57	25	72	58	58	**54**	2.7	1.1	3.5	2.7	3.1	**2.6**
		Δc [%]	8.8	-10.2	17.5	-4.1	10.9	**4.6**	12.0	-9.3	18.7	-2.5	16.0	**7.0**
	PET + PVC (NIR)	c	60	27	67	67	60	**56**	2.8	1.2	3.2	3.0	3.2	**2.7**
		Δc [%]	13.5	-1.5	10.0	10.1	14.3	**9.3**	15.8	-2.1	9.4	10.2	18.3	**10.3**
Combinations of Screening and state-of-the-art NIR sorting or manual removal of black materials	0–5 mm + PET (NIR)	c	61	27	71	59	57	**55**	2.6	1.1	3.1	2.5	2.7	**2.4**
		Δc [%]	15.4	-1.8	15.5	-2.5	9.0	**7.1**	7.6	-13.5	7.4	-8.5	-1.2	**-1.7**
	0–10 mm + PET (NIR)	c	60	25	73	59	59	**55**	2.6	1.0	3.2	2.5	2.7	**2.4**
		Δc [%]	13.3	-8.4	19.0	-3.6	13.2	**6.7**	4.8	-22.6	9.2	-10.1	0.8	**-3.6**
	0–20 mm + PET (NIR)	c	32	25	75	39	54	**45**	1.3	1.0	3.3	1.6	2.4	**1.9**
		Δc [%]	-39.8	-7.9	22.8	-36.1	2.2	**-11.8**	-45.3	-23.7	11.8	-40.9	-10.9	**-21.8**
	0–5 mm + PVC (NIR)	c	57	23	64	56	53	**51**	2.5	0.9	2.9	2.4	2.5	**2.2**
		Δc [%]	8.8	-17.4	5.2	-7.9	0.6	**-2.1**	1.3	-26.2	-0.7	-13.4	-8.7	**-9.6**
	0–10 mm + PVC (NIR)	c	56	21	66	55	55	**51**	2.4	0.8	2.9	2.3	2.5	**2.2**
		Δc [%]	6.5	-25.4	7.9	-9.1	4.2	**-3.2**	-1.6	-35.7	0.8	-15.1	-7.1	**-11.8**
	0–20 mm + PVC (NIR)	c	29	20	68	37	49	**41**	1.2	0.8	3.0	1.6	2.2	**1.8**
		Δc [%]	-44.4	-26.7	10.7	-39.4	-6.8	**-21.3**	-49.4	-38.0	2.7	-43.8	-18.6	**-29.4**
	0–5 mm + PET (NIR) + PVC (NIR)	c	64	24	71	61	60	**56**	2.8	1.0	3.2	2.6	2.8	**2.5**
		Δc [%]	21.3	-11.5	16.5	0.0	13.8	**8.0**	13.4	-22.3	8.2	-6.6	3.9	**-0.7**
	0–10 mm + PET (NIR) + PVC (NIR)	c	63	22	74	60	62	**56**	2.7	0.8	3.2	2.5	2.9	**2.4**
		Δc [%]	19.5	-19.7	20.1	-1.1	18.8	**7.5**	10.7	-32.5	10.2	-8.3	6.2	**-2.7**
	0–20 mm + PET (NIR) + PVC (NIR)	c	33	22	76	39	56	**45**	1.4	0.8	3.3	1.6	2.5	**1.9**
		Δc [%]	-37.8	-20.5	24.1	-35.5	7.0	**-12.5**	-43.4	-34.6	12.9	-40.8	-6.5	**-22.5**
	0–5 mm + b&g	c	61	21	77	51	58	**54**	2.7	0.9	3.4	2.2	2.8	**2.4**
		Δc [%]	15.8	-22.6	25.2	-15.8	10.0	**2.5**	9.3	-31.1	17.8	-19.8	2.6	**-4.2**
	0–10 mm + b&g	c	60	19	79	50	60	**54**	2.6	0.7	3.5	2.2	2.8	**2.4**
		Δc [%]	13.6	-32.5	29.3	-17.4	14.2	**1.4**	6.3	-42.4	20.2	-21.8	4.8	**-6.6**
	0–20 mm + b&g	c	29	18	82	30	54	**43**	1.2	0.7	3.6	1.3	2.5	**1.9**
		Δc [%]	-45.3	-35.0	34.1	-51.4	3.4	**-18.8**	-49.6	-45.6	23.7	-54.4	-7.0	**-26.6**
	0–5 mm + b&g + PVC (NIR)	c	64	18	77	52	60	**55**	2.8	0.7	3.5	2.3	2.9	**2.4**
		Δc [%]	22.3	-33.4	26.5	-14.1	14.9	**3.2**	15.9	-41.0	19.0	-18.5	8.3	**-3.2**
	0–10 mm + b&g + PVC (NIR)	c	63	15	80	51	63	**55**	2.8	0.6	3.5	2.2	3.0	**2.4**
		Δc [%]	20.4	-45.3	30.8	-15.7	19.9	**2.0**	13.1	-53.6	21.5	-20.6	10.9	**-5.7**
	0–20 mm + b&g + PVC (NIR)	c	30	14	83	29	57	**43**	1.3	0.5	3.7	1.2	2.6	**1.9**
		Δc [%]	-43.6	-49.5	35.8	-51.9	8.3	**-20.2**	-47.9	-58.1	25.1	-55.0	-2.0	**-27.6**
	0–5 mm + b&g + PET (NIR)	c	69	23	88	56	66	**60**	3.1	0.9	3.8	2.4	3.2	**2.7**
		Δc [%]	31.6	-16.5	42.9	-8.4	25.6	**15.0**	25.1	-27.2	31.9	-13.1	18.5	**7.0**
	0–10 mm + b&g + PET (NIR)	c	68	20	91	55	69	**61**	3.0	0.8	3.9	2.3	3.3	**2.7**
		Δc [%]	30.2	-26.9	48.8	-9.9	31.5	**14.7**	22.6	-39.3	35.2	-15.2	21.6	**5.0**
	0–20 mm + b&g + PET (NIR)	c	33	20	96	31	63	**48**	1.4	0.7	4.1	1.3	2.9	**2.1**
		Δc [%]	-37.4	-28.9	56.1	-49.2	20.2	**-7.8**	-42.1	-42.6	40.3	-52.6	8.6	**-17.7**
	0–5 mm + b&g + PET (NIR) + PVC (NIR)	c	74	20	89	57	70	**62**	3.3	0.8	3.9	2.5	3.4	**2.8**
		Δc [%]	40.9	-28.5	45.0	-5.8	33.5	**17.0**	34.7	-38.0	33.7	-11.1	27.6	**9.4**
	0–10 mm + b&g + PET (NIR) + PVC (NIR)	c	74	16	93	56	74	**63**	3.2	0.6	4.0	2.4	3.6	**2.8**
		Δc [%]	40.1	-41.3	51.1	-7.3	40.7	**16.7**	32.6	-51.7	37.2	-13.3	31.6	**7.3**
	0–20 mm + b&g + PET (NIR) + PVC (NIR)	c	35	15	97	31	68	**49**	1.5	0.5	4.2	1.3	3.2	**2.1**
		Δc [%]	-34.2	-45.7	59.0	-49.5	28.7	**-8.3**	-38.9	-56.6	42.6	-53.3	17.4	**-17.8**

More targeted removal	PVC (FTIR) + b&g PVC	c	51	26	61	62	52	**50**	2.4	1.2	2.9	2.8	2.7	**2.4**
		Δc [%]	-3.2	-6.8	-1.0	1.3	-0.3	**-2.0**	-3.1	-6.9	-0.9	0.9	-0.4	**-2.1**
	0–5 mm + PVC (FTIR) + b&g PVC	c	53	23	63	56	51	**49**	2.3	0.9	2.9	2.4	2.4	**2.2**
		Δc [%]	0.7	-16.9	3.5	-8.6	-3.0	**-4.8**	-6.5	-25.7	-2.3	-14.2	-12.6	**-12.2**
	0–10 mm + PVC (FTIR) + b&g PVC	c	52	21	65	55	53	**49**	2.2	0.8	2.9	2.3	2.4	**2.1**
		Δc [%]	-1.9	-24.7	6.1	-9.7	0.2	**-6.0**	-9.6	-35.1	-0.8	-15.8	-11.1	**-14.5**
	0–20 mm + PVC (FTIR) + b&g PVC	c	26	20	67	37	47	**39**	1.1	0.8	2.9	1.6	2.1	**1.7**
		Δc [%]	-50.7	-26.0	8.7	-39.4	-10.2	**-23.5**	-55.2	-37.3	1.0	-43.9	-21.8	**-31.4**
	PVC (NIR) + b&g PVC	c	52	26	61	62	54	**51**	2.5	1.2	2.9	2.8	2.8	**2.4**
		Δc [%]	-0.2	-7.0	-0.5	2.0	2.9	**-0.6**	0.5	-7.0	-0.4	1.9	4.3	**-0.1**
	0–5 mm + PVC (NIR) + b&g PVC	c	55	23	64	56	53	**50**	2.4	0.9	2.9	2.4	2.5	**2.2**
		Δc [%]	4.4	-17.3	4.1	-8.0	0.6	**-3.2**	-2.8	-26.1	-1.7	-13.6	-8.7	**-10.6**
	0–10 mm + PVC (NIR) + b&g PVC	c	54	21	65	55	55	**50**	2.3	0.8	2.9	2.3	2.5	**2.2**
		Δc [%]	1.9	-25.3	6.8	-9.2	4.2	**-4.3**	-5.9	-35.7	-0.3	-15.3	-7.0	**-12.8**
	0–20 mm + PVC (NIR) + b&g PVC	c	26	20	67	37	49	**40**	1.1	0.8	3.0	1.5	2.2	**1.7**
		Δc [%]	-50.1	-26.6	9.5	-39.7	-6.8	**-22.8**	-54.6	-37.9	1.6	-44.2	-18.5	**-30.7**
	PET (FTIR) + Textiles + b&g PET	c	56	28	65	64	56	**54**	2.6	1.3	3.1	2.9	2.9	**2.6**
		Δc [%]	7.1	2.5	5.7	4.9	6.6	**5.4**	7.3	2.1	5.6	4.7	7.4	**5.4**
	0–5 mm + PET (FTIR) + Textiles + b&g PET	c	59	26	68	58	55	**53**	2.6	1.0	3.0	2.5	2.6	**2.3**
		Δc [%]	13.1	-5.7	11.2	-4.9	4.9	**3.7**	4.6	-16.4	4.4	-10.8	-5.5	**-4.7**
	0–10 mm + PET (FTIR) + Textiles + b&g PET	c	58	24	70	57	57	**53**	2.5	0.9	3.1	2.4	2.6	**2.3**
		Δc [%]	11.0	-12.5	14.3	-6.0	8.7	**3.1**	1.8	-25.3	6.1	-12.4	-3.7	**-6.7**
	0–20 mm + PET (FTIR) + Textiles + b&g PET	c	31	24	72	38	51	**43**	1.3	0.9	3.2	1.6	2.3	**1.9**
		Δc [%]	-40.8	-12.4	17.5	-36.9	-2.0	**-14.9**	-46.6	-26.6	8.4	-41.7	-15.0	**-24.3**
	b&g Other	c	56	24	71	57	55	**53**	2.6	1.1	3.3	2.6	2.9	**2.5**
		Δc [%]	7.2	-11.8	15.7	-7.0	5.7	**2.0**	6.2	-12.4	14.6	-7.7	5.6	**1.3**
	0–5 mm + b&g Other	c	60	21	75	50	55	**52**	2.5	0.8	3.3	2.1	2.5	**2.3**
		Δc [%]	13.4	-24.3	22.9	-18.6	4.0	**-0.5**	3.3	-33.5	13.6	-24.2	-7.0	**-9.6**
	0–10 mm + b&g Other	c	58	18	78	49	56	**52**	2.5	0.7	3.4	2.0	2.6	**2.2**
		Δc [%]	11.2	-34.0	26.8	-20.2	7.7	**-1.7**	0.4	-44.5	15.7	-26.2	-5.3	**-12.0**
	0–20 mm + b&g Other	c	30	18	80	29	51	**41**	1.2	0.7	3.5	1.2	2.3	**1.8**
		Δc [%]	-43.0	-36.6	31.2	-52.7	-2.9	**-20.8**	-49.7	-47.7	18.7	-56.7	-16.3	**-30.4**
	PVC (FTIR) + b&g PVC + b&g Other	c	55	22	70	57	55	**52**	2.5	1.0	3.3	2.6	2.8	**2.4**
		Δc [%]	3.7	-19.5	14.6	-5.8	5.4	**-0.3**	2.8	-20.1	13.7	-6.9	5.2	**-1.1**
	0–5 mm + PVC (FTIR) + b&g PVC + b&g Other	c	57	18	75	50	54	**51**	2.4	0.7	3.3	2.1	2.5	**2.2**
		Δc [%]	9.4	-34.0	21.8	-17.6	3.6	**-3.4**	-0.4	-42.3	12.6	-23.8	-7.5	**-12.3**
	0–10 mm + PVC (FTIR) + b&g PVC + b&g Other	c	56	15	77	49	56	**51**	2.4	0.6	3.3	2.1	2.5	**2.2**
		Δc [%]	6.9	-45.3	25.7	-19.2	7.3	**-4.9**	-3.6	-54.2	14.8	-25.8	-5.8	**-14.9**
	0–20 mm + PVC (FTIR) + b&g PVC + b&g Other	c	27	14	80	29	51	**40**	1.1	0.5	3.4	1.2	2.2	**1.7**
		Δc [%]	-49.0	-49.3	30.1	-52.9	-3.4	**-24.9**	-55.0	-58.5	17.7	-57.1	-17.0	**-34.0**
	PVC (NIR) + b&g PVC + b&g Other	c	57	22	71	58	57	**53**	2.6	1.0	3.3	2.6	3.0	**2.5**
		Δc [%]	7.5	-19.8	15.4	-5.2	9.3	**1.4**	7.3	-20.4	14.5	-6.0	10.8	**1.2**
	0–5 mm + PVC (NIR) + b&g PVC + b&g Other	c	60	18	75	50	57	**52**	2.5	0.7	3.3	2.1	2.6	**2.3**
		Δc [%]	14.3	-34.7	22.8	-17.3	8.0	**-1.4**	4.2	-42.9	13.5	-23.4	-2.9	**-10.3**
	0–10 mm + PVC (NIR) + b&g PVC + b&g Other	c	59	15	78	49	59	**52**	2.5	0.6	3.4	2.1	2.7	**2.2**
		Δc [%]	12.0	-46.3	26.8	-18.9	12.3	**-2.8**	1.0	-55.1	15.7	-25.6	-0.9	**-13.0**
	0–20 mm + PVC (NIR) + b&g PVC + b&g Other	c	27	14	80	28	53	**40**	1.1	0.5	3.5	1.2	2.3	**1.7**
		Δc [%]	-48.1	-50.5	31.4	-53.8	0.9	**-24.0**	-54.3	-59.5	18.8	-58.0	-13.0	**-33.2**
	b&g Other + b&g PVC	c	54	24	70	57	55	**52**	2.5	1.1	3.3	2.5	2.9	**2.5**
		Δc [%]	3.2	-11.8	14.5	-7.1	5.8	**0.9**	2.4	-12.4	13.5	-7.8	5.6	**0.3**
	0–5 mm + b&g Other + b&g PVC	c	57	21	75	49	55	**51**	2.4	0.8	3.3	2.1	2.5	**2.2**
		Δc [%]	8.8	-24.2	21.7	-18.7	4.0	**-1.7**	-0.9	-33.4	12.5	-24.4	-6.9	**-10.7**
	0–10 mm + b&g Other + b&g PVC	c	56	18	77	48	56	**51**	2.3	0.7	3.3	2.0	2.6	**2.2**
		Δc [%]	6.3	-34.0	25.5	-20.4	7.7	**-3.0**	-4.1	-44.4	14.6	-26.5	-5.3	**-13.1**
	0–20 mm + b&g Other + b&g PVC	c	27	18	80	28	51	**41**	1.1	0.7	3.4	1.2	2.3	**1.7**
		Δc [%]	-49.2	-36.5	29.9	-53.2	-2.9	**-22.4**	-55.1	-47.7	17.5	-57.2	-16.3	**-31.8**

B.27. Sr

Table B.27: Relative concentration change (Δc, in %) of Sr caused by the removal of different material or particle size fractions referring to mg/kg and mg/MJ, both calculated for dry mass without hard impurities

	Removed fractions	Conc. after removal	mg/kg$_{DM}$ S01	S02	S03	S04	S05	Avr	mg/MJ S01	S02	S03	S04	S05	Avr
Single process steps	0–5 mm	c	78	90	54	59	62	**69**	3.4	3.6	2.4	2.5	2.9	**3.0**
		Δc [%]	-26.0	-31.9	-28.0	-21.6	-41.5	**-29.8**	-31.2	-39.0	-32.1	-26.0	-47.2	**-35.1**
	0–10 mm	c	75	80	50	56	57	**64**	3.2	3.1	2.2	2.4	2.6	**2.7**
		Δc [%]	-29.0	-39.1	-33.0	-24.8	-46.9	**-34.5**	-34.5	-47.3	-37.4	-29.5	-52.8	**-40.3**
	0–20 mm	c	71	76	48	56	47	**60**	3.0	2.9	2.1	2.4	2.1	**2.5**
		Δc [%]	-32.8	-42.2	-36.3	-25.4	-55.6	**-38.5**	-39.0	-50.8	-40.9	-30.5	-61.2	**-44.5**
	PET (NIR)	c	113	137	79	80	115	**105**	5.3	6.2	3.7	3.6	6.0	**5.0**
		Δc [%]	8.0	4.1	5.0	6.1	8.3	**6.3**	9.3	3.5	4.3	6.3	10.2	**6.7**
	PVC (NIR)	c	109	132	73	76	111	**100**	5.1	5.9	3.5	3.5	5.8	**4.8**
		Δc [%]	3.6	-0.2	-3.2	1.6	4.4	**1.2**	4.3	-0.2	-3.1	1.5	5.8	**1.7**
	b&g	c	120	140	80	76	114	**106**	5.8	6.4	3.9	3.5	6.1	**5.1**
		Δc [%]	14.5	5.9	7.2	0.9	7.0	**7.1**	17.9	6.9	8.3	2.6	11.9	**9.5**
	PET + PVC (NIR)	c	118	137	76	81	122	**107**	5.6	6.2	3.6	3.7	6.5	**5.1**
		Δc [%]	12.5	4.0	1.5	8.2	14.1	**8.0**	14.8	3.4	0.9	8.3	18.1	**9.1**
Combinations of Screening and state-of-the-art NIR sorting or manual removal of black materials	0–5 mm + PET (NIR)	c	84	92	55	62	66	**72**	3.6	3.7	2.4	2.6	3.1	**3.1**
		Δc [%]	-19.9	-30.1	-26.5	-17.4	-37.9	**-26.4**	-25.3	-38.4	-31.7	-22.5	-43.8	**-32.4**
	0–10 mm + PET (NIR)	c	81	82	51	59	60	**67**	3.5	3.1	2.2	2.5	2.7	**2.8**
		Δc [%]	-23.0	-37.9	-32.2	-20.9	-44.0	**-31.6**	-28.8	-47.5	-37.8	-26.3	-50.1	**-38.1**
	0–20 mm + PET (NIR)	c	77	77	48	59	49	**62**	3.3	2.9	2.1	2.5	2.2	**2.6**
		Δc [%]	-26.4	-41.3	-36.0	-21.4	-53.9	**-35.8**	-33.1	-51.4	-41.7	-27.4	-59.9	**-42.7**
	0–5 mm + PVC (NIR)	c	80	88	51	59	64	**69**	3.5	3.6	2.3	2.5	3.0	**3.0**
		Δc [%]	-23.6	-32.9	-32.1	-20.9	-40.1	**-29.9**	-28.8	-40.1	-35.9	-25.7	-45.7	**-35.2**
	0–10 mm + PVC (NIR)	c	77	78	47	57	58	**63**	3.3	3.1	2.1	2.4	2.6	**2.7**
		Δc [%]	-26.7	-40.5	-37.3	-24.3	-46.0	**-34.9**	-32.3	-48.7	-41.5	-29.3	-51.8	**-40.7**
	0–20 mm + PVC (NIR)	c	73	74	44	56	47	**59**	3.1	2.8	2.0	2.4	2.1	**2.5**
		Δc [%]	-30.5	-43.9	-40.9	-24.9	-55.5	**-39.1**	-36.8	-52.5	-45.2	-30.4	-61.1	**-45.2**
	0–5 mm + PET (NIR) + PVC (NIR)	c	88	91	52	63	68	**72**	3.8	3.6	2.3	2.7	3.2	**3.1**
		Δc [%]	-16.7	-31.2	-31.2	-16.5	-36.0	**-26.3**	-22.1	-39.7	-36.1	-22.0	-41.6	**-32.3**
	0–10 mm + PET (NIR) + PVC (NIR)	c	84	80	47	60	61	**66**	3.6	3.0	2.1	2.5	2.8	**2.8**
		Δc [%]	-19.9	-39.4	-37.2	-20.1	-42.6	**-31.9**	-25.8	-49.1	-42.4	-25.9	-48.7	**-38.4**
	0–20 mm + PET (NIR) + PVC (NIR)	c	81	75	44	60	49	**62**	3.4	2.8	1.9	2.5	2.2	**2.6**
		Δc [%]	-23.0	-43.2	-41.4	-20.5	-53.6	**-36.3**	-29.9	-53.3	-46.7	-27.0	-59.5	**-43.3**
	0–5 mm + b&g	c	90	93	55	57	65	**72**	3.9	3.7	2.5	2.5	3.1	**3.1**
		Δc [%]	-14.5	-29.5	-26.4	-23.8	-39.2	**-26.7**	-19.3	-37.2	-30.7	-27.4	-43.2	**-31.6**
	0–10 mm + b&g	c	87	82	51	54	58	**66**	3.8	3.2	2.2	2.3	2.8	**2.9**
		Δc [%]	-17.5	-37.7	-32.5	-27.6	-45.2	**-32.1**	-22.8	-46.8	-37.3	-31.5	-49.7	**-37.6**
	0–20 mm + b&g	c	84	77	48	54	48	**62**	3.6	2.9	2.1	2.3	2.2	**2.6**
		Δc [%]	-20.2	-41.3	-36.6	-28.5	-55.2	**-36.4**	-26.5	-50.9	-41.6	-32.9	-59.7	**-42.3**
	0–5 mm + b&g + PVC (NIR)	c	94	91	52	58	67	**72**	4.1	3.7	2.3	2.5	3.2	**3.2**
		Δc [%]	-10.6	-30.7	-31.4	-23.2	-37.3	**-26.6**	-15.2	-38.5	-35.4	-27.1	-41.0	**-31.4**
	0–10 mm + b&g + PVC (NIR)	c	91	80	47	55	60	**66**	4.0	3.1	2.1	2.3	2.8	**2.9**
		Δc [%]	-13.6	-39.3	-37.9	-27.2	-44.0	**-32.4**	-18.8	-48.5	-42.3	-31.4	-48.2	**-37.8**
	0–20 mm + b&g + PVC (NIR)	c	89	75	43	54	48	**62**	3.8	2.8	1.9	2.3	2.2	**2.6**
		Δc [%]	-15.6	-43.3	-42.5	-28.1	-55.0	**-36.9**	-22.1	-52.9	-47.0	-32.9	-59.3	**-42.8**
	0–5 mm + b&g + PET (NIR)	c	100	96	57	61	70	**77**	4.4	3.8	2.5	2.6	3.4	**3.3**
		Δc [%]	-5.1	-27.1	-24.3	-19.3	-34.6	**-22.1**	-9.7	-36.5	-30.1	-23.5	-38.3	**-27.6**
	0–10 mm + b&g + PET (NIR)	c	97	84	51	57	62	**70**	4.2	3.2	2.2	2.5	3.0	**3.0**
		Δc [%]	-7.9	-36.1	-31.5	-23.5	-41.5	**-28.1**	-13.3	-47.0	-37.7	-28.0	-45.9	**-34.4**
	0–20 mm + b&g + PET (NIR)	c	96	79	48	57	50	**66**	4.1	2.9	2.0	2.4	2.3	**2.8**
		Δc [%]	-8.7	-40.1	-36.3	-24.3	-53.1	**-32.5**	-15.5	-51.6	-42.8	-29.4	-57.6	**-39.4**
	0–5 mm + b&g + PET (NIR) + PVC (NIR)	c	106	94	52	61	73	**77**	4.7	3.7	2.3	2.6	3.6	**3.4**
		Δc [%]	0.6	-28.3	-30.1	-18.3	-31.8	**-21.6**	-3.8	-37.8	-35.6	-22.9	-34.8	**-27.0**
	0–10 mm + b&g + PET (NIR) + PVC (NIR)	c	103	82	47	58	64	**71**	4.5	3.0	2.0	2.5	3.1	**3.0**
		Δc [%]	-2.1	-37.9	-37.9	-22.8	-39.5	**-28.0**	-7.4	-48.8	-43.6	-27.7	-43.4	**-34.2**
	0–20 mm + b&g + PET (NIR) + PVC (NIR)	c	104	76	42	57	50	**66**	4.5	2.7	1.8	2.4	2.4	**2.8**
		Δc [%]	-1.4	-42.3	-43.5	-23.5	-52.7	**-32.7**	-8.4	-53.9	-49.3	-29.2	-56.8	**-39.5**

More targeted removal	PVC (FTIR) + b&g PVC	c	106	132	73	75	107	**98**	4.9	5.9	3.5	3.4	5.5	**4.6**
		Δc [%]	0.5	-0.2	-3.2	-0.4	0.4	**-0.6**	0.6	-0.3	-3.1	-0.7	0.4	**-0.6**
	0–5 mm + PVC (FTIR) + b&g PVC	c	78	89	51	58	62	**68**	3.4	3.6	2.3	2.5	2.9	**2.9**
		Δc [%]	-25.6	-32.6	-31.8	-22.6	-41.4	**-30.8**	-30.9	-39.8	-35.6	-27.4	-47.2	**-36.2**
	0–10 mm + PVC (FTIR) + b&g PVC	c	75	79	47	56	57	**63**	3.2	3.1	2.1	2.4	2.6	**2.7**
		Δc [%]	-28.7	-40.0	-37.0	-26.0	-46.8	**-35.7**	-34.2	-48.3	-41.1	-31.0	-52.8	**-41.5**
	0–20 mm + PVC (FTIR) + b&g PVC	c	71	75	45	55	47	**59**	3.0	2.9	2.0	2.3	2.1	**2.5**
		Δc [%]	-32.5	-43.3	-40.5	-26.7	-55.6	**-39.7**	-38.7	-52.0	-44.8	-32.2	-61.4	**-45.8**
	PVC (NIR) + b&g PVC	c	109	132	73	76	111	**100**	5.1	5.9	3.5	3.4	5.8	**4.8**
		Δc [%]	3.9	-0.1	-3.0	0.8	4.4	**1.2**	4.6	-0.1	-2.9	0.7	5.9	**1.6**
	0–5 mm + PVC (NIR) + b&g PVC	c	81	88	51	59	64	**69**	3.5	3.6	2.3	2.5	3.0	**3.0**
		Δc [%]	-23.3	-32.9	-32.0	-21.9	-40.1	**-30.0**	-28.6	-40.1	-35.8	-26.7	-45.7	**-35.4**
	0–10 mm + PVC (NIR) + b&g PVC	c	77	79	47	56	58	**63**	3.3	3.1	2.1	2.4	2.6	**2.7**
		Δc [%]	-26.4	-40.4	-37.2	-25.3	-45.9	**-35.1**	-32.0	-48.7	-41.4	-30.3	-51.8	**-40.8**
	0–20 mm + PVC (NIR) + b&g PVC	c	73	74	44	56	47	**59**	3.1	2.8	2.0	2.3	2.1	**2.5**
		Δc [%]	-30.2	-43.8	-40.8	-26.0	-55.5	**-39.3**	-36.5	-52.5	-45.1	-31.5	-61.1	**-45.3**
	PET (FTIR) + Textiles + b&g PET	c	112	134	78	78	113	**103**	5.2	6.0	3.7	3.5	5.8	**4.9**
		Δc [%]	6.3	1.9	4.4	3.7	5.6	**4.4**	6.6	1.4	4.3	3.5	6.5	**4.5**
	0–5 mm + PET (FTIR) + Textiles + b&g PET	c	83	91	56	61	65	**71**	3.6	3.6	2.5	2.6	3.0	**3.1**
		Δc [%]	-21.1	-31.1	-25.2	-19.0	-39.1	**-27.1**	-27.0	-38.9	-29.8	-24.1	-45.1	**-33.0**
	0–10 mm + PET (FTIR) + Textiles + b&g PET	c	80	81	52	58	59	**66**	3.4	3.1	2.3	2.5	2.7	**2.8**
		Δc [%]	-24.1	-38.6	-30.5	-22.4	-44.9	**-32.1**	-30.4	-47.6	-35.4	-27.7	-51.2	**-38.5**
	0–20 mm + PET (FTIR) + Textiles + b&g PET	c	76	77	50	58	49	**62**	3.2	2.9	2.2	2.4	2.2	**2.6**
		Δc [%]	-27.6	-41.9	-33.9	-22.9	-54.4	**-36.1**	-34.7	-51.3	-39.0	-28.8	-60.5	**-42.9**
	b&g Other	c	115	137	79	75	111	**103**	5.3	6.1	3.7	3.4	5.7	**4.8**
		Δc [%]	9.5	3.9	5.2	-0.7	4.0	**4.4**	8.5	3.2	4.2	-1.4	3.9	**3.7**
	0–5 mm + b&g Other	c	86	91	54	57	64	**70**	3.6	3.6	2.4	2.4	2.9	**3.0**
		Δc [%]	-18.5	-30.9	-27.5	-24.4	-40.0	**-28.2**	-25.7	-39.3	-33.0	-29.7	-46.3	**-34.8**
	0–10 mm + b&g Other	c	83	80	50	54	58	**65**	3.5	3.1	2.2	2.3	2.6	**2.7**
		Δc [%]	-21.5	-38.9	-33.4	-28.1	-45.7	**-33.5**	-29.2	-48.6	-39.2	-33.5	-52.2	**-40.6**
	0–20 mm + b&g Other	c	79	76	47	53	48	**61**	3.3	2.8	2.0	2.2	2.1	**2.5**
		Δc [%]	-24.6	-42.6	-37.4	-29.0	-55.1	**-37.7**	-33.4	-52.7	-43.4	-35.0	-61.3	**-45.1**
	PVC (FTIR) + b&g PVC + b&g Other	c	116	137	76	74	111	**103**	5.3	6.1	3.6	3.3	5.7	**4.8**
		Δc [%]	10.1	3.8	1.5	-1.1	4.5	**3.8**	9.2	2.9	0.6	-2.2	4.3	**3.0**
	0–5 mm + PVC (FTIR) + b&g PVC + b&g Other	c	86	90	51	56	64	**69**	3.6	3.6	2.2	2.3	2.9	**2.9**
		Δc [%]	-18.0	-31.7	-32.0	-25.7	-39.8	**-29.4**	-25.3	-40.2	-37.1	-31.3	-46.3	**-36.0**
	0–10 mm + PVC (FTIR) + b&g PVC + b&g Other	c	83	79	46	53	58	**64**	3.5	3.0	2.0	2.2	2.6	**2.7**
		Δc [%]	-21.0	-40.0	-38.2	-29.5	-45.6	**-34.9**	-28.8	-49.7	-43.6	-35.3	-52.3	**-41.9**
	0–20 mm + PVC (FTIR) + b&g PVC + b&g Other	c	80	74	43	52	48	**59**	3.3	2.7	1.9	2.2	2.1	**2.4**
		Δc [%]	-24.1	-43.8	-42.6	-30.6	-55.1	**-39.2**	-33.0	-54.0	-48.1	-36.8	-61.4	**-46.7**
	PVC (NIR) + b&g PVC + b&g Other	c	120	137	76	75	116	**105**	5.6	6.1	3.6	3.4	6.1	**5.0**
		Δc [%]	14.6	3.9	1.8	0.2	9.1	**5.9**	14.3	3.2	0.9	-0.7	10.6	**5.7**
	0–5 mm + PVC (NIR) + b&g PVC + b&g Other	c	90	90	51	56	66	**70**	3.8	3.5	2.2	2.4	3.0	**3.0**
		Δc [%]	-14.8	-32.0	-32.2	-25.0	-38.3	**-28.5**	-22.3	-40.5	-37.4	-30.6	-44.6	**-35.1**
	0–10 mm + PVC (NIR) + b&g PVC + b&g Other	c	86	78	46	53	59	**65**	3.6	3.0	2.0	2.2	2.7	**2.7**
		Δc [%]	-17.9	-40.5	-38.5	-28.9	-44.6	**-34.1**	-25.9	-50.2	-43.9	-34.7	-51.1	**-41.2**
	0–20 mm + PVC (NIR) + b&g PVC + b&g Other	c	83	73	43	53	48	**60**	3.4	2.7	1.8	2.2	2.1	**2.5**
		Δc [%]	-20.6	-44.4	-43.0	-30.0	-54.9	**-38.6**	-30.0	-54.5	-48.5	-36.3	-61.1	**-46.1**
	b&g Other + b&g PVC	c	115	137	79	74	111	**103**	5.3	6.2	3.7	3.3	5.7	**4.8**
		Δc [%]	9.8	4.0	5.4	-1.4	4.0	**4.4**	8.9	3.3	4.4	-2.2	3.9	**3.7**
	0–5 mm + b&g Other + b&g PVC	c	86	91	55	56	64	**70**	3.6	3.6	2.4	2.4	2.9	**3.0**
		Δc [%]	-18.2	-30.8	-27.4	-25.5	-40.0	**-28.4**	-25.5	-39.3	-32.9	-30.7	-46.3	**-34.9**
	0–10 mm + b&g Other + b&g PVC	c	83	81	50	53	58	**65**	3.5	3.1	2.2	2.2	2.6	**2.7**
		Δc [%]	-21.2	-38.9	-33.3	-29.2	-45.7	**-33.7**	-28.9	-48.5	-39.1	-34.6	-52.2	**-40.7**
	0–20 mm + b&g Other + b&g PVC	c	80	76	47	52	48	**61**	3.3	2.8	2.0	2.2	2.1	**2.5**
		Δc [%]	-24.3	-42.5	-37.3	-30.2	-55.1	**-37.9**	-33.1	-52.6	-43.3	-36.1	-61.3	**-45.3**

B.28. Ti

Table B.28: Relative concentration change (Δc, in %) of Ti caused by the removal of different material or particle size fractions referring to mg/kg and mg/MJ, both calculated for dry mass without hard impurities

	Removed fractions	Conc. after removal	mg/kg$_{DM}$						mg/MJ					
			S01	S02	S03	S04	S05	Avr	S01	S02	S03	S04	S05	Avr
Single process steps	0–5 mm	c	1569	1254	1064	1203	1596	**1337**	68	51	48	52	74	**58**
		Δc [%]	-0.6	-11.6	-13.0	-3.0	-10.1	**-7.7**	-7.7	-20.9	-18.0	-8.5	-18.8	**-14.8**
	0–10 mm	c	1591	1283	1041	1201	1586	**1340**	68	50	46	51	73	**58**
		Δc [%]	0.8	-9.6	-15.0	-3.2	-10.6	**-7.5**	-7.1	-21.8	-20.6	-9.2	-20.6	**-15.8**
	0–20 mm	c	1691	1327	1041	1218	1596	**1375**	71	51	46	52	72	**58**
		Δc [%]	7.2	-6.5	-15.0	-1.8	-10.1	**-5.2**	-2.6	-20.4	-21.1	-8.6	-21.5	**-14.9**
	PET (NIR)	c	1631	1429	1217	1121	1816	**1443**	77	64	58	51	95	**69**
		Δc [%]	3.3	0.6	-0.5	-9.6	2.4	**-0.8**	4.6	0.1	-1.2	-9.5	4.2	**-0.4**
	PVC (NIR)	c	1582	1418	1210	1188	1745	**1429**	74	64	58	54	91	**68**
		Δc [%]	0.2	-0.1	-1.2	-4.3	-1.6	**-1.4**	0.9	-0.1	-1.0	-4.3	-0.3	**-1.0**
	b&g	c	1670	1389	1327	1173	1675	**1447**	80	63	64	54	90	**70**
		Δc [%]	5.8	-2.1	8.5	-5.5	-5.6	**0.2**	8.9	-1.2	9.6	-3.8	-1.3	**2.4**
	PET + PVC (NIR)	c	1638	1427	1201	1056	1787	**1422**	78	64	57	48	95	**68**
		Δc [%]	3.8	0.5	-1.9	-14.9	0.7	**-2.3**	5.9	-0.1	-2.4	-14.8	4.3	**-1.4**
Combinations of Screening and state-of-the-art NIR sorting or manual removal of black materials	0–5 mm + PET (NIR)	c	1629	1248	1034	1063	1618	**1318**	71	50	46	45	76	**57**
		Δc [%]	3.2	-12.1	-15.5	-14.3	-8.8	**-9.5**	-3.7	-22.6	-21.5	-19.6	-17.3	**-16.9**
	0–10 mm + PET (NIR)	c	1657	1280	1005	1055	1608	**1321**	71	49	44	45	74	**56**
		Δc [%]	5.0	-9.9	-17.8	-15.0	-9.4	**-9.4**	-2.9	-23.8	-24.6	-20.7	-19.3	**-18.3**
	0–20 mm + PET (NIR)	c	1787	1329	1003	1063	1622	**1361**	75	50	44	45	73	**57**
		Δc [%]	13.2	-6.3	-18.0	-14.3	-8.6	**-6.8**	3.0	-22.4	-25.3	-20.8	-20.4	**-17.2**
	0–5 mm + PVC (NIR)	c	1572	1248	1045	1142	1545	**1311**	68	50	47	49	72	**57**
		Δc [%]	-0.4	-12.1	-14.6	-7.9	-12.9	**-9.6**	-7.3	-21.5	-19.4	-13.5	-21.0	**-16.5**
	0–10 mm + PVC (NIR)	c	1596	1277	1021	1137	1532	**1313**	68	50	45	48	70	**56**
		Δc [%]	1.1	-10.0	-16.6	-8.3	-13.6	**-9.5**	-6.6	-22.5	-22.1	-14.4	-23.0	**-17.7**
	0–20 mm + PVC (NIR)	c	1706	1322	1020	1151	1539	**1348**	72	51	45	48	69	**57**
		Δc [%]	8.1	-6.8	-16.7	-7.2	-13.2	**-7.2**	-1.7	-21.2	-22.7	-14.0	-24.2	**-16.8**
	0–5 mm + PET (NIR) + PVC (NIR)	c	1637	1241	1011	985	1562	**1287**	71	49	45	42	73	**56**
		Δc [%]	3.7	-12.5	-17.3	-20.6	-12.0	**-11.7**	-3.0	-23.3	-23.2	-25.9	-19.7	**-19.0**
	0–10 mm + PET (NIR) + PVC (NIR)	c	1669	1273	981	973	1548	**1289**	72	48	43	41	71	**55**
		Δc [%]	5.7	-10.3	-19.8	-21.6	-12.8	**-11.7**	-2.0	-24.6	-26.4	-27.3	-22.0	**-20.5**
	0–20 mm + PET (NIR) + PVC (NIR)	c	1814	1324	978	976	1558	**1330**	77	49	42	41	70	**56**
		Δc [%]	14.9	-6.7	-20.1	-21.3	-12.2	**-9.1**	4.7	-23.3	-27.3	-27.7	-23.3	**-19.4**
	0–5 mm + b&g	c	1676	1190	1143	1121	1453	**1317**	73	48	51	49	70	**58**
		Δc [%]	6.2	-16.2	-6.6	-9.7	-18.1	**-8.9**	0.2	-25.4	-12.0	-13.9	-23.6	**-14.9**
	0–10 mm + b&g	c	1710	1215	1118	1115	1435	**1318**	74	47	49	48	68	**57**
		Δc [%]	8.3	-14.4	-8.7	-10.1	-19.1	**-8.8**	1.4	-27.0	-15.1	-14.9	-25.8	**-16.3**
	0–20 mm + b&g	c	1864	1259	1123	1128	1435	**1362**	80	48	49	48	66	**58**
		Δc [%]	18.1	-11.3	-8.2	-9.1	-19.1	**-5.9**	8.8	-25.8	-15.4	-14.6	-27.3	**-14.9**
	0–5 mm + b&g + PVC (NIR)	c	1689	1181	1122	1045	1380	**1283**	74	47	50	45	67	**57**
		Δc [%]	7.0	-16.8	-8.3	-15.8	-22.2	**-11.2**	1.4	-26.2	-13.7	-20.1	-26.7	**-17.1**
	0–10 mm + b&g + PVC (NIR)	c	1727	1205	1095	1035	1356	**1284**	75	46	48	44	65	**56**
		Δc [%]	9.5	-15.1	-10.5	-16.5	-23.6	**-11.3**	2.8	-27.9	-16.9	-21.3	-29.3	**-18.5**
	0–20 mm + b&g + PVC (NIR)	c	1903	1251	1099	1043	1348	**1329**	82	47	48	44	63	**57**
		Δc [%]	20.6	-11.9	-10.2	-15.9	-24.0	**-8.3**	11.4	-26.9	-17.3	-21.4	-31.2	**-17.1**
	0–5 mm + b&g + PET (NIR)	c	1769	1175	1119	943	1455	**1292**	78	46	49	41	71	**57**
		Δc [%]	12.1	-17.3	-8.5	-24.0	-18.0	**-11.1**	6.6	-27.8	-15.6	-27.9	-22.6	**-17.5**
	0–10 mm + b&g + PET (NIR)	c	1816	1201	1087	928	1434	**1293**	79	45	47	40	68	**56**
		Δc [%]	15.1	-15.4	-11.1	-25.2	-19.2	**-11.2**	8.4	-29.8	-19.3	-29.6	-25.3	**-19.1**
	0–20 mm + b&g + PET (NIR)	c	2031	1251	1091	928	1433	**1347**	87	46	47	39	67	**57**
		Δc [%]	28.7	-11.9	-10.8	-25.2	-19.2	**-7.7**	19.1	-28.9	-19.9	-30.3	-27.0	**-17.4**
	0–5 mm + b&g + PET (NIR) + PVC (NIR)	c	1795	1164	1093	842	1367	**1252**	80	46	48	36	67	**55**
		Δc [%]	13.7	-18.0	-10.6	-32.1	-22.9	**-14.0**	8.7	-28.8	-17.6	-35.9	-26.3	**-20.0**
	0–10 mm + b&g + PET (NIR) + PVC (NIR)	c	1849	1189	1059	822	1338	**1251**	81	44	46	35	64	**54**
		Δc [%]	17.1	-16.2	-13.5	-33.8	-24.6	**-14.2**	10.9	-31.0	-21.5	-38.0	-29.5	**-21.8**
	0–20 mm + b&g + PET (NIR) + PVC (NIR)	c	2104	1240	1061	812	1326	**1308**	91	45	45	34	62	**55**
		Δc [%]	33.3	-12.6	-13.3	-34.6	-25.3	**-10.5**	23.8	-30.2	-22.3	-39.4	-31.8	**-20.0**

More targeted removal	PVC (FTIR) + b&g PVC	c	1564	1424	1214	1158	1732	**1418**	73	64	58	52	89	**67**
		Δc [%]	-0.9	0.3	-0.8	-6.6	-2.4	**-2.1**	-0.9	0.2	-0.7	-6.9	-2.5	**-2.2**
	0–5 mm + PVC (FTIR) + b&g PVC	c	1552	1257	1052	1110	1544	**1303**	67	51	47	47	72	**57**
		Δc [%]	-1.7	-11.4	-14.0	-10.5	-13.0	**-10.1**	-8.7	-20.9	-18.8	-16.0	-21.6	**-17.2**
	0–10 mm + PVC (FTIR) + b&g PVC	c	1573	1287	1028	1104	1532	**1305**	67	50	46	47	70	**56**
		Δc [%]	-0.3	-9.4	-16.0	-11.0	-13.6	**-10.1**	-8.1	-21.9	-21.5	-17.0	-23.4	**-18.4**
	0–20 mm + PVC (FTIR) + b&g PVC	c	1673	1332	1027	1115	1539	**1337**	71	51	45	47	69	**57**
		Δc [%]	6.0	-6.1	-16.1	-10.1	-13.3	**-7.9**	-3.7	-20.5	-22.1	-16.8	-24.5	**-17.5**
	PVC (NIR) + b&g PVC	c	1568	1418	1207	1168	1744	**1421**	73	64	58	53	91	**68**
		Δc [%]	-0.7	-0.1	-1.4	-5.9	-1.7	**-1.9**	0.0	-0.1	-1.2	-6.0	-0.4	**-1.5**
	0–5 mm + PVC (NIR) + b&g PVC	c	1555	1248	1042	1119	1544	**1302**	67	50	47	48	72	**57**
		Δc [%]	-1.4	-12.1	-14.8	-9.8	-13.0	**-10.2**	-8.2	-21.5	-19.6	-15.3	-21.1	**-17.1**
	0–10 mm + PVC (NIR) + b&g PVC	c	1578	1277	1018	1114	1531	**1304**	68	50	45	47	70	**56**
		Δc [%]	0.0	-10.0	-16.8	-10.2	-13.7	**-10.2**	-7.6	-22.6	-22.3	-16.2	-23.1	**-18.4**
	0–20 mm + PVC (NIR) + b&g PVC	c	1686	1322	1016	1126	1538	**1338**	71	51	45	47	69	**57**
		Δc [%]	6.8	-6.9	-16.9	-9.2	-13.3	**-7.9**	-2.8	-21.2	-22.9	-16.0	-24.3	**-17.4**
	PET (FTIR) + Textiles + b&g PET	c	1619	1429	1223	1253	1838	**1472**	75	64	58	57	95	**70**
		Δc [%]	2.6	0.6	-0.1	1.0	3.6	**1.5**	2.8	0.2	-0.1	0.8	4.4	**1.6**
	0–5 mm + PET (FTIR) + Textiles + b&g PET	c	1616	1257	1052	1214	1652	**1358**	69	50	47	52	77	**59**
		Δc [%]	2.4	-11.4	-14.0	-2.1	-6.9	**-6.4**	-5.3	-21.5	-19.3	-8.2	-16.1	**-14.1**
	0–10 mm + PET (FTIR) + Textiles + b&g PET	c	1643	1288	1026	1212	1643	**1362**	70	50	45	51	75	**58**
		Δc [%]	4.1	-9.3	-16.1	-2.3	-7.4	**-6.2**	-4.5	-22.5	-22.1	-9.0	-18.0	**-15.2**
	0–20 mm + PET (FTIR) + Textiles + b&g PET	c	1765	1336	1025	1231	1659	**1403**	74	51	45	52	74	**59**
		Δc [%]	11.9	-5.9	-16.2	-0.8	-6.5	**-3.5**	0.8	-21.1	-22.8	-8.4	-18.9	**-14.1**
	b&g Other	c	1725	1443	1353	1213	1804	**1508**	79	65	64	55	93	**71**
		Δc [%]	9.3	1.7	10.6	-2.2	1.7	**4.2**	8.3	1.0	9.5	-2.9	1.6	**3.5**
	0–5 mm + b&g Other	c	1741	1263	1178	1168	1617	**1393**	74	50	52	49	74	**60**
		Δc [%]	10.3	-11.0	-3.7	-5.8	-8.9	**-3.8**	0.5	-21.9	-11.0	-12.3	-18.5	**-12.6**
	0–10 mm + b&g Other	c	1776	1297	1155	1165	1607	**1400**	74	49	50	49	73	**59**
		Δc [%]	12.5	-8.6	-5.6	-6.1	-9.4	**-3.5**	1.5	-23.0	-13.9	-13.2	-20.3	**-13.8**
	0–20 mm + b&g Other	c	1930	1350	1162	1181	1620	**1448**	79	50	50	49	72	**60**
		Δc [%]	22.3	-4.9	-5.0	-4.8	-8.7	**-0.2**	8.0	-21.6	-14.1	-12.8	-21.3	**-12.4**
	PVC (FTIR) + b&g PVC + b&g Other	c	1711	1448	1343	1123	1759	**1477**	79	65	63	50	90	**70**
		Δc [%]	8.4	2.0	9.8	-9.5	-0.9	**2.0**	7.5	1.2	8.8	-10.5	-1.1	**1.2**
	0–5 mm + PVC (FTIR) + b&g PVC + b&g Other	c	1724	1267	1165	1065	1562	**1356**	73	50	51	45	72	**58**
		Δc [%]	9.2	-10.8	-4.8	-14.2	-12.0	**-6.5**	-0.6	-21.9	-12.0	-20.6	-21.4	**-15.3**
	0–10 mm + PVC (FTIR) + b&g PVC + b&g Other	c	1759	1302	1140	1057	1549	**1361**	74	49	50	44	70	**57**
		Δc [%]	11.4	-8.3	-6.8	-14.8	-12.7	**-6.2**	0.5	-23.1	-14.9	-21.8	-23.3	**-16.5**
	0–20 mm + PVC (FTIR) + b&g PVC + b&g Other	c	1911	1357	1147	1066	1558	**1408**	78	50	49	44	69	**58**
		Δc [%]	21.1	-4.4	-6.3	-14.1	-12.2	**-3.2**	6.9	-21.7	-15.2	-21.9	-24.5	**-15.3**
	PVC (NIR) + b&g PVC + b&g Other	c	1724	1442	1337	1132	1774	**1482**	80	65	63	51	93	**70**
		Δc [%]	9.2	1.6	9.2	-8.7	0.0	**2.3**	9.0	0.9	8.4	-9.6	1.3	**2.0**
	0–5 mm + PVC (NIR) + b&g PVC + b&g Other	c	1740	1257	1155	1073	1563	**1358**	74	50	51	45	72	**58**
		Δc [%]	10.3	-11.5	-5.6	-13.5	-11.9	**-6.4**	0.5	-22.6	-12.8	-19.9	-20.8	**-15.1**
	0–10 mm + PVC (NIR) + b&g PVC + b&g Other	c	1779	1291	1130	1065	1549	**1363**	75	49	49	44	70	**57**
		Δc [%]	12.7	-9.1	-7.6	-14.1	-12.7	**-6.2**	1.7	-23.9	-15.8	-21.1	-23.0	**-16.4**
	0–20 mm + PVC (NIR) + b&g PVC + b&g Other	c	1950	1345	1136	1075	1559	**1413**	80	50	49	44	69	**58**
		Δc [%]	23.5	-5.2	-7.2	-13.3	-12.2	**-2.9**	8.9	-22.5	-16.1	-21.2	-24.2	**-15.0**
	b&g Other + b&g PVC	c	1711	1443	1350	1192	1803	**1500**	79	65	64	54	93	**71**
		Δc [%]	8.4	1.6	10.4	-3.9	1.6	**3.6**	7.5	1.0	9.4	-4.6	1.5	**2.9**
	0–5 mm + b&g Other + b&g PVC	c	1724	1263	1175	1145	1615	**1384**	73	50	52	48	74	**60**
		Δc [%]	9.2	-11.0	-4.0	-7.7	-9.0	**-4.5**	-0.5	-21.9	-11.3	-14.2	-18.5	**-13.3**
	0–10 mm + b&g Other + b&g PVC	c	1758	1297	1151	1140	1606	**1391**	74	49	50	48	73	**59**
		Δc [%]	11.4	-8.6	-5.9	-8.1	-9.5	**-4.1**	0.5	-23.1	-14.1	-15.1	-20.4	**-14.4**
	0–20 mm + b&g Other + b&g PVC	c	1910	1350	1158	1155	1618	**1438**	78	50	50	48	72	**60**
		Δc [%]	21.0	-4.9	-5.3	-6.9	-8.8	**-1.0**	6.9	-21.6	-14.4	-14.8	-21.4	**-13.1**

B.29. V

Table B.29: Relative concentration change (Δc, in %) of V caused by the removal of different material or particle size fractions referring to mg/kg and mg/MJ, both calculated for dry mass without hard impurities

	Removed fractions	Conc. after removal	mg/kg$_{DM}$ S01	S02	S03	S04	S05	Avr	mg/MJ S01	S02	S03	S04	S05	Avr
Single process steps	0–5 mm	c	3.7	4.3	2.5	4.7	6.9	**4.4**	0.16	0.17	0.11	0.20	0.32	**0.19**
		Δc [%]	-42.6	-11.0	-30.0	-12.6	-28.4	**-24.9**	-46.7	-20.3	-33.9	-17.6	-35.3	**-30.8**
	0–10 mm	c	3.6	4.2	2.2	4.6	6.5	**4.2**	0.15	0.16	0.10	0.20	0.30	**0.18**
		Δc [%]	-44.1	-13.0	-37.4	-13.7	-31.9	**-28.0**	-48.5	-24.8	-41.5	-19.1	-39.5	**-34.7**
	0–20 mm	c	3.3	4.3	1.9	4.7	6.3	**4.1**	0.14	0.16	0.08	0.20	0.28	**0.17**
		Δc [%]	-49.3	-11.5	-46.6	-13.1	-34.4	**-31.0**	-53.9	-24.7	-50.4	-19.1	-42.8	**-38.2**
	PET (NIR)	c	6.9	4.9	3.6	5.5	9.8	**6.1**	0.33	0.22	0.17	0.25	0.51	**0.30**
		Δc [%]	7.5	2.5	-0.1	3.0	1.9	**2.9**	8.8	1.9	-0.8	3.2	3.8	**3.4**
	PVC (NIR)	c	6.5	4.8	3.5	5.5	9.0	**5.9**	0.30	0.22	0.17	0.25	0.47	**0.28**
		Δc [%]	0.3	0.2	-0.9	3.0	-5.8	**-0.6**	1.0	0.2	-0.8	2.9	-4.6	**-0.3**
	b&g	c	7.2	4.0	3.2	4.5	9.6	**5.7**	0.35	0.18	0.15	0.21	0.51	**0.28**
		Δc [%]	12.3	-17.9	-9.7	-15.4	-0.3	**-6.2**	15.6	-17.1	-8.8	-13.9	4.3	**-4.0**
	PET + PVC (NIR)	c	7.0	5.0	3.5	5.7	9.2	**6.1**	0.33	0.22	0.17	0.26	0.49	**0.29**
		Δc [%]	8.3	2.7	-1.2	6.5	-4.5	**2.4**	10.5	2.1	-1.7	6.6	-1.1	**3.3**
Combinations of Screening and state-of-the-art NIR sorting or manual removal of black materials	0–5 mm + PET (NIR)	c	3.9	4.4	2.3	4.8	6.7	**4.4**	0.17	0.17	0.10	0.20	0.31	**0.19**
		Δc [%]	-39.3	-9.1	-34.5	-10.9	-30.3	**-24.8**	-43.4	-19.9	-39.1	-16.4	-36.8	**-31.1**
	0–10 mm + PET (NIR)	c	3.8	4.3	2.0	4.7	6.3	**4.2**	0.16	0.16	0.09	0.20	0.29	**0.18**
		Δc [%]	-40.8	-11.0	-43.2	-12.1	-34.5	**-28.3**	-45.3	-24.8	-47.9	-18.1	-41.7	**-35.5**
	0–20 mm + PET (NIR)	c	3.5	4.4	1.6	4.8	6.0	**4.0**	0.15	0.16	0.07	0.20	0.27	**0.17**
		Δc [%]	-46.3	-9.1	-54.2	-11.3	-37.6	**-31.7**	-51.1	-24.7	-58.3	-18.0	-45.7	**-39.6**
	0–5 mm + PVC (NIR)	c	3.5	4.3	2.4	4.8	6.0	**4.2**	0.15	0.17	0.11	0.21	0.28	**0.18**
		Δc [%]	-45.1	-11.1	-31.6	-9.9	-37.8	**-27.1**	-48.9	-20.6	-35.5	-15.3	-43.6	**-32.8**
	0–10 mm + PVC (NIR)	c	3.4	4.2	2.2	4.8	5.6	**4.0**	0.15	0.16	0.10	0.20	0.25	**0.17**
		Δc [%]	-46.9	-13.1	-39.3	-10.9	-42.1	**-30.5**	-51.0	-25.2	-43.3	-16.8	-48.3	**-36.9**
	0–20 mm + PVC (NIR)	c	3.0	4.3	1.8	4.8	5.2	**3.8**	0.13	0.16	0.08	0.20	0.23	**0.16**
		Δc [%]	-53.1	-11.6	-48.7	-10.1	-45.6	**-33.8**	-57.3	-25.1	-52.4	-16.7	-52.5	**-40.8**
	0–5 mm + PET (NIR) + PVC (NIR)	c	3.7	4.4	2.3	4.9	5.6	**4.2**	0.16	0.17	0.10	0.21	0.26	**0.18**
		Δc [%]	-41.9	-9.1	-36.4	-7.7	-41.5	**-27.3**	-45.7	-20.2	-41.0	-13.8	-46.6	**-33.5**
	0–10 mm + PET (NIR) + PVC (NIR)	c	3.6	4.3	1.9	4.9	5.1	**4.0**	0.16	0.16	0.08	0.21	0.24	**0.17**
		Δc [%]	-43.8	-11.1	-45.5	-8.8	-46.7	**-31.2**	-47.9	-25.2	-50.0	-15.4	-52.4	**-38.2**
	0–20 mm + PET (NIR) + PVC (NIR)	c	3.2	4.4	1.5	4.9	4.7	**3.7**	0.14	0.16	0.07	0.21	0.21	**0.16**
		Δc [%]	-50.4	-9.1	-56.9	-7.7	-51.4	**-35.1**	-54.8	-25.2	-60.8	-15.3	-57.6	**-42.7**
	0–5 mm + b&g	c	4.0	3.1	1.9	3.6	6.4	**3.8**	0.18	0.13	0.08	0.16	0.31	**0.17**
		Δc [%]	-37.5	-35.3	-47.7	-32.0	-32.8	**-37.1**	-41.0	-42.4	-50.8	-35.2	-37.3	**-41.3**
	0–10 mm + b&g	c	3.9	2.8	1.5	3.5	6.0	**3.6**	0.17	0.11	0.07	0.15	0.29	**0.16**
		Δc [%]	-39.1	-41.0	-57.7	-34.1	-37.0	**-41.8**	-43.0	-49.7	-60.7	-37.6	-42.2	**-46.6**
	0–20 mm + b&g	c	3.6	2.8	1.0	3.5	5.7	**3.3**	0.15	0.10	0.05	0.15	0.26	**0.14**
		Δc [%]	-44.8	-42.7	-70.6	-34.8	-40.4	**-46.6**	-49.1	-52.1	-72.9	-38.8	-46.4	**-51.9**
	0–5 mm + b&g + PVC (NIR)	c	3.8	3.1	1.8	3.7	5.4	**3.6**	0.17	0.12	0.08	0.16	0.26	**0.16**
		Δc [%]	-40.3	-36.1	-50.2	-30.0	-44.1	**-40.1**	-43.4	-43.3	-53.1	-33.6	-47.4	**-44.2**
	0–10 mm + b&g + PVC (NIR)	c	3.7	2.8	1.4	3.6	4.8	**3.3**	0.16	0.11	0.06	0.16	0.23	**0.14**
		Δc [%]	-42.1	-42.2	-60.6	-32.1	-49.5	**-45.3**	-45.7	-50.9	-63.4	-36.0	-53.3	**-49.8**
	0–20 mm + b&g + PVC (NIR)	c	3.3	2.7	0.9	3.6	4.4	**3.0**	0.14	0.10	0.04	0.15	0.20	**0.13**
		Δc [%]	-49.2	-44.1	-74.0	-32.7	-54.4	**-50.9**	-53.1	-53.6	-76.0	-37.2	-58.7	**-55.7**
	0–5 mm + b&g + PET (NIR)	c	4.3	3.1	1.5	3.6	6.2	**3.7**	0.19	0.12	0.07	0.15	0.30	**0.17**
		Δc [%]	-32.6	-36.0	-56.7	-33.0	-35.8	**-38.8**	-35.9	-44.2	-60.0	-36.5	-39.4	**-43.2**
	0–10 mm + b&g + PET (NIR)	c	4.2	2.8	1.1	3.5	5.7	**3.4**	0.19	0.10	0.05	0.15	0.27	**0.15**
		Δc [%]	-34.0	-42.6	-69.1	-35.4	-41.0	**-44.4**	-37.8	-52.4	-71.9	-39.2	-45.5	**-49.4**
	0–20 mm + b&g + PET (NIR)	c	3.9	2.7	0.5	3.4	5.2	**3.1**	0.17	0.10	0.02	0.14	0.24	**0.13**
		Δc [%]	-39.7	-44.9	-85.6	-36.4	-45.4	**-50.4**	-44.2	-55.5	-87.0	-40.7	-50.7	**-55.6**
	0–5 mm + b&g + PET (NIR) + PVC (NIR)	c	4.2	3.0	1.4	3.7	4.8	**3.4**	0.18	0.12	0.06	0.16	0.24	**0.15**
		Δc [%]	-35.3	-36.9	-59.9	-30.7	-49.8	**-42.5**	-38.1	-45.3	-63.0	-34.6	-52.0	**-46.6**
	0–10 mm + b&g + PET (NIR) + PVC (NIR)	c	4.0	2.7	1.0	3.6	4.2	**3.1**	0.18	0.10	0.04	0.15	0.20	**0.13**
		Δc [%]	-37.1	-44.0	-72.9	-33.2	-56.6	**-48.8**	-40.5	-53.9	-75.4	-37.5	-59.4	**-53.3**
	0–20 mm + b&g + PET (NIR) + PVC (NIR)	c	3.6	2.6	0.3	3.5	3.5	**2.7**	0.15	0.09	0.01	0.15	0.16	**0.12**
		Δc [%]	-44.5	-46.6	-90.2	-34.1	-63.4	**-55.8**	-48.4	-57.3	-91.2	-39.0	-66.7	**-60.5**

More targeted removal	PVC (FTIR) + b&g PVC	c	6.5	4.9	3.6	5.4	9.6	**6.0**	0.30	0.22	0.17	0.25	0.49	**0.29**
		Δc [%]	0.6	1.0	0.03	1.0	0.3	**0.6**	0.6	0.8	0.2	0.7	0.3	**0.5**
	0–5 mm + PVC (FTIR) + b&g PVC	c	3.7	4.3	2.5	4.7	6.9	**4.4**	0.16	0.18	0.11	0.20	0.32	**0.19**
		Δc [%]	-42.3	-10.0	-30.2	-11.8	-28.3	**-24.5**	-46.4	-19.6	-34.1	-17.3	-35.4	**-30.6**
	0–10 mm + PVC (FTIR) + b&g PVC	c	3.6	4.2	2.2	4.7	6.5	**4.3**	0.15	0.17	0.10	0.20	0.30	**0.18**
		Δc [%]	-43.8	-11.9	-37.8	-12.9	-31.8	**-27.6**	-48.2	-24.1	-41.8	-18.8	-39.5	**-34.5**
	0–20 mm + PVC (FTIR) + b&g PVC	c	3.3	4.3	1.9	4.7	6.3	**4.1**	0.14	0.17	0.08	0.20	0.28	**0.17**
		Δc [%]	-49.1	-10.2	-47.1	-12.3	-34.4	**-30.6**	-53.8	-24.0	-50.8	-18.8	-42.9	**-38.0**
	PVC (NIR) + b&g PVC	c	6.5	4.8	3.5	5.5	9.0	**5.9**	0.30	0.22	0.17	0.25	0.47	**0.28**
		Δc [%]	0.6	0.3	-0.8	2.8	-5.8	**-0.6**	1.3	0.3	-0.7	2.7	-4.5	**-0.2**
	0–5 mm + PVC (NIR) + b&g PVC	c	3.5	4.3	2.4	4.8	6.0	**4.2**	0.15	0.17	0.11	0.21	0.28	**0.18**
		Δc [%]	-45.1	-11.0	-31.6	-10.2	-37.8	**-27.1**	-48.9	-20.5	-35.4	-15.7	-43.5	**-32.8**
	0–10 mm + PVC (NIR) + b&g PVC	c	3.4	4.2	2.2	4.8	5.6	**4.0**	0.15	0.16	0.10	0.20	0.25	**0.17**
		Δc [%]	-46.8	-13.0	-39.2	-11.3	-42.1	**-30.5**	-50.9	-25.1	-43.2	-17.2	-48.3	**-37.0**
	0–20 mm + PVC (NIR) + b&g PVC	c	3.0	4.3	1.8	4.8	5.2	**3.8**	0.13	0.16	0.08	0.20	0.23	**0.16**
		Δc [%]	-53.0	-11.4	-48.7	-10.5	-45.6	**-33.9**	-57.3	-25.1	-52.4	-17.2	-52.5	**-40.9**
	PET (FTIR) + Textiles + b&g PET	c	6.8	4.9	3.6	5.4	9.7	**6.1**	0.32	0.22	0.17	0.24	0.50	**0.29**
		Δc [%]	5.7	0.8	0.4	0.4	1.3	**1.7**	5.9	0.3	0.3	0.3	2.1	**1.8**
	0–5 mm + PET (FTIR) + Textiles + b&g PET	c	3.9	4.3	2.4	4.7	6.7	**4.4**	0.17	0.17	0.11	0.20	0.31	**0.19**
		Δc [%]	-40.0	-10.6	-31.7	-13.1	-29.6	**-25.0**	-44.5	-20.7	-35.9	-18.5	-36.6	**-31.3**
	0–10 mm + PET (FTIR) + Textiles + b&g PET	c	3.8	4.2	2.1	4.6	6.4	**4.2**	0.16	0.16	0.09	0.19	0.29	**0.18**
		Δc [%]	-41.6	-12.6	-39.7	-14.3	-33.6	**-28.4**	-46.4	-25.4	-44.1	-20.2	-41.2	**-35.5**
	0–20 mm + PET (FTIR) + Textiles + b&g PET	c	3.4	4.3	1.8	4.6	6.1	**4.0**	0.14	0.16	0.08	0.19	0.27	**0.17**
		Δc [%]	-47.0	-11.0	-49.8	-13.7	-36.5	**-31.6**	-52.2	-25.4	-53.7	-20.3	-45.0	**-39.3**
	b&g Other	c	7.1	3.9	3.3	4.6	9.4	**5.6**	0.33	0.18	0.15	0.21	0.48	**0.27**
		Δc [%]	9.8	-18.6	-8.2	-13.9	-2.3	**-6.7**	8.8	-19.2	-9.1	-14.6	-2.4	**-7.3**
	0–5 mm + b&g Other	c	4.0	3.1	2.0	3.8	6.4	**3.9**	0.17	0.12	0.09	0.16	0.29	**0.17**
		Δc [%]	-37.1	-35.6	-44.8	-29.6	-33.2	**-36.1**	-42.7	-43.5	-49.0	-34.5	-40.3	**-42.0**
	0–10 mm + b&g Other	c	4.0	2.8	1.6	3.7	6.0	**3.6**	0.17	0.11	0.07	0.15	0.27	**0.15**
		Δc [%]	-38.5	-41.2	-54.3	-31.5	-37.3	**-40.6**	-44.5	-50.5	-58.3	-36.7	-44.8	**-47.0**
	0–20 mm + b&g Other	c	3.6	2.8	1.2	3.6	5.7	**3.4**	0.15	0.10	0.05	0.15	0.25	**0.14**
		Δc [%]	-43.6	-42.9	-66.5	-32.0	-40.4	**-45.1**	-50.2	-52.9	-69.7	-37.7	-48.7	**-51.8**
	PVC (FTIR) + b&g PVC + b&g Other	c	7.1	4.0	3.3	4.7	9.4	**5.7**	0.33	0.18	0.15	0.21	0.48	**0.27**
		Δc [%]	10.5	-17.8	-8.3	-13.2	-2.0	**-6.2**	9.6	-18.5	-9.1	-14.2	-2.2	**-6.9**
	0–5 mm + PVC (FTIR) + b&g PVC + b&g Other	c	4.1	3.1	2.0	3.8	6.4	**3.9**	0.17	0.12	0.09	0.16	0.29	**0.17**
		Δc [%]	-36.7	-34.9	-45.3	-29.3	-33.2	**-35.9**	-42.4	-43.1	-49.4	-34.6	-40.3	**-42.0**
	0–10 mm + PVC (FTIR) + b&g PVC + b&g Other	c	4.0	2.9	1.6	3.7	6.0	**3.6**	0.17	0.11	0.07	0.15	0.27	**0.15**
		Δc [%]	-38.2	-40.5	-54.9	-31.2	-37.3	**-40.4**	-44.2	-50.2	-58.9	-36.8	-44.9	**-47.0**
	0–20 mm + PVC (FTIR) + b&g PVC + b&g Other	c	3.7	2.8	1.2	3.7	5.7	**3.4**	0.15	0.10	0.05	0.15	0.25	**0.14**
		Δc [%]	-43.3	-42.1	-67.3	-31.7	-40.4	**-45.0**	-49.9	-52.6	-70.4	-37.9	-48.8	**-51.9**
	PVC (NIR) + b&g PVC + b&g Other	c	7.2	3.9	3.2	4.7	8.7	**5.6**	0.33	0.18	0.15	0.21	0.46	**0.27**
		Δc [%]	11.1	-18.8	-9.4	-11.7	-8.7	**-7.5**	10.9	-19.4	-10.1	-12.5	-7.5	**-7.7**
	0–5 mm + PVC (NIR) + b&g PVC + b&g Other	c	3.9	3.1	1.9	3.9	5.4	**3.6**	0.16	0.12	0.08	0.16	0.25	**0.16**
		Δc [%]	-39.5	-36.4	-47.1	-28.1	-43.9	**-39.0**	-44.9	-44.4	-51.1	-33.4	-49.6	**-44.7**
	0–10 mm + PVC (NIR) + b&g PVC + b&g Other	c	3.8	2.8	1.5	3.8	4.9	**3.3**	0.16	0.11	0.07	0.16	0.22	**0.14**
		Δc [%]	-41.2	-42.3	-57.0	-30.0	-48.9	**-43.9**	-47.0	-51.7	-60.8	-35.7	-54.9	**-50.0**
	0–20 mm + PVC (NIR) + b&g PVC + b&g Other	c	3.4	2.7	1.1	3.7	4.5	**3.1**	0.14	0.10	0.05	0.15	0.20	**0.13**
		Δc [%]	-47.4	-44.1	-69.7	-30.5	-53.4	**-49.0**	-53.7	-54.3	-72.6	-36.8	-59.8	**-55.4**
	b&g Other + b&g PVC	c	7.1	3.9	3.3	4.6	9.4	**5.6**	0.33	0.18	0.15	0.21	0.48	**0.27**
		Δc [%]	10.0	-18.6	-8.1	-14.3	-2.3	**-6.6**	9.1	-19.1	-9.0	-14.9	-2.4	**-7.3**
	0–5 mm + b&g Other + b&g PVC	c	4.1	3.1	2.0	3.7	6.4	**3.9**	0.17	0.12	0.09	0.16	0.29	**0.17**
		Δc [%]	-37.0	-35.6	-44.7	-30.1	-33.2	**-36.1**	-42.6	-43.5	-48.9	-35.0	-40.3	**-42.0**
	0–10 mm + b&g Other + b&g PVC	c	4.0	2.8	1.6	3.6	6.0	**3.6**	0.17	0.11	0.07	0.15	0.27	**0.15**
		Δc [%]	-38.4	-41.1	-54.3	-32.0	-37.3	**-40.6**	-44.4	-50.5	-58.3	-37.2	-44.8	**-47.0**
	0–20 mm + b&g Other + b&g PVC	c	3.6	2.8	1.2	3.6	5.7	**3.4**	0.15	0.10	0.05	0.15	0.25	**0.14**
		Δc [%]	-43.5	-42.8	-66.5	-32.6	-40.4	**-45.2**	-50.1	-52.9	-69.7	-38.3	-48.6	**-51.9**

B.30. W

Table B.30: Relative concentration change (Δc, in %) of W caused by the removal of different material or particle size fractions referring to mg/kg and mg/MJ, both calculated for dry mass without hard impurities

	Removed fractions	Conc. after removal	mg/kg$_{DM}$ S01	S02	S03	S04	S05	Avr	mg/MJ S01	S02	S03	S04	S05	Avr
Single process steps	0–5 mm	c	22	79	34	14	12	**32**	0.95	3.18	1.51	0.60	0.55	**1.36**
		Δc [%]	-59.5	1.5	-12.0	-37.5	-43.4	**-30.2**	-62.3	-9.0	-16.9	-41.0	-48.9	**-35.7**
	0–10 mm	c	20	84	34	12	11	**32**	0.85	3.28	1.51	0.51	0.52	**1.33**
		Δc [%]	-63.4	8.6	-11.1	-46.9	-46.0	**-31.7**	-66.2	-6.0	-16.9	-50.2	-52.0	**-38.3**
	0–20 mm	c	18	90	35	12	6	**32**	0.75	3.45	1.56	0.52	0.27	**1.31**
		Δc [%]	-67.3	16.1	-7.6	-45.8	-71.5	**-35.2**	-70.2	-1.2	-14.3	-49.6	-75.2	**-42.1**
	PET (NIR)	c	59	83	43	25	23	**47**	2.77	3.74	2.03	1.13	1.22	**2.18**
		Δc [%]	8.9	7.6	12.3	10.4	11.5	**10.2**	10.3	7.0	11.6	10.6	13.5	**10.6**
	PVC (NIR)	c	57	78	39	23	22	**44**	2.65	3.54	1.85	1.06	1.17	**2.05**
		Δc [%]	4.9	1.3	1.7	3.8	7.2	**3.8**	5.6	1.3	1.8	3.7	8.6	**4.2**
	b&g	c	63	86	46	25	23	**49**	3.01	3.94	2.20	1.15	1.25	**2.31**
		Δc [%]	16.6	11.7	19.7	10.7	11.4	**14.0**	20.0	12.7	21.0	12.6	16.5	**16.6**
	PET + PVC (NIR)	c	62	84	44	26	25	**48**	2.95	3.79	2.07	1.18	1.34	**2.27**
		Δc [%]	15.0	9.2	14.6	15.3	20.7	**14.9**	17.3	8.5	13.9	15.4	25.0	**16.0**
Combinations of Screening and state-of-the-art NIR sorting or manual removal of black materials	0–5 mm + PET (NIR)	c	23	86	38	16	13	**35**	1.02	3.42	1.69	0.67	0.62	**1.48**
		Δc [%]	-56.6	11.1	0.0	-30.6	-36.3	**-22.5**	-59.5	-2.1	-7.1	-34.9	-42.3	**-29.2**
	0–10 mm + PET (NIR)	c	21	93	39	13	13	**36**	0.91	3.55	1.69	0.56	0.58	**1.46**
		Δc [%]	-60.9	20.3	1.5	-41.0	-39.0	**-23.8**	-63.8	1.7	-6.8	-45.0	-45.7	**-31.9**
	0–20 mm + PET (NIR)	c	19	101	41	14	7	**36**	0.80	3.77	1.76	0.57	0.30	**1.44**
		Δc [%]	-64.9	30.2	6.3	-39.4	-68.3	**-27.2**	-68.1	7.8	-3.2	-44.0	-72.4	**-36.0**
	0–5 mm + PVC (NIR)	c	23	80	34	15	13	**33**	0.98	3.22	1.54	0.62	0.60	**1.39**
		Δc [%]	-57.9	3.2	-10.3	-35.1	-39.0	**-27.8**	-60.8	-7.8	-15.4	-39.0	-44.6	**-33.5**
	0–10 mm + PVC (NIR)	c	21	86	35	12	12	**33**	0.88	3.33	1.54	0.53	0.56	**1.37**
		Δc [%]	-62.0	10.7	-9.3	-44.9	-41.6	**-29.4**	-64.9	-4.7	-15.4	-48.5	-47.9	**-36.3**
	0–20 mm + PVC (NIR)	c	18	92	36	13	6	**33**	0.78	3.51	1.59	0.53	0.29	**1.34**
		Δc [%]	-66.0	18.6	-5.7	-43.7	-69.5	**-33.2**	-69.0	0.4	-12.5	-47.8	-73.3	**-40.5**
	0–5 mm + PET (NIR) + PVC (NIR)	c	25	88	39	16	15	**36**	1.07	3.47	1.72	0.69	0.68	**1.53**
		Δc [%]	-54.6	13.2	2.1	-27.5	-30.4	**-19.4**	-57.5	-0.6	-5.1	-32.3	-36.5	**-26.4**
	0–10 mm + PET (NIR) + PVC (NIR)	c	22	95	40	14	14	**37**	0.95	3.61	1.73	0.59	0.64	**1.51**
		Δc [%]	-59.1	23.1	3.8	-38.3	-33.1	**-20.7**	-62.1	3.5	-4.8	-42.8	-40.2	**-29.3**
	0–20 mm + PET (NIR) + PVC (NIR)	c	20	103	42	14	7	**37**	0.84	3.84	1.80	0.60	0.32	**1.48**
		Δc [%]	-63.2	33.6	8.8	-36.5	-65.4	**-24.5**	-66.5	9.9	-1.0	-41.7	-69.8	**-33.8**
	0–5 mm + b&g	c	25	90	41	16	13	**37**	1.11	3.62	1.84	0.67	0.64	**1.58**
		Δc [%]	-53.0	16.5	7.3	-30.9	-36.1	**-19.2**	-55.7	3.7	1.0	-34.1	-40.4	**-25.1**
	0–10 mm + b&g	c	23	98	42	13	13	**38**	1.00	3.79	1.85	0.57	0.60	**1.56**
		Δc [%]	-57.4	27.0	9.3	-41.4	-38.8	**-20.3**	-60.2	8.4	1.6	-44.5	-43.8	**-27.7**
	0–20 mm + b&g	c	21	107	44	14	7	**38**	0.90	4.04	1.93	0.58	0.31	**1.55**
		Δc [%]	-61.3	38.3	15.0	-39.8	-67.8	**-23.1**	-64.3	15.6	6.0	-43.5	-71.1	**-31.5**
	0–5 mm + b&g + PVC (NIR)	c	27	92	42	16	15	**38**	1.18	3.68	1.88	0.70	0.71	**1.63**
		Δc [%]	-50.5	18.9	9.8	-27.7	-30.2	**-15.9**	-53.1	5.4	3.4	-31.4	-34.3	**-22.0**
	0–10 mm + b&g + PVC (NIR)	c	24	101	43	14	14	**39**	1.06	3.86	1.89	0.59	0.67	**1.61**
		Δc [%]	-55.1	30.1	11.9	-38.8	-32.9	**-17.0**	-57.9	10.4	4.0	-42.3	-37.9	**-24.7**
	0–20 mm + b&g + PVC (NIR)	c	22	110	45	14	7	**40**	0.95	4.12	1.98	0.60	0.34	**1.60**
		Δc [%]	-58.9	42.2	18.0	-36.9	-64.9	**-20.1**	-62.0	18.1	8.7	-41.0	-68.3	**-28.9**
	0–5 mm + b&g + PET (NIR)	c	28	100	48	18	15	**42**	1.23	3.95	2.11	0.76	0.75	**1.76**
		Δc [%]	-48.4	29.6	26.0	-21.7	-26.6	**-8.2**	-50.9	13.0	16.3	-25.8	-30.8	**-15.6**
	0–10 mm + b&g + PET (NIR)	c	25	111	49	15	15	**43**	1.11	4.16	2.14	0.64	0.70	**1.75**
		Δc [%]	-53.2	43.7	29.4	-33.5	-29.2	**-8.6**	-55.9	19.2	17.5	-37.5	-34.5	**-18.2**
	0–20 mm + b&g + PET (NIR)	c	23	123	53	16	8	**44**	1.00	4.49	2.25	0.66	0.36	**1.75**
		Δc [%]	-56.8	59.3	37.9	-31.0	-63.2	**-10.8**	-60.0	28.5	23.8	-35.7	-66.7	**-22.0**
	0–5 mm + b&g + PET (NIR) + PVC (NIR)	c	30	103	49	19	17	**44**	1.32	4.03	2.17	0.80	0.84	**1.83**
		Δc [%]	-44.9	32.8	29.6	-17.4	-18.3	**-3.7**	-47.3	15.2	19.5	-22.1	-21.9	**-11.3**
	0–10 mm + b&g + PET (NIR) + PVC (NIR)	c	27	114	51	16	17	**45**	1.19	4.26	2.20	0.67	0.80	**1.82**
		Δc [%]	-50.0	48.0	33.2	-29.9	-20.8	**-3.9**	-52.7	21.8	20.9	-34.4	-25.9	**-14.1**
	0–20 mm + b&g + PET (NIR) + PVC (NIR)	c	25	128	54	16	9	**46**	1.09	4.61	2.32	0.69	0.40	**1.82**
		Δc [%]	-53.2	64.9	42.3	-26.9	-58.9	**-6.3**	-56.5	31.8	27.6	-32.3	-62.6	**-18.4**

More targeted removal	PVC (FTIR) + b&g PVC	c	54	78	38	23	21	**43**	2.53	3.53	1.84	1.04	1.08	**2.00**
		Δc [%]	0.8	1.2	0.9	2.2	0.8	**1.2**	0.8	1.1	1.0	1.8	0.7	**1.1**
	0–5 mm + PVC (FTIR) + b&g PVC	c	22	80	34	14	12	**32**	0.95	3.22	1.52	0.61	0.55	**1.37**
		Δc [%]	-59.1	3.1	-11.1	-36.2	-42.9	**-29.3**	-62.0	-8.0	-16.1	-40.1	-48.6	**-35.0**
	0–10 mm + PVC (FTIR) + b&g PVC	c	20	85	34	12	11	**33**	0.85	3.32	1.53	0.52	0.52	**1.35**
		Δc [%]	-63.1	10.5	-10.2	-45.8	-45.5	**-30.8**	-65.9	-4.8	-16.1	-49.4	-51.7	**-37.6**
	0–20 mm + PVC (FTIR) + b&g PVC	c	18	91	36	12	6	**33**	0.75	3.50	1.58	0.52	0.27	**1.32**
		Δc [%]	-67.0	18.3	-6.7	-44.6	-71.3	**-34.3**	-70.0	0.2	-13.3	-48.8	-75.0	**-41.4**
	PVC (NIR) + b&g PVC	c	57	78	39	24	22	**44**	2.66	3.54	1.86	1.07	1.17	**2.06**
		Δc [%]	5.3	1.4	1.9	4.4	7.2	**4.0**	6.0	1.4	2.1	4.3	8.7	**4.5**
	0–5 mm + PVC (NIR) + b&g PVC	c	23	80	34	15	13	**33**	0.99	3.22	1.54	0.63	0.60	**1.40**
		Δc [%]	-57.7	3.3	-10.1	-34.7	-38.9	**-27.6**	-60.6	-7.8	-15.2	-38.7	-44.6	**-33.4**
	0–10 mm + PVC (NIR) + b&g PVC	c	21	86	35	12	12	**33**	0.89	3.33	1.54	0.53	0.56	**1.37**
		Δc [%]	-61.8	10.9	-9.1	-44.6	-41.6	**-29.3**	-64.7	-4.6	-15.1	-48.3	-47.9	**-36.1**
	0–20 mm + PVC (NIR) + b&g PVC	c	18	92	36	13	6	**33**	0.78	3.51	1.59	0.54	0.29	**1.34**
		Δc [%]	-65.8	18.8	-5.5	-43.3	-69.4	**-33.1**	-68.9	0.5	-12.3	-47.6	-73.3	**-40.3**
	PET (FTIR) + Textiles + b&g PET	c	58	80	41	24	23	**45**	2.70	3.60	1.93	1.09	1.17	**2.10**
		Δc [%]	7.2	3.6	6.2	6.2	7.7	**6.2**	7.4	3.2	6.1	6.0	8.5	**6.2**
	0–5 mm + PET (FTIR) + Textiles + b&g PET	c	23	82	36	15	13	**34**	1.00	3.29	1.60	0.64	0.59	**1.43**
		Δc [%]	-56.9	6.1	-6.0	-33.4	-38.7	**-25.8**	-60.1	-5.9	-11.8	-37.5	-44.8	**-32.0**
	0–10 mm + PET (FTIR) + Textiles + b&g PET	c	21	88	36	13	12	**34**	0.90	3.41	1.61	0.54	0.56	**1.40**
		Δc [%]	-61.0	14.2	-4.9	-43.3	-41.4	**-27.3**	-64.3	-2.5	-11.7	-47.2	-48.1	**-34.8**
	0–20 mm + PET (FTIR) + Textiles + b&g PET	c	19	95	38	13	6	**34**	0.79	3.59	1.66	0.55	0.28	**1.38**
		Δc [%]	-65.0	22.7	-0.8	-42.0	-69.5	**-30.9**	-68.4	2.8	-8.5	-46.4	-73.5	**-38.8**
	b&g Other	c	60	84	44	24	22	**47**	2.76	3.78	2.09	1.09	1.14	**2.17**
		Δc [%]	11.0	8.9	16.2	7.6	6.2	**10.0**	10.0	8.2	15.1	6.8	6.1	**9.2**
	0–5 mm + b&g Other	c	24	87	40	15	13	**36**	1.03	3.46	1.74	0.64	0.58	**1.49**
		Δc [%]	-54.9	12.9	3.8	-32.6	-39.5	**-22.0**	-58.9	-0.9	-4.0	-37.2	-45.8	**-29.4**
	0–10 mm + b&g Other	c	22	95	40	13	12	**36**	0.93	3.60	1.75	0.54	0.55	**1.47**
		Δc [%]	-59.1	22.5	5.6	-42.7	-42.1	**-23.2**	-63.1	3.1	-3.7	-47.0	-49.1	**-32.0**
	0–20 mm + b&g Other	c	20	103	42	13	6	**37**	0.82	3.82	1.82	0.55	0.28	**1.46**
		Δc [%]	-62.9	32.8	10.8	-41.3	-69.5	**-26.0**	-67.2	9.4	0.2	-46.2	-73.7	**-35.5**
	PVC (FTIR) + b&g PVC + b&g Other	c	61	85	45	25	22	**48**	2.79	3.82	2.12	1.12	1.15	**2.20**
		Δc [%]	12.0	10.4	17.4	10.2	7.1	**11.4**	11.0	9.5	16.4	8.9	6.9	**10.5**
	0–5 mm + PVC (FTIR) + b&g PVC + b&g Other	c	25	89	40	16	13	**36**	1.04	3.51	1.76	0.65	0.59	**1.51**
		Δc [%]	-54.5	14.8	5.0	-30.9	-38.9	**-20.9**	-58.6	0.4	-2.9	-36.1	-45.4	**-28.5**
	0–10 mm + PVC (FTIR) + b&g PVC + b&g Other	c	22	97	41	13	12	**37**	0.93	3.65	1.77	0.55	0.55	**1.49**
		Δc [%]	-58.7	24.8	6.8	-41.3	-41.6	**-22.0**	-62.8	4.6	-2.5	-46.1	-48.7	**-31.1**
	0–20 mm + PVC (FTIR) + b&g PVC + b&g Other	c	20	105	43	14	6	**38**	0.83	3.88	1.85	0.56	0.28	**1.48**
		Δc [%]	-62.5	35.6	12.2	-39.8	-69.3	**-24.7**	-66.9	11.1	1.5	-45.2	-73.6	**-34.6**
	PVC (NIR) + b&g PVC + b&g Other	c	64	86	45	25	24	**49**	2.95	3.84	2.14	1.15	1.25	**2.26**
		Δc [%]	17.7	10.7	18.9	12.9	14.4	**14.9**	17.5	9.9	17.9	11.8	16.0	**14.6**
	0–5 mm + PVC (NIR) + b&g PVC + b&g Other	c	26	89	41	16	14	**37**	1.09	3.52	1.79	0.67	0.64	**1.54**
		Δc [%]	-52.5	15.2	6.5	-29.2	-34.3	**-18.9**	-56.7	0.7	-1.6	-34.5	-40.9	**-26.6**
	0–10 mm + PVC (NIR) + b&g PVC + b&g Other	c	23	97	41	14	13	**38**	0.98	3.67	1.80	0.57	0.60	**1.52**
		Δc [%]	-57.0	25.5	8.3	-39.9	-36.9	**-20.0**	-61.2	5.0	-1.2	-44.8	-44.3	**-29.3**
	0–20 mm + PVC (NIR) + b&g PVC + b&g Other	c	21	106	43	14	7	**38**	0.87	3.90	1.87	0.58	0.31	**1.51**
		Δc [%]	-60.7	36.6	13.9	-38.1	-67.0	**-23.1**	-65.4	11.7	3.0	-43.8	-71.6	**-33.2**
	b&g Other + b&g PVC	c	60	84	44	24	22	**47**	2.77	3.78	2.10	1.10	1.14	**2.18**
		Δc [%]	11.4	9.0	16.5	8.3	6.2	**10.3**	10.4	8.3	15.4	7.4	6.1	**9.5**
	0–5 mm + b&g Other + b&g PVC	c	24	87	40	15	13	**36**	1.04	3.47	1.75	0.65	0.58	**1.50**
		Δc [%]	-54.7	13.0	4.1	-32.1	-39.4	**-21.8**	-58.8	-0.8	-3.8	-36.9	-45.8	**-29.2**
	0–10 mm + b&g Other + b&g PVC	c	22	95	40	13	12	**37**	0.93	3.61	1.76	0.55	0.55	**1.48**
		Δc [%]	-59.0	22.6	5.8	-42.3	-42.1	**-23.0**	-63.0	3.2	-3.4	-46.7	-49.1	**-31.8**
	0–20 mm + b&g Other + b&g PVC	c	20	103	42	13	6	**37**	0.83	3.83	1.83	0.55	0.28	**1.46**
		Δc [%]	-62.7	33.0	11.1	-40.9	-69.5	**-25.8**	-67.1	9.5	0.5	-45.9	-73.7	**-35.3**

B.31. Zn

Table B.31: Relative concentration change (Δc, in %) of Zn caused by the removal of different material or particle size fractions referring to mg/kg and mg/MJ, both calculated for dry mass without hard impurities

	Removed fractions	Conc. after removal	mg/kg$_{DM}$ S01	S02	S03	S04	S05	Avr	mg/MJ S01	S02	S03	S04	S05	Avr
Single process steps	0–5 mm	c	1586	571	506	401	782	**769**	68	23	23	17	36	**34**
		Δc [%]	9.9	-45.3	-15.9	-6.7	4.7	**-10.7**	2.1	-51.0	-20.7	-12.0	-5.5	**-17.4**
	0–10 mm	c	1562	540	495	361	792	**750**	67	21	22	15	36	**32**
		Δc [%]	8.2	-48.2	-17.8	-16.2	6.0	**-13.6**	-0.3	-55.2	-23.3	-21.4	-5.8	**-21.2**
	0–20 mm	c	1603	524	463	346	768	**741**	68	20	20	15	34	**31**
		Δc [%]	11.1	-49.8	-23.2	-19.6	2.8	**-15.7**	0.9	-57.3	-28.7	-25.1	-10.3	**-24.1**
	PET (NIR)	c	1514	1091	579	442	807	**887**	71	49	27	20	42	**42**
		Δc [%]	4.8	4.6	-3.8	2.8	8.0	**3.3**	6.1	4.0	-4.5	3.0	9.9	**3.7**
	PVC (NIR)	c	1414	1052	595	402	689	**830**	66	47	28	18	36	**39**
		Δc [%]	-2.0	0.8	-1.2	-6.6	-7.8	**-3.4**	-1.4	0.8	-1.1	-6.7	-6.6	**-3.0**
	b&g	c	933	1109	660	420	657	**756**	45	51	32	19	35	**36**
		Δc [%]	-35.4	6.3	9.5	-2.3	-12.1	**-6.8**	-33.5	7.3	10.6	-0.6	-8.1	**-4.8**
	PET + PVC (NIR)	c	1485	1101	570	411	746	**863**	70	49	27	19	40	**41**
		Δc [%]	2.9	5.5	-5.3	-4.5	-0.2	**-0.3**	5.0	4.9	-5.8	-4.4	3.4	**0.6**
Combinations of Screening and state-of-the-art NIR sorting or manual removal of black materials	0–5 mm + PET (NIR)	c	1687	581	467	411	858	**801**	73	23	21	18	40	**35**
		Δc [%]	16.8	-44.3	-22.5	-4.4	14.9	**-7.9**	9.0	-50.9	-28.0	-10.3	4.1	**-15.2**
	0–10 mm + PET (NIR)	c	1665	549	452	365	873	**781**	71	21	20	15	40	**34**
		Δc [%]	15.3	-47.4	-25.0	-15.1	16.9	**-11.1**	6.6	-55.6	-31.1	-20.9	4.0	**-19.4**
	0–20 mm + PET (NIR)	c	1732	531	412	349	851	**775**	73	20	18	15	38	**33**
		Δc [%]	20.0	-49.1	-31.6	-19.0	13.9	**-13.2**	9.2	-57.9	-37.7	-25.1	-0.7	**-22.5**
	0–5 mm + PVC (NIR)	c	1562	568	496	368	717	**742**	68	23	22	16	33	**32**
		Δc [%]	8.2	-45.5	-17.6	-14.4	-4.0	**-14.7**	0.7	-51.4	-22.3	-19.6	-12.9	**-21.1**
	0–10 mm + PVC (NIR)	c	1534	537	484	324	725	**721**	66	21	22	14	33	**31**
		Δc [%]	6.2	-48.6	-19.6	-24.7	-2.9	**-17.9**	-1.9	-55.7	-24.9	-29.7	-13.4	**-25.1**
	0–20 mm + PVC (NIR)	c	1574	519	451	306	693	**709**	66	20	20	13	31	**30**
		Δc [%]	9.1	-50.3	-25.1	-28.9	-7.2	**-20.5**	-0.8	-57.9	-30.5	-34.1	-18.9	**-28.5**
	0–5 mm + PET (NIR) + PVC (NIR)	c	1667	579	454	374	790	**773**	72	23	20	16	37	**34**
		Δc [%]	15.5	-44.5	-24.6	-13.1	5.8	**-12.2**	8.0	-51.3	-29.9	-18.9	-3.5	**-19.1**
	0–10 mm + PET (NIR) + PVC (NIR)	c	1641	545	439	323	803	**750**	71	21	19	14	37	**32**
		Δc [%]	13.7	-47.8	-27.2	-24.8	7.5	**-15.7**	5.4	-56.1	-33.2	-30.3	-3.8	**-23.6**
	0–20 mm + PET (NIR) + PVC (NIR)	c	1711	525	397	303	772	**742**	72	20	17	13	35	**31**
		Δc [%]	18.5	-49.6	-34.1	-29.7	3.4	**-18.3**	7.9	-58.6	-40.0	-35.4	-9.7	**-27.2**
	0–5 mm + b&g	c	1009	578	548	386	681	**641**	44	23	25	17	33	**28**
		Δc [%]	-30.1	-44.6	-9.0	-10.2	-8.8	**-20.6**	-34.0	-50.7	-14.4	-14.5	-14.9	**-25.7**
	0–10 mm + b&g	c	942	543	536	338	687	**609**	41	21	24	15	32	**27**
		Δc [%]	-34.7	-48.0	-11.1	-21.3	-8.0	**-24.6**	-38.9	-55.6	-17.3	-25.5	-15.6	**-30.6**
	0–20 mm + b&g	c	868	523	498	320	651	**572**	37	20	22	14	30	**25**
		Δc [%]	-39.9	-49.9	-17.3	-25.7	-12.9	**-29.1**	-44.6	-58.1	-23.8	-30.2	-21.6	**-35.7**
	0–5 mm + b&g + PVC (NIR)	c	929	575	537	347	595	**597**	41	23	24	15	29	**26**
		Δc [%]	-35.6	-44.9	-10.9	-19.4	-20.3	**-26.2**	-39.0	-51.1	-16.1	-23.5	-24.9	**-30.9**
	0–10 mm + b&g + PVC (NIR)	c	850	538	524	294	597	**561**	37	21	23	13	28	**24**
		Δc [%]	-41.1	-48.4	-13.1	-31.6	-20.0	**-30.8**	-44.7	-56.2	-19.2	-35.5	-26.0	**-36.3**
	0–20 mm + b&g + PVC (NIR)	c	747	517	484	271	548	**513**	32	19	21	12	26	**22**
		Δc [%]	-48.3	-50.4	-19.6	-37.0	-26.6	**-36.4**	-52.2	-58.9	-25.9	-41.1	-33.6	**-42.3**
	0–5 mm + b&g + PET (NIR)	c	1042	591	505	395	752	**657**	46	23	22	17	36	**29**
		Δc [%]	-27.8	-43.3	-16.1	-8.2	0.6	**-19.0**	-31.3	-50.6	-22.6	-12.9	-5.1	**-24.5**
	0–10 mm + b&g + PET (NIR)	c	966	553	488	340	763	**622**	42	21	21	15	36	**27**
		Δc [%]	-33.1	-47.0	-18.9	-20.9	2.1	**-23.6**	-37.0	-56.0	-26.3	-25.6	-5.5	**-30.1**
	0–20 mm + b&g + PET (NIR)	c	882	531	439	318	726	**579**	38	19	19	13	34	**25**
		Δc [%]	-38.9	-49.1	-27.1	-26.0	-2.8	**-28.8**	-43.5	-58.9	-34.5	-31.0	-12.1	**-36.0**
	0–5 mm + b&g + PET (NIR) + PVC (NIR)	c	951	588	491	350	658	**608**	42	23	22	15	32	**27**
		Δc [%]	-34.1	-43.6	-18.5	-18.7	-12.0	**-25.4**	-37.0	-51.1	-24.9	-23.3	-15.8	**-30.4**
	0–10 mm + b&g + PET (NIR) + PVC (NIR)	c	858	548	472	289	665	**566**	38	20	20	12	32	**25**
		Δc [%]	-40.5	-47.5	-21.6	-32.9	-11.0	**-30.7**	-43.7	-56.7	-28.8	-37.2	-16.8	**-36.7**
	0–20 mm + b&g + PET (NIR) + PVC (NIR)	c	732	525	420	260	611	**510**	32	19	18	11	29	**22**
		Δc [%]	-49.3	-49.7	-30.3	-39.5	-18.1	**-37.4**	-52.9	-59.8	-37.5	-44.0	-25.4	**-43.9**

More targeted removal	PVC (FTIR) + b&g PVC	c	1454	1051	602	428	749	**857**	68	47	29	19	39	**40**
		Δc [%]	0.7	0.8	0.0	-0.4	0.3	**0.3**	0.8	0.6	0.1	-0.8	0.2	**0.2**
	0–5 mm + PVC (FTIR) + b&g PVC	c	1600	574	505	399	785	**772**	69	23	23	17	36	**34**
		Δc [%]	10.8	-45.0	-16.1	-7.4	5.1	**-10.5**	2.9	-50.9	-20.8	-13.1	-5.3	**-17.4**
	0–10 mm + PVC (FTIR) + b&g PVC	c	1575	543	494	356	795	**753**	67	21	22	15	36	**32**
		Δc [%]	9.1	-48.0	-18.1	-17.2	6.4	**-13.5**	0.6	-55.2	-23.4	-22.7	-5.6	**-21.3**
	0–20 mm + PVC (FTIR) + b&g PVC	c	1620	526	461	341	771	**744**	68	20	20	14	35	**32**
		Δc [%]	12.2	-49.6	-23.5	-20.7	3.2	**-15.7**	1.9	-57.3	-28.9	-26.7	-10.2	**-24.2**
	PVC (NIR) + b&g PVC	c	1419	1052	596	398	689	**831**	66	48	28	18	36	**39**
		Δc [%]	-1.7	0.8	-1.1	-7.5	-7.8	**-3.4**	-1.0	0.8	-1.0	-7.6	-6.6	**-3.1**
	0–5 mm + PVC (NIR) + b&g PVC	c	1568	569	497	363	717	**743**	68	23	22	16	33	**32**
		Δc [%]	8.6	-45.5	-17.5	-15.5	-3.9	**-14.8**	1.2	-51.3	-22.2	-20.7	-12.9	**-21.2**
	0–10 mm + PVC (NIR) + b&g PVC	c	1541	537	485	319	725	**721**	66	21	22	14	33	**31**
		Δc [%]	6.7	-48.6	-19.5	-25.9	-2.9	**-18.0**	-1.4	-55.7	-24.8	-30.9	-13.4	**-25.3**
	0–20 mm + PVC (NIR) + b&g PVC	c	1583	519	451	300	693	**709**	67	20	20	13	31	**30**
		Δc [%]	9.6	-50.3	-25.1	-30.2	-7.2	**-20.6**	-0.3	-57.9	-30.5	-35.4	-18.9	**-28.6**
	PET (FTIR) + Textiles + b&g PET	c	1502	1061	617	438	788	**881**	70	48	29	20	41	**42**
		Δc [%]	4.0	1.7	2.5	1.8	5.6	**3.1**	4.2	1.3	2.4	1.6	6.4	**3.2**
	0–5 mm + PET (FTIR) + Textiles + b&g PET	c	1668	570	516	408	835	**799**	72	23	23	17	39	**35**
		Δc [%]	15.6	-45.4	-14.4	-5.2	11.7	**-7.5**	6.9	-51.6	-19.6	-11.1	0.7	**-14.9**
	0–10 mm + PET (FTIR) + Textiles + b&g PET	c	1646	538	504	364	848	**780**	70	21	22	15	39	**33**
		Δc [%]	14.0	-48.5	-16.4	-15.4	13.5	**-10.5**	4.5	-56.0	-22.3	-21.2	0.5	**-18.9**
	0–20 mm + PET (FTIR) + Textiles + b&g PET	c	1708	520	470	348	825	**774**	71	20	21	15	37	**33**
		Δc [%]	18.3	-50.2	-22.0	-19.0	10.5	**-12.5**	6.6	-58.3	-28.1	-25.2	-4.2	**-21.8**
	b&g Other	c	889	1086	649	416	633	**735**	41	49	31	19	33	**34**
		Δc [%]	-38.4	4.1	7.7	-3.4	-15.2	**-9.1**	-39.0	3.4	6.6	-4.1	-15.3	**-9.7**
	0–5 mm + b&g Other	c	953	566	540	382	653	**619**	40	22	24	16	30	**27**
		Δc [%]	-34.0	-45.7	-10.4	-11.2	-12.6	**-22.8**	-39.9	-52.4	-17.2	-17.3	-21.8	**-29.7**
	0–10 mm + b&g Other	c	887	531	527	336	657	**588**	37	20	23	14	30	**25**
		Δc [%]	-38.5	-49.1	-12.5	-21.8	-12.0	**-26.8**	-44.5	-57.2	-20.1	-27.7	-22.6	**-34.4**
	0–20 mm + b&g Other	c	810	510	491	318	621	**550**	33	19	21	13	28	**23**
		Δc [%]	-43.9	-51.1	-18.5	-26.0	-16.9	**-31.3**	-50.4	-59.7	-26.3	-32.2	-28.4	**-39.4**
	PVC (FTIR) + b&g PVC + b&g Other	c	895	1095	649	413	635	**737**	41	49	31	19	33	**34**
		Δc [%]	-38.0	5.0	7.7	-4.0	-15.0	**-8.9**	-38.5	4.1	6.8	-5.1	-15.2	**-9.6**
	0–5 mm + PVC (FTIR) + b&g PVC + b&g Other	c	961	569	539	378	654	**620**	41	22	24	16	30	**27**
		Δc [%]	-33.4	-45.5	-10.6	-12.1	-12.4	**-22.8**	-39.4	-52.3	-17.3	-18.7	-21.8	**-29.9**
	0–10 mm + PVC (FTIR) + b&g PVC + b&g Other	c	895	533	526	331	659	**589**	37	20	23	14	30	**25**
		Δc [%]	-38.0	-48.9	-12.7	-23.1	-11.8	**-26.9**	-44.1	-57.2	-20.3	-29.4	-22.6	**-34.7**
	0–20 mm + PVC (FTIR) + b&g PVC + b&g Other	c	818	513	489	312	622	**551**	34	19	21	13	28	**23**
		Δc [%]	-43.4	-50.9	-18.9	-27.5	-16.7	**-31.5**	-50.0	-59.8	-26.6	-34.1	-28.4	**-39.8**
	PVC (NIR) + b&g PVC + b&g Other	c	822	1097	642	380	562	**700**	38	49	30	17	29	**33**
		Δc [%]	-43.1	5.1	6.5	-11.8	-24.8	**-13.6**	-43.2	4.3	5.7	-12.6	-23.8	**-13.9**
	0–5 mm + PVC (NIR) + b&g PVC + b&g Other	c	878	563	529	339	569	**576**	37	22	23	14	26	**25**
		Δc [%]	-39.2	-46.0	-12.2	-21.2	-23.8	**-28.5**	-44.5	-52.8	-18.8	-27.1	-31.5	**-35.0**
	0–10 mm + PVC (NIR) + b&g PVC + b&g Other	c	802	526	516	288	570	**541**	34	20	22	12	26	**23**
		Δc [%]	-44.5	-49.6	-14.3	-33.0	-23.7	**-33.0**	-49.9	-57.8	-21.9	-38.5	-32.6	**-40.1**
	0–20 mm + PVC (NIR) + b&g PVC + b&g Other	c	698	504	478	266	522	**493**	29	19	21	11	23	**20**
		Δc [%]	-51.7	-51.7	-20.7	-38.3	-30.1	**-38.5**	-57.4	-60.5	-28.4	-43.9	-39.7	**-46.0**
	b&g Other + b&g PVC	c	893	1087	649	412	634	**735**	41	49	31	19	33	**34**
		Δc [%]	-38.2	4.1	7.8	-4.3	-15.2	**-9.2**	-38.7	3.4	6.8	-5.1	-15.3	**-9.8**
	0–5 mm + b&g Other + b&g PVC	c	957	566	540	377	653	**619**	40	22	24	16	30	**27**
		Δc [%]	-33.7	-45.7	-10.3	-12.3	-12.6	**-22.9**	-39.6	-52.4	-17.1	-18.4	-21.8	**-29.9**
	0–10 mm + b&g Other + b&g PVC	c	891	531	528	331	657	**588**	37	20	23	14	30	**25**
		Δc [%]	-38.3	-49.1	-12.4	-23.0	-12.0	**-27.0**	-44.3	-57.2	-20.0	-28.9	-22.6	**-34.6**
	0–20 mm + b&g Other + b&g PVC	c	814	510	491	313	621	**550**	33	19	21	13	28	**23**
		Δc [%]	-43.6	-51.1	-18.5	-27.3	-16.9	**-31.5**	-50.2	-59.7	-26.2	-33.5	-28.4	**-39.6**

B.32. Compliance with legal limit values (Austrian WIO)

Table B.32: Compliance of contaminant concentrations with legal limit values for the use of SRF in cement plants listed in the Austrian WIO, expressed as % of limit value

			Cr					Co					Ni					As					Cd					Sb					Hg					Pb				
			S01	S02	S03	S04	S05	S01	S02	S03	S04	S05	S01	S02	S03	S04	S05	S01	S02	S03	S04	S05	S01	S02	S03	S04	S05	S01	S02	S03	S04	S05	S01	S02	S03	S04	S05	S01	S02	S03	S04	S05
Single process steps	0–5 mm	80th p.	17	6	4	8	11	5	11	9	14	9	16	7	3	6	5	9	4	4	4	5	26	10	49	27	11	147	142	38	139	274	17	14	9	7	9	60	15	15	49	10
		Median	26	9	6	12	16	9	19	16	26	16	29	13	6	10	9	14	6	6	6	8	52	19	97	53	22	210	203	54	198	392	35	27	18	14	18	108	27	27	89	18
	0–10 mm	80th p.	16	5	4	6	10	5	10	9	14	8	15	6	3	5	4	10	4	4	4	5	27	10	49	27	11	153	152	38	142	278	18	14	9	7	9	56	15	15	47	10
		Median	23	7	5	9	15	9	19	16	26	15	27	11	6	8	8	15	6	6	5	7	53	19	98	54	22	218	217	54	203	397	35	28	17	14	18	101	28	26	85	17
	0–20 mm	80th p.	15	5	3	6	9	5	10	9	15	8	14	6	3	5	3	10	4	4	4	5	21	10	46	23	11	144	164	39	118	280	19	14	9	7	8	60	15	15	50	8
		Median	22	7	5	9	13	8	19	16	27	14	26	10	5	8	6	16	6	6	5	7	42	19	93	47	22	205	235	55	169	400	38	29	17	14	15	109	28	26	89	14
	PET (NIR)	80th p.	62	13	7	10	16	12	13	11	16	12	61	15	6	8	8	11	5	7	5	8	28	12	42	13	10	146	137	38	127	293	21	17	12	12	10	100	17	16	50	10
		Median	91	19	10	15	24	21	24	19	29	22	110	26	11	15	15	16	8	11	7	11	57	23	84	26	19	208	196	54	182	418	43	33	24	24	20	180	31	28	90	17
	PVC (NIR)	80th p.	57	12	7	10	16	11	13	11	16	12	55	14	6	8	8	10	5	7	5	8	26	7	25	27	11	91	133	30	138	192	21	16	12	12	10	95	13	13	13	11
		Median	84	18	10	15	23	20	23	19	28	22	100	25	10	14	14	15	8	10	7	12	52	15	50	54	22	131	190	43	198	275	41	32	23	24	20	171	24	23	23	19
	b&g	80th p.	67	13	7	10	14	13	13	7	7	12	66	13	6	8	8	11	5	7	5	8	31	12	56	27	11	161	70	23	98	164	23	17	12	12	10	108	18	18	53	12
		Median	100	19	11	15	21	23	24	13	12	22	120	24	11	14	15	17	7	11	7	12	61	25	113	55	22	230	99	32	141	235	45	34	25	25	21	194	33	33	96	22
	PET + PVC (NIR)	80th p.	62	13	7	10	17	12	13	11	17	13	62	15	6	9	9	11	5	7	5	8	29	7	15	12	9	92	140	29	120	210	22	16	12	12	10	107	14	12	10	9
		Median	92	19	10	15	26	21	24	19	30	23	111	27	11	16	16	16	8	10	7	12	59	14	31	25	18	131	200	41	171	301	45	33	24	25	21	193	25	22	18	16
Combinations of Screening and state-of-the-art NIR sorting or manual removal of black materials	0–5 mm + PET (NIR)	80th p.	18	6	4	8	12	5	11	9	15	9	17	7	3	6	5	10	4	4	4	5	29	9	42	12	9	155	150	38	120	304	19	14	9	7	9	67	16	14	51	8
		Median	26	9	6	11	17	9	20	16	27	16	30	13	6	11	9	15	6	6	6	8	58	19	84	24	18	221	214	54	171	434	37	28	18	14	19	121	28	26	92	15
	0–10 mm + PET (NIR)	80th p.	16	5	4	6	11	5	11	9	15	8	16	6	3	5	5	11	4	4	4	5	30	9	42	12	9	162	162	38	123	309	19	14	9	7	9	63	16	14	49	8
		Median	24	7	5	8	17	9	19	16	27	15	28	11	6	9	8	16	6	6	5	7	60	19	84	24	17	231	231	55	176	442	38	29	17	14	18	113	29	25	89	14
	0–20 mm + PET (NIR)	80th p.	15	4	3	6	9	4	11	9	16	8	15	6	3	5	3	12	4	4	4	4	24	9	39	7	9	153	176	39	95	313	21	15	9	7	8	69	16	14	52	5
		Median	23	6	5	9	14	8	19	16	28	14	27	10	5	9	6	17	6	6	5	6	48	19	77	14	17	218	252	55	136	448	42	30	17	14	15	125	29	26	94	10
	0–5 mm + PVC (NIR)	80th p.	15	6	4	7	11	5	11	9	15	9	13	7	3	6	5	10	4	4	4	5	27	5	25	27	10	96	145	30	132	198	18	13	9	7	9	64	11	12	11	9
		Median	22	9	6	11	17	9	19	16	26	16	23	13	6	11	9	14	6	6	6	8	54	10	49	53	21	137	207	43	189	283	36	27	18	14	18	115	20	21	21	17
	0–10 mm + PVC (NIR)	80th p.	13	5	3	6	11	5	10	9	15	8	12	6	3	5	4	10	4	4	4	5	27	4	24	27	10	99	156	30	135	200	18	14	9	7	9	59	12	11	9	9
		Median	19	7	5	8	16	9	19	16	27	15	21	11	6	8	8	15	6	6	5	8	55	9	48	54	20	142	222	43	193	286	37	27	17	14	18	107	21	20	15	16
	0–20 mm + PVC (NIR)	80th p.	12	5	3	6	9	4	10	9	15	8	11	6	3	5	3	11	4	4	4	5	21	4	20	23	10	81	169	30	110	198	20	14	9	7	8	65	11	11	9	7
		Median	18	7	5	8	13	8	19	16	28	14	20	10	5	8	5	16	6	6	5	7	43	8	41	47	20	116	241	43	157	283	40	28	17	14	15	117	20	20	15	12
	0–5 mm + PET (NIR) + PVC (NIR)	80th p.	15	6	4	7	12	5	11	9	16	9	13	7	3	6	5	10	4	4	4	5	30	4	14	11	8	97	153	29	111	218	19	14	9	7	9	72	12	11	9	7
		Median	23	9	5	10	18	9	20	16	28	16	24	13	6	11	9	16	6	6	6	8	61	8	29	23	16	138	219	41	159	311	39	27	18	14	19	130	21	19	16	13
	0–10 mm + PET (NIR) + PVC (NIR)	80th p.	15	6	4	7	12	5	11	9	16	9	13	7	3	6	5	10	4	4	4	5	30	4	14	11	8	97	153	29	111	218	19	14	9	7	9	72	12	11	9	7
		Median	23	9	5	10	18	9	20	16	28	16	24	13	6	11	9	16	6	6	6	8	61	8	29	23	16	138	219	41	159	311	39	27	18	14	19	130	21	19	16	13
	0–20 mm + PET (NIR) + PVC (NIR)	80th p.	12	4	3	5	10	4	11	9	16	8	11	6	3	5	3	12	4	4	4	4	25	3	9	6	7	80	181	29	84	220	22	15	9	7	8	76	11	10	5	4
		Median	17	6	4	8	14	8	19	16	30	14	20	10	5	9	5	18	6	6	5	6	50	6	18	12	15	114	259	42	120	315	44	29	17	14	15	136	21	19	9	6
	0–5 mm + b&g	80th p.	20	6	4	8	9	6	11	5	5	9	18	6	3	6	5	11	3	4	4	6	32	10	57	27	10	172	76	22	89	169	20	14	9	7	10	73	17	17	55	11
		Median	29	8	6	11	14	10	19	9	9	15	33	10	6	10	9	16	5	6	6	8	64	20	114	54	21	246	108	32	127	241	39	29	18	14	19	131	30	31	99	20
	0–10 mm + b&g	80th p.	18	4	4	6	9	5	10	5	5	8	17	4	3	4	5	11	3	4	4	5	33	10	57	28	10	181	82	22	91	170	20	15	9	7	9	68	17	17	53	11
		Median	27	6	5	8	13	10	19	9	8	15	31	7	5	7	8	17	5	6	5	8	66	20	115	56	20	258	117	31	130	243	40	30	18	14	19	123	31	30	95	19
	0–20 mm + b&g	80th p.	18	4	3	6	7	5	10	5	5	7	17	3	3	4	3	13	3	4	4	5	27	10	55	24	10	174	89	22	60	166	23	16	9	7	8	76	17	17	56	8
		Median	26	5	5	9	10	9	19	9	8	13	30	6	5	7	5	19	5	6	5	7	53	21	109	47	20	249	127	31	86	237	45	31	18	14	16	137	31	31	100	15

	0–5 mm + b&g + PVC (NIR)	80th p.	17	6	4	7	10	6	11	5	5	9	15	6	3	6	5	11	3	4	4	6	33	5	27	27	10	109	78	12	78	65	21	14	9	7	10	79	13	13	11	10
		Median	25	8	6	10	14	10	19	9	9	16	27	10	6	10	9	17	5	6	6	8	67	9	55	55	19	156	111	17	112	92	41	28	18	14	20	142	23	24	20	18
	0–10 mm + b&g + PVC (NIR)	80th p.	15	4	3	5	9	5	10	5	5	8	13	4	3	4	5	12	3	4	4	5	34	4	27	28	9	115	84	12	80	63	21	15	9	7	10	74	13	13	7	10
		Median	22	6	5	7	14	10	18	9	8	15	24	7	5	7	8	17	5	6	5	8	69	8	54	56	18	164	120	16	114	90	43	29	17	14	19	133	23	23	13	17
	0–20 mm + b&g + PVC (NIR)	80th p.	14	4	3	5	7	5	10	5	5	7	12	3	3	4	3	13	3	4	4	5	28	4	22	23	9	94	92	11	47	51	24	15	9	7	8	84	12	13	8	7
		Median	20	5	4	7	10	9	18	8	8	13	22	6	5	7	5	20	5	5	5	7	56	7	45	47	18	134	131	15	67	73	49	31	17	14	16	152	22	23	14	12
	0–5 mm + b&g + PET (NIR)	80th p.	21	5	4	7	10	6	11	4	4	9	20	6	3	6	5	12	3	4	4	5	37	10	50	10	8	186	79	20	59	185	22	15	9	7	10	84	18	17	58	9
		Median	31	8	6	11	15	10	20	8	8	16	35	10	6	11	10	18	5	6	6	8	74	20	99	20	16	266	113	28	85	264	43	30	18	14	20	152	32	30	105	16
	0–10 mm + b&g + PET (NIR)	80th p.	19	4	3	5	10	5	11	4	4	8	18	4	3	4	5	13	3	4	4	5	38	10	50	10	7	197	86	19	61	187	22	16	9	7	10	80	18	17	56	8
		Median	28	6	5	8	14	10	19	7	7	15	33	7	5	8	9	19	5	6	5	7	77	20	100	20	15	282	122	28	87	268	45	31	18	14	20	144	33	30	101	15
	0–20 mm + b&g + PET (NIR)	80th p.	19	3	3	5	7	5	11	4	4	7	18	3	3	4	3	15	3	4	4	4	32	10	46	4	7	193	94	19	23	184	26	17	9	7	8	92	19	17	60	5
		Median	28	5	4	8	10	9	19	7	7	13	33	6	5	8	6	22	5	6	5	6	64	20	93	8	15	276	135	27	32	262	51	33	18	14	16	166	34	31	107	10
	0–5 mm + b&g + PET (NIR) + PVC (NIR)	80th p.	18	5	4	7	11	6	11	4	4	9	16	6	3	6	6	13	3	4	4	5	39	4	15	9	6	113	81	8	45	61	23	15	9	7	10	93	13	12	8	8
		Median	27	8	5	10	16	10	20	8	8	16	28	10	6	11	10	19	5	6	6	8	78	7	30	18	13	161	115	11	65	87	46	30	18	14	21	167	23	22	14	14
	0–10 mm + b&g + PET (NIR) + PVC (NIR)	80th p.	15	4	3	4	10	5	11	4	4	8	14	4	3	4	5	13	3	4	4	5	41	3	14	9	6	120	88	7	46	59	24	15	9	7	10	88	13	12	3	7
		Median	23	6	5	6	15	10	19	7	7	15	26	7	5	8	9	20	5	6	5	7	82	6	28	18	11	171	126	10	66	84	48	31	18	14	20	159	24	22	6	12
	0–20 mm + b&g + PET (NIR) + PVC (NIR)	80th p.	14	3	3	4	7	5	11	4	4	7	13	3	2	4	3	16	3	4	4	4	34	2	8	2	6	95	97	6	4	44	28	16	9	7	8	105	13	12	3	3
		Median	21	4	4	6	11	9	19	6	7	13	24	6	4	8	5	23	5	5	5	6	69	4	15	5	11	135	139	8	6	62	57	33	18	14	16	188	23	22	5	6
More targeted removal	PVC (FTIR) + b&g PVC	80th p.	57	12	7	10	15	11	13	11	15	12	56	14	6	8	8	10	5	7	5	7	25	7	38	27	11	88	131	35	125	199	20	16	12	12	10	90	14	14	12	11
		Median	84	18	10	14	22	20	23	19	28	21	101	25	10	14	14	15	8	10	7	11	50	15	76	53	23	126	188	50	179	284	40	32	23	23	20	162	25	26	22	20
	0–5 mm + PVC (FTIR) + b&g PVC	80th p.	17	6	4	7	11	5	11	9	14	9	16	7	3	6	5	9	4	4	4	5	25	5	38	27	11	92	143	35	118	204	17	14	9	7	9	60	12	13	11	10
		Median	26	9	6	11	16	9	20	16	26	15	29	13	6	11	9	14	6	6	5	8	51	10	75	53	22	131	204	50	169	291	35	27	18	14	18	108	21	24	20	18
	0–10 mm + PVC (FTIR) + b&g PVC	80th p.	16	5	4	5	10	5	11	9	15	8	15	6	3	5	4	9	4	4	4	5	26	5	38	27	11	95	153	35	121	206	18	14	9	7	9	56	12	13	8	9
		Median	23	7	5	8	15	9	19	16	26	15	27	11	6	8	8	14	6	6	5	7	52	9	75	54	21	136	219	51	173	295	36	28	17	14	18	100	22	23	15	17
	0–20 mm + PVC (FTIR) + b&g PVC	80th p.	15	5	3	6	9	5	11	9	15	7	15	6	3	5	3	10	4	4	4	4	20	4	35	23	11	78	166	36	96	205	19	14	9	7	8	60	12	13	8	7
		Median	22	7	5	8	13	8	19	16	27	13	26	10	5	8	6	15	6	6	5	7	40	8	69	47	22	111	237	51	137	292	38	29	17	14	15	108	21	23	15	13
	PVC (NIR) + b&g PVC	80th p.	57	12	7	10	16	11	13	11	16	12	56	14	6	8	8	10	5	7	5	8	26	7	25	27	11	89	133	28	125	193	21	16	12	12	10	95	13	13	12	11
		Median	84	18	10	15	23	20	23	19	28	22	100	25	10	15	14	15	8	10	7	12	52	15	50	54	22	127	189	40	178	275	41	32	23	24	20	171	24	23	22	19
	0–5 mm + PVC (NIR) + b&g PVC	80th p.	15	6	4	7	11	5	11	9	15	9	13	7	3	6	5	10	4	4	4	5	27	5	25	27	10	93	144	28	118	198	18	13	9	7	9	64	11	11	11	9
		Median	22	9	6	11	17	9	19	16	27	16	23	13	6	11	9	14	6	6	5	8	54	10	49	54	21	133	206	39	168	283	36	27	18	14	18	114	20	21	20	17
	0–10 mm + PVC (NIR) + b&g PVC	80th p.	13	5	3	6	11	5	10	9	15	8	12	6	3	5	4	10	4	4	4	5	28	4	24	27	10	96	155	28	121	200	19	14	9	7	9	59	12	11	8	9
		Median	19	7	5	8	16	9	19	16	27	15	21	11	6	8	8	15	6	6	5	8	55	9	48	55	20	138	222	40	172	286	37	27	17	14	18	106	21	20	15	16
	0–20 mm + PVC (NIR) + b&g PVC	80th p.	12	5	3	6	9	4	10	9	15	8	11	6	3	5	3	11	4	4	4	5	22	4	20	23	10	78	168	28	94	198	20	14	9	7	8	64	11	11	8	7
		Median	18	7	5	8	13	8	19	16	28	14	20	10	5	8	5	16	6	6	5	7	43	8	41	47	20	111	240	40	135	283	40	28	17	14	15	116	20	20	15	12
	PET (FTIR) + Textiles + b&g PET	80th p.	60	13	7	10	16	11	13	11	16	12	59	14	6	8	8	11	5	7	5	8	27	12	51	14	9	142	133	36	146	284	21	16	12	12	10	97	17	15	48	9
		Median	88	19	10	15	23	20	24	20	28	22	107	25	10	15	14	16	8	10	7	12	55	24	102	27	19	203	190	51	209	406	42	32	24	24	20	174	30	27	87	17
	0–5 mm + PET (FTIR) + Textiles + b&g PET	80th p.	17	6	4	7	11	5	11	9	15	9	16	7	3	6	5	10	4	4	4	6	28	10	51	13	9	150	145	36	140	294	18	14	9	7	9	65	15	14	50	8
		Median	26	9	6	11	17	9	20	17	27	16	29	13	6	11	9	15	6	6	6	8	56	20	103	25	17	215	207	52	200	420	36	27	18	14	18	117	27	25	89	14
	0–10 mm + PET (FTIR) + Textiles + b&g PET	80th p.	16	5	4	6	11	5	11	9	15	8	15	6	3	5	5	10	4	4	4	5	29	10	52	13	8	157	156	36	144	299	19	14	9	7	9	61	16	13	48	7
		Median	23	7	5	8	16	9	19	17	27	15	28	11	6	8	8	15	6	6	5	8	58	20	103	25	17	224	223	52	205	427	37	28	17	14	18	109	28	24	86	13
	0–20 mm + PET (FTIR) + Textiles + b&g PET	80th p.	15	5	3	6	9	4	11	9	16	8	15	6	3	5	3	11	4	4	4	5	23	10	49	8	8	147	169	37	118	302	20	15	9	7	8	66	15	14	50	5
		Median	22	7	5	8	13	8	19	17	28	14	27	10	5	8	5	17	6	6	5	7	46	20	98	16	17	210	242	53	169	432	41	29	17	14	15	120	28	24	90	9
	b&g Other	80th p.	62	12	7	10	13	12	13	7	7	12	61	13	6	7	8	11	5	7	5	7	28	12	54	26	12	152	68	35	108	154	21	17	12	12	10	99	18	18	50	12
		Median	92	18	11	14	19	21	23	13	12	21	110	23	11	13	14	16	7	11	7	11	56	24	109	51	24	217	97	50	155	220	42	33	24	24	20	178	32	32	91	21
	0–5 mm + b&g Other	80th p.	19	5	4	7	9	5	10	5	5	8	17	5	3	5	5	10	3	4	4	5	29	10	55	26	11	161	74	35	100	158	18	14	9	7	9	66	16	17	52	11
		Median	28	8	6	11	13	10	19	9	10	14	31	10	6	9	9	15	5	6	5	8	58	20	110	51	23	231	106	50	143	225	37	28	18	14	18	119	29	30	93	19
	0–10 mm + b&g Other	80th p.	17	4	4	5	8	5	10	5	5	8	16	4	3	4	4	10	3	4	4	5	30	10	55	26	11	169	79	35	102	159	19	14	9	7	9	62	17	16	50	10
		Median	25	6	5	8	12	9	18	9	9	14	29	7	5	7	8	16	5	6	5	7	59	20	111	52	22	241	113	50	146	227	38	29	17	14	18	111	30	30	90	18

0–20 mm + b&g Other	80th p.	16	4	3	5	6	5	10	5	5	7	16	3	3	4	3	11	3	4	4	4	24	10	53	22	11	161	86	36	74	155	21	15	9	7	8	68	17	17	52	8
	Median	24	5	5	8	9	9	18	8	9	12	29	6	5	7	5	17	5	6	5	7	47	20	106	44	23	230	123	51	106	221	41	30	17	14	15	122	30	30	94	15
PVC (FTIR) + b&g PVC + b&g Other	80th p.	62	12	7	9	13	12	13	7	7	11	62	13	6	8	8	10	5	7	5	7	27	7	42	26	12	95	68	32	87	82	21	17	12	12	10	99	15	16	12	12
	Median	92	18	10	14	19	21	23	13	12	21	111	23	11	14	14	16	7	11	7	11	55	15	85	52	24	136	97	45	124	117	42	33	24	24	20	178	26	29	21	21
0–5 mm + PVC (FTIR) + b&g PVC + b&g Other	80th p.	19	6	4	7	9	5	10	5	5	8	17	5	3	5	5	10	3	4	4	5	28	5	42	26	11	100	74	32	77	82	18	14	9	7	9	66	12	15	10	10
	Median	28	8	6	10	13	10	19	9	10	14	31	10	6	10	9	15	5	6	5	8	56	10	85	51	23	142	106	45	110	117	37	28	18	14	18	119	22	27	19	19
0–10 mm + PVC (FTIR) + b&g PVC + b&g Other	80th p.	17	4	3	5	8	5	10	5	5	8	16	4	3	4	4	10	3	4	3	5	29	4	42	26	11	104	80	32	79	81	19	14	9	7	9	62	13	15	7	10
	Median	25	6	5	7	12	9	18	9	9	14	29	7	5	7	8	15	5	6	5	7	58	9	85	52	22	148	114	46	112	116	38	29	17	14	18	111	23	26	13	18
0–20 mm + PVC (FTIR) + b&g PVC + b&g Other	80th p.	17	4	3	5	6	5	10	5	5	7	16	3	3	4	3	11	3	4	3	4	23	4	39	22	11	85	86	32	49	72	21	15	9	7	8	68	12	15	7	8
	Median	25	5	4	7	9	9	18	8	9	12	29	6	5	7	5	17	5	6	5	6	45	8	78	44	23	122	123	46	69	103	42	30	17	14	15	122	22	27	13	14
PVC (NIR) + b&g PVC + b&g Other	80th p.	63	12	7	9	14	12	13	7	7	12	62	13	6	8	8	11	5	7	5	8	29	7	28	26	11	96	69	23	85	64	22	16	12	12	10	105	14	14	12	11
	Median	93	18	10	14	20	22	23	13	13	21	111	24	11	14	15	16	7	11	7	12	58	15	55	52	23	137	98	33	122	92	44	33	24	24	20	190	26	26	21	20
0–5 mm + PVC (NIR) + b&g PVC + b&g Other	80th p.	16	6	4	7	9	5	10	5	5	8	14	5	3	5	5	10	3	4	4	5	30	5	27	26	11	101	75	23	75	64	19	14	9	7	9	71	12	13	10	10
	Median	24	8	5	10	13	10	19	9	10	15	25	10	6	10	9	15	5	6	5	8	60	9	54	51	22	145	107	33	107	91	39	28	18	14	18	127	22	23	19	17
0–10 mm + PVC (NIR) + b&g PVC + b&g Other	80th p.	14	4	3	5	8	5	10	5	5	8	13	4	3	4	4	11	3	4	3	5	31	4	27	26	10	106	81	23	77	62	20	14	9	7	9	66	12	12	7	9
	Median	21	6	5	7	13	9	18	8	9	14	23	7	5	7	8	16	5	6	5	7	62	8	53	53	21	151	115	33	110	89	40	28	17	14	18	119	22	22	13	17
0–20 mm + PVC (NIR) + b&g PVC + b&g Other	80th p.	13	4	3	5	6	5	10	5	5	7	12	3	3	4	3	12	3	4	3	4	25	4	22	22	11	86	88	23	45	52	22	15	9	7	8	74	12	12	7	7
	Median	19	5	4	7	9	8	18	8	9	12	21	6	5	7	5	18	5	6	5	6	49	7	45	44	21	122	125	32	65	74	44	30	17	14	15	132	22	22	13	12
b&g Other + b&g PVC	80th p.	62	12	7	10	13	12	13	7	7	12	61	13	6	7	8	11	5	7	5	7	28	12	55	26	12	150	67	32	94	154	21	17	12	12	10	99	18	18	50	12
	Median	92	18	11	15	19	21	23	13	12	21	110	23	11	13	14	16	7	11	7	11	56	24	109	52	24	214	96	46	135	220	42	33	24	24	20	177	32	32	91	21
0–5 mm + b&g Other + b&g PVC	80th p.	19	6	4	7	9	5	10	5	5	8	17	5	3	5	5	10	3	4	4	5	29	10	55	26	11	159	73	32	85	158	18	14	9	7	9	66	16	16	52	11
	Median	28	8	6	11	13	10	19	9	10	14	31	10	6	9	9	15	5	6	5	8	58	20	110	51	23	227	105	46	122	225	37	28	18	14	18	119	29	30	93	19
0–10 mm + b&g Other + b&g PVC	80th p.	17	4	4	5	8	5	10	5	5	8	16	4	3	4	4	10	3	4	3	5	30	10	56	26	11	166	79	33	87	159	19	14	9	7	9	62	17	16	50	10
	Median	25	6	5	8	12	9	18	9	9	14	29	7	5	7	8	16	5	6	5	7	59	20	111	52	22	237	112	47	124	227	38	29	17	14	18	111	30	29	90	18
0–20 mm + b&g Other + b&g PVC	80th p.	16	4	3	5	6	5	10	5	5	7	16	3	3	4	3	11	3	4	3	4	24	10	53	22	11	157	85	33	58	155	21	15	9	7	8	68	17	16	52	8
	Median	24	5	5	8	9	9	18	8	9	12	29	6	5	7	5	17	5	6	5	7	48	20	106	44	23	225	122	47	83	221	41	30	17	14	15	122	30	30	94	15

Ph.inishe**D.**